12-12-2022

The Solar Neighborhood Complete Survey of Stars and Planets Orbiting K Stars

Leonardo A. Paredes
Georgia State University

The Solar Neighborhood Complete Survey of Stars and Planets Orbiting K Stars

by

Leonardo A. Paredes

A Dissertation Submitted in Partial Fulfillment of the Requirements for the Degree of

Doctor of Philosophy

in the College of Arts and Sciences

Georgia State University

2022

ABSTRACT

Here I present a comprehensive study of the multiplicity of a volume-complete sample of K stars within 33 pc, a part of the RECONS K Star project (RKS), a large effort with the objective of searching for stellar, substellar, and planetary companions using three observational techniques to cover separations from 10 000 AU to 0.1 AU. In this work, I present the results of the companion search for 804 K dwarf type stars using the radial velocity (RV) technique. The survey extends for five years so far using the CHIRON Spectrograph at the CTIO/SMARTS 1.5m, achieving precisions down to 7 m/s for K dwarfs with V magnitudes between 7.0-11.5. Of the 804 K dwarfs within 33 pc and between DEC $+30^{\circ}$ and -30°, a sample of 562 K dwarfs did not have high precision RV measurements before, and are now the target of our volume-complete survey. Among the 804 stars we have found 124 RV perturbations consistent with companions never detected before, of which 38 are newly discovered stellar/sub-stellar orbits, 4 are likely planet candidates, and 82 are strong candidates for companions. Combining these results with known companions, we present here a detailed portrait of K dwarf systems unveiling a stellar multiplicity fraction of 22%, when only RV surveys are considered. The results remain consistent between the 25 pc and 33 pc, even when the 33 pc is almost doubling the stars in the 25 pc sample. The orbital architectures given by RVs and presented here, show that the lack of brown dwarfs in short period regimes still applies, and shows circular orbits become more rare with increasing orbital period. All of which starts to provide insights into formation processes around K stars. Ultimately, by providing a careful defined sample, a systematic search, and the combination of previous

studies, this thesis research aims to set basis for understanding star and planet formation processes for decades to come.

INDEX WORDS: Astronomical techniques (1684); Extrasolar gas giants (509); Spectroscopic binary stars (1557); Radial velocity (1332); Solar neighborhood (1509); Surveys (1671)

The Solar Neighborhood Complete Survey of Stars and Planets Orbiting K Stars

by

Leonardo A. Paredes

Committee Chair:	Todd J. Henry
Committee:	Russel J. White
	Douglas R. Gies
	Sebastién Lépine
	David R. Ciardi

Electronic Version Approved:

Office of Graduate Studies

College of Arts and Sciences

Georgia State University

December 2022

DEDICATION

I'd like to dedicate this thesis and hard-work to produce it to my mother, Jeannette Alvarez Defranchi, my family, and my advisor Todd J. Henry. Their unconditional support kept me going every step of the way.

TABLE OF CONTENTS

LIST OF TABLES

LIST OF FIGURES

CHAPTER 1

K Dwarf Stars and Their Companions

1.1 Overview

Welcome dear reader to my doctoral dissertation, where I would like to invite you to join me in a journey through the space beyond the confines of our Solar System to meet some of our stellar neighbors. The solar neighborhood is our tiny community in the vast city called the Milky Way Galaxy, a barred, spiral-armed galaxy that hosts our Solar System in its disc, about 8 kiloparsecs away from its center. The neighborhood we live in is a diverse place because the stars that "live" in our vicinity have different properties that dictate how they evolve throughout their lives. They can be hotter or colder than the Sun, more or less luminous than the Sun, and have relatively short or very, very, long lives. The Solar System has managed to be a place quiet enough to host and sustain an Earth with life on it, for long enough to have some of its inhabitants to be self-aware of their own existence, and to be curious enough to look for the *answer to the ultimate question of life, universe, and everything.*

The questions are often more important than the answers themselves, so let's start then with some questions: *Are we alone in our solar neighborhood, our Milky Way Galaxy, or even the broader Universe?* and *What are we able to learn about our place in the Universe?* If we *are* alone in the Universe, *Are we in a special place?*. We sometimes feel like we are special, but under the Copernican principle the answer is likely no. So, as a potentially common part of the Universe, we should look around and try to answer some of the big

questions, such as *How do stars form?*, *How do planets form?*, and *Which stellar hosts offer better conditions for sustainable life?*.

The solar neighborhood excels in providing stars in close proximity that have properties similar to the Sun, offering unmatched opportunities to study them in detail. An important consideration when trying to answer the questions posed involves determining how we can generalize findings of a surveyed sample of stars to the broader populations of stars in the Universe. Ideally, we really can only understand the answers in context if we find and characterize *all* stars of a given type in a sample. That is one of the key goals of the research presented here.

Even with the nearest stars it is not an easy task to fully characterize a given point of light as a single or multiple star system. Stars are hiding everywhere, and without searching for unseen companions, we do not really understand the nature of the target we are studying. Stars in a system orbiting very close to one another may pose as a single bright source, and some companions are so faint that they are overwhelmed in brightness by their stellar host. In some stellar systems there are components with masses that appear to be low enough to be planets and not stars ... or are they sneaky low mass stars just posing as planets?

Motivated by these questions and in pursuit of answers, I present to you here my study of our stellar neighbors, with a particular emphasis on how to "catchém all". Specifically, I target a complete sample of stellar systems with a main sequence K dwarf star as the primary component in our solar neighborhood. My goal is to reveal companions orbiting the K dwarfs, and to determine if each companion is a star or a planet.

1.2 Counting Stars

Stars have been counted before, but as time passes, new technologies allow deeper and more detailed searches. This work builds upon previous studies and presents new and updated stellar counts for a volume-complete sample of K dwarfs. For comparison, the study led by Raghavan et al. (2010), focused on 454 primarily G dwarf systems within 25 pc, and found that 50% are, in fact, multi-star systems. At lower masses, Winters et al. (2019) reported a lower stellar multiplicity rate of only 26% for 1120 M dwarfs within 25 pc. Between the G and M types in mass, temperature, and luminosity, the K dwarfs have not received the attention of their larger and smaller cousins. Stellar multiplicity rates are clearly correlated with the masses of the primary stars in the systems, but because most surveys to date for K dwarfs have only targeted ∼100 stars, we can only anticipate that the overall multiplicity rate will fall between 30% and 50%. In addition, because of their brightnesses, K dwarfs are easier to study than faint M dwarfs, and are somewhat less massive than G dwarfs, so lower mass companions can be detected. Thus, K dwarfs fall in a sweet spot for detecting a wide variety of companions orbiting a large sample of stars, all accomplished with a reasonable amount of telescope time.

In essence, the work described here has three main objectives. The primary objective is to determine an accurate stellar multiplicity rate for K dwarfs. We will count every single "orange" point in the sky, survey each of them for companions, and as a result know how many are single vs. multiple. The second objective is to complete the count in a volume-complete sample of stars, so that characteristics of the stars and their companions can be

determined with statistical accuracy. Finally, the third objective is to unveil the orbital architectures of the multiple systems that are found by mapping the orbits of their stellar, brown dwarf, and/or giant exoplanet companions.

1.3 K Dwarfs vs. Other Types of Stars

Stars of spectral type K in the main sequence stage (hydrogen-burning) of its evolution have surface temperatures between T_{eff} = 3930–5270 K (Gray & Corbally 2009; Pecaut & Mamajek 2013) and have masses between M = 0.59–0.88$M_{\odot}$ (Henry & McCarthy 1993; Eker et al. 2015). They fall between the hotter and more massive G dwarf stars and the cooler, less massive M dwarf stars. Compared to G dwarfs like our Sun that make up only 5% of stars in the solar neighborhood, K dwarfs are more abundant at 12% and have longer lives burning hydrogen in the main sequence, thereby potentially making them better companion hosts than G dwarfs (Cuntz & Guinan 2016; Richey-Yowell et al. 2019, 2022).

When searching for the smallest unresolved companions, the radial velocity technique excels, and possibilities of detection of lower mass companions in K dwarfs, such as brown dwarfs and exoplanets increase compared to G dwarfs. The reflex motion on K dwarfs produced and measured through radial velocities is larger compared to G dwarfs for an equivalent companion. Compared to M dwarfs, K dwarfs are also brighter in optical bands, therefore easier to find. At same time, higher signal to noise ratios allow the use of higher spectral resolving power, important for extracting radial velocities even more sensitive to the presence of companions. The spectral energy distribution of K dwarfs peaks in the

optical region, and offers generous numbers of unblended spectral lines formed in Earth's atmosphere, far enough from the spectral region contaminated by telluric spectral lines, which tend to contaminate the Doppler effect produced by the companion in the host star.

Magnetic activity on the stellar surface has an impact in both exoplanet detection and habitability. In terms of detection, M dwarfs show more activity and flaring than K dwarfs and other earlier type stars because their evolution is slower and they have longer lives. Activity in the photosphere and chromosphere, in the form of oscillation, granulation, and/or magnetic field spots, has significant effects on the spectral line profiles, mimicking Doppler shifts produced by a planet size companion, when in reality the shifts results from inhomogenieties in the rotating stellar host surface.

From the planet habitability perspective, K dwarfs may be the best host for long term sustainable life. Cuntz & Guinan (2016) call early and mid type K dwarfs "Goldilocks" life-hosting stars and rank them at the top of the real estate market value offerings. In their analysis, they develop the "Habitable-Planetary-Real-Estate Parameter" (HabPREP) considering a variety of aspects that ultimately show a strong dependence with the stellar host fundamental parameters. In their own words the aspects to consider are: "(1) the frequency of the various types of stars, (2) the speed of stellar evolution in their lifetimes, (3) the size of the stellar climatological habitable zones (CLI-HZs), (4) the strengths and persistence of their magnetic-dynamo-generated X-ray-UV emissions, and (5) the frequency and severity of flares, including superflares; both (4) and (5) greatly reduce the suitability of red dwarfs to host life-bearing planets".

1.4 K Dwarfs with Stellar Companions

In a recent *Annual Reviews* article, Duchêne & Kraus (2013) omit an assessment of K dwarf multiplicity altogether, addressing solar-type stars with masses greater than 0.7 $M_{\odot}$ and red dwarfs less massive than 0.5 $M_{\odot}$, skipping most of the K dwarfs due to the dearth of survey work. As can be seen by examining the list of stellar multiplicity surveys in Table 1.1 ranked by the number of K dwarf systems observed), relatively few K dwarfs have actually been explored.

Previous searches for companions to nearby stars similar to the Sun have typically included a few hundred stars. In their pioneering work, Duquennoy & Mayor (1991) found that roughly half of 164 F and G stars in a volume-limited survey were multiples. Subsequent updates (Udry et al. 2000; Raghavan et al. 2010) have built upon these results, and reached similar conclusions. The largest survey of solar-type stars to date includes 4847 F and G stars byTokovinin (2014), in which he estimates that ∼80% of stellar companions have been detected, but in which only ∼30% of tertiaries and additional companions have been identified. However, these studies have not *systematically* sampled *all* separation regimes, relying instead on programs reporting companions found during various heterogeneous imaging and RV efforts that did not search all stars in the samples.

At lower masses, the most comprehensive studies are those of Ward-Duong et al. (2015), who surveyed 245 K and M dwarfs within 15 pc from 3–1000 AU using adaptive optics and wide-field searches, and that of Winters et al. (2019), who searched 1120 M dwarfs within 25 pc, at regions from 2″ outward, with additions for closer systems as available. Both

studies found a multiplicity rate of ∼25%. A radial velocity survey of 1000+ M dwarfs is currently beyond most programs (see, e.g., Bonfils et al. (2013), who observed 102 M dwarfs), although CARMENES is targeting 324 M dwarfs (Reiners et al. 2018) and Winters is currently observing a similar number within 15 pc.

Two things complicate results from most of these surveys: (1) some stars are omitted from observing lists entirely, e.g., binaries from RV surveys, and (2) null detections are often not reported, resulting in the need for various, sometimes uncertain, correction factors. In a comprehensive assessment of RV surveys, Grether & Lineweaver (2006) showed that among stars within 25 pc selected using *Hipparcos* results, ∼90% of K0V stars, 50% of K5V stars, and only 10% of K9V stars were being targeted for planets. They sum up the problem well, even for Sun-like stars: "Doppler survey target selection criteria often exclude close binaries (separation $<2''$) from the target lists and are not focused on detecting stellar companions. Some stars have also been left off the target lists because of high stellar chromospheric activity." In my work, I attempt to address these problems by observing *all* stars in the sample.

Table 1.1: Surveys of Nearby Stars for Companions

Reference	Spectral Types	# Total Systems	# K Systems	Search Region	Technique	Notes
Bonfils et al. (2013)	M	102	0	P < 6 yrs	radial velocities	11 pc
Duquennoy & Mayor (1991)	FG	164	0	P < 13 yrs	radial velocities	
Reiners et al. (2018)	M	324	0	recent start	radial velocities	CARMENES
Winters et al. (2019)	M	1120	0	0–1000 AU	various	25 pc
Tokovinin (2014)	FG	4847	0	0–1000+ AU	various	67 pc
Ward-Duong et al. (2015)	KM	245	11	3–10000 AU	adaptive optics	15 pc
Valenti & Fischer (2005)	FGK	1040	66	none	radial velocities	not companion survey
Gaidos et al. (2013)	K	110	85	P < 4 yrs	radial velocities	
Horch et al. (2012)	AFGK	384	99	$0.05–2''$	speckle imaging	multiples only
Horch et al. (2011)	AFGK	497	118	$0.05–2''$	speckle imaging	

Table 1.1: Surveys of Nearby Stars for Companions

Reference	Spectral Types	# Total Systems	# K Systems	Search Region	Technique	Notes
Raghavan et al. (2010)	FGK	454	165	0–1000 AU	various	25 pc
Tokovinin (1992)	KM	200	167	P < 3000 days	radial velocities	
Halbwachs et al. (2018)	GK	269	261	P < 13 yrs	radial velocities	

1.5 K Dwarfs with Planetary Companions

K dwarfs have generally not been systematically surveyed for planets. Most RV and transit programs target either FGK samples in which the bluer, brighter stars dominate the sample, or M dwarfs that permit the smallest planet detections. Most surveyors have systematically discarded obvious binaries, thereby preventing comprehensive assessments of companions. Furthermore, an exoplanet transit detection might be misrepresenting the planet's radii by a factor of 1.5 on average if the host star is assumed to be single, and by a factor of 1.2 for K stars, as demonstrated by the study on Kepler Object of Interest with derived radii (Ciardi et al. 2015).

As of 2022 October the NASA Exoplanet Archive, a trusted repository for confirmed exoplanets, reports 39 K dwarfs with at least one orbiting planet confirmed in the 33 pc horizon solar neighborhood, 3 of which were presented in Paredes et al. (2021) as results of this work. An additional exoplanet orbiting a K dwarf, HIP 65, was follow-up and characterized in this work. The exoplanet detection was first spotted by the first batch of TESS Object of Interest, and served as test-bed for the on-going symbiosis between CHIRON RVs and TESS transit detections. The growth in observational resources destined for exoplanets searches in recent years, have started to fill gap in K dwarfs monitoring, but still remains

to be done. To date, among the 804 K dwarfs will be presented here 587 have at least one timeseries from TESS. In this aspect, the work presented here also pretends to pave part of the road for new discoveries in these unexplored regimes in our solar neighborhood, and be ready for the ambitious exoplanet endeavors of the next decade.

1.6 Steps to Surveying Hundreds of K Dwarfs for Companions

In Chapter 1 we have outlined the reasons why K dwarfs were selected for this survey, which focuses on finding companions to these stars using the radial velocity (RV) technique. Stars exhibiting RV variations are likely, but not always, being perturbed by an orbiting companion. The process to extract the RVs from the spectra of K dwarfs is discussed in Chapter 2, where I detail the construction of a custom-tailored data processing pipeline for spectra from the CHIRON instrument at the CTIO/SMARTS 1.5m telescope.

The second step is to construct a sample of K dwarf primary stars. Ideally, we want a reasonable compromise in the number of K dwarfs to target in an RV survey. A sample that is too small will not yield statistically reliable results. On the other hand, a sample that is too large means that a huge number of high-resolution spectra must be obtained, and such a survey cannot be completed in a reasonable amount of time. Here we target a sample of several hundred stars that is sufficient for statistically significant results, and can be surveyed in $\sim$5 years. I rely on a combination of new data and results from other groups who have observed some stars previously. This sample is also large enough that it can be subdivided into groups such as metal-poor/metal-rich, active/inactive, or young/old, that

remain sufficiently large that general properties and correlations can be revealed. In Chapter 3, I detail the criteria adopted to identify which stars are K dwarfs, the steps taken to select a volume-complete sample of stars to be observed, and the strategy used to survey them.

The third step is to analyze the series of RV observations acquired for each K dwarf to determine whether or not a companion has been detected using the data available. Criteria used to determine verdicts of companion vs. no companion are based on the capabilities of the CHIRON instrument used to measure the RVs, the observing strategy executed, and information available previously in the literature for each star. In Chapter 4, I show the results obtained for each K dwarf in the survey and show the evidence supporting the companion or no companion verdict.

In Chapter 5, the results are analyzed as a whole in two curated sub-samples with horizons of 25 pc and 33 pc. I discuss the findings shown in this thesis and future prospects of surveys for K dwarf companions.

Finally, in Chapter 6 I provide details about some additional experiences I had while carrying out the research presented here. In particular, I provide details about my contributions as the SMARTS Fellow for the 1.5m Telescope. This included reopening the telescope with the CHIRON Spectrograph in 2017, establishing instrument, computer, and data reduction protocols, and assisting users of the facility. As a result, I have helped expand the research options available to RECONS group members and other groups in the Department of Physics and Astronomy at Georgia State University, as well as many researchers in the U.S., Chile, and Europe.

CHAPTER 2

Technique, Instrument, and Data Processing

2.1 Gravitational Signatures

As in our Solar System, gravitational interactions between a host star (or primary star) in another system and its companions — other stellar companions, brown dwarfs, and/or planets — dictate positions, velocities, and evolution in the orbital motion of each component of the system. Kepler's Laws of orbital motion describe mathematically the phenomena of the interacting bodies, relating the orbital characteristics of the motion and the physical properties of the components, primarily their masses. When monitoring the primary star, the presence of an unseen companion produces a reflex motion, and clues to the companion's nature can be gathered by measuring the host star's velocity in the line of sight, i.e., its radial velocity (RV), and analyzing its variations over time. For a gravitational two-body problem, Kepler's Laws can be arranged to establish relations between observational measurements, such as the RV time-series of the primary star and masses of the components. The most useful arrangement for the work presented here establishes the relation between the RV semi-amplitude K_1 of the time-series with the masses of the primary star m_1 and its companion m_2 as

$$K_1 = \frac{28.4329 \text{ m s}^{-1}}{\sqrt{1-e^2}} \frac{m_2 \sin i}{M_{\text{Jup}}} \left(\frac{m_1+m_2}{M_\odot}\right)^{-2/3} \left(\frac{P}{\text{yr}}\right)^{-1/3} \tag{2.1}$$

where e is the eccentricity, i is the inclination, and P is the period of the orbital motion. If the goal is to determine precise orbital parameters using Eq. 2.1, a precise RV semi-amplitude

K_1 must be derived using multiple RV measurements.

2.2 Doppler Technique

Measurements of the RV of a star at given times are needed to reveal and characterize a companion, and photons collected can provide the necessary measurements by using the well-known Doppler Effect. In its most fundamental form, the Doppler Effect describes how the wavelength of an emitted photon $\lambda_{\rm emit}$ in the rest frame of the source will shift to a different wavelength $\lambda_{\rm meas}$ as seen by an observer moving with respect to the emitter. This produces a dimensionless quantity known as the redshift, $z_{\rm meas}$, given by

$$z_{\rm meas} = \frac{\lambda_{\rm meas} - \lambda_{\rm emit}}{\lambda_{\rm emit}} \tag{2.2}$$

In practice, stellar spectra are obtained from each observation of a target star, providing $\lambda_{\rm meas}$ from the positions of the spectral features, while $\lambda_{\rm emit}$ is the reference wavelength for those features. The measured redshift, $z_{\rm meas}$, is then derived after correcting for the velocity shift of the observer's motion around the Solar System's barycenter, z_B, leaving the true redshift of the star independent of the motion of observer at the Earth, as in

$$z_{\rm true} = z_{\rm meas} + z_B + z_{\rm meas} z_B \tag{2.3}$$

The final RV of the star is derived after measuring the redshifts $z_{\rm meas}$ and z_B, and is simply the speed of light times the result, $cz_{\rm true}$, to convert the dimensionless redshift into a velocity. A detailed description of the z_B calculation is beyond the scope of this work, but

details can be found in Wright & Eastman (2014) and their code "barycorr." Their work provides a barycentric correction at $\sim$1 cm s^{-1} precision level, and incorporates relativistic effects, telescope position, observation timing, stellar position, and stellar motion. Note that $z_{\rm meas}$ measures not only changes in the star's overall velocity via wavelength shifts of stellar atmosphere spectral features, but changes in the velocity of the star's atmosphere in the radial direction as well. Fortunately, for most K dwarfs such atmospheric motions are not severe, and are not a worry at the RV precisions of $\sim$5–20 m s^{-1} achieved for this work. Positions of the wavelengths of absorption/emission lines in each stellar spectrum are compared to known reference wavelength positions to provide the RV value. The precision of the RV measured depends strongly on the richness of information in each spectrum, generally favoring prominent spectral line features rather than continuum flux. FGKM dwarf stellar spectra are particularly rich in features at optical wavelengths because their cool atmospheres produce numerous strong, narrow spectral line profiles.

The radial motion of the star equally affects photons emitted by the star at various wavelengths, so a relative Doppler shift between two epochs can be computed by applying a cross-correlation function (CCF) to two spectra across many wavelengths. The CCF compares spectra of the same star at two different times, or compares one spectrum against a reference, to obtain its relative RV.

Consider two spectra of the same star, as shown in Fig. 2.1, where an observed spectrum $f(n)$ is shown in blue and the reference or template spectrum $g(n)$ is shown in red, both expressed in terms of bin number, n, where $n = A \ln \lambda + B$, for which any spectrum shift

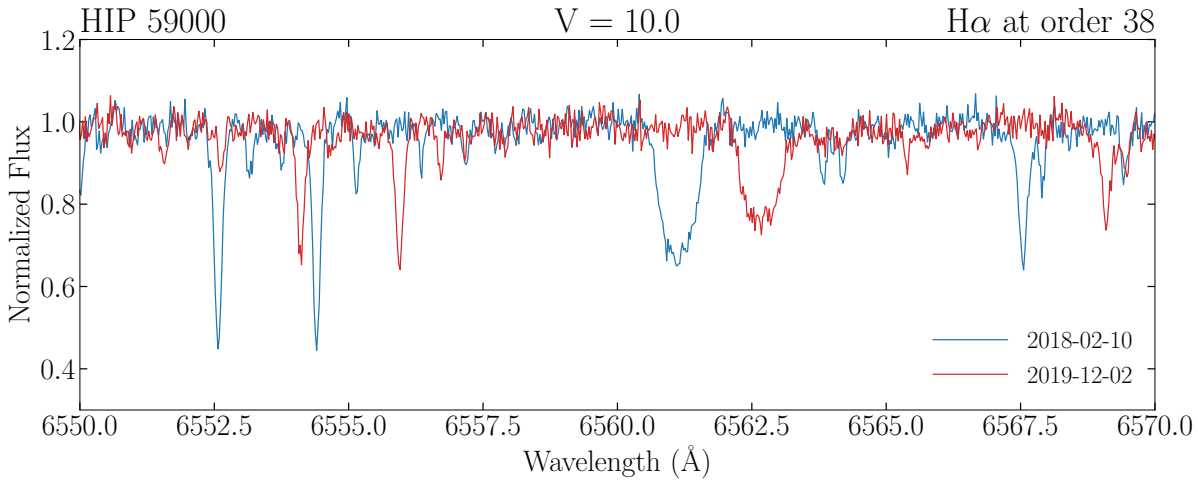

Figure 2.1 Two normalized and flattened spectra of the same star. A selected template spectrum obtained at one epoch is shown in red and a second spectrum secured at a different time is shown in blue. For illustration purposes, neither spectrum is corrected for the barycentric motion of the Earth, so the Doppler shift is more evident.

corresponds to a uniform linear Doppler shift. Each spectrum's wavelength scale is resampled so that the log-wavelength shift (proportional to the RV) is uniform at any part of the spectrum. Each spectrum is also continuum subtracted and flattened, i.e., having zero mean, $\sum_n f(n) = 0, \sum_n g(n) = 0$, with the number of bins typically large.

The normalized CCF, $C(s)$, between the f and g spectra is defined by

$$C(s) = \frac{\frac{1}{N}\sum_n f(n)g(n-s)}{\frac{1}{N}\sum_n f^2(n)\ \frac{1}{N}\sum_n g^2(n)} \tag{2.4}$$

where s is the shift between the f and g spectra. The CCF is constructed by sampling shifts in the log-wavelength axis, n, and calculating $C(s)$ for each s, as shown in Fig. 2.2. The shift $\hat{s}$ is the velocity at which the CCF is maximized, i.e., where f and g match the best.

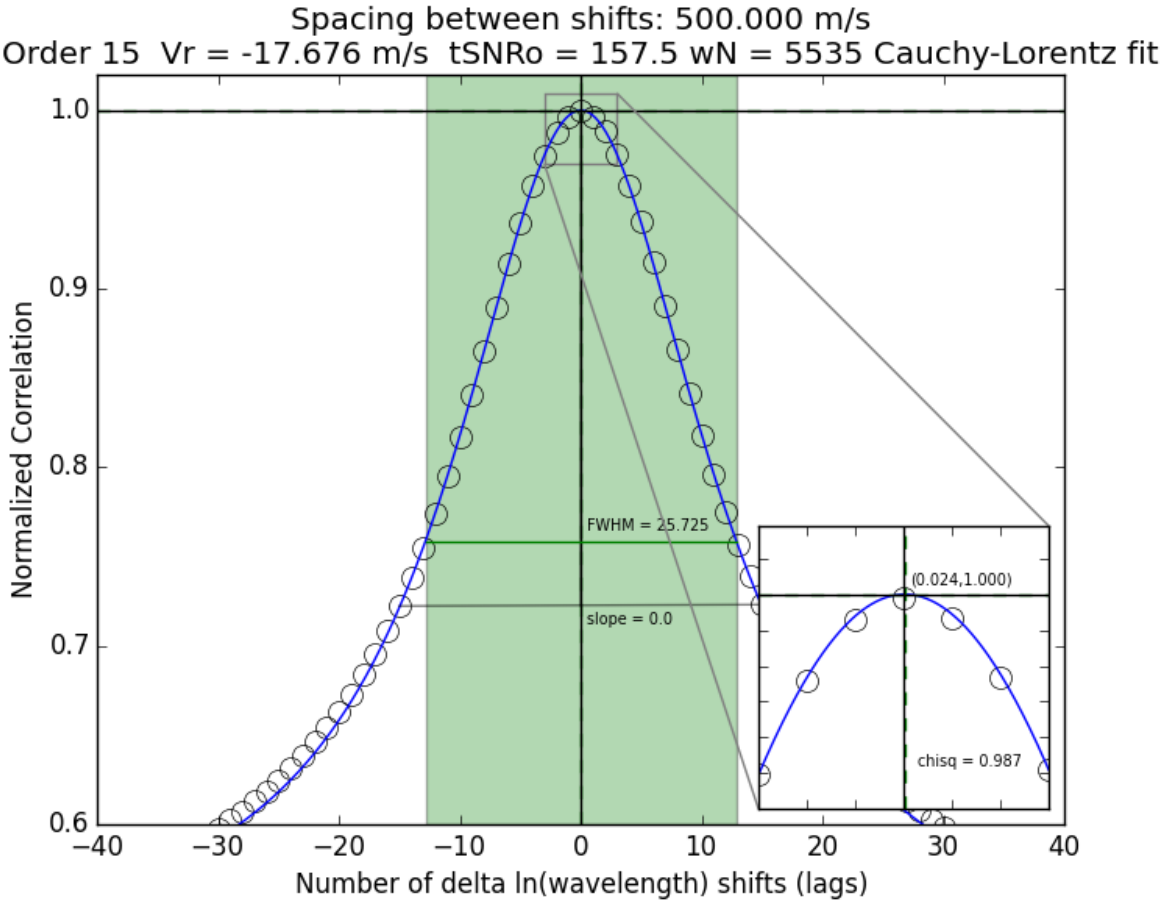

Figure 2.2 CCF applied to two spectra called f and g in the text. Open circles are the CCF values, $C(s)$, for each shift s in the n log-wavelength axis. The blue line is a Cauchy-Lorentz model that best fits the series of s,$C(s)$ data. The zoomed region is centered on $\hat{s}$, the value of s for which $C(s)$ is maximized — $\hat{s}$ is the value used for the RV measurement.

The result is the velocity solely from the Doppler shift of the star at the time of the observed spectrum with respect to the template spectrum, and is given by $c\hat{s}$.

The precision of the velocity derived from the Doppler shift between the two spectra depends on both instrumental factors and astrophysical phenomena occurring in the target star and the space between the star and the observer. For the Earth-based portion, the

precision is determined by the light throughput of the telescope/instrument combination, the resolution of the spectrograph, and the quality of the wavelength calibration. For the wavelength calibration, the near-simultaneous reference technique is one of the most widely use methods to extract RVs from data taken with spectrographs. The method consists of establishing an accurate wavelength scale by exposing the spectrograph to a comparison lamp immediate before or after each science observation. The comparison lamp used for this work is a Thorium-Argon (ThAr) lamp, which offers numerous strong and stable emission lines to provide a contemporaneous CCD pixel-to-wavelength map for science observations. Further improvements to reach higher precision RVs involve the implementation of temperature and pressure controls of the optical system; typically these improvements can increase the precision from $\sim$7 $\mathrm{m\,s^{-1}}$ to $\sim$1 $\mathrm{m\,s^{-1}}$.

The shape of the CCF can provide information such as the quality of the input spectra as well as the nature of physical processes associated with the light we collect from the star. Low S/N input spectra typically results in a CCF with a peak much less prominent or not present at all. If the input spectral regions have enough S/N but do not exhibit prominent spectral lines, i.e., input spectral regions are mostly continuum, then the shape of CCF shows a peak but is wider. Among the astrophysical processes affecting the shape of the CCF are fast rotation, stellar activity, and the presence of stellar companions of comparable brightness. When the input spectra comes from a fast rotating star ($v \sin i \gg 10$ $\mathrm{km\,s^{-1}}$), spectral lines exhibit rotational broadening proportional to the stellar rotation speed. The CCF peak is present but the shape is wider and also proportional to the stellar rotation speed. This case

is very similar to the case of spectral regions lacking spectral lines, because the broadened lines could get shallow enough to blend with continuum. Stellar activity introduces time dependent asymmetries in the profile of the spectral lines, resulting in the CCF having a moving peak that is not due to changes in the radial velocity of the star. Lastly, multiple peaks in the CCF are typically because the light of two or more stellar sources combine into a single spectrum, spectral features of the different stars appear in the same spectrum but shifted by their radial velocity difference. A binary system resolved from this spectral characteristics are named spectroscopic binary type 2 (SB2).

For the remaining sections of this Chapter, the focus is on how the Doppler technique is applied to data from the CHIRON instrument (Tokovinin et al. 2013) operating at the CTIO/SMARTS 1.5m Telescope at Cerro Tololo, Chile. CHIRON is a high-resolution echelle optical spectrograph specifically designed for extracting precise RVs with resulting precisions on the order of $\sim$7 $\mathrm{m\,s^{-1}}$.

2.3 CTIO/SMARTS 1.5m Telescope

The CTIO/SMARTS 1.5m telescope has been operated by the SMARTS Consortium (Subasavage et al. 2010) since 2003. The telescope is primarily operated by onsite CTIO/SMARTS staff observers, although occasional runs are done by individual SMARTS Consortium members. The 1.5m has had a few different instruments available since SMARTS began, but the primary instrument over the past decade, and the only one in operation since 2015, is the CHIRON high-resolution spectrograph (Tokovinin et al. 2013). CHIRON was commissioned

in 2011, upgraded in 2012, and was used until the 1.5m closed in 2016, when the primary observing program at the time ended. The 1.5m was reopened in June 2017 by the author of this dissertation and his advisor, in concert with CTIO staff members, and the K dwarf RV program commenced.

2.4 Observing Queue Management

Since June 2017, the RECONS team has overseen the management and operations of the 1.5m and CHIRON. This includes financial management, staffing, scientific support, the construction of observing queues, data processing, and data distribution. Queue management is carried out via a web-based platform at *chiron.astro.gsu.edu* in which time allocations, target requests, desired observing cadences, and on-site telescope operations are fully integrated. Programs from users who purchase observing time and those awarded time via the NOAO/NOIRLab and Chilean TACs are scheduled simultaneously.

Once observing time is allocated, PIs and their collaborators access the queue management platform to submit their targets and observing requirements, managing the use of the observing time that they have been granted. Our queue management team then sorts the various observing requests from multiple PIs to create the nightly schedule, and the observing sequence is executed by a CTIO/SMARTS observer using the same web-based platform. The observer is able to add, remove, or re-sequence observations as sky conditions permit, and can complete the arc of some science programs through a 7-night shift or prepare the next shift's observer to carry on longer programs. From October 2017 through July 2019, the

facility was operated every other week, while beginning in August 2019, operations expanded to full-time nightly coverage.

2.5 Telescope Operations

A typical night of CHIRON operations starts with a fixed set of calibrations for all observing modes, detailed in Table 2.1, that commence in the afternoon. At astronomical twilight, the on-site observer accesses the night's observing schedule using the web platform and executes the queue, reporting back the status and/or any issues that may affect the observations. For some programs, an Atlanta-based team member is available real-time to assist in interpretation of the science requirements. The web platform is directly connected to the instrument controller; therefore, for each target acquired the requested instrument setup is passed directly to the instrument and telescope control system (TCS), increasing efficiency and reducing configuration errors. At the end of the night, another fixed set of calibrations is secured. More details about the website and related operational systems are provided in Brewer et al. (2014).

2.6 CHIRON Spectrograph

CHIRON covers an optical wavelength range of 415 to 880 nm, cross-dispersed into 66 to 136 spectral orders, and is able to acquire targets up to ∼18 mag through a fiber that is 2.7″ in diameter on the sky. The primary resource for details about CHIRON is Tokovinin et al. (2013), which outlines the four different slit setups available, ranging in resolution from 28,000 to 136,000 (see Table 2.1). A user's choice of setup is determined by science goals

and target brightnesses.

Table 2.1: Modes available for observing with CHIRON.

Slit Mode	Binning	R	Throughput	Element Size
Fiber	4x4	28 000	1.00	4 000 $\mathrm{m\,s^{-1}}$
Slicer	3x1	80 000	0.75	1 000 $\mathrm{m\,s^{-1}}$
Slit	3x1	90 000	0.40	1 000 $\mathrm{m\,s^{-1}}$
Narrow Slit	3x1	136 000	0.20	1 000 $\mathrm{m\,s^{-1}}$

CHIRON offers two wavelength calibration options — a ThAr comparison lamp and an iodine cell. The latter can be used to achieve instrumental precision better than 5 $\mathrm{m\,s^{-1}}$ on targets brighter than $V \sim 6$, at the expense of requiring large amounts of observing time to reach a sufficient signal-to-noise ratios (S/N) for such precision. The work we present here utilizes CHIRON in slicer mode and the ThAr lamp for wavelength calibration, which is more versatile than the iodine cell and is the most popular among users.

2.7 Data Management

The raw data and calibration files are backed up and transferred for processing daily to computer facilities in Atlanta. The files consist of two-dimensional CCD frames containing the echelle orders and header information, where telescope, ephemerides, spectrograph, and exposure meter (EM) data are recorded. The default data processing consists of bias and flat-field corrections, cosmic ray removal, echelle order extractions, and wavelength calibrations using ThAr comparison lamps.[1] The algorithms used are based on the REDUCE IDL

[1] An iodine cell is available, but few CHIRON PIs have used the iodine cell since reopening and wavelength calibrations

package (Piskunov & Valenti 2002) and were adapted to CHIRON data with the goal of deriving precise radial velocity measurements. Reduced data are produced in FITS file format, containing for each extracted order the flux in photo-electrons and topocentric wavelength in Angstroms per pixel. A portion of the spectra in the blue-end is not extracted, mainly because of the designers decision to favor the light throughput closer to 5000Å, where the technique using Iodine wavelength calibration is used. Additional specifics of the data reduction process are described in detail in Tokovinin et al. (2013). Once a night of observations is fully processed, calibration files, raw data, logs, and reduced data are grouped into individual PI programs and placed in secure directories on servers in Atlanta. PIs are then notified and instructed how to retrieve their data products. The entire process from raw data acquisition to the delivery of fully processed data products can be completed within a day, although batches are more typically made available every two weeks.

2.8 Radial Velocity Pipeline

The desire to apply the Doppler technique described in § 2.2 to the CHIRON data described in § 2.6 motivated the creation of a pipeline (here after the RV pipeline) developed in python by the author. The RV pipeline is able to process large volumes of spectra taken with CHIRON to extract radial velocities for hundreds of stars. It was optimized specifically for our K dwarf survey at the 1.5m and follows a recipe that has nine steps.

1. *Input spectra.* Each wavelength-calibrated spectrum (Figure 1) enters the RV pipeline once it has been confirmed to have the proper target identification, as well as cor-

based on iodine lines are not part of routine operations.

rect observational parameters, such as coordinates, hour angle, time of exposure, and airmass.

2. *Flattening spectra.* The removal of the blaze function embedded in each order of the echelle spectra is crucial for extracting precise radial velocities. The Doppler information contained in the spectrum is most valuable in regions where changes in the slope of the flux per wavelength are steepest, i.e., for sharp lines. The flattening process starts with a recursive sigma clipping algorithm to remove the spectral lines over subsections of the order to be able to map the continuum. Then, a 5th-order polynomial is fit using the remaining data points in a particular order. Finally, the original unfiltered spectral order is divided by the blaze function fit to get a flattened, normalized version (Figure 2). Removing the blaze function to flatten each order ensures that Doppler shifts are the result of shifting lines due to a star's velocity, rather than from changes in the instrument response along the order. Figure 2 illustrates three spectral regions after removing the blaze function and normalization. These spectral regions include many key features found in K dwarf spectra: Cr I, Fe I, Hα, Li I, Na I, and Ti I.

3. *Barycentric correction.* The motion of the Earth around the barycenter of the Solar System produces a large ($\pm$30 km s^{-1}) Doppler oscillation present in all sequences of spectra. These variations must be removed with high precision to derive the final radial velocities for a targeted star. We use the algorithm "barycorr" by Wright & Eastman (2014) that calculates corrections appropriate for radial velocity precisions to at least better than 3 cm s^{-1}into cm s^{-1}. The three ingredients used to calculate the correction

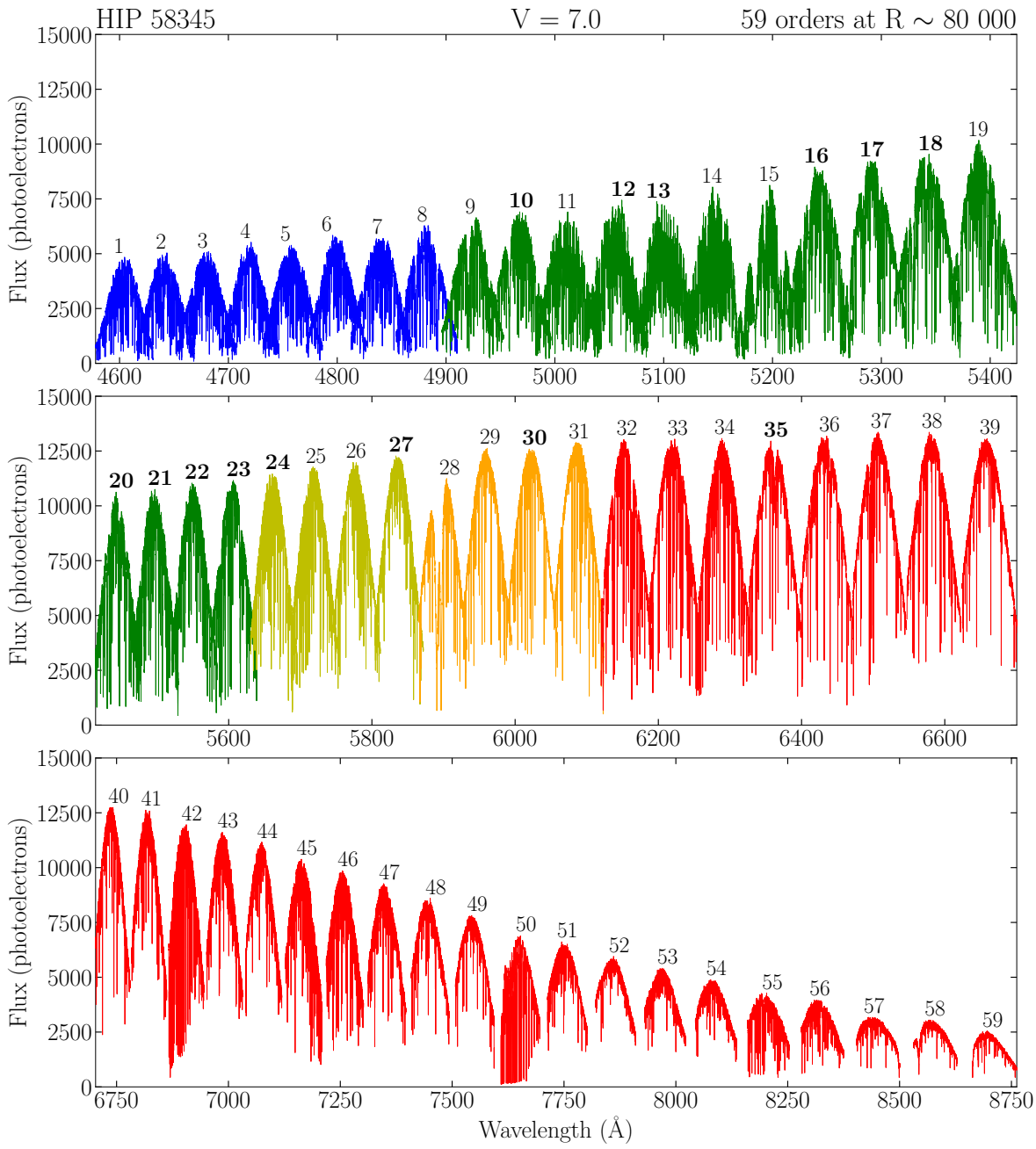

Figure 2.3 All 59 echelle spectral orders in slicer mode (R ∼ 80000) for the K dwarf HIP 58345 extracted by the CHIRON basic reduction pipeline are shown. A fixed set of 14 of these orders (boldface numbers) are used to derive our radial velocities.

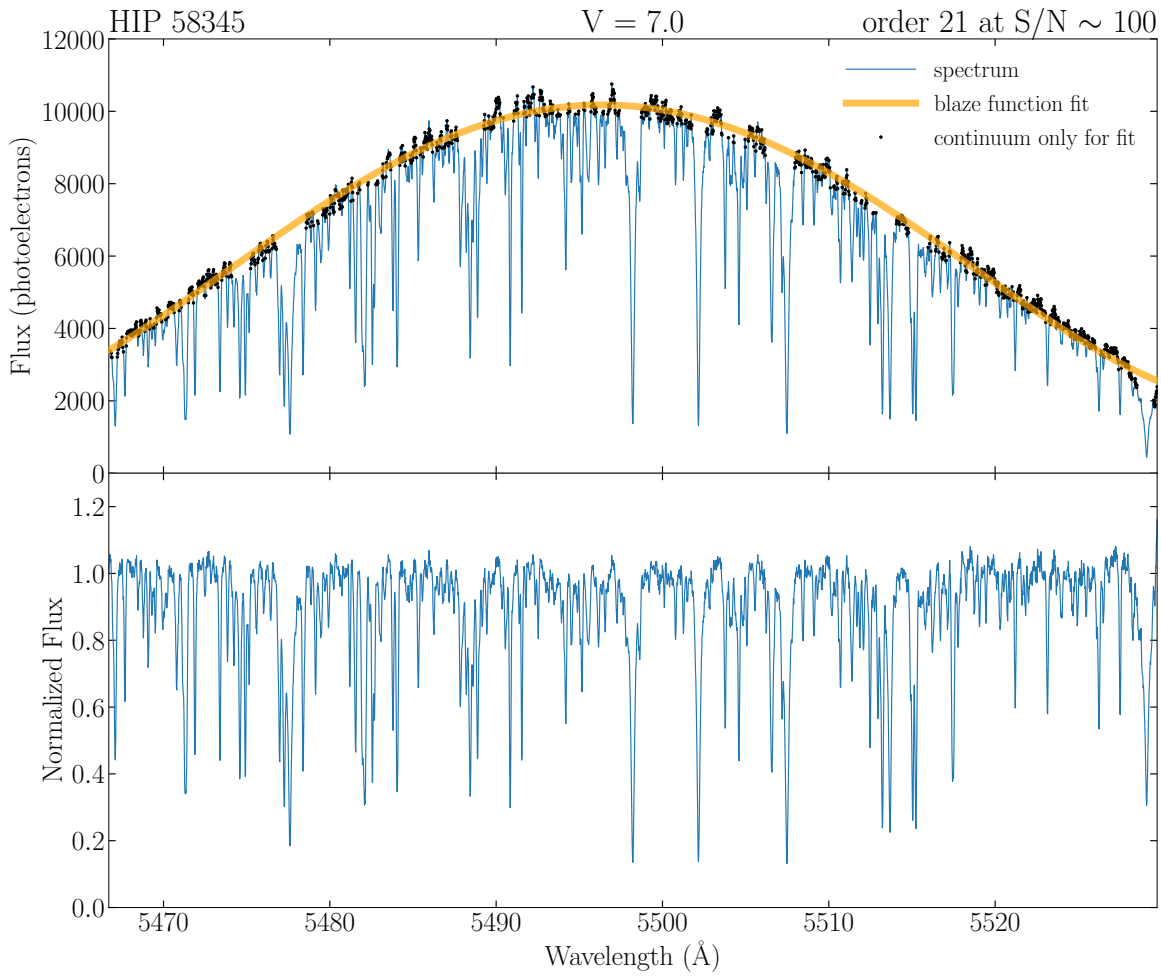

Figure 2.4 Spectrum of order 21 (∼5460 to 5530 Å) of HIP 58345 taken in slicer mode (R ∼ 80,000) at S/N ∼ 100. *top:* Spectrum before the removal of the blaze function, where the black dots are the data points from the original spectrum (blue line) used to fit the blaze function (yellow line). *bottom:* Normalized spectrum after the removal of the blaze function, illustrating a flattened spectrum.

are (1) the geographical position of the CHIRON spectrograph on Earth, using GPS measurements by Mamajek (2012), (2) the time stamp of the observation, taken as the midpoint of the exposure weighted by photon counts as measured via the exposure meter of CHIRON, saved in the image header under keyword EMMNWOB, and (3) astrometric information for the target star, including its RA, DEC, proper motion and

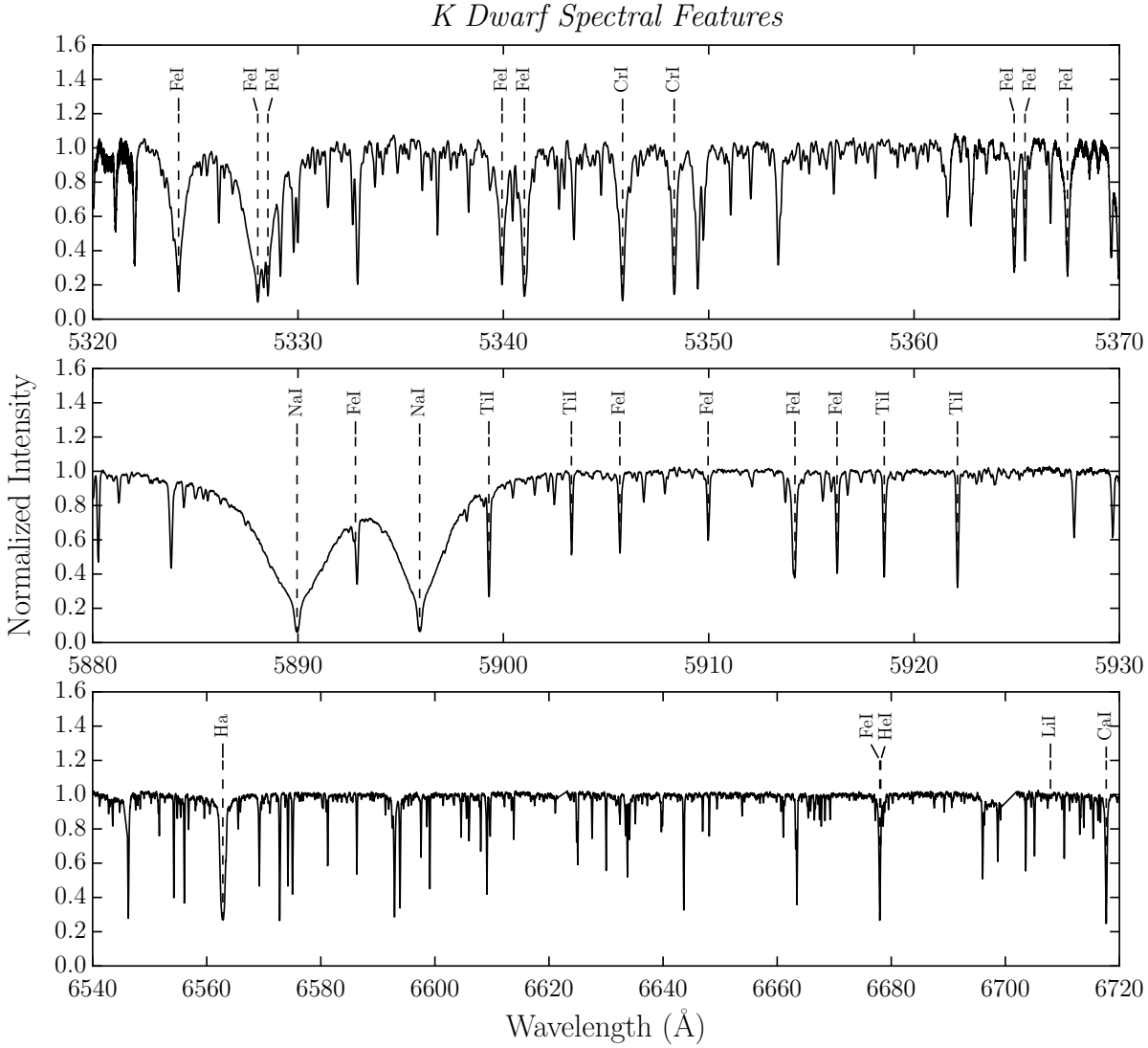

Figure 2.5 Examples of three spectral regions of the K dwarf HIP 73184 observed with CHIRON, after removing the blaze function and normalizing each order.

parallax. For each spectrum, a barycentric julian date in days is obtained that becomes the time-stamp for the corrected radial velocity, and a barycentric velocity correction in $\mathrm{m\,s^{-1}}$ is obtained that is used to determine the RV measurement at the moment of the observation.

4. *Choose template spectrum.* We calculate a radial velocity at each epoch relative to a single epoch observation we call the template spectrum for each star. We select the best quality spectrum as the template, considering weather conditions, Moon illumination and S/N.

5. *Re-sample spectrum.* The spectrum is re-sampled to match the same wavelength grid as the template spectrum to enable direct positional comparisons for the cross-correlation matches. Once the template spectrum is selected, each order is interpolated into a linear log-wavelength grid and oversampled two times the total number of pixels (6400 pixels per order). The result is that any single pixel Doppler shift across the spectrum corresponds to a radial velocity shift of 500 $\mathrm{m\,s^{-1}}$ in the slicer mode used for this survey.

6. *Order selection.* One of the advantages of working with spectra from a single spectral type of star and luminosity class – in this case K dwarfs – is that spectral features do not vary significantly from one star to another. Therefore, we select a set of spectral orders out of the full set of 59 orders provided by CHIRON in slicer mode that provides the best Doppler results. The quality of the Doppler information given within a single order depends on the number of spectral lines present, the shapes of those lines, the prevalence of telluric lines that pollute the spectrum, and the S/N across the order. Better precision in the radial velocity calculation comes from orders with more numerous spectral lines that are sharp and deep, with few telluric lines, and with less noise. Following these criteria, we omit orders at the blue and red ends of the total

wavelength range that have relatively low S/N — these are also furthest in wavelength scale from the instrument's peak efficiency at 5500 Å, as well as being relatively far from the blackbody peaks of K dwarfs. In addition, some orders were omitted because they simply have too few lines or are severely contaminated by telluric lines. Finally, orders were removed that have sources of contamination to the radial velocity signal resulting from broad spectral lines and lines sensitive to stellar activity, such as Hα, Hβ, and the Na doublet. In the end, we use a set of 14 orders selected from the 59 available in slicer mode: 10, 12, 13, 16, 17, 18, 20, 21, 22, 23, 24, 27, 30, 35. Numerous test were conducted using RV standard star calibrators of different magnitudes, which confirmed the selection, and allowed to spot additional orders that consistently deviate from the typical RV. Note that these are arbitrary order number labels assigned for the reduced data products of CHIRON, where the central wavelength of order n in Å is given by $\lambda_n = 565754/(124 - n)$.

7. *Cross-correlation function.* The RV at a given epoch is calculated relative to the RV at the epoch of the selected template spectrum. The wavelength grid of each spectrum is matched to the template spectrum, and then the cross-correlation function (CCF) is calculated for each order pair. The radial velocity derived from the order corresponds to the location of the peak in the CCF, for which the location is determined by fitting a Cauchy-Lorentz function. Additional parameters of the fitted function such as FWHM and amplitude are also obtained and used to determine the uncertainty in the RV measurement.

8. *Uncertainty estimation.* The uncertainty in the RV extracted from each order is closely related to the criteria described in step (6), in concert with the resulting shape of the derived CCF. We estimate a velocity uncertainty for a single order following the prescription by Zucker (2003) by quantifying the relative amplitude and sharpness of its CCF. The CCF shape and quality are directly related to the S/N of the spectrum; therefore, the errors estimated this way are photon errors. Instrumental errors and astrophysical noise are not reflected in this value, so the error for a single order may underestimate the total uncertainty.

9. *Radial velocity calculation.* Once each order from a given spectrum is cross-correlated with its respective order in the template, a final RV and its uncertainty are computed as in step 7. The final value and uncertainty for the epoch's observation is derived using the individual values and their uncertainties from the 14 orders by determining a weighted mean value and the standard error on the weighted mean.

CHAPTER 3

Getting K Dwarfs Together

3.1 The Sample

The observed stars presented in this dissertation are a portion of an effort targeting ∼5000 stellar systems containing a K dwarf primary star within 50 pc. The main selection criteria to construct the full sample are based on the primary star's photometric properties, i.e., its color and absolute magnitude, and its astrometric properties, i.e., its distance from the Solar System and position in the sky. A secondary criterion takes into account whether or not a K dwarf primary needs to be searched for companions via RVs with CHIRON or if the star can be considered well-covered by previous RV studies. If sufficient RV coverage is already available in selected catalogs and data archives, a star will not be included in the CHIRON target list. The sample is curated so that it only includes systems in which the K dwarf is the primary component, and for which the distance and color can be confirmed with *Gaia* Data Release 2 (DR2) (Evans et al. 2018). The initial target list included stars from *Hipparcos* and significant updates were made using results from *Gaia* in both DR1 released in September 2016 and DR2 released in April 2018. The observing program began in June 2017, before DR2 results were available and it remains important to consider stars in *Hipparcos* because a few stars are either too bright for *Gaia* to provide accurate astrometry, or do not have astrometric results in *Gaia* because of companions in orbits that so far prevent accurate astrometric solutions, thereby resulting in *Gaia* entries with no parallaxes.

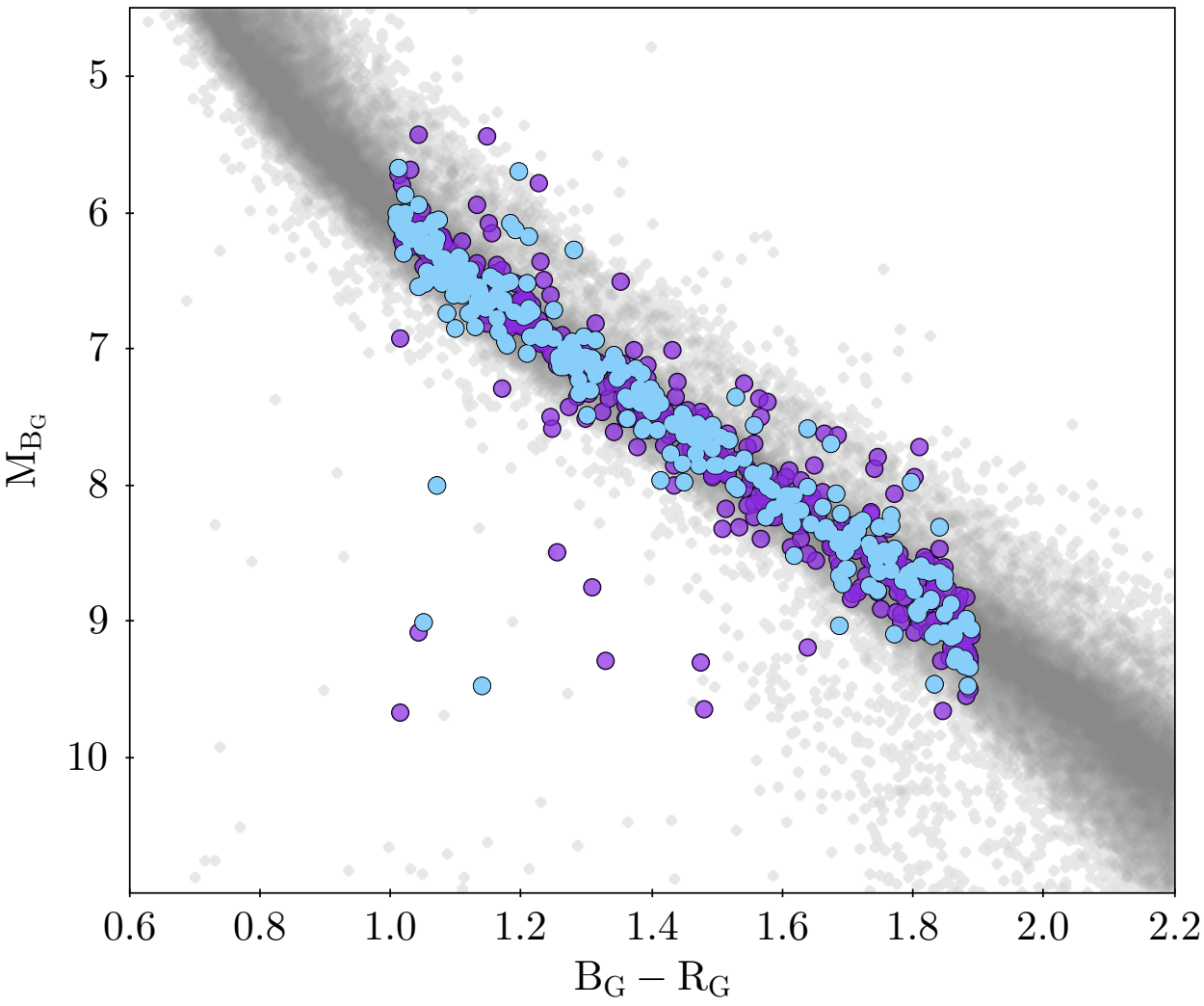

Figure 3.1 Observational HR Diagram of the 25PC (blue) and 33PC samples (purple) in the context of stars within 100 pc (gray). *Gaia* DR2 photometry is used to set the absolute magnitude and color axes.

3.1.1 K Dwarf Colors

Stars of spectral type K were chosen using careful assessments of the regions in color and luminosity on the HR Diagram where dividing lines between the G/K and K/M spectral types are found. Spectral types are a notoriously finicky business because various researchers

use different wavelength coverage, spectral resolution, and S/N that affects features used to determine a spectral type. The dividing lines adopted here were derived using studies that provide spectral types determined using systems applied to large numbers of nearby stars, in particular Gray & Corbally (2009) for the G/K line and Gray & Corbally (2009) supplemented with RECONS types for the K/M line. To define the blue and red ends of the K dwarf sequence, stars with spectral types in those datasets were matched to members of the RECONS 25 pc sample that have been carefully vetted for close companions, enabling us to use presumably single stars uncorrupted by secondaries to map K dwarf spectral types to $V - K$ colors. We initially adopted colors for K dwarfs spanning $V - K$ = 1.90–3.70, and applied an additional constraint of M_V = 5.80–8.80 to eliminate evolved stars and white dwarfs. The $V - K$ values were accumulated for the sample stars using V from Tycho (Høg et al. 2000) and K from 2MASS (Skrutskie et al. 2006). Once GDR2 data were available, these color and absolute magnitude limits were translated into comparable *Gaia* regimes, which were adopted for the final K dwarf sample: $B_G - R_G$ = 1.01–1.89 and M_{B_G} = 5.30–9.90. Two horizons of 25 pc and 33 pc were considered for the observing program — because of the amount of observing required, stars were targeted by distance and data accumulated as time progressed. The two samples of stars, separated by distances of 0–25 pc and 25–30 pc, are considered to be unaffected by extinction and are shown on the HR Diagram in Figure 3.1.

3.1.2 The Solar Neighborhood K Dwarfs

A total of 804 K dwarfs comprise the solar neighborhood sample considered here and are listed in Table 1. Stars were selected to have parallaxes of at least 30 mas, initially from *Hipparcos* (van Leeuwen 2007) and later from *Gaia* DR2, placing them all within 33 pc of the Sun. We restricted our sample to all K dwarfs between +30 and −30 deg declination in order to create an equatorial sample in which each star can be observed from major observatories in both hemispheres. This sky region is particularly useful now for our complementary speckle survey, and the sample of ∼2000 K dwarfs in this region constitutes a legacy sample that can be considered for future investigations such as exoplanet searches.

Initially, the sample was constructed with parallaxes solely from *Hipparcos*, in which 472 K dwarfs were reported to be within 33 pc. The observations with CHIRON on this sample commenced in June 2017, before *Gaia* DR2 (Evans et al. 2018) results were available, and focused on 300 K dwarfs. The remaining 172 stars are considered to be sufficiently observed for RV coverage by the HARPS (Mayor et al. 2003) and HIRES (Vogt et al. 1994) teams. The sample was then updated using parallaxes from *Gaia* DR1 and then DR2, which increased the total number of stars considered in this dissertation to 804. Each K dwarf in this larger sample satisfies our main selection criteria from at least one of the astrometric surveys. Most of the members are consistent in both surveys, but there are 53 stars to be discussed here that originally appeared to be within 33 pc in *Hipparcos* but have now been found to be more distant in *Gaia* DR2. There are also 10 stars in *Hipparcos* that are not in GDR2 because they are very bright or because companions corrupt the astrometric solutions, as

mentioned above. There are two reasons for the marked increase in sample size. First, as shown in Figure 3.2 for the full-sky 50 pc sample, *Hipparcos* provided 1048 K dwarfs with decreasing completeness in the sample in each equal-volume bin after 25 pc. This is simply caused by *Hipparcos'* brightness limit. *Gaia* DR1 provided another 776 K dwarfs within 50 pc and GDR2 effectively completed the sample.[1] Second, the sample size has increased also through the addition of stars due to the superior technical capabilities of *Gaia*. In particular, *Gaia* provides accurate photometry for all K dwarfs within 50 pc down to a resolution limit of 2″ (Arenou et al. 2018) and is able to resolve even closer pairs to less than 1″ projected separations when brightness ratios are not extreme.

While the 804 K dwarfs presented here are an ensemble from *Hipparcos* and *Gaia* DR2, the statistical analysis on the sample discussed in §5.8 and §5.9 only considers K dwarfs with parallaxes and photometry from *Gaia* DR2, with an additional careful vetting to consider only systems in which a K dwarf when is the primary component. This leaves a final sample of 278 K dwarf primaries within 25 pc and 678 K dwarf primaries within 33 pc, labeled 25PC and 33PC respectively in the Sample column of Table 1. The remaining 126 sources labeled XTRA (for "extra") in Table 1 are not part of the statistical K dwarf companion survey, but are included here because our observations and subsequent detections of potentially interesting secondaries began before *Gaia* DR2.

A considerable effort went into constructing and curating this sample, beyond the photometric and astrometric cuts. A key challenge has been to match accurately the stars to entries

[1]The slight excess in the population of K dwarfs between 45.4 and 47.8 pc is due to the Hyades cluster members.

in other catalogs, in particular when stars in close projected proximity are not resolved in the same way across the catalogs. Accurate source matching is imperative when scheduling observations, assessing the natures of newly discovered companions, and for the complete statistical analysis. For this purpose, a look-up table (Table 4) is provided in §B containing additional star names, namely from *Hipparcos* (van Leeuwen 2007), the *TESS* Input Catalog v8 (Stassun et al. 2018, 2019), *Gaia* DR2 (Evans et al. 2018), the Ninth Spectroscopic Binary Catalog (SB9) (Pourbaix et al. 2004), the Washington Double Star Catalog (WDS) (Mason et al. 2001), and the main identifier selected by the SIMBAD Object Database (Wenger et al. 2000).

3.1.3 K Dwarfs Already Monitored

Several of these nearby K dwarfs have already been observed in previous studies to obtain RV time series, with some having extensive coverage in campaigns with precise RV instruments to detect orbiting planets, and others having published spectroscopic binary orbital solutions. In both cases, following the secondary criterion mentioned earlier, these stars were not observed again with CHIRON because they are considered covered by others. To be specific, a star is considered to be "covered by others" when there are 10 or more RV measurements found in the data archives of either the HARPS (Mayor et al. 2003) or HIRES (Vogt et al. 1994) efforts, or when an orbital solution is found and published in the SB9 catalog (Pourbaix et al. 2004). These three sources are constantly being updated with more observations and orbital solutions as time progresses, and the cutoff date adopted for the assessments provided here is 2020 July. In this dissertation, the number of observations considered by these large

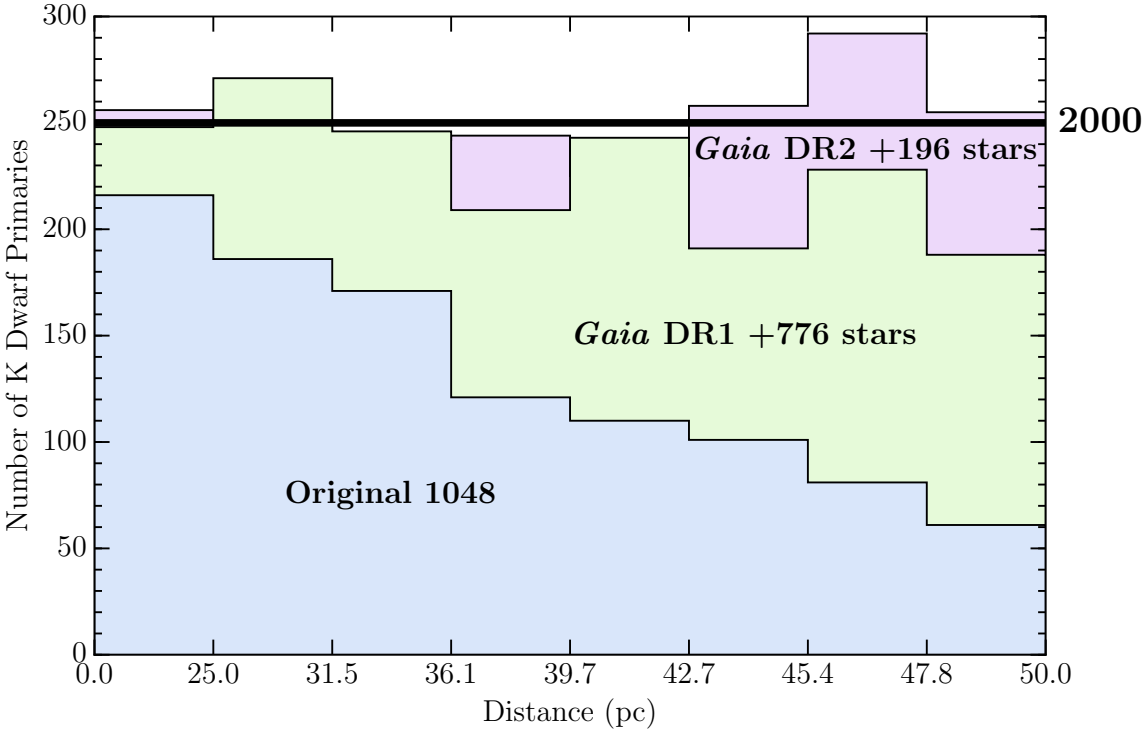

Figure 3.2 Number of equatorial K dwarfs found in eight equal volume bins out to 50 pc from the Sun (note that the numbers represent the full-sky counts, whereas the histograms are for the equatorial sample). The blue histogram represents the initial sample from *Hipparcos*; note the steady decline in numbers due to brightness limits. The green histogram shows the increases using parallaxes from *Gaia* DR1. the purple shows the final adopted sample using parallaxes from *Gaia* DR2. The consistent number of K dwarfs in each volume segment found in *Gaia* DR2 indicates that the sample is effectively complete and not limited by magnitude. The slight excess of K dwarfs between 45.4 and 47.8 pc shows an overdensity is due to Hyades cluster members located at ∼47 pc.

programs is the number of RVs compiled and published for HARPS in Trifonov et al. (2020) and for HIRES in Butler et al. (2017); Tal-Or et al. (2019) — these data included in the RV time series presented here.

Using Gaia photometry, parallaxes, and derived absolute magnitudes, the K dwarfs lie along a narrow, well-defined main sequence in the HR diagram of solar neighborhood stars (Figure 3.1). This characteristic makes it relatively easy to identify over-luminous K stars above the main sequence as potential multiple systems, or K stars below the main sequence as subdwarfs, compared to their bluer G and redder M spectral type neighbors. The solar neighborhood sample of G spectral type stars includes over-luminous stars because a portion of the population has evolved, whereas at masses lower than K dwarfs, M stars span a much larger mass range in which a variety of physical processes, such as magnetic activity, flares, and interior structures that change from partially to fully convective, result in a wide range of luminosities. For the K dwarf sample, I am confident that the list presented here includes the best sample currently feasible and is effectively complete for K dwarfs in the equatorial volume out to 33 pc. This is supported by Figure 3.2, which shows that in each of the eight equal-volume bins, the numbers are statistically equivalent (except for the known overdensity due to the Hyades). This suggests that the completeness of detections with *Gaia* is not limited by magnitude or distance.

3.2 Observing Program

The K dwarfs are being observed with CHIRON in slicer mode, which provides a resolution of 80,000 and spreads the spectrum into 59 orders. Integration times are uniformly set to 900 seconds except for a few stars brighter than $V \sim 6$ for which the exposure is typically stopped when the S/N reaches 100 at 5500Å. After each science exposure, a single ThAr lamp exposure of 0.4 seconds is taken to use for wavelength calibration. In poor seeing or partial cloud cover, the 900 second integration time is maintained in an effort to permit coverage of targets in the large program and to provide insight into how precision changes under various sky conditions. The consistent 900 second integration times for stars with $V \sim$ 6–12 also enables straightforward evaluations of the changes in RV precision with magnitude, as well as permitting direct comparisons of fluxes received for individual stars throughout their coverage during the survey.

3.2.1 RV search

Our RV search is designed to perform a systematic reconnaissance for companions, so each K dwarf in our sample gets at least 6, and ideally 9, observations using the slicer instrument setup described in §3.2. The observing cadence goal is to secure 2–3 spectra within a few days, then repeat the sequence after a month, and then repeat it again after a year, with labels "D", "M", and "Y" respectively shown in Table 2. The cadence is not necessarily strict and is subject to weather conditions, schedule constraints, and technical mishaps of the instrument/telescope. The daily and monthly cadences are aimed to detect short period

RV perturbations, and the yearly cadence is suited to detect RV trends due to companions in long period orbits. As detailed above, the sample experienced upgrades since it was first assembled, and RV observations were always prioritized for closer stars in the sample, i.e., first to 25 pc, then to 33 pc. When a perturbation is seen in the RV series, the star is then assigned additional observations to reveal the nature of the companion and ideally to solve for its complete orbit. Such perturbations are evaluated on a case-by-case basis, paying close attention to the RV trends, RV accelerations, and RV curvatures. When a periodicity is found, ephemerides are calculated so that new RVs taken at appropriate times can be used to further constrain or discard an orbital solution.

3.2.2 Current Status of Observations for RV

Table 3.1 gives details about the observing coverage for the sample. From 2017 June through 2022 May, a total of 7522 high resolution spectra were obtained with CHIRON and successfully processed to measure RVs for the 804 stars in the full sample under consideration. For the 278 K dwarfs in the 25PC sample, there are 3142 CHIRON RVs with each star observed at least once, including single observations used to characterize the stars even if they have been previously observed by HARPS or HIRES, or have orbits in SB9. Coverage of the 678 K dwarfs in the full equatorial sample out to 33PC includes 6259 CHIRON RVs, with 674 K dwarfs having at least one successful observation.

Table 3.1: Survey completion per sample until 2022 May.

Sample	Total	Aim	# Stars covered by		
			HIRES/HARPS/SB9	CHIRON (DMY)	Combined
25PC	278	143	135	118 (82%)	253 (91%)
33PC	678	464	214	315 (68%)	529 (78%)
All	804	562	242	386 (69%)	628 (78%)

The portion of the RV survey completed is measured for the K dwarfs in the sample that have not been previously monitored using HARPS, HIRES, or do not have an orbital solution published (§3.1.3) — these numbers are given in the Aim column of Table 3.1. As of 2022 May, each K dwarf in the sample labeled "DMY" (see §3.2) in Table 2 is considered to have a complete set of RV time series observations with CHIRON. For the total sample of 804 K dwarfs, there are 562 targets for CHIRON, of which 386 have DMY cadence coverage (69% complete). For the 678 K dwarfs in the 33PC sample, 464 are targets for CHIRON, of which 315 have DMY cadence coverage (68% complete). Finally, for the 278 K dwarfs in the 25PC sample, 143 are targets for CHIRON, of which 118 have DMY cadence coverage (83% complete). By adding targets with at least two of the three DMY survey cadences achieved, the coverage increases to 77%, 77%, and 90% in the All, 33PC, and 25PC samples, respectively. As shown in Table 3.1, when combining the CHIRON and previous efforts by others, 91% of the K dwarfs within 25 pc and in the equatorial region of the sky now have sufficient RV coverage to make an assessment on the presence of possible companions, and overall multiplicity of a volume complete sample (§5.8).

3.2.3 Complementary Wide-Field and Speckle Surveys

A detailed discussion of the complementary wide-field and speckle surveys of K dwarfs within 50 pc by the RECONS team is beyond the scope of this dissertation, but a few details are warranted here. Led by Elliott Horch at Southern Connecticut State University, a search for companions in *Gaia* with separations larger than 2.″0 is being carried out, and results are compared to the WDS to confirm if the companions are previously known or are new discoveries. Led by Todd Henry at Georgia State University, a search for companions using optical speckle interferometry is being done, using primarily the Differential Speckle Survey Instrument (DSSI) (Horch et al. 2009) on the Lowell Discovery 4.3m Telescope, the Gemini North and South 8.1m telescopes, and the Apache Point 3.5m to resolve companions at separations of 0.″01 to 2.″50 down to ∼6 magnitudes fainter than the K dwarf primary. The speckle survey overlaps the Solar System scale region targeted in the RV survey, whereas the wide-field effort sweeps up companions at larger separations. It is not the goal of this thesis work to dive into the speckle technique, but detections made so far are referenced here to provide context for some of the RV detections and the overall multiplicity, given that in cases such as long RV trends, there is overlap in the detections in both the RV and speckle surveys that are due to the same companion.

CHAPTER 4

Results: The Search For Companions

4.1 Observations Included in this Thesis

Observations of K dwarfs made with CHIRON from 2017 June until 2022 May are presented in this thesis (§3.2.2). Included in the sample are three RV standard stars and 5 stars with known exoplanets that were observed to test the sensitivity and reliability of CHIRON. We break the discussion of RV results into four categories of (usually) K dwarfs observed: (1) RV standard stars, (2) stars known to have exoplanets, (3) survey K dwarfs with no companion detected, and (4) survey K dwarfs with companions found via the CHIRON observations.

Results for each star in this work are presented in a series of Figures in Appendix A, with two stars displayed on each page. There remain 26 stars in the sample of 804 with no CHIRON observations to date, leaving 778 that do have a least one spectrum. The name at the top in bold font is usually the name adopted for the broader RECONS survey of ∼5000 K dwarfs, where RKS stands for RECONS K Star and the RA and DEC are used for numbering. For a few stars, the *Hipparcos* HIP name is given because the star is now reported to be beyond 50 pc and is not formally in the RKS survey. Below and to the left of this name are two lines including RA and DEC, a V magnitude (those with approximate symbols are *Gaia* B_G magnitudes converted to V), the total number of observations found in HARPS plus HIRES publications ($N_{H/H}$) and the number of successful CHIRON observations (N_C). Also given is the "DMY" code representing whether or not data were acquired with CHIRON on daily, monthly, and/or yearly timescales, as described in §3.2. Additional names are given

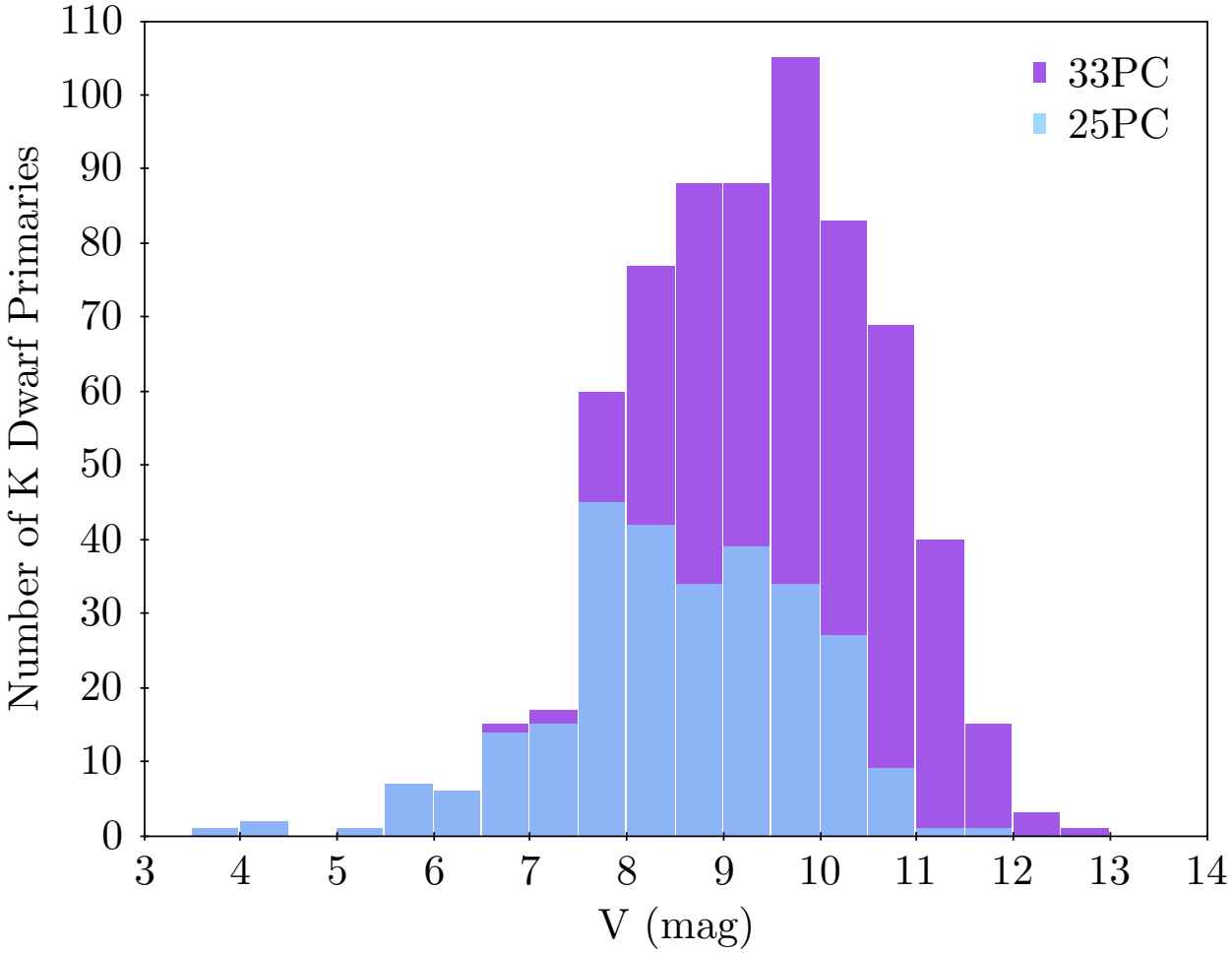

Figure 4.1 Distribution of V magnitudes for the K dwarfs within 25 pc (blue bins) and 33 pc (purple bins).

below and to the right of the RKS name; refer to Table 4 for the full list of names pertinent to stars in this survey. Below the header lines are four panels for each star. In the upper left are the RV timeseries, if available, from the HARPS (Trifonov et al. 2020) and HIRES (Tal-Or et al. 2019) databases. Both datasets are plotted with a fixed scale of 24 years from 1995–2019, the longest time span of observations available if the star was observed; if not, a label of "NO DATA" is displayed. In the upper right are results for CHIRON observations

for the available data acquired at the CTIO/SMARTS 1.5m, spanning a fixed time scale of 6 years (2017–2023). Both of the upper panels include the calculation of the Median Absolute Deviation (MAD), ∼0.8 times the standard deviation of normally distribute data, which we use as a measure of variability for each of the RV datasets for all stars. The lower-left and lower-right panels, a periodogram of the CHIRON RV timeseries and a phased orbit model, are part of the analysis when searching for the orbital solution when enough data is available and is described in further in this Chapter in §4.6.1.

The V magnitudes given with the plots in Appendix B and listed in Table 1 are represented in the histogram of Figure 4.1, which shows K dwarfs within 33 pc, the primary focus of this survey. These stars have V = 3.5–13.0, with most stars having V = 7.0–12.0, which means they are fairly bright for 1-m class telescopes like the CTIO/SMARTS 1.5m. However, CHIRON was designed primarily to look for planets orbiting α Cen A ($V \sim 0.0$) and α Cen B ($V \sim 1.3$) at very high spectral resolution. So, at the beginning of the K dwarf survey there was no clear understanding of the RV precision at fainter magnitudes. One of the main results of this thesis is determining how effective using CHIRON in slicer mode with spectral resolution $\sim$ 80,000 can be for main sequence stars with V $<$ 13 mag; these results are discussed in §4.5.

4.2 Calibrators: RV Standard Stars

The V magnitude distribution (Figure 4.1) of the K dwarfs studied here shows that the majority of targets have V = 7.0–12.0. It was decided that the appropriate RV standards

to check the sensitivity and stability of CHIRON would be K dwarfs that were somewhat brighter and overlapping the bright end of this range. Three K dwarfs were chosen for monitoring, HIP 3535 ($V = 8.0$, K3V), HIP 58345 ($V = 7.0$, K4V), and HIP 73184 ($V = 5.8$, K4V). These three stars were selected as RV standards because they have significant datasets from previous RV programs indicating that they have variations of only 3–7 $\mathrm{m\,s^{-1}}$ over years (Butler et al. 2017), sufficiently low for our purposes to consider them RV standard stars. RV time series for all three stars are shown in Figure 4.2 as published in Paredes et al. (2021), where the panels illustrate the stability of CHIRON on three timescales: over a night (top panel), a month (middle panel), and the first two and a half years of CHIRON operations since reopening in June 2017 (bottom panel). Note that in the bottom panel results for two RV standards (HIP 3535 and HIP 58345) are shown to provide a consistent stream of data as they compensate for one another's seasonal gaps. Over a few years, there are occasional outlier points, in particular for HIP 3535, the faintest of the three standards and the most prone to suffer from weather mishaps. Details of CHIRON's stability from these tests over all three timescales are as follows. Updated RVs are shown in Figure 4.3 and rffiglupdatedrvstd2.

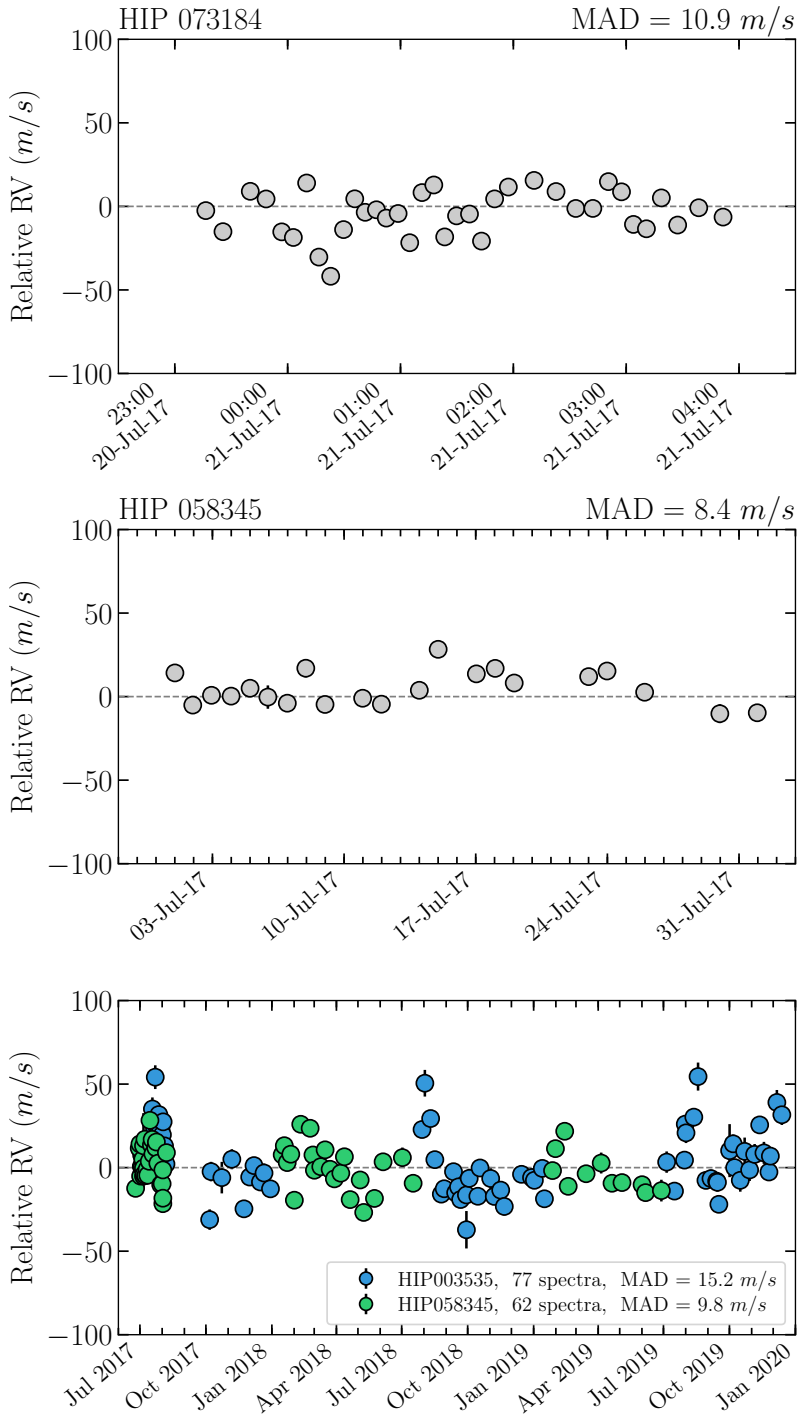

Figure 4.2 Three K dwarfs observed as RV standards to monitor the stability of CHIRON. *top*: HIP 73184 observed for ∼4.5 hr on a single night. *middle*: HIP 58345 observed roughly once per night for a month; skipped nights were due to unfavorable weather conditions. *bottom*: HIP 3535 and HIP 58345 observed between 2017 June and 2019 December with a typical cadence of one observation every 7–10 days.

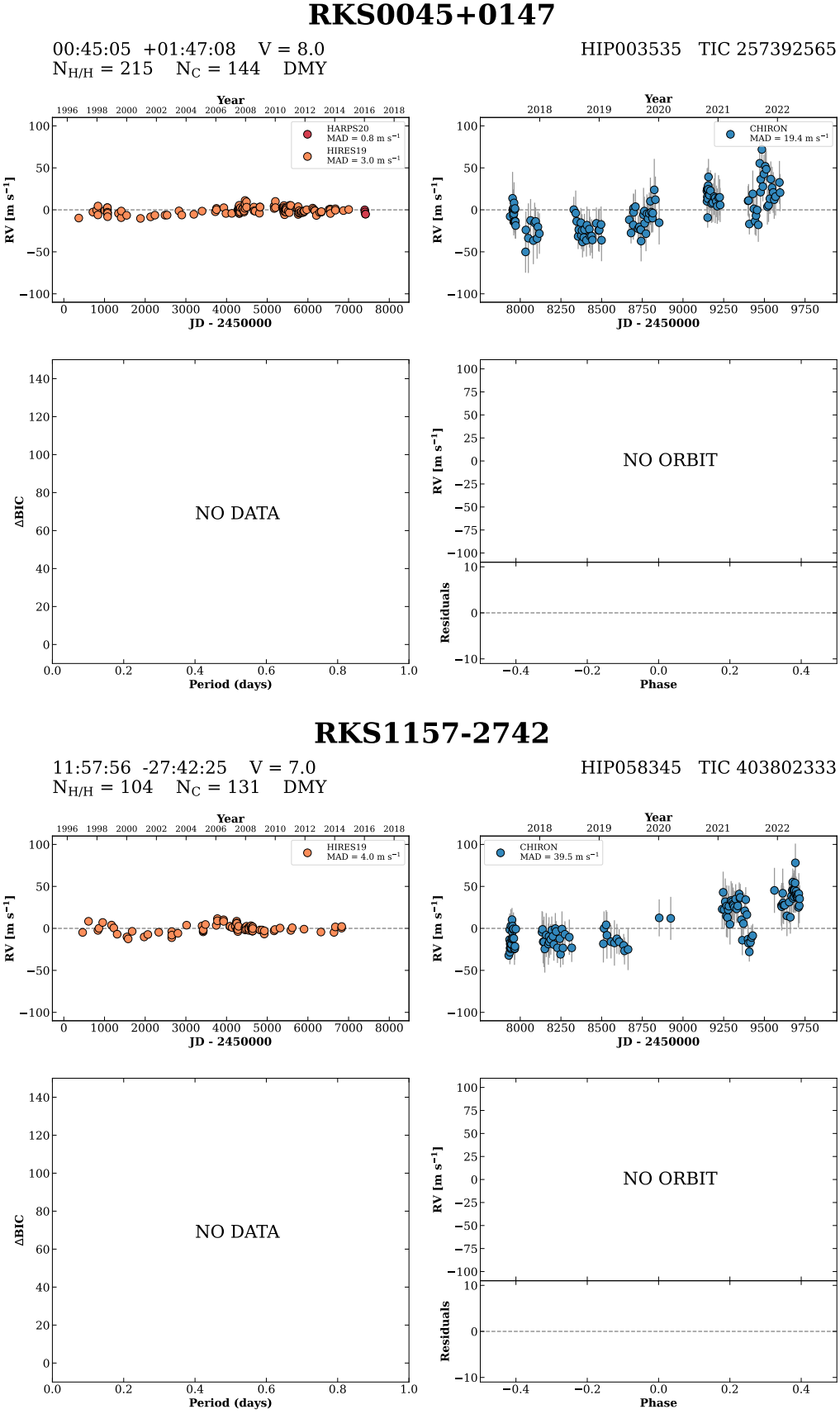

Figure 4.3 Updated RV results for RV standards HIP 3535 (top) and HIP 58345 (bottom).

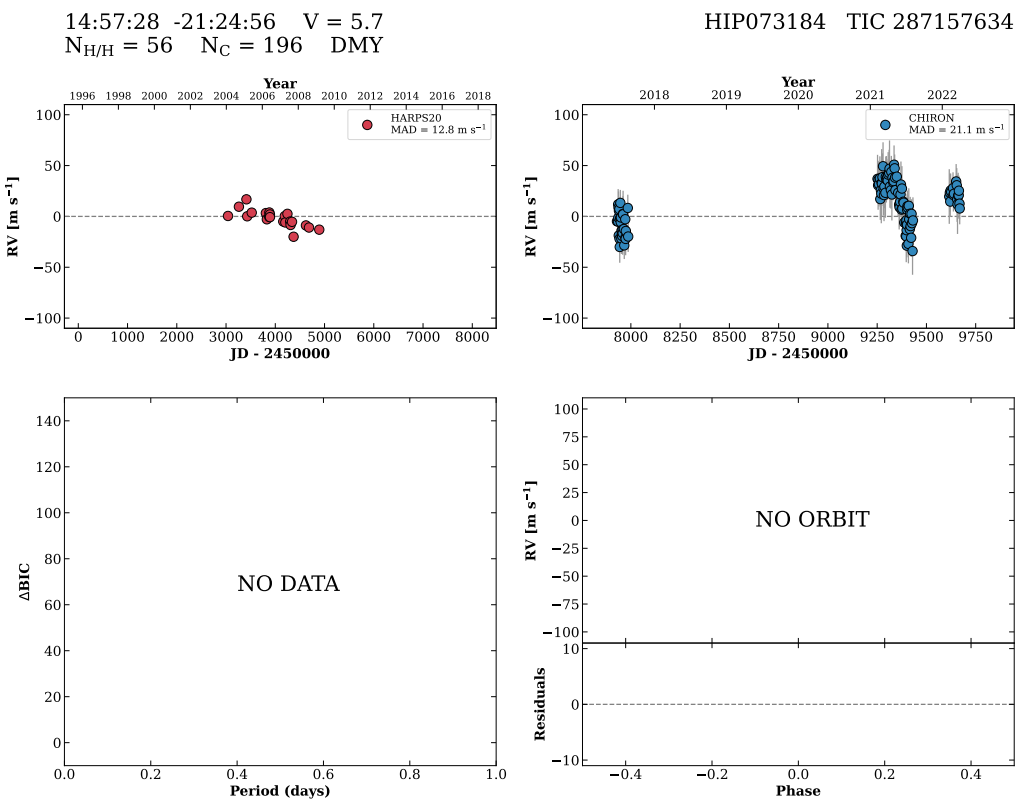

Figure 4.1 Updated RV results for RV standard HIP 73184.

1. *Stability over hours.* HIP 73184 was observed 36 times on the night of 2017 July 17 to test the stability of CHIRON over a period of ∼4.5 hours. Observations were taken on a clear night with seeing of 0.7–1.0″, while the airmass changed from 1.012–1.674. The top panel of Figure 4.2 shows that the MAD is 10.9 $\mathrm{m\,s^{-1}}$ during the series of observations. Note that HIP 73184 is known to host two wide stellar companions (B and C) at a separation of 25″ and a wide brown dwarf companion (D) at 258″. CHIRON is sufficiently sensitive that the slow RV drift caused by the BC pair is evident in the updated RV timeseries (Figure 252), so HIP 73184 has been dropped as an RV standard.

2. *Stability over 1 month.* As shown in middle panel of Figure 4.2, HIP 58345 was observed on 21 nights over a one month period in 2017. Nights when there are no data are typically weather dropouts. There are few RV measurements lying far from the

mean value, with a resulting MAD of 8.4 $\mathrm{m\,s^{-1}}$ for the data series.

3. *Stability over 2+ yr.* The bottom panel of Figure 4.2 includes data sequences for HIP 3535 (77 spectra, MAD value 15.2 $\mathrm{m\,s^{-1}}$) and HIP 58345 (62 spectra, MAD value 9.8 $\mathrm{m\,s^{-1}}$) together, as observations are dove-tailed throughout the year to provide an unbroken series of RV standard observations. It is evident that there are several stretches of time when RV offsets are found in the HIP 3535 data sequence. We have examined various quantities in an attempt to reveal the cause(s) of the offsets for individual measurements. It appears that the drifts in the HIP 3535 data are *not* caused solely by (a) varying S/N in the spectra (primarily because nearly all spectra, 62 out of 77, have S/N $>$ 50) — out of the 15 RVs where the S/N is below 50, only four deviate by more than 15 $\mathrm{m\,s^{-1}}$ from the mean, (b) airmass, and (c) temperature changes in the Coude room where CHIRON is housed. We suspect that the poorer precision is due to shifts in the spectral resolution: values computed from the individual spectra indicate that when the resolution dips by more than $\sim$1%, the final RV points are offset. Resolution offsets occur when the focus of the spectrum onto the CCD drifts slightly, and shows that it is critical to keep the lines consistently as narrow as possible on the chip. We also find a correlation between the RVs with offsets $>$15 $\mathrm{m\,s^{-1}}$ from the mean and their individual uncertainties. This is consistent with the fact that our error bars reflect mostly photon noise in combination with instrumental errors, but because HIP 3535 is a relatively bright star ($V = 8.0$), in this case the latter reason appears to dominate.

The error associated with each RV measurement on a night is highly correlated with the photon flux received by the CHIRON detector and relates to the variance across the 14 orders from which individual RVs are extracted. As can be seen in the time series for HIP 3535 (blue points in the bottom panel of Figure 4.2), the dispersion as measured by the MAD of the points overall (15 $\mathrm{m\,s^{-1}}$) is larger than errors on most of the individual points (typically 3–10 $\mathrm{m\,s^{-1}}$). The roughly factor of two difference is presumably due to systematic errors, with the leading culprits being changes in the focus of lines on the CCD and temperature fluctuations inside the chamber that houses the CHIRON instrument. It is emphasized that these results are for K dwarfs observed during our survey; other types of stars will not necessarily provide similar results, i.e., hotter stars with fewer lines available for RV extraction, or rapidly rotating stars with broad lines.

The results of these tests indicate that for K dwarfs with $V = 5.8$–8.0, the combination of the 1.5m, CHIRON, and our RV pipeline can yield RV precisions of 8–15 $\mathrm{m\,s^{-1}}$over timescales from hours to years. An assessment of stars as faint as $V = 12.0$ is given in §4.5 below, after discussion of the other set of standards — stars know to have exoplanet candidates.

Figure 4.5 illustrates the RV MAD values for the 351 of the 804 stars for which a verdict of no companion was determined and were monitored for at least two cadences of the survey. The points are color coded by the amount of time coverage currently available in the RV time series. Most stars brighter than $V = 11.0$ have MAD values less than 15 $\mathrm{m\,s^{-1}}$, whereas fainter stars have values that climb to 40 $\mathrm{m\,s^{-1}}$, and in five cases are even higher. Stars with observations spanning a longer timeline (yellow), tend to have slightly higher MADs, because

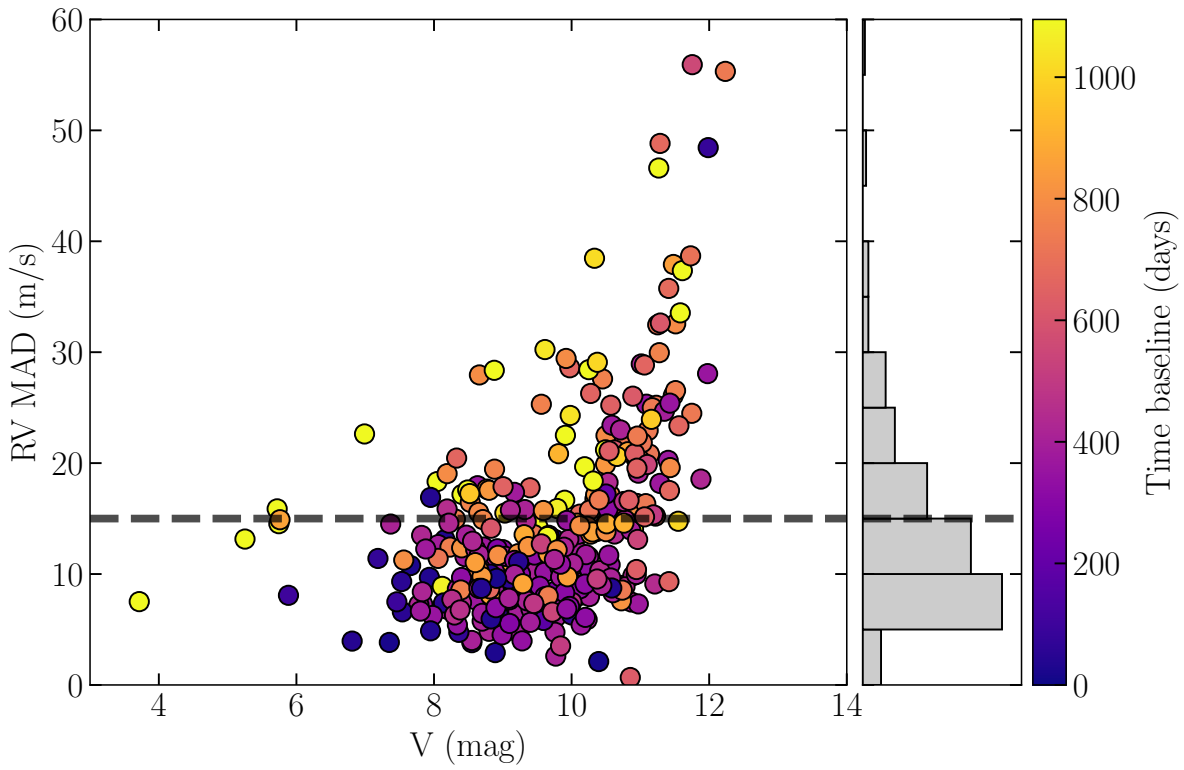

Figure 4.5 RV MAD vs. V magnitude of K dwarfs with flat RV timeseries.

with more observations there are more chances to encounter weather/technical problems, and because they put to test stability of CHIRON at at the longest timescales, almost 5 yrs so far. There are a few other stars that appear to hover above the main distribution of points, and each is worthy of continued observation, but at the present time they are considered to be single stars.

In addition to mapping the dependence of RV precision given by the MAD of the time series with target brightness, because sky conditions and telescope tracking vary, it is useful to map the precision given by the uncertainty calculated for each RV measurement as a

function of the S/N of its corresponding spectrum (Figure 4.2), in the case of CHIRON spectra in slicer mode, measured at order 21 in the pixels around 5500Å, i.e. the blaze peak. According to equation (1) in Tokovinin et al. (2013), the S/N at the blaze peak for slicer mode is given by,

$$S/N = \frac{N_{ph}}{\sqrt{N_{ph} + KR^2}}, \tag{4.1}$$

where N_{ph} the number of stellar photons per spectral pixel collected during the exposure time (considering a peak efficiency of 6% of CHIRON), with $K = 9$ as the number of pixel binned across the order, and $R = 5.5$, as the CCD readout noise in electrons. The results are shown in Figure 4.2 relates the S/N values for 2745 individual spectra of the 351 K dwarfs to the resulting RV uncertainties. Overall, for S/N values of at least 40, the uncertainties are less than 15 $\mathrm{m\,s^{-1}}$, whereas for S/N ∼20, the uncertainties increase to 30 $\mathrm{m\,s^{-1}}$ and above. It is therefore recommended that to reach a precision of 15 $\mathrm{m\,s^{-1}}$ in slicer mode with CHIRON, observers targeting K dwarfs or similar stars anticipate exposure times of 900 sec (our standard exposure time) for stars with $V \lesssim 10.5$. As a rule of thumb, to obtain at best a single measurement error in RV of ∼10 $\mathrm{m\,s^{-1}}$, it is necessary to reach S/N ∼100 at 5500 Å. This is possible for a K dwarf brighter than V ∼ 9 in 900 seconds exposure in slicer mode. Therefore, for stars like those observed in our program, the expected precision can be predicted using:

$$\sigma_{RV} \sim \frac{10000}{\mathrm{S/N}^2} + 10\ \mathrm{m\,s^{-1}} \tag{4.2}$$

In Paredes et al. (2021) I presented the RV uncertainty dependence with the S/N calculated from CHIRON's exposure meter. The S/N from the exposure meter is given in real-time for the observer and allows to limit the exposure time automatically when enough S/N is reach, or to increase the exposure time to compensate for cloud cover, seeing, and telescope tracking, all of which can affect how much light is injected into the fiber. The exposure meter picks off about 1% of the collimated light at 5450Å with a bandwidth of 900Å (Tokovinin et al. 2013). Until 2019 July 18, S/N from the exposure meter mapped directly to the S/N from the spectrum at the blaze peak, providing a straightforward method to evaluate individual exposures, as shown by circle points in Figure 4.2. After this date, a major repair took place and resulted in a realignment of the fiber collecting the light from the telescope. CHIRON was able to collect more light after, but at the cost of changing the relation between the S/N estimated from the exposure meter counts presented in Eq. 2 in Paredes et al. (2021), as shown in Figure 4.2 (top-right) by the slope differences between circle data points (pre-repair) and triangles data points (post-repair).

As outlined in §2.8, the individual RV measurements have been determined using the weighted standard error of the RVs measured for the 14 orders adopted in the pipeline. From Figure 4.2 is evident that the RV uncertainly is strongly dependant on the quality of the spectra, mainly determined by its S/N, or as expected RV errors being lower for brighter stars and higher S/N spectra. Therefore, RV uncertainties appear slightly overestimated compared to the MAD of an entire RV dataset and to the RMS residual fits from orbits derived later in this Chapter where several measurement contribute to a solution, instead there are more

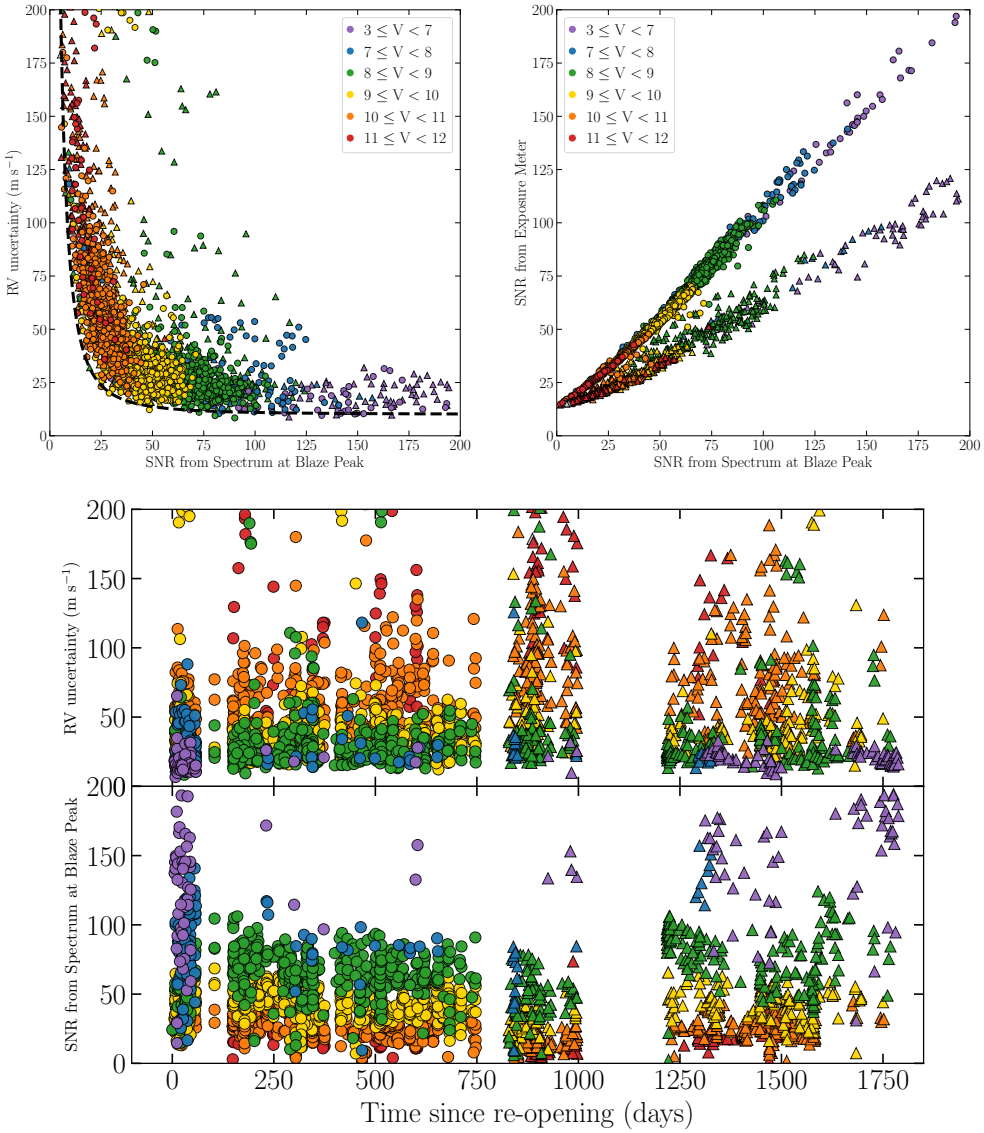

Figure 4.6 *Top-left:* RV uncertainty for individual spectra versus S/N calculated from CHIRON's spectra at the blaze peak. The dashed line is described by Eq. (4.2) *Top-right:* Relation between S/N of spectrum estimated from the exposure meter counts and the S/N measured in the blaze peak of the spectrum. *Bottom:* Temporal evolution of the RV uncertainty estimated and the S/N from spectrum at blaze peak since the reopening of the telescope in 2017 June. *All:* Each of the 2745 data points represents a single spectrum with exposure times of 900 seconds of a K dwarf with no companions found, color coded by stellar V magnitude. The circles and triangles indicate data taken before and after to 2019 July 18, where a major repair and fiber alignment took place.

an indicative of the relative internal data quality rather than strictly an indicative of the global RV accuracy. While there are other errors, such as systematic instrumental offsets to be considered in future work when larger datasets are available, for this characterization of our K dwarf survey prospects, the reported errors are only the result of the statistical results based on individual RVs extracted from the 14 different orders calculated and combined uniformly for the entire sample here presented.

The large numbers of RV data points measured in stars with no companions in diverse observational scenarios, allows exploration of other correlations with RV precision, either to discard or confirm possible causes of anomalous RV changes. In Paredes et al. (2021) I showed that RV precision is not affected by airmass, which was an initial concern for having a survey reaching targets up to +30 degrees in declination with airmass $\sim$2. Nowadays, after 5 years running, the main priority is to maintain the stability of the instrument, by keeping close monitoring of the temporal evolution in the quality of the data, so we promptly be able to spot, correct and/or characterize undesired effects in the RVs produced.

4.3 Calibrators: Stars with Known Exoplanets

A set of five K dwarfs with exoplanet candidates reported via RV measurements were selected to provide proof-of-concept datasets for CHIRON. All five are (presumed) single planet systems, and observations commenced during the initial reopening observing run of the CTIO/SMARTS 1.5m in 2017 June. These test systems provided opportunities to test end-to-end processes from observing protocols through RV extraction from the spectra, thereby

measuring the efficacy of CHIRON for the K dwarf survey. The instrument setup, data reduction, and RV calculation methods were as described in Chapters 2 and 3. In Table 4.1 we provide previous orbital solutions and new solutions from CHIRON data for the five systems, in which the exoplanet candidates have orbital periods of 2–24 days. Their respective orbital fits from the CHIRON data are shown in Figure 4.7. The new orbital solutions presented here have been calculated solely based on the CHIRON observations and therefore are independent from the previously reported solutions. In most cases the CHIRON orbits are superior to previously published orbits, e.g., eccentricities have been determined explicitly here, whereas in three of the five systems, eccentricities were assumed to be zero or were poorly defined in published orbits. Each system is described briefly here.

4.3.1 HIP 2350

This star (V = 9.37, K1V) was reported by Moutou et al. (2005) to have a hot Jupiter of minimum mass 0.48 $M_{\rm Jup}$ with an orbital period of 3.444 days. We obtained 24 spectra of HIP 2350 between 2017 July 16 and August 08 and confirm a 0.50 $M_{\rm Jup}$ minimum mass planet with an orbital period of 3.458 days, consistent with the previous result. The 73 $\rm m\,s^{-1}$ RV semi-amplitude is $\sim$7 times larger than the typical uncertainty for K dwarfs in our program, indicating that hot Jupiters of this type are easily revealed by CHIRON. HIP 2350 has a lower mass stellar companion detected with RoboAO at Palomar (Baranec et al. 2012) at a separation of 0.5″ and fainter by 3.3 mag at 754 nm (Sloan i' filter) by Riddle et al. (2015) and Roberts et al. (2015). The companion was confirmed with DSSI at Gemini North (Horch et al. 2009) at a separation of 0.5″ and fainter by 3.8 mag at 692 nm (Wittrock

et al. 2016). The companion is likely an M1V with an estimated orbital period of ∼130 yrs from the projected separation, and it should not pose a serious threat to the detection, nor the orbital stability of the planet. Shaya & Olling (2011) and later Oh et al. (2017) reported HIP 2350 to be part of a co-moving wide pair where the primary component is HIP 2292, another solar-type star, at projected separation of 897″ (∼0.2 pc). While the system could still be a wide multiple, Oh et al. (2017) also discuss the possibility that systems such as these could have formed together but are now drifting apart.

4.3.2 HIP 57370

This star (V = 8.05, K0V) was reported by Ge et al. (2006) to have a hot Jupiter with a minimum mass 0.49 $M_{\rm Jup}$ in an orbit with a period of 4.114 days. We obtained 20 spectra of HIP 57370 between 2017 June 29 and 2017 July 26, and the same minimum mass of 0.49 $M_{\rm Jup}$ in an orbital period of 4.079 days. The single point with a large error near phase 0.8 in the panel for this star in Figure 4.7 was taken at the beginning of the night on 2017 July 26, when clouds were present and the seeing expanded to 2.5″, resulting in poor S/N for this observation. This data point is included to illustrate the relative quality of a poor observation suffering from high photon noise error compared to more typical measurements. The lack of speckle companions (Henry et al. 2022, in prep), nor any known visual stellar companions makes this detection robust. Despite being a non-transiting planet, Guilluy et al. (2019) use this hot Jupiter (HD 102195 b) to demonstrate the feasibility of detailed studies of exoplanet atmospheres using the GIANO spectrograph (Oliva et al. 2006) mounted at Telescopio Nazionale Galileo (TNG), a 4-m class telescope.

4.3.3 HIP 72339

This star (V = 8.04, K0V) is near the celestial equator, but at $V - K_s$ = 1.81 is slightly bluer than the blue cutoff we used for our K dwarf sample; thus, it is not part of the larger survey but was observed strictly as a benchmark. This star has a known hot Jupiter with minimum mass 1.02 $M_{\rm Jup}$ and orbital period 10.720 days (Udry et al. 2000). We confirm the companion via 28 spectra to have a somewhat larger minimum mass of 1.09 $M_{\rm Jup}$ and a virtually identical orbital period of 10.721 days. Our phased RV curve spans 3.5 full orbits for data taken in 2017 from June 24 to August 7, and this is the star with a known planet for which we have the longest time coverage at 42 days. Given the RV variation of K = 112 $\mathrm{m\,s^{-1}}$ seen, this potentially Jupiter-like exoplanet is clearly detected, indicating that CHIRON reveals such candidates easily. No visual stellar companions are known in the system and the planet is not found to be transiting. While this system has been revisited by Wittenmyer et al. (2009) and Hinkel et al. (2015), the candidate exoplanet's properties have not changed significantly since the initial discovery.

4.3.4 HIP 98505

We obtained 31 observations of HIP 98505 (V = 7.66, K2V) between 2017 June 24 and August 4, spanning 40 days, to reveal a companion with minimum mass 1.17 $M_{\rm Jup}$ in a 2.218 day orbit. This planet (HD 189733 b) was discovered by Bouchy et al. (2005) and reported to have a minimum mass of 1.15 $M_{\rm Jup}$ in a 2.219 day orbit; the system has been extensively studied since then with no significant changes in the orbital parameters. At an orbital incli-

nation of ∼85 degrees, the exoplanet transits its host star, allowing detailed determination of its fundamental parameters, which combined with the proximity and brightness of the star have made the system an ideal laboratory for exoplanet atmosphere studies (e.g., Redfield et al. 2008 and Guilluy et al. 2020 and references therein). Bakos et al. (2006) reports a lower mass companion 11.2″ from HIP 98505 that is 3.7 magnitudes fainter in K_s. Using astrometry, proper motion, radial velocity, and photometry, they derive an orbit for the stellar companion nearly perpendicular to the planet's transiting orbit, i.e. nearly face-on. However, at a projected separation of 218 AU and orbital period of 3200 years, the orbit is highly uncertain.

4.3.5 HIP 99711

We found for this star ($V = 7.76$, K2V) a 0.63 $M_{\rm Jup}$ companion with the longest orbital period (23.646 days) and the smallest RV amplitude (55.3 $\mathrm{m\,s^{-1}}$) of the five selected benchmark stars. Nonetheless, the RV perturbation is clear in the CHIRON data, and the values are consistent with those in the discovery paper (Santos et al. 2000). The companion (HD 192263 b) is among the earliest exoplanet candidates, but was called into question by Henry et al. (2002), who argued that the RV signal detected is due to stellar magnetic activity rather than the stellar reflex motion caused by a companion. However, Santos et al. (2003) then provided further proof to improve the planet's orbit, and confirmed the discovery, which is also supported by our measurements. We suspect that the slight differences in the orbital solution we found are due to contamination of the RV signal by the same stellar magnetic activity that led to the initial dispute about the discovery.

Table 4.1: New orbital solutions for known exoplanets in Paredes et al. (2021)

Star	M_*	Period	$m \sin i$	e	ω	K	a	T_p	RMS	No.	Ref.
	$M_\odot$	days	$M_{\rm Jup}$		deg	$\rm m\,s^{-1}$	AU	JD - 2450000	$\rm m\,s^{-1}$	Obs.	
Previously Known Exoplanet Systems											
HIP 2350	0.92	$3.458^{+0.0081}_{-0.0083}$	0.50	0.187	37.28	$72.5^{+4.6}_{-4.4}$	0.044	7948.482	12.8	24	Paredes et al. (2021)
	0.93	3.444	0.48	0.000	126.90	67.4	0.044	3323.206	...	28	Moutou et al. (2005)
HIP 57370	0.92	$4.079^{+0.0142}_{-0.0146}$	0.49	0.167	206.16	$66.9^{+3.5}_{-3.3}$	0.049	7933.659	26.1	20	Paredes et al. (2021)
	0.93	4.114	0.49	<0.140	143.40	63.4	0.049	3732.700	16.0	59	Ge et al. (2006)
HIP 72339	0.85	$10.721^{+0.0033}_{-0.0031}$	1.09	0.063	281.05	$112.3^{+4.6}_{-4.5}$	0.090	7928.965	9.9	28	Paredes et al. (2021)
	0.79	10.720	1.02	0.044	203.63	115.0	0.088	1287.380	15.4	118	Udry et al. (2000)
HIP 98505	0.84	$2.218^{+0.0010}_{-0.0009}$	1.17	0.028	136.42	$204.7^{+2.6}_{-2.5}$	0.031	7929.288	21.5	31	Paredes et al. (2021)
	0.82	2.219	1.15	0 (fix)	...	205.0	0.031	...	...	35	Bouchy et al. (2005)
HIP 99711	0.74	$23.646^{+0.2304}_{-0.2082}$	0.63	0.154	188.21	$55.3^{+2.1}_{-2.2}$	0.146	7912.820	13.5	32	Paredes et al. (2021)
	0.75	24.348	0.72	0 (fix)	0.00	61.0	0.150	...	...	182	Santos et al. (2003)

4.4 Classification of Companion Detections and Non-detections with RVs

Having investigated the detection sensitivity of CHIRON via RV standards and the set of five K dwarfs previously known to harbor exoplanets, it is now important to define a classification scheme for which a K dwarf primary is considered to have a stellar, brown dwarf, or planetary companion, or if it should instead be considered to be a single star to the limits reached with CHIRON in this survey. The resulting assessments fall into three categories, as noted for target stars in Table 2 and determined as follows:

- **No RV companion detected**
  - *Flat RV curve (F):* is assigned to RV datasets that show no significant change in the RV over the given timescale δt, as determined by its $\rm MAD_{RV}$ and/or ΔRV when compared to other survey stars of comparable brightness. Typically a K dwarf with $\rm MAD_{RV}$ below 40–50 $\rm m\,s^{-1}$($\sim$3 times the MAD of the RV standards)

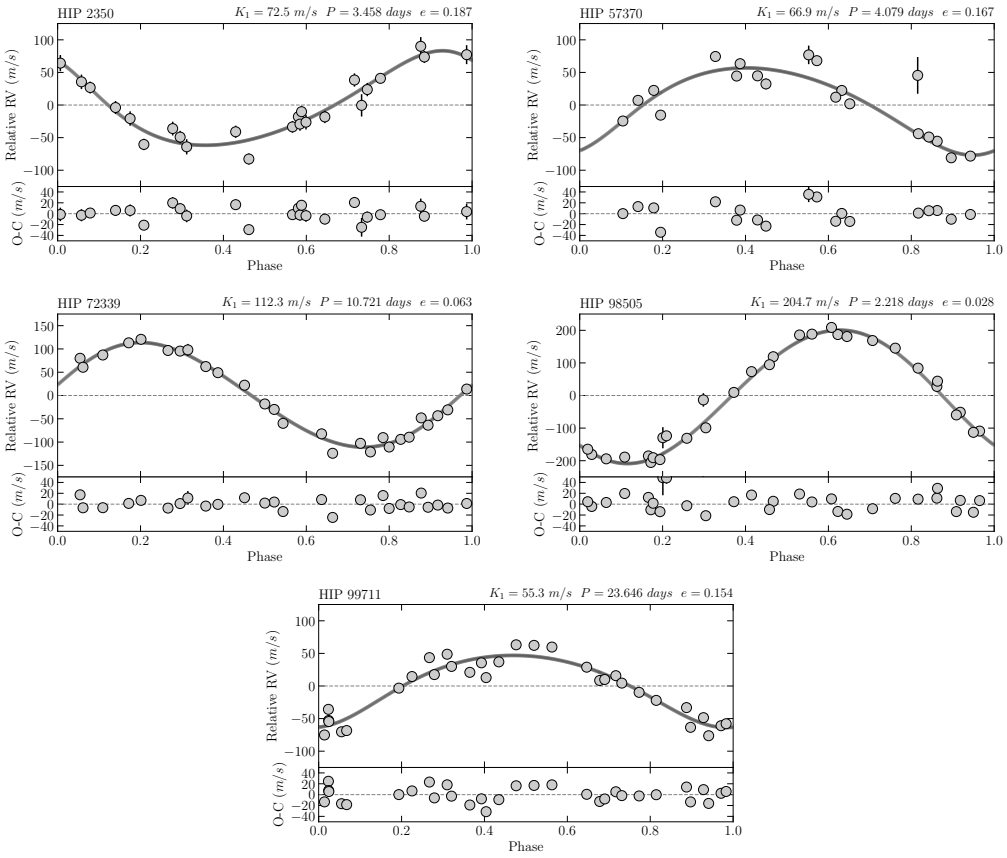

Figure 4.7 Phase-folded RV curves and residuals derived from CHIRON spectra for five K dwarfs previously reported to have exoplanet candidates in orbit. Phase zero indicates the time of periastron passage (T_p).

is deemed to have no detectable component within the time coverage. If enough data are available, a Lomb-Scargle periodogram showing no peaks above the FAP threshold confirms the assessment by the MAD, therefore concluding that no companion is found in the timescale covered. Noteworthy examples are the RV standards that I have been monitoring since the reopening, updated plots for standards HIP 3535 (Figure 13), HIP 58345 (Figure 198), HIP 73184 (Figure 252), and other stars HIP013258 (Figure 52) and HIP 4022 (Figure 14), among

others. *For the statistical treatment of stellar multiplicity discussed in Chapter 5, these stars (F) are considered to be single.*

- **RV companion detected?**
  - *Perturbation RV curve (P):* is assigned to RV datasets in which significant RV variations are evident, but the cause of the variable RVs is not yet determined. In most cases, additional data are needed for a more definitive classification. Causes include (1) the presence of a real companion with an indeterminate orbital period, (2) light contamination from a close source drifting in and out the fiber, and/or (3) signal limitation due to weather or intrinsic low brightness.
  - *Active RV curve (A):* is assigned to RV datasets in which significant RV variations are seen that are presumably due to stellar activity. Such signals may be correlated with the star's rotation and appear periodic, or may appear erratic with no periodicity evident. Activity levels can be estimated by inspecting key spectral lines sensitive to activity in the stellar chromosphere, such as Hα and Ca II. Additional information from chromospheric activity catalogs (Henry et al. 1996; Arriagada 2011) are used to decide whether or not to pursue more observations beyond the RV survey minimum. *For the statistical treatment of stellar multiplicity discussed in Chapter 5, this category of stars — Active (A) — is considered to be single.*

- **RV companion detected!**

– *Trend RV curve (T):* is assigned when the RV dataset shows a steady change in the RV values without a significant RV curvature to show periodicity; such trends are indicative of long orbital period companions. A few noteworthy examples include (1) HIP 11452 for which Agati et al. (2015) report an SB2 type companion with an orbital period of $\sim$ 25 years fitted spectroscopic and visually, while the CHIRON data exhibit a long-term trend over 1.46 years with maximum change of 531.8 $\mathrm{m\,s^{-1}}$ (Figure 43), and (2) RKS1418-0636A (Figure 239) for which speckle observations reveal a companion separated by $0.1675''$. Although this type of detection is not sufficient to pinpoint the nature of the companion, the trend offers a rough estimate of the minimum RV semi-amplitude as half the maximum RV variation in the trend, ΔRV/2, and minimum period as two times the observation time baseline, 2Δt. Stars with companion candidates of this type can be found in Table 3. These companions are ideal for confirmation via the speckle survey, in which stellar companions at separations of several AU can be detected directly.

– *Orbit RV curve (O):* is assigned when a companion is confirmed via a complete orbital solution that is well-constrained. For companions in circular or nearly-circular orbits, it is ideal to obtain RV data covering most or all orbital phases, for example, RKS0022-2701 (Figure 9) and RKS0112+0058 (Figure 22). For companions in highly eccentric orbits, the solution can be well-constrained with observations secured near the epoch of periastron. Noteworthy examples are RKS0701-2556A and RKS1518-1837 with orbital periods of 2745.3 days and 1635.7 days,

respectively and RV curves shown in Figure 119 and Figure 261 . The set of 42 new discoveries made during this survey have orbital solutions presented in Table 3. *For the statistical treatment of stellar multiplicity discussed in Chapter 5, both categories of stars — trends (T) and orbits (O) — are considered to be multiple.*

Table 2 summarizes the companion search results for all 804 stars considered to date for the K dwarf sample. For CHIRON data, included are the number of successful RV observations made with CHIRON, the DMY cadence coverage, the timespan over which the CHIRON observations were obtained, the full range of RVs measured, and the MAD values for the RV series. The RV Det. Type column indicates the verdict for the type of detection inferred from the RV profile, as described above, where F = flat, P = Perturbation (unsolved), A = Active, T = Trend (unsolved, but companion evident), and O = Orbit (solved). Following these CHIRON columns are data from the external datasets considered, including the number of observations from HIRES reported in Tal-Or et al. (2019), the number of observations by HARPS given in Trifonov et al. (2020), the status as planet host listed in NASA Exoplanet Archive (NEA), the SB9 spectroscopic catalog, and the WDS double star catalog.

4.5 K Dwarfs with no Detected Companions

A K dwarf is considered to have no RV companion detected by CHIRON when its RV time series shows no variation or perturbation in the time observed, manifested as points approximating a flat line with individual RV data points having values close to the 0 $\mathrm{m\,s^{-1}}$ relative RV line. Considering the sensitivities established from the RV standards and the handful of stars with known planets, it is clear that a K dwarf with MAD below 40–50 $\mathrm{m\,s^{-1}}$ ($\sim$3 times the MAD of the RV standards) has no detectable component within the time coverage. If enough data are available, e.g., >12 total frames, a Lomb-Scargle periodogram showing

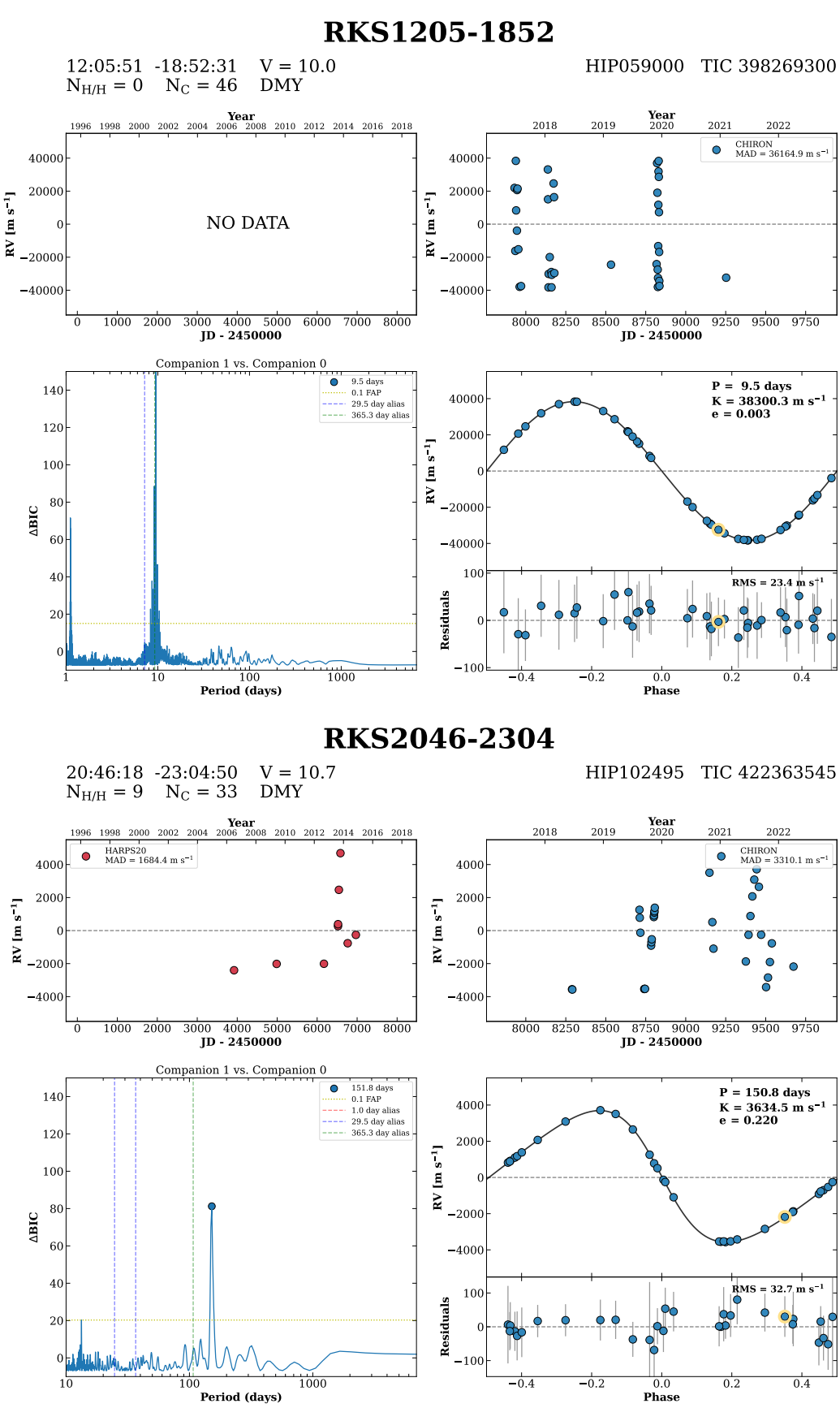

Figure 4.8 RV results for RKS1205-1852 (top) and RKS2046-2304 (bottom).

no peaks above the FAP threshold confirms the assessment by the MAD that no detectable companion is present. In Table 2, K dwarfs with no companions detected with CHIRON are labeled with an F under the column RV Status.

To understand the sensitivity of the survey to companions, a few examples are illustrative. Here we use circular orbits observed edge-on for objects orbiting a K dwarf with mass 0.8 $M_{\odot}$ to provide guidelines for companions that can be detected. The lowest mass star with mass of 0.075 $M_{\odot}$ would cause RV perturbations of ∼15000 $\mathrm{m\,s^{-1}}$ in a 1-day orbit, ∼4000 $\mathrm{m\,s^{-1}}$ in a 100-day orbit, and ∼800 $\mathrm{m\,s^{-1}}$ in a 10,000-day (27-year) orbit. Thus, all would be detected in the RV survey, although a complete orbit would not be possible in the latter case with only one year of data. A Jupiter-mass planet would cause RV perturbations of ∼200 $\mathrm{m\,s^{-1}}$ in a 1-day orbit, 50 $\mathrm{m\,s^{-1}}$ in a 100-day orbit, and ∼10 $\mathrm{m\,s^{-1}}$ in a 10,000-day orbit. Thus, exoplanets with orbital periods out to 100 days would be revealed in the CHIRON survey, but those in longer period orbits would likely be missed. Overall, the 1-day orbits correspond to orbital semimajor axes of ∼0.02 AU, the 100-day orbits to ∼0.4 AU and the 10000-day orbits to ∼8.4 AU. The survey is therefore sensitive to most companions down to the mass of Jupiter within ∼1 AU and to stellar companions out to at least 5 AU. Note that companions further than ∼1 AU from their primaries can also be revealed through our high-resolution speckle survey of the same stars.

Of the 118 stars covered at all three DMY cadences by CHIRON in the 25 pc sample, 89 (75%) are considered to have no detected companions. Similarly, for the 315 stars observed in the 33 pc sample, 228 (72%) have no companions, and for the 386 stars in the full sample

of K dwarfs considered here, 280 (73%) are single stars. These stars should become high-priority targets for terrestrial planet searches because we now know that they do not have stellar (or brown dwarf) companions within a few AU, nor do they have hot or warm Jupiters within ∼1 AU.

4.6 K Dwarfs with Detected Companions

4.6.1 Orbital fitting procedures

Orbits for known and new exoplanet candidates have been derived using the code `Systemic2` (Meschiari et al. 2009)[1], which provides a functional interface written in `R` that can be used to calculate Lomb-Scargle periodograms and to explore orbital fits interactively given a set of RV data. Interactive fits are a useful exploratory tool because each RV dataset is may be affected by poor quality data or RV calculations that need to be refined, but interaction is not always feasible when dealing with large data sets counted by thousands, or when detections are desired to be uniformly treated for statistical purposes. For this case, I complemented the analysis with the tools provided in the package for RV modeling `RadVel` (Fulton et al. 2018)[2], and tools from the package `RVsearch` (Rosenthal et al. 2021)[3]. Both packages are written in `python`, and I adapted them for seamless integration with the workflow I have designed to organize, process, and analyse the RV data from CHIRON in the search for companions.

The orbital fitting process starts with the calculated RVs by the pipeline described in

[1] github.com/stefano-meschiari/Systemic2
[2] github.com/California-Planet-Search/radvel
[3] github.com/California-Planet-Search/rvsearch

§2.8 as inputs into the orbital fitters to search for periodic signals. Prominent peaks in the periodogram of the RV dataset above the false alarm probability (FAP) level hint the presence of a periodic change. Keplerian orbits fit results for the strongest periodic signals of the CHIRON RV dataset are visually inspected for vetting and refinement if needed. Initial fits are made using circular orbits in order to avoid very high eccentricity orbits that may fit the datasets but are astrophysically unlikely. The set of orbital parameters to fit are the orbital period P, the RV semi-amplitude K, the epoch of the periastron passage T_P, the eccentricity e, and the argument of the periapsis ω.

The two lower panels in 4.8 shows the results of the orbital fit analysis. The lower left panel shows the periodogram of the CHIRON data, where the Bayesian Information Criterion (BIC) is measured for three models fitted, a no-companion model (Companion 0), an RV trend/curvature model, and a one companion model (Companion 1). If the ΔBIC between Companion 1 and Companion 0 model is favored, and the highest peak becomes the most likely period for one companion model applied to the data. Step sizes of 0.001 days are used to fine tune the orbital period, while the fitting process is carried out using chi-square minimization until each orbit fit converges, determined when the RMS of the fit reaches $\sim$20 $\mathrm{m\,s^{-1}}$. I have chosen limit given the typical RV scatter and uncertainties seen for the 351 K dwarfs with no detected companions, as shown in Figure 4.5 and Figure 4.2. The yellow dashed line indicates the 10% FAP threshold below which a periodic signal is deemed unrealiable. The vertical dashed lines mark regions of potential aliasing produced at 1.00, 29.50, and 365.25 days, used to keep track of false detections due to nightly data

acquisition, moon influence, and barycentric motion of the Earth. In the lower right panel a phased orbital fit and residuals are shown for the CHIRON (only) data if a solution could be obtained. The RV curve is centered at phase zero when the transit over RV = 0 occurs. The last RV data point measured is encircled in yellow, and the Period (P), the RV semi-amplitude (K), eccentricity (e), and root mean square of the fit (RMS) are given for the one companion orbital solution. If it wasn't possible to solve an orbit for one companion "NO ORBIT" is displayed. Finally, I get them through a final step in the orbital parameter determinations, to derive the intervals of confidence for parameters using MCMC simulations included in `Systemic2` code, starting with the model best fitted, a total ∼10000 steps, in 2 chains, and skipping the first 1000 iterations.

Orbits already published in Paredes et al. (2021) shown here in Figures 4.7 and 5.7 and Tables 4.1 and 5.1 include errors for nine K dwarf + exoplanet systems. To estimate the companion $m \sin i$ values and compare with the known orbital solutions from their discovery publication, masses for the primary stars have been derived using V magnitudes converted from V_T magnitudes (Høg et al. 2000) and the mass-luminosity relation in M_V of Henry & McCarthy (1993). Updated orbital parameters for the K dwarfs and their companions published in Paredes et al. (2021) are included in Table 3 and in the series of Figures in Appendix A.

4.6.2 Complete Orbits Derived

In the first block in table Table 3 I present 42 new orbits of companions of K dwarfs found solely with CHIRON RV data collected until 2022 May. On each line, the star ID and Sample

label is accompanied with the five relevant orbital parameters, Period, RV Semi-amplitude, eccentricity, argument of the periapsis and epoch of the periastron passage, derived with the procedures described in §4.6.1. The RMS of the orbital fit and number of observations as a way to assess how reliable the orbital solution is. Orbital solutions resulting from low number of observations and/or poor orbital phase coverage, with either high RMS (ex. $>100\ \mathrm{m\,s^{-1}}$) or low RMS (ex. $<100\ \mathrm{m\,s^{-1}}$), hints that the solution found could not be well constrained and more data is needed at specific times. High RMS values could be the result of feeding the orbital fit with RV data with poor quality or with anomalous changes, while low RMS values can be the result over-fitting. An example of keeping track of orbital phase coverage while considering seasonal visibility is shown for in Figure 4.9

The K dwarf RKS0914+0426A (Figure 156) is an example of an orbital fit not well constrained, where a low RMS is just the result of over-fitting 40 RVs that do not fully cover the orbital phase.

An opposite case is seen in the orbital solution of RKS0840-0628A a.k.a HIP 42507 (Figure 149), where RV semi-amplitude is large enough to be detected, yet RV measurement uncertainties and the high RMS make the orbital fit not well constrained. In fact, close inspection of its spectra line features shows double lines (Figure 4.10), evidencing a spectroscopic binary type 2 detection (SB2). The RV extraction procedures designed for this work intended for orbital detection of SB1 and planets, where the spectra is mostly produced by the primary star. Despite this limitation for the characterization of the companion, it is possible at the very least detect its presence and flag them for further analysis.

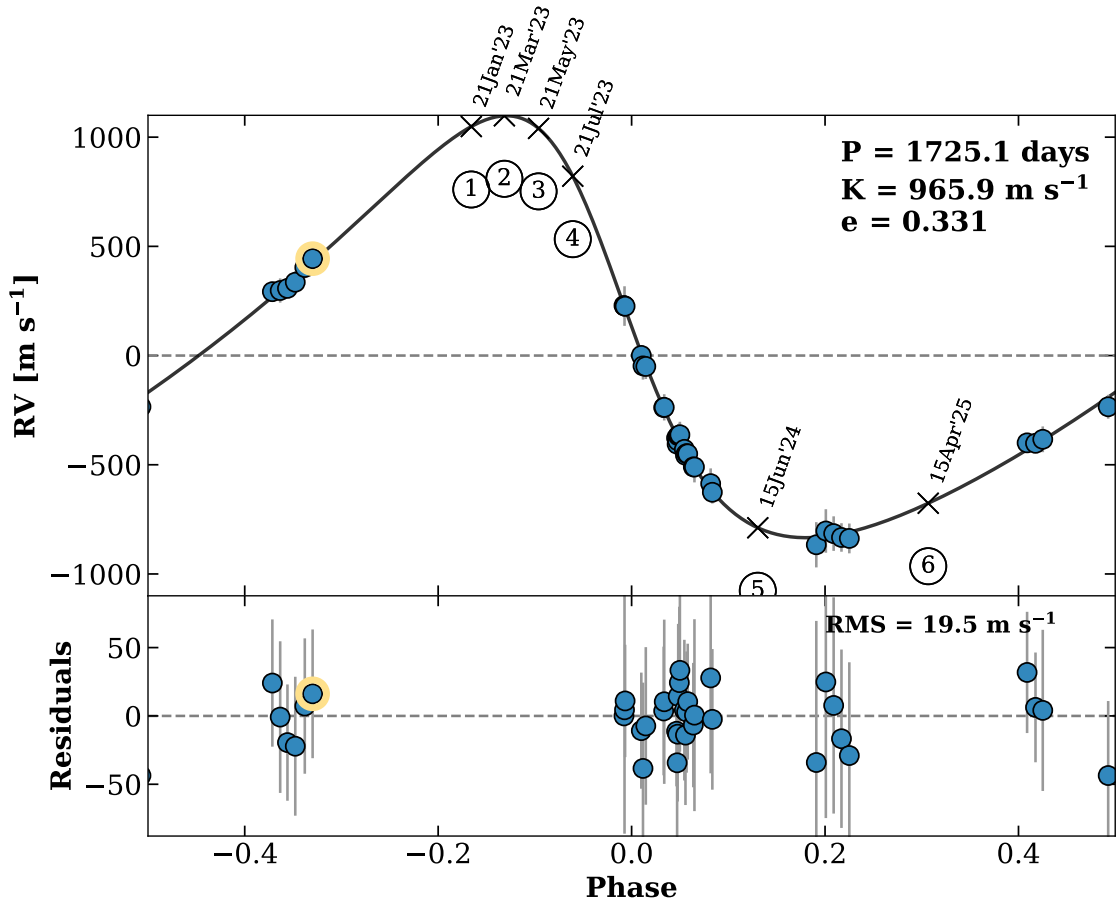

Figure 4.9 RKS1154+2844 as an example of how ephemerides phase coverage is followed-up. The circled numbers mark the upcoming observation needed along with the ideal night for it.

Orbital periods for new companions presented in Table 3 range from ∼4 days, RKS0329-2406 and RKS2041-2219 (Figures 346 and 63), to 7560 days, RKS1121-2027 (Figure 188). Note that despite the 22 RVs measured over the span of 1238 days are not covering sufficiently the 7560 day period orbital phase, I still consider the orbital solution acceptable because the orbital fit is likely the result of the prominent RV curvature seen in its RV timeseries.

Eccentricities are not fixed to obtain the each orbital solution so they range freely from

circular to highly eccentric orbits. The three orbits with lowest eccentricities are RKS2041-2219 (Figure 346), RKS1205-1852 (Figure 202), and RKS0329-2406 (Figure 63), also are also short period orbits. The most eccentric orbit, $e = 0.922$, is obtained for RKS1518-1837 (Figure 261) and while is a long period orbit of 1635 days, RVs were timely measured close before and after the time of of the periastron.

RV semi-amplitudes are closely related to the mass-ratio between companion(s) and stellar host and range between 95 $\mathrm{m\,s^{-1}}$and 70.5 $\mathrm{km\,s^{-1}}$, which for a K dwarf of 0.8 $M_{\odot}$ correspond to 0.61 M_{Jup} and 0.68 $M_{\odot}$, respectively.

4.6.3 SB2s

The primary goals of this phase of the survey are to determine the multiplicity rate for K dwarfs and to solve orbits for single objects in SB1s. Thus, while a few SB2 systems are evident in our data — these are included in the counts for multiplicity — we do not solve their orbits at this time. SB2s are spotted first in the RV timeseries, usually exhibiting drastic changes in RVs, as individual components light contribution to the spectrum is changing with the orbital phase.

Having said this, we acknowledge the scenario where stellar companions that are relatively bright and similar in spectral classification to the primary star will probably create a measurable signal in the derived CCF. If the relative velocity separation is larger than the characteristic width of the CCF (FWHM =13 $\mathrm{km\ s^{-1}}$, which is set primarily by the thermal broadening of the spectral absorption lines; see Fig. 2.2???), then the blending of the CCFs of the two components will be small and the resulting affect on the RV of the primary is

minimal. On the other hand, if the relative velocity separation is small, $|v_r| <$ FWHM, then the measured peak RV assigned to the primary will be shifted slightly in the direction of the secondary component and cause a slight underestimate of the absolute value of velocity difference. This will happen when the component orbital velocity curves cross and when the semi-amplitudes K_1, K_2 are small compared to FWHM. In the limit $|v_r| \ll$ FWHM, the primary velocity will be shifted by an amount that is approximately $v_r f_2/(f_1 + f_2)$, where f_1 and f_2 are the monochromatic fluxes of the primary and secondary components. In such small semi-amplitude cases, the derived semi-amplitude will be smaller than the actual semi-amplitude by a factor of $(1 - \frac{f_2}{f_1+f_2}\frac{K_1+K+2}{K_1})$. As an example, suppose we encountered a system of a K0 V+K4 V pair with a long period (or small inclination) with $f_2/f_1 = 0.33$ and $K_2/K_1 = M_1/M_2 = 1.20$. Then the ratio of the measured to true semi-amplitude of the primary would be approximately 0.45. Consequently, the semi-amplitudes reported in Table 3??? for stellar companions may be underestimates in the cases of low K_1 (private communication with Douglas Gies).

In this line, the future work in this project involves adding further diagnostics for low semi-amplitude detections, to make sure that they are not the result of blended CCFs canceling each other.

4.7 Active K Dwarfs

Stellar activity in the surface of stars, usually seen in young stars, can mimic exoplanet-like periodic signals in the RV data. Affects the spectral line profiles superimposing a period

associated to the rotation rate of the star. Activity indicators can be found in the spectrum of stars and used to trace active regions, the most famous being the Ca II H&K lines chromospheric index (Wilson 1978). Unfortunately, CHIRON was not designed to cover the spectral region that includes Ca II H&K lines, therefore bisector velocity span was explored as an alternative. This technique measures variations in the spectral line profile by mapping changes in its width at different depths. This method sensitive in active stars and can confirm or discard a dubious detections at the exoplanet level. It is not feasible to trace shifting spectral lines on large numbers, so an effective way is to use the same cross correlation function to extract RVs as an average or proxy of the spectral lines used. The overall results from bisector velocity span are not addressed here, because early testing in non-active stars not necessary have yielded consistent results. Regardless, stars with signs of activity, either from the literature or spectral characteristics, are labeled "A" in Table 2 under the column "RV Det. Type". Although this is not a final assessment, it let us to keep track for further monitoring and analysis. After describing the type of results derived from this research, in Chapter 5 I cover results of the survey as whole and discuss the statistical aspects derived from this survey.

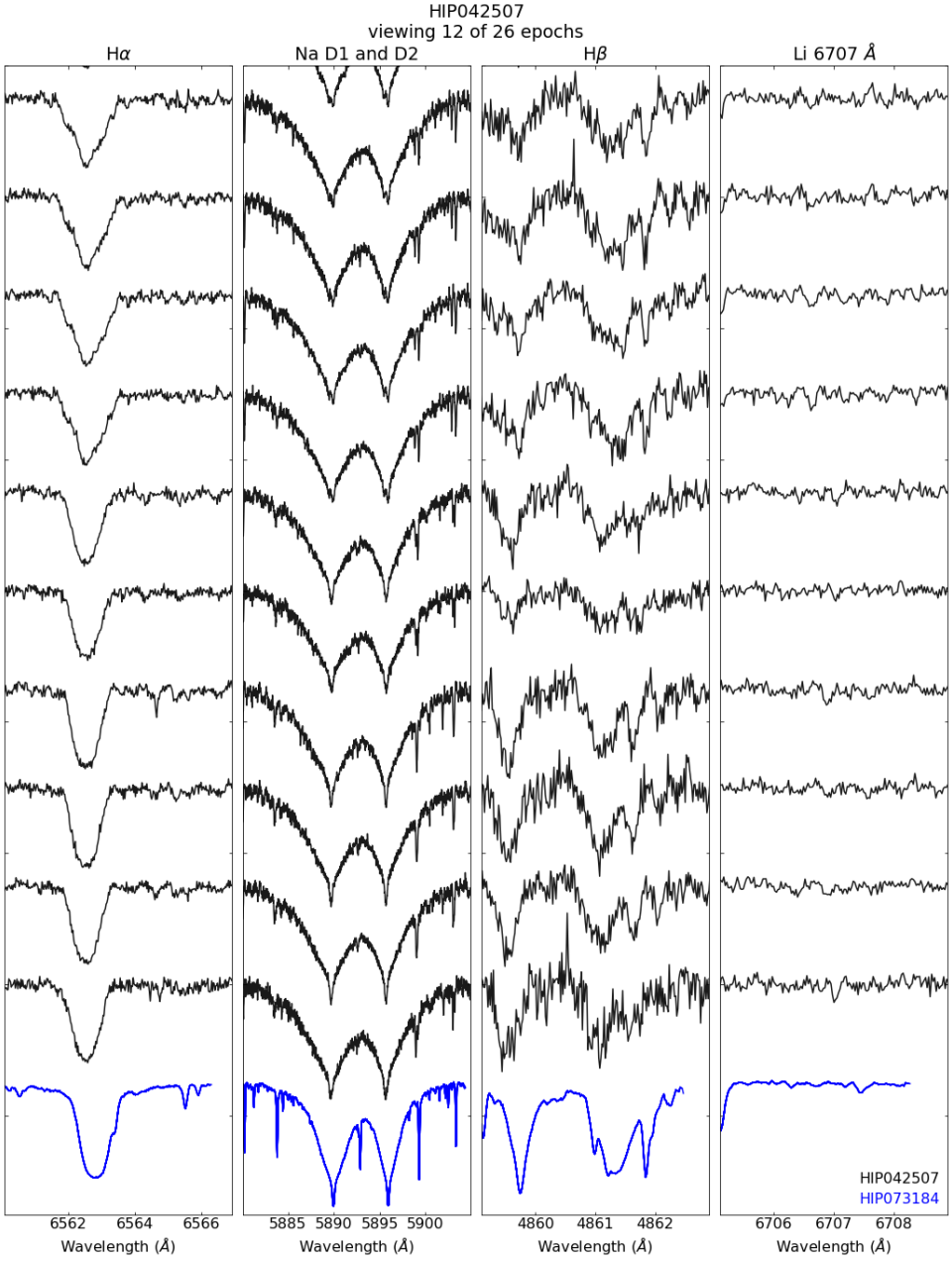

Figure 4.10 Spectral features Hα, Na D1 and D2, Hβ and Li 6707Åshown in black lines of RKS0840-0628A a.k.a HIP 42507, arranged vertically in timeseries from bottom to top. The blue spectrum correspond to one of the standards with high S/N for reference. The double lines characteristic of SB2 companions are more noticeable in the Hα and Na D1/D2 profiles towards the bluer side starting at the 5th epoch from bottom and up. It ca be noticed as well that Na D1/D2 go from single sharp core to a double minimum core (from bottom to top) SB2 components increase their velocity separation.

CHAPTER 5

Discussion

5.1 Detected Companions

Figures 5.1, 5.3, 5.5 summarize the key results of the K dwarf RV survey, addressing the 25 pc, 33 pc, and all K dwarfs observed results, respectively. This results are an update to the findings presented in Paredes et al. (2020). The plots illustrate the RV semi-amplitudes (K_1) in $\mathrm{m\,s^{-1}}$ vs. orbital periods in days created by companions for a typical K dwarf, for which a mass of 0.8 $M_\odot$ has been assumed for all stars. Diagonal lines are modeling the K_1 signatures by one companions in circular, edge-on orbits for the lowest mass stars at 75 M_{Jup}, the lowest mass brown dwarfs at 13 $M_{\rm Jup}$, and an exoplanet of 1 $M_{\rm Jup}$sampling orbital periods from less than 1 day to 100,000 days (274 years). Each line is limiting an area to define the type of companion found to each K dwarf. For additional context, the signatures due to E(arth), J(upiter), S(aturn), U(ranus), and N(eptune) are shown with corresponding letters as if they were each orbiting a K dwarf with mass 0.8 $M_\odot$.

Points on each plot show the RV signatures, broken into two types — simple and with arrows. Simple points represent companions with fully mapped orbits having solutions that provide minimum masses, broken into various subsets. Blue and purple points are known companions published in the literature as of 2022 October. Blue points represent stellar companions with orbits compiled in the SB9 catalog and purple points are confirmed exoplanets compiled by the NASA Exoplanet Archive. Green points represent new discoveries from this survey for companions of all three types. Gray points with arrows are companions

causing trends in the RV time series for which only minimum K_1 values and orbital periods can be estimated.

In all three Figures, a light blue horizontal line is plotted at the RV MAD value for each star for which no companion was detected. The ensemble of lines accumulating right above the 5 $m\,s^{-1}$level shown by the dotted blue line represent another evidence of the companion detection sensitivity of CHIRON for K dwarfs in the survey. A few percentage of lines is way below the 5$m\,s^{-1}$level, this is because fewer RV data points are available, or they are spread over a much shorter time baselines, which from Figure 4.5, tends to lead lower MAD values.

5.2 Required Caveat for RV Results

It is important to note that for systems with wrapped orbits, the *sini* ambiguity in inclination limits the characterization of the companion to a minimum mass. In addition, for cases where trends are seen rather than wrapped orbits, only mass estimates can be made for companions. So, in both cases the assignments of brown dwarf and exoplanet may be incorrect and the companion may be stellar. What can be stated with confidence is that if the minimum mass is greater than 75 Jupiter masses, the companion must be stellar. While a detailed analysis of the intersection between the RV and speckle survey results is beyond the scope of this dissertation, we have found that at least 35 of the RV companions (with orbits or trends) to have speckle detections.

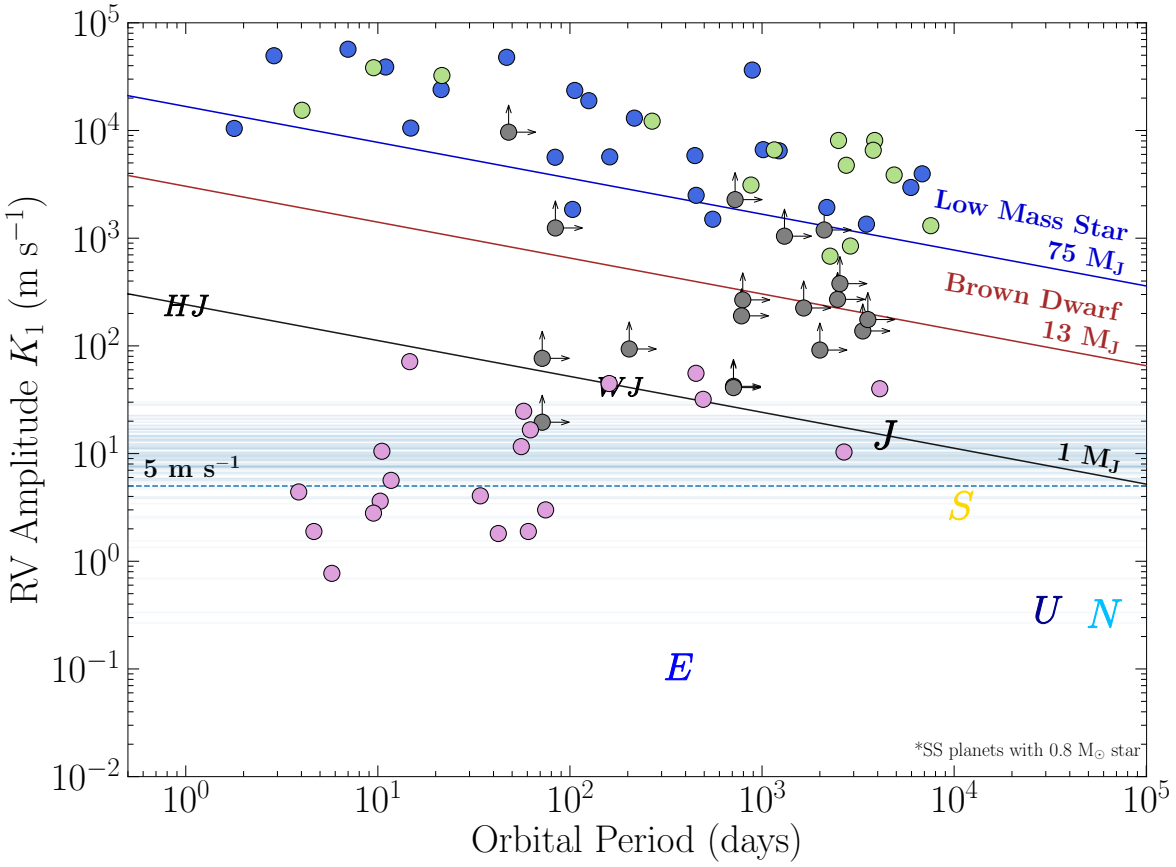

Figure 5.1 Companion detections via RV techniques for K dwarfs within 25 pc. Diagonal lines represent K_1 values for the lowest mass star, lowest mass brown dwarf, and 1 Jupiter-mass planet for orbital periods of less than 1 to 10^5 days. Simple points represent companions with derived orbits and arrowed points are for incomplete orbits, e.g., trends. Blue and purple points are for known stellar and brown dwarf/exoplanet candidates, respectively. Green points represent new companions discovered in the CHIRON survey. Gray points are CHIRON detections without complete orbits, with arrows indicating minimum K_1 values and shortest orbital periods. Light blue lines are placed at the RV MAD values for stars with no companion detections.

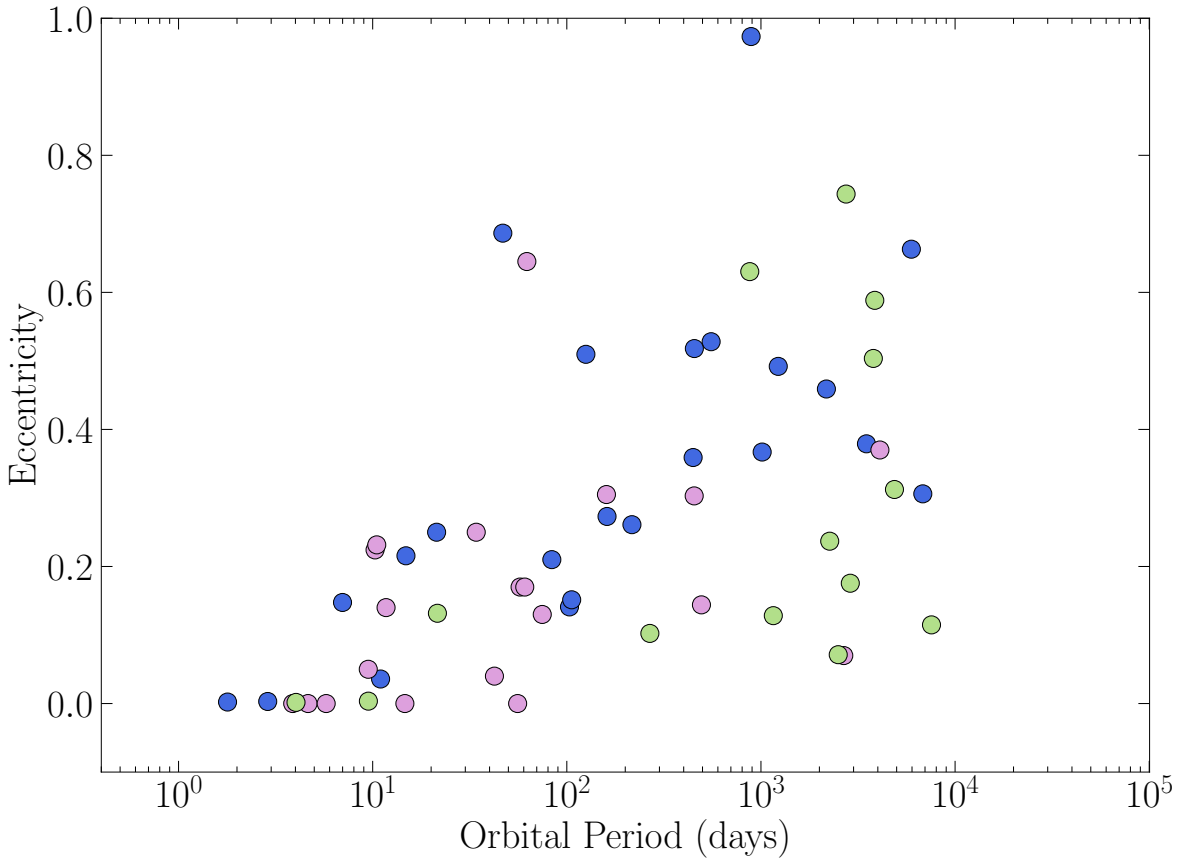

Figure 5.2 Orbital architectures from the e vs P plot for the detections via RV techniques for K dwarfs within 25 pc. Blue and purple points are for known stellar and brown dwarf/exoplanet candidates, respectively. Green points represent new companions discovered in the CHIRON survey.

5.3 Results for the 25 Parsec Sample

Of the 278 K dwarfs in the 25 pc equatorial sample, 135 were covered in HARPS, HIRES, or SB9, leaving 143 to be surveyed with CHIRON. Of these, 118 have full DMY cadence coverage and 89 have detected companions. As shown in Figure 5.1 there are 12 new stellar companions found in this survey, a significant contribution given that only 20 were previously

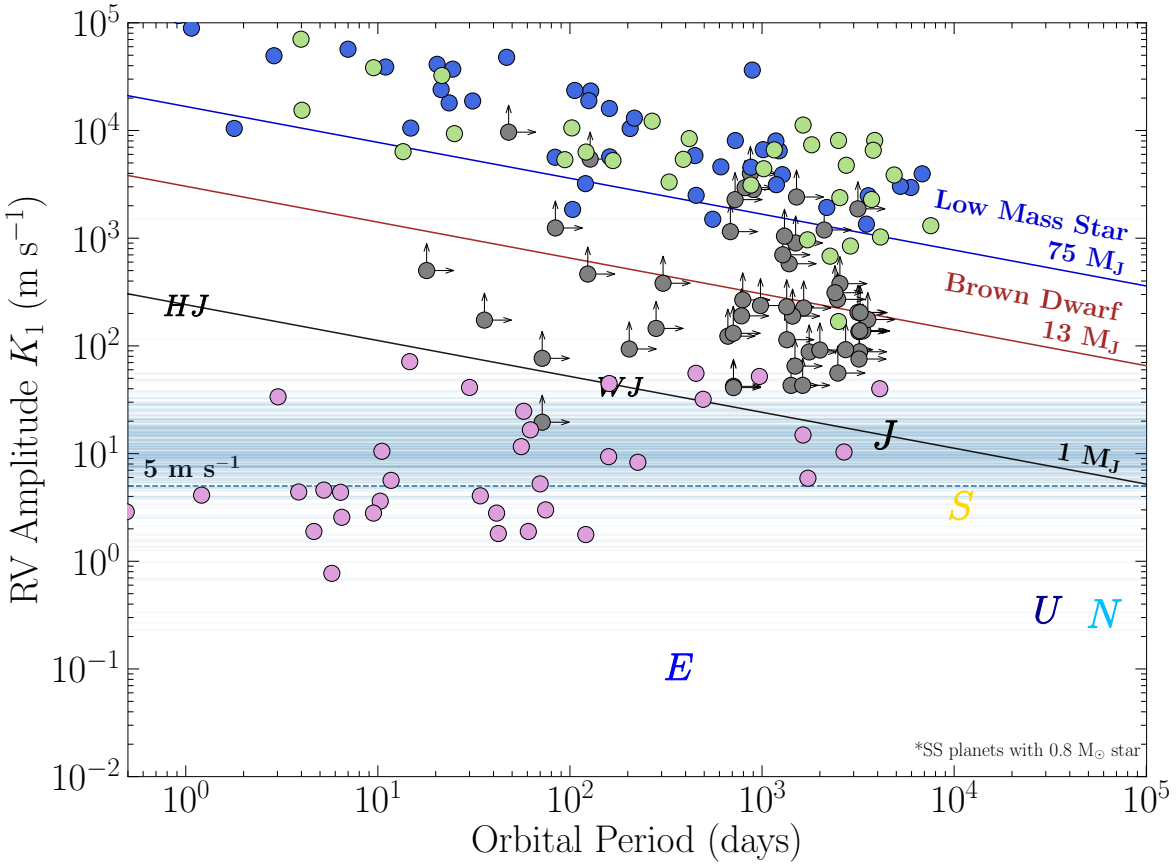

Figure 5.3 Companion detections via RV techniques for K dwarfs within 33 pc. Diagonal lines represent K_1 values for the lowest mass star, lowest mass brown dwarf, and 1 Jupiter-mass planet for orbital periods of less than 1 to 10^5 days. Simple points represent companions with derived orbits and arrowed points are for incomplete orbits, e.g., trends. Blue and purple points are for known stellar and brown dwarf/exoplanet candidates, respectively. Green points represent new companions discovered in the CHIRON survey. Gray points are CHIRON detections without complete orbits, with arrows indicating minimum K_1 values and shortest orbital periods. Light blue lines are placed at the RV MAD values for stars with no companion detections.

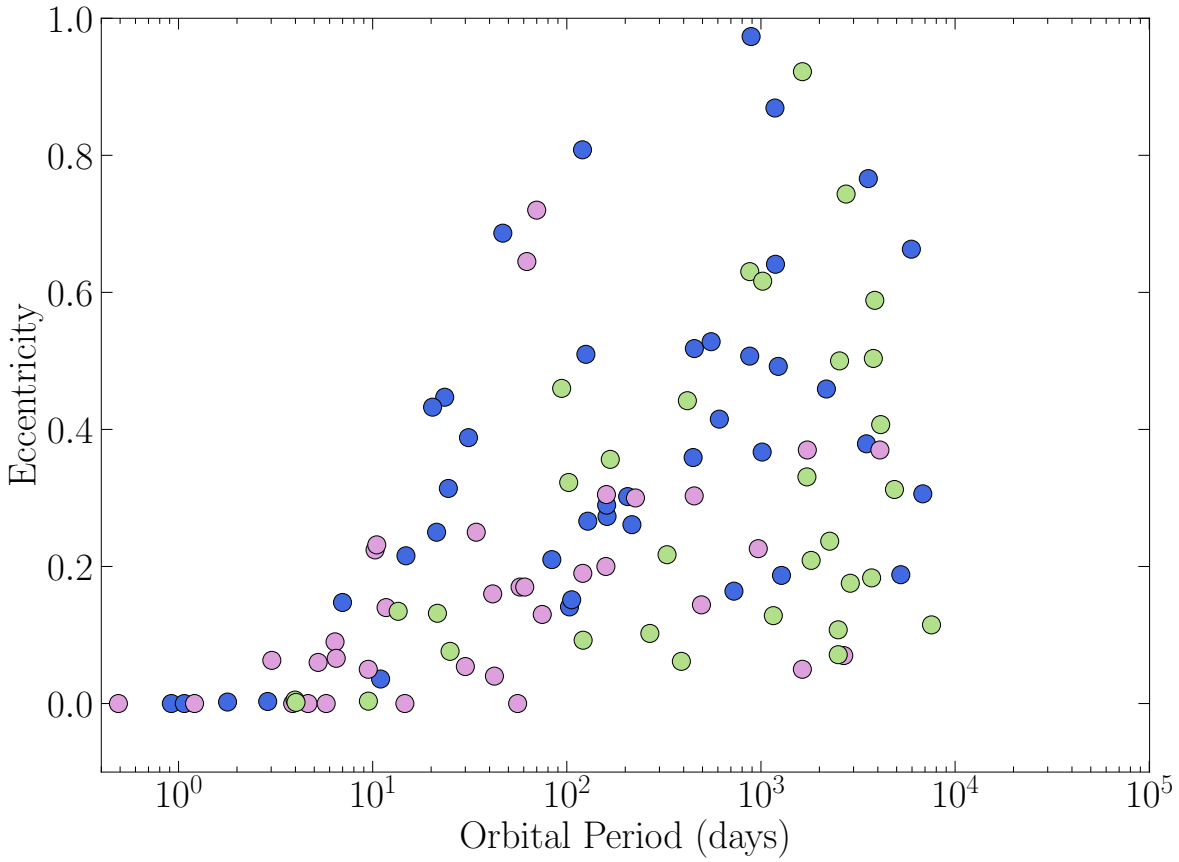

Figure 5.4 Orbital architectures from the e vs P plot for the detections via RV techniques for K dwarfs within 33 pc. Blue and purple points are for known stellar and brown dwarf/exoplanet candidates, respectively. Green points represent new companions discovered in the CHIRON survey.

known. In addition, 2 new brown dwarf candidates were found, boosting the total sample of such objects to 5.

This 25 pc sample will be considered for the multiplicity statistics described in §5.8, given that 253 (91%) of the 278 stars nearer than this horizon can be considered to be fully explored for companions within a few AU. Note that there are 17 additional companions

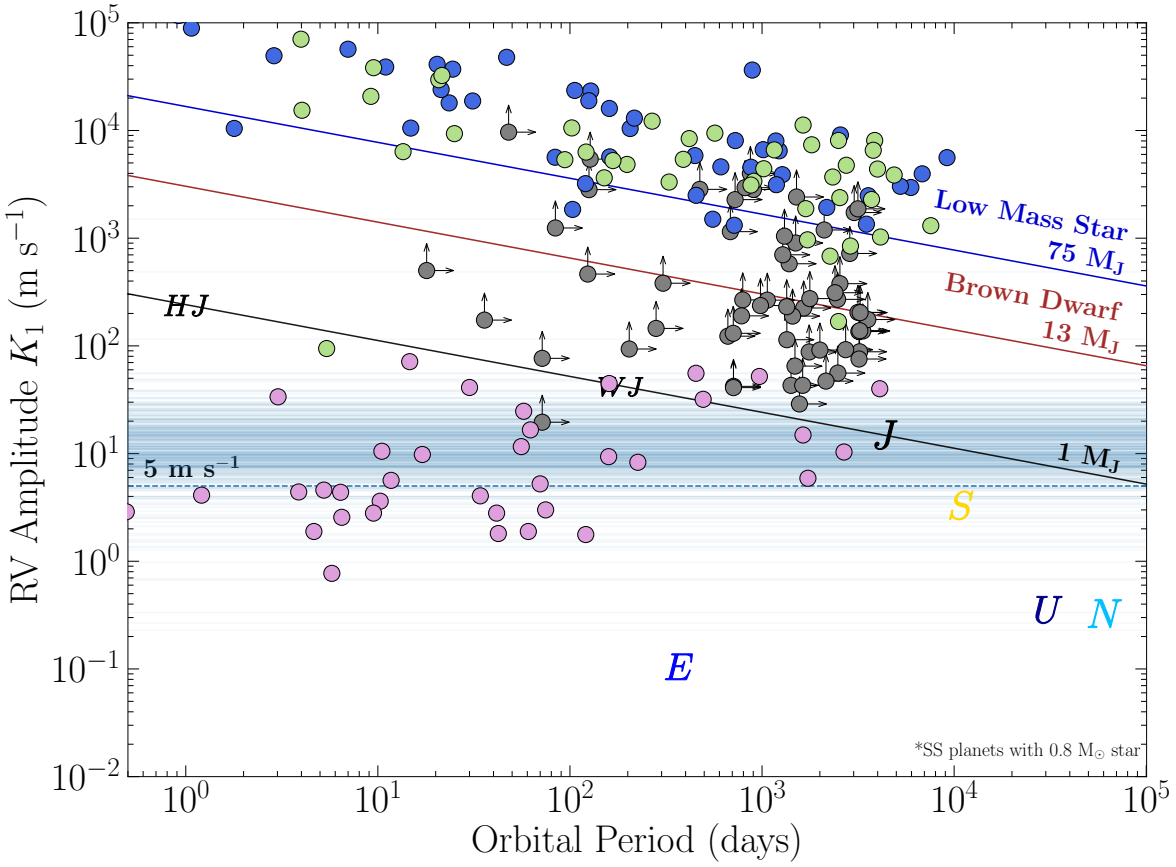

Figure 5.5 Companion detections via RV techniques for K dwarfs in the sample of all 804 stars observed with CHIRON. Diagonal lines represent K_1 values for the lowest mass star, lowest mass brown dwarf, and 1 Jupiter-mass planet for orbital periods of less than 1 to 10^5 days. Simple points represent companions with derived orbits and arrowed points are for incomplete orbits, e.g., trends. Blue and purple points are for known stellar and brown dwarf/exoplanet candidates, respectively. Green points represent new companions discovered in the CHIRON survey. Gray points are CHIRON detections without complete orbits, with arrows indicating minimum K_1 values and shortest orbital periods. Light blue lines are placed at the RV MAD values for stars with no companion detections.

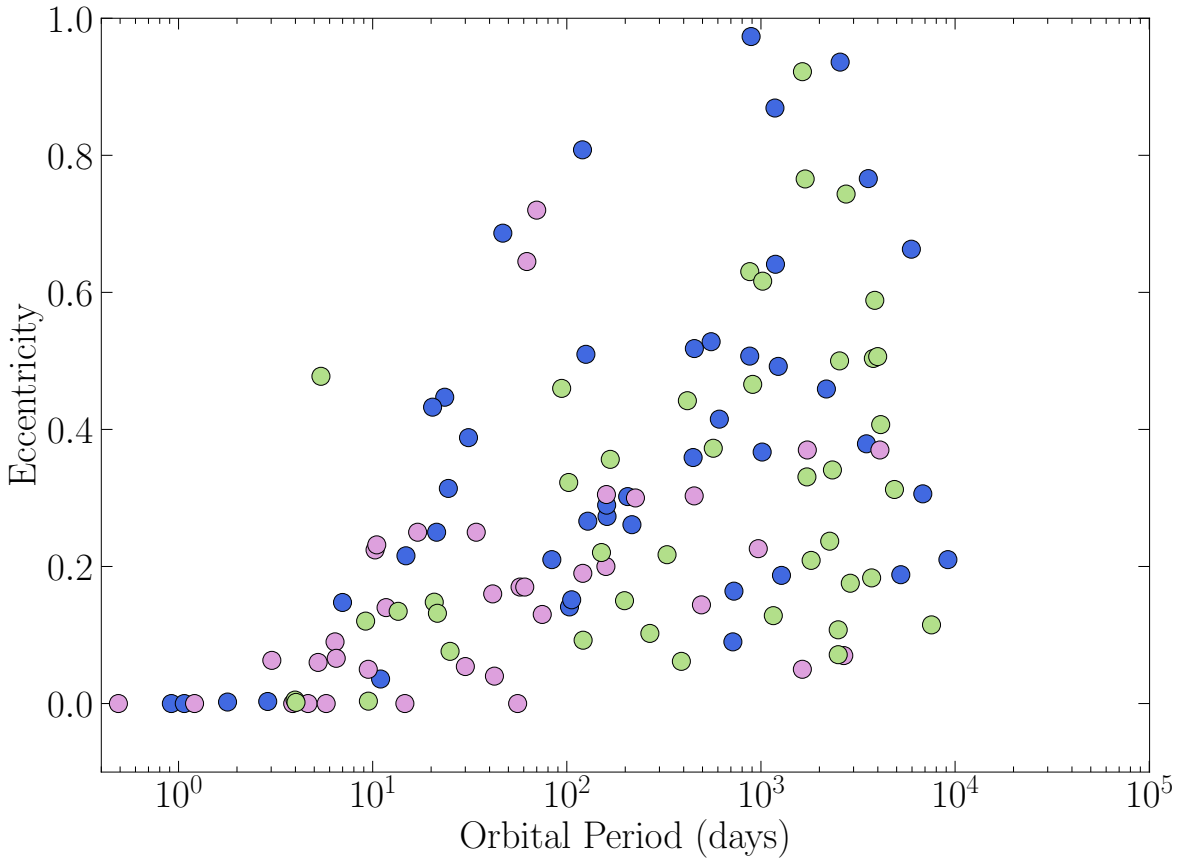

Figure 5.6 Orbital architectures from the e vs P plot for the detections via RV techniques for K dwarfs in the sample of all 804 stars observed with CHIRON. Blue and purple points are for known stellar and brown dwarf/exoplanet candidates, respectively. Green points represent new companions discovered in the CHIRON survey.

shown with the arrowed gray points evident in the RV time series as trends that do not yet have complete orbital solutions, but these will be included in the multiplicity calculation.

5.4 Results for the 33 Parsec Sample

The goal of this initial K dwarf RV survey is to complete RV coverage for all 678 K dwarfs in the 33 pc equatorial sample. Of these, 214 are considered to be covered by HARPS or

HIRES, or have orbits in SB9, leaving 464 to be surveyed with CHIRON. To date, 315 have full DMY cadence coverage with CHIRON, nearly tripling the number of stars observed in the 25 pc sample. The remaining stars continue to be observed with CHIRON, with a plan to complete the coverage for all 678 stars in the sample in the future. Previously known companions and new discoveries via this CHIRON survey are plotted using the same colors as for the 25 pc sample. The detections fall into previously known/new companions as follows: stars 35/29, brown dwarf candidates 2/3, and exoplanet candidates 33/3 from Paredes et al. (2021).

5.5 Results for All K Dwarfs Considered

As described in Chapter 3, in total there are 804 K dwarfs considered in the CHIRON survey, including the 33 pc sample stars described above, as well as stars from the initial *Hipparcos* list and calibration stars. While this sample is neither as volume-limited nor volume-complete as the 25 pc and 33 pc samples, it is discussed here to capture all of the discoveries made during the 5-year CHIRON campaign. Figure 5.5 shows all companions found so far. Focusing on the green points that represent new discoveries, there are 39 stellar companions, 3 brown dwarf candidates, and 4 exoplanet candidates. The exoplanet candidates are discussed further in §5.6.

A key result seen in this plot is the prevalence of both low mass stellar companions and exoplanets orbiting K dwarfs. In contrast, the few brown dwarf candidates revealed in this survey are found only at orbital periods longer than 1000 days, this result is very

compelling since it is derived from a uniformly treated sample of uniform stellar spectral type, providing an undisputed evidence to confirm the concept known as the "brown dwarf desert", and further supporting that they may undergo a different formation process than low-mass stars. Another key result seen in this plot, is an slight tilt in the trend in the low-mass star region. This suggest that close stellar companions in envelopes are shown in the plot as higher mass-ratios at shorter periods than longer periods.

There is a large population of arrowed gray points in the region of companions with minimum masses of 1–75 M_{Jup}. The datasets for these stars have perturbations with indeterminate K_1 values and orbital periods, and hence these companions may be massive planets, brown dwarfs, or stars. Therefore, it is apparent that there are many stellar companions, few brown dwarfs, and many exoplanets in orbit around K dwarfs. While some orbits are still unfinished, the census for each type of companion have maintained proportions since the first analysis done in Paredes et al. (2020). The completion of long period orbits will be more suitable for the speckle and wide survey.

Another point of discussion is the relation between the orbital eccentricity and period. Figures 5.2, 5.4, and 5.4 show the orbital architectures of the K dwarfs with stellar with at least one stellar companion (blue and green points) and with at least one planet companion (purple). The tendency already hinted in §4.6.2. At higher orbital periods, orbits tend to be more eccentric, circular orbits become non-existent around 10-day period for stellar-type orbits and from 50-day period for planet-type companions. The tendency is the same in all three samples and applies for stellar and planets orbits. It is important to remark that

the presence multiple companions vs. one companion could be affecting the shape of some orbits, so it is very likely that despite the clear tendency seen, better characterization of multi-companion systems could provide more reliable limits to the distribution of orbital architectures.

5.6 Four Exoplanet Candidates

Phase-folded RV curves for the 4 exoplanet candidates are presented in Figure 5.7. Their minimum masses range from 0.51 M_{Jup} to 2.95 M_{Jup}, exhibit semi-amplitudes in the RV data series of 41–735 $m\,s^{-1}$, and have orbital periods of 0.98–160 days. One of the four, HIP 65, has been found to eclipse in *TESS*, and therefore has been confirmed to be a hot Jupiter in a nearly circular (e = 0.009), 0.98-day orbit.

5.6.1 TESS target HIP 65 (NLTT 57844)

A possible low mass companion was found to transit HIP 65 (TOI 129, $V = 11.13$, K4V) in the first set of data released from *TESS* in sector 2, and later in sectors 28, 29. At 61.9 pc, this star is beyond the 50 pc cutoff of our K dwarf survey, but was observed as an early possible discovery by *TESS* that could be quickly verified with CHIRON data. Initial RVs were collected with CHIRON starting 2018 September 8 and within two weeks of the first *TESS* data release, an orbit was published at www.recons.org on 2018 September 10. The quick turnaround was possible because of the nimble system established to acquire CHIRON observations. A total of 58 spectroscopic observations have been secured between 2018 September 8 to 2020 January 12 and we find an RV signal consistent with the *TESS* transit

signal detected. Our analysis yields to a giant planet companion with mass 2.95 $M_{\rm Jup}$ in an orbital period of 0.981 days, consistent with the orbit published by Nielsen et al. (2020). The properties of the ∼1 day orbit and massive planet make this an excellent candidate for detailed exoplanet atmospheric studies.

5.6.2 HIP 5763

This K dwarf survey star (V = 9.86, K6V) shows a perturbation with a period 30 days in the RVs due to a companion with minimum mass 0.51 $M_{\rm Jup}$. A total of 19 observations spanning two years were secured between 2017 November 20 and 2019 December 17. This planet candidate has the smallest RV amplitude (41.1 $\rm m\,s^{-1}$) of the four new detections reported here, but this amplitude is clearly offset from results for stars of similar brightness in Figure 4.5, indicating that the companion is likely real. In addition, the RMS of the residuals to the orbital fit (16.2 $\rm m\,s^{-1}$) is similar to the RMS values we find after fitting orbits for the five known planetary systems. HIP 5763 is not known to have visual stellar companions reported in the Washington Double Star Catalog (WDS) (Mason et al. 2001), nor any spectroscopic binary companions reported in The Ninth Catalogue of Spectroscopic Binary Orbits (SB9) (Pourbaix et al. 2004). *TESS* observed this target in sector 17 from 2019 October 8 to 2019 November 2 (25 days) at 2 minute cadence; the *TESS* SPOC (Science Processing Operations Center) pipeline does not report transit events.

5.6.3 HIP 34222

At $V = 10.23$, this K7V star is one of the fainter K dwarfs in the sample, which is reflected in the relatively large error bars on individual points. We obtained 19 spectra spread over two years between 2017 December 15 and 2019 December 18. The dataset indicates a possible companion with minimum mass 0.83 $M_{\rm Jup}$ in an orbit with $e = 0.301$, which is the most eccentric of the nine systems discussed here. With a derived orbital period of 160 days, the relatively high eccentricity is not precluded by tidal circularization, which happens only for systems with orbital periods less than a few weeks (Halbwachs et al. 2005); nonetheless, we consider this to be the least precise orbit presented here. The WDS reports WDS J07057+2728B as a visual companion 4.6 magnitudes fainter at 13.5″, but no parallax nor reliable proper motion is available to confirm it is bound to HIP 34222. Although WDS lists five stars as nearby, none are physical companions. No spectroscopic companion is listed in SB9 catalog.

5.6.4 HIP 86221

This star ($V = 9.20$, K5V) is among the most northern in our equatorial sample, with DEC $\sim +28$ deg. We find a classic hot Jupiter candidate in a 2.2 day orbit with minimum mass 0.71 $M_{\rm Jup}$. Although we have only 9 observations to date for this star, the semi-amplitude of the orbital fit, 130 $\mathrm{m\,s^{-1}}$, is more than 10 times CHIRON's typical MAD value for K dwarfs of this brightness, so we consider the detection secure. The HIP 86221 system is known to be a stellar triple. The AB components are separated by a few tenths of an arcsecond, with B

fainter than A by 0.59 mag in the optical. A visual binary orbit has been determined for AB using astrometry and speckle interferometry, yielding a period of 23.991 years, semi-major axis of 0.″2884, and eccentricity 0.2053 (Söderhjelm 1999; Mason et al. 1999; Malkov et al. 2012). No spectroscopic companion is listed in the SB9 catalog. Thus, the companion we detect is not the stellar secondary, and presumably orbits the primary given that the flux in the spectra is heavily weighted to the brighter primary component. The third star in the system is NLTT 45161 at a distance of 9.4″ and is 2.26 magnitudes fainter in the V band than the combined AB pair (Mason et al. 2001; Gould & Chanamé 2004). Given the proximity we do not reject that the contamination from the nearby stellar companions into a blended CCF, could result in the understimation of the primary star RV semi-amplitude, as stated in §4.6.3, so more data and further analysis is on-going. Among FGK dwarf systems, 12% are triple star systems (Raghavan et al. 2010; Tokovinin 2014), and as of May 2021 the NASA Exoplanet Archive reports 3260 stellar systems hosting at least one confirmed exoplanet of which 41 are triple star systems, so if deeper analysis confirms the exoplanet nature of the detection, it will be rare among the known exoplanet population.

Table 5.1: Orbital solutions for new exoplanet candidates in Paredes et al. (2021)

Star	M_*	Period	$m \sin i$	e	ω	K	a	T_p	RMS	No.	Ref.
	$M_\odot$	days	$M_{\rm Jup}$		deg	$\mathrm{m\,s^{-1}}$	AU	JD - 2450000	$\mathrm{m\,s^{-1}}$	Obs.	
TESS Exoplanet System											
HIP 65	0.74	0.981 (fix)	2.95	0.009	291.42	$734.6^{+4.6}_{-4.5}$	0.017	8368.833	20.4	58	Paredes et al. (2021)
	0.78	0.981	3.21	0 (fix)	...	753.7	0.017	...	...	34	Nielsen et al. (2020)
New Candidate Exoplanet Systems											
HIP 5763	0.72	$30.014^{+0.1528}_{-0.2842}$	0.51	0.054	271.08	$41.1^{+8.8}_{-11.2}$	0.170	8056.731	16.2	19	Paredes et al. (2021)
HIP 34222	0.62	$159.986^{+2.6753}_{-2.9256}$	0.83	0.305	31.80	$44.7^{+9.1}_{-8.3}$	0.492	8023.220	12.7	19	Paredes et al. (2021)
HIP 86221	0.79	$2.224^{+0.0004}_{-0.0005}$	0.71	0.086	208.93	$129.6^{+34.5}_{-19.6}$	0.031	7947.283	12.8	9	Paredes et al. (2021)

Table 5.1 summarizes the orbital elements for the four systems discussed here. The values

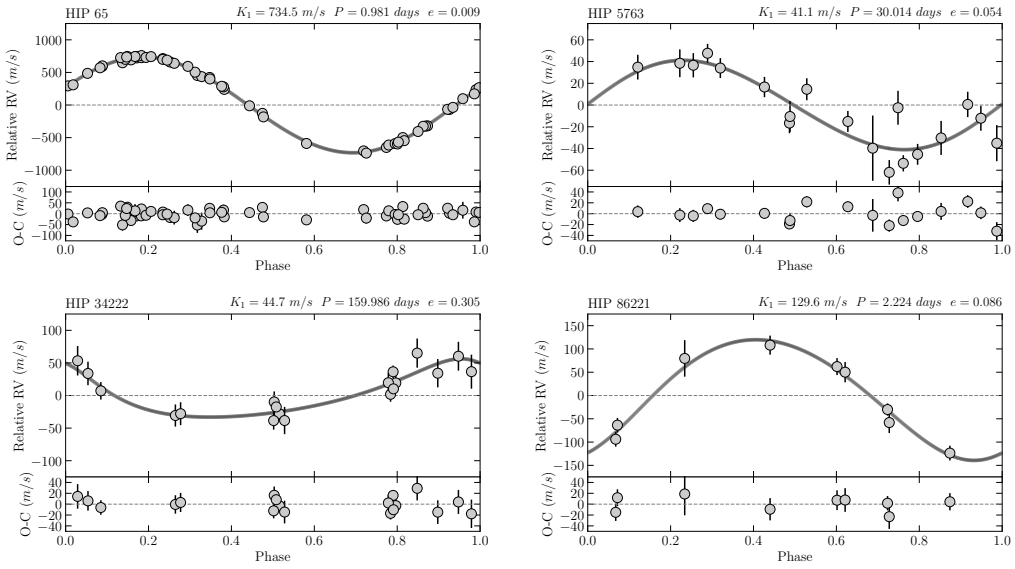

Figure 5.7 Phase-folded RV curves and residuals derived from CHIRON spectra for four K dwarfs discovered to have exoplanet candidates in orbit. Phase zero indicates the time of periastron passage (T_p).

listed include the first orbits from the discovery references, and our orbit. We have not added any points from other efforts to ours from CHIRON to enable direct comparisons between results. For the five stars used to check the veracity of our observing and reduction efforts with CHIRON discussed in Chapter 4, we find that our orbits are in good agreement with those found in the discovery papers. We note that we have been able to reach similar orbital solutions with less data compared to the discovery papers, primarily because of CHIRON's RV precision for this type of star.

5.7 K Dwarf Multiplicity

"If you don't know the multiplicity of your star you will have on average 1.5 times uncertainty on Radii of your newly found transiting planet" - David Ciardi (Ciardi et al. 2015), "Know

Thy Star, Know Thy Planet" Conference, Pasadena, 2017. One of the primary goals of the overall K dwarf survey is to determine the multiplicity fraction for this population of stars. At this date a complete assessment at all separations will require the addition of results of speckle and wide-field surveys, both of which have not been published yet. This RV study is considering the 25 pc and 33 pc samples because they are well-defined and effectively volume-complete. The following discussion includes results from all RV sources described in Chapters 3 and 4, from HARPS (Trifonov et al. 2020), HIRES (Butler et al. 2017; Tal-Or et al. 2019), and the CHIRON survey (Paredes et al. (2020, 2021) and this work), as well orbits reported in SB9. It does not consider companions found in the speckle or wide-field surveys. Another caveat is that in K dwarfs considered single, stellar companions might still be missing, therefore the multiplicity fractions presented are minimum values, until addressing the biases and completeness in a more rigorous statistical analysis.

5.8 Multiplicity of 25 Parsec Sample

Recall from Chapter 3 that 253 (91%) of the 278 K dwarfs in the equatorial 25 pc sample have been searched for companions using the RV technique. Of these, 62 have stellar-type companions, 208 are single, and 8 are not covered enough for definitive assessment. The stellar multiplicity fraction is 22%. Given the reasonably large sample, in Figure 5.8 the sample is split into five histogram bins determined using K dwarf $B_G - R_G$ colors. Blue portions indicate companions, orange portions are for flatline, single stars, and the few gray regions represent the 25 (9%) of stars with incomplete RV coverage by this survey o any other

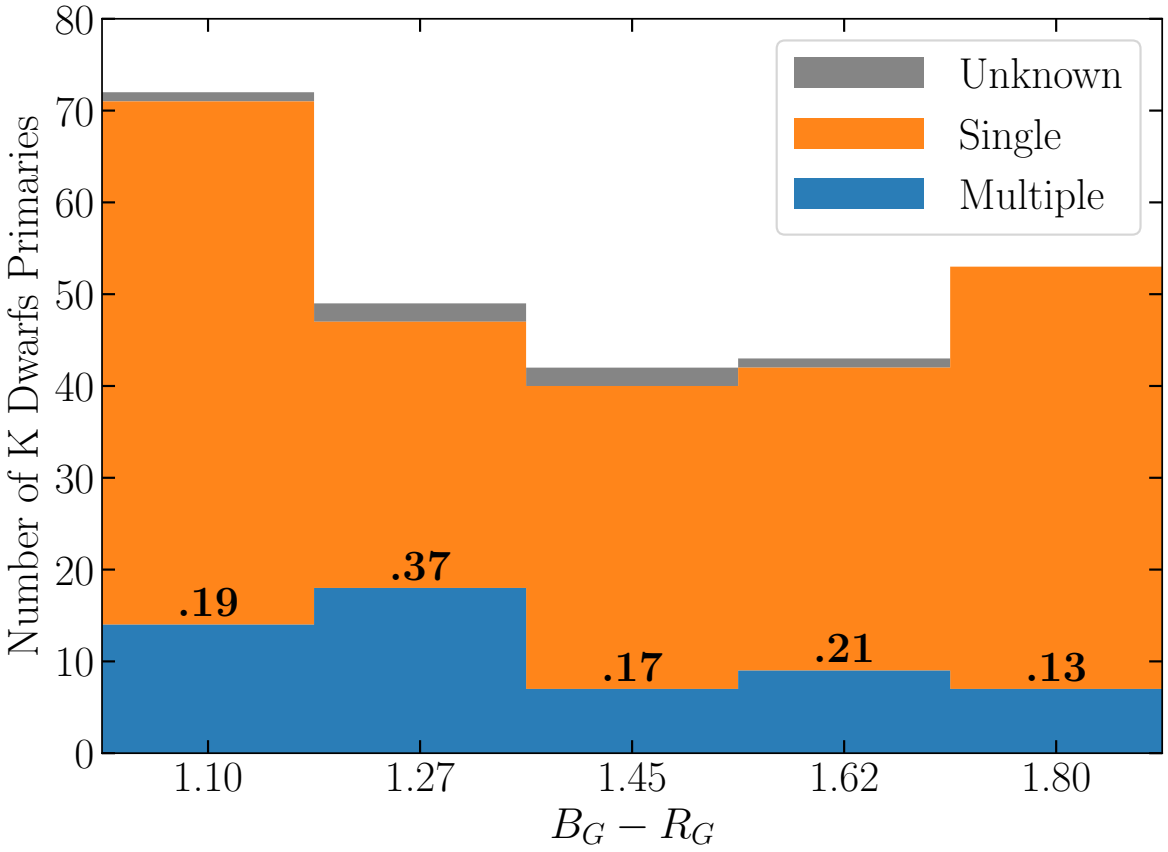

Figure 5.8 Multiplicity of K dwarfs within 25 pc for companions discovered using RV techniques.

considered here at this time. While it is not possible to make a definitive call on any trend in the multipliclity rate given only 50–70 stars per bin, there is a hint that redder, i.e., lower mass, K dwarfs have somewhat fewer companions than their more massive counterparts. What is needed is a larger sample to make a better evaluation? Fortunately, the 33 pc sample offers that opportunity.

5.9 Multiplicity of 33 Parsec Sample

Figure 5.9 shows the sample expanded to 33 pc, in which 529 (78%) of the 678 K dwarfs have RV coverage by HARPS, HIRES, or CHIRON, or have companions with orbits given in SB9. There are now 100–140 stars per bin and a multiplicity trend is evident — within a few AU of the stars where the RV surveys have sampled, bluer, higher mass K dwarfs have somewhat more companions than redder, lower mass K dwarfs. This is consistent with the fact that solar-type stars have companions roughly twice as often as M dwarfs, as outlined in Chapter 1. Even within the narrow mass range of K dwarfs, there is evidence for a slow decline in companion rates. For the 33 pc sample, 150 are found with at least an stellar companion found by the RV sources described here, 474 are found to be single, 54 do not have enough RV coverage. The stellar multiplicity fraction for the 33 pc sample is 22%, number that remain consisted with the results found in the 25 pc sample.

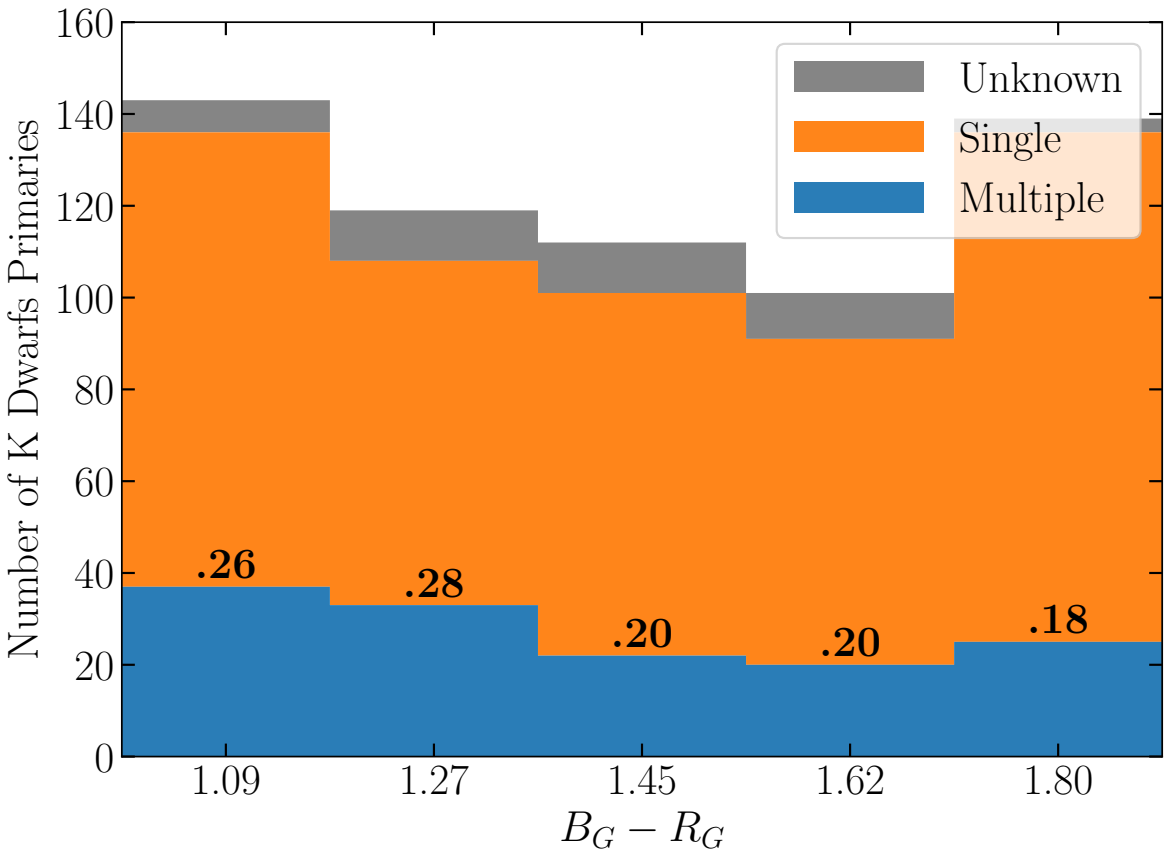

Figure 5.9 Multiplicity of K dwarfs within 33 pc for companions discovered using RV techniques.

CHAPTER 6

Overall Results, and Opening New Horizons For Research

6.1 Key Science Results

Here I summarize some of the results presented in this thesis.

- The work in this thesis has establish the foundations of the volume-complete sample of ∼5000 K dwarfs stars within 50 pc.

- 804 equatorial K dwarfs systems within 33 pc are surveyed here in detail. The curation and careful vetting, result in samples of 678 K dwarf primaries within 33 pc and 278 K dwarf primaries within 25 pc.

- The RV surveys presents the data gathered from ∼7500 high resolution spectra from CHIRON over ∼5 years, and in combination with RV data from HARPS, HIRES, and orbital solutions from SB9 catalog, reach a survey coverage of 97% in the 25 pc sample and 92% in the 33 pc sample.

- 42 newly discovered orbital solutions are presented, 38 are stellar/sub-stellar in nature, and 4 are solutions for exoplanet candidates.

- The stellar multiplicity fraction of K dwarfs is 22%, when considering companions searches using RV. The multiplicity fraction per color bin of K dwarfs exhibit an slight increase towards early spectral sub-types, which is consistent with the starting hypothesis that multiplicity increase with the mass of the primary, across all spectral types.

- The work involved in this thesis has successfully put back in science operations the CHIRON spectrograph for our entire astronomical community, and has proved its RV precision and stability for detecting exoplanets down to Jupiter-size and for executing long-term companion survey searches.

- This work has shown that between CHIRON and exoplanet transit space missions such as *TESS* there is an strong symbiosis, and is already producing meaningful scientific discoveries in the exoplanet field.

Finally, revisiting the observational HR diagram, the known and newly found companions to K dwarf systems within 33 pc are shown in (Figure 6.1).

6.2 1.5m CTIO/SMARTS Fellow

Now back from our journey to the solar neighborhood in the search for the hidden companions, join me one more time and allow me to share with you, dear reader, the journey of my professional development during my doctoral research years. Conducting the RV survey during my Ph.D. studies has give me the opportunity to accumulate valuable research experiences and have helped shape my present and future professional career in Astronomy. First and foremost are the ability to carry out the large-scale observational effort you have read about in the previous Chapters, and second, to be the primary contact scientist and operations support for a research-grade facility at Cerro-Tololo Inter American Observatory (CTIO), the 1.5m CTIO/SMARTS Telescope + CHIRON Spectrograph, used by dozens of other scientific groups. In the beginnings of the research endeavour presented here, my advi-

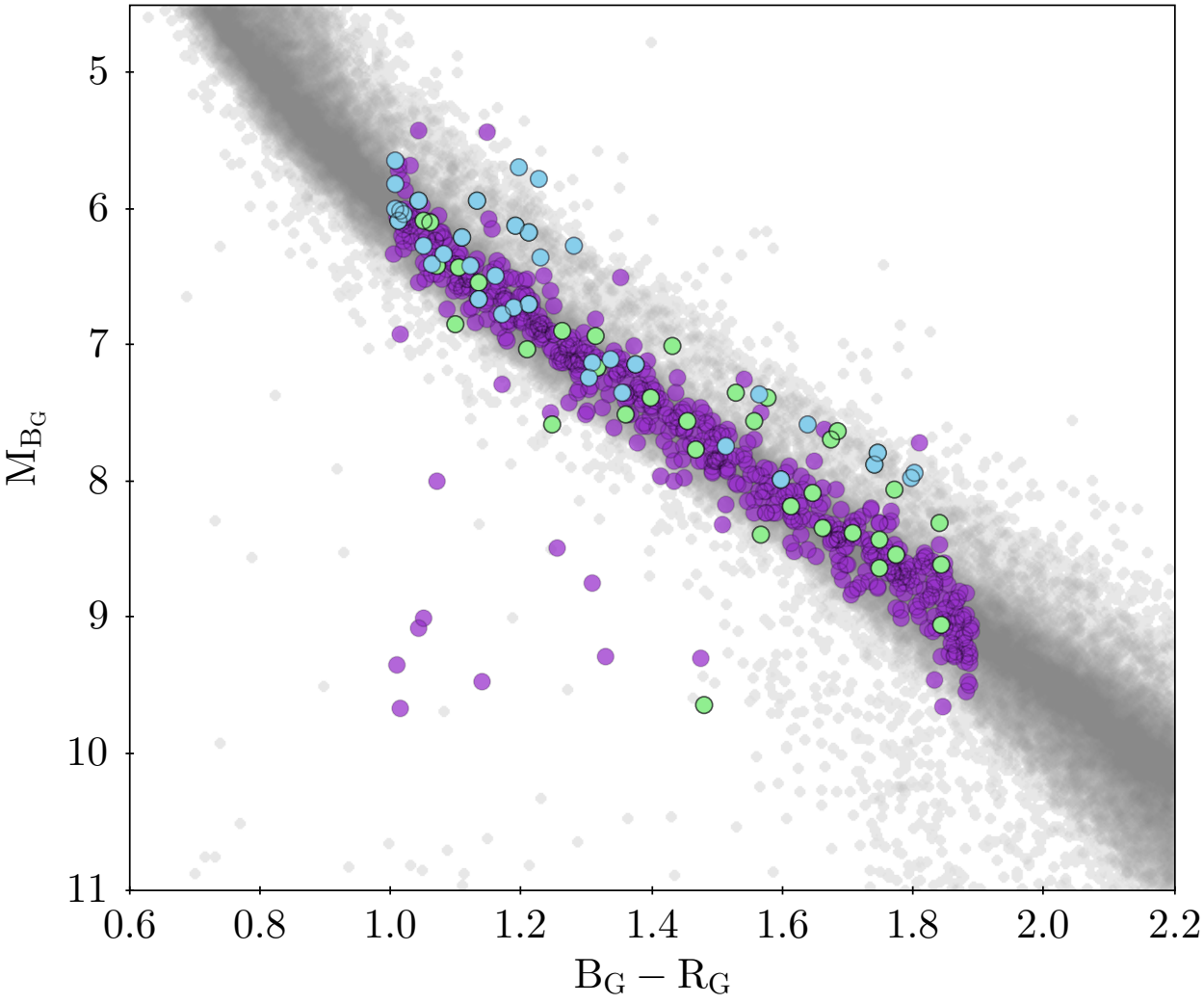

Figure 6.1 Observational HR diagram of the K dwarfs within 33 pc. In purple points, single systems. In blue points, systems with known companions from SB9. In green points, systems with newly discovered companions. A handful of stars of the survey are located below the main sequence, if photometry and astrometry from Gaia is not highly uncertain, these are potential K sub-dwarfs (sdB) stars or K plus white dwarfs pairs (K+WD).

sor, Todd J. Henry and I, could not have foreseen where this project would take us, but the goal was always clear. I decided to accept the challenge and I was appointed by Dr. Henry, director of the RECONS group, and the Department of Physics and Astronomy at Georgia State University to be the 1.5m CTIO/SMARTS Telescope Fellow.

Along side with developing my research, I was tasked with leading the reopening of the telescope, which at the time had been shutdown and cut funding indefinitely. The main objectives were resuming full-time operations with the CHIRON spectrograph, and prove its capabilities for short and long-term precise search for exoplanets and multiple star systems, for the astronomical community and for my research. To overcome the challenging process of recommissioning, I took several responsibilities and got involved in both the technical and scientific aspects of the 1.5m CTIO/SMARTS Telescope. These included: observing for several weeks straight on-site, during which I established scheduling and observing procedures; carrying out troubleshooting of telescope and instrument issues (remotely and in-site); developing documentation; and designing data analysis tools, all which are still being use to date. When queue observing operations began, telescope operator jobs were created, and I directed the training of two telescope operators, first in 2017 Dr. Rodrigo Hinojosa and in 2019 Mr. Roberto Aviles, and continued supporting their work throughout the years after. In the process, I coordinated efforts with all of the observatory teams in CTIO: telescope operations staff, electronic engineers, mechanical engineers, instrument/software developers, scientific staff. The collaboration has served the day-to-day observation operations, promptly solutions of technical problems affecting the science produced, and has served in the imple-

mentation of procedures that benefit the effectiveness and efficiency of science done with CHIRON for its users in our astronomical community. This team effort has resulted in a successful re-invigoration of the facility that now enables 20+ different observing projects to be established each semester in queue mode from different institutions and research groups in the SMARTS, NASA, NOIRLab, and Chilean astronomical communities.

The research presented in this thesis is the accumulation of incremental results obtained by the author over the years since the recommission of CHIRON, the findings have been published and promoted in different instances within the astronomical community, such as the Astronomical Journal, the annual American Astronomical Society meetings, in topical meetings in the stellar and exoplanet fields, and have supported research funding proposals for the National Science Foundation (NSF), NASA and Georgia State University. CHIRON spectrograph is nowadays part of a long term partnership with NASA Exoplanet division through the NN-Explore Program, as one of the ground-base facilities to follow-up exoplanet discoveries by TESS space mission, and to facilitate exoplanet science in line with NASA research goal. Even with the CHIRON spectrograph and 1.5m Telescope not being the newest or the most cutting-edge facility around, technologically speaking, it has become in one of the most subscribed instruments for RV work and exoplanets science, and has been praised by its users for its efficiency in the delivery of science products, promptly scientific support for its users, and the unparalleled flexibility offered for scheduling and management of observing time allocated, a rare feature but most needed in an era where new exoplanet candidates discoveries are announced every month. Personally, I will add that the praise is

fruit of the tremendous commitment and professional investment that each one, from the RECONS group leadership to all members of the teams supporting CHIRON, have shown to maintain this endeavour going.

After the successful recommissioning process, I oversaw and got involved in every step of journey of the photons, since the preparation for their acquisition until they become part of published scientific results. The following sections describes the steps and how they were accomplished.

6.2.1 Reconstructing the Scheduling Procedures for Queue Observing Programs

The CHIRON Spectrograph was constructed with an scheduling web interface hosted and managed by the Exoplanet research group at Yale University. The design is described by its lead developer in Brewer et al. (2014), where is highlighted the motivation and advantages of managing the nightly schedule and user target requests in this way. Unfortunately by the year 2015, the managing team was starting to move out to different endeavors and I personally witnessed, as telescope operator as CTIO at the time, that the necessary maintenance of the scheduling system became harder to execute. When the RECONS group took the lead to resume observations after one year CHIRON ceased operations, with myself now being part their ranks, we faced the challenge of understand and reconstruct a necessary scheduling system.

The motivation was to put back on track the broken system and reinstate communication between the parts involved in the operations, i.e., communications between nightly scheduling

target list, instrument and telescope control, the storage and transfer of data acquired nightly, and registry and log of observations reported back to an SQL database accessible by the users. Even more challenging implement a new configuration so the system could be hosted in a new server in GSU.

In my telescope operator days at the 1.5m Telescope at CTIO, I experienced first hand the efficiency of the scheduling system when fully functional. I was motivated and confident enough that the reconstruction was a worthy try, so I took the initiative to lead the effort in reconstructing the scheduling system in the way it was intended to work. My purpose was in the benefit of the users for easier management and monitoring of their observing programs, in the benefit of the telescope operators for easing their night tasks during the long working hours, and in our own benefit as daily target schedulers and program coordinators.

The task require me to taught myself enough web development (`HTML/PHP/Javascript`), database management (`SQL`), and network protocols to be able to host and communicate the involved systems remotely between GSU and CTIO servers, without any prior experience and under the constraints of the existing system designed to work in the Yale University servers. Unfortunately, the original scheduler and its coded parts did not included extensive documentation, and even less for rebuilding it in a different host server. Regardless, after almost 9 months of work in 2018 March, the scheduling system was put fully functional and hosted in our servers at the Dep. of Physics and Astronomy of GSU.

The first two years I was the only person scheduling targets to observe in a nightly basis, and despite all the benefits of the integrated system describe before, it was a daunting task

to accommodate every day each individual observing requests by the PIs, especially when their requests involved observing in specific ephemerides or unusual observing strategies, all that when the total targets requests of all programs of a given semester were increasing to be counted by the thousands.

With the objective of decrease the hours I spent daily puzzling together observing lists, I started to design functionalities in the web scheduler system with my newly gained experience at the reconstruction. The main upgrade that I implemented was motivated by the increasing number of targets where PIs requested careful timing for their observations. At the moment this was only requested in comments with no standardized format or by direct communication by email with the PIs, making very hard to keep track of. With this in mind, I build upon the existing target adding interface, and introduced standarized date fields, so users in their end can attach their time windows desired for their targets, without ambiguity and error proof. While in the scheduler end, I implemented filters by date requests and added highlighted labels in time sensitive target requests. As result, the pool with all the thousands decreased drastically to hundreds, making the daily scheduling tasks much easier to handle and to keep track of. In addition, the correction of few existing code bugs in the original programming of the scheduler, and the addition of some changes in the visual style, the daily time I spent scheduling was reduced from hours to 1 hour at most. At the same time, the PIs were also benefited with these constant upgrades, by now having less chances of missing their targets with important ephemerides, and in general by improving the ways for communicating they request successfully. In 2019, CHIRON went from operating every other week to every week

with two telescope operators in seven-day shifts. The daily scheduling duties increased and were now a collaborative task shared between more members of the RECONS group.

6.3 Reconstructing CHIRON Standard Data Reduction Procedures and Distribution

The data reduction routines implemented by the instrument designers worked more independently from the systems integrated with the scheduler, but they were still very tied up to the servers and configurations of Yale University. Besides the reconstruction of the scheduler, I lead the transferring of the standard data reduction pipeline to our servers in GSU. The pipeline in its current configuration have processed CHIRON data since its commissioning in 2011, so one of the main objectives was to ensure the consistency of data processing for the returning users. In 2018 March, I was able to successfully transfer and have fully working the `IDL` scripts that process the science data and calibrations from CHIRON. Although the data distribution system was not transferable, I developed a new one where PIs receive automatic emails to notify them when their data was processed and ready to be downloaded.

6.4 Observing Runs and Support for Telescope Operations and PIs

One of the main commitments during my involvement in this project was to always make sure that the telescope, operators and users were well supported. I personally directed the training of the two telescope operators currently working, sharing my experience and knowledge for their successful development as key members of our team. I committed my availability and disposition for technical support 24/7 in events of unexpected technical

failures, providing remote assistance (even once remotely connected during an international flight at 35,000 feet), and having an active participation in fixing the technical mishaps that interfered smooth observing.

Often PIs who had been awarded observing time will require assistance and scientific support, especially if they are new to CHIRON. I provided help in issues such as observing strategies, data troubleshooting, and general assistance. In occasions by sharing data analysis codes or just providing guidance for their specific needs with the CHIRON data.

I conducted several observing runs in-site over the years, especially before CHIRON started to run every week with two telescope operators, where I planned and executed observations in night working shifts from 10 up to 31 days straight at the observatory. I participated in crucial instrument repair events, helping in the diagnosis of the instrument problems, testing procedures, and in the execution of the fixing procedures, usually along side the operations staff at the mountain and the instrument support astronomer at CTIO Dr. Andrei Tokovinin. Some of these events include: telescope mechanical balancing, telescope mirror maintenance, instrument optical components maintenance, optical fiber alignments, calibration lamps system repair, among others. In all of them participating either in the diagnostic and/or the fixing, or at the very least in assistance.

My involvement in telescope operations was not limited to the 1.5m Telescope only. When needed, I also covered several observing runs at the 0.9m SMARTS Telescope, where other fellow members of the RECONS group get imaging data for their research. This became particularly crucial when the COVID-19 pandemic was preventing foreign travel

of astronomers from US to Chile, and observations needed for their projects could not be executed otherwise. I then willingly stayed longer in Chile and put myself at disposition for 14+ day observing runs every few months.

Although the enterprise as fellow had me as a protagonist while conducting the doctoral research I am presenting you here, I've been passing on my experience to newer members of our group, so that the 1.5m+CHIRON facility can remain available for astronomers henceforth.

6.5 Scientific Collaborations Through CHIRON

In the wake of a blooming era of exoplanet discoveries with transit missions as TESS, several scientific collaborations formed, many of them resulting in fruitful studies published in refereed journals. Since 2019 to date, collaborations and shared goals between scientific groups has materialized into my involvement in 14 refereed publications[1], one of which I am the first author.

Among the scientific opportunities brought by CHIRON recommissioning, are the rich spectra datasets available for new members of the RECONS group and for other astronomy research groups at GSU. The availability of CHIRON time is and datasets is, and has supported around 10 different Ph.D. research works in GSU in its 5-year run, and is currently opening new research venues and professional development opportunities for new RECONS group members, in addition to the existing opportunities with the 0.9m Telescope and its

[1]Paredes et al. (2021); Vanderspek et al. (2019); Wang et al. (2019); Jones et al. (2019); Dorval et al. (2020); Huang et al. (2020); Zhou et al. (2020); Mireles et al. (2020); Rodríguez Martínez et al. (2020); Davis et al. (2020); Silverstein et al. (2022); Nisak et al. (2022); Lester et al. (2022); Hubbard-James et al. (2022)

unique 25+ year long on-going astrometry research.

6.6 Development of Professional Skills

The journey above described allowed me the development of skills of all kinds, some of which I've never experienced before. Multi-disciplinary team work, scientific support and collaborations are among the most relevant, but programming skills were by far the most recurring. I was privileged of having access to work with the data presented here. The handling of ∼7500 science spectra, ∼24000 calibration frames, each conformed by 60 spectral orders, all taken in variety of quality conditions, and other few thousands of telemetry and header information associated to the 804 targets presented in this thesis work, required me almost always the implementation of some level of automatization, pipeline-type of processing, and in all cases a programming codes that could manage exceptions, errors or unforeseen effects on CHIRON data. The RV pipeline and the code development for the related data quality assessments procedures that I've presented you in this work, was always a necessary but many times an immensely challenging endeavour to pursue, because in this author's humble opinion, is best way for the effective use of resources invested in this research.

6.7 The Future

The future of the research presented here is continuing the systematic exploration of the solar neighborhood, not just because large number statistics, but also because these stellar systems are within human-kind reach, maybe not for the present times but for the future generations of interstellar explorers. Since the genesis of this research, the aim has been

to complete searches where coverage was missing in previous surveys, at the very least leaving a trusted repository of the exploration conducted for other to build upon. If this study contributes in a small way to the foundations of future discoveries in star formation, exoplanet detection, formation and habitability, this author and all those who supported this research will consider them self accomplished.

Appendices

A RV Timeseries and Orbital Solution Plots of the K dwarfs.

Page left intentionally blank.

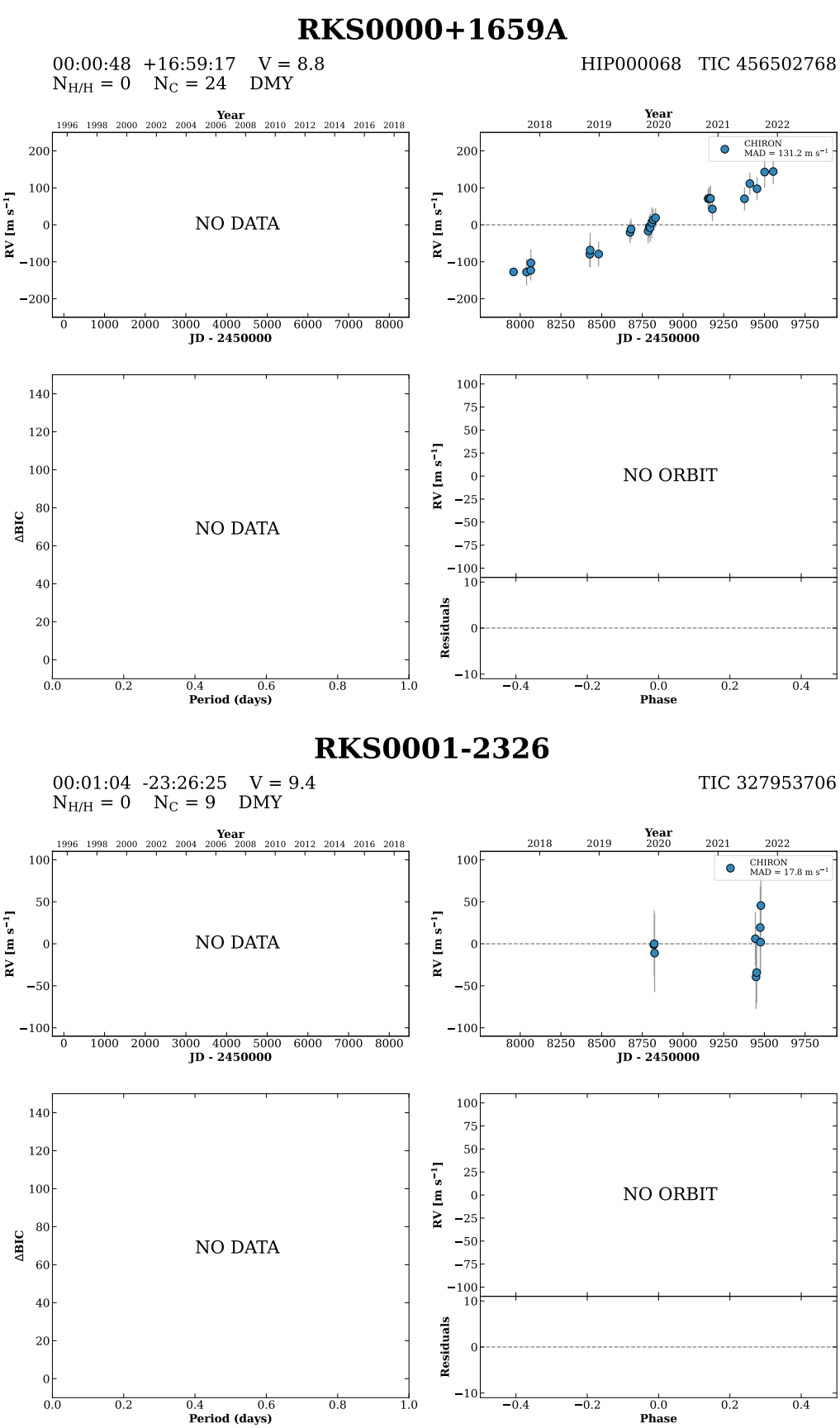

Figure 2 RV results for RKS0000+1659A (top) and RKS0001-2326 (bottom).

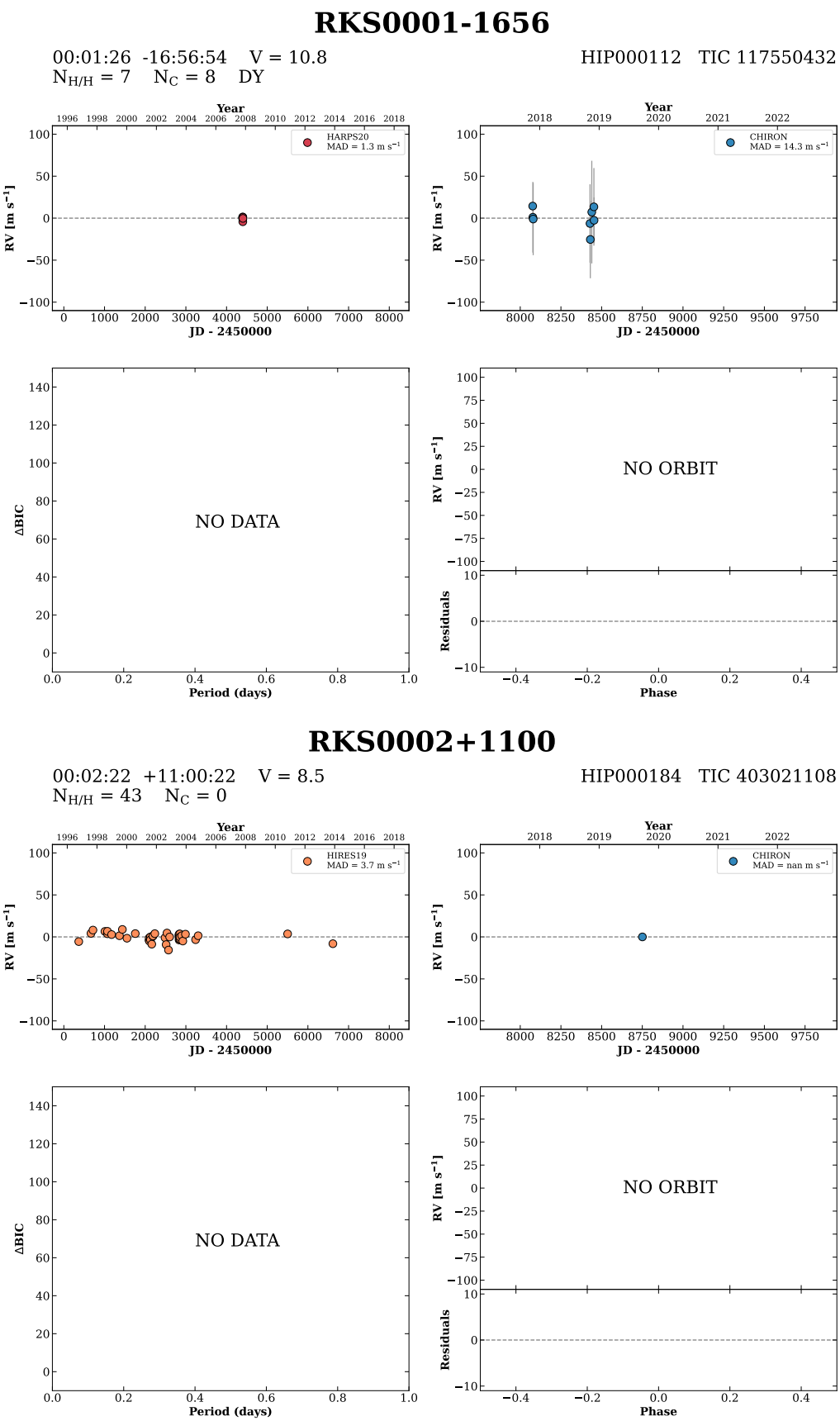

Figure 3 RV results for RKS0001-1656 (top) and RKS0002+1100 (bottom).

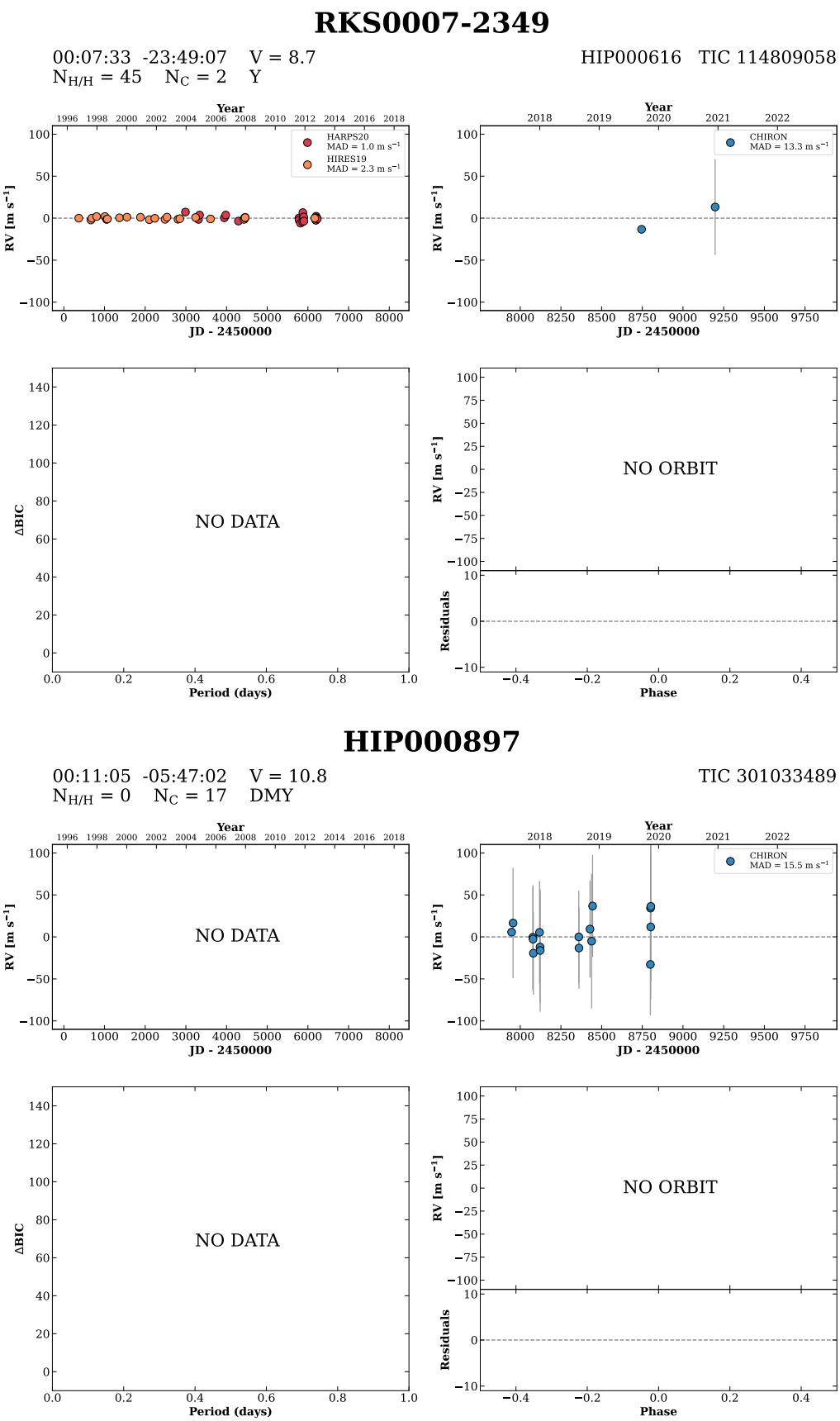

Figure 4 RV results for RKS0007-2349 (top) and HIP000897 (bottom).

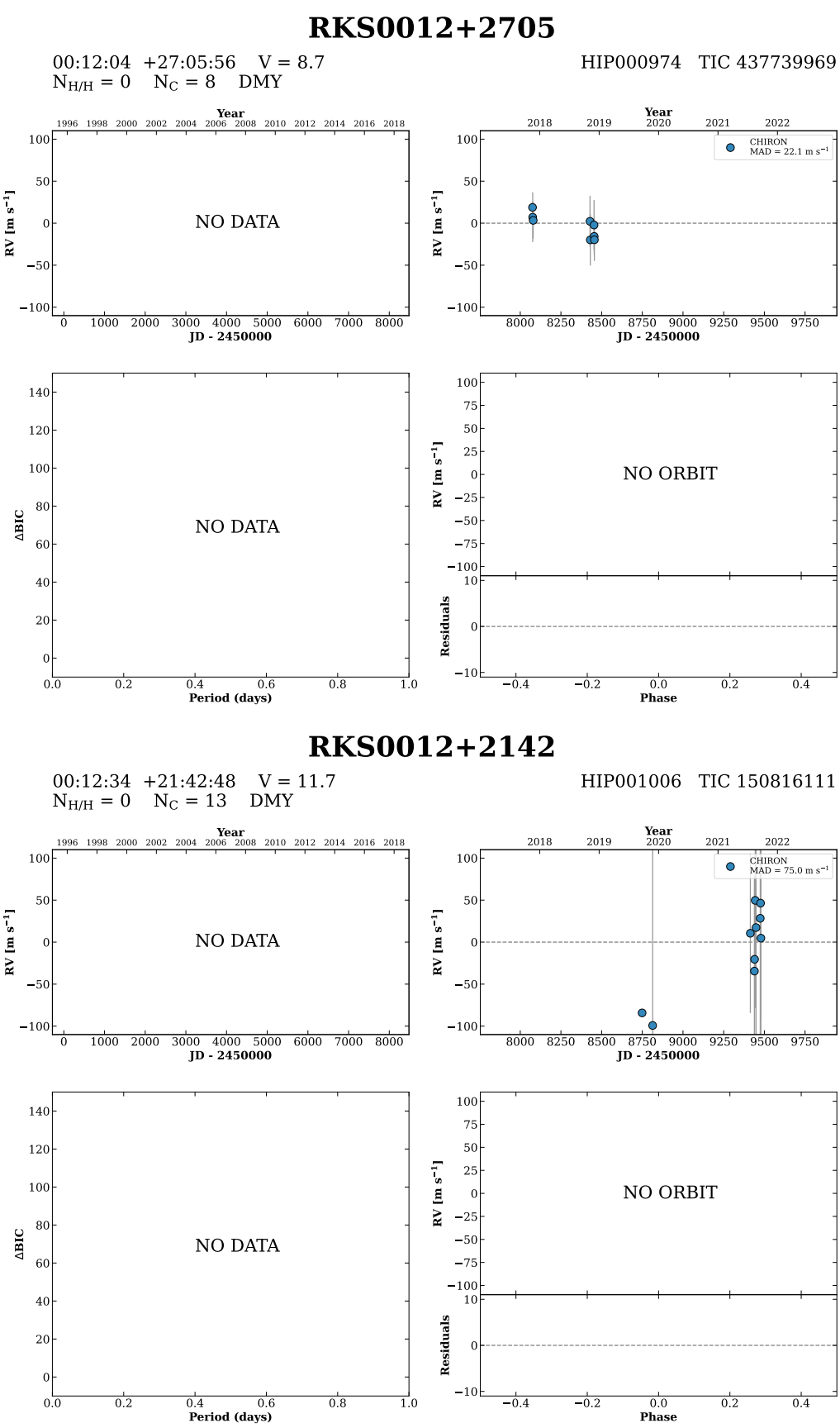

Figure 5 RV results for RKS0012+2705 (top) and RKS0012+2142 (bottom).

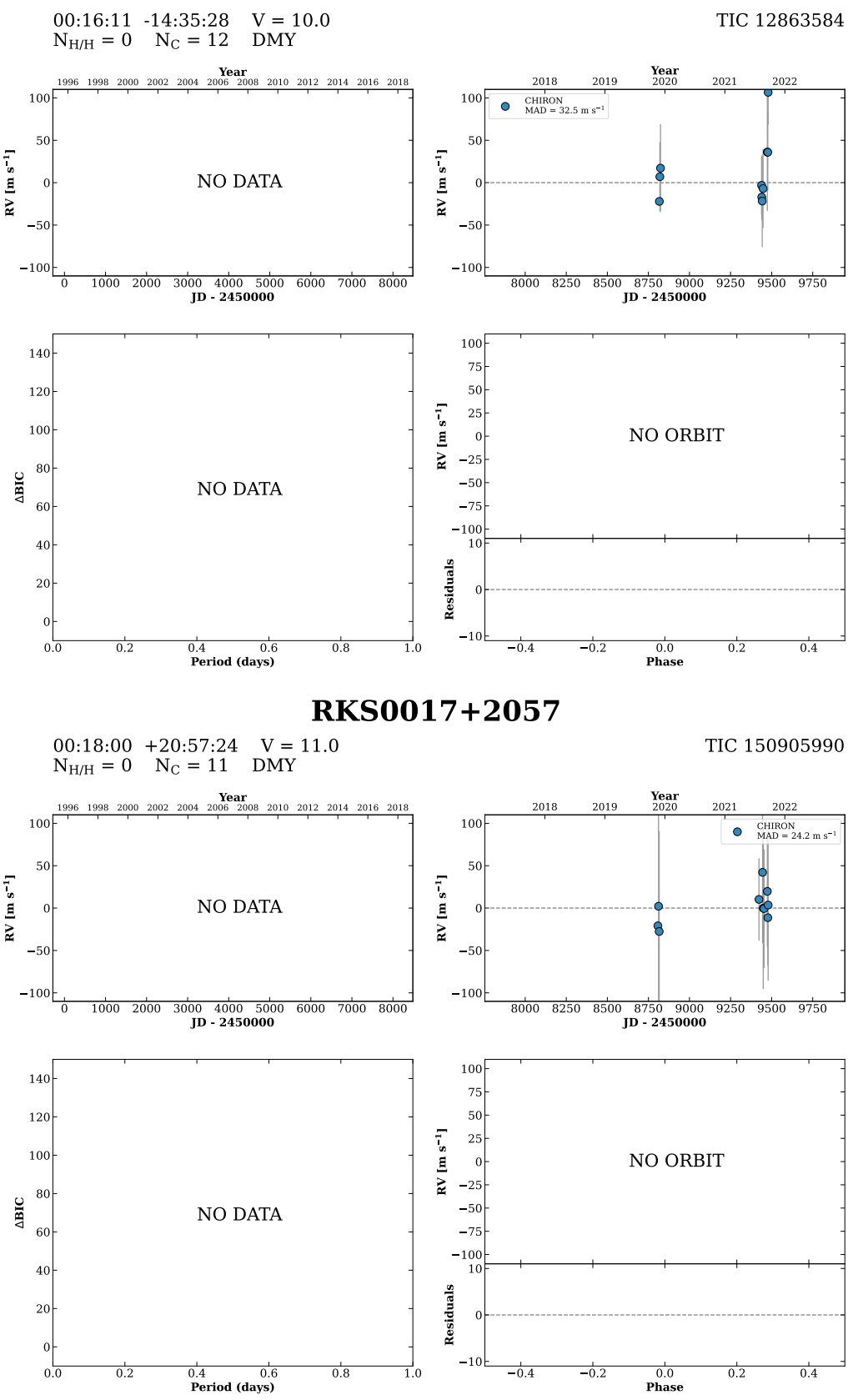

Figure 6 RV results for RKS0016-1435 (top) and RKS0017+2057 (bottom).

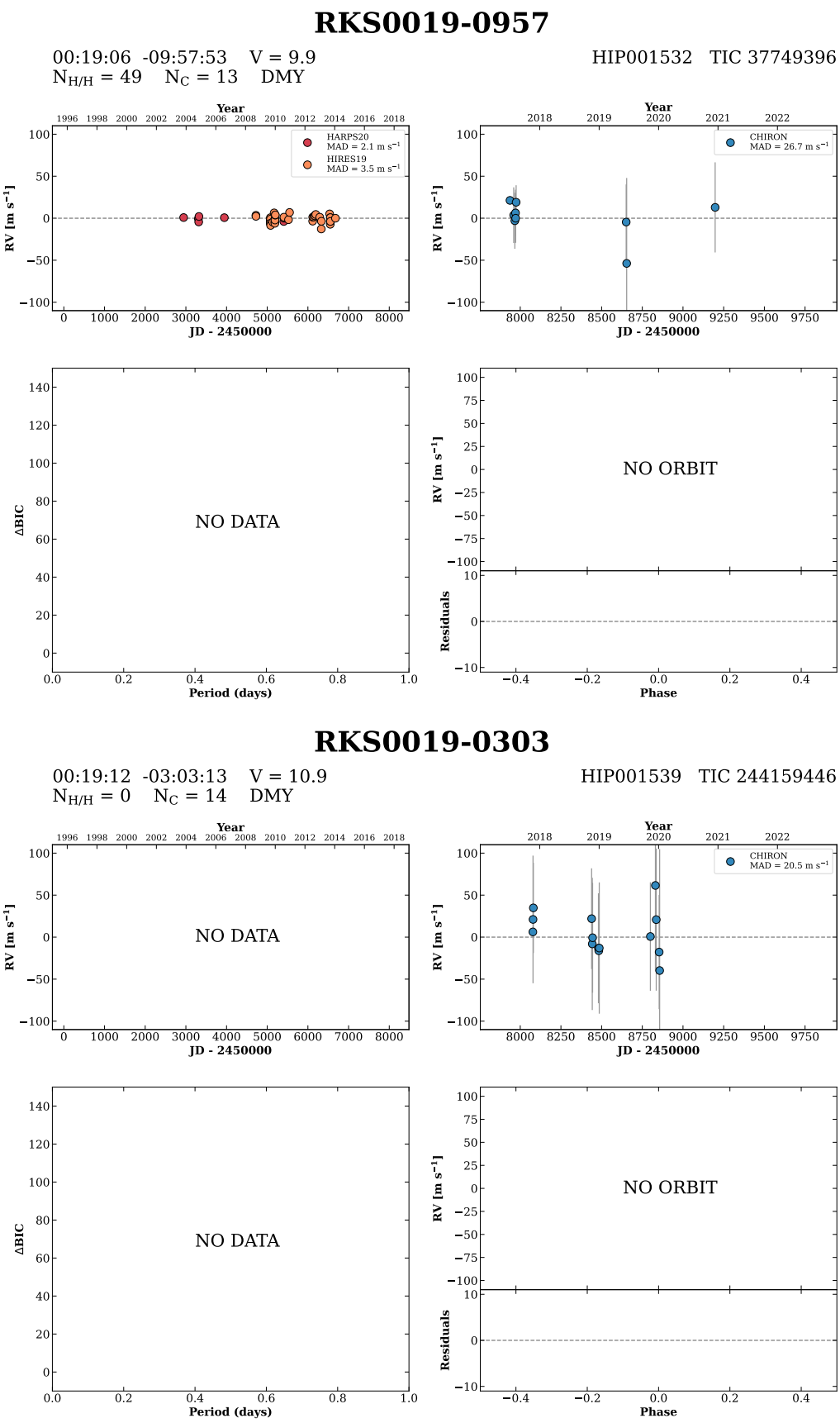

Figure 7 RV results for RKS0019-0957 (top) and RKS0019-0303 (bottom).

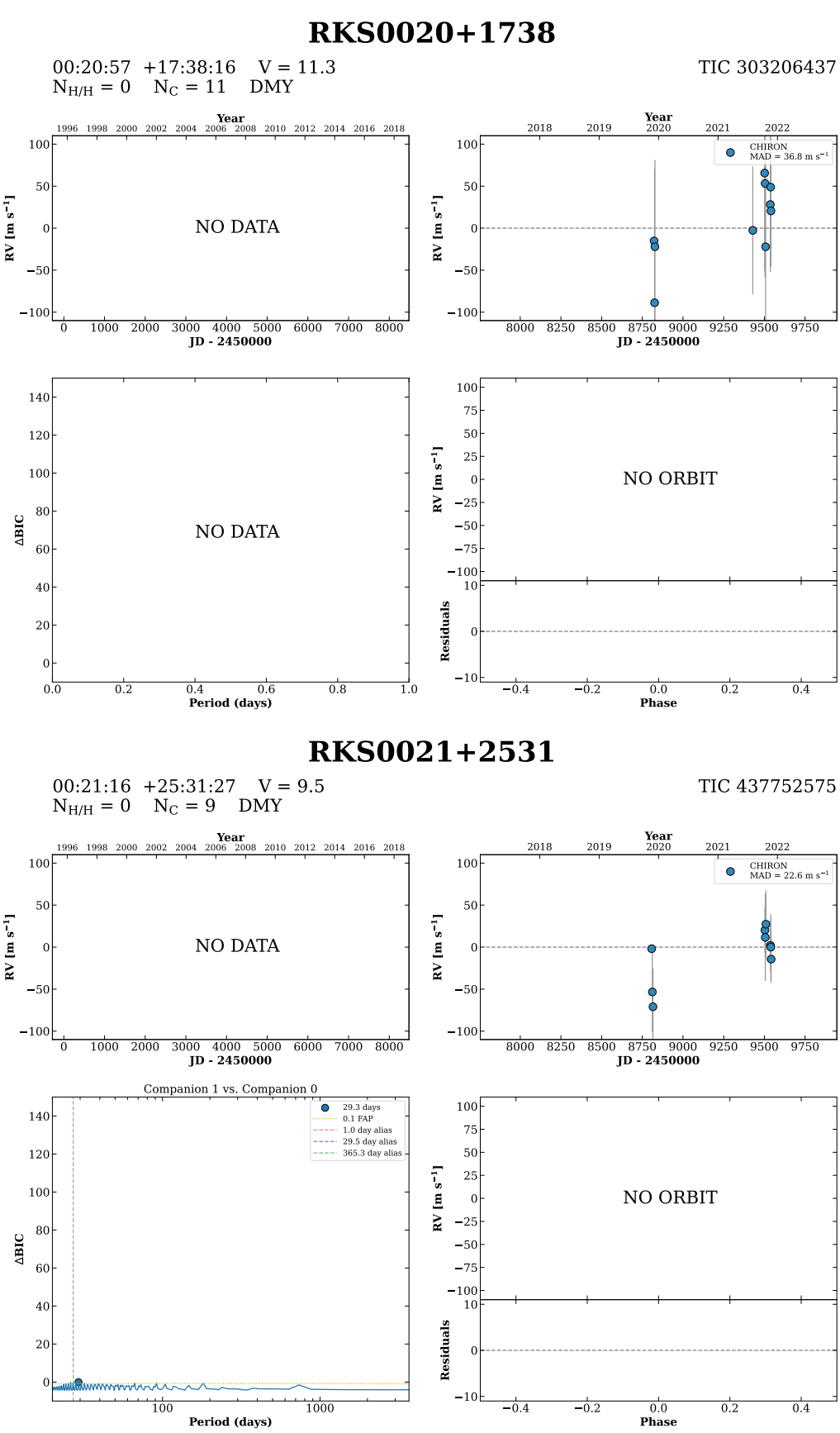

Figure 8 RV results for RKS0020+1738 (top) and RKS0021+2531 (bottom).

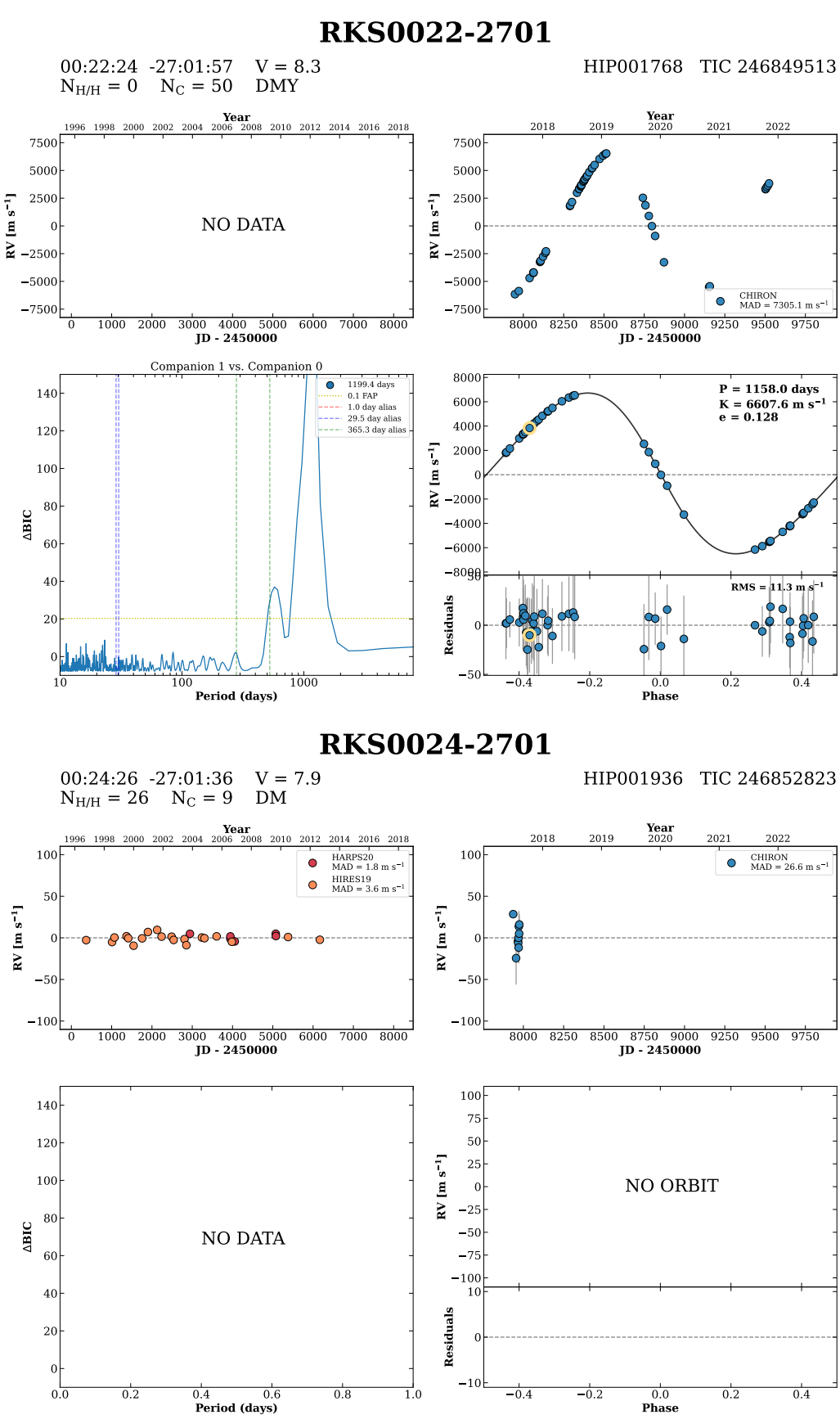

Figure 9 RV results for RKS0022-2701 (top) and RKS0024-2701 (bottom).

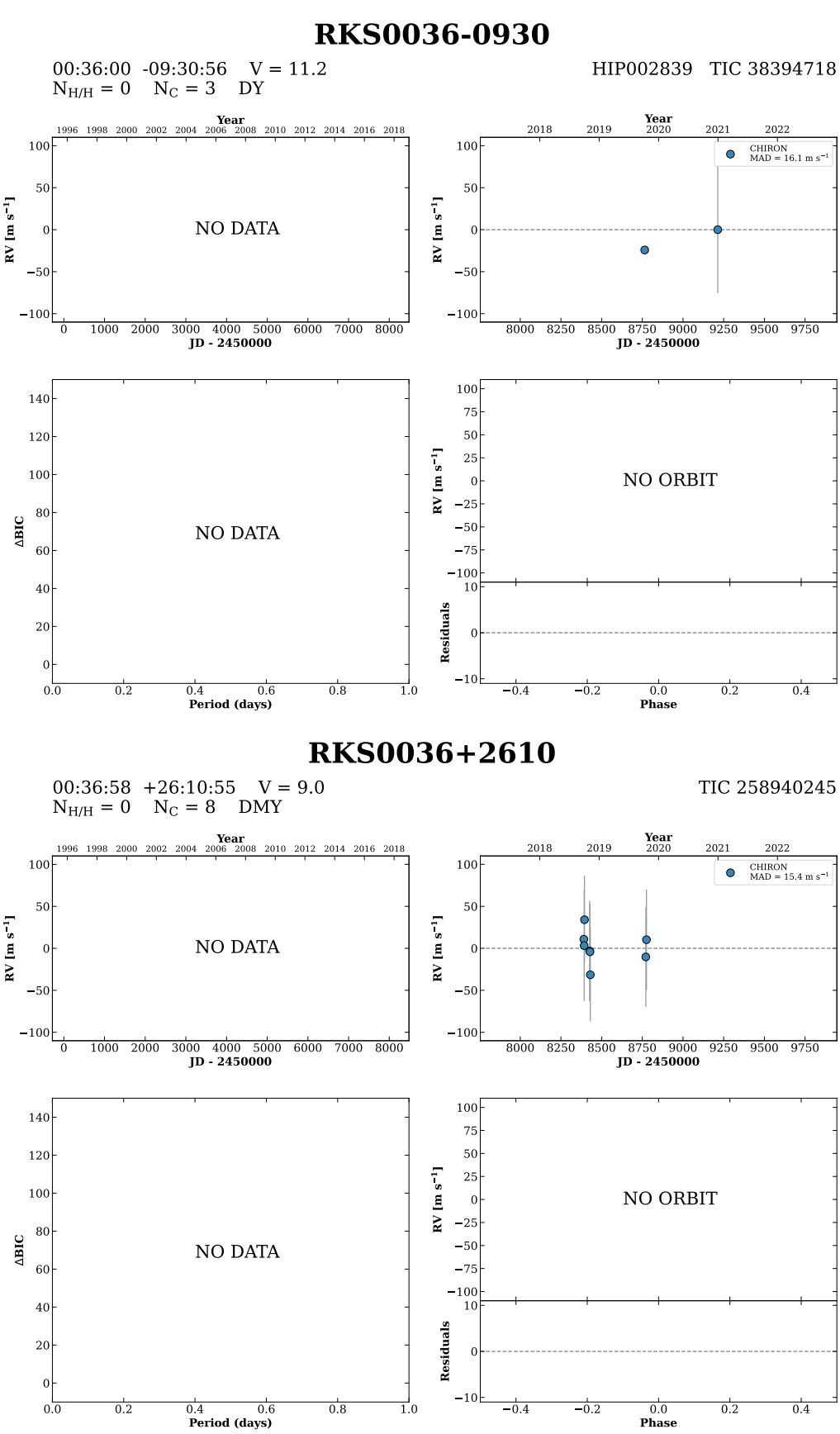

Figure 10 RV results for RKS0036-0930 (top) and RKS0036+2610 (bottom).

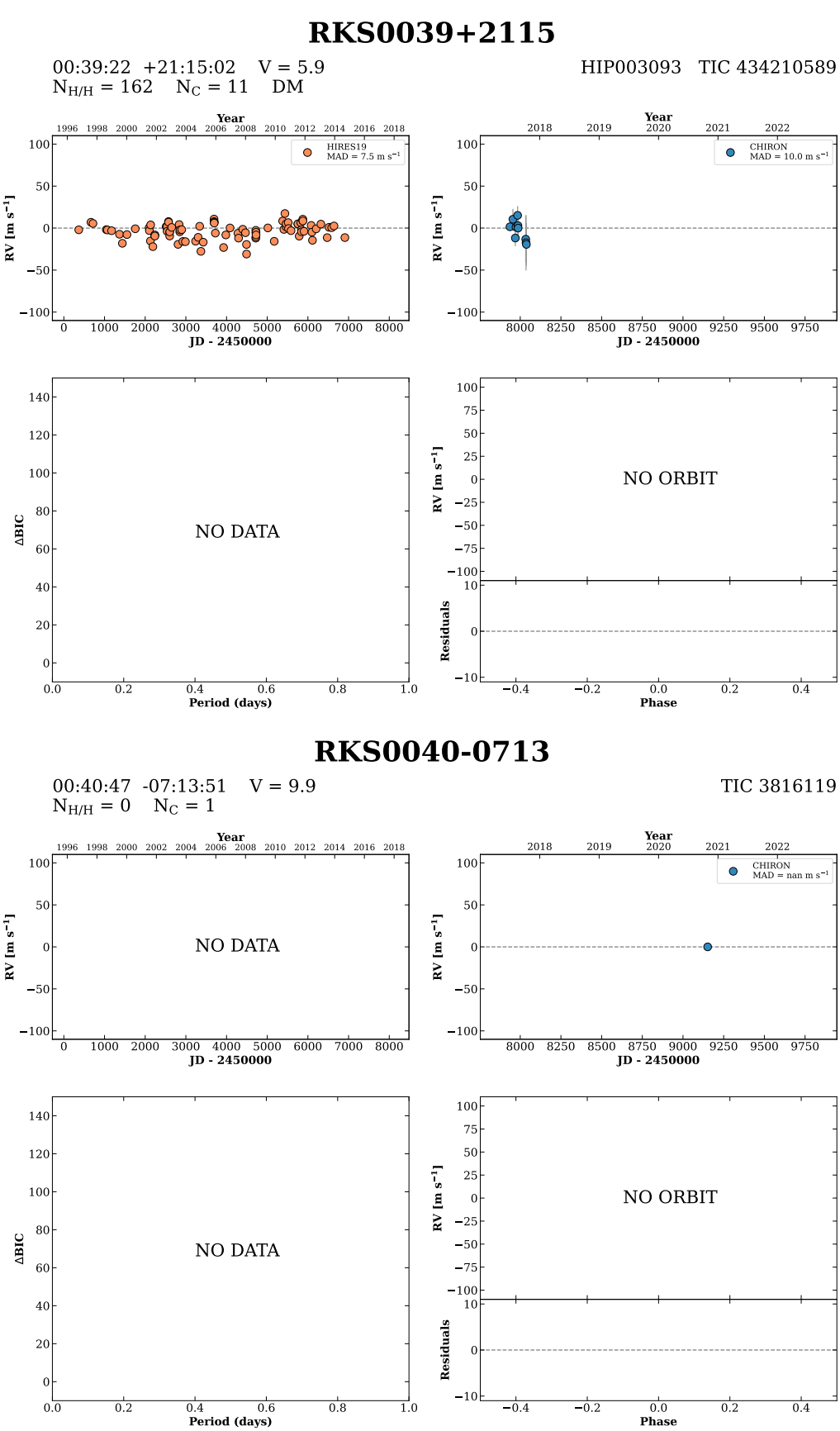

Figure 11 RV results for RKS0039+2115 (top) and RKS0040-0713 (bottom).

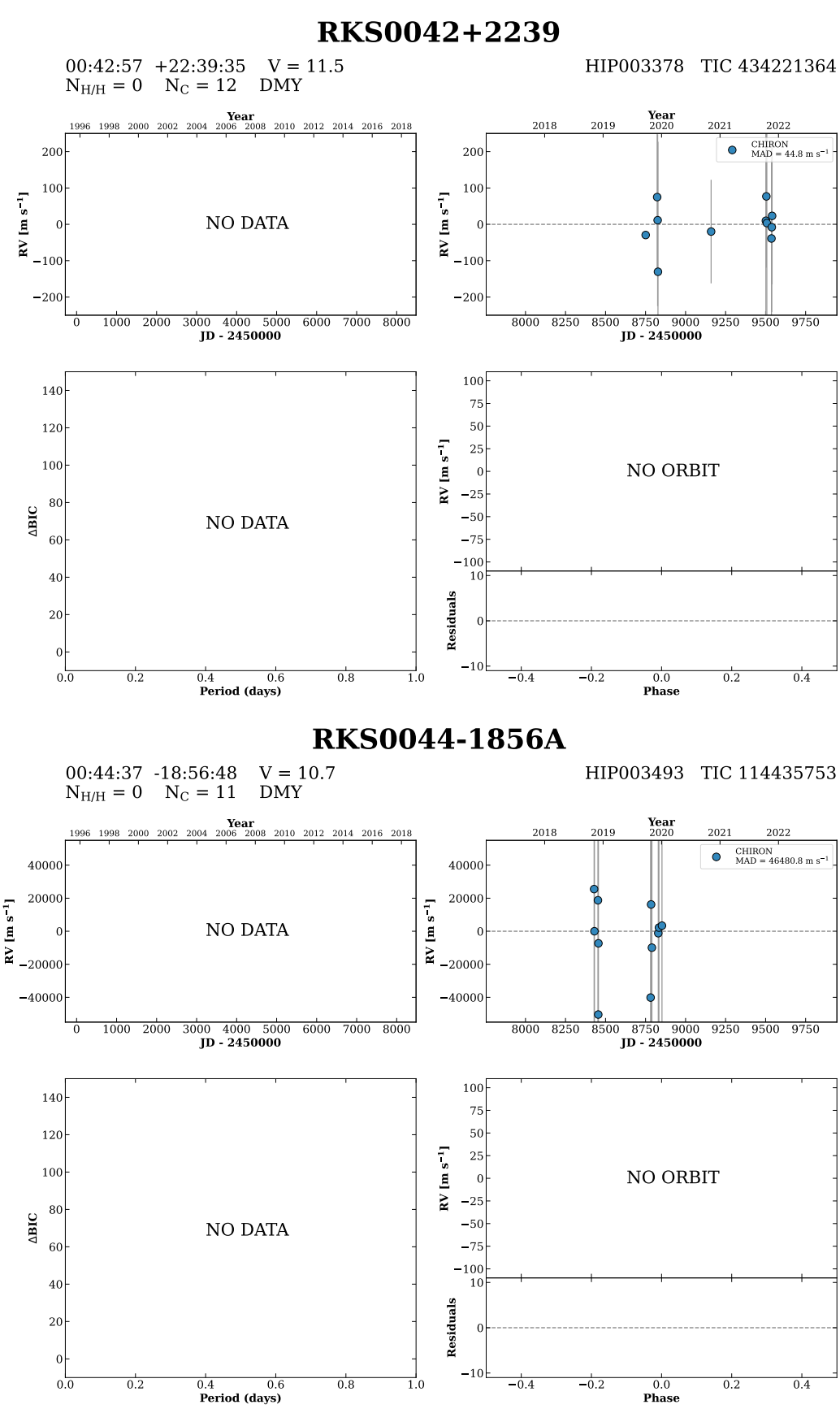

Figure 12 RV results for RKS0042+2239 (top) and RKS0044-1856A (bottom).

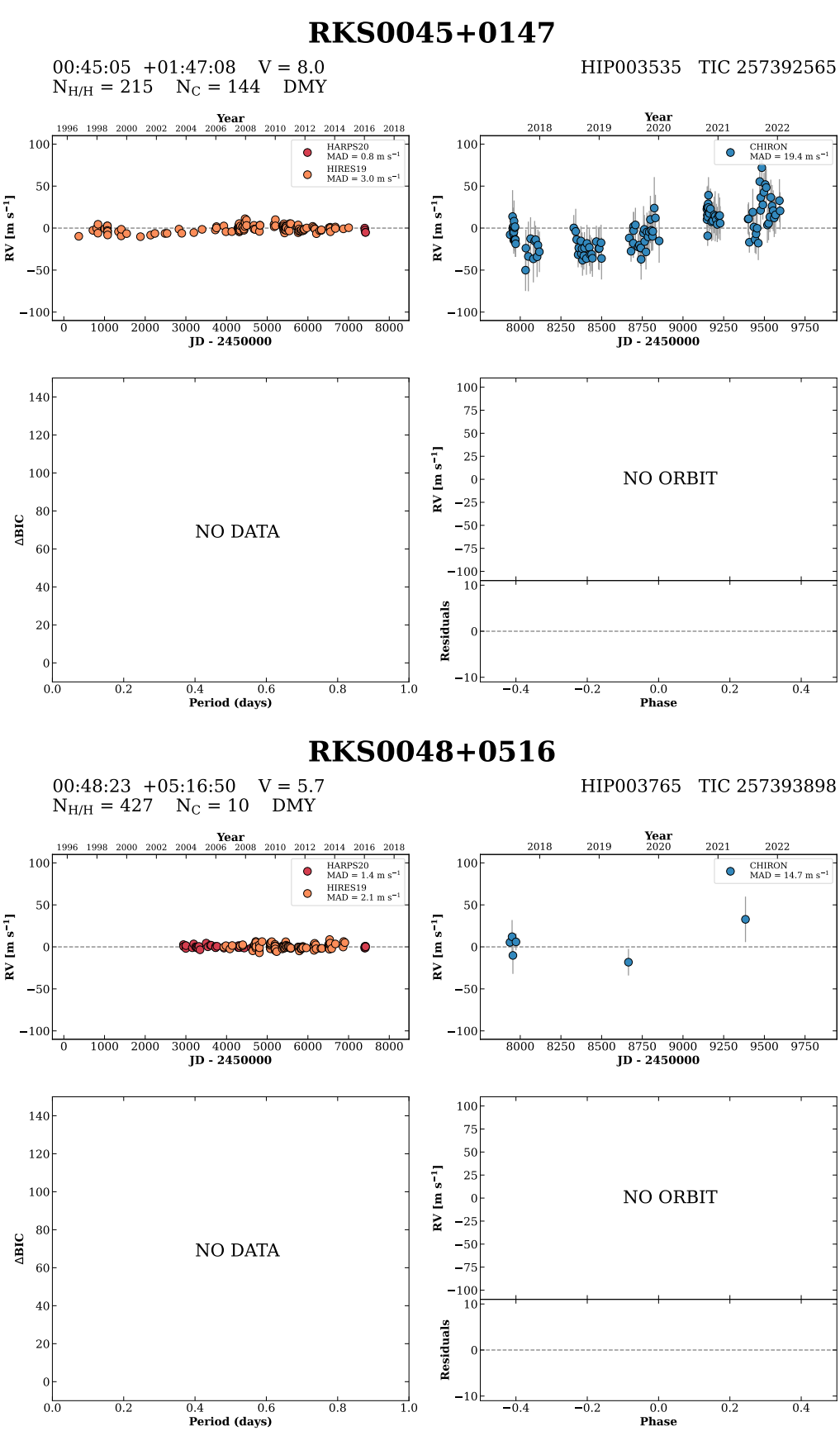

Figure 13 RV results for RKS0045+0147 (top) and RKS0048+0516 (bottom).

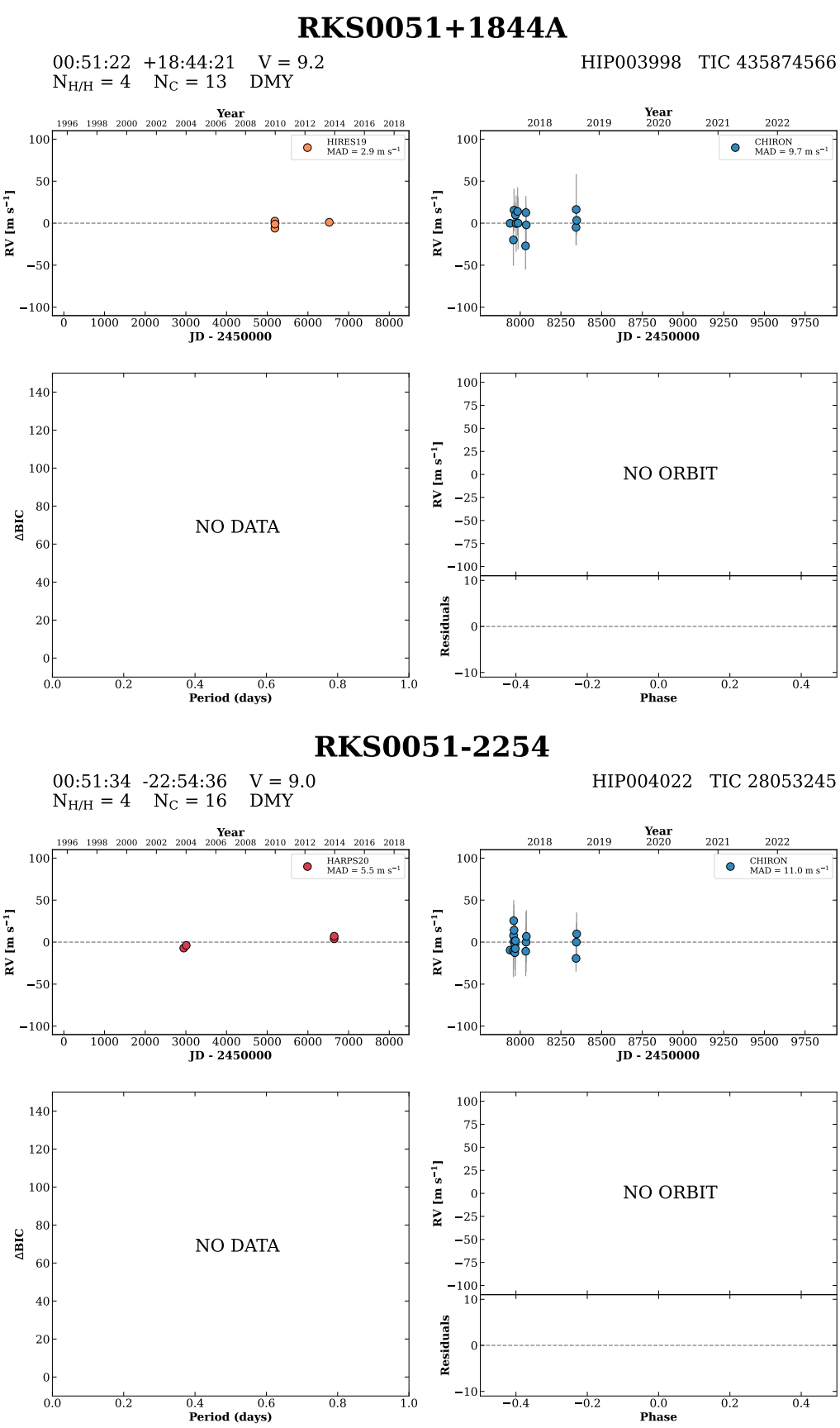

Figure 14 RV results for RKS0051+1844A (top) and RKS0051-2254 (bottom).

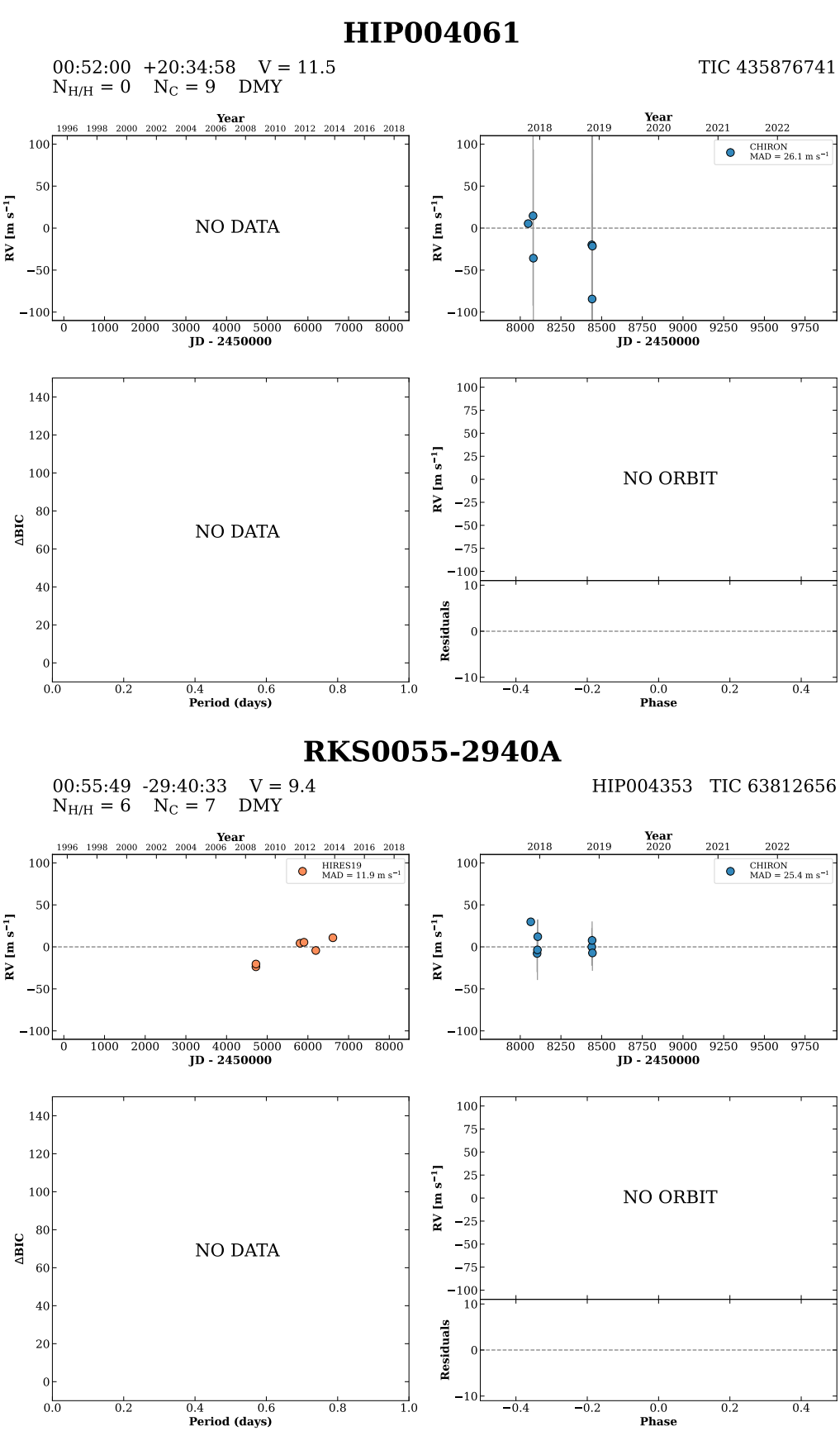

Figure 15 RV results for HIP004061 (top) and RKS0055-2940A (bottom).

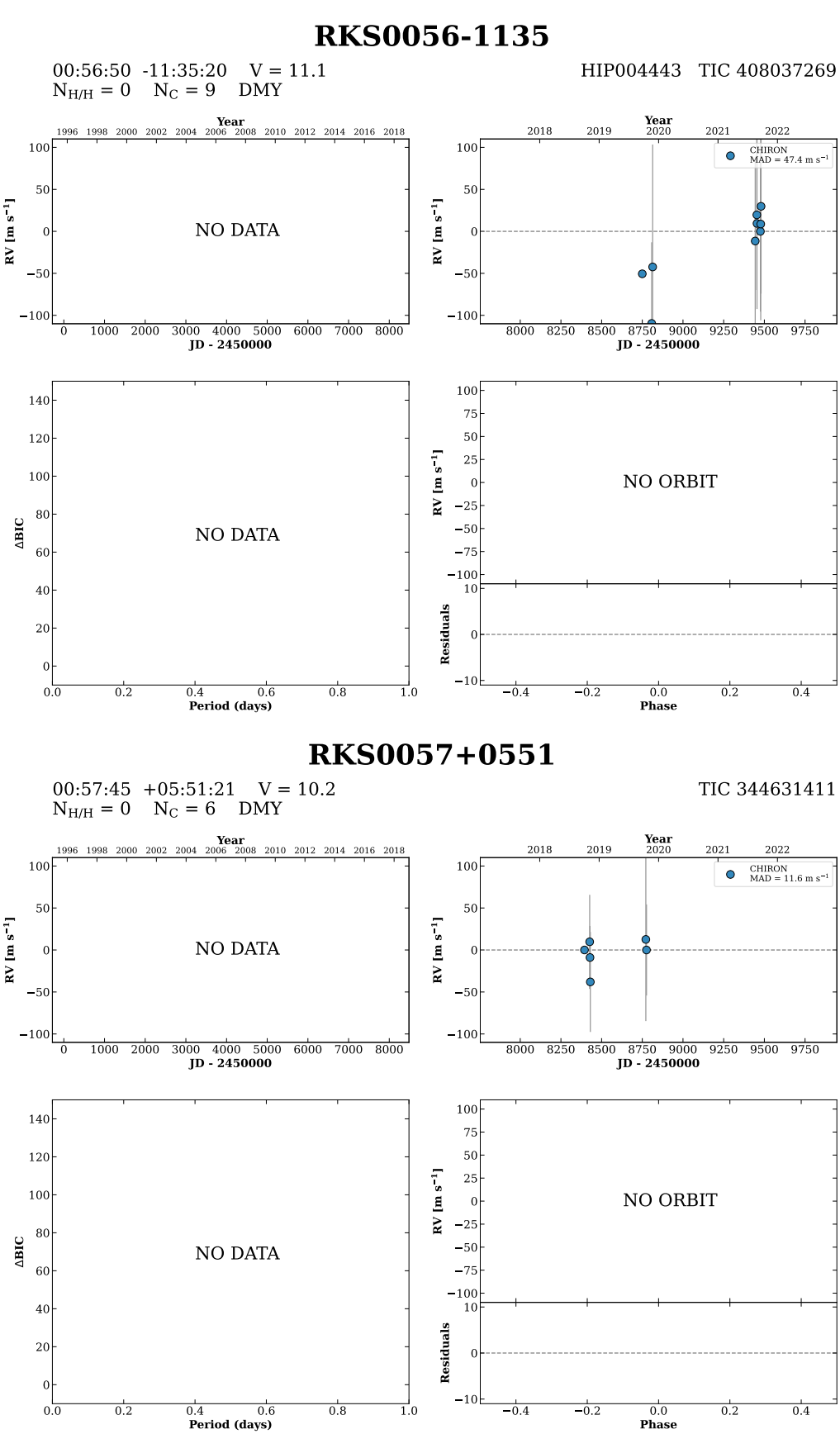

Figure 16 RV results for RKS0056-1135 (top) and RKS0057+0551 (bottom).

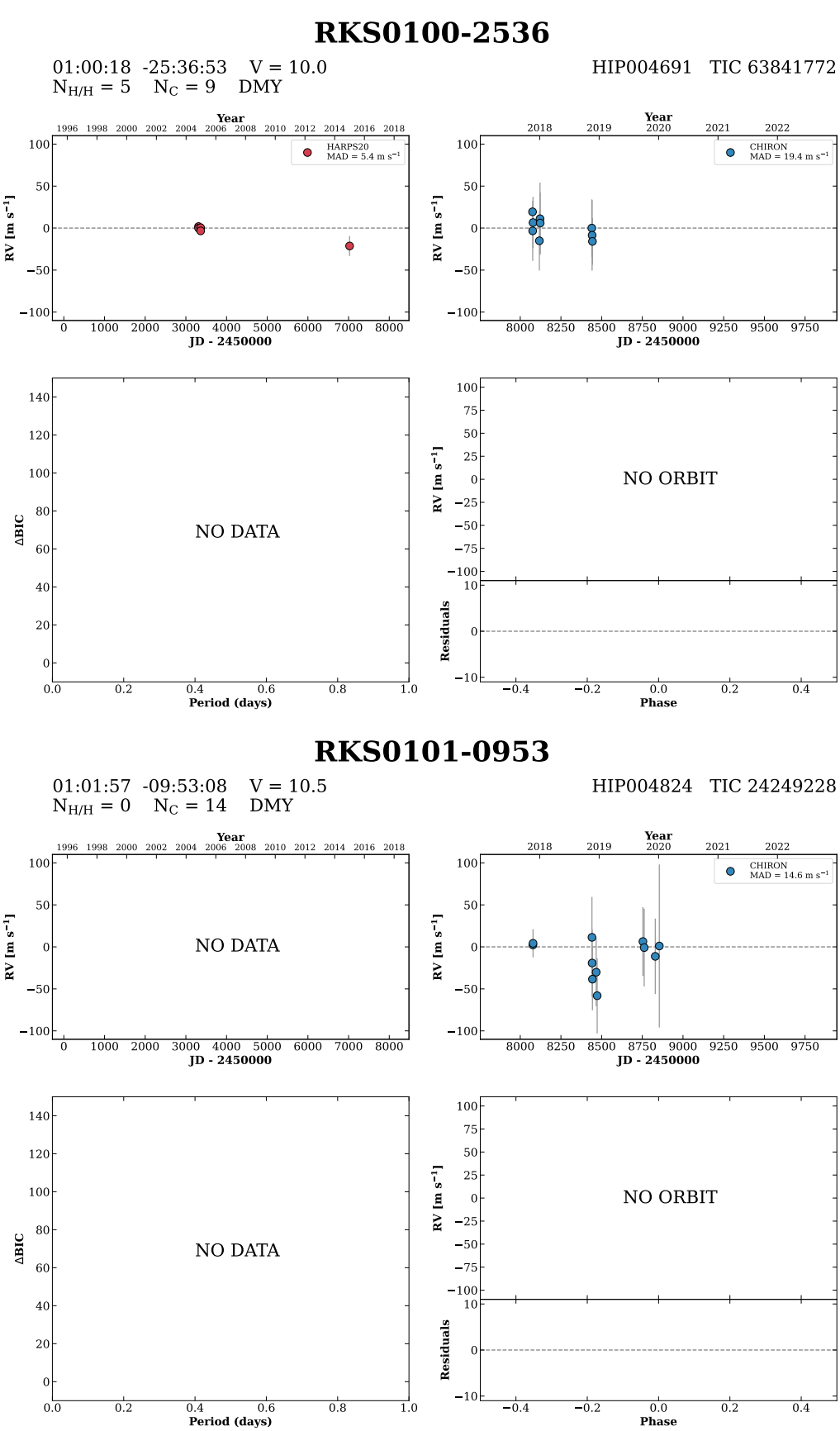

Figure 17 RV results for RKS0100-2536 (top) and RKS0101-0953 (bottom).

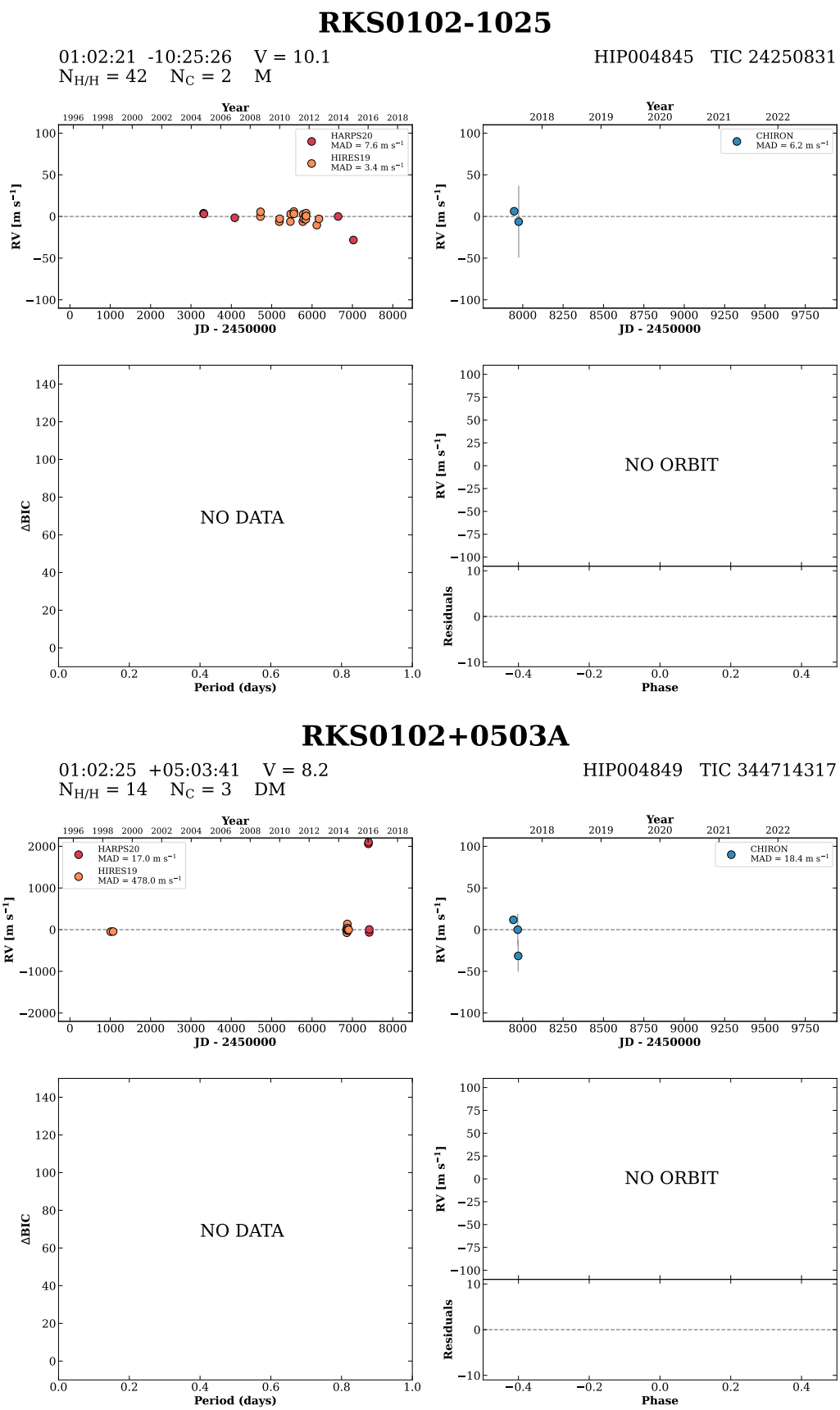

Figure 18 RV results for RKS0102-1025 (top) and RKS0102+0503A (bottom).

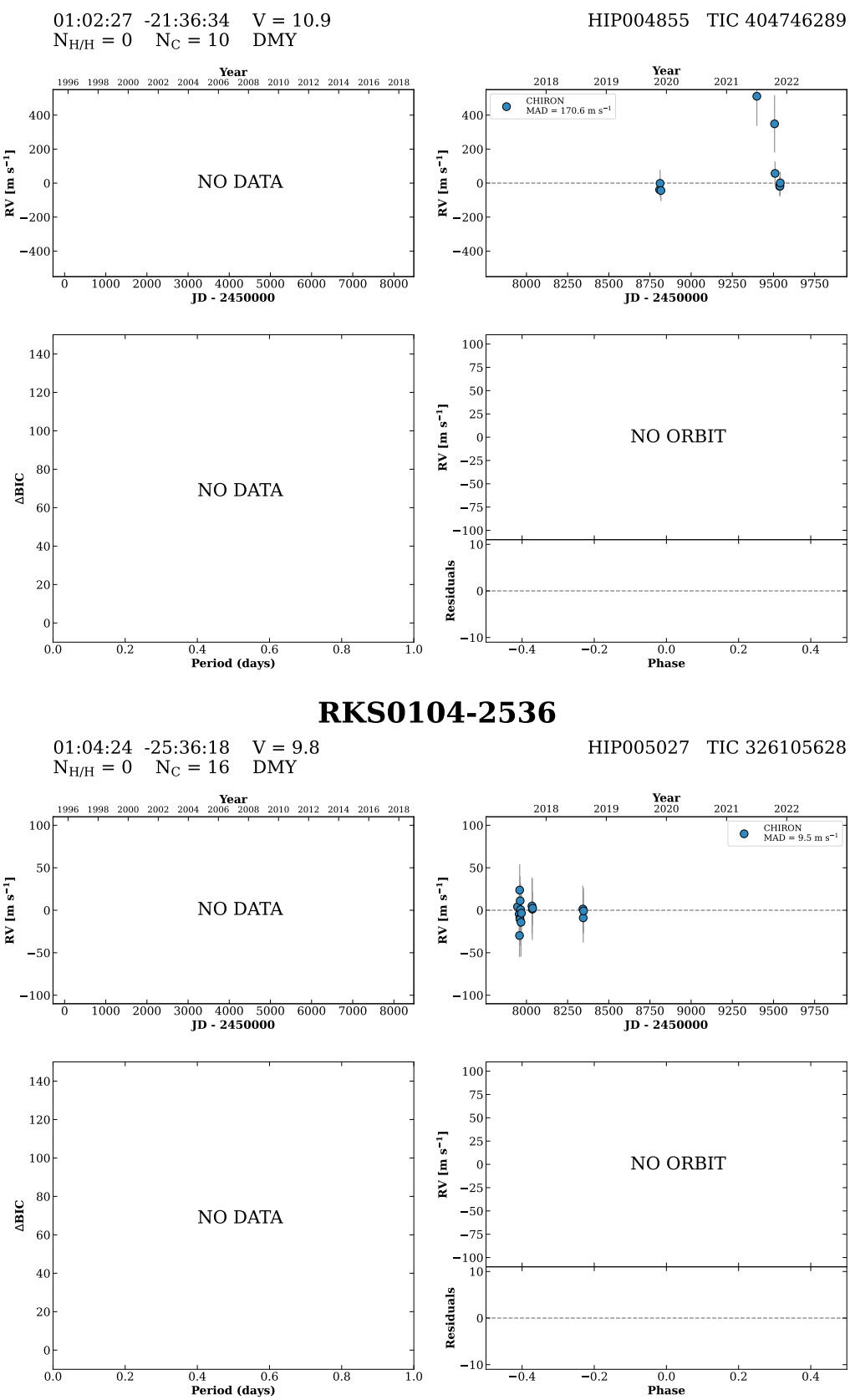

Figure 19 RV results for RKS0102-2136 (top) and RKS0104-2536 (bottom).

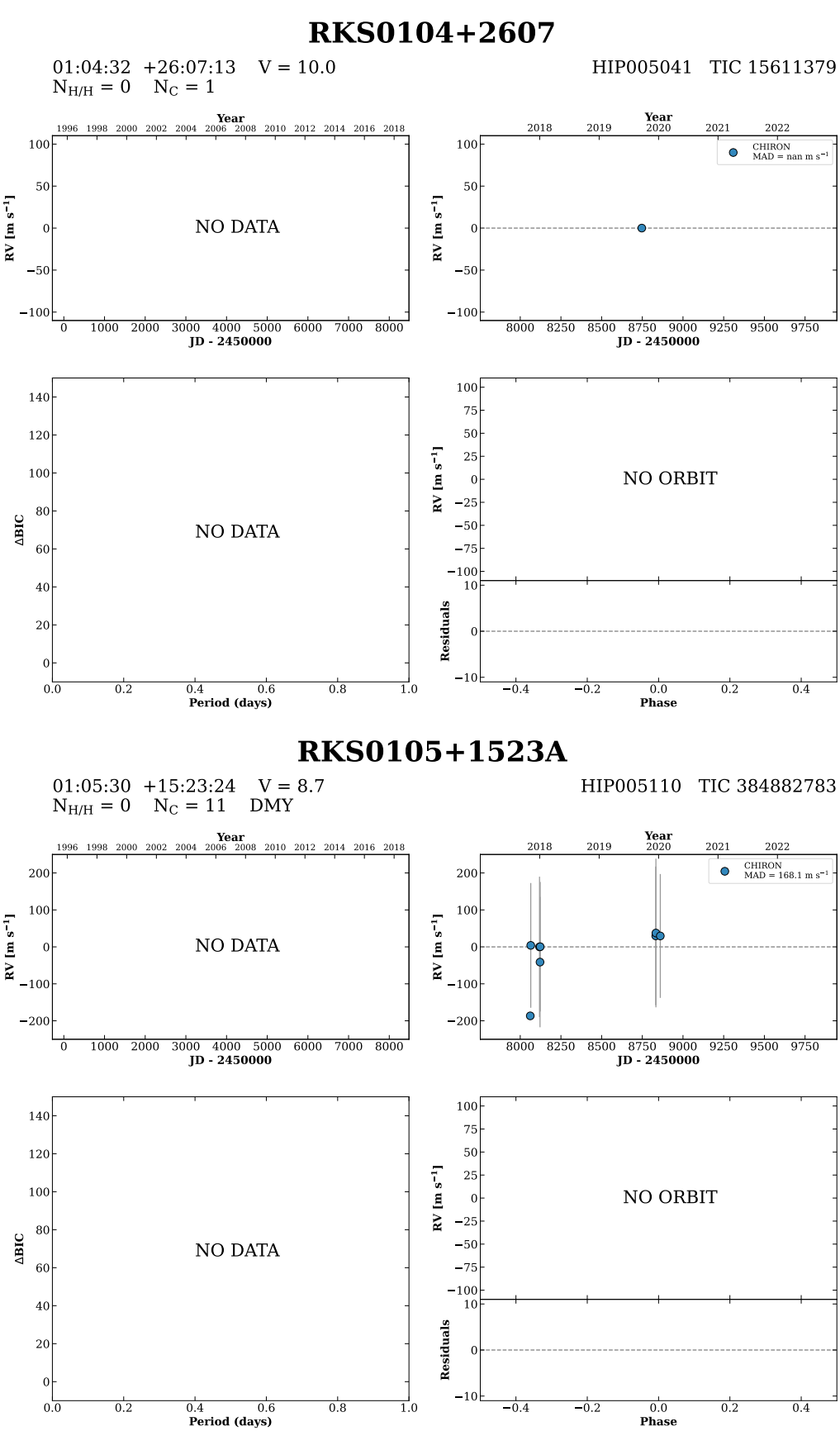

Figure 20 RV results for RKS0104+2607 (top) and RKS0105+1523A (bottom).

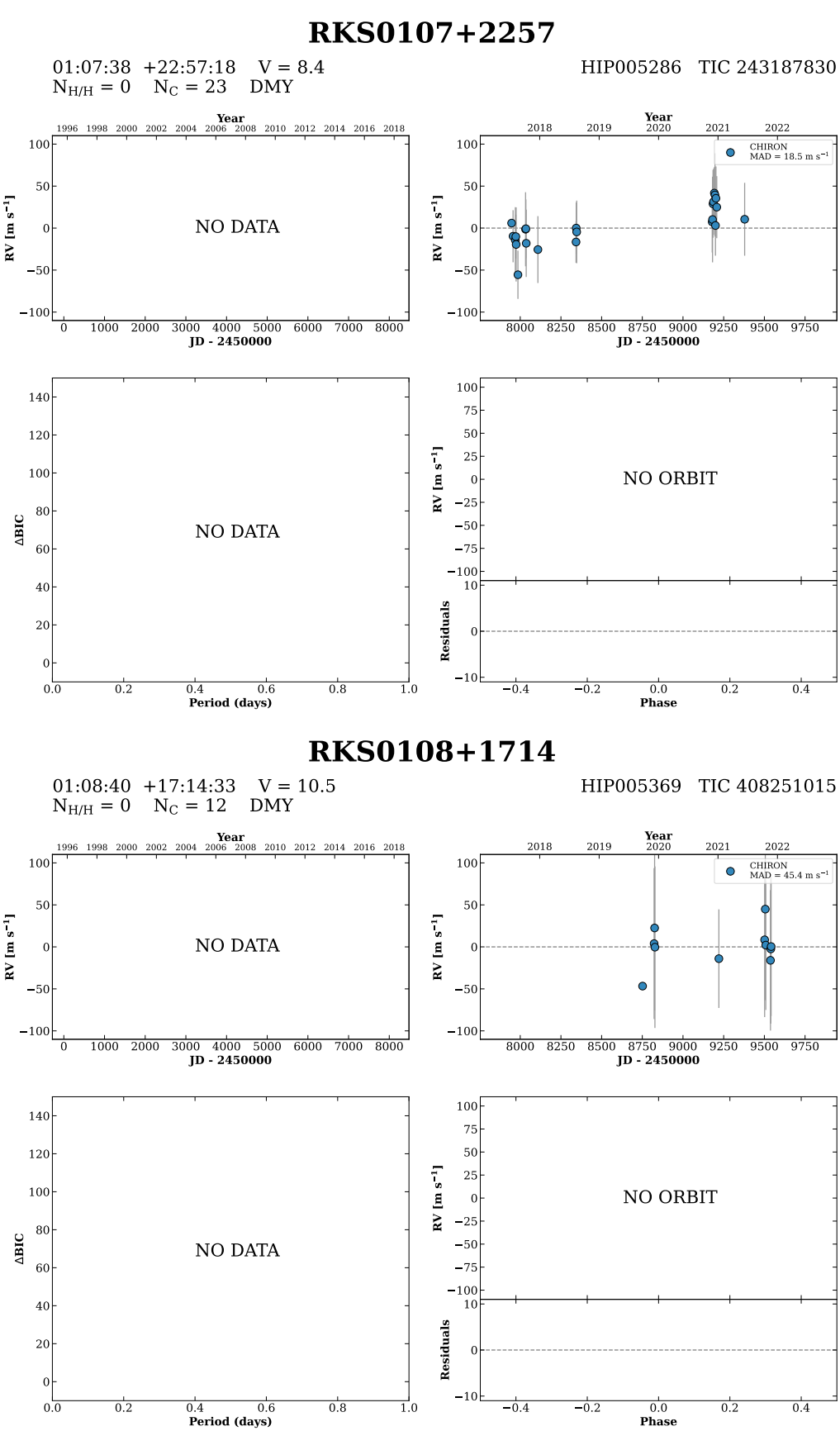

Figure 21 RV results for RKS0107+2257 (top) and RKS0108+1714 (bottom).

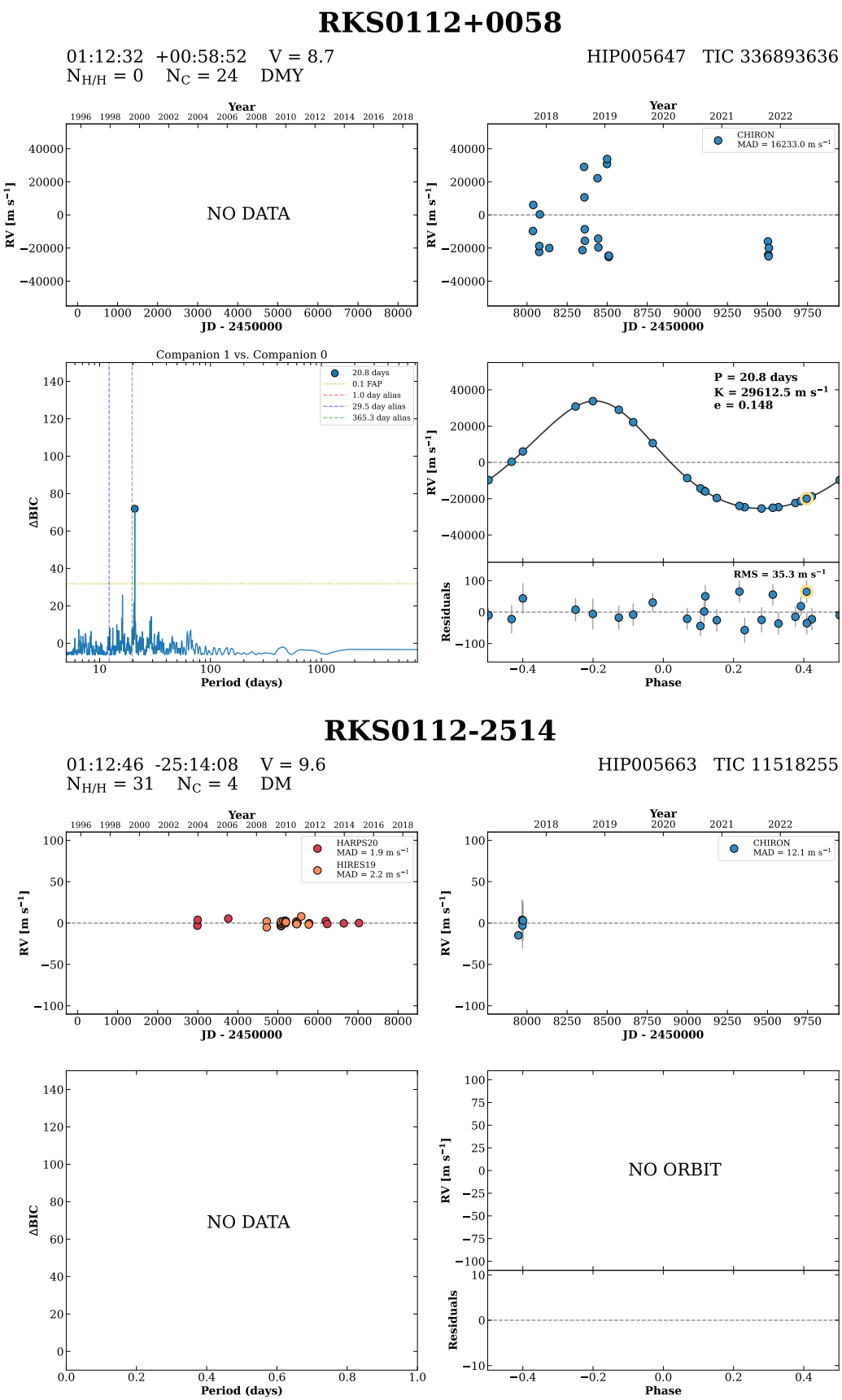

Figure 22 RV results for RKS0112+0058 (top) and RKS0112-2514 (bottom).

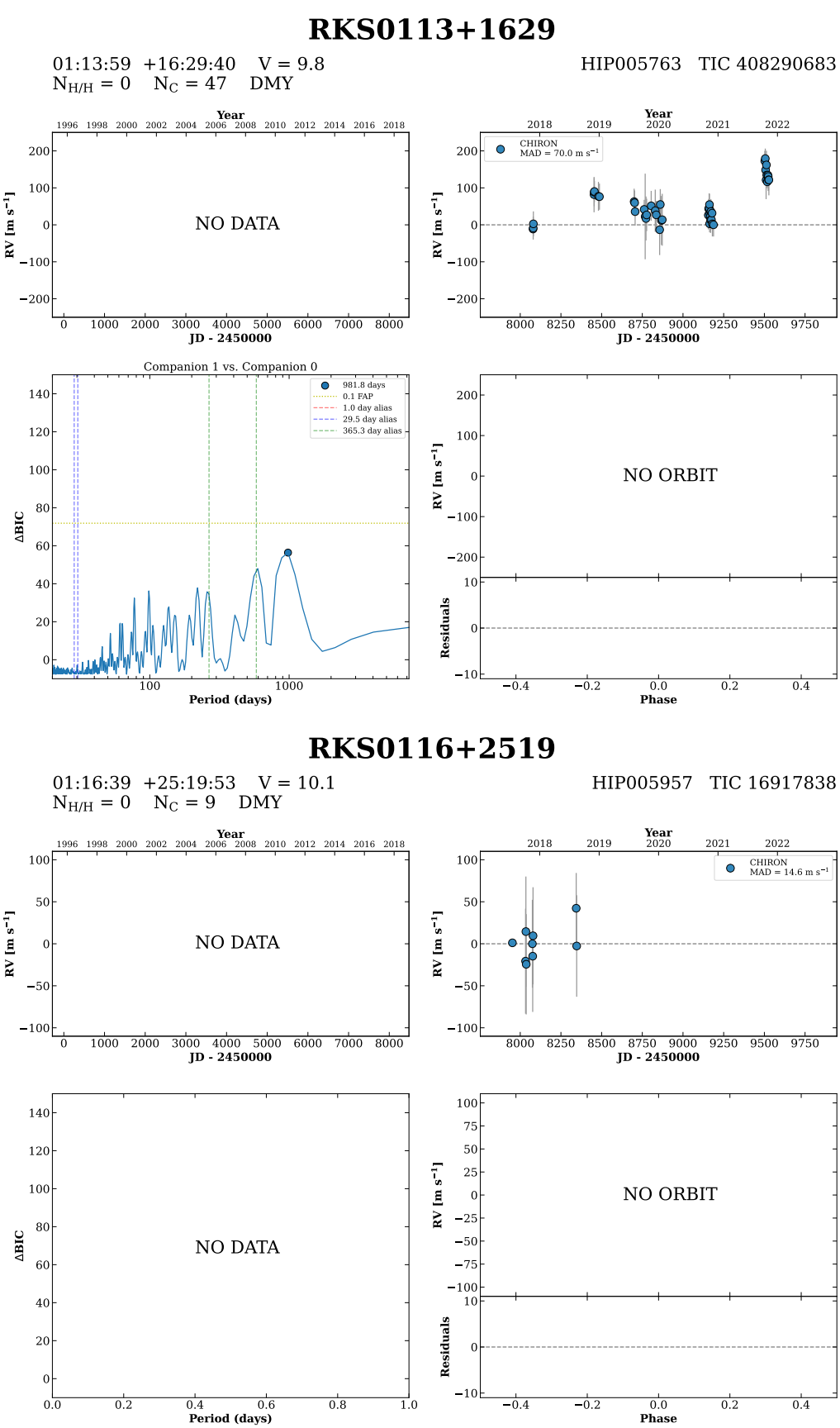

Figure 23 RV results for RKS0113+1629 (top) and RKS0116+2519 (bottom).

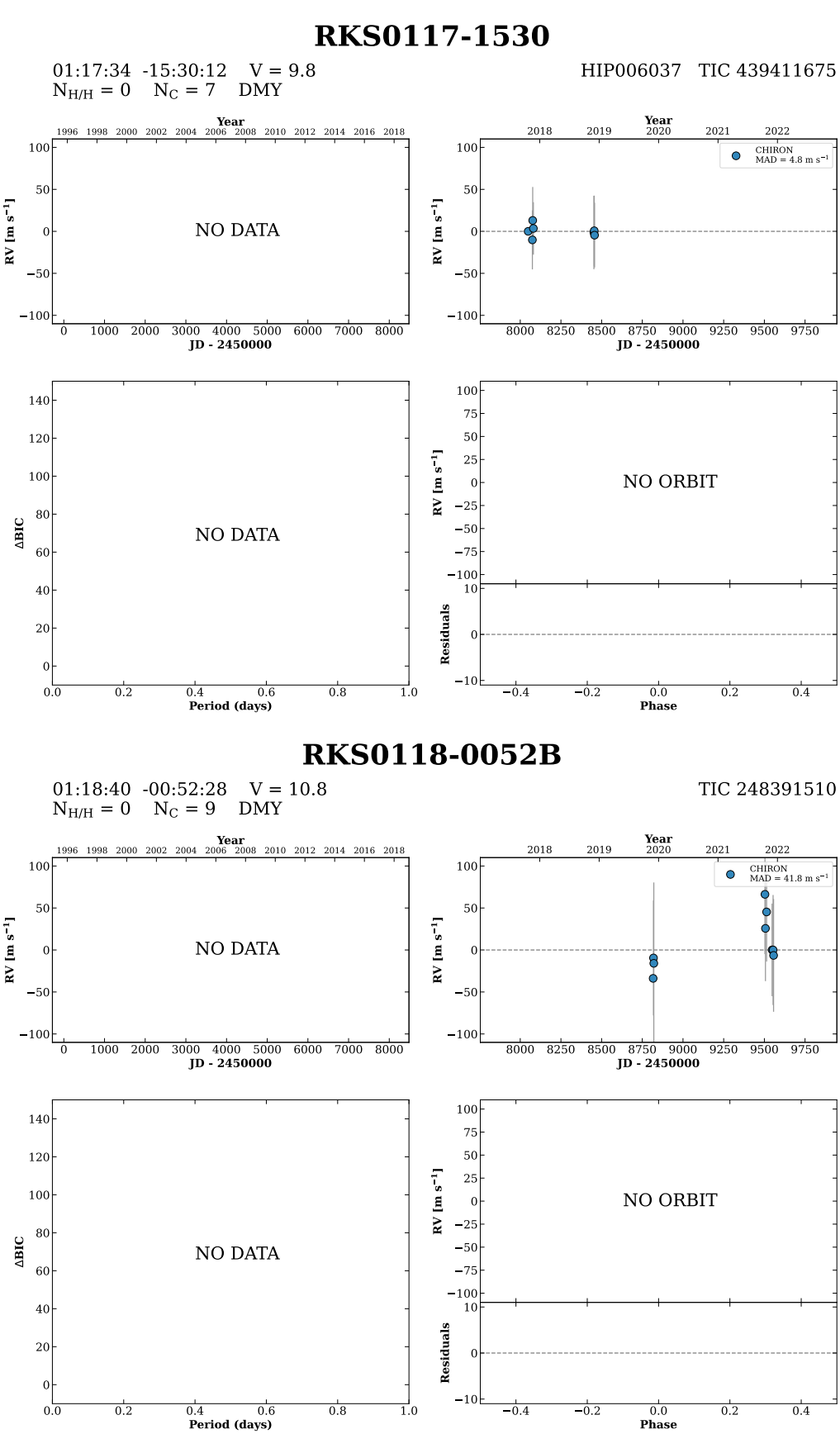

Figure 24 RV results for RKS0117-1530 (top) and RKS0118-0052B (bottom).

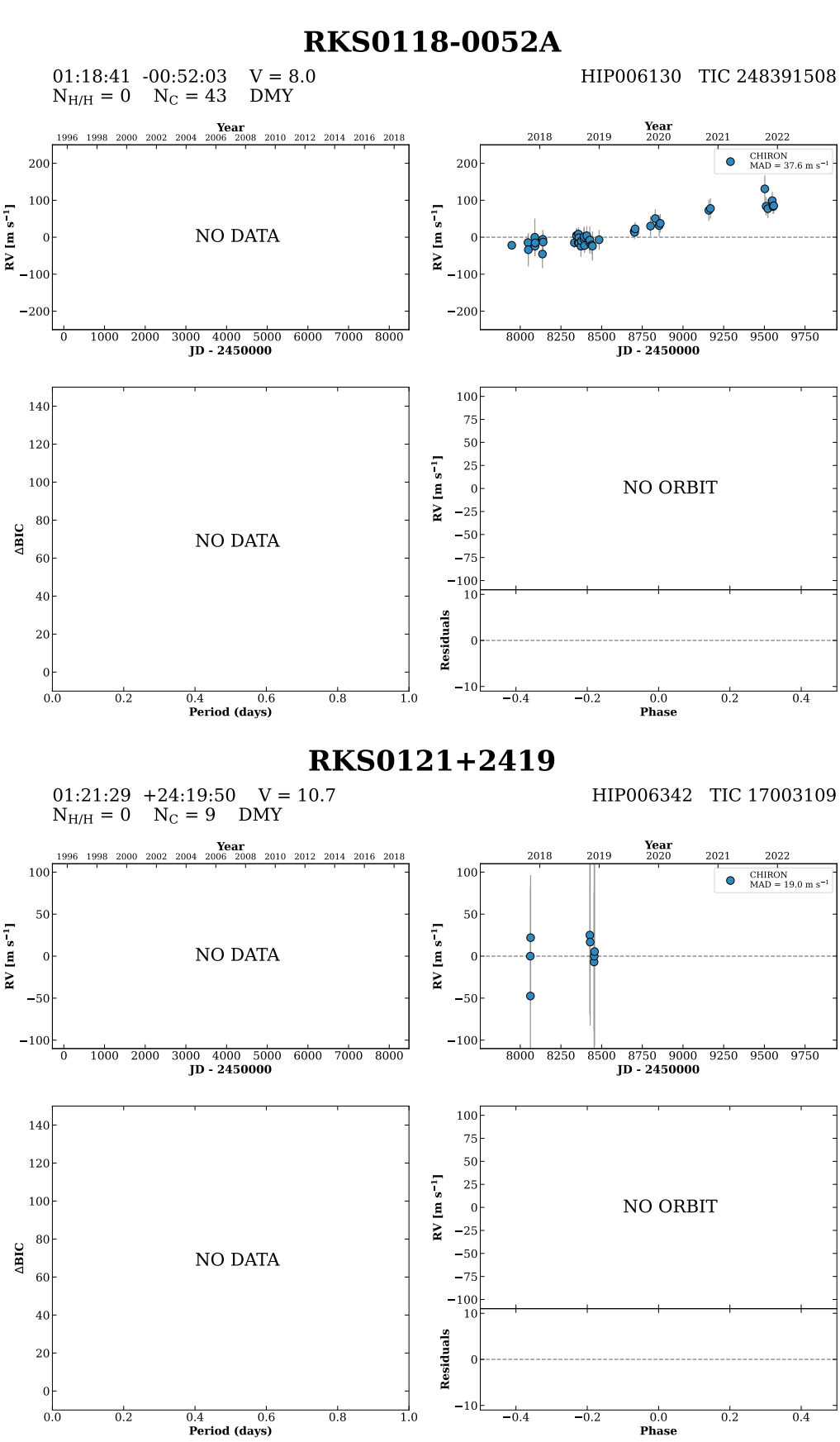

Figure 25 RV results for RKS0118-0052A (top) and RKS0121+2419 (bottom).

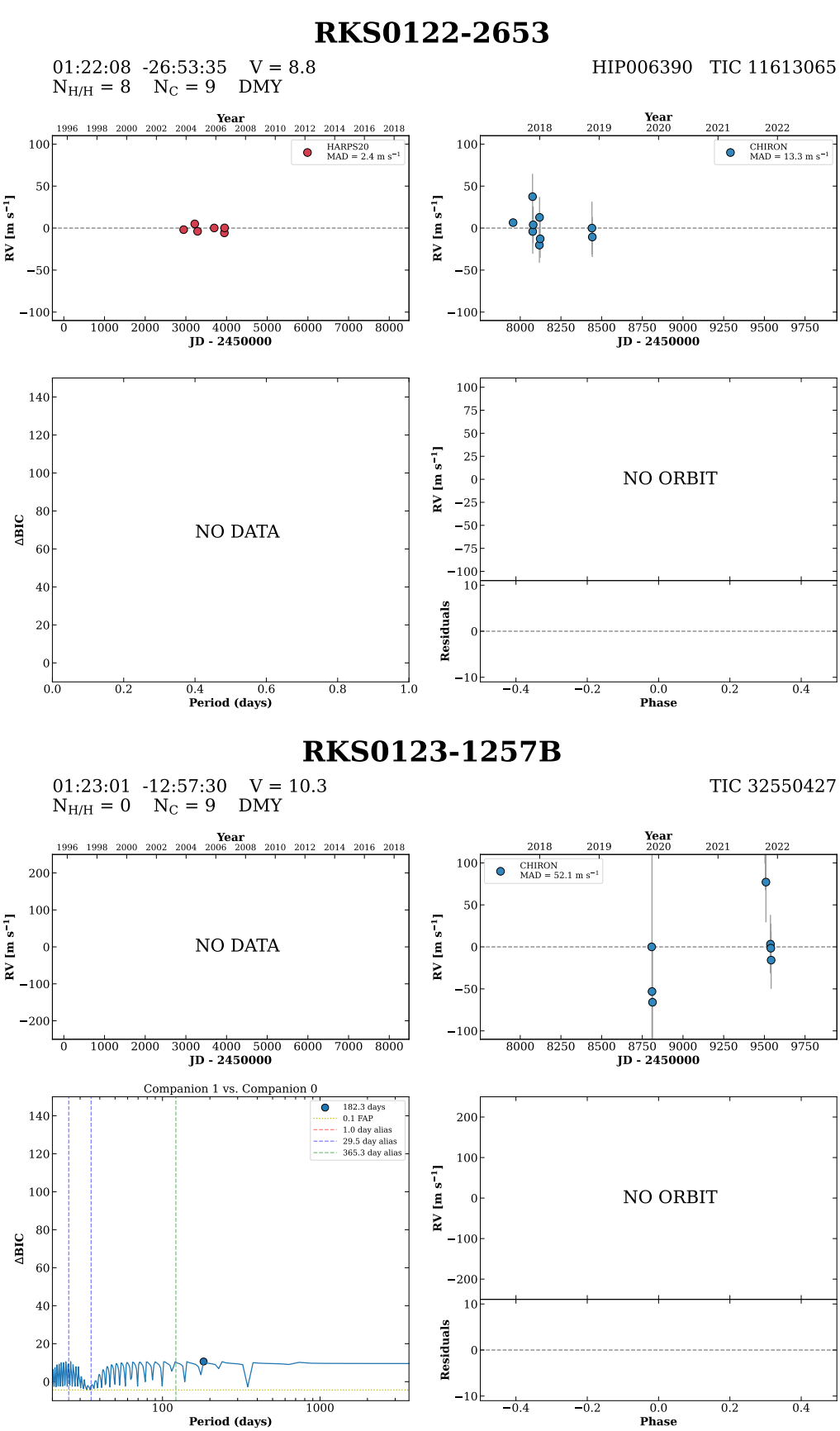

Figure 26 RV results for RKS0122-2653 (top) and RKS0123-1257B (bottom).

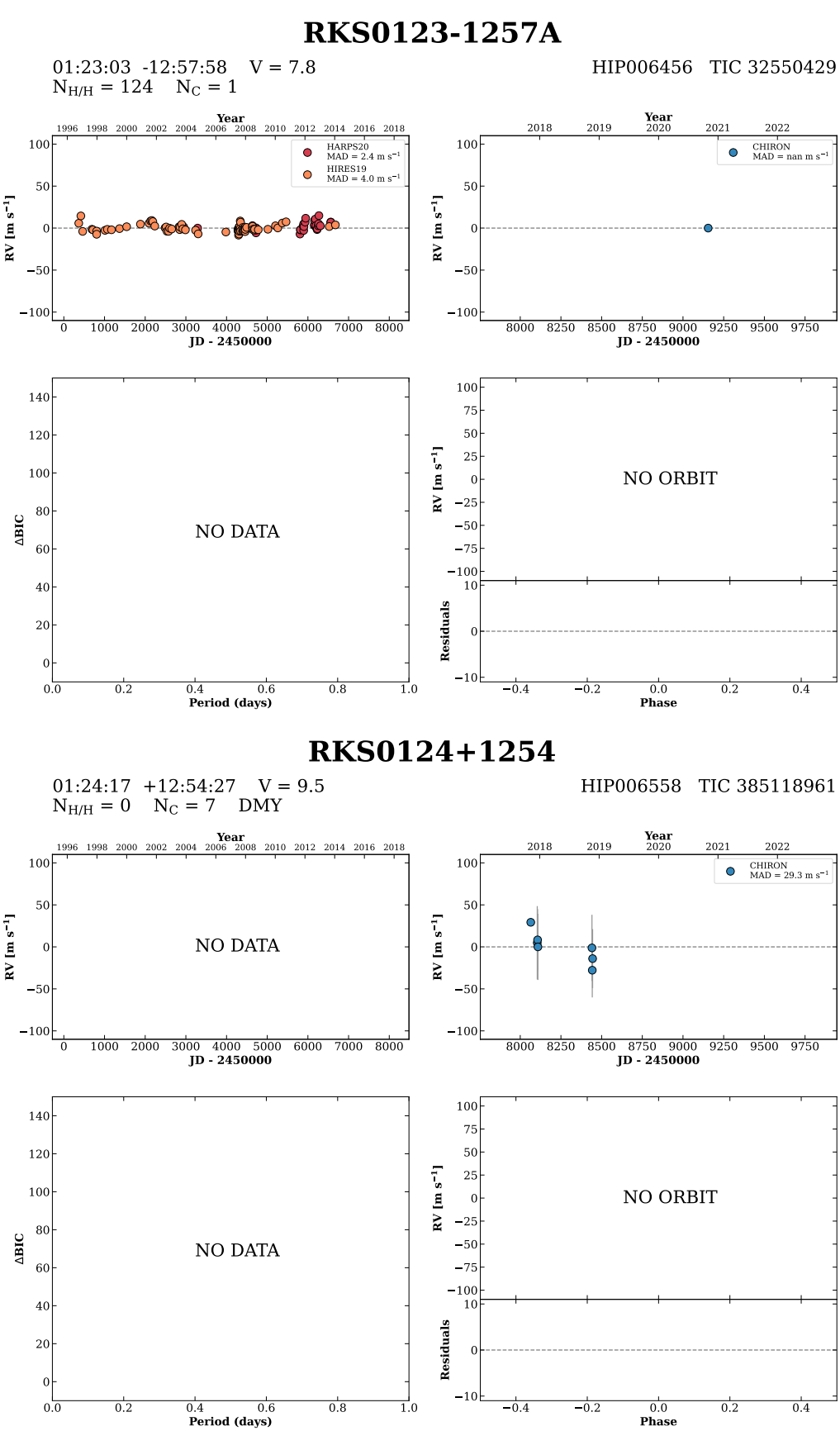

Figure 27 RV results for RKS0123-1257A (top) and RKS0124+1254 (bottom).

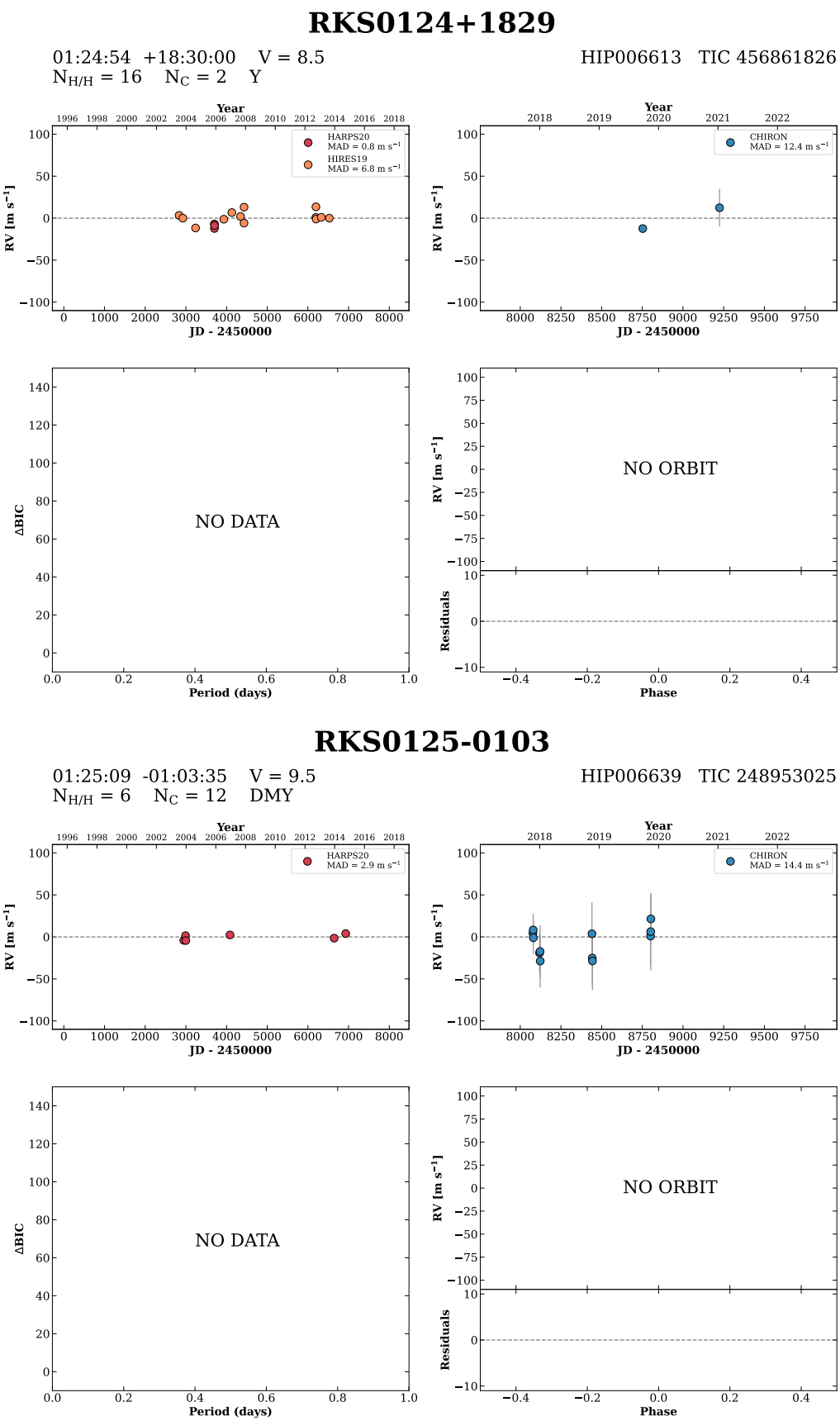

Figure 28 RV results for RKS0124+1829 (top) and RKS0125-0103 (bottom).

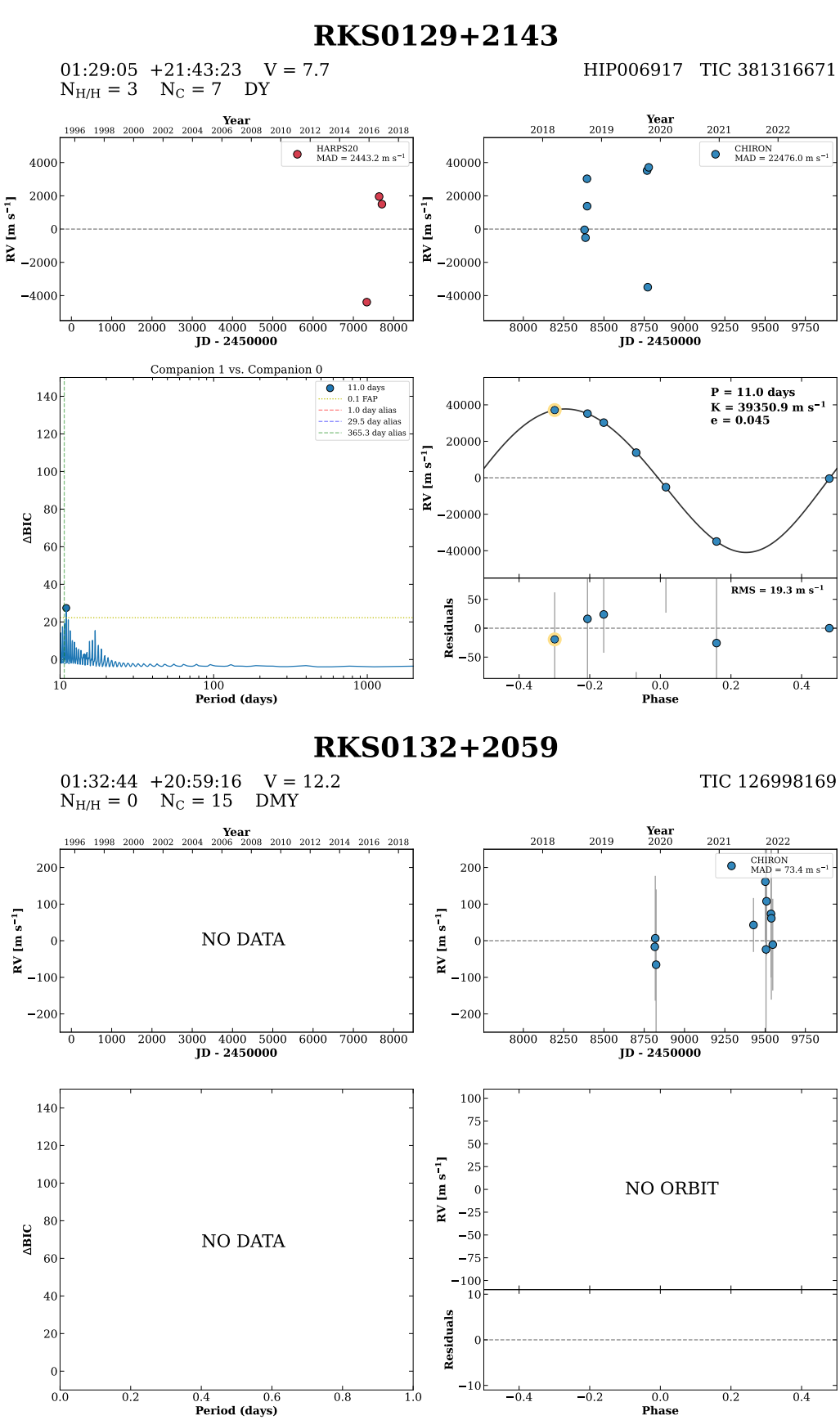

Figure 29 RV results for RKS0129+2143 (top) and RKS0132+2059 (bottom).

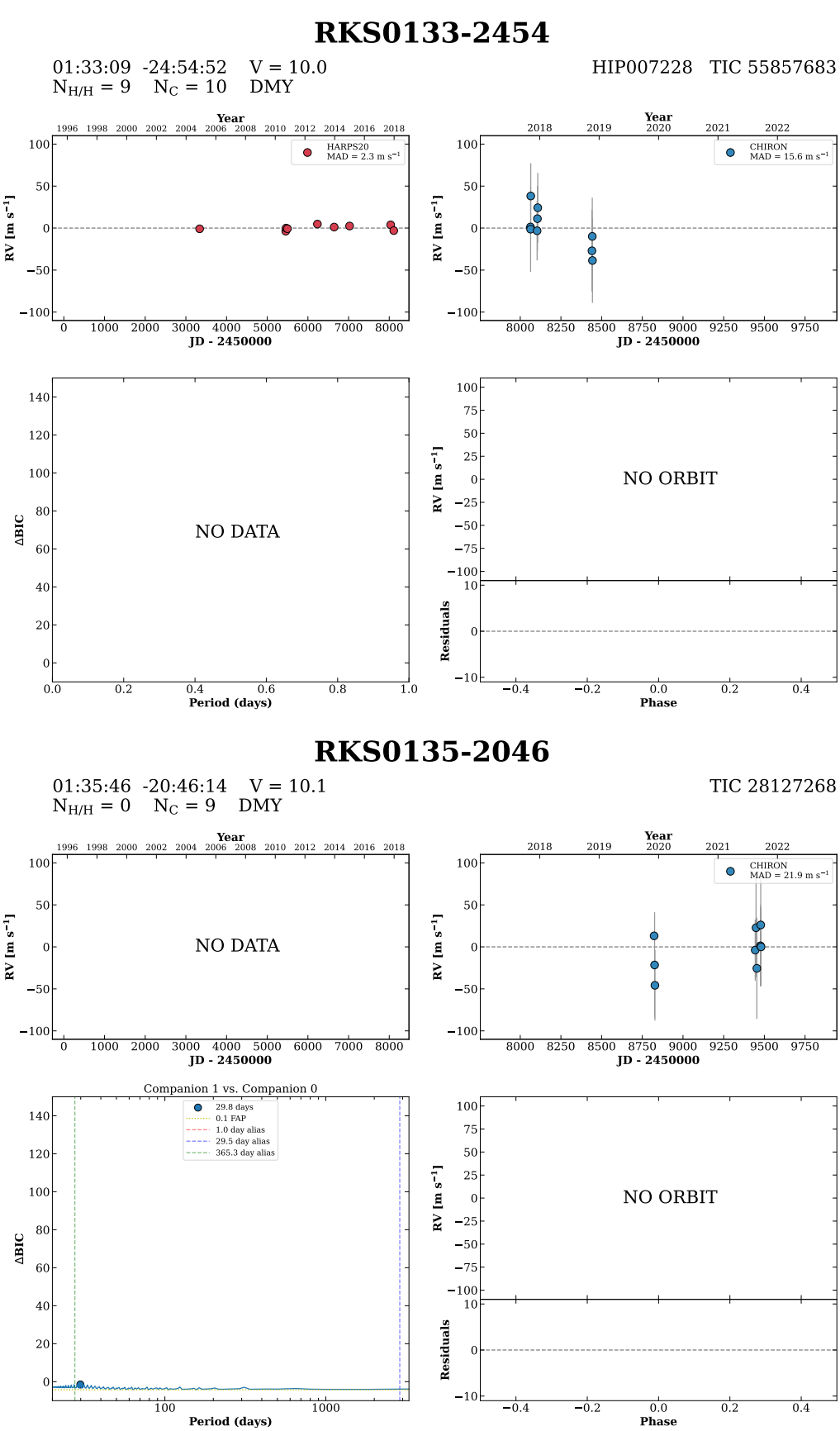

Figure 30 RV results for RKS0133-2454 (top) and RKS0135-2046 (bottom).

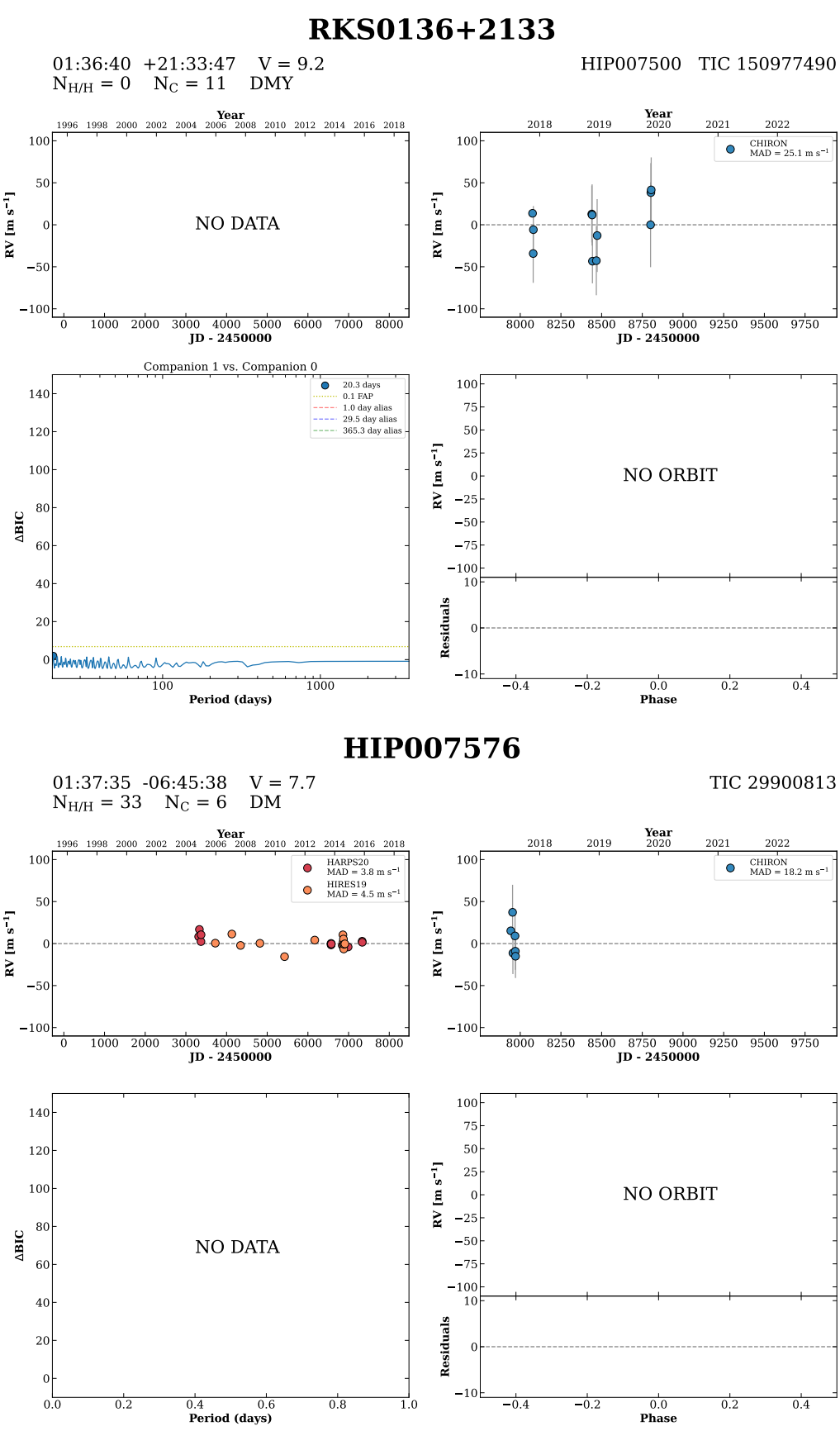

Figure 31 RV results for RKS0136+2133 (top) and HIP007576 (bottom).

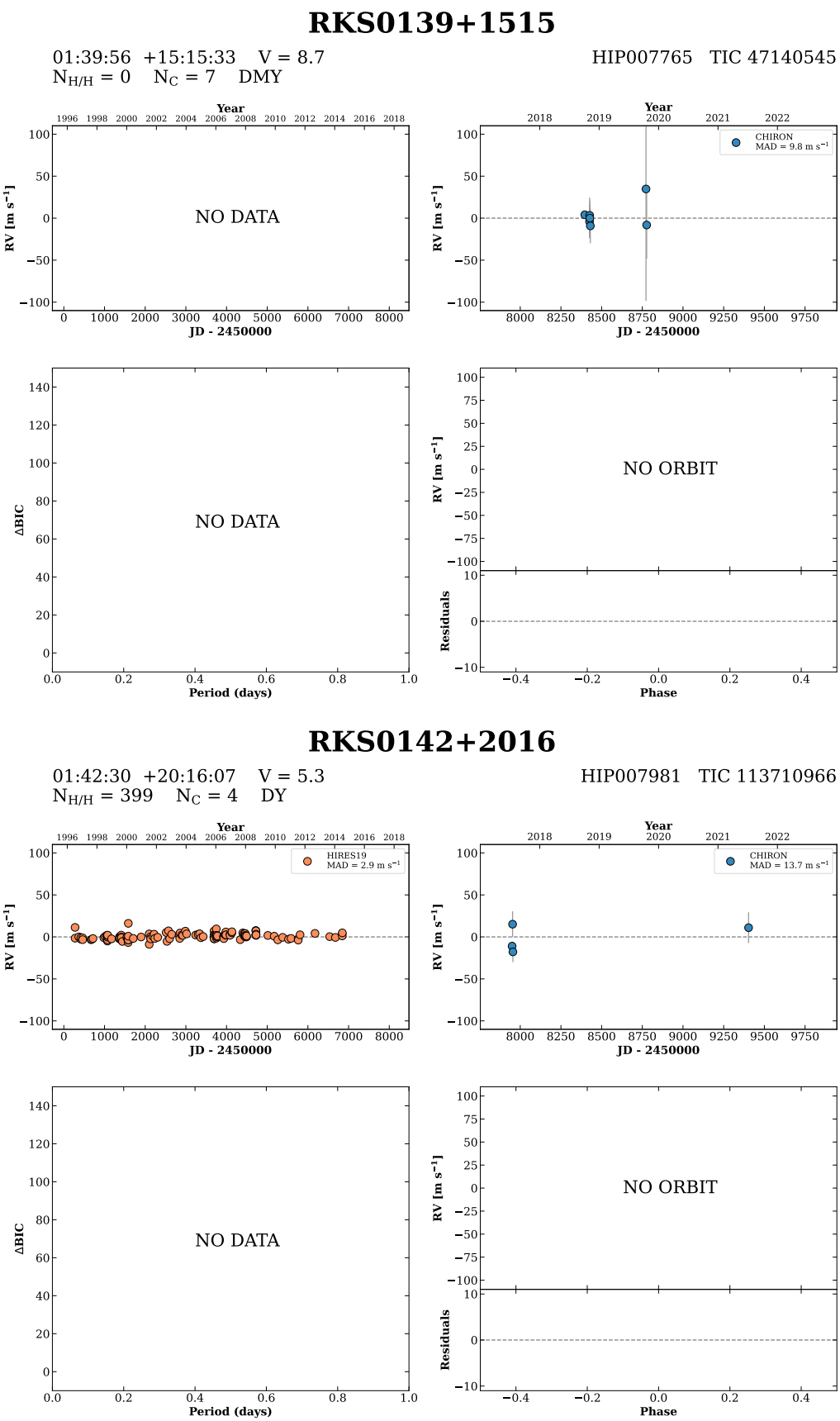

Figure 32 RV results for RKS0139+1515 (top) and RKS0142+2016 (bottom).

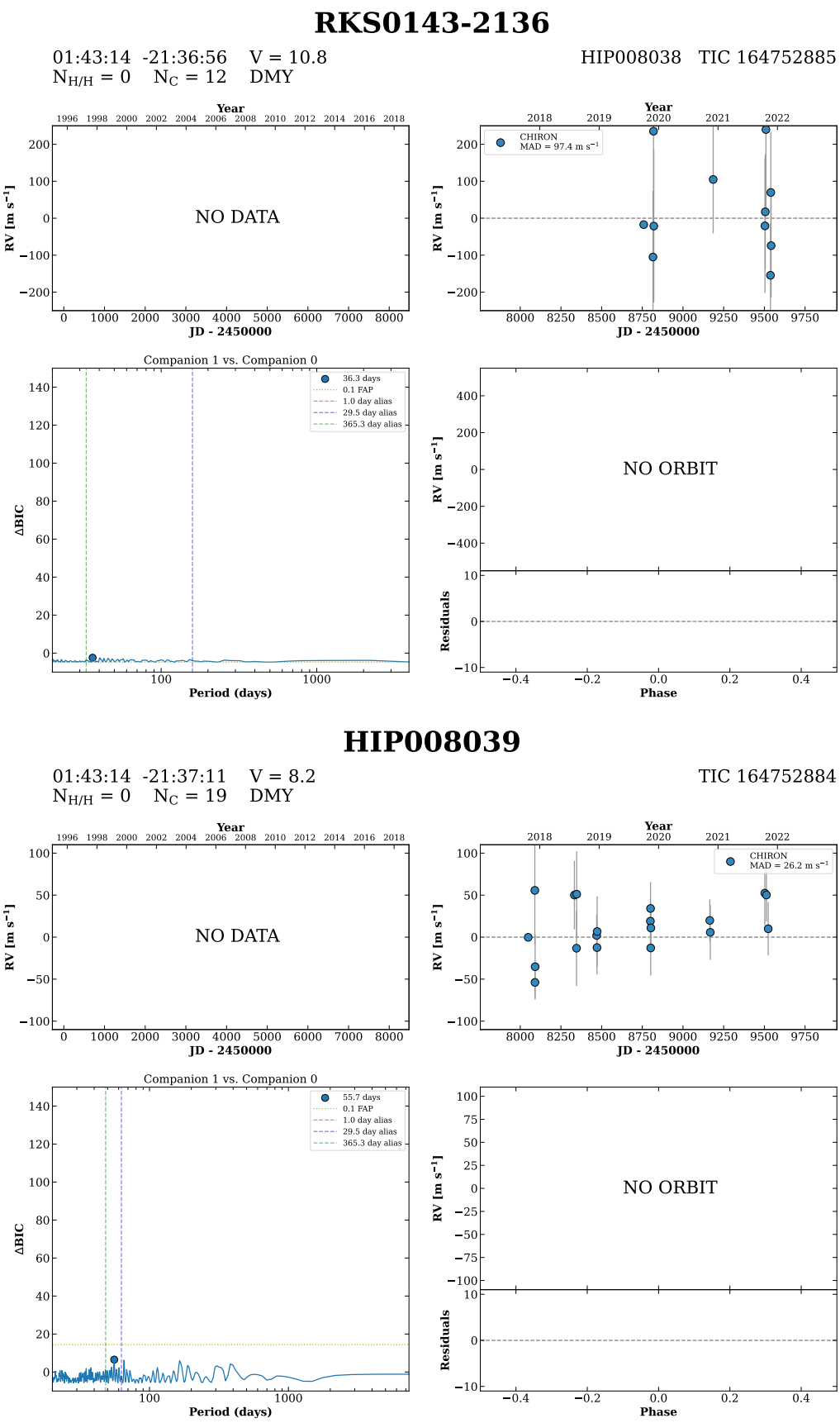

Figure 33 RV results for RKS0143-2136 (top) and HIP008039 (bottom).

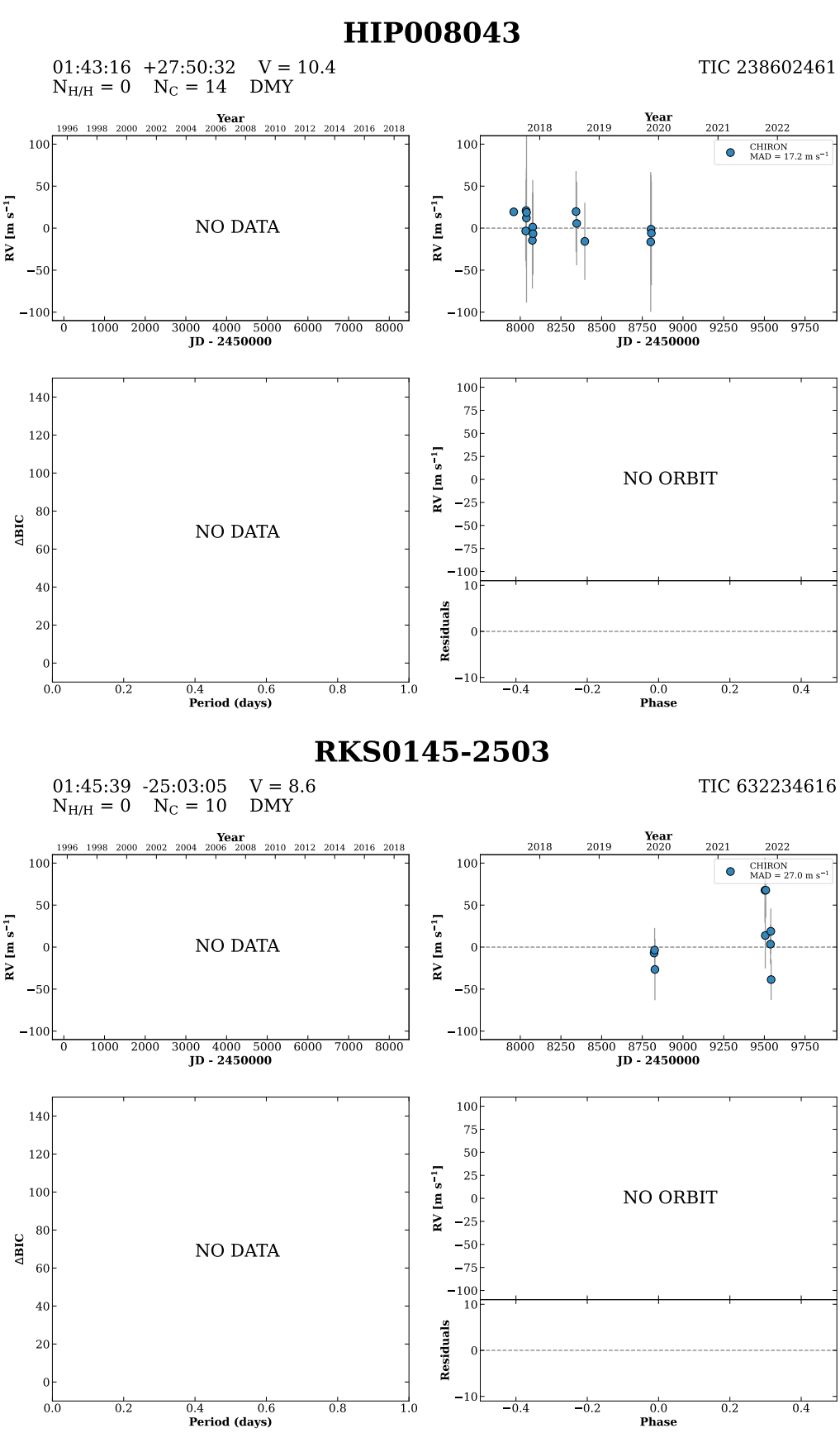

Figure 34 RV results for HIP008043 (top) and RKS0145-2503 (bottom).

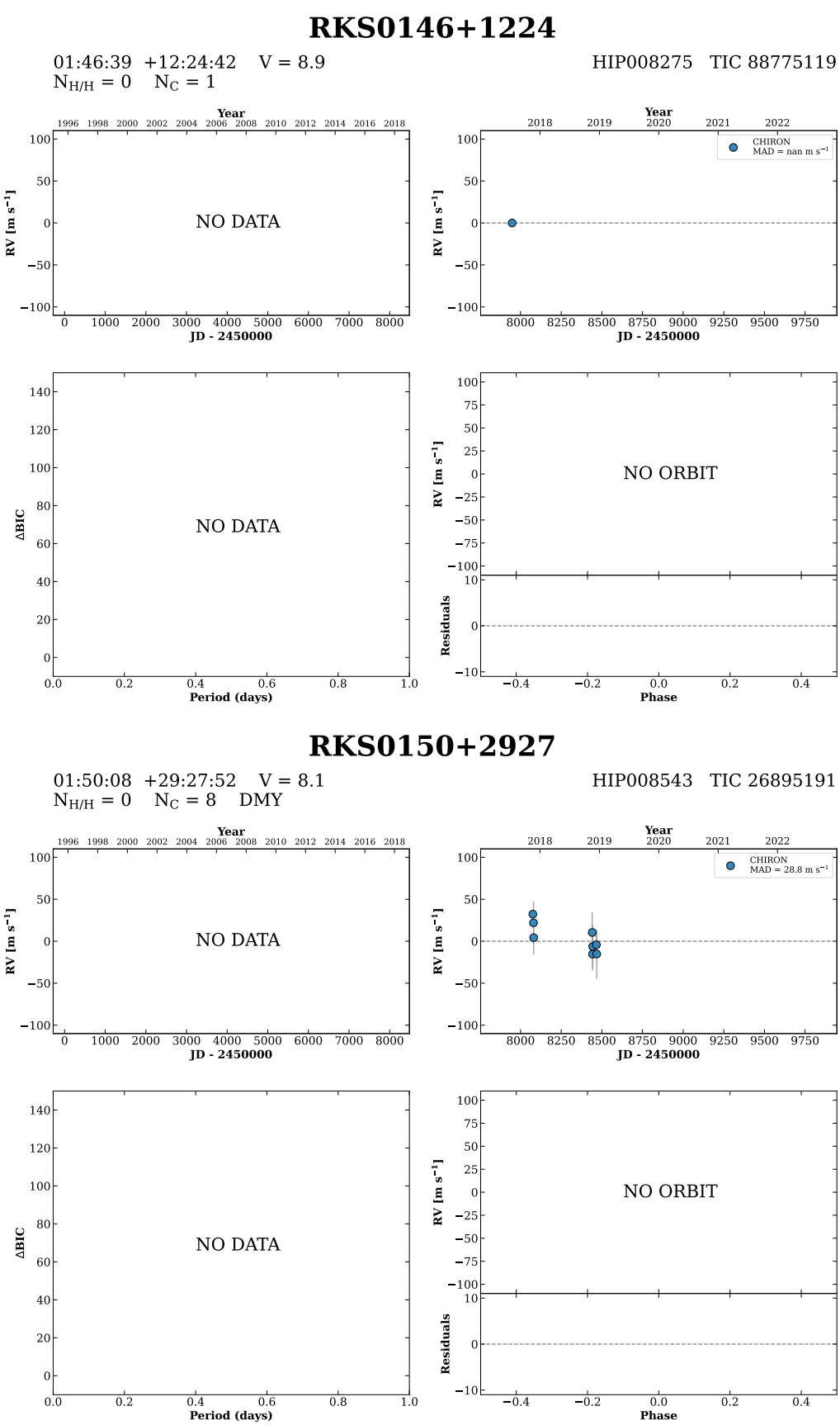

Figure 35 RV results for RKS0146+1224 (top) and RKS0150+2927 (bottom).

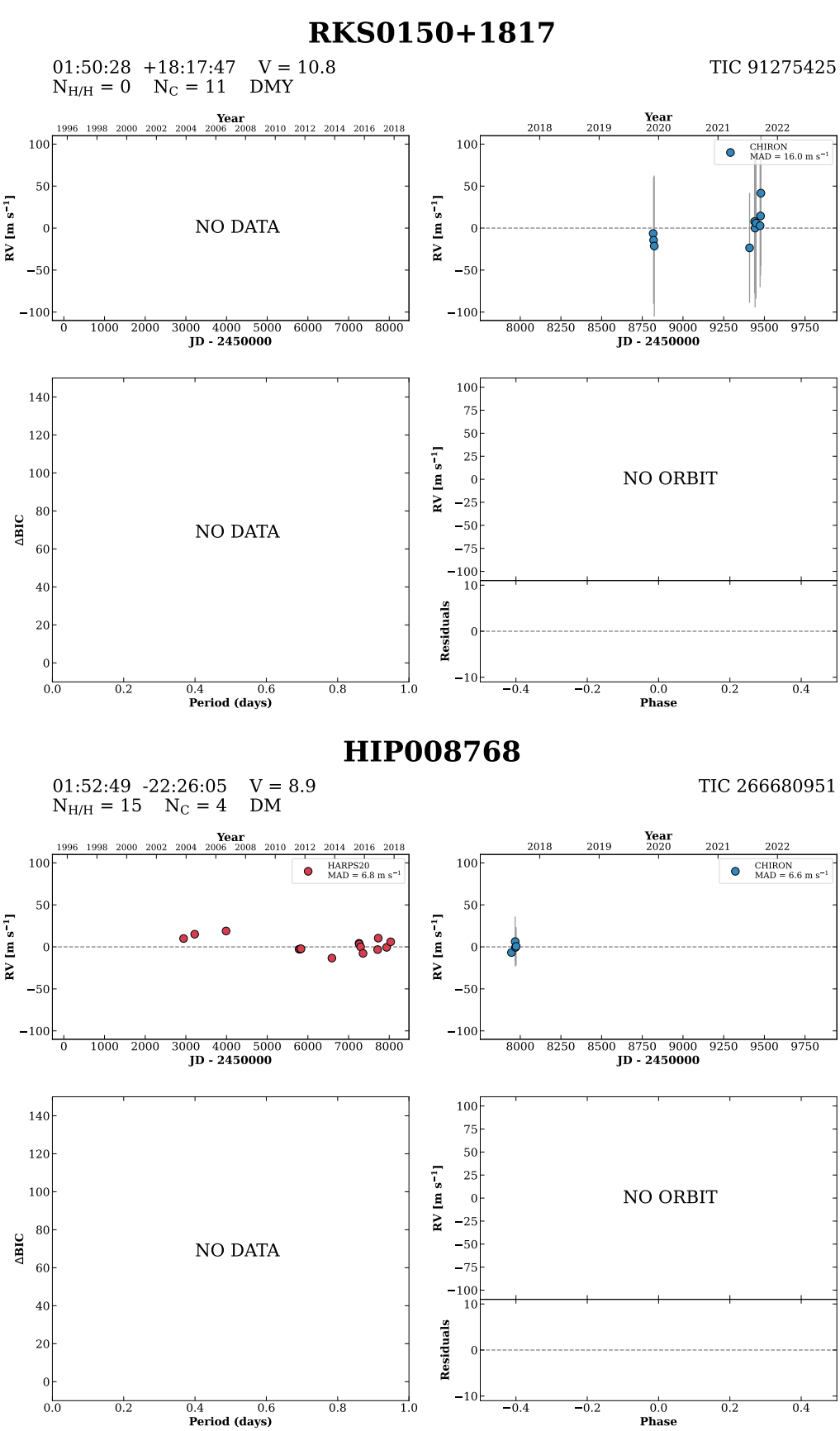

Figure 36 RV results for RKS0150+1817 (top) and HIP008768 (bottom).

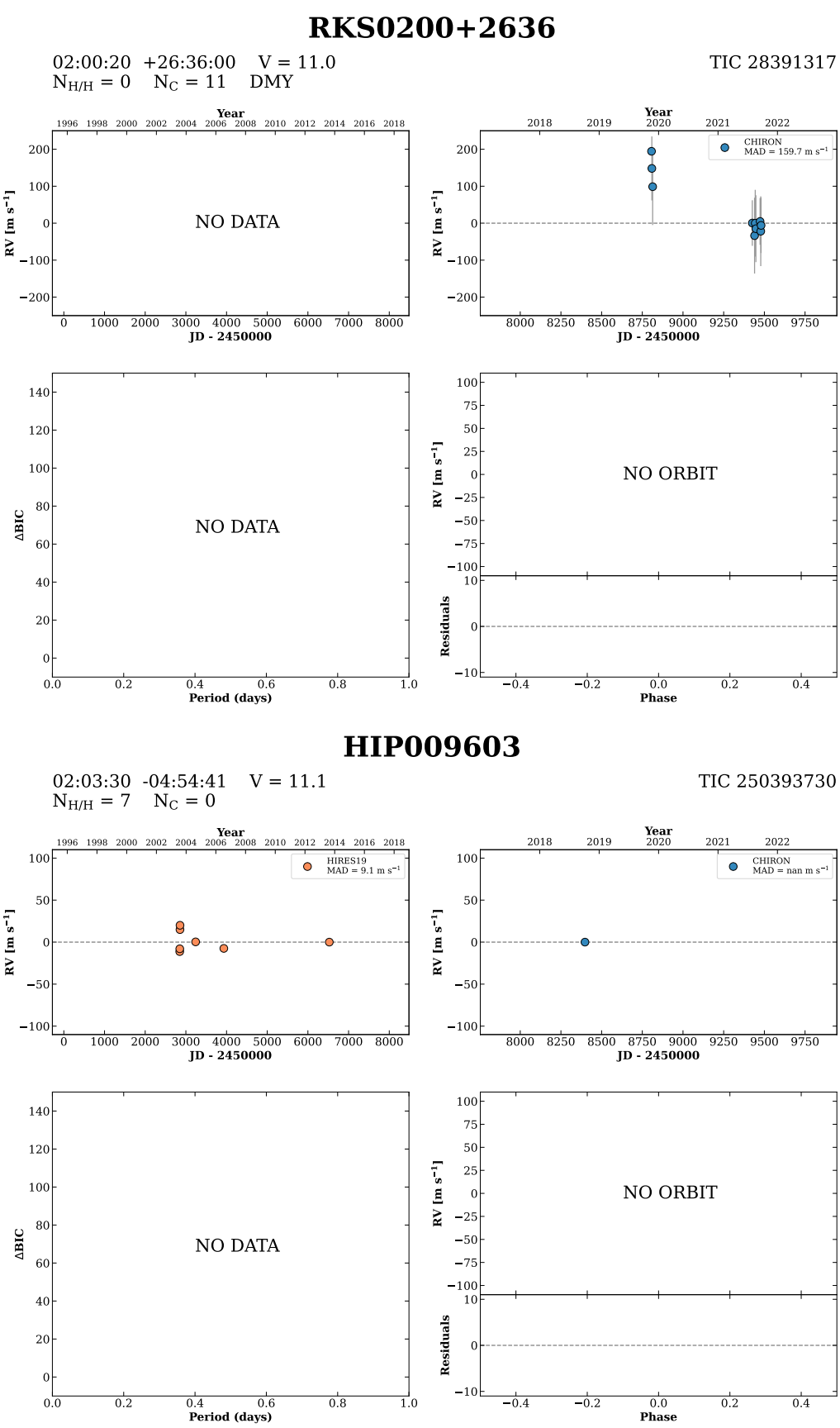

Figure 37 RV results for RKS0200+2636 (top) and HIP009603 (bottom).

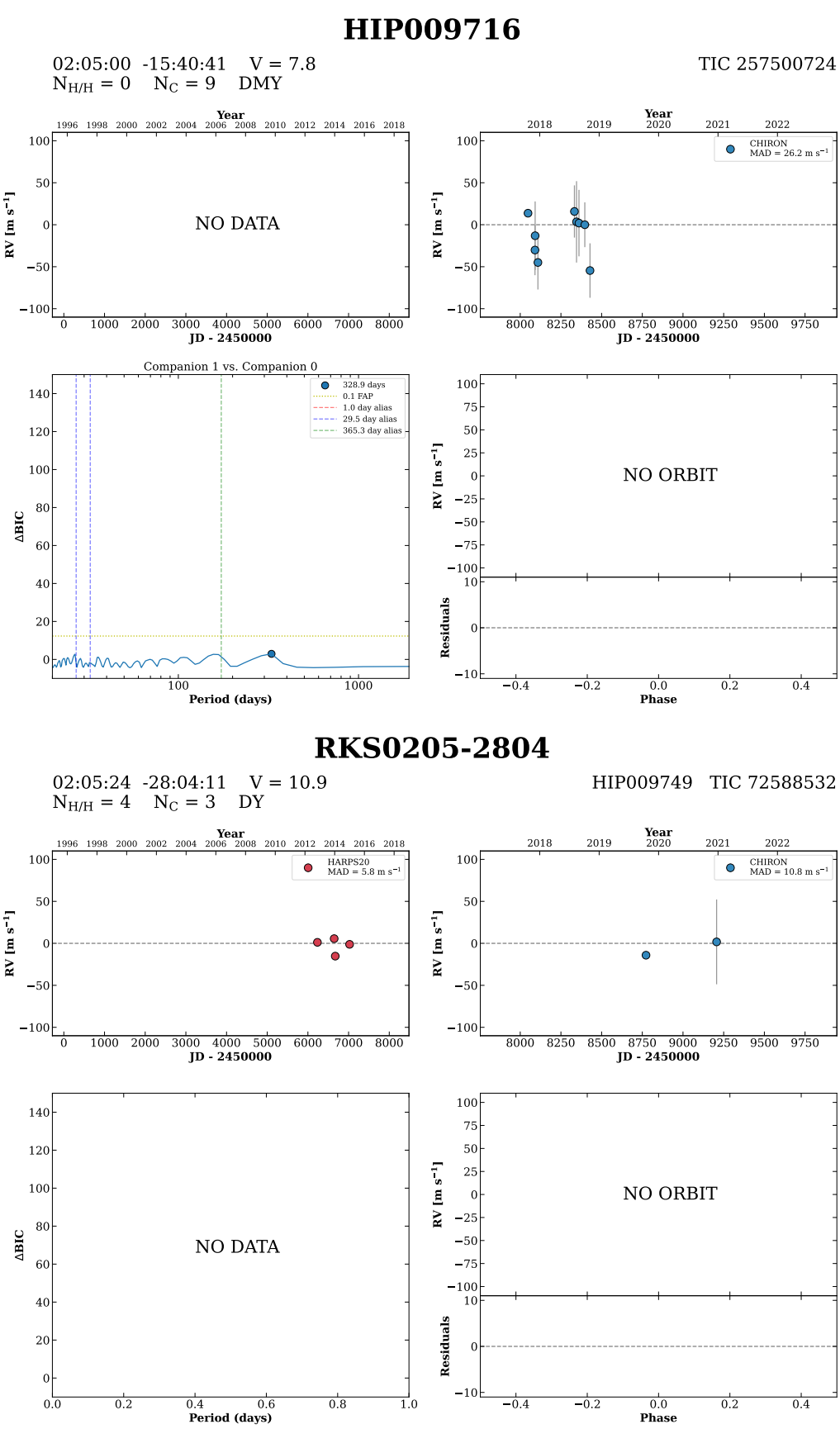

Figure 38 RV results for HIP009716 (top) and RKS0205-2804 (bottom).

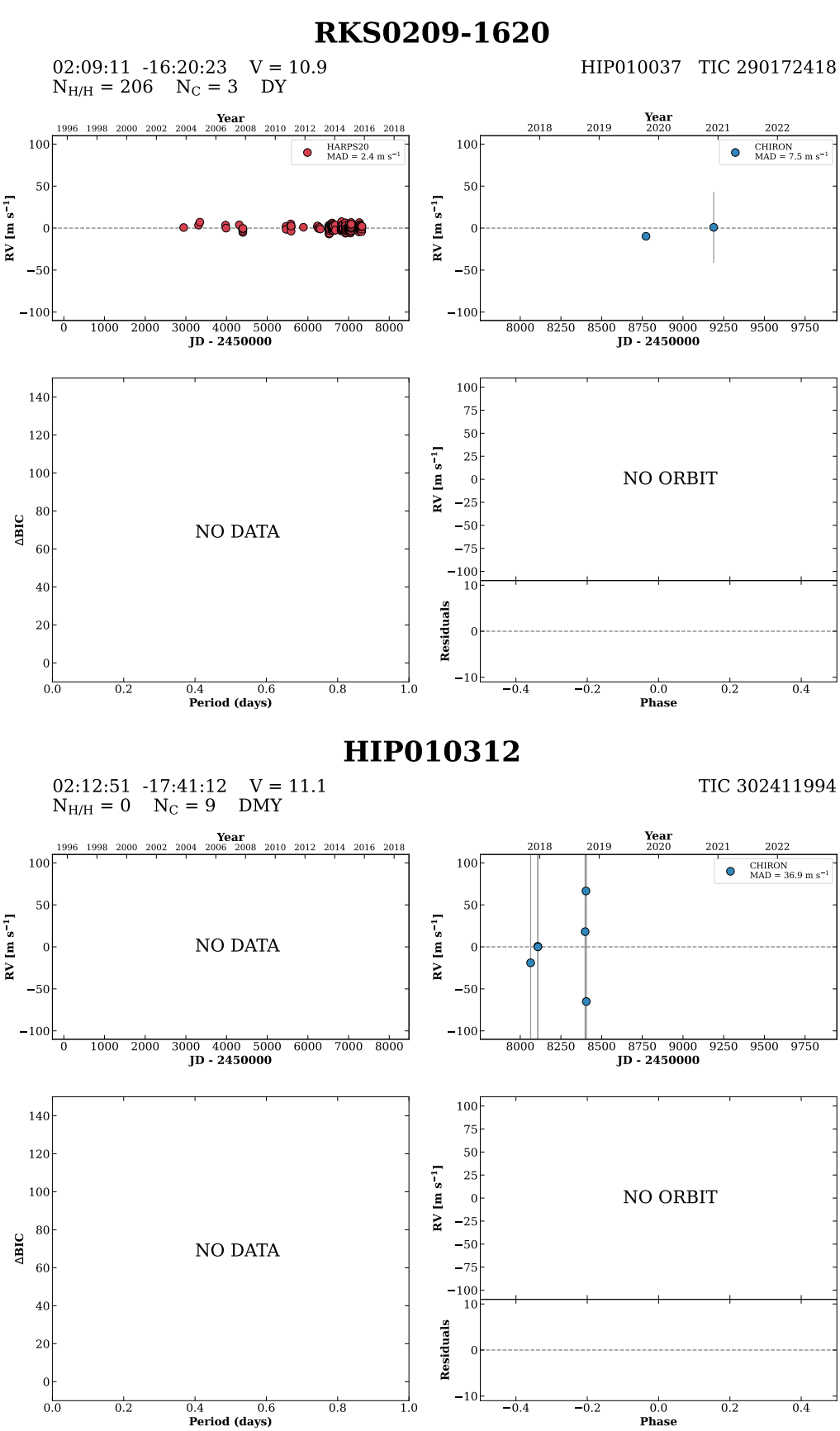

Figure 39 RV results for RKS0209-1620 (top) and HIP010312 (bottom).

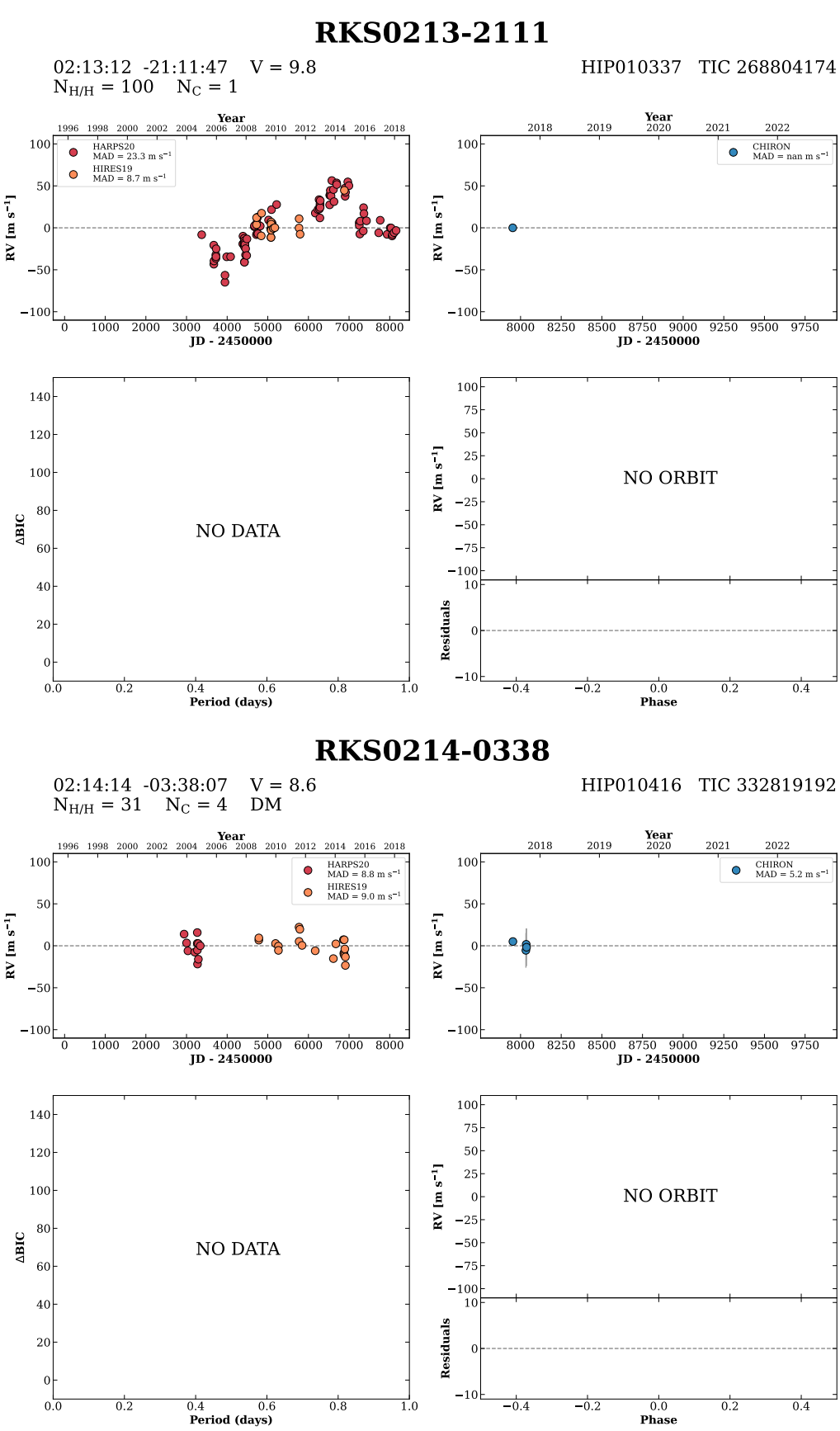

Figure 40 RV results for RKS0213-2111 (top) and RKS0214-0338 (bottom).

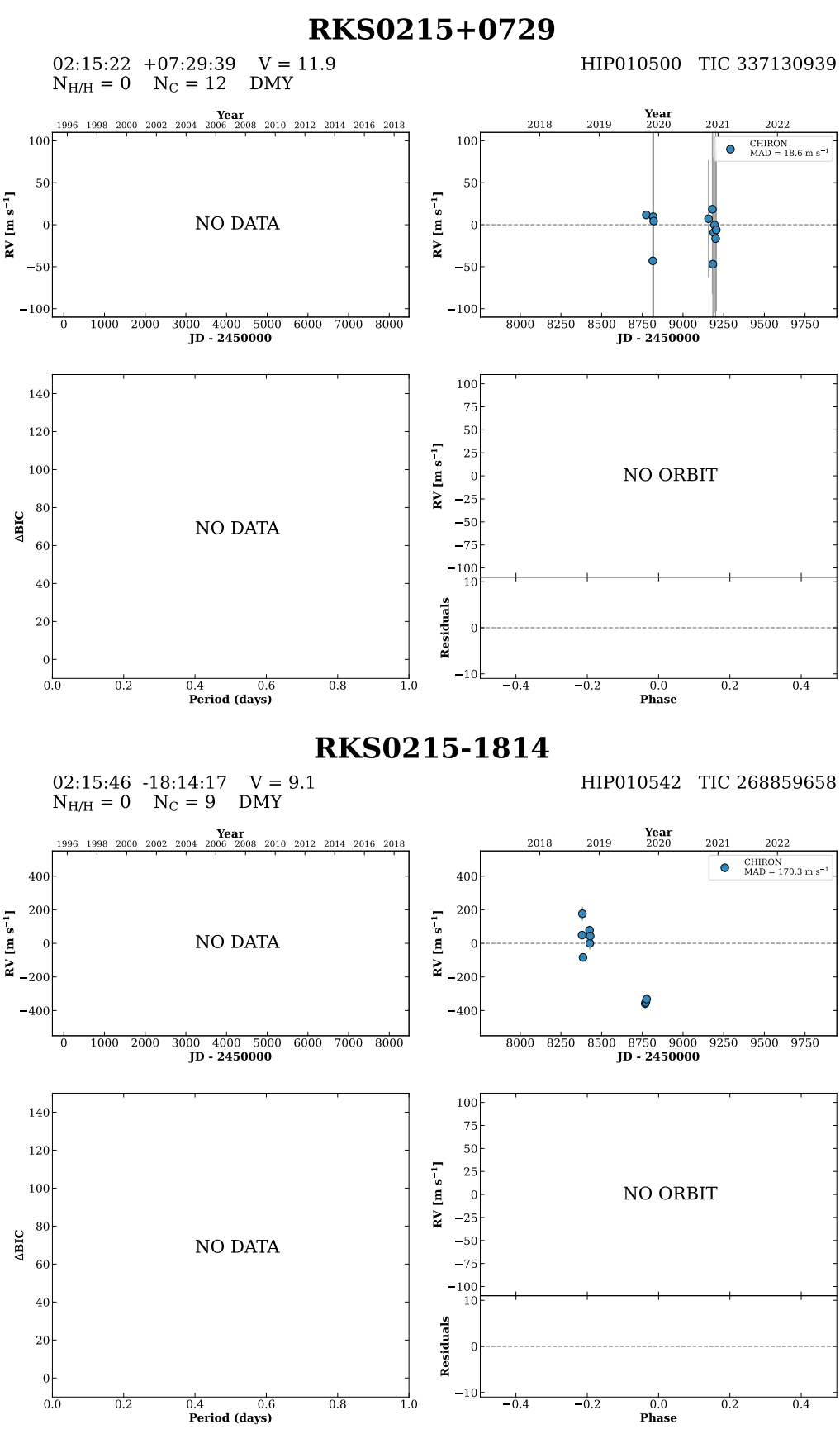

Figure 41 RV results for RKS0215+0729 (top) and RKS0215-1814 (bottom).

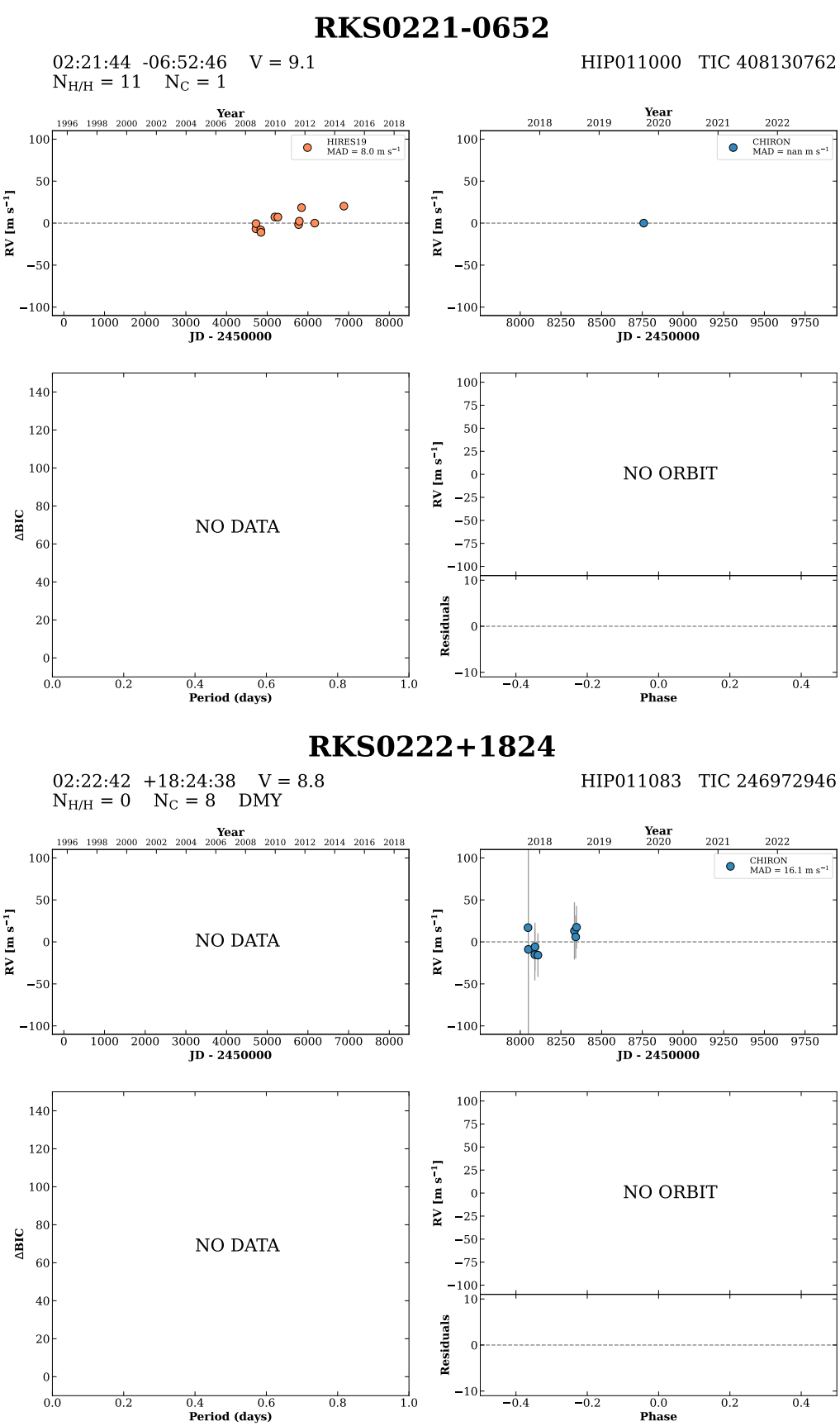

Figure 42 RV results for RKS0221-0652 (top) and RKS0222+1824 (bottom).

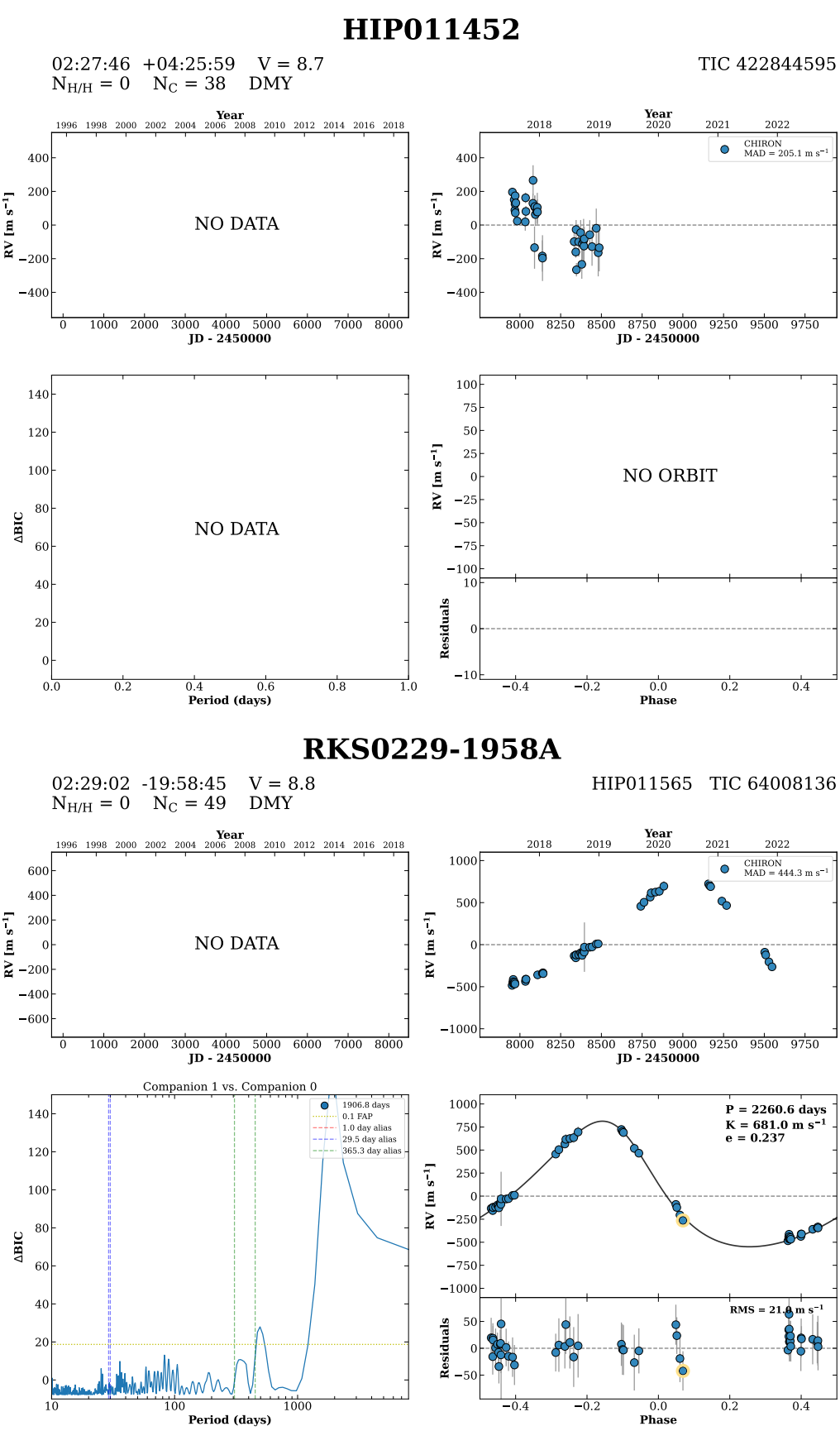

Figure 43 RV results for HIP011452 (top) and RKS0229-1958A (bottom).

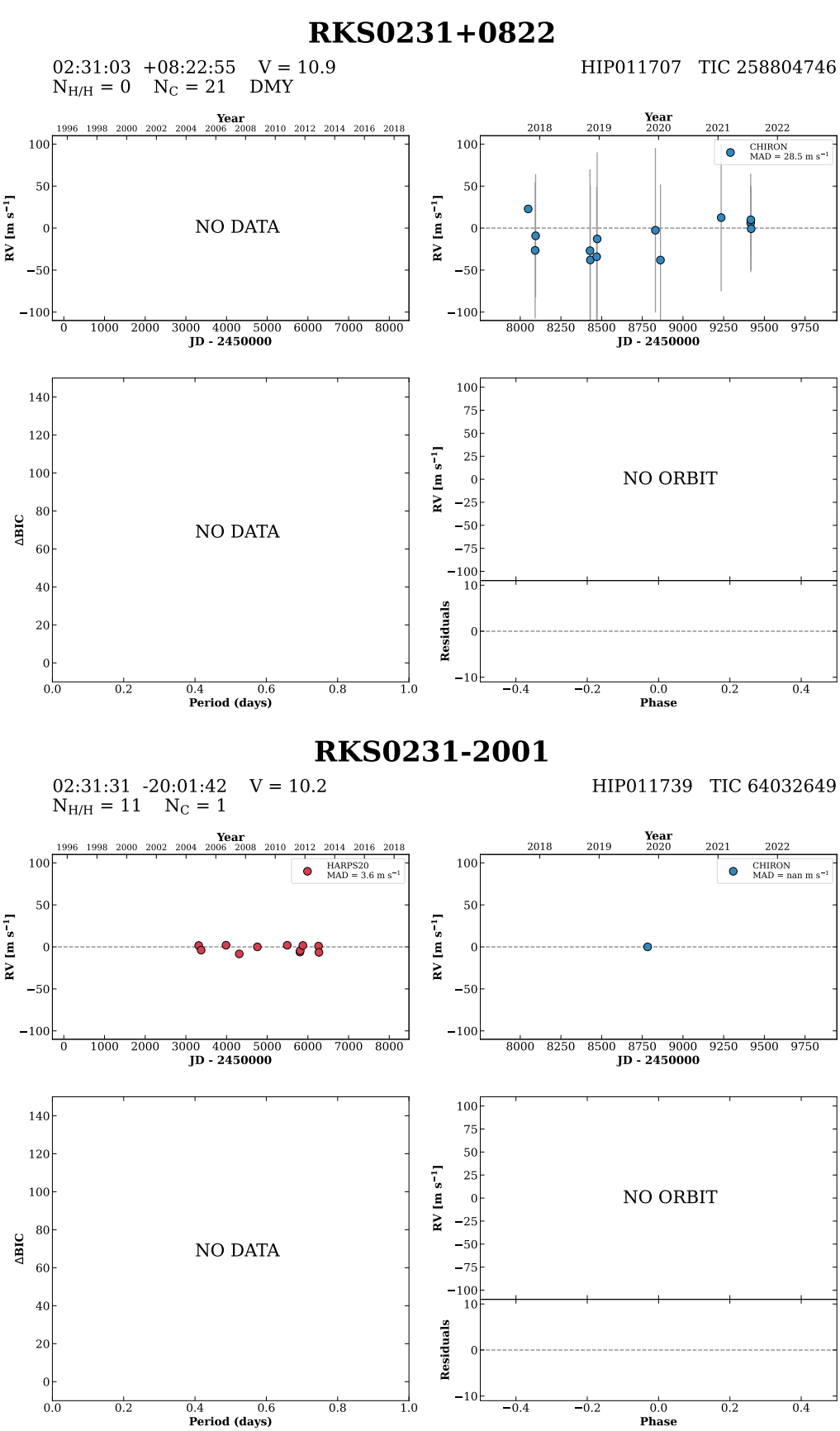

Figure 44 RV results for RKS0231+0822 (top) and RKS0231-2001 (bottom).

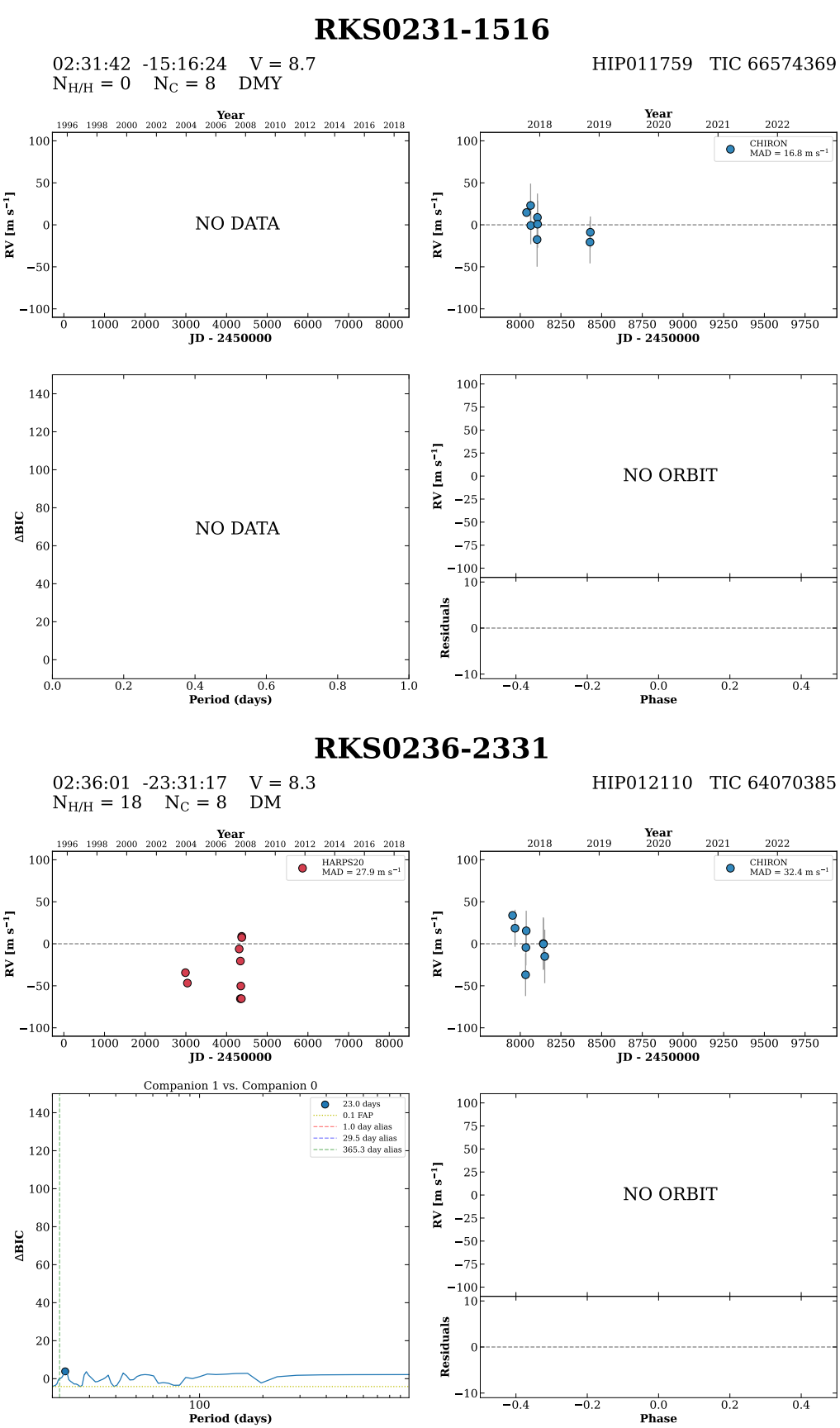

Figure 45 RV results for RKS0231-1516 (top) and RKS0236-2331 (bottom).

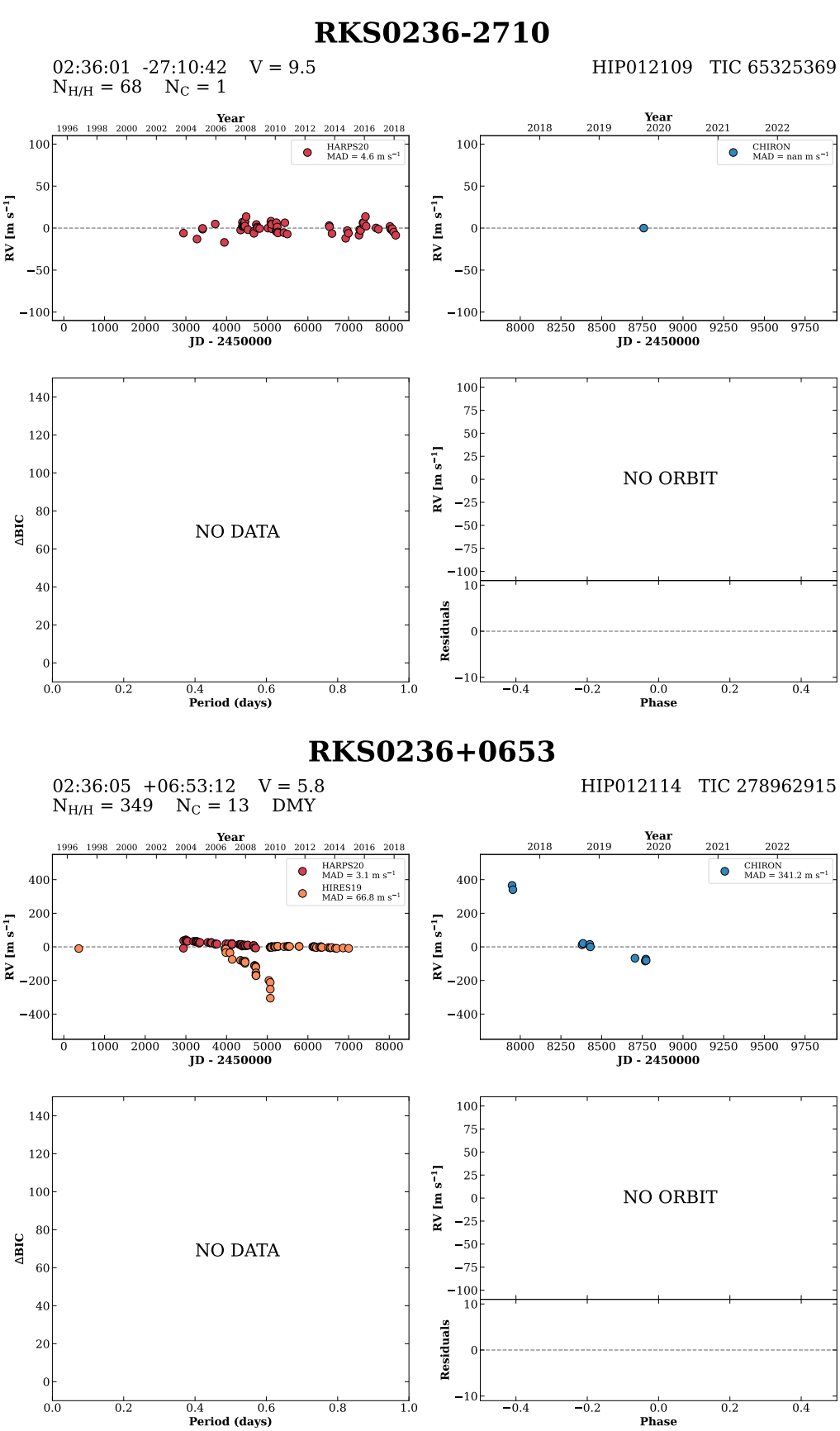

Figure 46 RV results for RKS0236-2710 (top) and RKS0236+0653 (bottom).

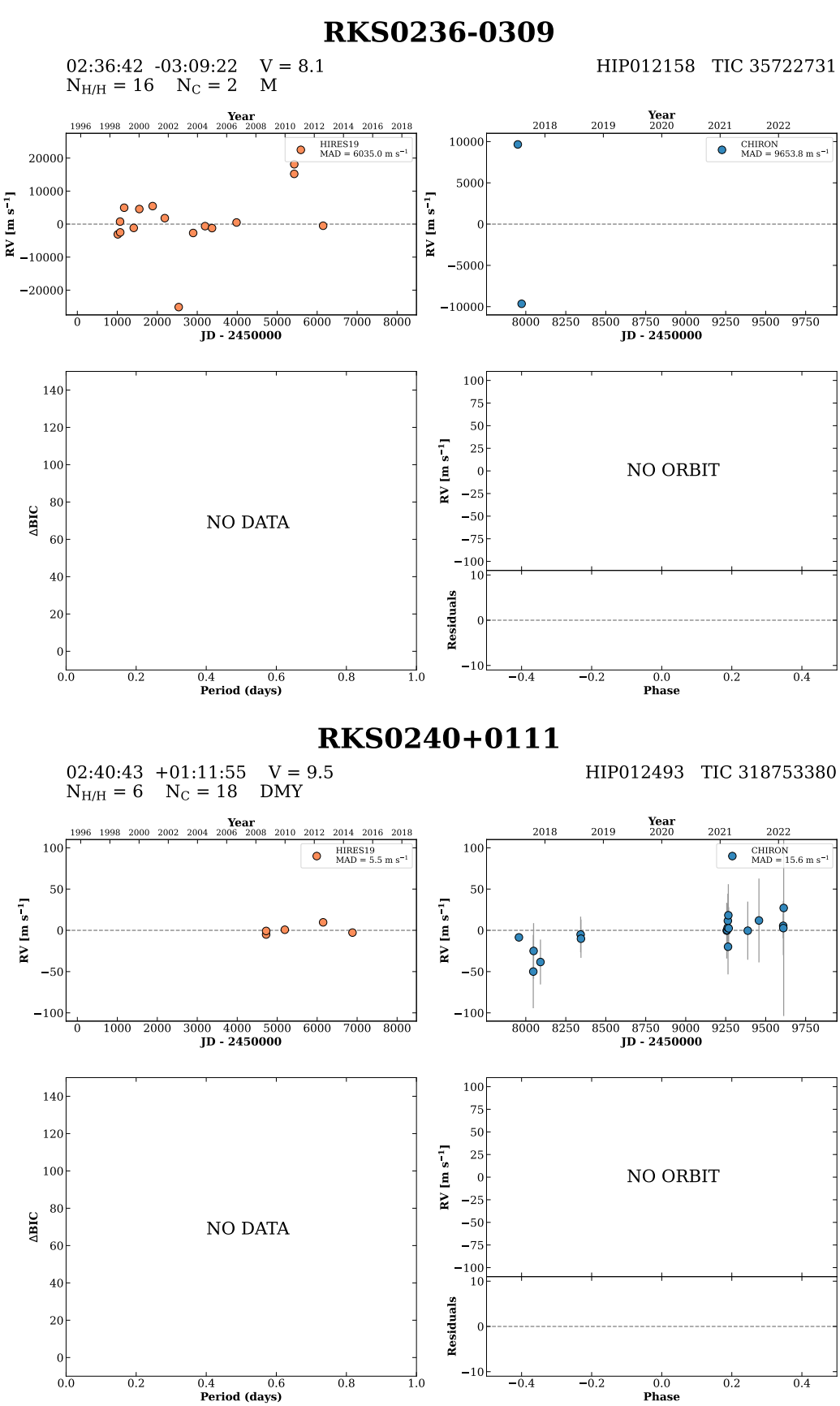

Figure 47 RV results for RKS0236-0309 (top) and RKS0240+0111 (bottom).

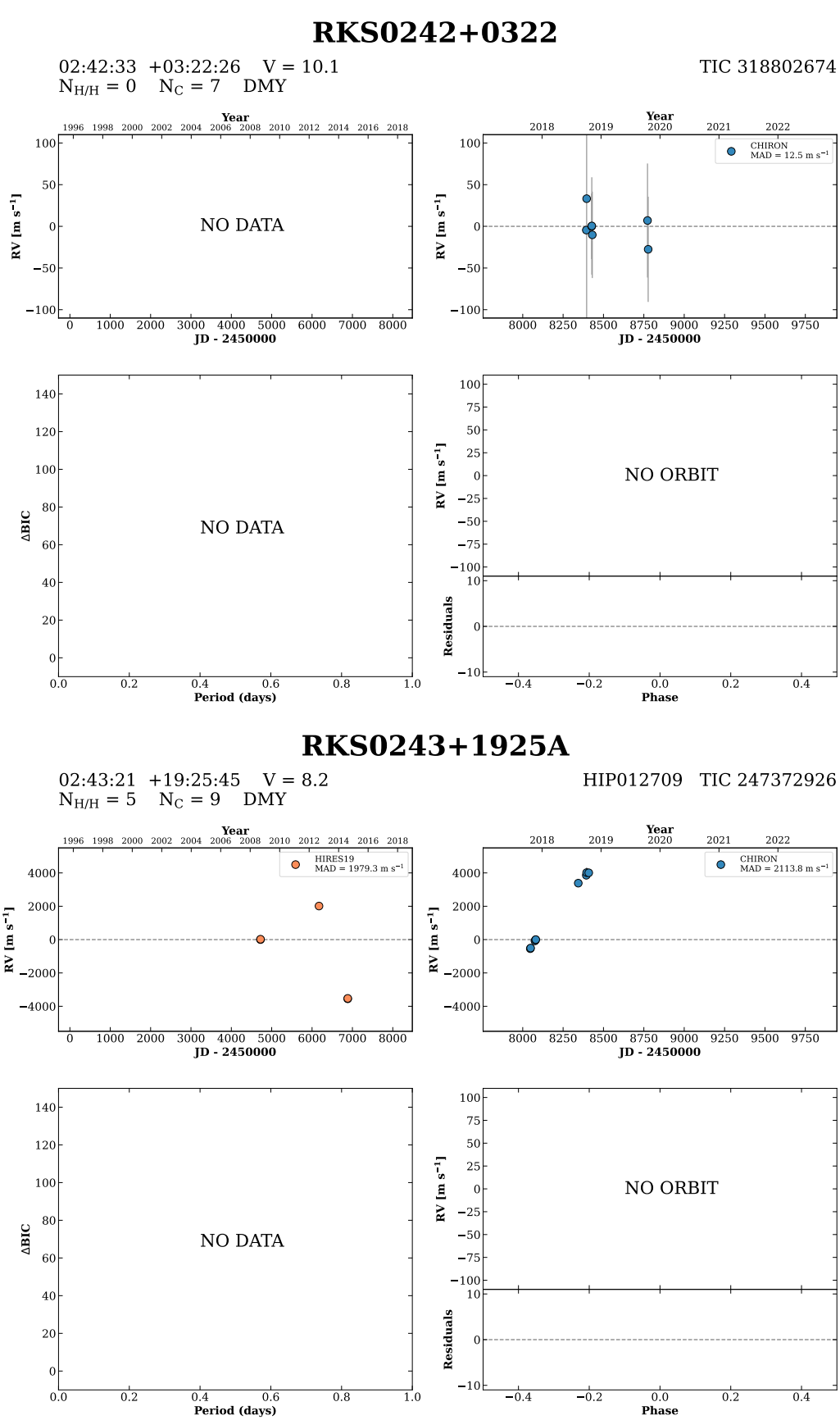

Figure 48 RV results for RKS0242+0322 (top) and RKS0243+1925A (bottom).

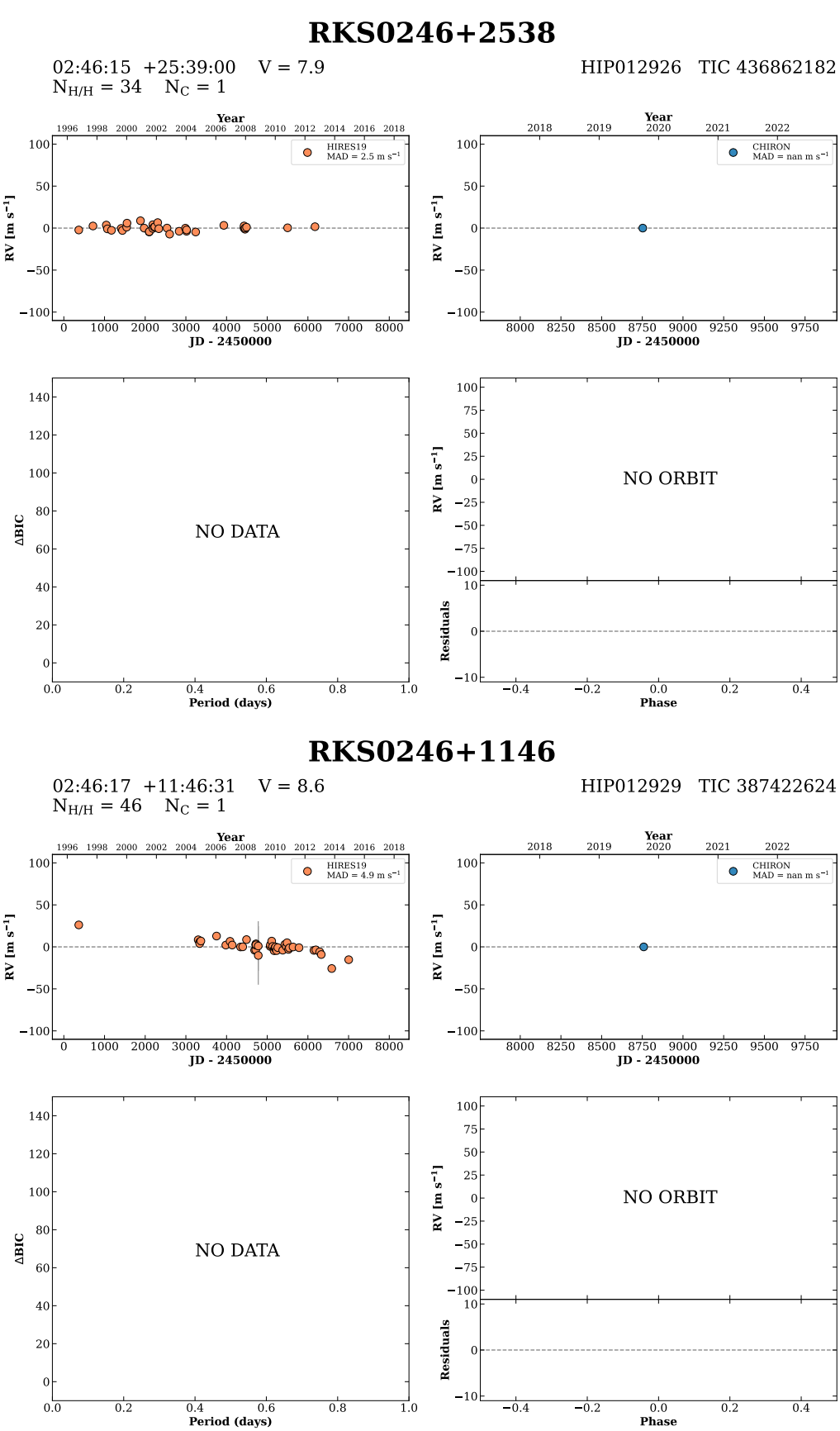

Figure 49 RV results for RKS0246+2538 (top) and RKS0246+1146 (bottom).

RKS0246-2305

02:46:43 -23:05:12 V = 10.2 HIP012961 TIC 204614039
$N_{H/H}$ = 48 N_C = 6 DM

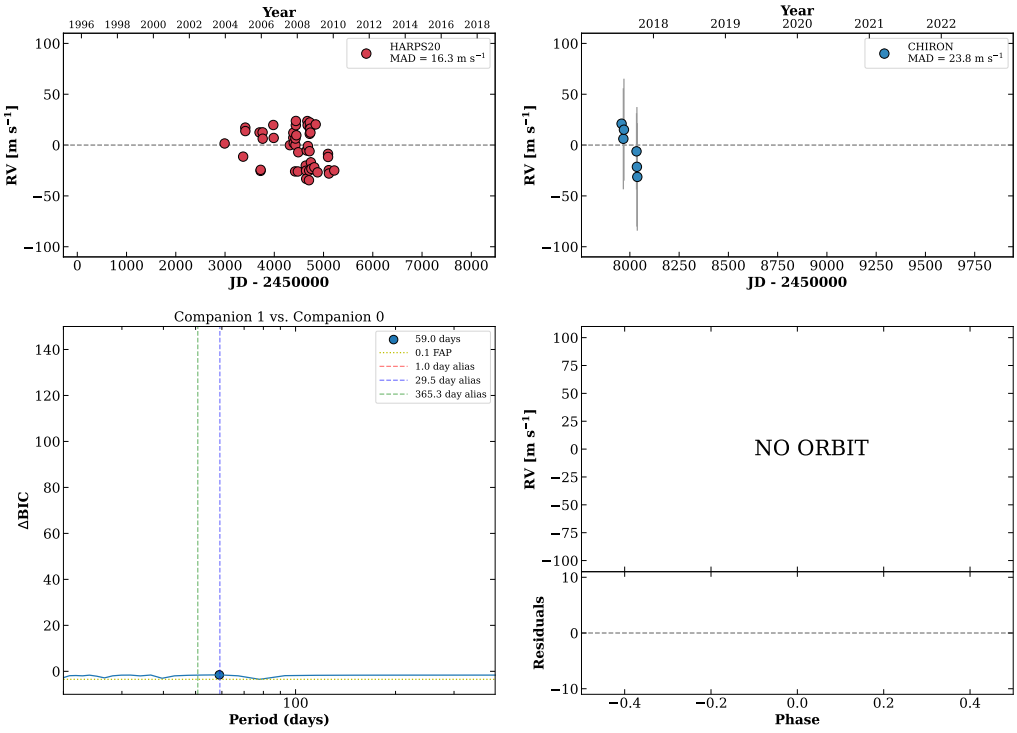

RKS0247+2842

02:47:56 +28:42:44 V = 11.1 HIP013065 TIC 397367857
$N_{H/H}$ = 0 N_C = 9 DMY

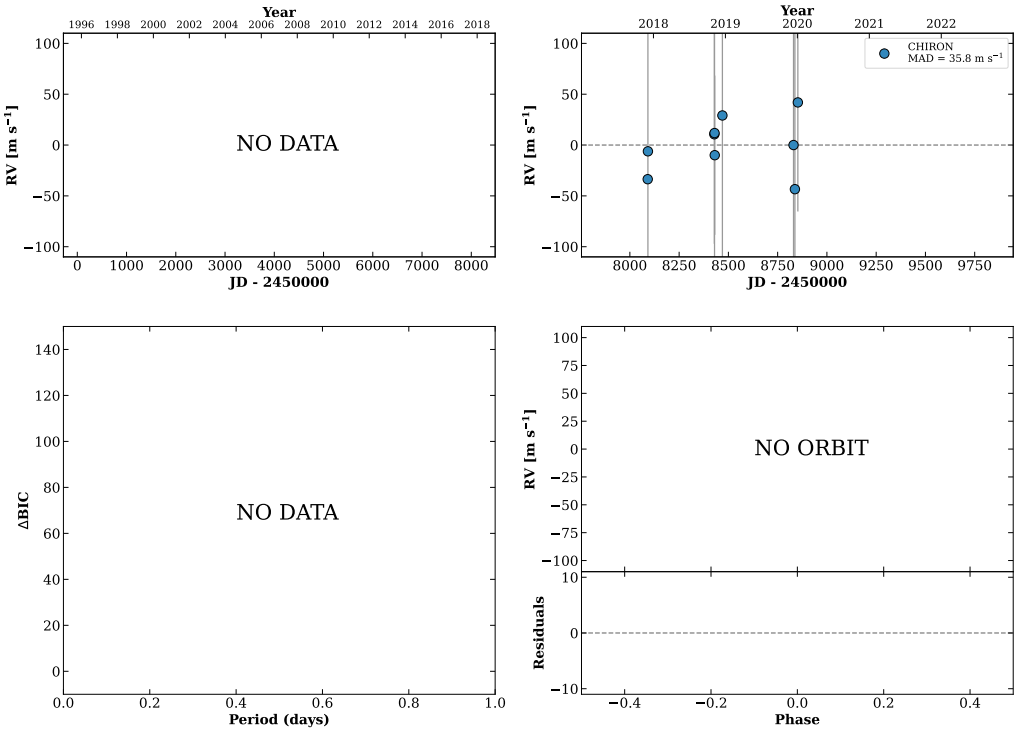

Figure 50 RV results for RKS0246-2305 (top) and RKS0247+2842 (bottom).

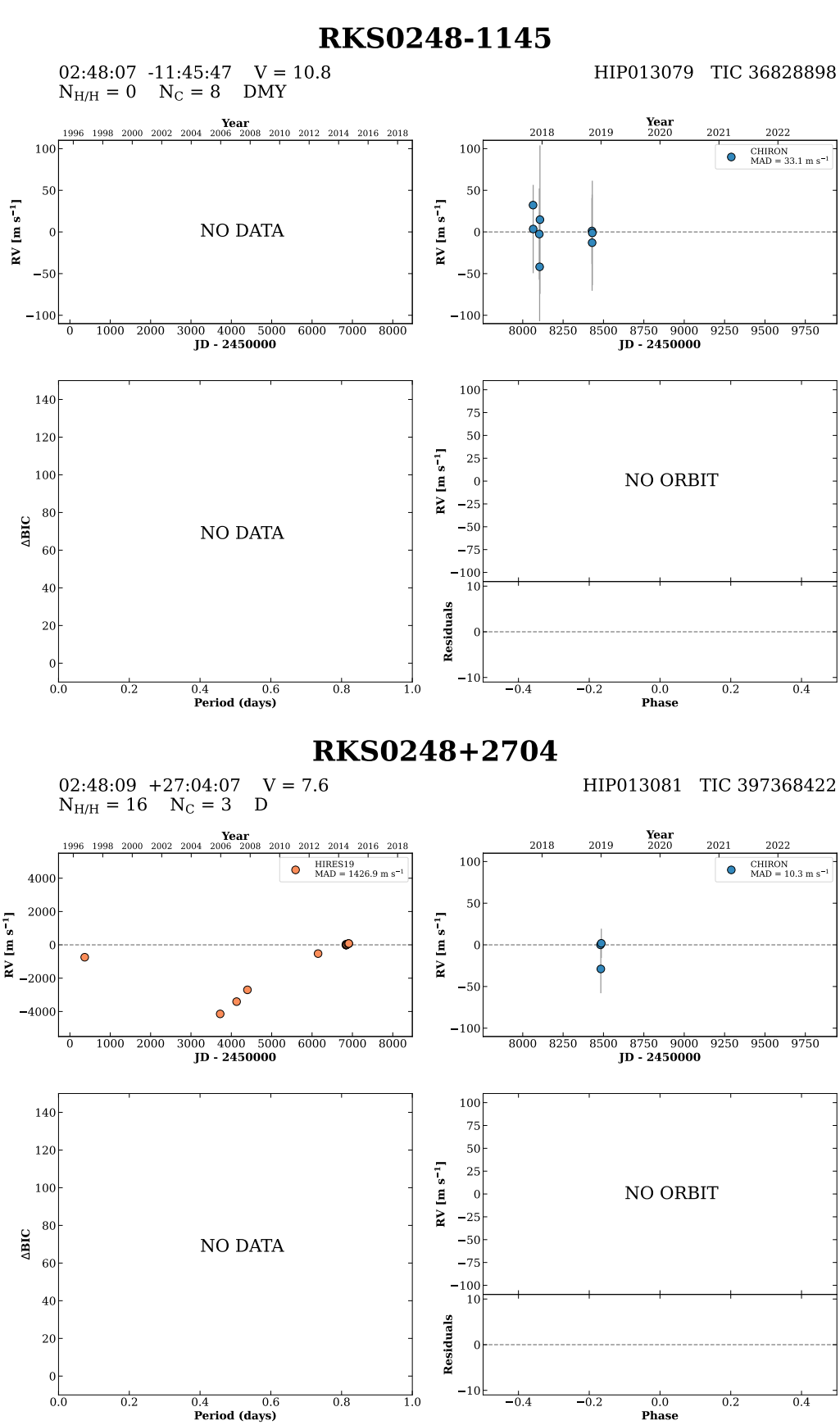

Figure 51 RV results for RKS0248-1145 (top) and RKS0248+2704 (bottom).

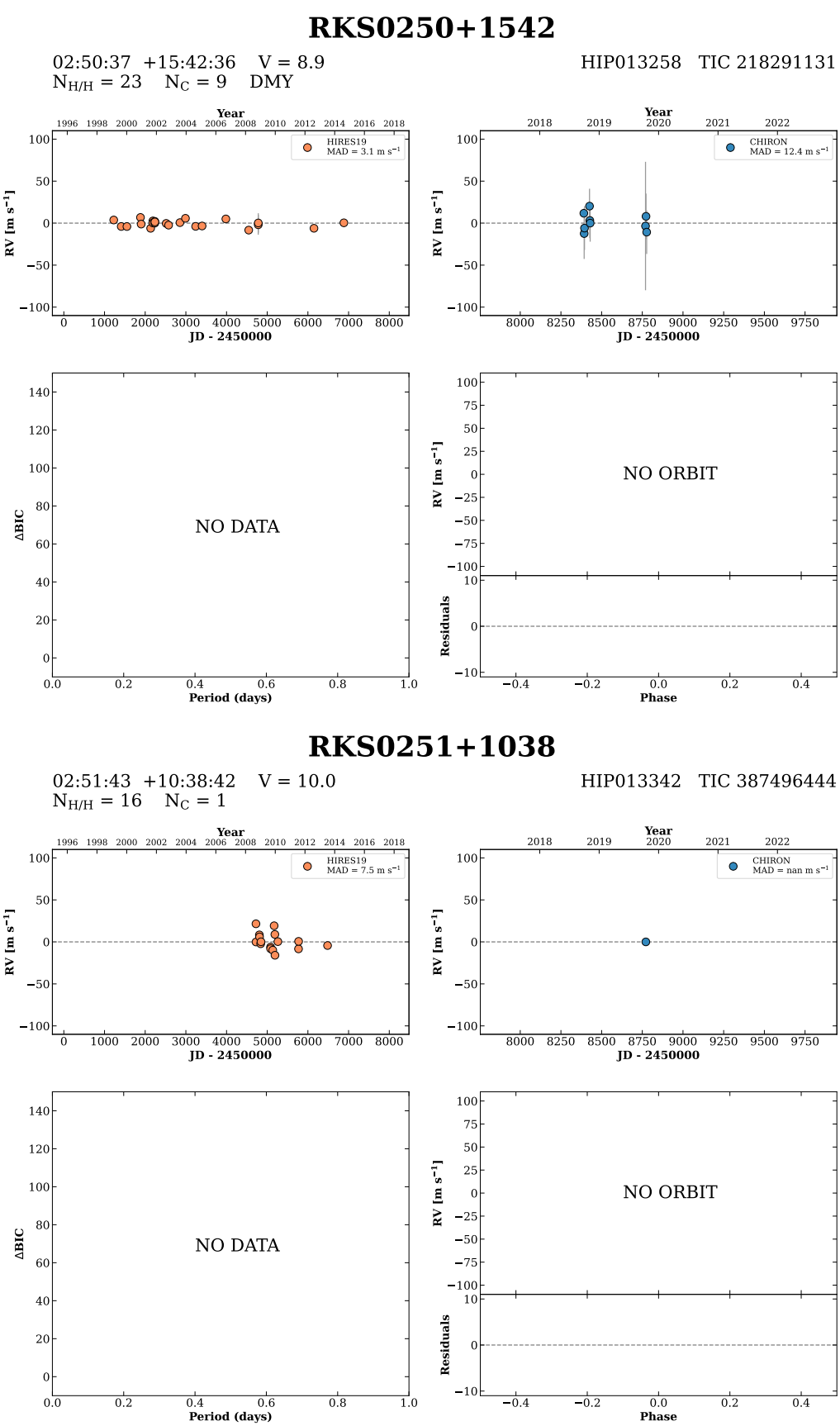

Figure 52 RV results for RKS0250+1542 (top) and RKS0251+1038 (bottom).

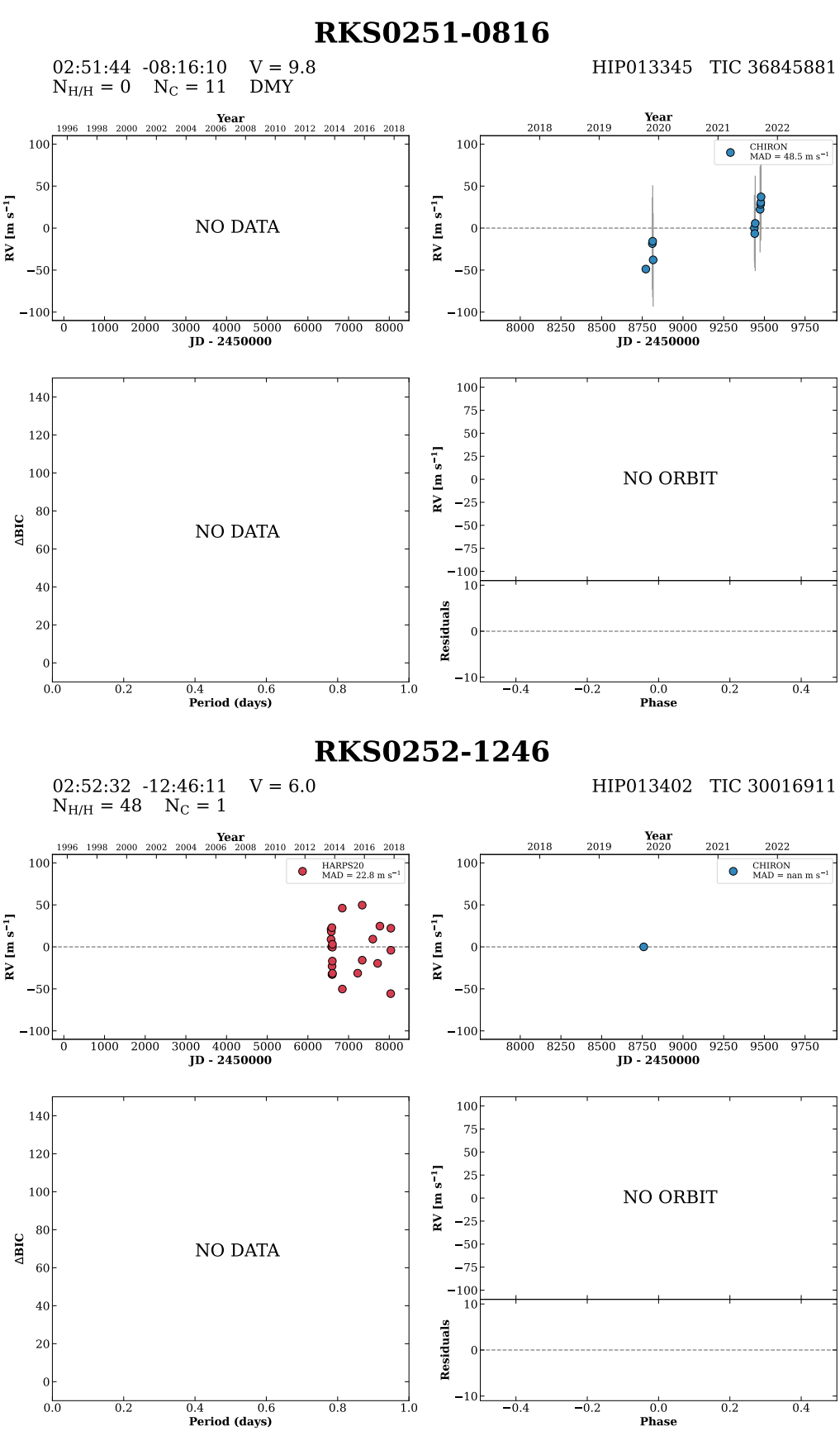

Figure 53 RV results for RKS0251-0816 (top) and RKS0252-1246 (bottom).

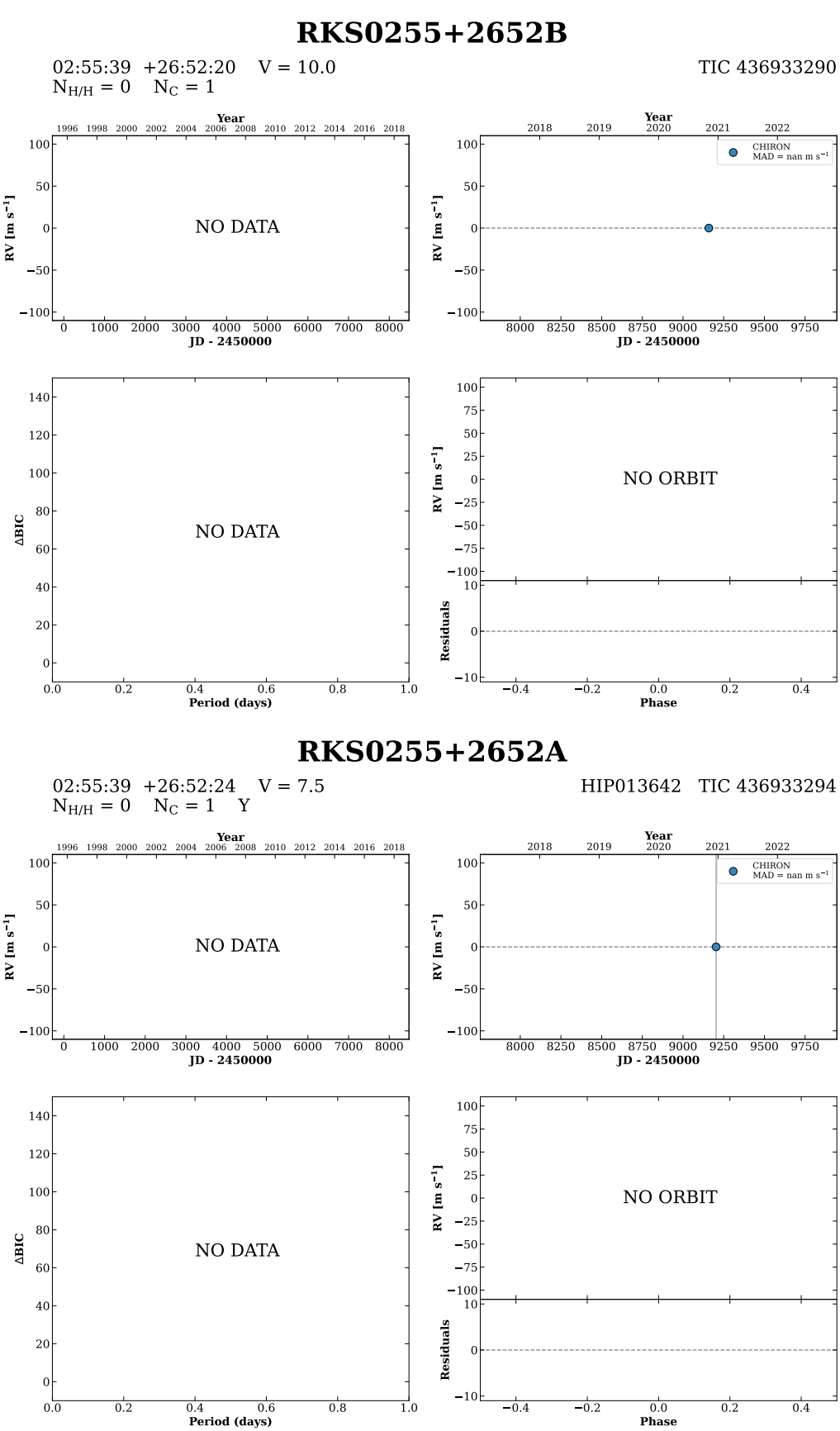

Figure 54 RV results for RKS0255+2652B (top) and RKS0255+2652A (bottom).

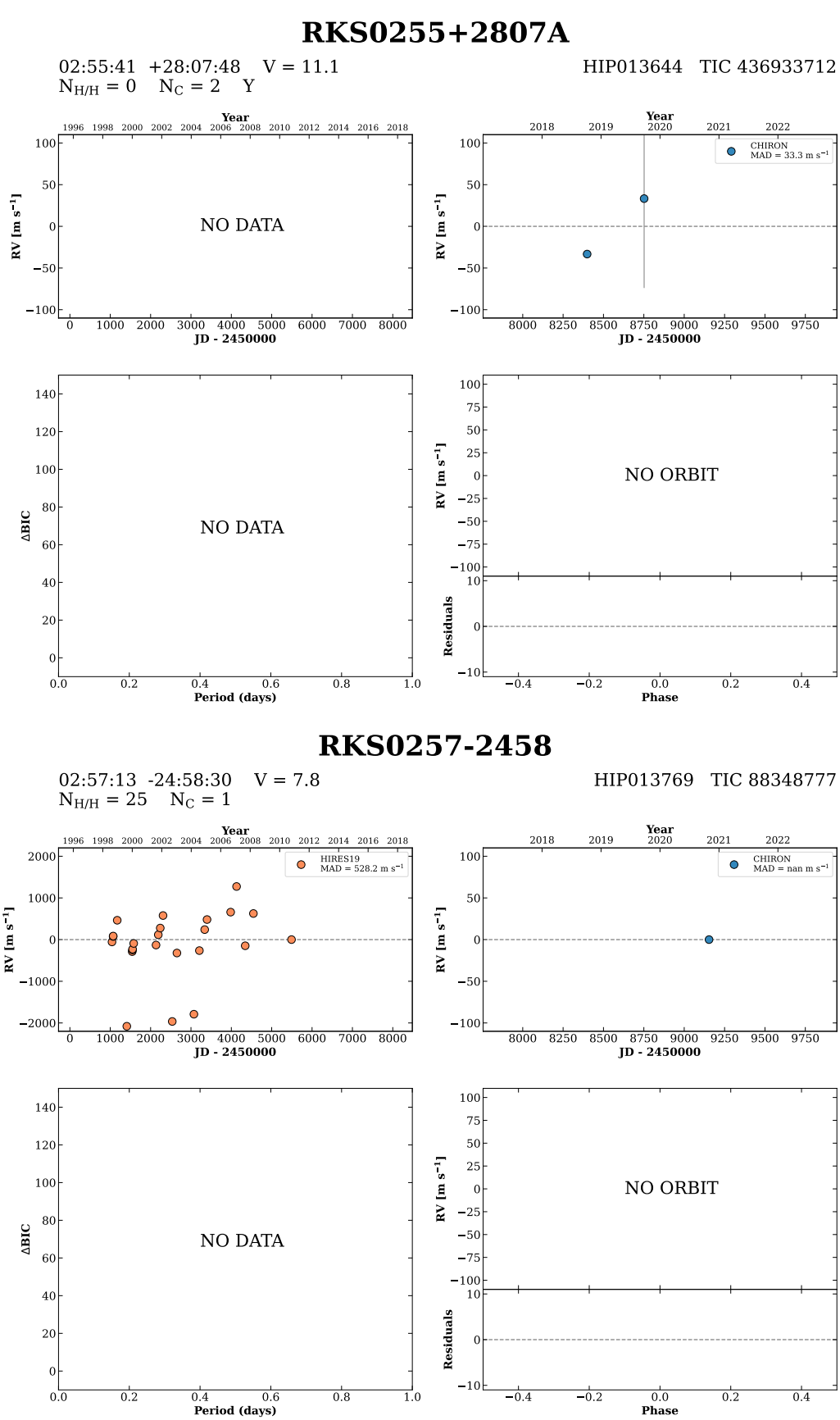

Figure 55 RV results for RKS0255+2807A (top) and RKS0257-2458 (bottom).

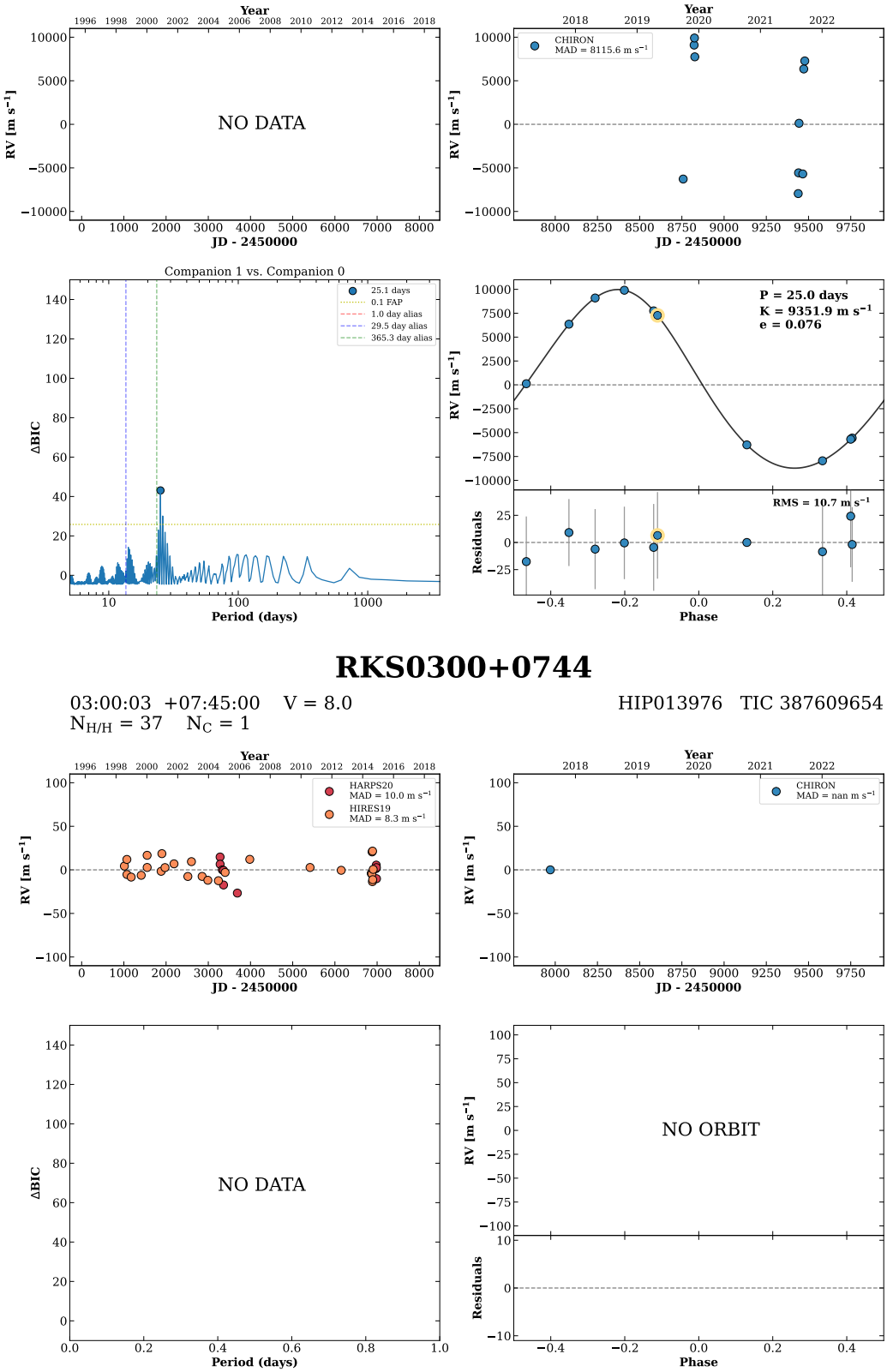

Figure 56 RV results for RKS0258+2646 (top) and RKS0300+0744 (bottom).

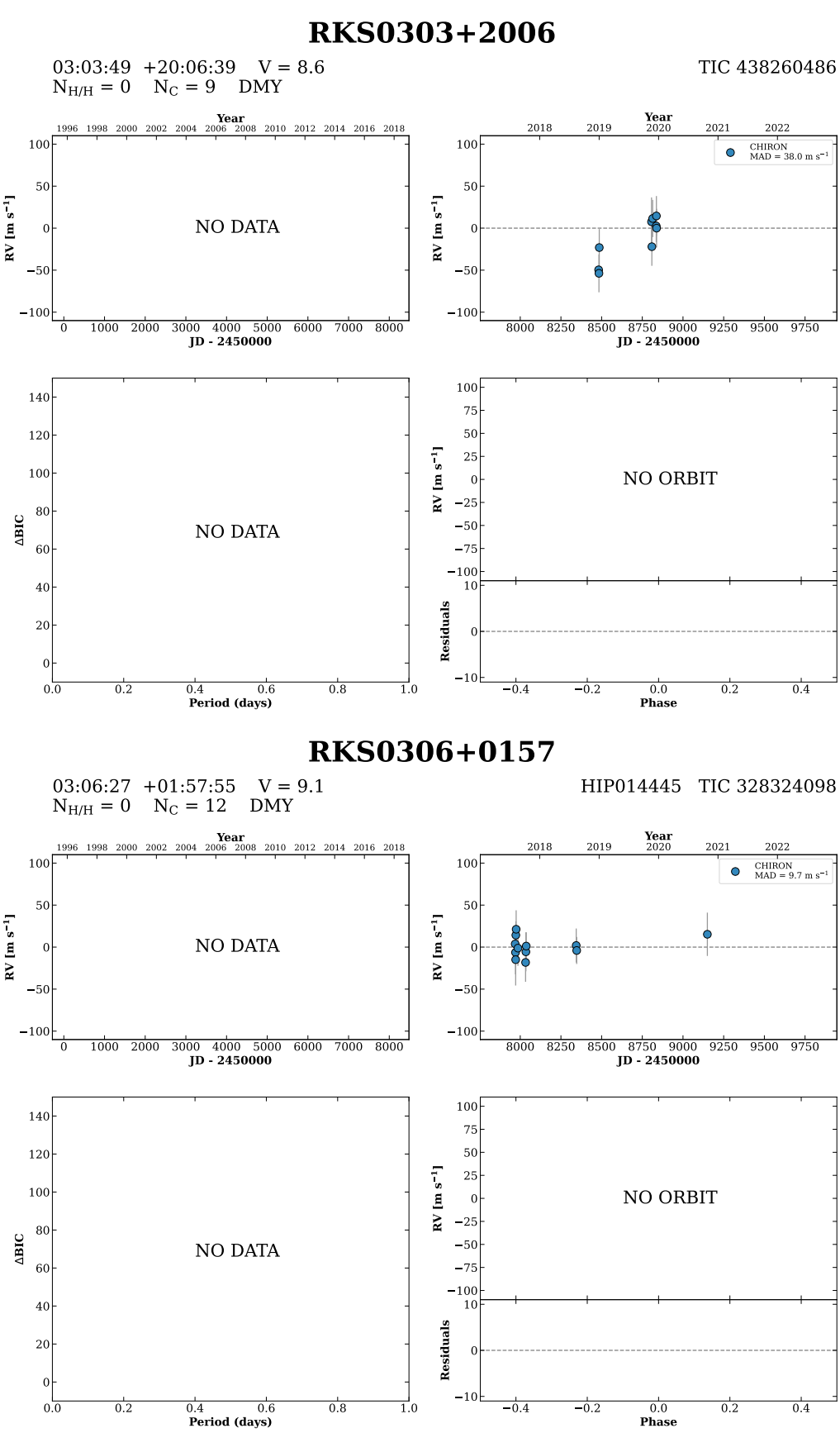

Figure 57 RV results for RKS0303+2006 (top) and RKS0306+0157 (bottom).

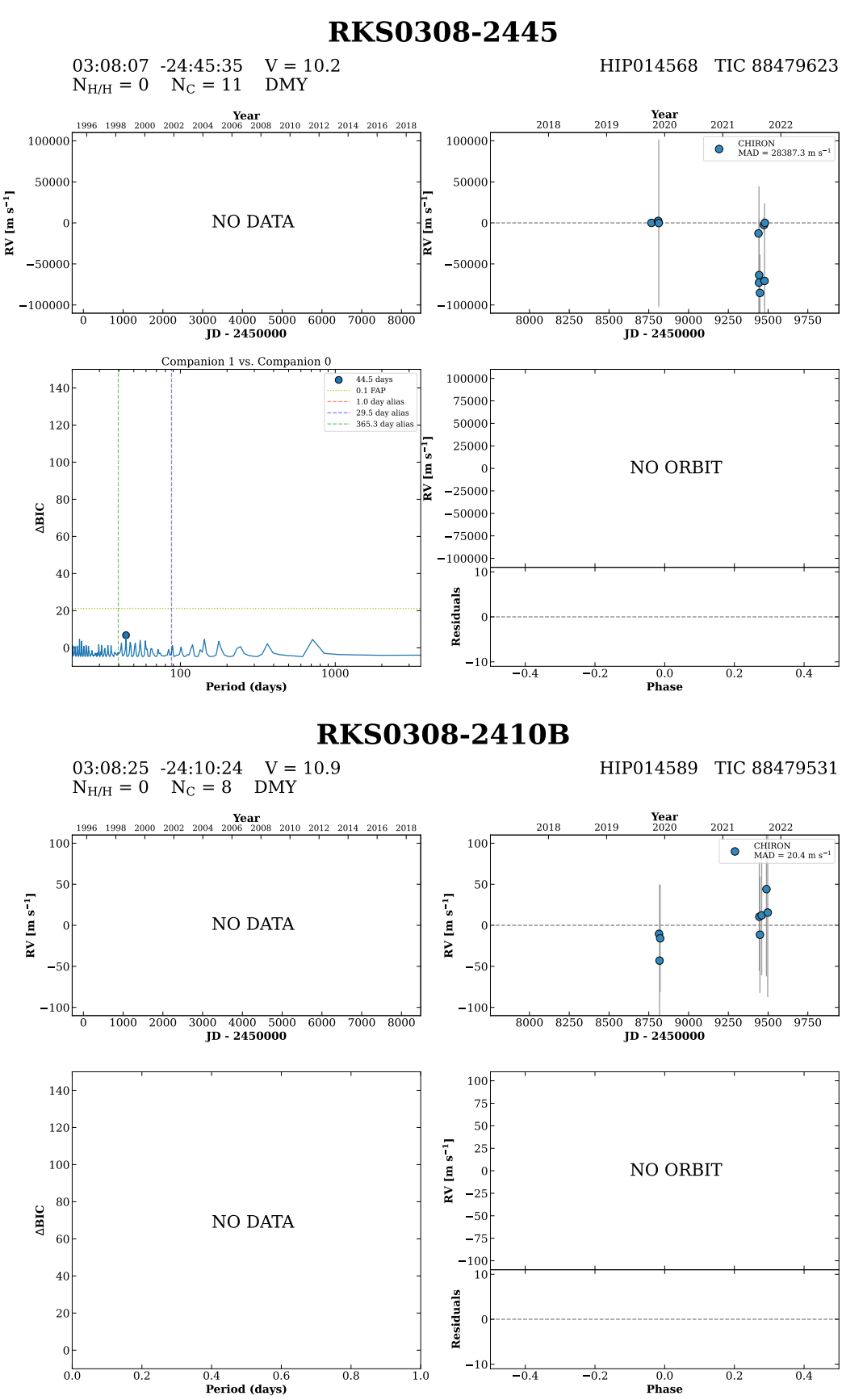

Figure 58 RV results for RKS0308-2445 (top) and RKS0308-2410B (bottom).

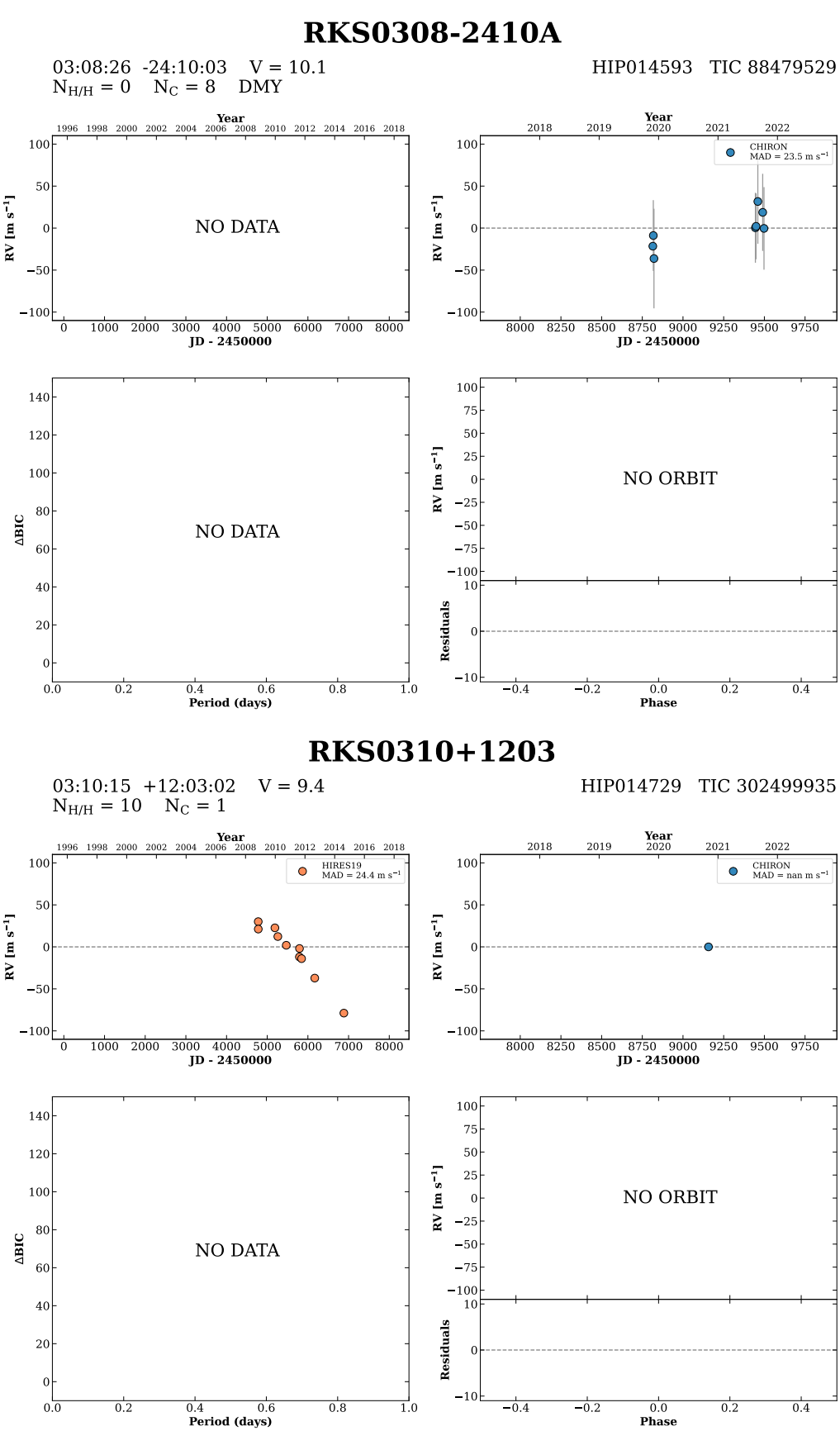

Figure 59 RV results for RKS0308-2410A (top) and RKS0310+1203 (bottom).

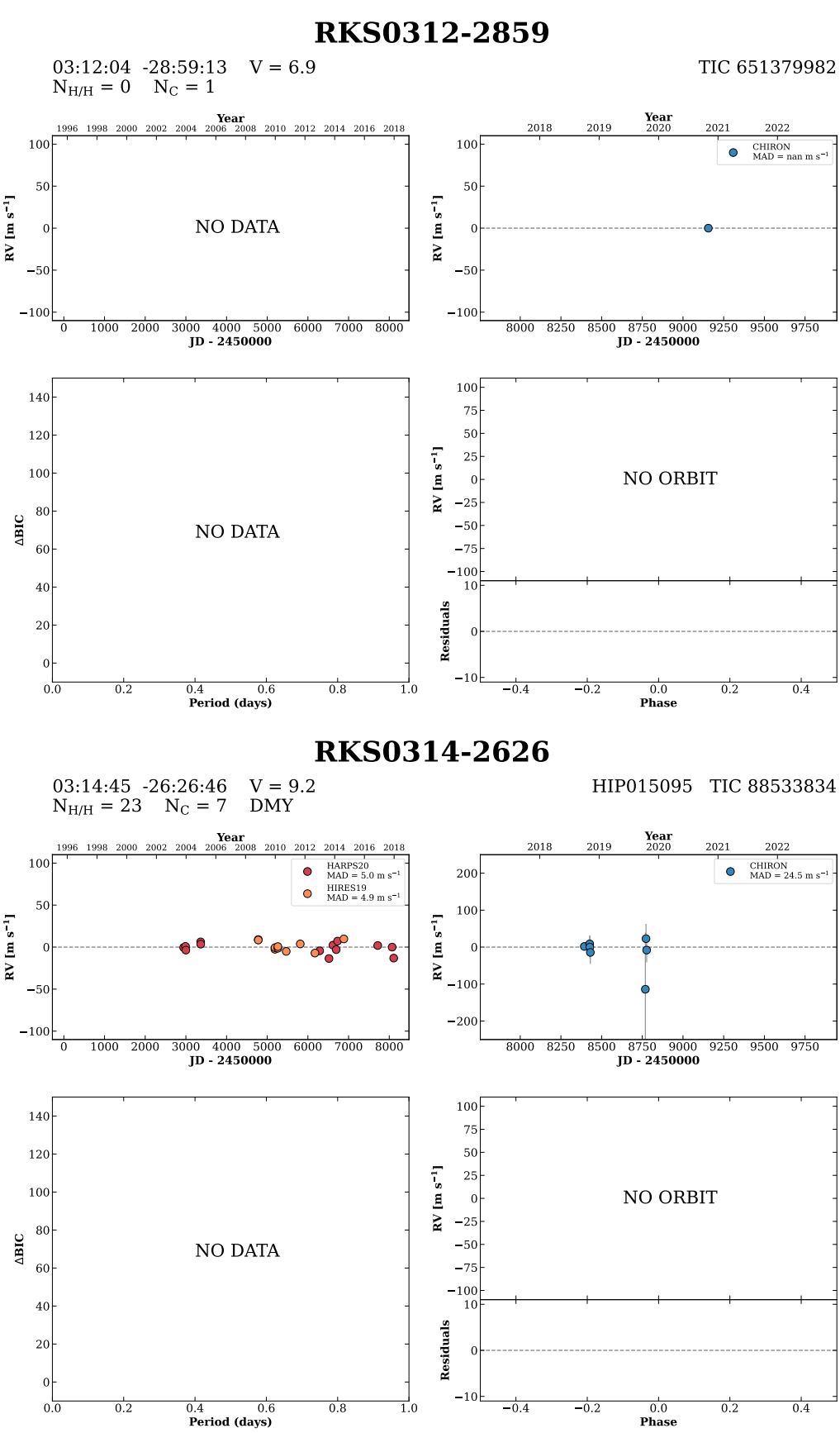

Figure 60 RV results for RKS0312-2859 (top) and RKS0314-2626 (bottom).

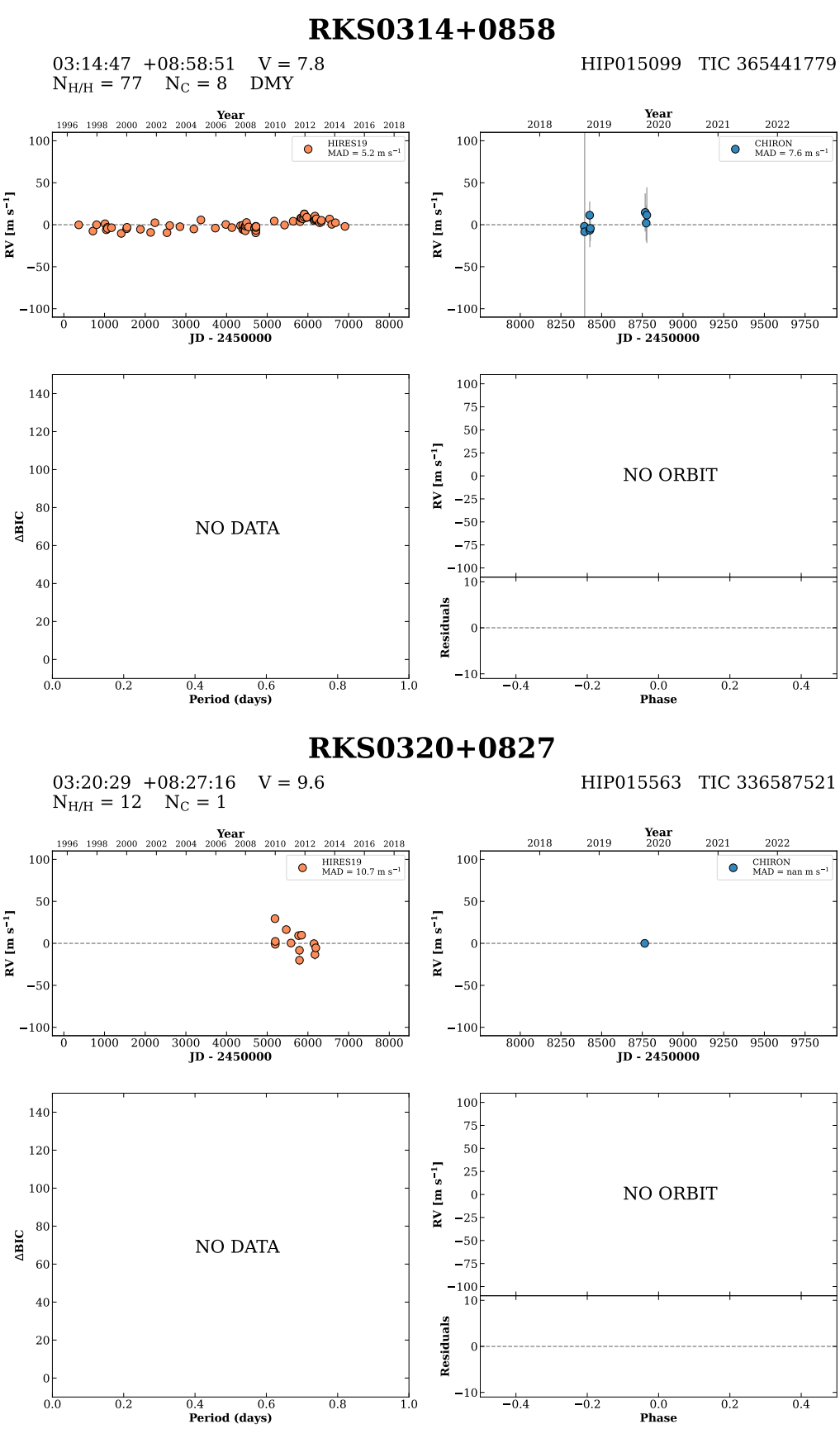

Figure 61 RV results for RKS0314+0858 (top) and RKS0320+0827 (bottom).

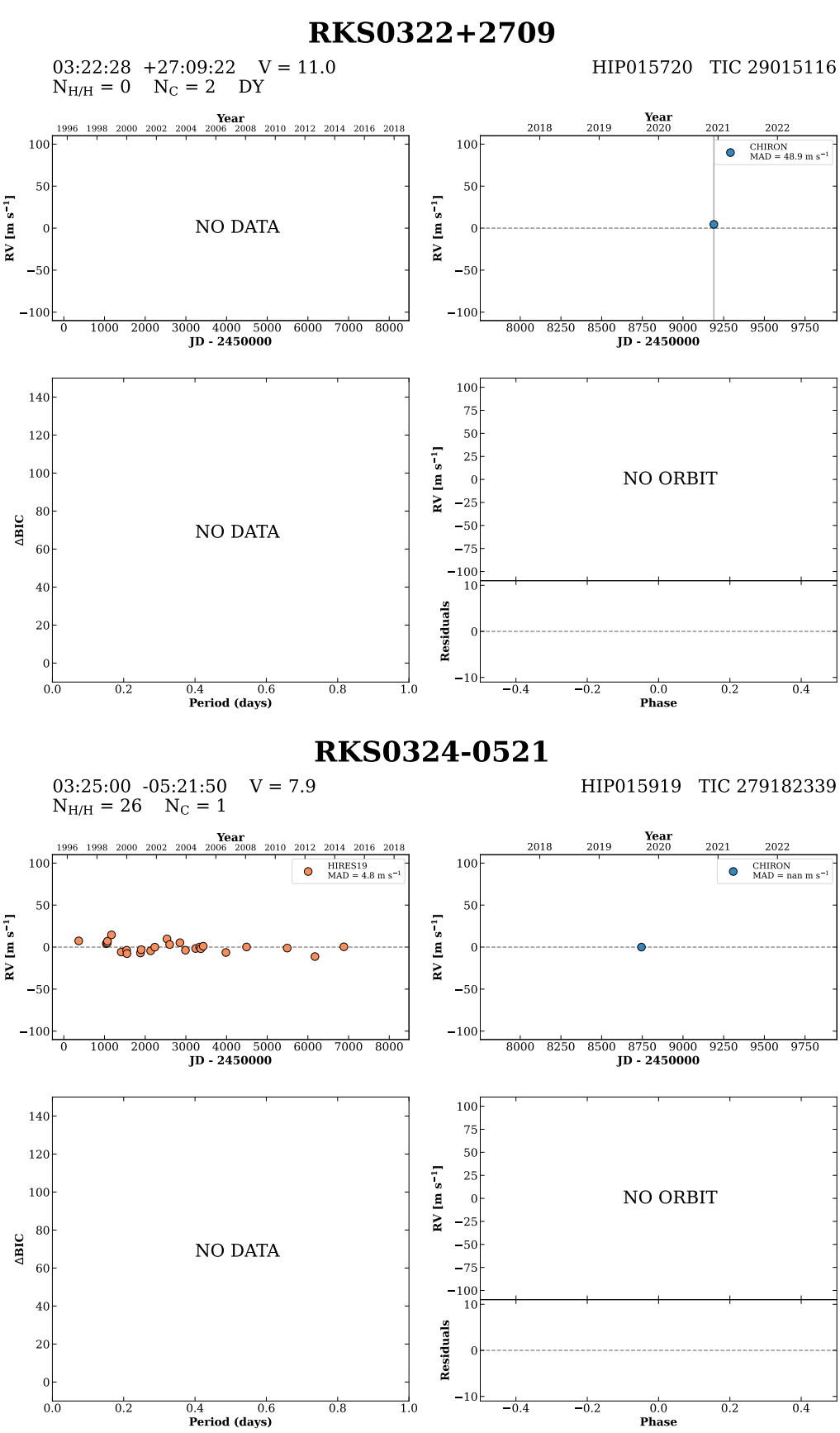

Figure 62 RV results for RKS0322+2709 (top) and RKS0324-0521 (bottom).

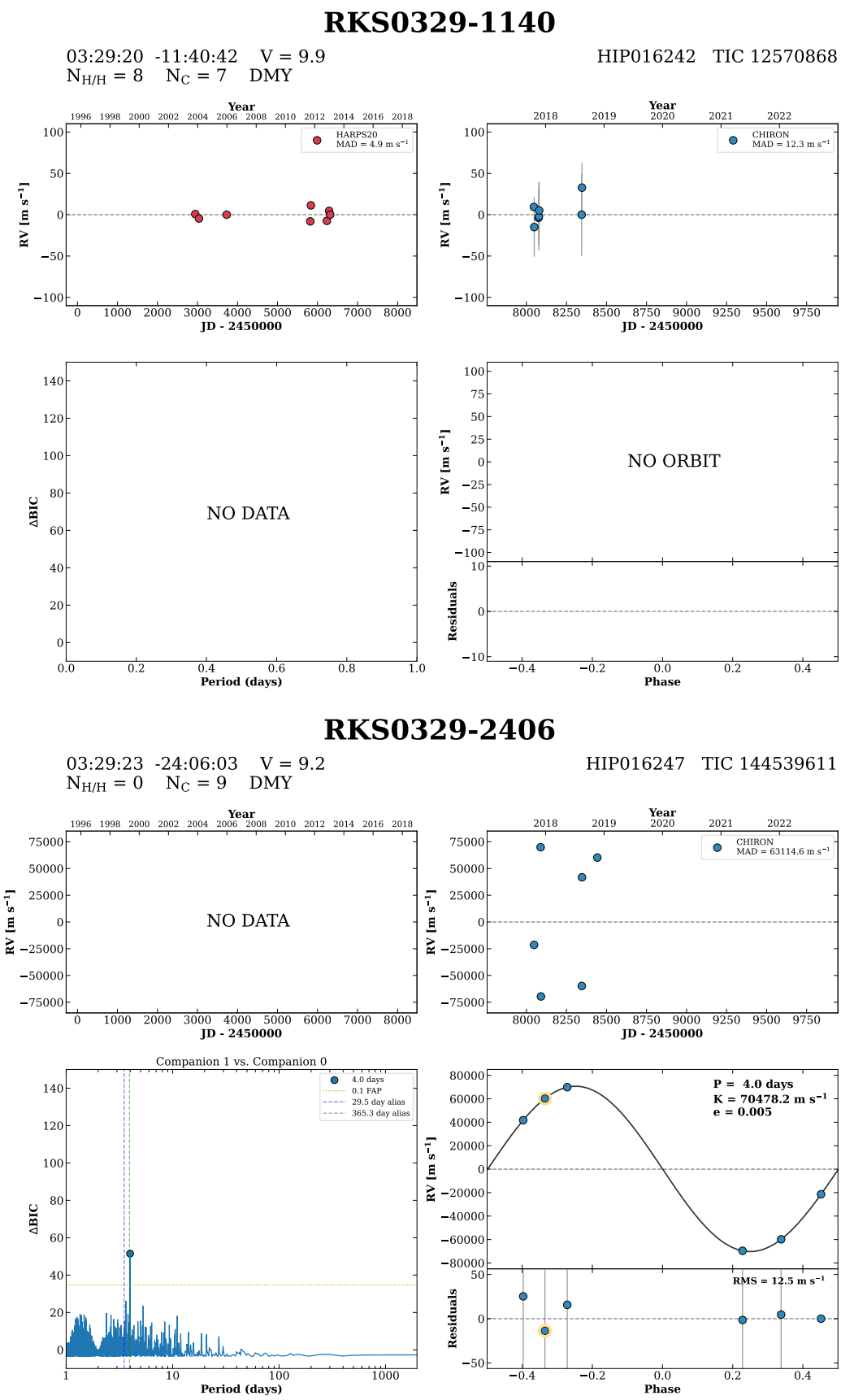

Figure 63 RV results for RKS0329-1140 (top) and RKS0329-2406 (bottom).

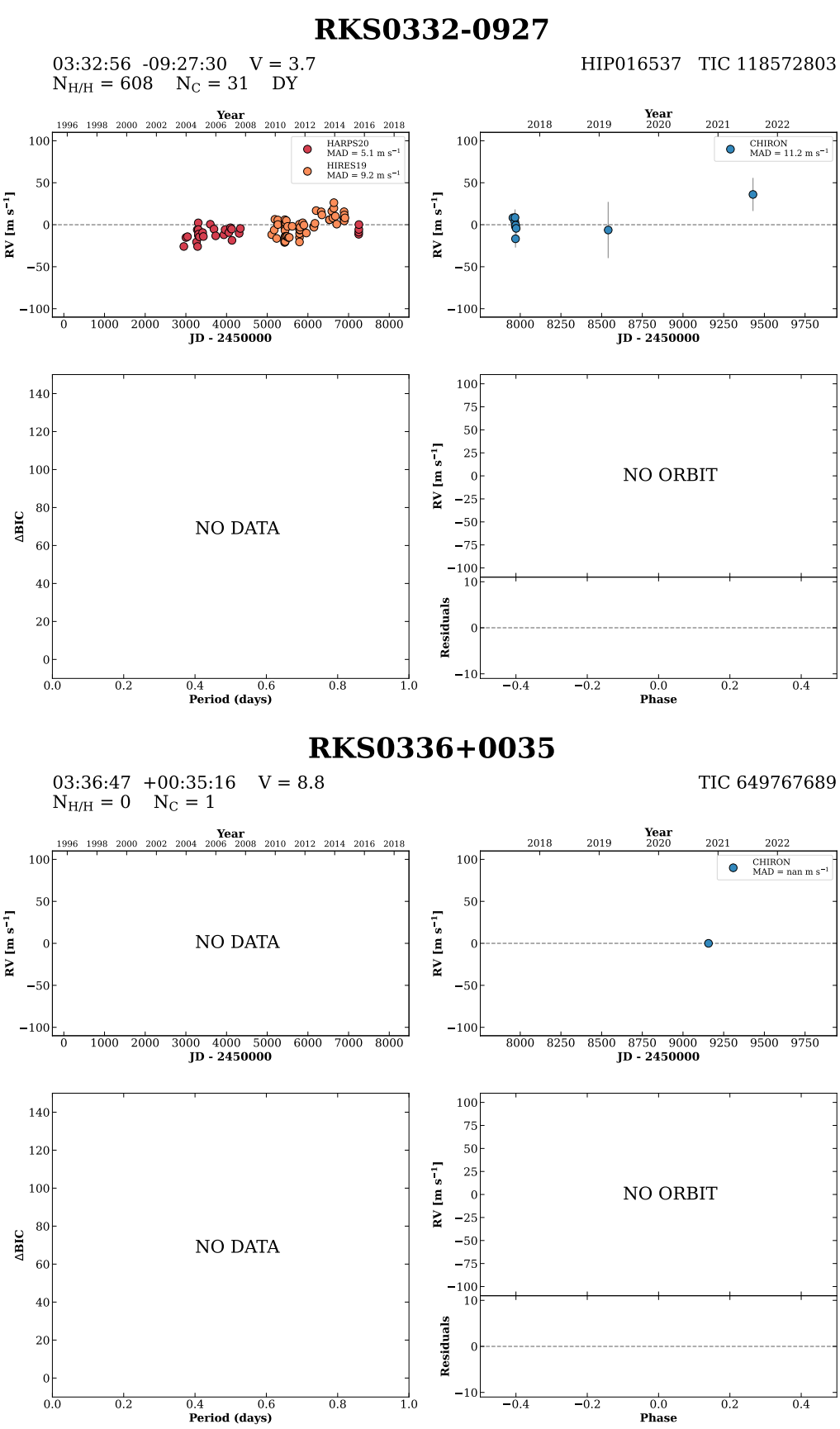

Figure 64 RV results for RKS0332-0927 (top) and RKS0336+0035 (bottom).

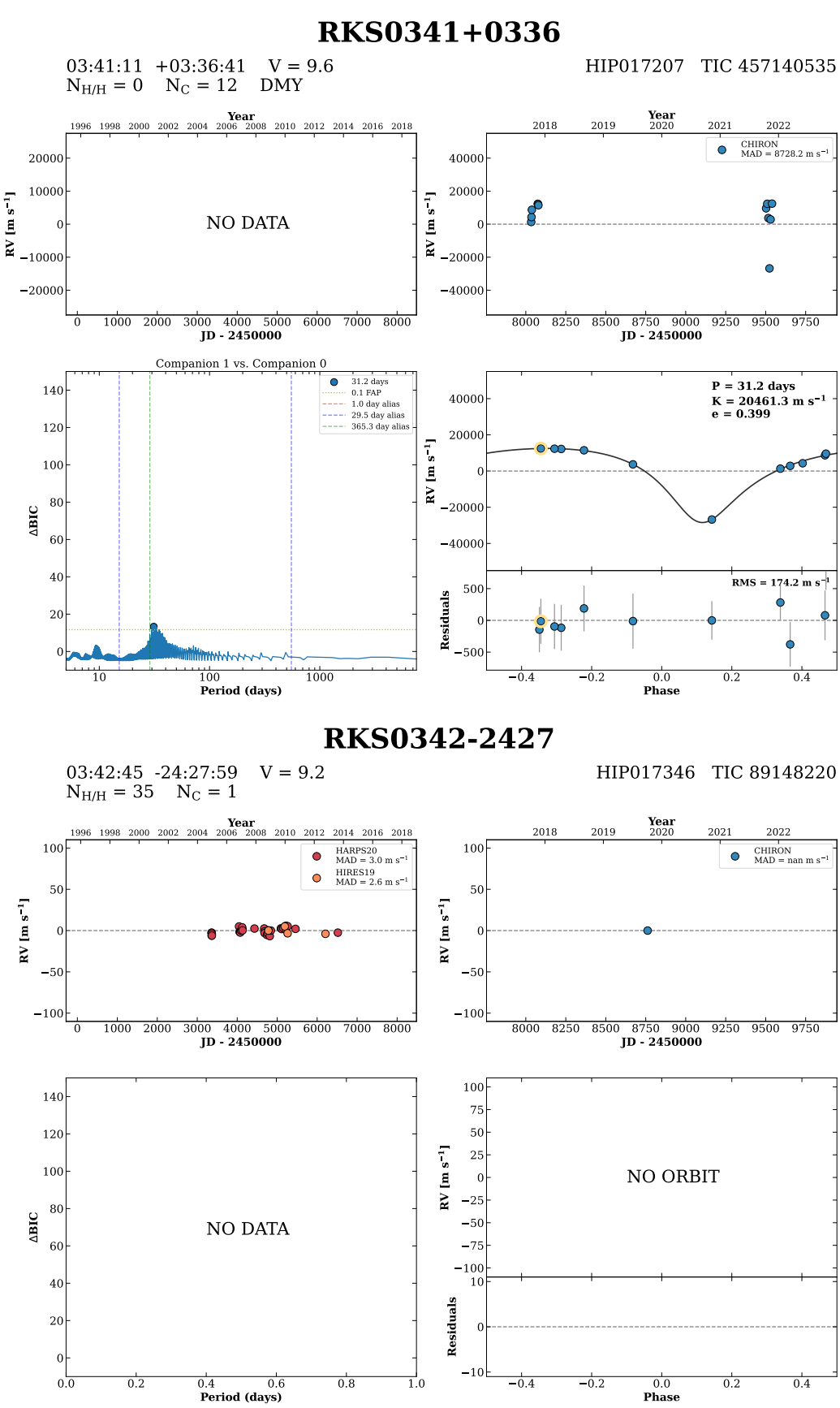

Figure 65 RV results for RKS0341+0336 (top) and RKS0342-2427 (bottom).

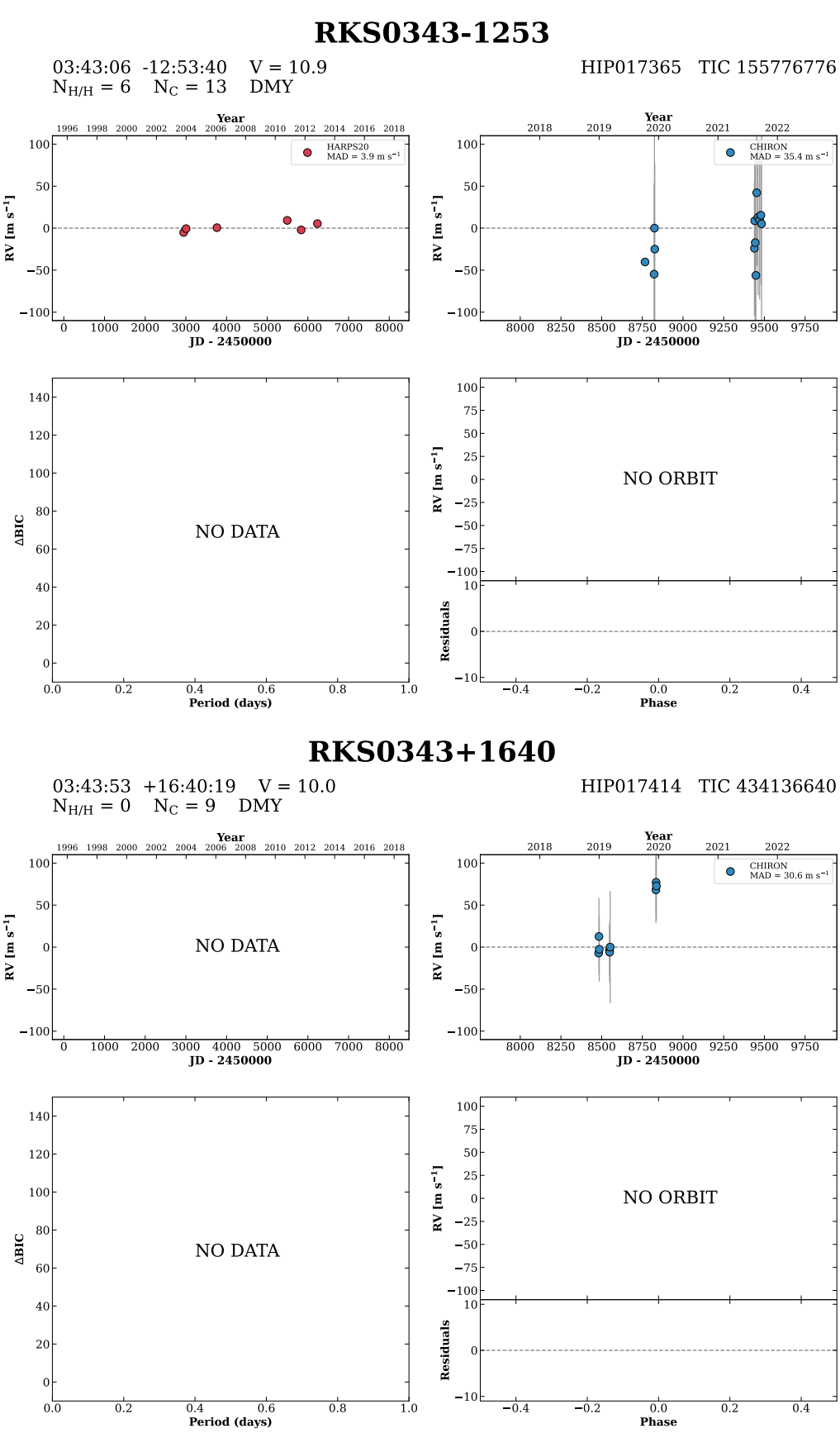

Figure 66 RV results for RKS0343-1253 (top) and RKS0343+1640 (bottom).

RKS0343-1906

03:43:55 -19:06:39 V = 7.1 HIP017420 TIC 121025936
$N_{H/H}$ = 110 N_C = 1

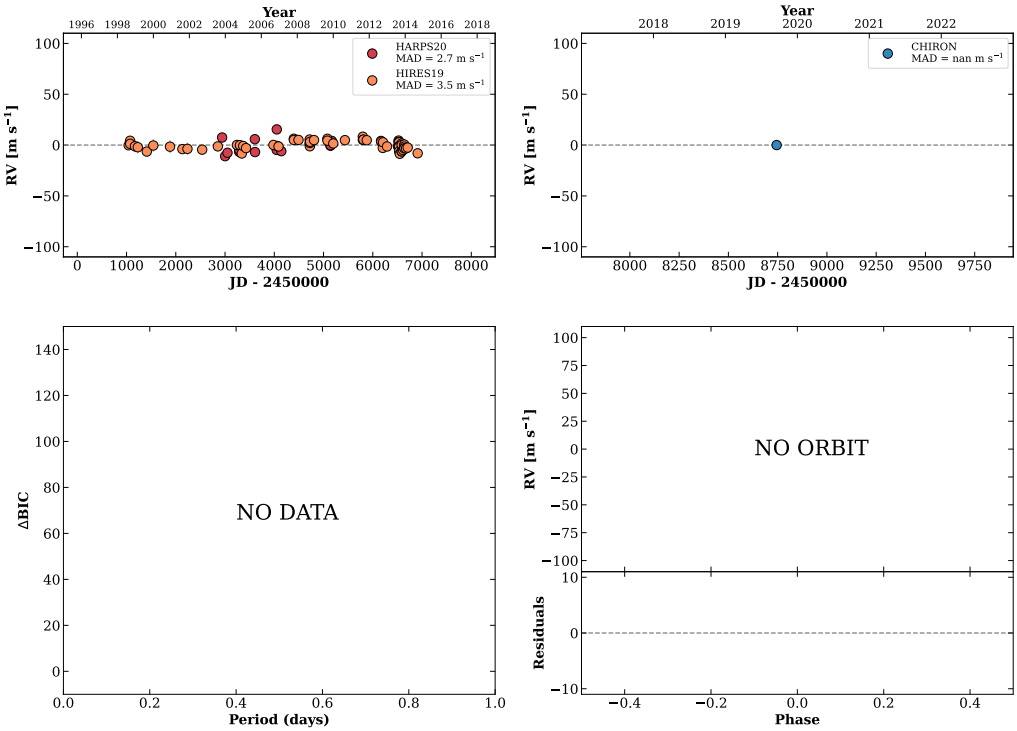

RKS0344+1155

03:44:51 +11:55:12 V = 9.2 HIP017496 TIC 434138790
$N_{H/H}$ = 4 N_C = 8 DMY

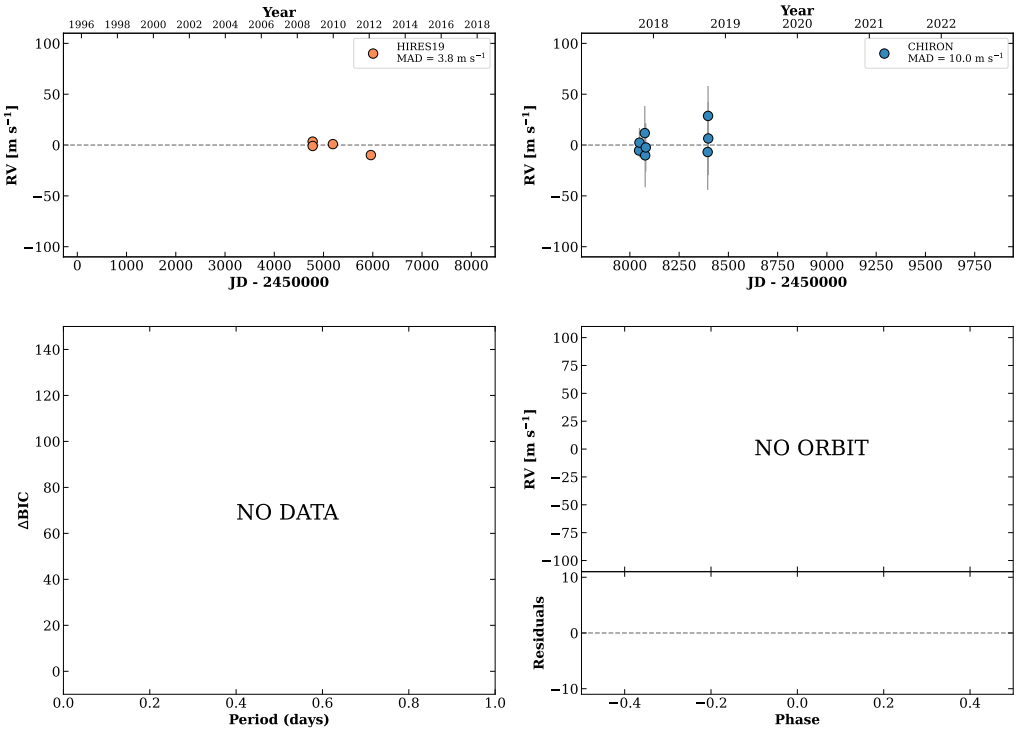

Figure 67 RV results for RKS0343-1906 (top) and RKS0344+1155 (bottom).

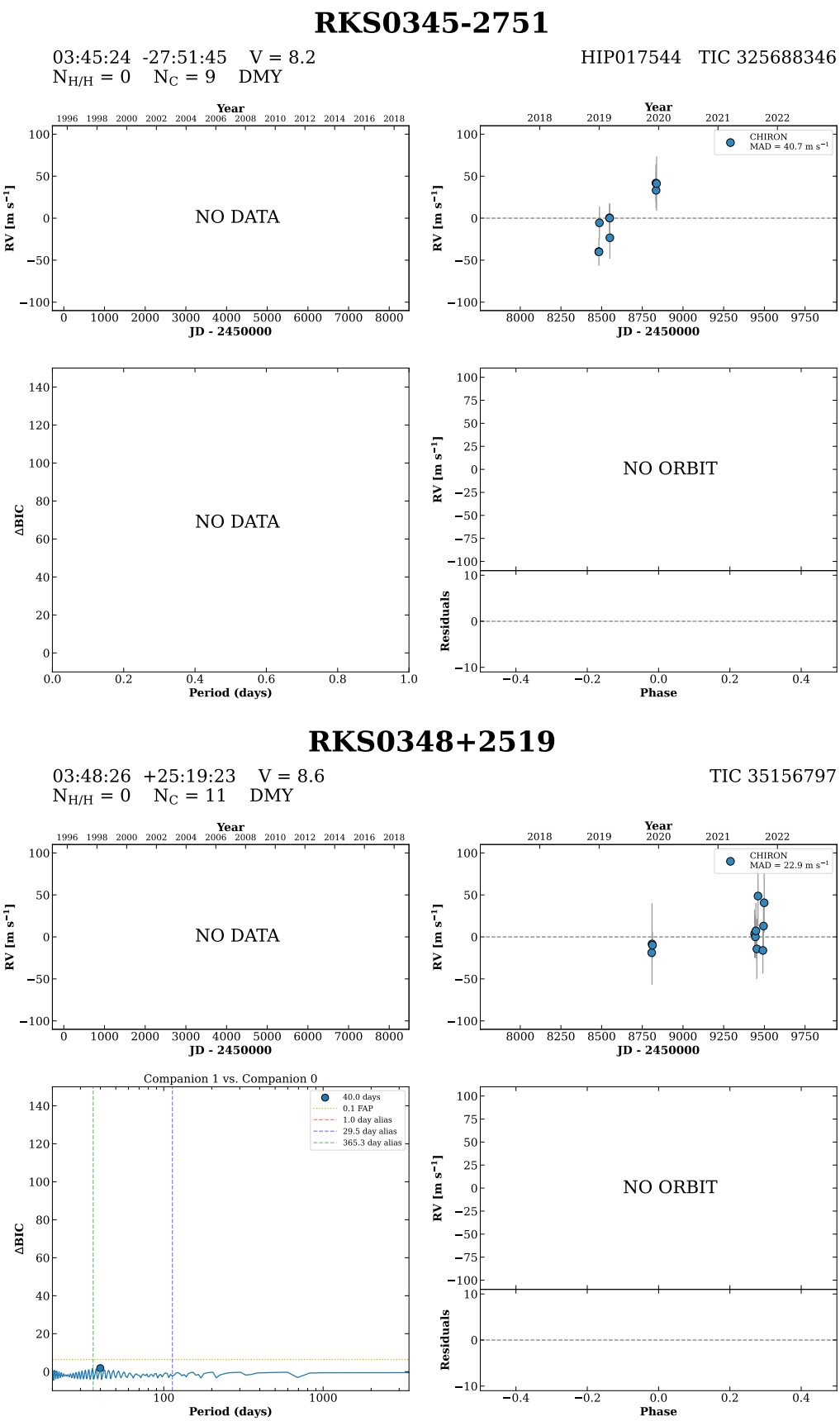

Figure 68 RV results for RKS0345-2751 (top) and RKS0348+2519 (bottom).

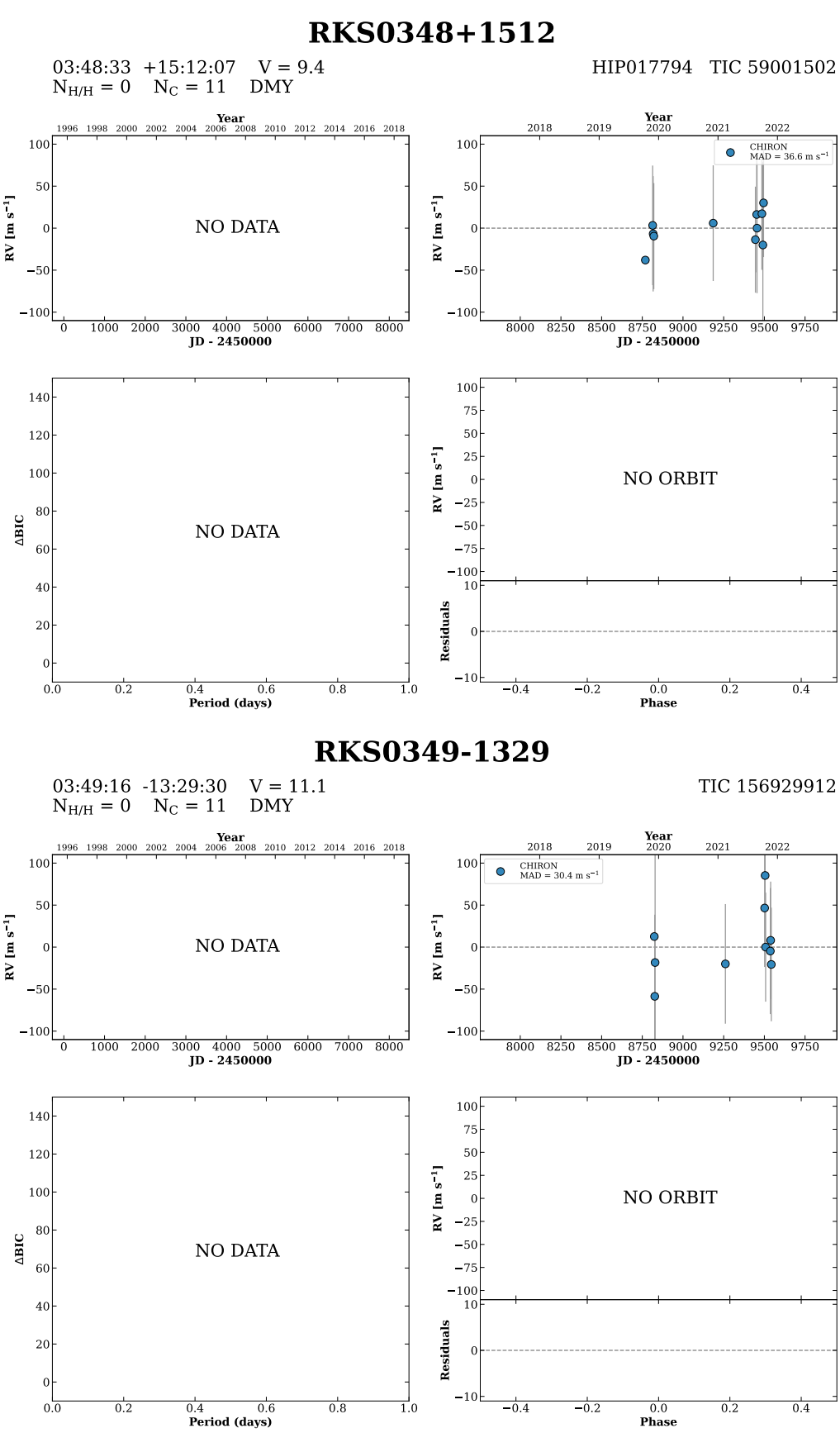

Figure 69 RV results for RKS0348+1512 (top) and RKS0349-1329 (bottom).

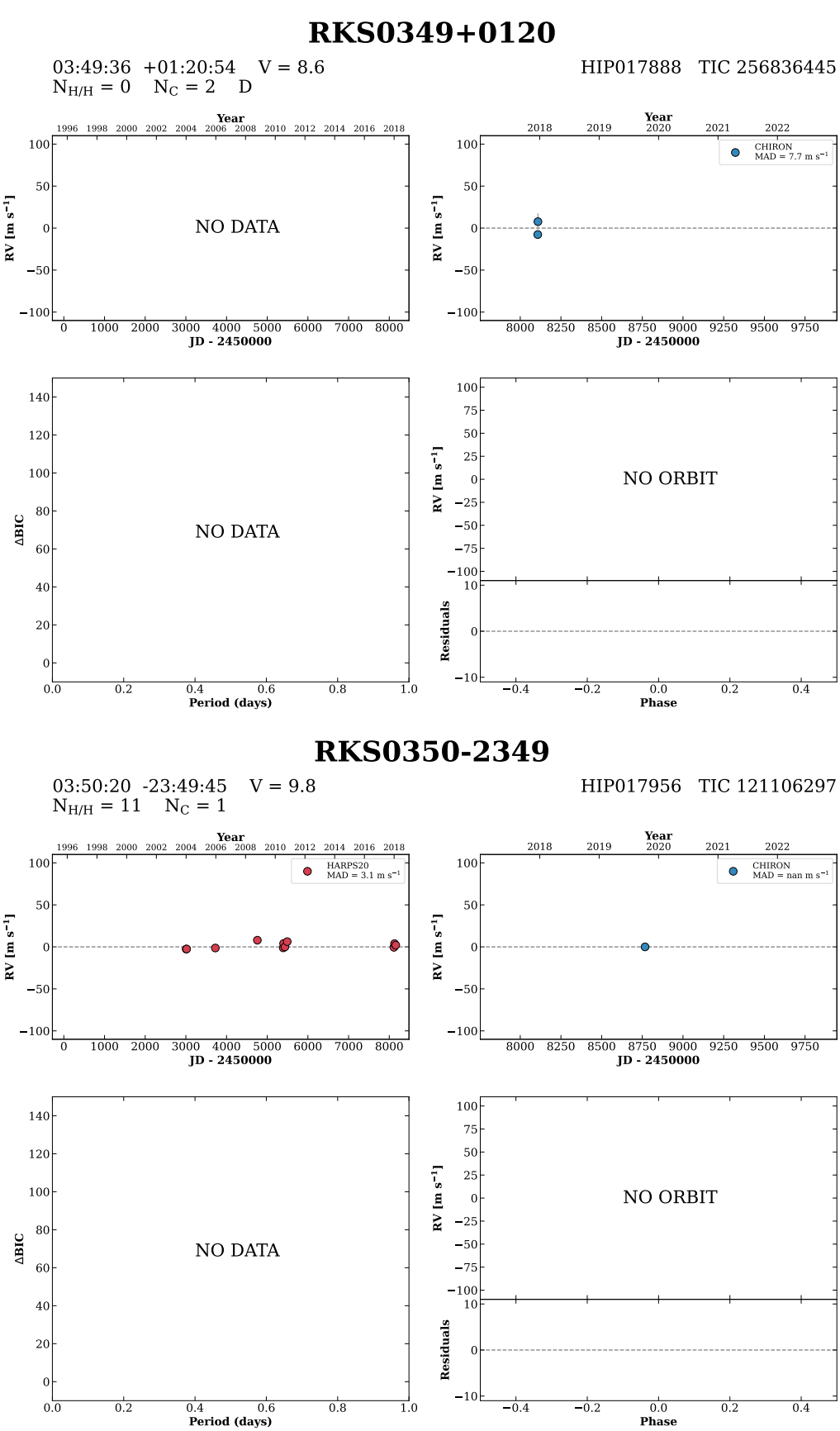

Figure 70 RV results for RKS0349+0120 (top) and RKS0350-2349 (bottom).

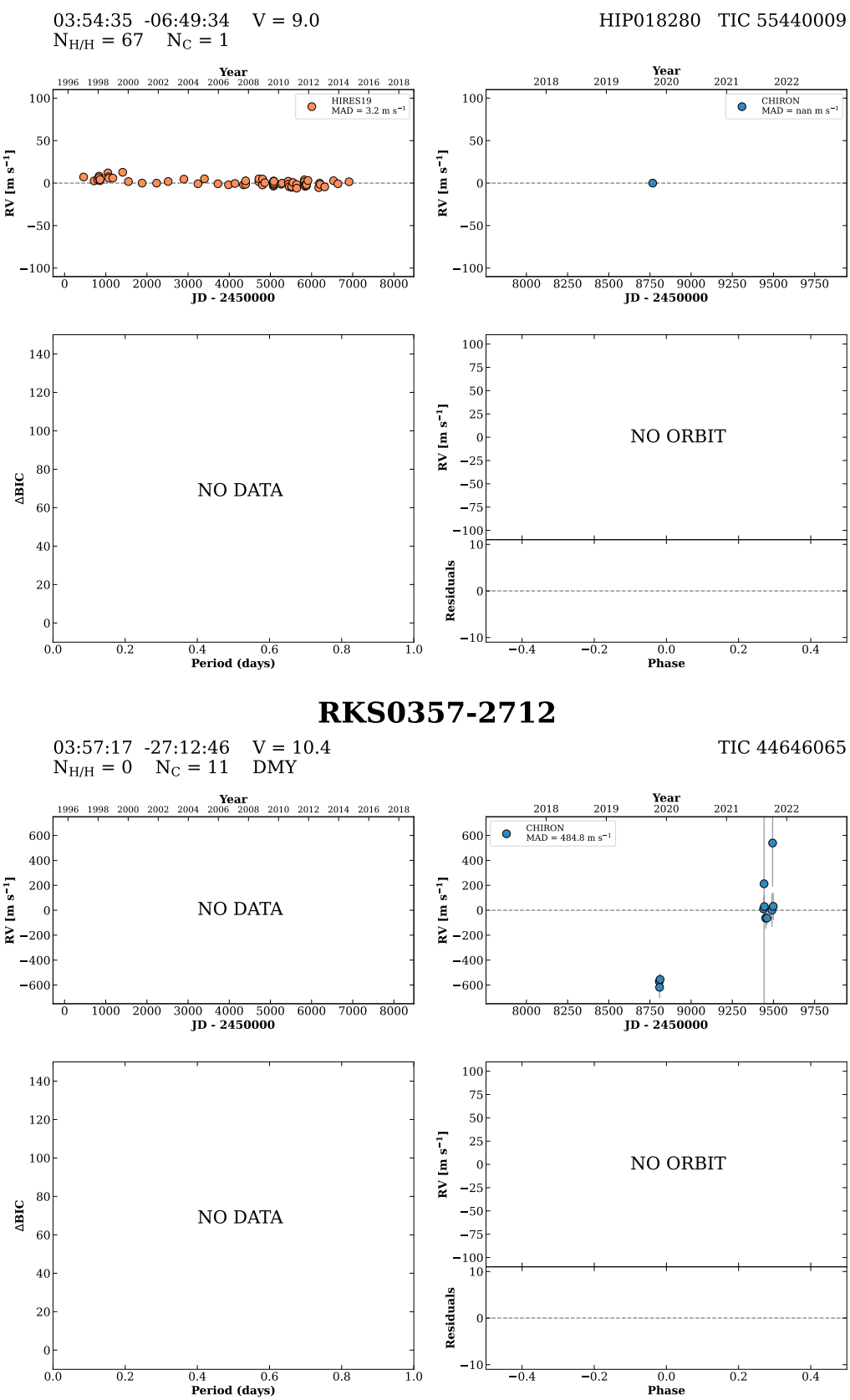

Figure 71 RV results for RKS0354-0649 (top) and RKS0357-2712 (bottom).

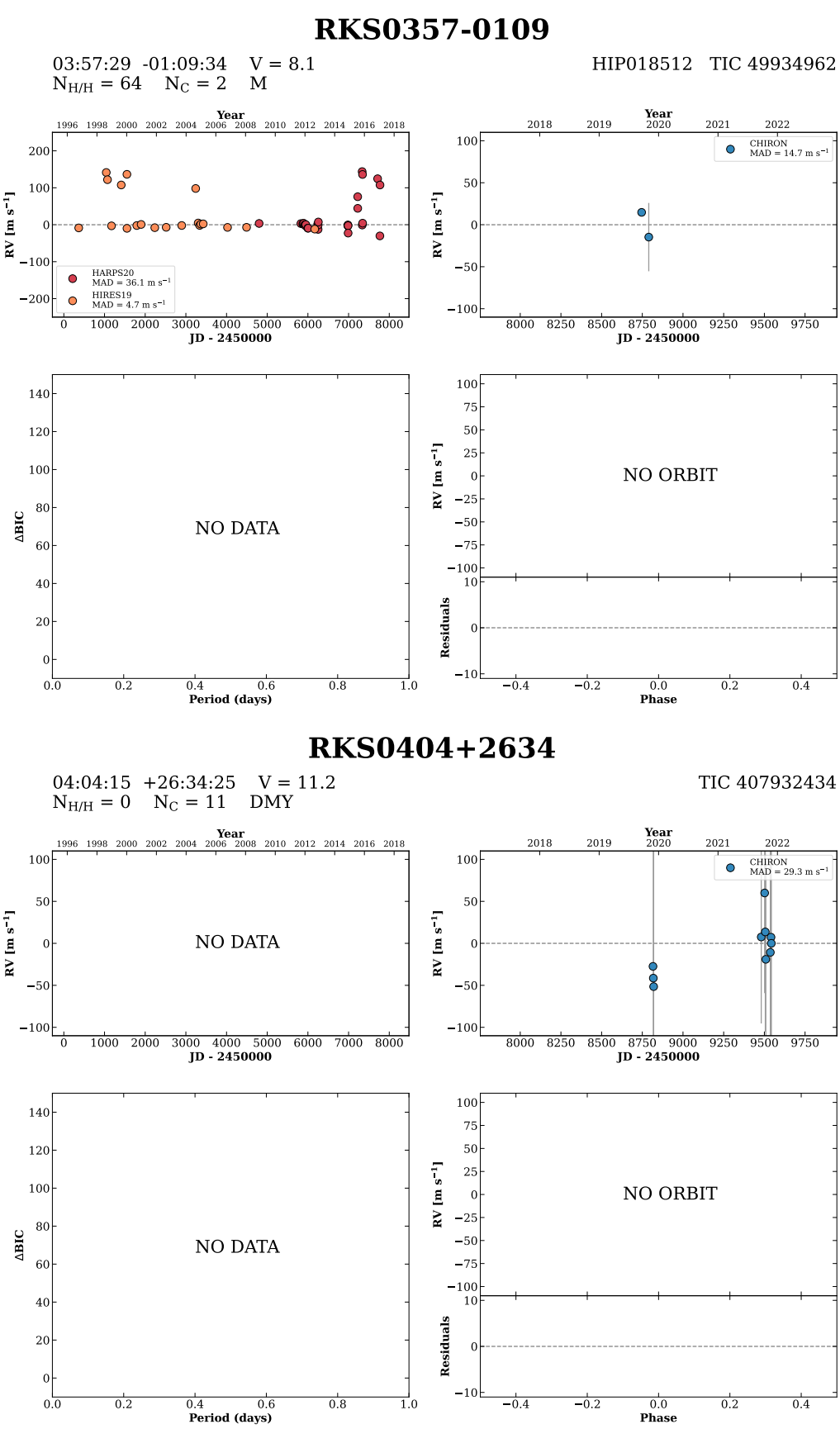

Figure 72 RV results for RKS0357-0109 (top) and RKS0404+2634 (bottom).

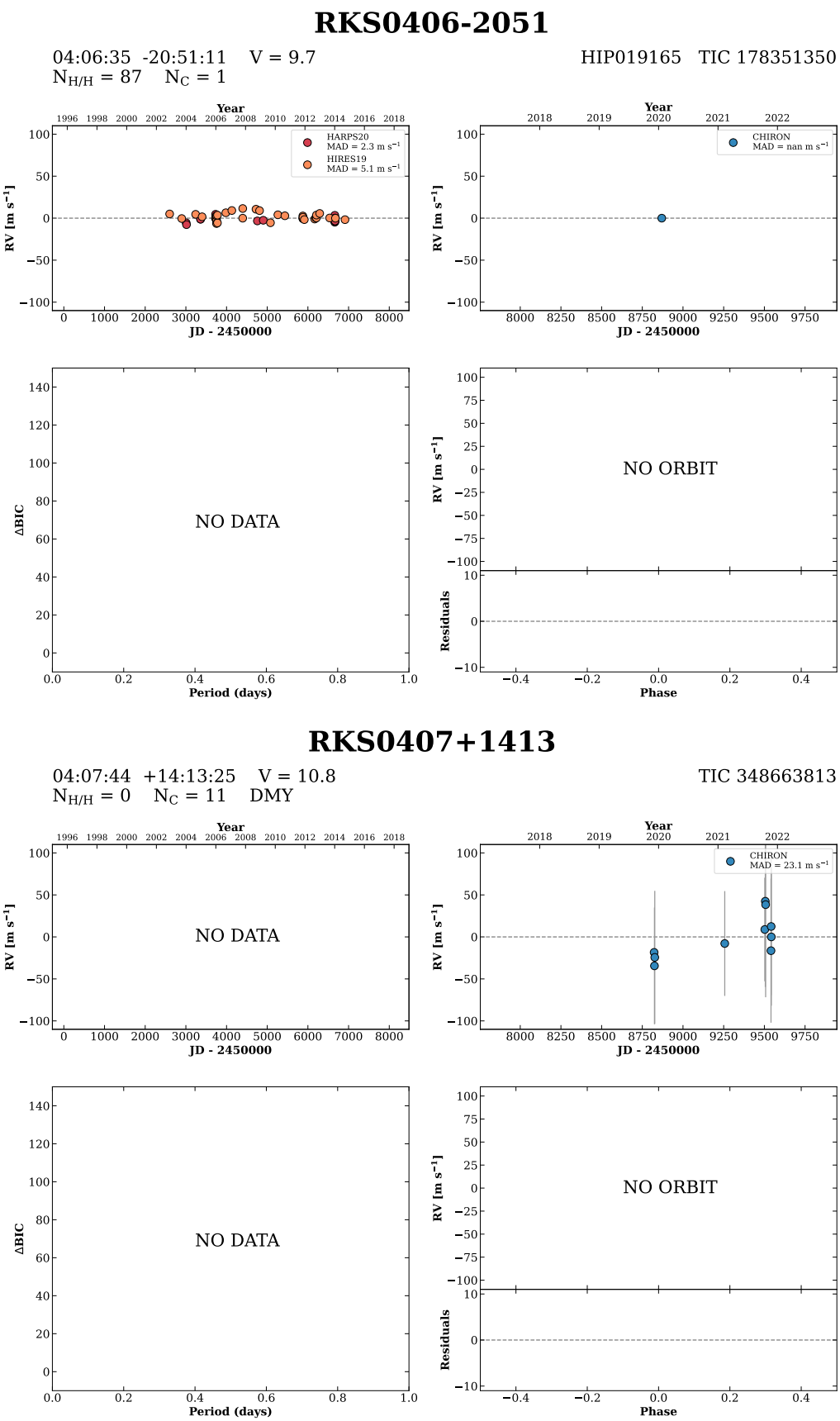

Figure 73 RV results for RKS0406-2051 (top) and RKS0407+1413 (bottom).

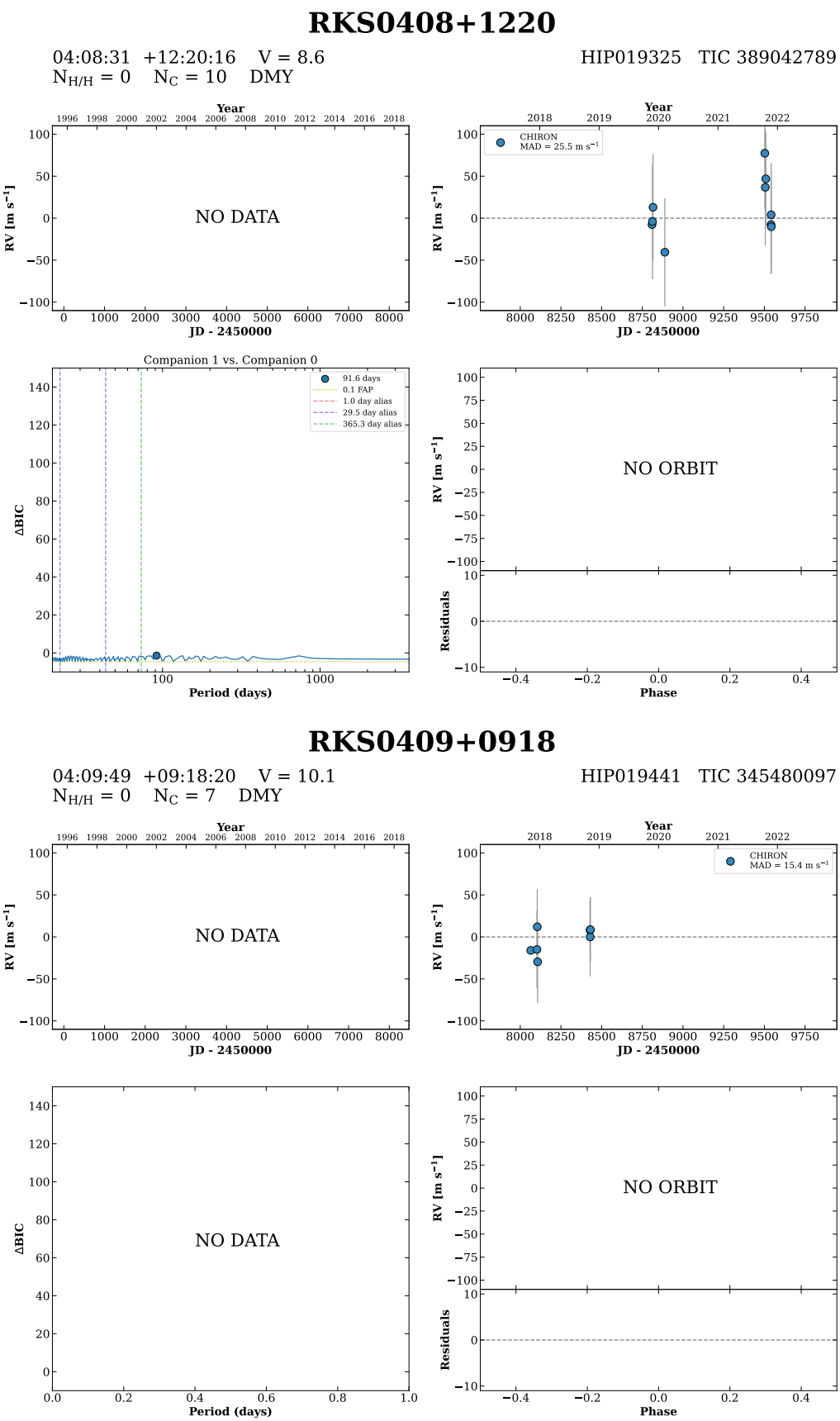

Figure 74 RV results for RKS0408+1220 (top) and RKS0409+0918 (bottom).

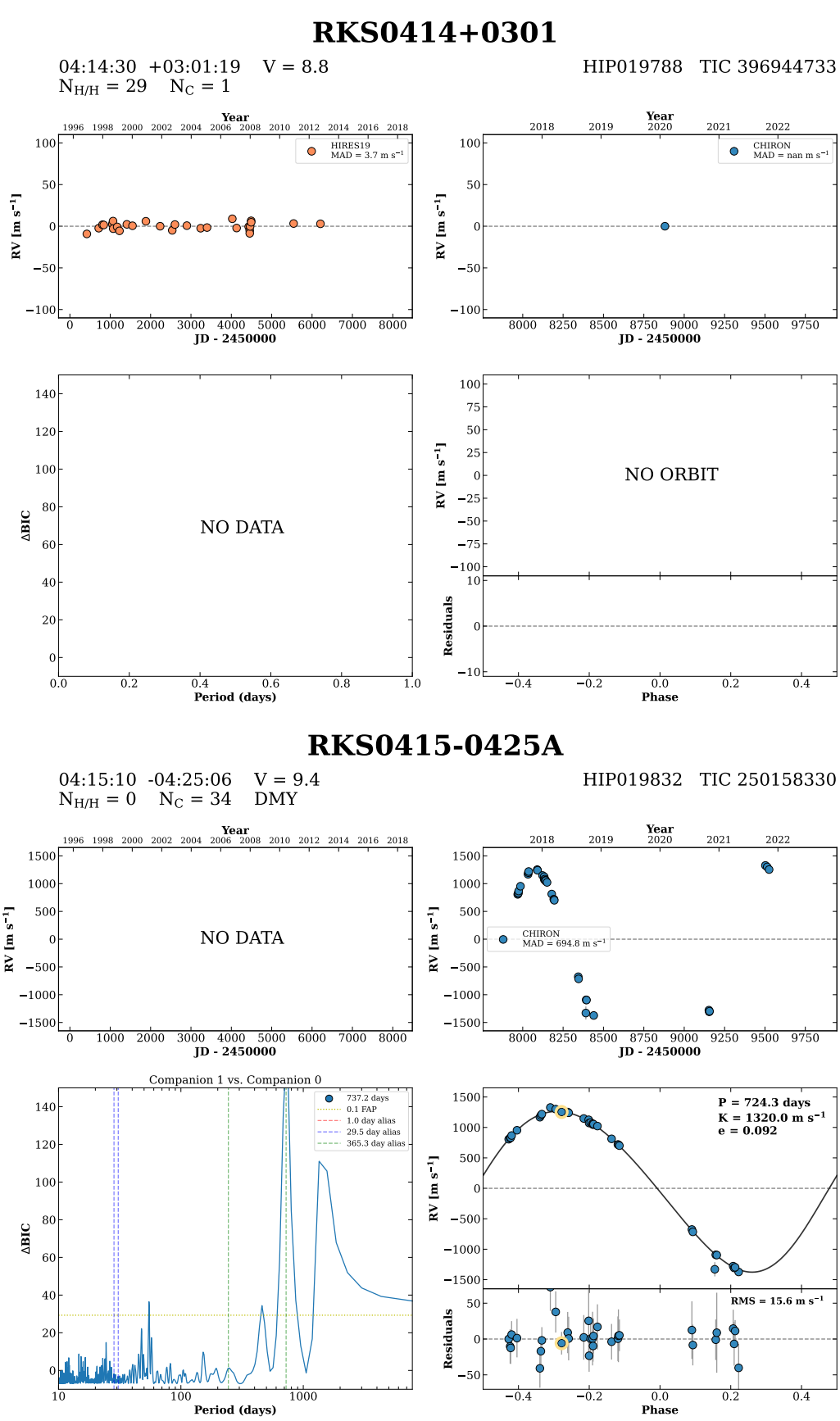

Figure 75 RV results for RKS0414+0301 (top) and RKS0415-0425A (bottom).

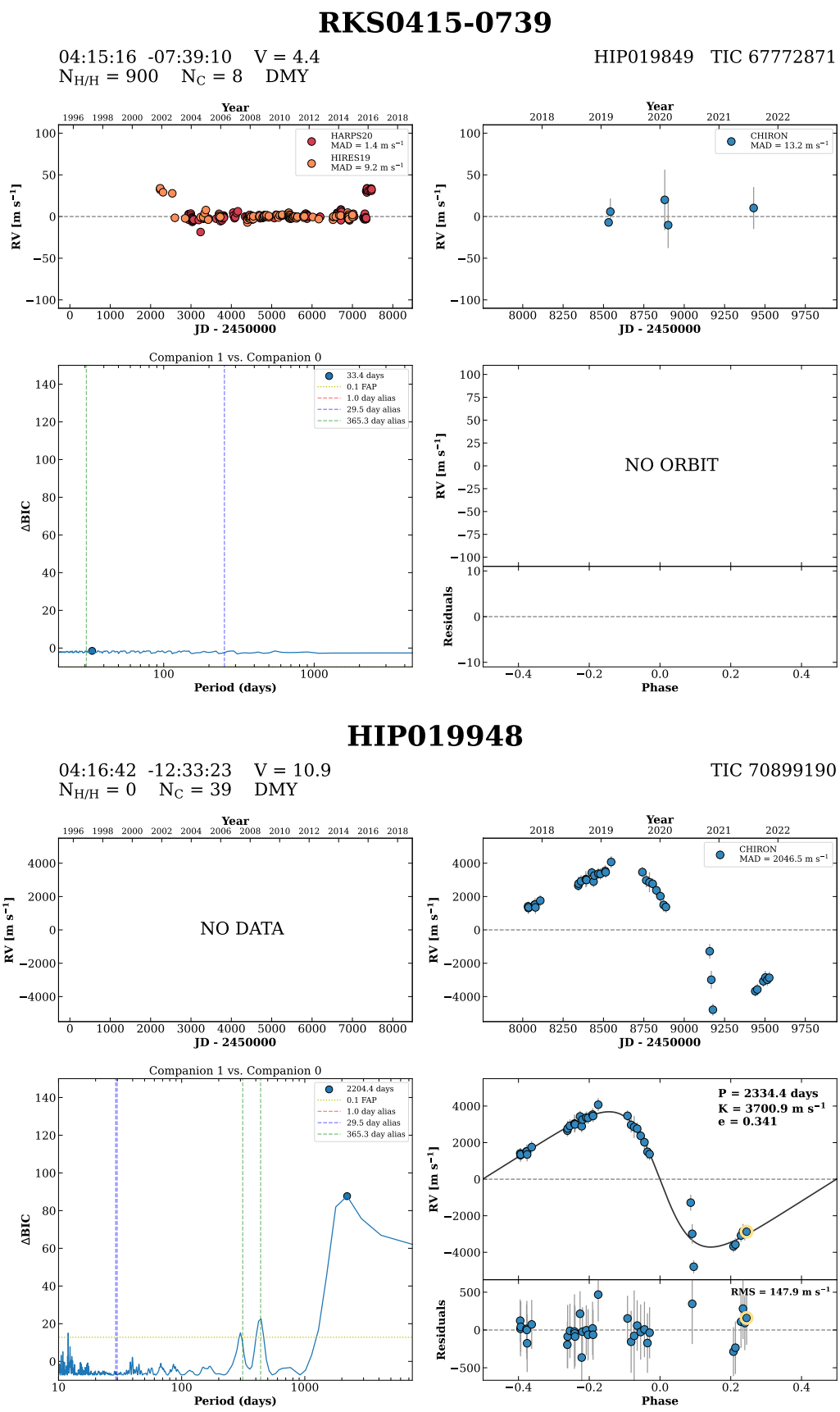

Figure 76 RV results for RKS0415-0739 (top) and HIP019948 (bottom).

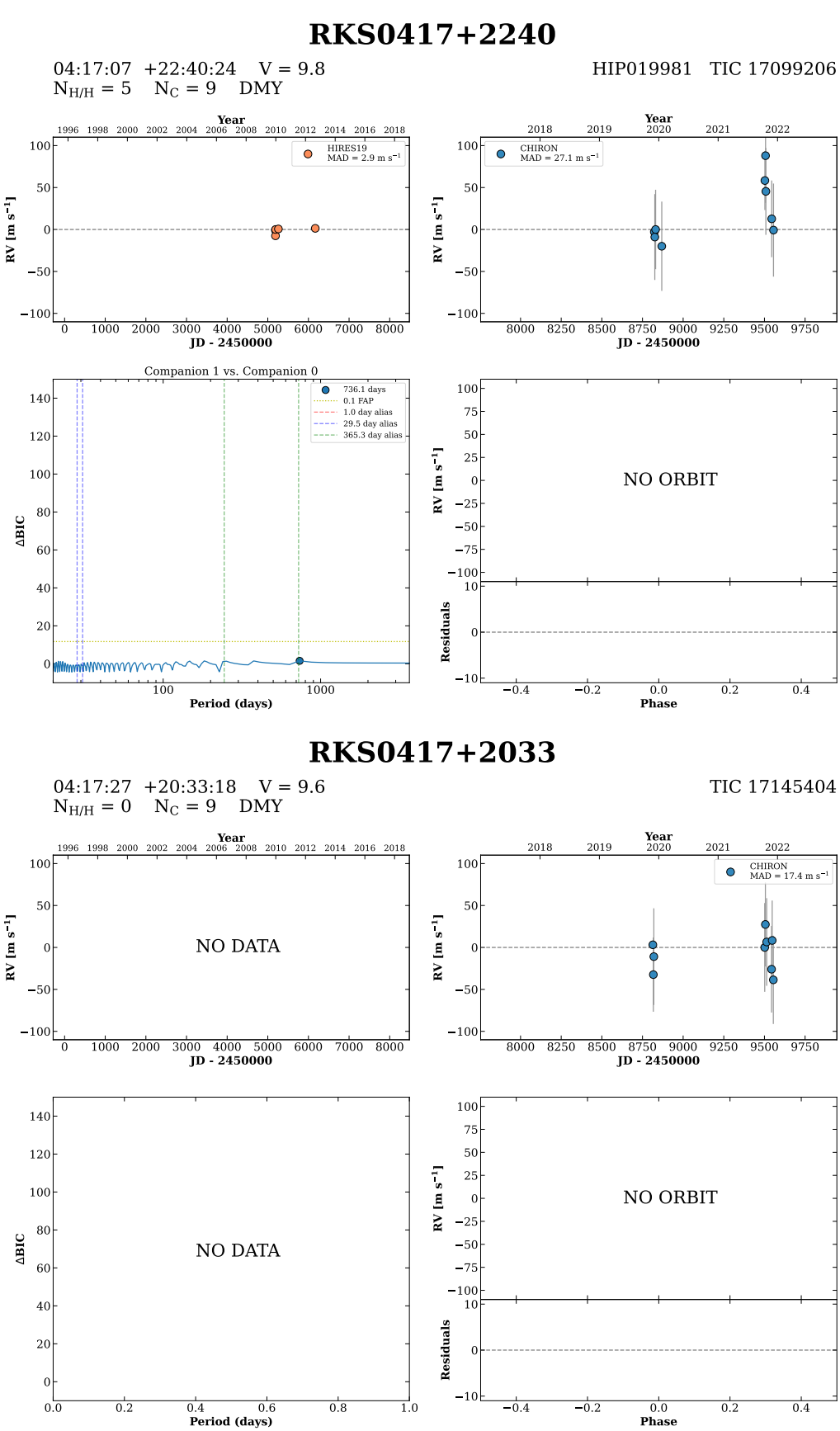

Figure 77 RV results for RKS0417+2240 (top) and RKS0417+2033 (bottom).

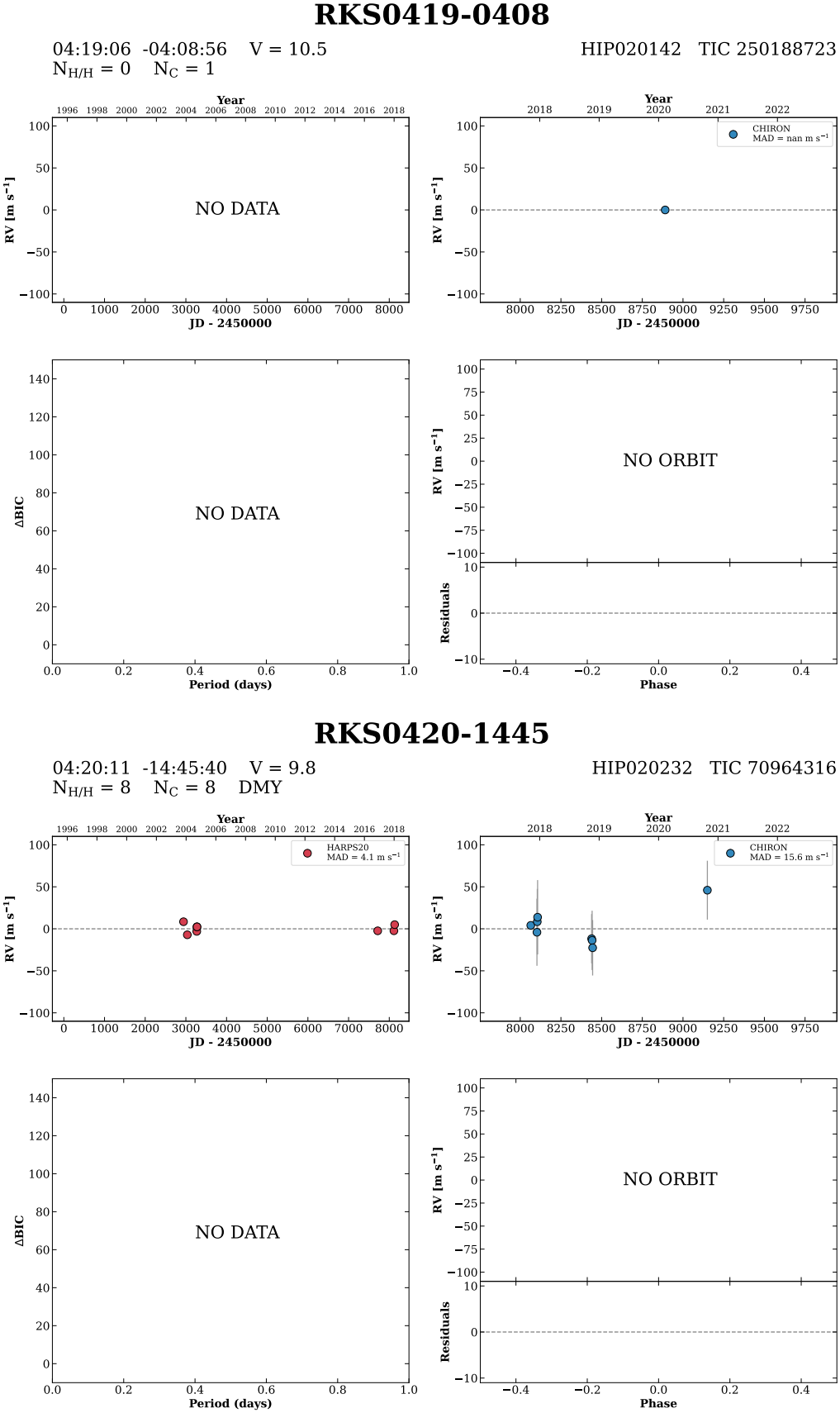

Figure 78 RV results for RKS0419-0408 (top) and RKS0420-1445 (bottom).

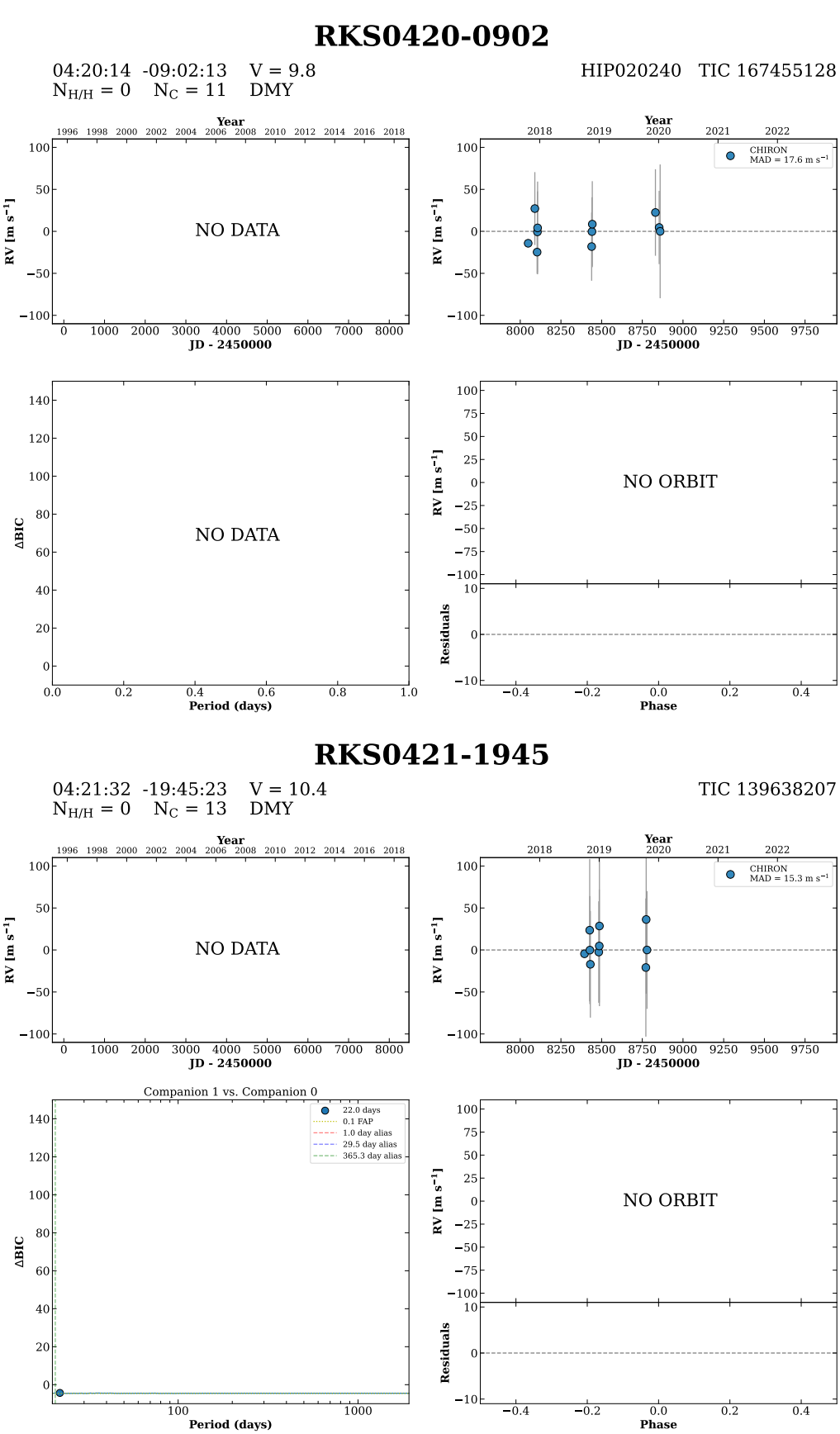

Figure 79 RV results for RKS0420-0902 (top) and RKS0421-1945 (bottom).

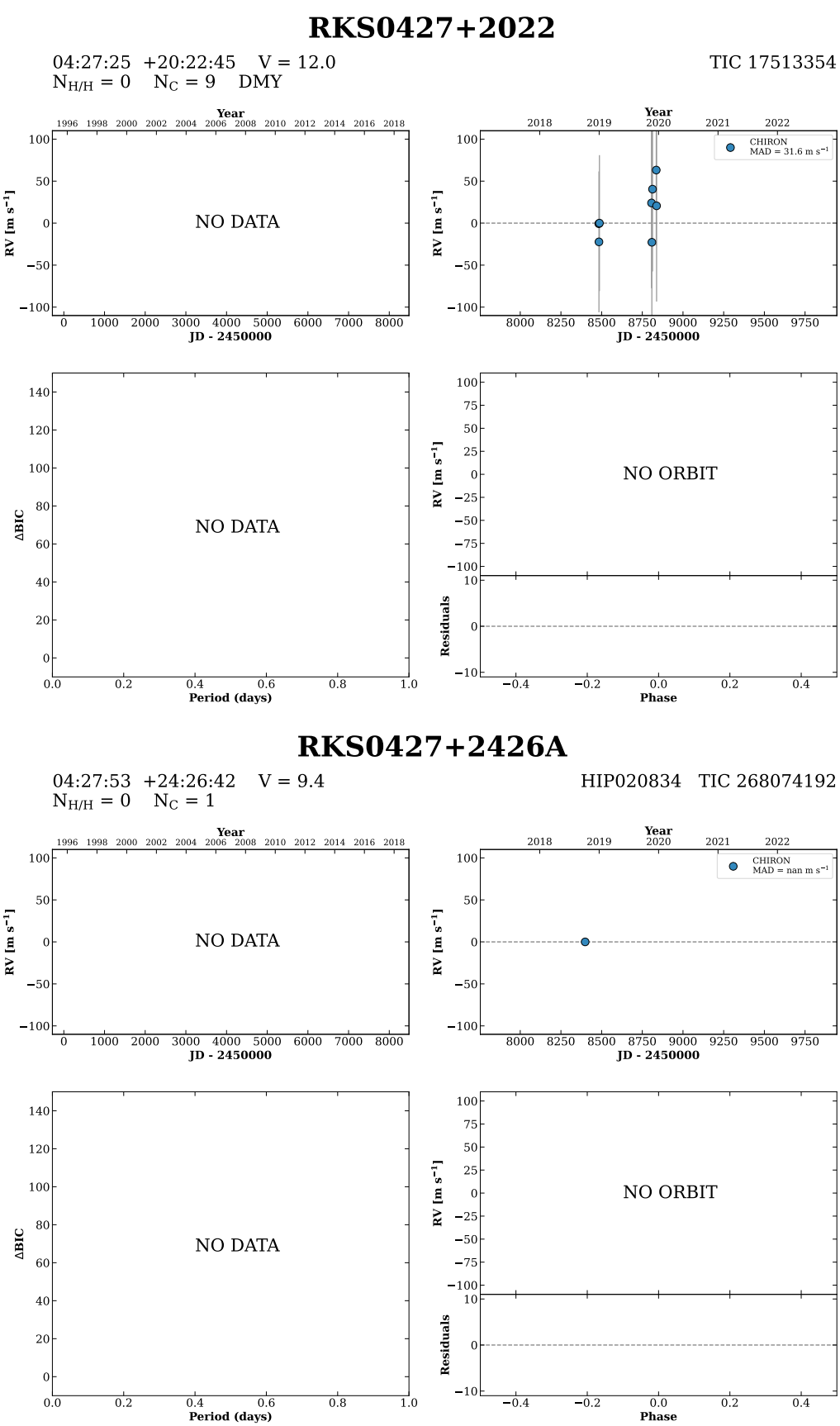

Figure 80 RV results for RKS0427+2022 (top) and RKS0427+2426A (bottom).

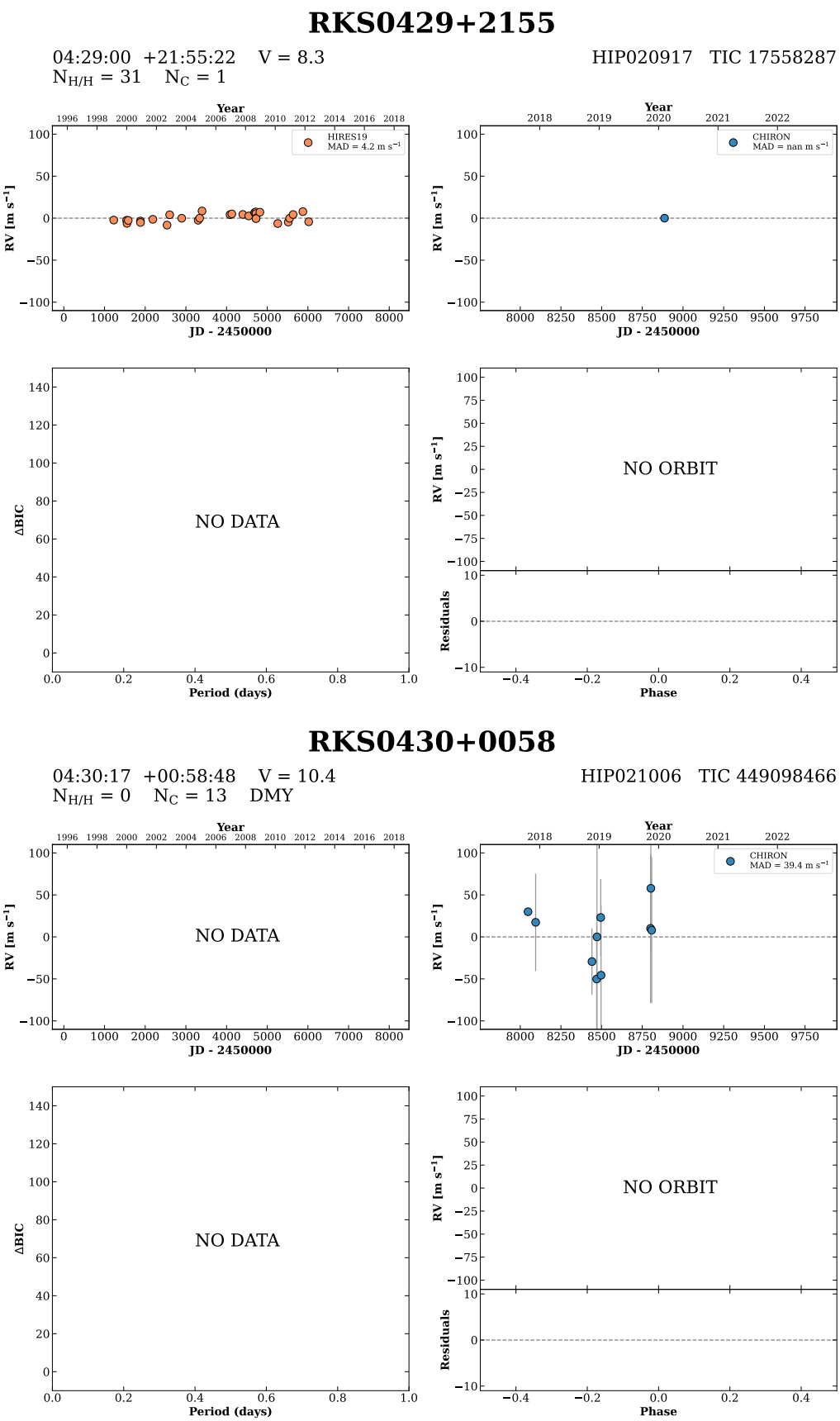

Figure 81 RV results for RKS0429+2155 (top) and RKS0430+0058 (bottom).

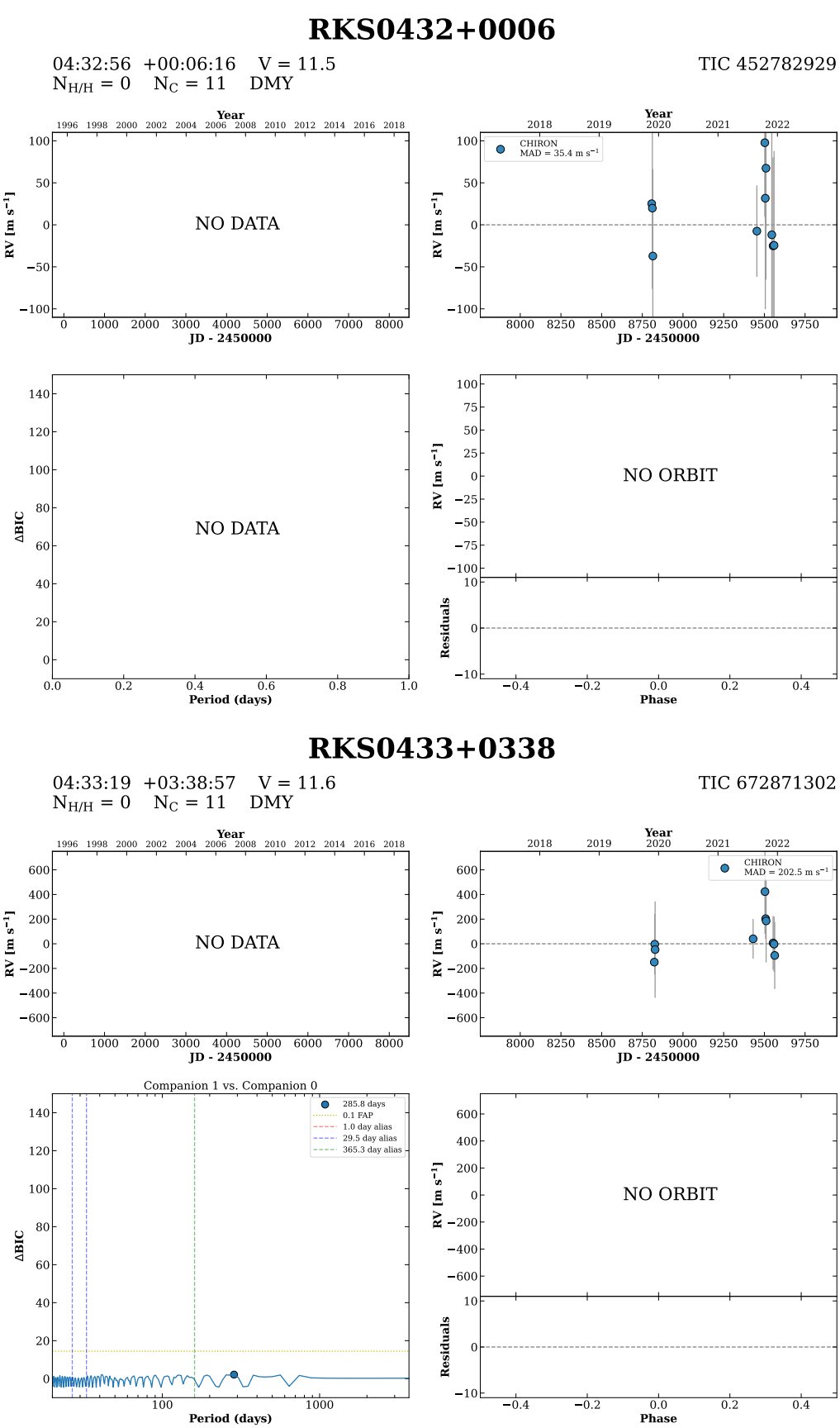

Figure 82 RV results for RKS0432+0006 (top) and RKS0433+0338 (bottom).

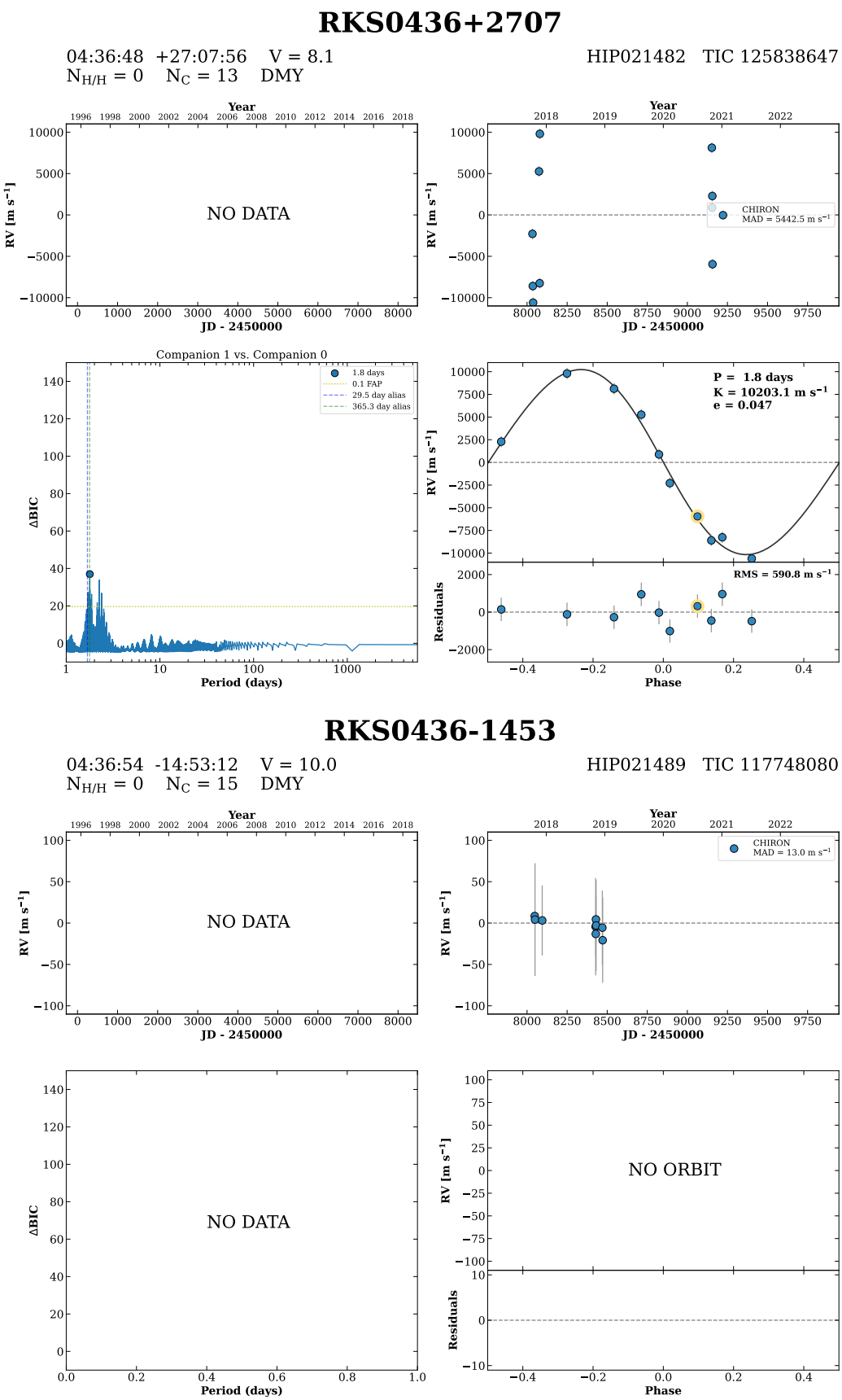

Figure 83 RV results for RKS0436+2707 (top) and RKS0436-1453 (bottom).

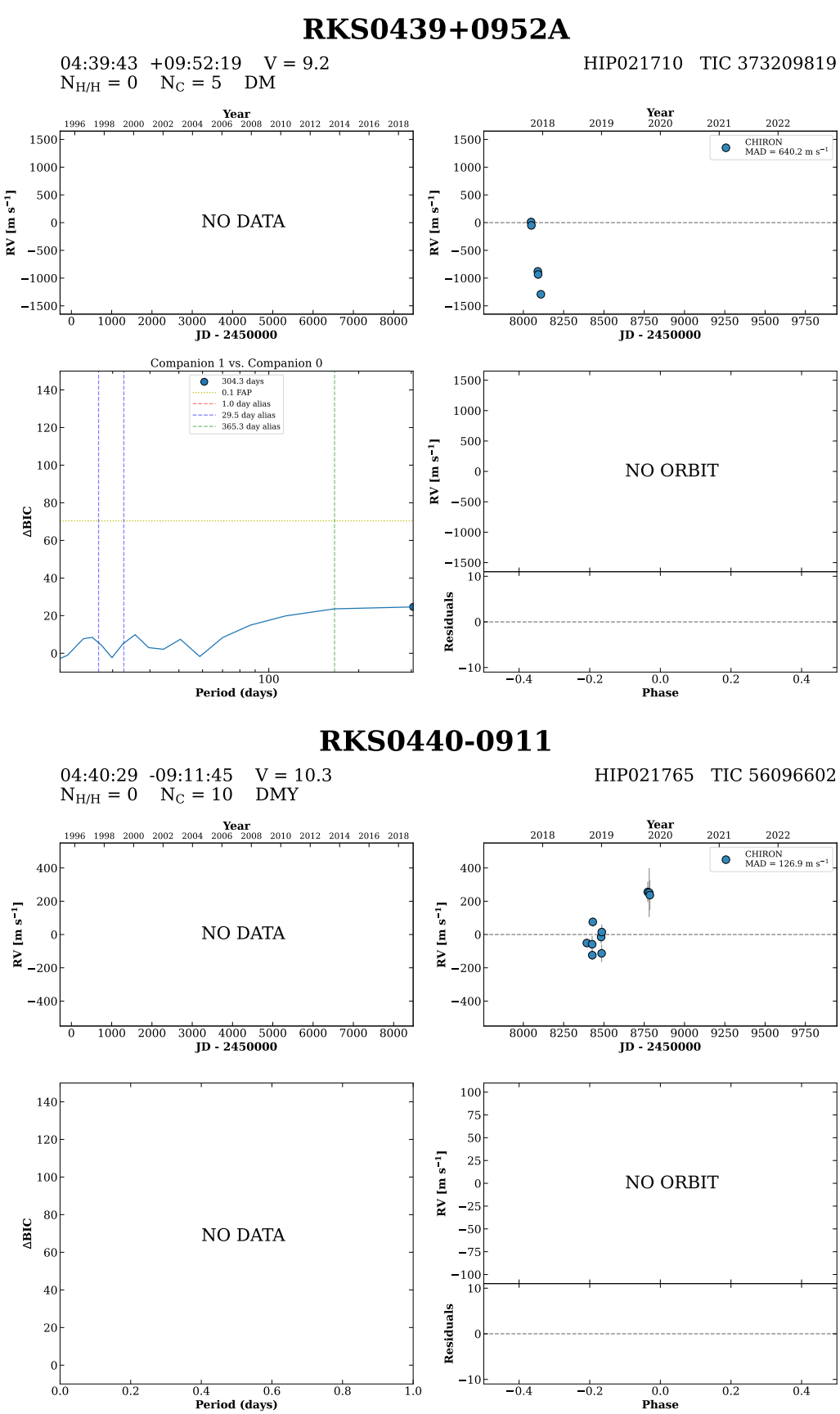

Figure 84 RV results for RKS0439+0952A (top) and RKS0440-0911 (bottom).

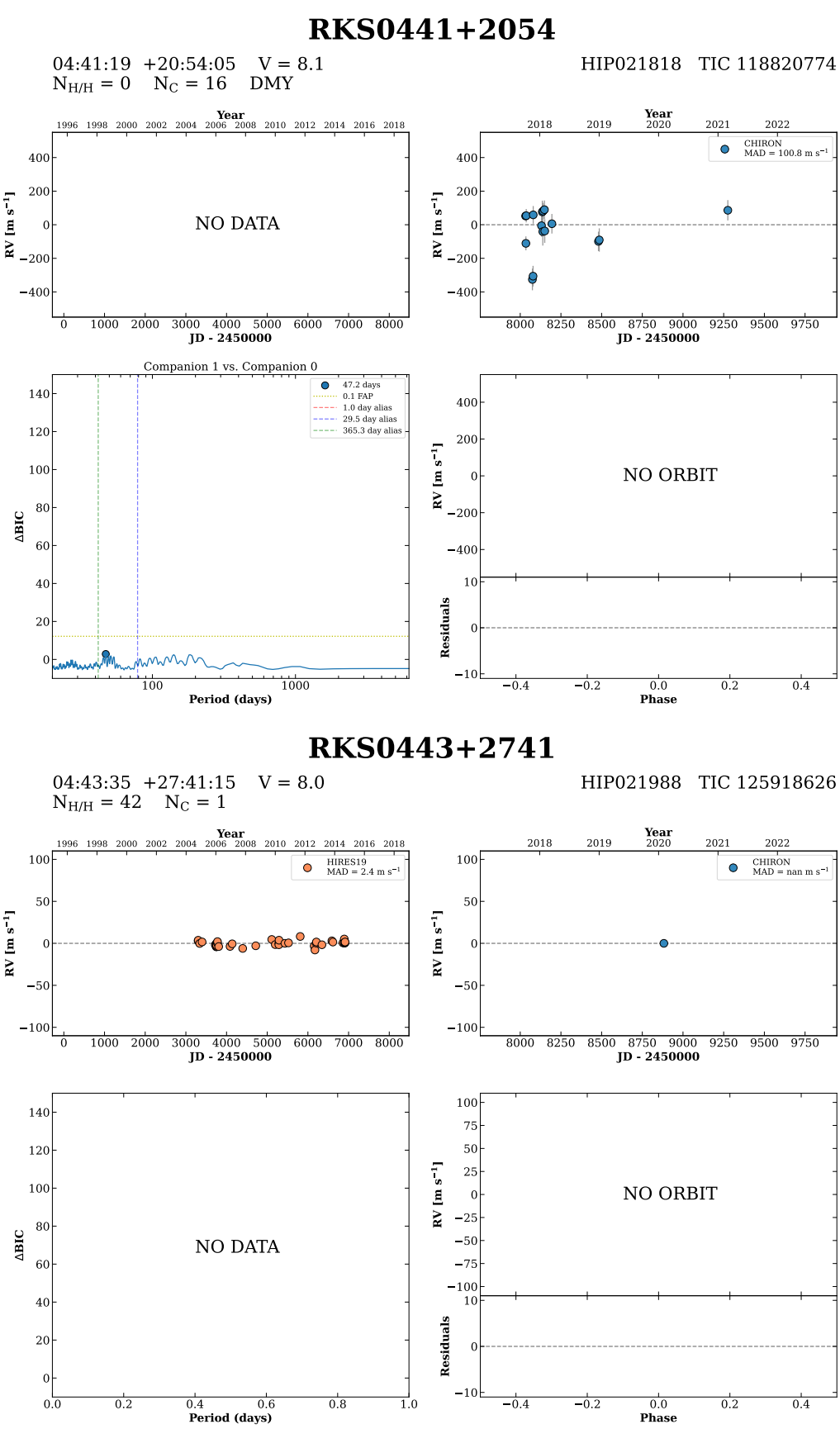

Figure 85 RV results for RKS0441+2054 (top) and RKS0443+2741 (bottom).

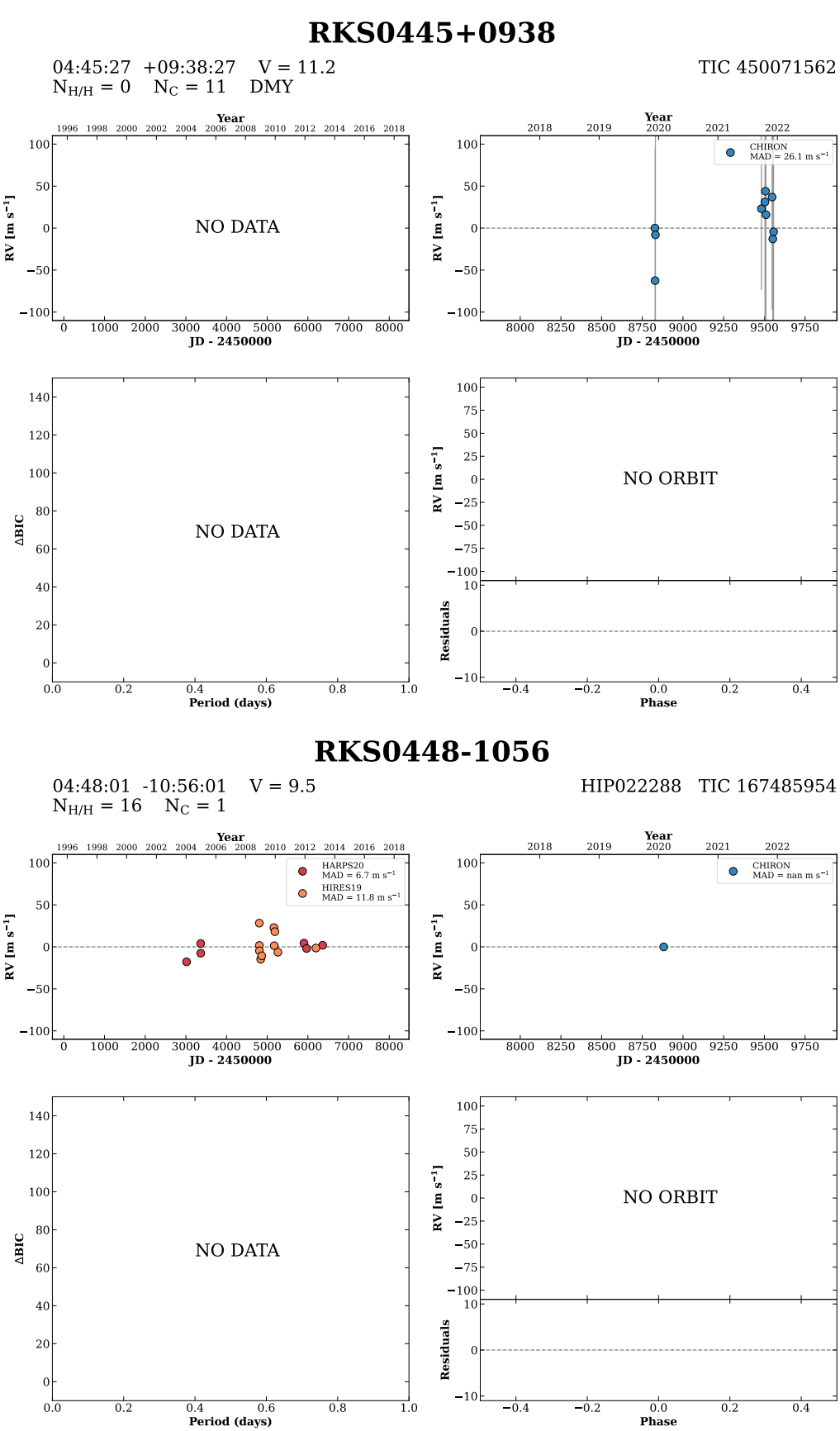

Figure 86 RV results for RKS0445+0938 (top) and RKS0448-1056 (bottom).

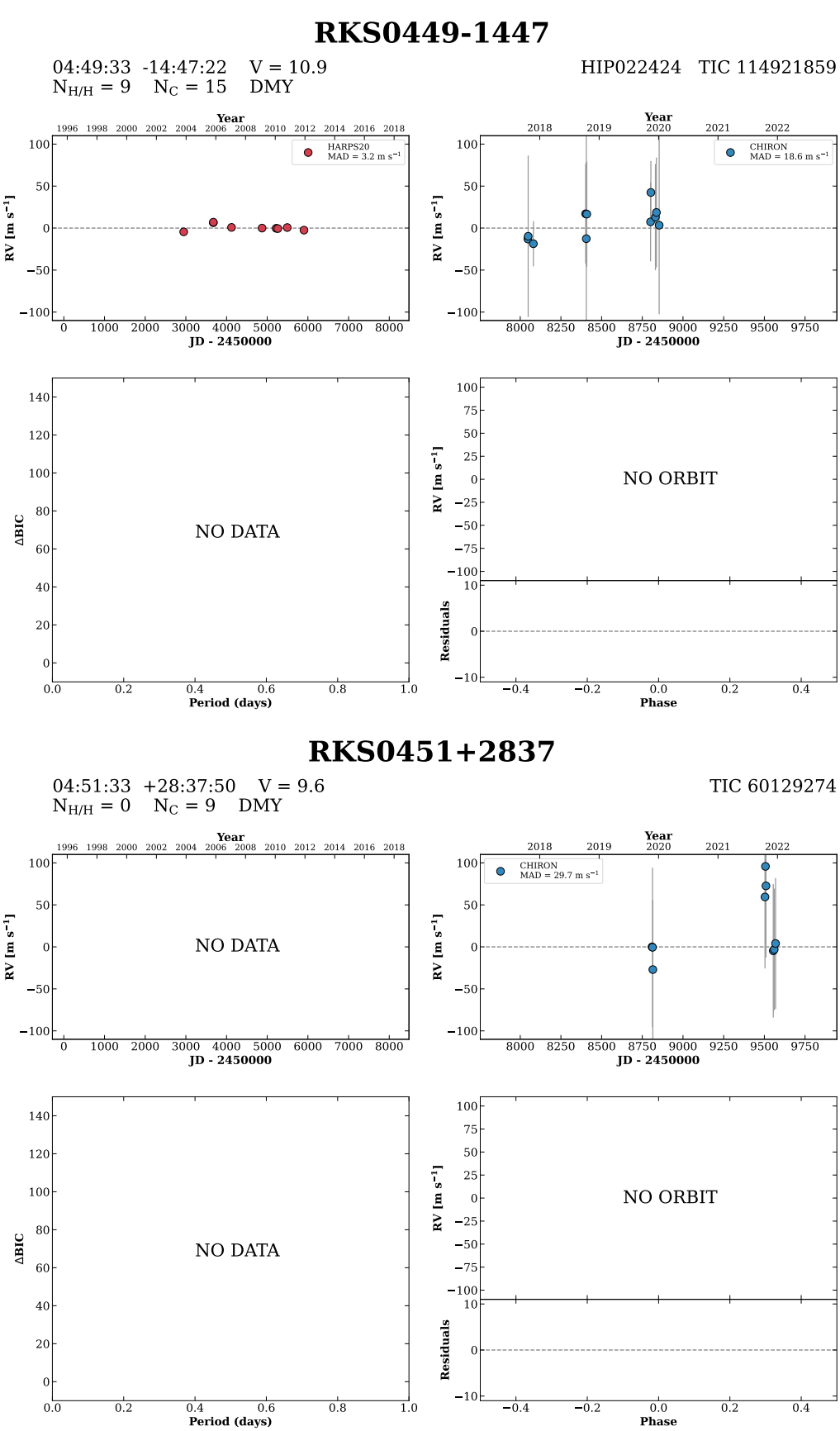

Figure 87 RV results for RKS0449-1447 (top) and RKS0451+2837 (bottom).

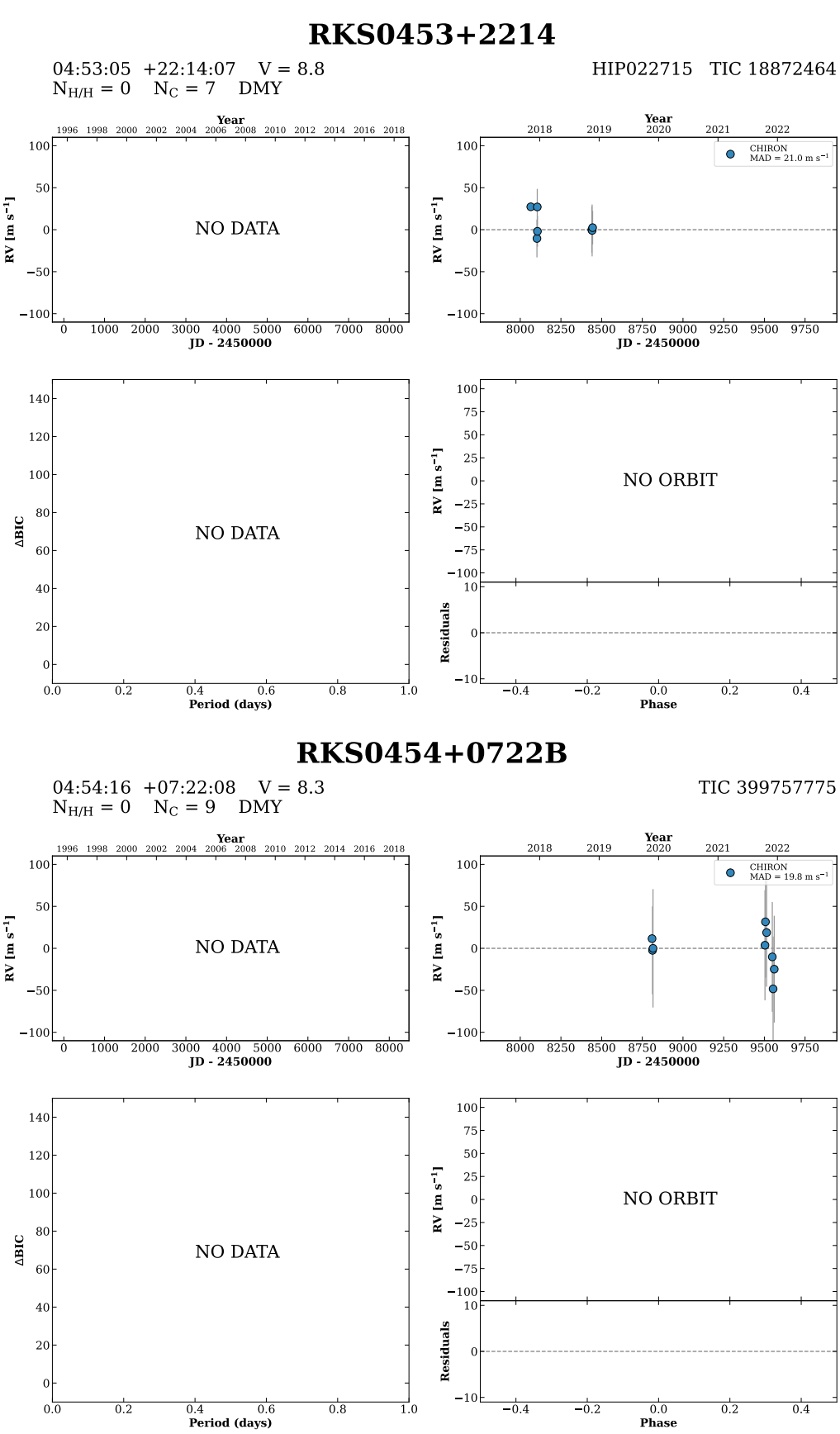

Figure 88 RV results for RKS0453+2214 (top) and RKS0454+0722B (bottom).

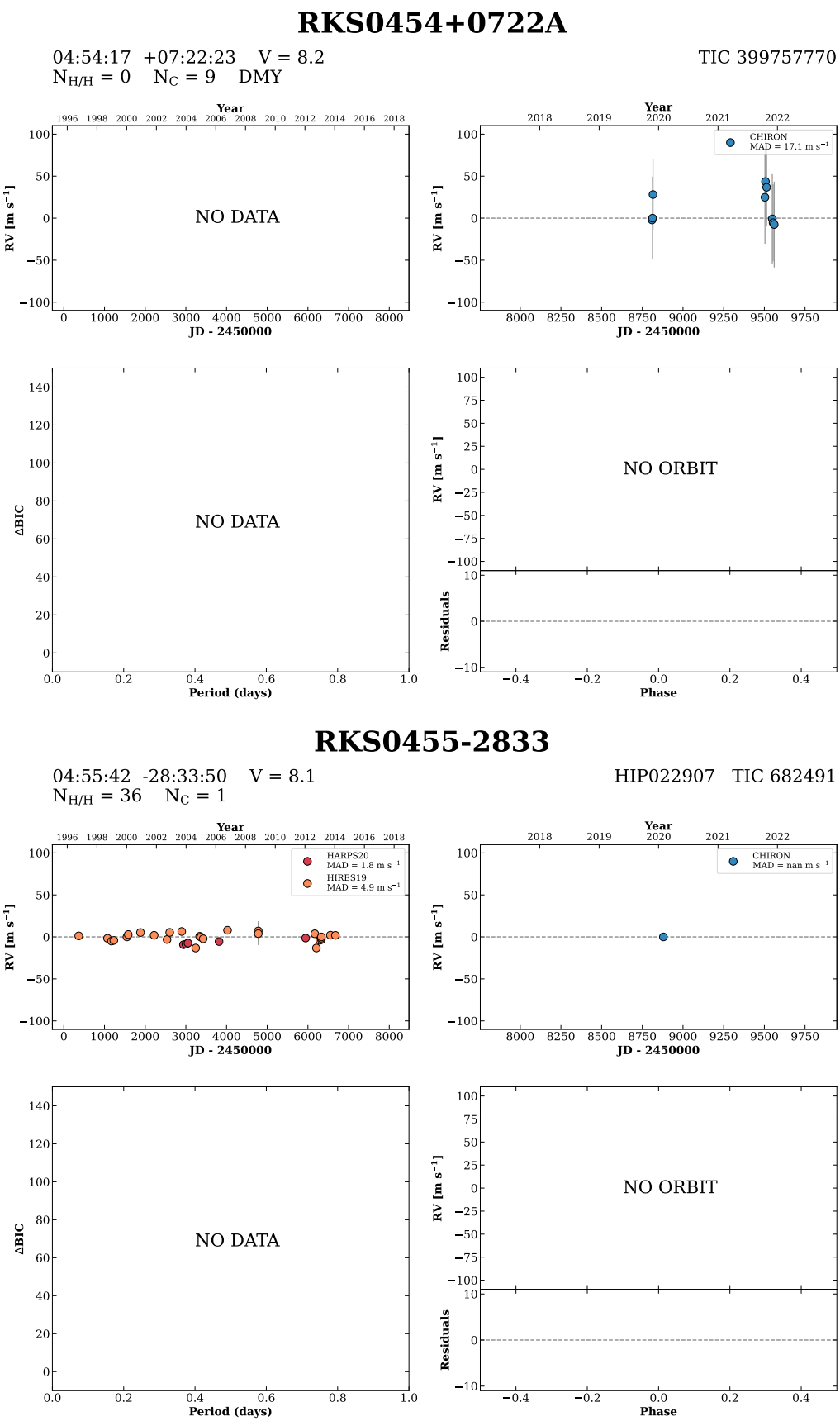

Figure 89 RV results for RKS0454+0722A (top) and RKS0455-2833 (bottom).

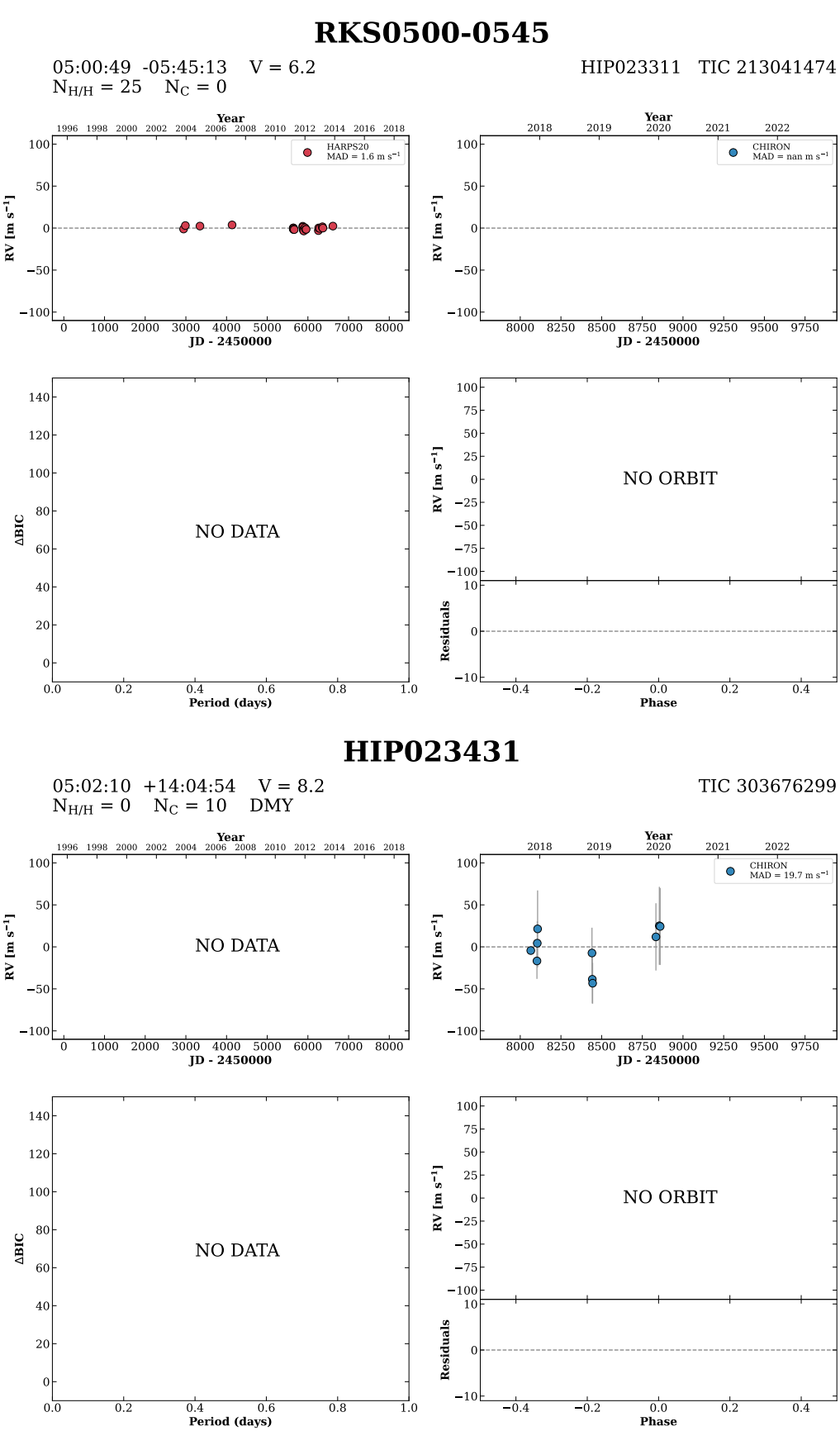

Figure 90 RV results for RKS0500-0545 (top) and HIP023431 (bottom).

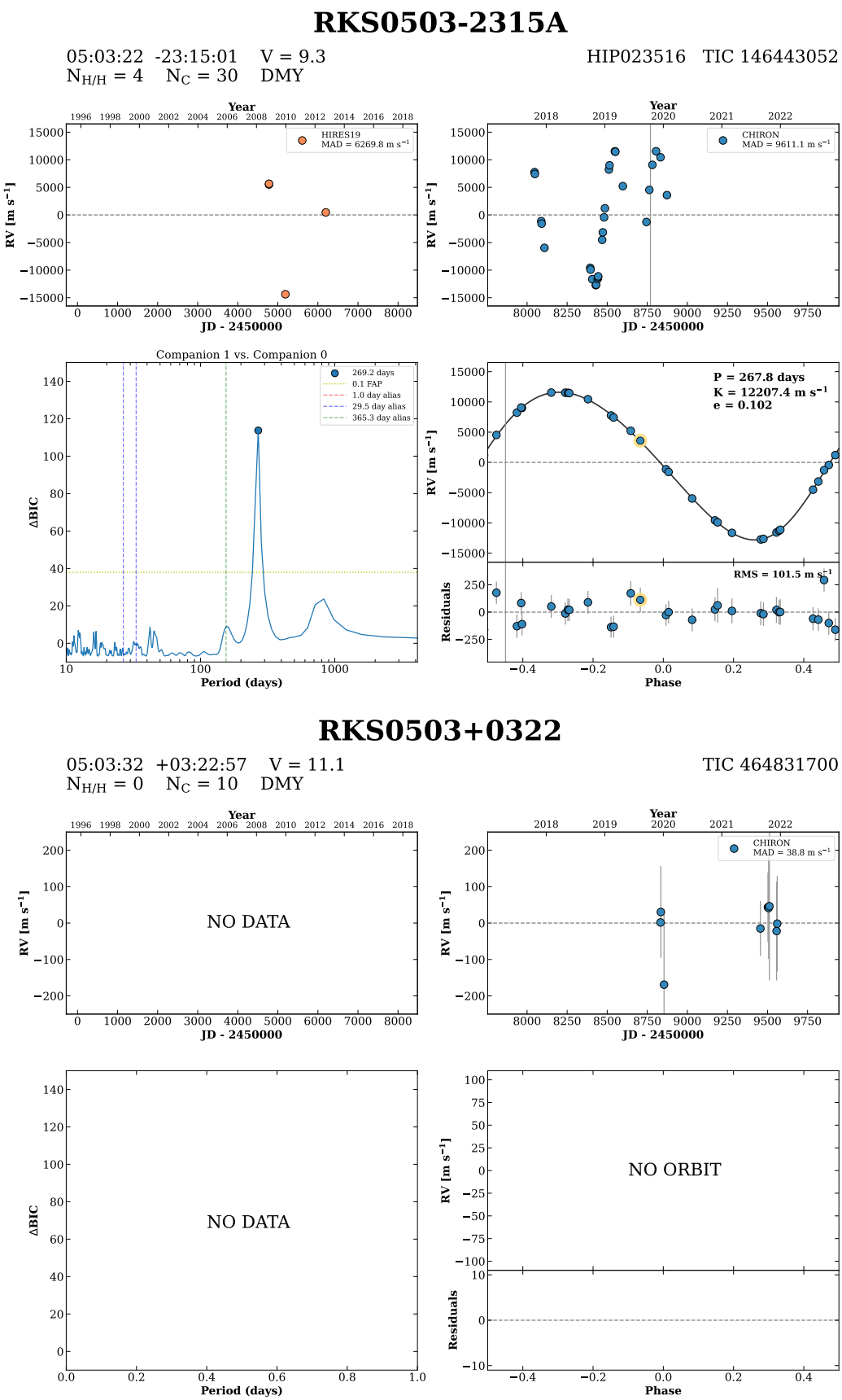

Figure 91 RV results for RKS0503-2315A (top) and RKS0503+0322 (bottom).

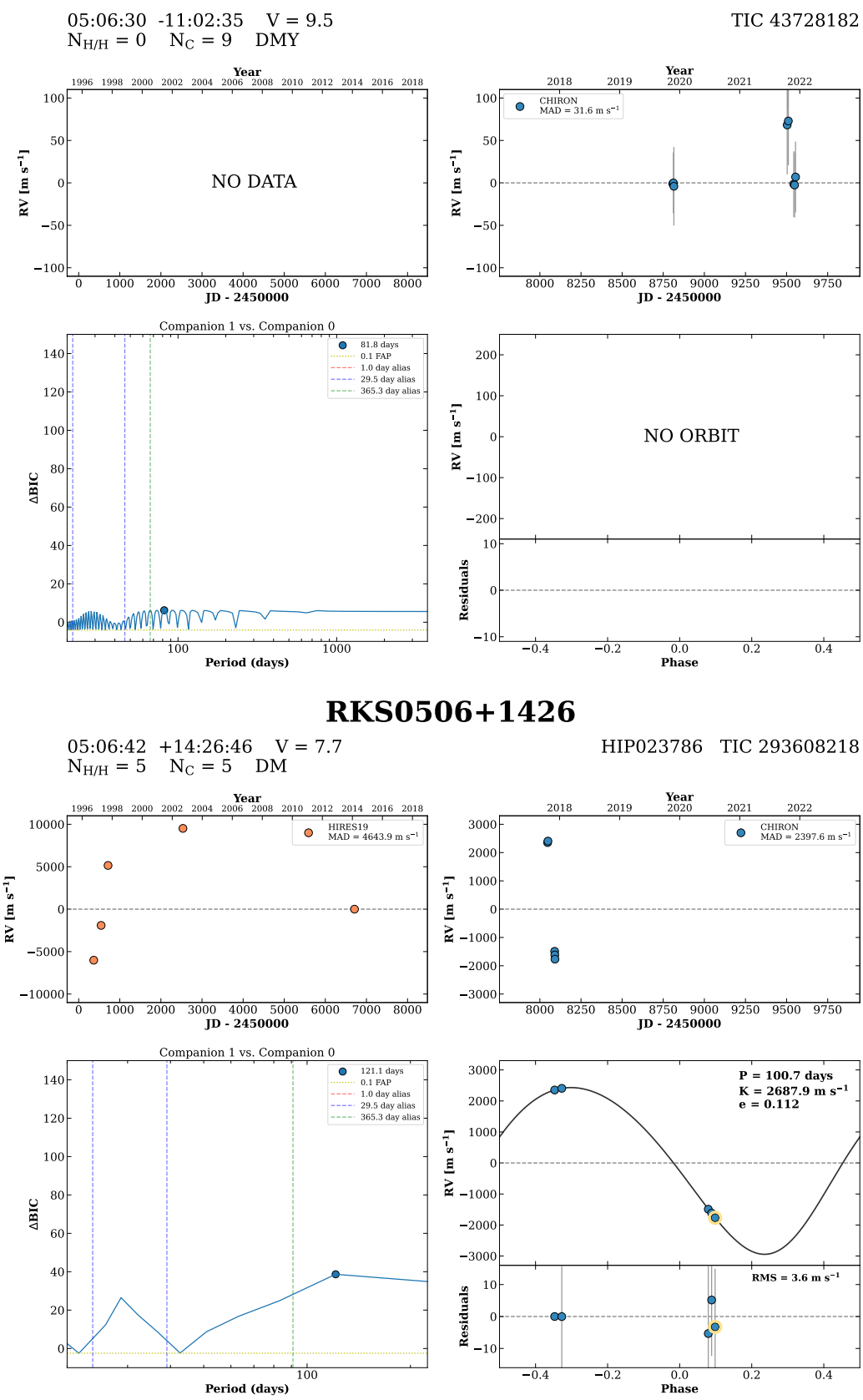

Figure 92 RV results for RKS0506-1102 (top) and RKS0506+1426 (bottom).

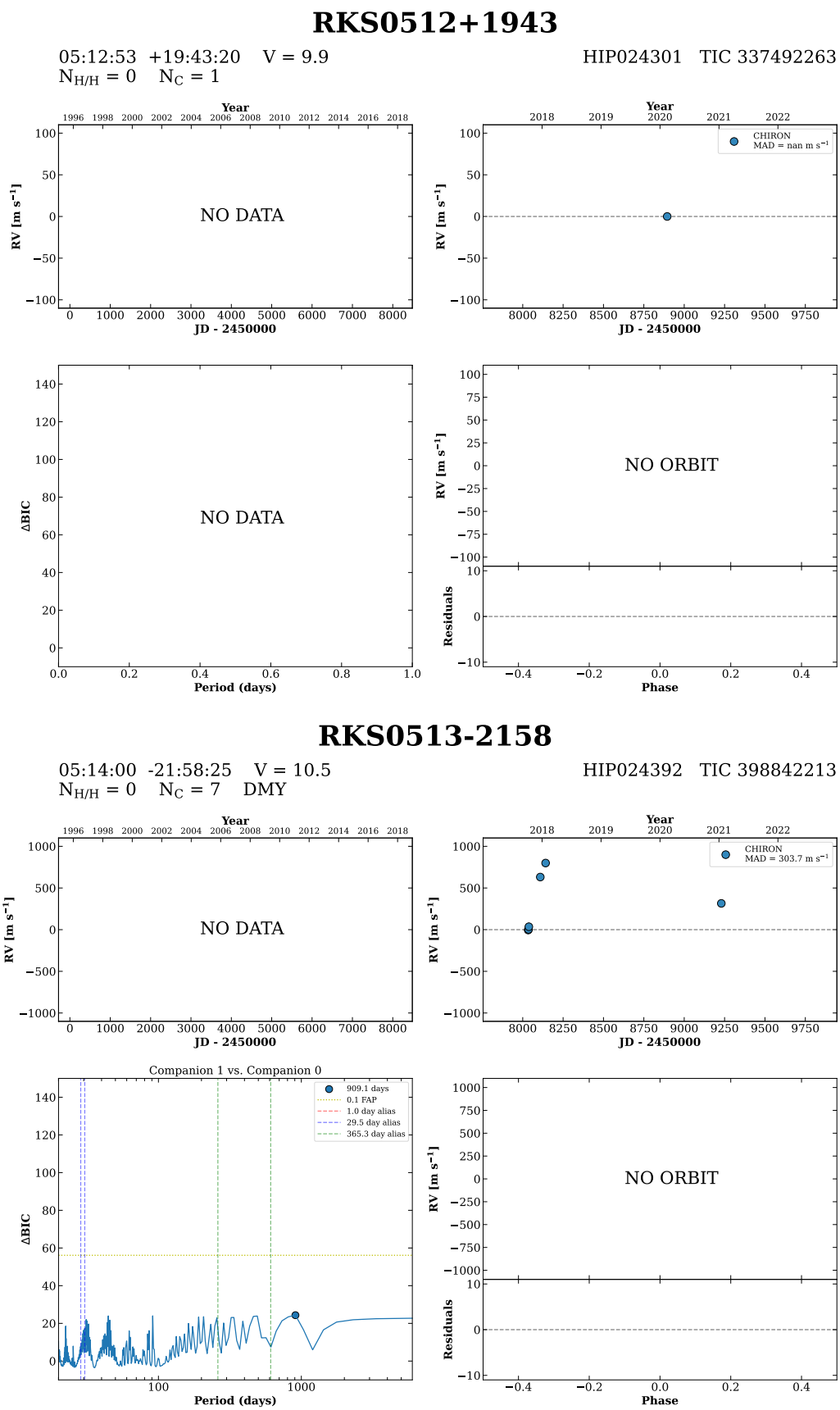

Figure 93 RV results for RKS0512+1943 (top) and RKS0513-2158 (bottom).

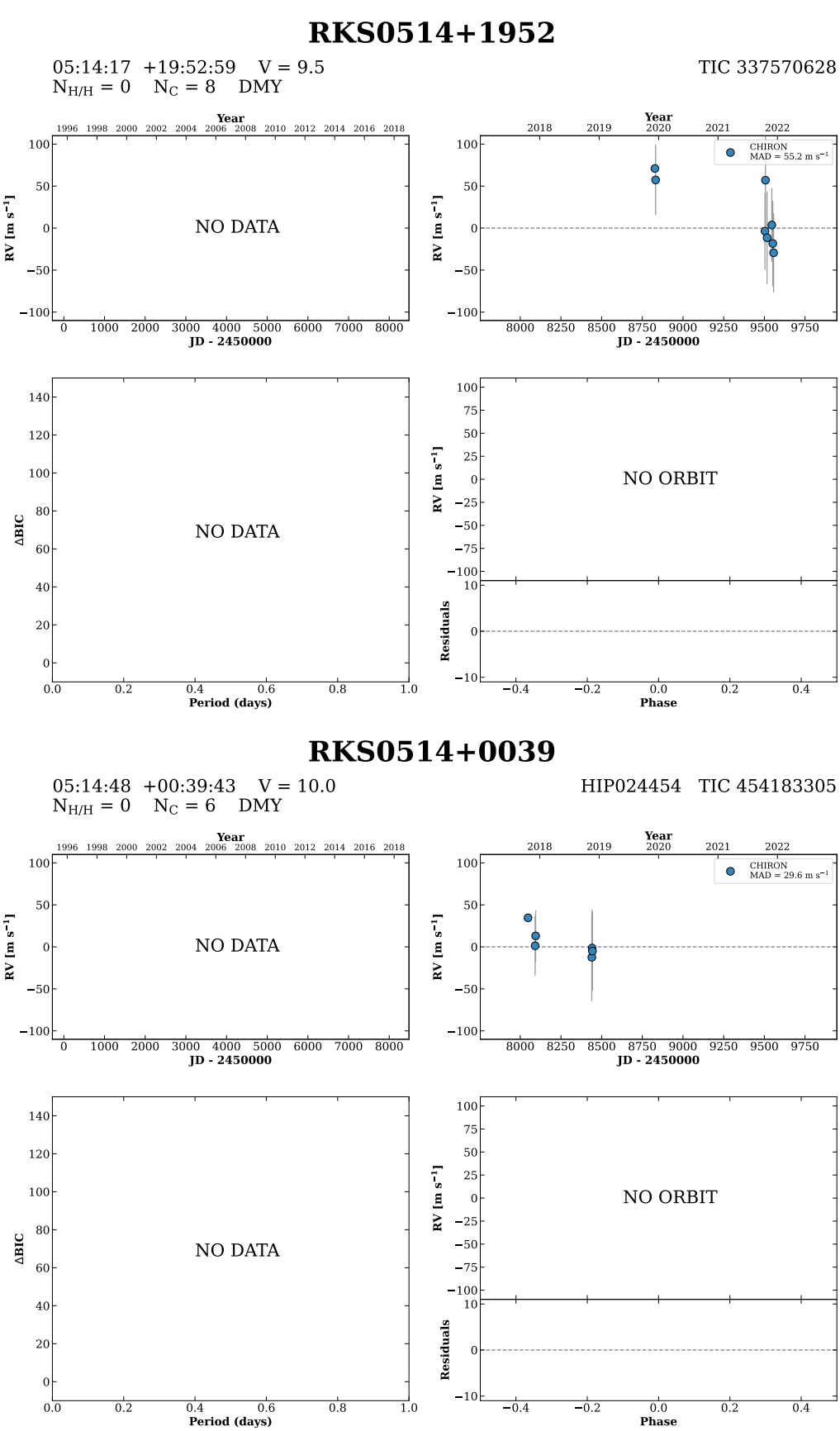

Figure 94 RV results for RKS0514+1952 (top) and RKS0514+0039 (bottom).

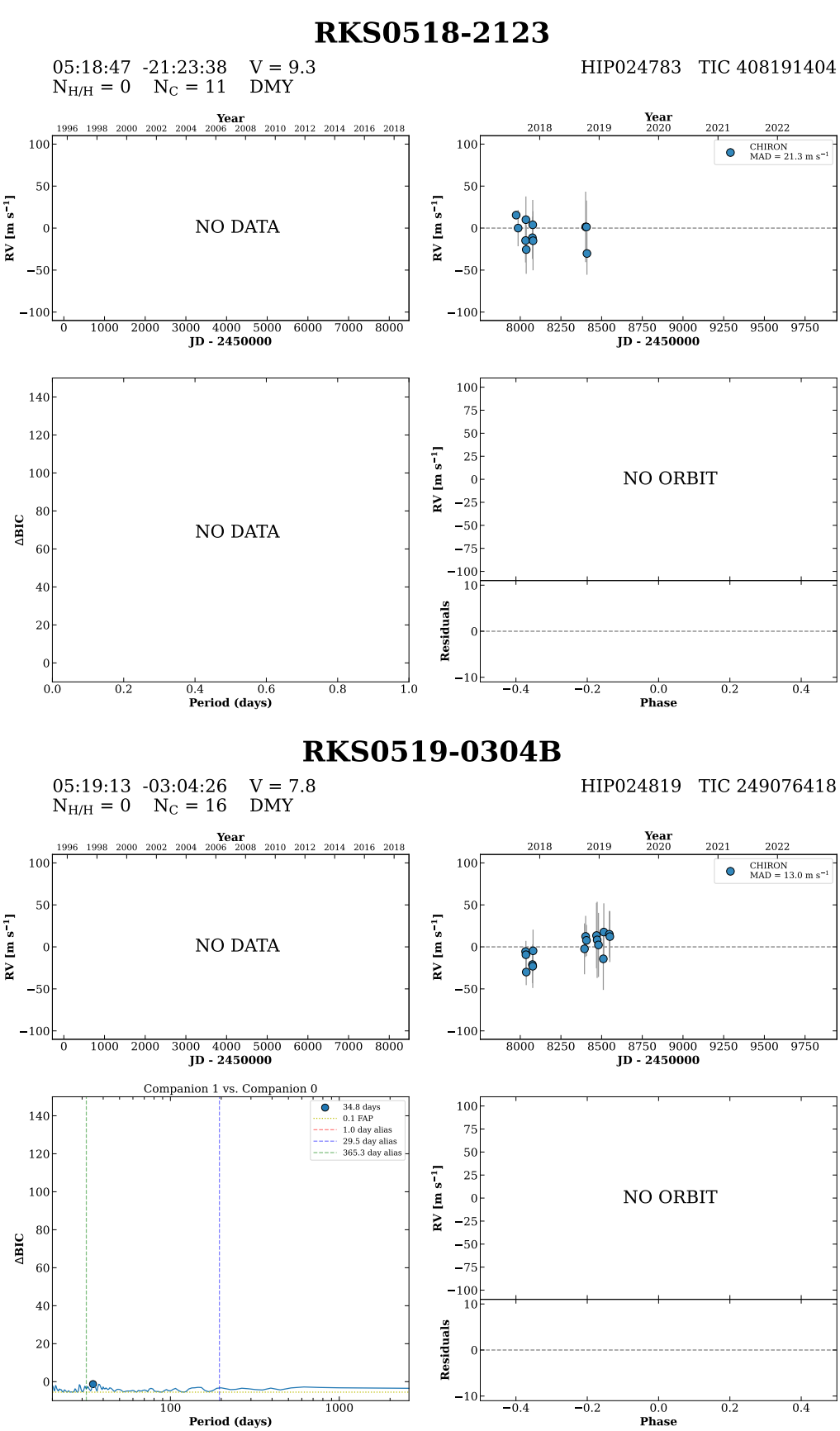

Figure 95 RV results for RKS0518-2123 (top) and RKS0519-0304B (bottom).

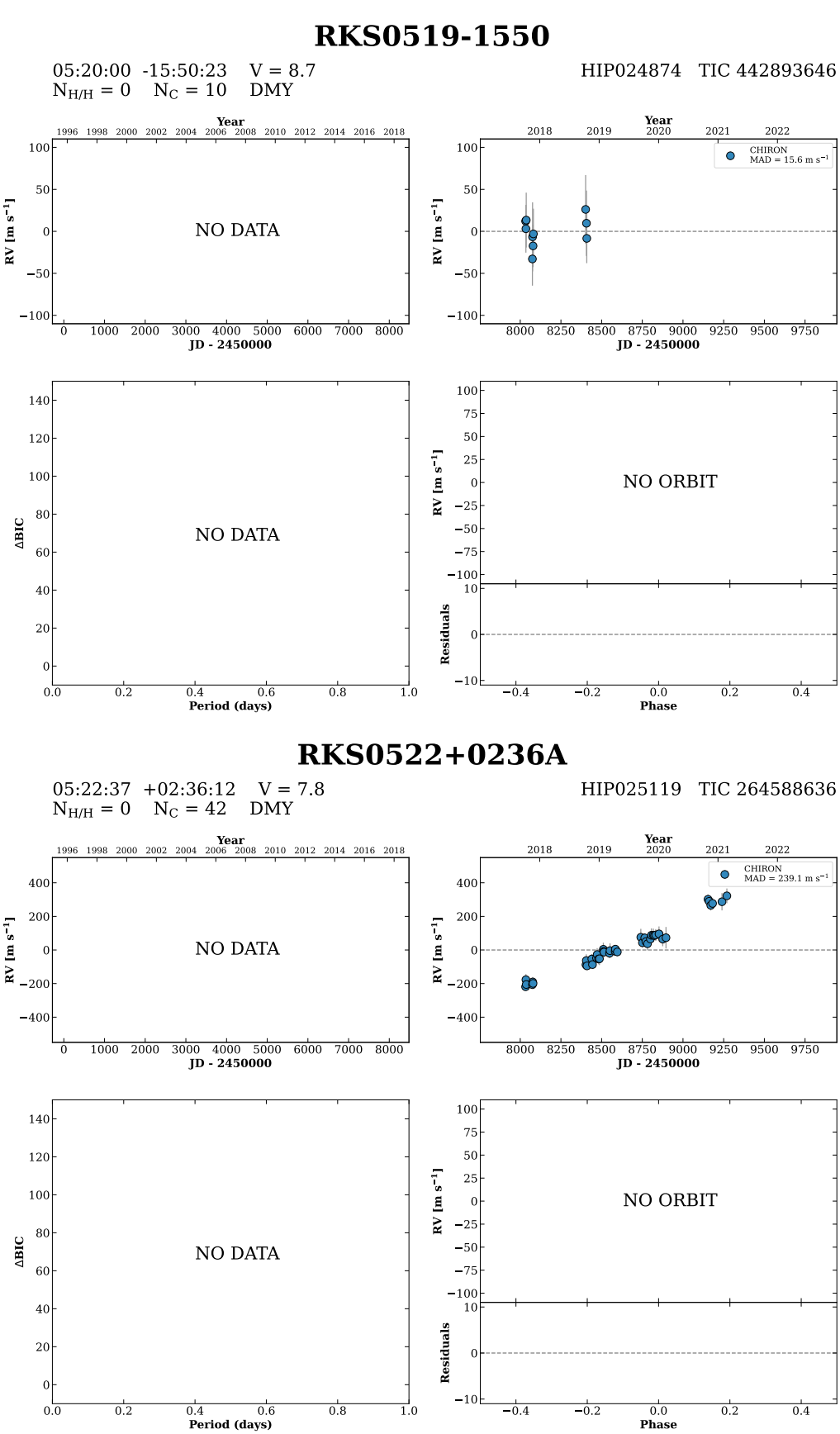

Figure 96 RV results for RKS0519-1550 (top) and RKS0522+0236A (bottom).

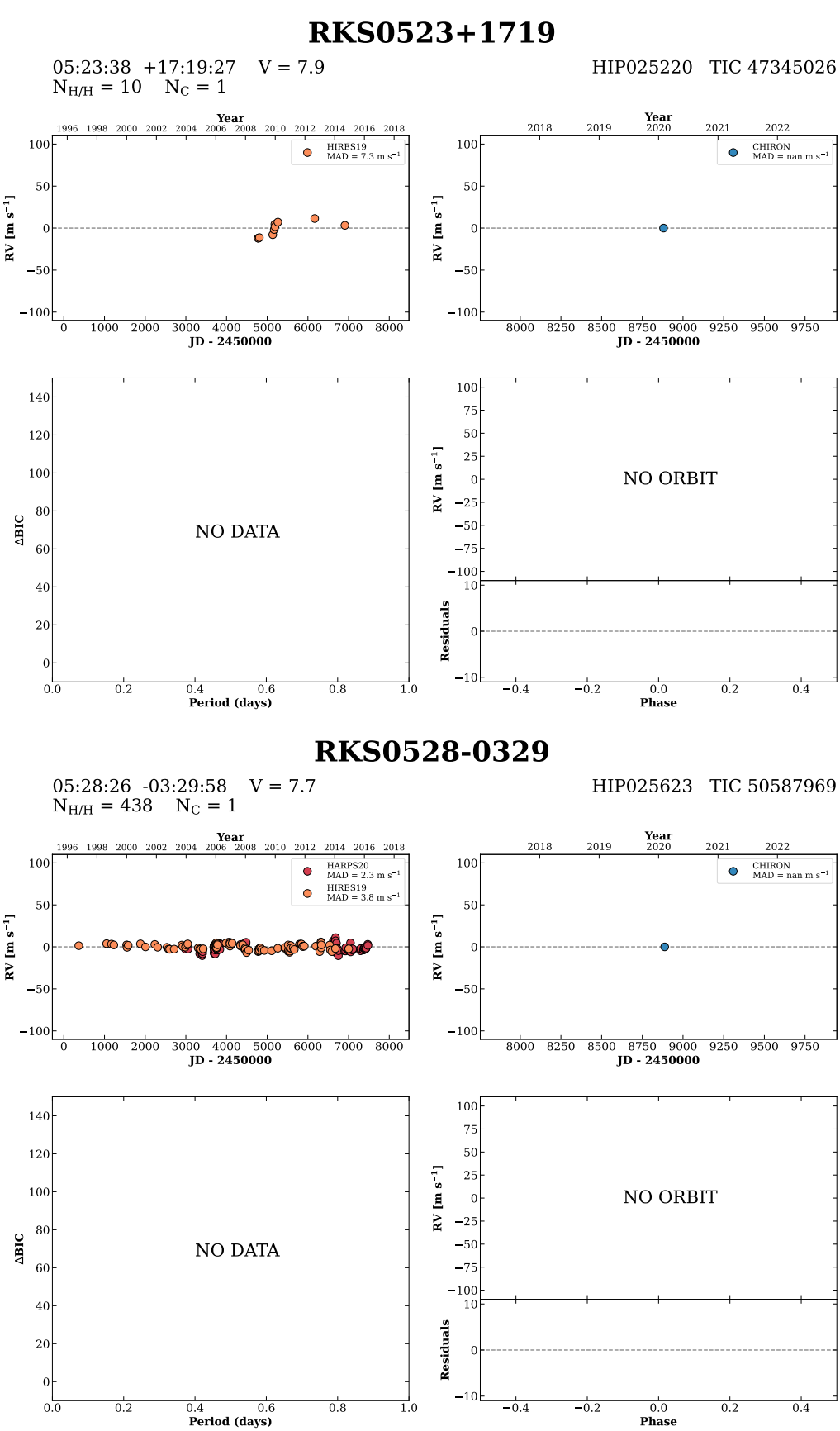

Figure 97 RV results for RKS0523+1719 (top) and RKS0528-0329 (bottom).

RKS0533-2643

05:33:05 -26:43:28 V = 9.1 HIP026013 TIC 31374837
$N_{H/H}$ = 51 N_C = 8 DMY

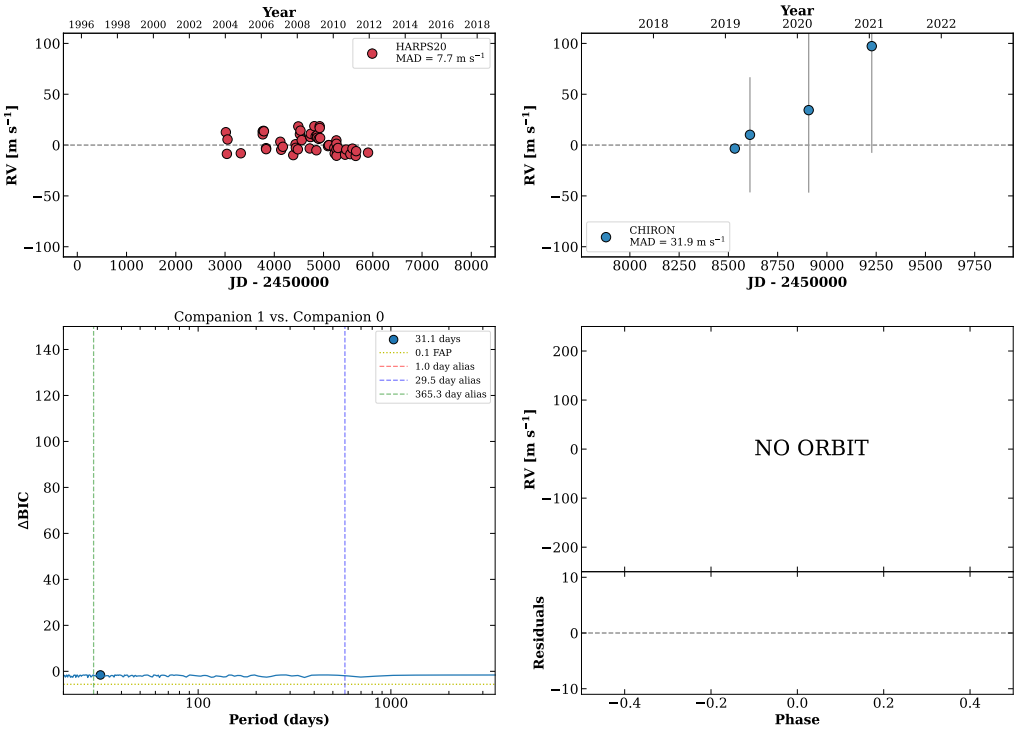

RKS0534-2328

05:34:49 -23:28:08 V = 8.8 HIP026175 TIC 92988866
$N_{H/H}$ = 0 N_C = 9 DMY

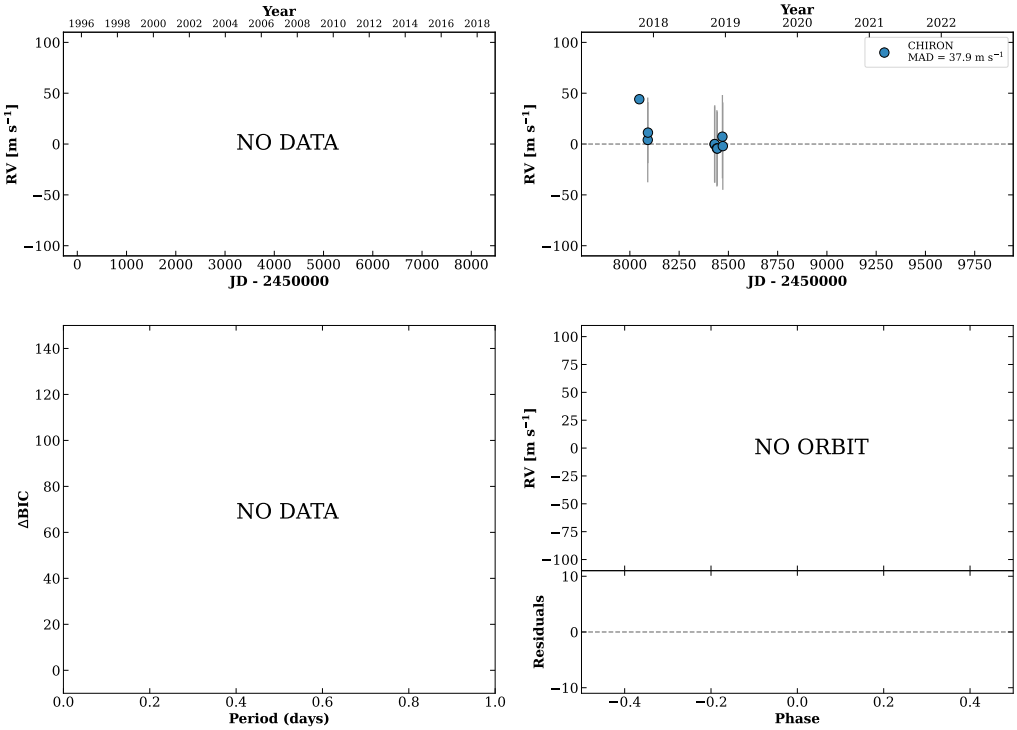

Figure 98 RV results for RKS0533-2643 (top) and RKS0534-2328 (bottom).

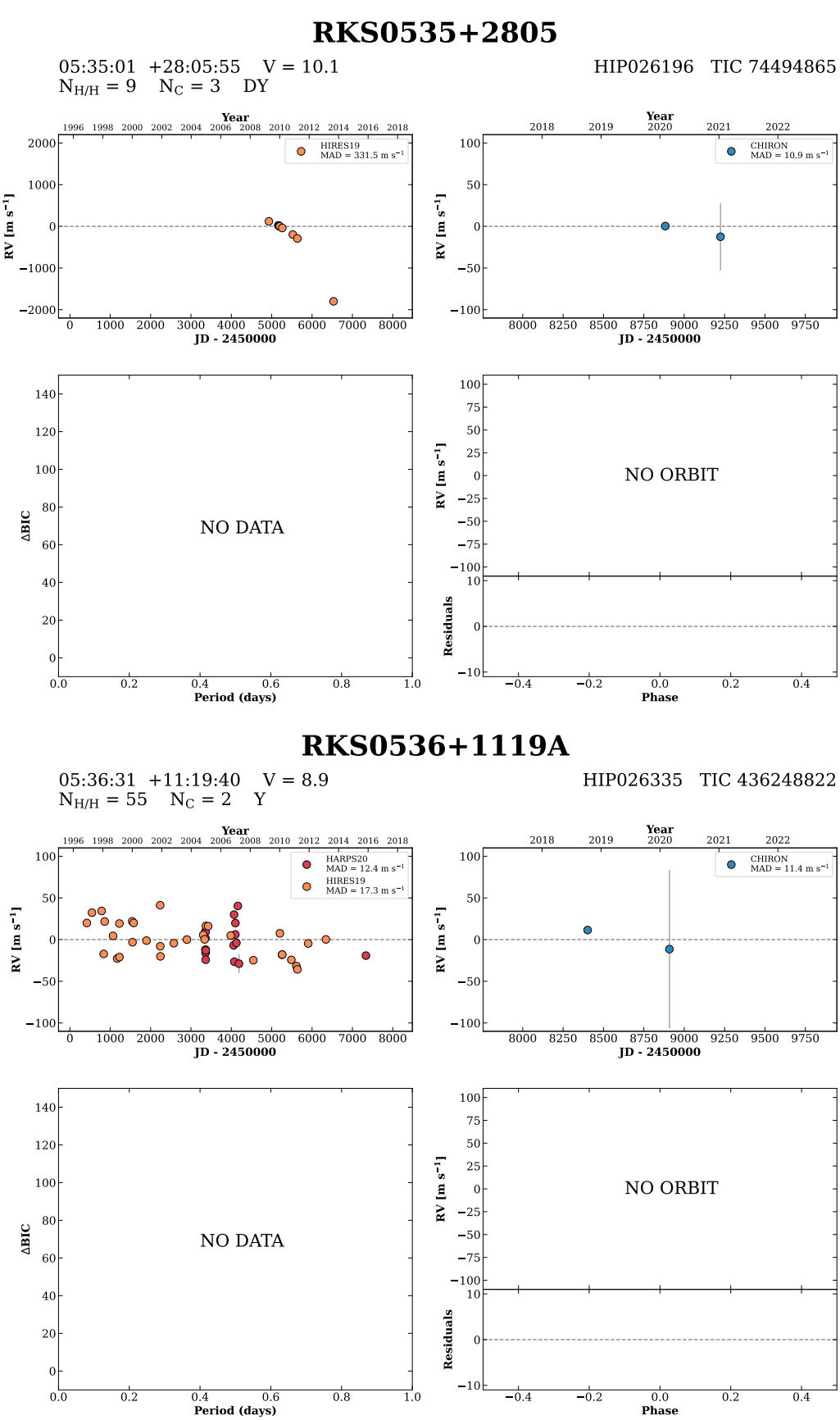

Figure 99 RV results for RKS0535+2805 (top) and RKS0536+1119A (bottom).

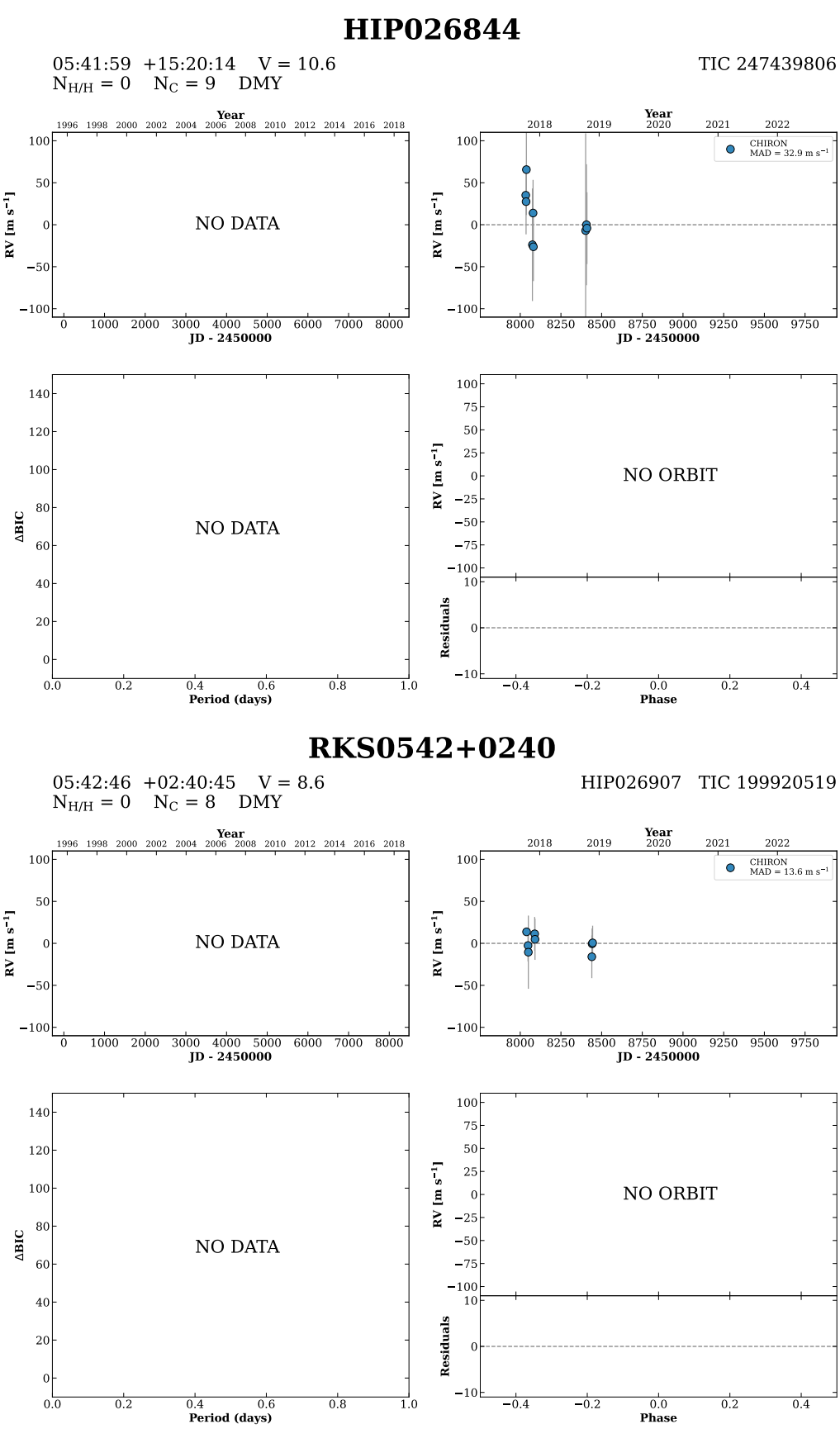

Figure 100 RV results for HIP026844 (top) and RKS0542+0240 (bottom).

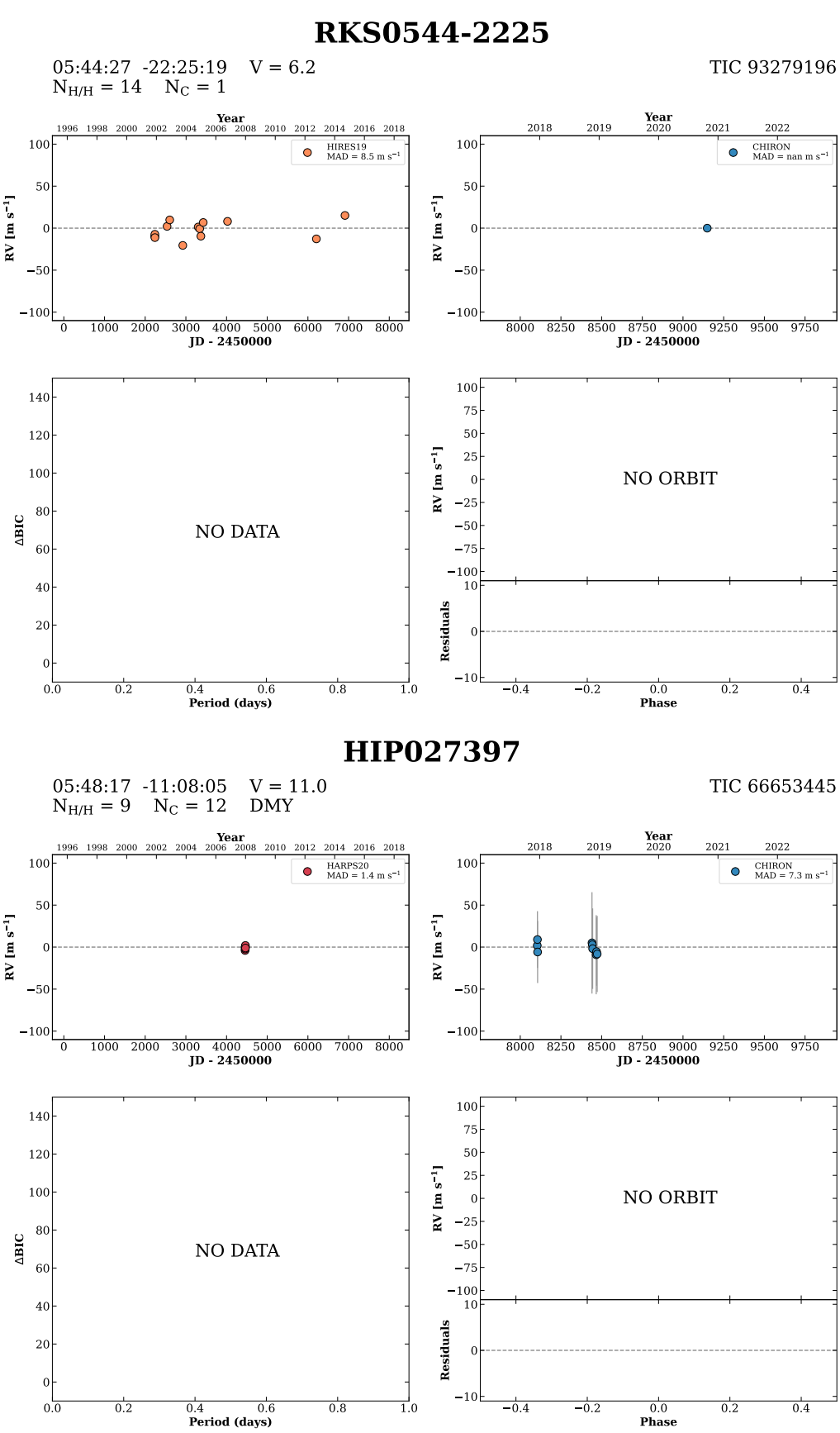

Figure 101 RV results for RKS0544-2225 (top) and HIP027397 (bottom).

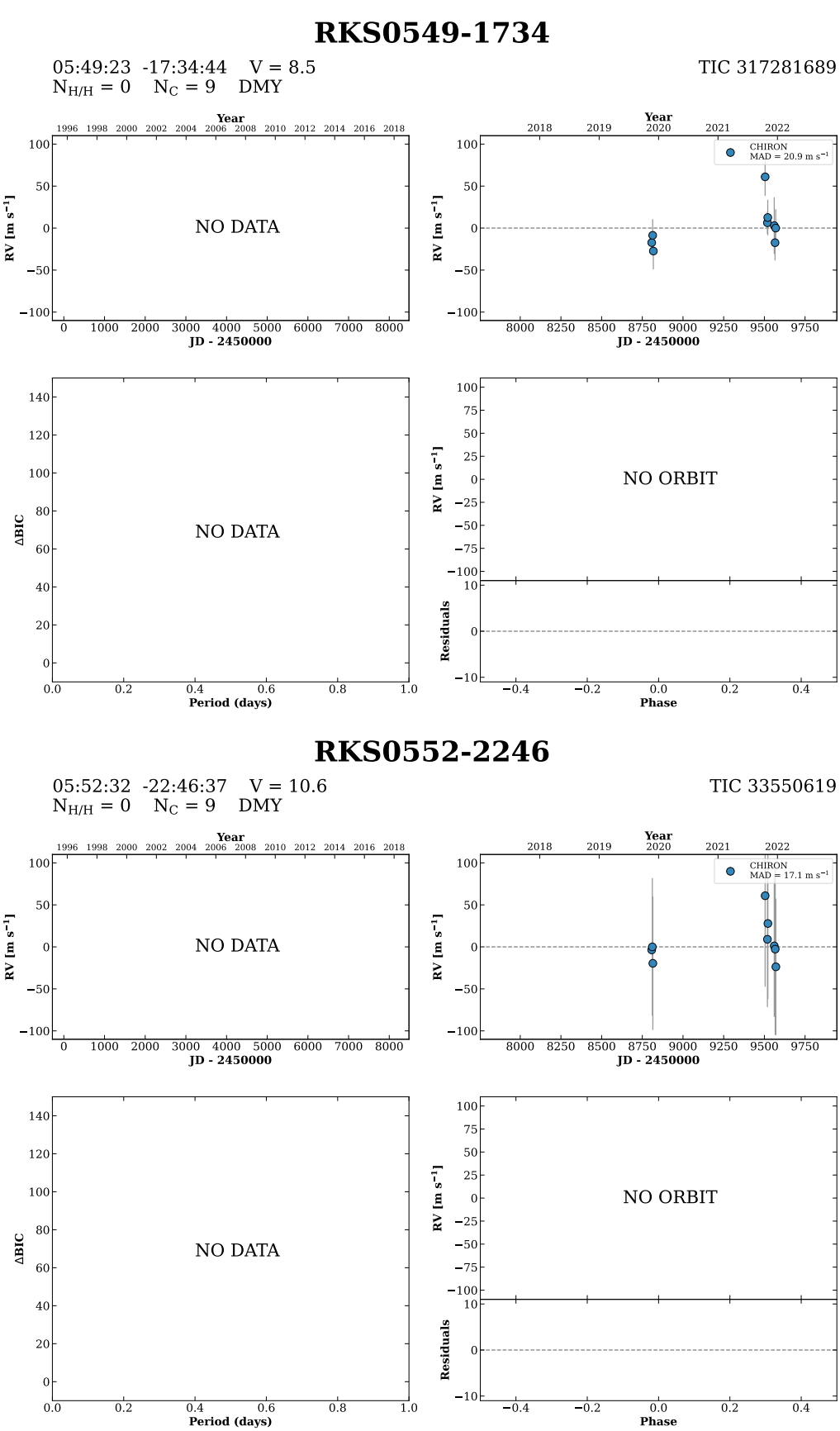

Figure 102 RV results for RKS0549-1734 (top) and RKS0552-2246 (bottom).

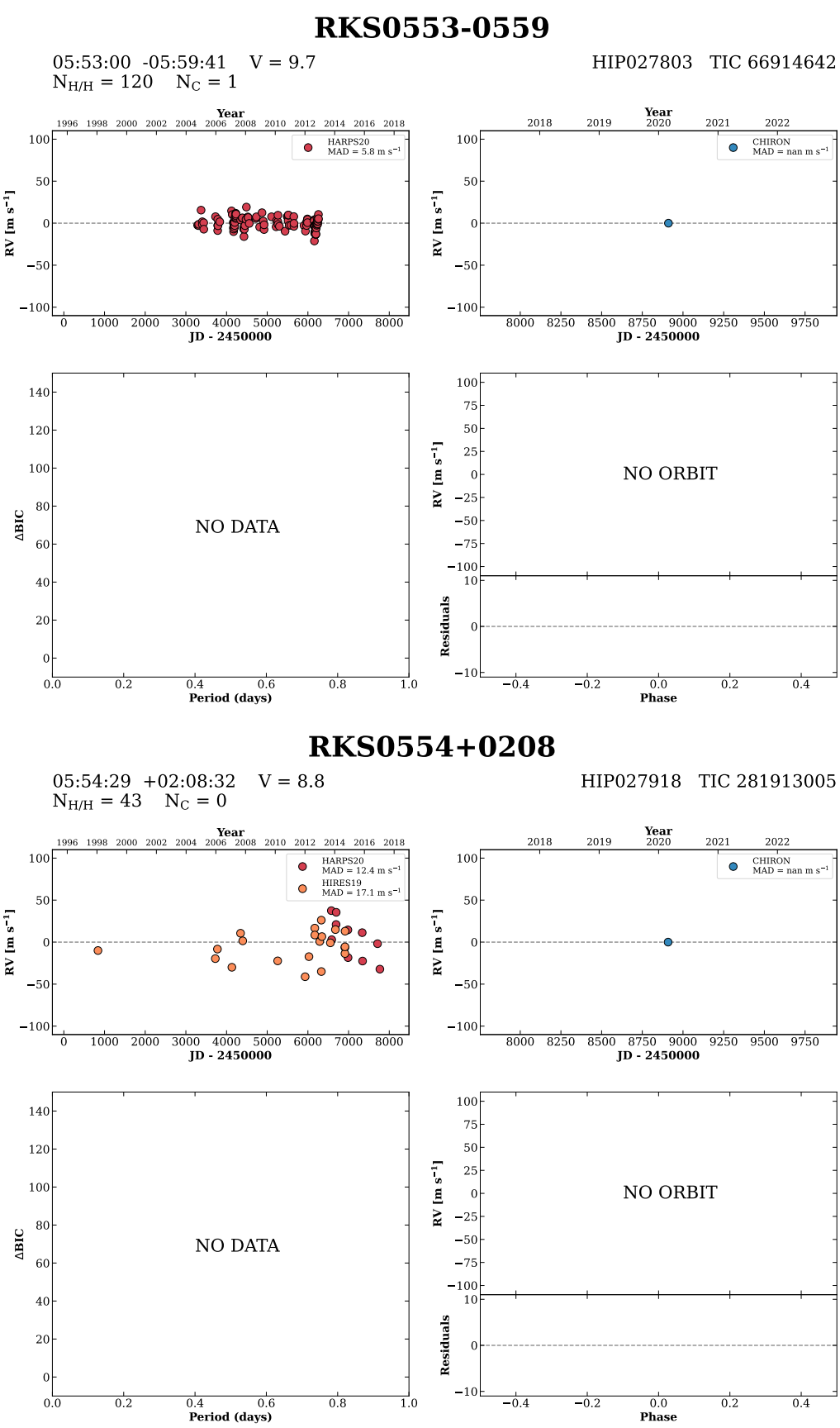

Figure 103 RV results for RKS0553-0559 (top) and RKS0554+0208 (bottom).

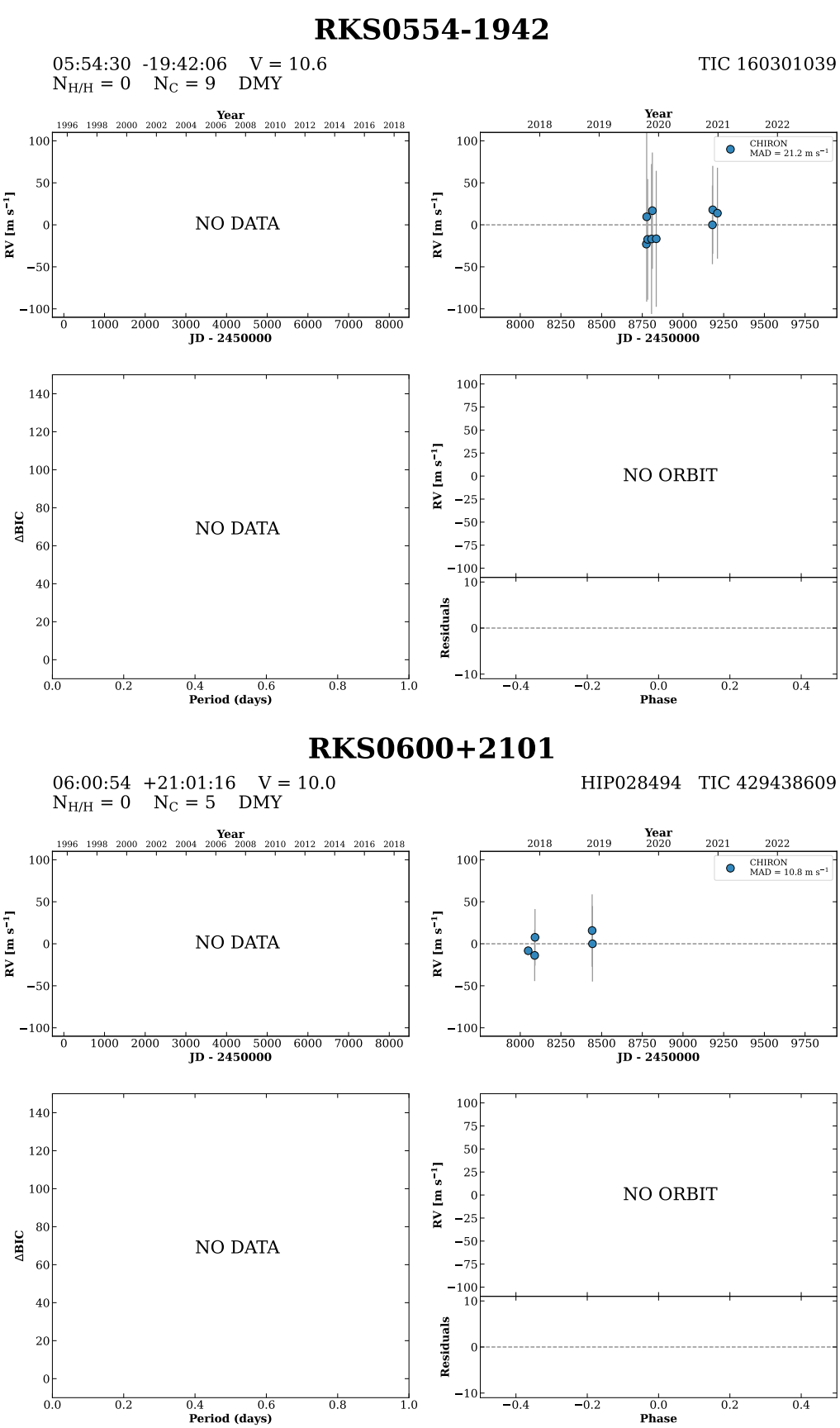

Figure 104 RV results for RKS0554-1942 (top) and RKS0600+2101 (bottom).

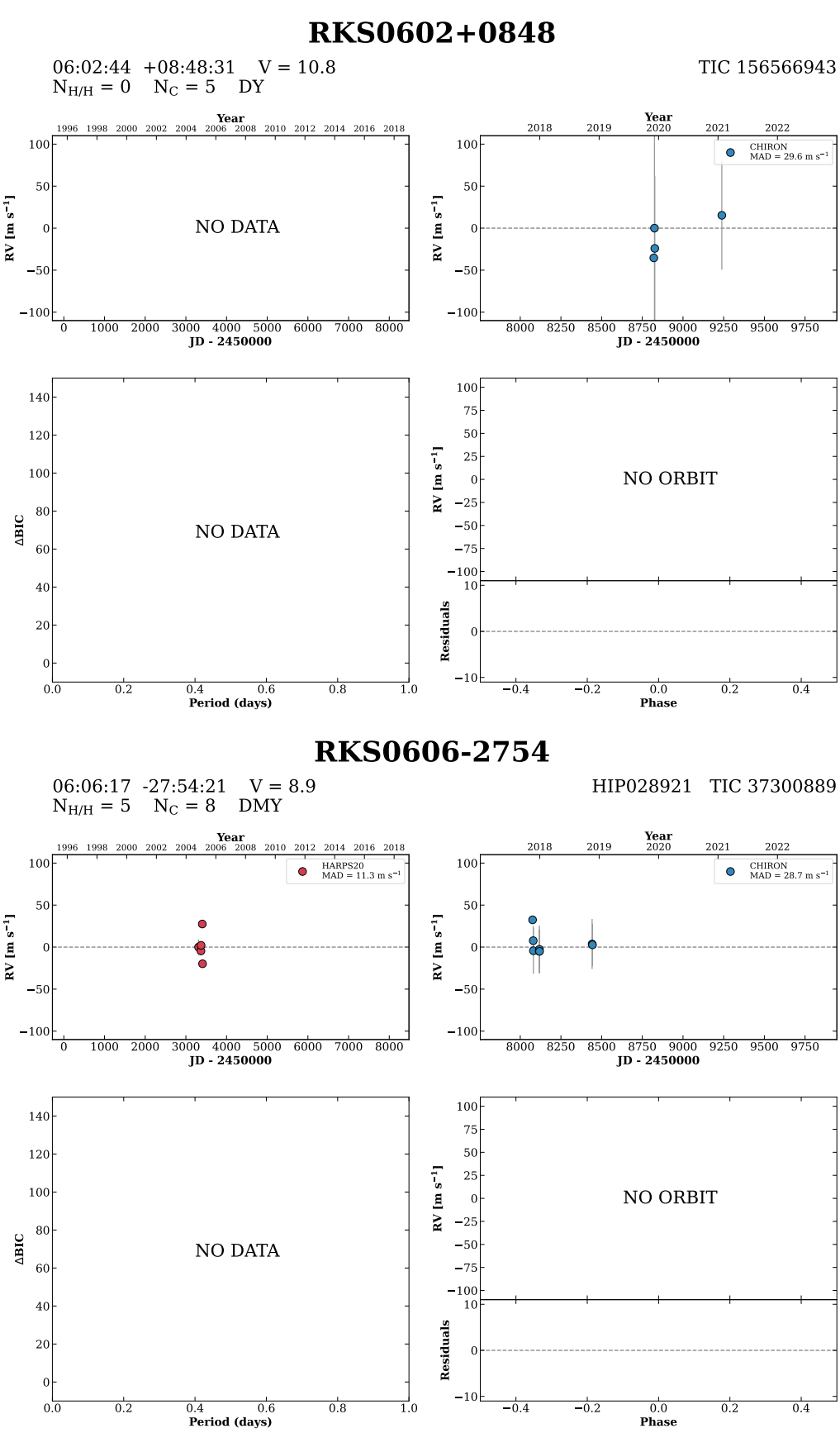

Figure 105 RV results for RKS0602+0848 (top) and RKS0606-2754 (bottom).

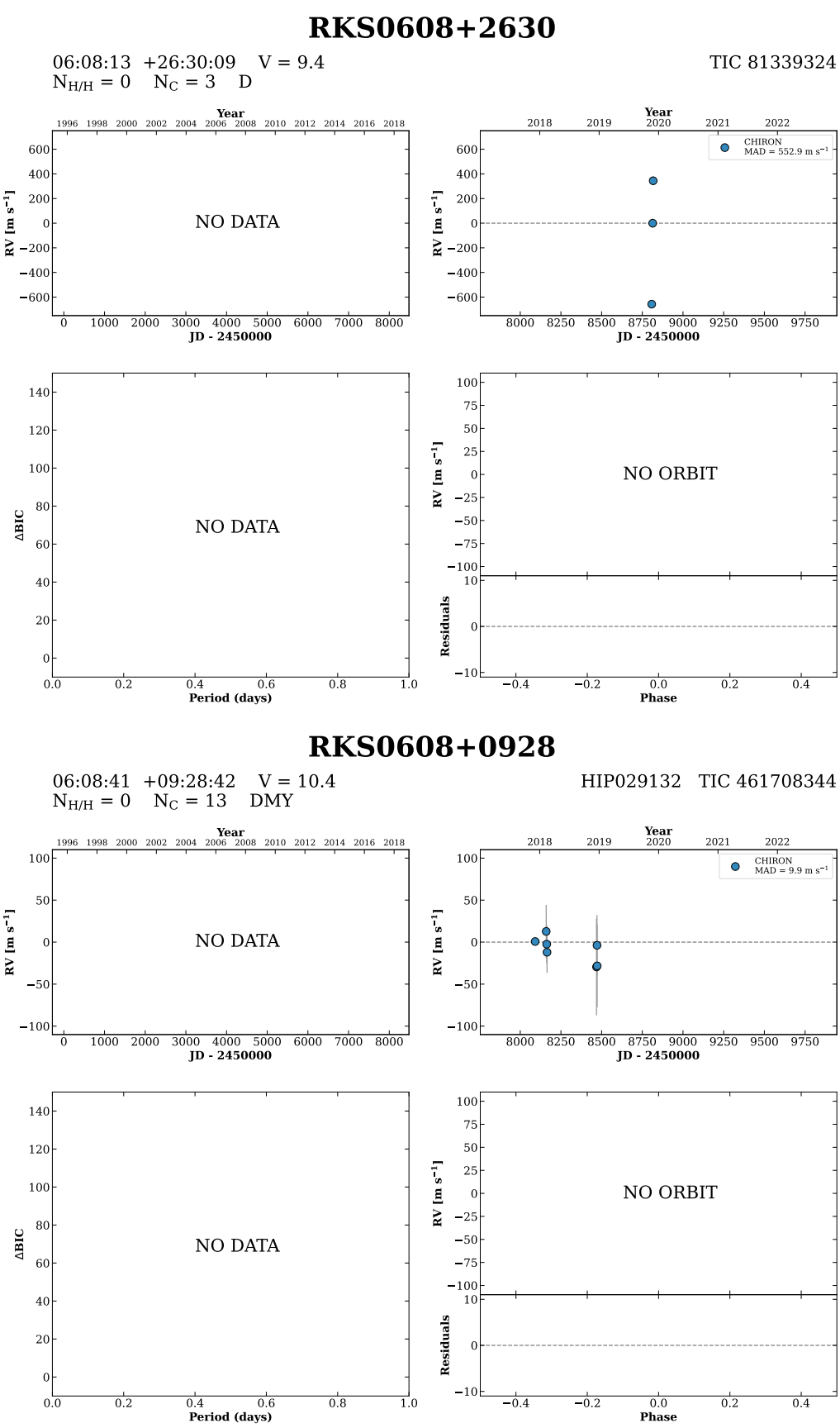

Figure 106 RV results for RKS0608+2630 (top) and RKS0608+0928 (bottom).

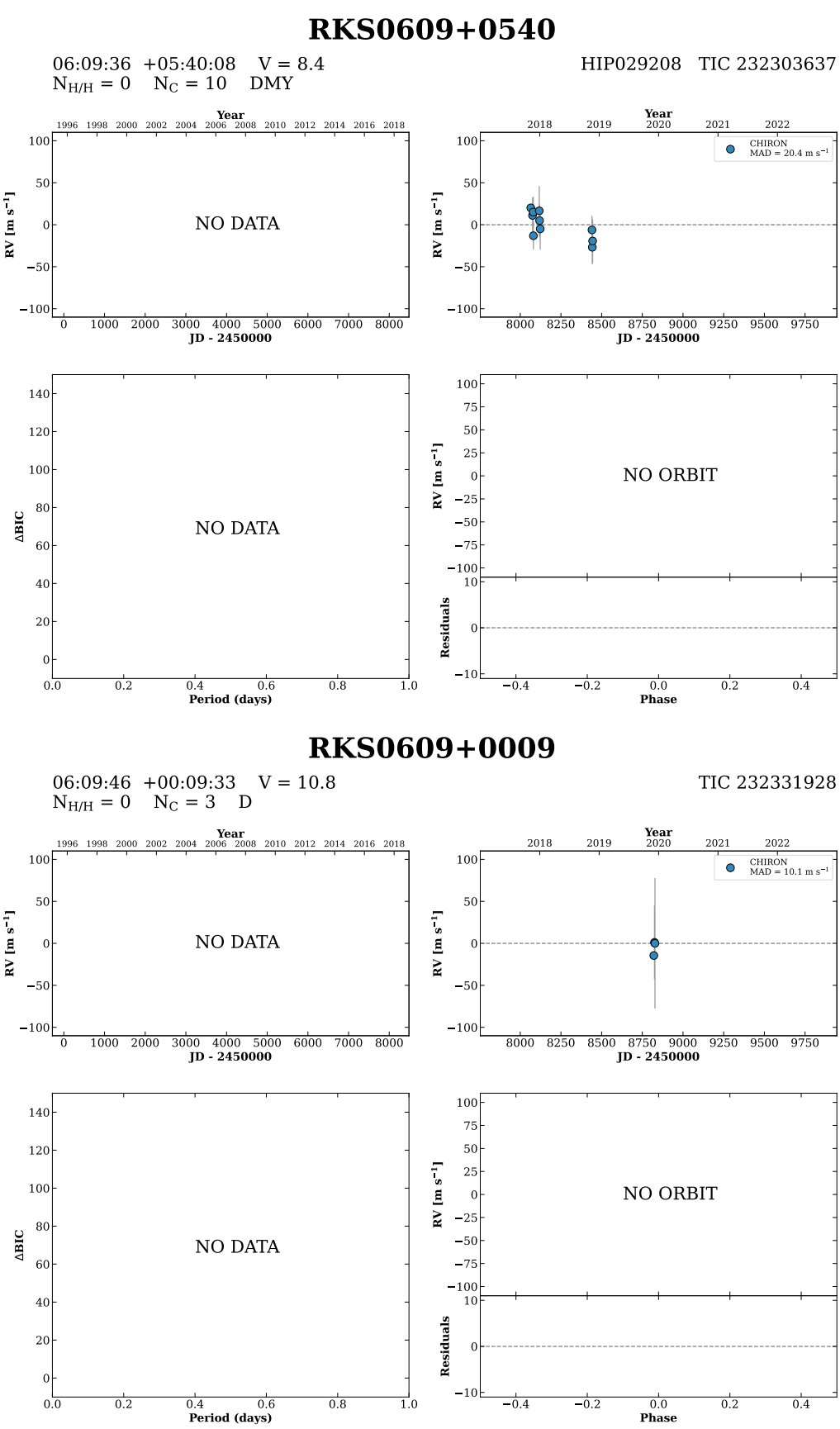

Figure 107 RV results for RKS0609+0540 (top) and RKS0609+0009 (bottom).

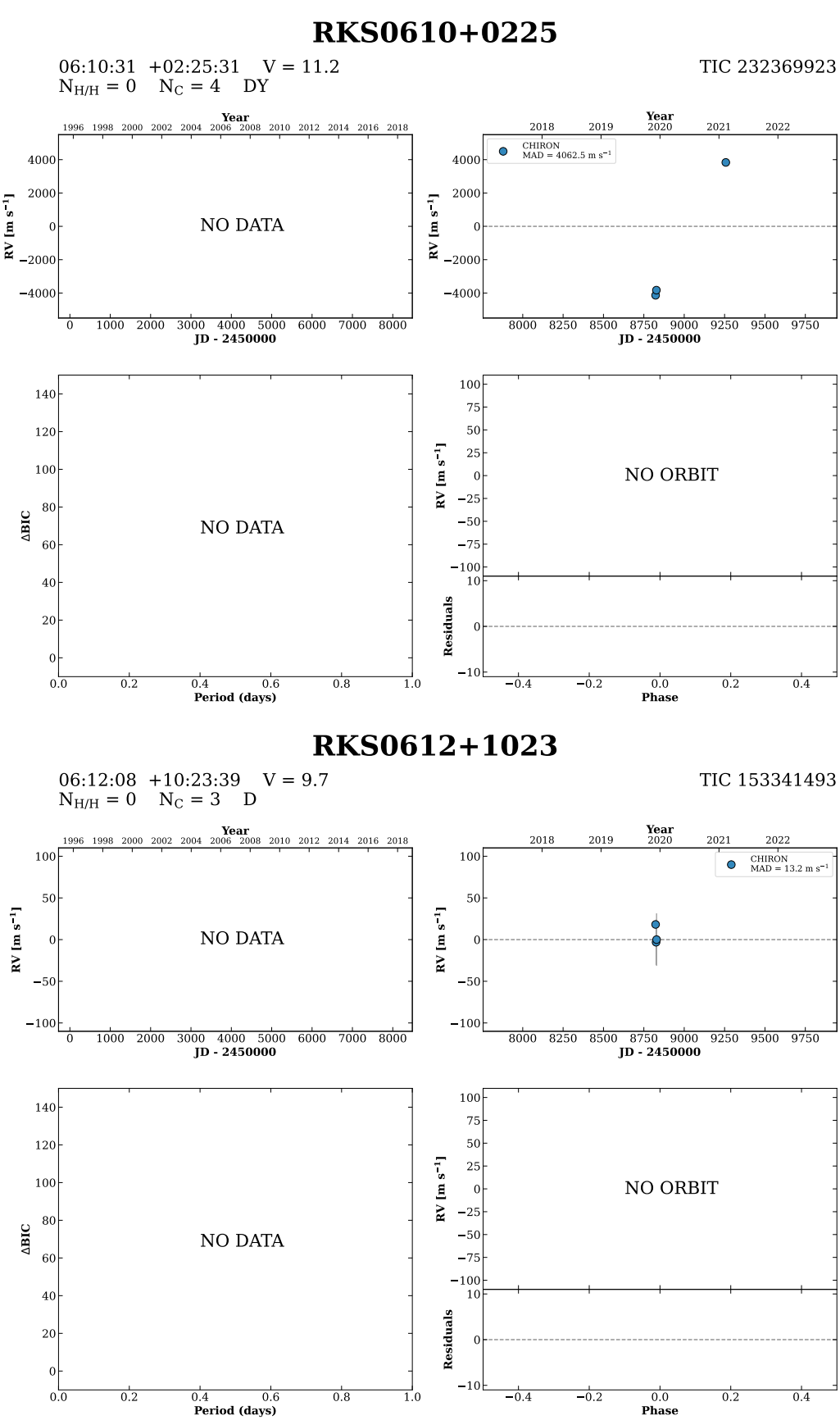

Figure 108 RV results for RKS0610+0225 (top) and RKS0612+1023 (bottom).

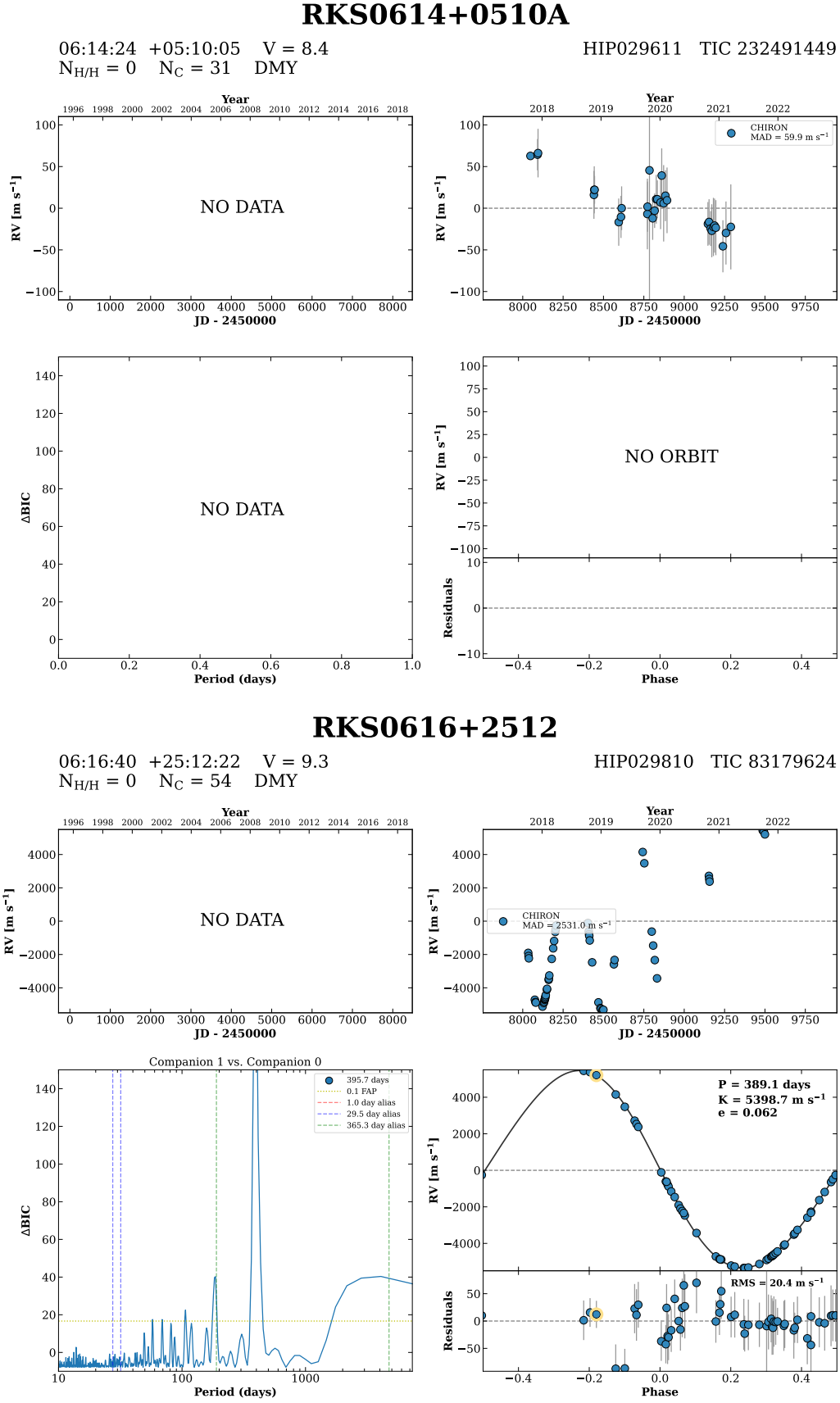

Figure 109 RV results for RKS0614+0510A (top) and RKS0616+2512 (bottom).

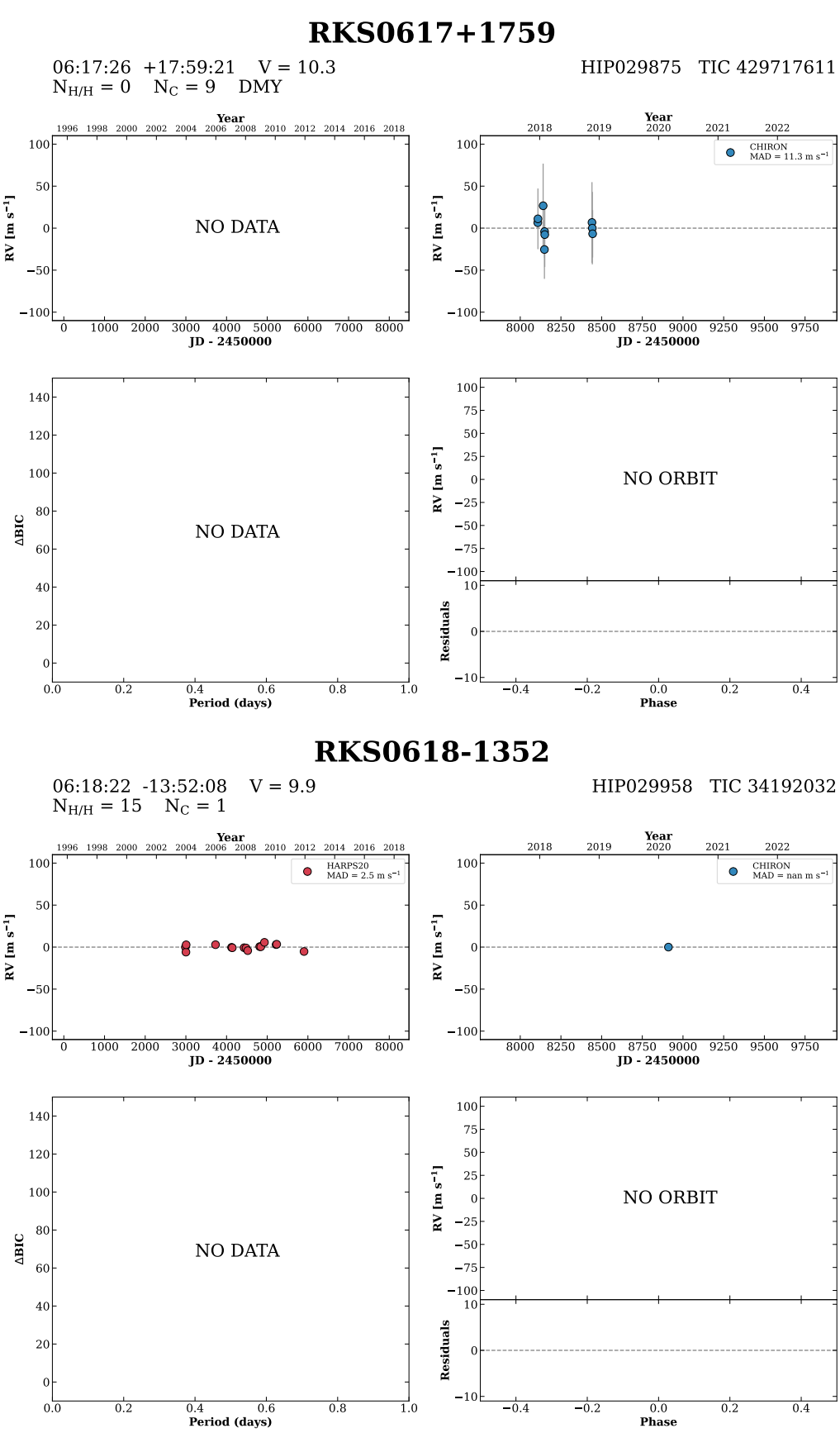

Figure 110 RV results for RKS0617+1759 (top) and RKS0618-1352 (bottom).

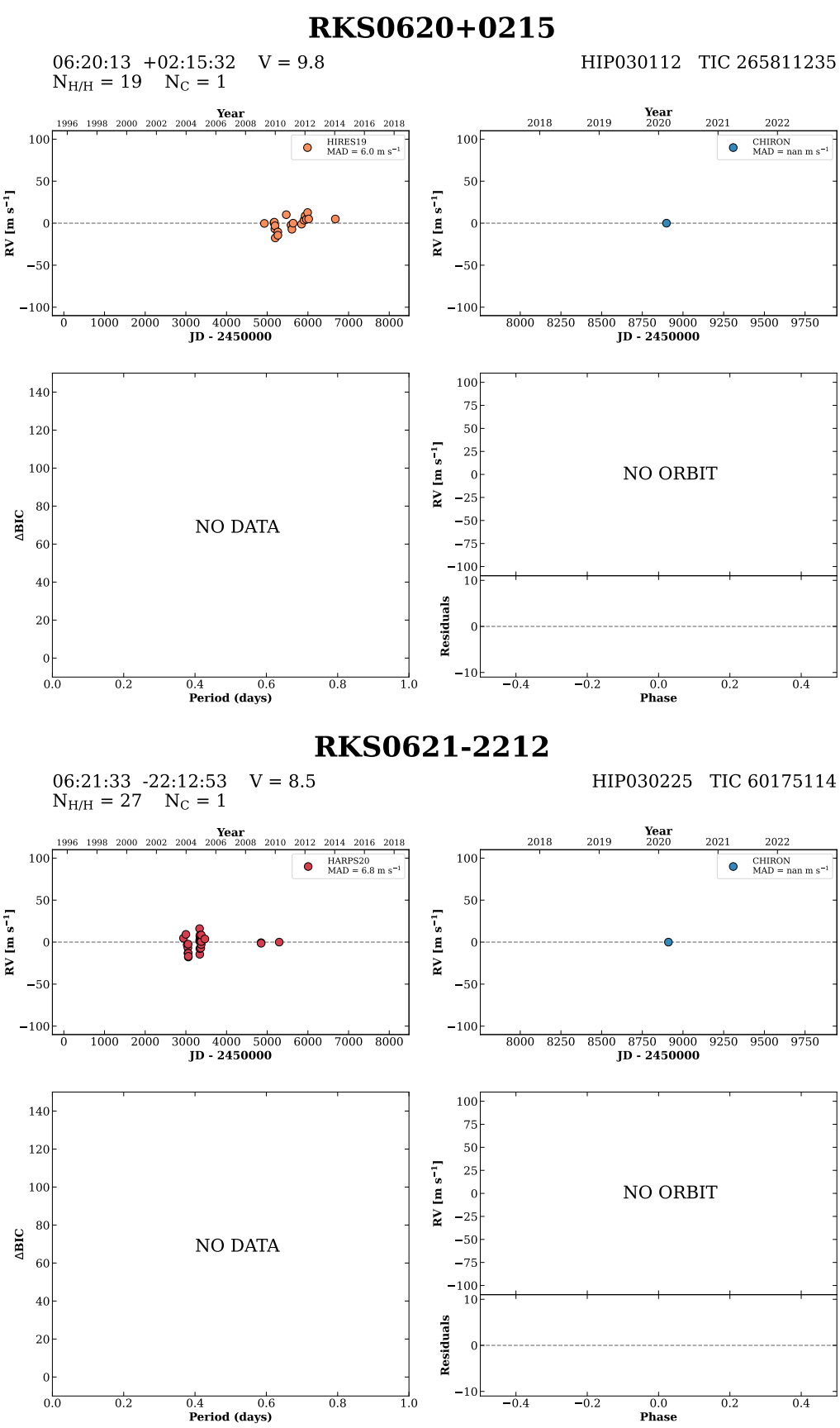

Figure 111 RV results for RKS0620+0215 (top) and RKS0621-2212 (bottom).

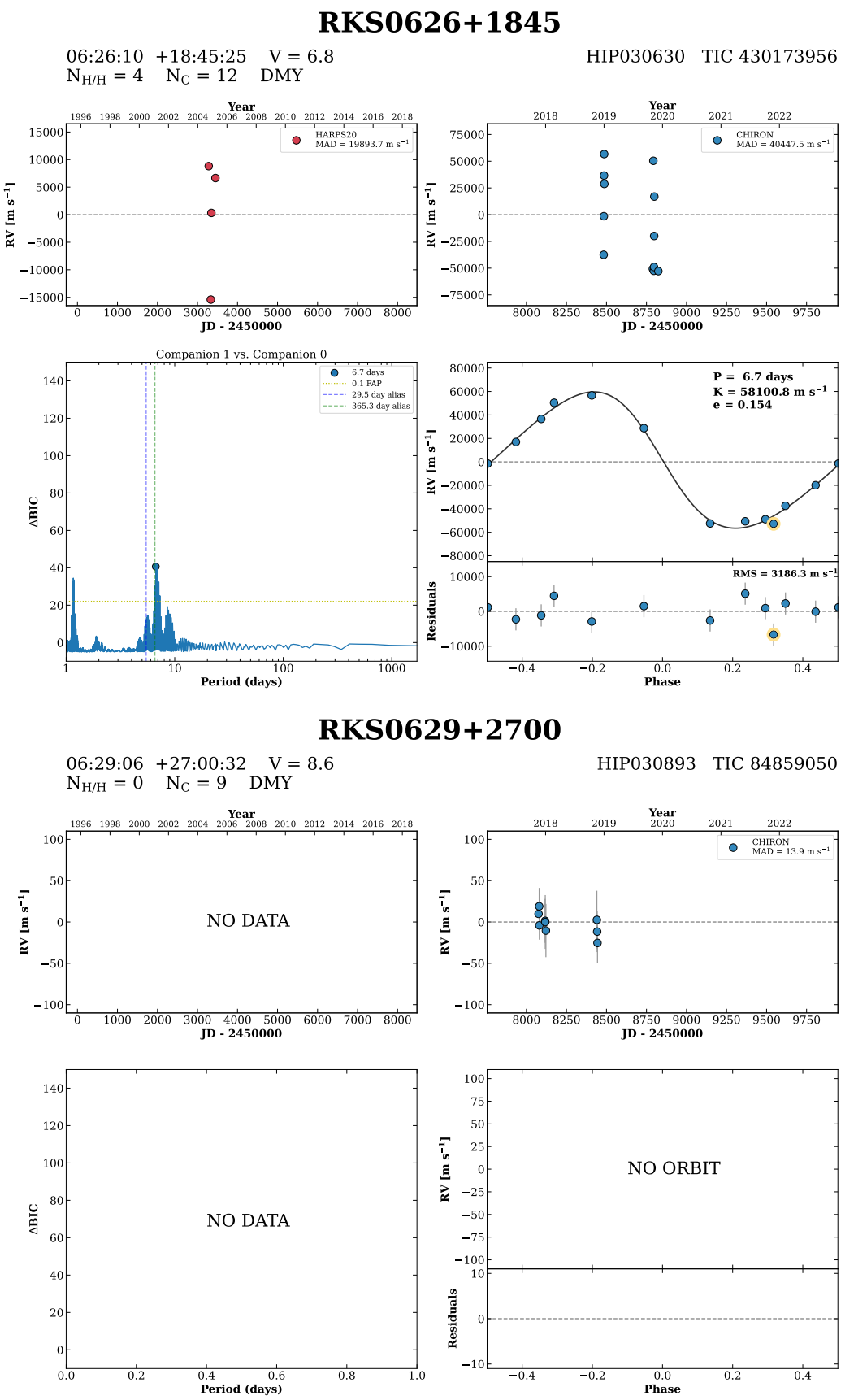

Figure 112 RV results for RKS0626+1845 (top) and RKS0629+2700 (bottom).

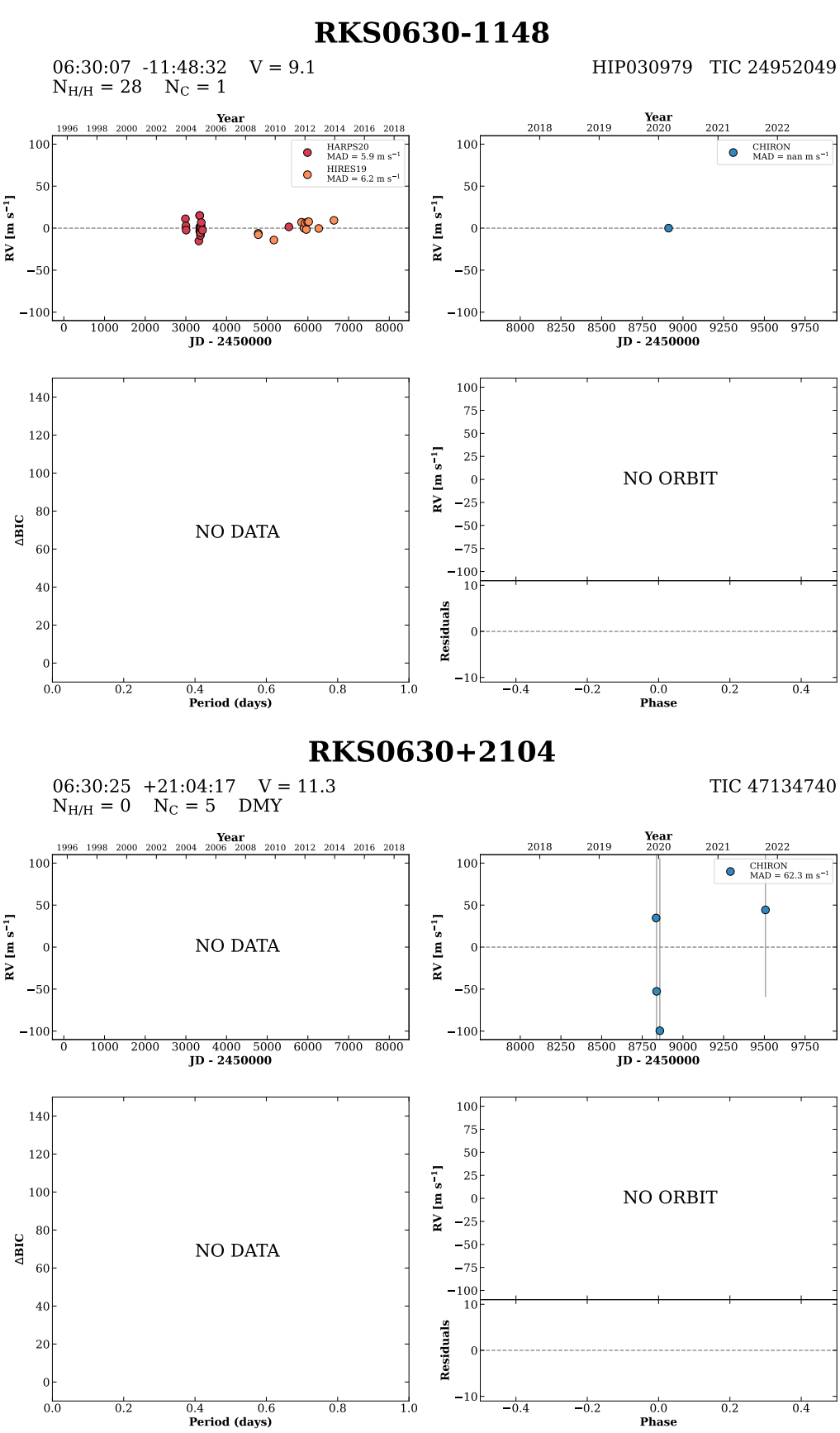

Figure 113 RV results for RKS0630-1148 (top) and RKS0630+2104 (bottom).

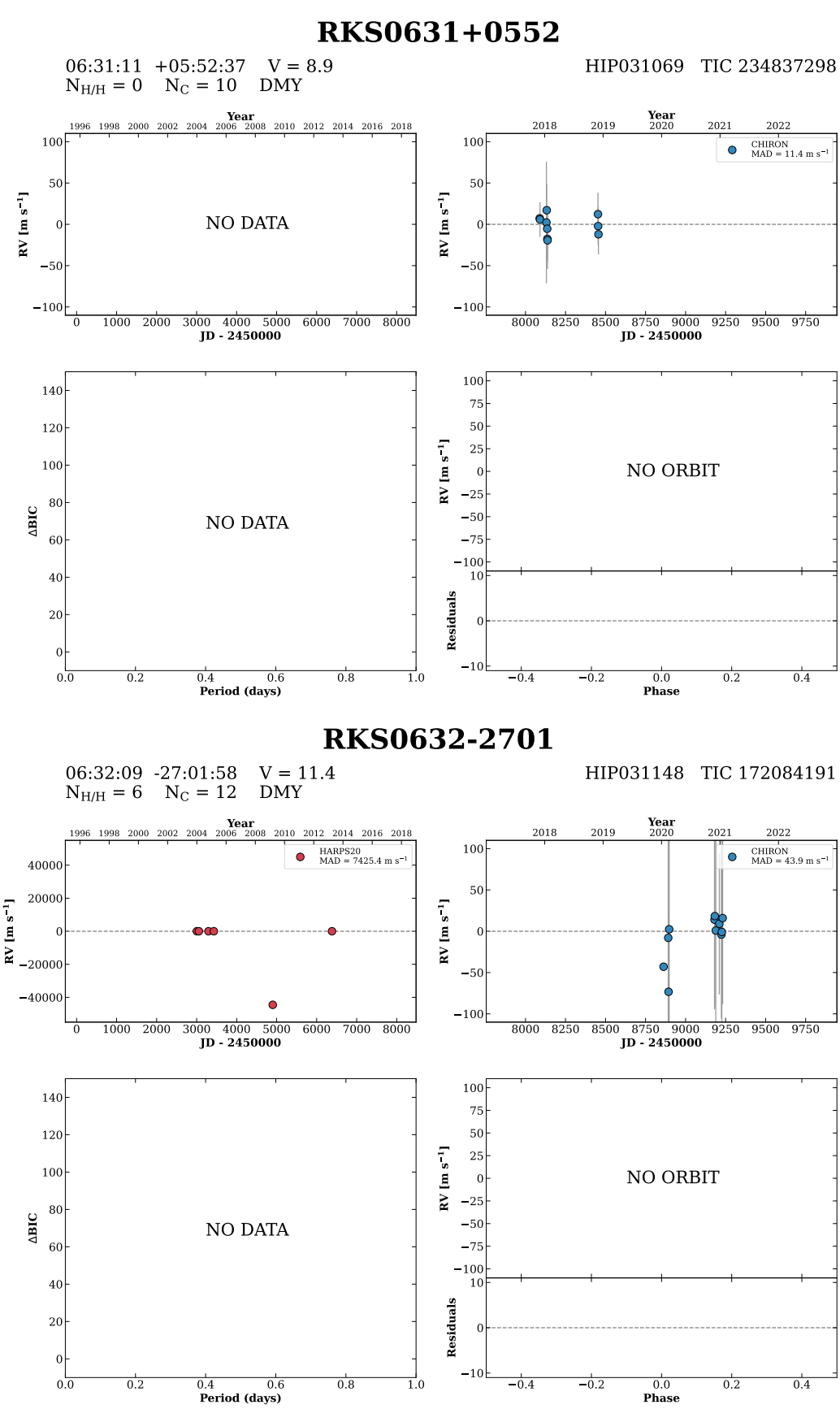

Figure 114 RV results for RKS0631+0552 (top) and RKS0632-2701 (bottom).

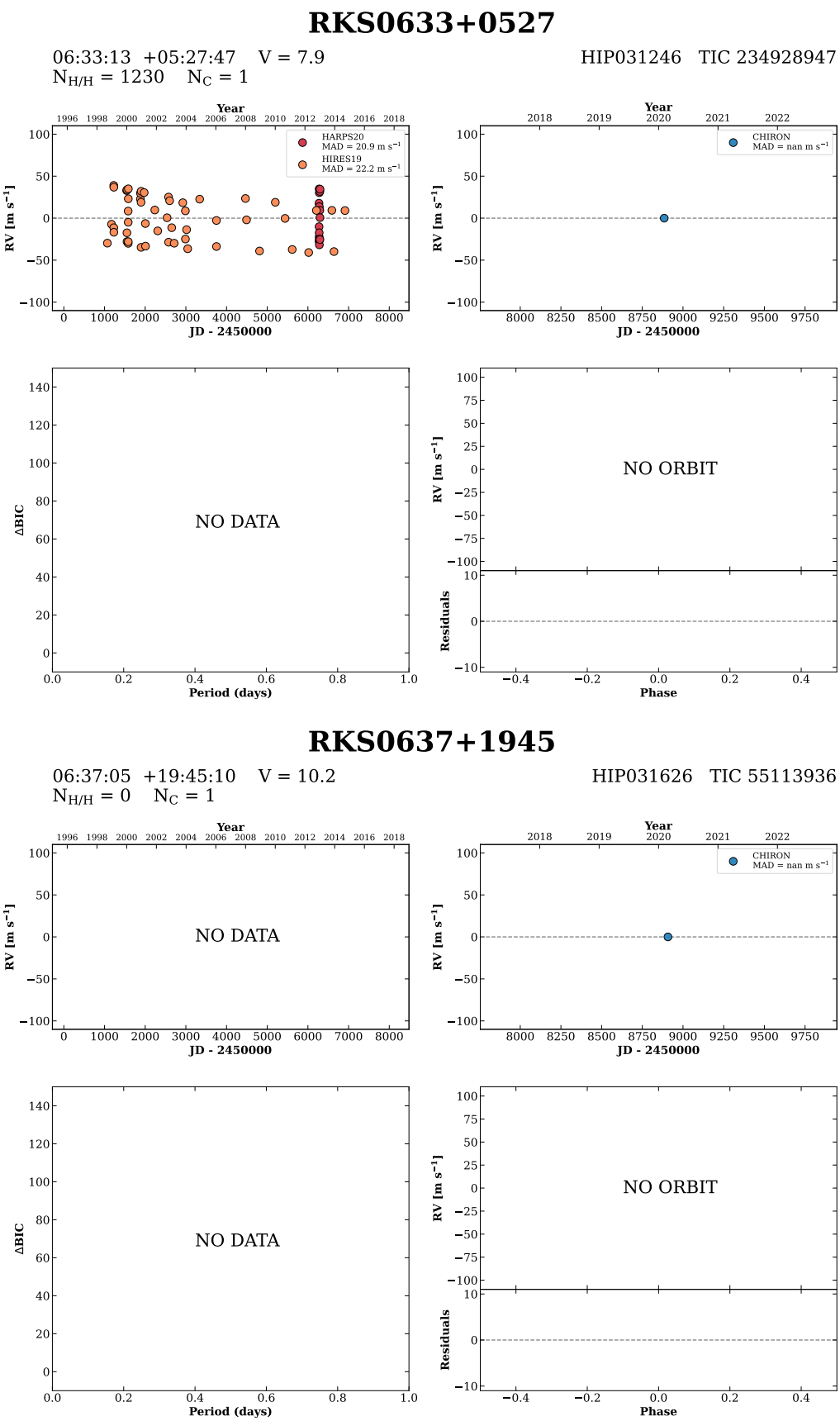

Figure 115 RV results for RKS0633+0527 (top) and RKS0637+1945 (bottom).

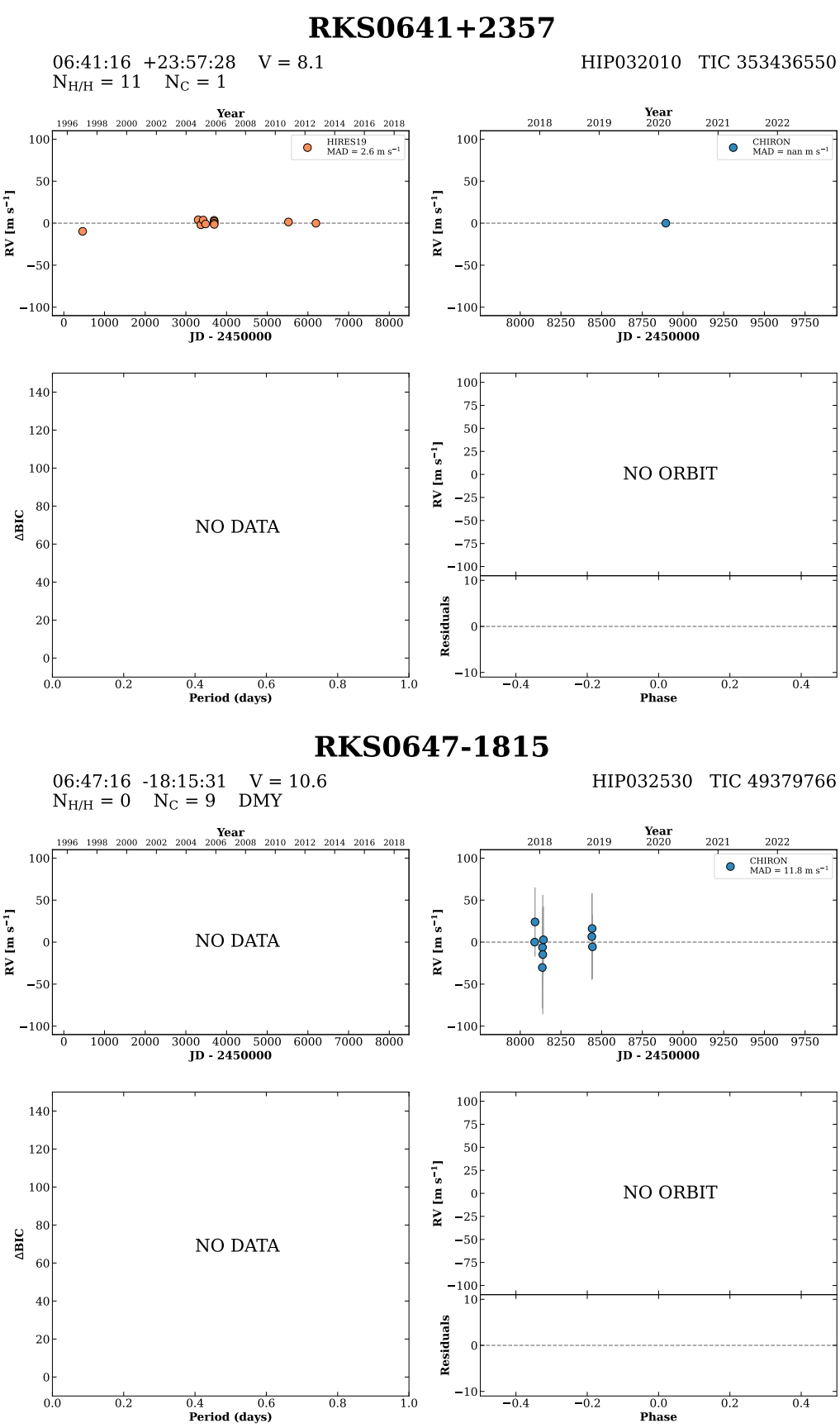

Figure 116 RV results for RKS0641+2357 (top) and RKS0647-1815 (bottom).

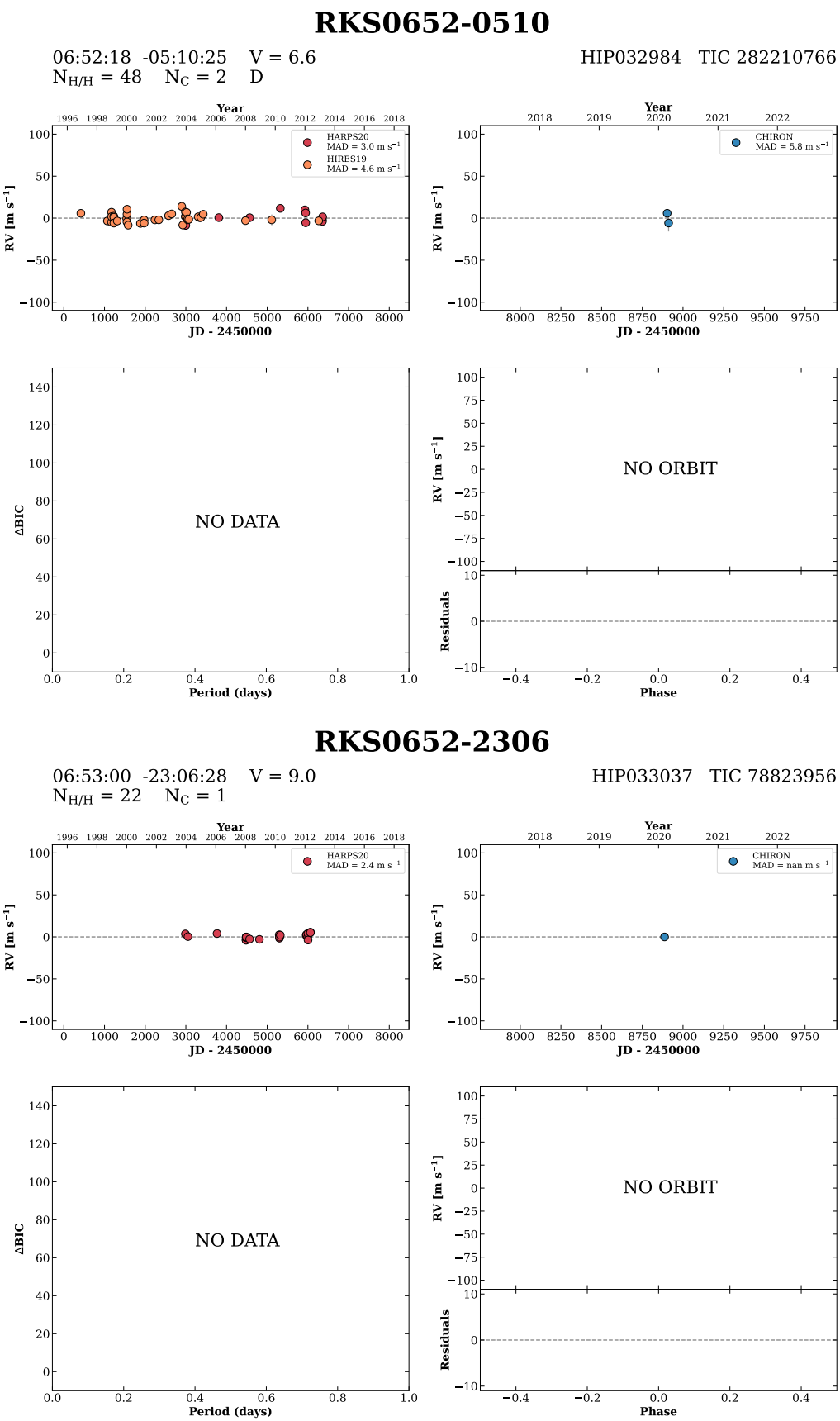

Figure 117 RV results for RKS0652-0510 (top) and RKS0652-2306 (bottom).

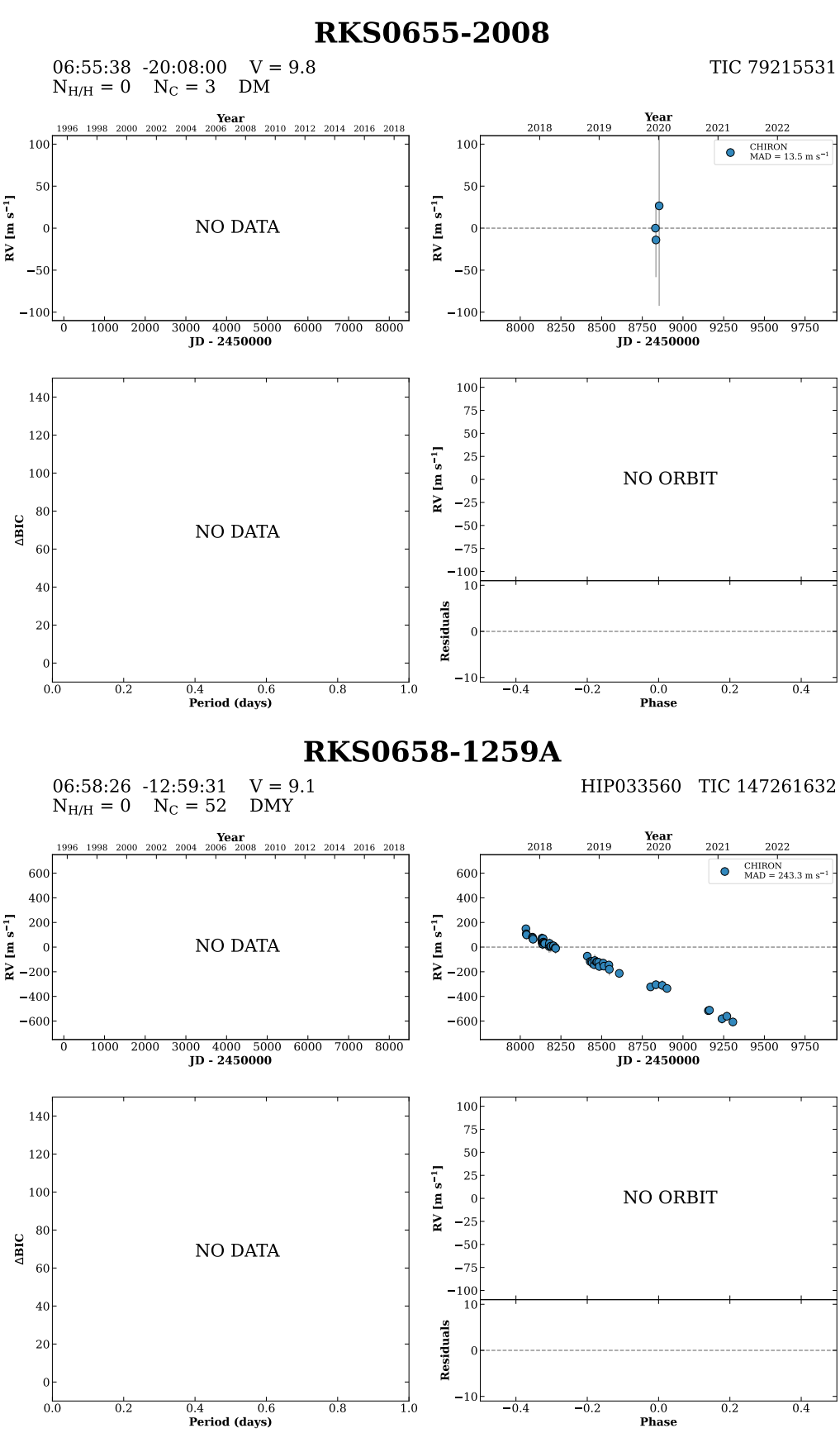

Figure 118 RV results for RKS0655-2008 (top) and RKS0658-1259A (bottom).

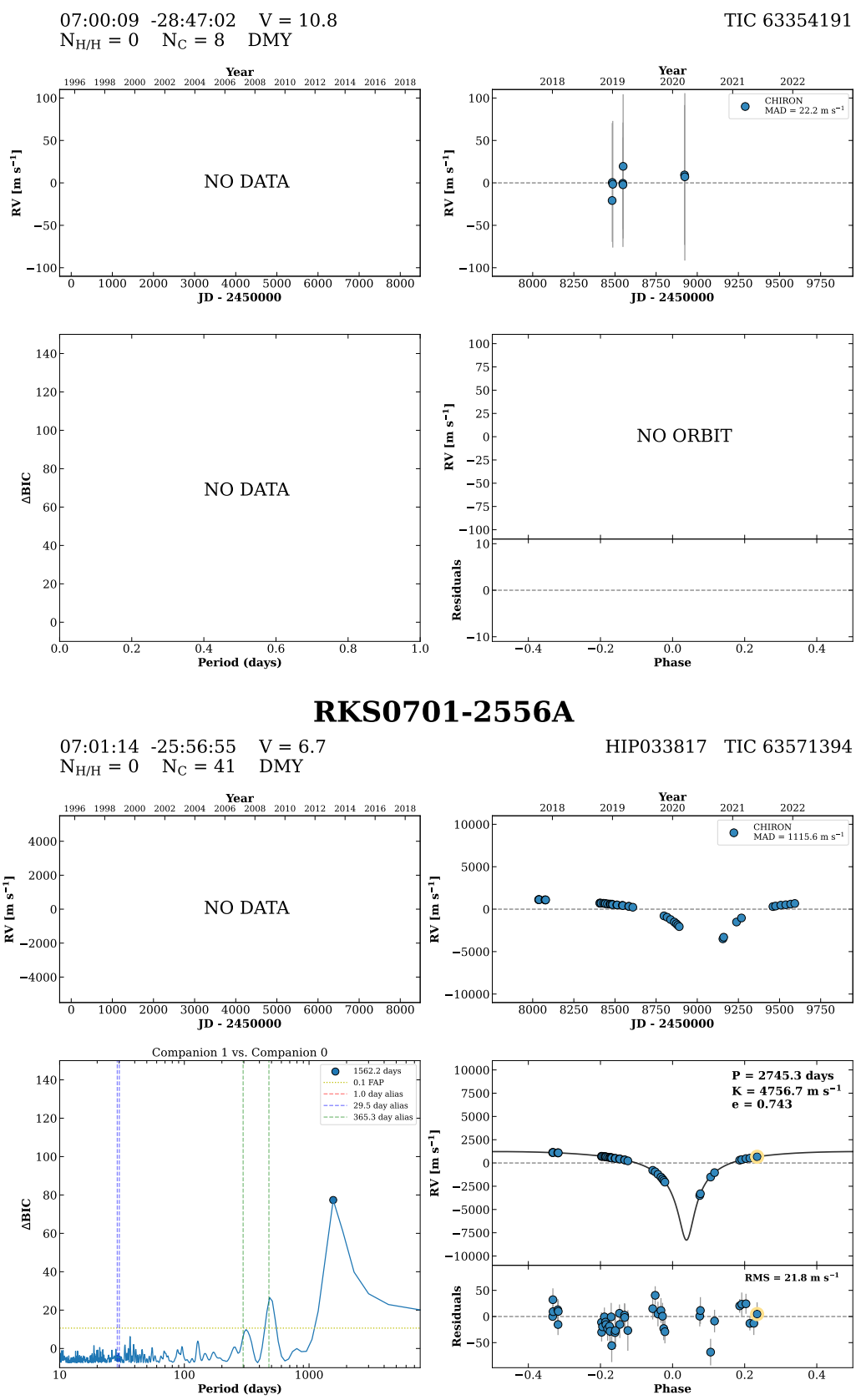

Figure 119 RV results for RKS0700-2847 (top) and RKS0701-2556A (bottom).

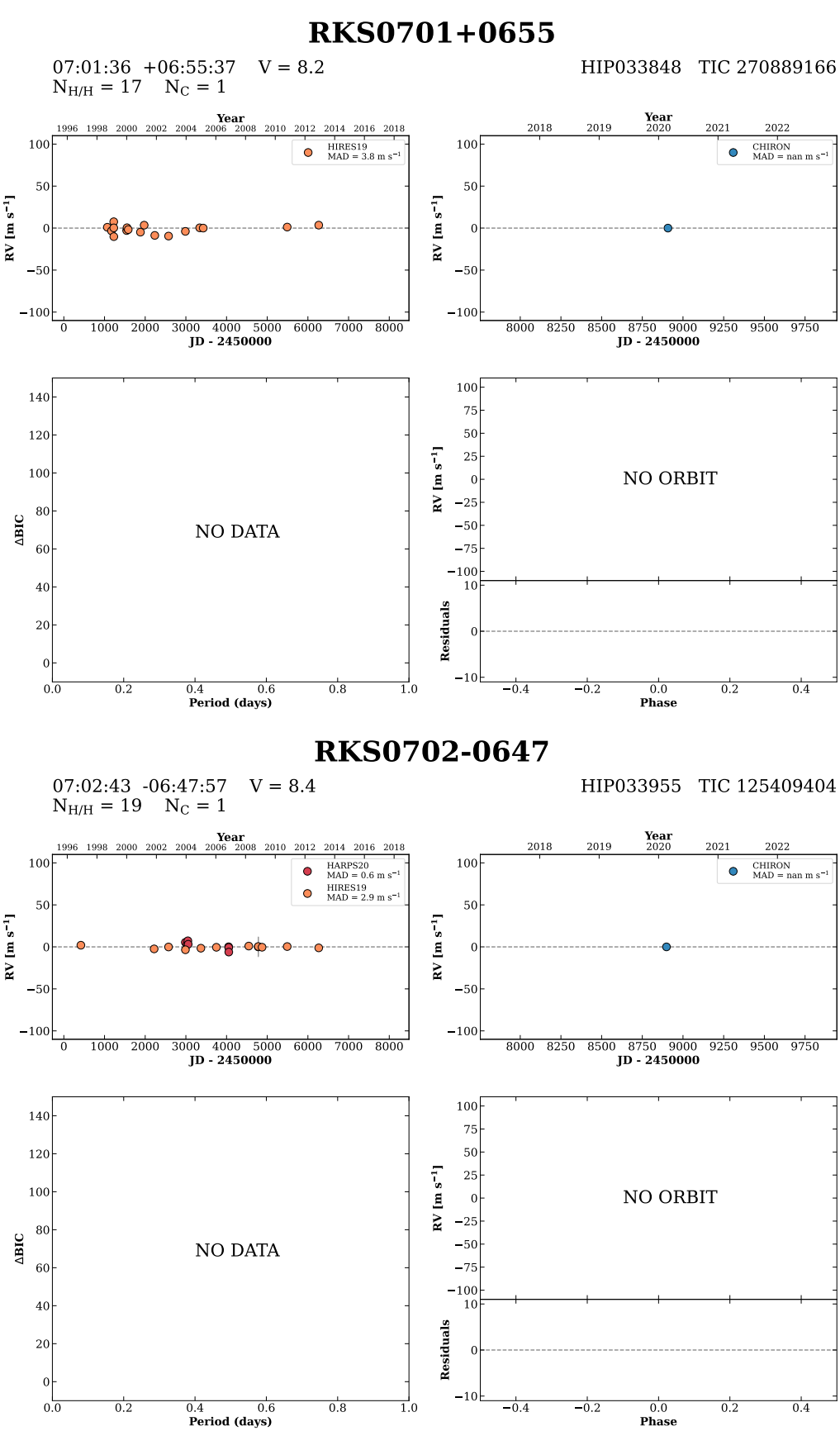

Figure 120 RV results for RKS0701+0655 (top) and RKS0702-0647 (bottom).

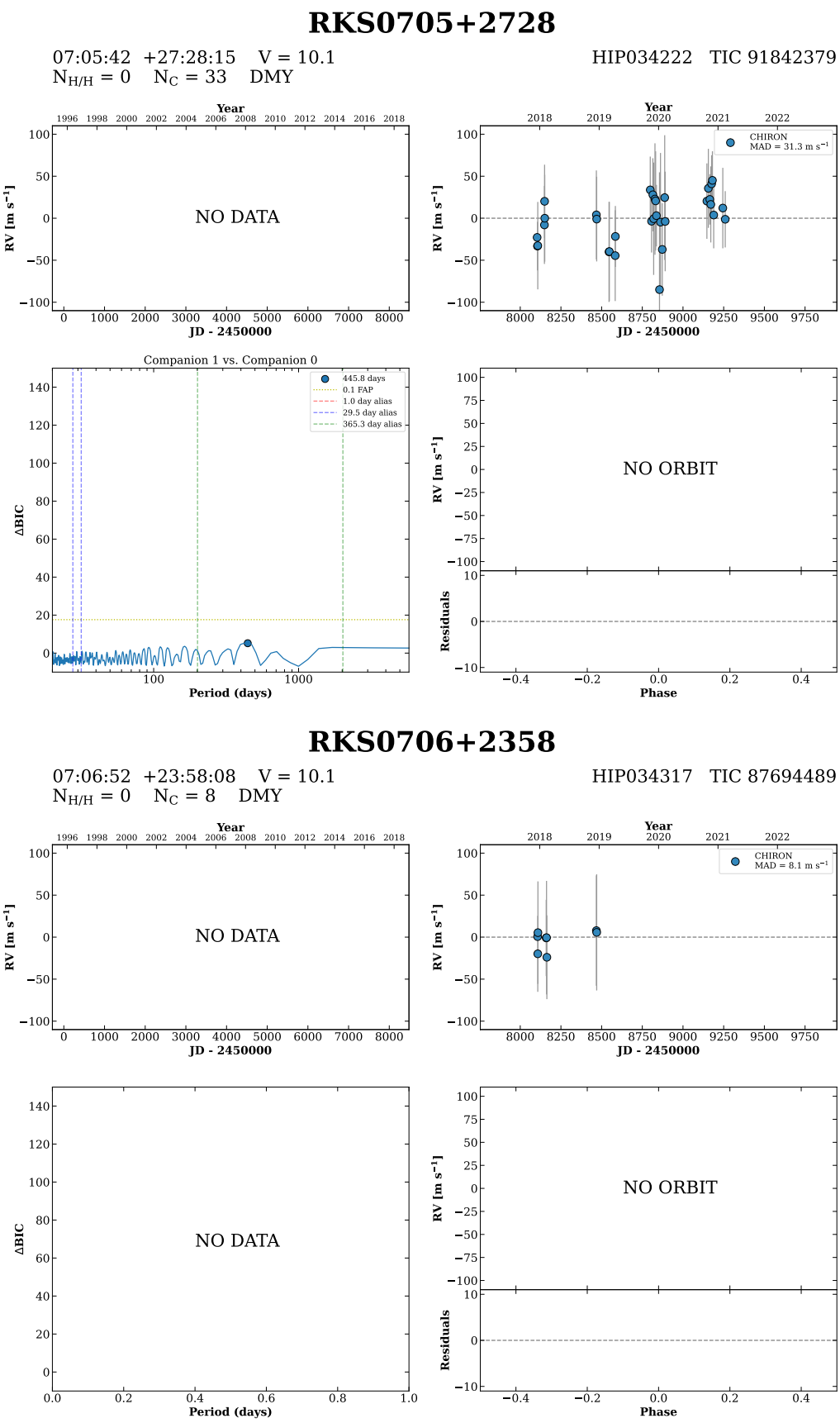

Figure 121 RV results for RKS0705+2728 (top) and RKS0706+2358 (bottom).

RKS0707+0326

07:07:09 +03:26:51 V = 9.8 HIP034341 TIC 292351181
$N_{H/H}$ = 0 N_C = 30 DMY

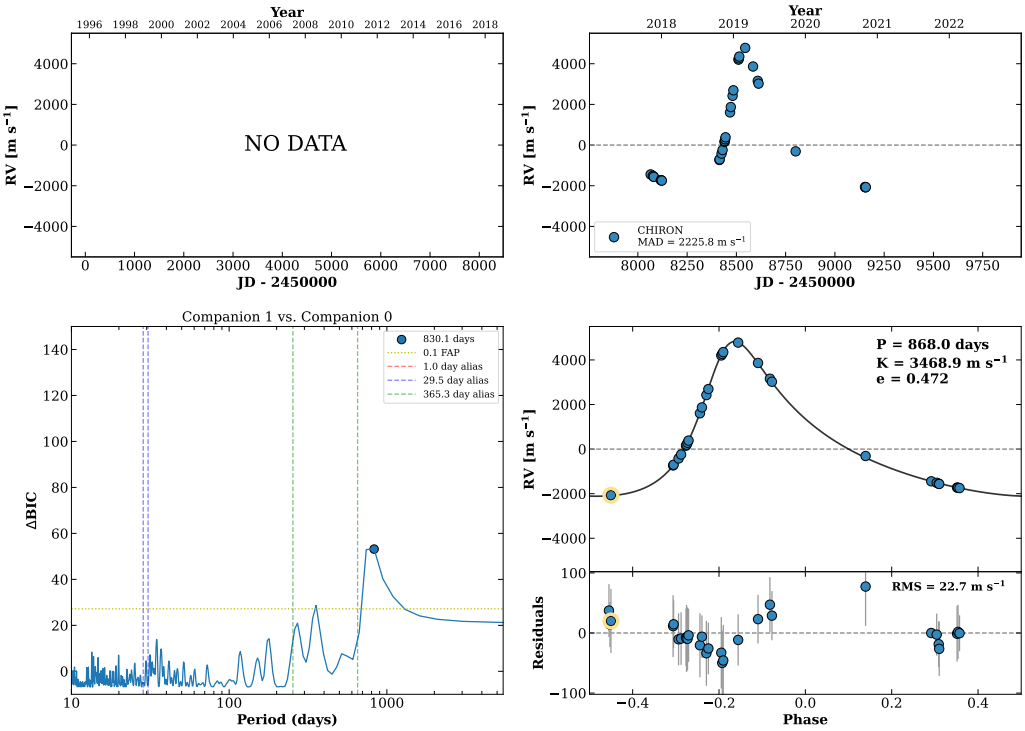

RKS0708+2950

07:08:04 +29:50:04 V = 8.3 HIP034414 TIC 87752739
$N_{H/H}$ = 0 N_C = 9 DMY

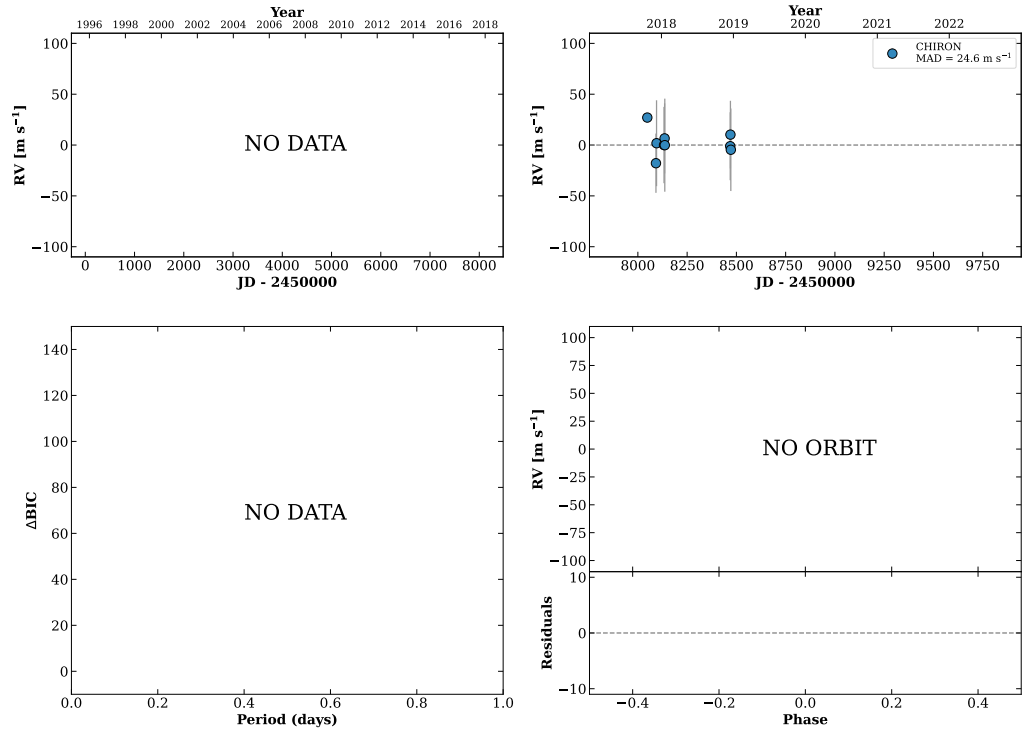

Figure 122 RV results for RKS0707+0326 (top) and RKS0708+2950 (bottom).

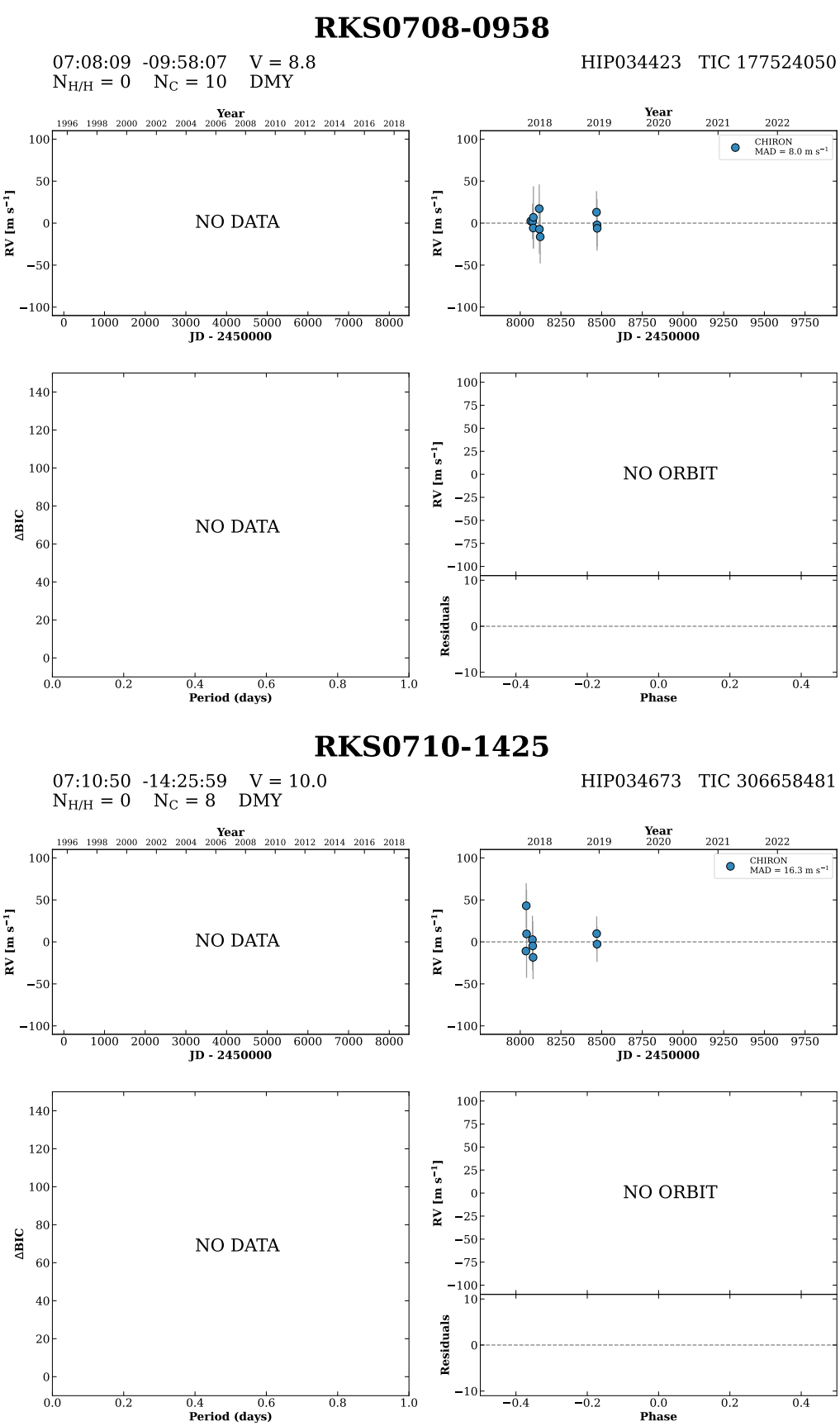

Figure 123 RV results for RKS0708-0958 (top) and RKS0710-1425 (bottom).

RKS0712-2453

07:12:05 -24:53:31 V = 10.4 HIP034785 TIC 65406275
$N_{H/H}$ = 15 N_C = 1

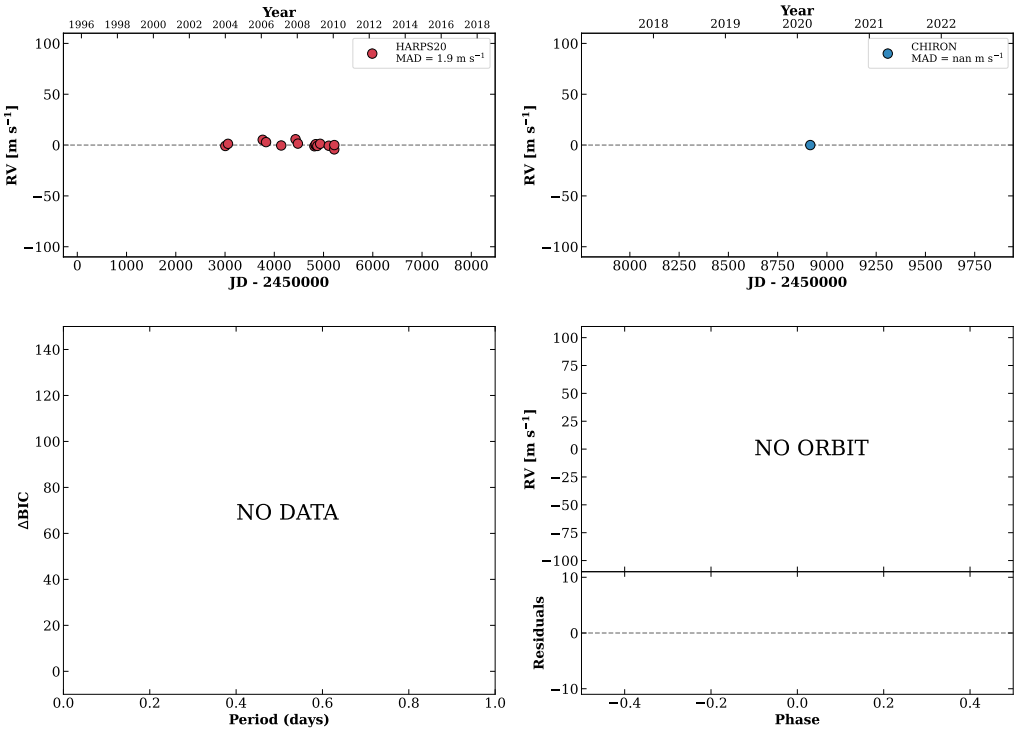

RKS0713+2500

07:13:53 +25:00:41 V = 8.4 HIP034950 TIC 101722543
$N_{H/H}$ = 0 N_C = 8 DMY

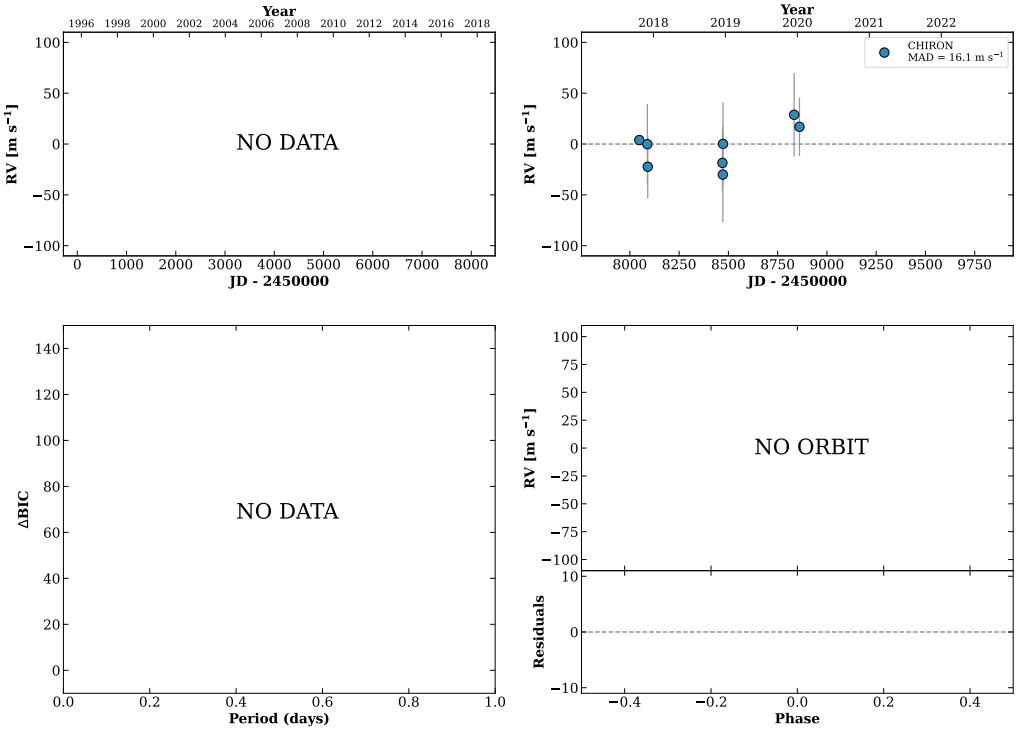

Figure 124 RV results for RKS0712-2453 (top) and RKS0713+2500 (bottom).

RKS0716-0339

07:16:11 -03:39:57 V = 9.0 HIP035173 TIC 50992589
$N_{H/H}$ = 0 N_C = 1

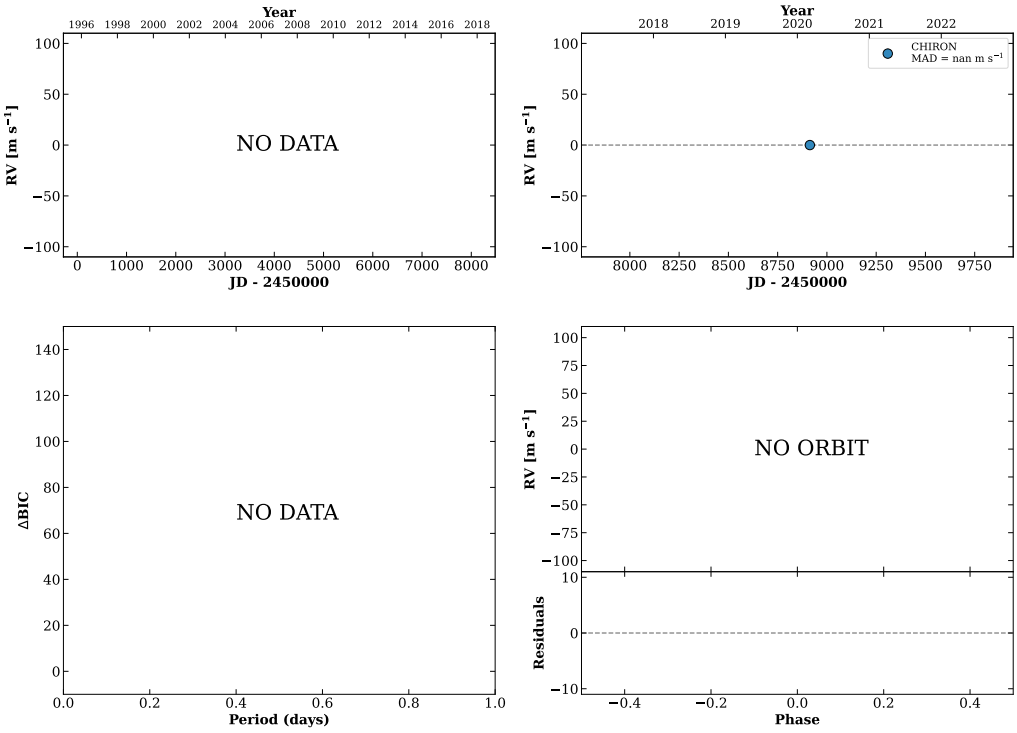

RKS0718+1632

07:18:06 +16:32:34 V = 9.9 TIC 440851540
$N_{H/H}$ = 0 N_C = 1

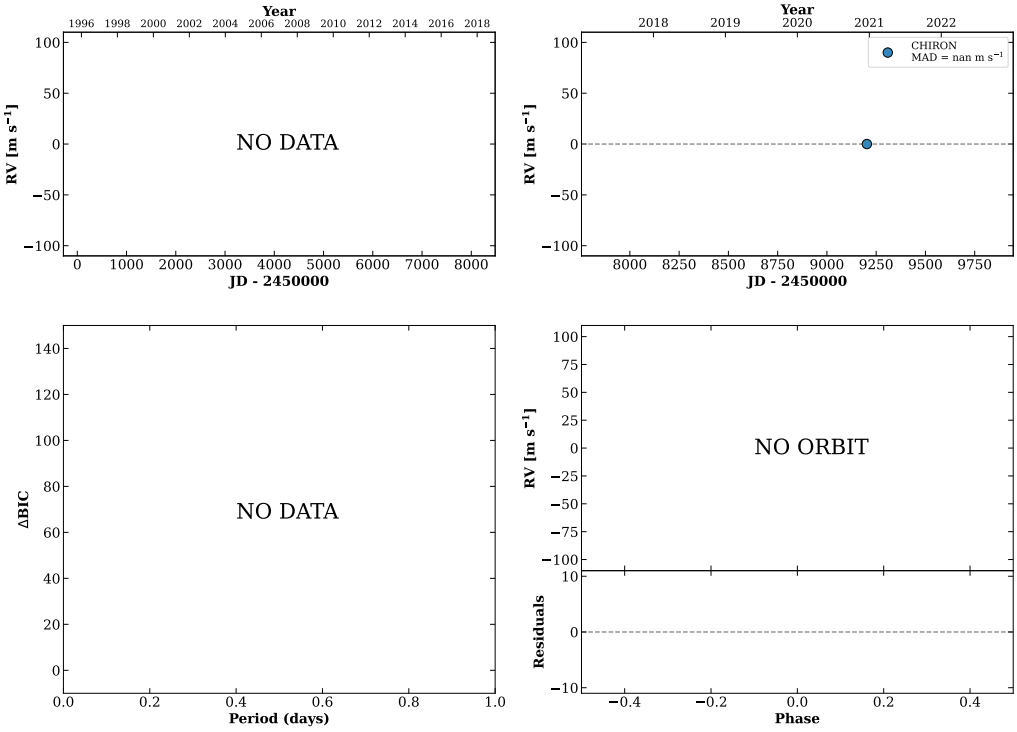

Figure 125 RV results for RKS0716-0339 (top) and RKS0718+1632 (bottom).

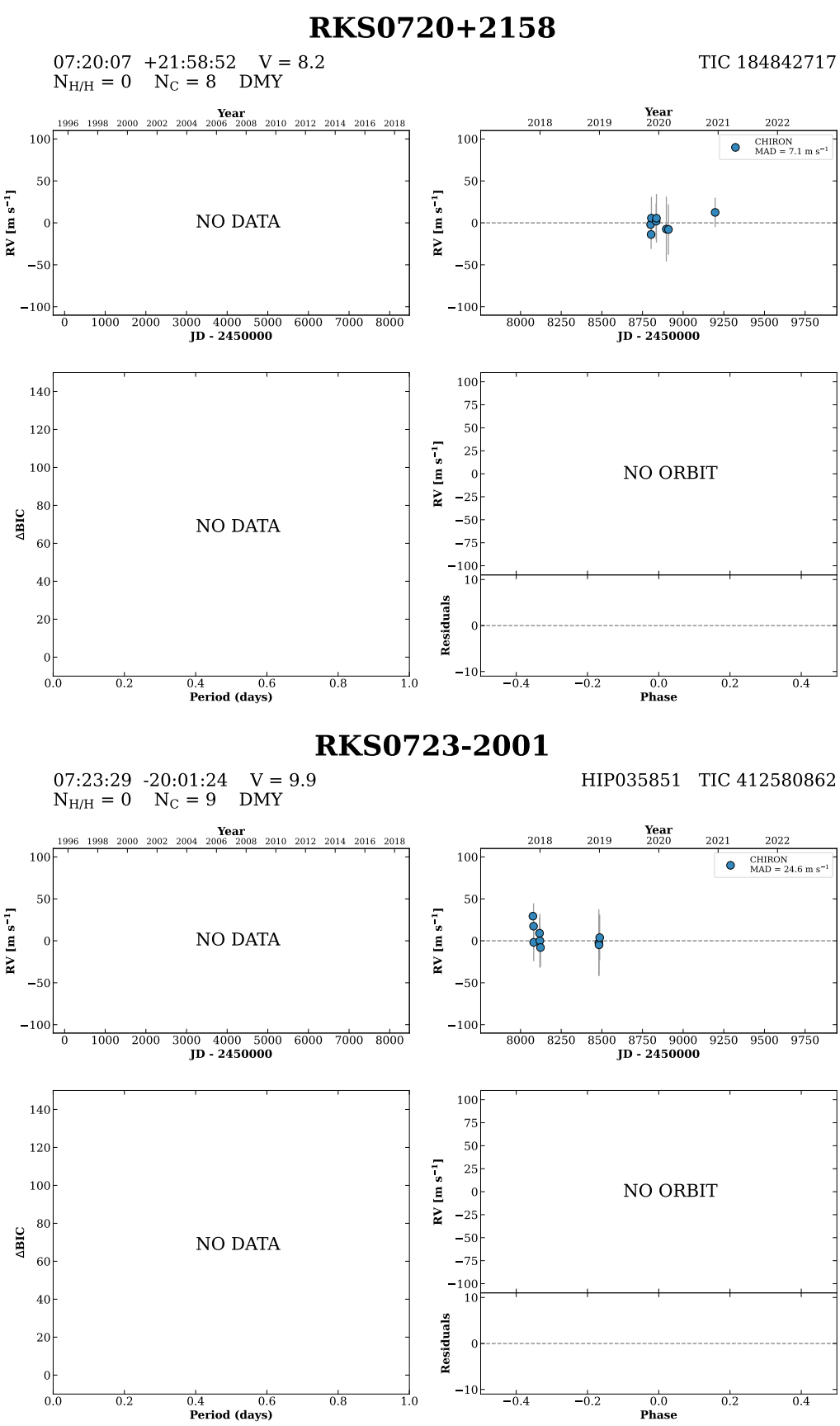

Figure 126 RV results for RKS0720+2158 (top) and RKS0723-2001 (bottom).

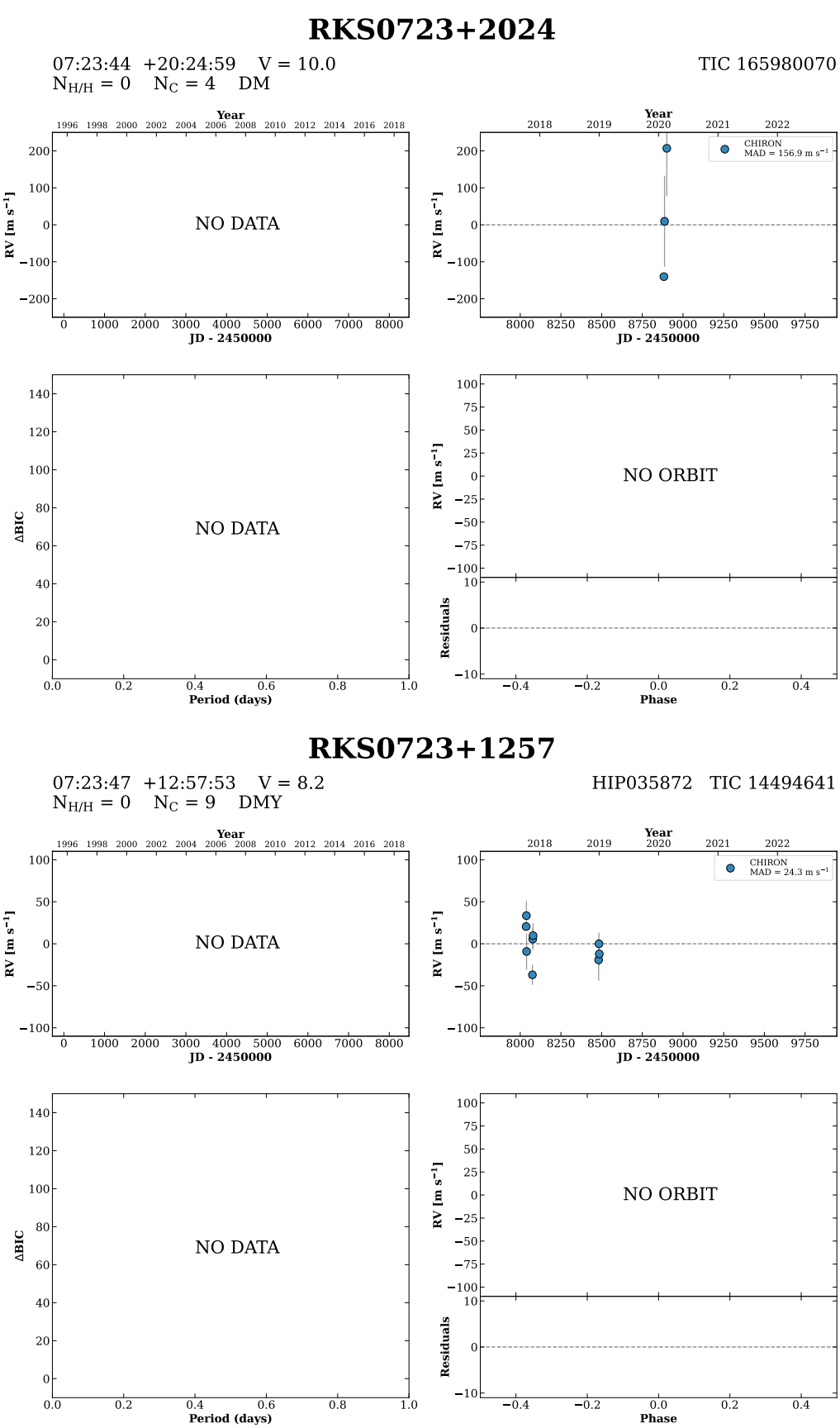

Figure 127 RV results for RKS0723+2024 (top) and RKS0723+1257 (bottom).

RKS0724-1753

07:24:34 -17:53:32 V = 10.3 HIP035943 TIC 412778373
$N_{H/H}$ = 7 N_C = 10 DMY

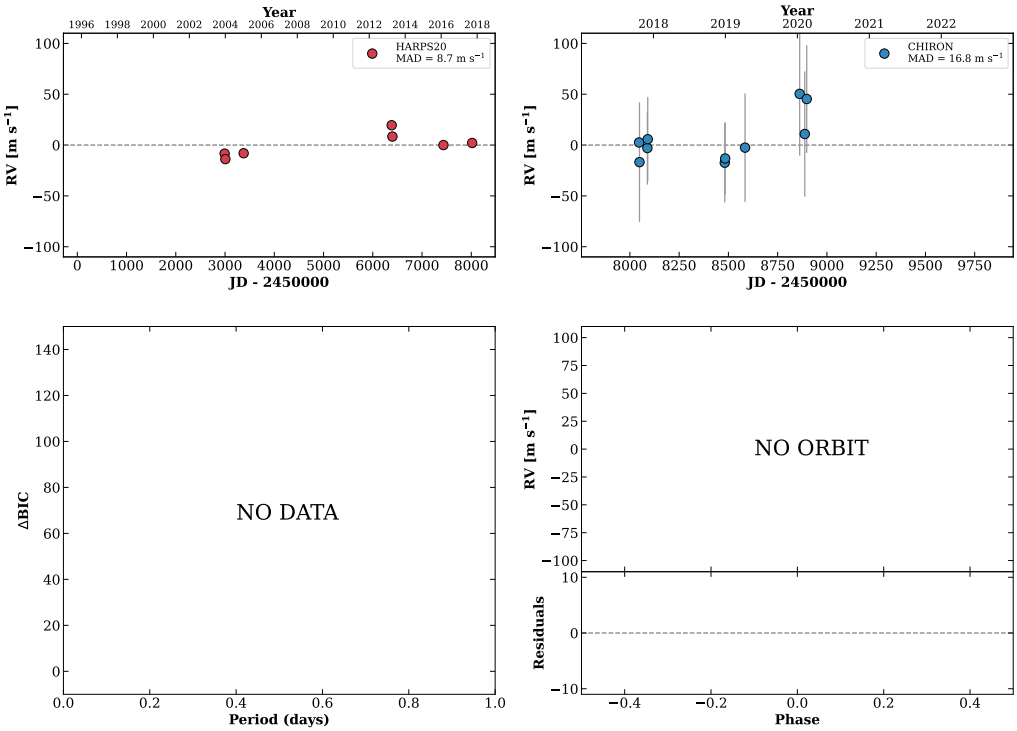

RKS0725-1041

07:25:30 -10:42:00 V = 11.6 TIC 403630804
$N_{H/H}$ = 0 N_C = 11 DMY

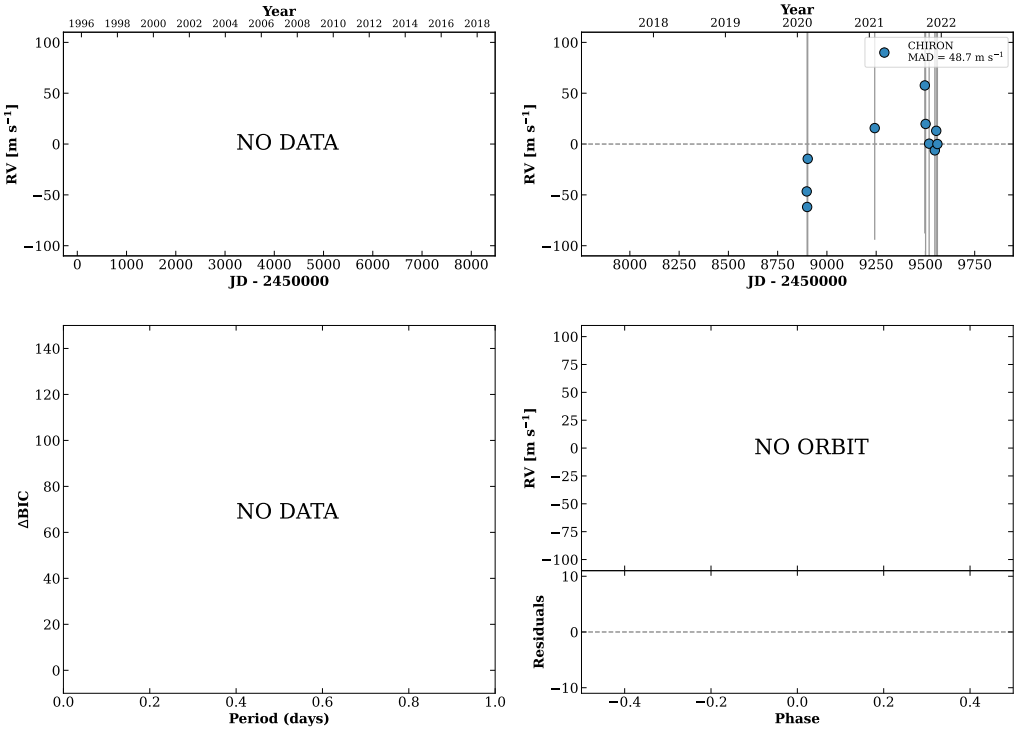

Figure 128 RV results for RKS0724-1753 (top) and RKS0725-1041 (bottom).

RKS0726-1546

07:26:27 -15:46:13 V = 9.2 HIP036121 TIC 386070101
$N_{H/H}$ = 0 N_C = 35 DMY

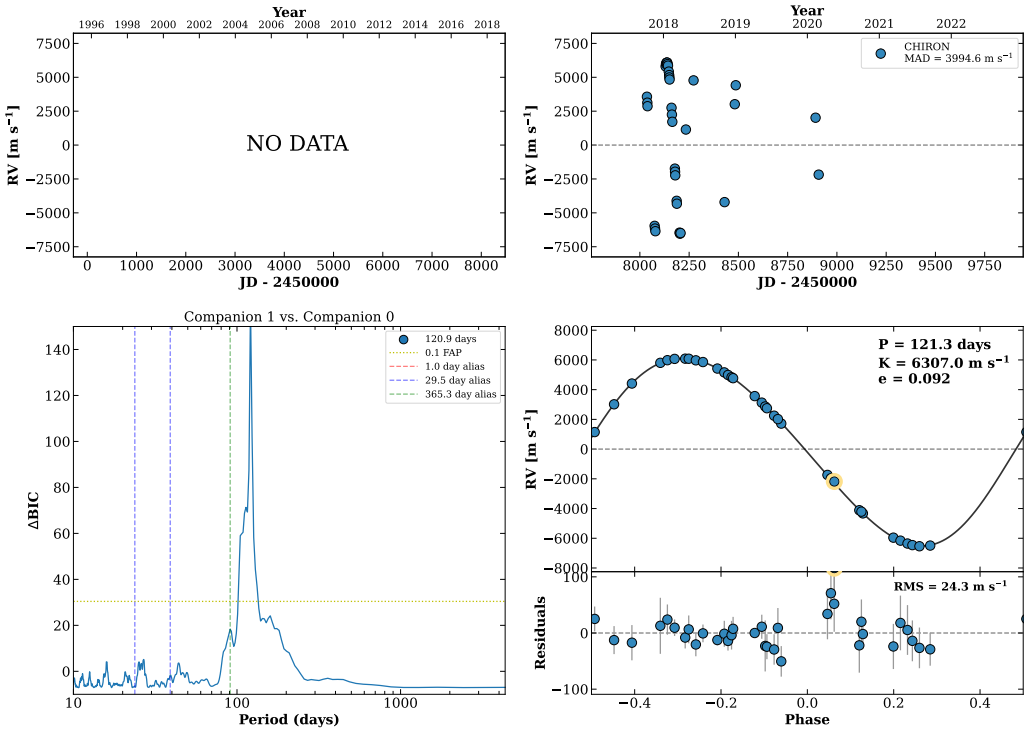

RKS0730-0340

07:30:18 -03:40:24 V = 10.4 TIC 65068595
$N_{H/H}$ = 0 N_C = 8 DMY

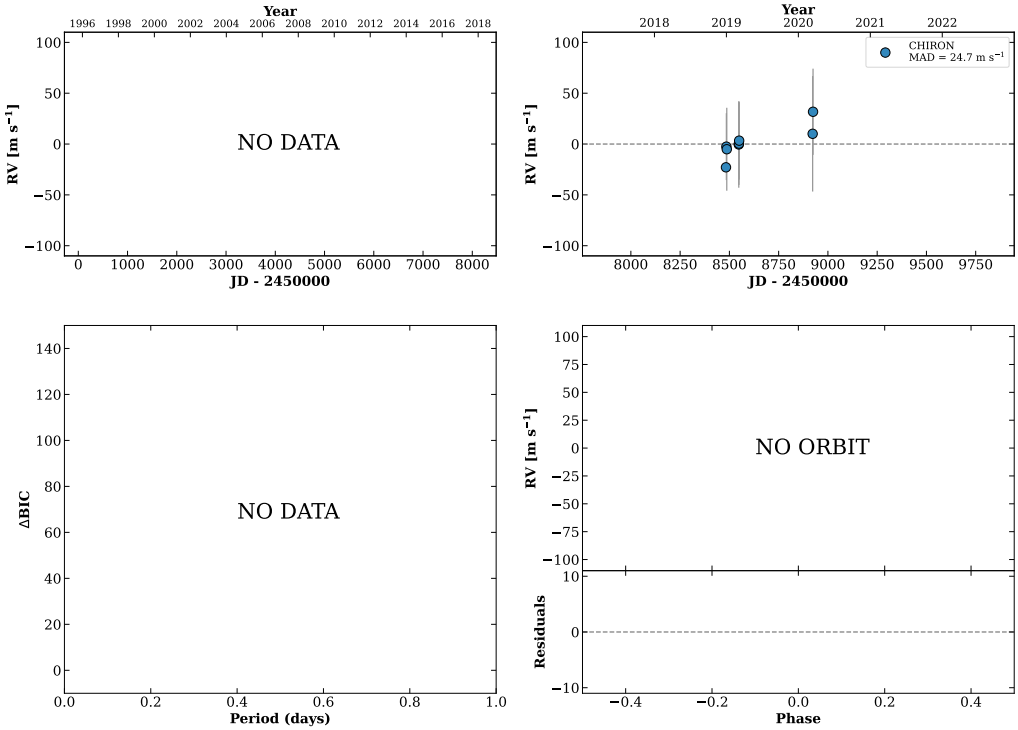

Figure 129 RV results for RKS0726-1546 (top) and RKS0730-0340 (bottom).

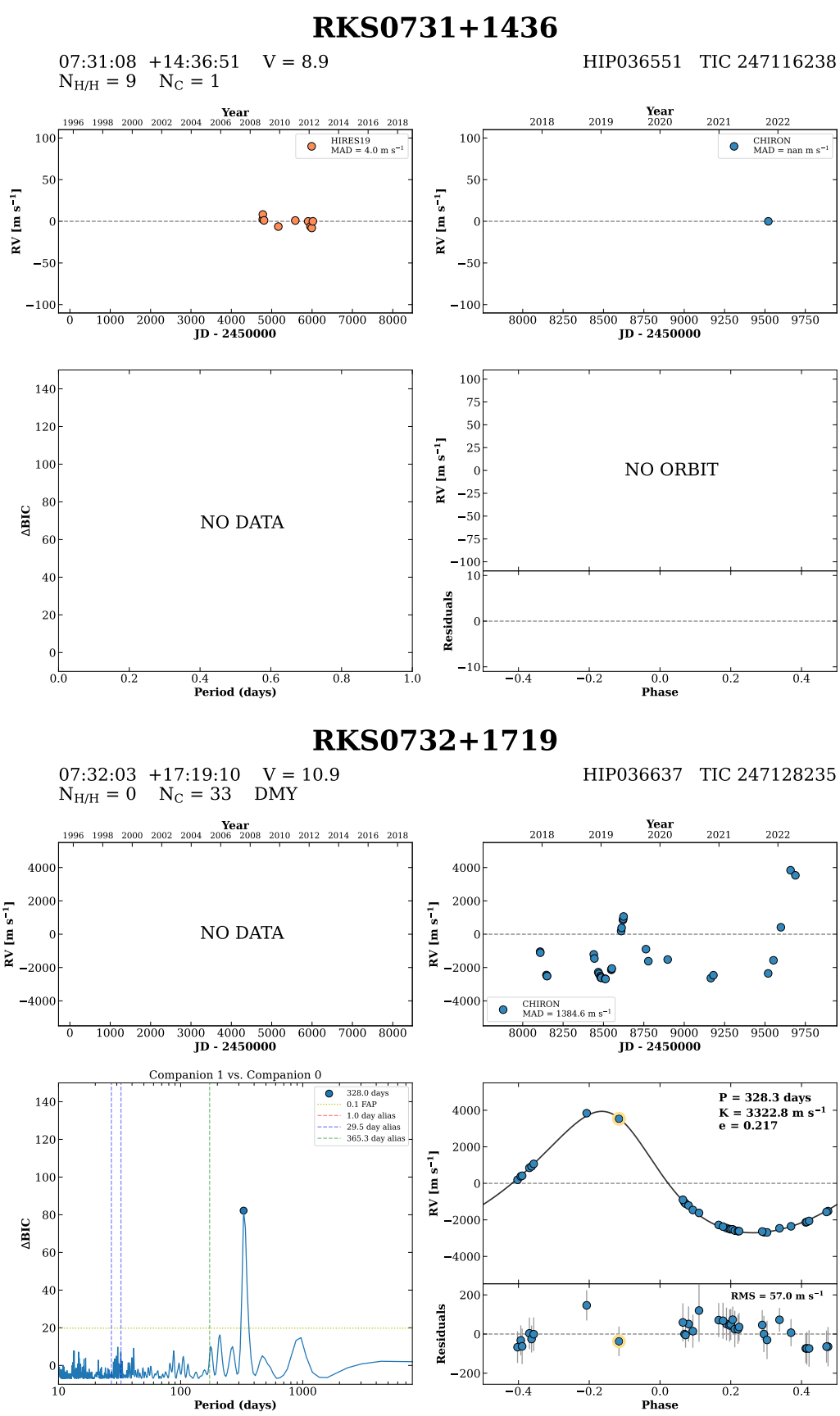

Figure 130 RV results for RKS0731+1436 (top) and RKS0732+1719 (bottom).

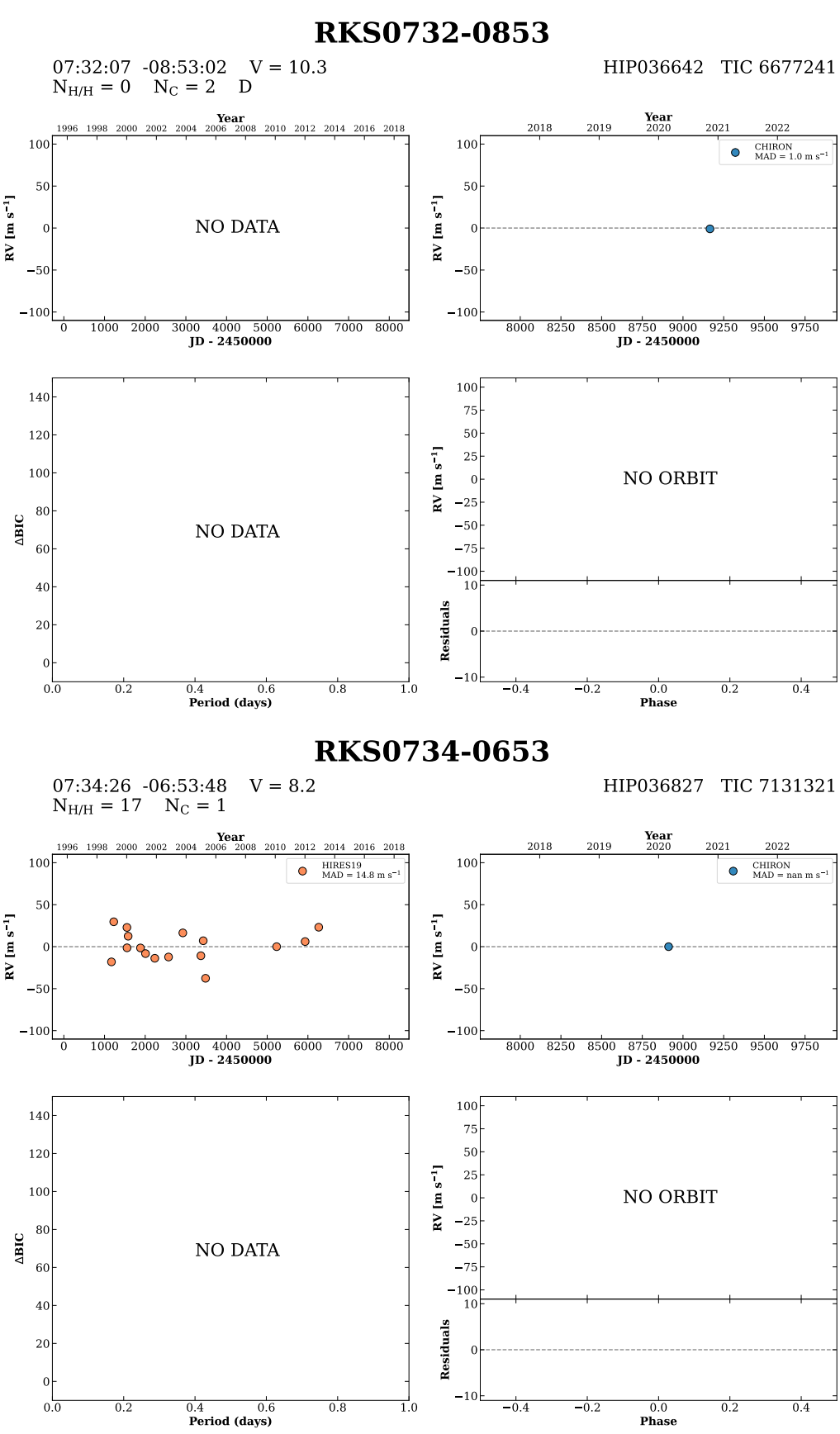

Figure 131 RV results for RKS0732-0853 (top) and RKS0734-0653 (bottom).

RKS0739-0335

07:40:00 -03:35:51 V = 7.2 HIP037349 TIC 66100263
$N_{H/H}$ = 17 N_C = 1

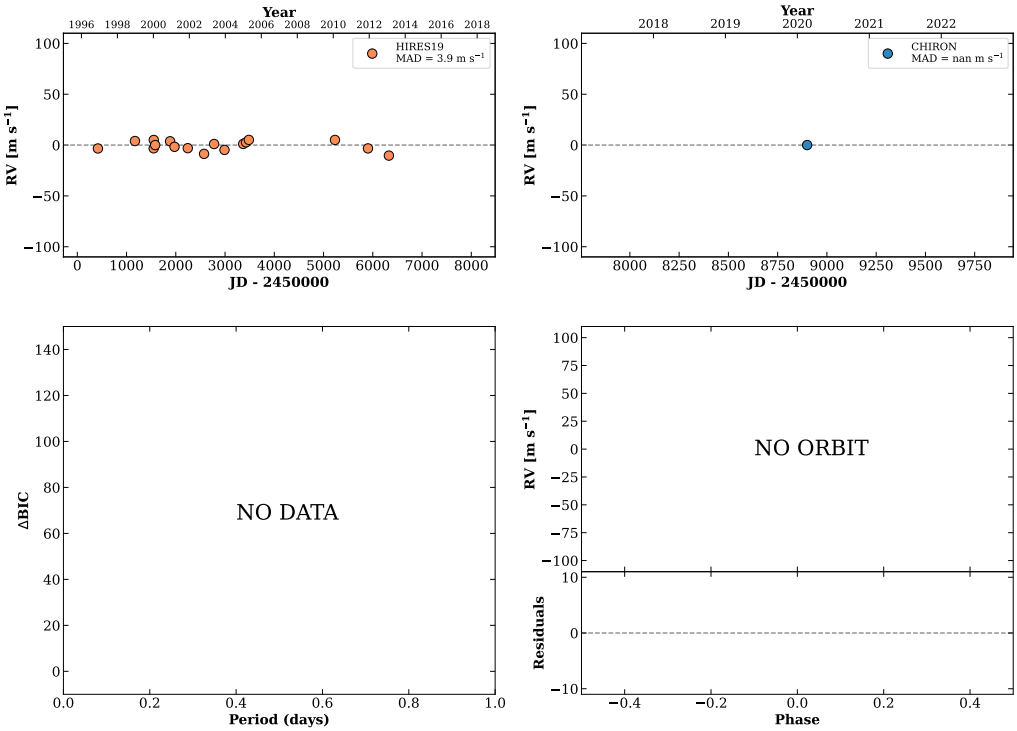

RKS0740-0336

07:40:03 -03:36:13 V = 8.9 TIC 66189398
$N_{H/H}$ = 9 N_C = 1

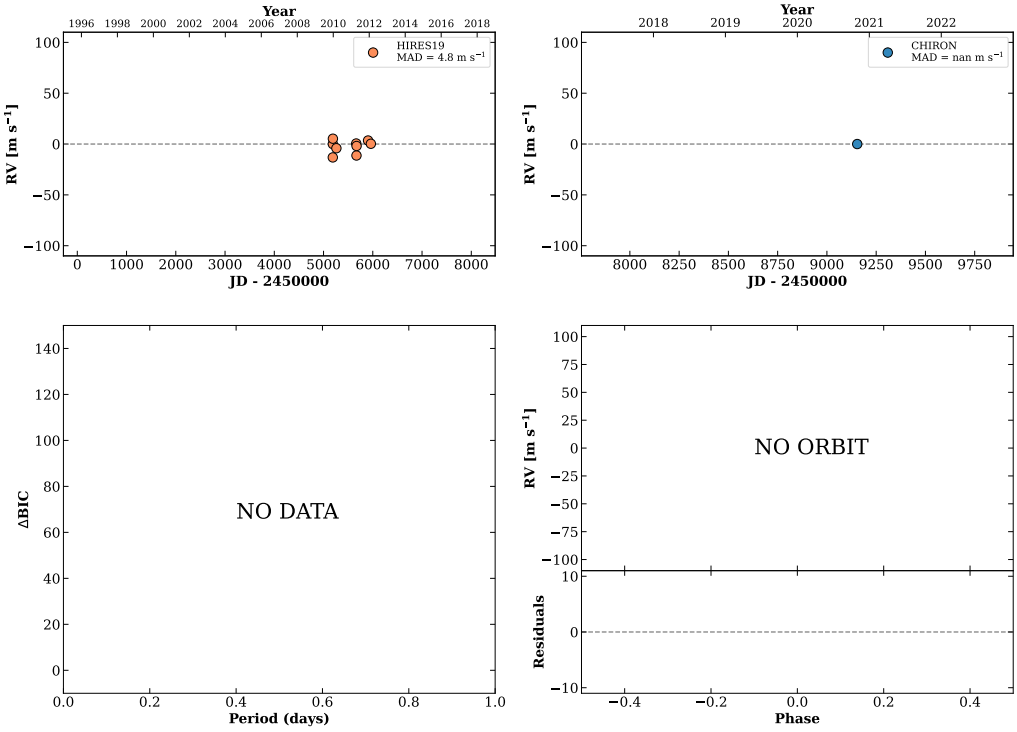

Figure 132 RV results for RKS0739-0335 (top) and RKS0740-0336 (bottom).

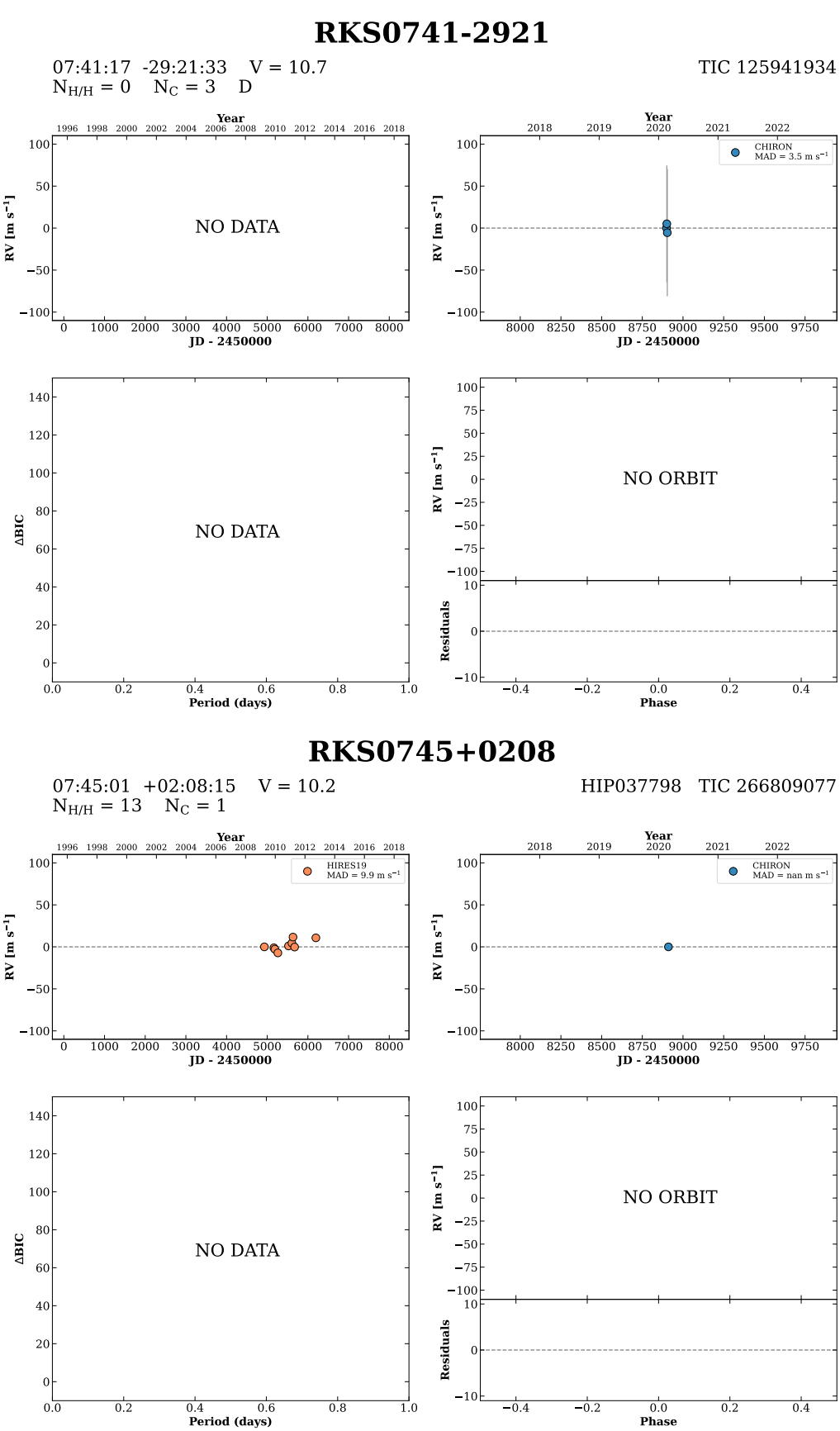

Figure 133 RV results for RKS0741-2921 (top) and RKS0745+0208 (bottom).

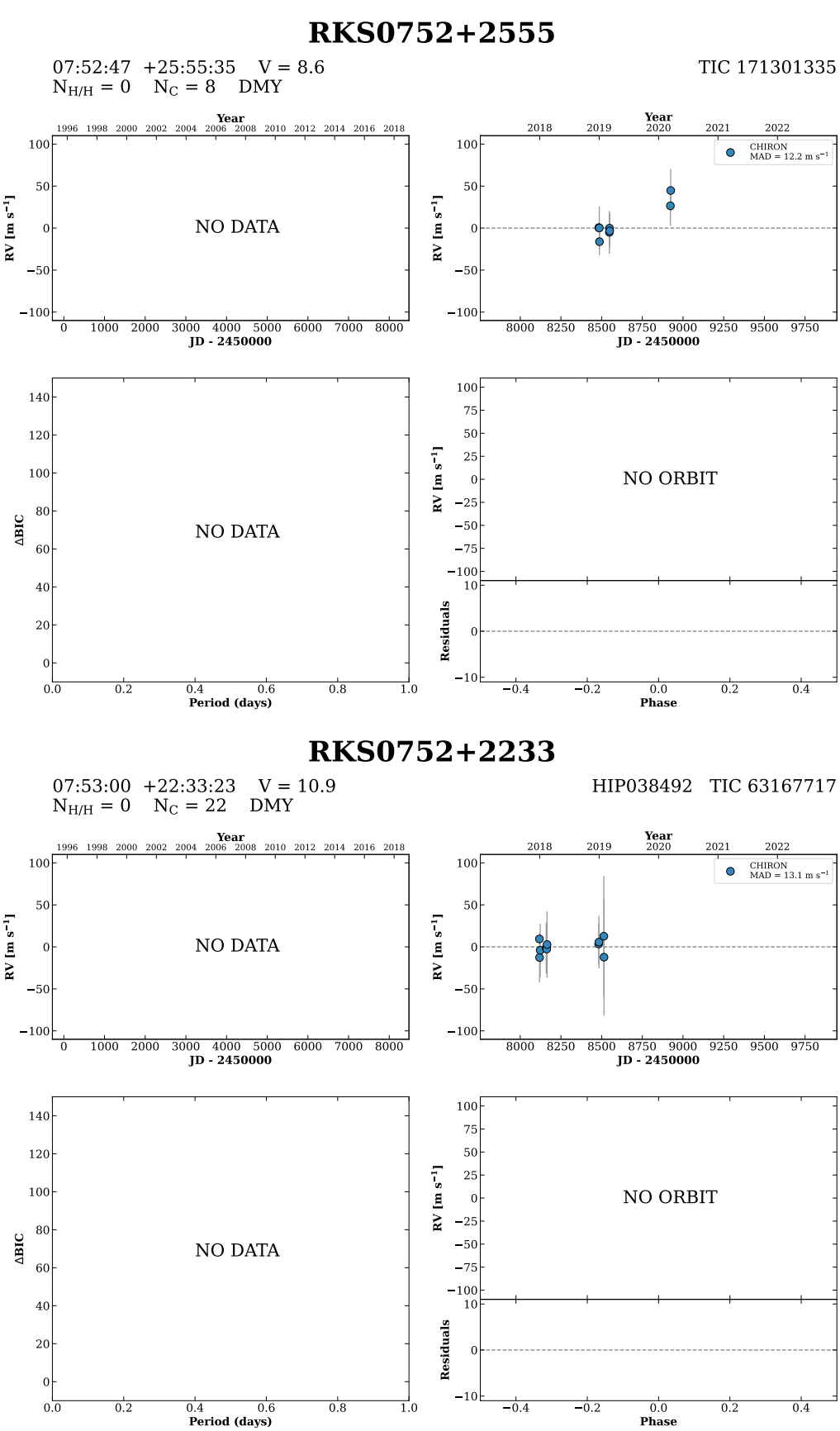

Figure 134 RV results for RKS0752+2555 (top) and RKS0752+2233 (bottom).

RKS0754-2518

07:54:11 -25:18:11 V = 9.8 HIP038594 TIC 128902569
$N_{H/H}$ = 17 N_C = 1

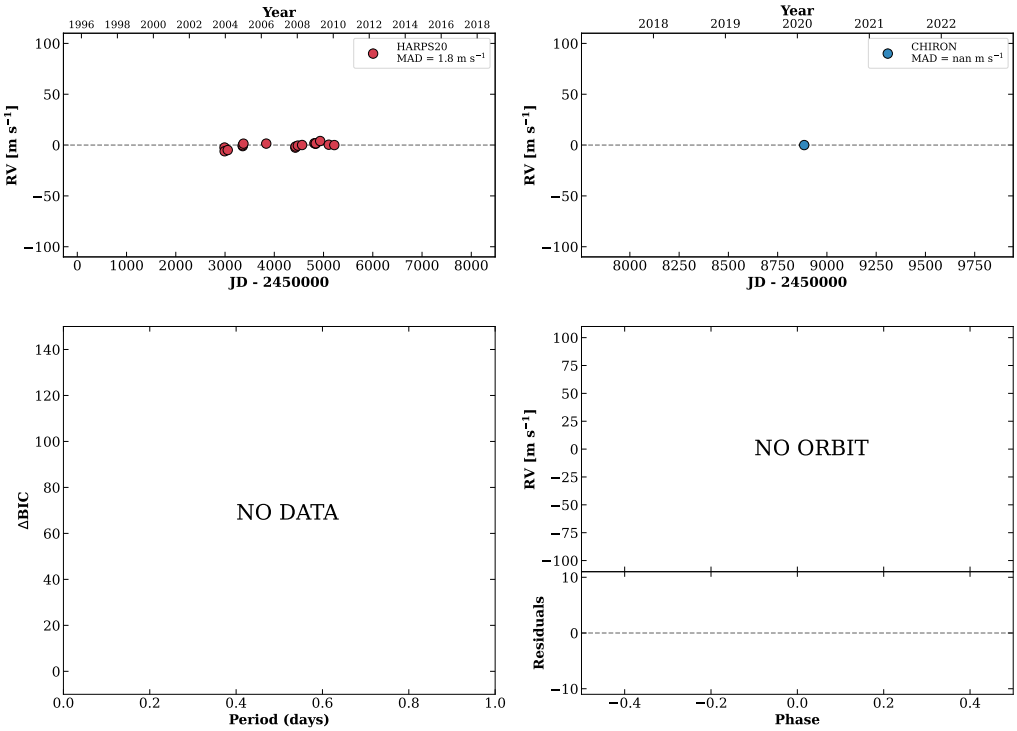

RKS0754-0124A

07:54:34 -01:24:44 V = 7.4 HIP038625 TIC 123089572
$N_{H/H}$ = 0 N_C = 3 DM

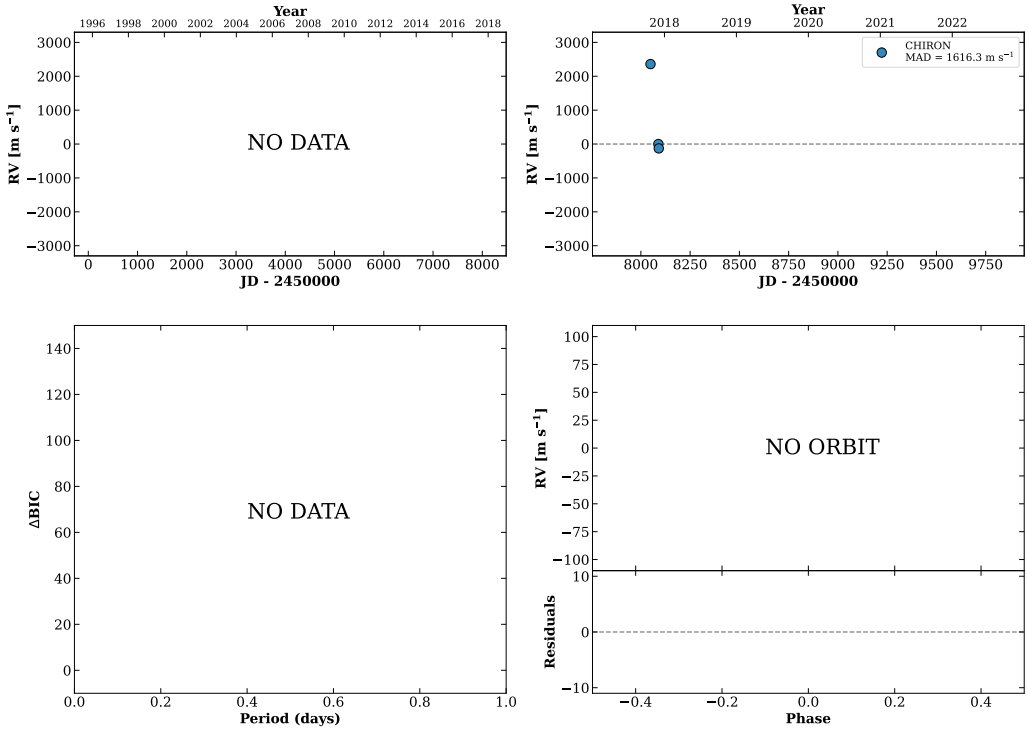

Figure 135 RV results for RKS0754-2518 (top) and RKS0754-0124A (bottom).

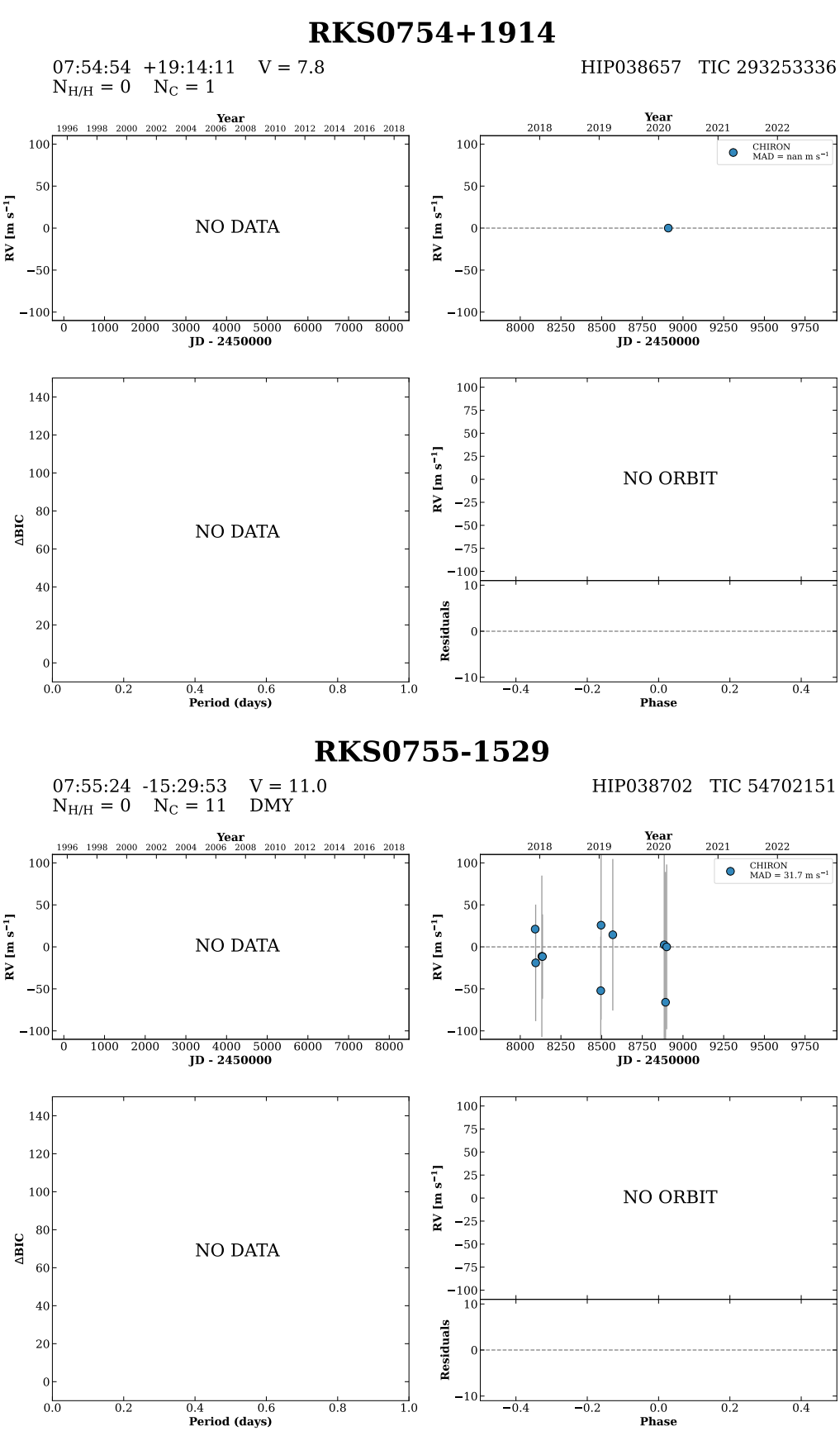

Figure 136 RV results for RKS0754+1914 (top) and RKS0755-1529 (bottom).

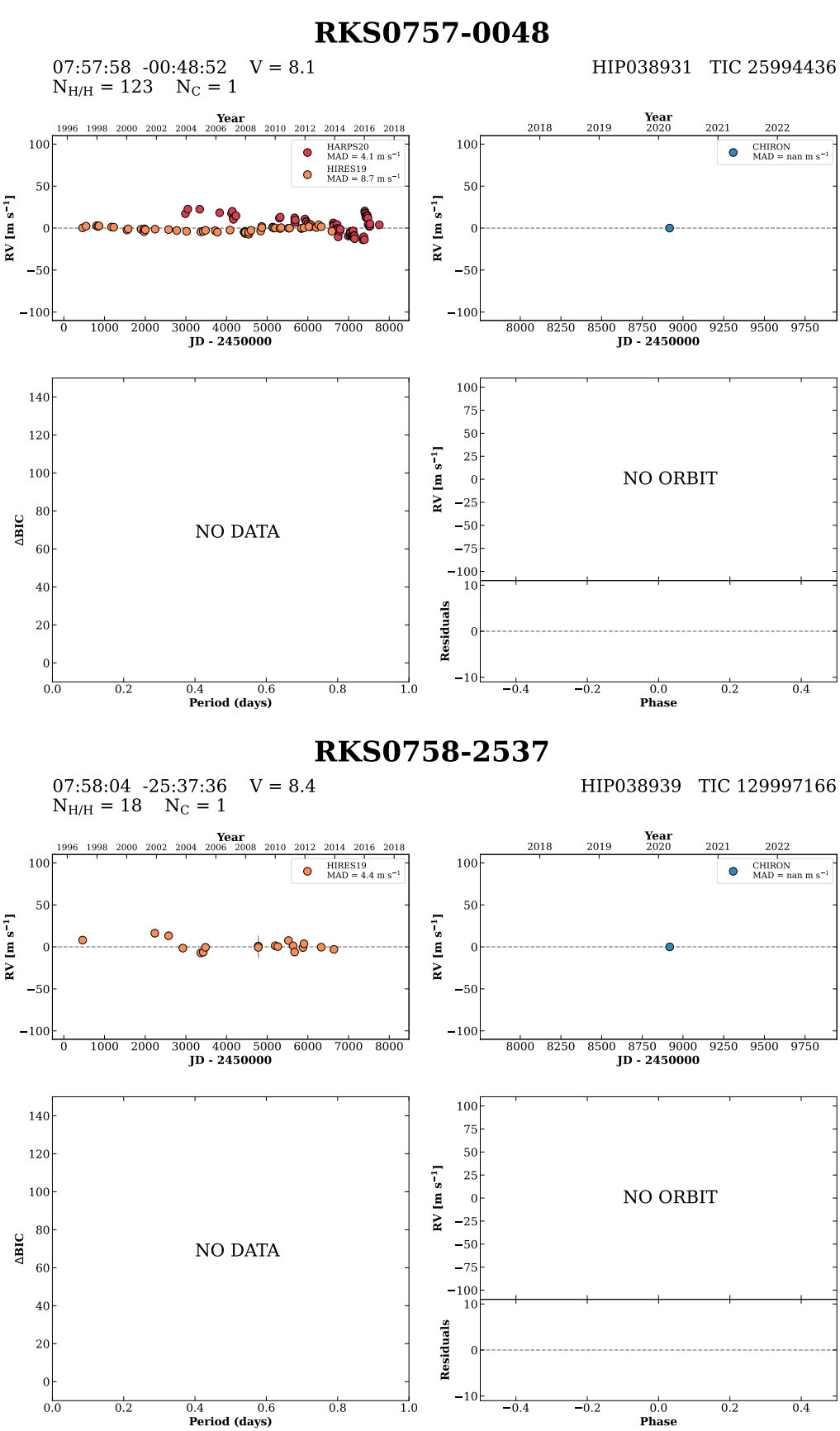

Figure 137 RV results for RKS0757-0048 (top) and RKS0758-2537 (bottom).

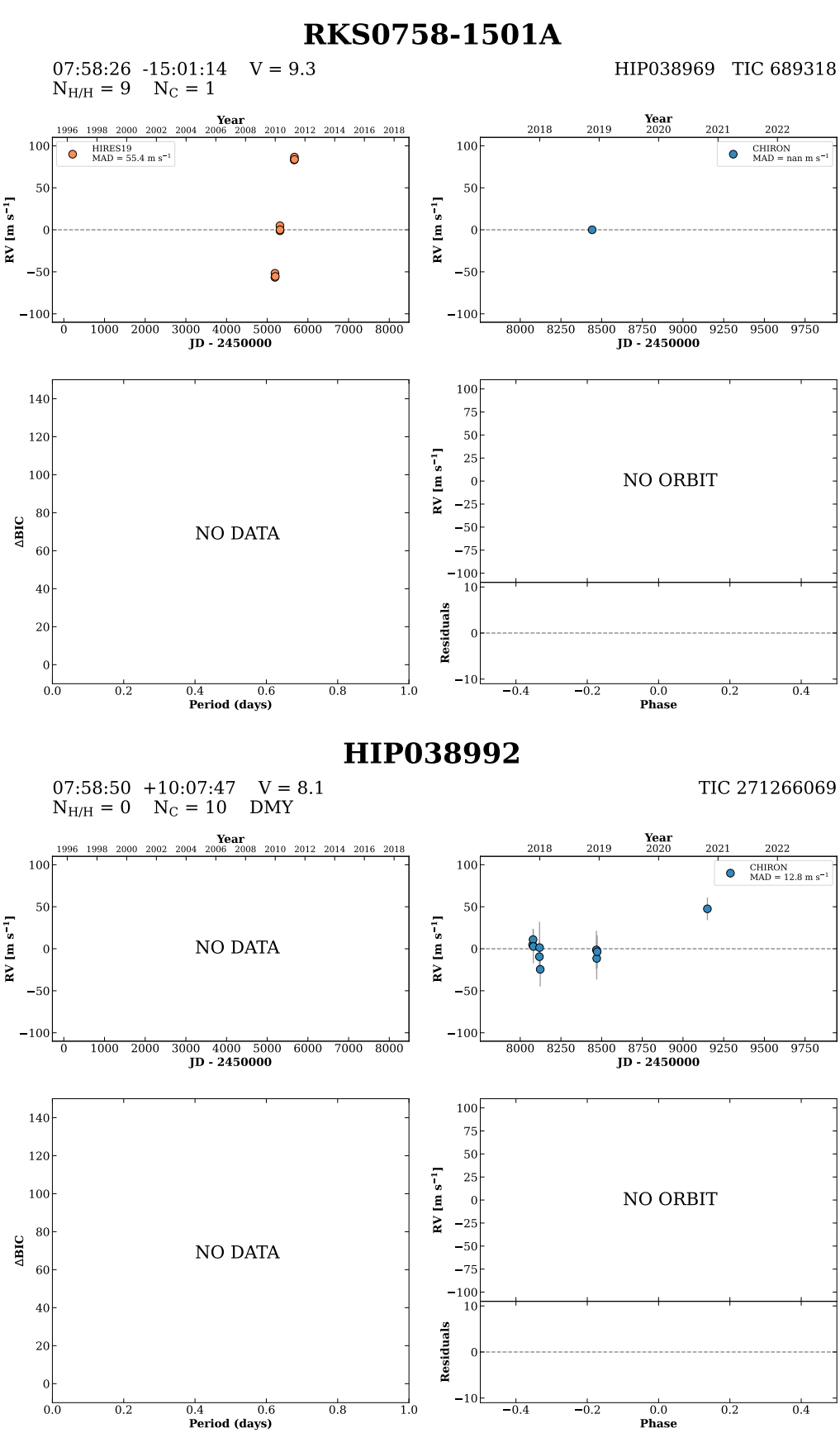

Figure 138 RV results for RKS0758-1501A (top) and HIP038992 (bottom).

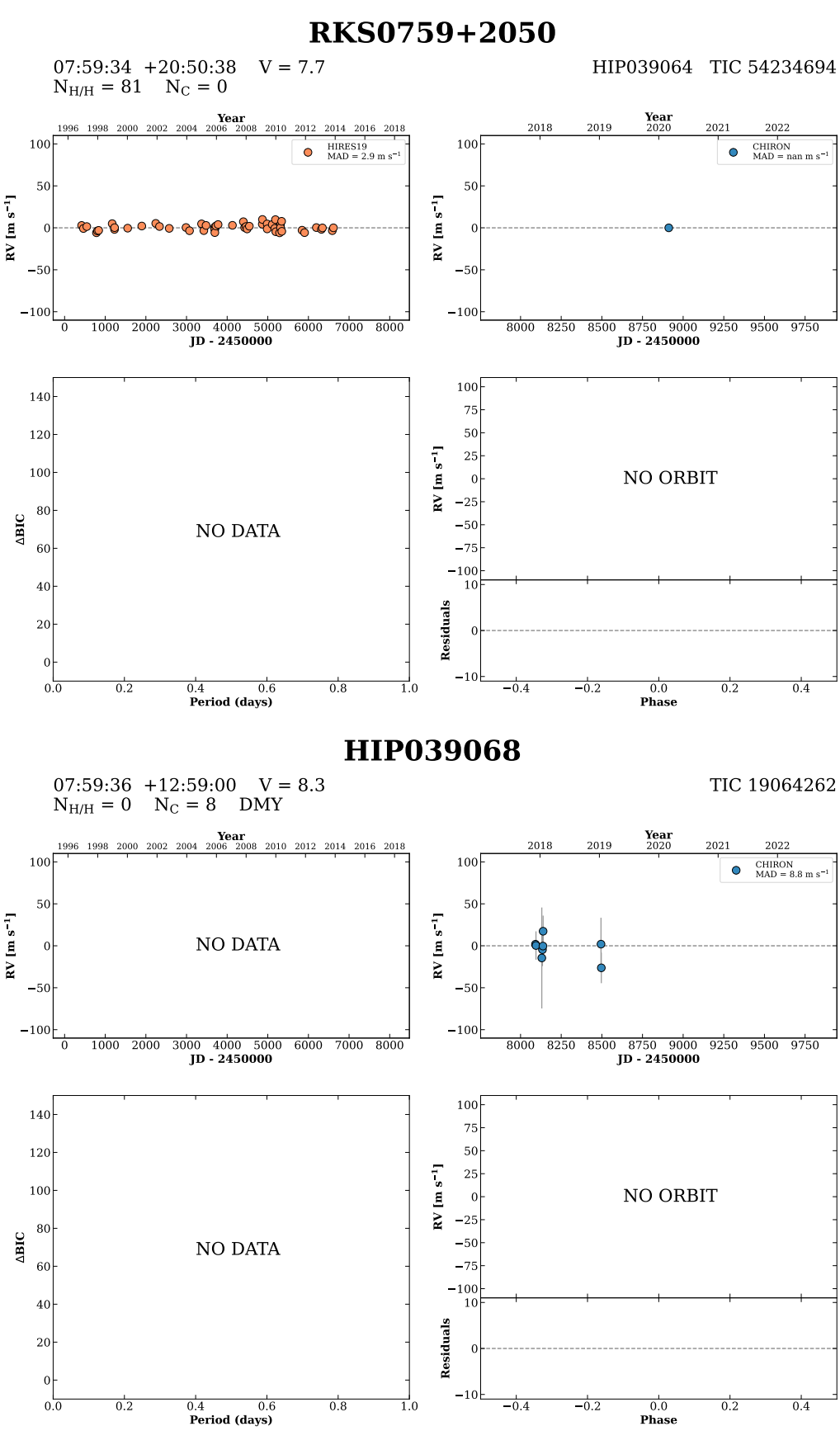

Figure 139 RV results for RKS0759+2050 (top) and HIP039068 (bottom).

RKS0804+1217

08:04:23 +12:17:19 V = 11.2 TIC 408816165
$N_{H/H}$ = 0 N_C = 3 D

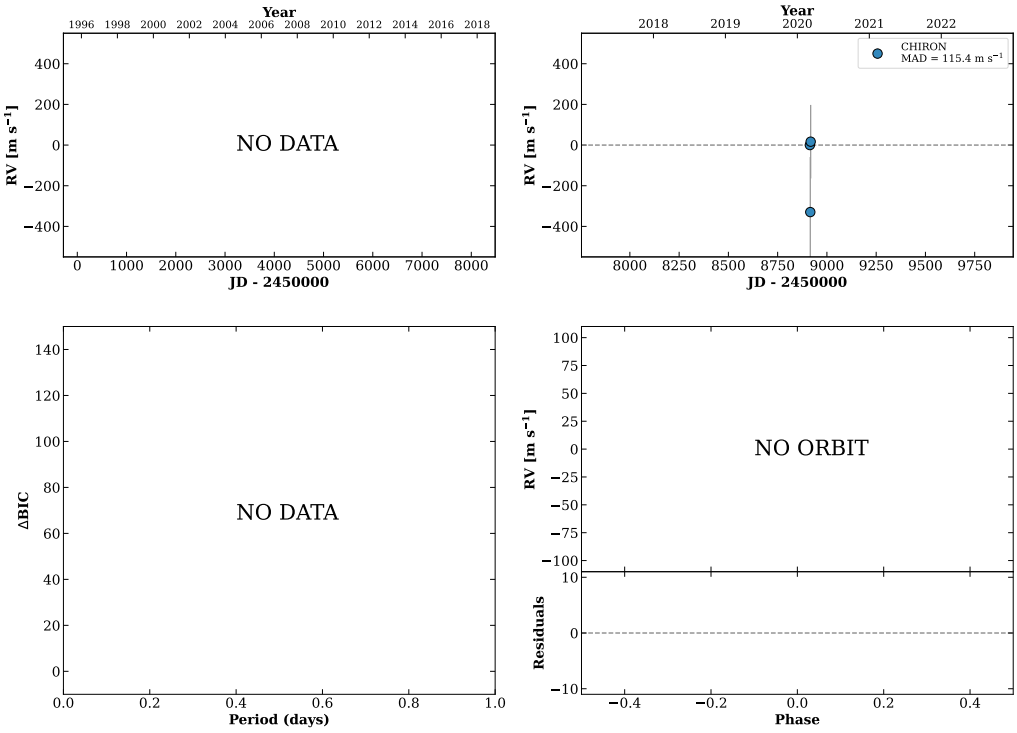

RKS0808+2106

08:08:13 +21:06:18 V = 9.4 HIP039826 TIC 386838171
$N_{H/H}$ = 0 N_C = 11 DMY

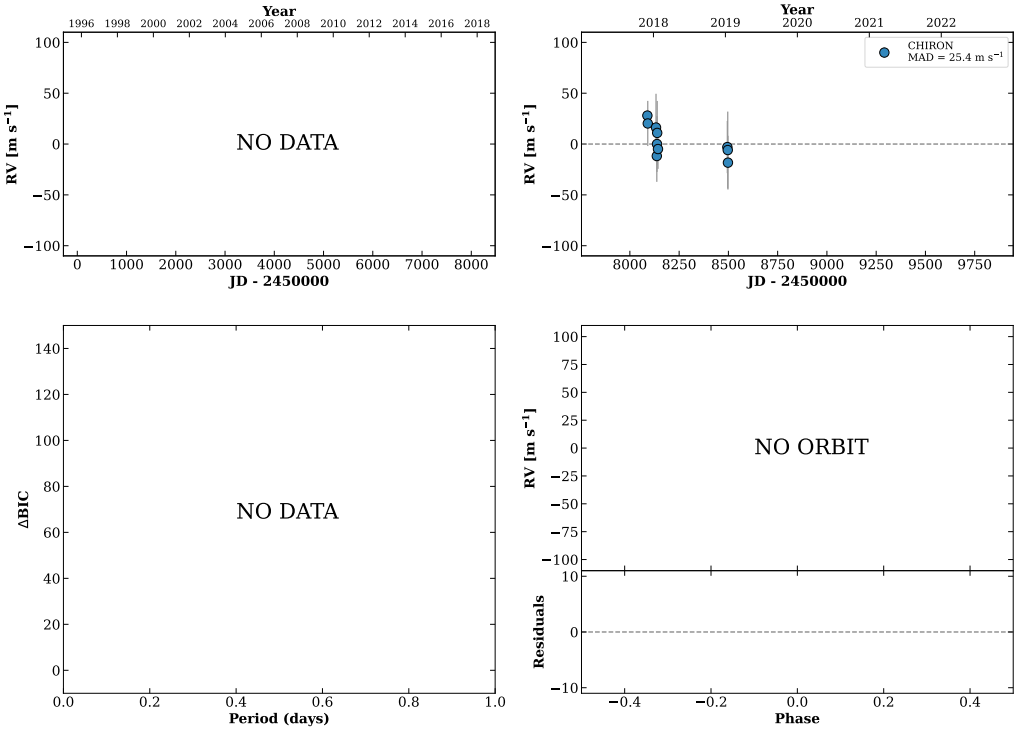

Figure 140 RV results for RKS0804+1217 (top) and RKS0808+2106 (bottom).

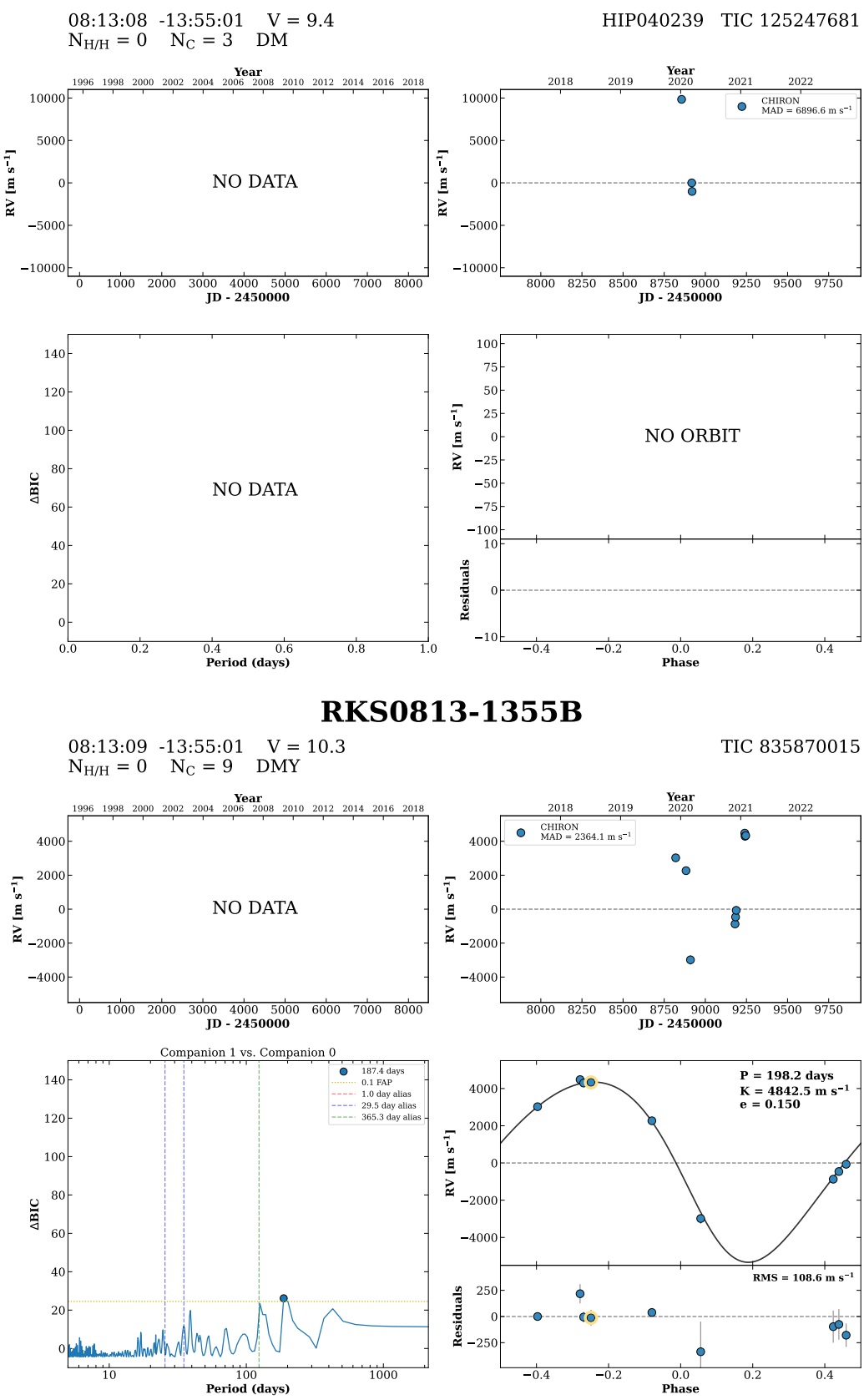

Figure 141 RV results for RKS0813-1355A (top) and RKS0813-1355B (bottom).

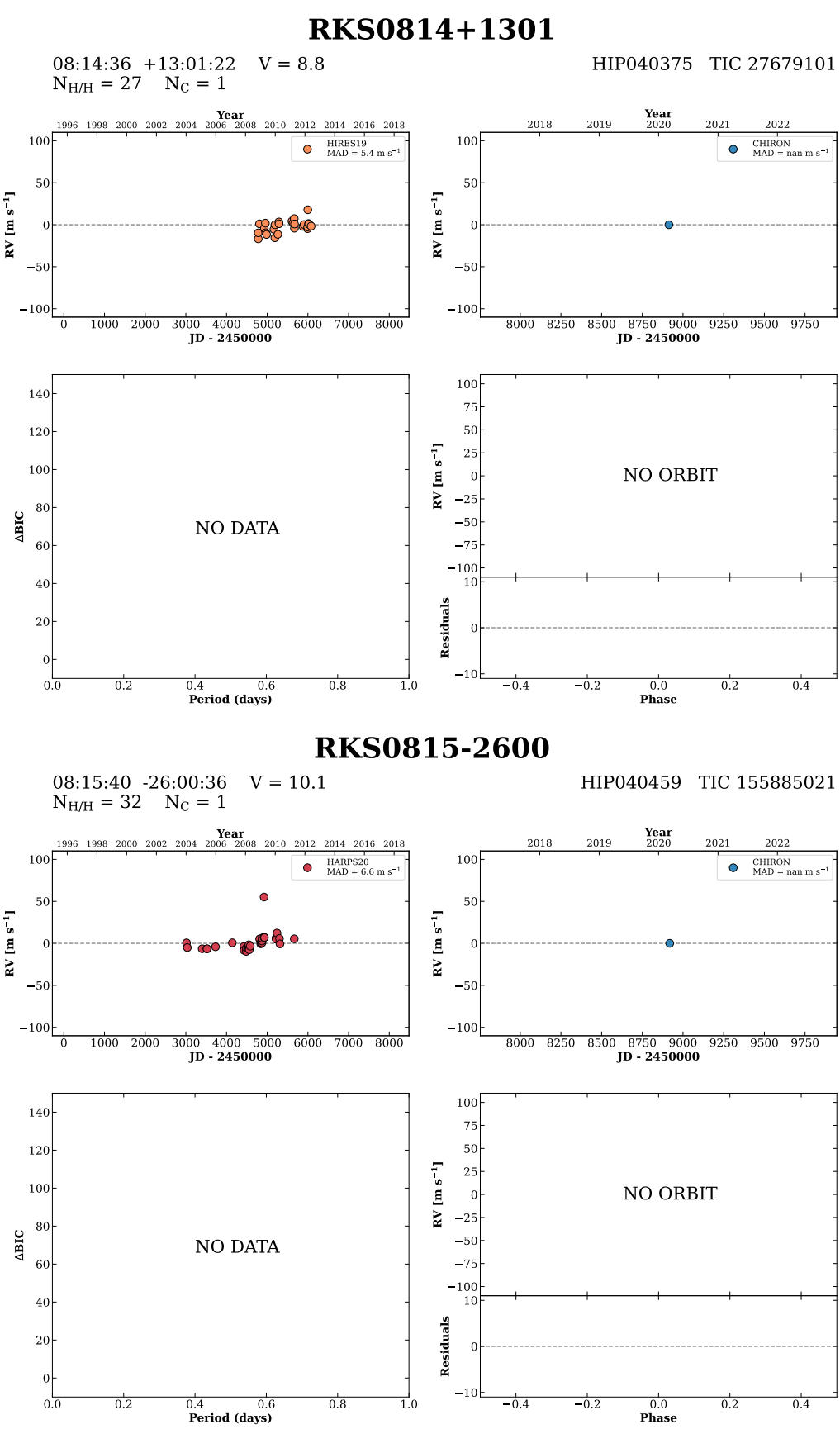

Figure 142 RV results for RKS0814+1301 (top) and RKS0815-2600 (bottom).

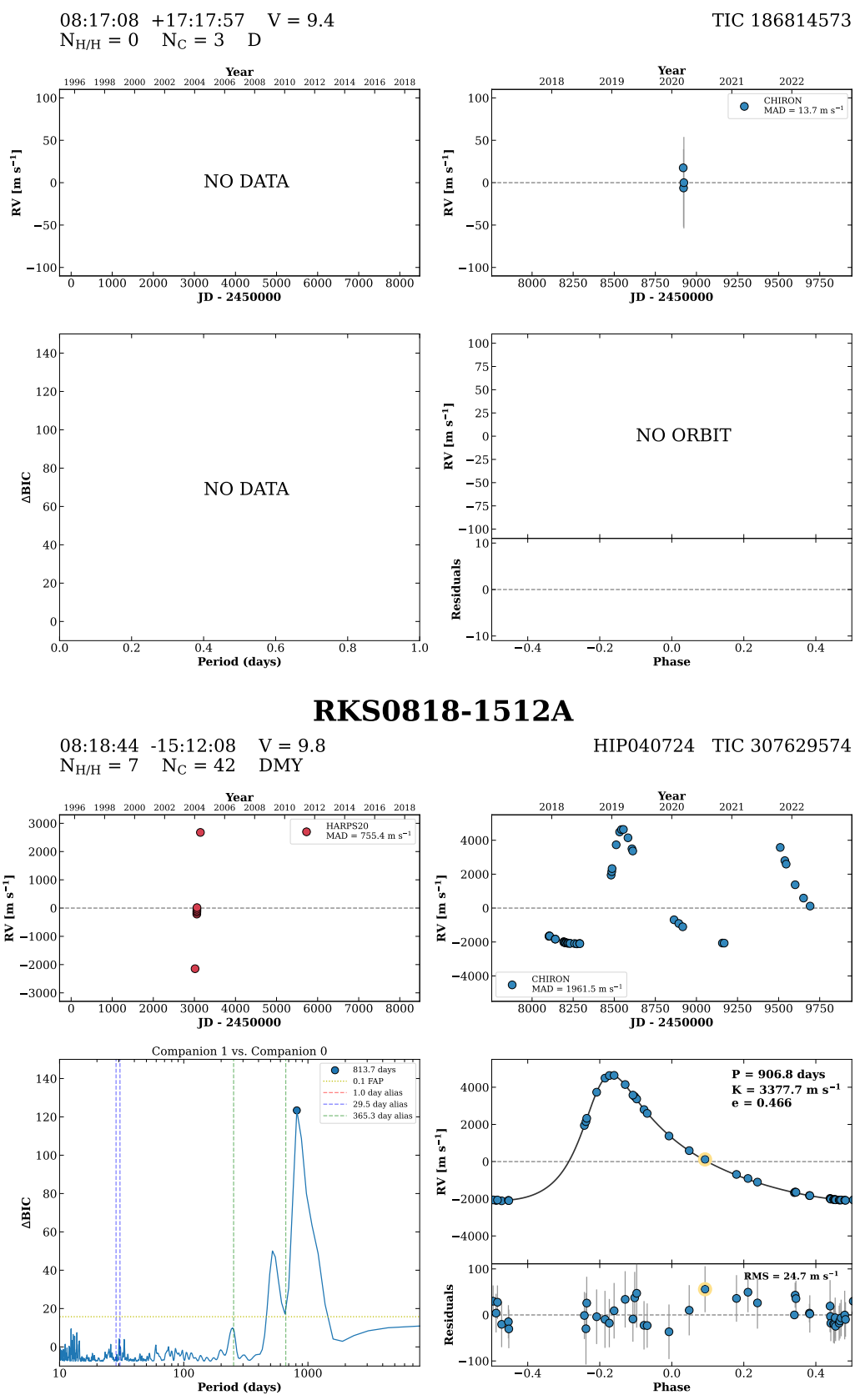

Figure 143 RV results for RKS0817+1717 (top) and RKS0818-1512A (bottom).

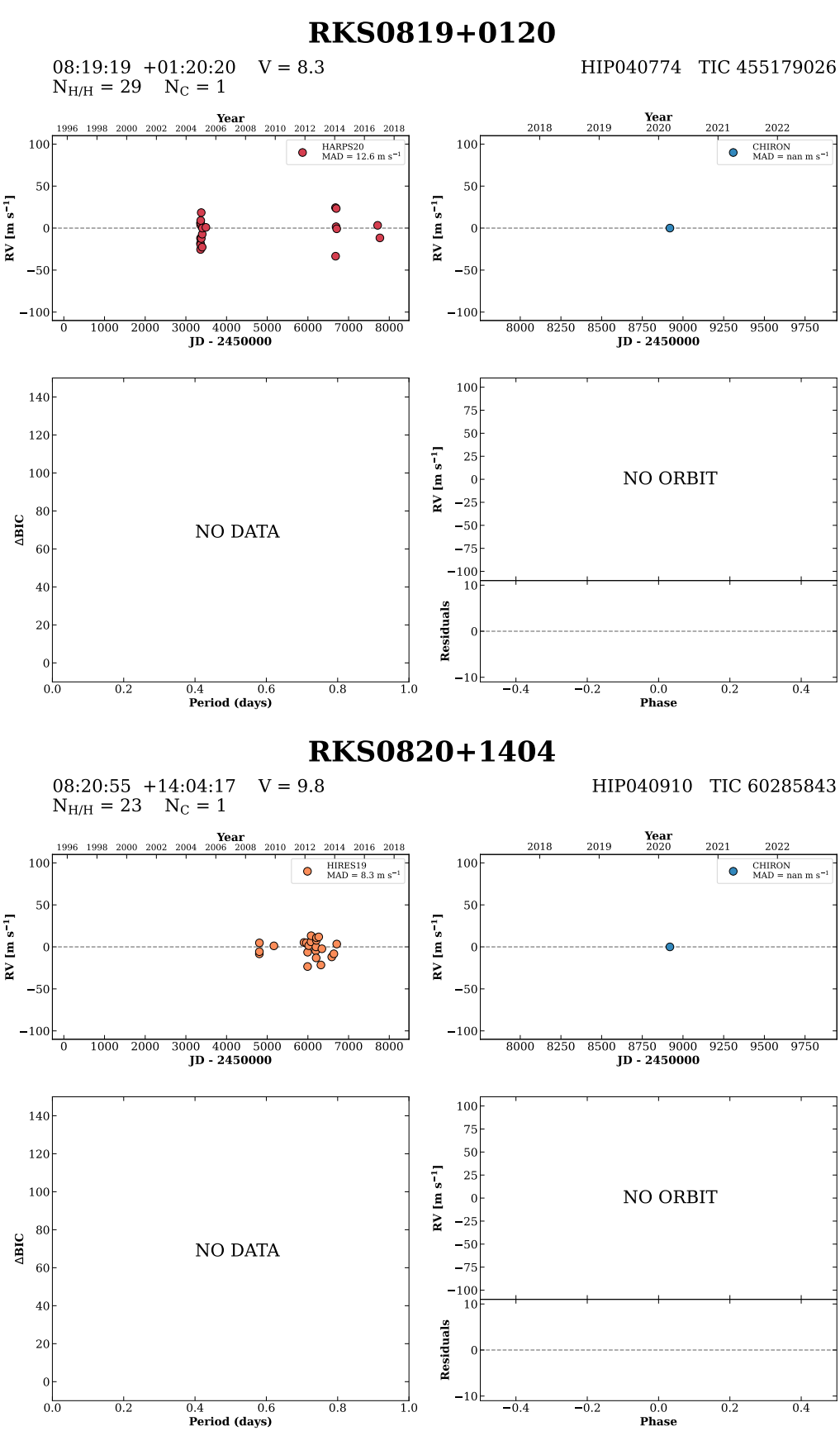

Figure 144 RV results for RKS0819+0120 (top) and RKS0820+1404 (bottom).

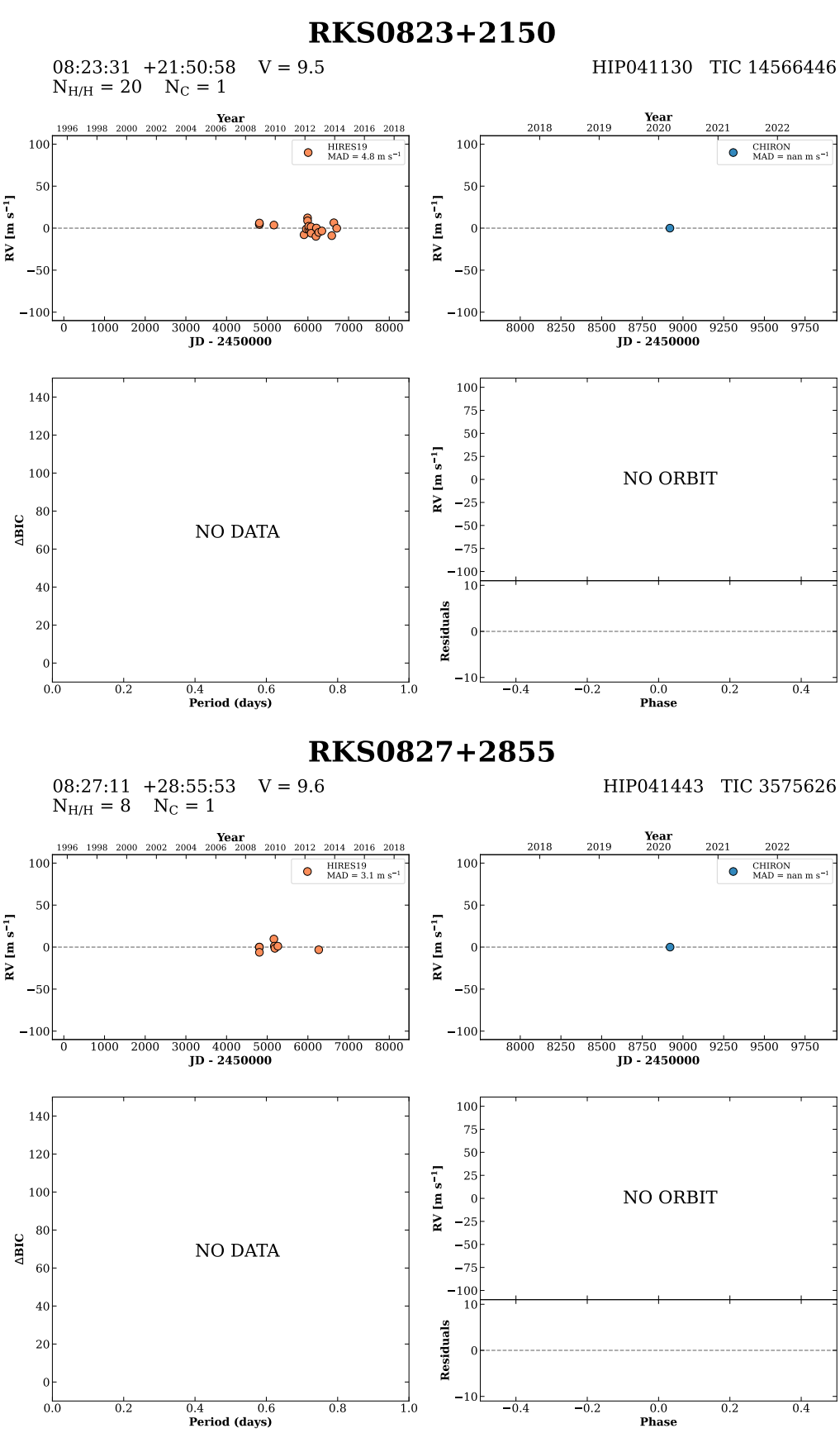

Figure 145 RV results for RKS0823+2150 (top) and RKS0827+2855 (bottom).

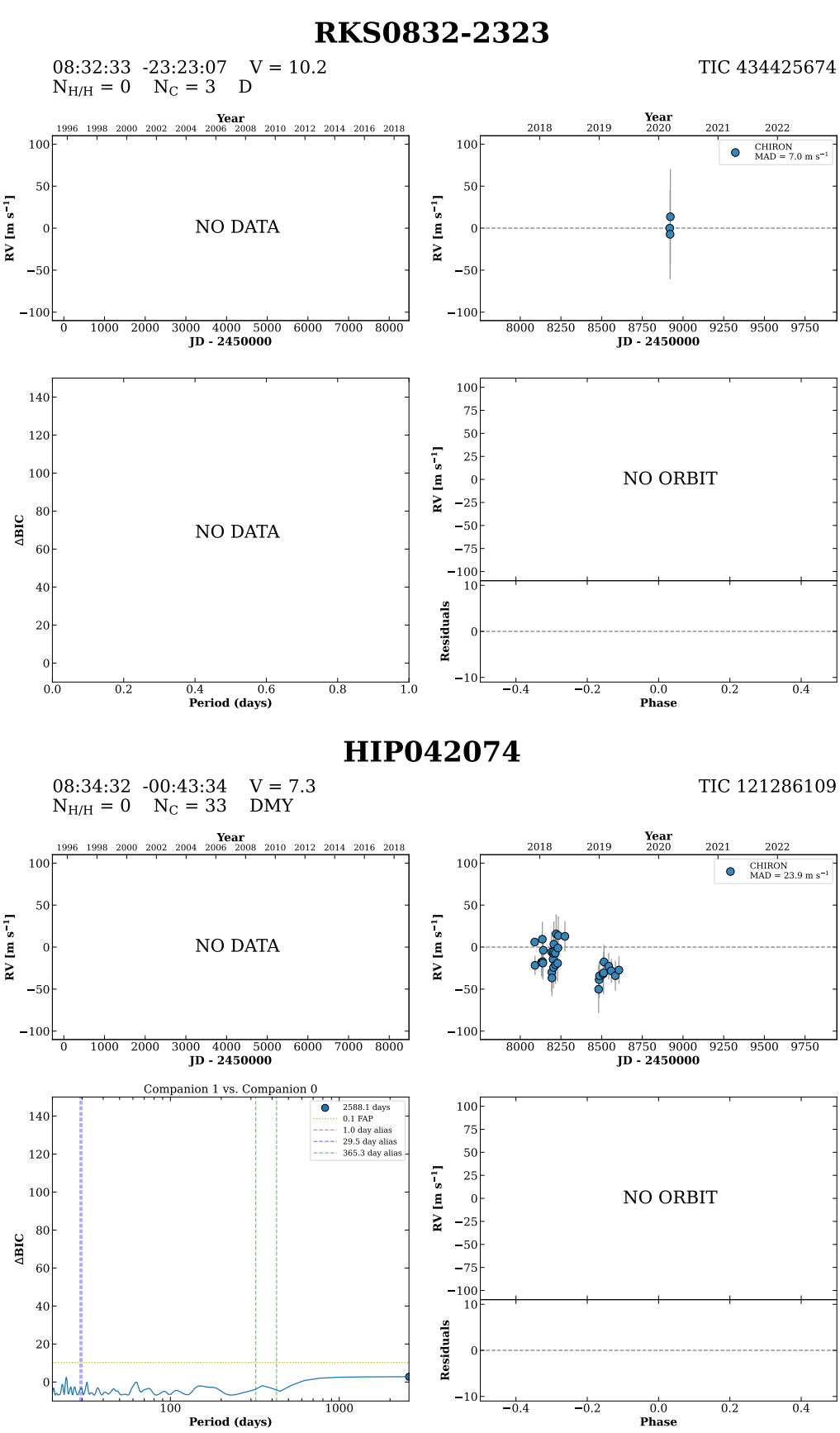

Figure 146 RV results for RKS0832-2323 (top) and HIP042074 (bottom).

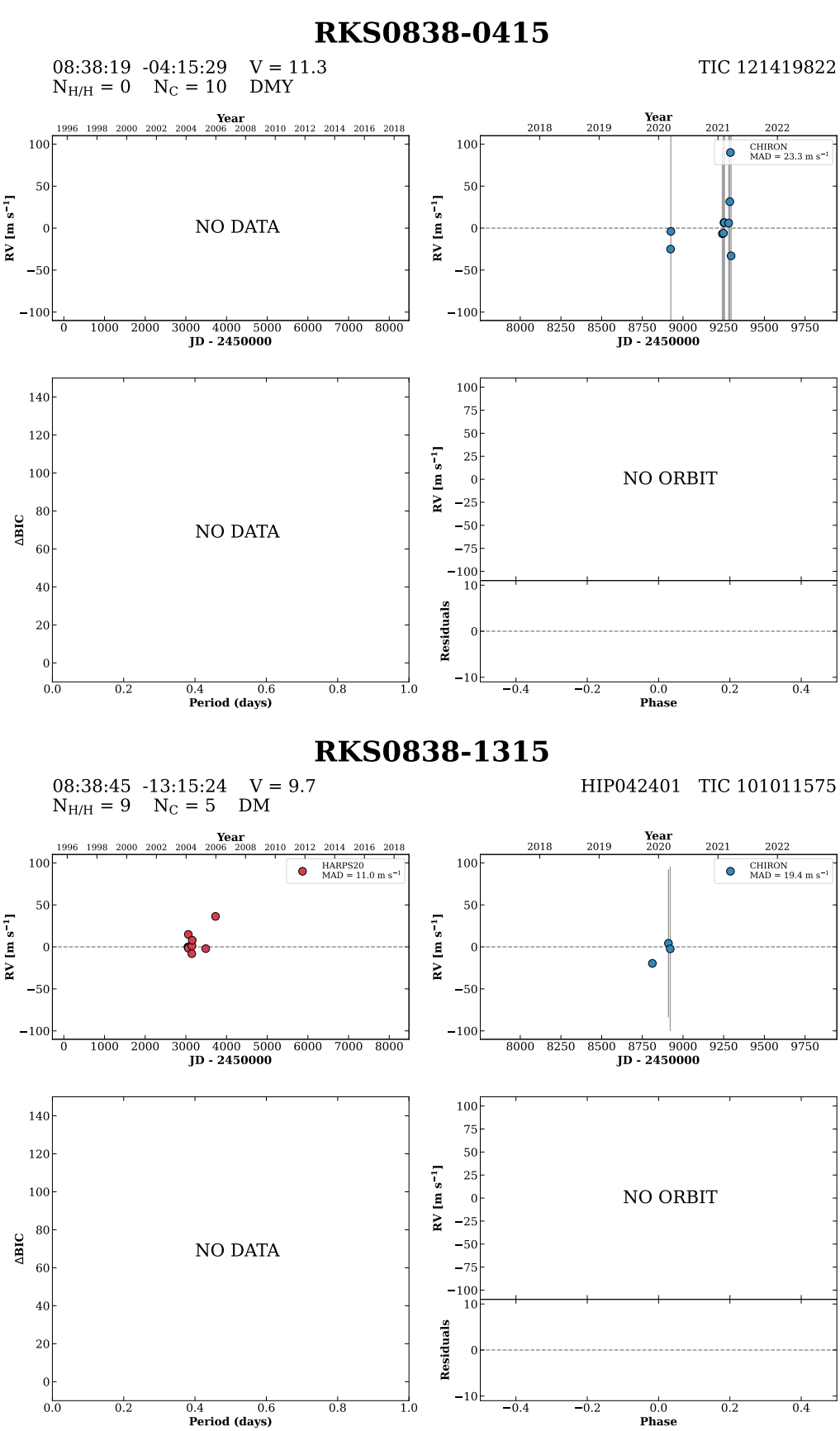

Figure 147 RV results for RKS0838-0415 (top) and RKS0838-1315 (bottom).

RKS0839+0657

08:39:00 +06:57:20 V = 7.9 HIP042418 TIC 458680441
$N_{H/H}$ = 0 N_C = 9 DMY

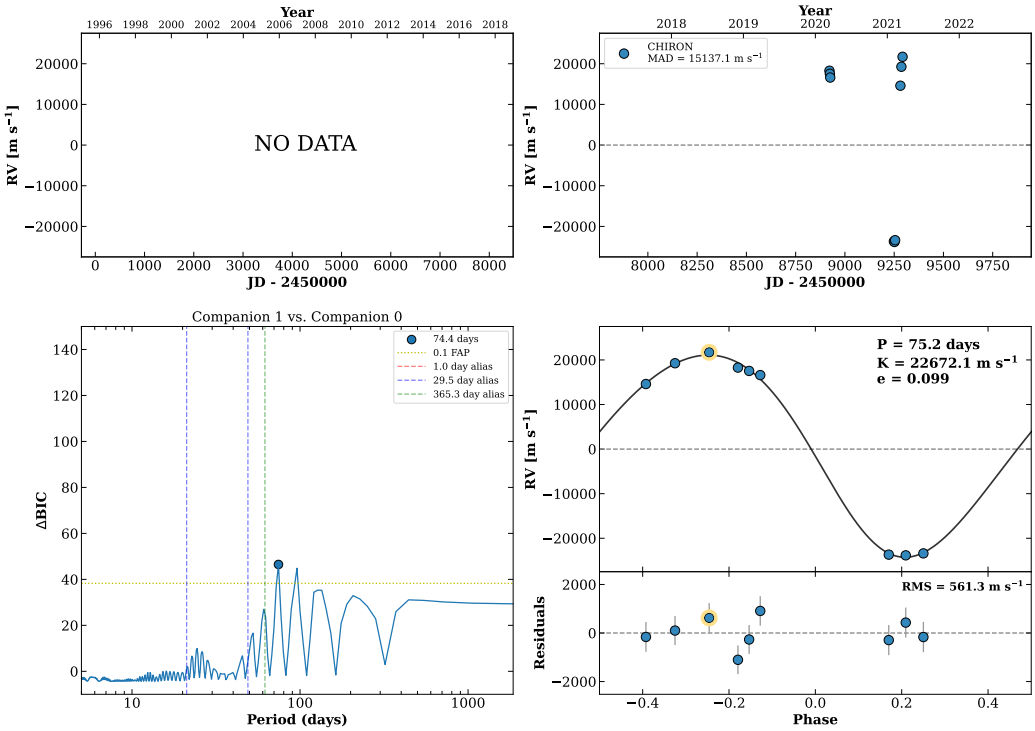

RKS0839+1131

08:39:51 +11:31:22 V = 7.6 HIP042499 TIC 443965212
$N_{H/H}$ = 59 N_C = 1

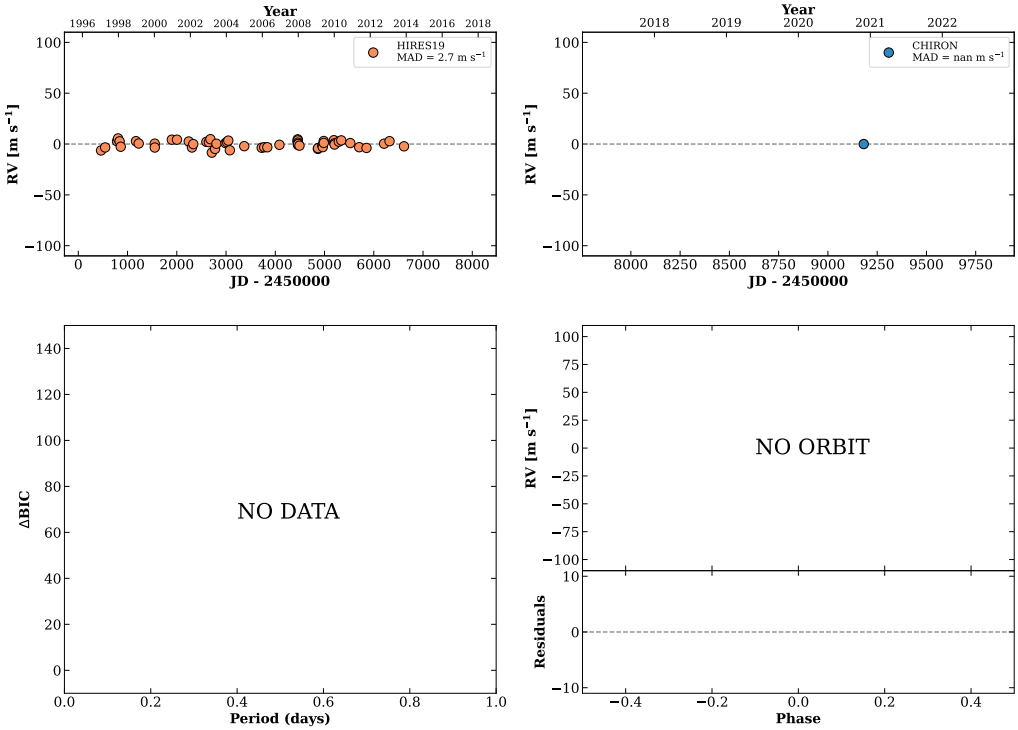

Figure 148 RV results for RKS0839+0657 (top) and RKS0839+1131 (bottom).

RKS0840-0628A

08:40:00 -06:28:33 V = 9.9 HIP042507 TIC 51624556
$N_{H/H}$ = 0 N_C = 37 DMY

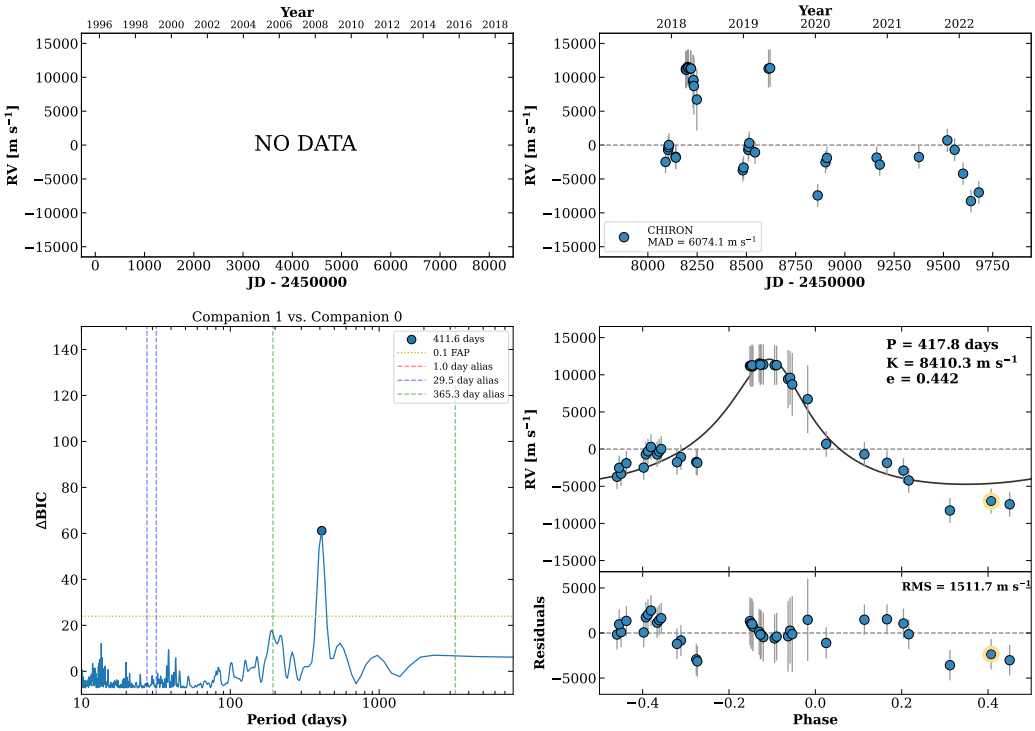

RKS0848+0628

08:48:26 +06:28:06 V = 10.3 HIP043233 TIC 444008058
$N_{H/H}$ = 0 N_C = 14 DMY

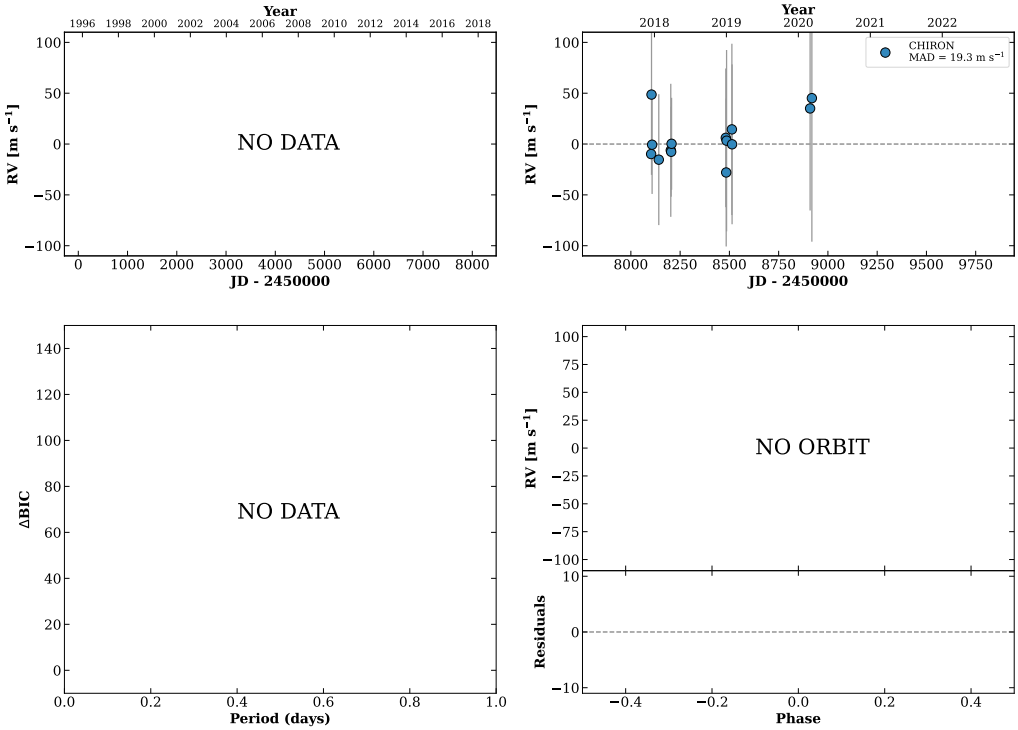

Figure 149 RV results for RKS0840-0628A (top) and RKS0848+0628 (bottom).

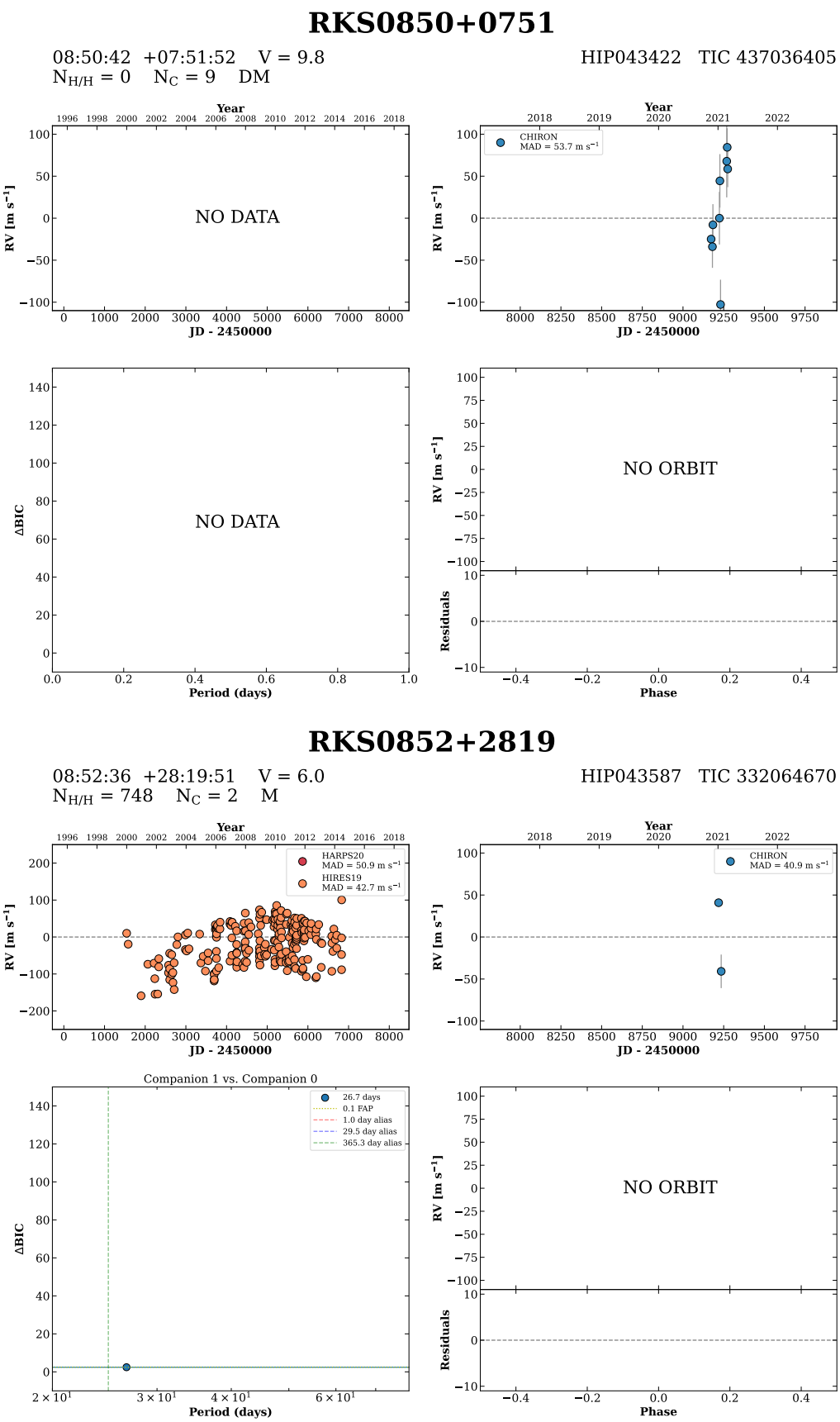

Figure 150 RV results for RKS0850+0751 (top) and RKS0852+2819 (bottom).

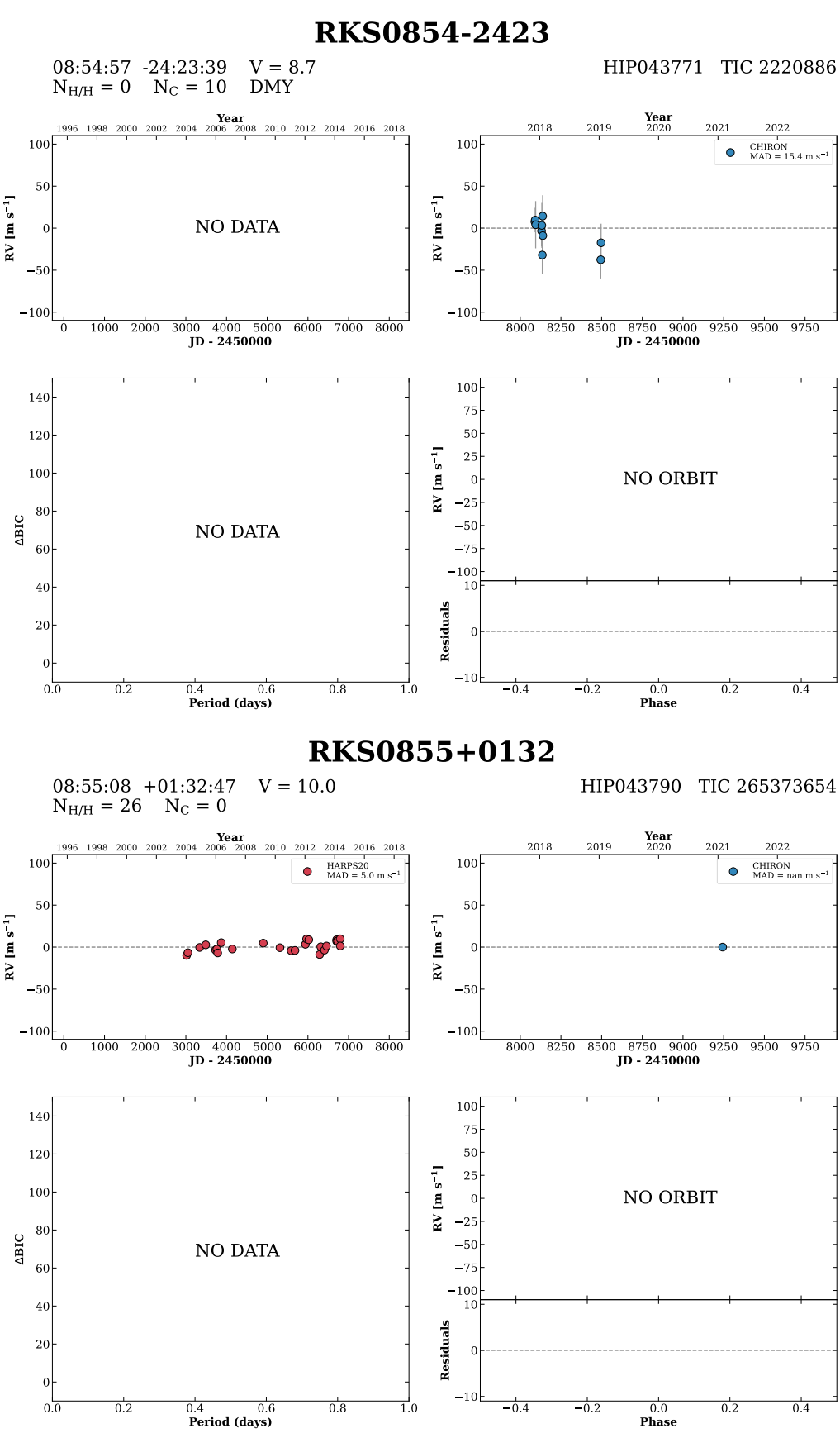

Figure 151 RV results for RKS0854-2423 (top) and RKS0855+0132 (bottom).

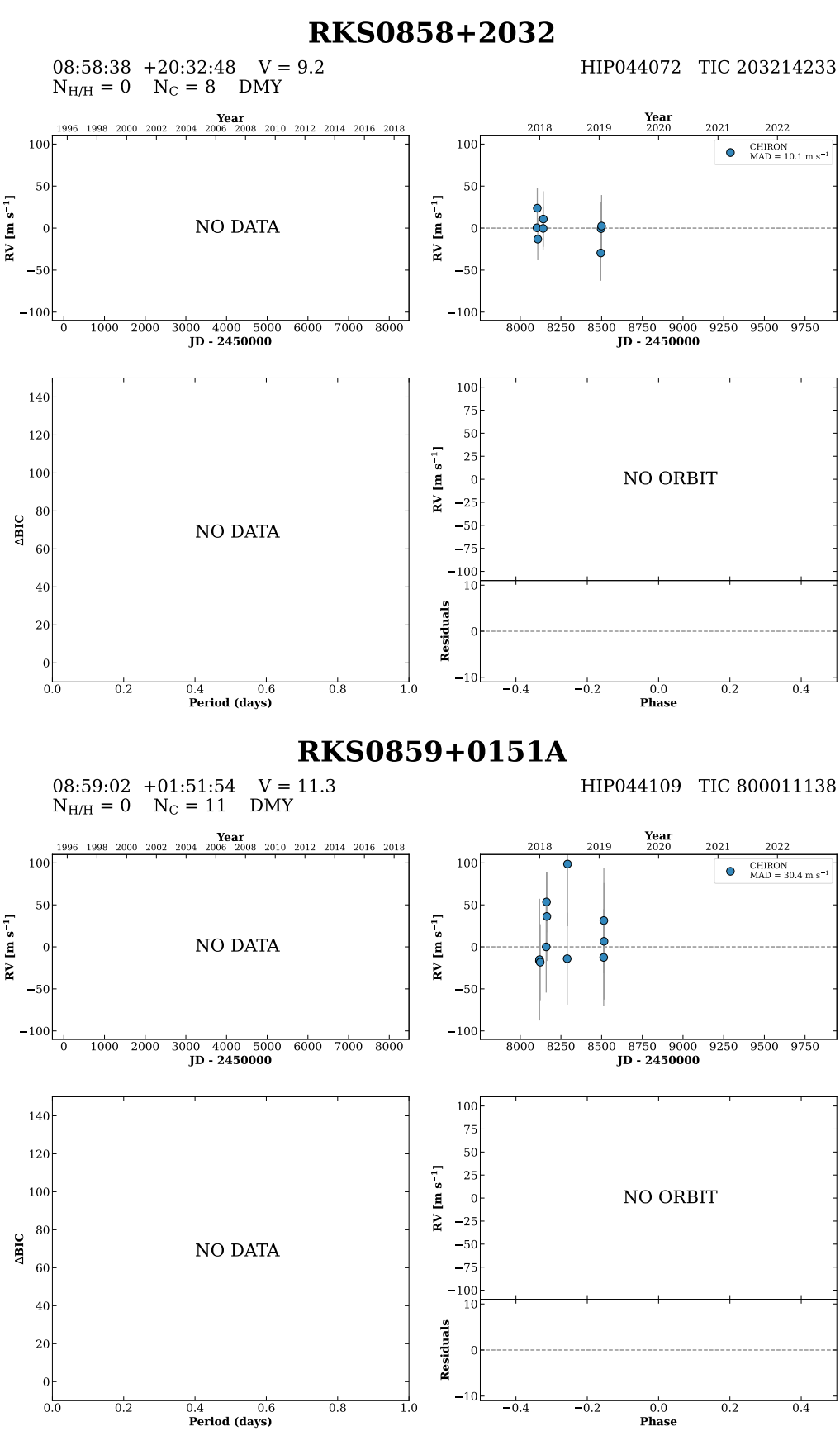

Figure 152 RV results for RKS0858+2032 (top) and RKS0859+0151A (bottom).

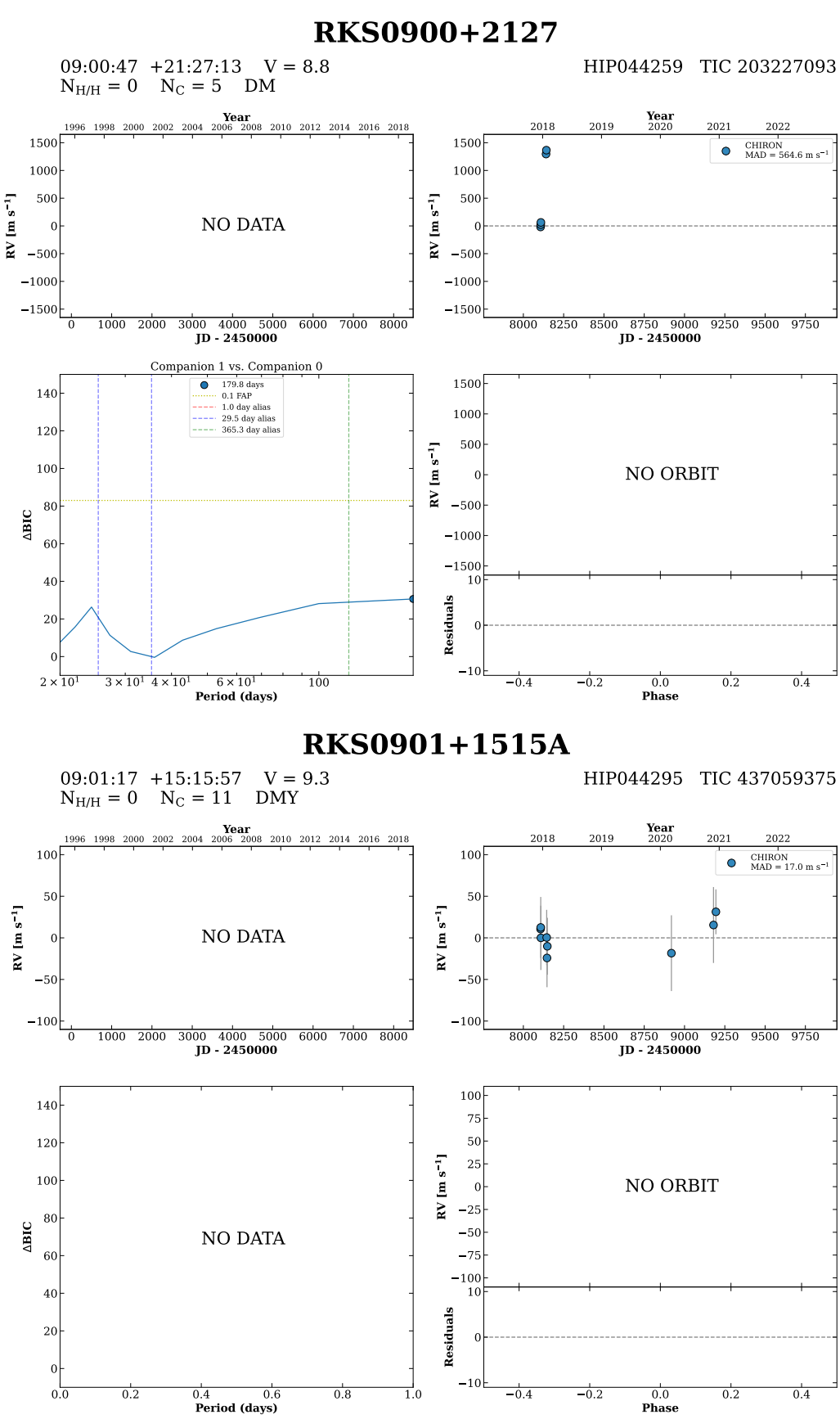

Figure 153 RV results for RKS0900+2127 (top) and RKS0901+1515A (bottom).

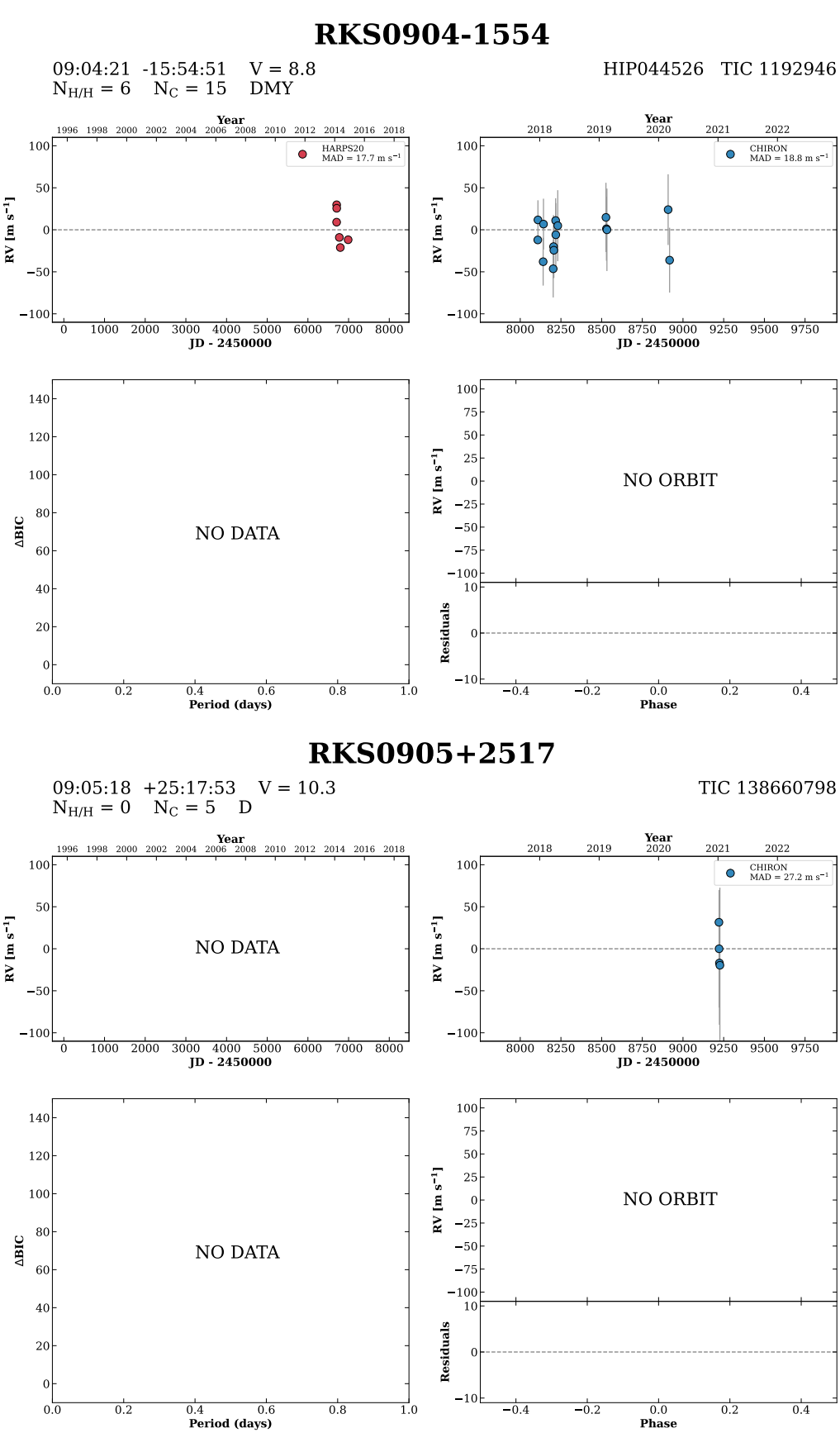

Figure 154 RV results for RKS0904-1554 (top) and RKS0905+2517 (bottom).

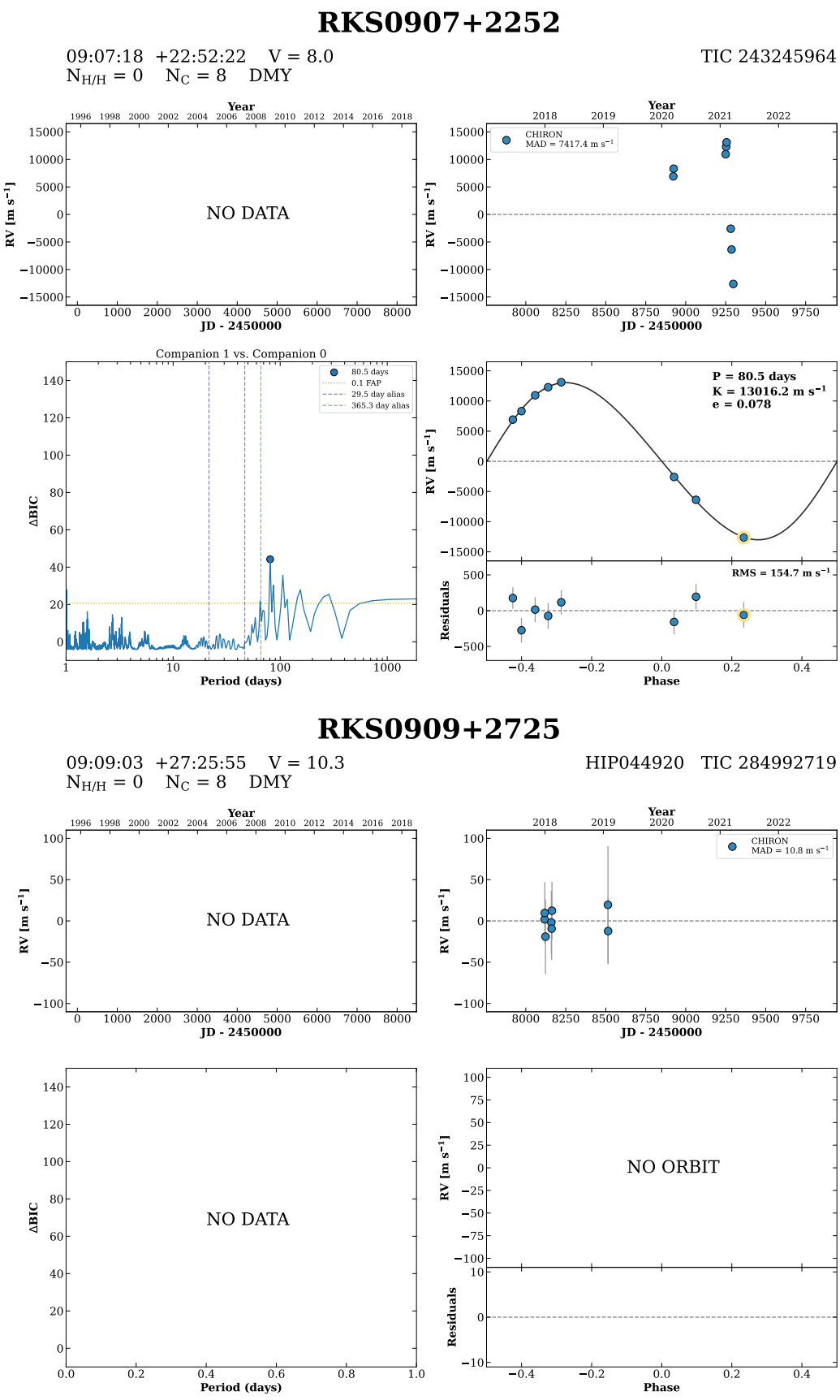

Figure 155 RV results for RKS0907+2252 (top) and RKS0909+2725 (bottom).

RKS0909+0512

09:09:54 +05:12:13 V = 8.4 TIC 270693260
$N_{H/H}$ = 0 N_C = 4 DM

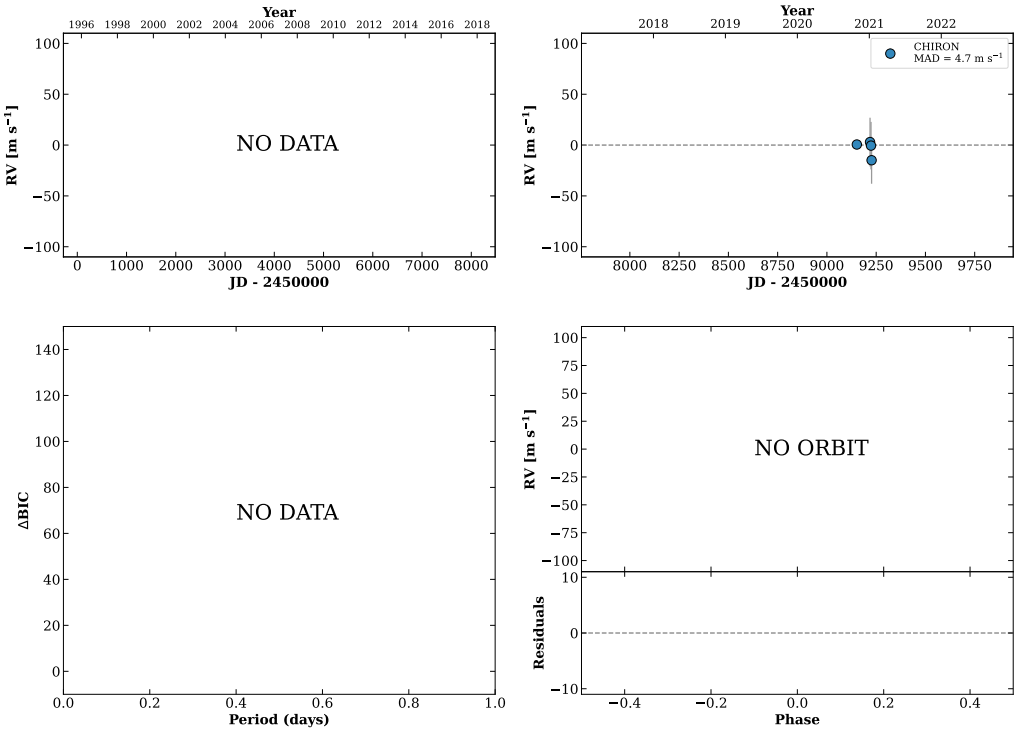

RKS0914+0426A

09:14:54 +04:26:34 V = 7.9 HIP045383 TIC 290468468
$N_{H/H}$ = 3 N_C = 40 DMY

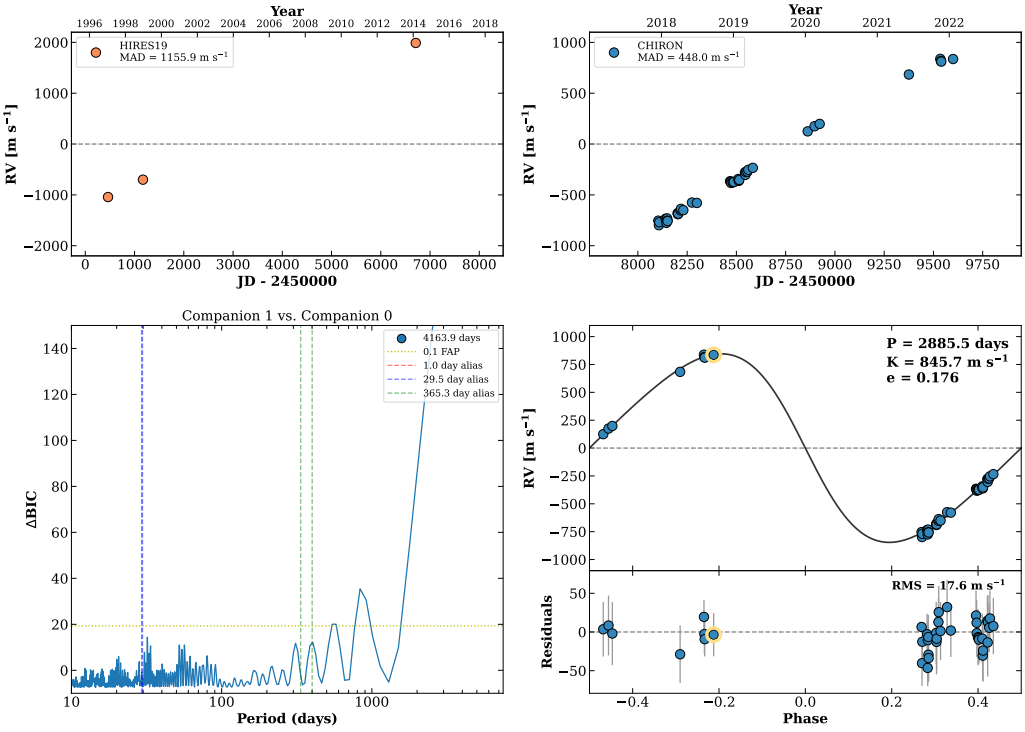

Figure 156 RV results for RKS0909+0512 (top) and RKS0914+0426A (bottom).

RKS0917-0323

09:17:55 -03:23:14 V = 7.8 HIP045621 TIC 170889511
$N_{H/H}$ = 0 N_C = 9 DY

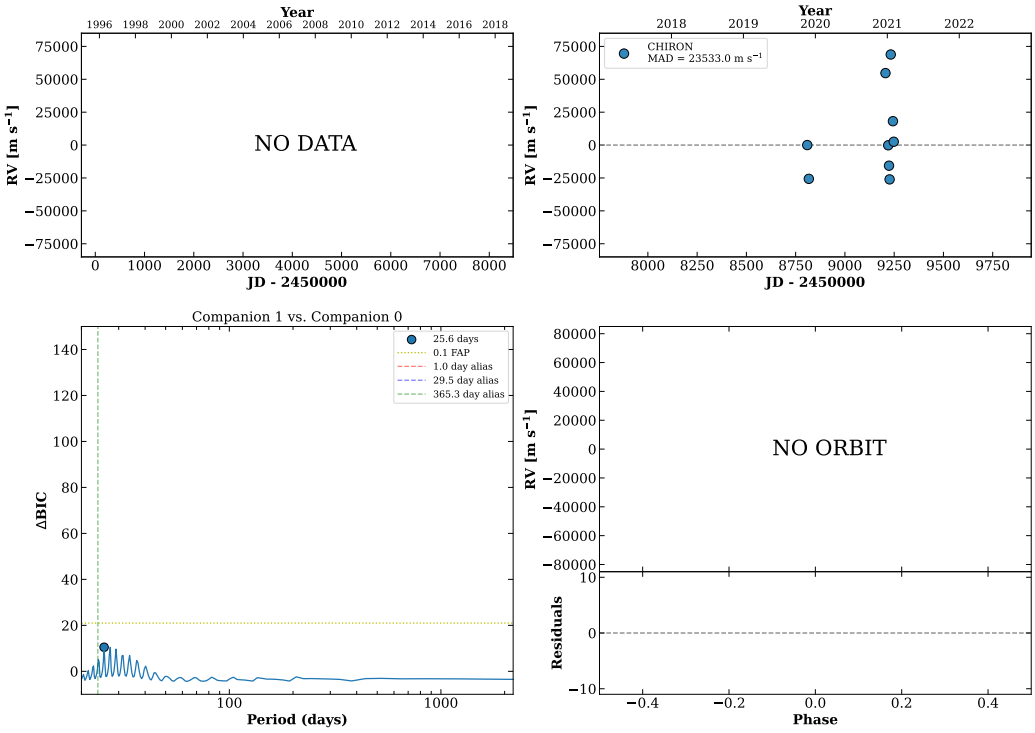

RKS0918+2718

09:18:22 +27:18:42 V = 9.5 TIC 149397312
$N_{H/H}$ = 4 N_C = 9 DM

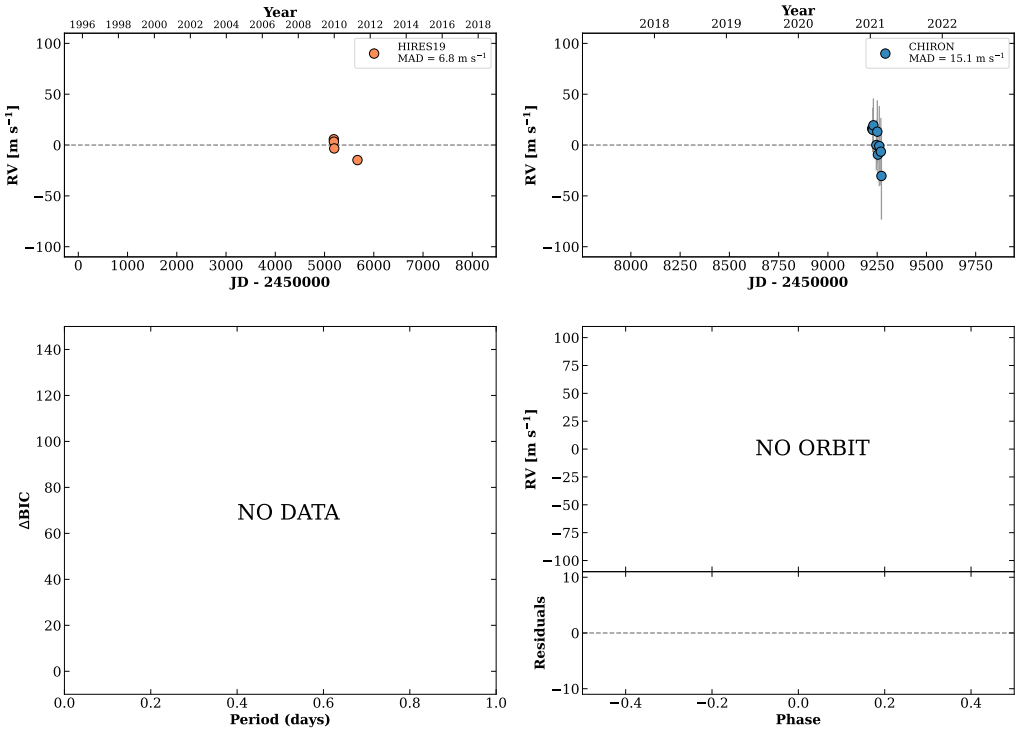

Figure 157 RV results for RKS0917-0323 (top) and RKS0918+2718 (bottom).

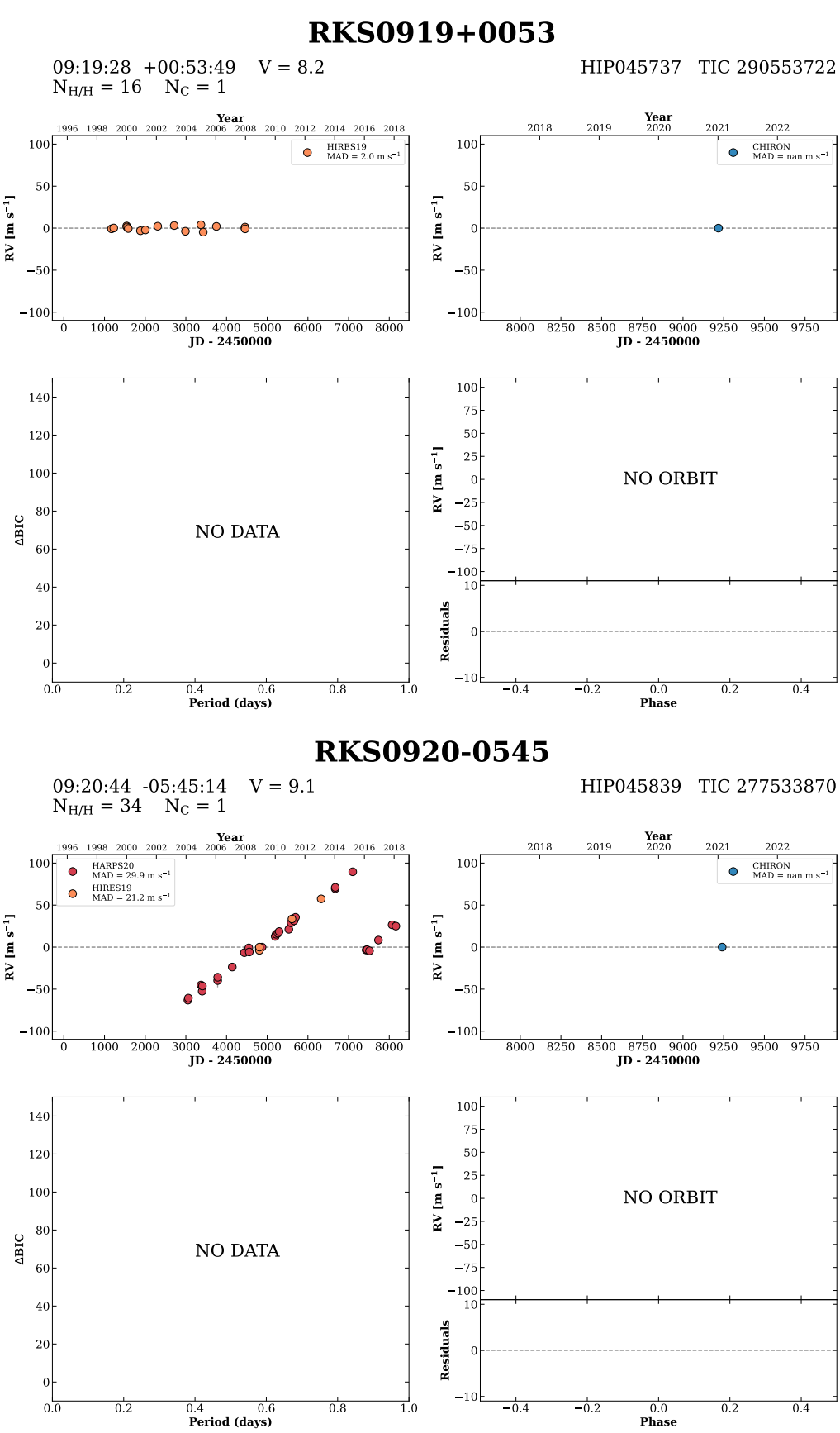

Figure 158 RV results for RKS0919+0053 (top) and RKS0920-0545 (bottom).

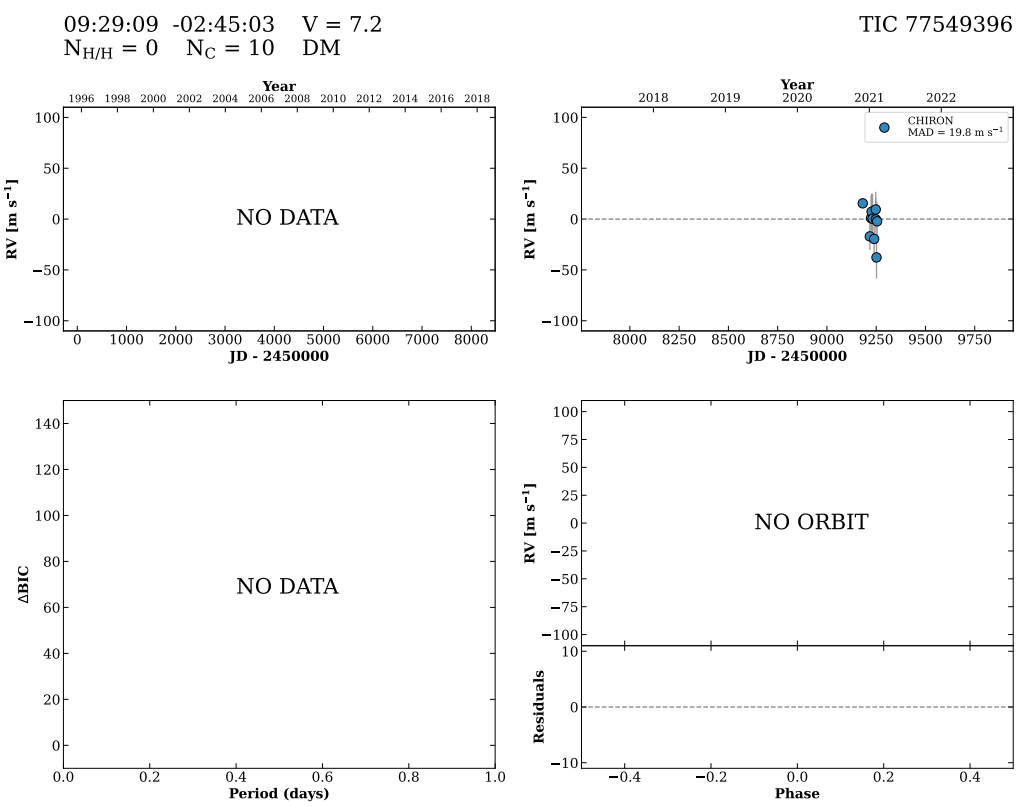

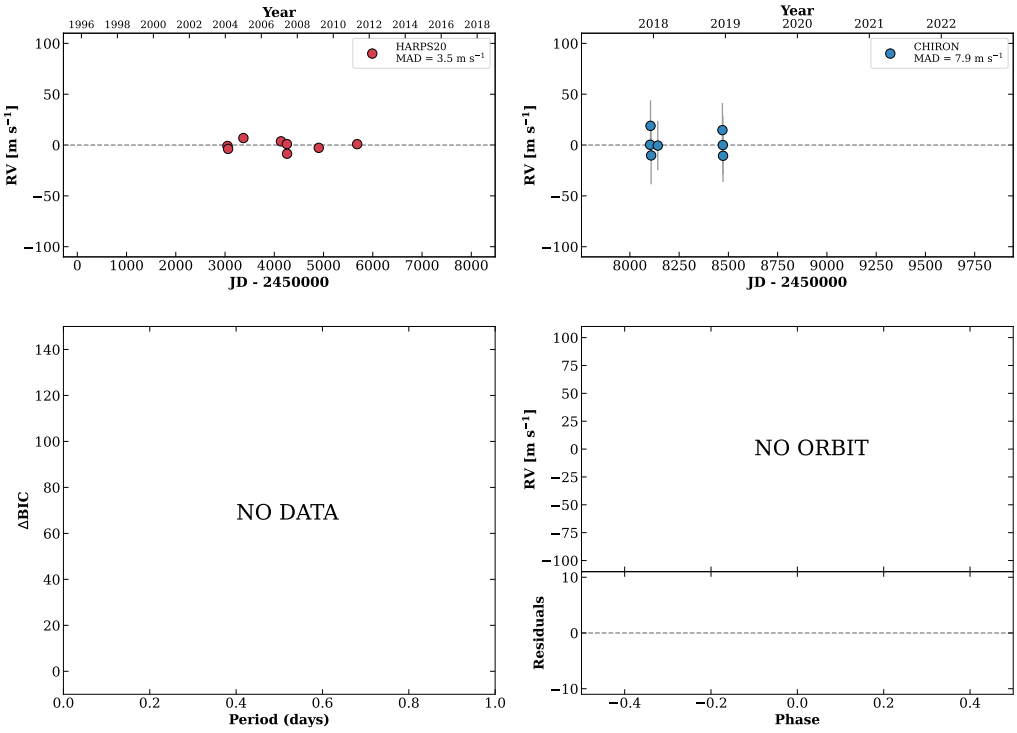

Figure 159 RV results for RKS0929-0245 (top) and RKS0929-0522 (bottom).

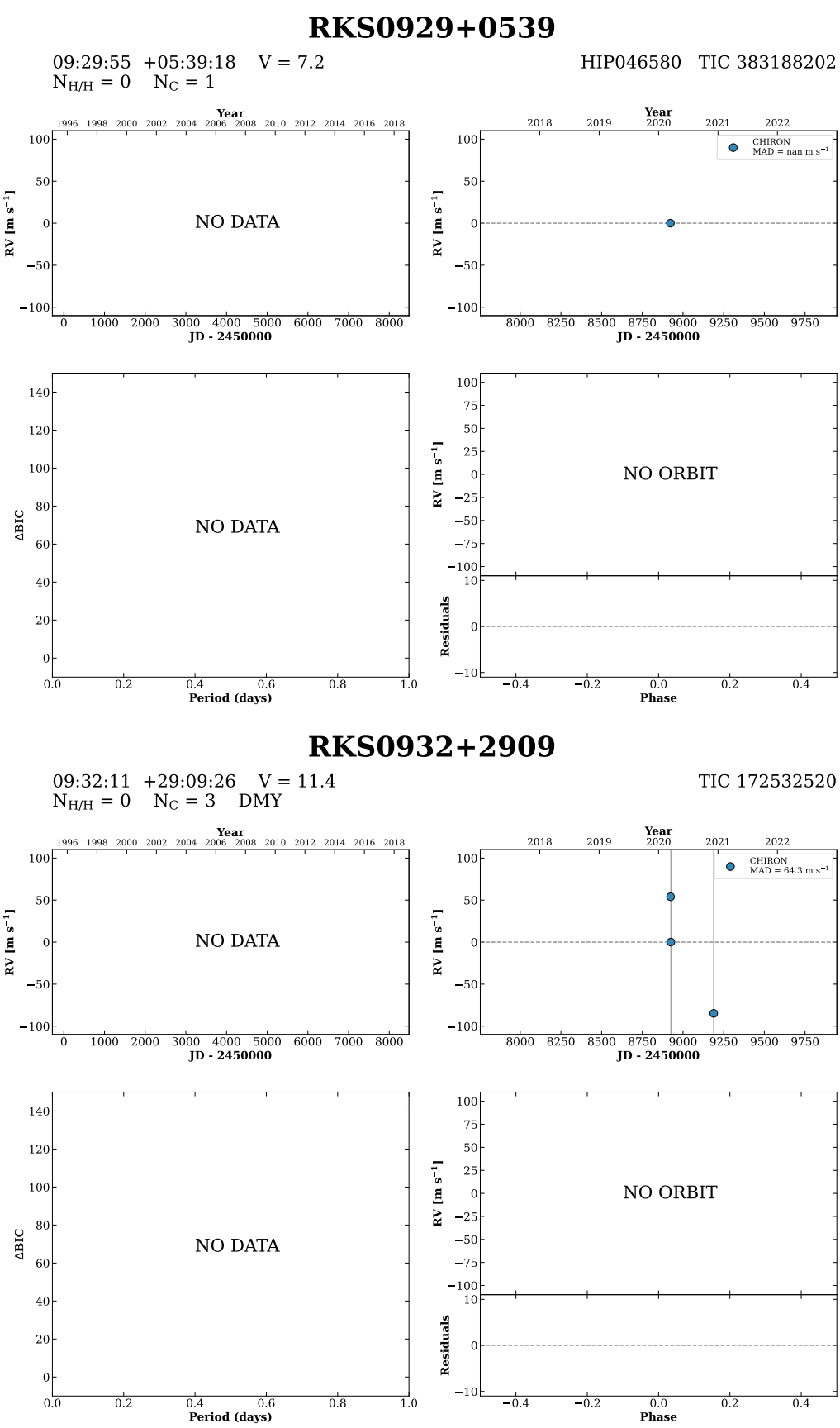

Figure 160 RV results for RKS0929+0539 (top) and RKS0932+2909 (bottom).

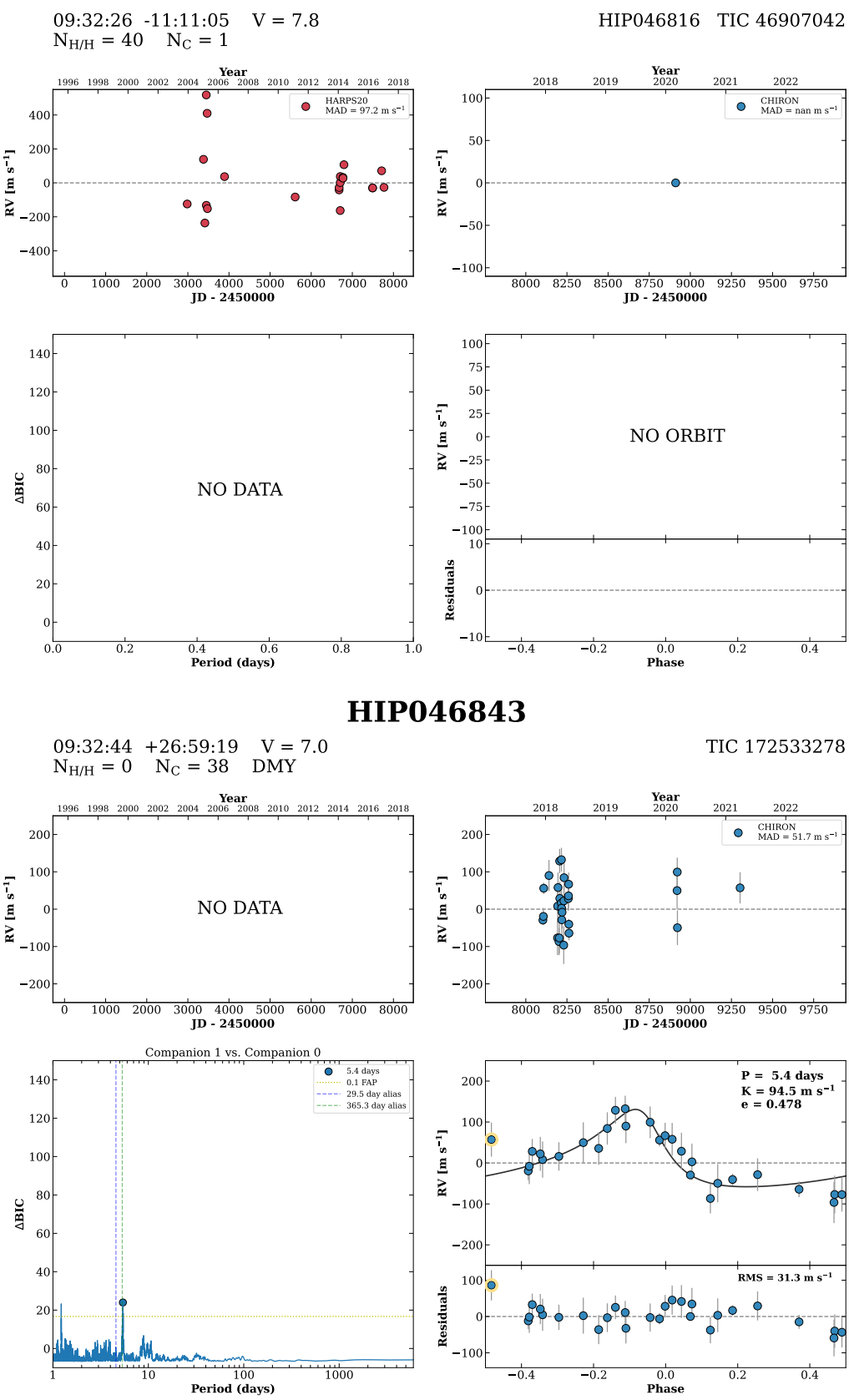

Figure 161 RV results for RKS0932-1111 (top) and HIP046843 (bottom).

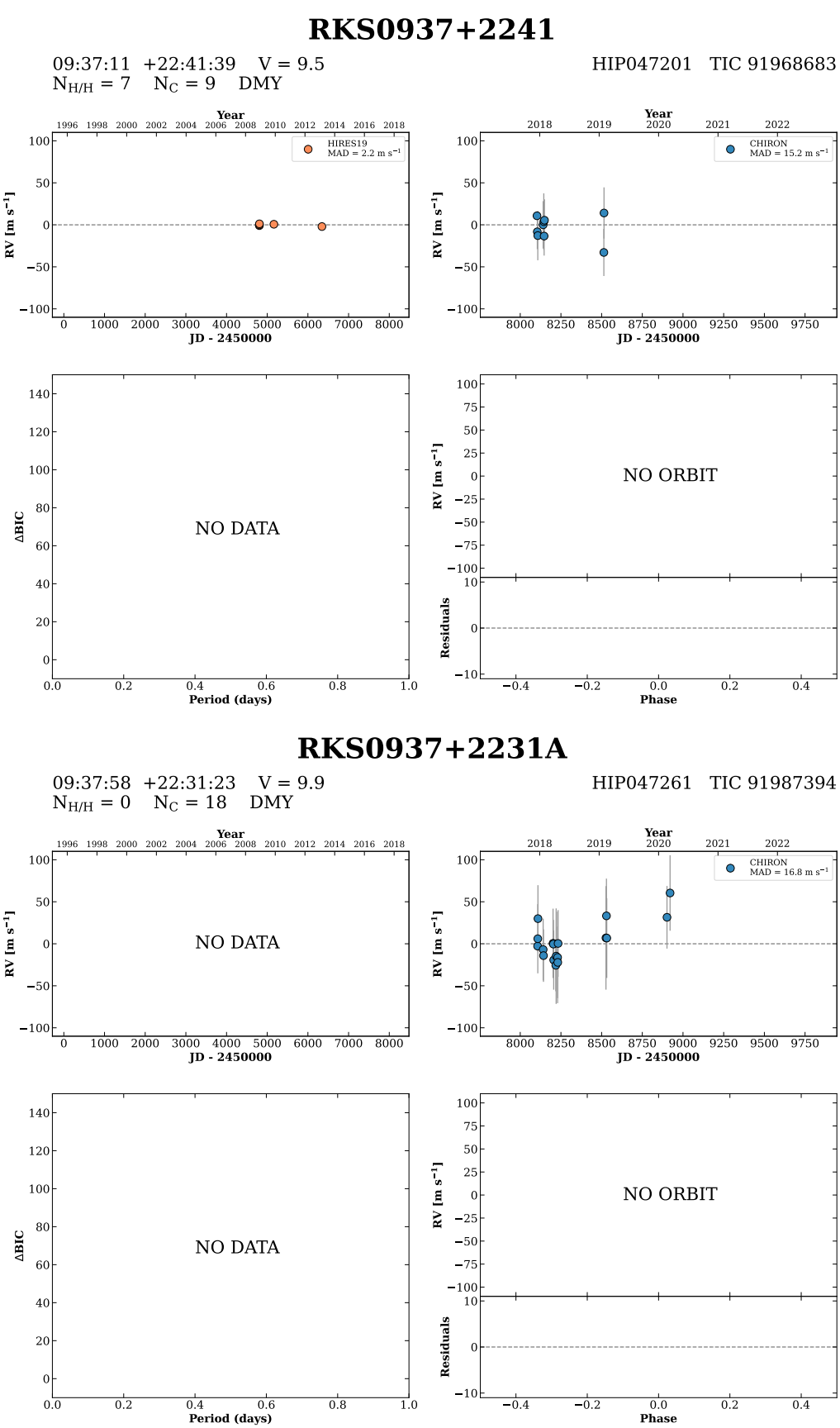

Figure 162 RV results for RKS0937+2241 (top) and RKS0937+2231A (bottom).

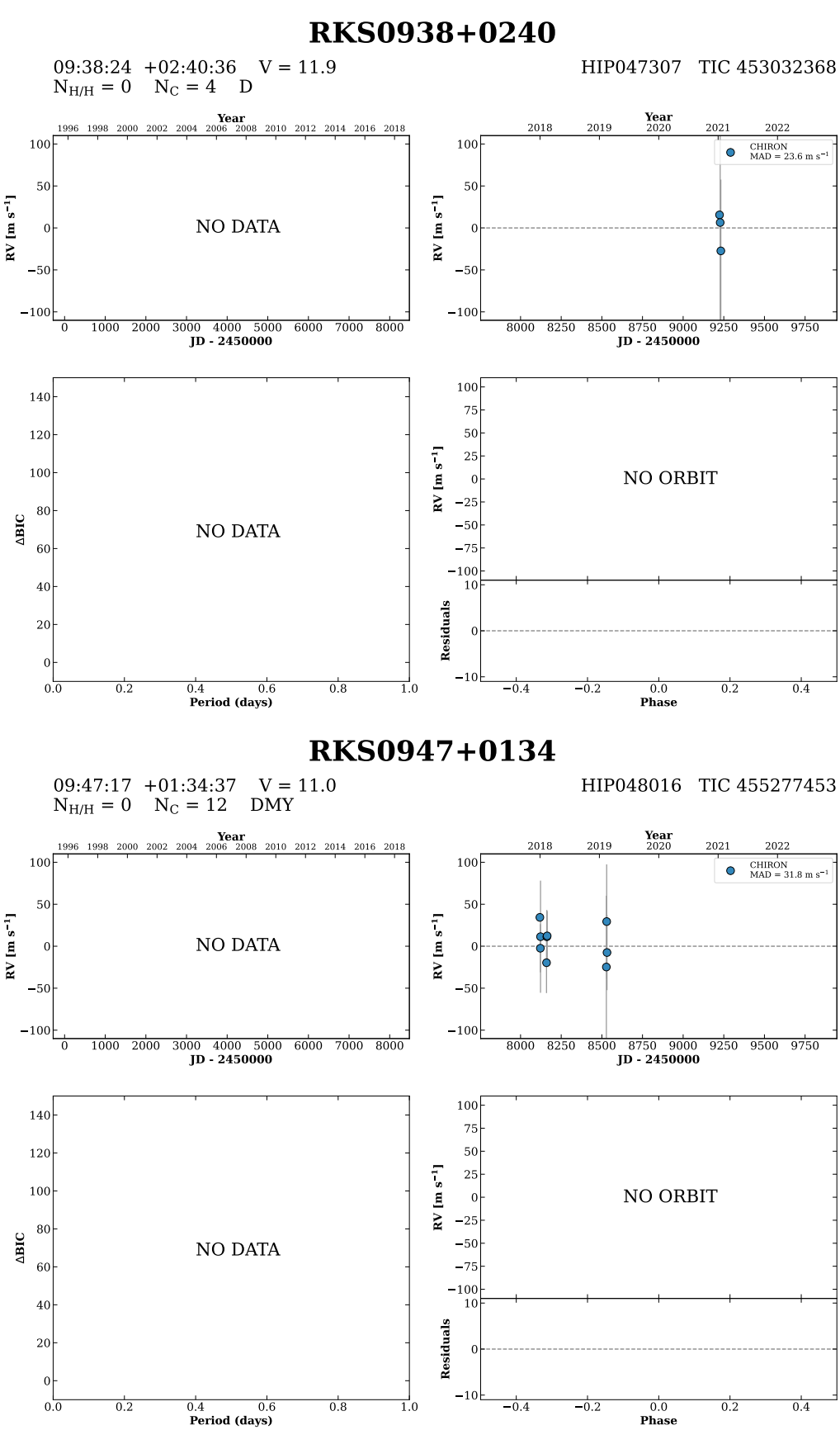

Figure 163 RV results for RKS0938+0240 (top) and RKS0947+0134 (bottom).

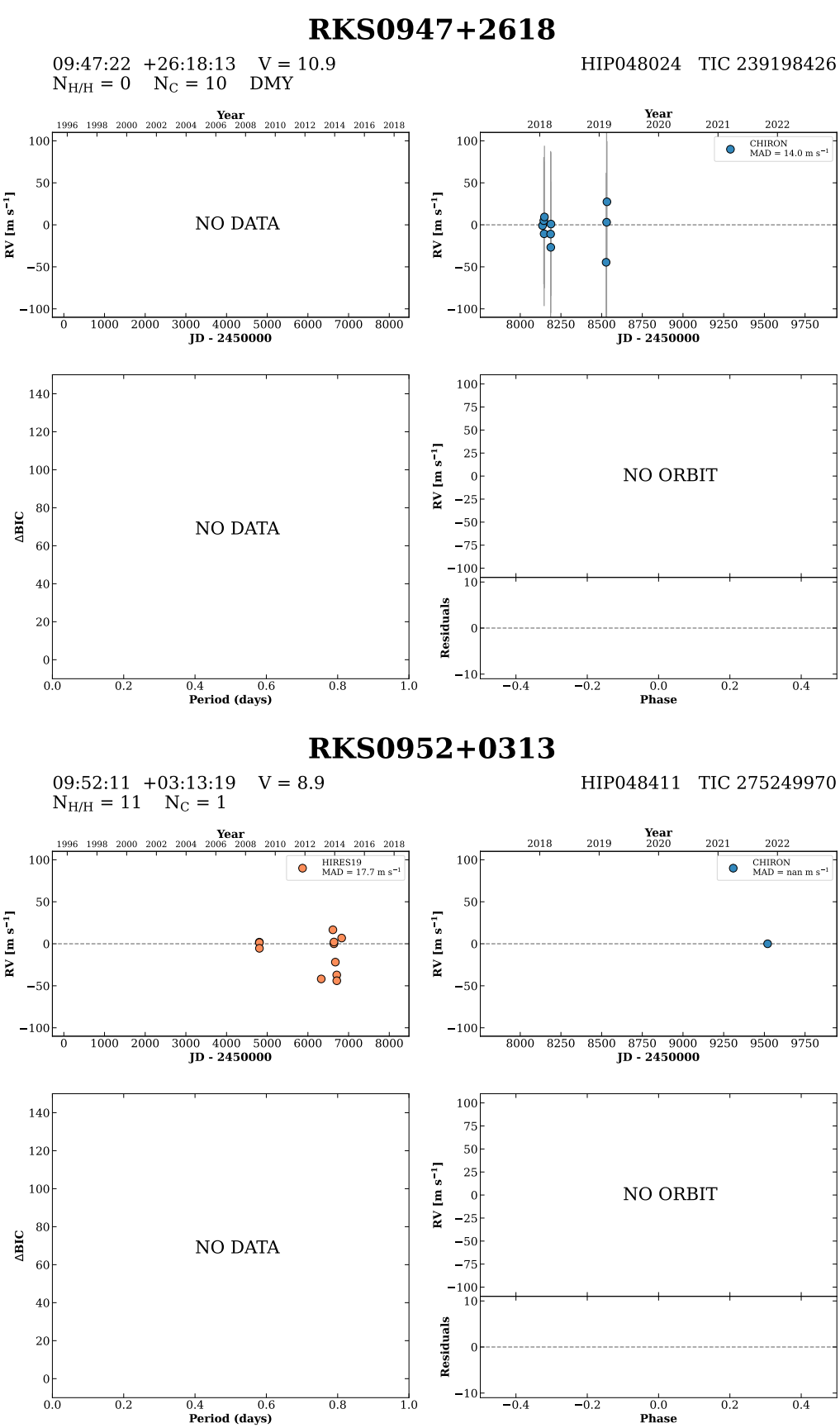

Figure 164 RV results for RKS0947+2618 (top) and RKS0952+0313 (bottom).

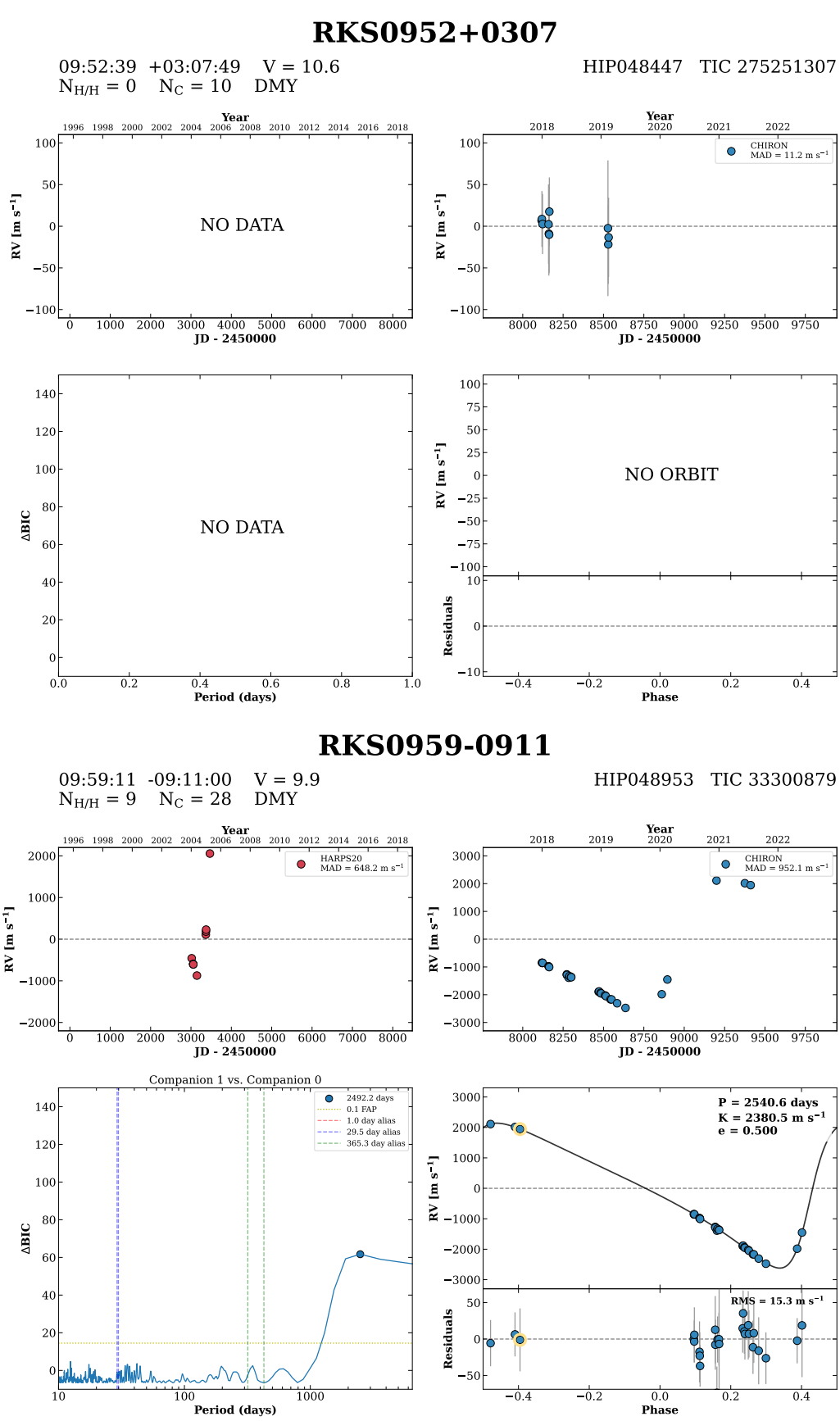

Figure 165 RV results for RKS0952+0307 (top) and RKS0959-0911 (bottom).

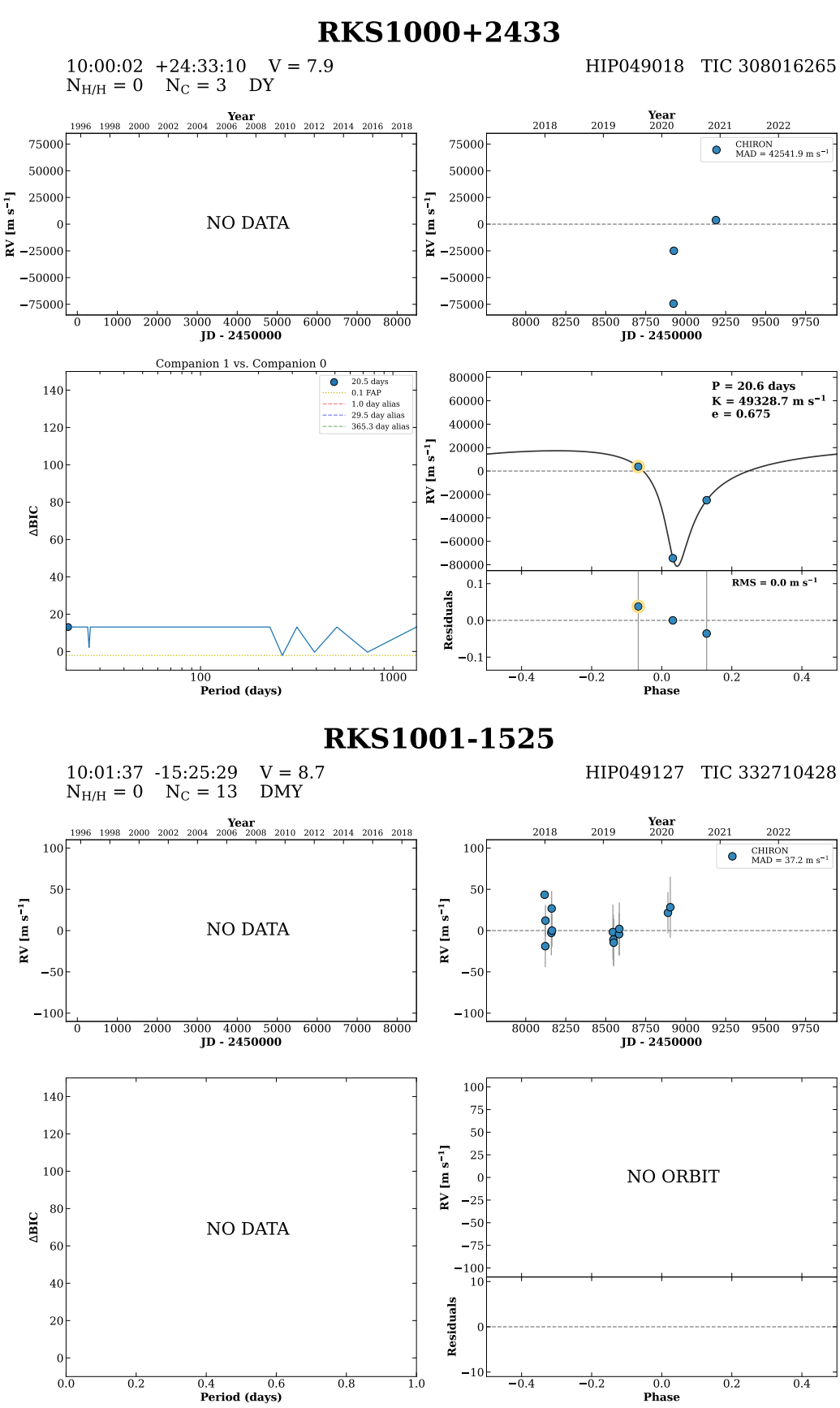

Figure 166 RV results for RKS1000+2433 (top) and RKS1001-1525 (bottom).

RKS1004-1143

10:04:38 -11:43:47 V = 8.2 HIP049366 TIC 26073633
$N_{H/H}$ = 18 N_C = 1

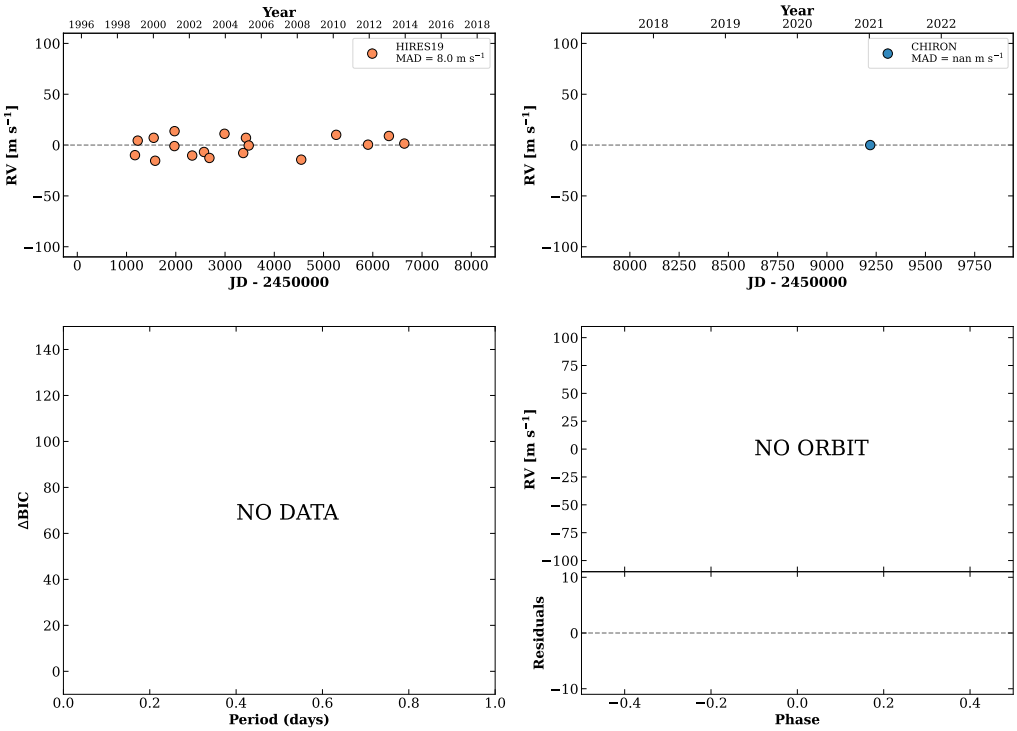

RKS1005+2629

10:05:27 +26:29:16 V = 9.1 HIP049429 TIC 3906145
$N_{H/H}$ = 0 N_C = 8 DMY

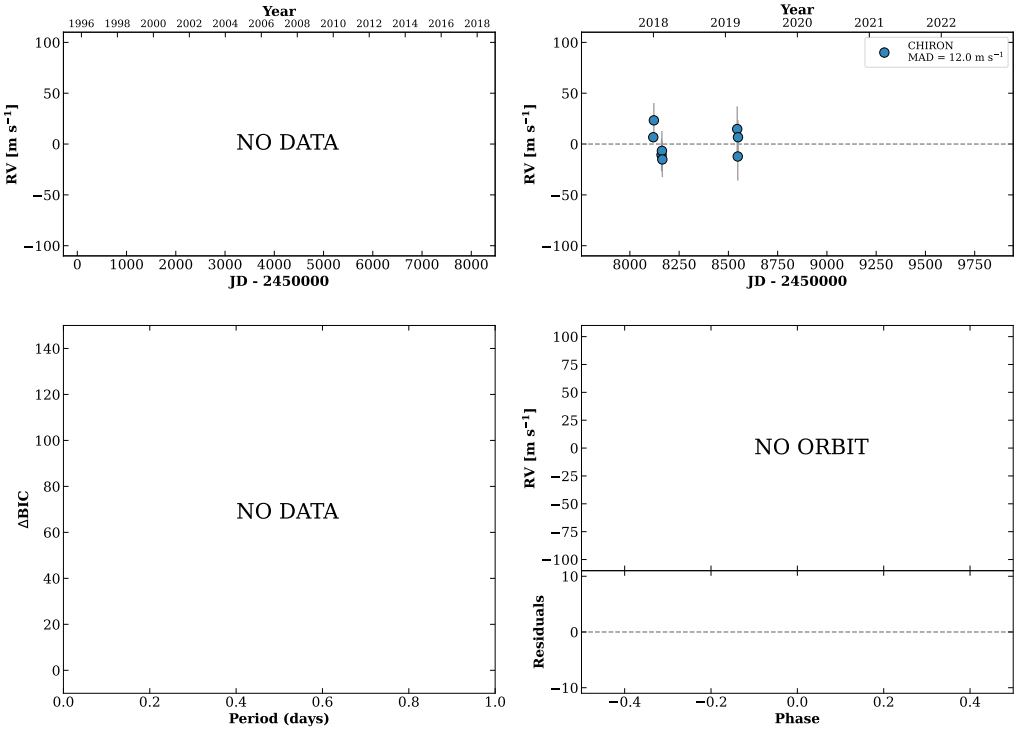

Figure 167 RV results for RKS1004-1143 (top) and RKS1005+2629 (bottom).

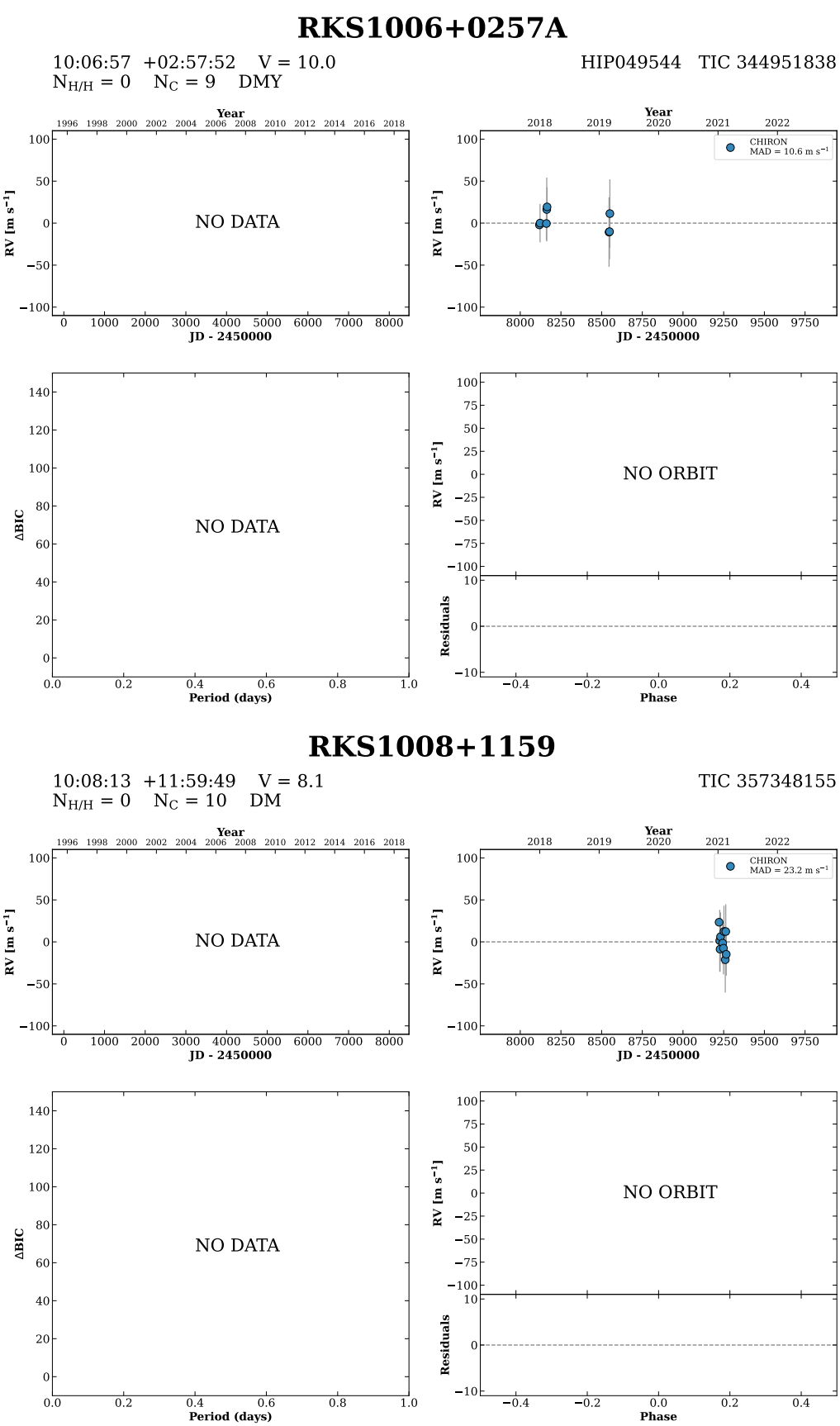

Figure 168 RV results for RKS1006+0257A (top) and RKS1008+1159 (bottom).

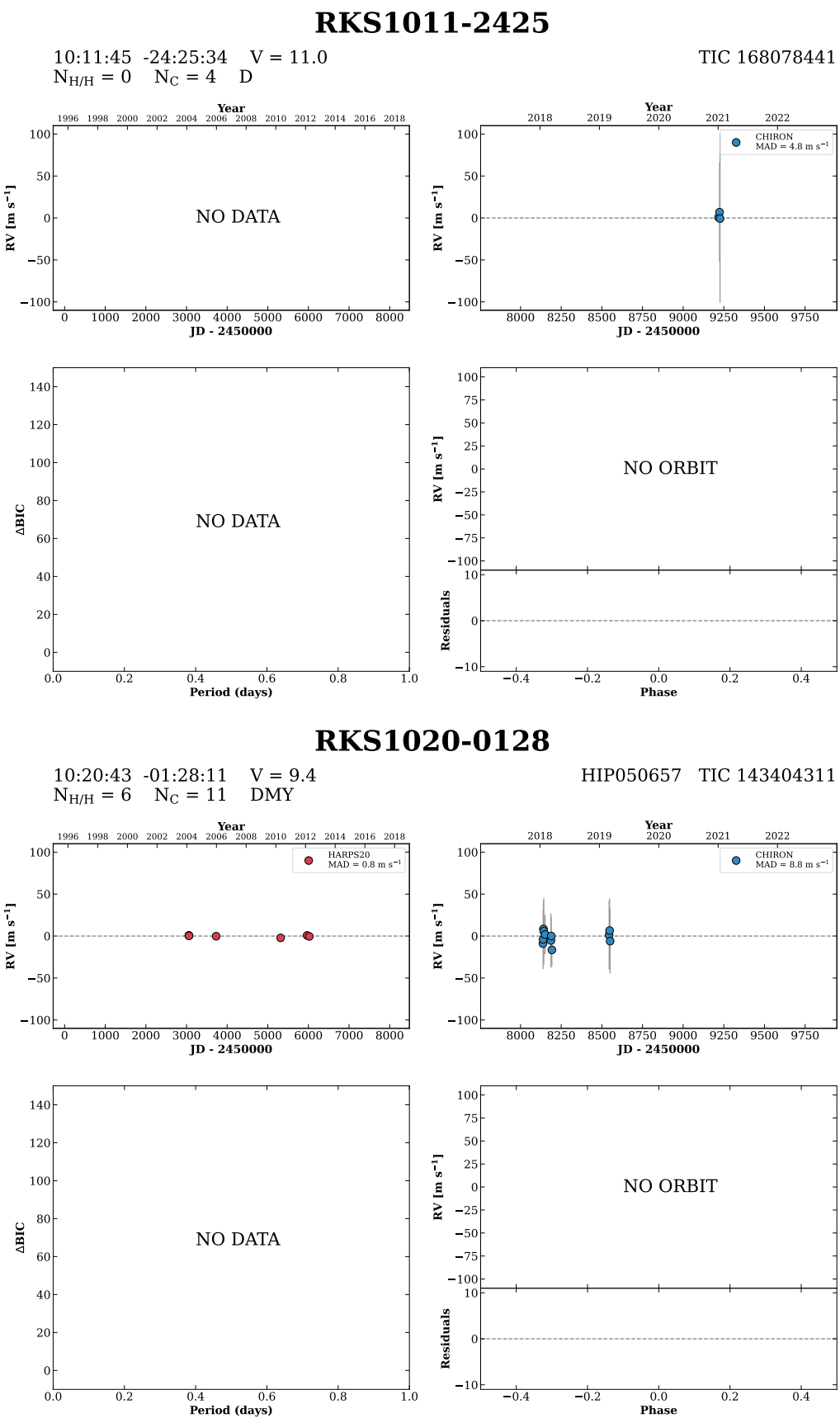

Figure 169 RV results for RKS1011-2425 (top) and RKS1020-0128 (bottom).

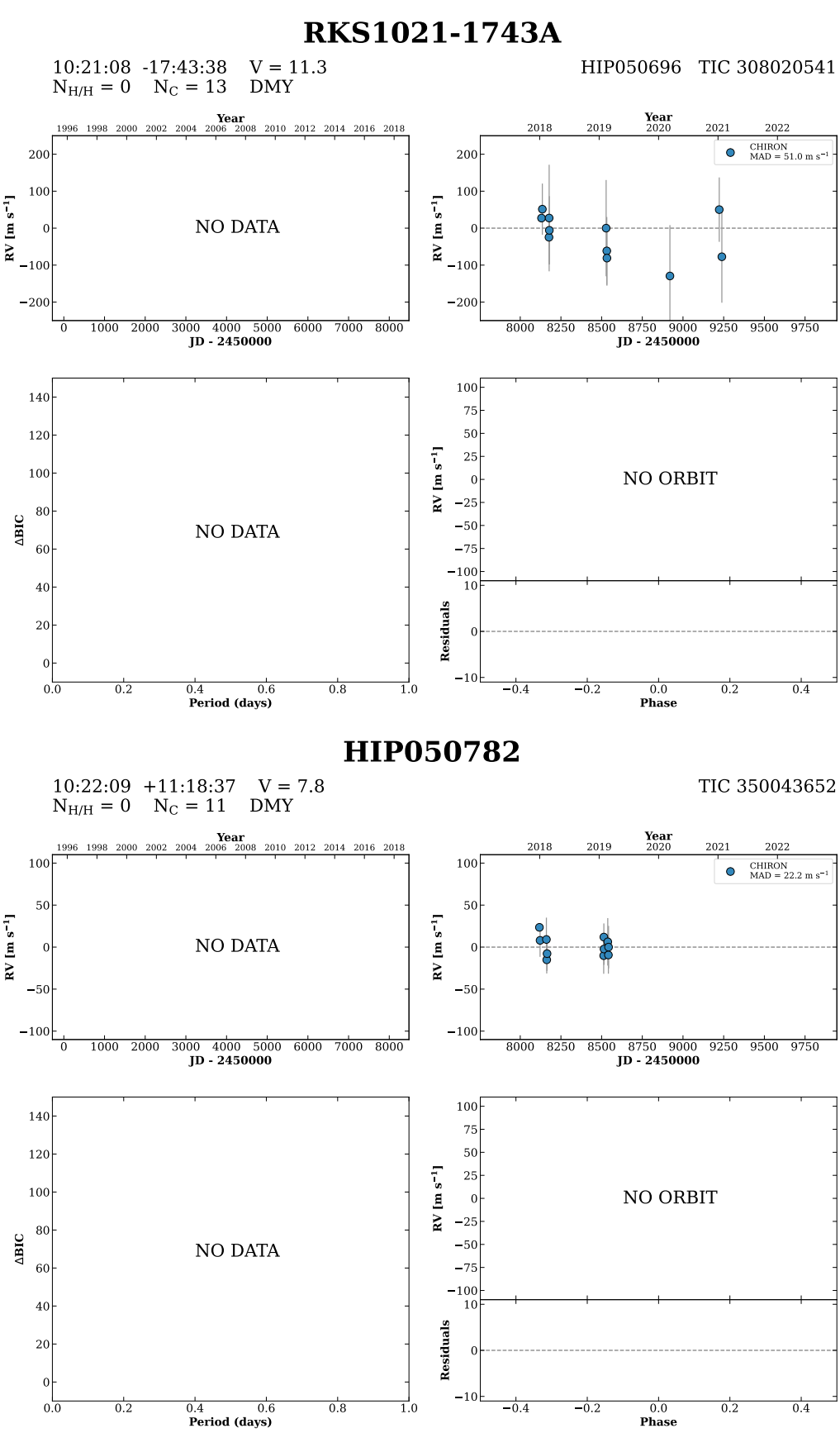

Figure 170 RV results for RKS1021-1743A (top) and HIP050782 (bottom).

RKS1024-1024

10:24:15 -10:24:21 V = 10.0 HIP050944 TIC 36841797
$N_{H/H}$ = 16 N_C = 1

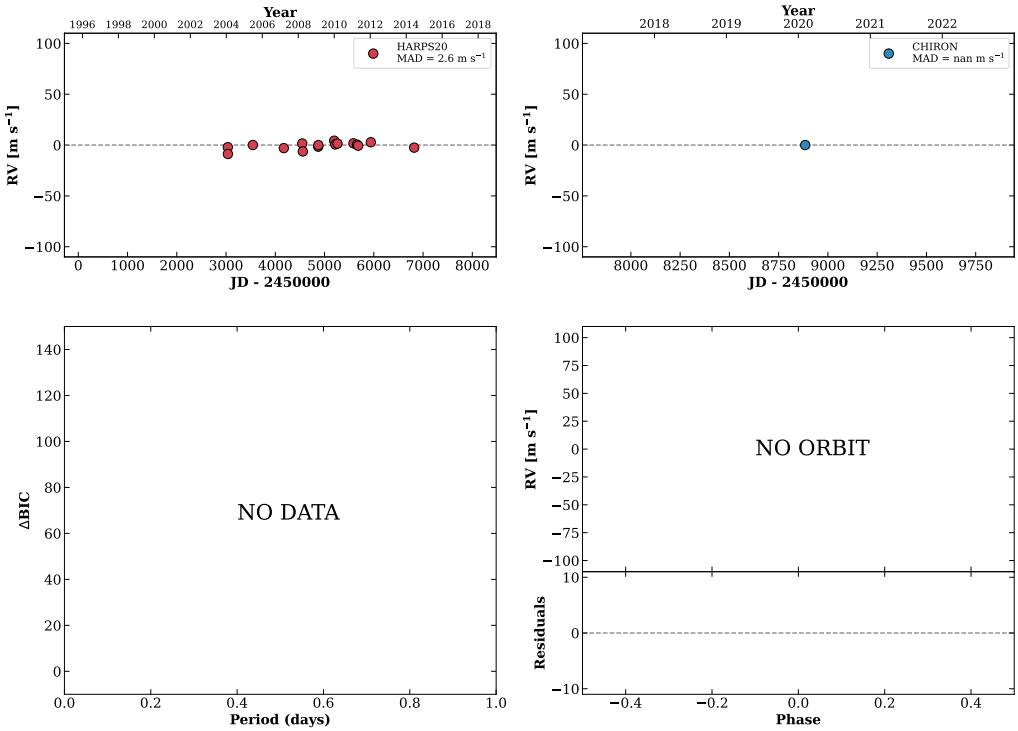

RKS1026-0631

10:26:41 -06:31:35 V = 9.8 HIP051127 TIC 36892736
$N_{H/H}$ = 0 N_C = 34 DMY

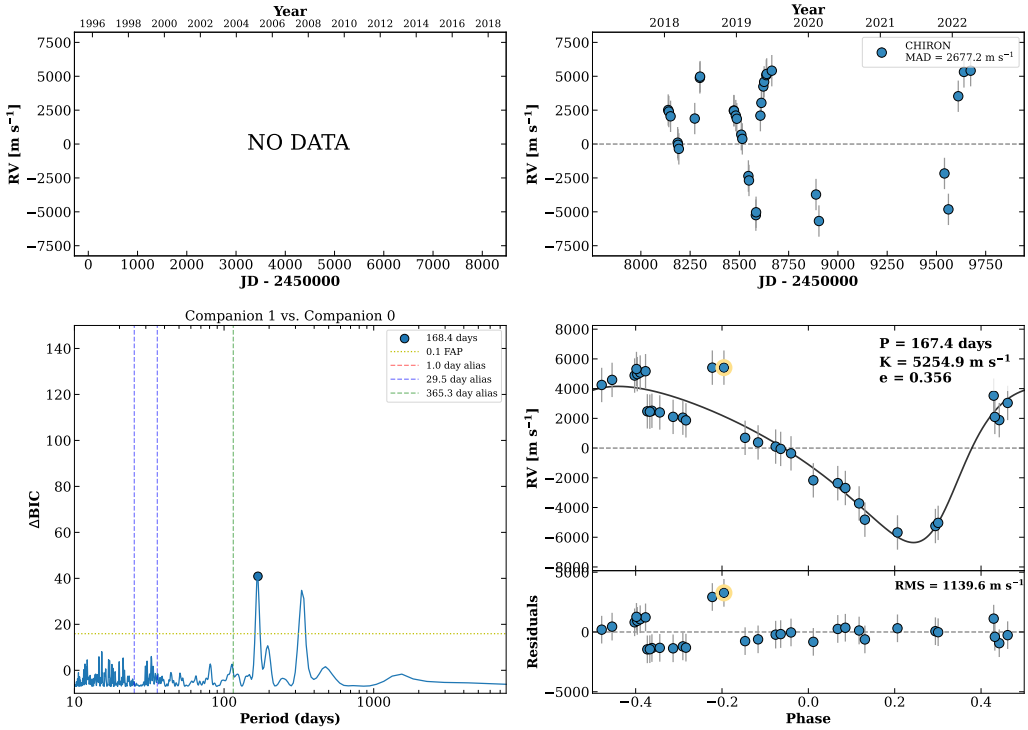

Figure 171 RV results for RKS1024-1024 (top) and RKS1026-0631 (bottom).

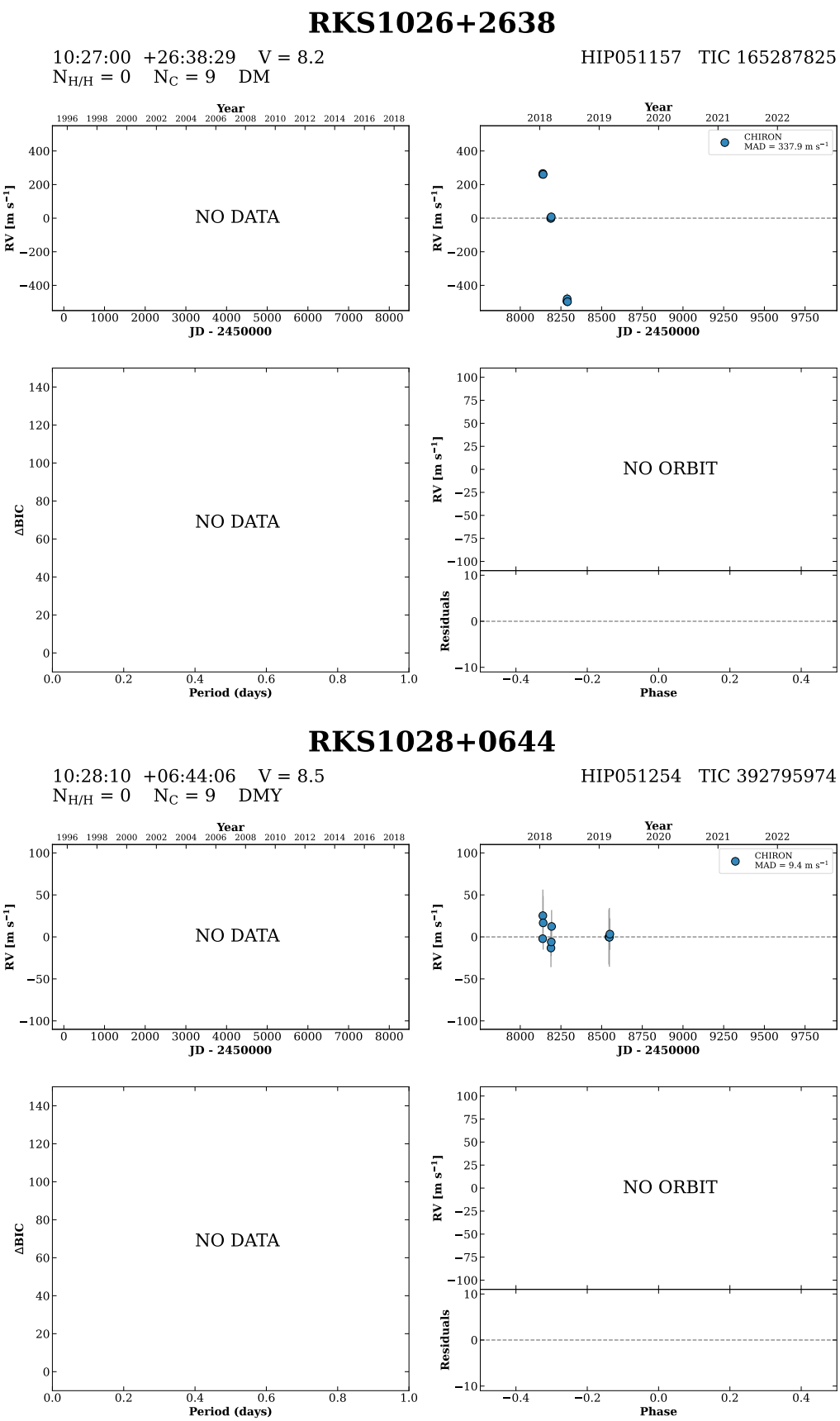

Figure 172 RV results for RKS1026+2638 (top) and RKS1028+0644 (bottom).

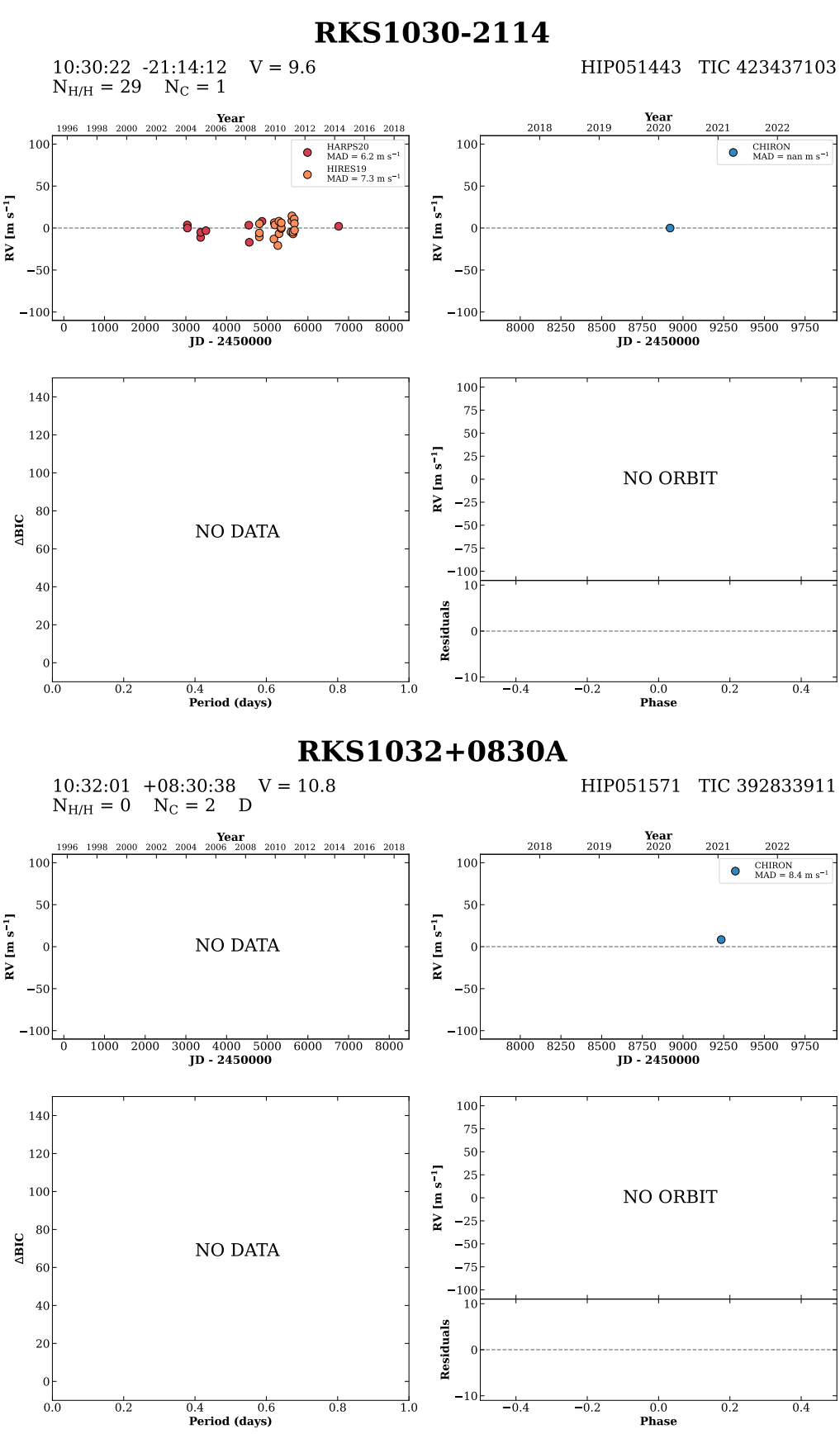

Figure 173 RV results for RKS1030-2114 (top) and RKS1032+0830A (bottom).

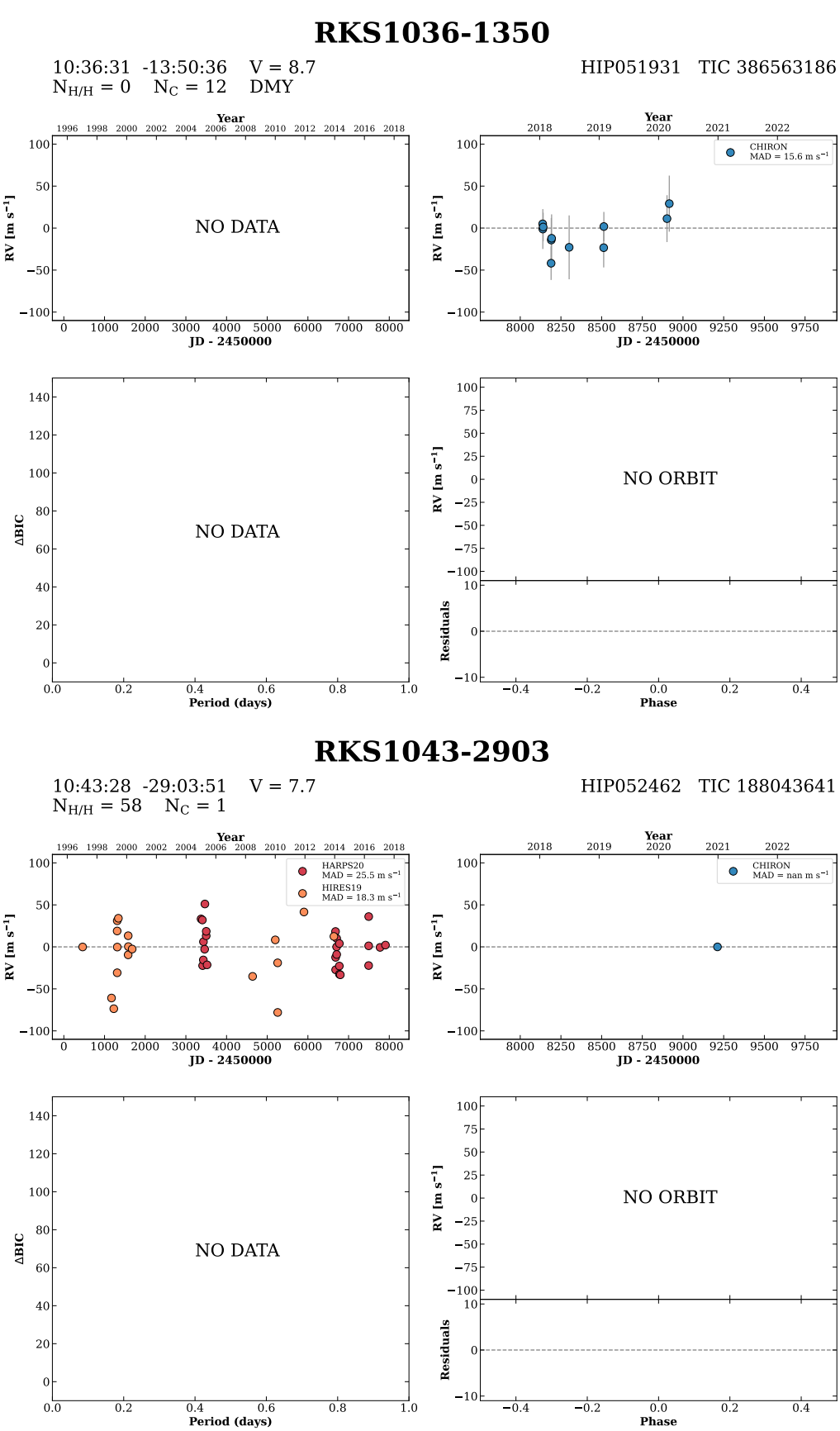

Figure 174 RV results for RKS1036-1350 (top) and RKS1043-2903 (bottom).

RKS1046-2435

10:46:37 -24:35:08 V = 9.4 HIP052708 TIC 188087957
$N_{H/H}$ = 5 N_C = 9 DMY

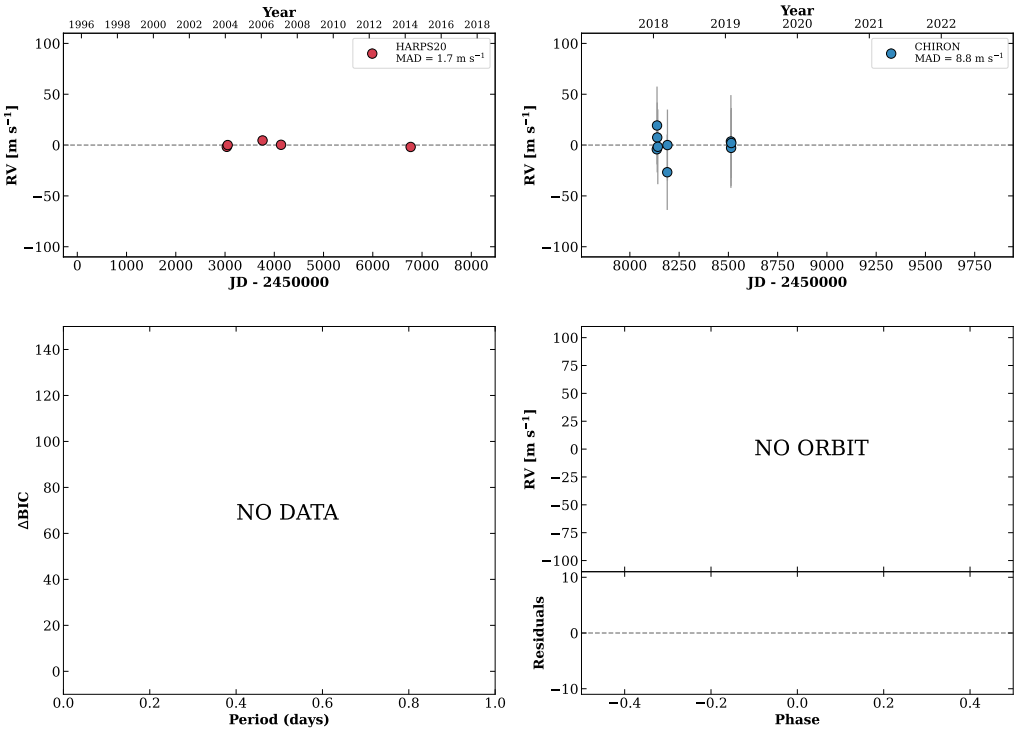

RKS1047+2129

10:47:19 +21:29:51 V = 10.1 HIP052765 TIC 95836951
$N_{H/H}$ = 0 N_C = 7 DMY

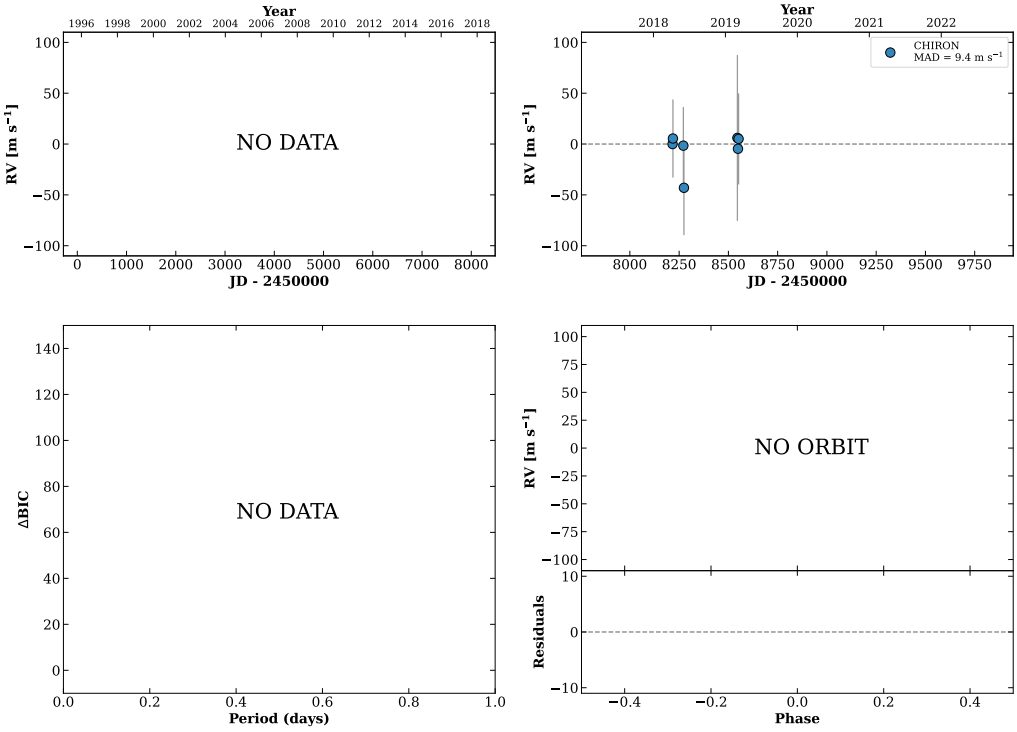

Figure 175 RV results for RKS1046-2435 (top) and RKS1047+2129 (bottom).

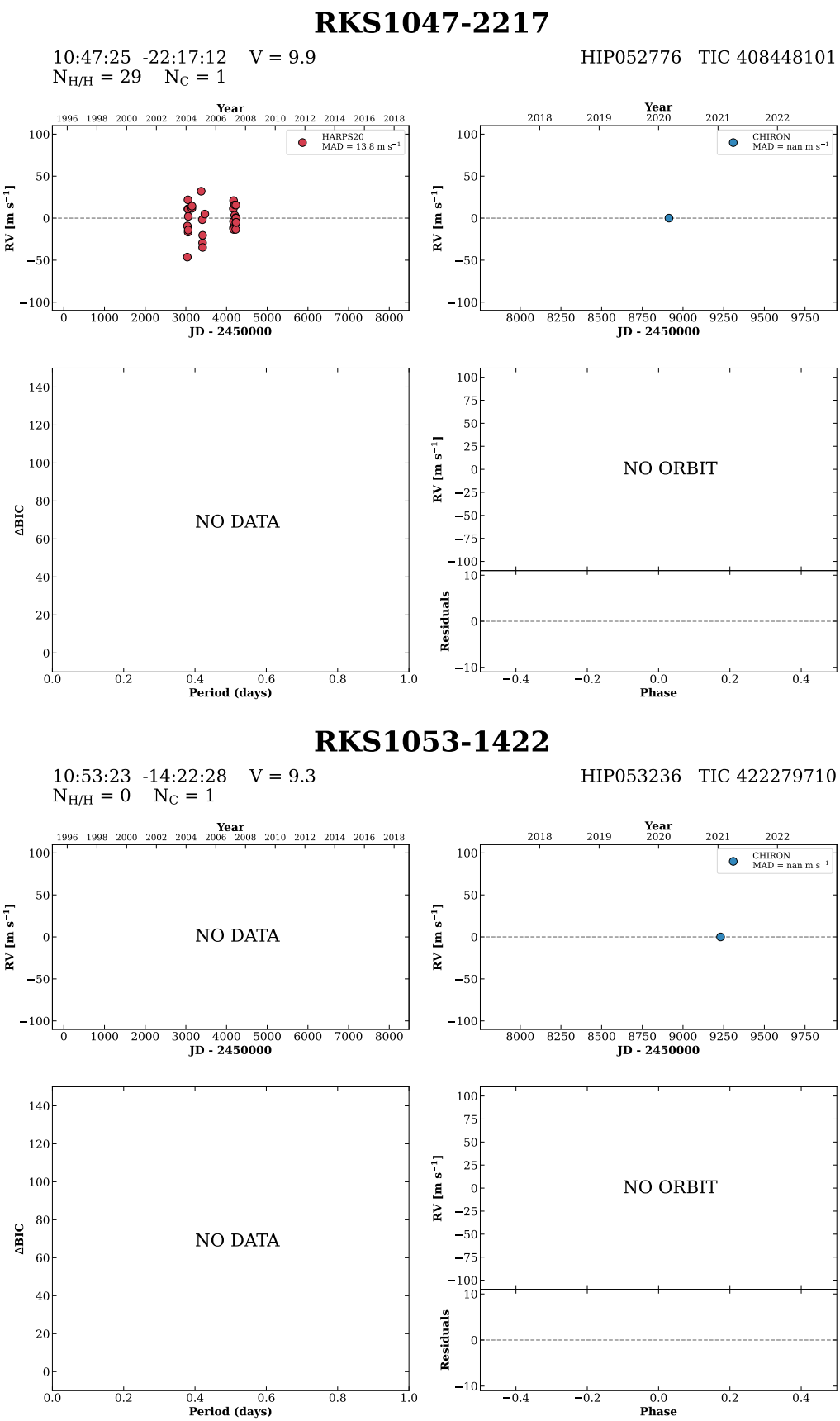

Figure 176 RV results for RKS1047-2217 (top) and RKS1053-1422 (bottom).

RKS1054-0432

10:54:49 -04:32:31 V = 10.4 TIC 14343469
$N_{H/H}$ = 0 N_C = 3 DM

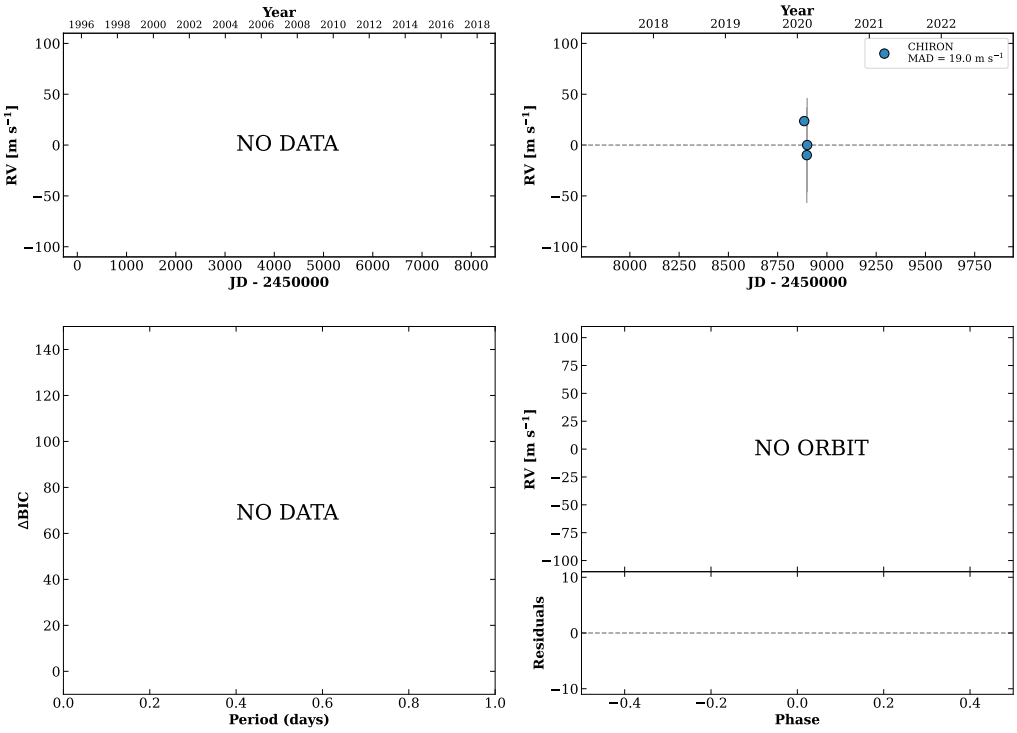

RKS1056+0723

10:56:31 +07:23:19 V = 7.4 HIP053486 TIC 365006720
$N_{H/H}$ = 6 N_C = 9 DMY

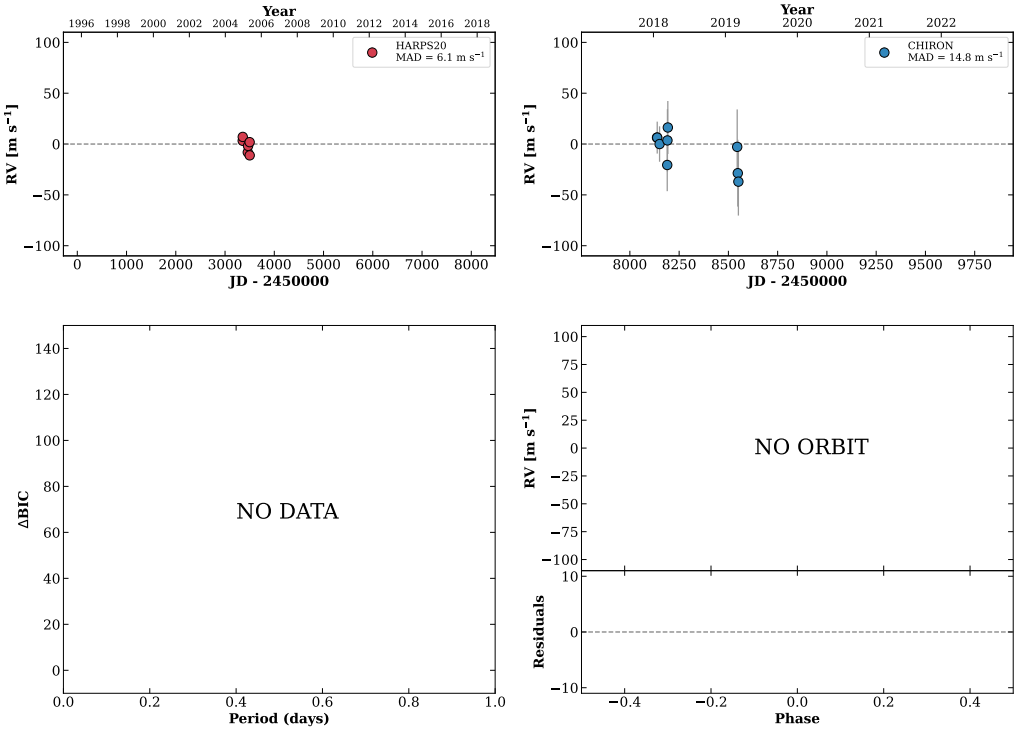

Figure 177 RV results for RKS1054-0432 (top) and RKS1056+0723 (bottom).

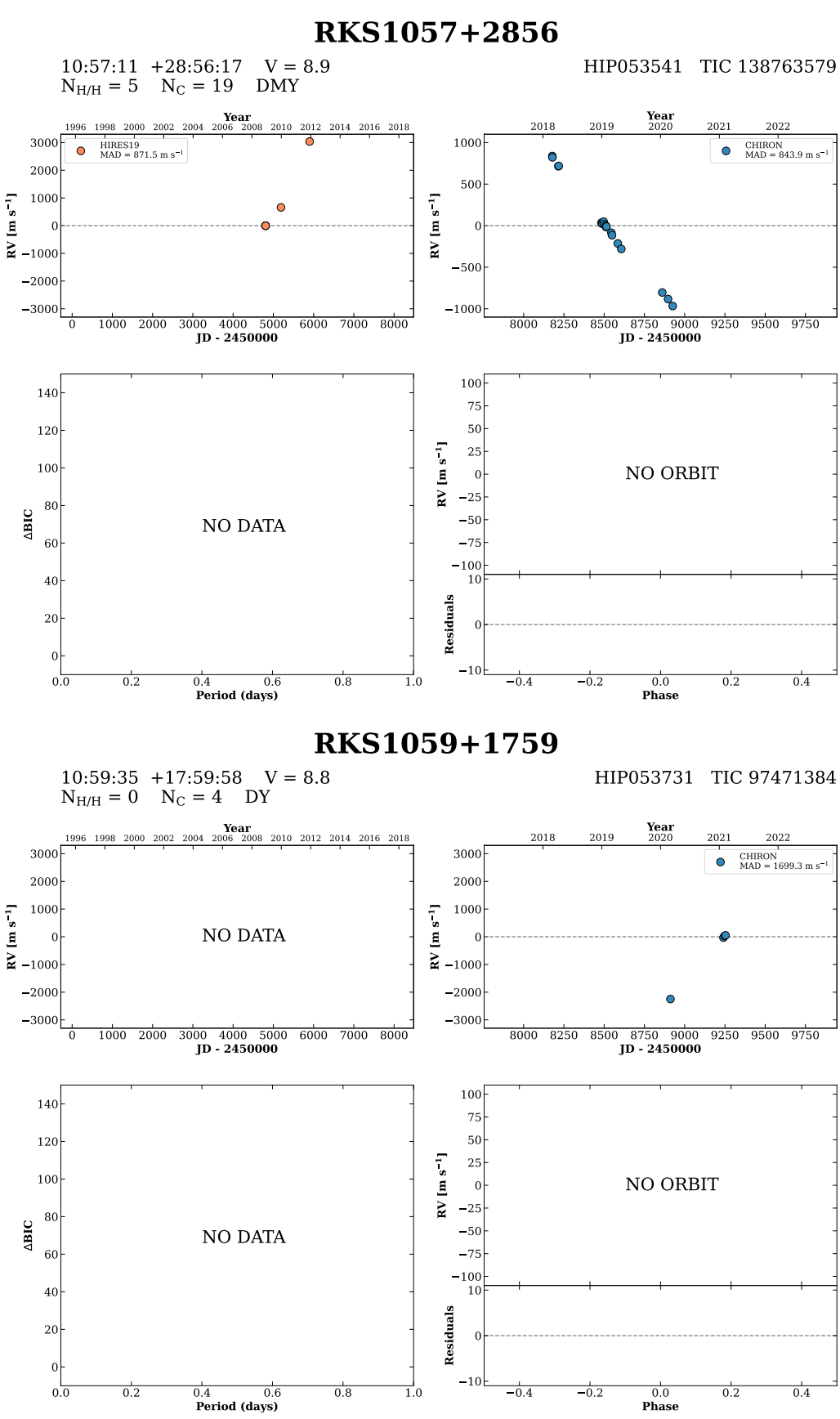

Figure 178 RV results for RKS1057+2856 (top) and RKS1059+1759 (bottom).

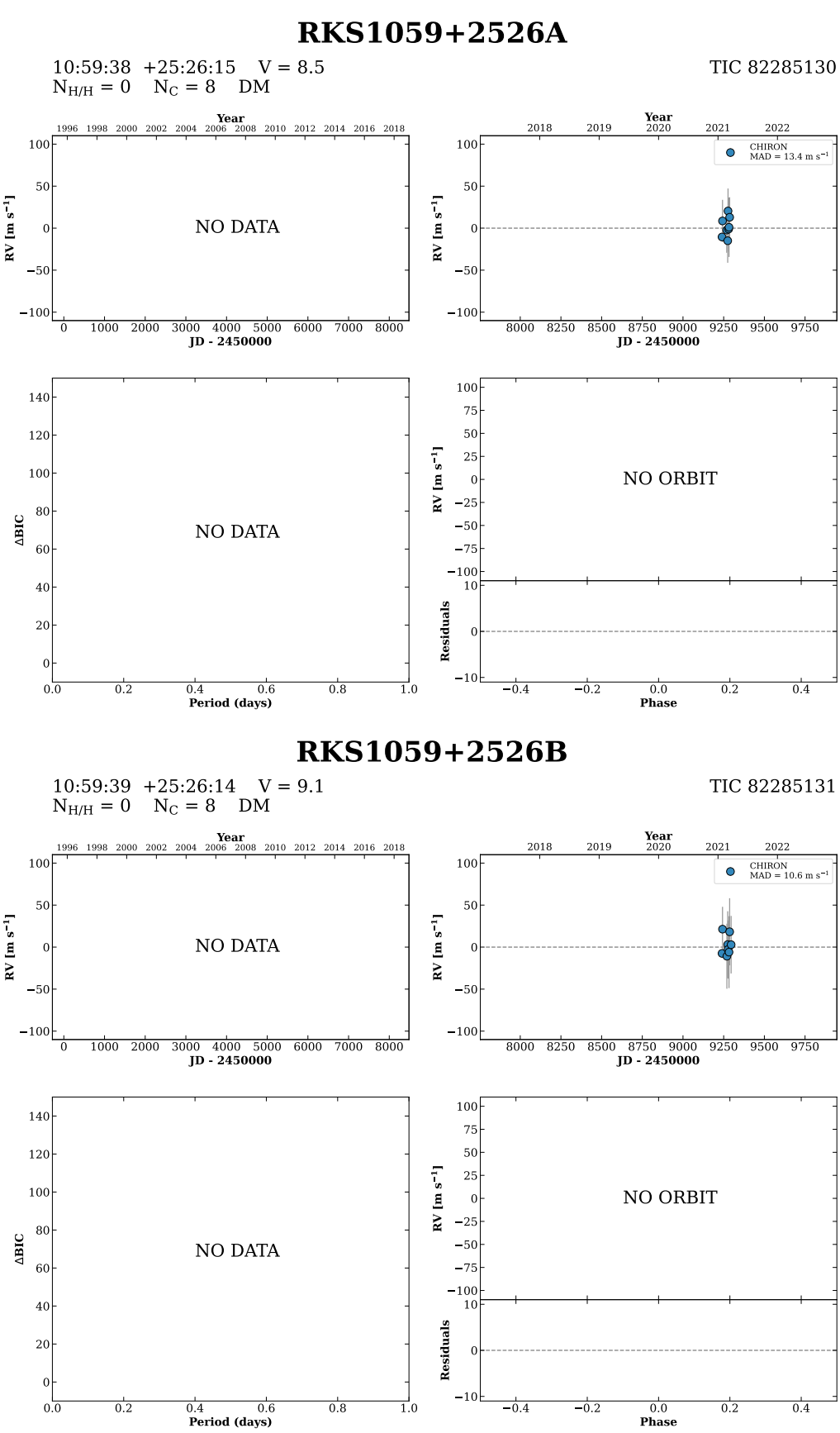

Figure 179 RV results for RKS1059+2526A (top) and RKS1059+2526B (bottom).

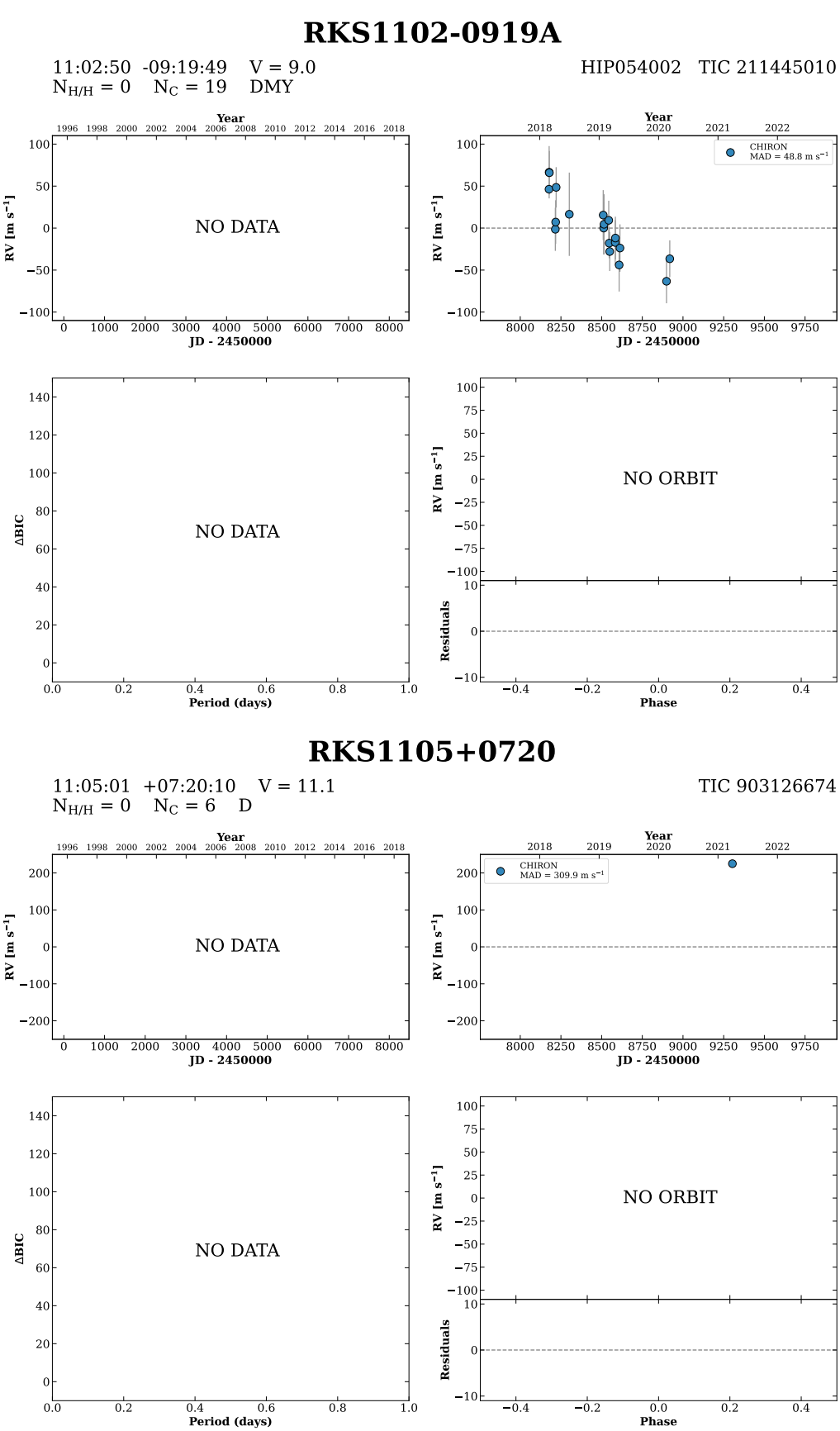

Figure 180 RV results for RKS1102-0919A (top) and RKS1105+0720 (bottom).

RKS1108-2816A

11:08:06 -28:16:05 V = 9.3 HIP054418 TIC 168453014
$N_{H/H}$ = 6 N_C = 29 DMY

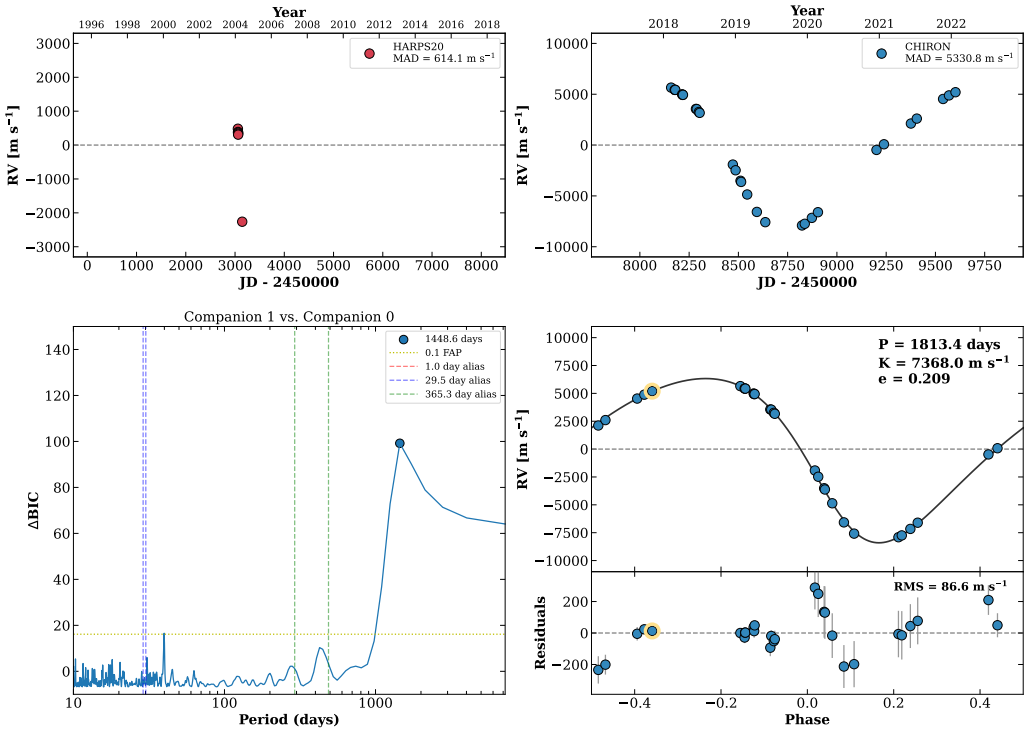

RKS1108+1546

11:08:32 +15:46:03 V = 9.8 HIP054459 TIC 77109256
$N_{H/H}$ = 12 N_C = 1

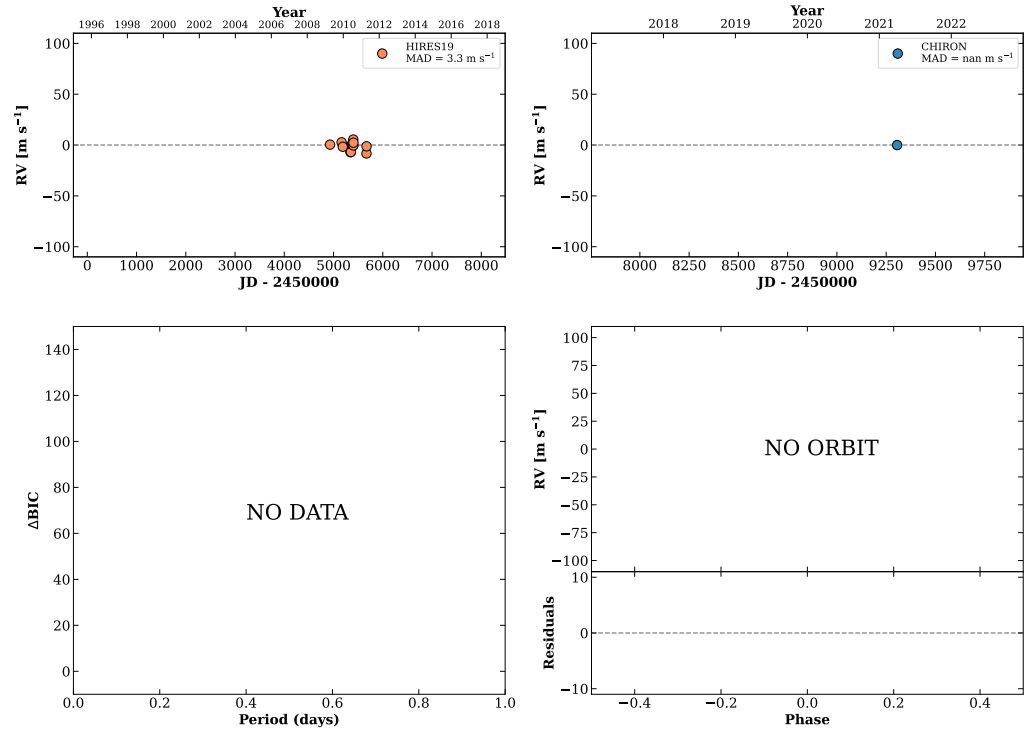

Figure 181 RV results for RKS1108-2816A (top) and RKS1108+1546 (bottom).

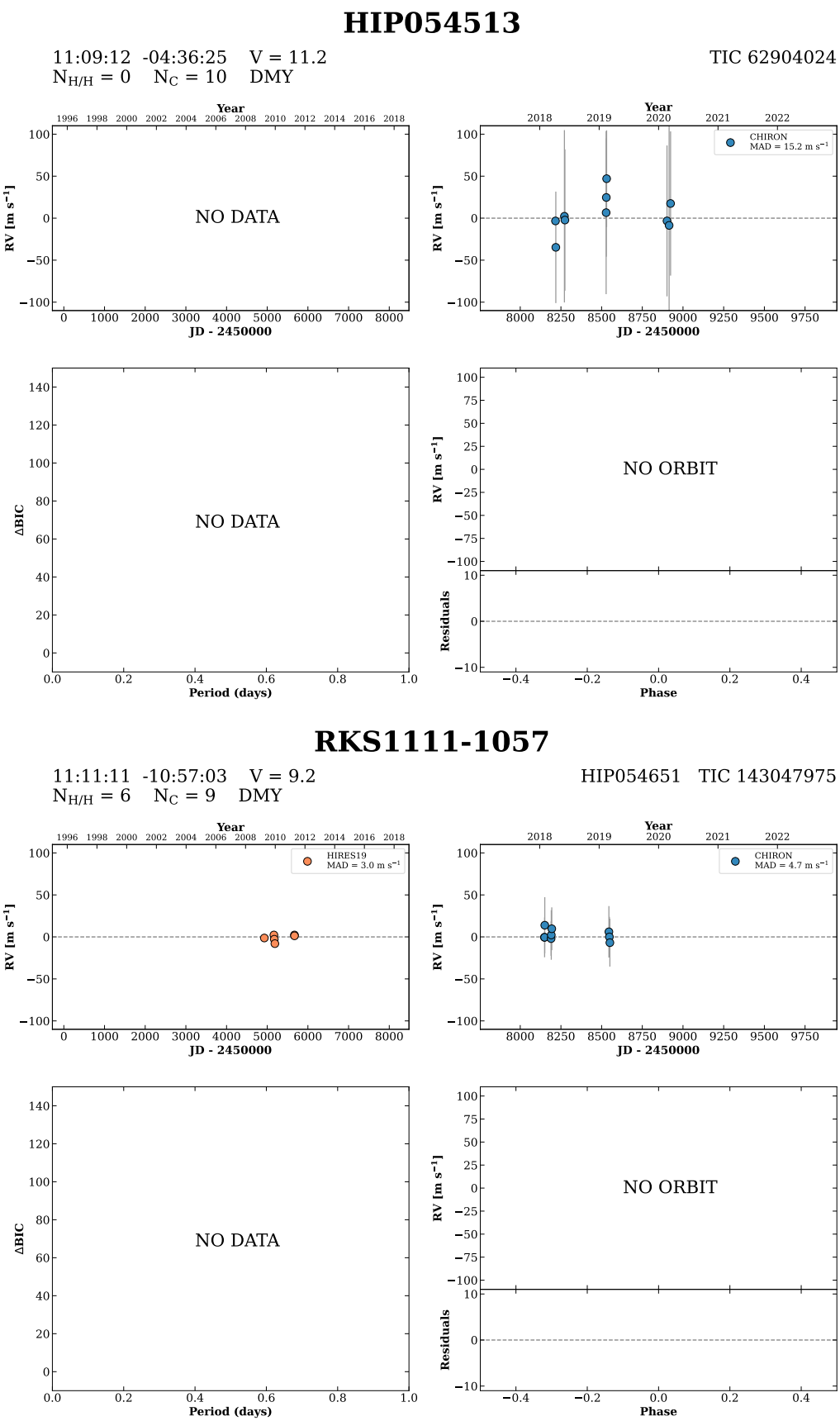

Figure 182 RV results for HIP054513 (top) and RKS1111-1057 (bottom).

RKS1111-1459A

11:11:33 -14:59:29 V = 9.1 HIP054677 TIC 308076910
$N_{H/H}$ = 0 N_C = 26 DMY

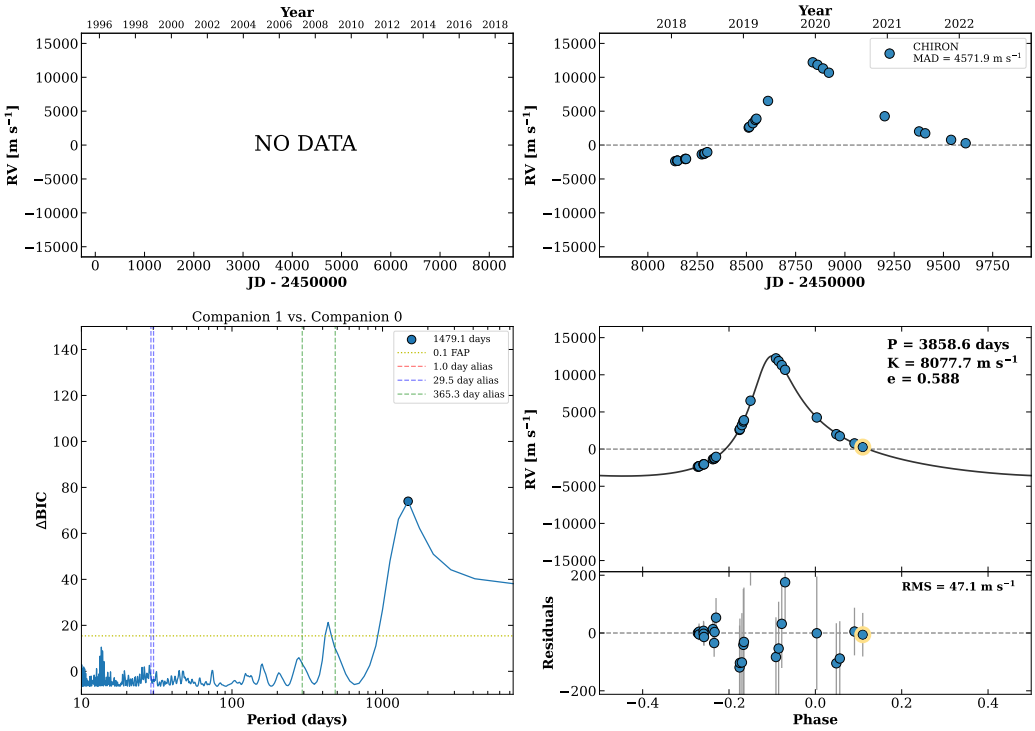

HIP054803

11:13:10 +00:14:17 V = 10.3 TIC 425283213
$N_{H/H}$ = 0 N_C = 10 DMY

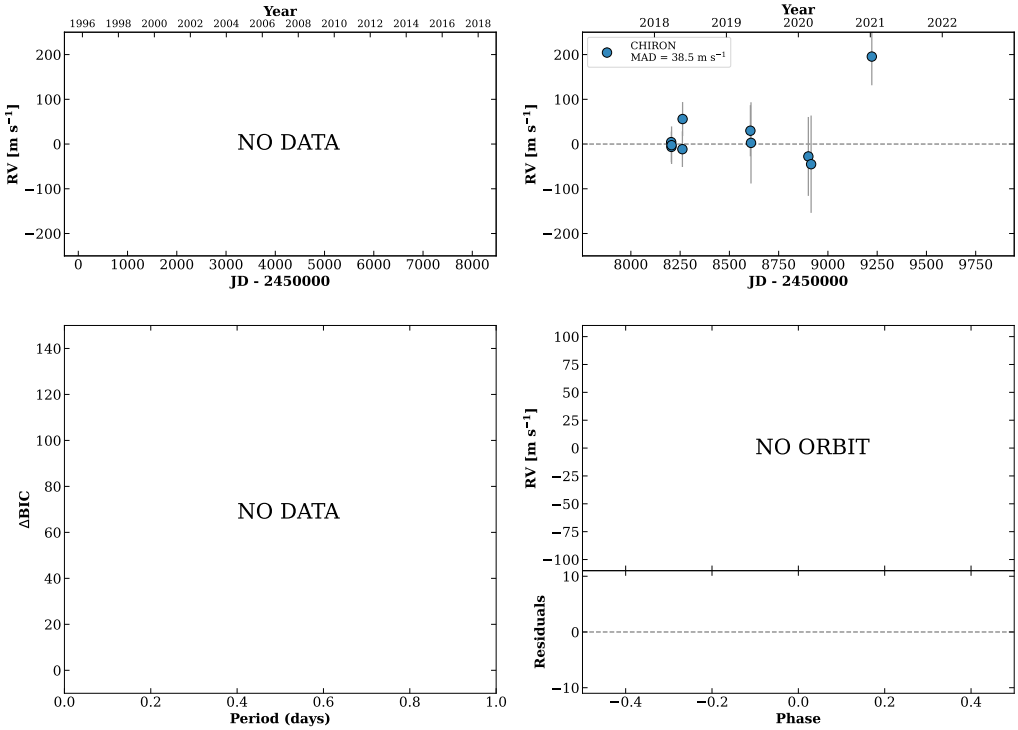

Figure 183 RV results for RKS1111-1459A (top) and HIP054803 (bottom).

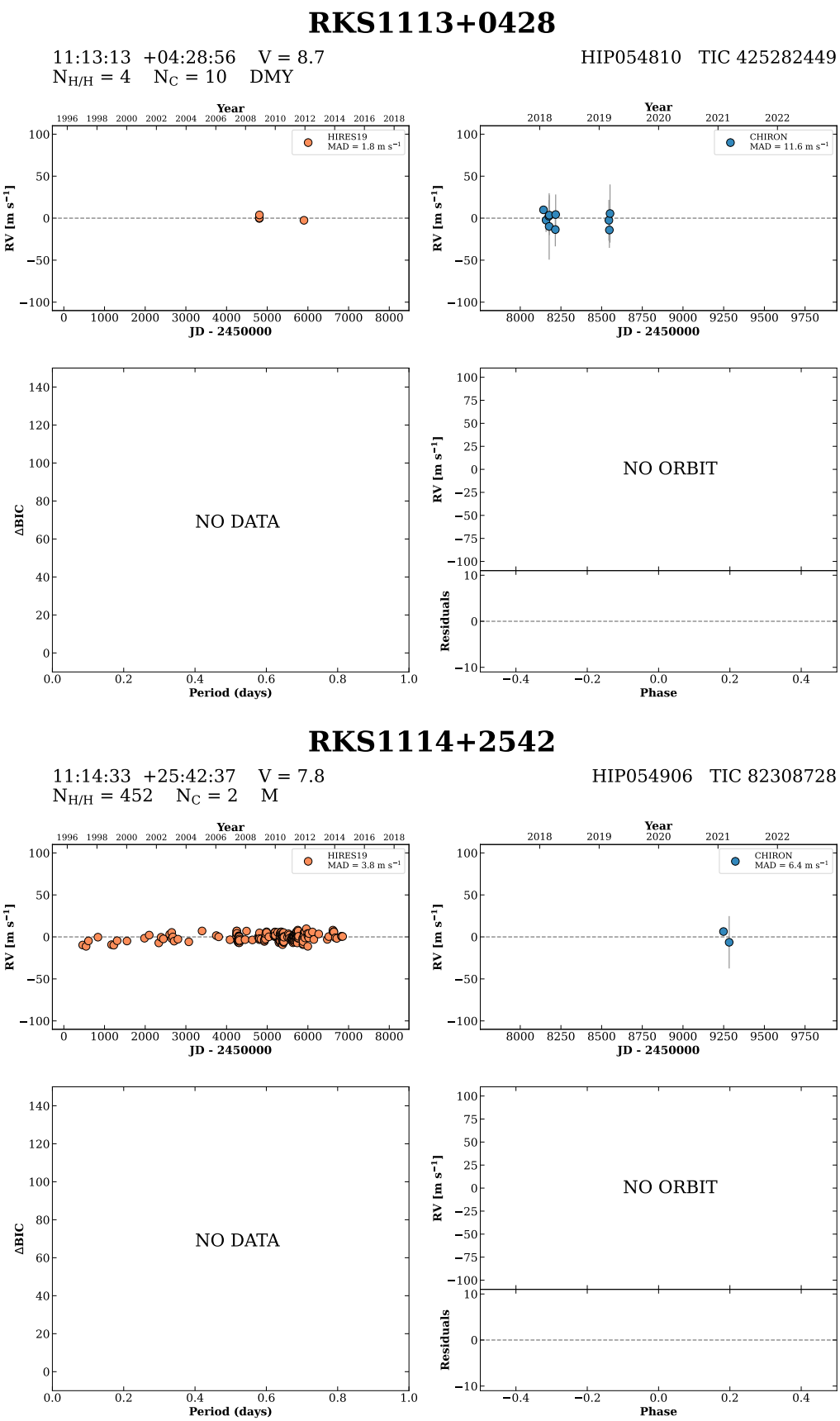

Figure 184 RV results for RKS1113+0428 (top) and RKS1114+2542 (bottom).

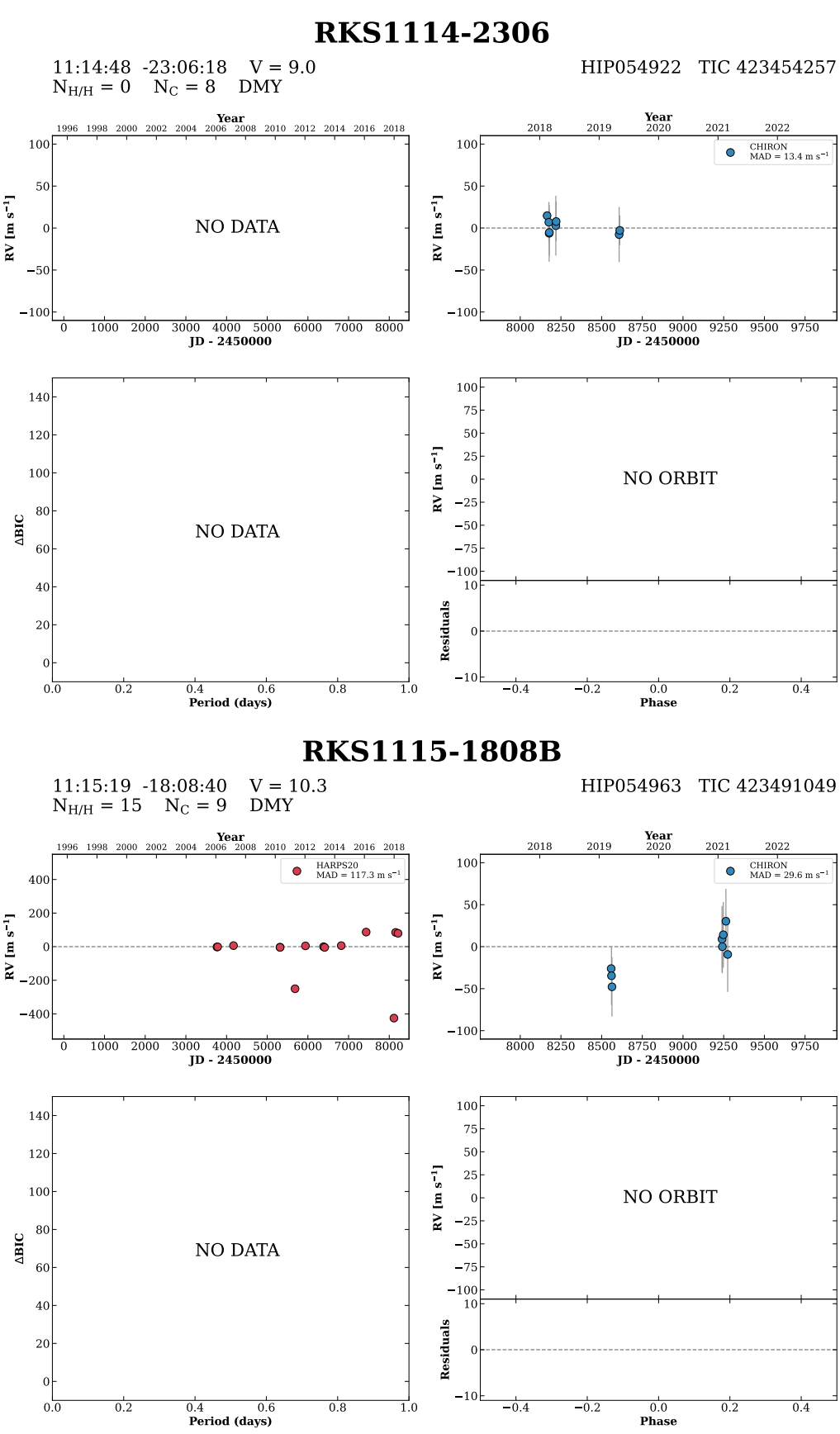

Figure 185 RV results for RKS1114-2306 (top) and RKS1115-1808B (bottom).

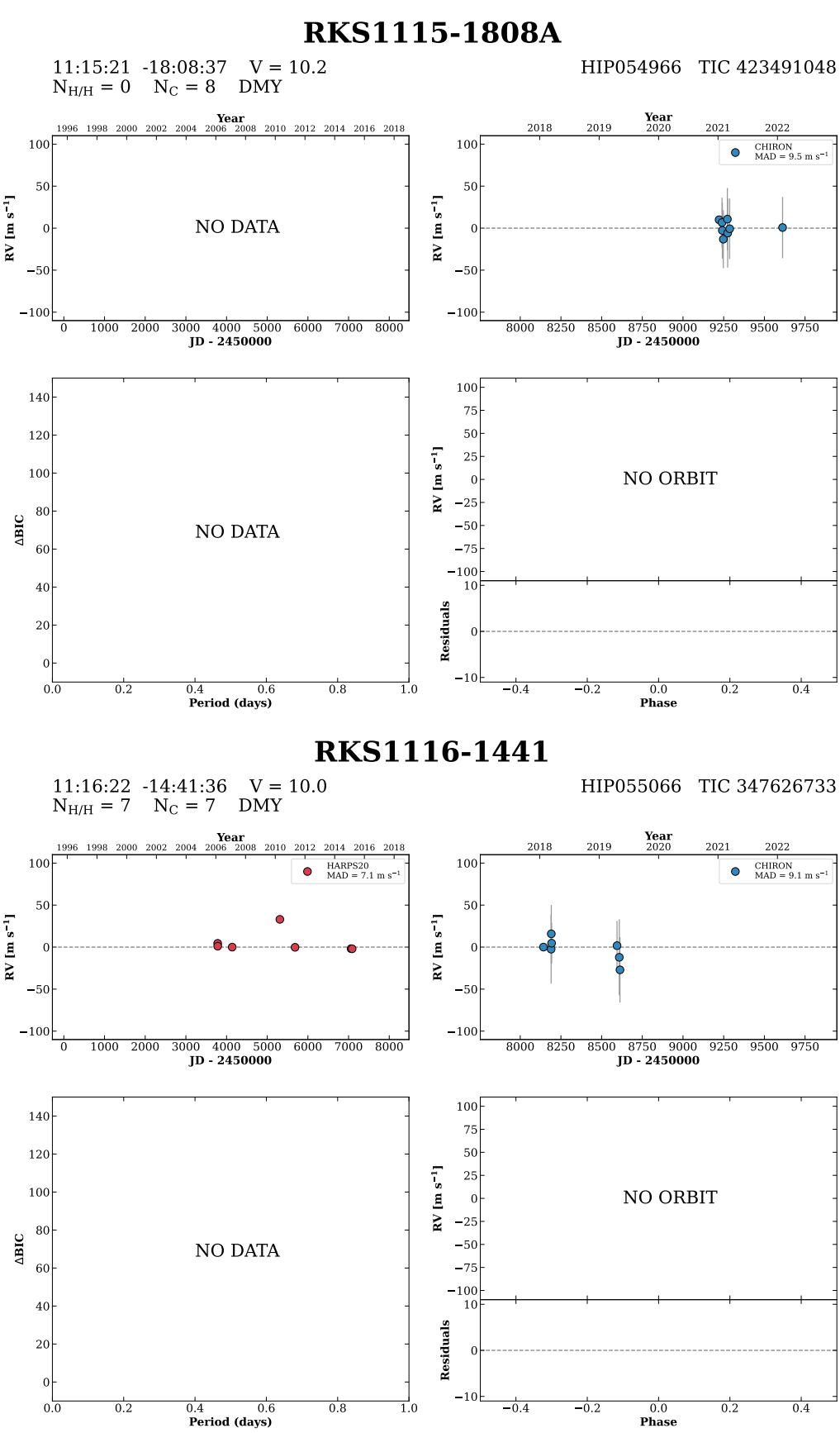

Figure 186 RV results for RKS1115-1808A (top) and RKS1116-1441 (bottom).

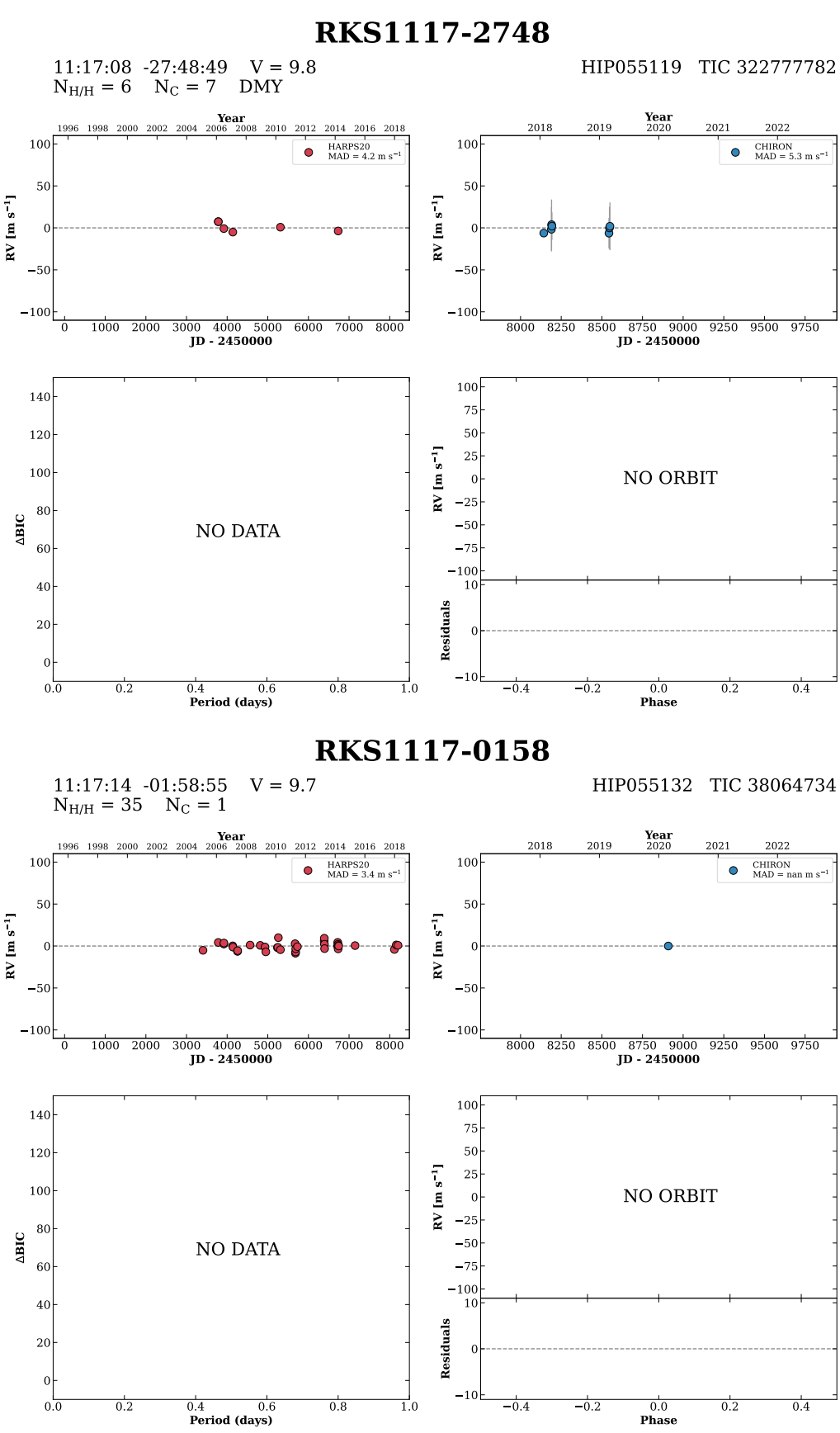

Figure 187 RV results for RKS1117-2748 (top) and RKS1117-0158 (bottom).

RKS1121-2027

11:21:27 -20:27:14 V = 8.6 HIP055454 TIC 437261156
$N_{H/H}$ = 0 N_C = 22 DMY

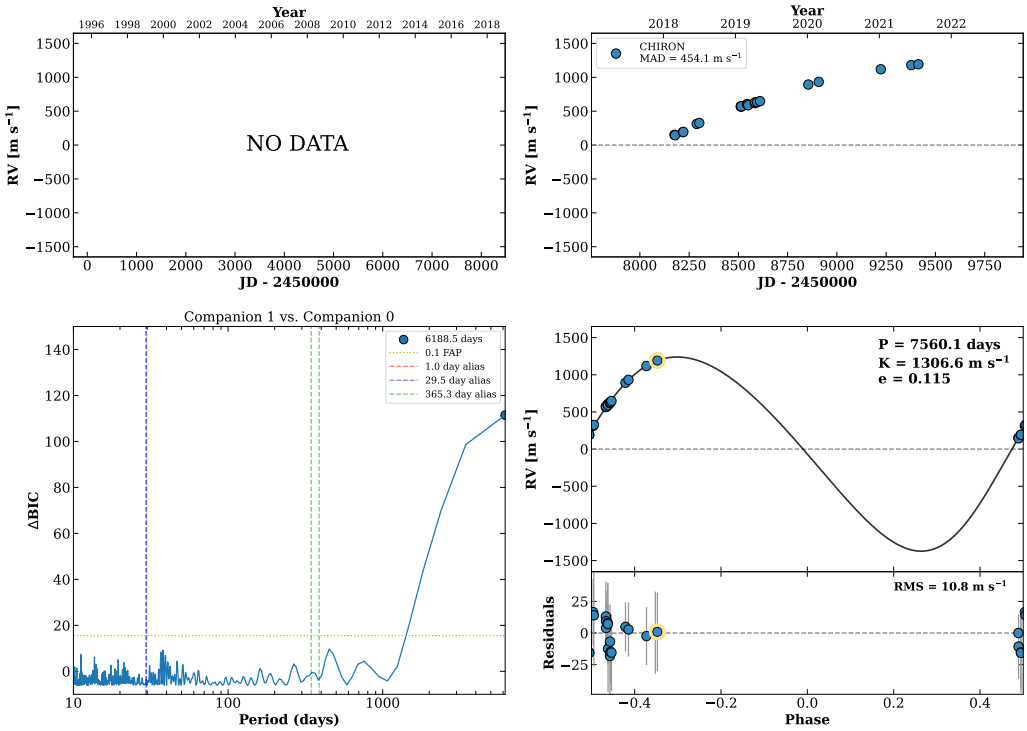

RKS1121+1811

11:21:49 +18:11:24 V = 7.9 HIP055486 TIC 3819571
$N_{H/H}$ = 7 N_C = 1

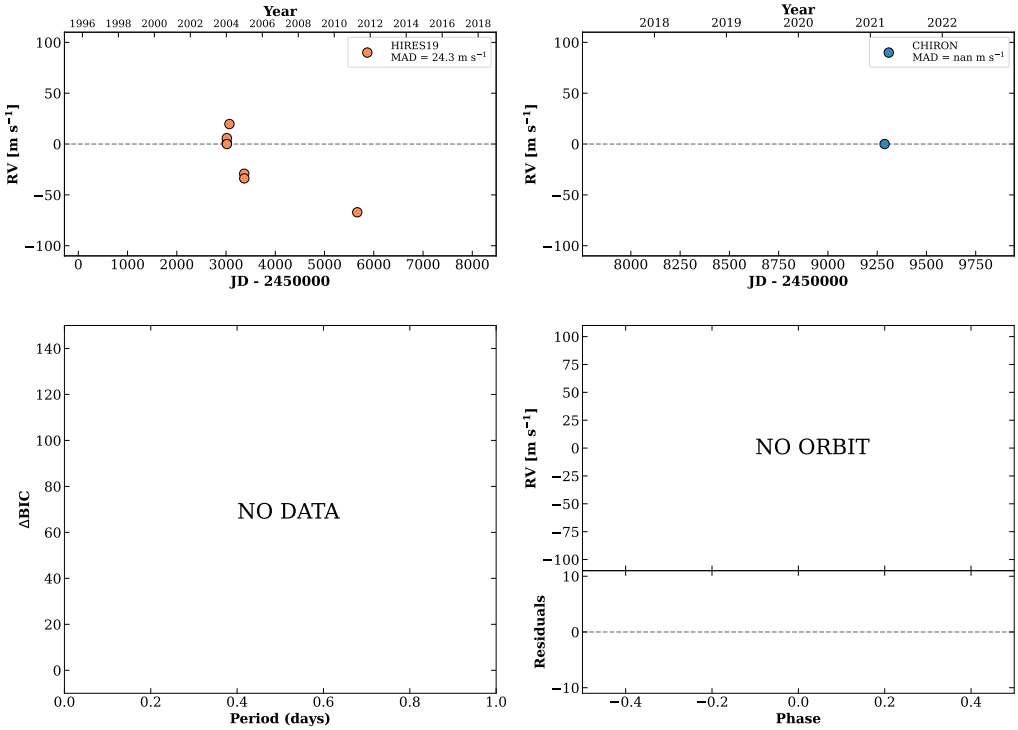

Figure 188 RV results for RKS1121-2027 (top) and RKS1121+1811 (bottom).

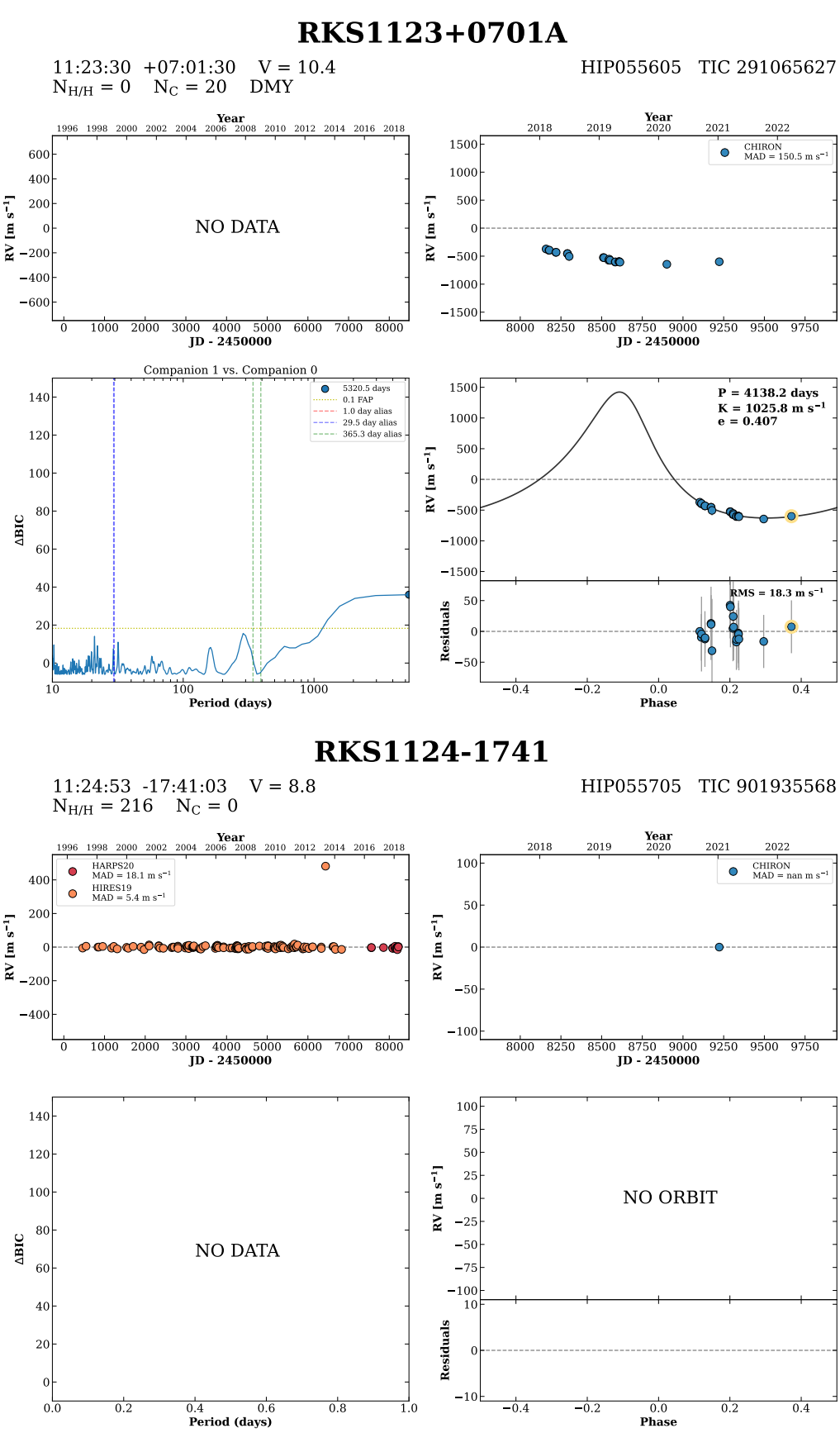

Figure 189 RV results for RKS1123+0701A (top) and RKS1124-1741 (bottom).

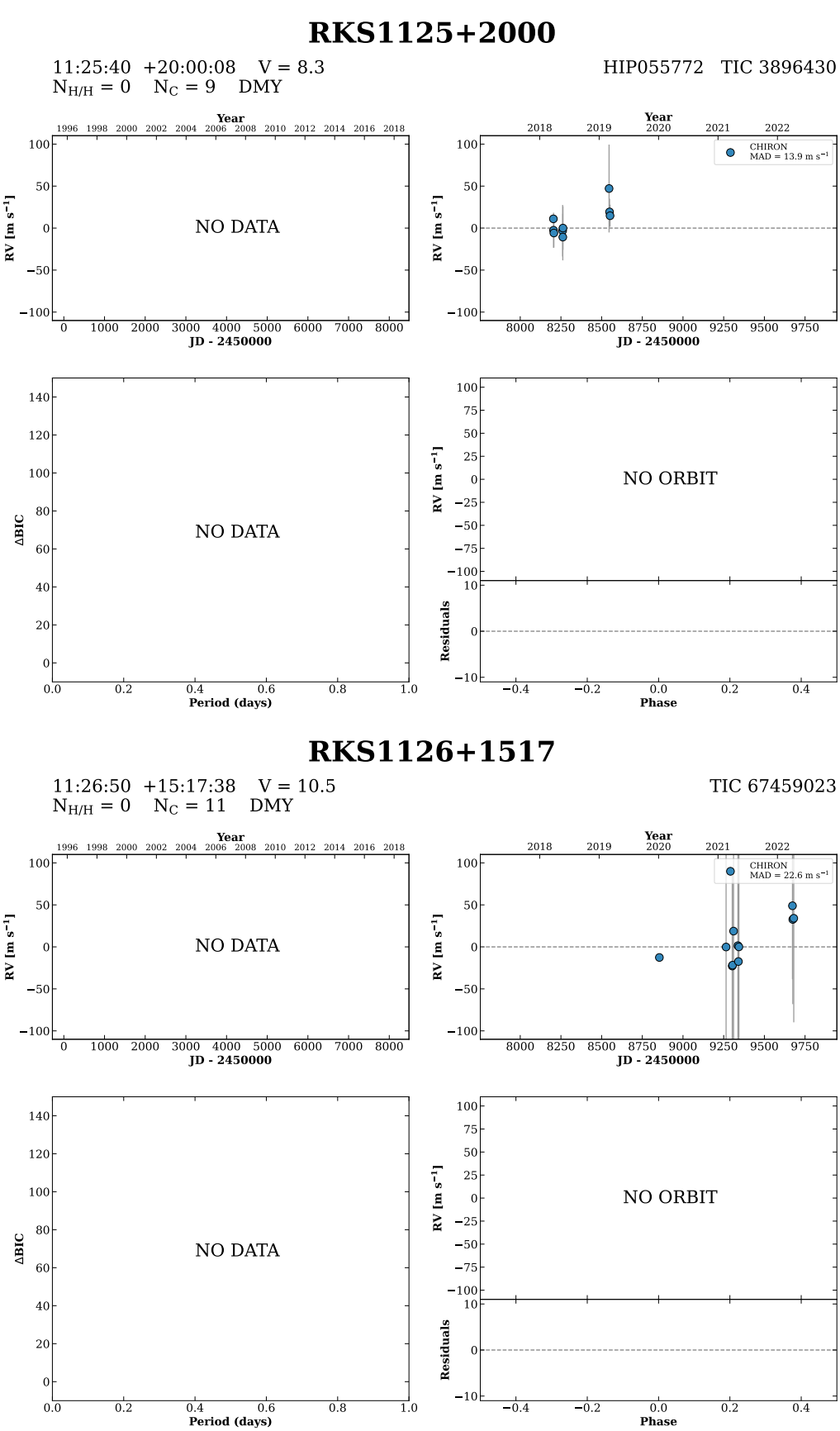

Figure 190 RV results for RKS1125+2000 (top) and RKS1126+1517 (bottom).

RKS1127+0358A

11:27:39 +03:58:36 V = 10.6 HIP055915 TIC 363570744
$N_{H/H}$ = 4 N_C = 17 DMY

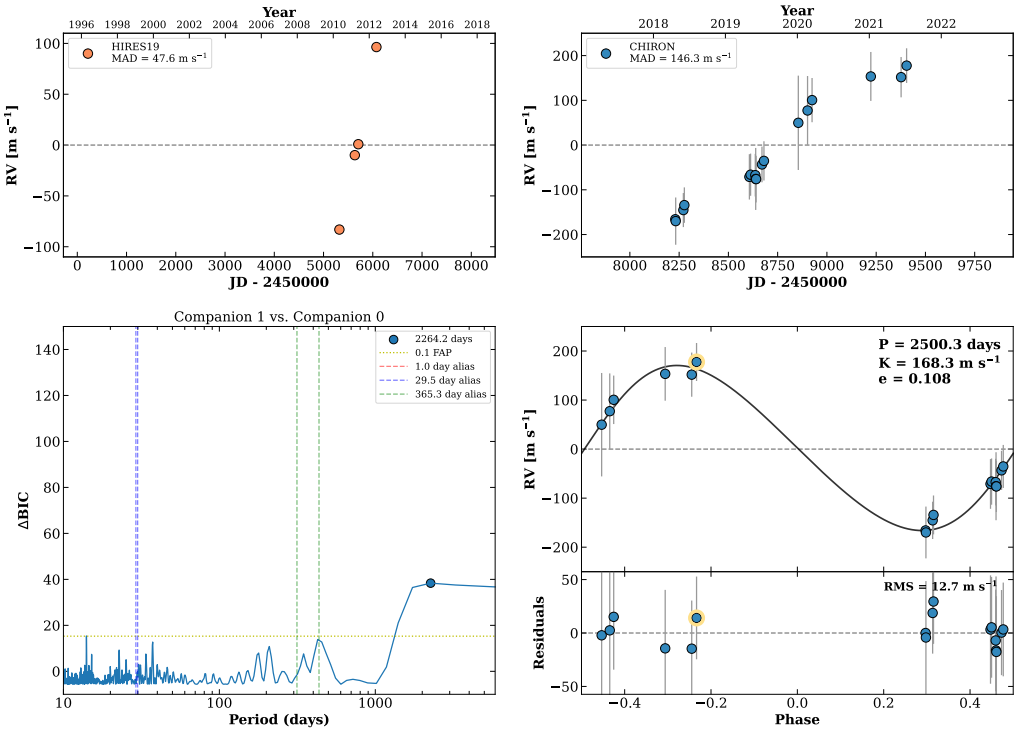

RKS1128+0731

11:28:28 +07:31:02 V = 10.2 HIP055988 TIC 388799527
$N_{H/H}$ = 0 N_C = 9 DMY

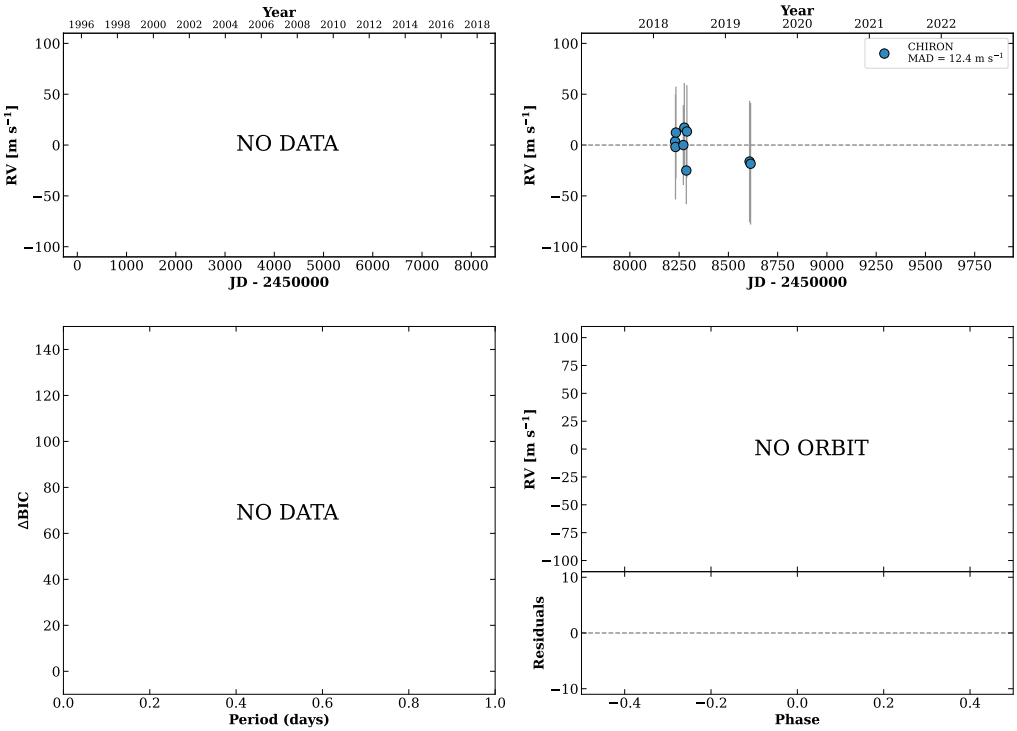

Figure 191 RV results for RKS1127+0358A (top) and RKS1128+0731 (bottom).

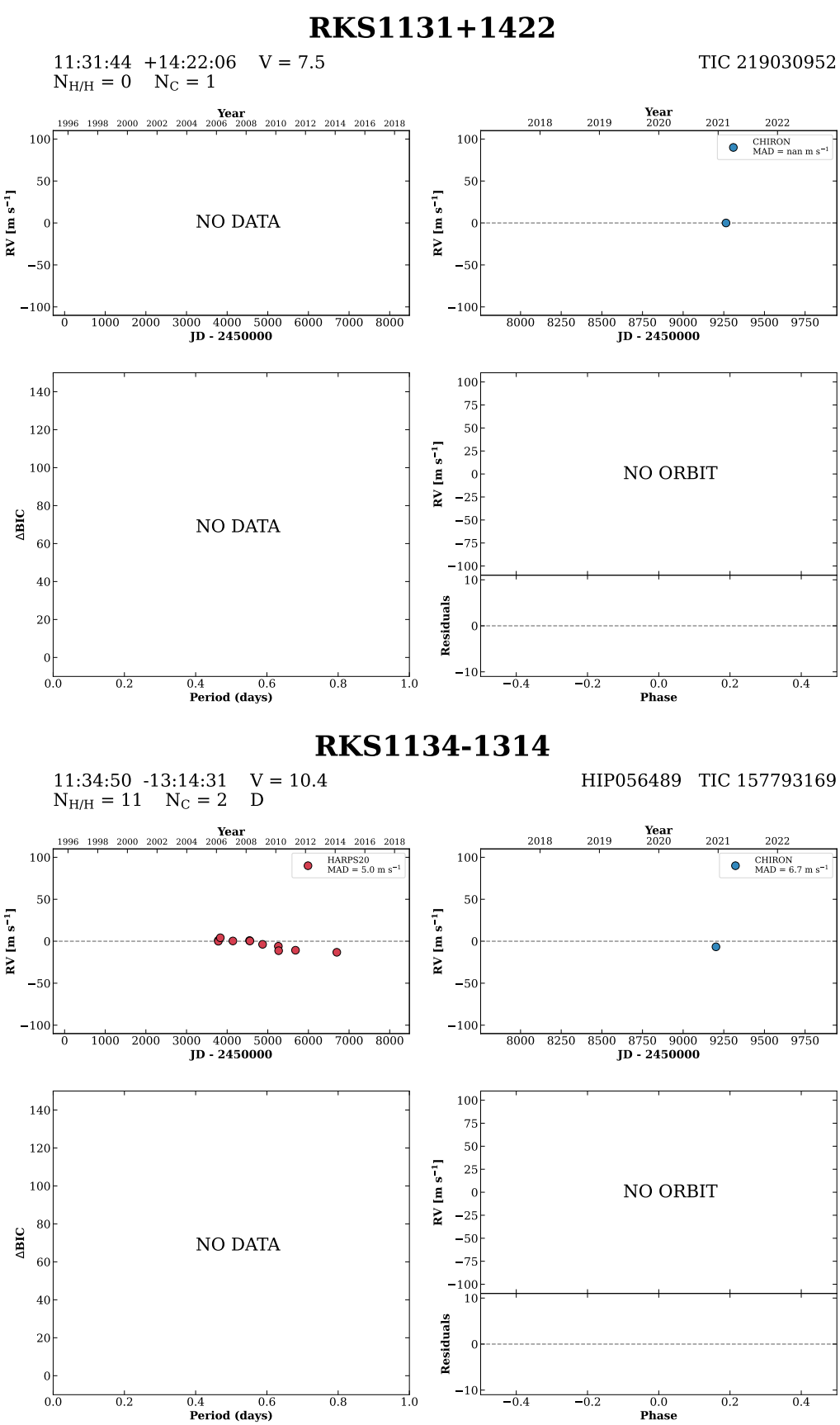

Figure 192 RV results for RKS1131+1422 (top) and RKS1134-1314 (bottom).

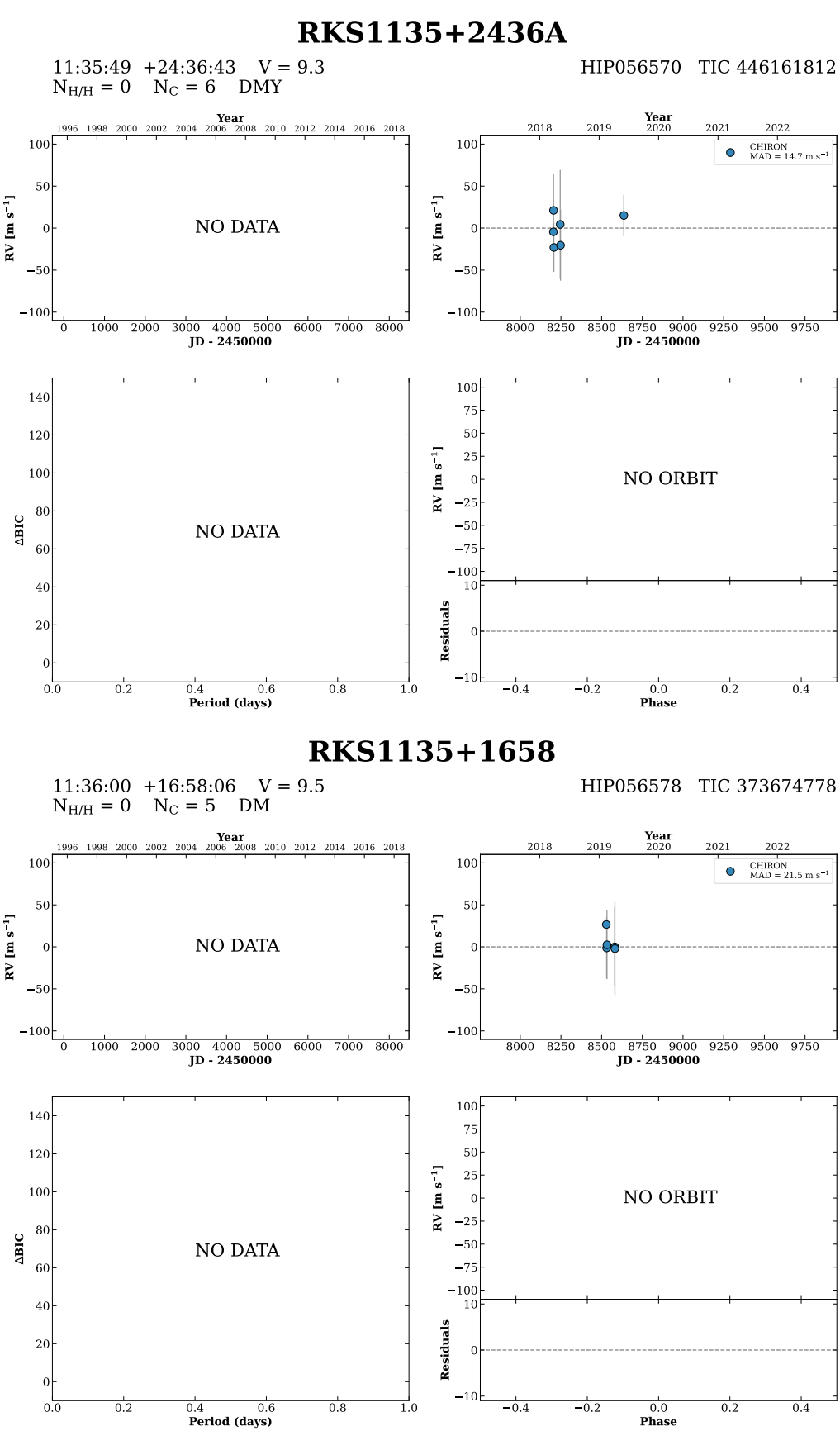

Figure 193 RV results for RKS1135+2436A (top) and RKS1135+1658 (bottom).

RKS1139-2741

11:39:08 -27:41:46 V = 10.0 HIP056838 TIC 14718770
$N_{H/H}$ = 12 N_C = 5 DM

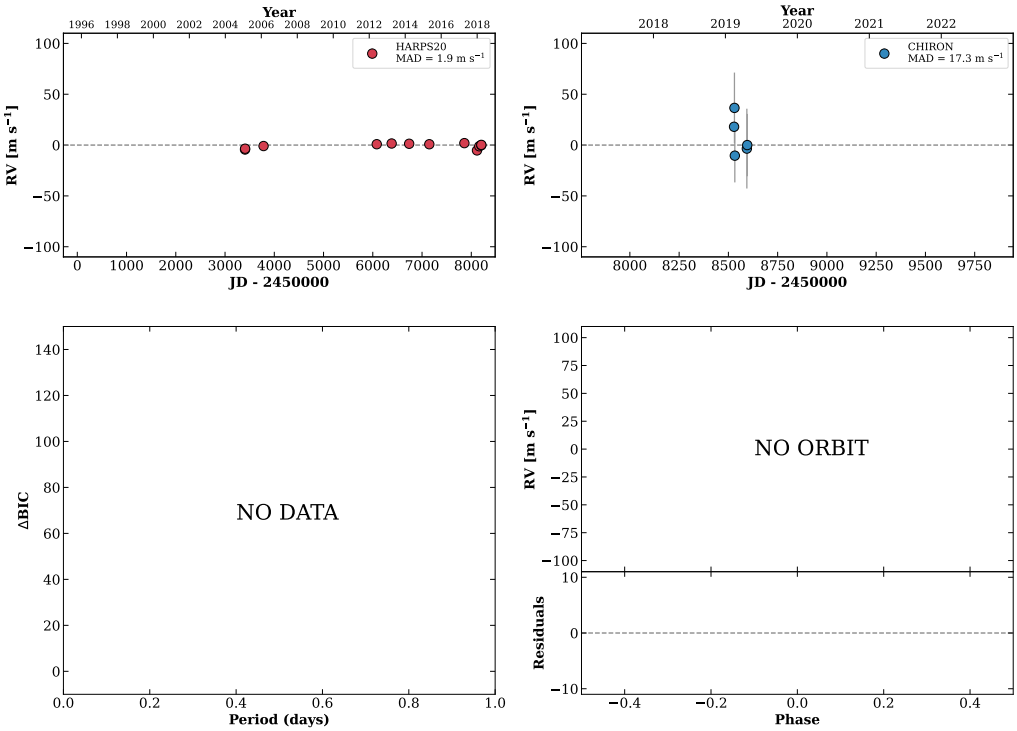

RKS1141+0508A

11:41:50 +05:08:26 V = 9.6 HIP057058 TIC 281906915
$N_{H/H}$ = 5 N_C = 7 DMY

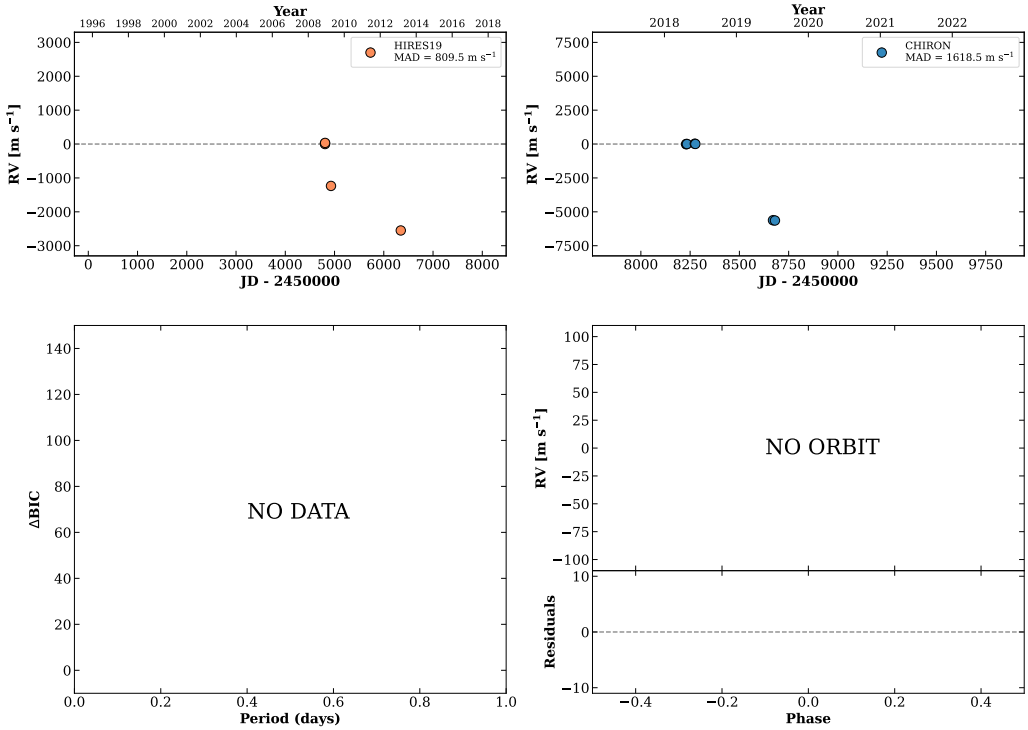

Figure 194 RV results for RKS1139-2741 (top) and RKS1141+0508A (bottom).

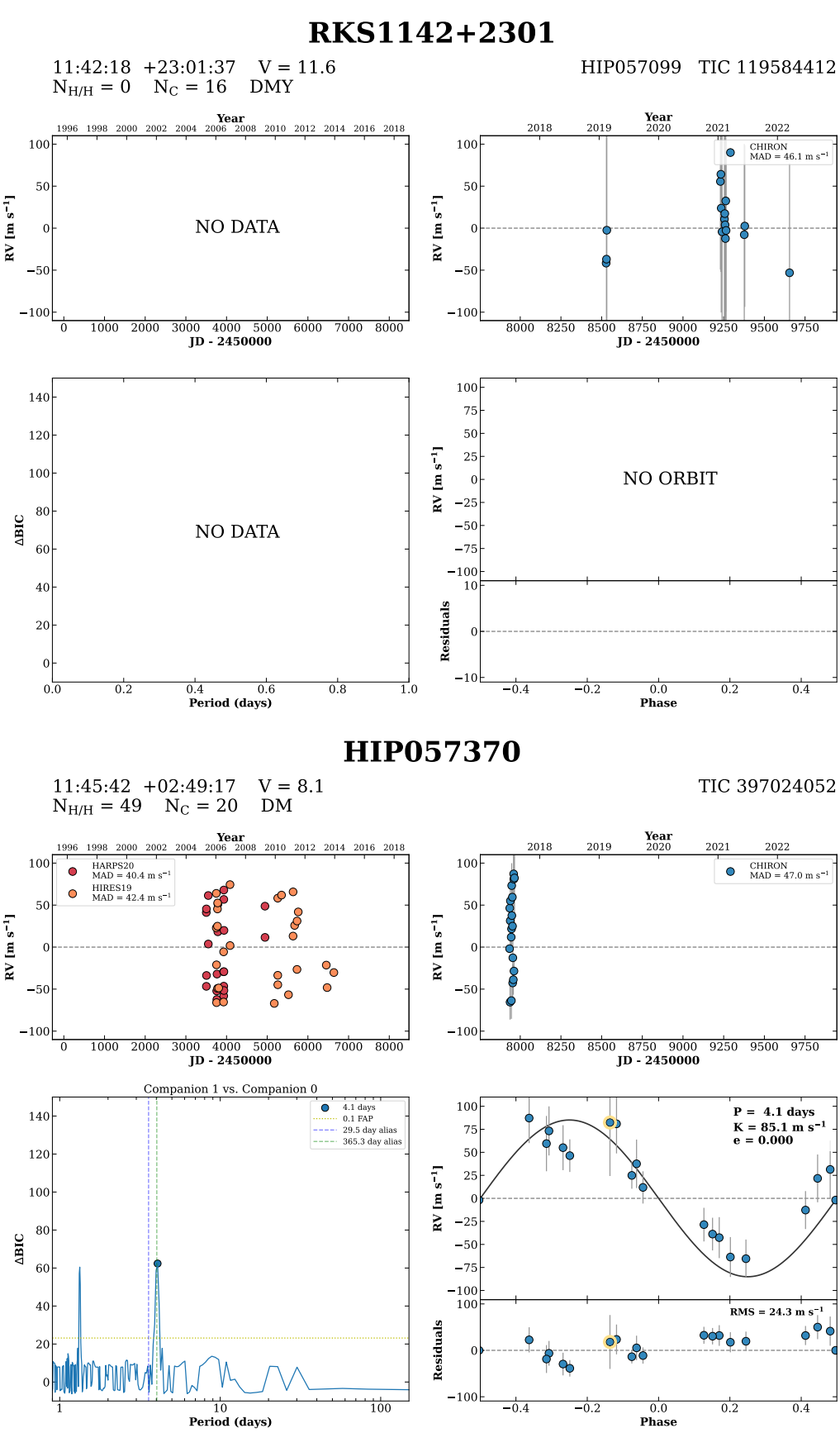

Figure 195 RV results for RKS1142+2301 (top) and HIP057370 (bottom).

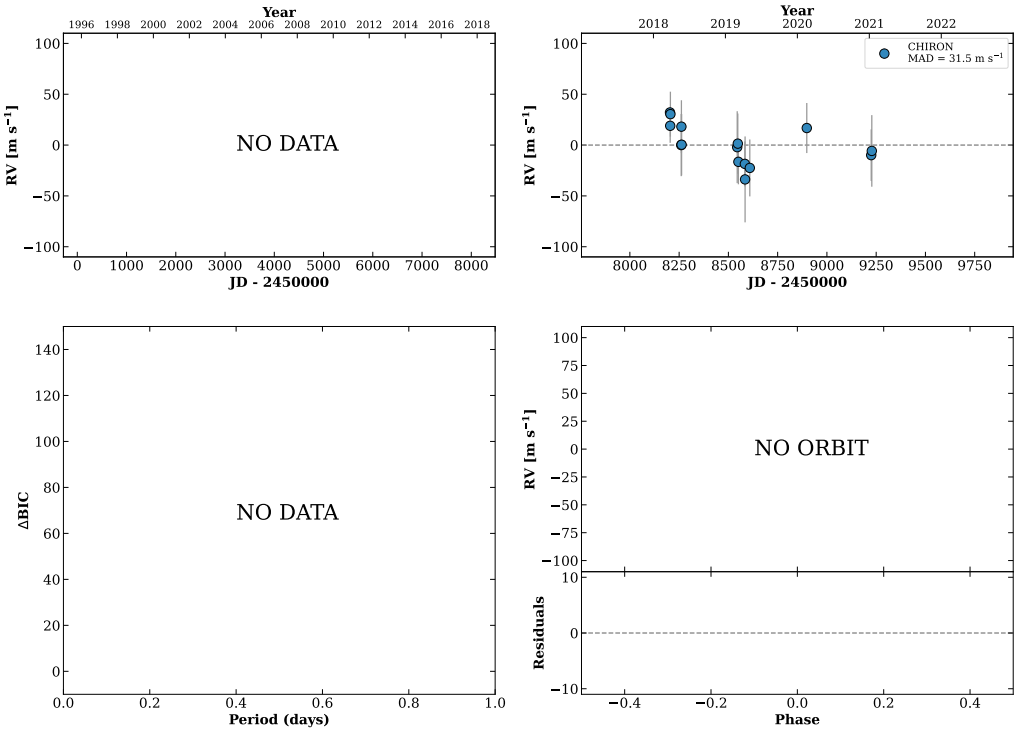

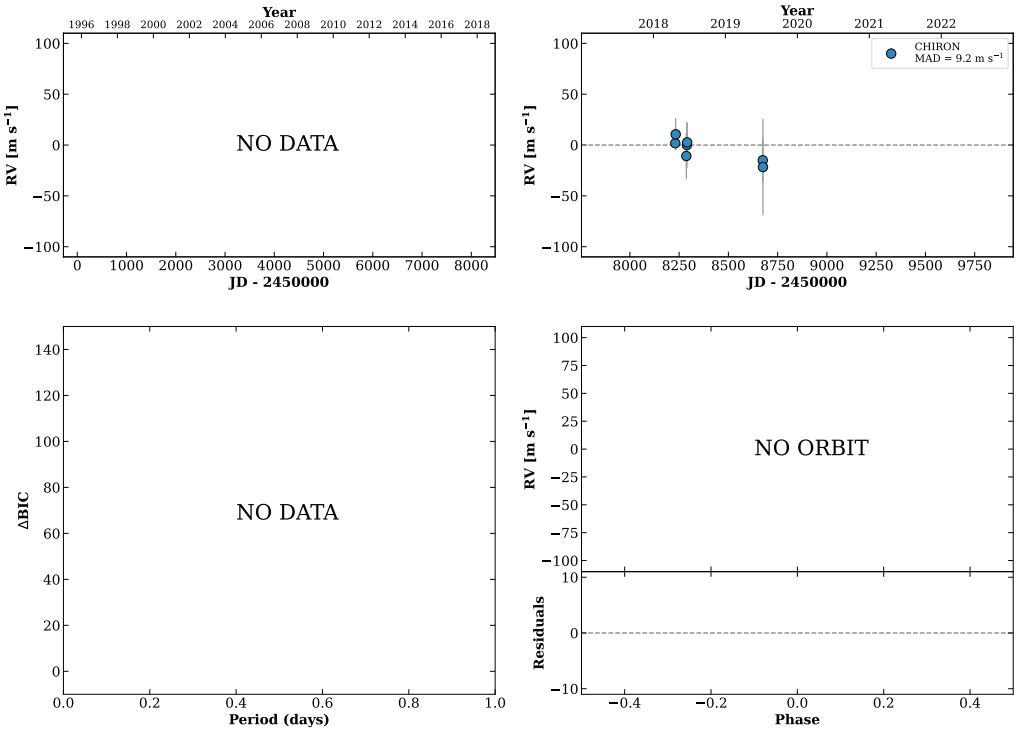

Figure 196 RV results for RKS1147-1149A (top) and RKS1152+1845 (bottom).

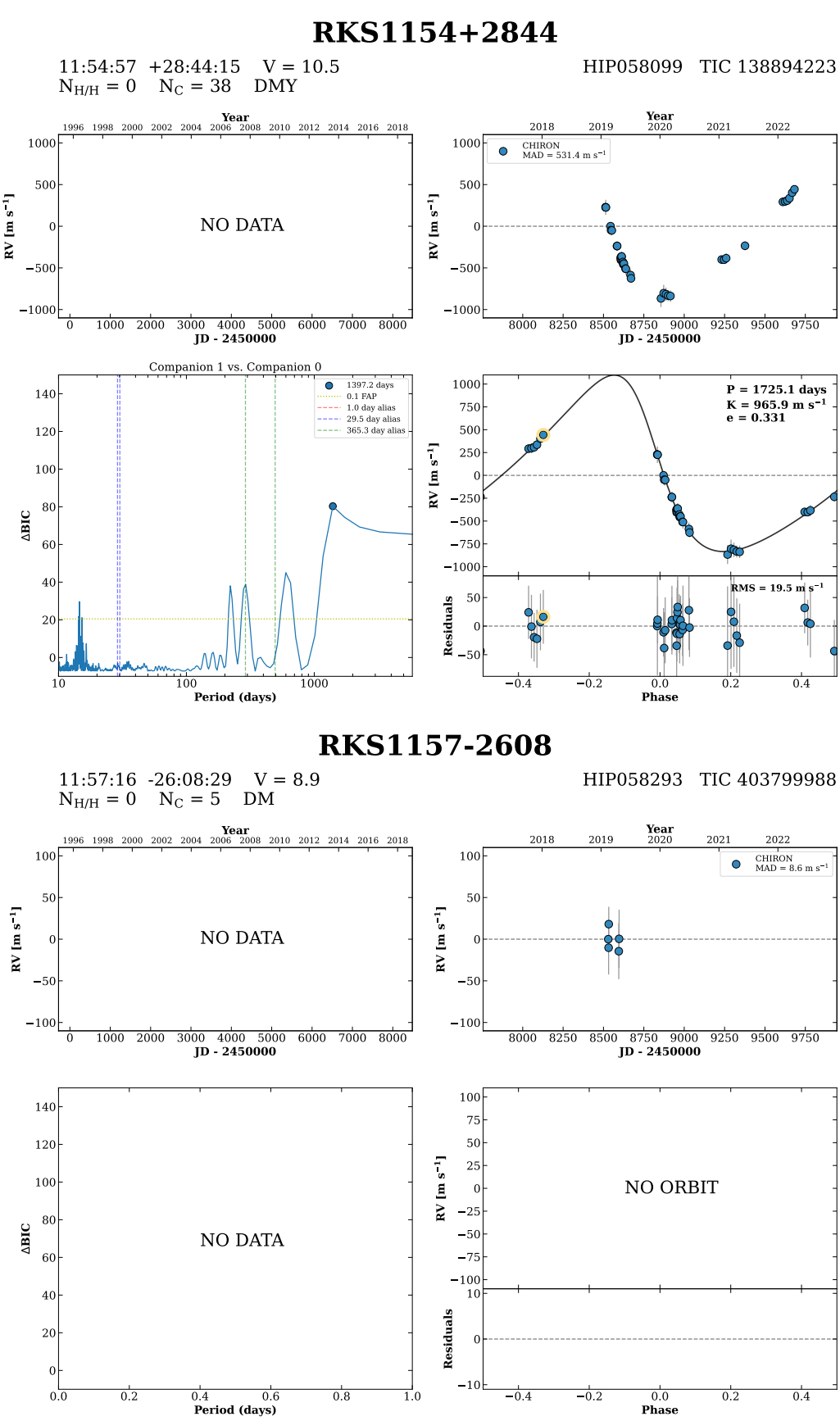

Figure 197 RV results for RKS1154+2844 (top) and RKS1157-2608 (bottom).

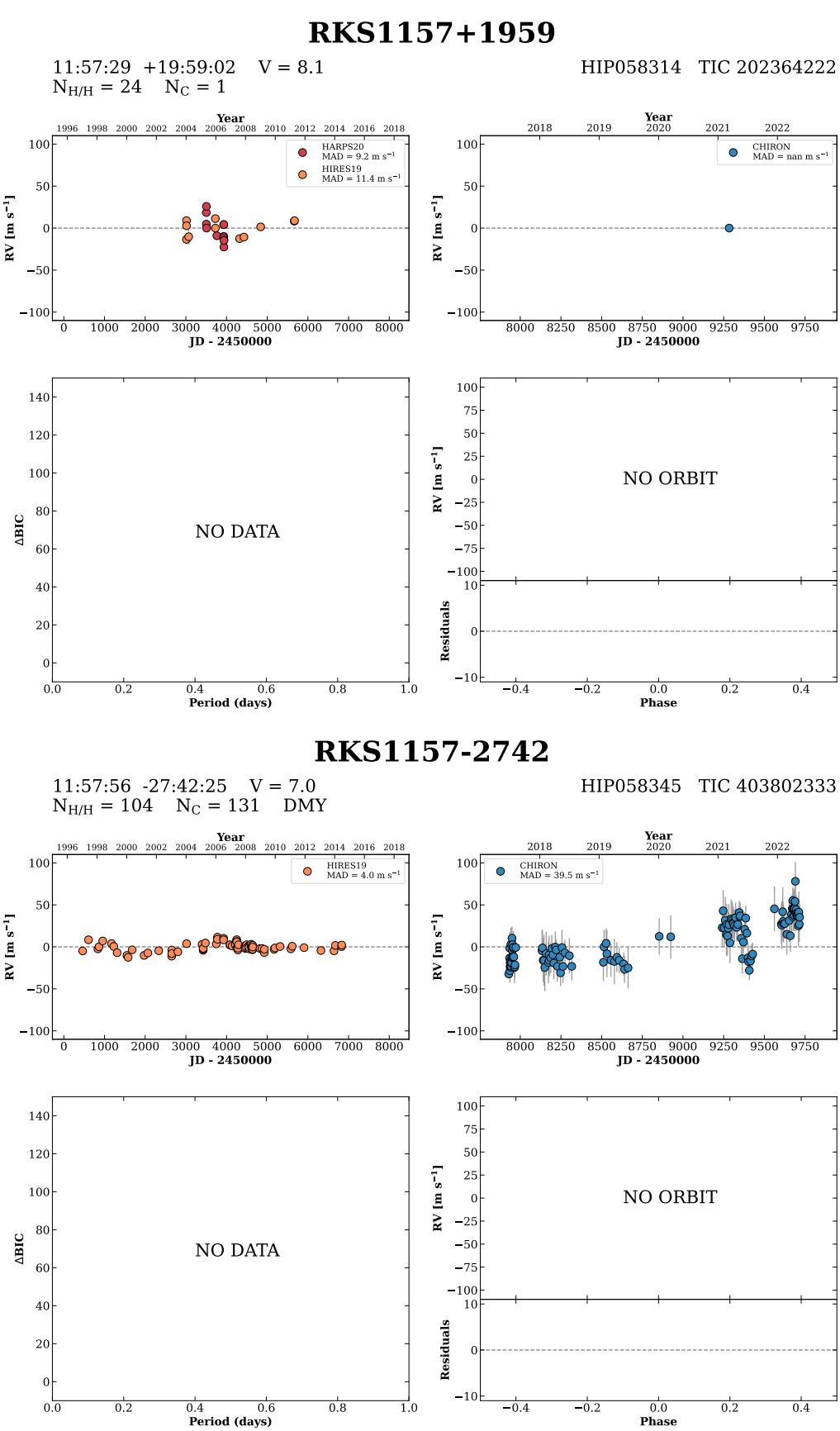

Figure 198 RV results for RKS1157+1959 (top) and RKS1157-2742 (bottom).

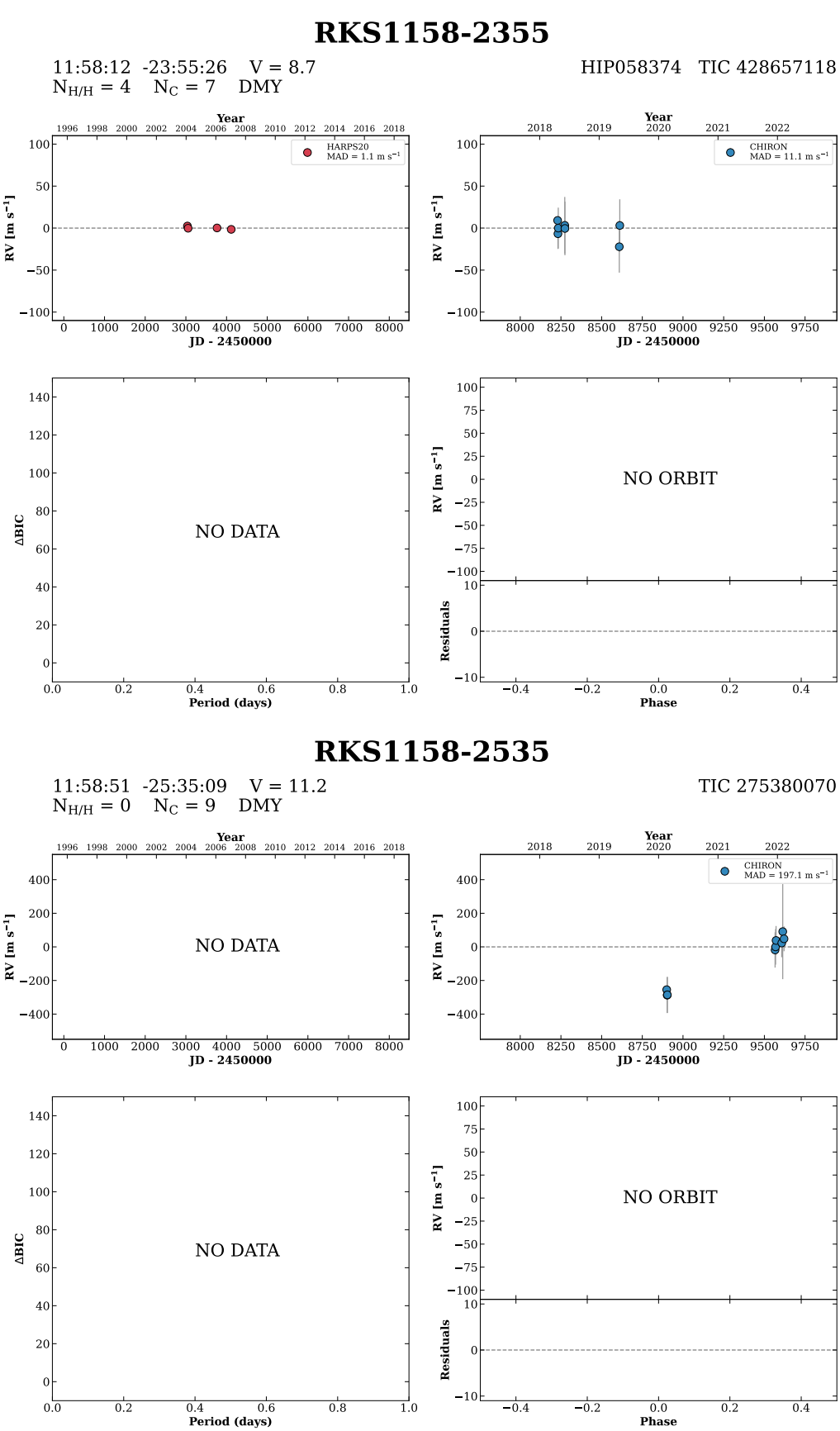

Figure 199 RV results for RKS1158-2355 (top) and RKS1158-2535 (bottom).

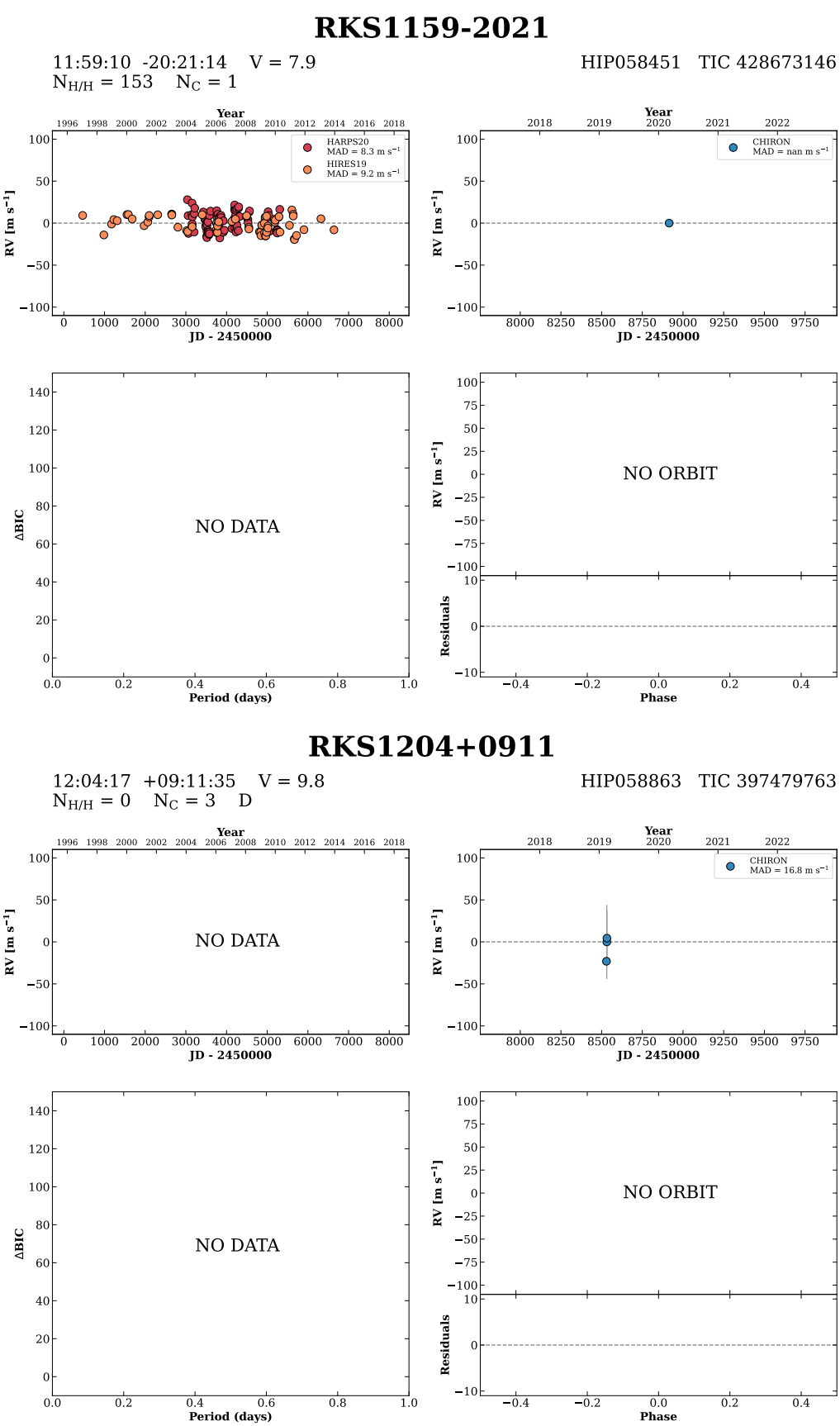

Figure 200 RV results for RKS1159-2021 (top) and RKS1204+0911 (bottom).

RKS1204-0013

12:04:48 -00:13:36 V = 10.8 HIP058908 TIC 96243247
$N_{H/H}$ = 0 N_C = 2 D

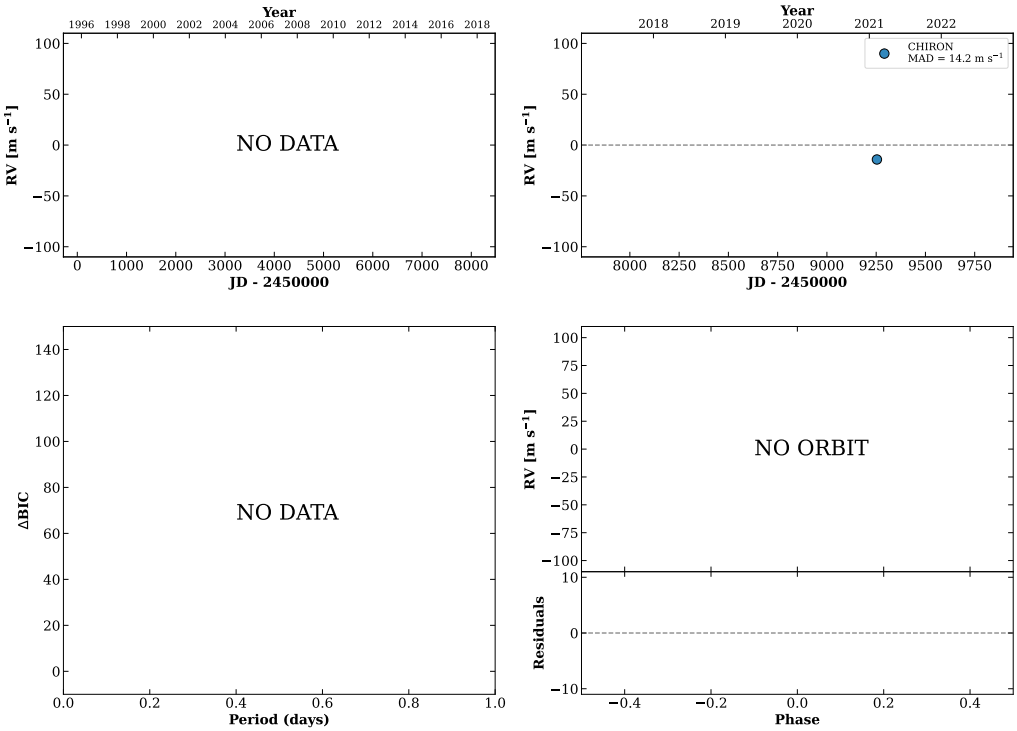

HIP058949

12:05:13 -01:30:33 V = 8.2 TIC 96243602
$N_{H/H}$ = 0 N_C = 3 D

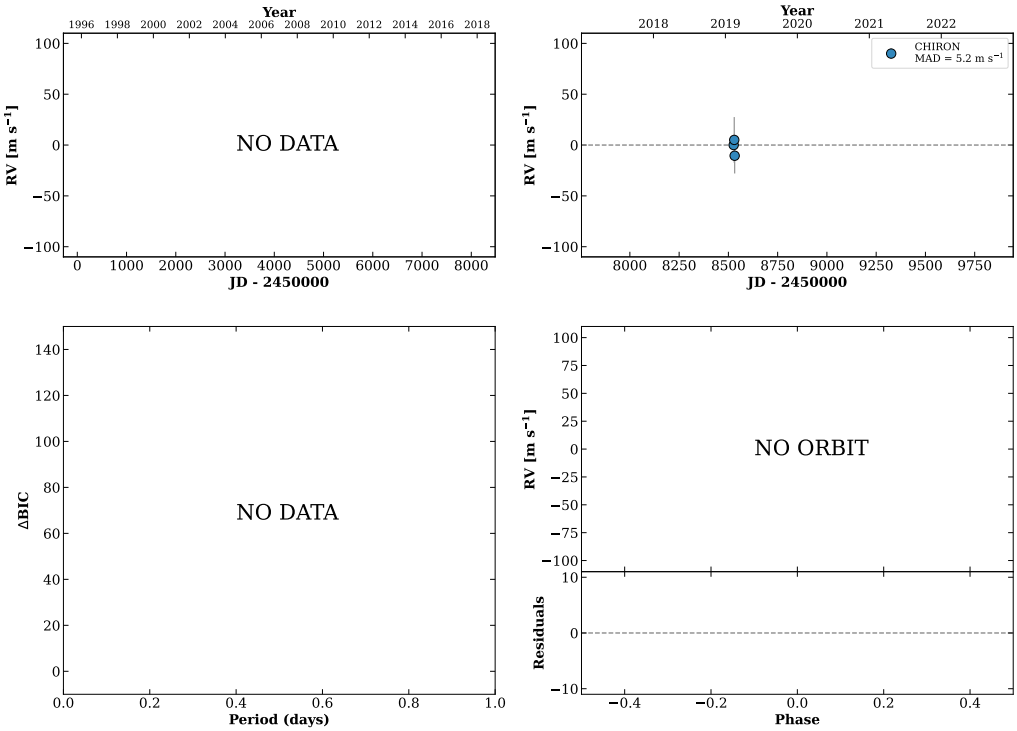

Figure 201 RV results for RKS1204-0013 (top) and HIP058949 (bottom).

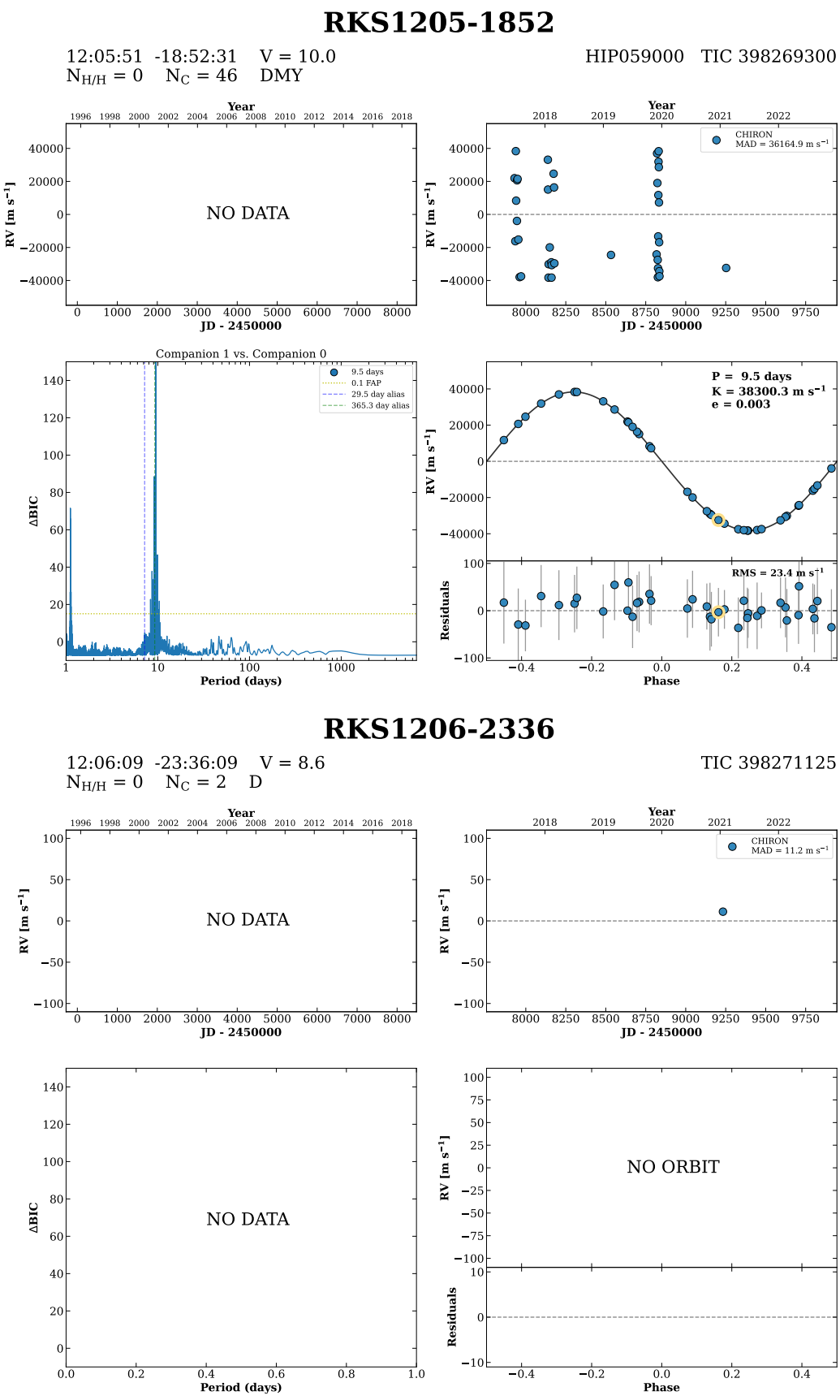

Figure 202 RV results for RKS1205-1852 (top) and RKS1206-2336 (bottom).

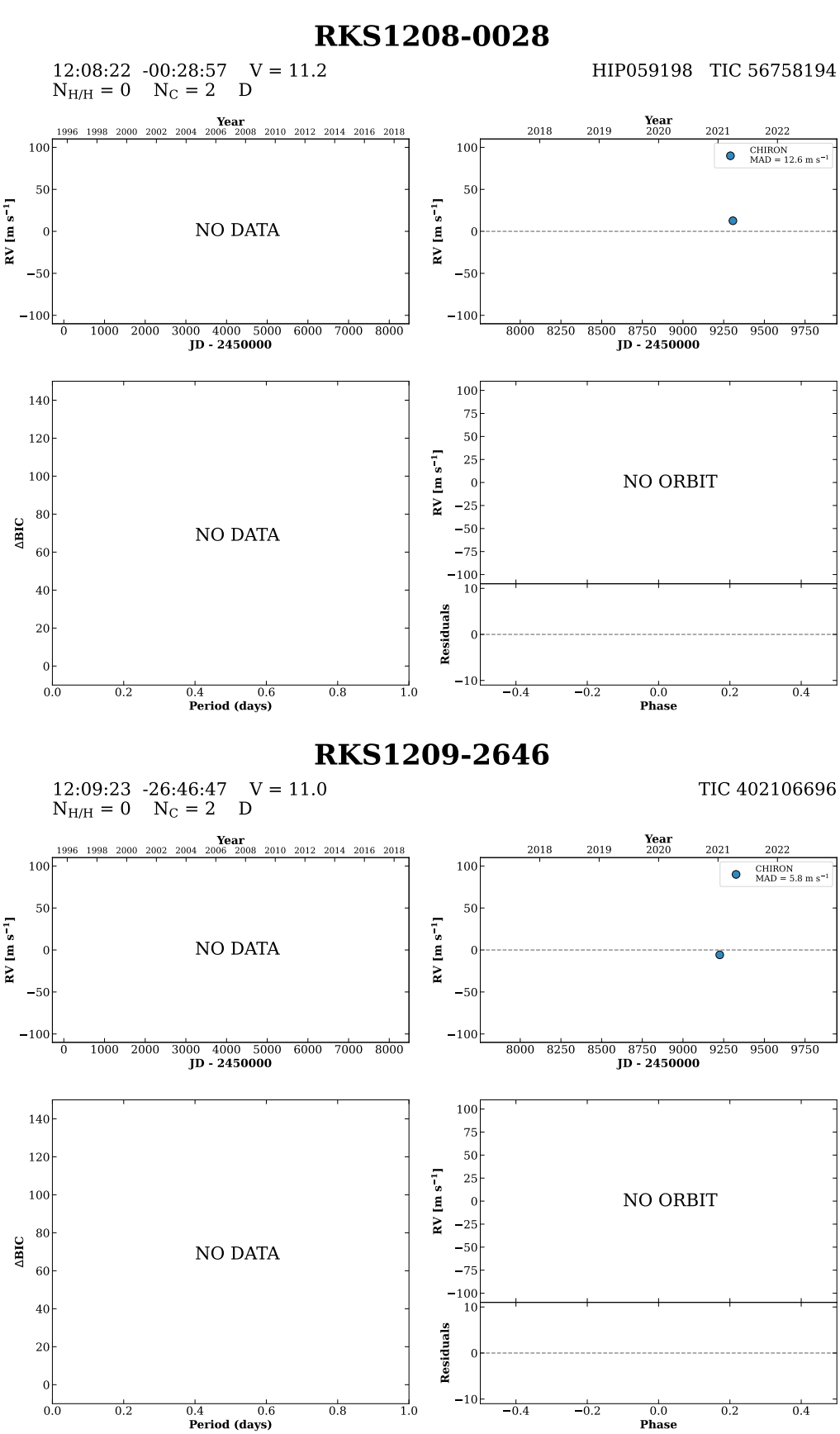

Figure 203 RV results for RKS1208-0028 (top) and RKS1209-2646 (bottom).

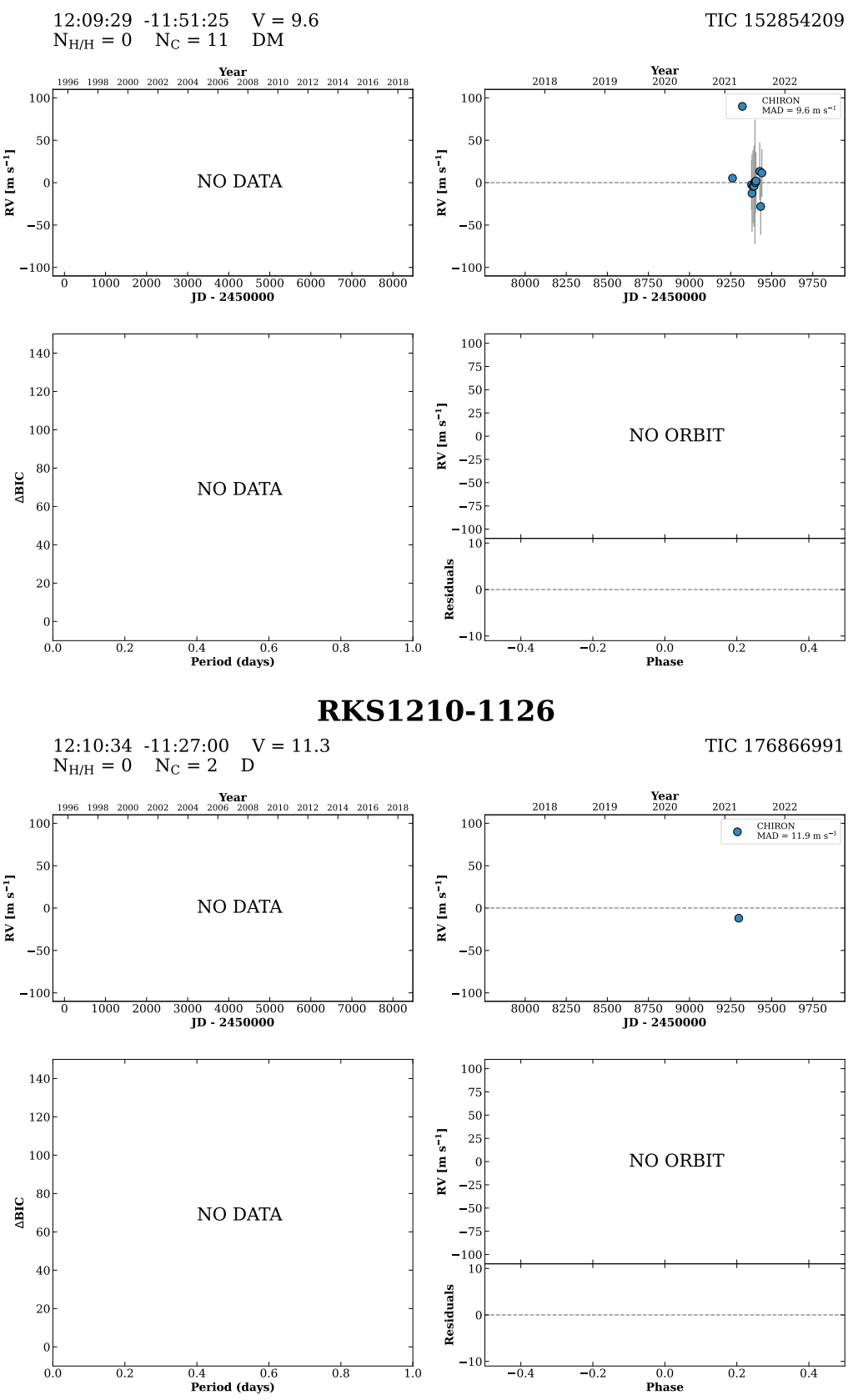

Figure 204 RV results for RKS1209-1151 (top) and RKS1210-1126 (bottom).

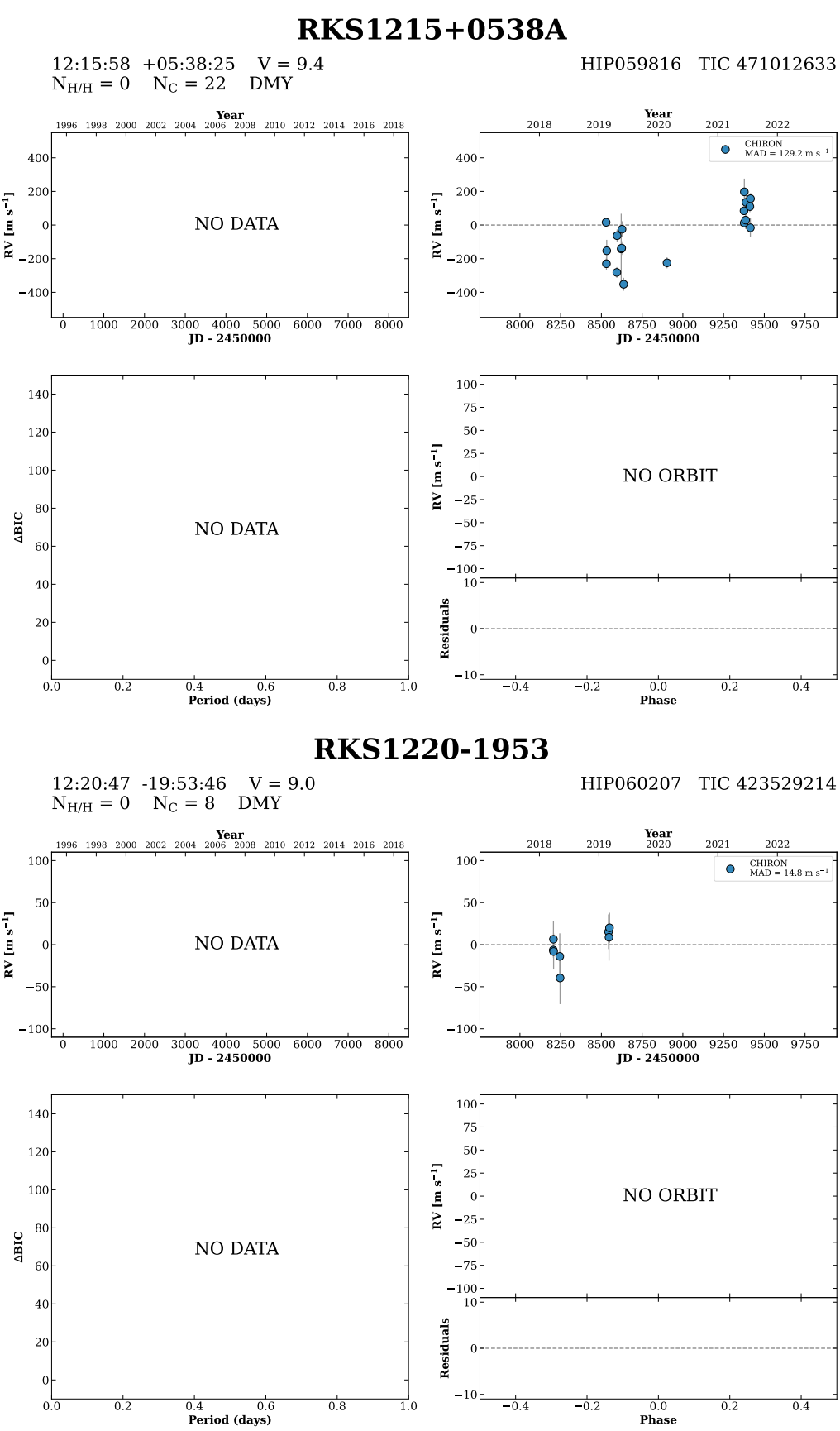

Figure 205 RV results for RKS1215+0538A (top) and RKS1220-1953 (bottom).

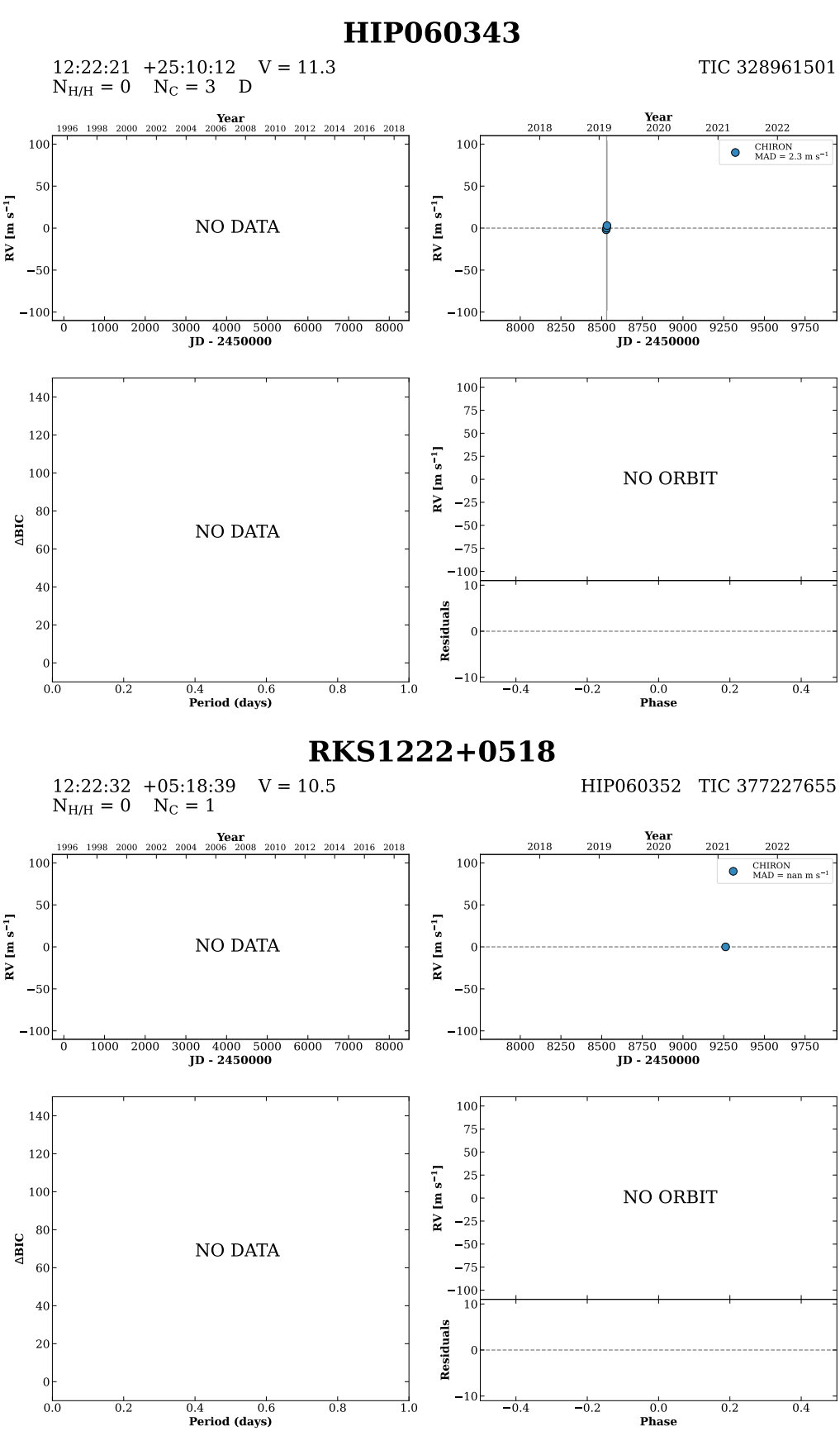

Figure 206 RV results for HIP060343 (top) and RKS1222+0518 (bottom).

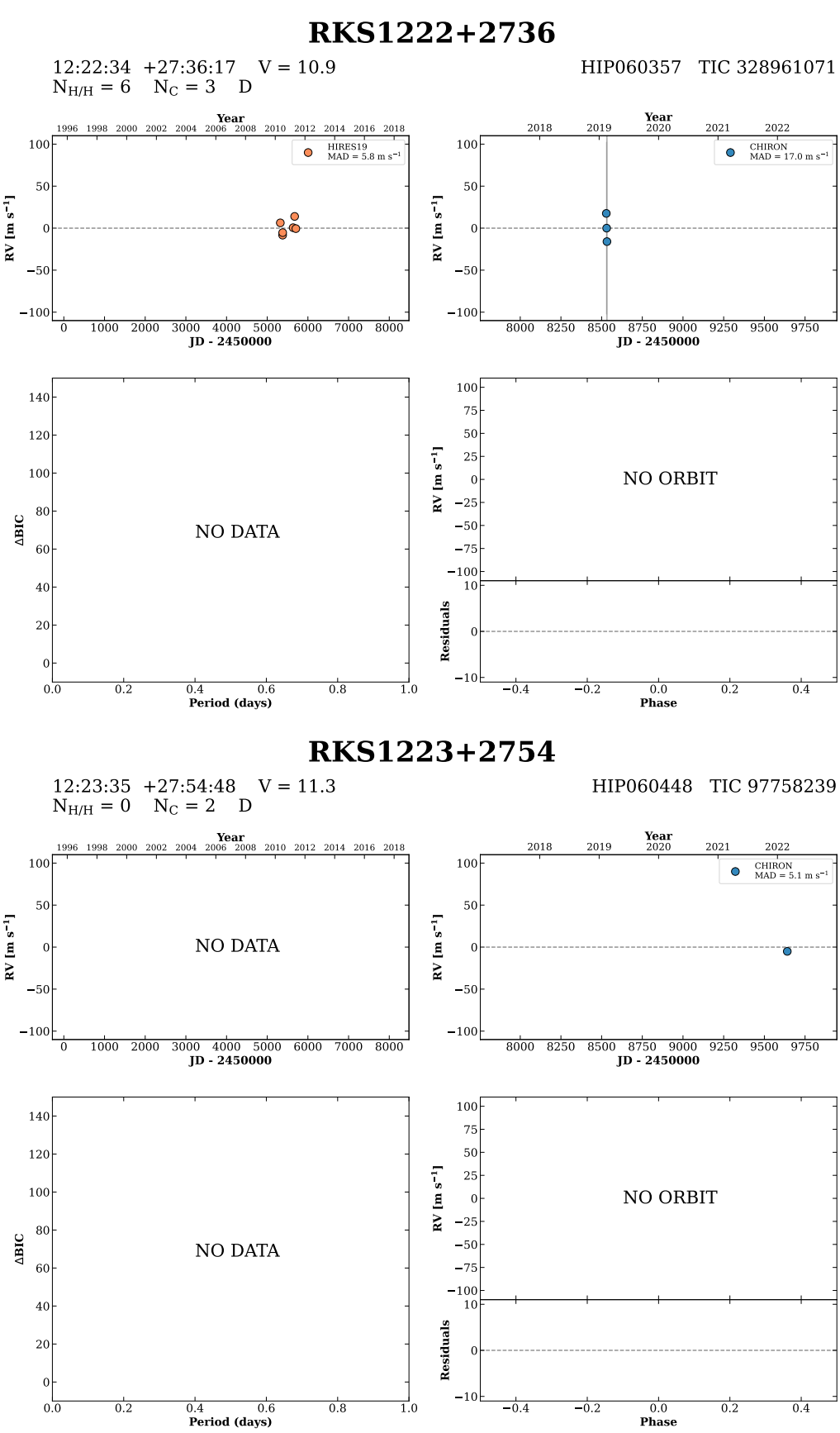

Figure 207 RV results for RKS1222+2736 (top) and RKS1223+2754 (bottom).

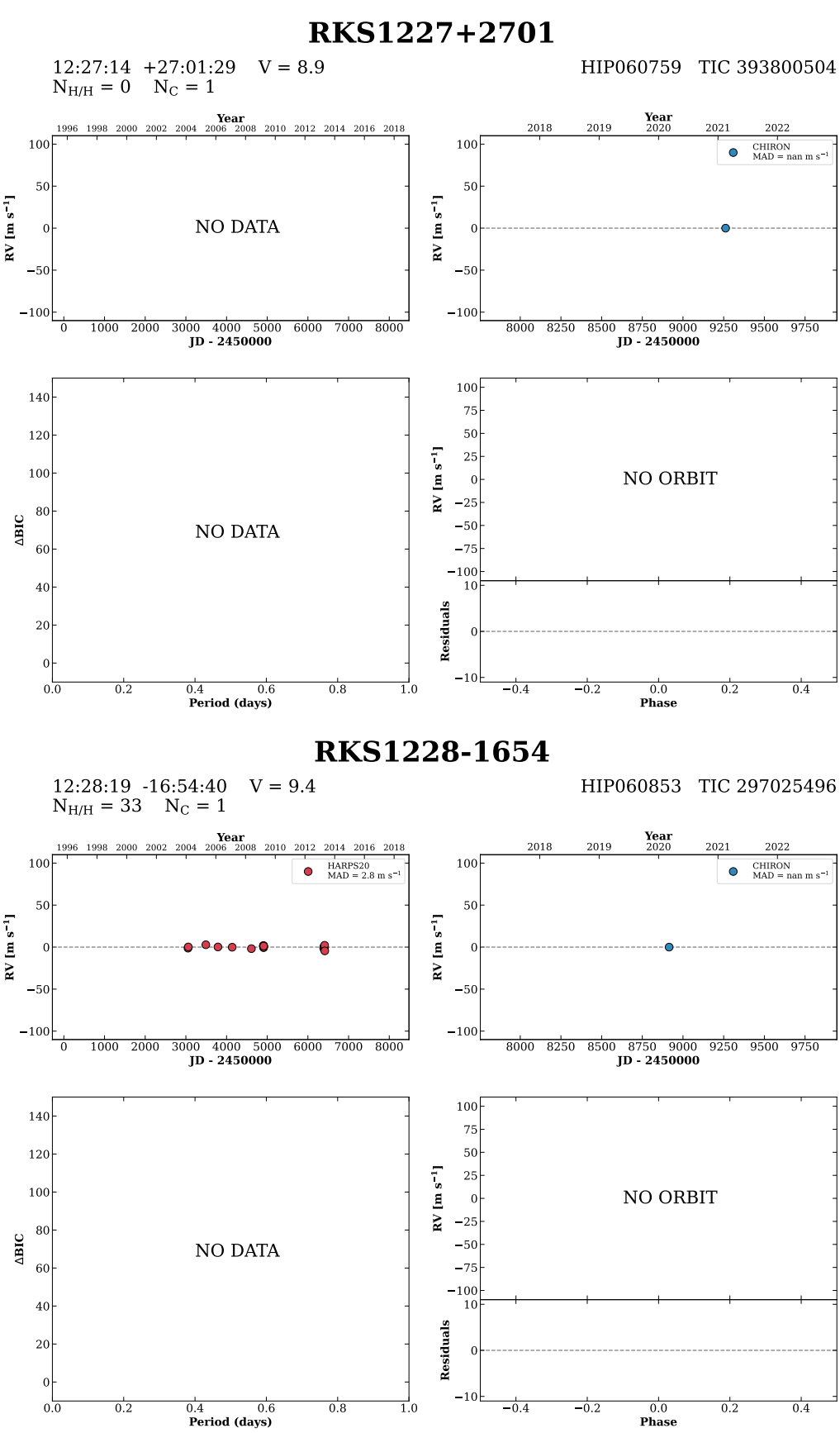

Figure 208 RV results for RKS1227+2701 (top) and RKS1228-1654 (bottom).

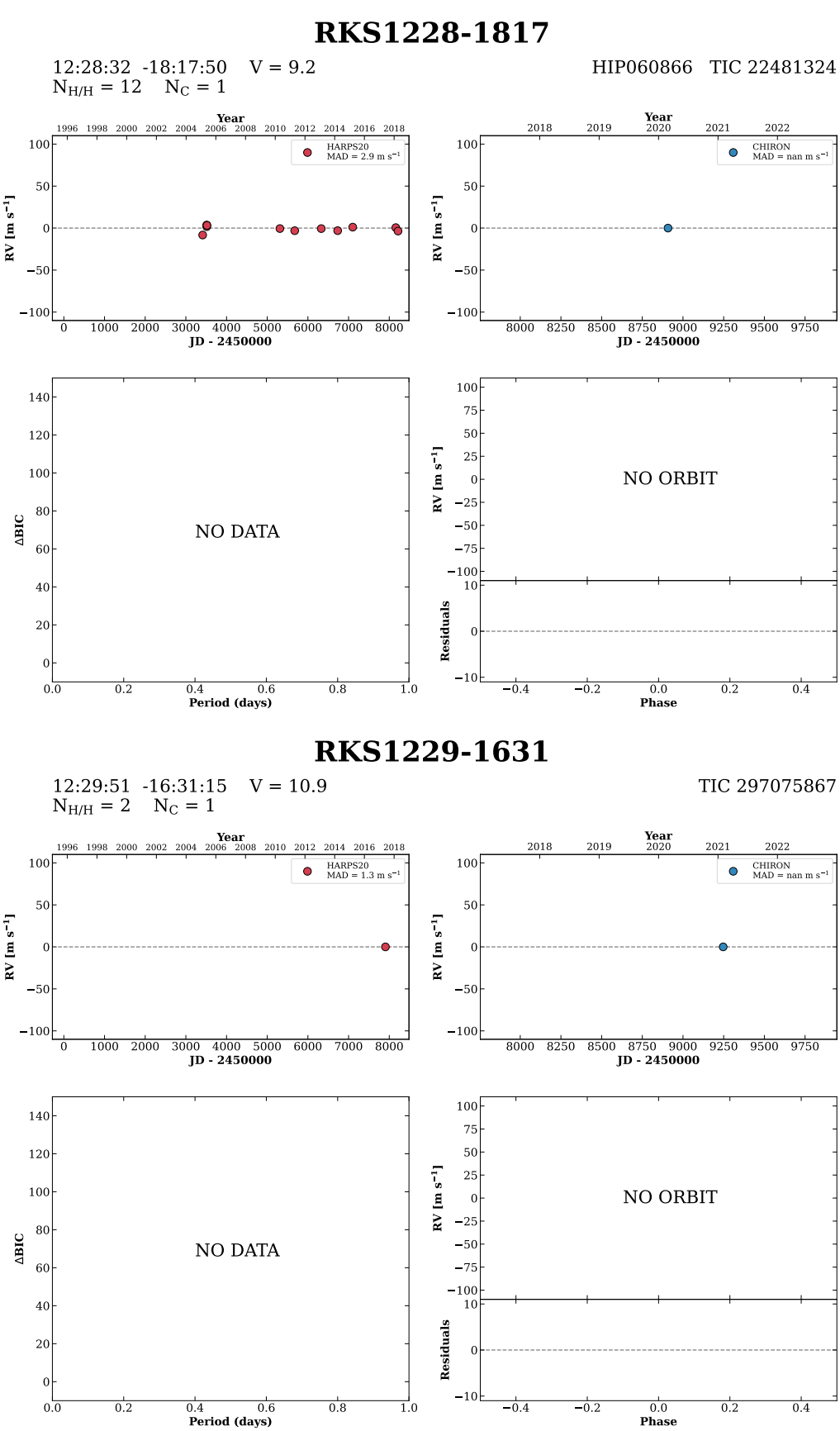

Figure 209 RV results for RKS1228-1817 (top) and RKS1229-1631 (bottom).

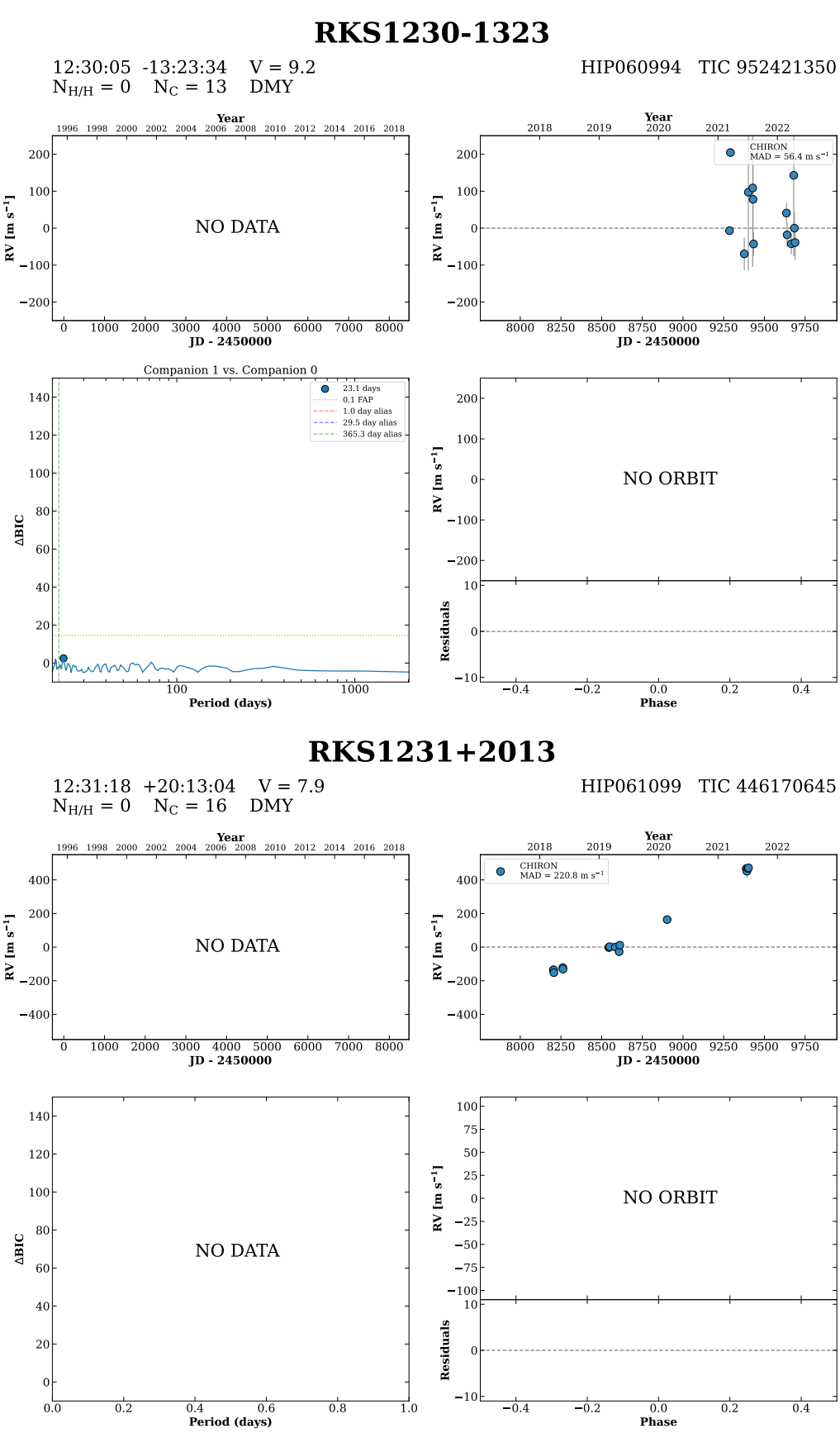

Figure 210 RV results for RKS1230-1323 (top) and RKS1231+2013 (bottom).

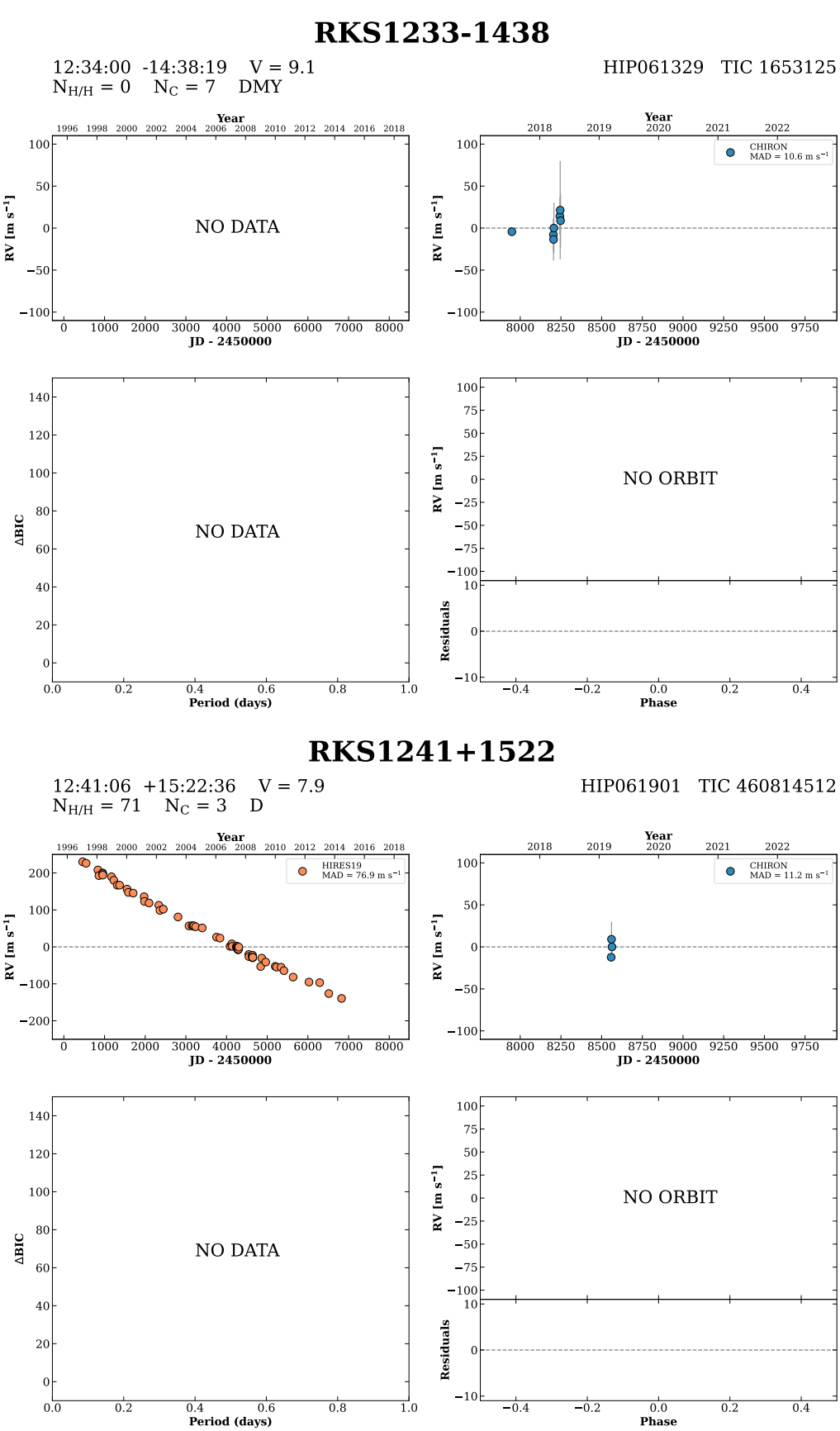

Figure 211 RV results for RKS1233-1438 (top) and RKS1241+1522 (bottom).

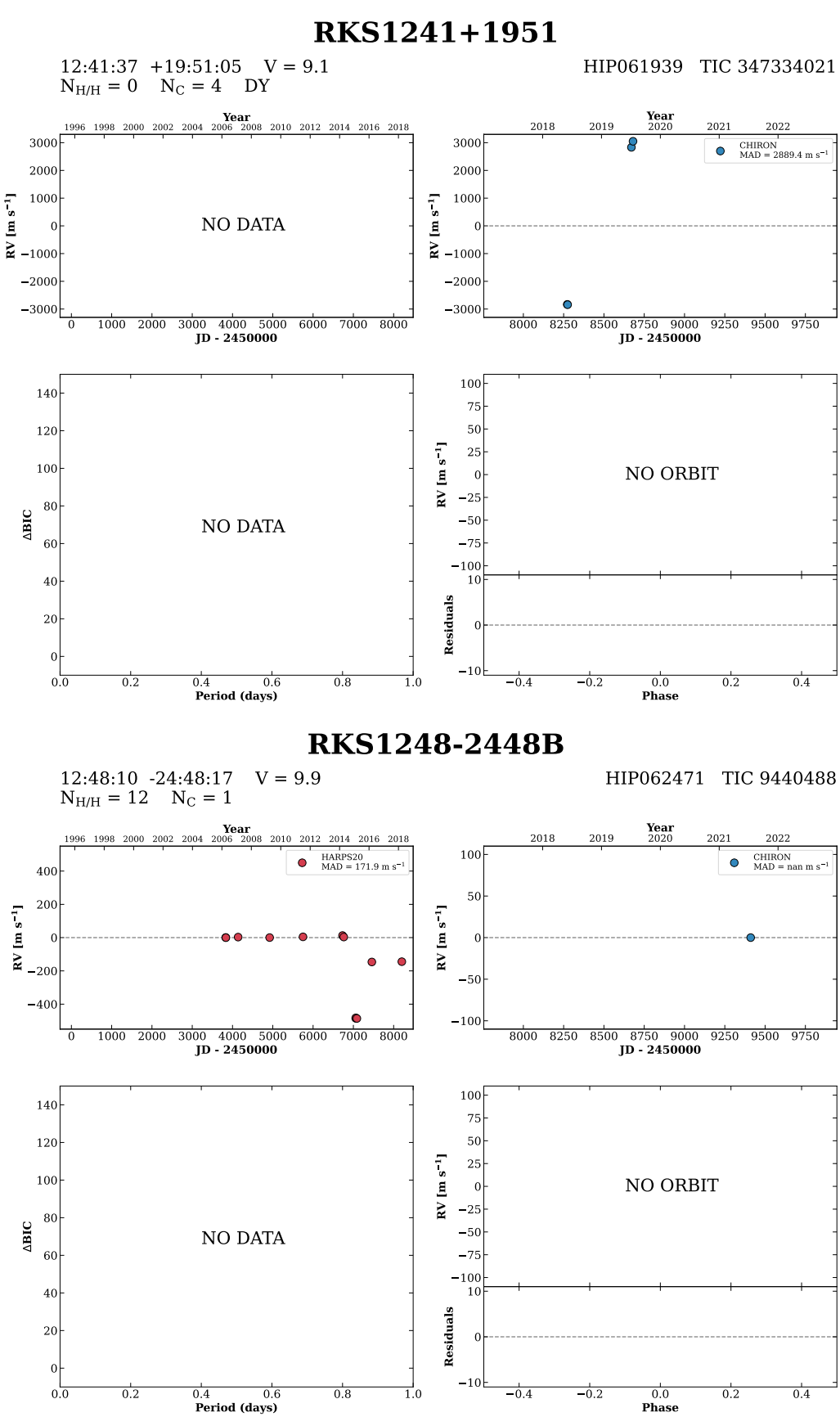

Figure 212 RV results for RKS1241+1951 (top) and RKS1248-2448B (bottom).

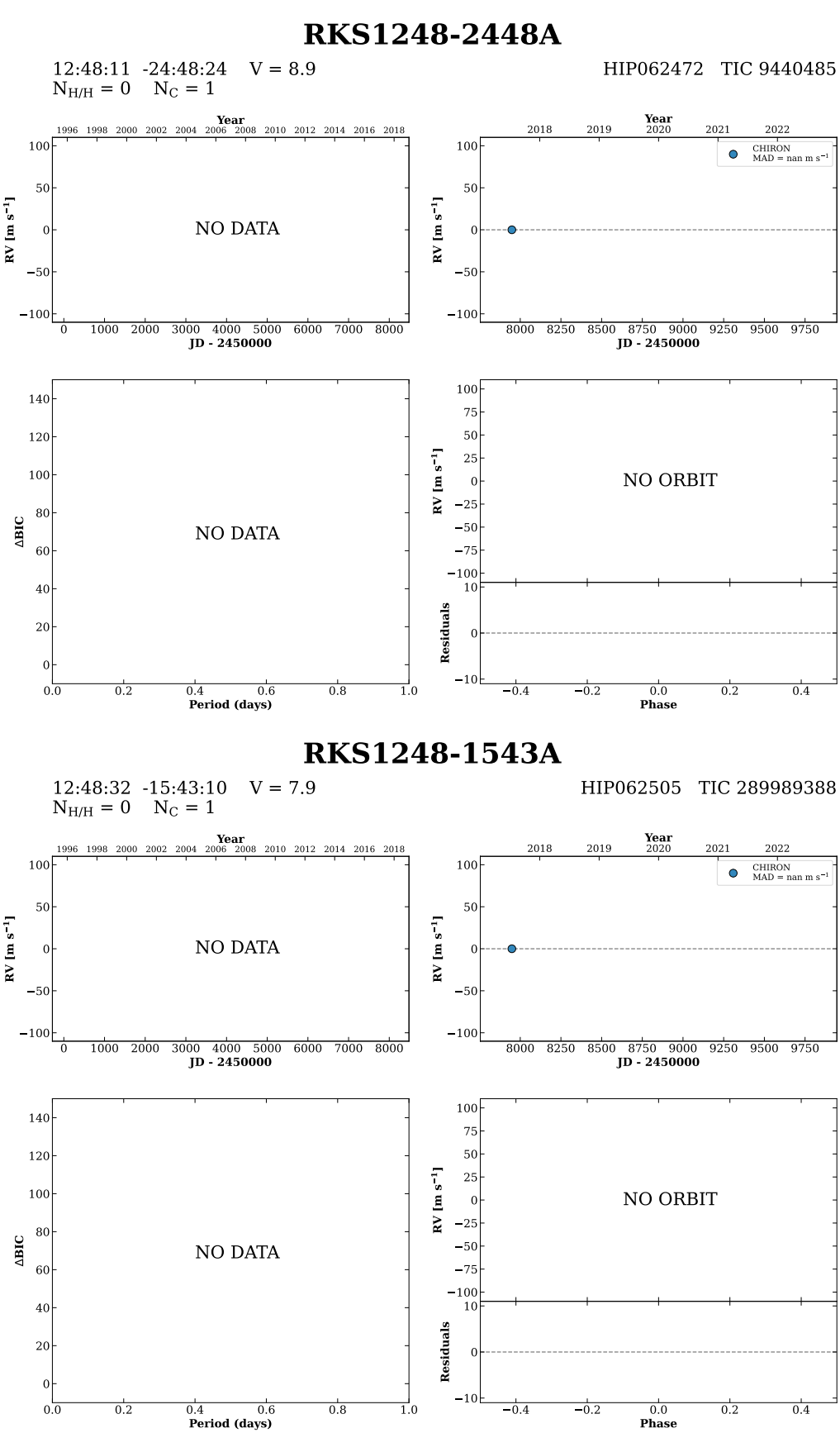

Figure 213 RV results for RKS1248-2448A (top) and RKS1248-1543A (bottom).

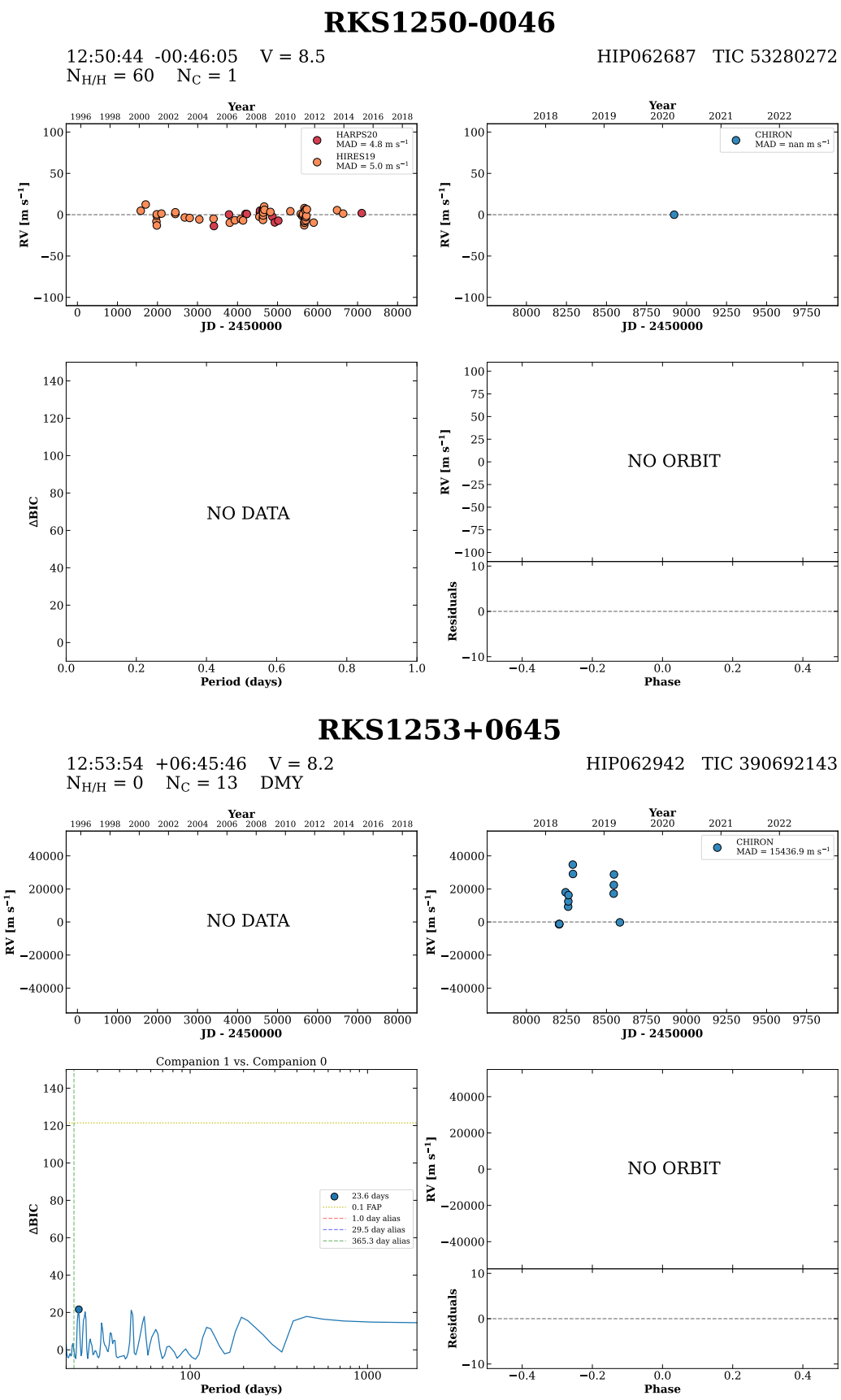

Figure 214 RV results for RKS1250-0046 (top) and RKS1253+0645 (bottom).

RKS1256-2455

12:56:30 -24:55:32 V = 10.0 HIP063157 TIC 228761127
$N_{H/H}$ = 40 N_C = 1

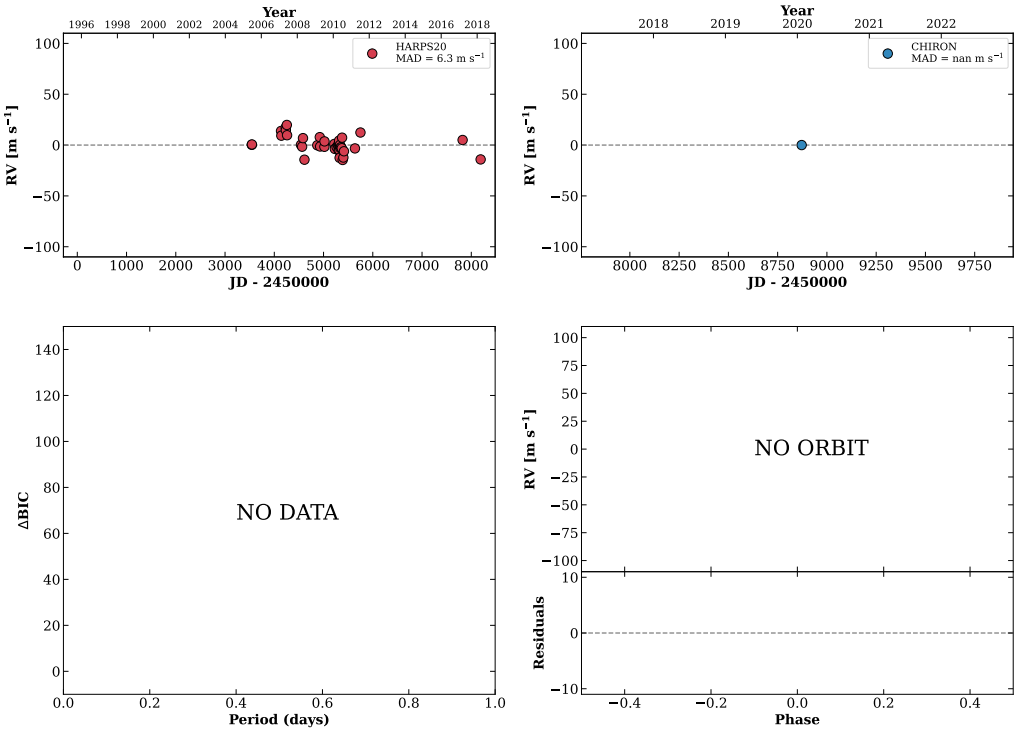

RKS1257-1427

12:57:44 -14:27:48 V = 9.1 HIP063257 TIC 2491738
$N_{H/H}$ = 4 N_C = 9 DMY

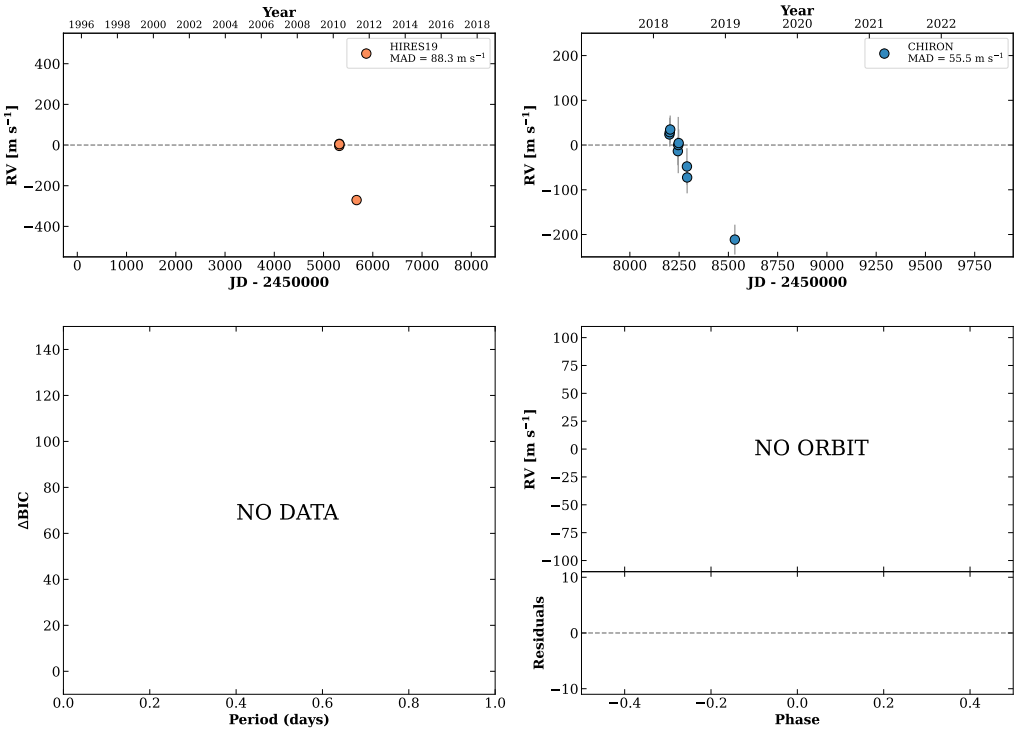

Figure 215 RV results for RKS1256-2455 (top) and RKS1257-1427 (bottom).

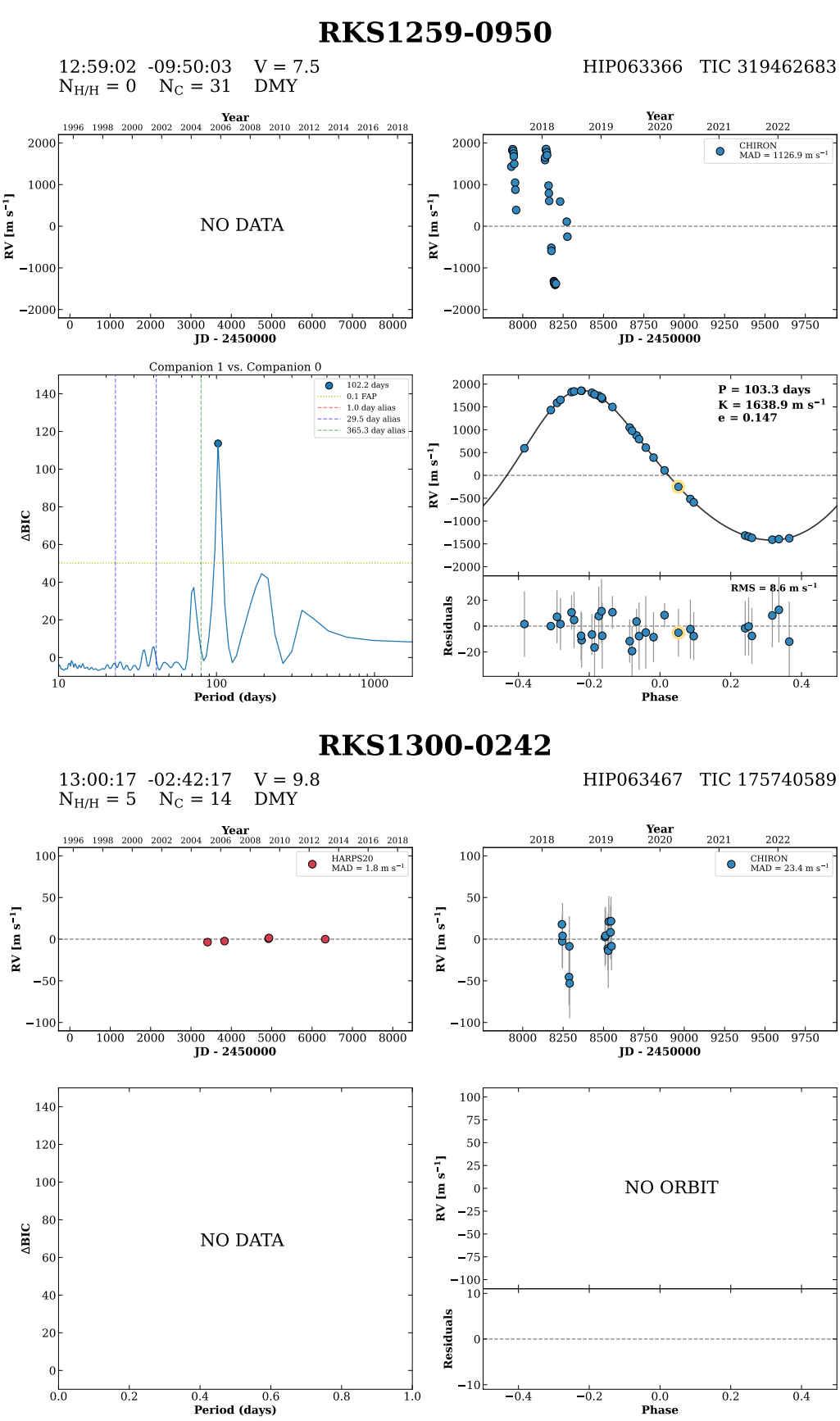

Figure 216 RV results for RKS1259-0950 (top) and RKS1300-0242 (bottom).

RKS1302-2647

13:02:21 -26:47:14 V = 8.3 HIP063618 TIC 229047482
$N_{H/H}$ = 7 N_C = 27 DMY

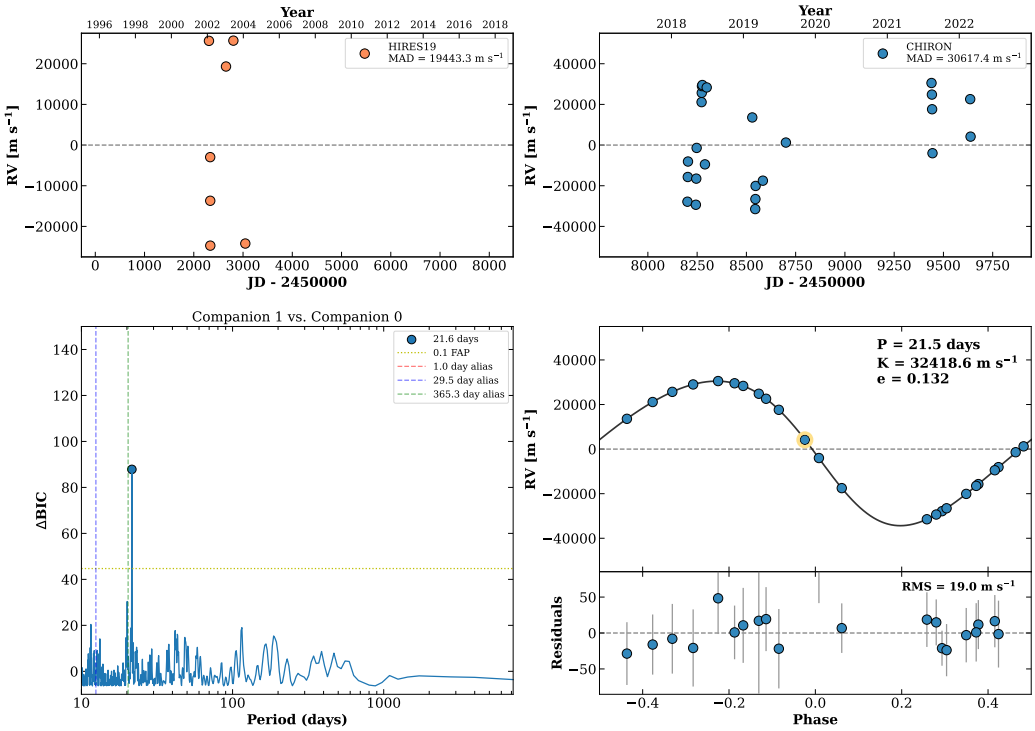

RKS1303-0509

13:03:50 -05:09:43 V = 7.7 HIP063742 TIC 124612531
$N_{H/H}$ = 20 N_C = 1

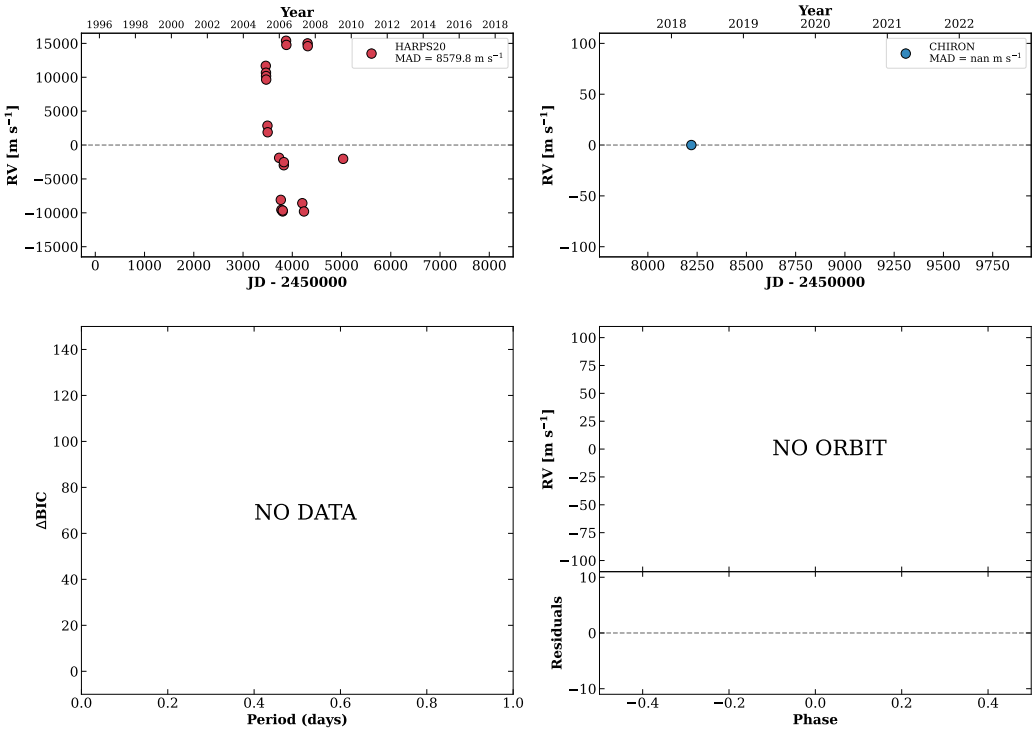

Figure 217 RV results for RKS1302-2647 (top) and RKS1303-0509 (bottom).

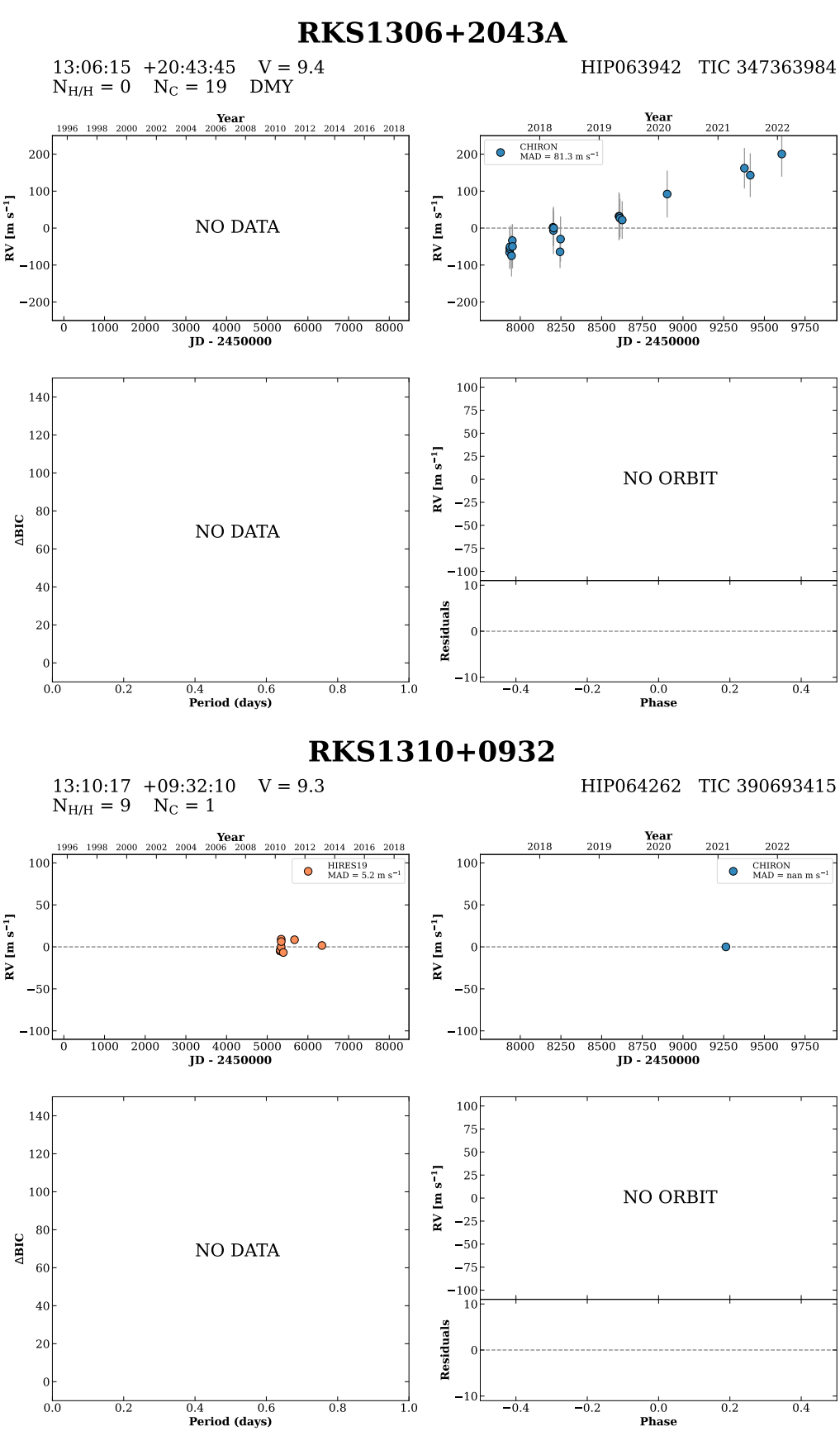

Figure 218 RV results for RKS1306+2043A (top) and RKS1310+0932 (bottom).

RKS1312-0215

13:12:44 -02:15:54 V = 7.6 HIP064457 TIC 292113181
$N_{H/H}$ = 227 N_C = 1

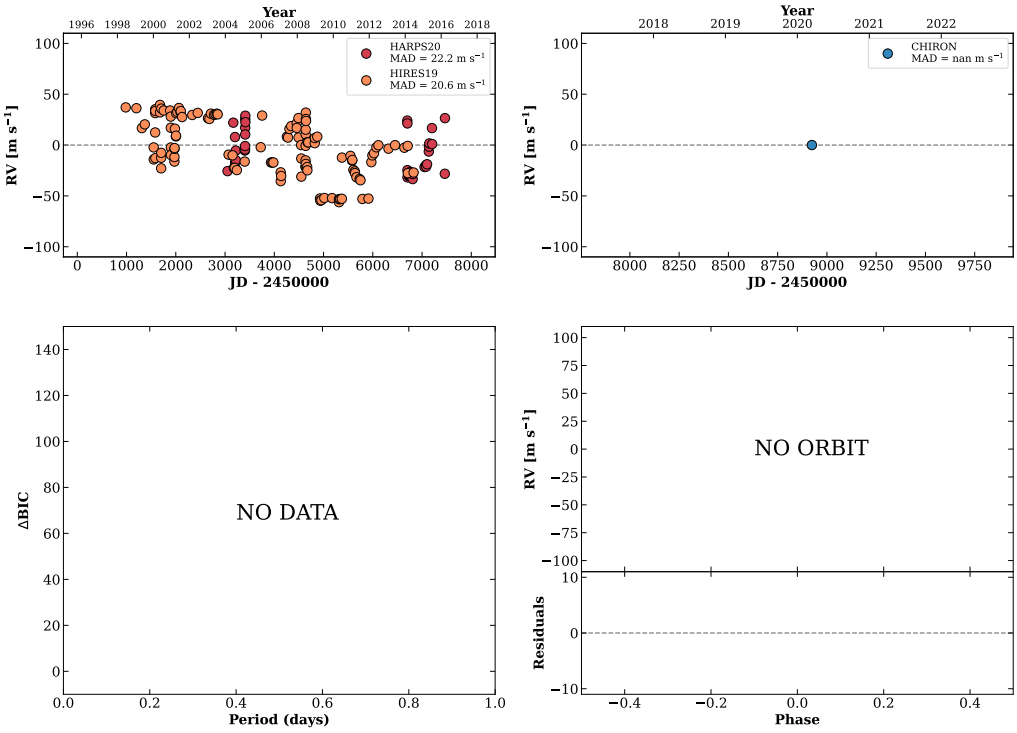

RKS1316+1701

13:16:51 +17:01:02 V = 6.5 HIP064797 TIC 373765355
$N_{H/H}$ = 18 N_C = 1

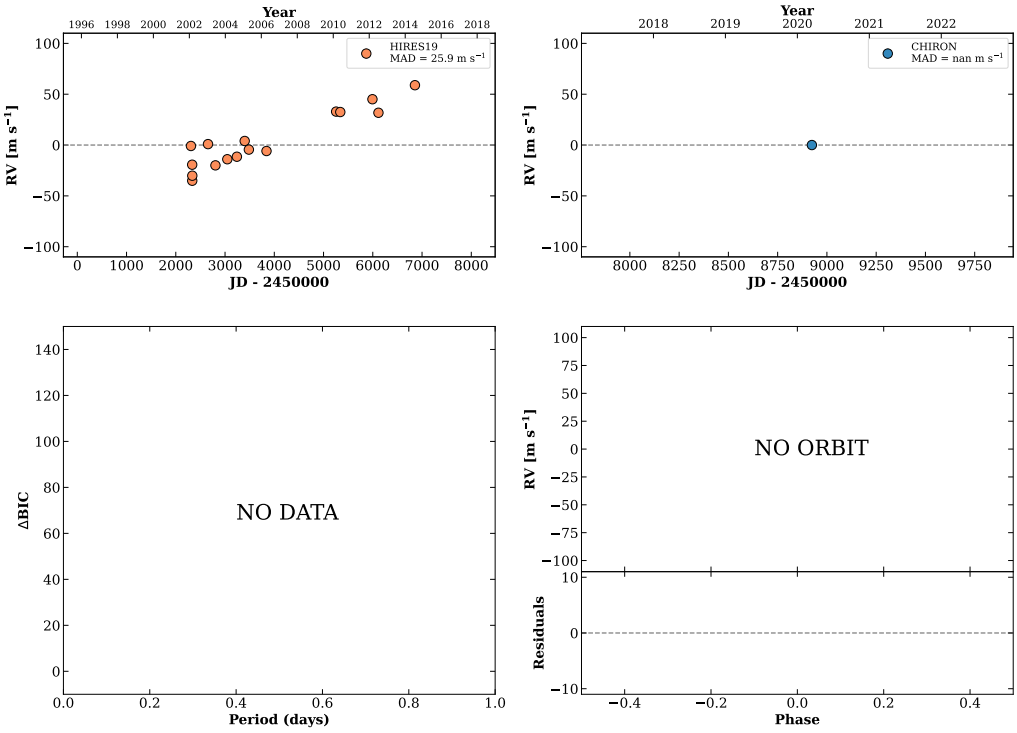

Figure 219 RV results for RKS1312-0215 (top) and RKS1316+1701 (bottom).

RKS1318-1446

13:18:06 -14:46:48 V = 10.9 HIP064895 TIC 335636504
$N_{H/H}$ = 0 N_C = 2 D

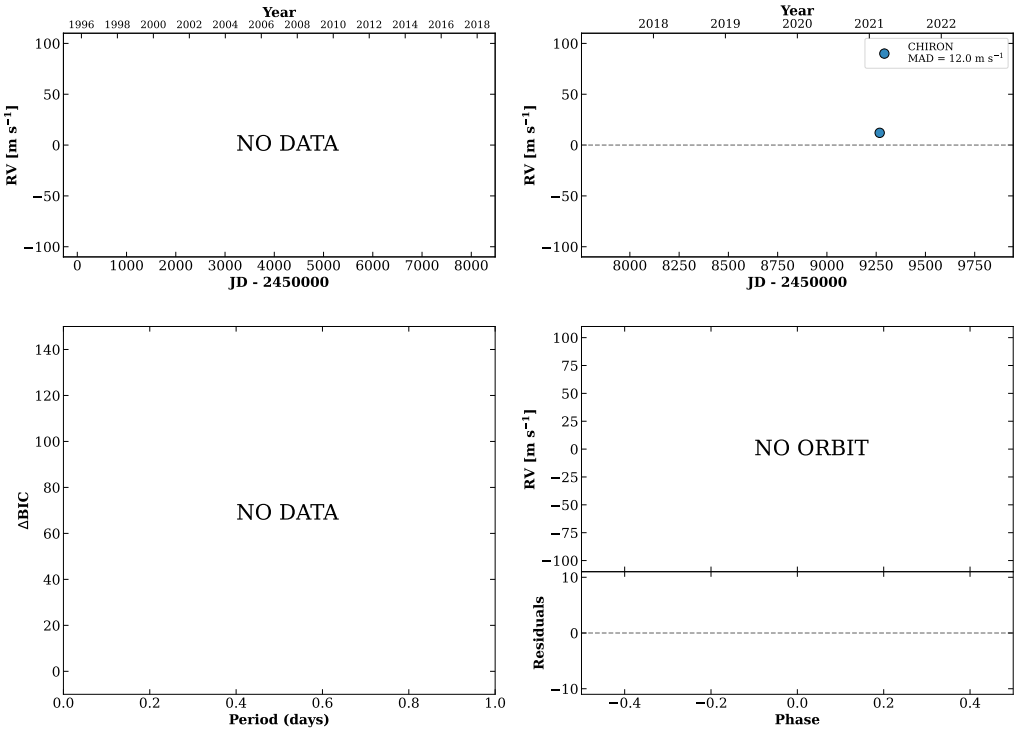

RKS1320+0407

13:20:44 +04:07:59 V = 8.6 HIP065121 TIC 393649309
$N_{H/H}$ = 0 N_C = 1

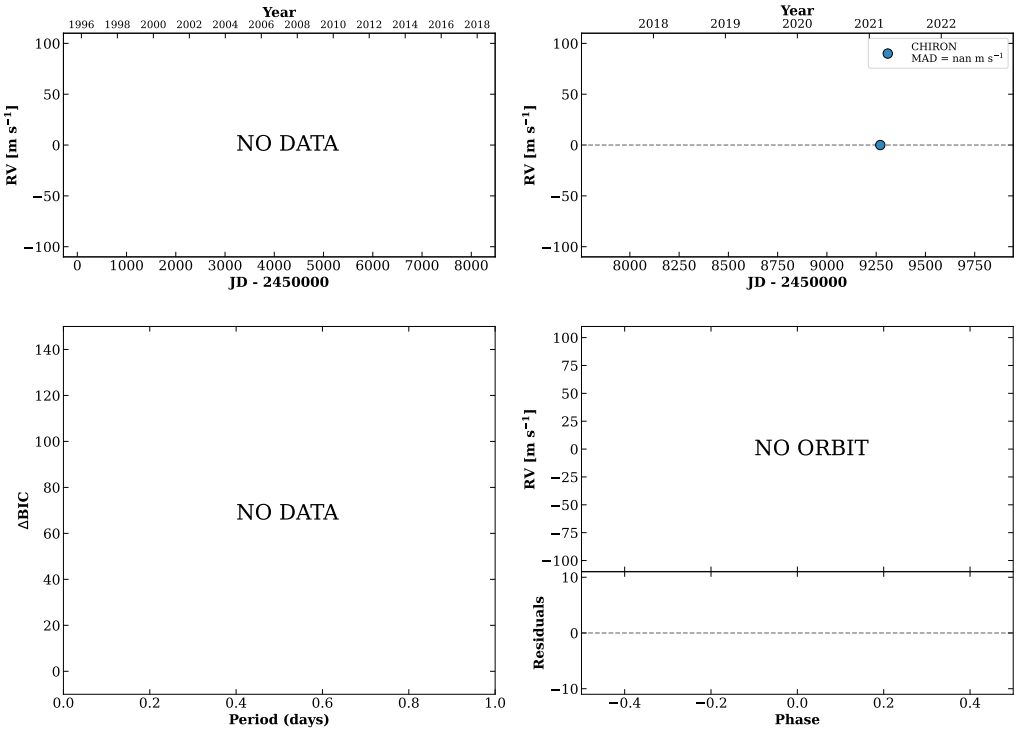

Figure 220 RV results for RKS1318-1446 (top) and RKS1320+0407 (bottom).

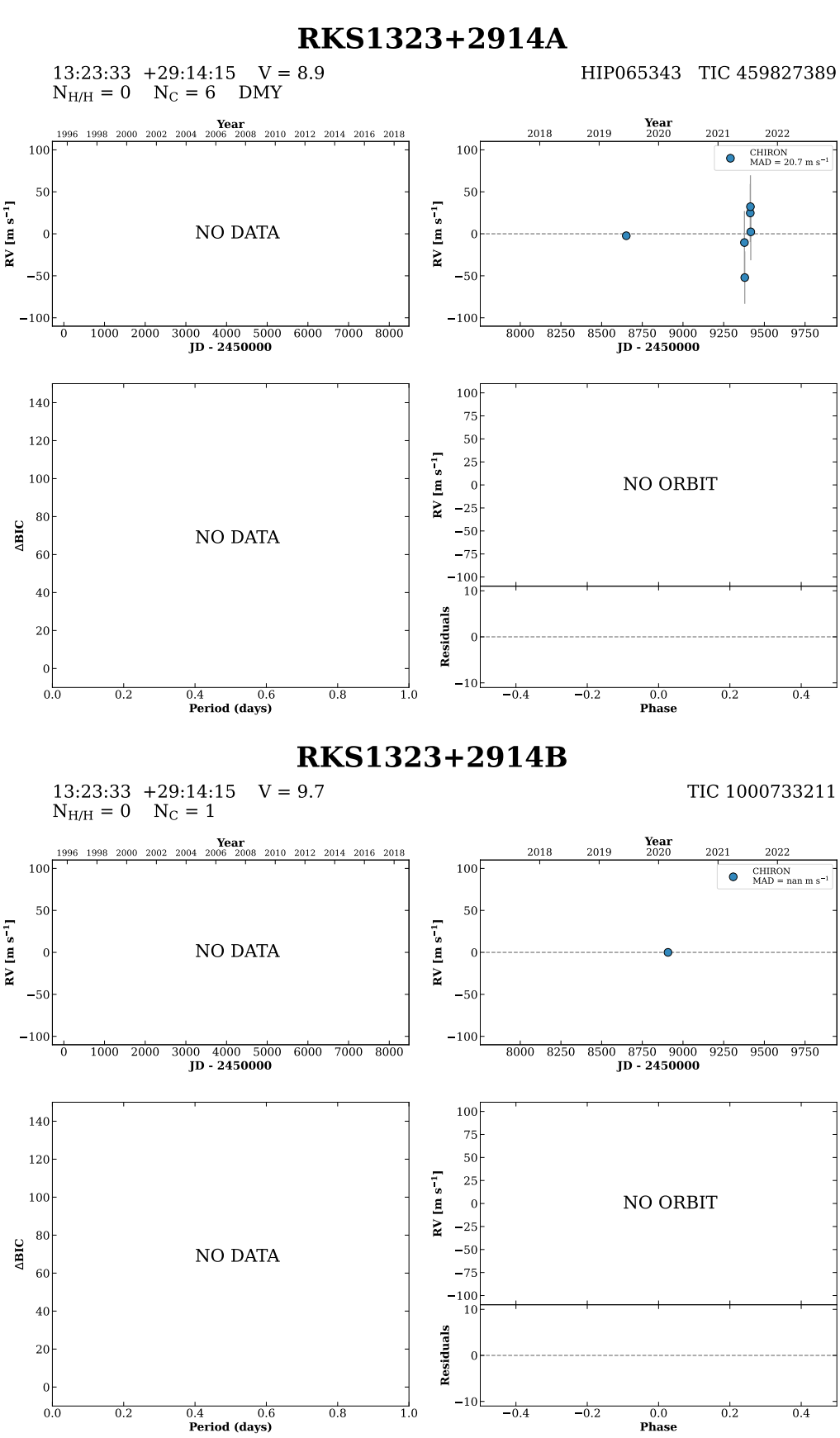

Figure 221 RV results for RKS1323+2914A (top) and RKS1323+2914B (bottom).

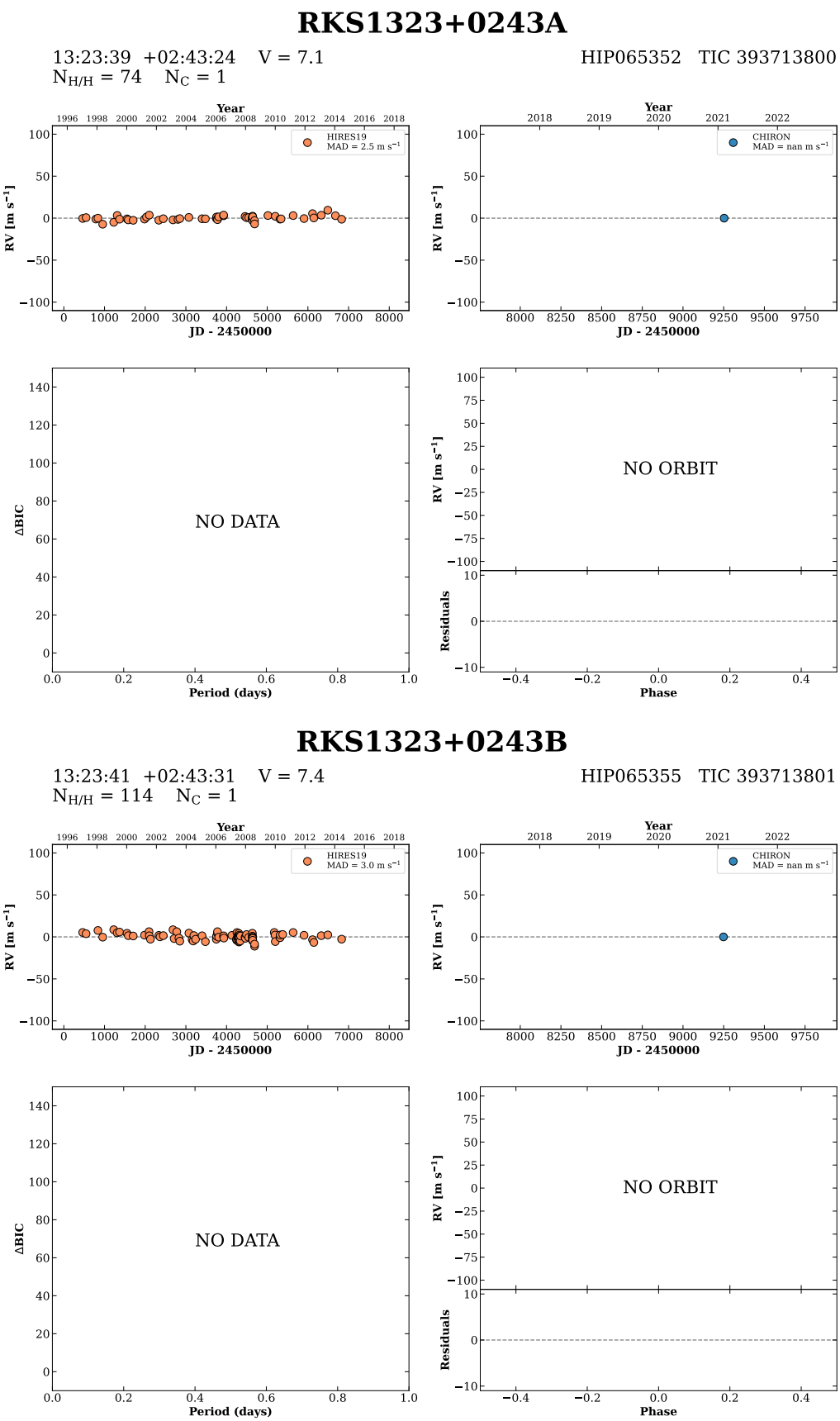

Figure 222 RV results for RKS1323+0243A (top) and RKS1323+0243B (bottom).

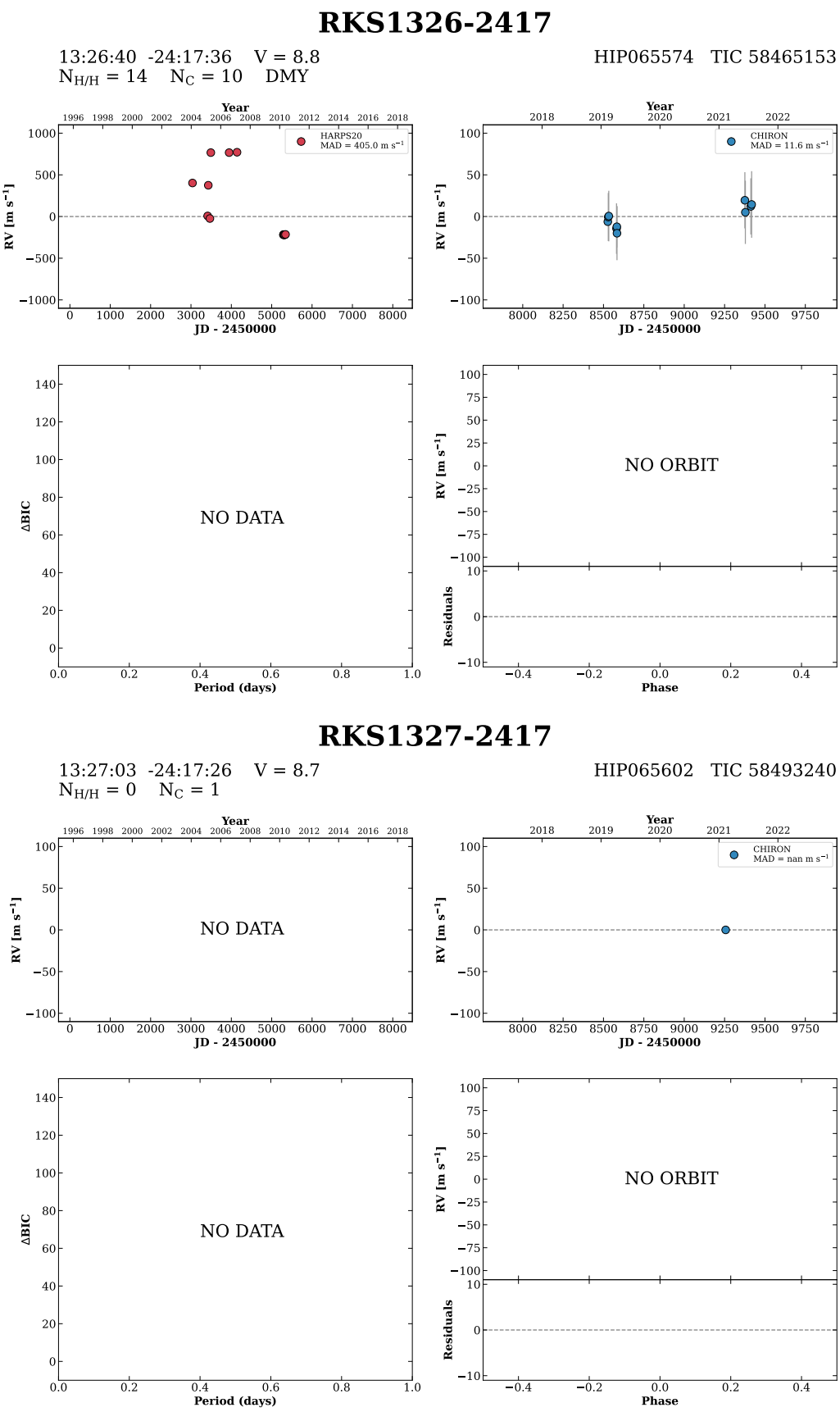

Figure 223 RV results for RKS1326-2417 (top) and RKS1327-2417 (bottom).

RKS1331-0219

13:31:40 -02:19:03 V = 7.3 HIP065982 TIC 130712175
$N_{H/H}$ = 0 N_C = 1

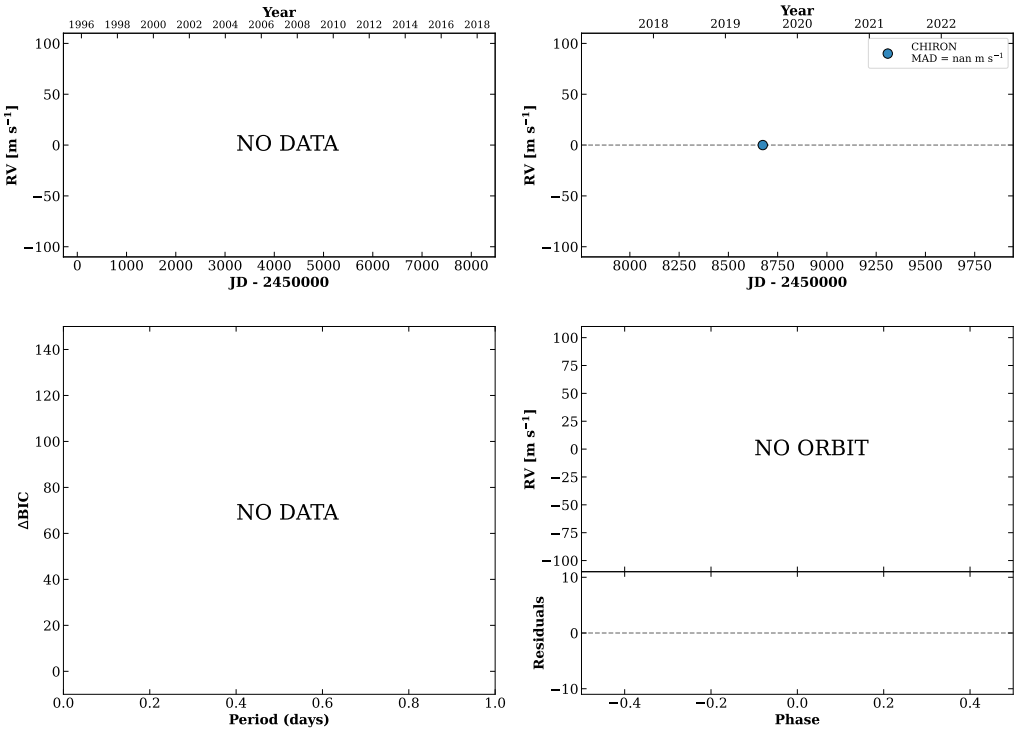

RKS1333+0835

13:33:32 +08:35:12 V = 8.0 HIP066147 TIC 378993741
$N_{H/H}$ = 24 N_C = 1

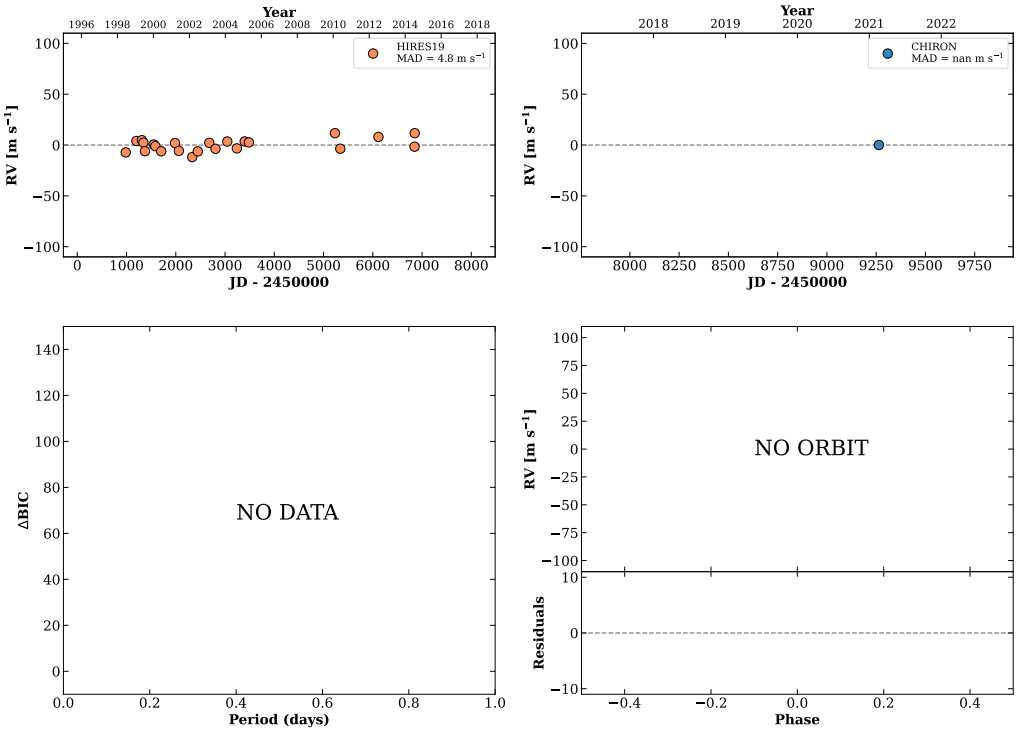

Figure 224 RV results for RKS1331-0219 (top) and RKS1333+0835 (bottom).

RKS1334-0018

13:34:16 -00:18:50 V = 7.4 HIP066212 TIC 130725942
$N_{H/H}$ = 0 N_C = 1

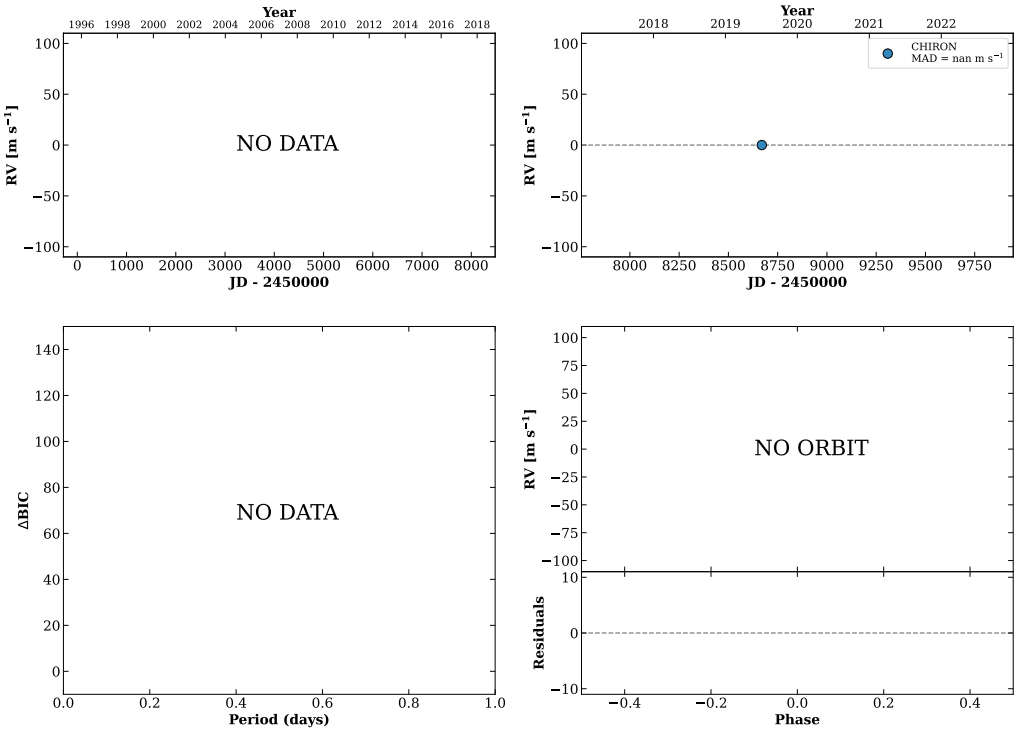

RKS1334+0440

13:34:22 +04:40:03 V = 9.9 HIP066222 TIC 365159477
$N_{H/H}$ = 12 N_C = 1

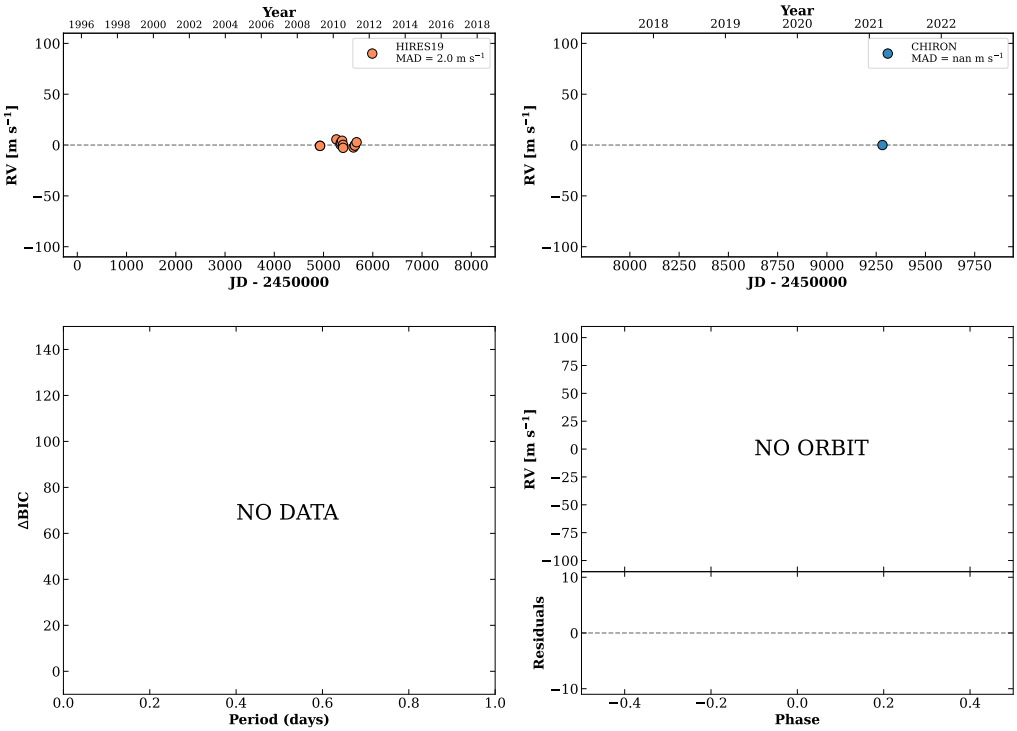

Figure 225 RV results for RKS1334-0018 (top) and RKS1334+0440 (bottom).

RKS1334-0820

13:34:43 -08:20:31 V = 9.2 HIP066252 TIC 659763
$N_{H/H}$ = 17 N_C = 1

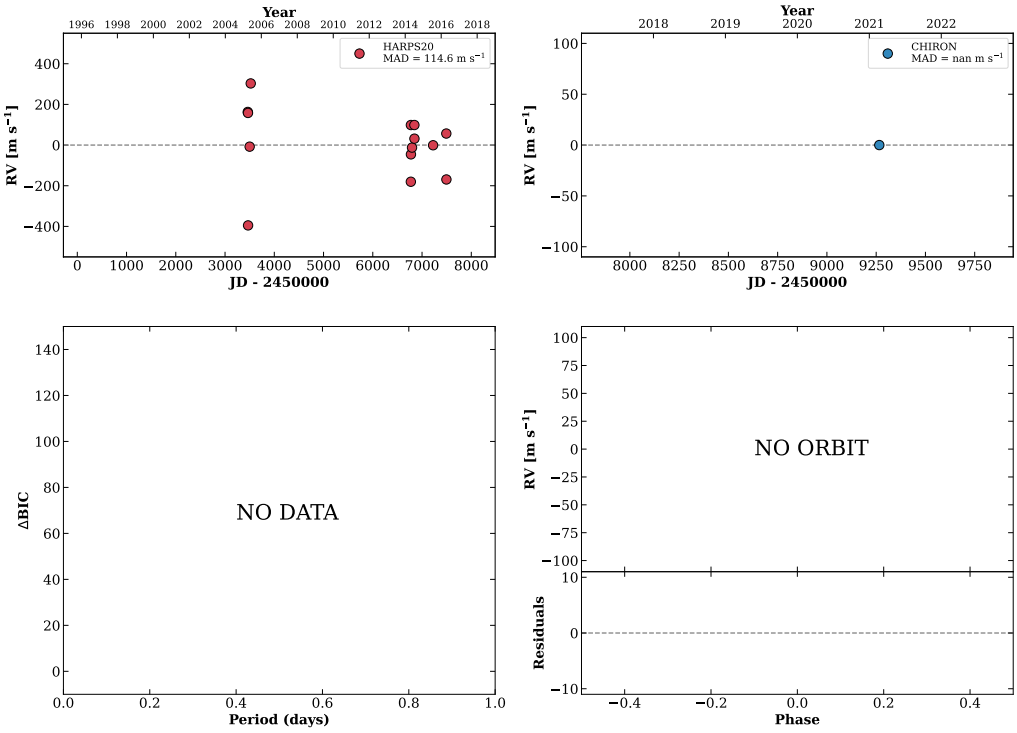

RKS1335+0650

13:35:06 +06:50:28 V = 8.9 HIP066283 TIC 379052876
$N_{H/H}$ = 7 N_C = 1

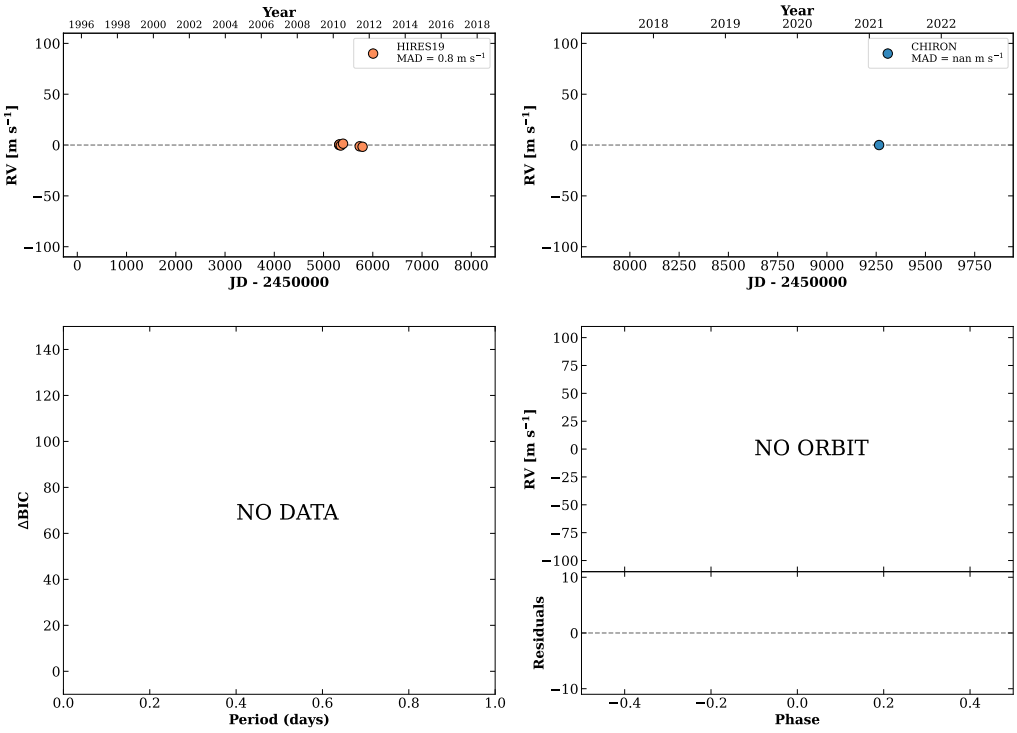

Figure 226 RV results for RKS1334-0820 (top) and RKS1335+0650 (bottom).

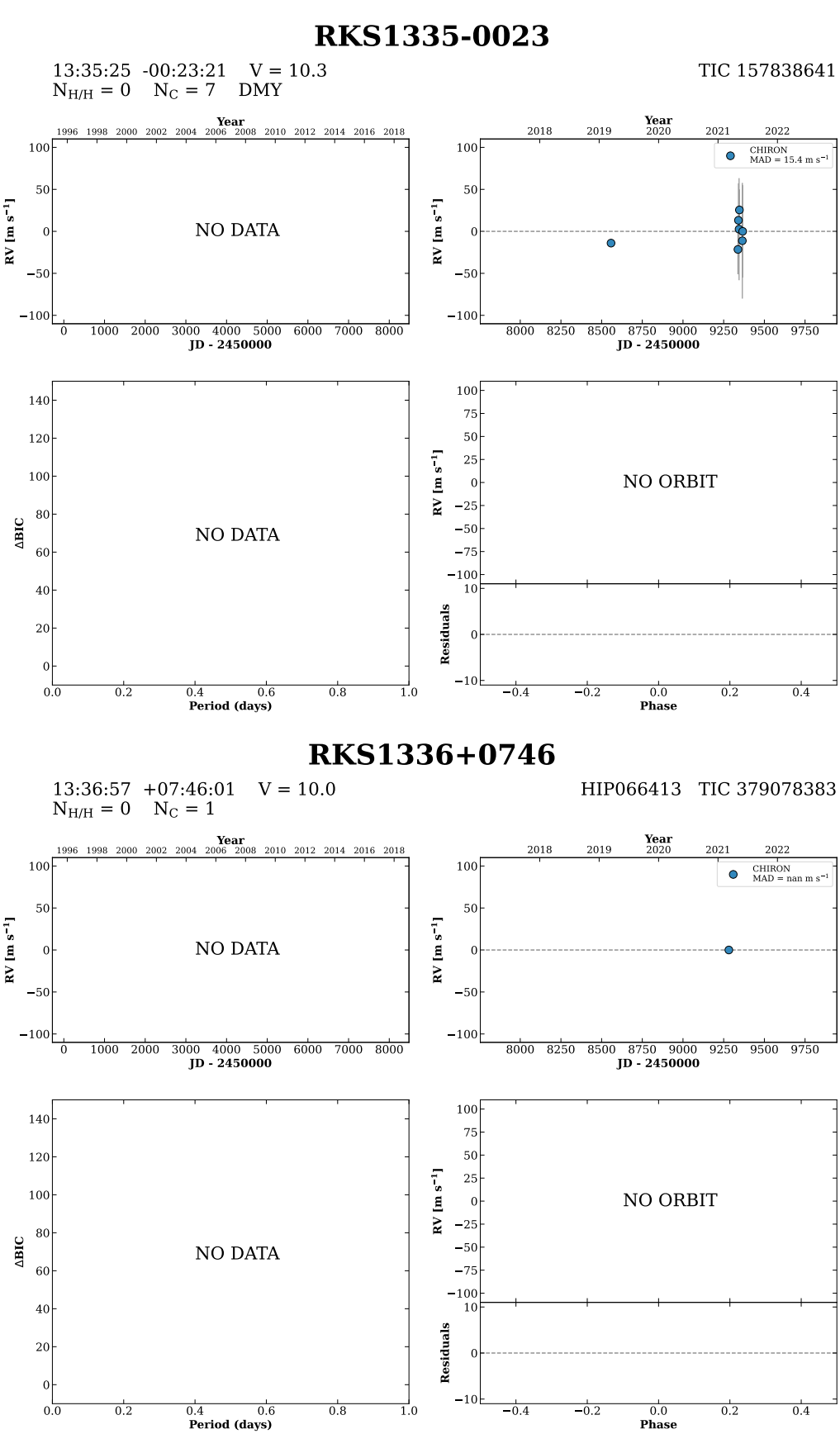

Figure 227 RV results for RKS1335-0023 (top) and RKS1336+0746 (bottom).

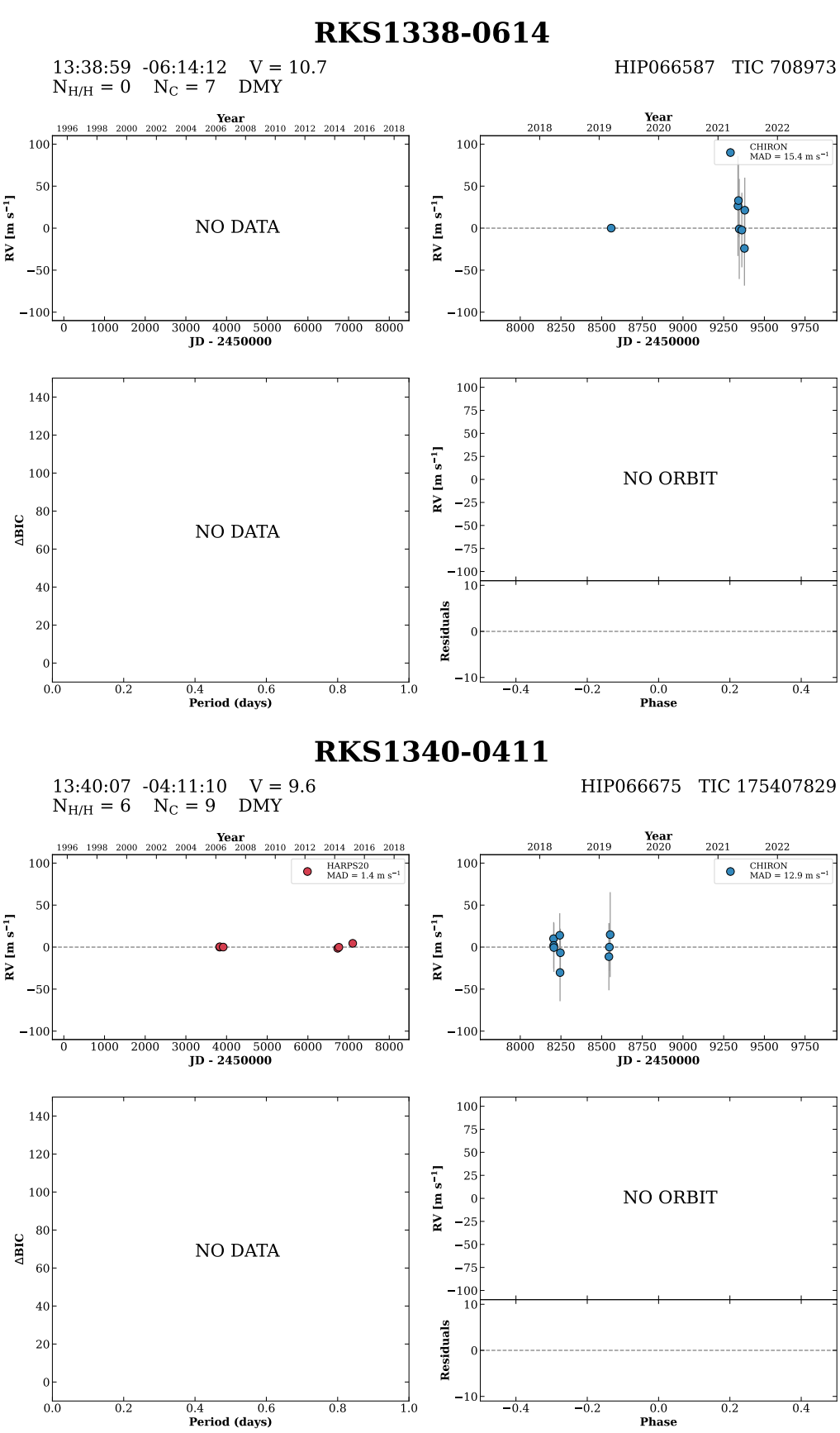

Figure 228 RV results for RKS1338-0614 (top) and RKS1340-0411 (bottom).

RKS1341-0007

13:41:56 -00:07:45 V = 9.8 HIP066840 TIC 61098813
$N_{H/H}$ = 13 N_C = 1

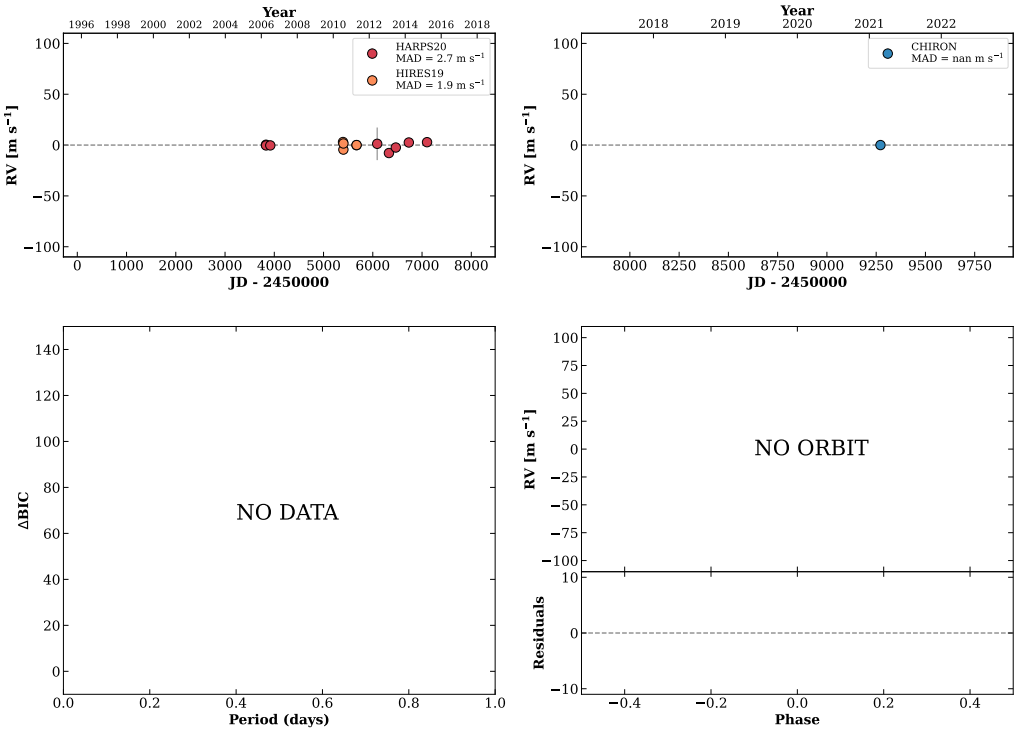

RKS1342-0141

13:42:26 -01:41:11 V = 9.2 HIP066886 TIC 61110114
$N_{H/H}$ = 0 N_C = 1

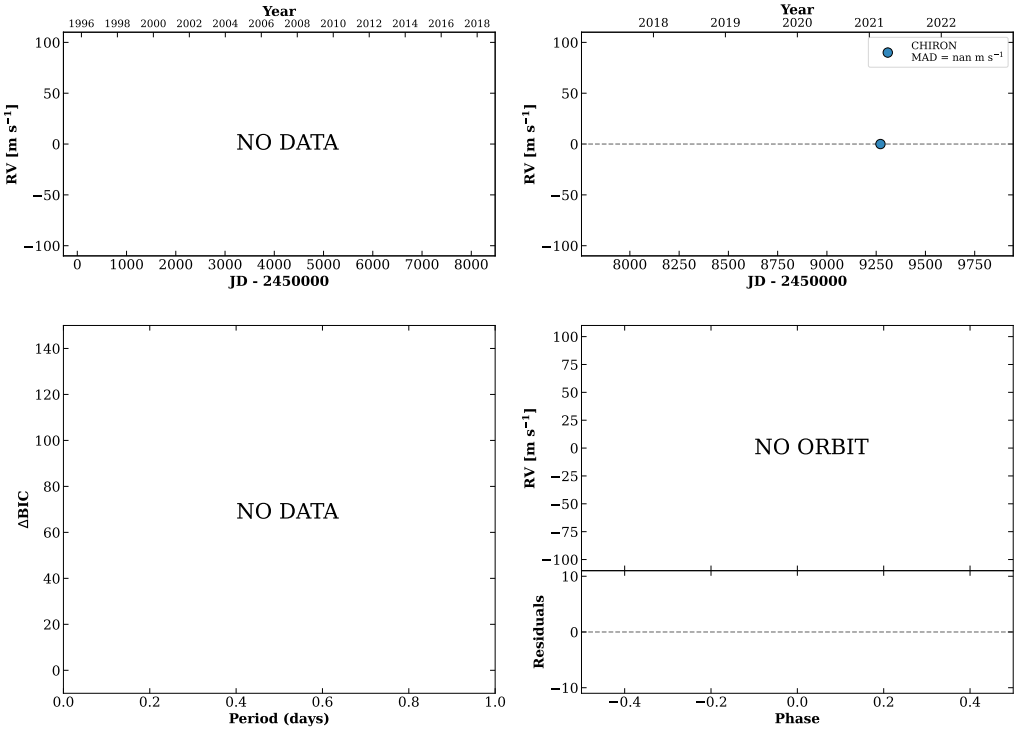

Figure 229 RV results for RKS1341-0007 (top) and RKS1342-0141 (bottom).

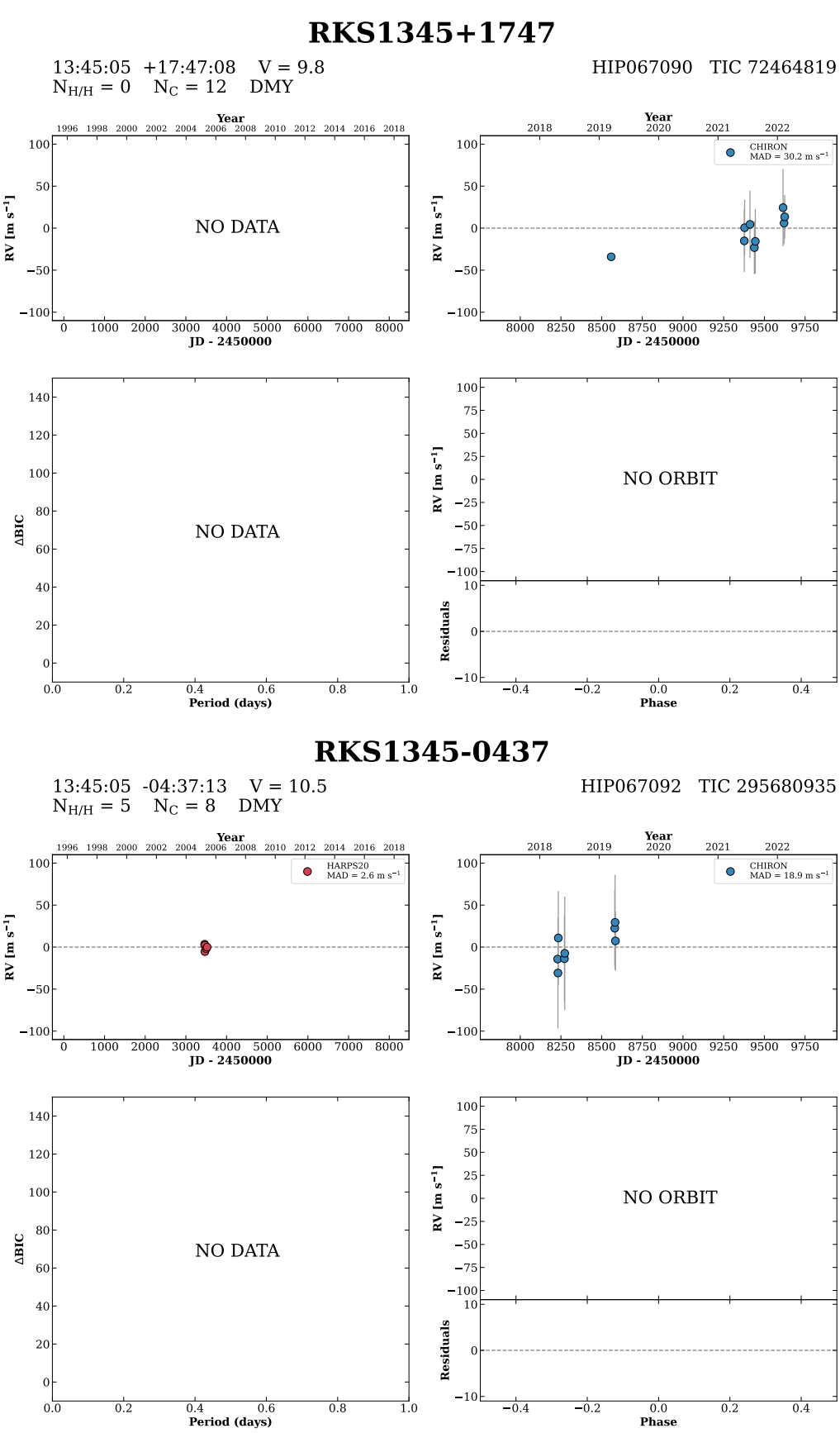

Figure 230 RV results for RKS1345+1747 (top) and RKS1345-0437 (bottom).

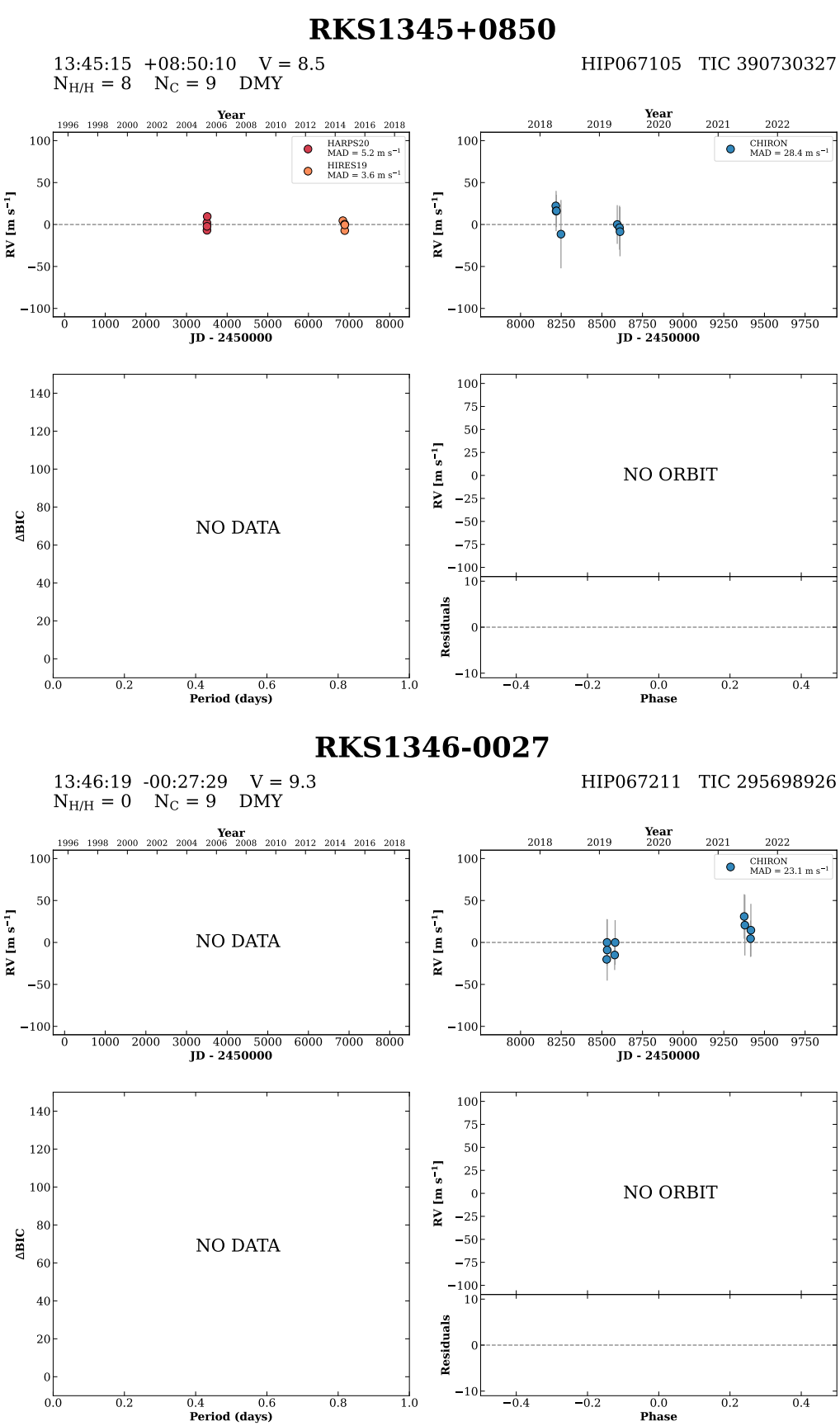

Figure 231 RV results for RKS1345+0850 (top) and RKS1346-0027 (bottom).

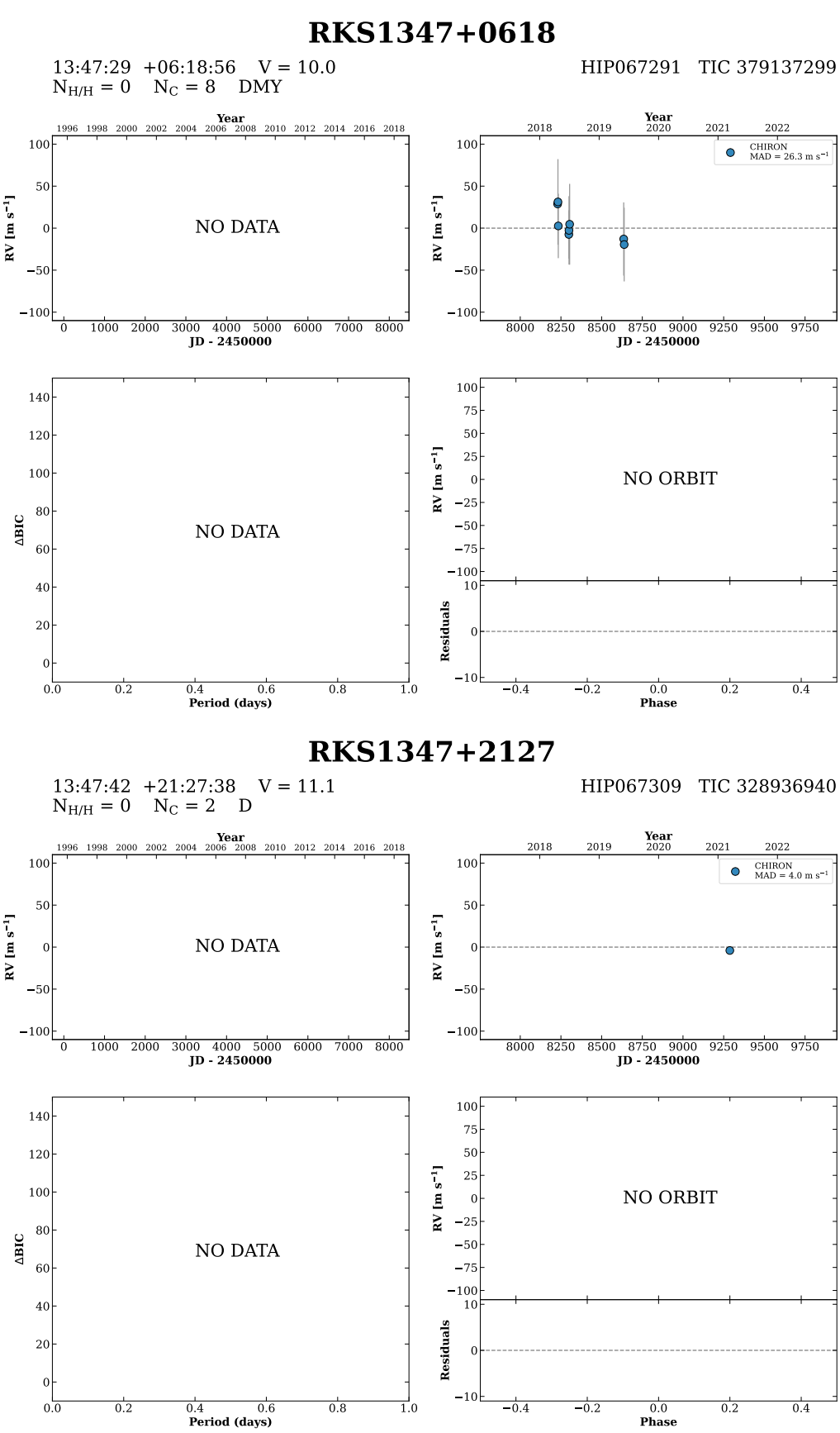

Figure 232 RV results for RKS1347+0618 (top) and RKS1347+2127 (bottom).

HIP067344

13:48:10 -10:47:20 V = 8.3 TIC 187309694
$N_{H/H}$ = 0 N_C = 9 DMY

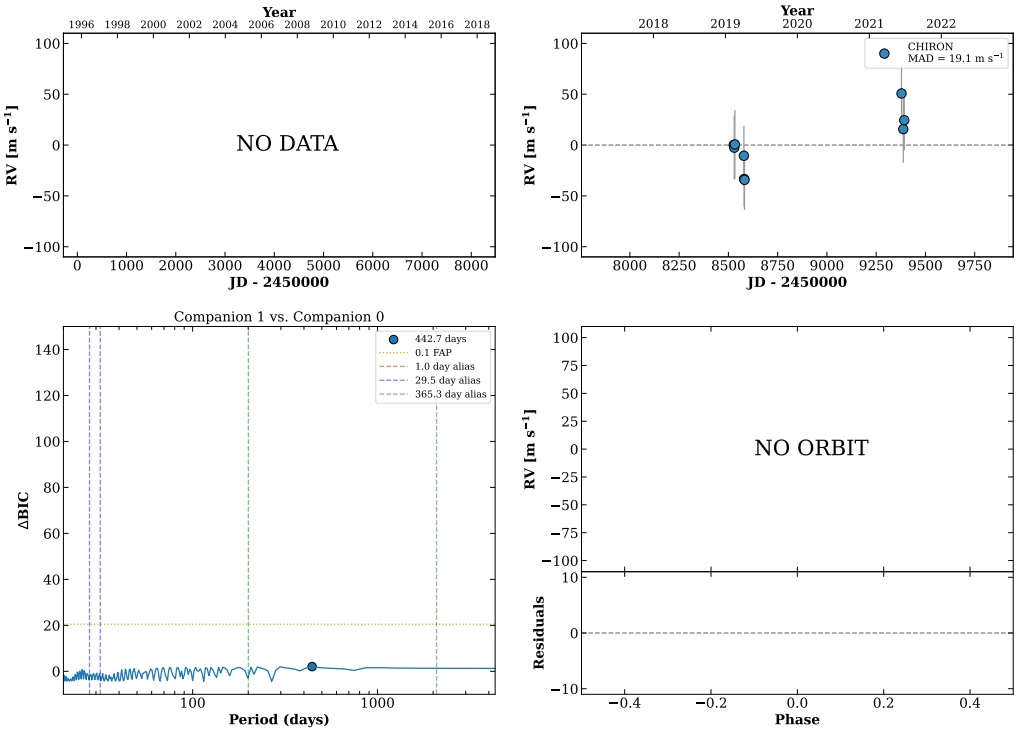

RKS1349+2658A

13:49:04 +26:58:48 V = 7.0 HIP067422 TIC 359220741
$N_{H/H}$ = 19 N_C = 1

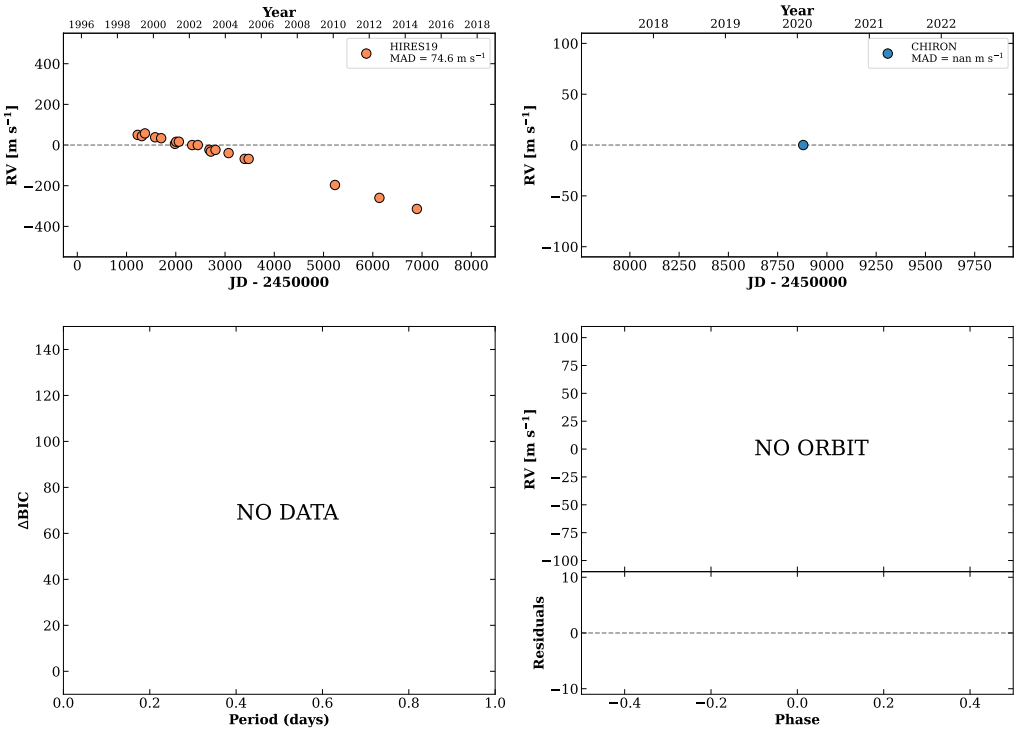

Figure 233 RV results for HIP067344 (top) and RKS1349+2658A (bottom).

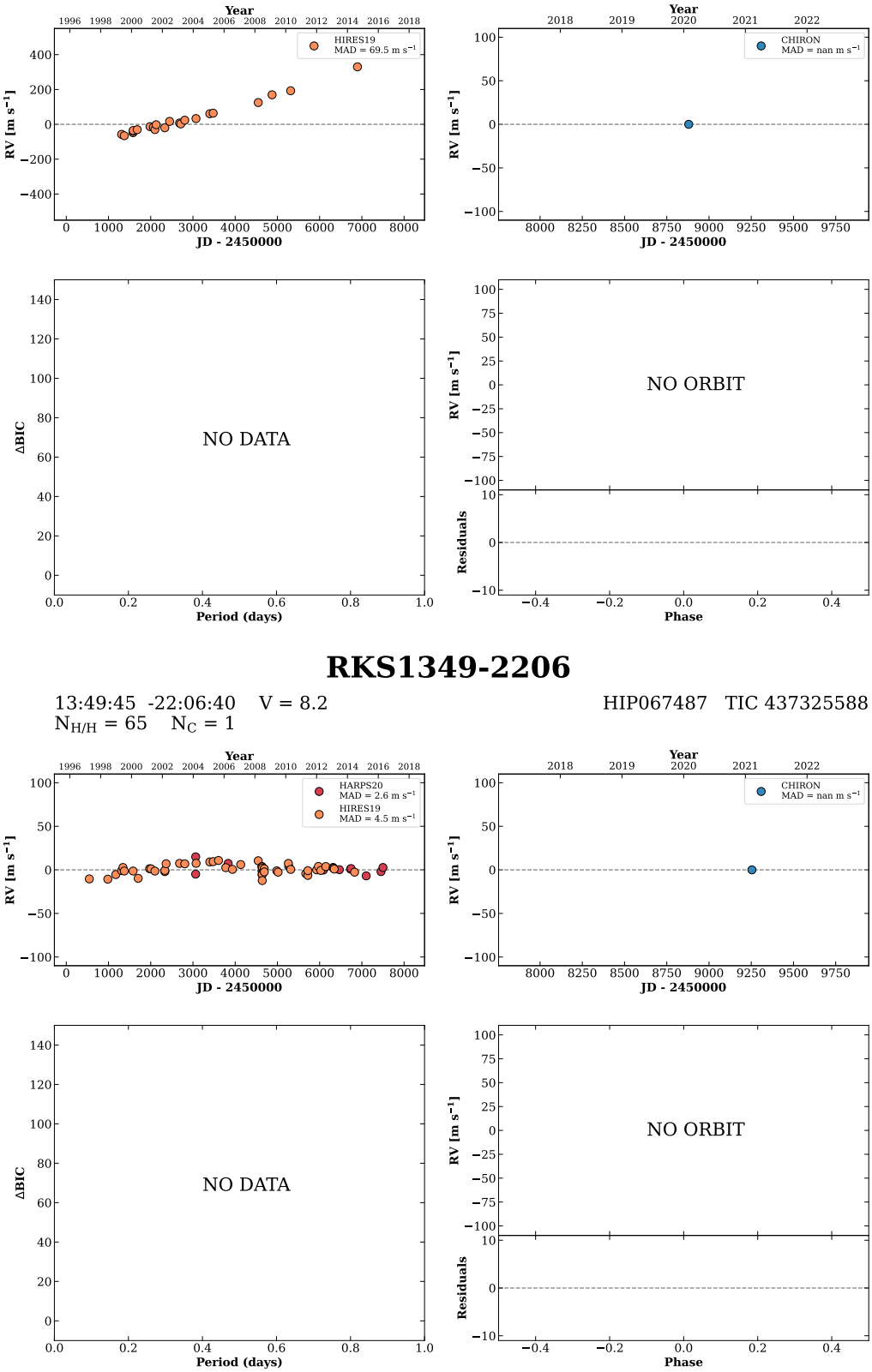

Figure 234 RV results for RKS1349+2658B (top) and RKS1349-2206 (bottom).

RKS1353+2748

13:53:05 +27:48:24 V = 8.4 HIP067773 TIC 258061897
$N_{H/H} = 0$ $N_C = 6$ DMY

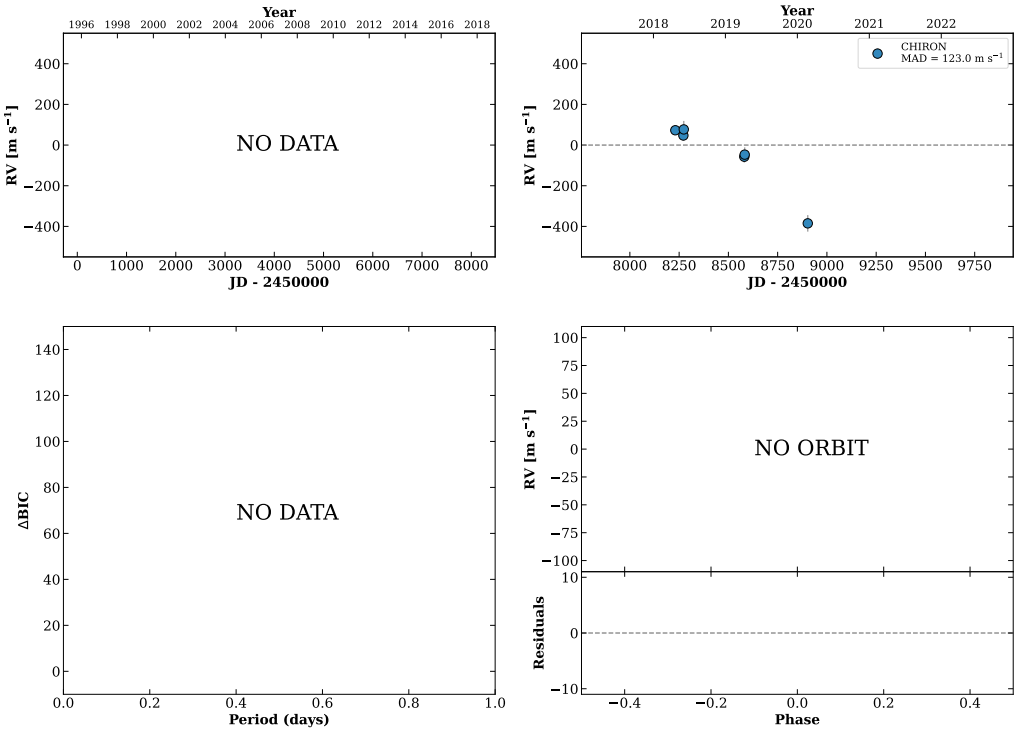

RKS1353+1256A

13:53:28 +12:56:33 V = 9.8 HIP067808 TIC 72578769
$N_{H/H} = 0$ $N_C = 39$ DMY

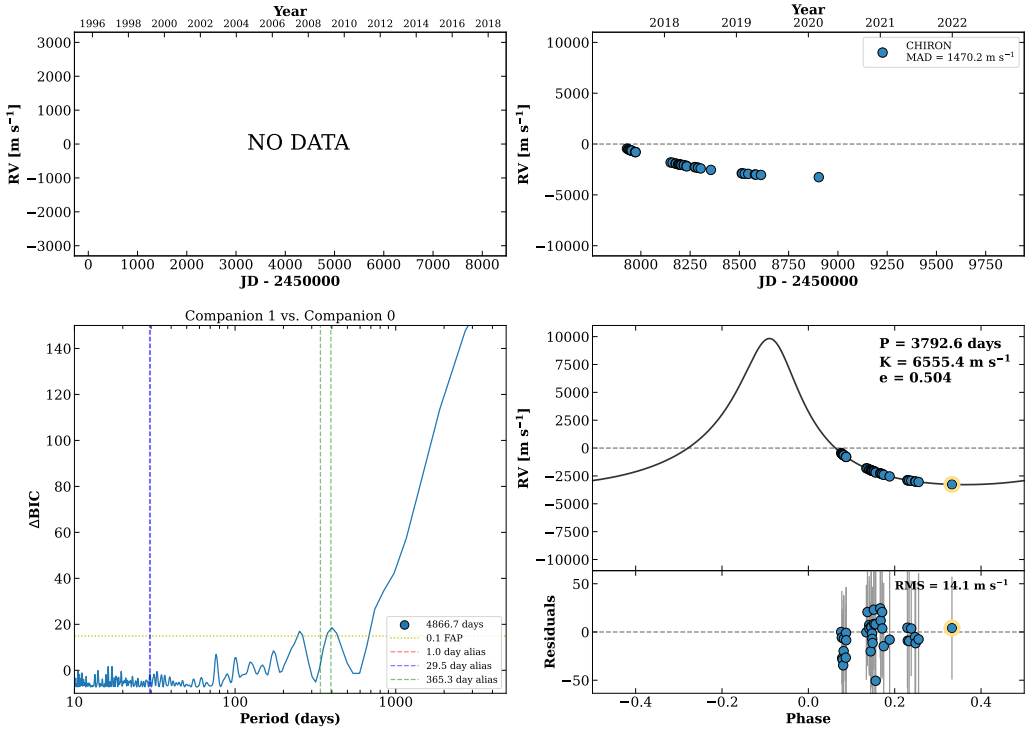

Figure 235 RV results for RKS1353+2748 (top) and RKS1353+1256A (bottom).

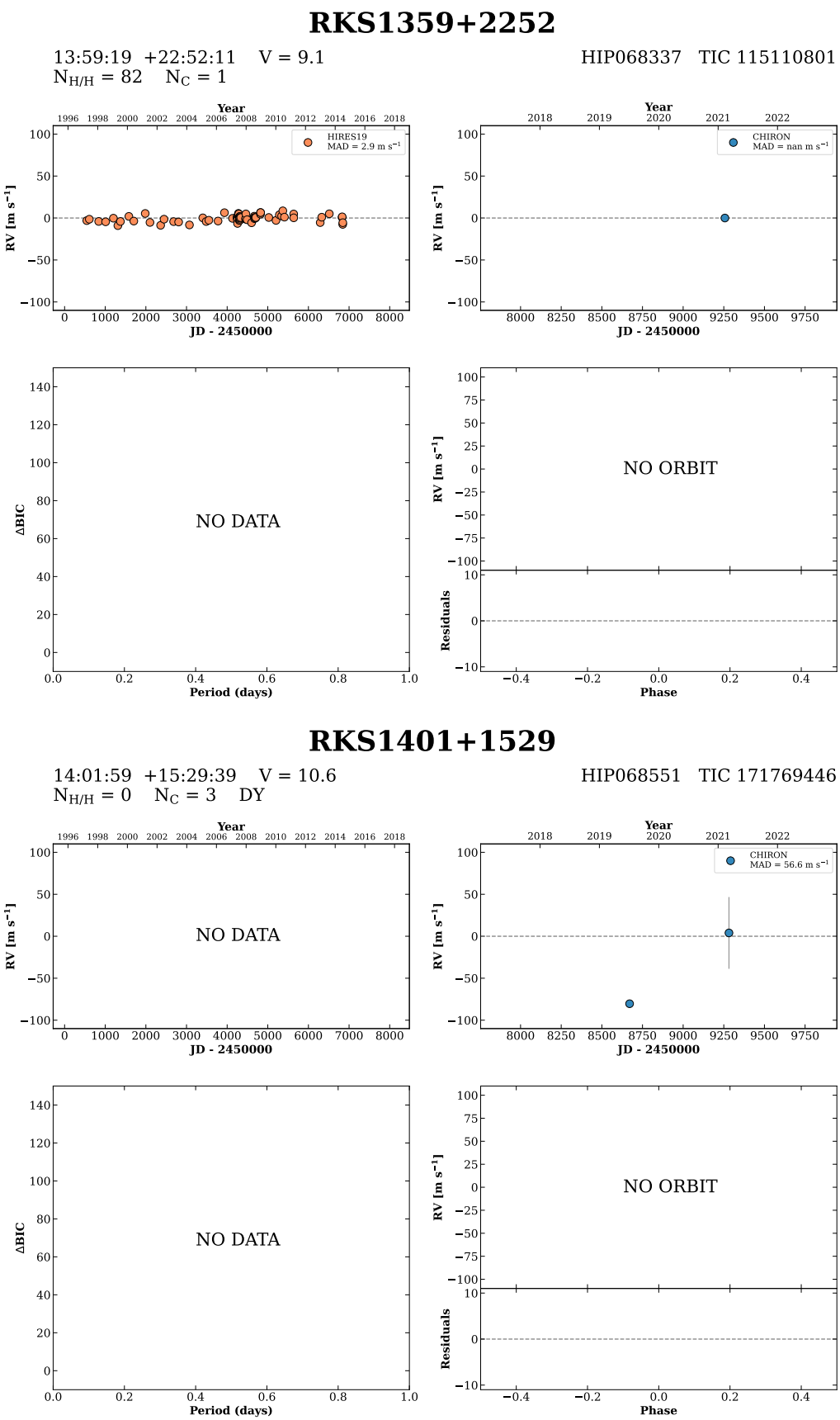

Figure 236 RV results for RKS1359+2252 (top) and RKS1401+1529 (bottom).

RKS1411-1236

14:11:46 -12:36:42 V = 7.9 HIP069357 TIC 308311310
$N_{H/H}$ = 37 N_C = 1

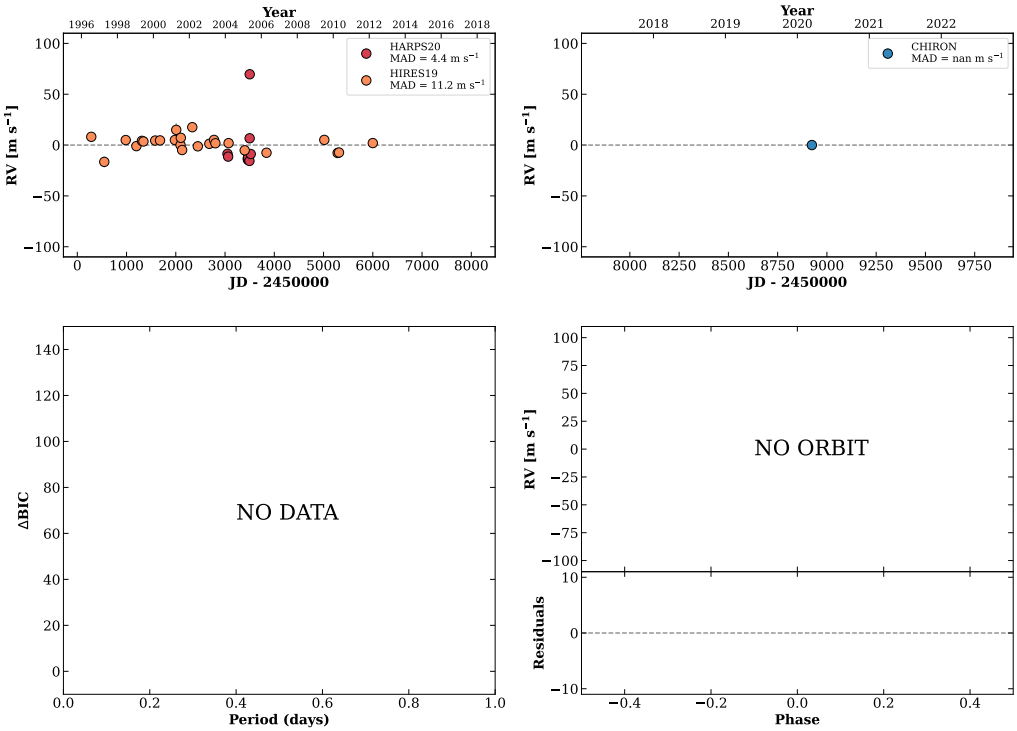

RKS1412+2348A

14:12:42 +23:48:52 V = 8.9 HIP069410 TIC 307797957
$N_{H/H}$ = 0 N_C = 10 DMY

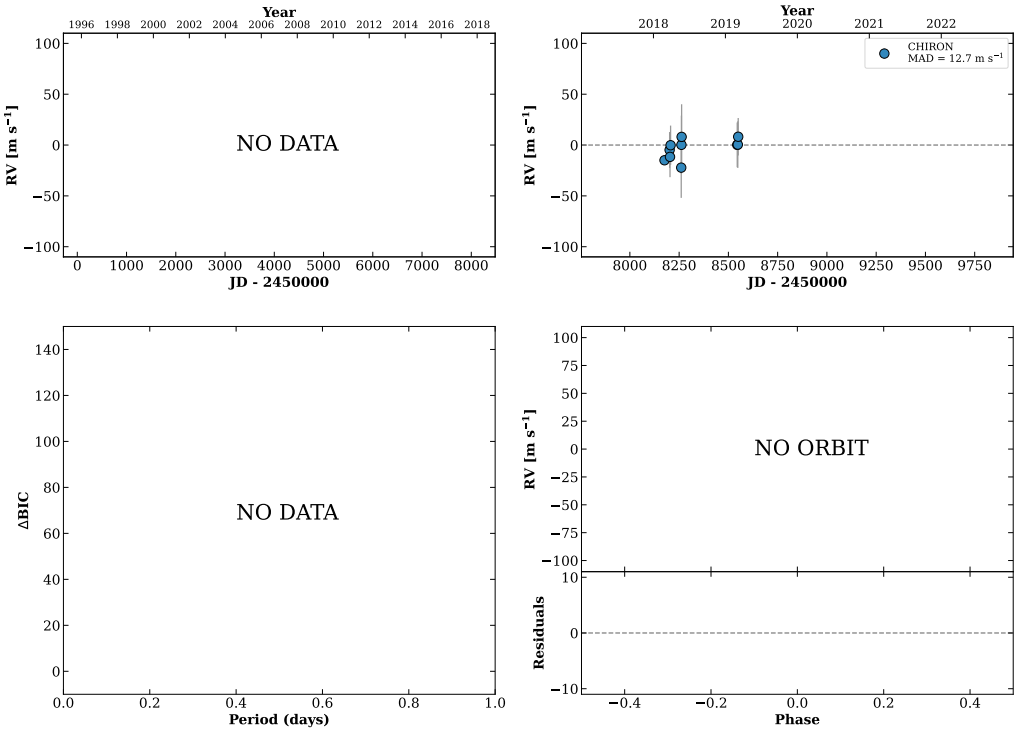

Figure 237 RV results for RKS1411-1236 (top) and RKS1412+2348A (bottom).

RKS1413-0657

14:13:31 -06:57:32 V = 10.1 HIP069485 TIC 5979133
$N_{H/H}$ = 6 N_C = 8 DMY

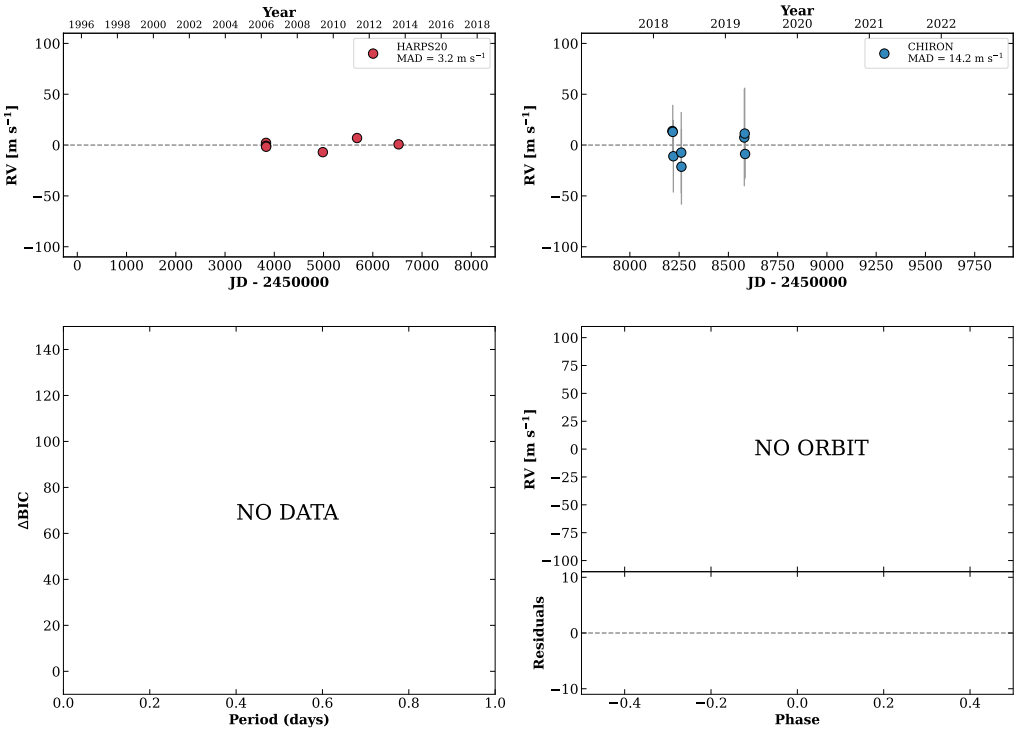

RKS1414-1521

14:14:21 -15:21:22 V = 10.2 HIP069562 TIC 157414031
$N_{H/H}$ = 0 N_C = 2 Y

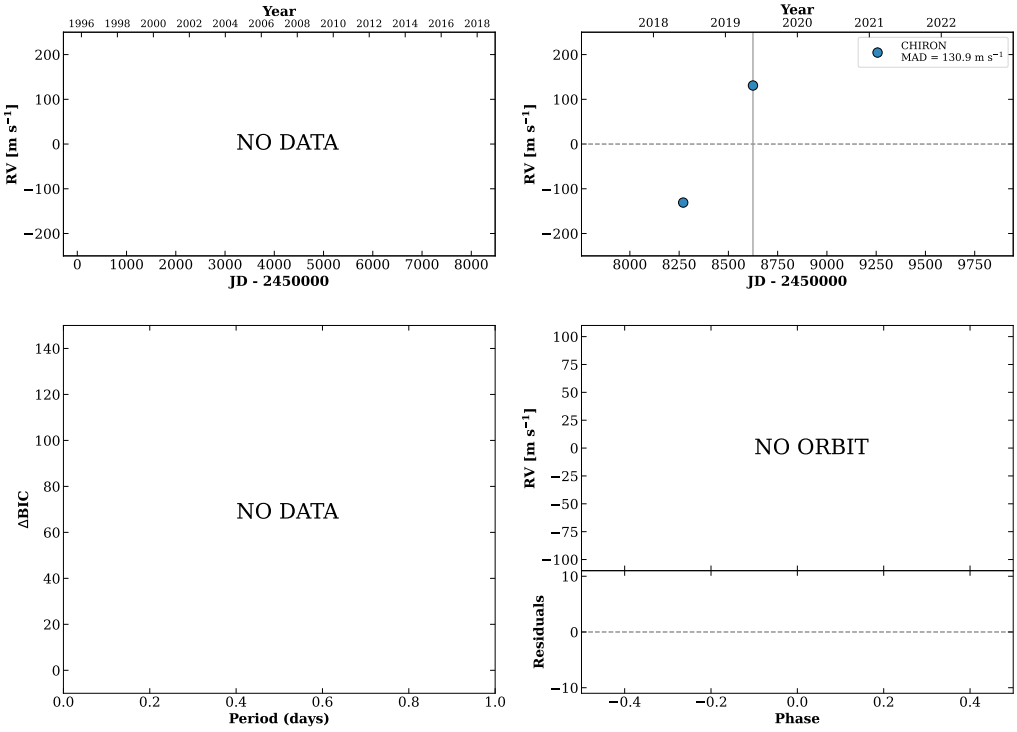

Figure 238 RV results for RKS1413-0657 (top) and RKS1414-1521 (bottom).

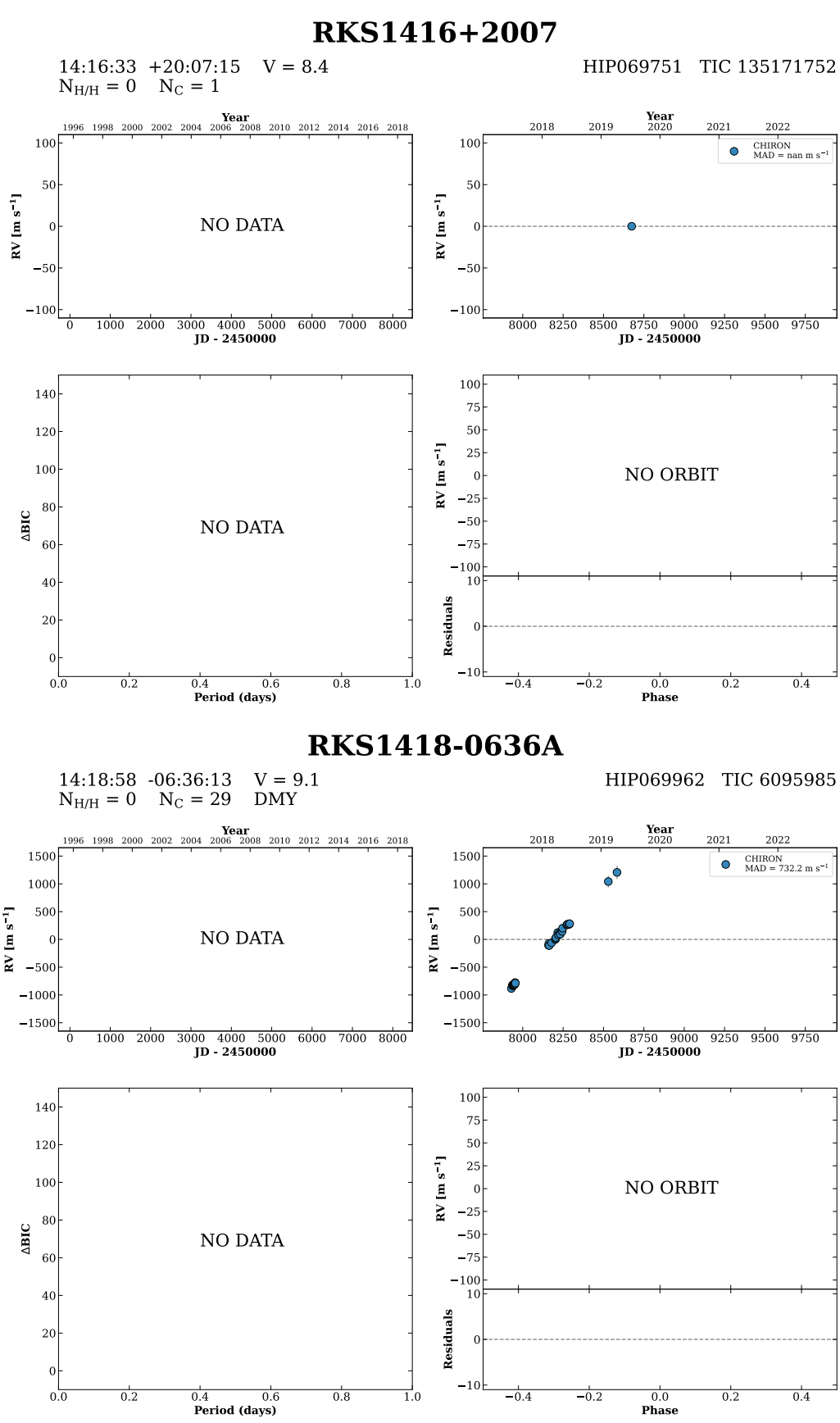

Figure 239 RV results for RKS1416+2007 (top) and RKS1418-0636A (bottom).

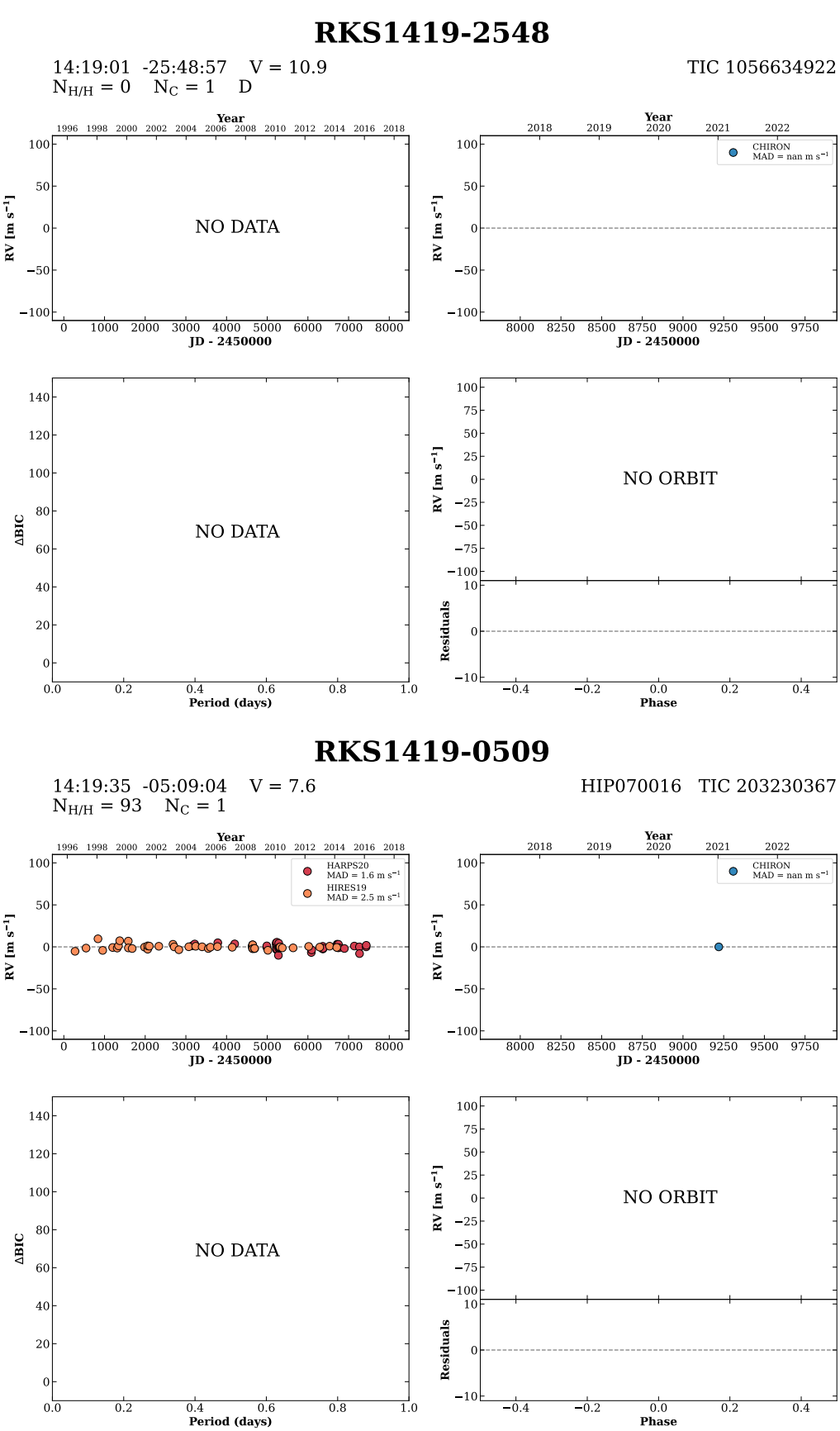

Figure 240 RV results for RKS1419-2548 (top) and RKS1419-0509 (bottom).

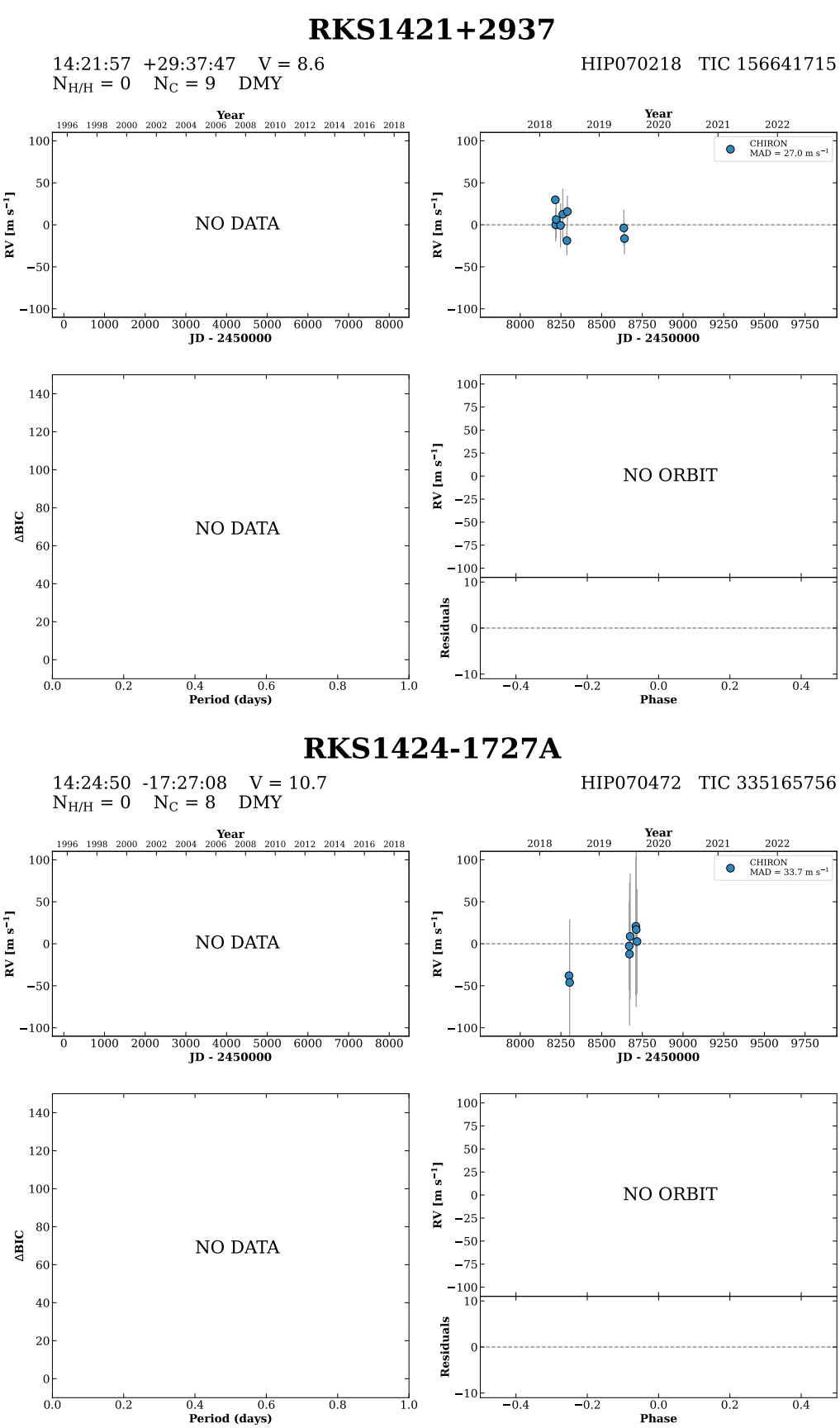

Figure 241 RV results for RKS1421+2937 (top) and RKS1424-1727A (bottom).

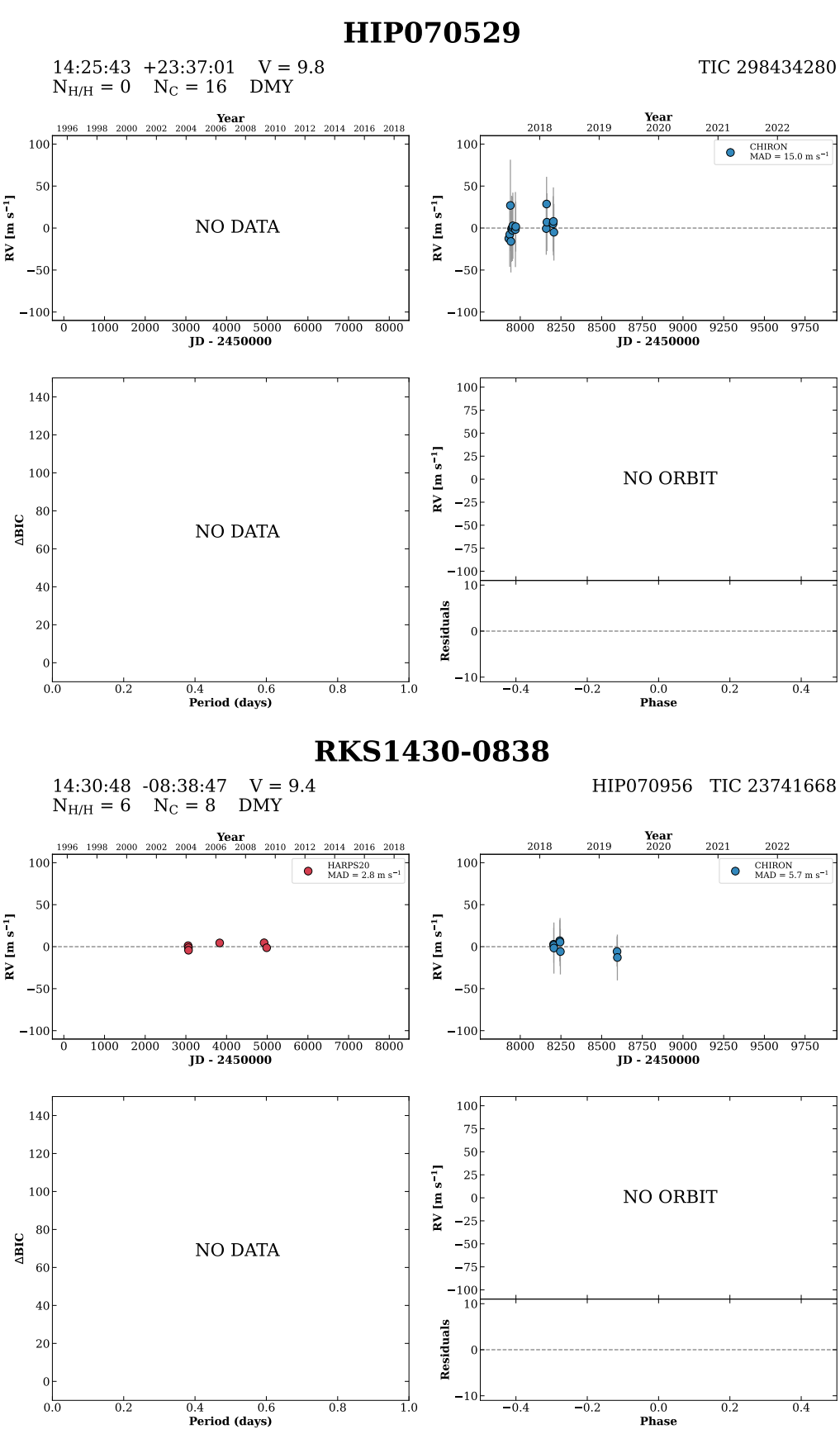

Figure 242 RV results for HIP070529 (top) and RKS1430-0838 (bottom).

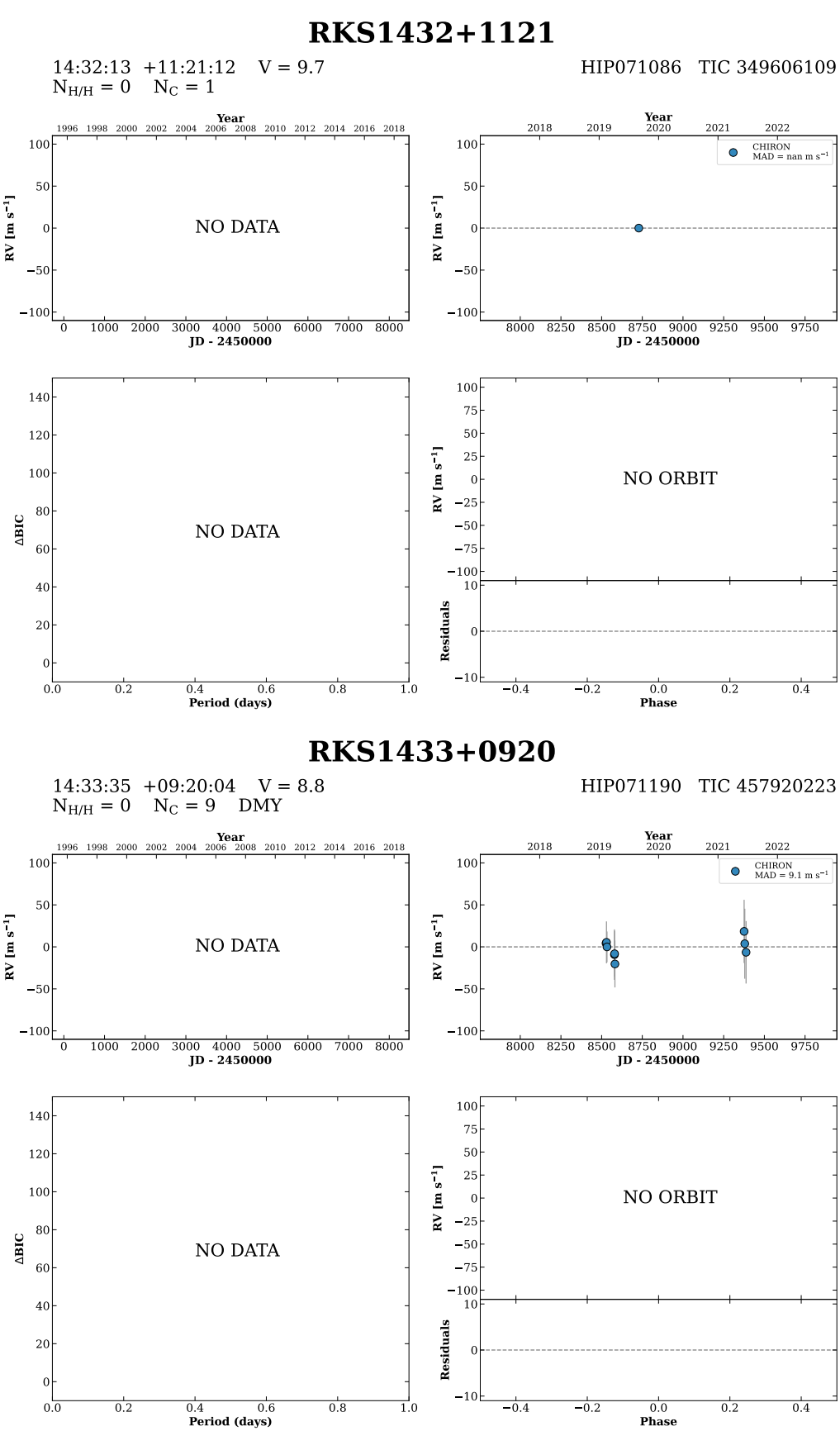

Figure 243 RV results for RKS1432+1121 (top) and RKS1433+0920 (bottom).

RKS1436+0944

14:36:01 +09:44:47 V = 7.5 HIP071395 TIC 349606708
$N_{H/H}$ = 133 N_C = 1

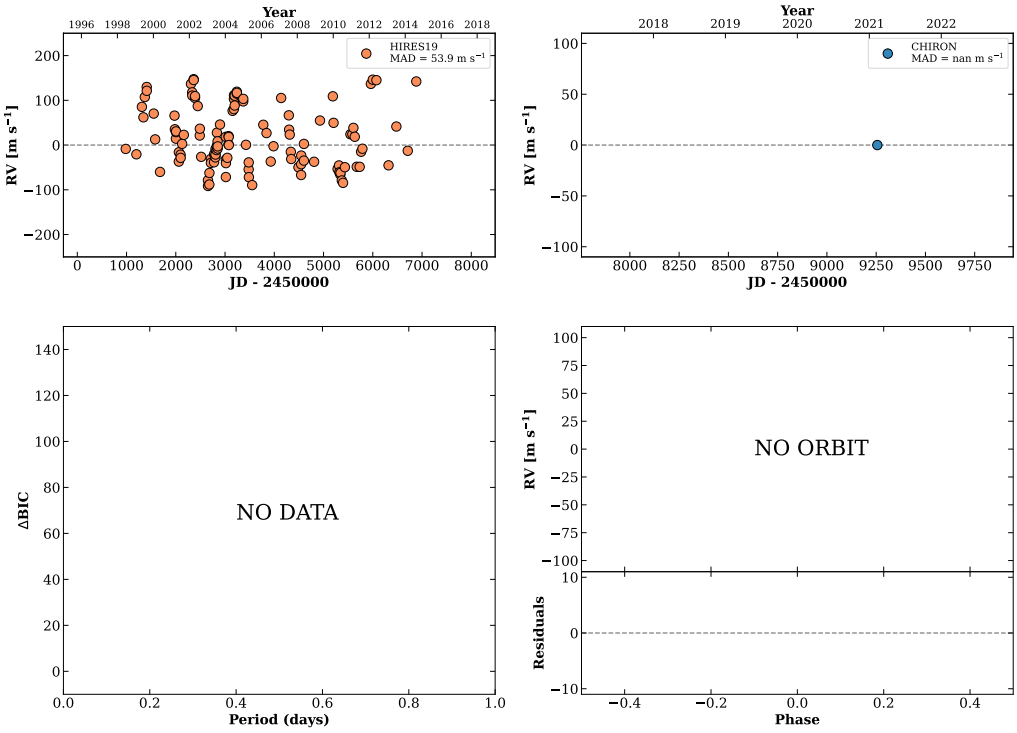

RKS1437-2548

14:37:05 -25:48:09 V = 8.3 HIP071481 TIC 16855
$N_{H/H}$ = 30 N_C = 2 D

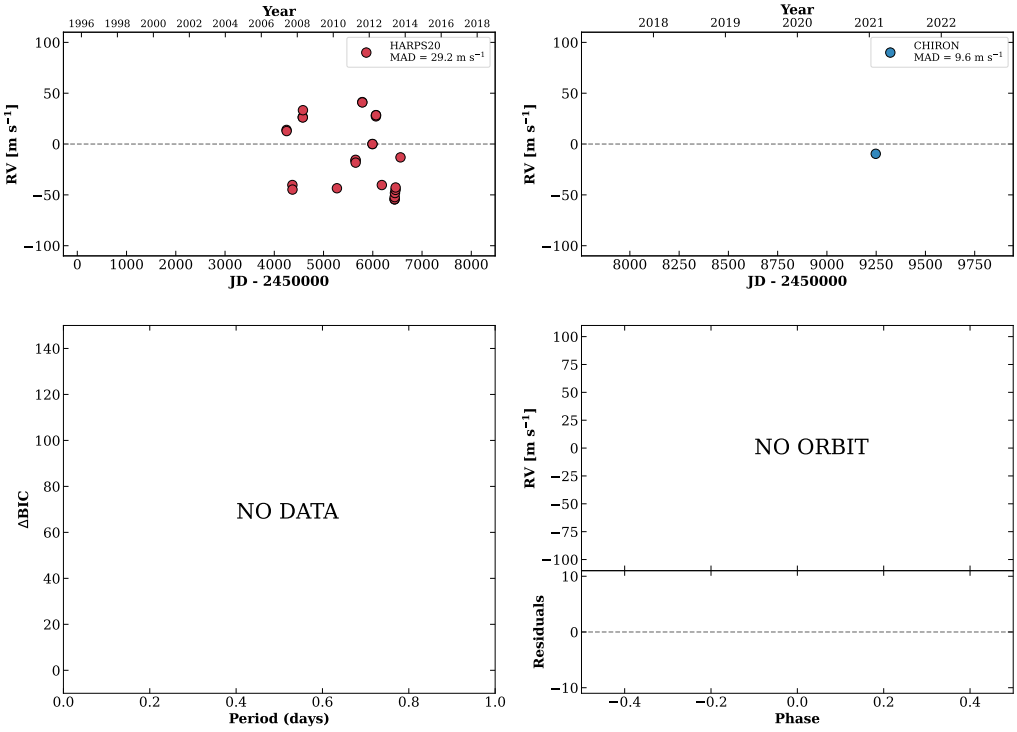

Figure 244 RV results for RKS1436+0944 (top) and RKS1437-2548 (bottom).

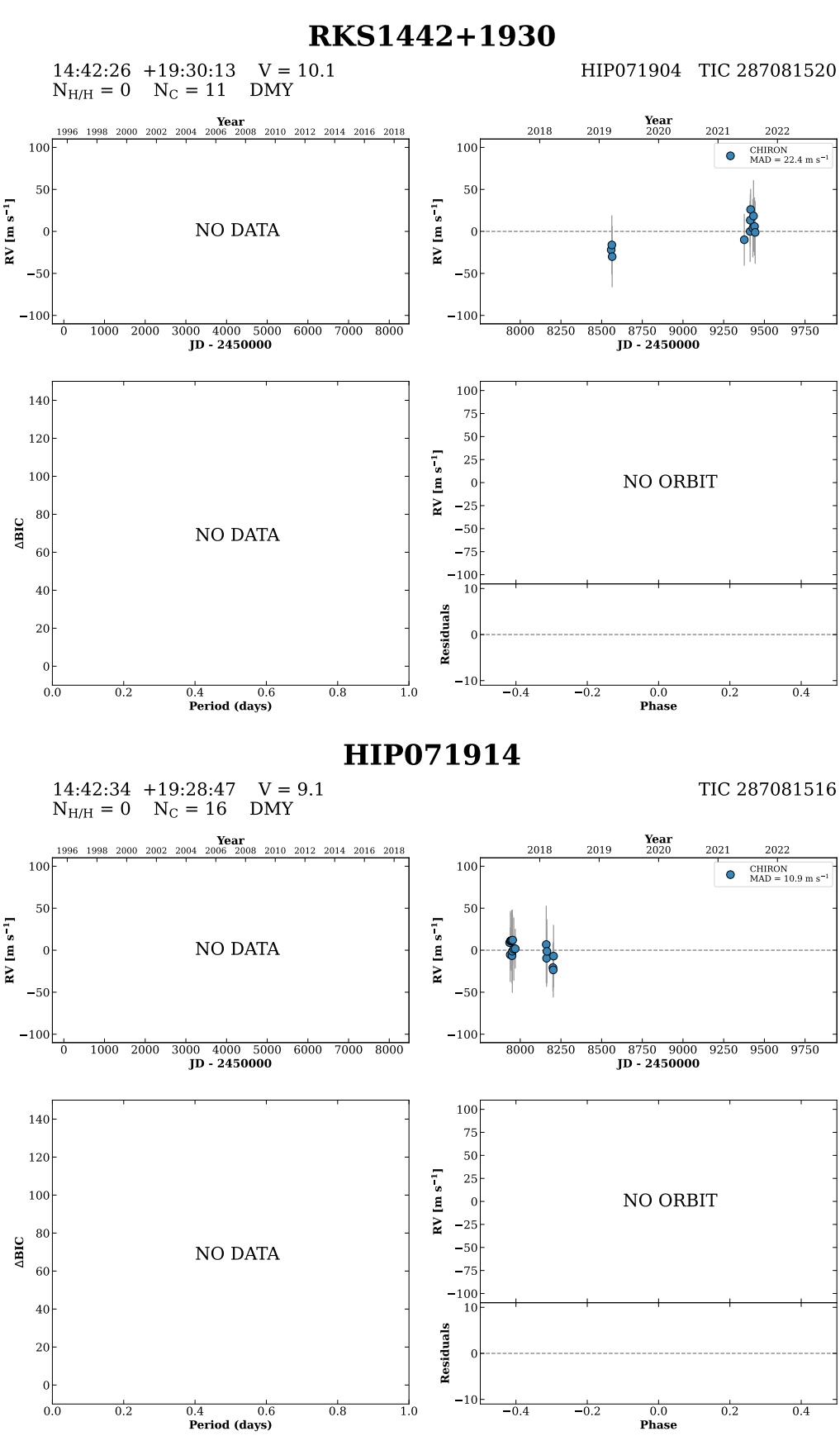

Figure 245 RV results for RKS1442+1930 (top) and HIP071914 (bottom).

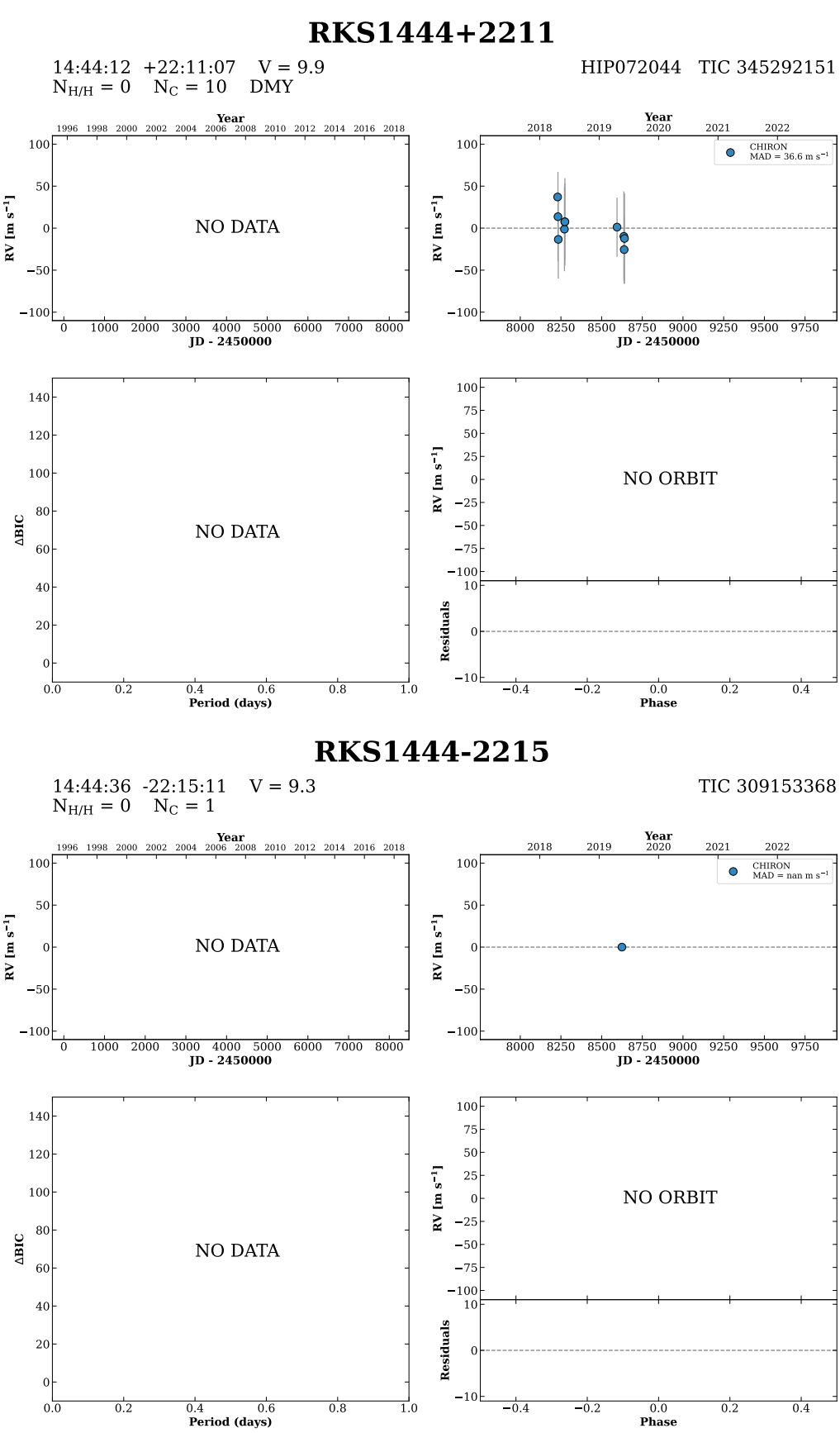

Figure 246 RV results for RKS1444+2211 (top) and RKS1444-2215 (bottom).

RKS1445+1350

14:45:24 +13:50:47 V = 7.9 HIP072146 TIC 450354414
$N_{H/H}$ = 13 N_C = 1

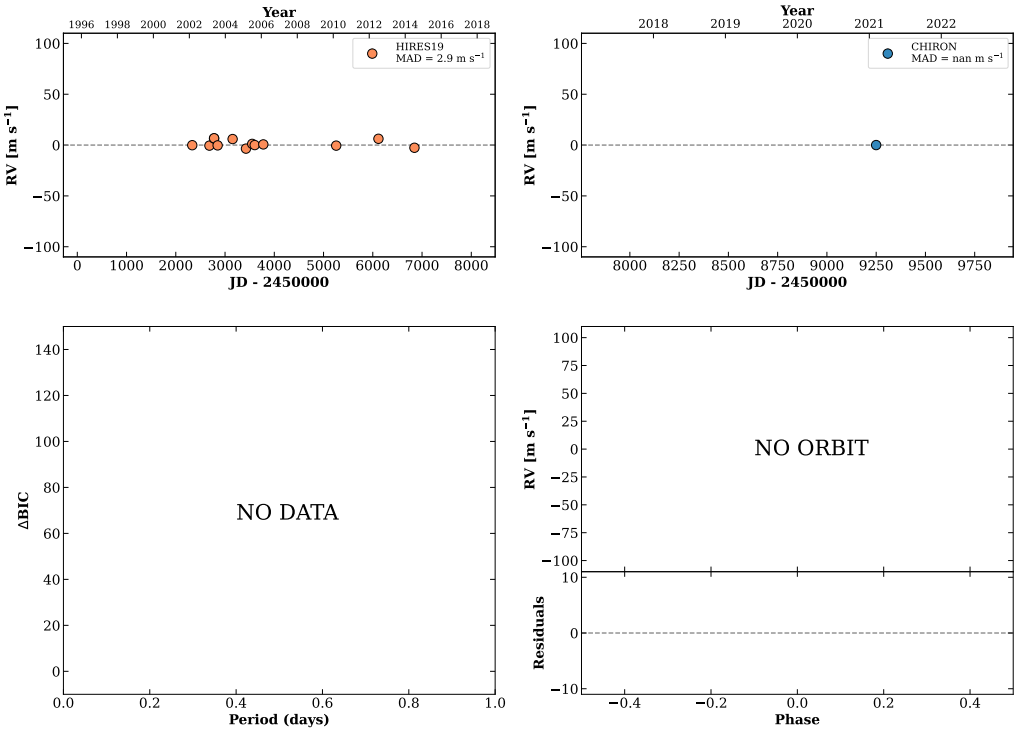

RKS1446+2730

14:46:03 +27:30:44 V = 8.0 HIP072200 TIC 219834010
$N_{H/H}$ = 0 N_C = 7 DMY

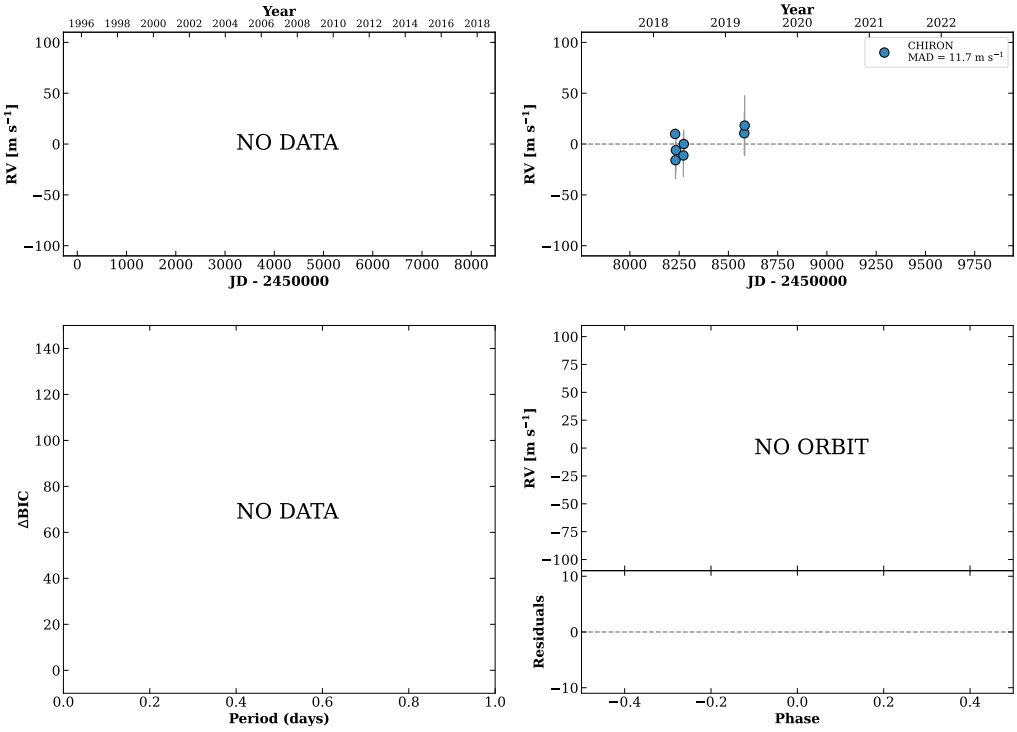

Figure 247 RV results for RKS1445+1350 (top) and RKS1446+2730 (bottom).

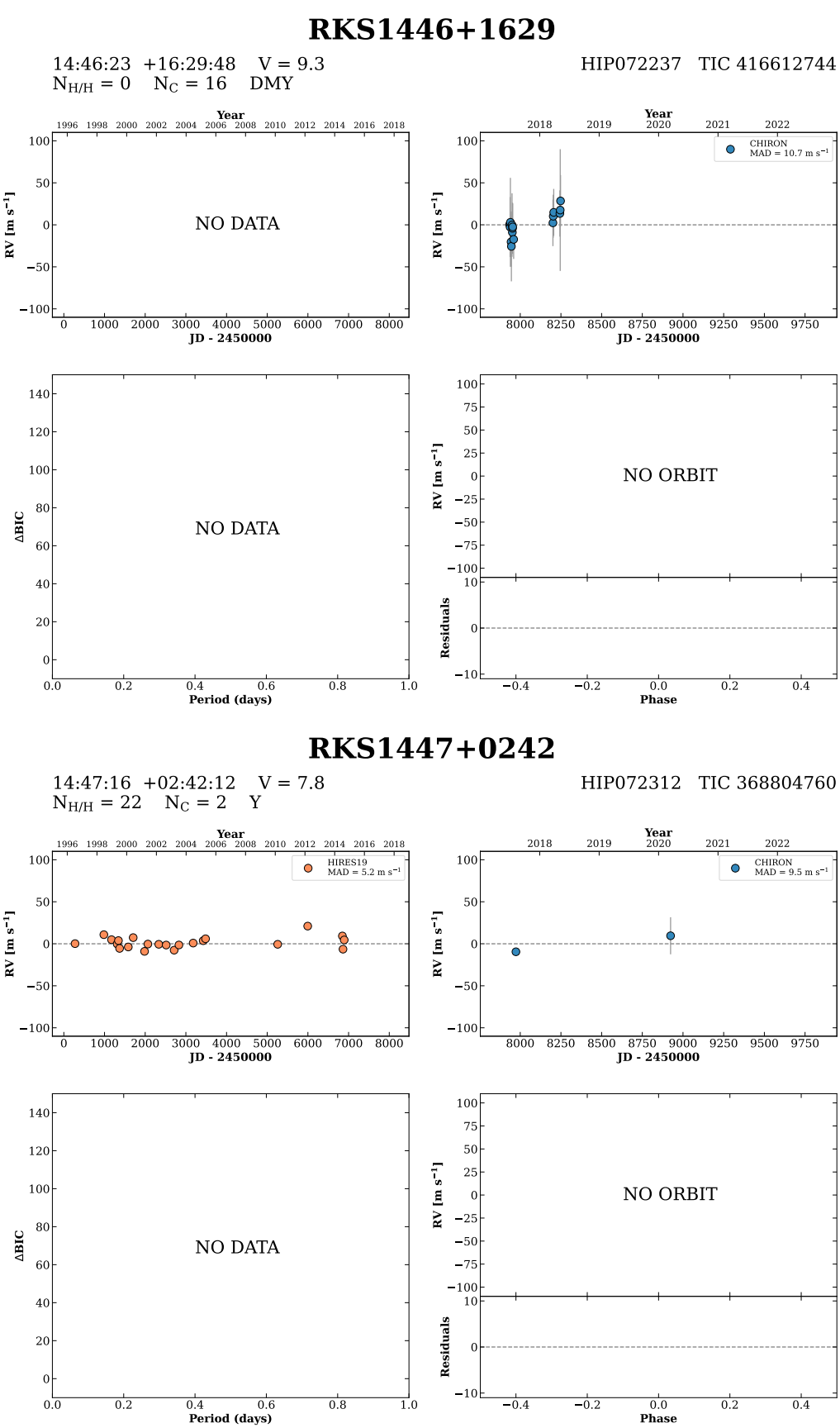

Figure 248 RV results for RKS1446+1629 (top) and RKS1447+0242 (bottom).

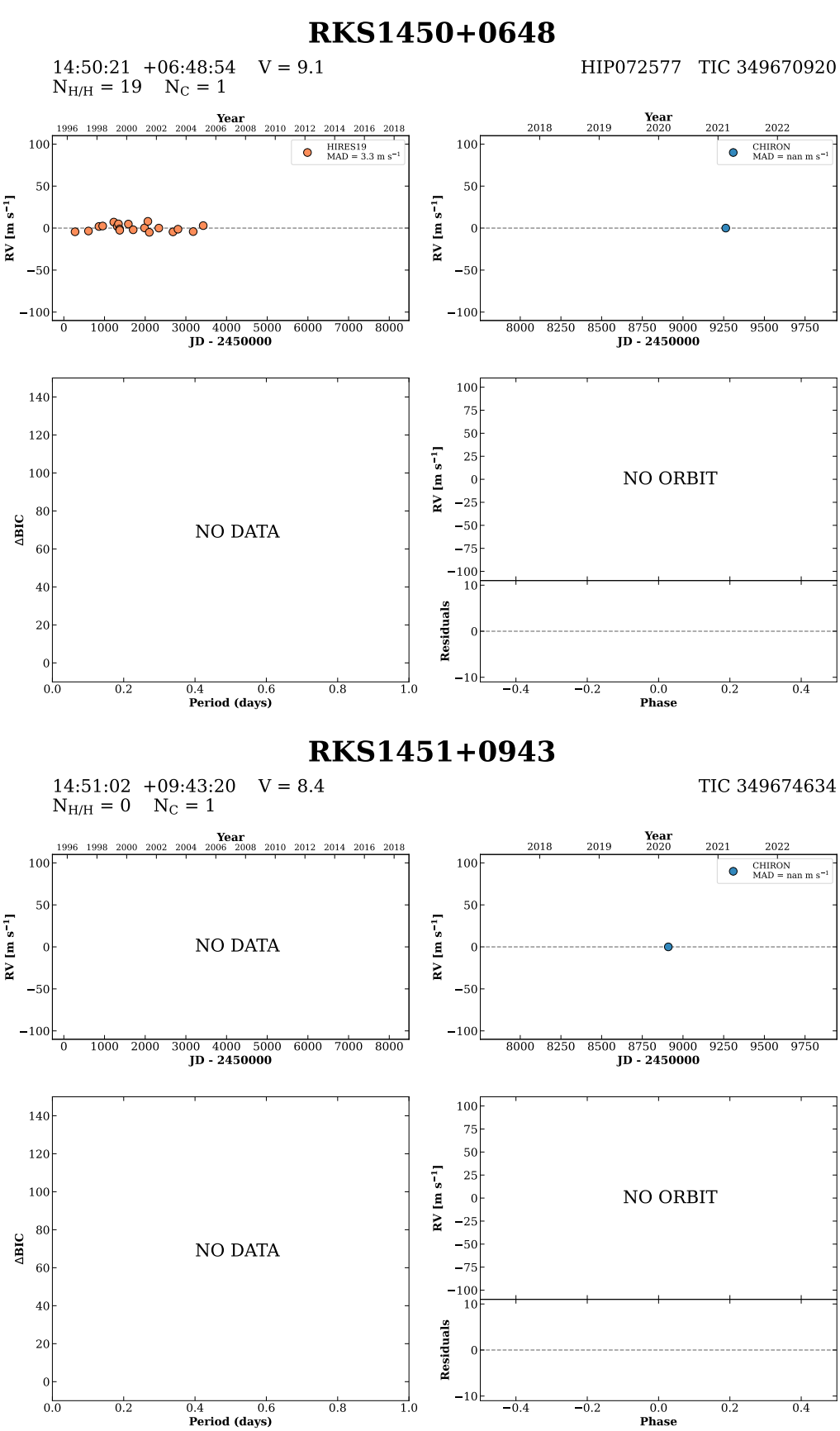

Figure 249 RV results for RKS1450+0648 (top) and RKS1451+0943 (bottom).

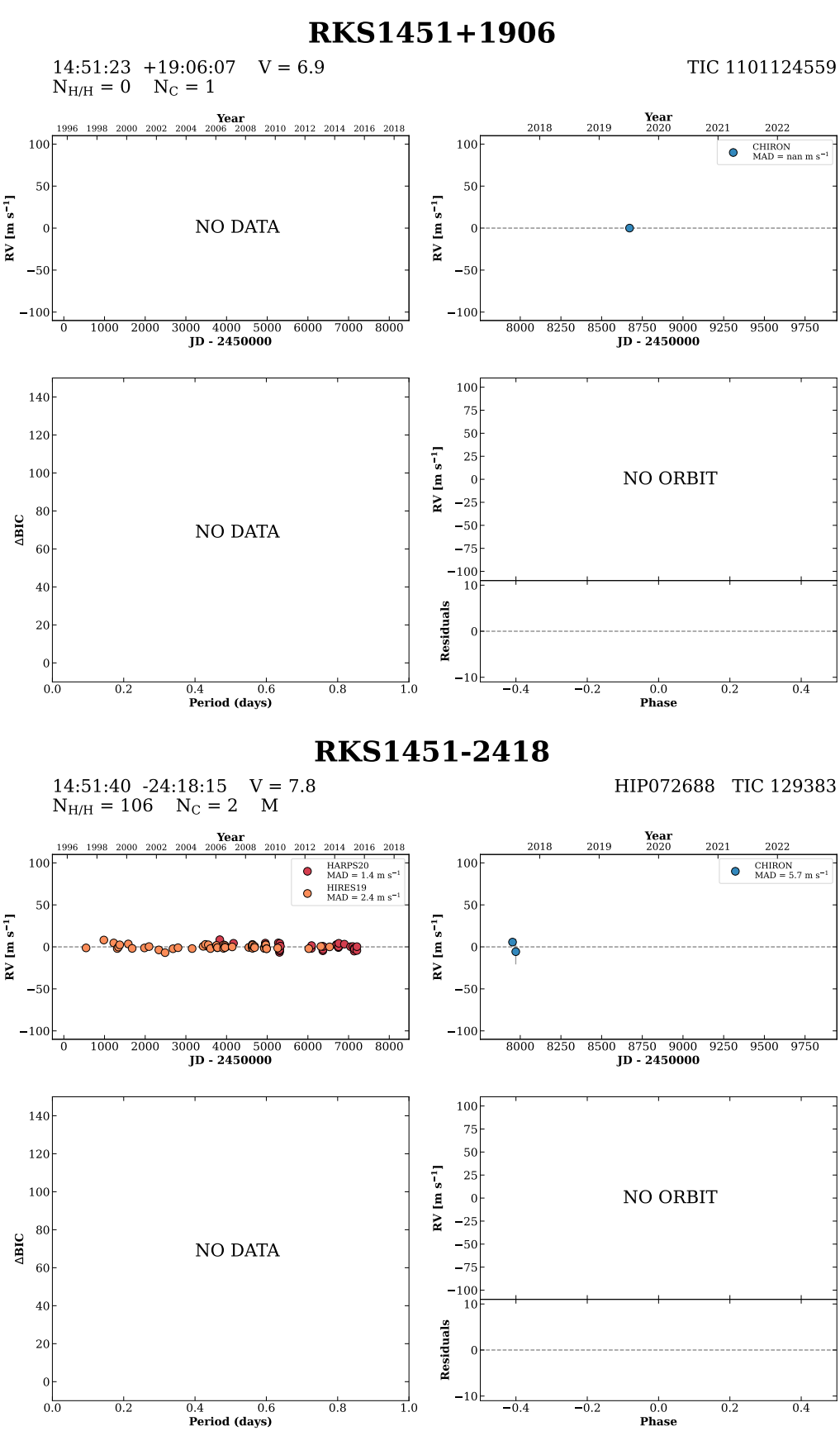

Figure 250 RV results for RKS1451+1906 (top) and RKS1451-2418 (bottom).

RKS1453+1909

14:53:24 +19:09:10 V = 6.0 HIP072848 TIC 267365256
$N_{H/H}$ = 0 N_C = 10 DMY

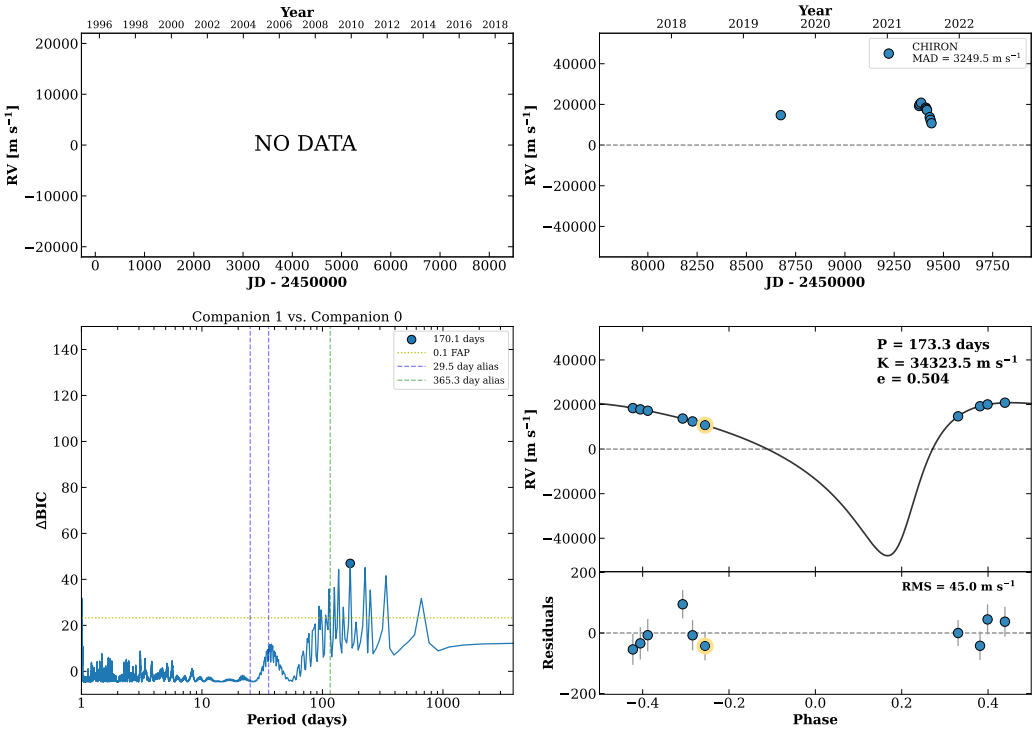

RKS1453+2320

14:53:42 +23:20:43 V = 8.7 HIP072875 TIC 311182515
$N_{H/H}$ = 0 N_C = 36 DMY

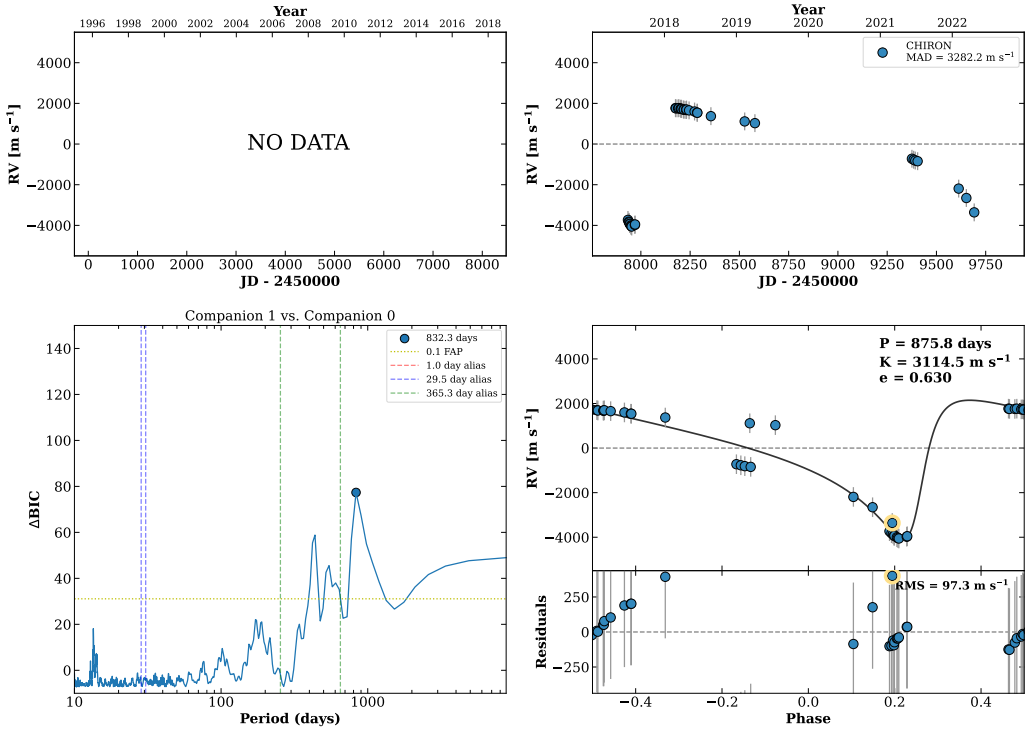

Figure 251 RV results for RKS1453+1909 (top) and RKS1453+2320 (bottom).

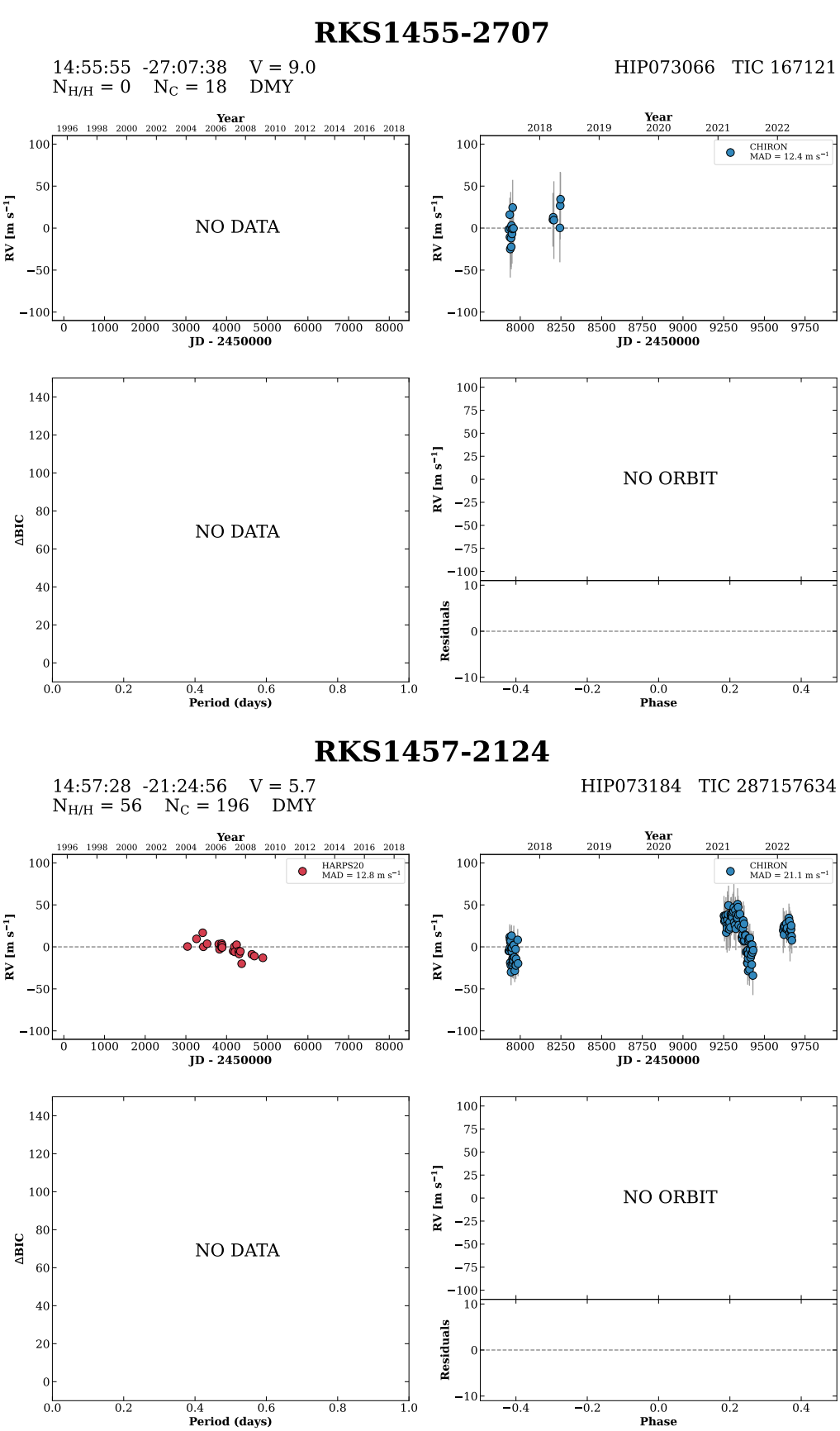

Figure 252 RV results for RKS1455-2707 (top) and RKS1457-2124 (bottom).

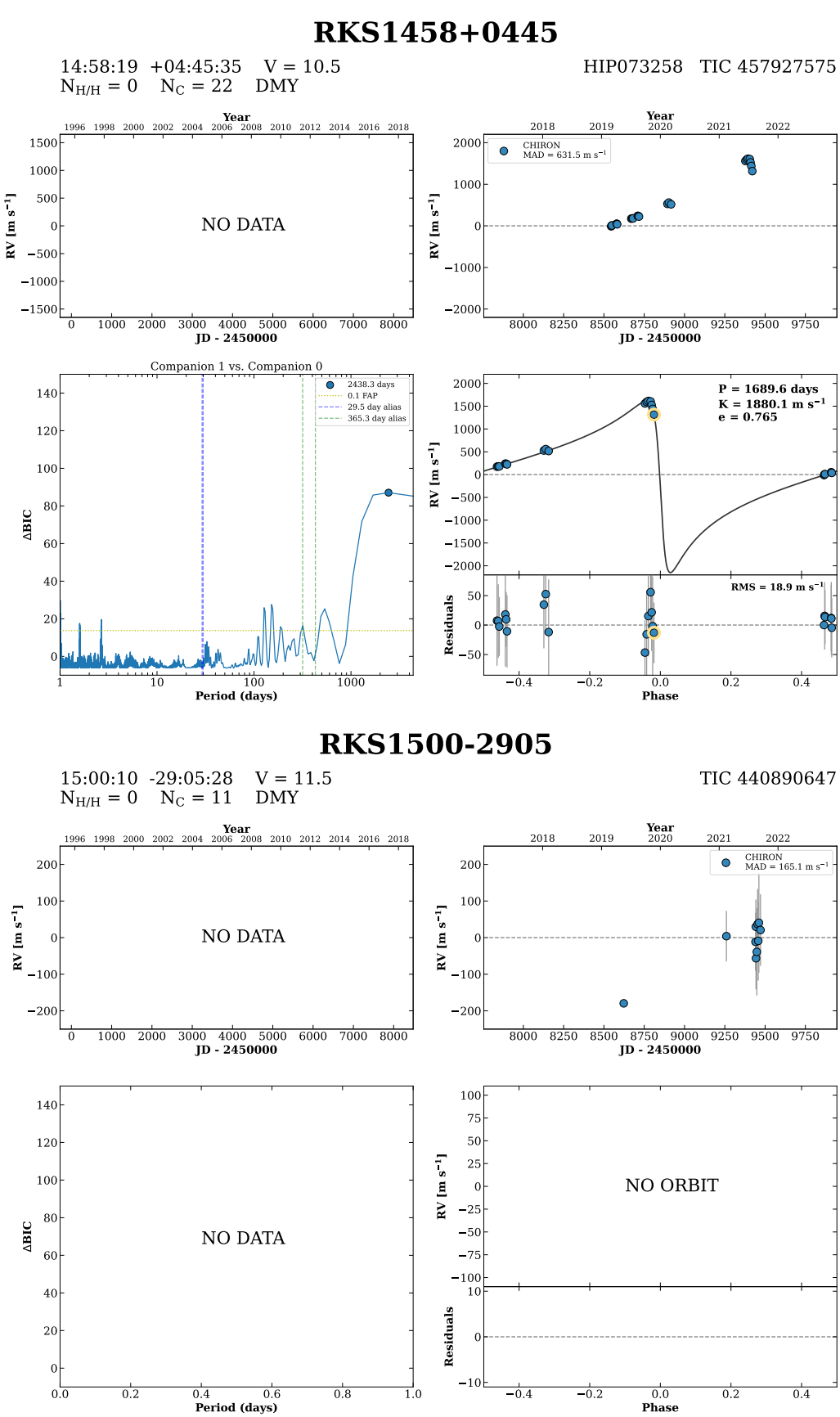

Figure 253 RV results for RKS1458+0445 (top) and RKS1500-2905 (bottom).

RKS1500-2427

15:00:19 -24:27:15 V = 9.9 HIP073427 TIC 440887364
$N_{H/H}$ = 11 N_C = 8 DMY

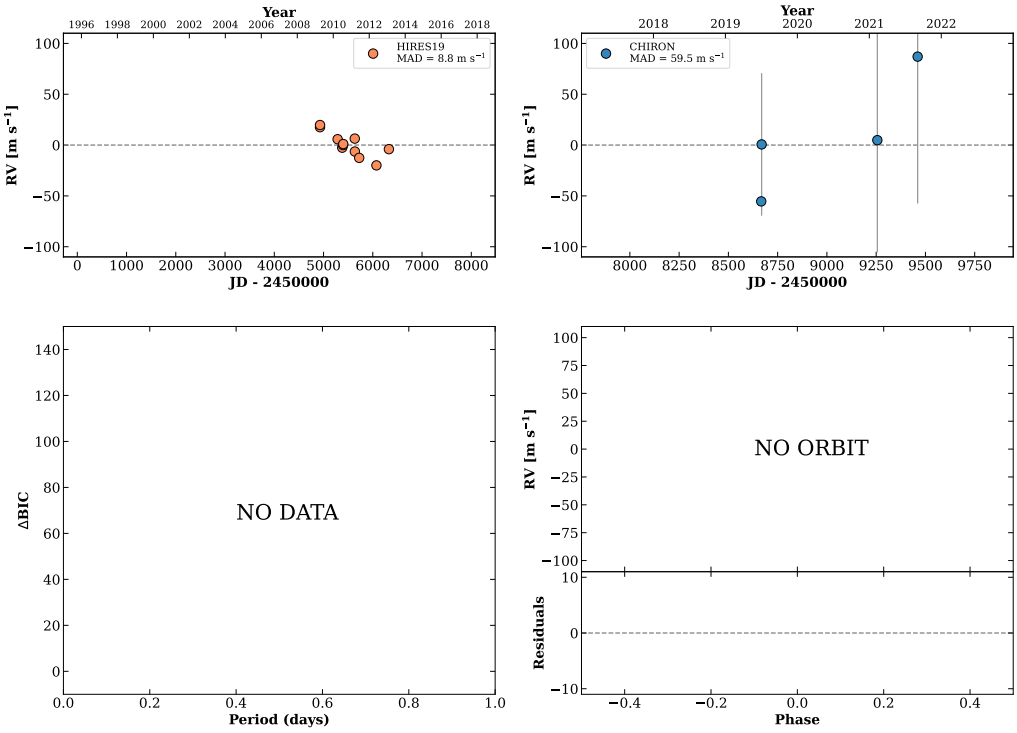

RKS1500-1108

15:00:43 -11:08:06 V = 9.5 HIP073457 TIC 192679501
$N_{H/H}$ = 5 N_C = 8 DMY

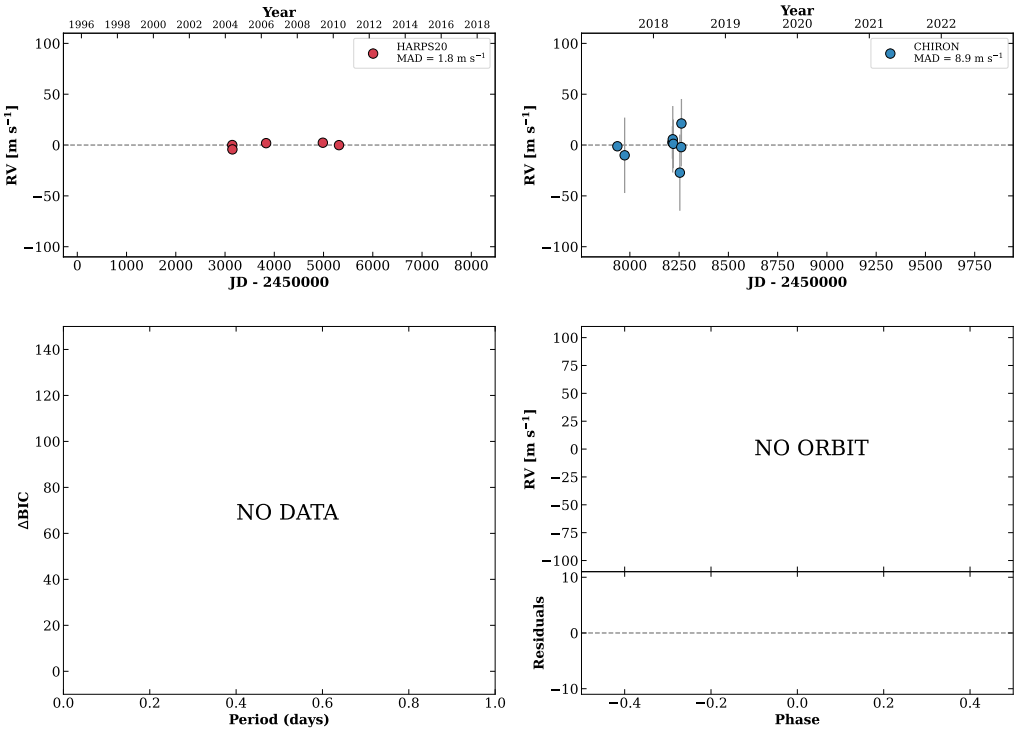

Figure 254 RV results for RKS1500-2427 (top) and RKS1500-1108 (bottom).

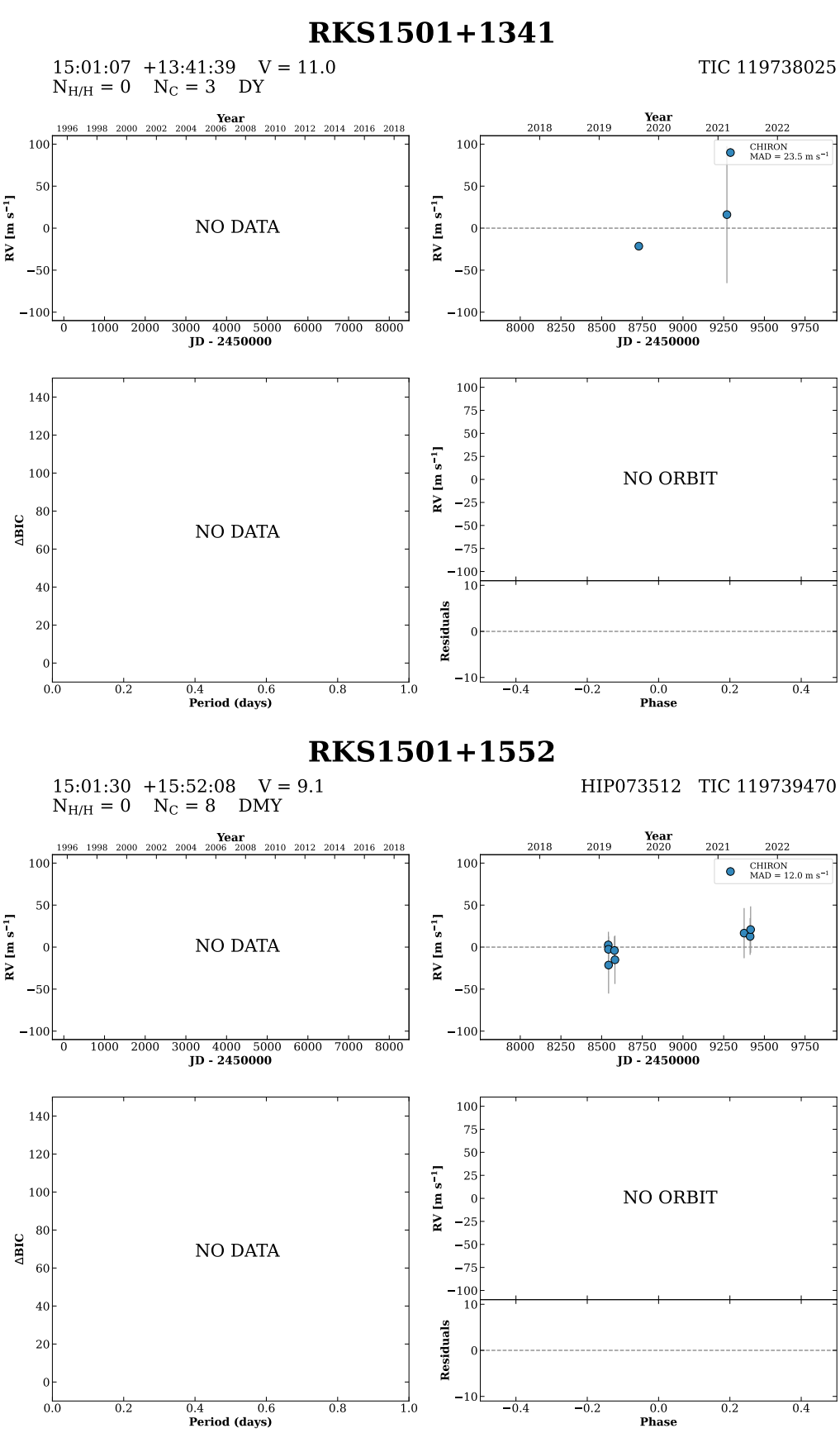

Figure 255 RV results for RKS1501+1341 (top) and RKS1501+1552 (bottom).

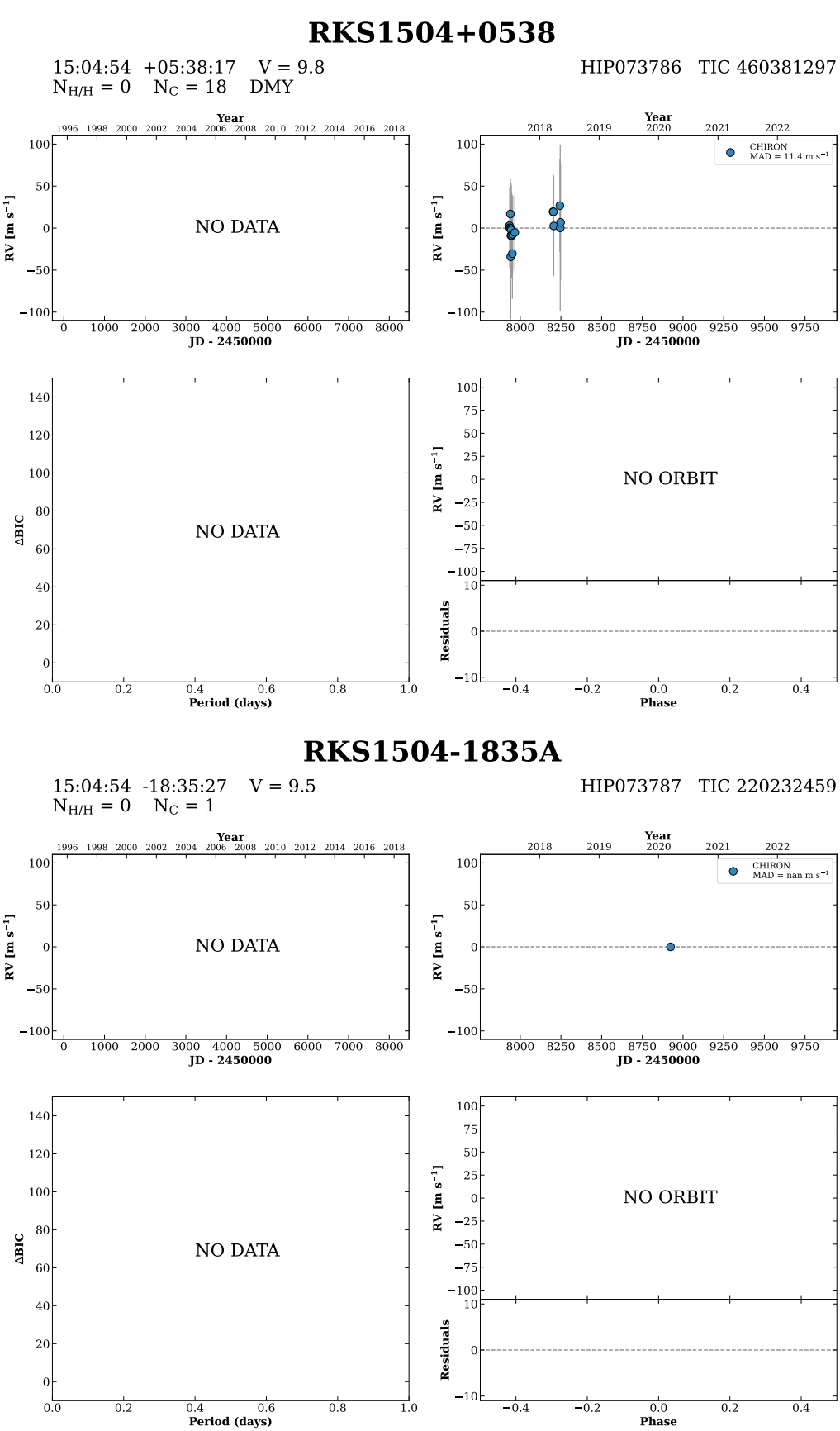

Figure 256 RV results for RKS1504+0538 (top) and RKS1504-1835A (bottom).

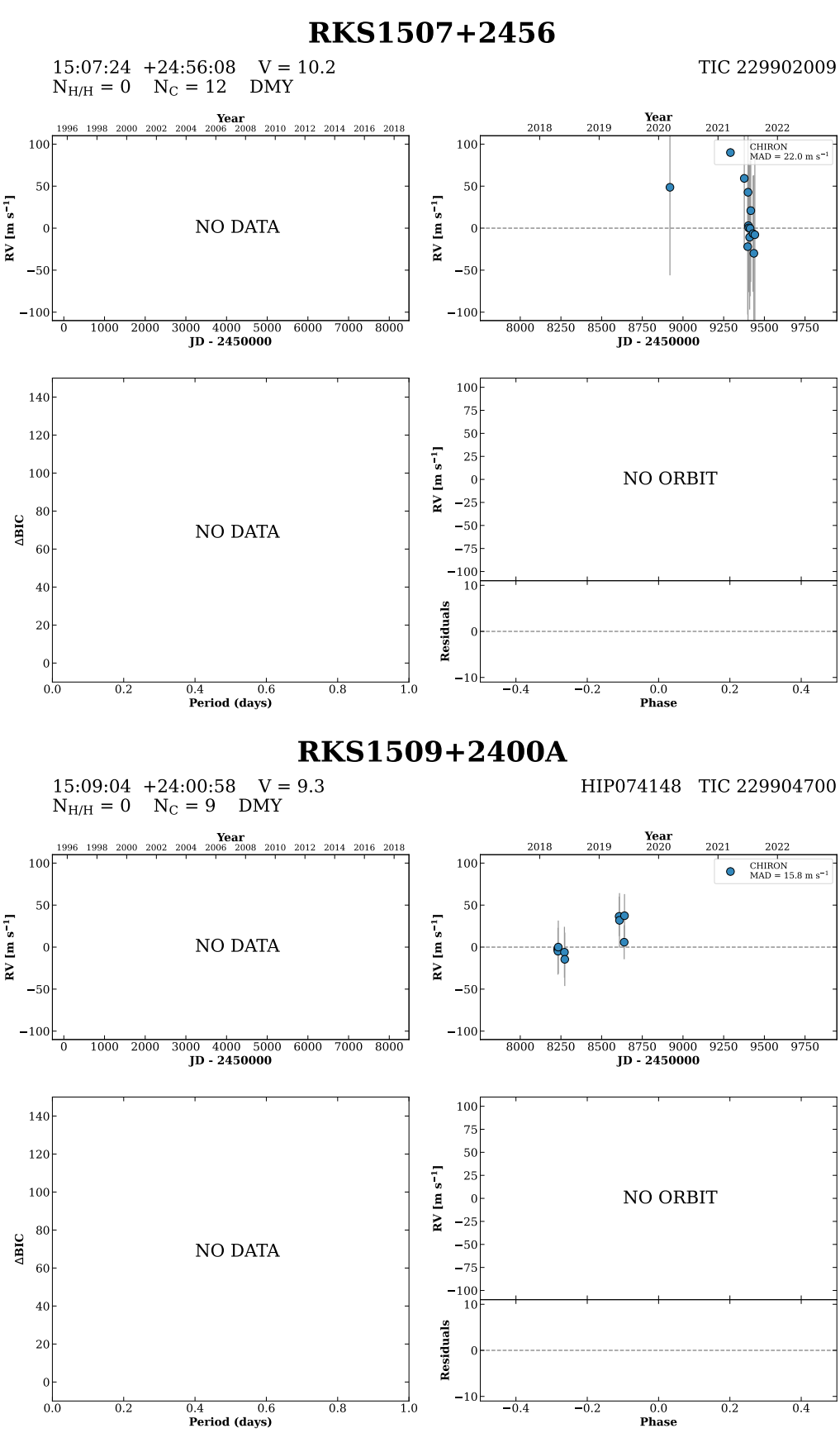

Figure 257 RV results for RKS1507+2456 (top) and RKS1509+2400A (bottom).

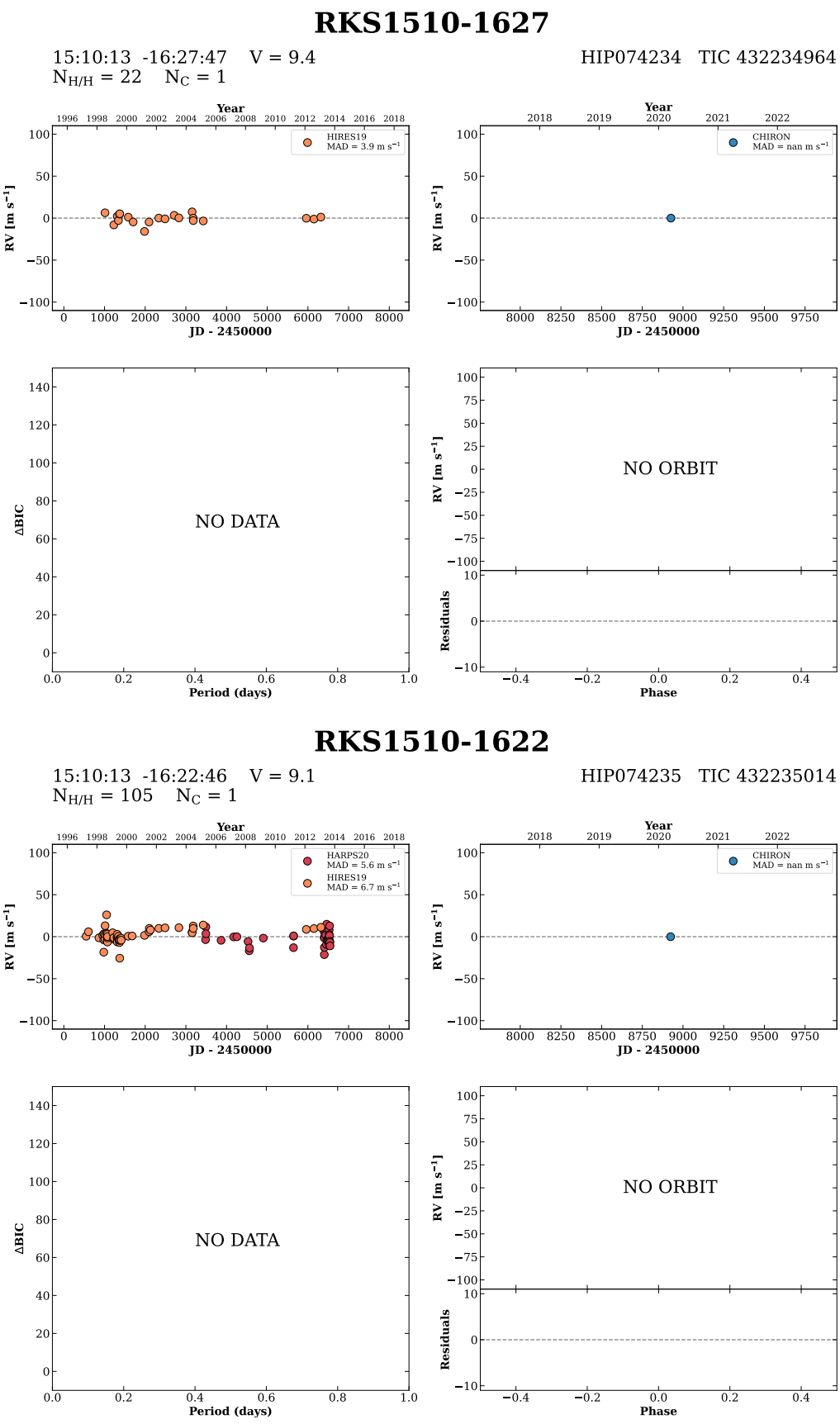

Figure 258 RV results for RKS1510-1627 (top) and RKS1510-1622 (bottom).

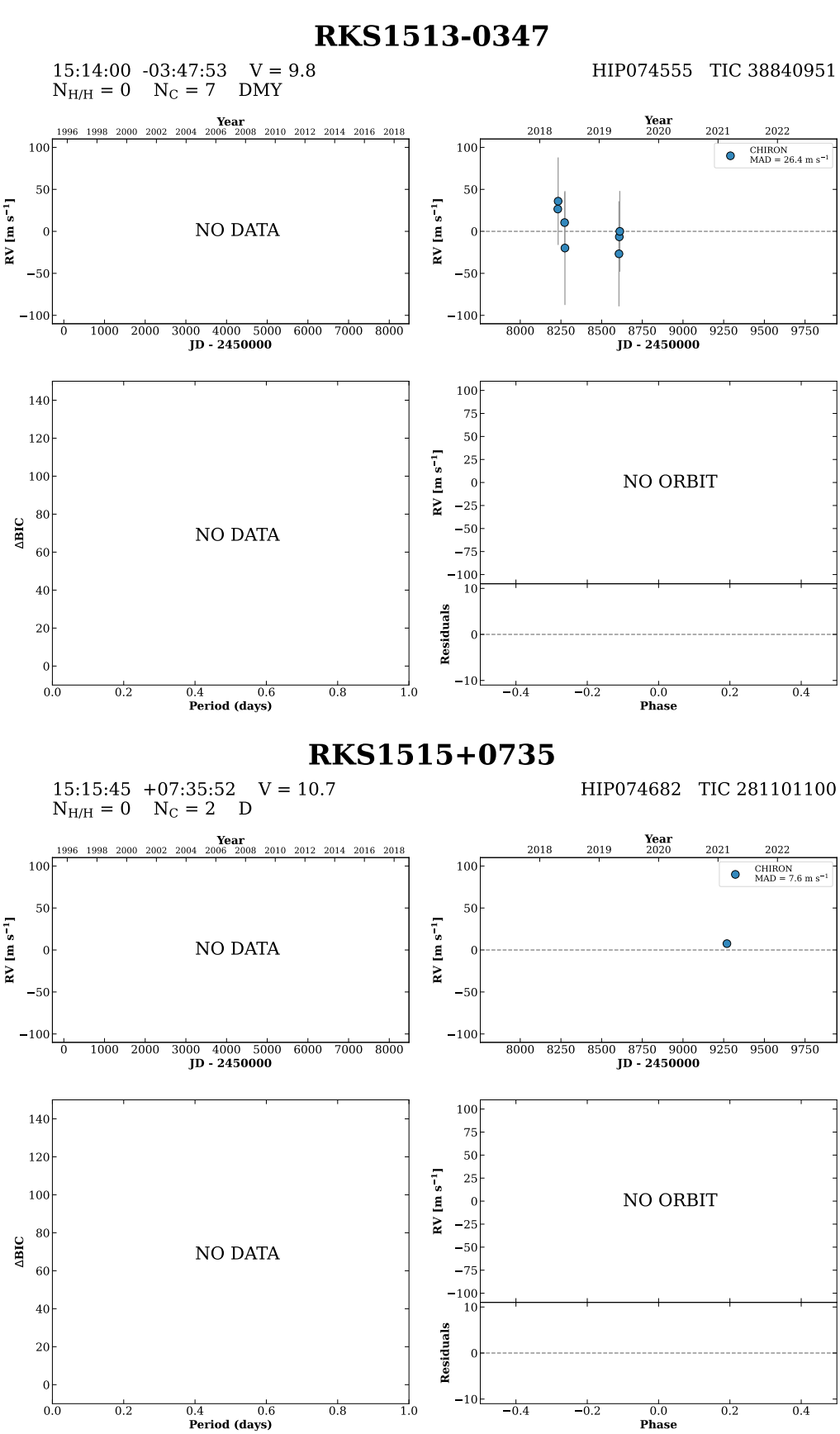

Figure 259 RV results for RKS1513-0347 (top) and RKS1515+0735 (bottom).

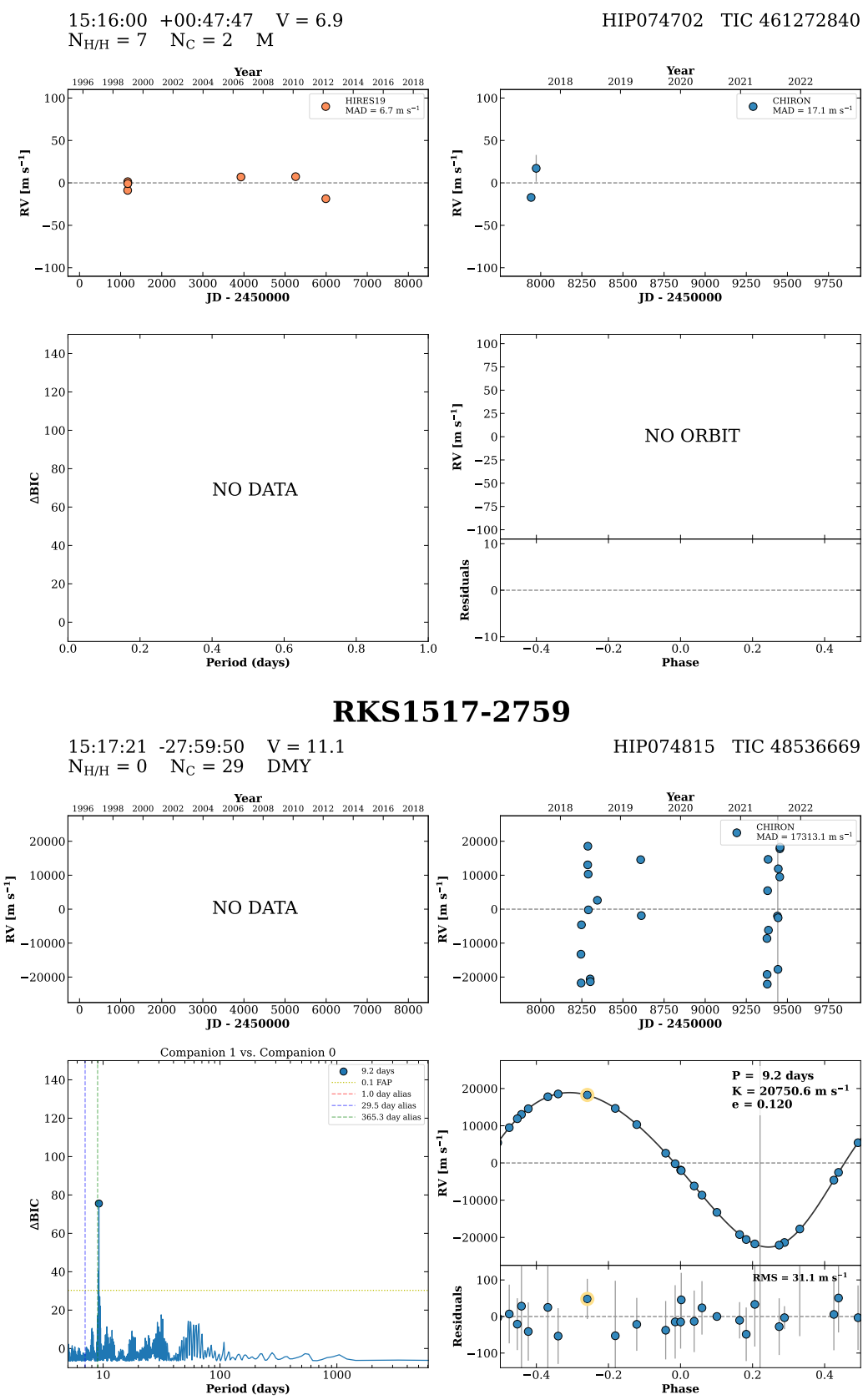

Figure 260 RV results for RKS1515+0047 (top) and RKS1517-2759 (bottom).

RKS1518-1837

15:18:40 -18:37:36 V = 10.3 HIP074926 TIC 438893825
$N_{H/H}$ = 0 N_C = 22 DMY

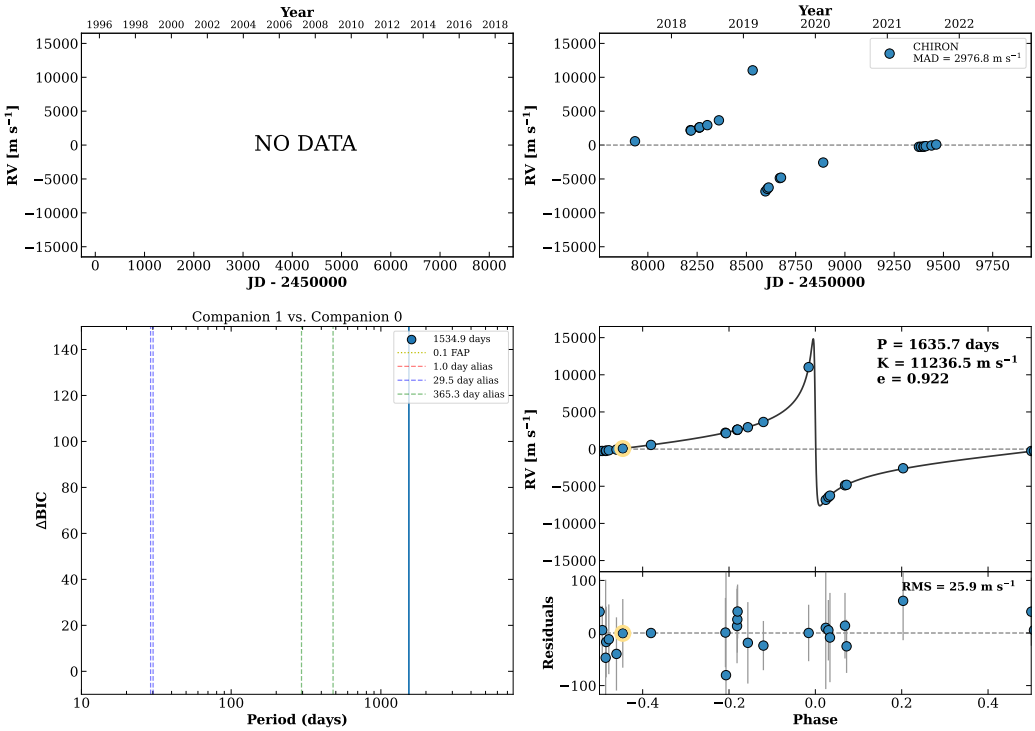

RKS1519+0146

15:19:19 +01:46:05 V = 9.9 TIC 461308071
$N_{H/H}$ = 0 N_C = 1

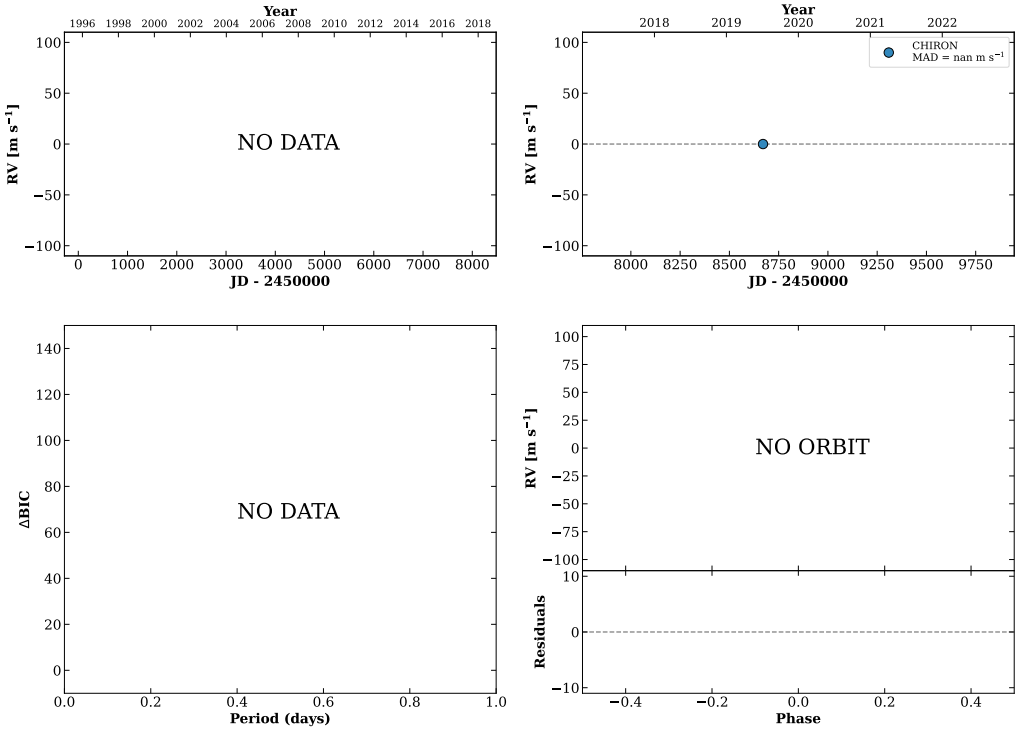

Figure 261 RV results for RKS1518-1837 (top) and RKS1519+0146 (bottom).

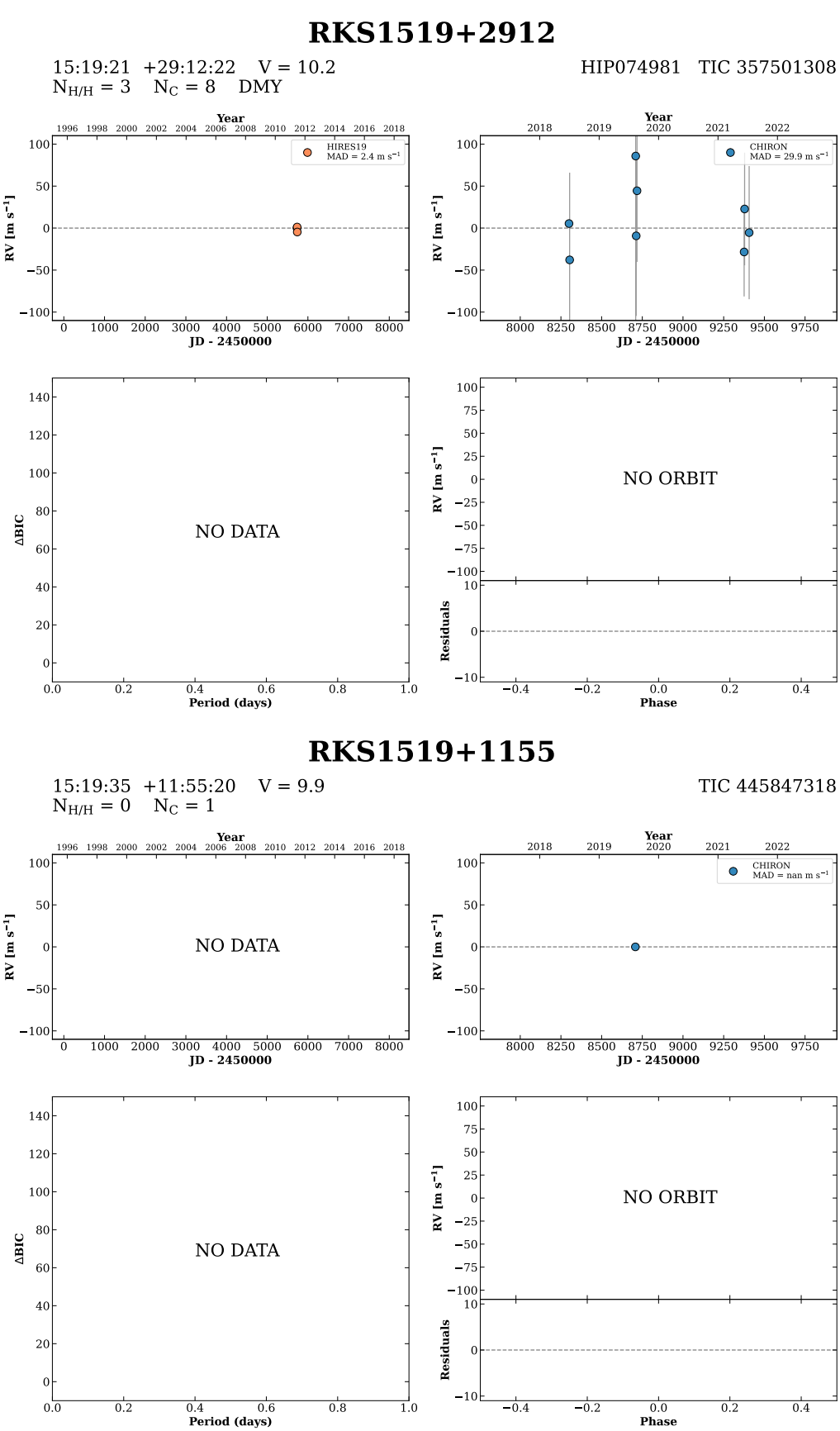

Figure 262 RV results for RKS1519+2912 (top) and RKS1519+1155 (bottom).

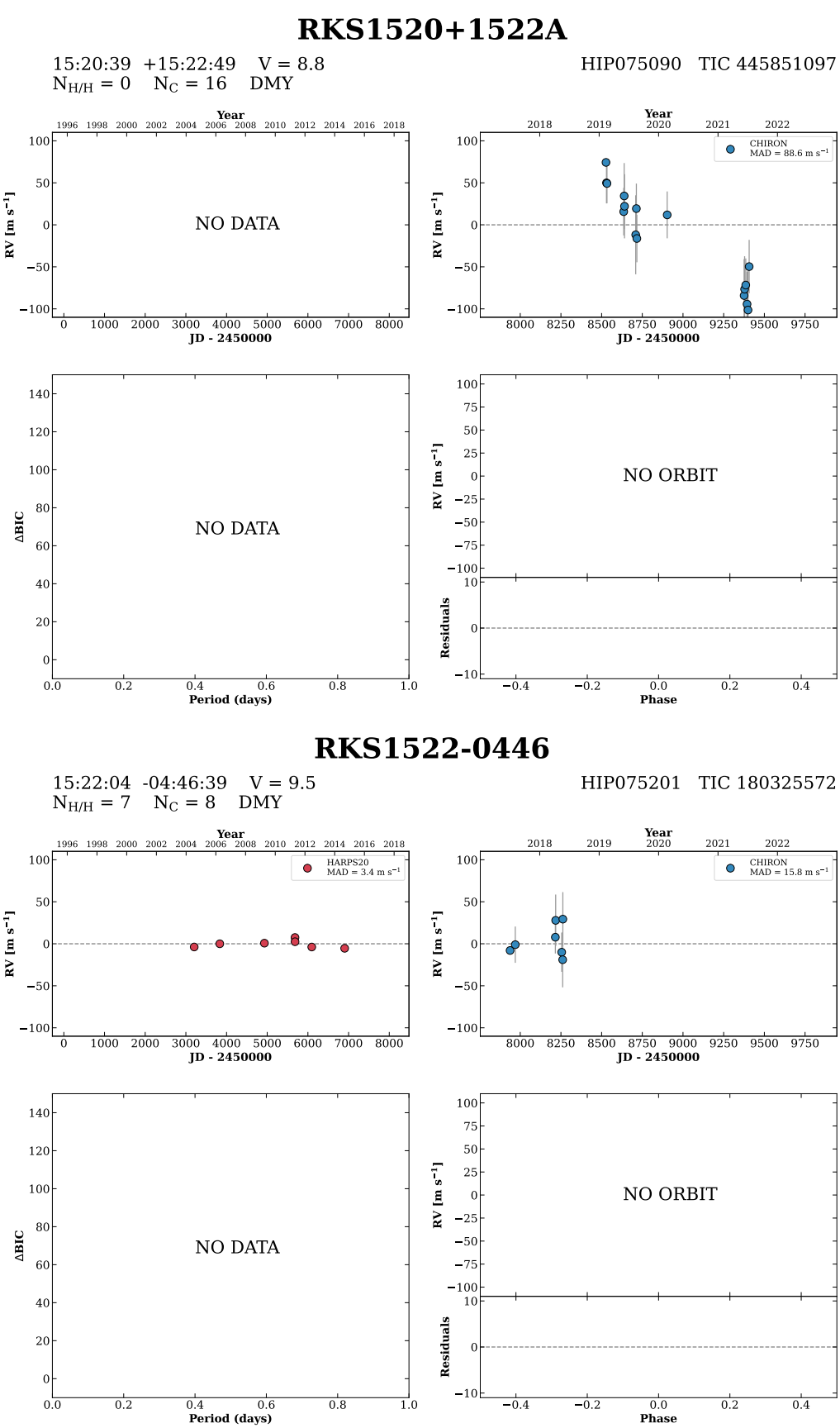

Figure 263 RV results for RKS1520+1522A (top) and RKS1522-0446 (bottom).

RKS1522-1039

15:22:37 -10:39:40 V = 8.0 HIP075253 TIC 36981205
$N_{H/H}$ = 198 N_C = 2 M

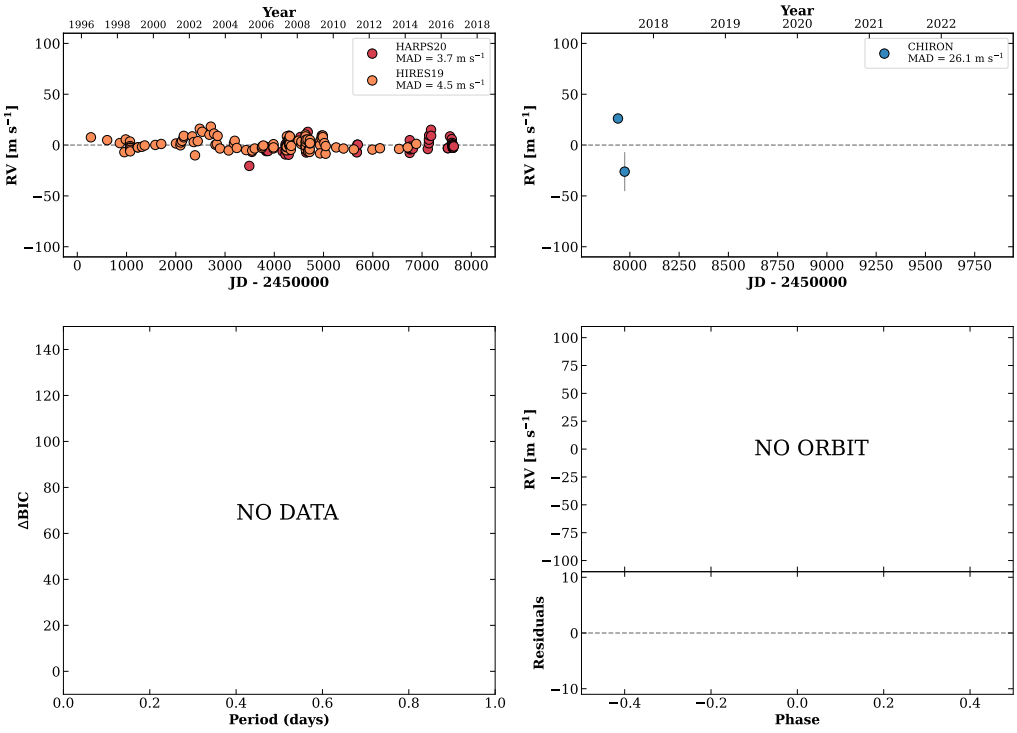

RKS1522+0125

15:22:43 +01:25:07 V = 8.3 HIP075266 TIC 461330181
$N_{H/H}$ = 21 N_C = 1

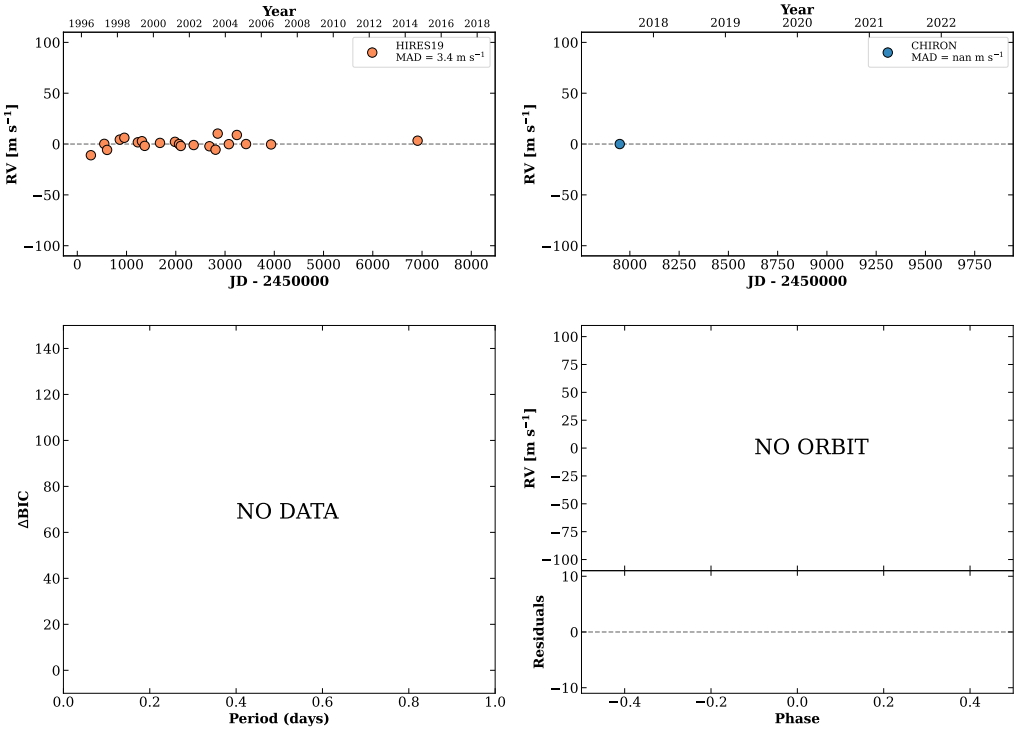

Figure 264 RV results for RKS1522-1039 (top) and RKS1522+0125 (bottom).

RKS1525-2642

15:25:59 -26:42:21 V = 8.8 HIP075542 TIC 388734737
$N_{H/H}$ = 16 N_C = 4 DM

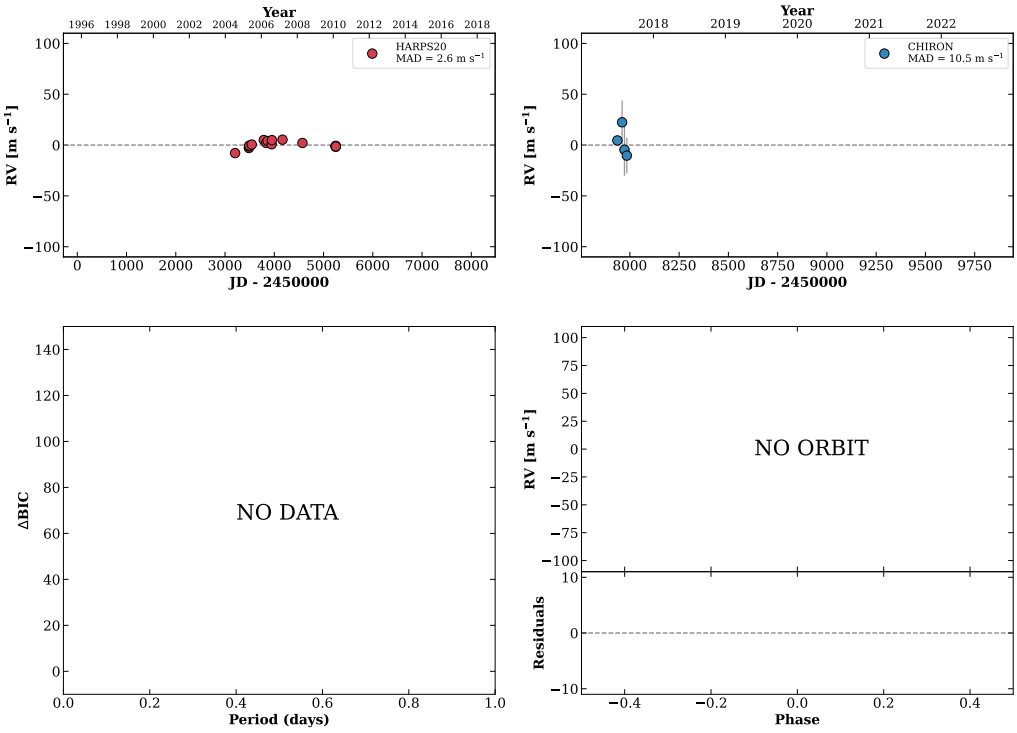

RKS1527+1035

15:27:38 +10:35:39 V = 9.9 HIP075672 TIC 392982986
$N_{H/H}$ = 4 N_C = 5 DMY

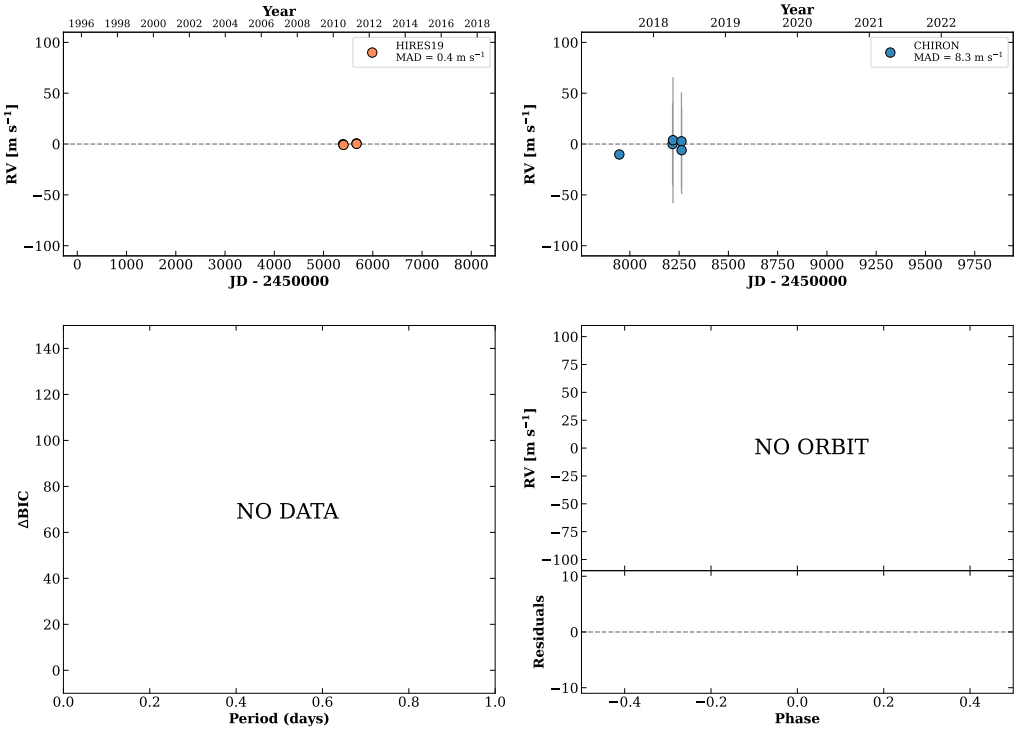

Figure 265 RV results for RKS1525-2642 (top) and RKS1527+1035 (bottom).

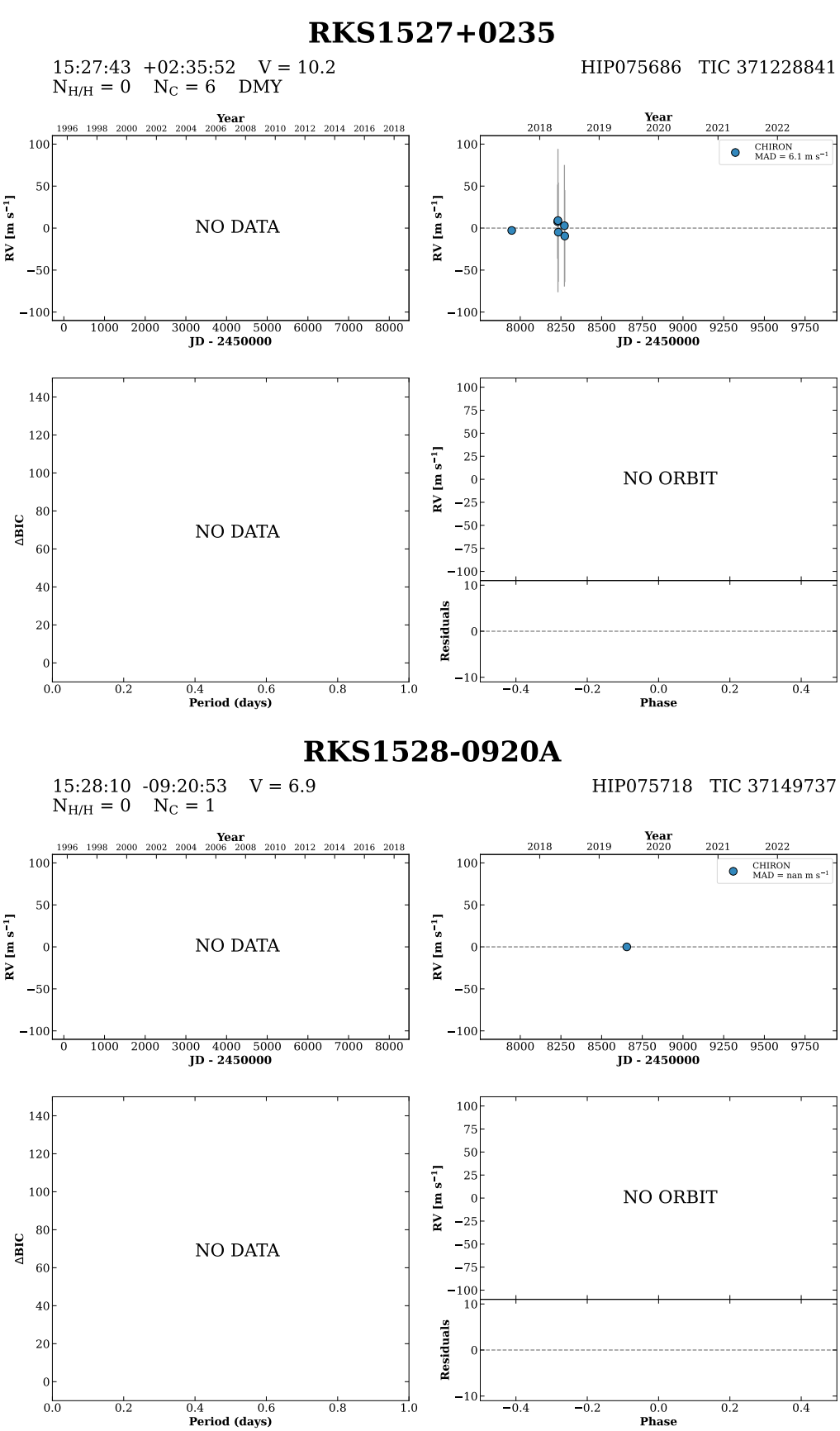

Figure 266 RV results for RKS1527+0235 (top) and RKS1528-0920A (bottom).

RKS1528-0921B

15:28:12 -09:21:28 V = 7.6 HIP075722 TIC 37149743
$N_{H/H}$ = 28 N_C = 1

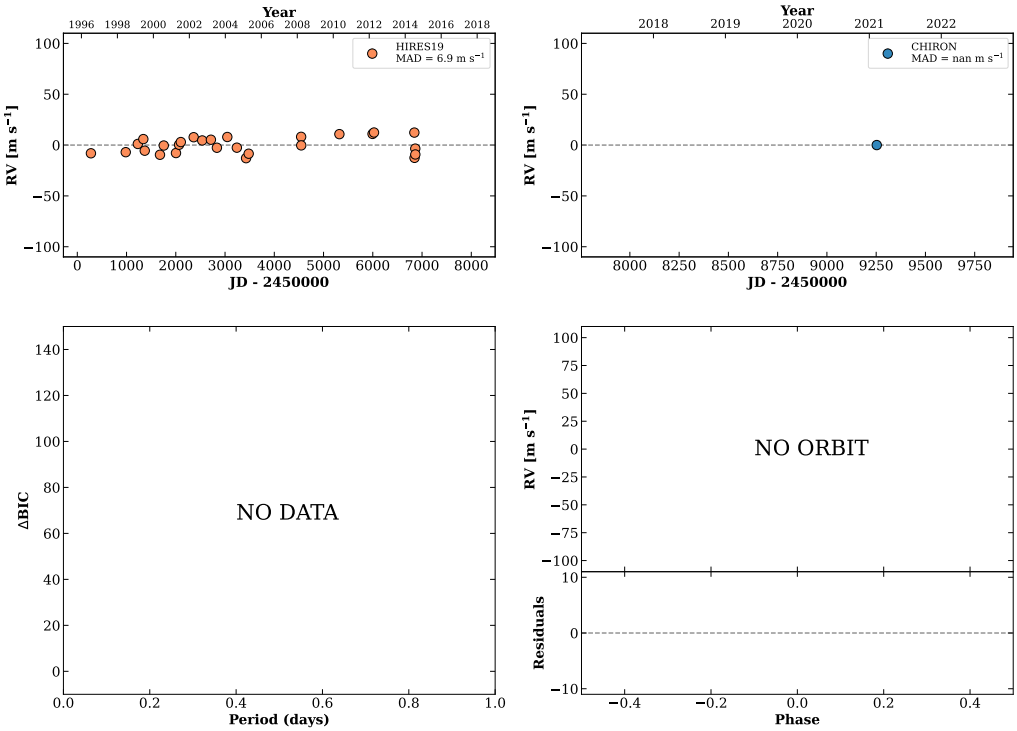

RKS1531-2916

15:31:40 -29:16:29 V = 11.3 TIC 185850907
$N_{H/H}$ = 0 N_C = 3 DY

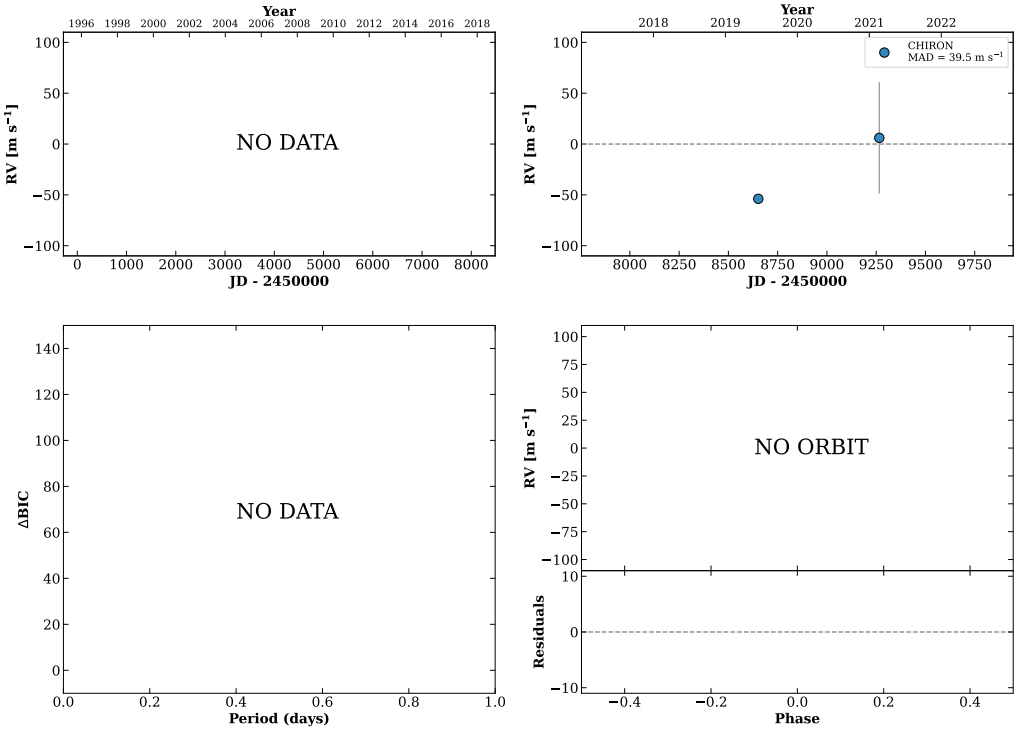

Figure 267 RV results for RKS1528-0921B (top) and RKS1531-2916 (bottom).

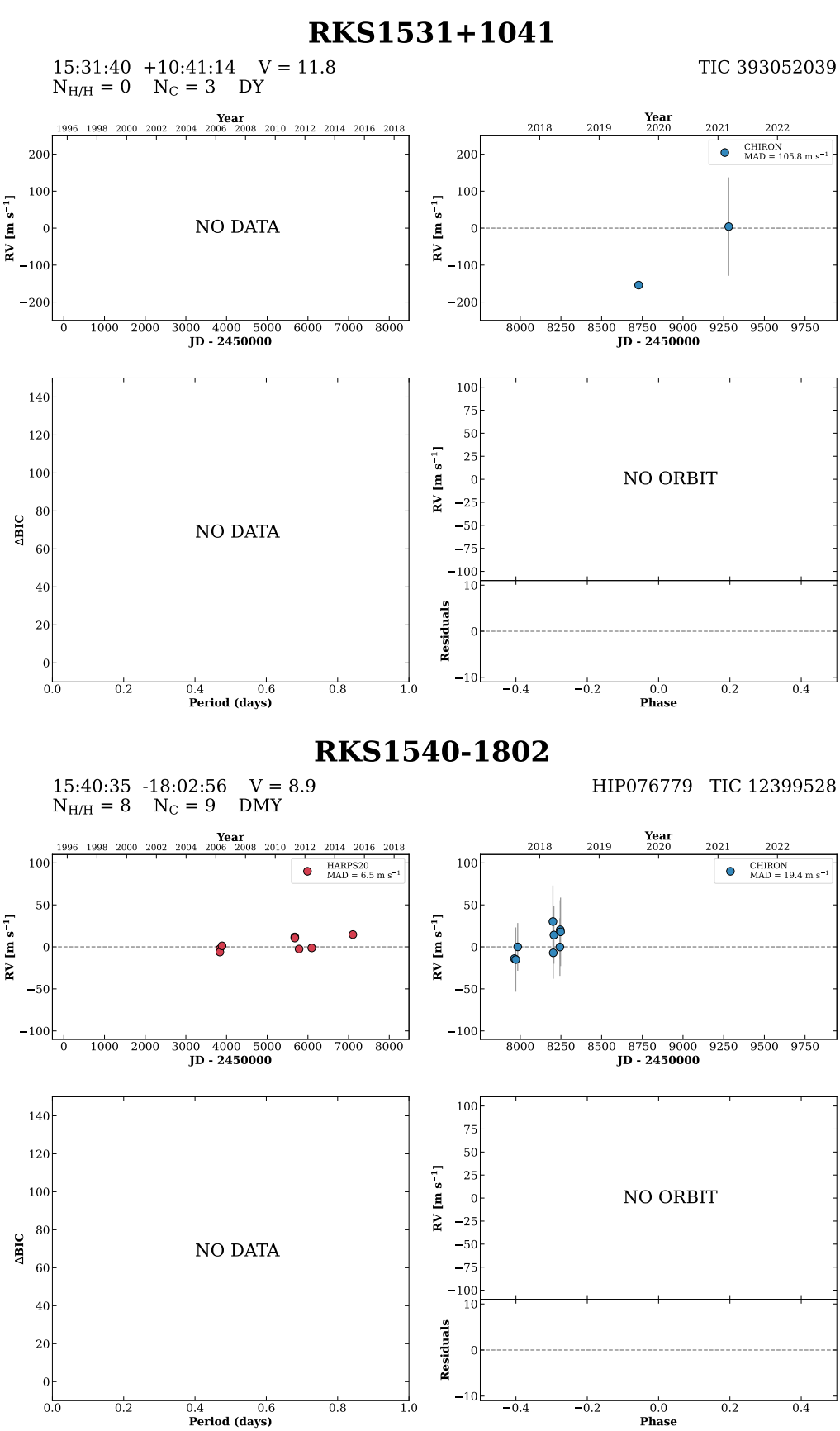

Figure 268 RV results for RKS1531+1041 (top) and RKS1540-1802 (bottom).

HIP077408

15:48:09 +01:34:18 V = 7.4 TIC 272595871
$N_{H/H}$ = 11 N_C = 4 DM

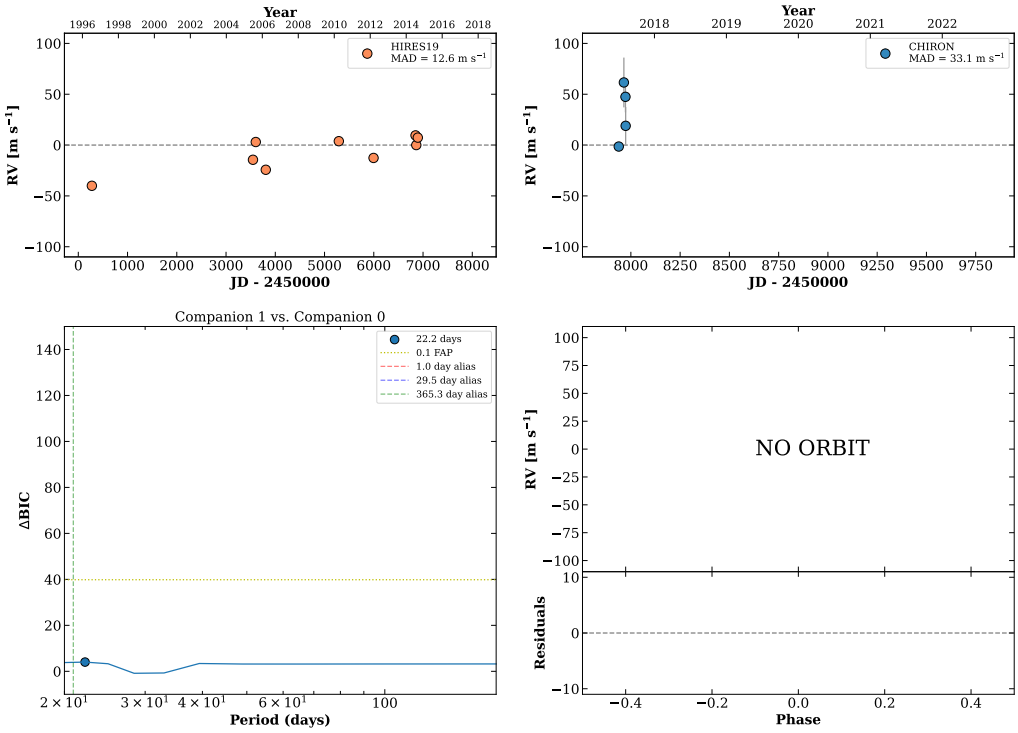

RKS1552+1052A

15:52:08 +10:52:28 V = 9.4 HIP077725 TIC 446193444
$N_{H/H}$ = 0 N_C = 12 DMY

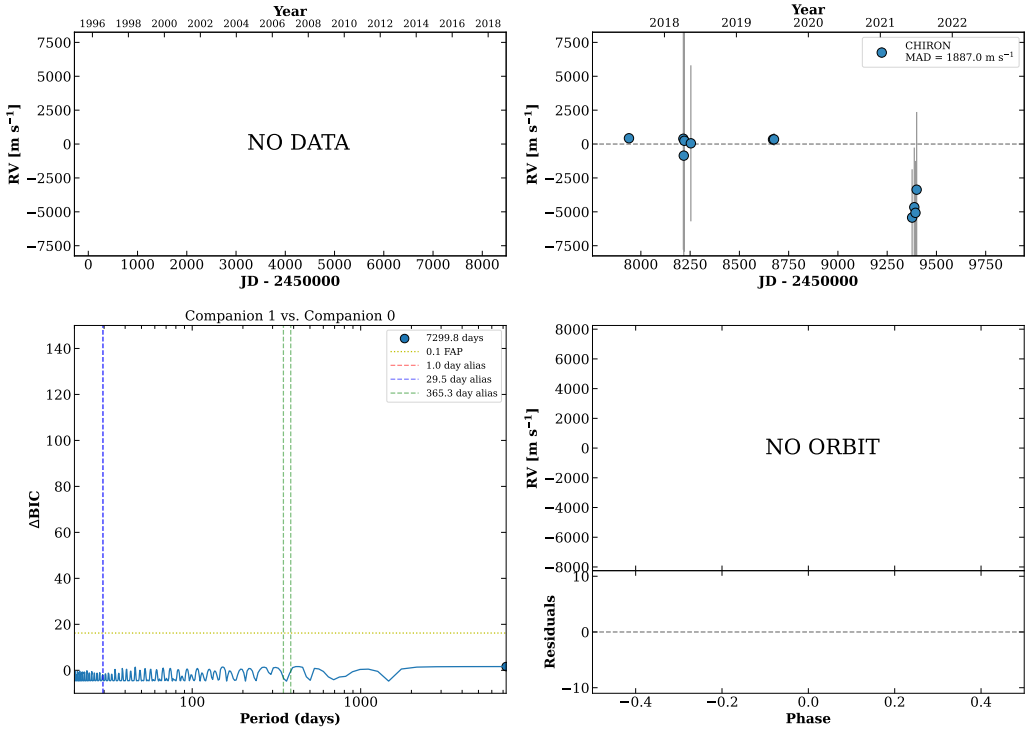

Figure 269 RV results for HIP077408 (top) and RKS1552+1052A (bottom).

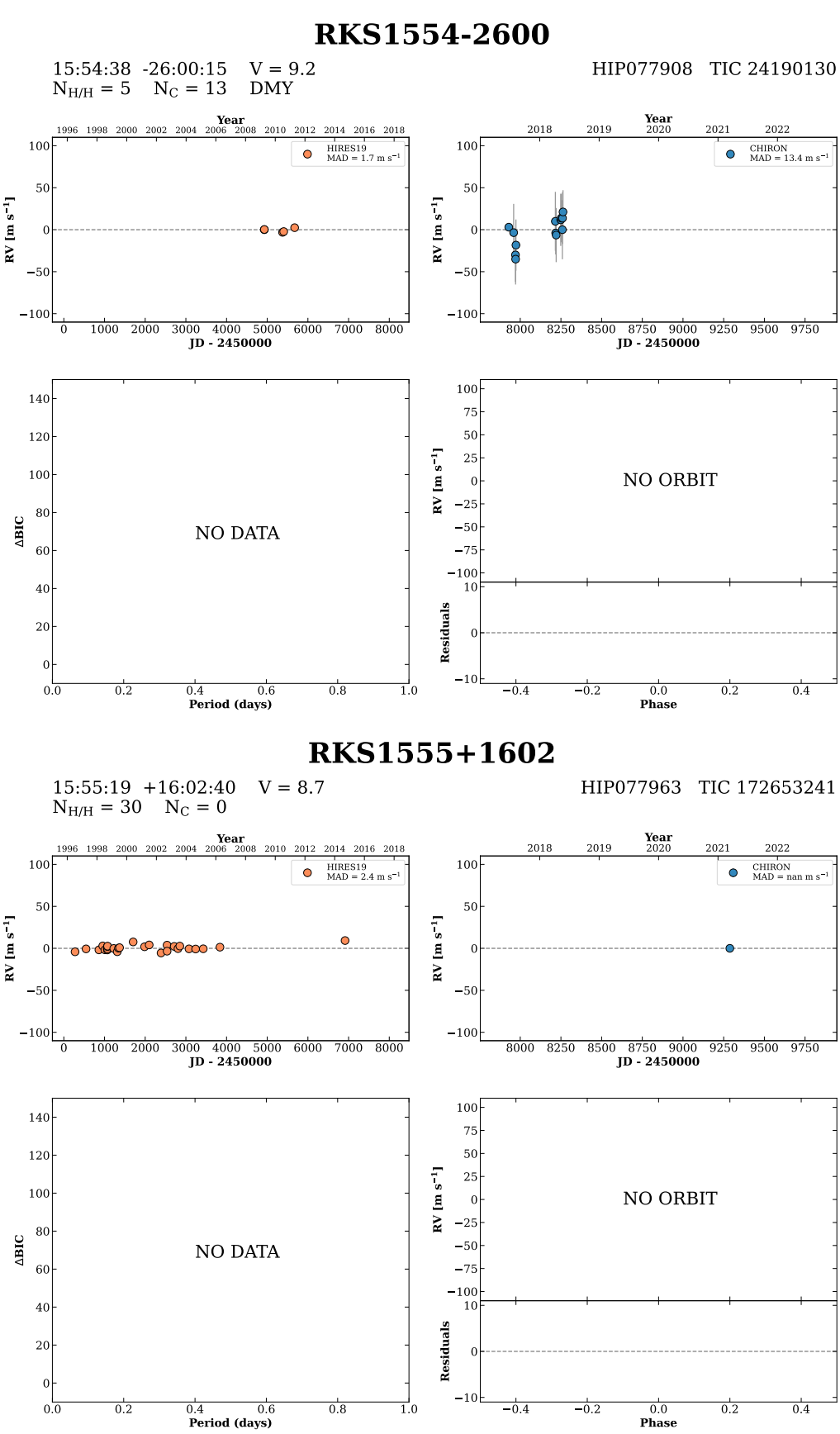

Figure 270 RV results for RKS1554-2600 (top) and RKS1555+1602 (bottom).

RKS1559-0504

15:59:42 -05:04:34 V = 9.0 HIP078336 TIC 168454208
$N_{H/H}$ = 0 N_C = 8 DMY

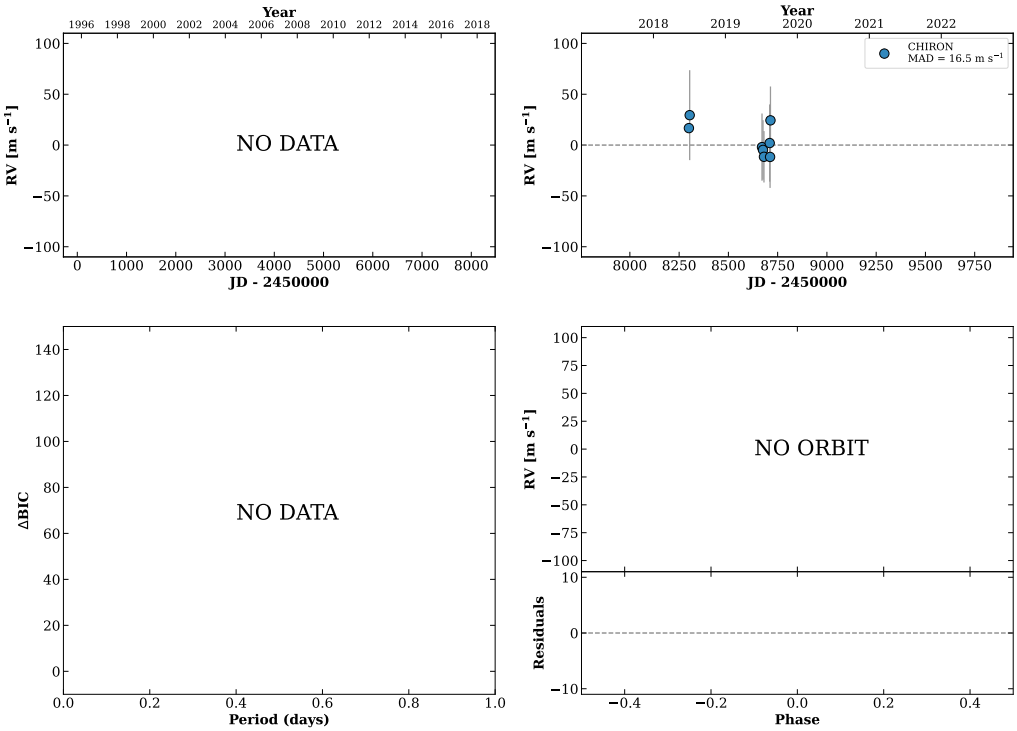

RKS1600-0147A

16:00:16 -01:47:56 V = 10.3 HIP078395 TIC 168457265
$N_{H/H}$ = 25 N_C = 2 D

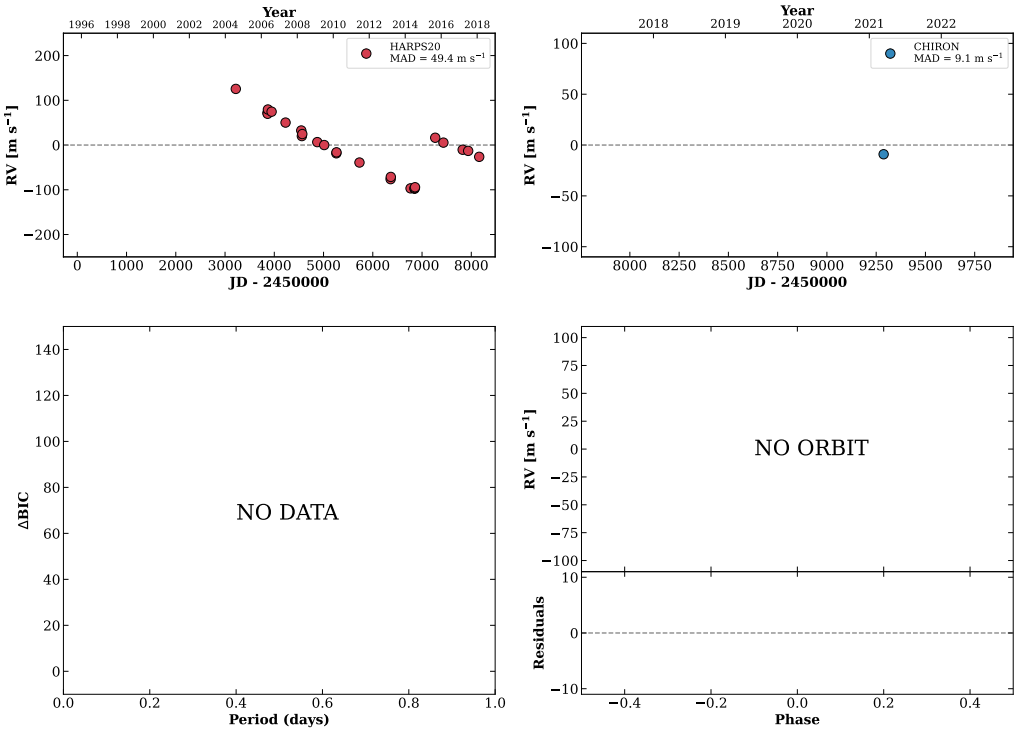

Figure 271 RV results for RKS1559-0504 (top) and RKS1600-0147A (bottom).

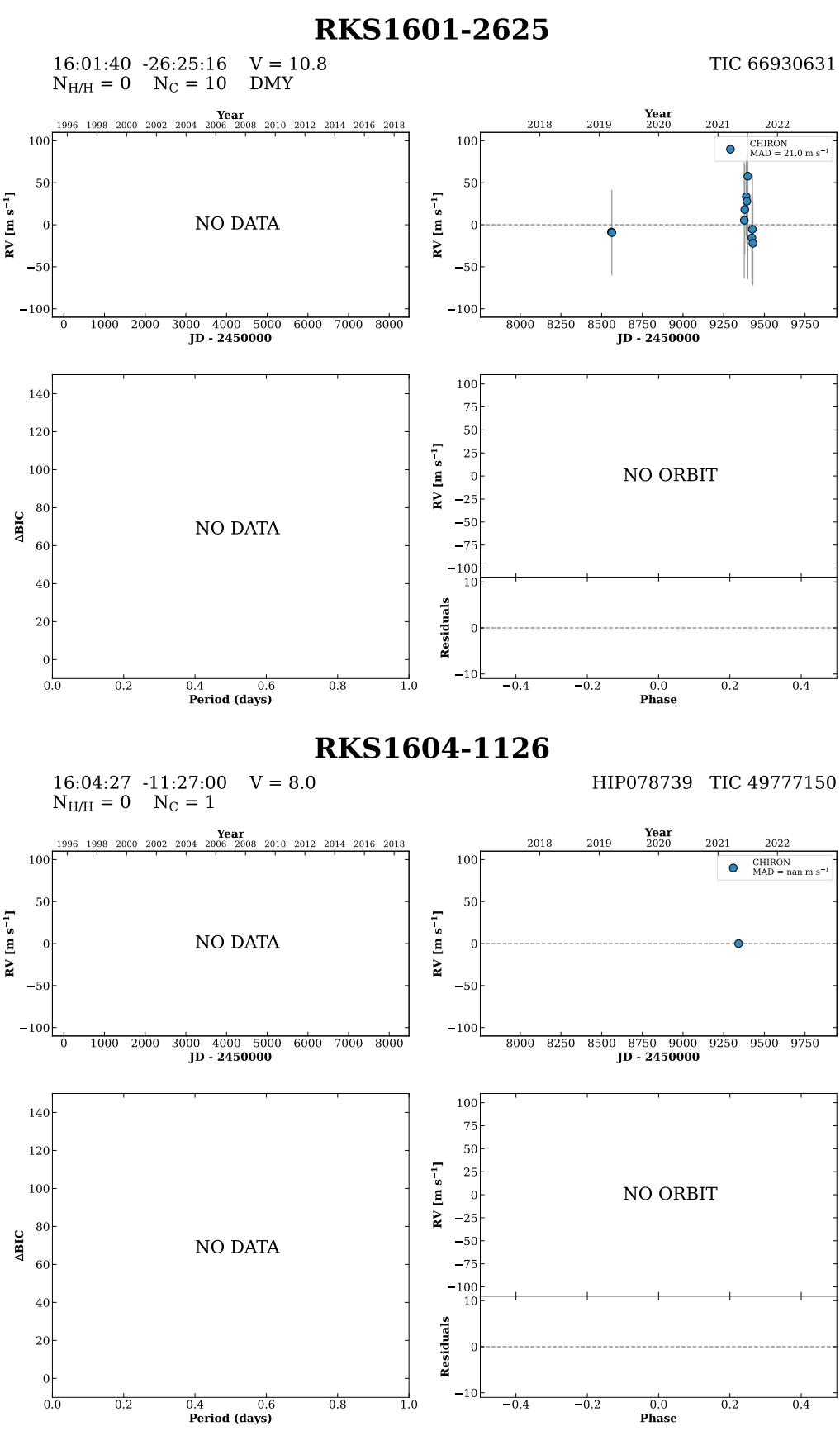

Figure 272 RV results for RKS1601-2625 (top) and RKS1604-1126 (bottom).

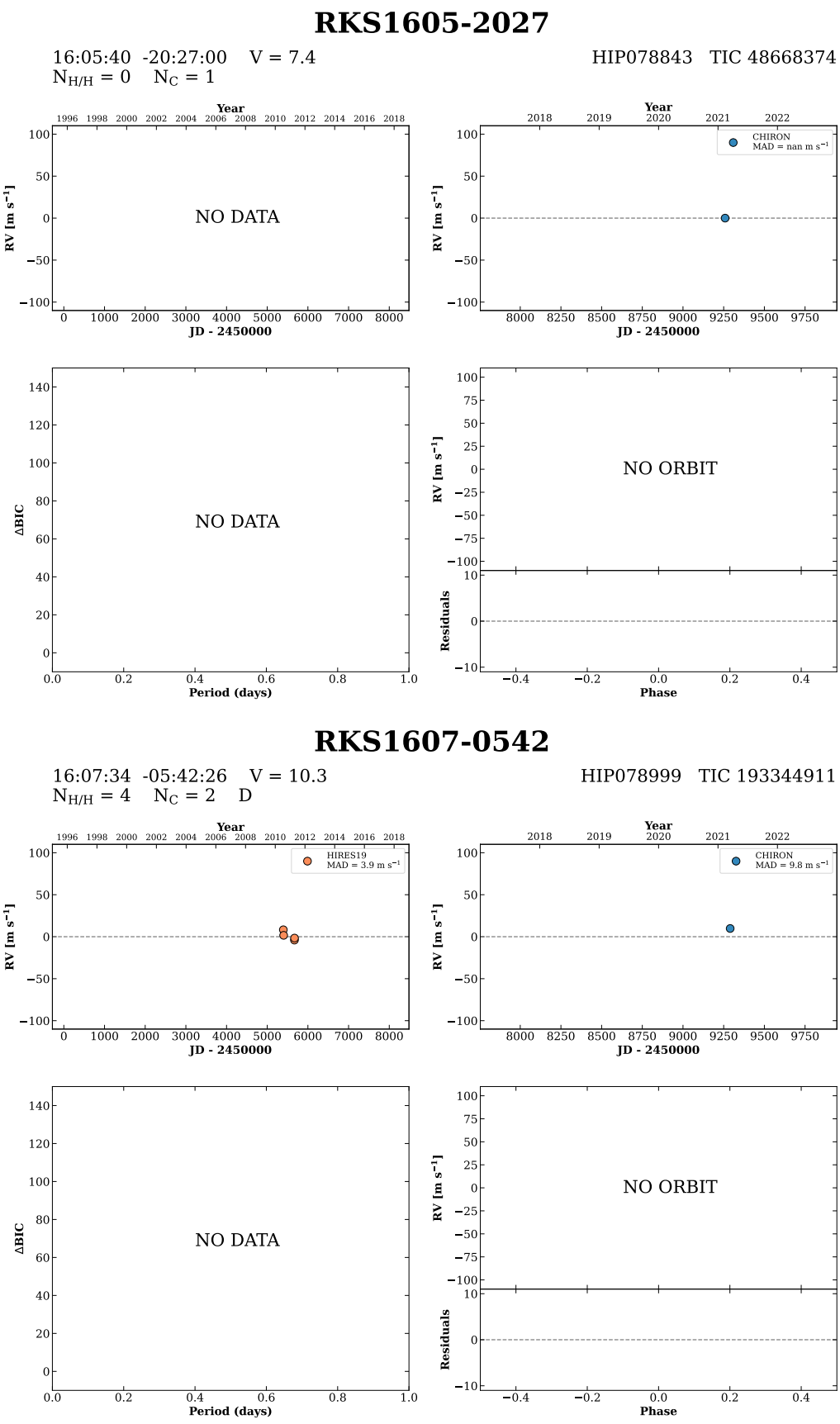

Figure 273 RV results for RKS1605-2027 (top) and RKS1607-0542 (bottom).

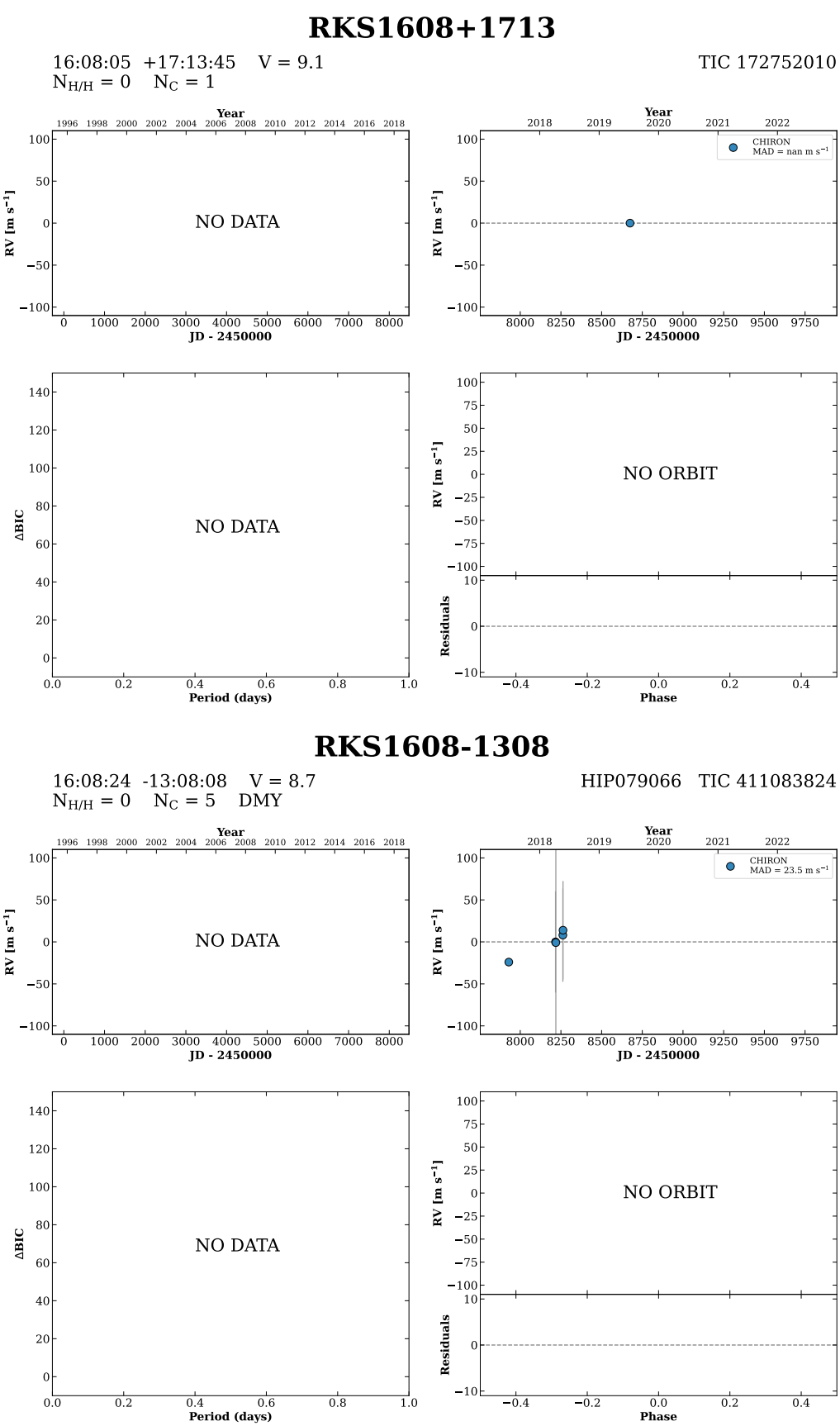

Figure 274 RV results for RKS1608+1713 (top) and RKS1608-1308 (bottom).

RKS1613+1331B

16:13:18 +13:31:41 V = 6.7 HIP079492 TIC 119985831
$N_{H/H}$ = 94 N_C = 2 M

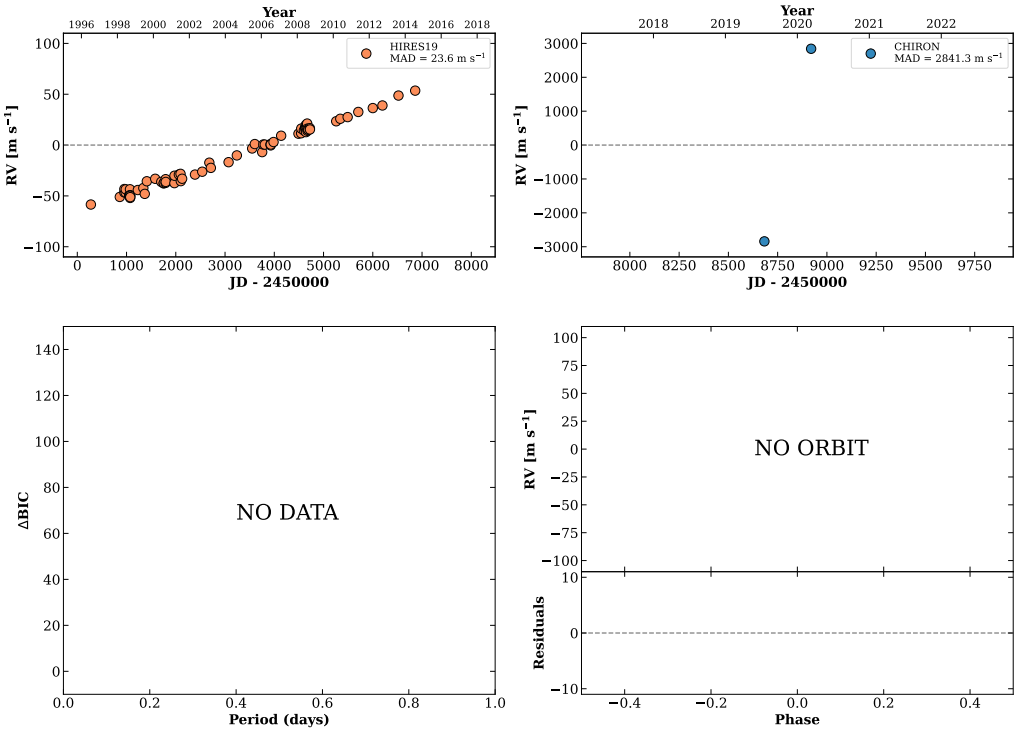

RKS1613+1331A

16:13:18 +13:31:37 V = 6.7 HIP079492 TIC 119985828
$N_{H/H}$ = 111 N_C = 1

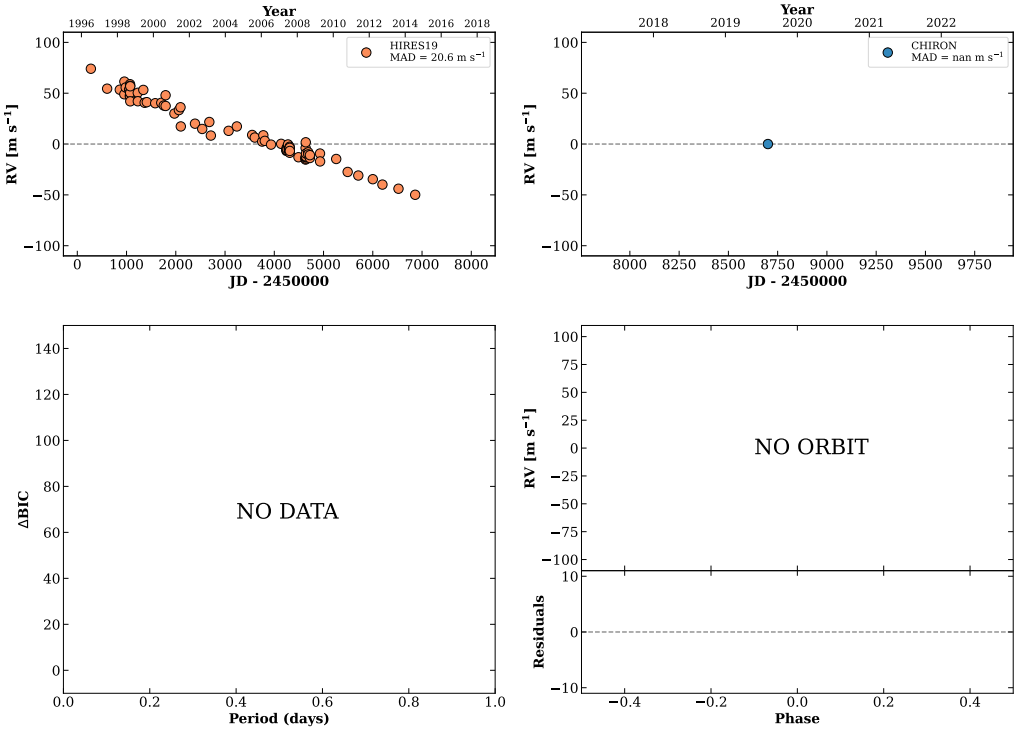

Figure 275 RV results for RKS1613+1331B (top) and RKS1613+1331A (bottom).

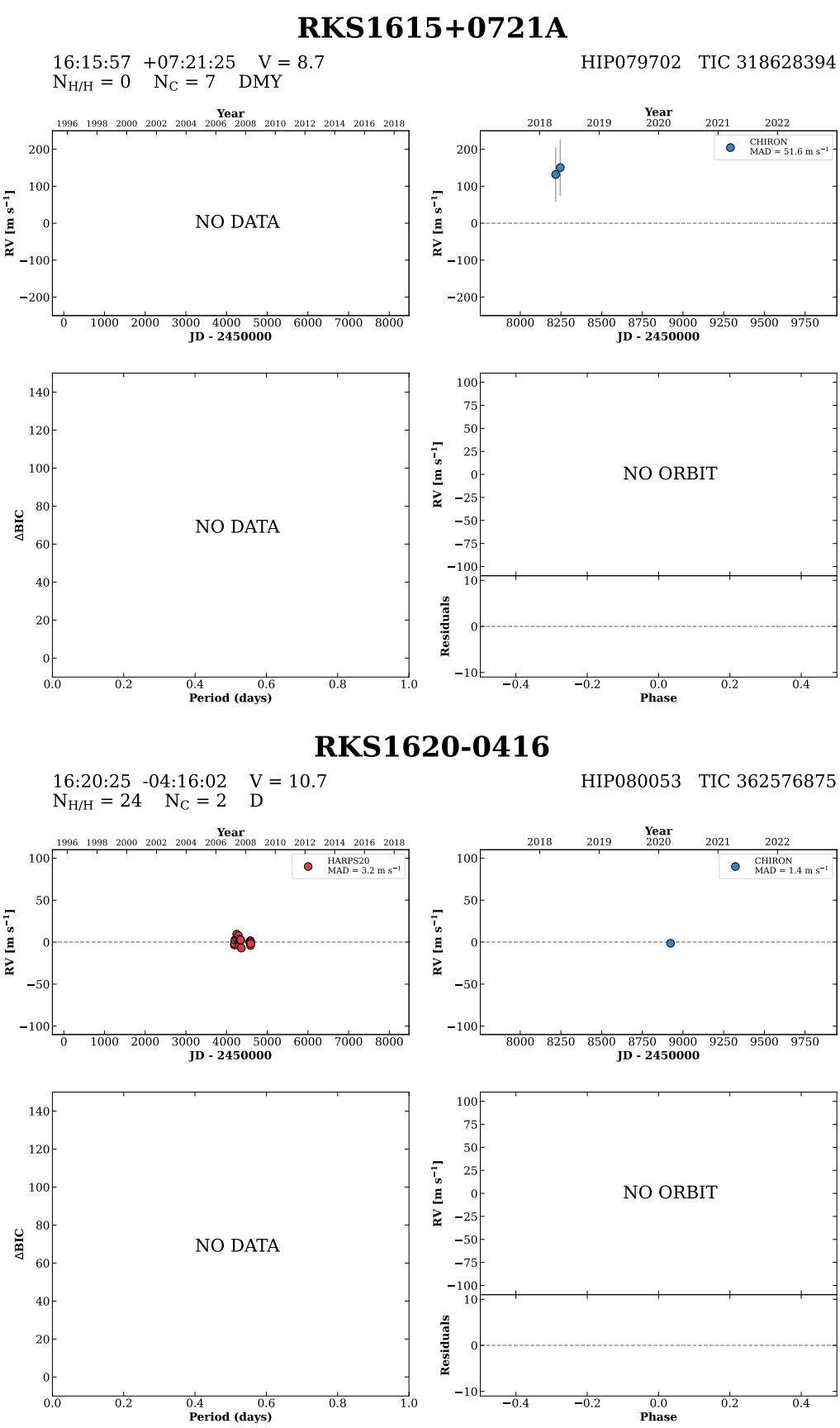

Figure 276 RV results for RKS1615+0721A (top) and RKS1620-0416 (bottom).

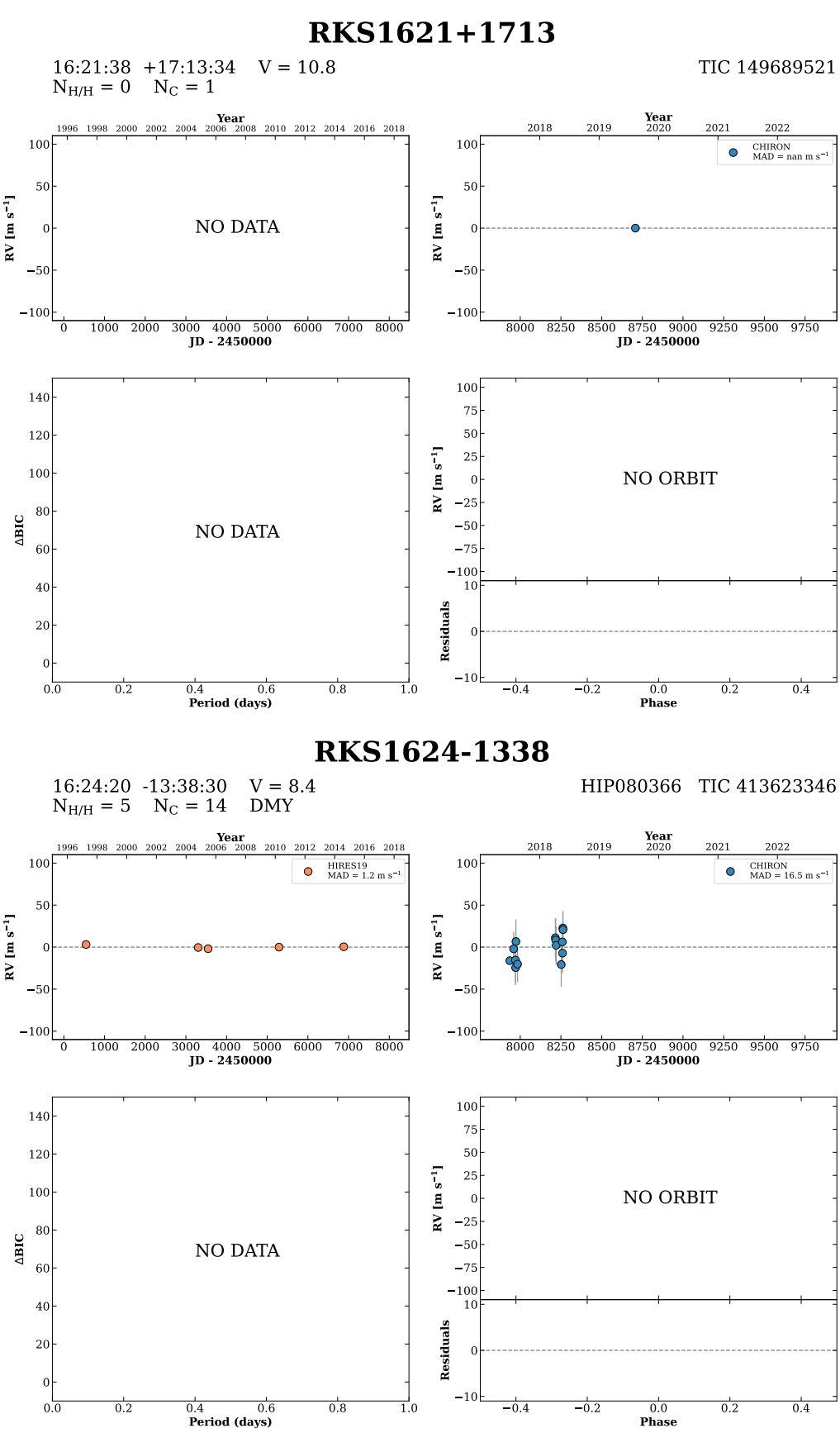

Figure 277 RV results for RKS1621+1713 (top) and RKS1624-1338 (bottom).

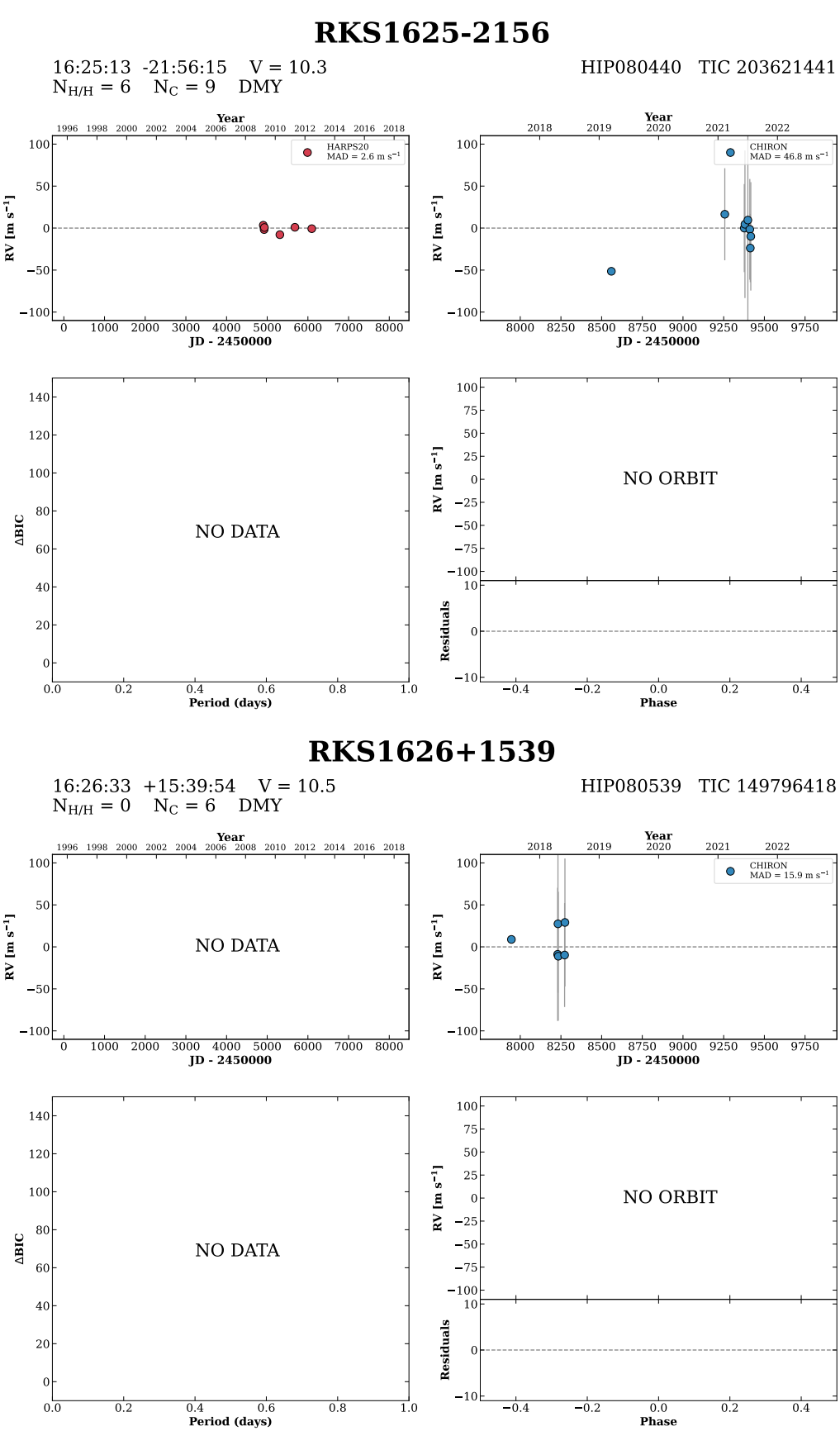

Figure 278 RV results for RKS1625-2156 (top) and RKS1626+1539 (bottom).

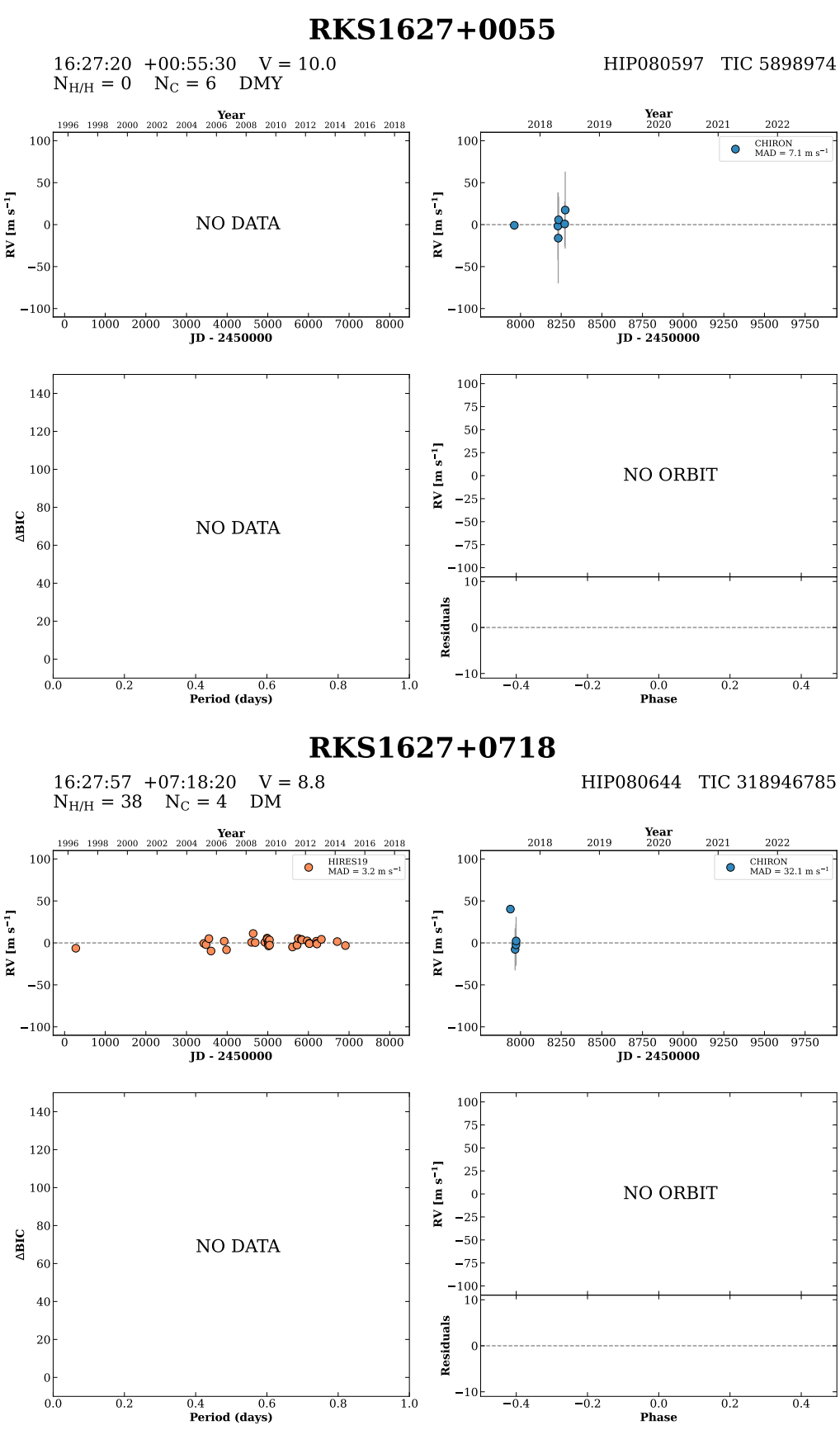

Figure 279 RV results for RKS1627+0055 (top) and RKS1627+0718 (bottom).

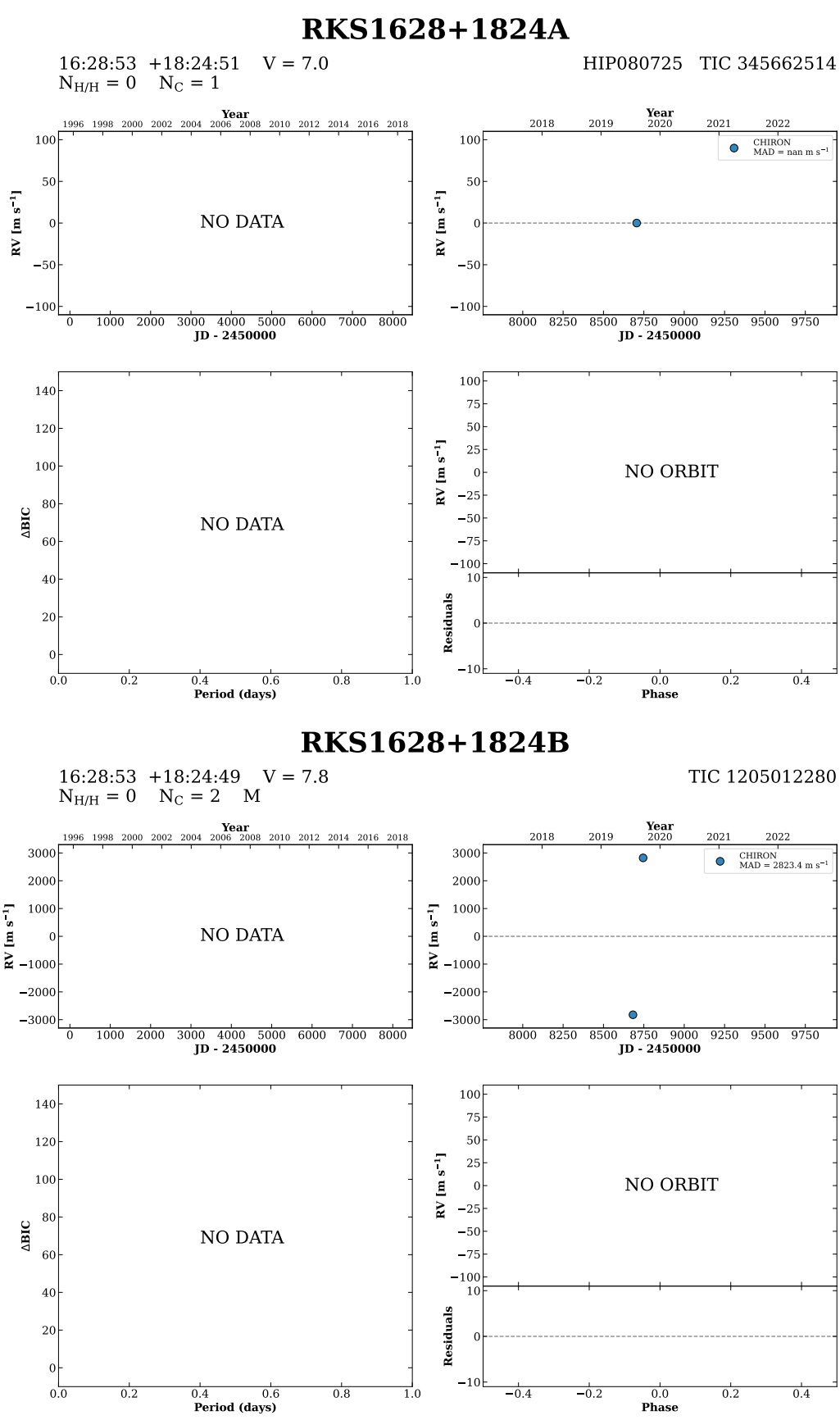

Figure 280 RV results for RKS1628+1824A (top) and RKS1628+1824B (bottom).

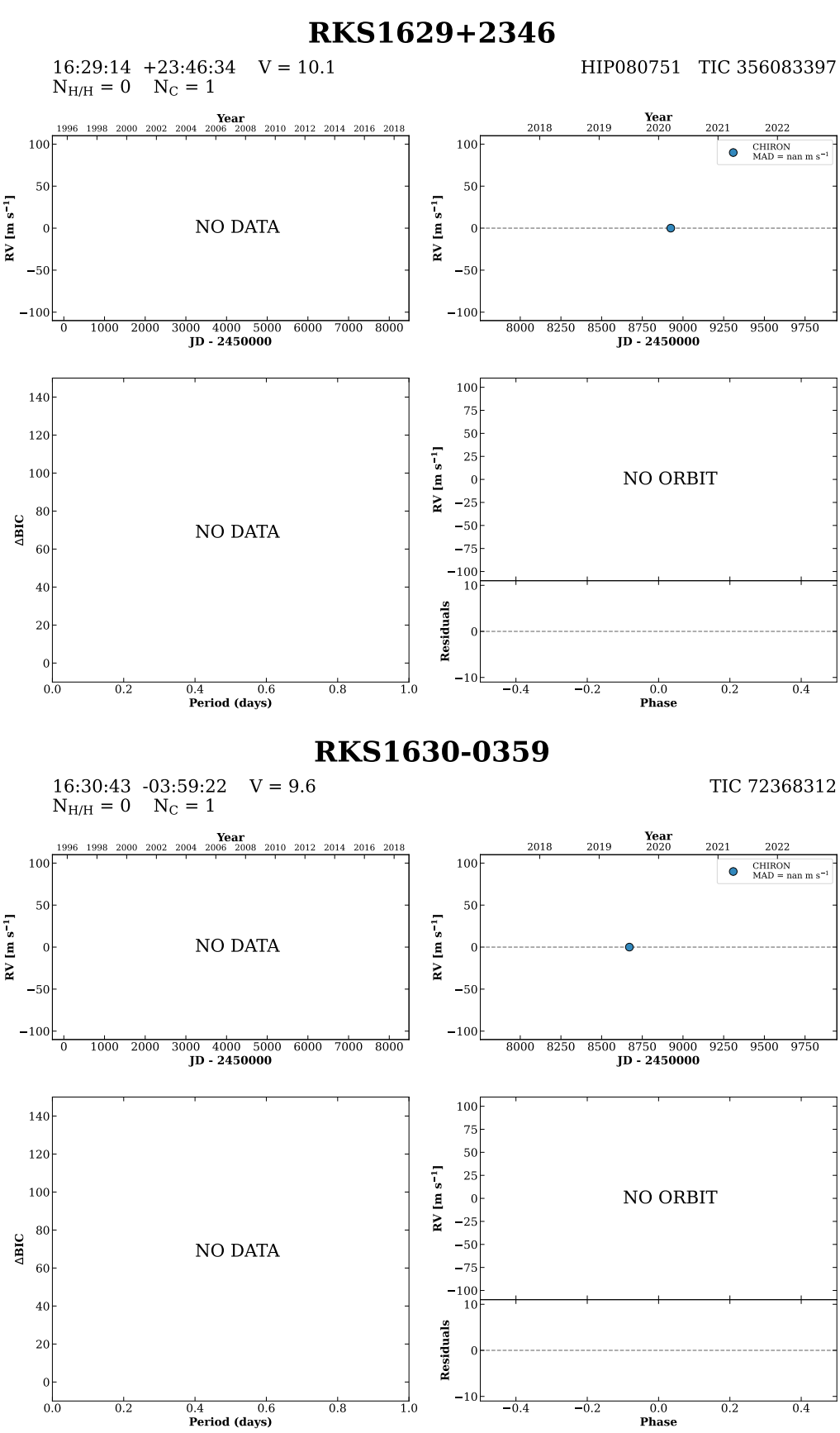

Figure 281 RV results for RKS1629+2346 (top) and RKS1630-0359 (bottom).

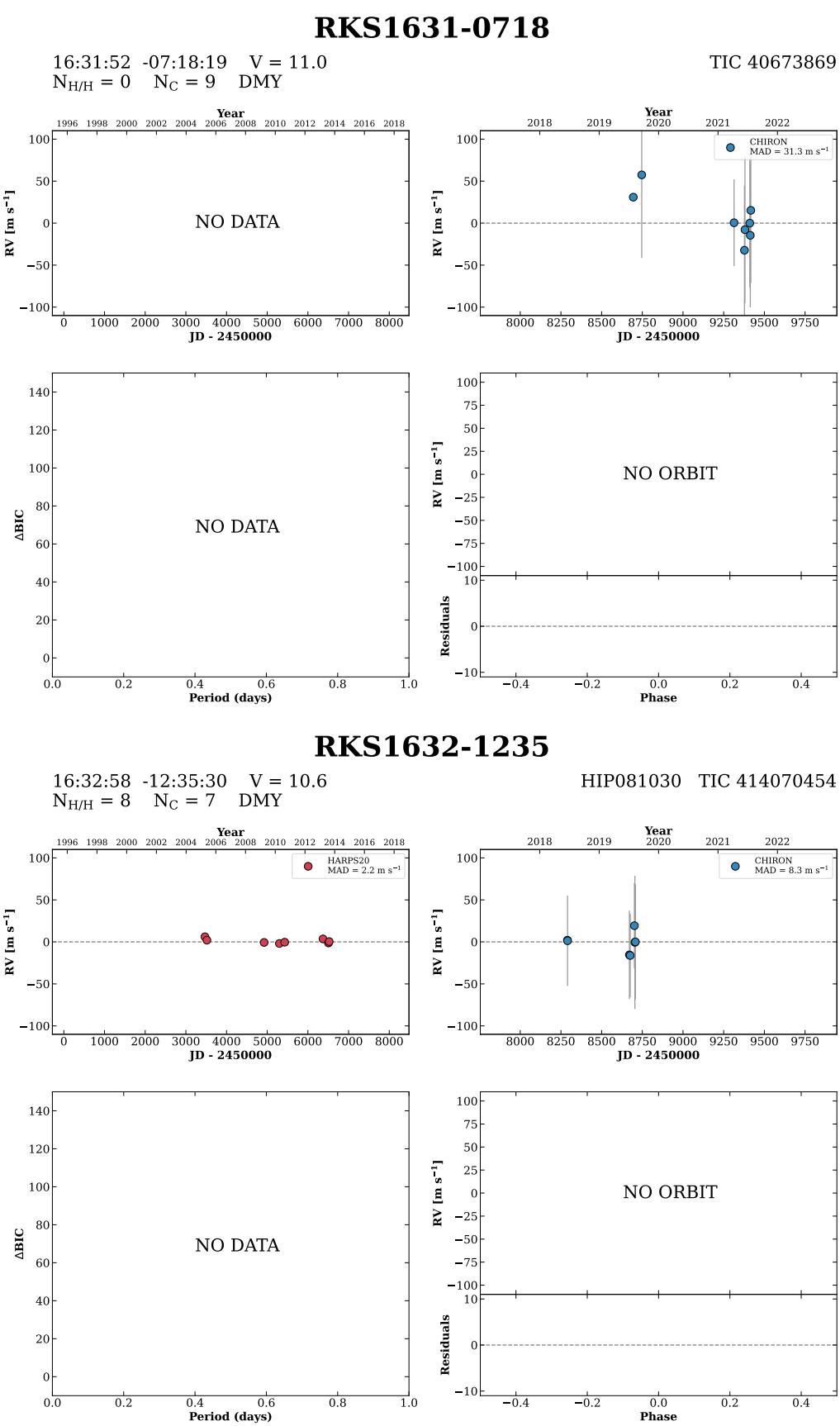

Figure 282 RV results for RKS1631-0718 (top) and RKS1632-1235 (bottom).

RKS1633-0933

16:33:42 -09:33:12 V = 11.3 HIP081084 TIC 40849632
$N_{H/H}$ = 33 N_C = 2 Y

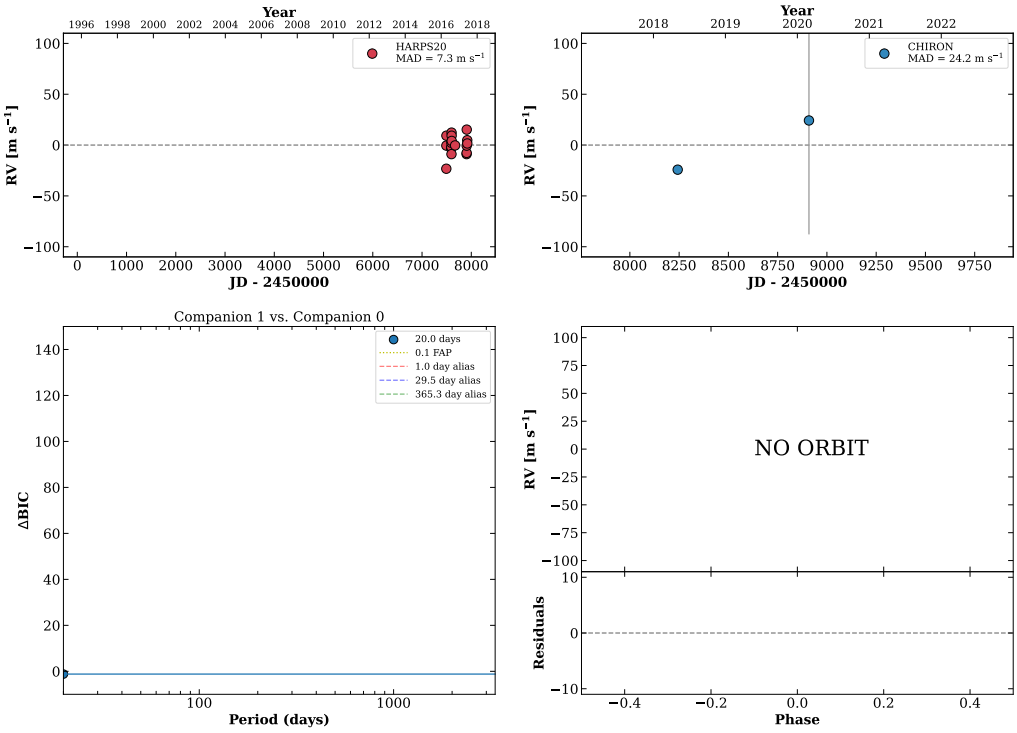

RKS1636-0219

16:36:21 -02:19:29 V = 5.8 HIP081300 TIC 58092025
$N_{H/H}$ = 67 N_C = 5 DMY

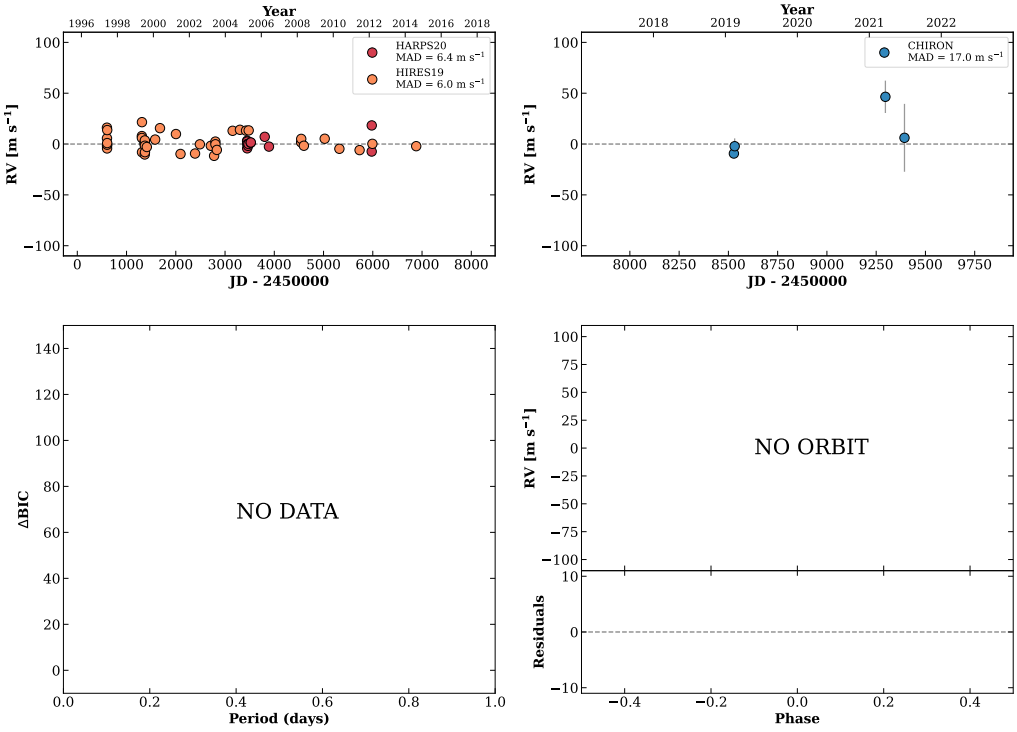

Figure 283 RV results for RKS1633-0933 (top) and RKS1636-0219 (bottom).

RKS1638-0501

16:38:20 -05:01:15 V = 10.4 HIP081465 TIC 58184907
$N_{H/H}$ = 9 N_C = 1

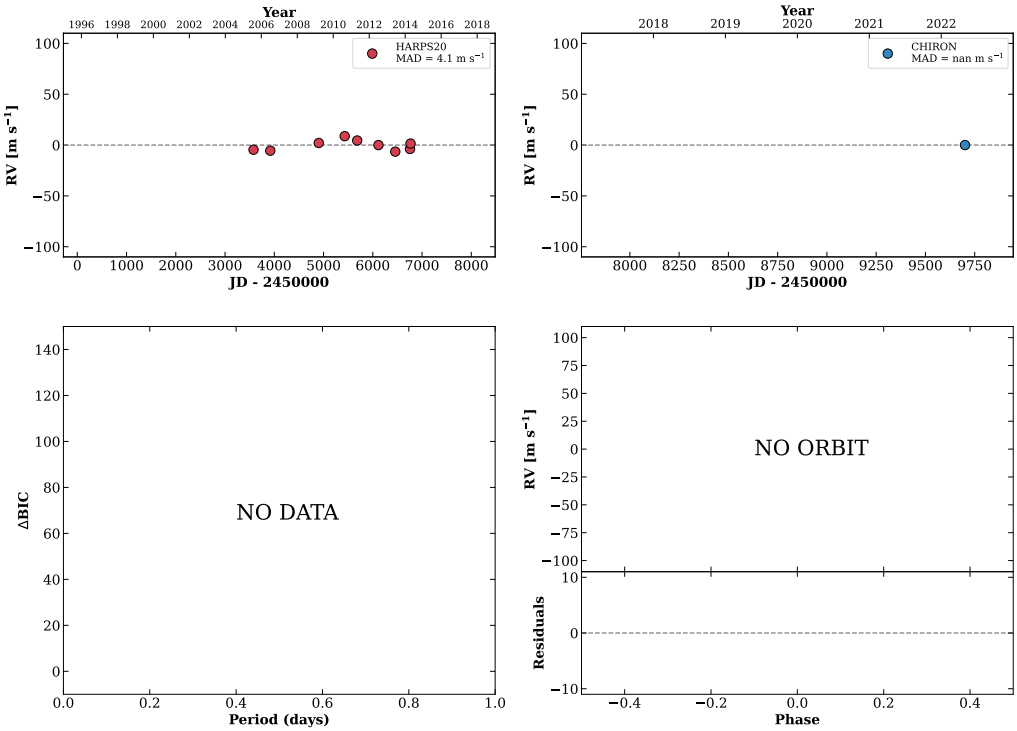

RKS1646+0531

16:46:51 +05:31:26 V = 10.9 TIC 315475193
$N_{H/H}$ = 0 N_C = 3 DY

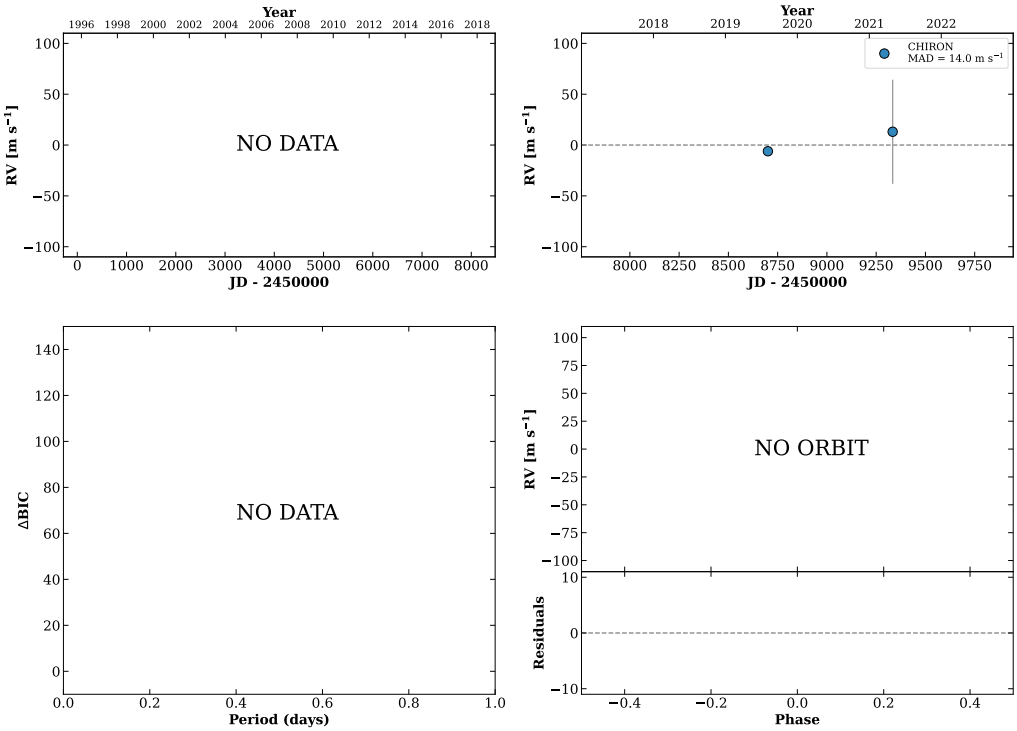

Figure 284 RV results for RKS1638-0501 (top) and RKS1646+0531 (bottom).

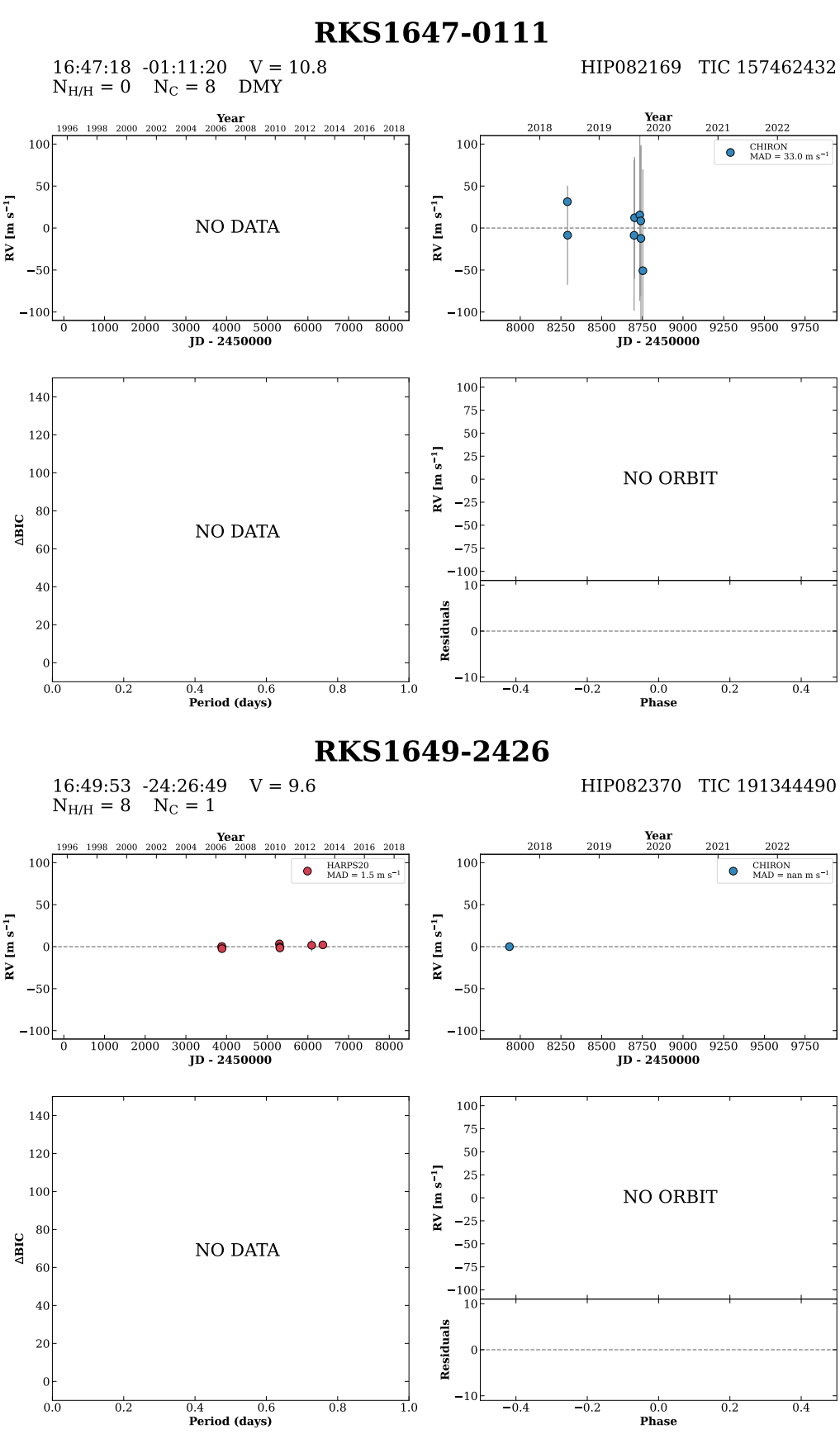

Figure 285 RV results for RKS1647-0111 (top) and RKS1649-2426 (bottom).

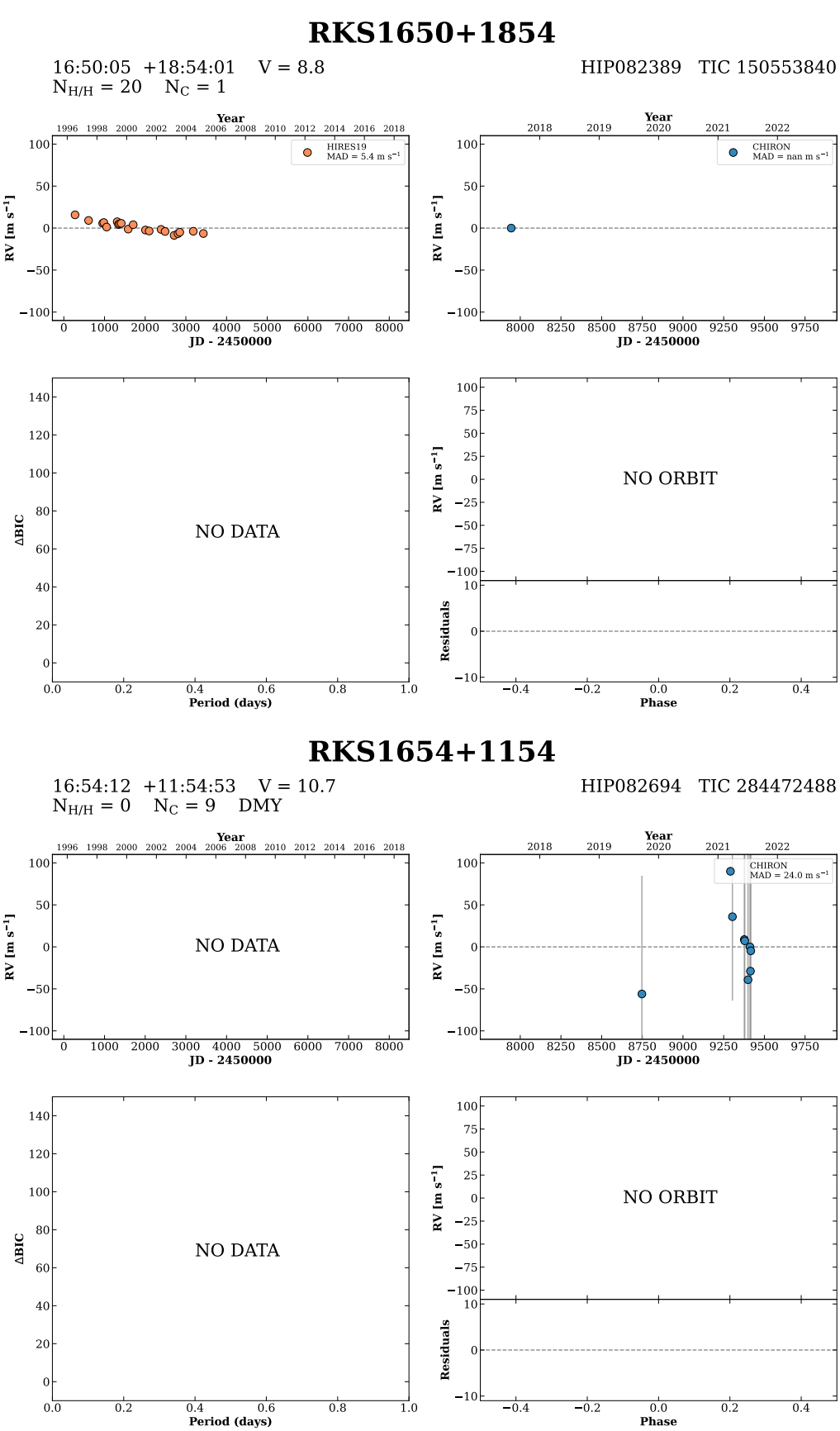

Figure 286 RV results for RKS1650+1854 (top) and RKS1654+1154 (bottom).

RKS1659-2616

16:59:33 -26:16:04 V = 10.4 HIP083147 TIC 18364458
$N_{H/H}$ = 0 N_C = 30 DMY

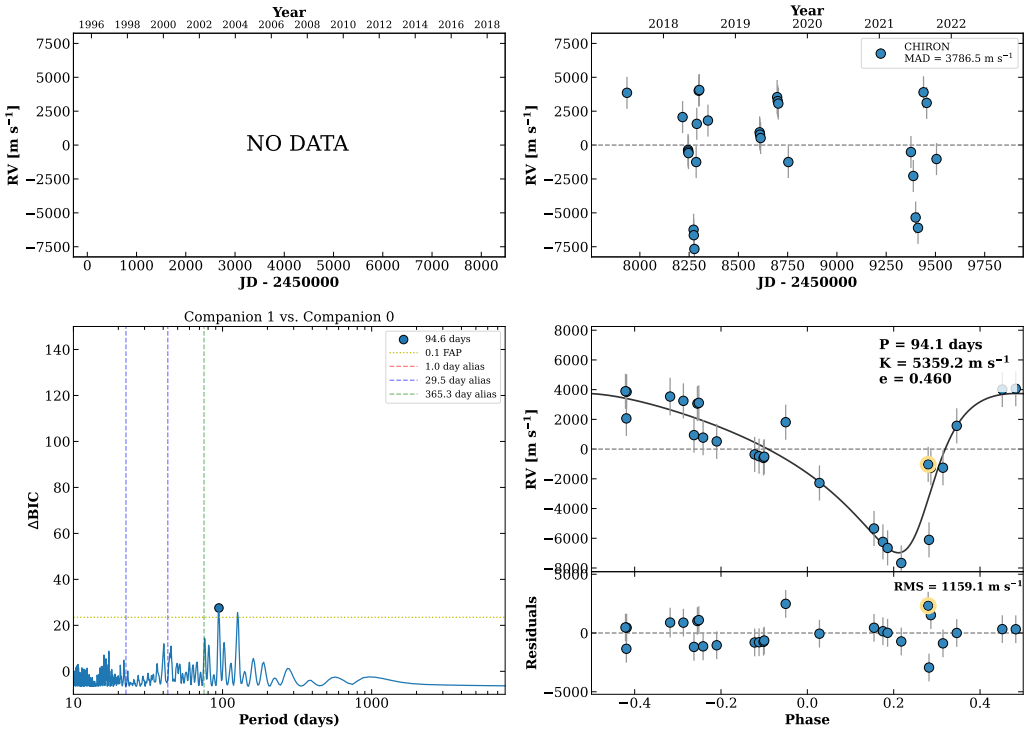

RKS1701+2256

17:02:00 +22:56:09 V = 8.8 HIP083343 TIC 349490623
$N_{H/H}$ = 0 N_C = 13 DMY

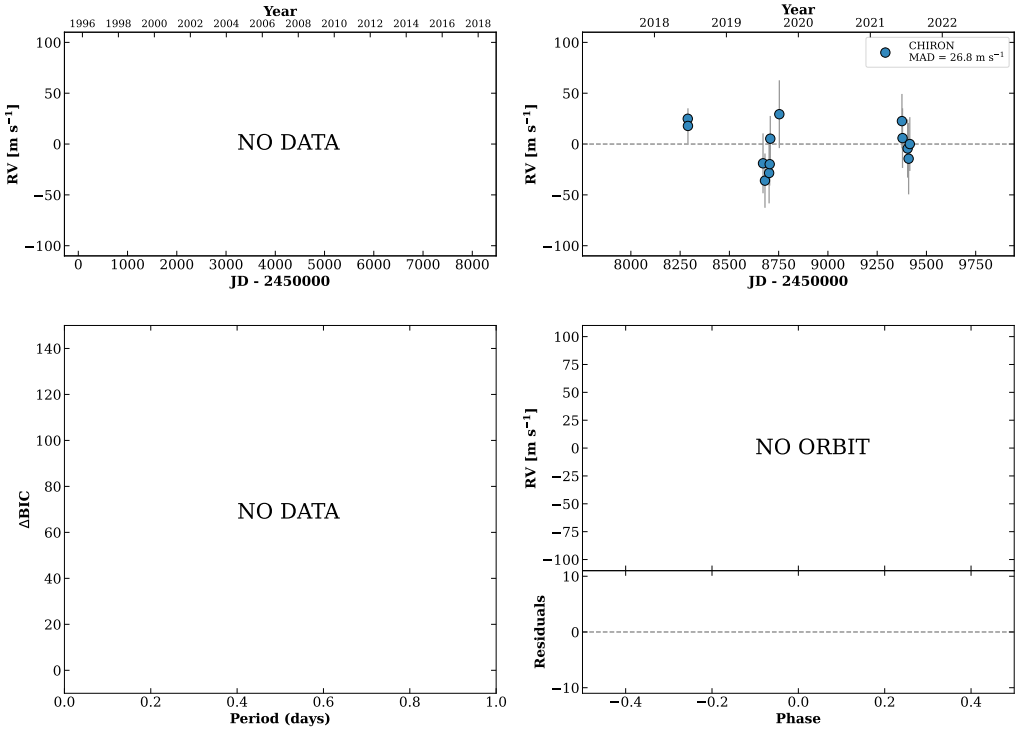

Figure 287 RV results for RKS1659-2616 (top) and RKS1701+2256 (bottom).

RKS1705-0503

17:05:03 -05:04:00 V = 7.7 HIP083591 TIC 142456308
$N_{H/H}$ = 143 N_C = 1

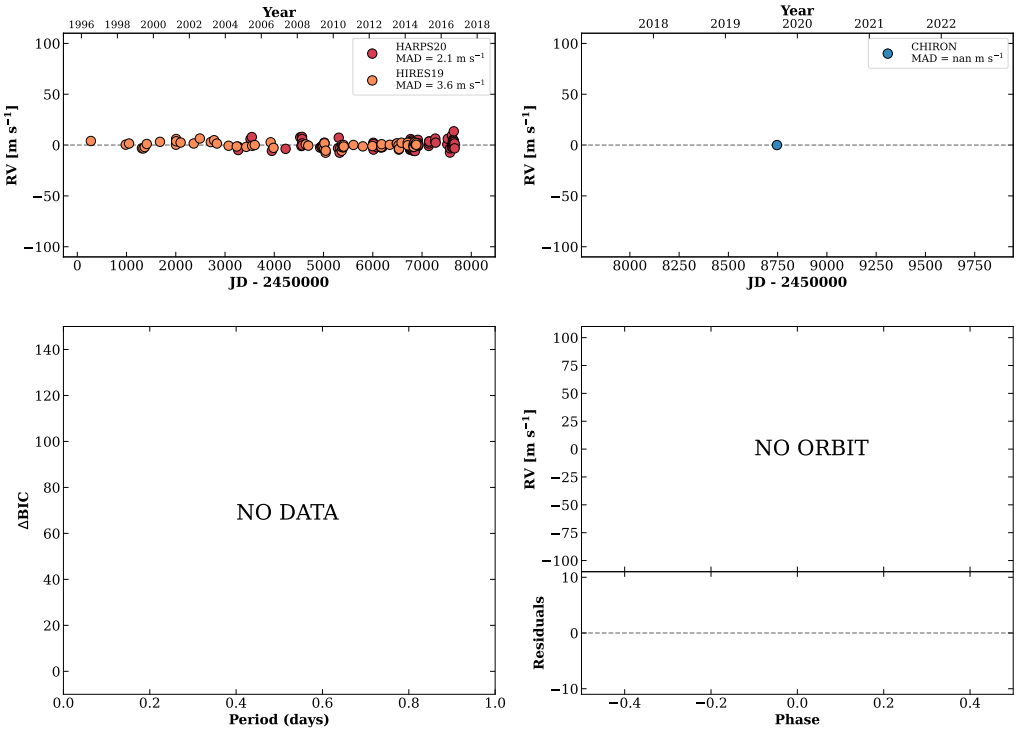

RKS1705-0147

17:05:09 -01:47:10 V = 9.5 TIC 142452434
$N_{H/H}$ = 0 N_C = 6 DMY

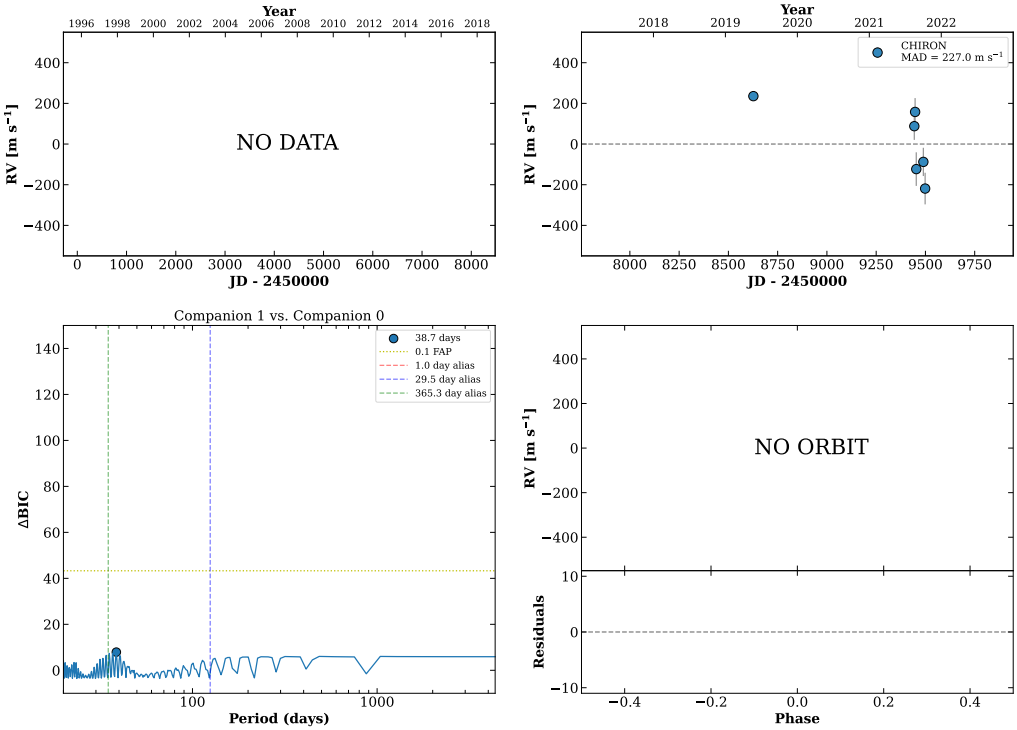

Figure 288 RV results for RKS1705-0503 (top) and RKS1705-0147 (bottom).

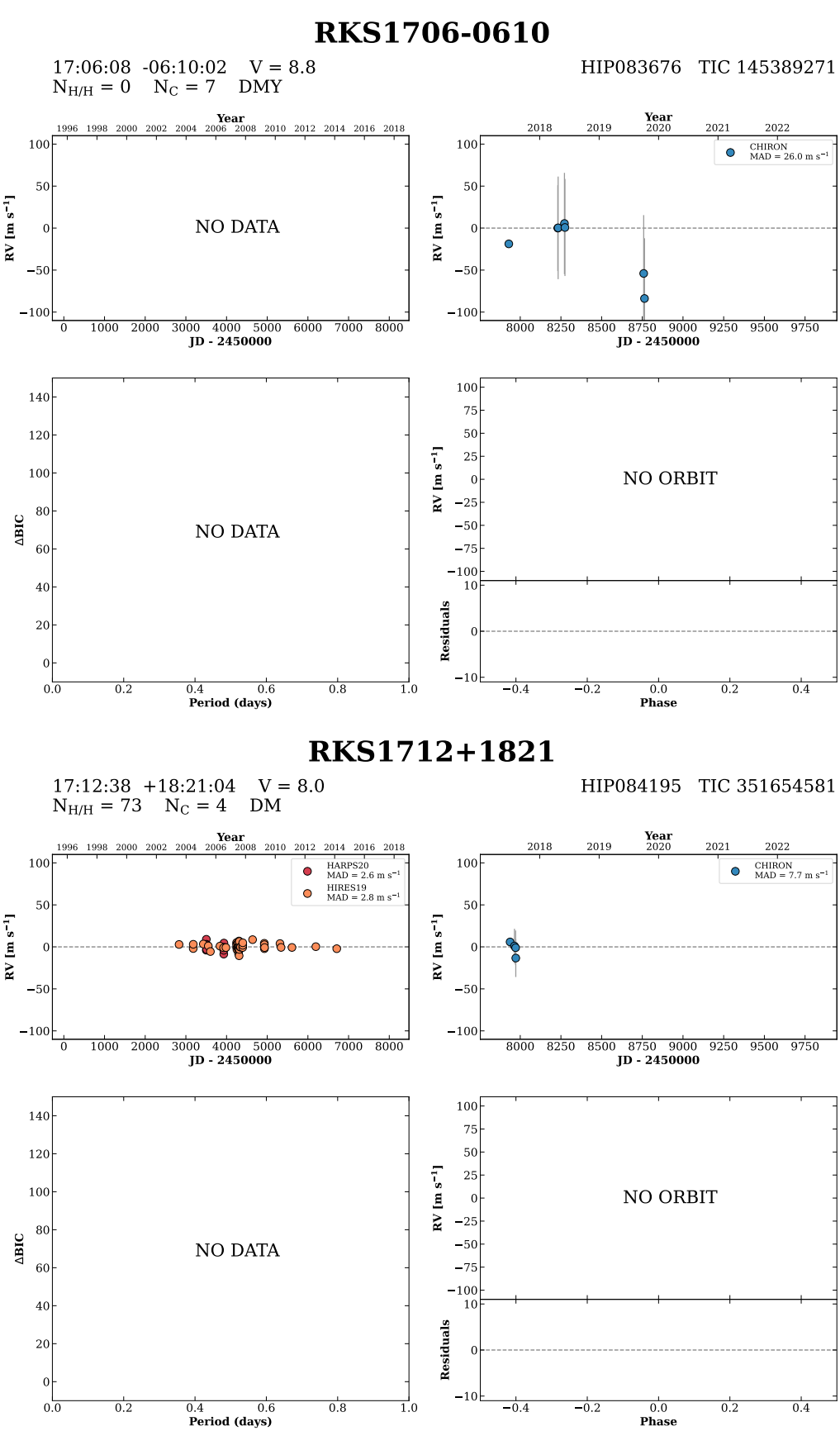

Figure 289 RV results for RKS1706-0610 (top) and RKS1712+1821 (bottom).

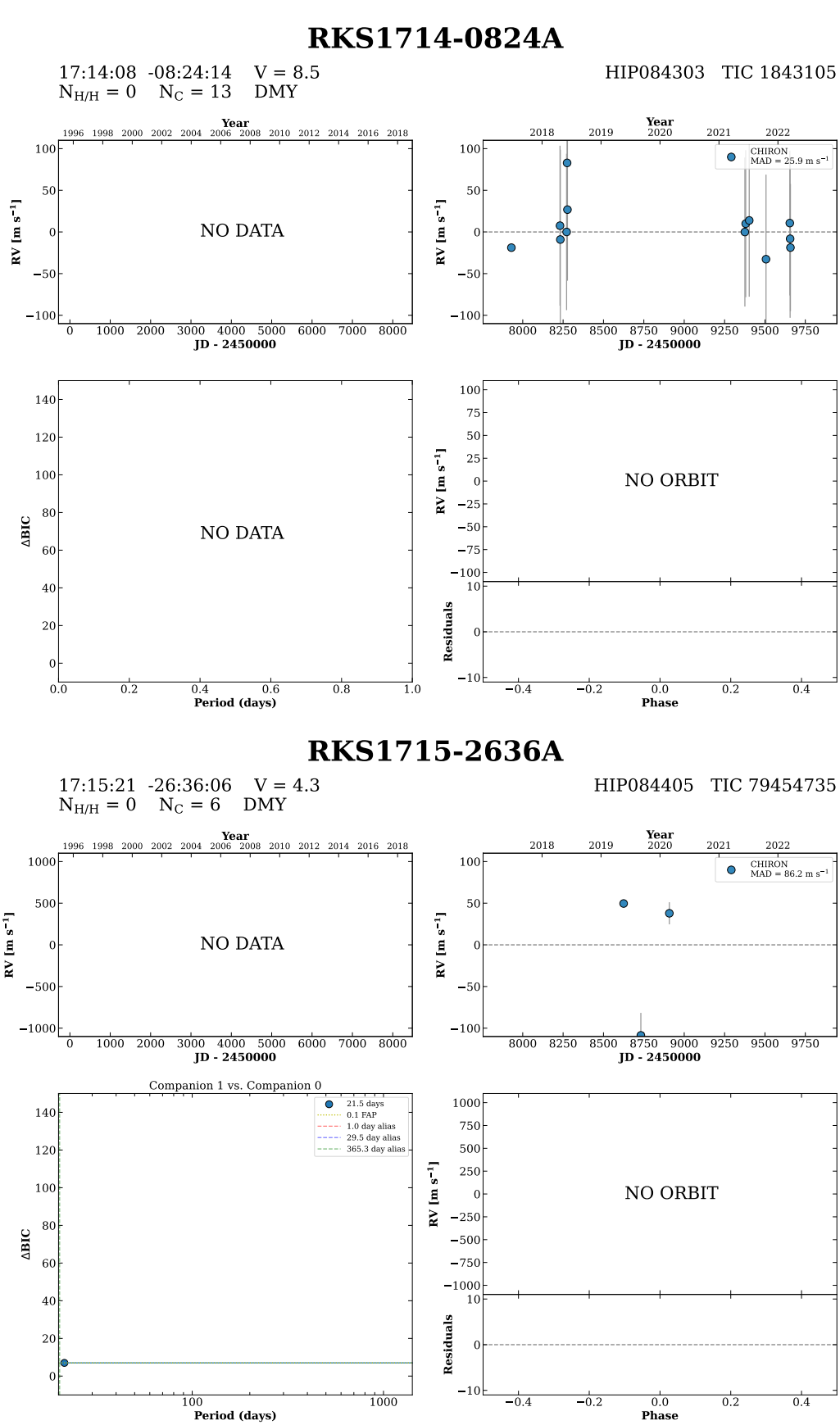

Figure 290 RV results for RKS1714-0824A (top) and RKS1715-2636A (bottom).

RKS1716-2632

17:16:13 -26:32:46 V = 6.3 HIP084478 TIC 79841001
$N_{H/H}$ = 27 N_C = 2 M

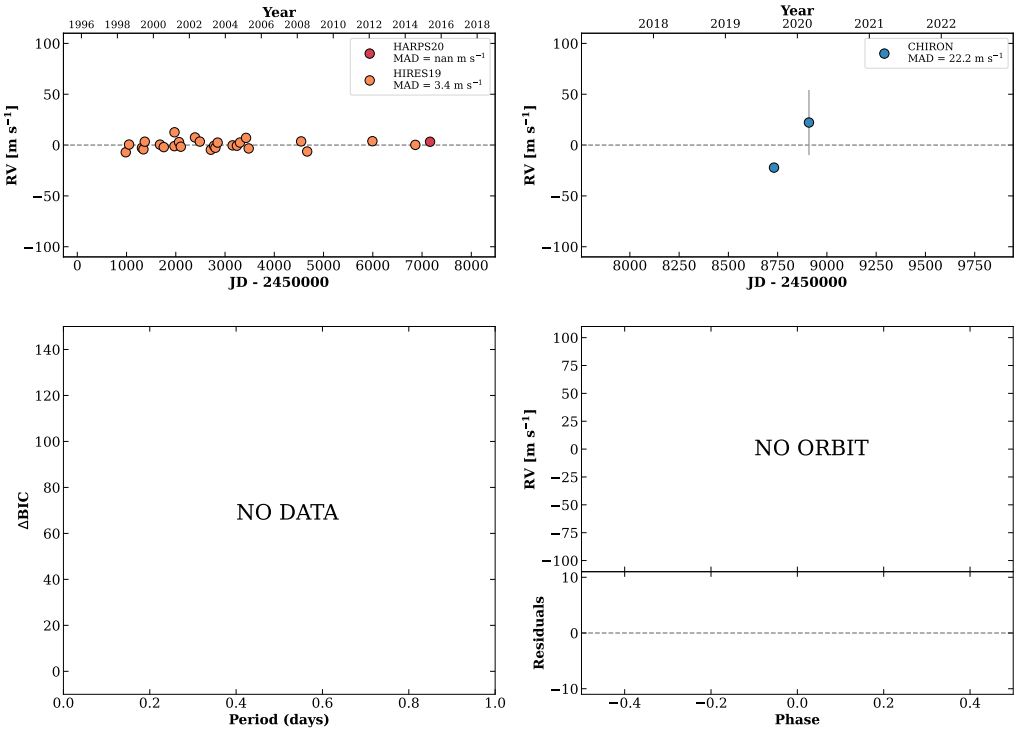

RKS1716-1210

17:16:20 -12:10:41 V = 10.5 HIP084487 TIC 435045600
$N_{H/H}$ = 7 N_C = 10 DMY

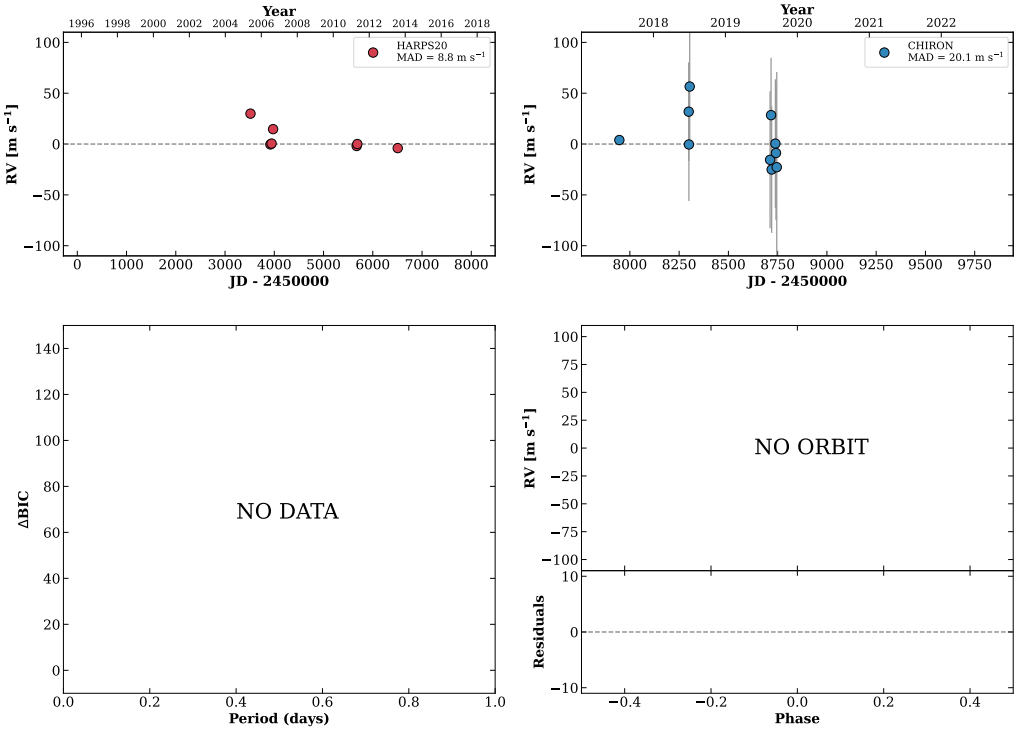

Figure 291 RV results for RKS1716-2632 (top) and RKS1716-1210 (bottom).

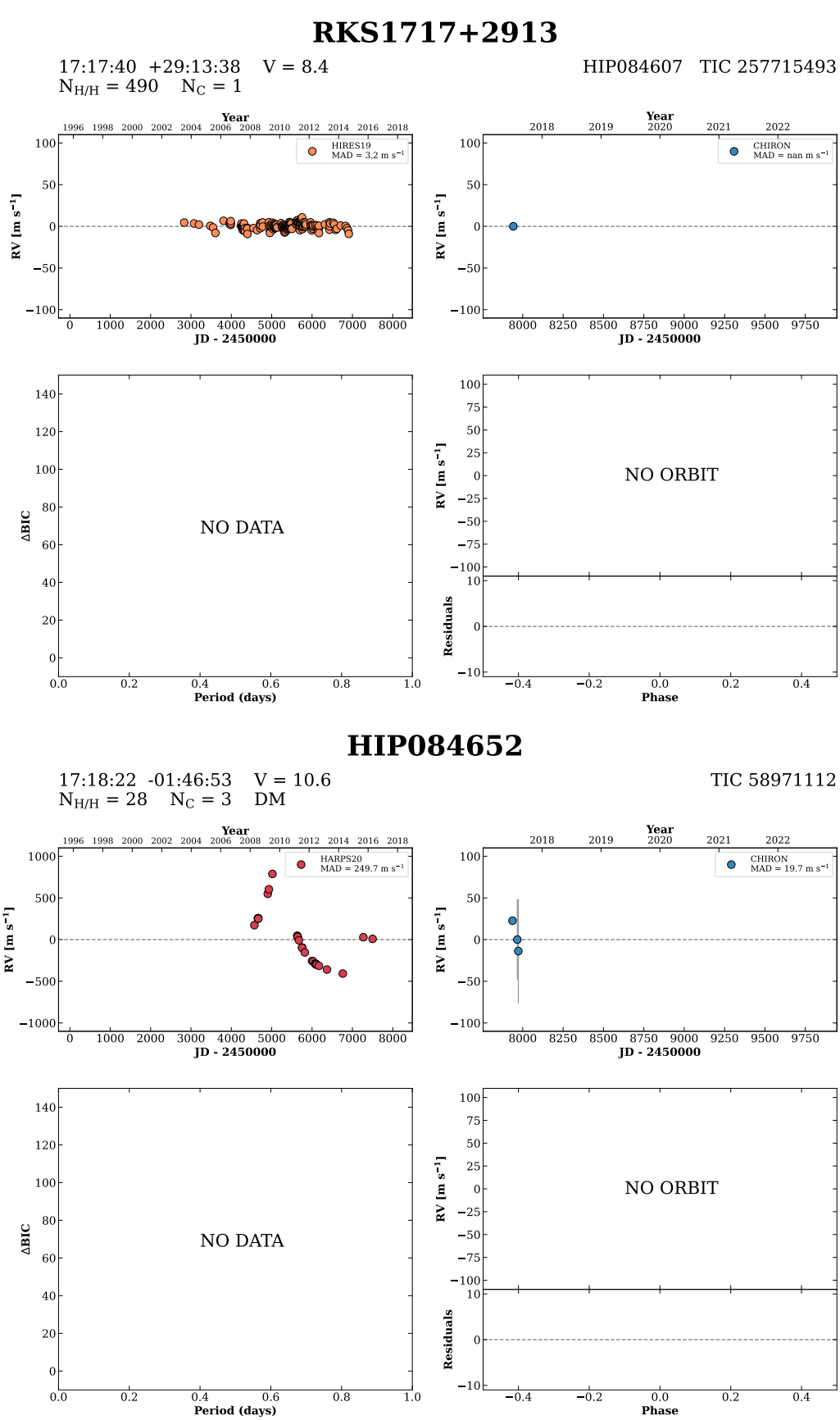

Figure 292 RV results for RKS1717+2913 (top) and HIP084652 (bottom).

RKS1721-2106

17:21:01 -21:06:43 V = 9.7 HIP084893 TIC 1455907039
$N_{H/H}$ = 0 N_C = 3 D

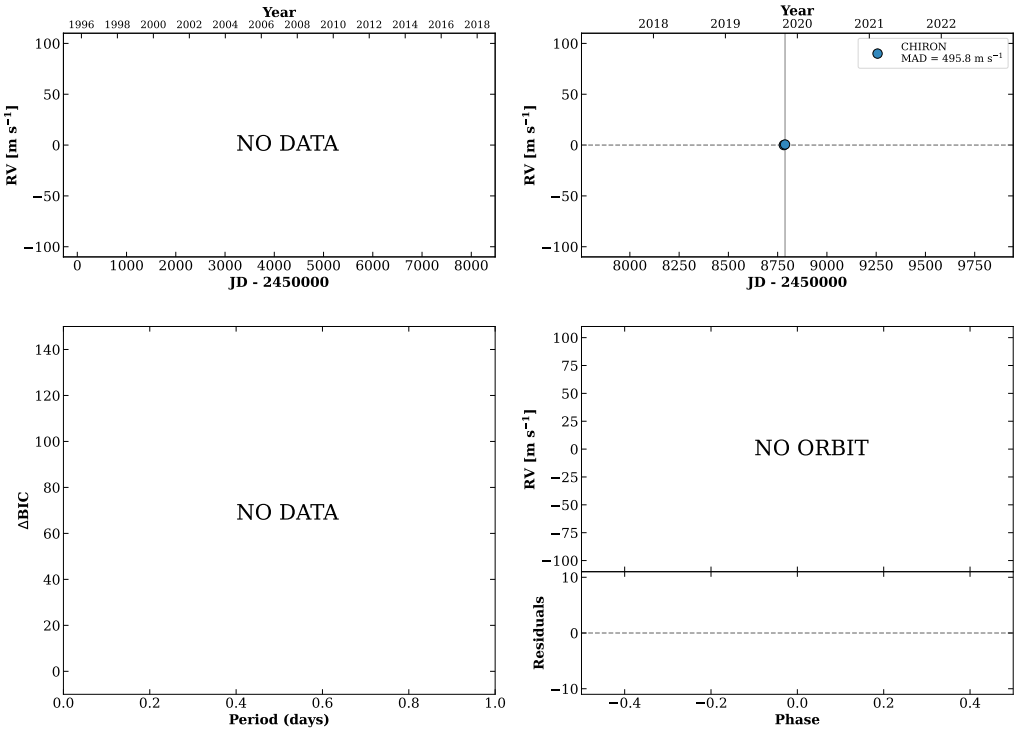

RKS1722-1457

17:22:43 -14:57:37 V = 10.9 HIP085026 TIC 429927313
$N_{H/H}$ = 0 N_C = 15 DMY

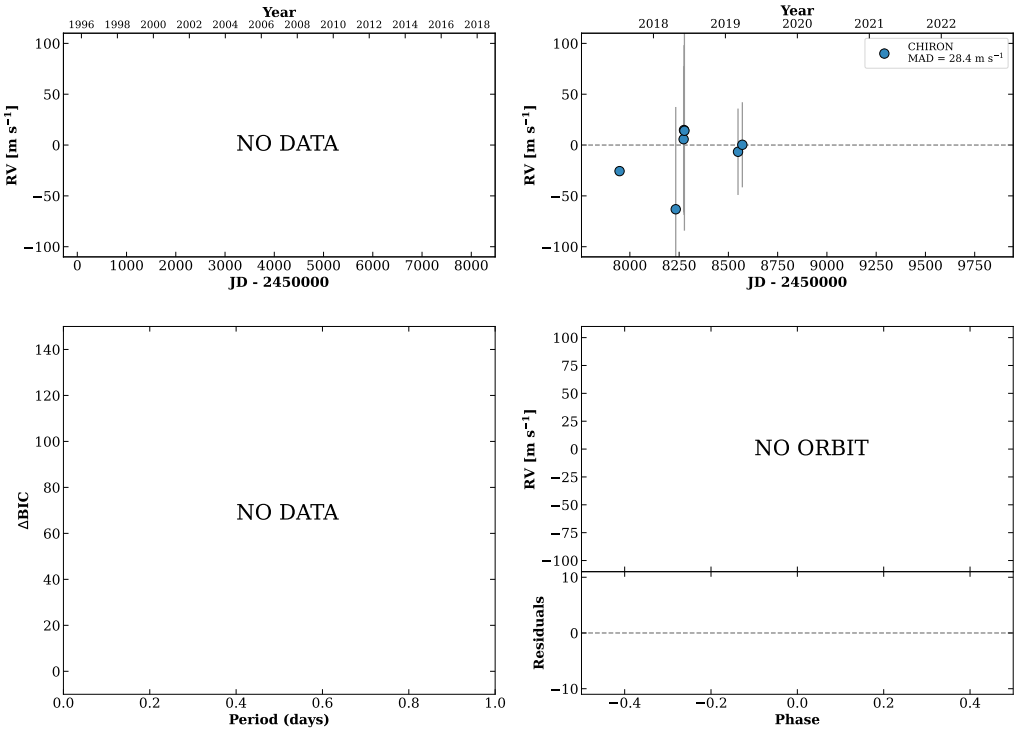

Figure 293 RV results for RKS1721-2106 (top) and RKS1722-1457 (bottom).

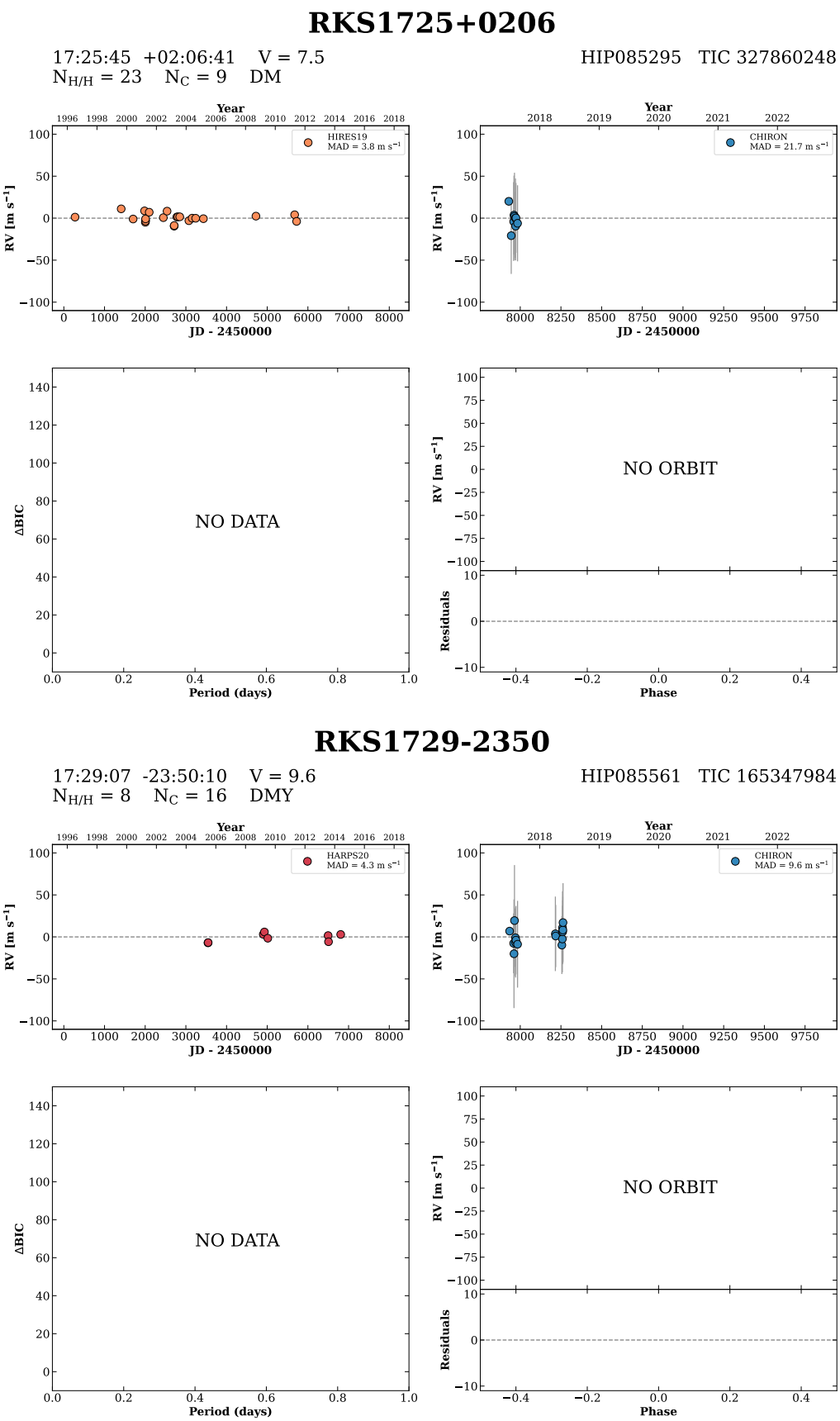

Figure 294 RV results for RKS1725+0206 (top) and RKS1729-2350 (bottom).

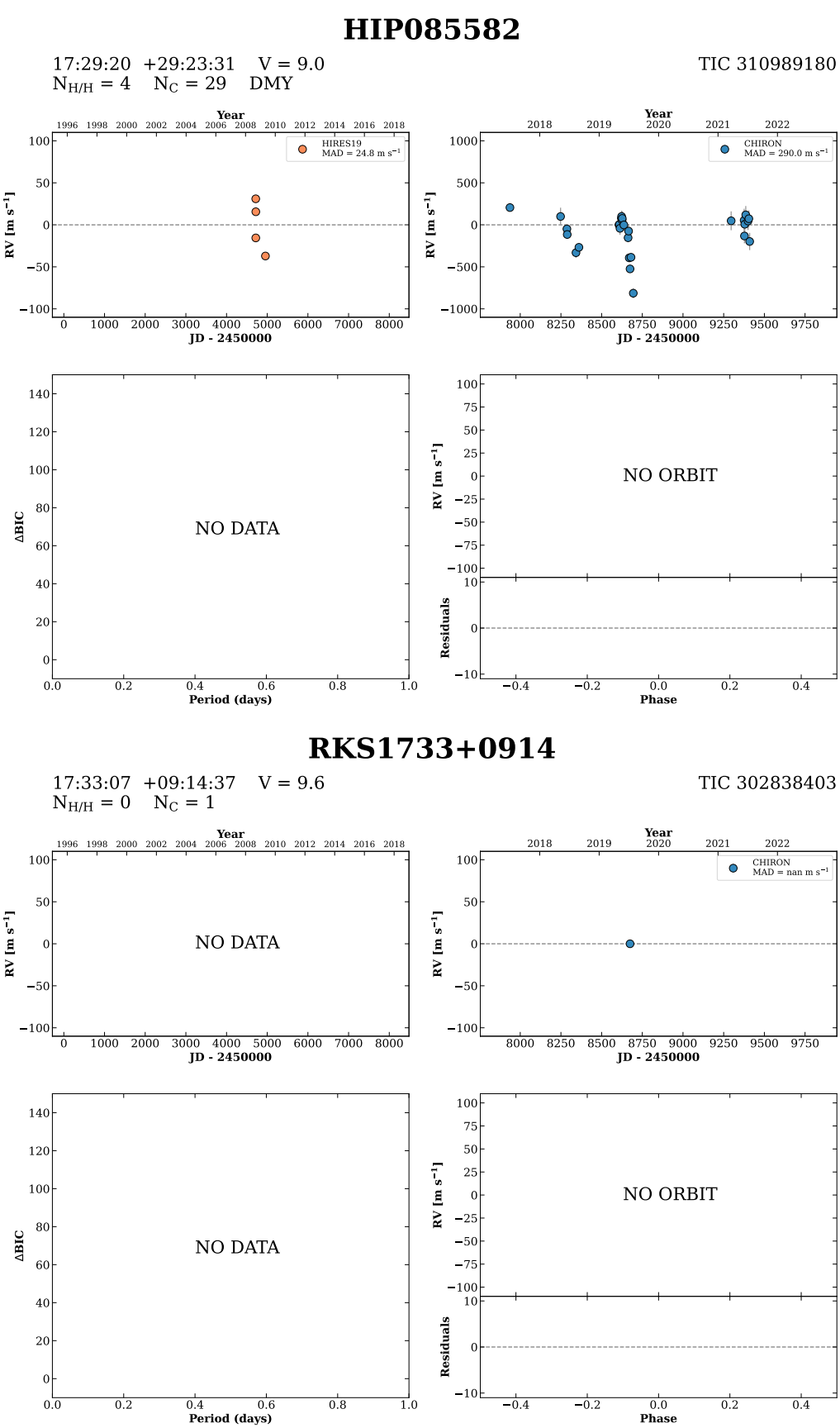

Figure 295 RV results for HIP085582 (top) and RKS1733+0914 (bottom).

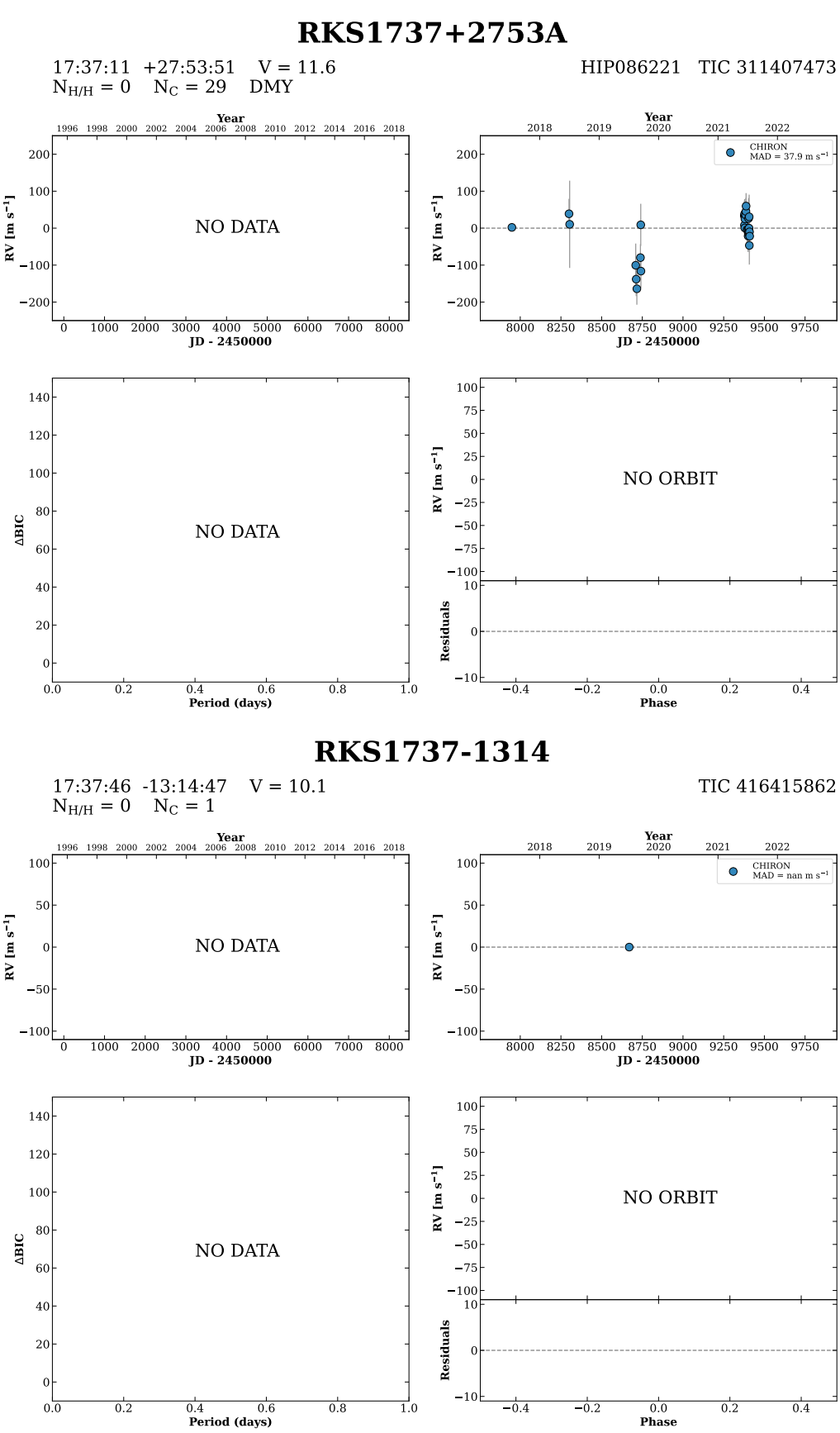

Figure 296 RV results for RKS1737+2753A (top) and RKS1737-1314 (bottom).

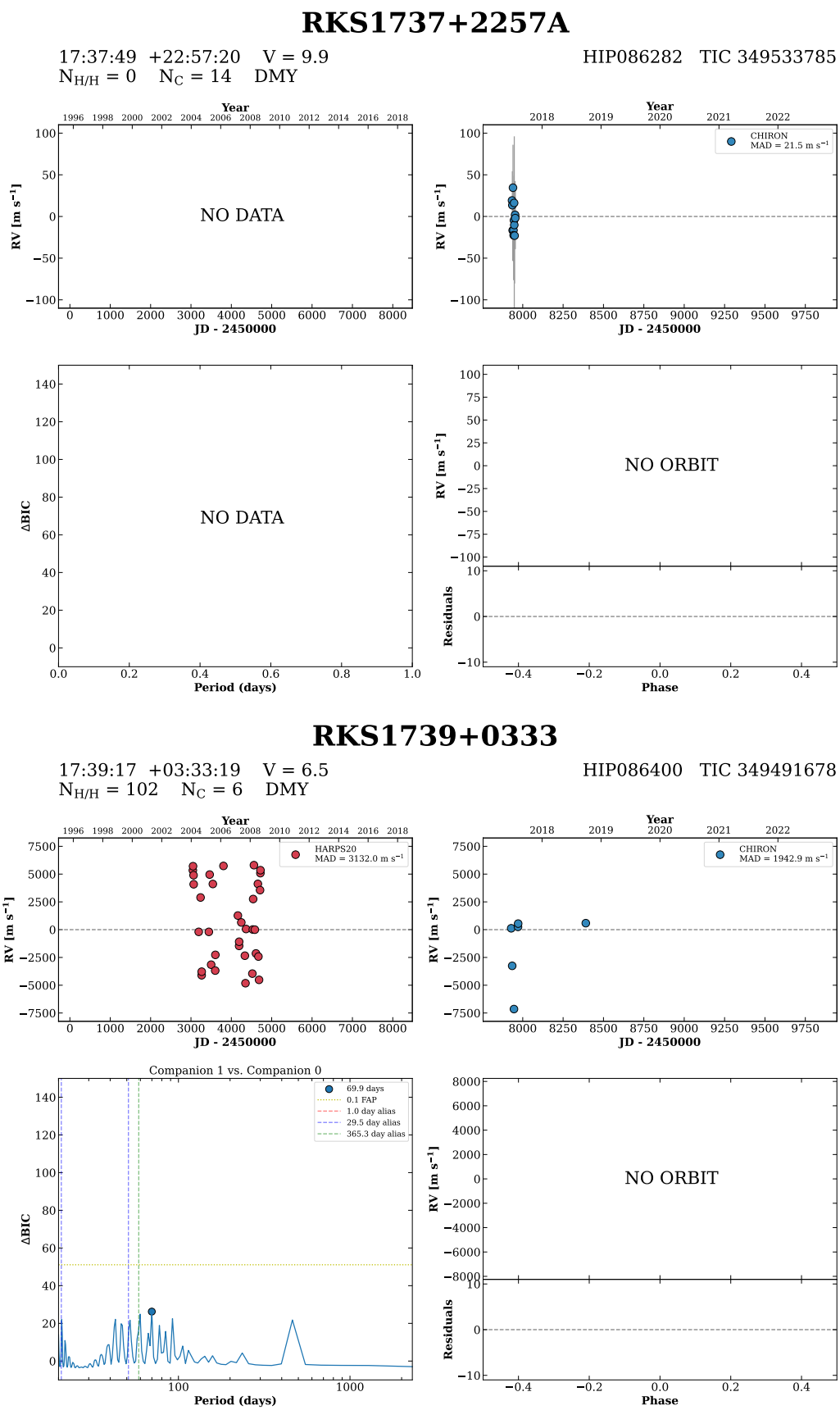

Figure 297 RV results for RKS1737+2257A (top) and RKS1739+0333 (bottom).

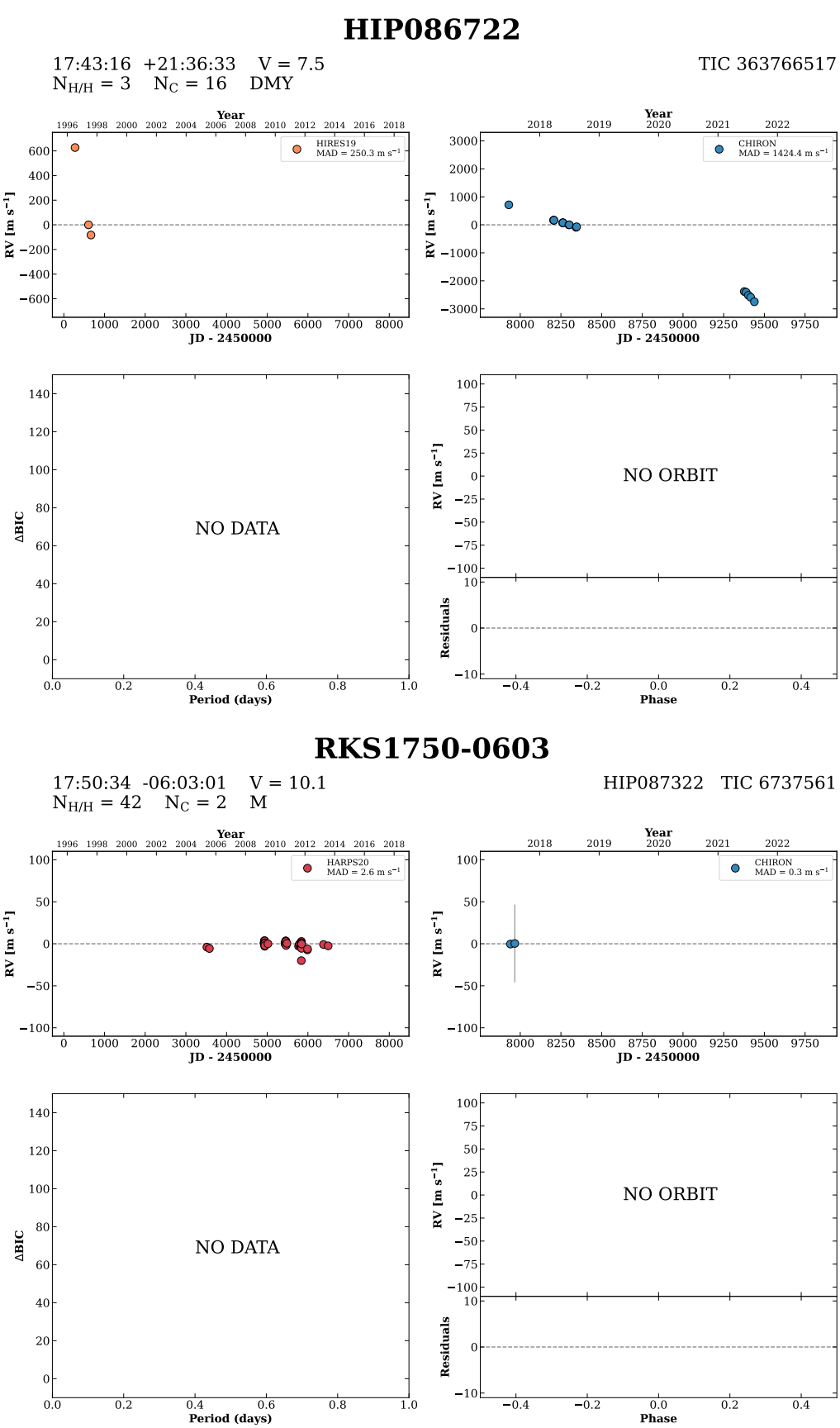

Figure 298 RV results for HIP086722 (top) and RKS1750-0603 (bottom).

RKS1752-0733

17:52:17 -07:33:37 V = 9.9 HIP087464 TIC 7095233
$N_{H/H}$ = 14 N_C = 9 DMY

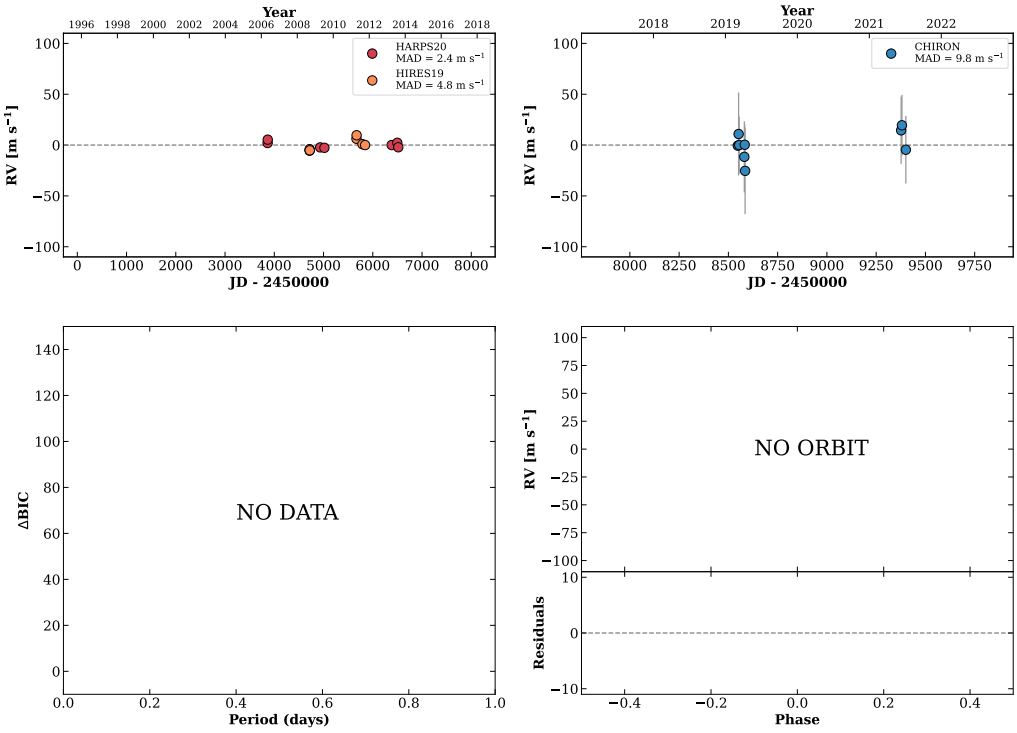

RKS1753+2119

17:53:30 +21:19:31 V = 8.5 HIP087579 TIC 275063206
$N_{H/H}$ = 2 N_C = 2 M

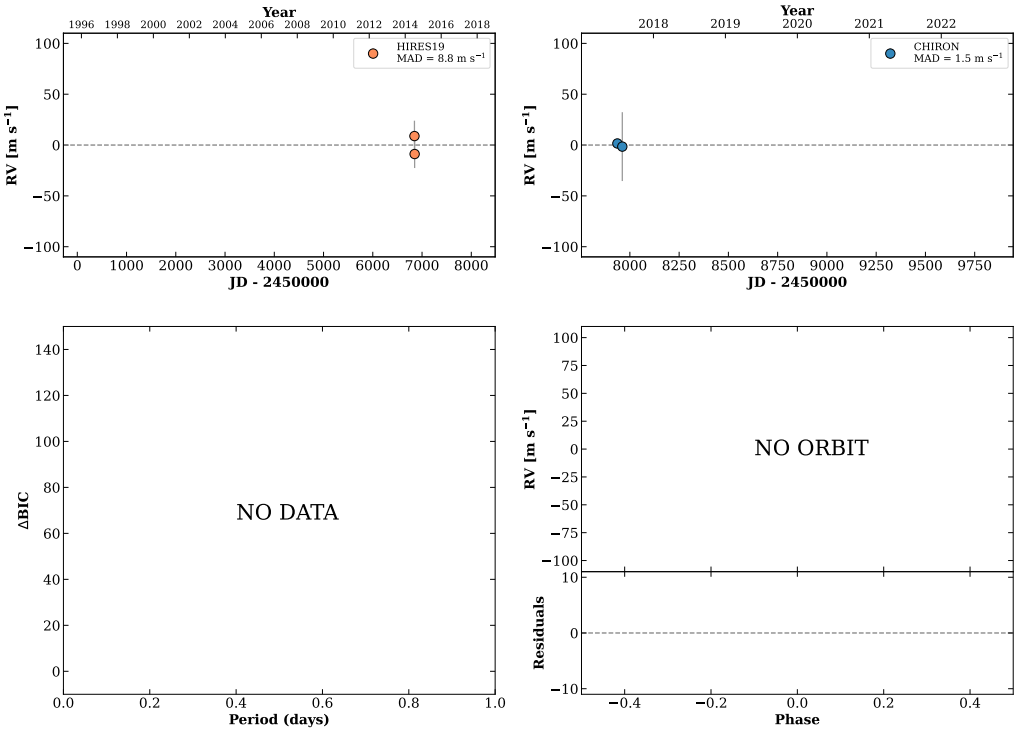

Figure 299 RV results for RKS1752-0733 (top) and RKS1753+2119 (bottom).

RKS1754-2649

17:54:54 -26:49:42 V = 10.3 TIC 133745276
$N_{H/H}$ = 0 N_C = 9 DMY

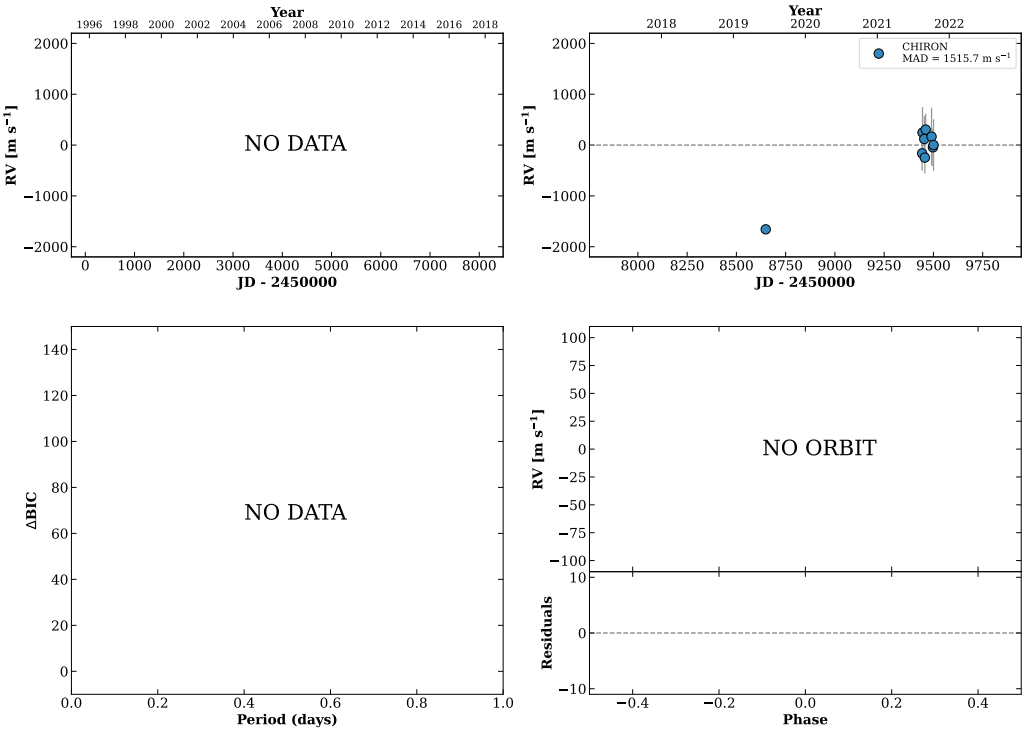

RKS1755+0345

17:55:25 +03:45:16 V = 10.1 HIP087745 TIC 325225116
$N_{H/H}$ = 0 N_C = 9 DMY

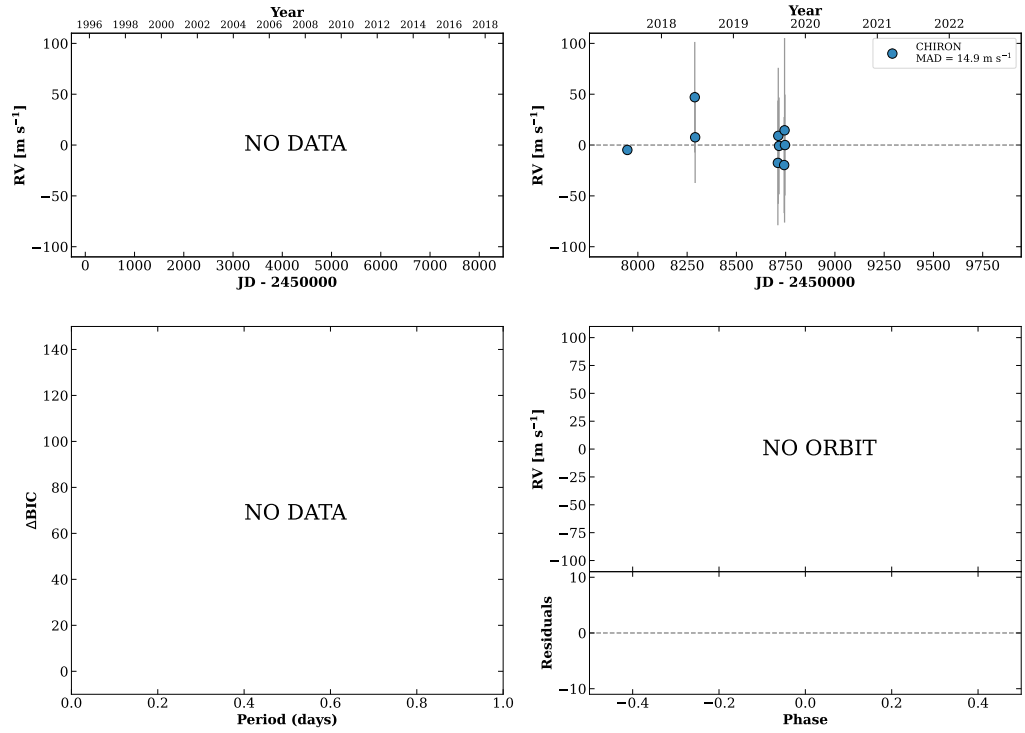

Figure 300 RV results for RKS1754-2649 (top) and RKS1755+0345 (bottom).

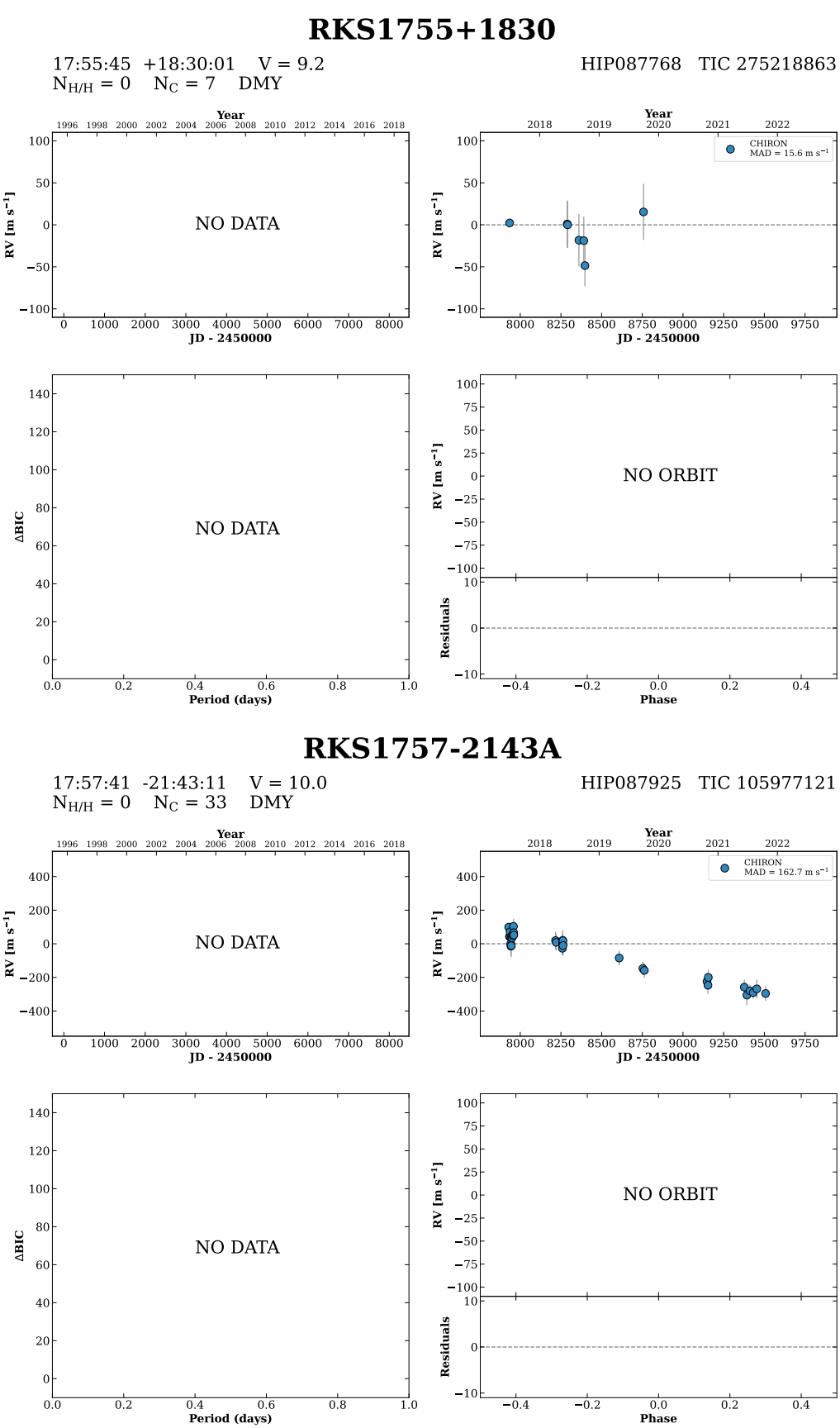

Figure 301 RV results for RKS1755+1830 (top) and RKS1757-2143A (bottom).

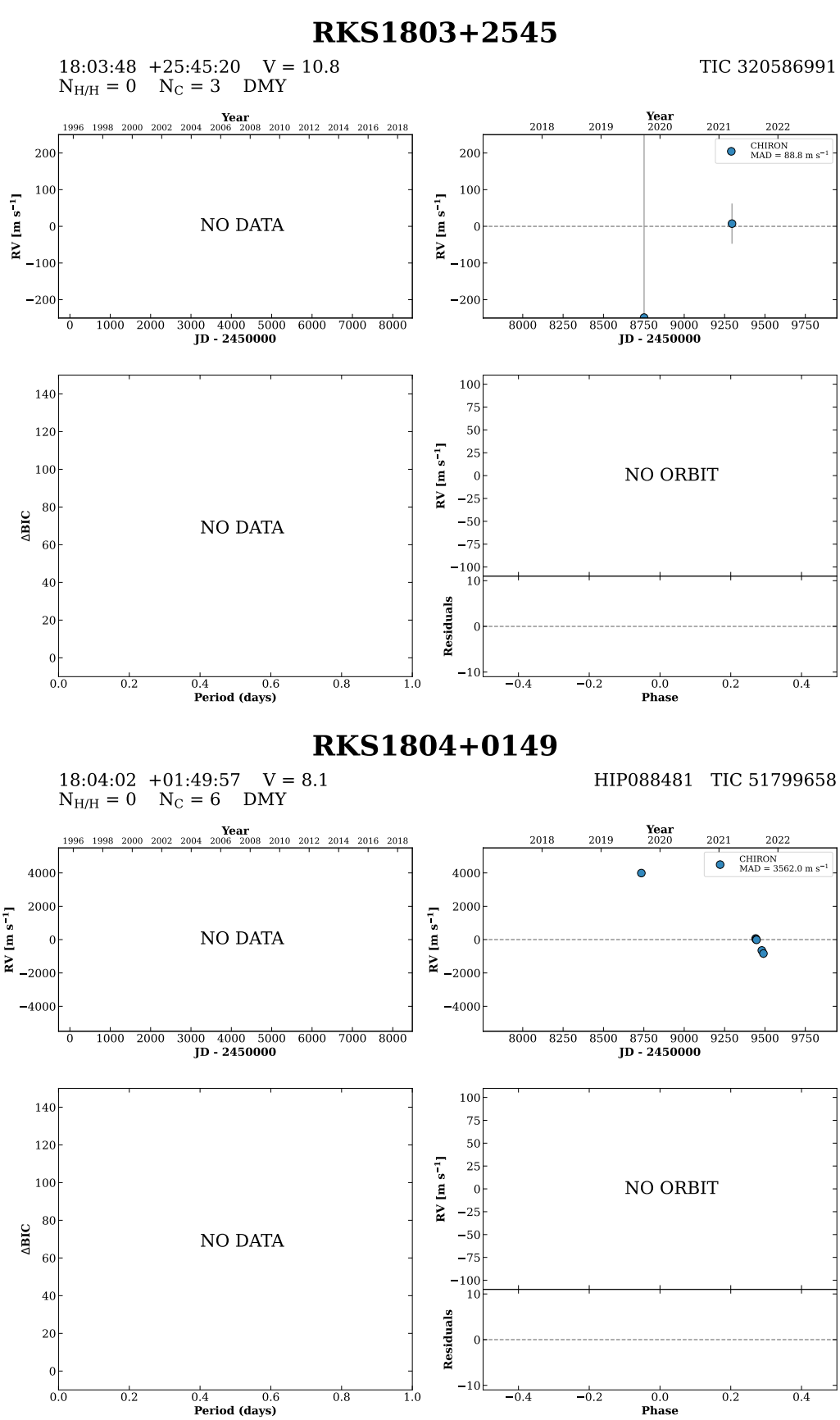

Figure 302 RV results for RKS1803+2545 (top) and RKS1804+0149 (bottom).

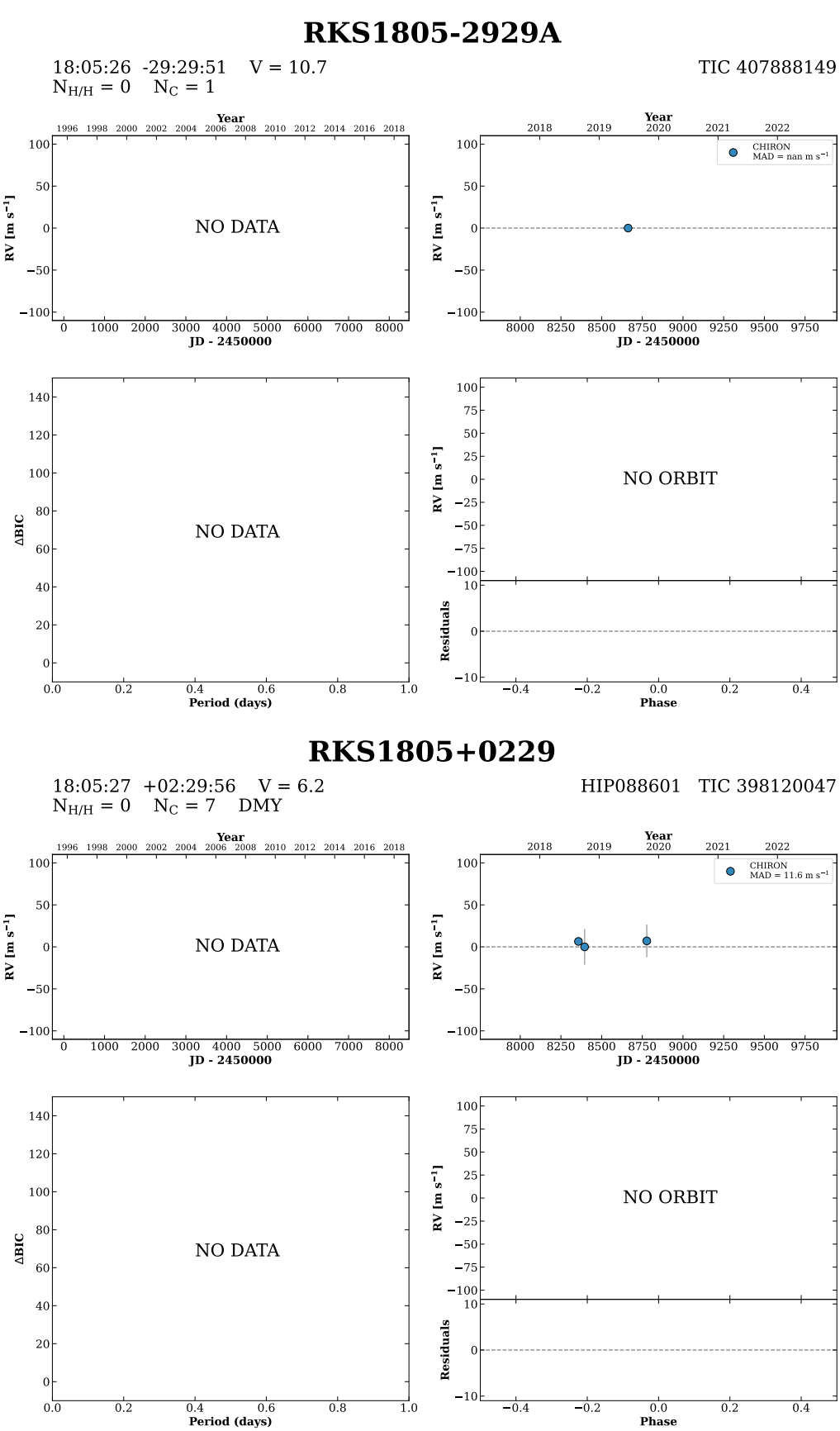

Figure 303 RV results for RKS1805-2929A (top) and RKS1805+0229 (bottom).

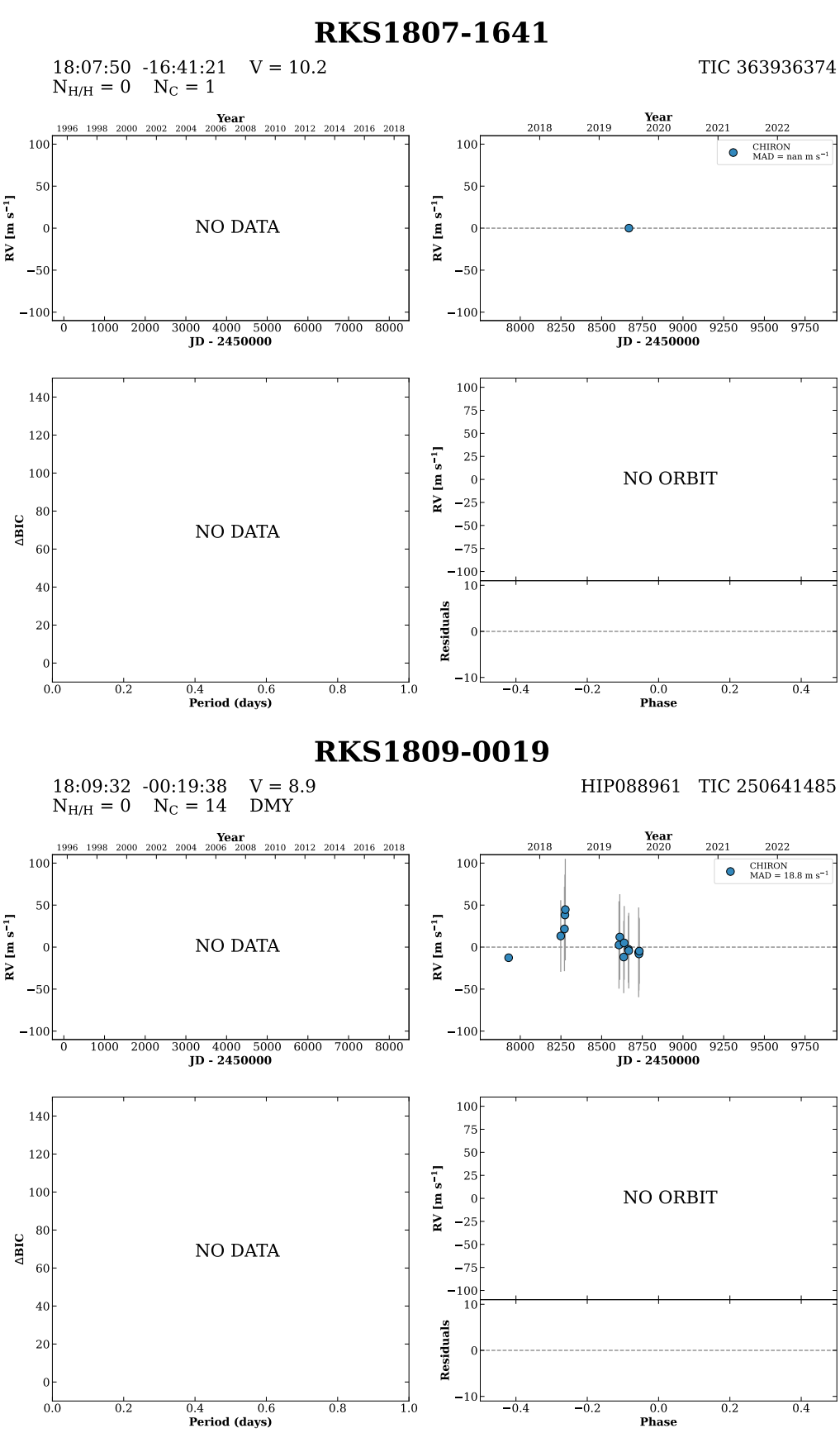

Figure 304 RV results for RKS1807-1641 (top) and RKS1809-0019 (bottom).

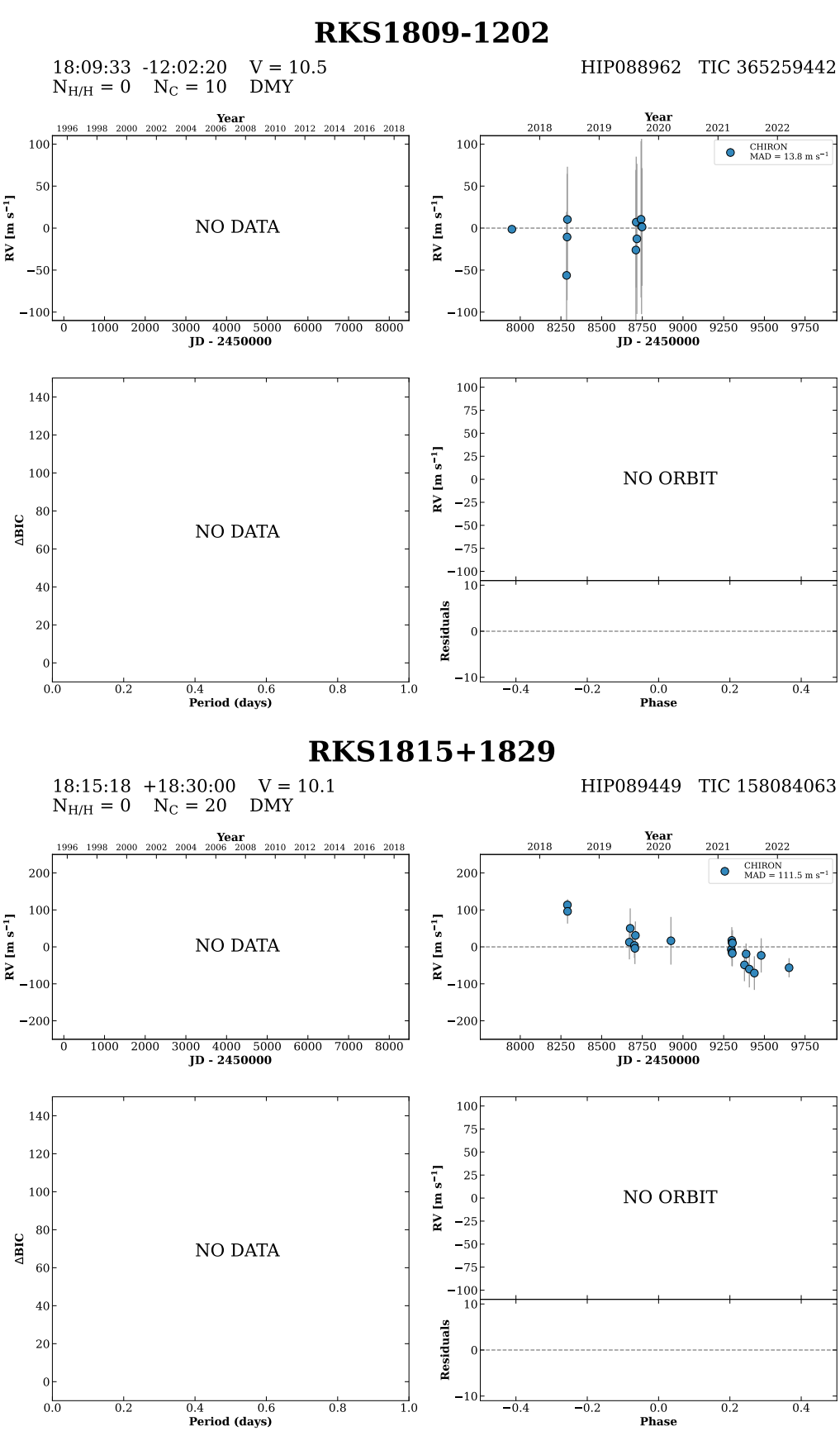

Figure 305 RV results for RKS1809-1202 (top) and RKS1815+1829 (bottom).

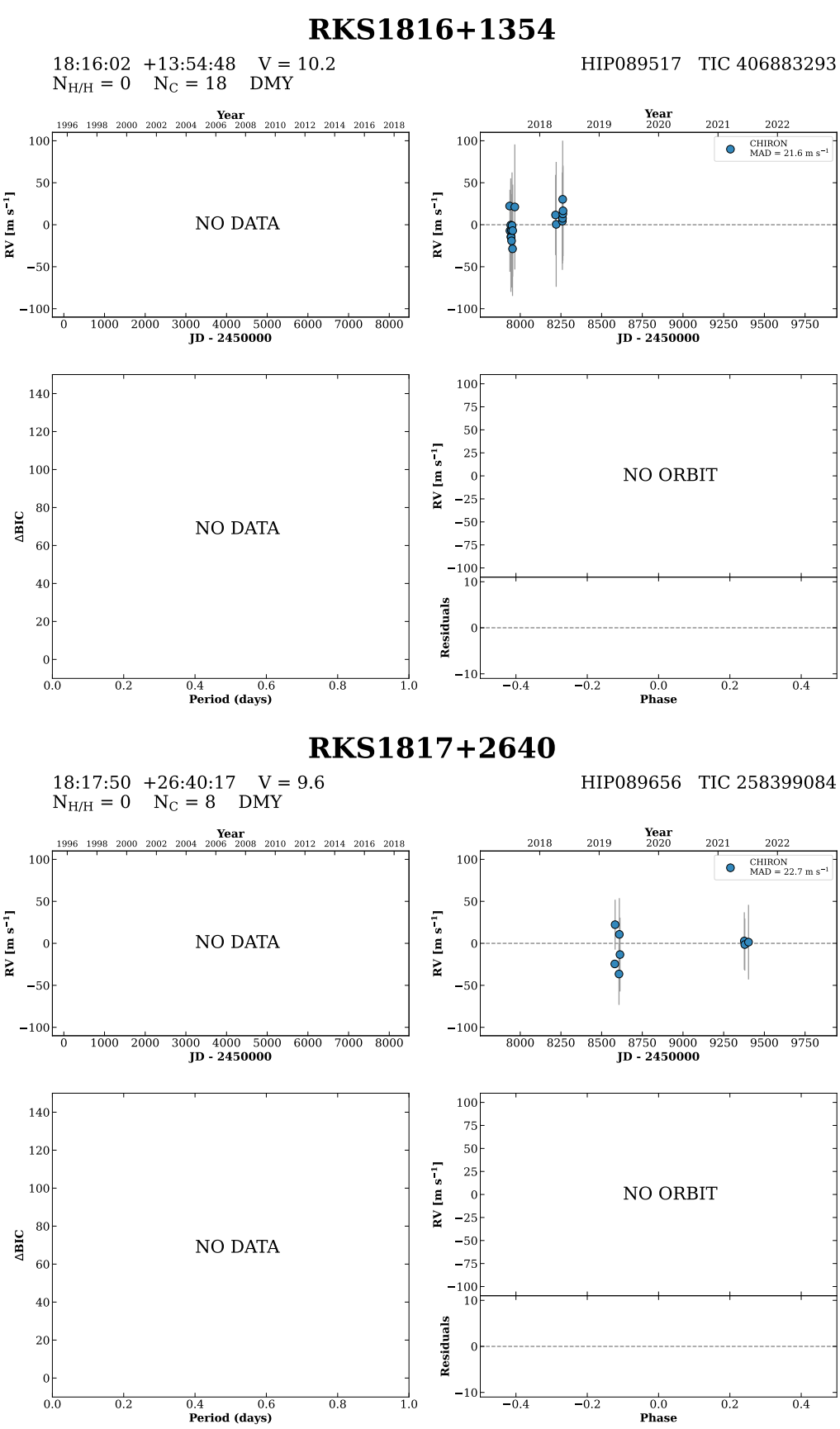

Figure 306 RV results for RKS1816+1354 (top) and RKS1817+2640 (bottom).

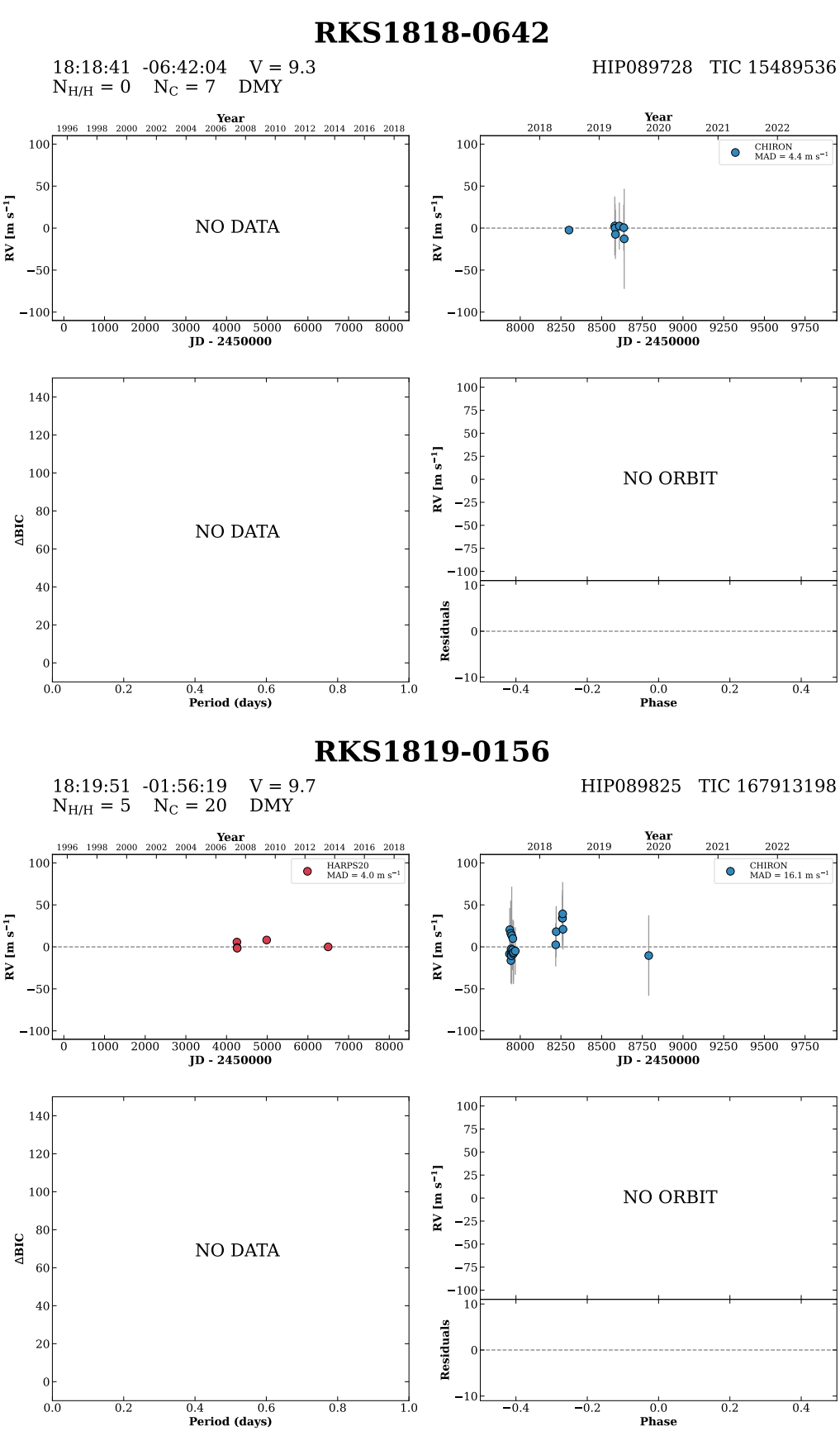

Figure 307 RV results for RKS1818-0642 (top) and RKS1819-0156 (bottom).

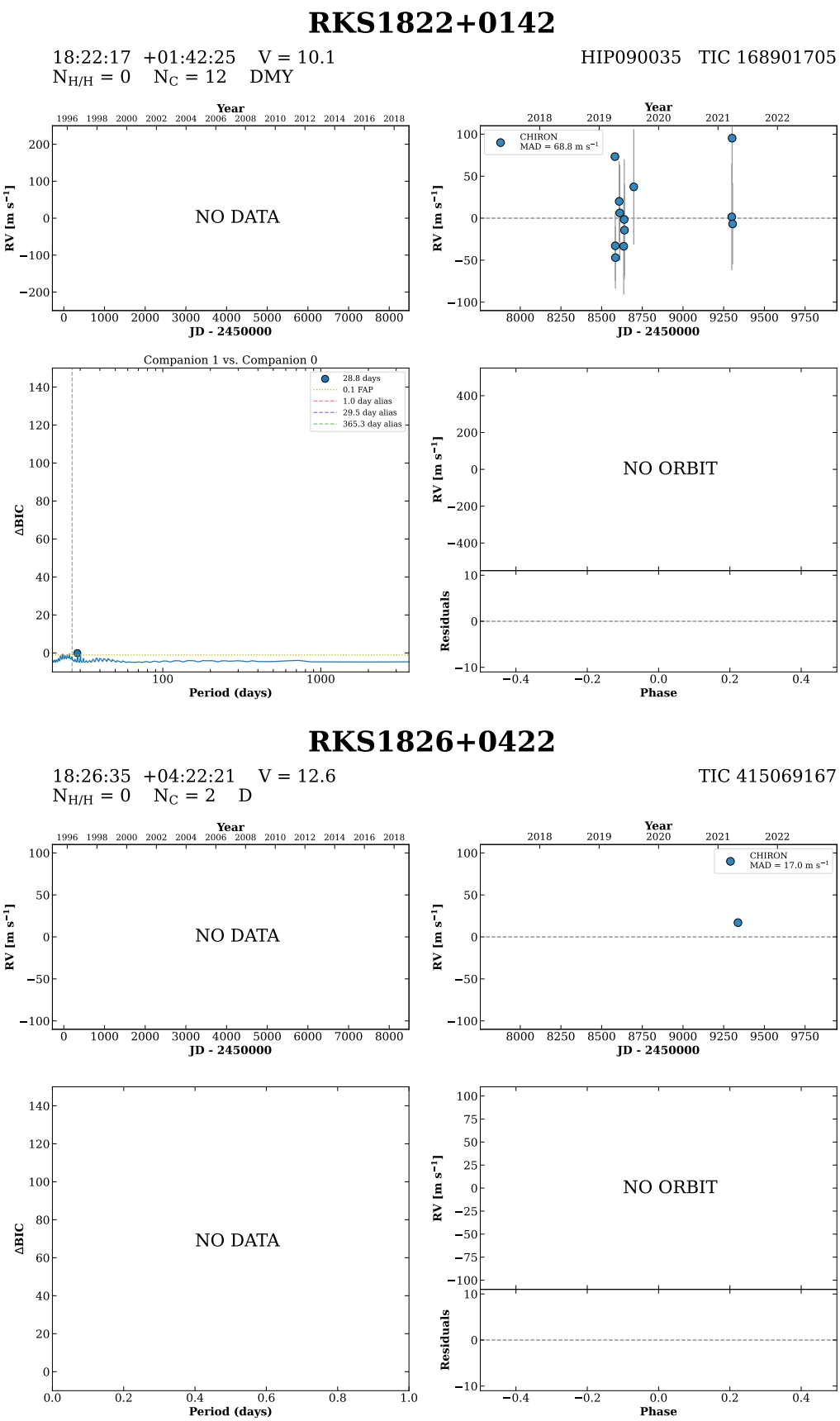

Figure 308 RV results for RKS1822+0142 (top) and RKS1826+0422 (bottom).

RKS1829-2758

18:29:22 -27:58:19 V = 9.4 HIP090611 TIC 324370520
$N_{H/H}$ = 8 N_C = 13 DMY

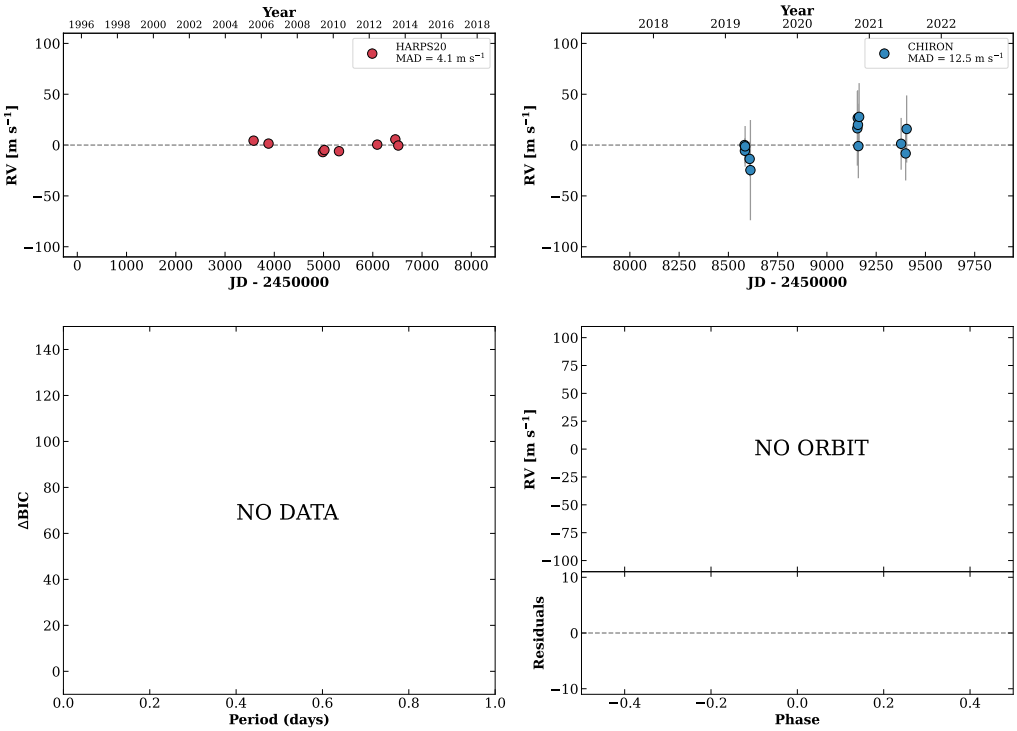

RKS1829+0903A

18:29:32 +09:03:44 V = 8.7 HIP090626 TIC 320508747
$N_{H/H}$ = 0 N_C = 10 DMY

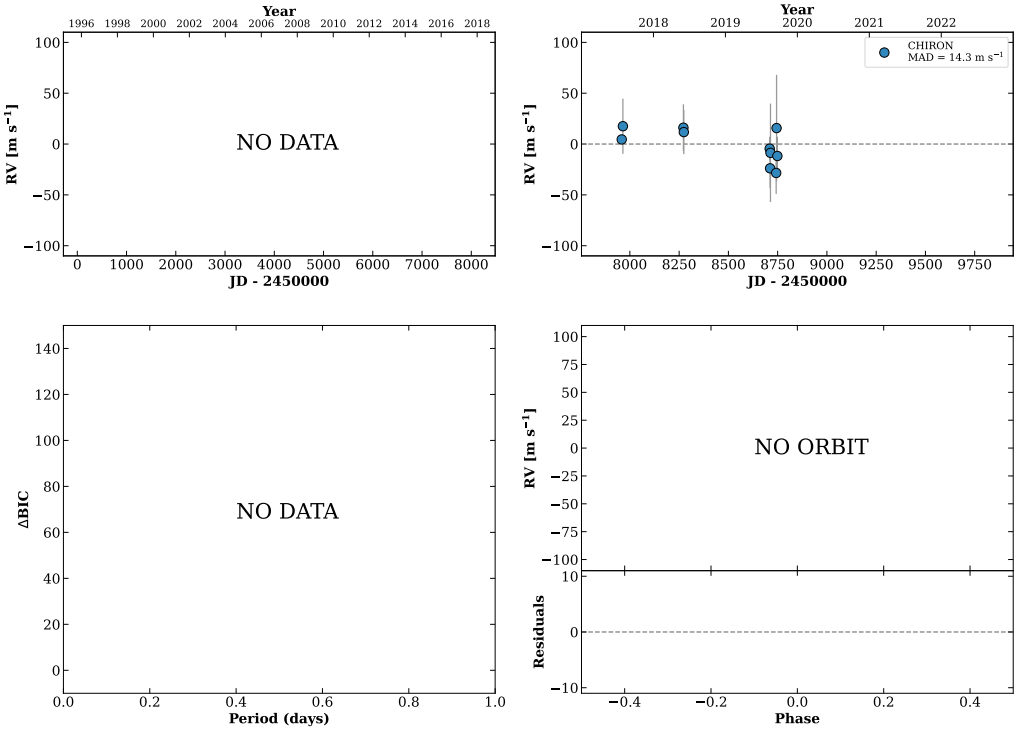

Figure 309 RV results for RKS1829-2758 (top) and RKS1829+0903A (bottom).

RKS1829-0149

18:29:52 -01:49:05 V = 8.0 HIP090656 TIC 133556737
$N_{H/H}$ = 122 N_C = 2 M

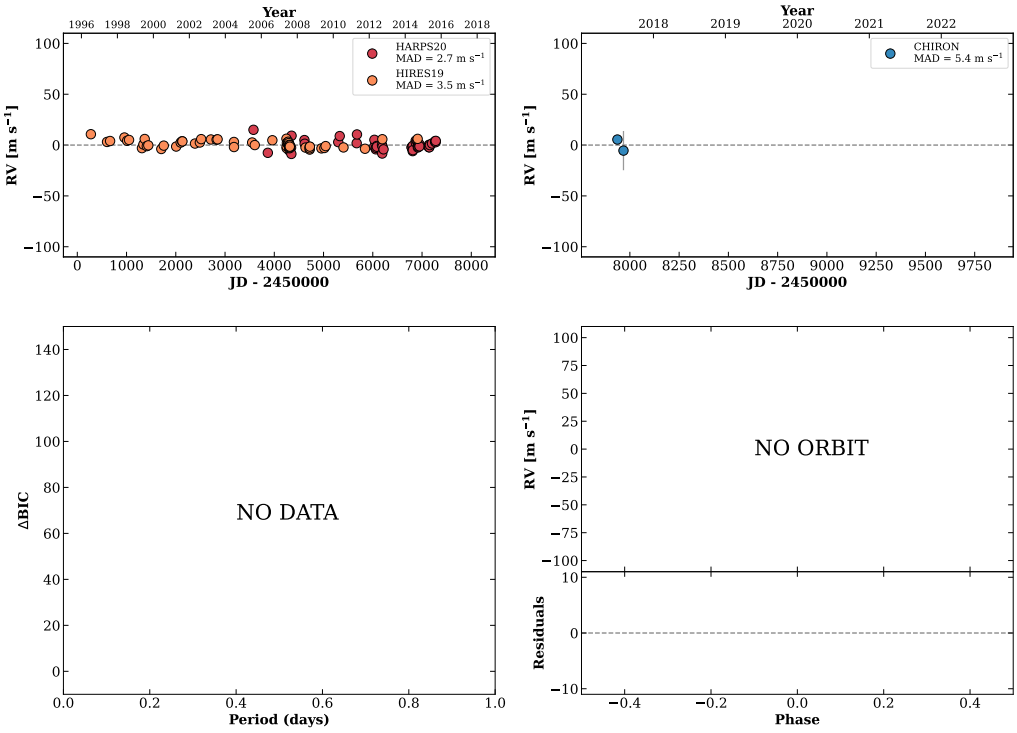

RKS1831-1854

18:31:19 -18:54:32 V = 6.8 HIP090790 TIC 186271747
$N_{H/H}$ = 47 N_C = 4 DM

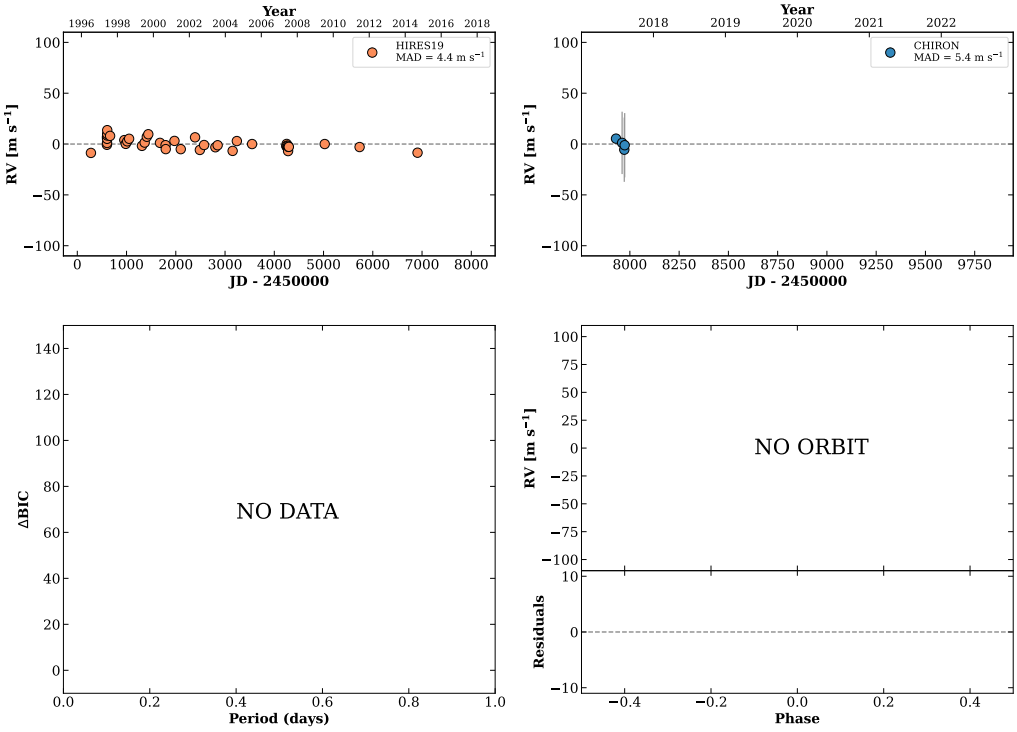

Figure 310 RV results for RKS1829-0149 (top) and RKS1831-1854 (bottom).

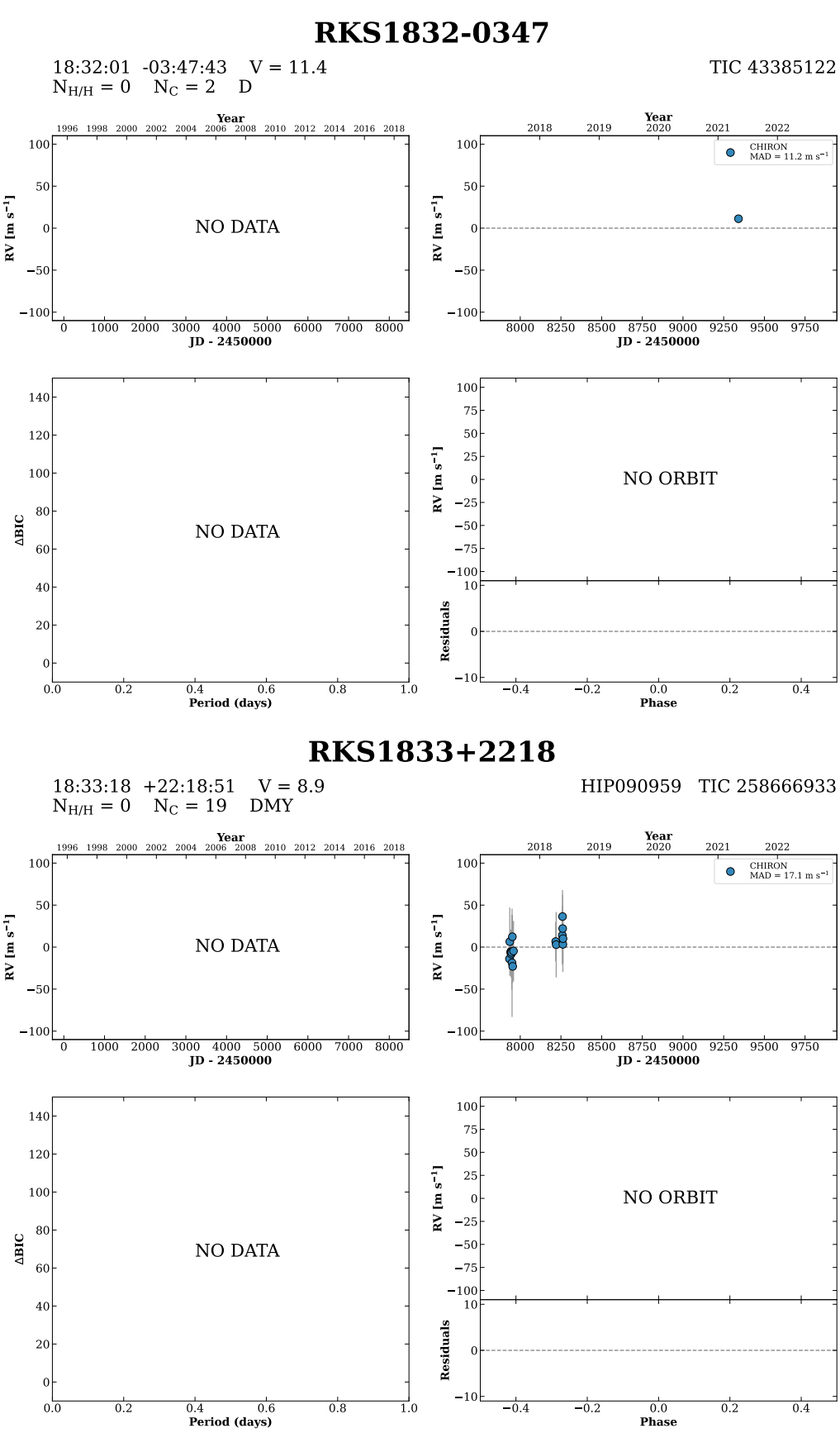

Figure 311 RV results for RKS1832-0347 (top) and RKS1833+2218 (bottom).

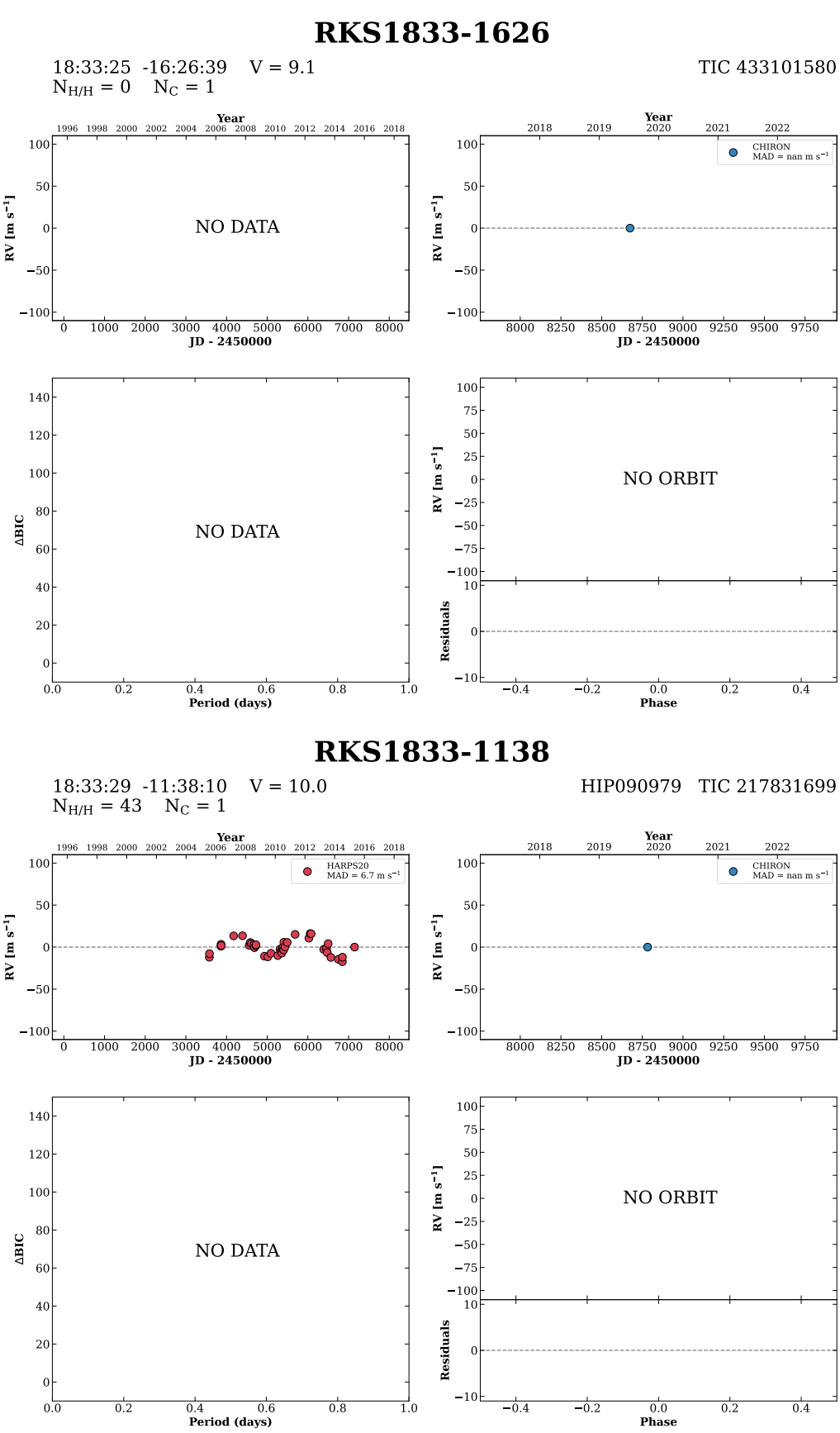

Figure 312 RV results for RKS1833-1626 (top) and RKS1833-1138 (bottom).

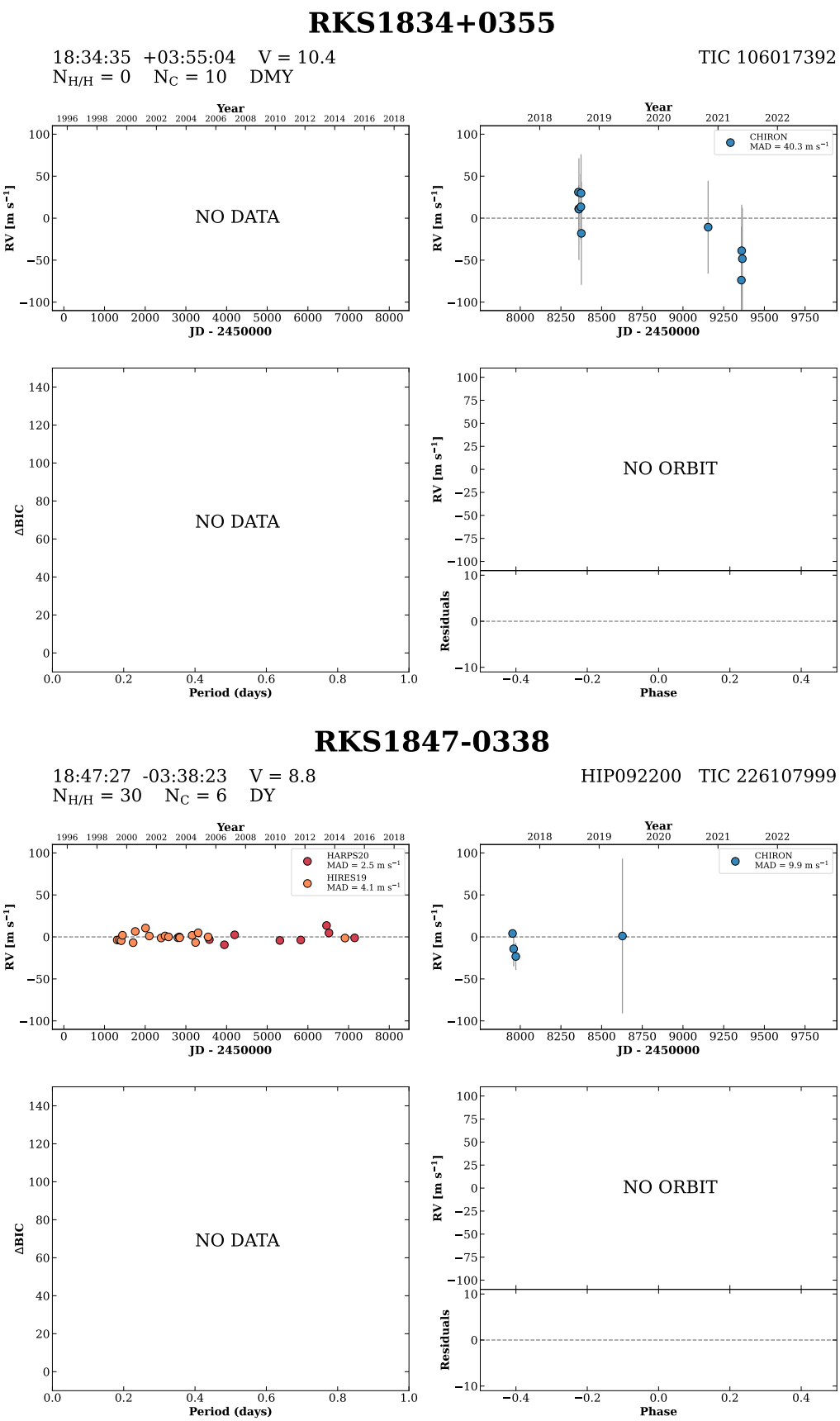

Figure 313 RV results for RKS1834+0355 (top) and RKS1847-0338 (bottom).

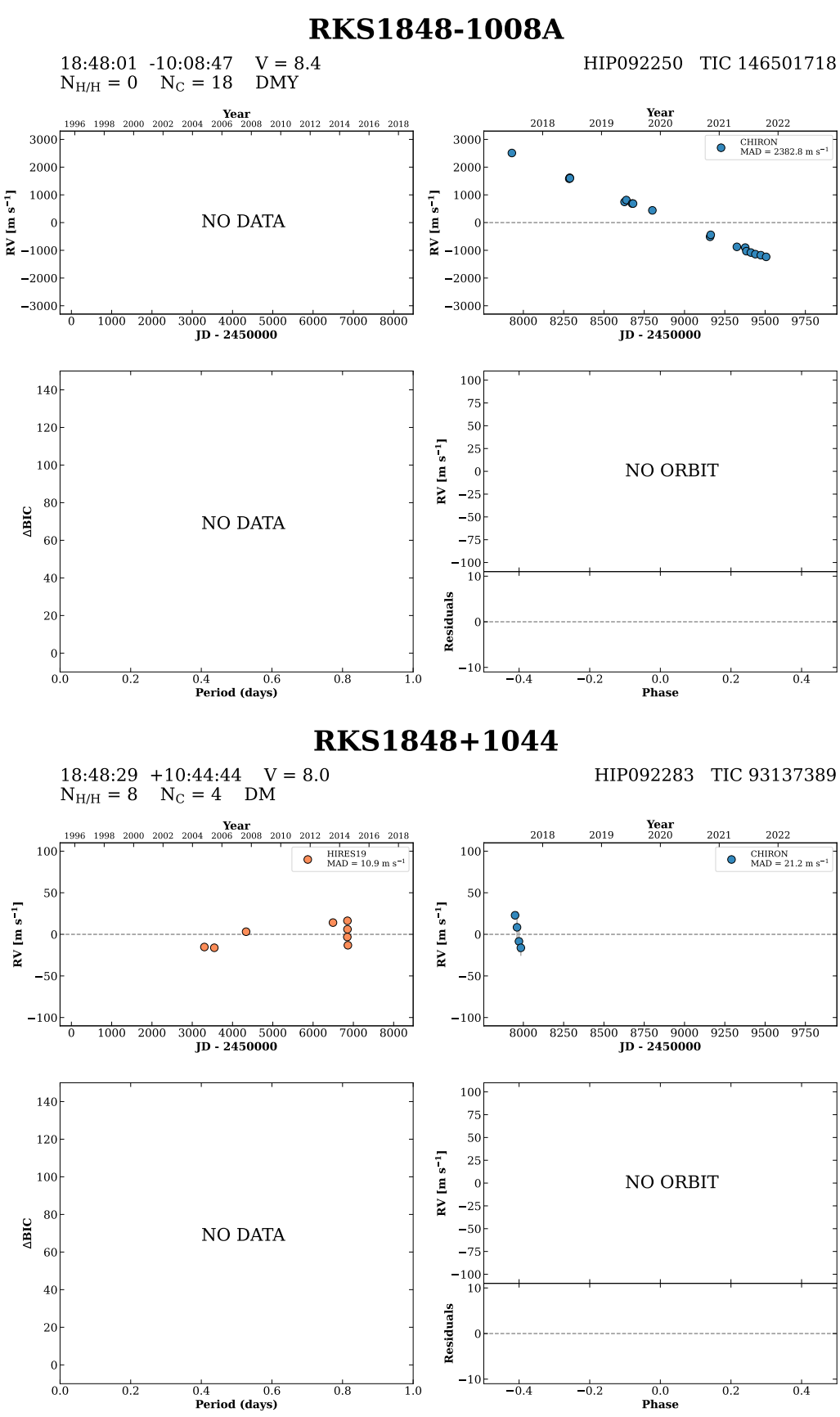

Figure 314 RV results for RKS1848-1008A (top) and RKS1848+1044 (bottom).

RKS1848+1726

18:48:52 +17:26:20 V = 9.2 HIP092311 TIC 224431102
$N_{H/H}$ = 0 N_C = 16 DMY

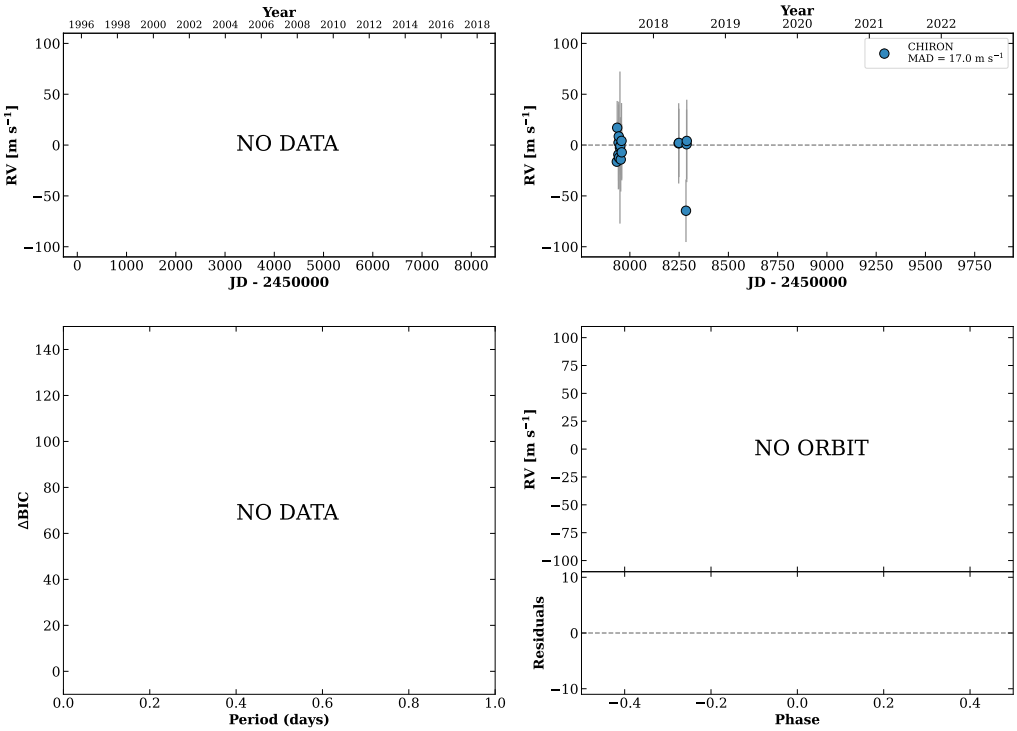

RKS1850-2655

18:50:21 -26:55:25 V = 9.7 HIP092444 TIC 89684637
$N_{H/H}$ = 7 N_C = 41 DMY

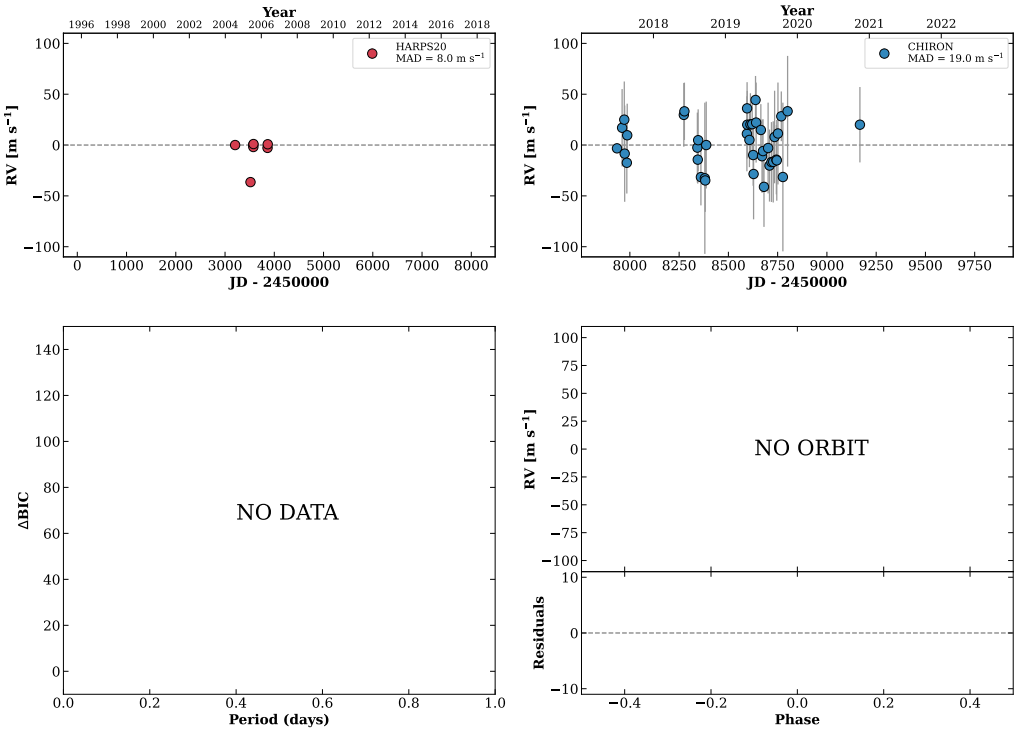

Figure 315 RV results for RKS1848+1726 (top) and RKS1850-2655 (bottom).

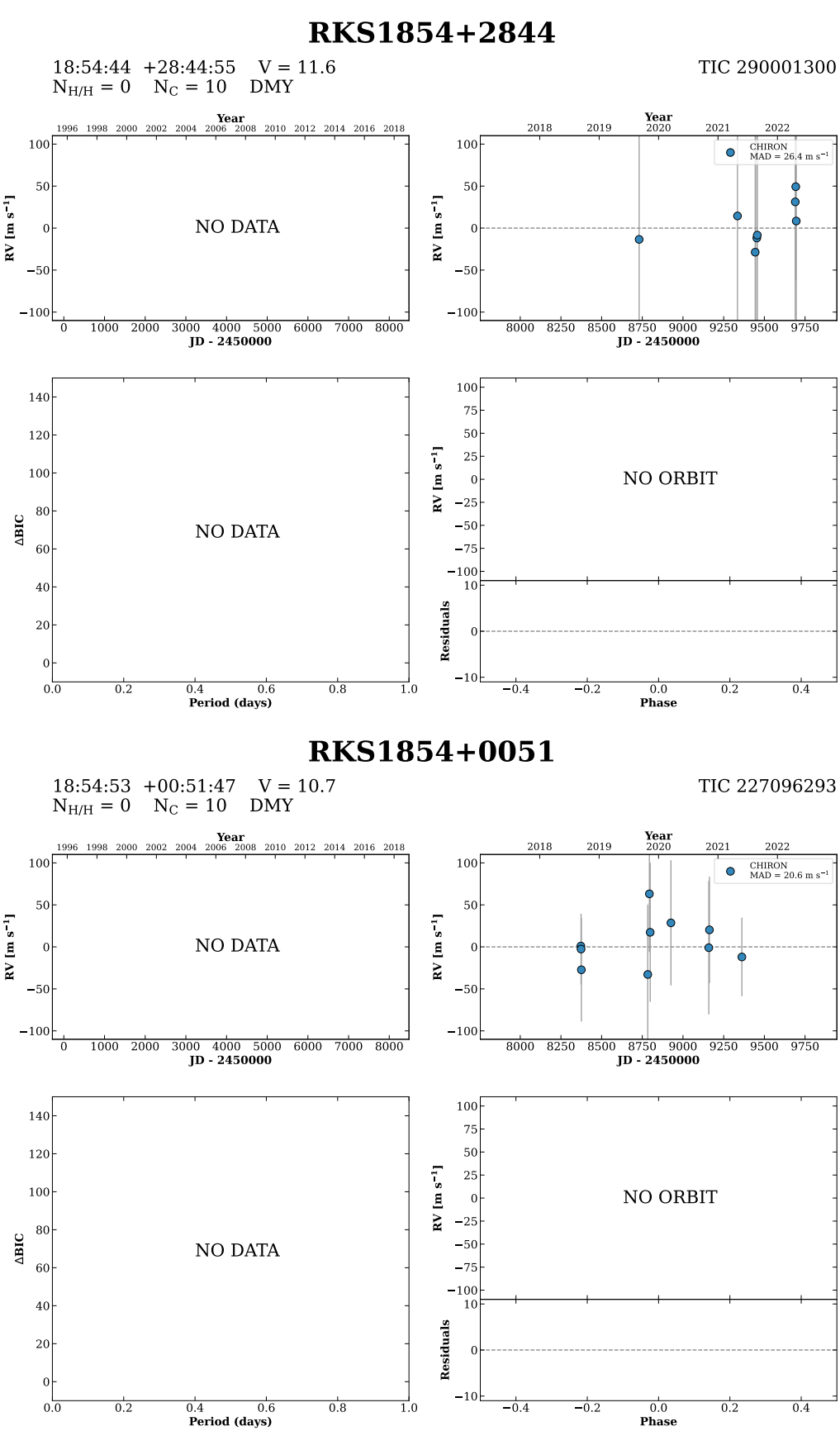

Figure 316 RV results for RKS1854+2844 (top) and RKS1854+0051 (bottom).

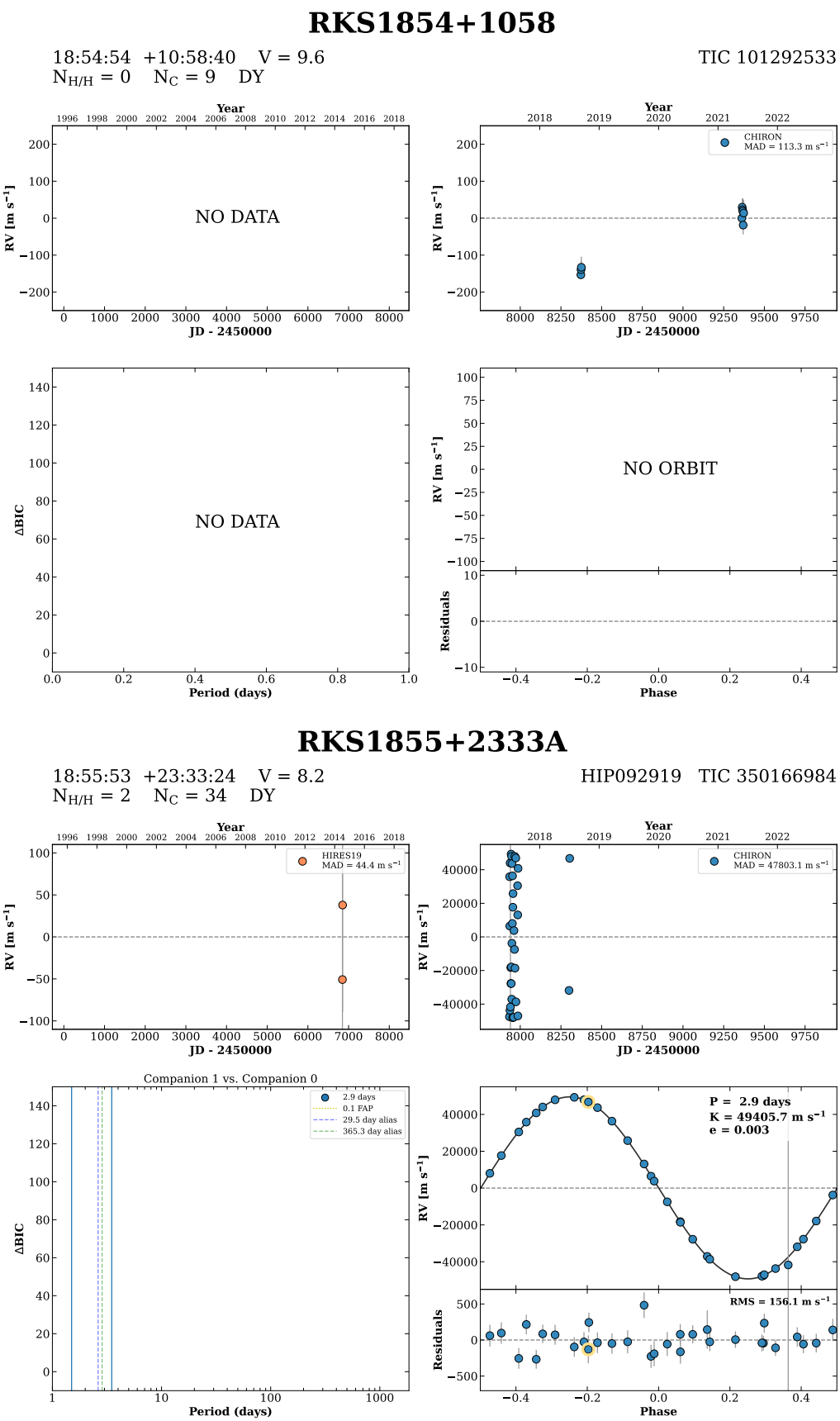

Figure 317 RV results for RKS1854+1058 (top) and RKS1855+2333A (bottom).

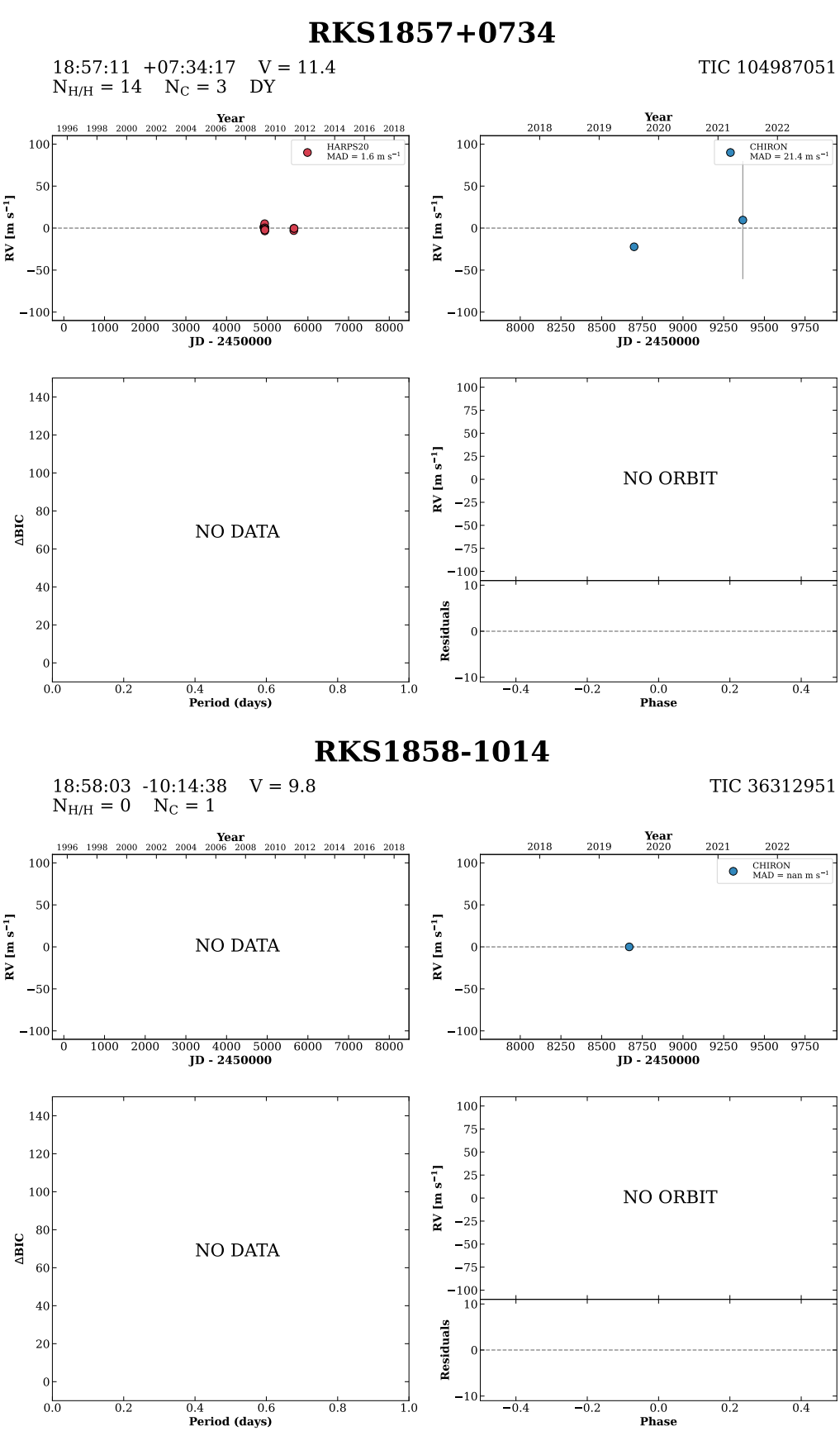

Figure 318 RV results for RKS1857+0734 (top) and RKS1858-1014 (bottom).

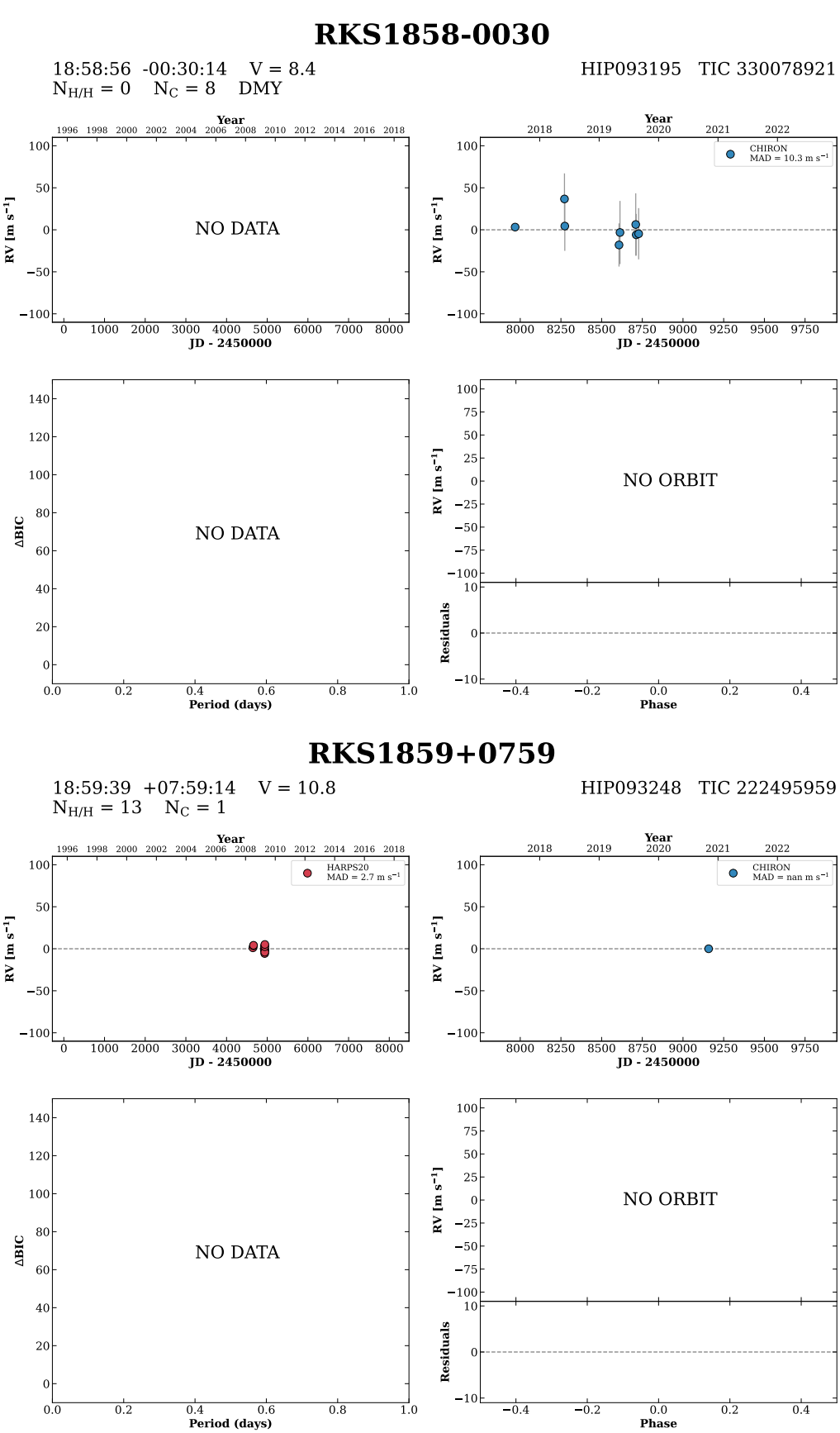

Figure 319 RV results for RKS1858-0030 (top) and RKS1859+0759 (bottom).

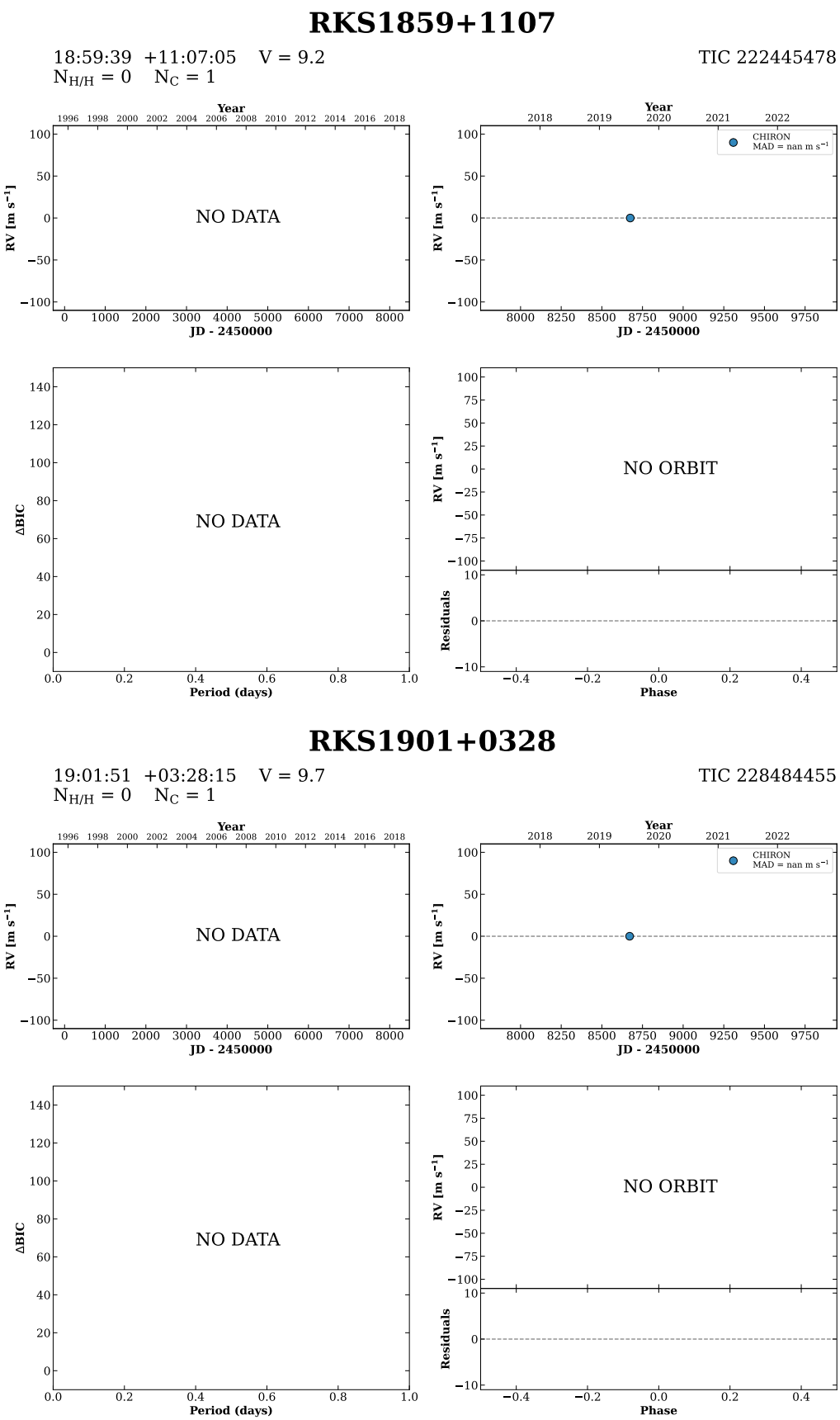

Figure 320 RV results for RKS1859+1107 (top) and RKS1901+0328 (bottom).

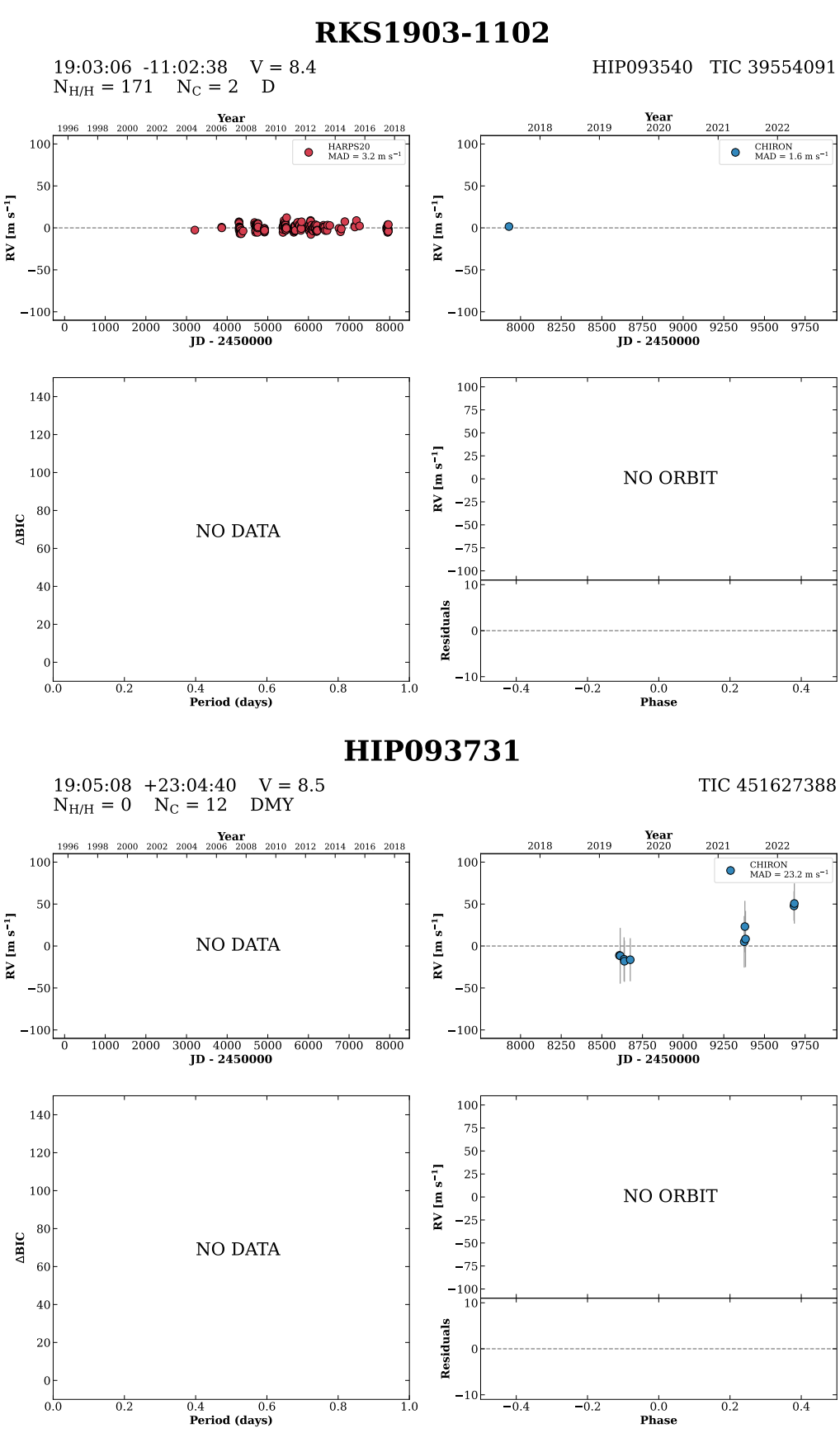

Figure 321 RV results for RKS1903-1102 (top) and HIP093731 (bottom).

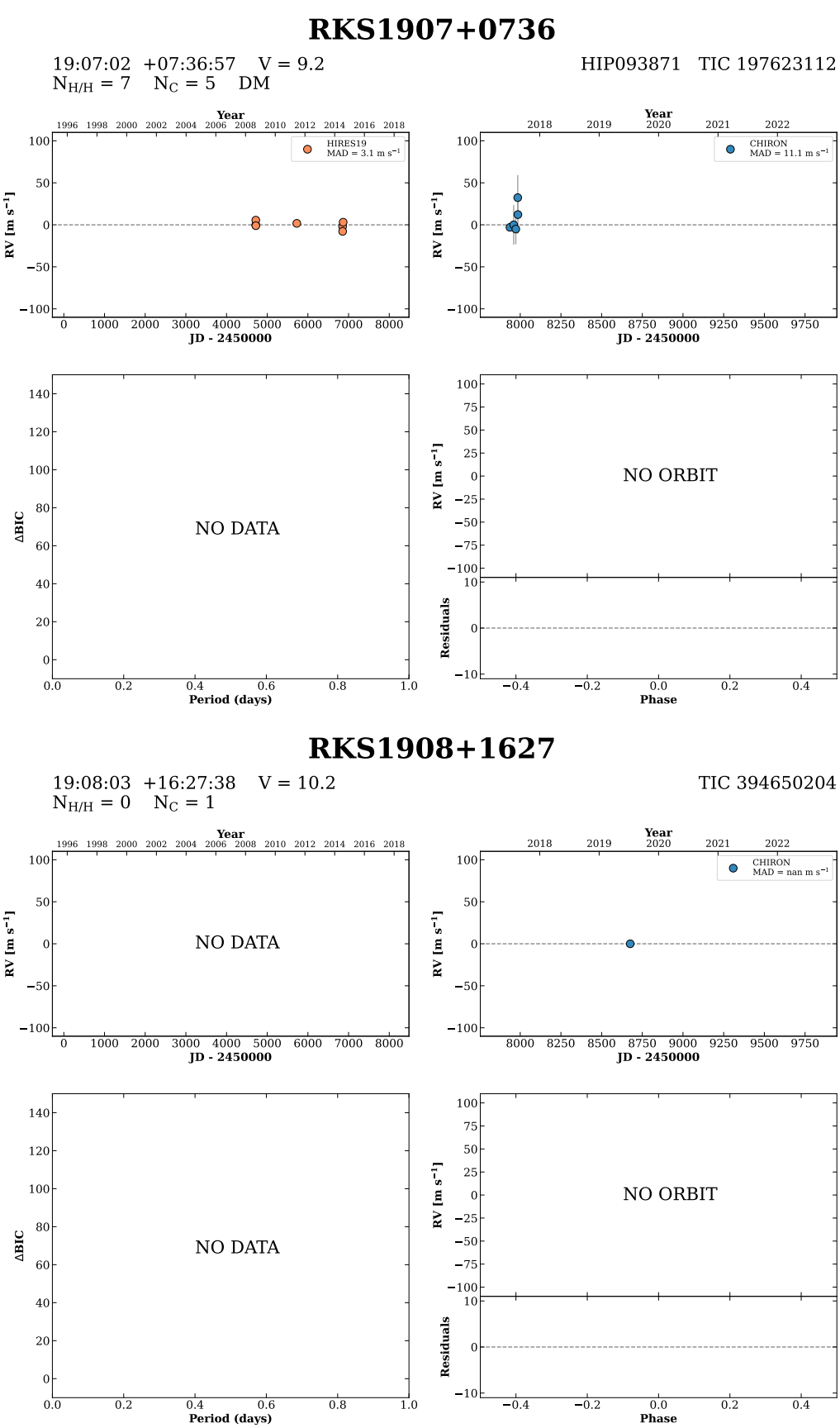

Figure 322 RV results for RKS1907+0736 (top) and RKS1908+1627 (bottom).

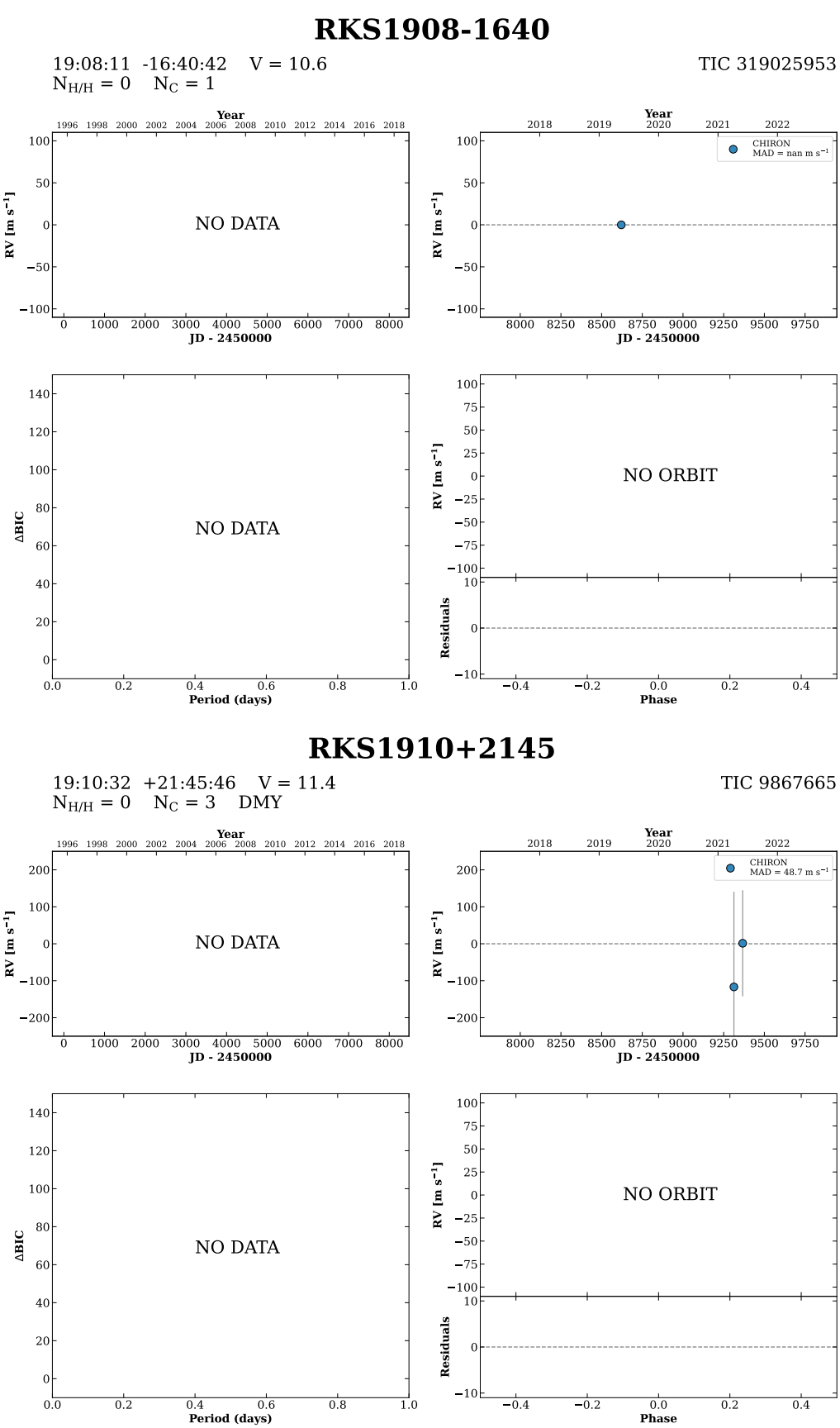

Figure 323 RV results for RKS1908-1640 (top) and RKS1910+2145 (bottom).

RKS1911+0500

19:11:48 +05:00:36 V = 11.4 TIC 181547479
$N_{H/H}$ = 0 N_C = 3 DY

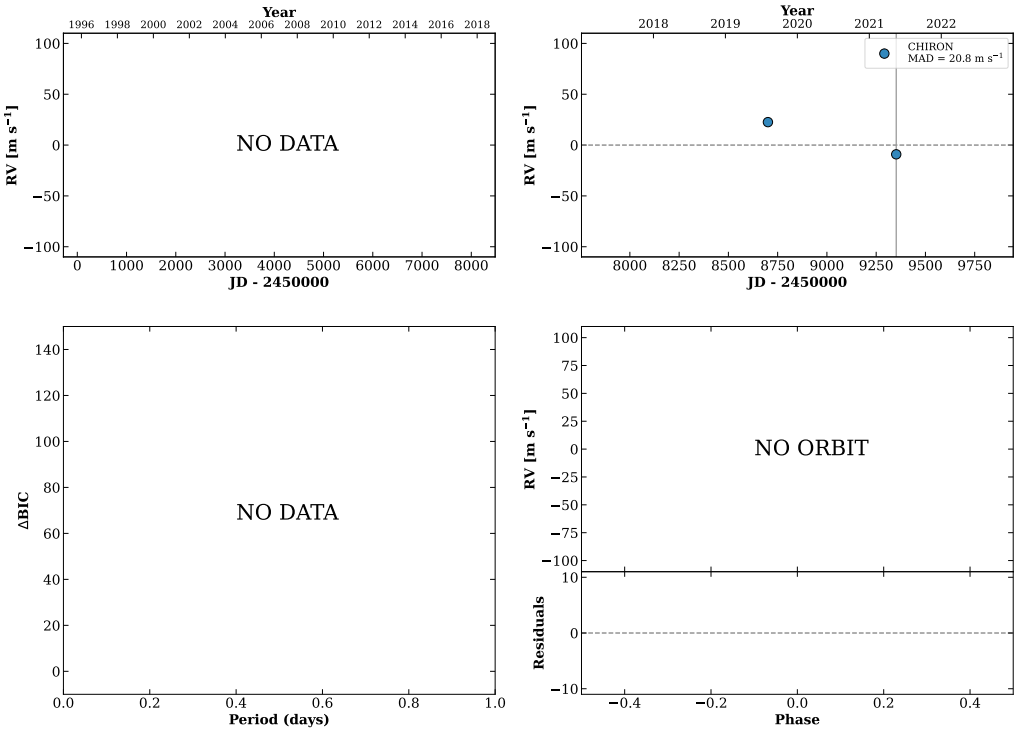

RKS1914+0209A

19:14:59 +02:09:55 V = 9.8 HIP094590 TIC 174696280
$N_{H/H}$ = 0 N_C = 4 DM

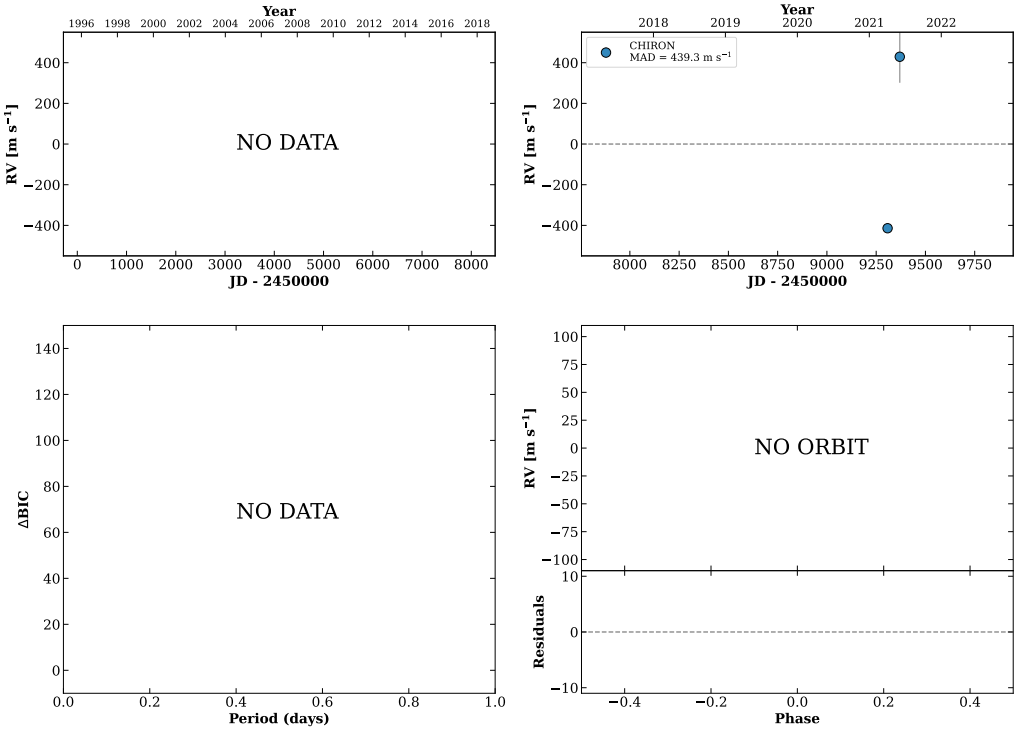

Figure 324 RV results for RKS1911+0500 (top) and RKS1914+0209A (bottom).

RKS1915+2453A

19:15:19 +24:53:49 V = 9.7 HIP094622 TIC 403613403
$N_{H/H}$ = 0 N_C = 30 DMY

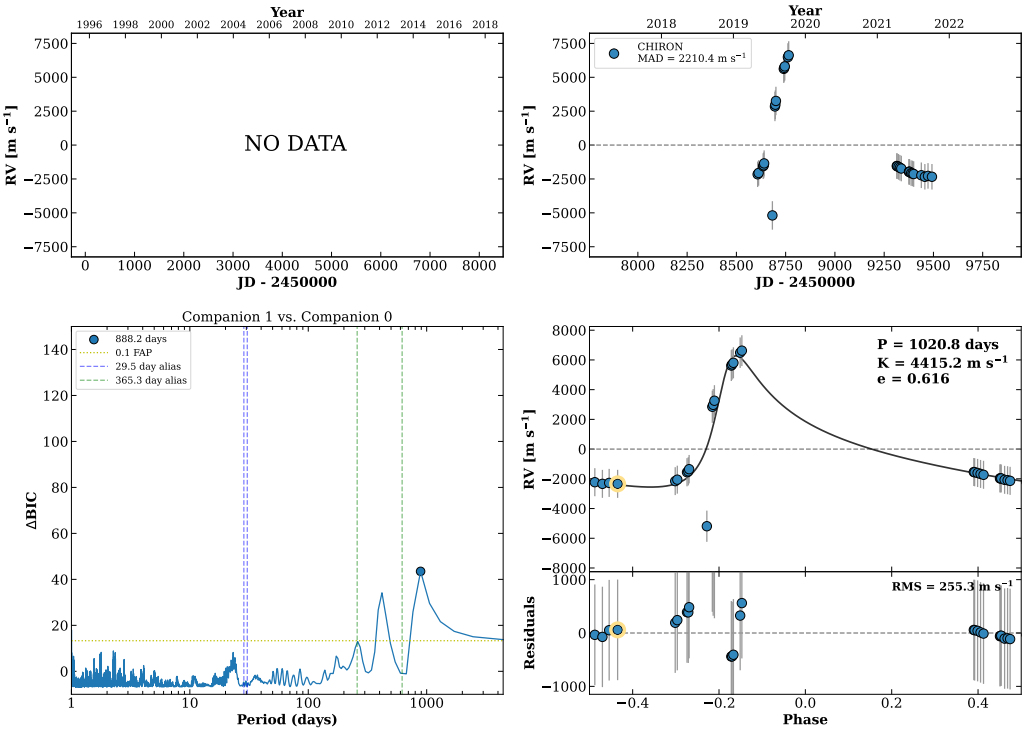

RKS1915+1133

19:15:35 +11:33:17 V = 8.1 HIP094650 TIC 210208396
$N_{H/H}$ = 8 N_C = 7 DMY

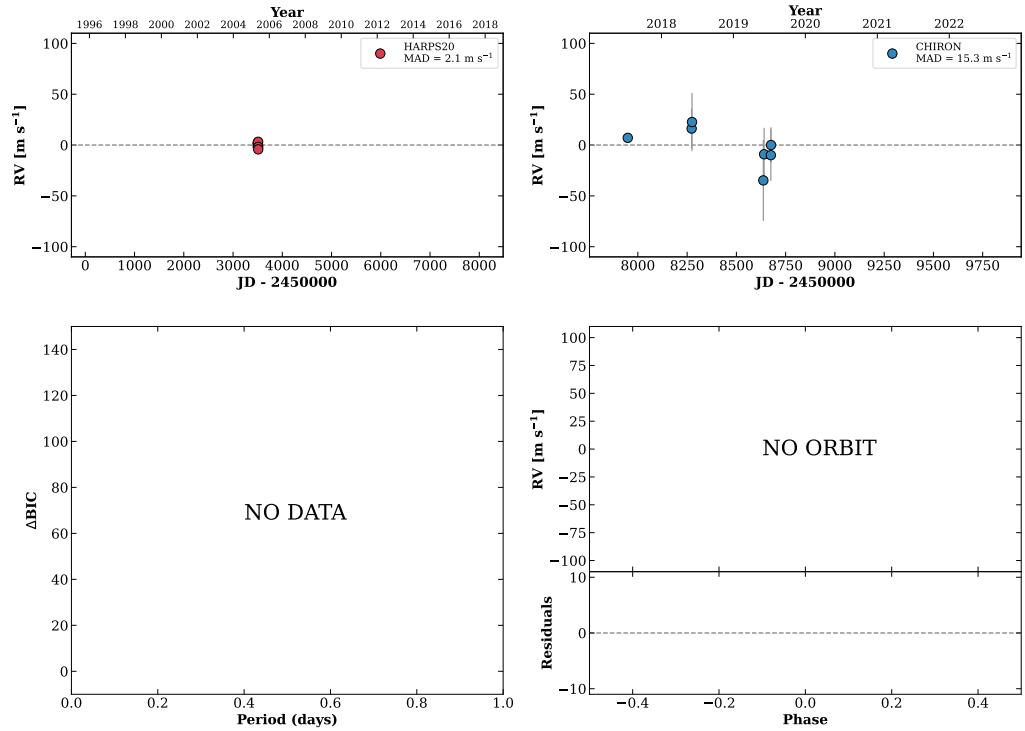

Figure 325 RV results for RKS1915+2453A (top) and RKS1915+1133 (bottom).

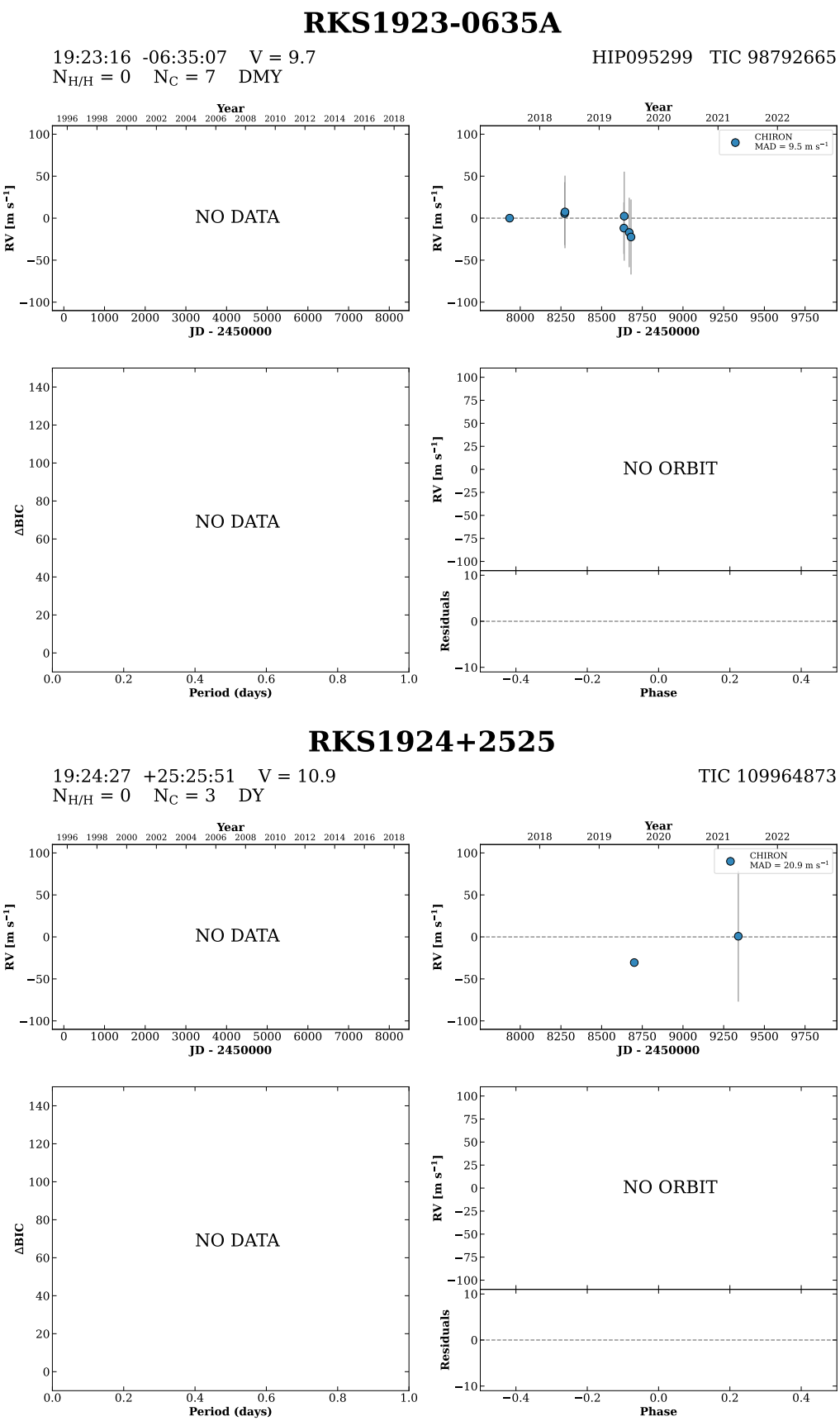

Figure 326 RV results for RKS1923-0635A (top) and RKS1924+2525 (bottom).

RKS1924-2203

19:24:34 -22:03:44 V = 10.9 HIP095417 TIC 118882363
$N_{H/H}$ = 8 N_C = 1

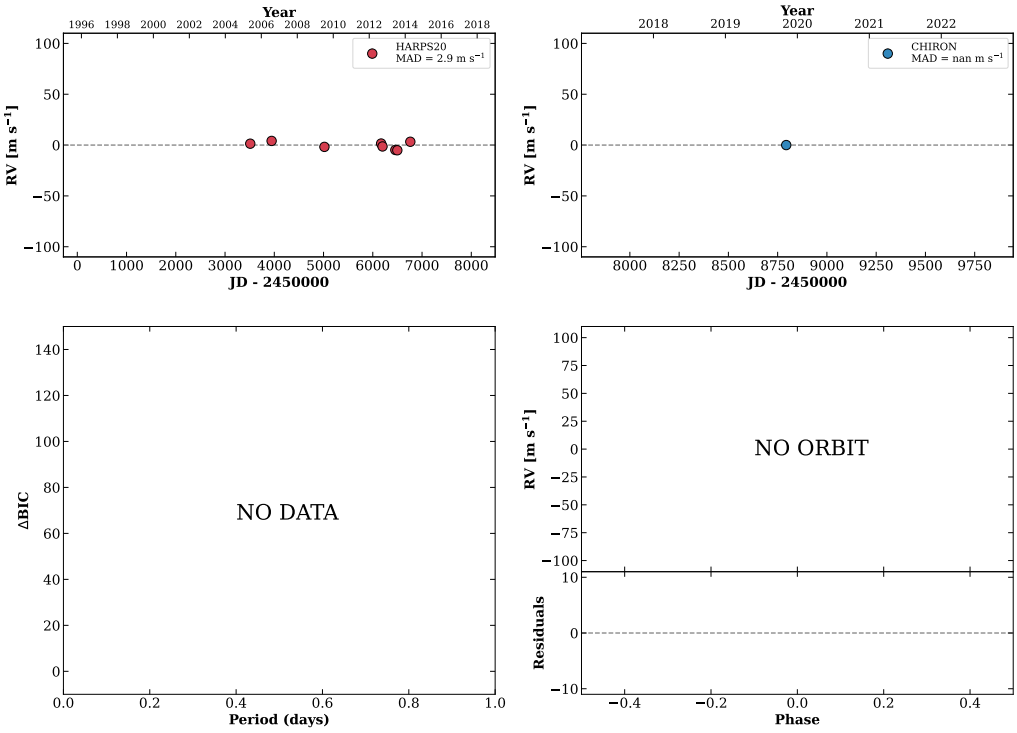

RKS1924+0832

19:24:42 +08:33:00 V = 11.2 HIP095429 TIC 132696054
$N_{H/H}$ = 0 N_C = 8 DMY

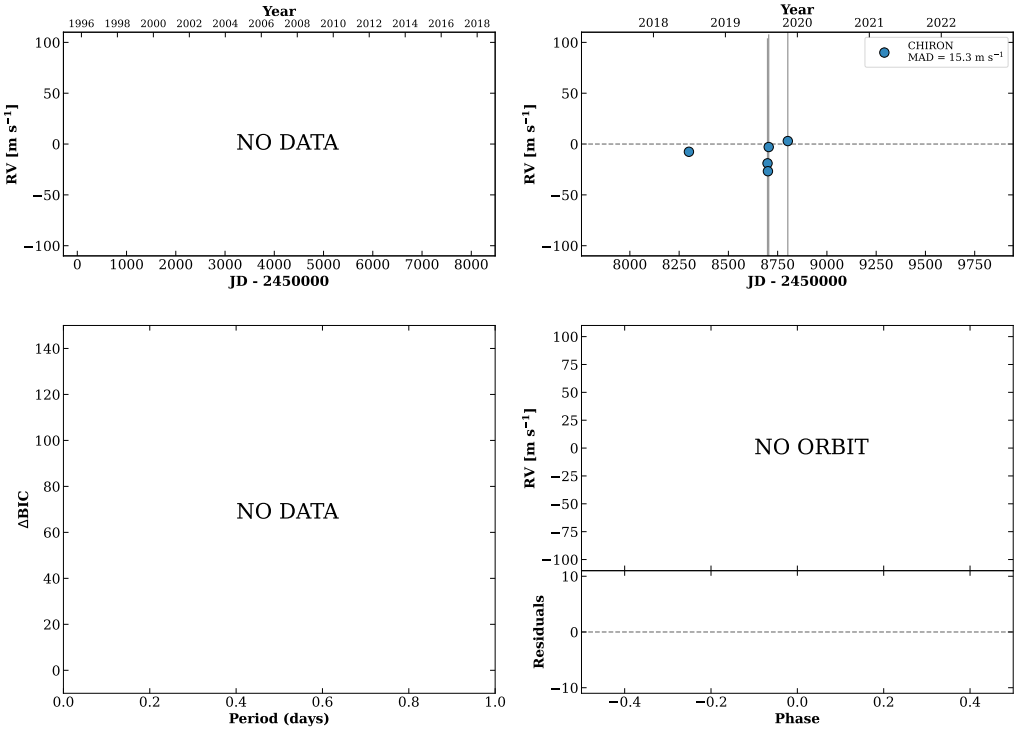

Figure 327 RV results for RKS1924-2203 (top) and RKS1924+0832 (bottom).

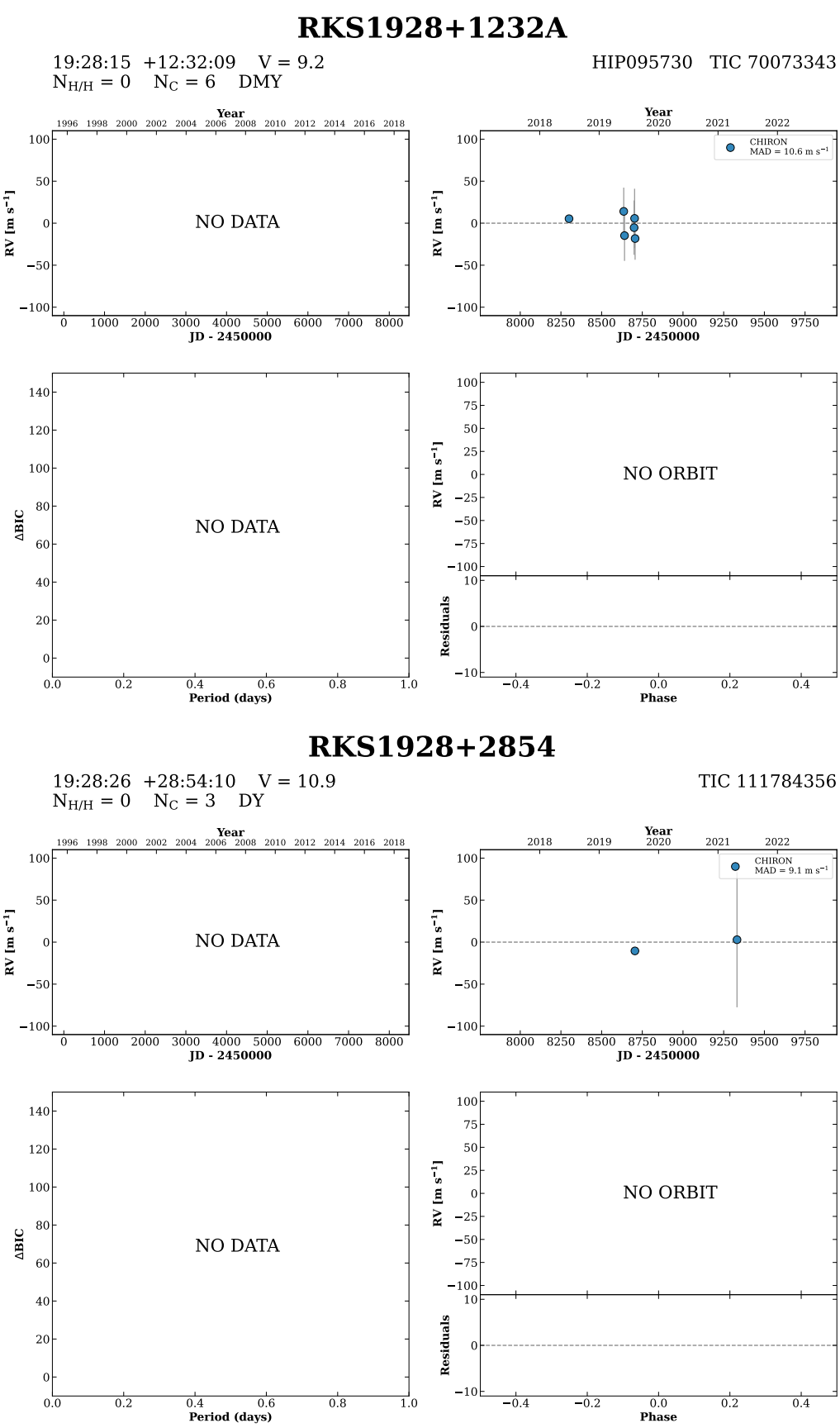

Figure 328 RV results for RKS1928+1232A (top) and RKS1928+2854 (bottom).

RKS1929+0709

19:29:05 +07:09:36 V = 10.5 TIC 134621509
$N_{H/H} = 0$ $N_C = 1$

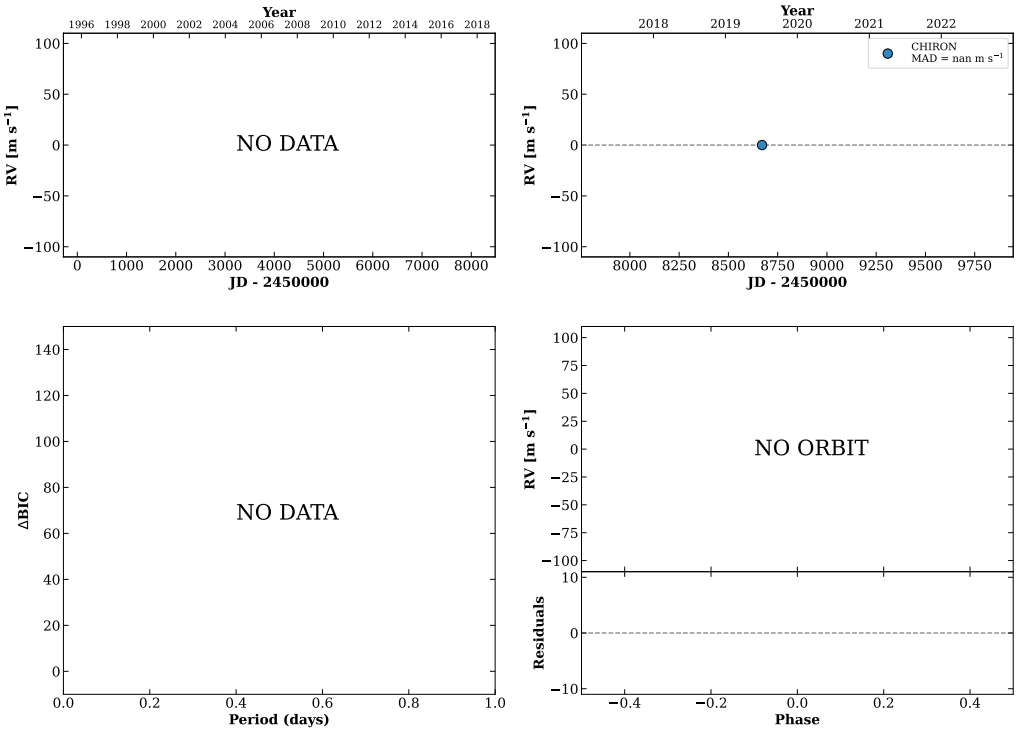

RKS1930+2140

19:30:05 +21:40:34 V = 10.0 HIP095890 TIC 370406321
$N_{H/H} = 0$ $N_C = 9$ DMY

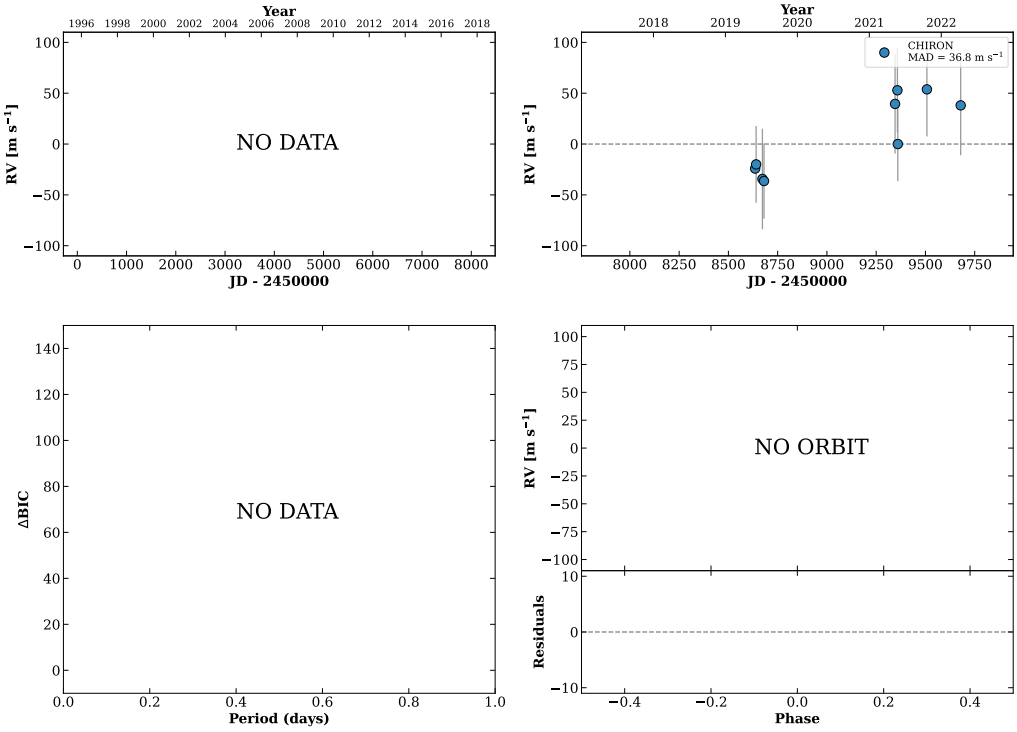

Figure 329 RV results for RKS1929+0709 (top) and RKS1930+2140 (bottom).

RKS1932-1116

19:32:07 -11:16:30 V = 7.5 HIP096085 TIC 100711809
$N_{H/H}$ = 31 N_C = 6 DM

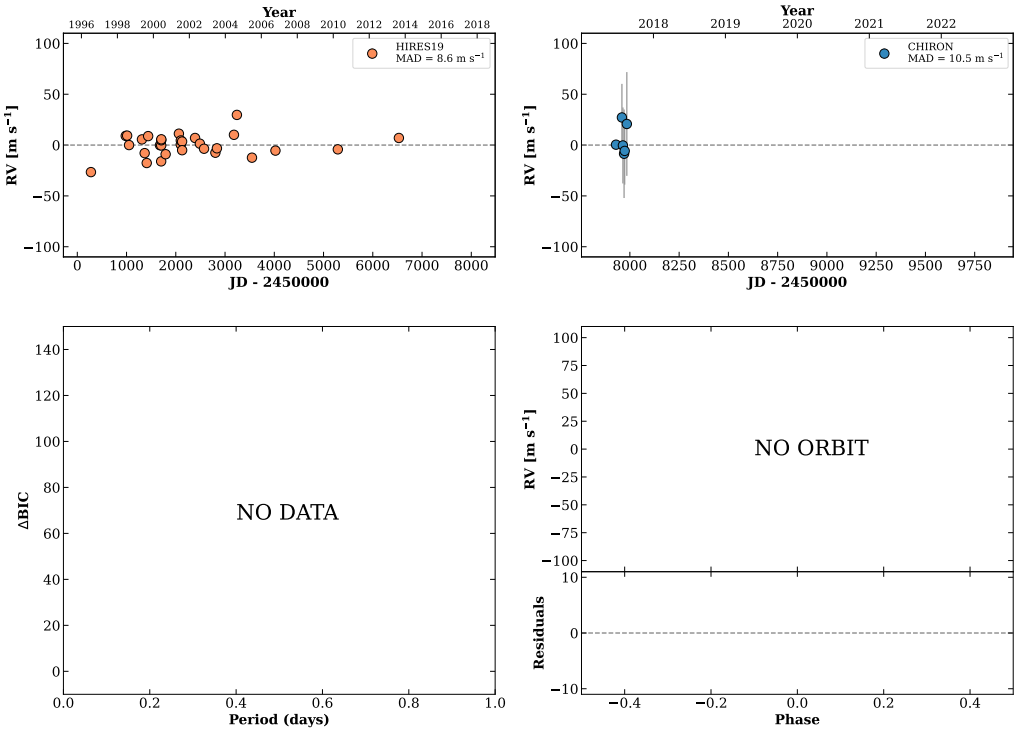

RKS1932+0034

19:32:38 +00:34:39 V = 10.4 HIP096121 TIC 113873448
$N_{H/H}$ = 0 N_C = 18 DMY

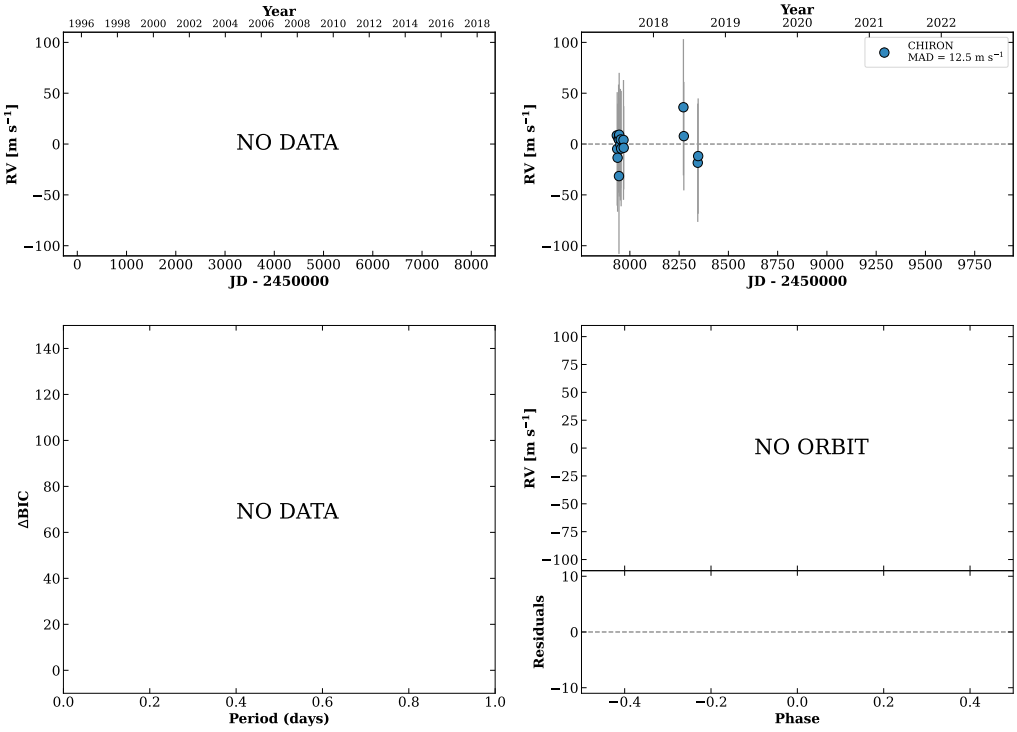

Figure 330 RV results for RKS1932-1116 (top) and RKS1932+0034 (bottom).

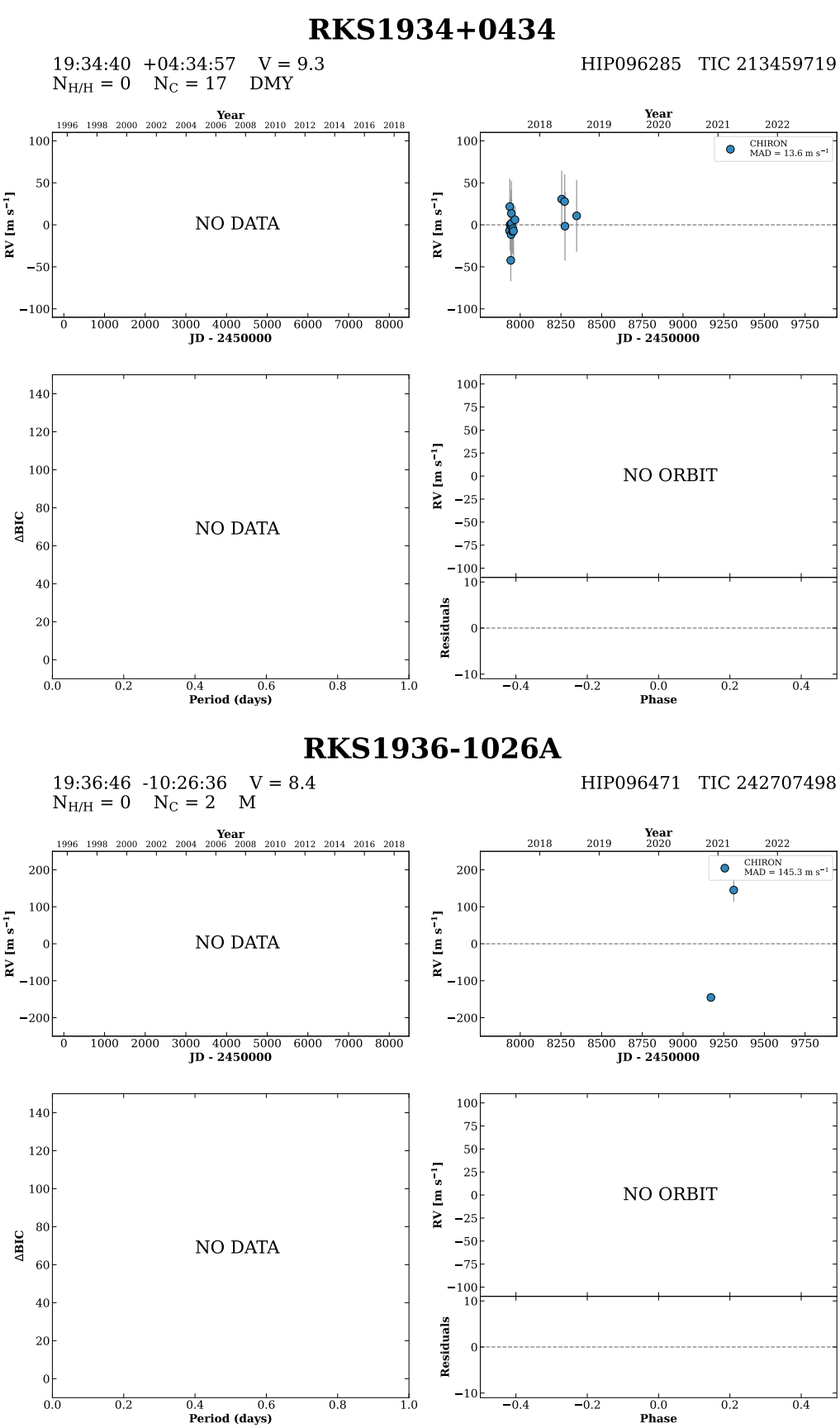

Figure 331 RV results for RKS1934+0434 (top) and RKS1936-1026A (bottom).

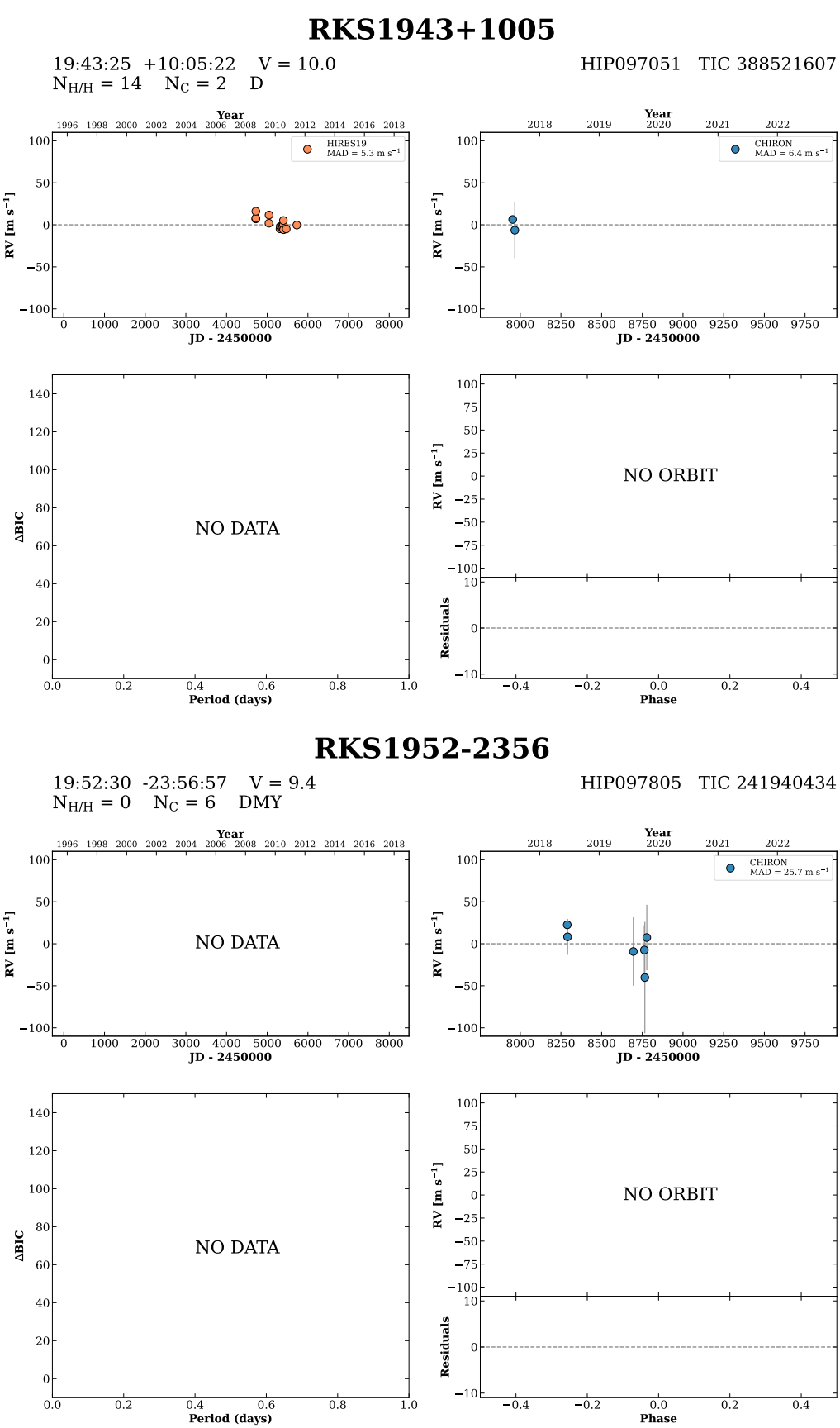

Figure 332 RV results for RKS1943+1005 (top) and RKS1952-2356 (bottom).

RKS1954-2356

19:54:18 -23:56:28 V = 6.2 HIP097944 TIC 241967968
$N_{H/H}$ = 42 N_C = 1

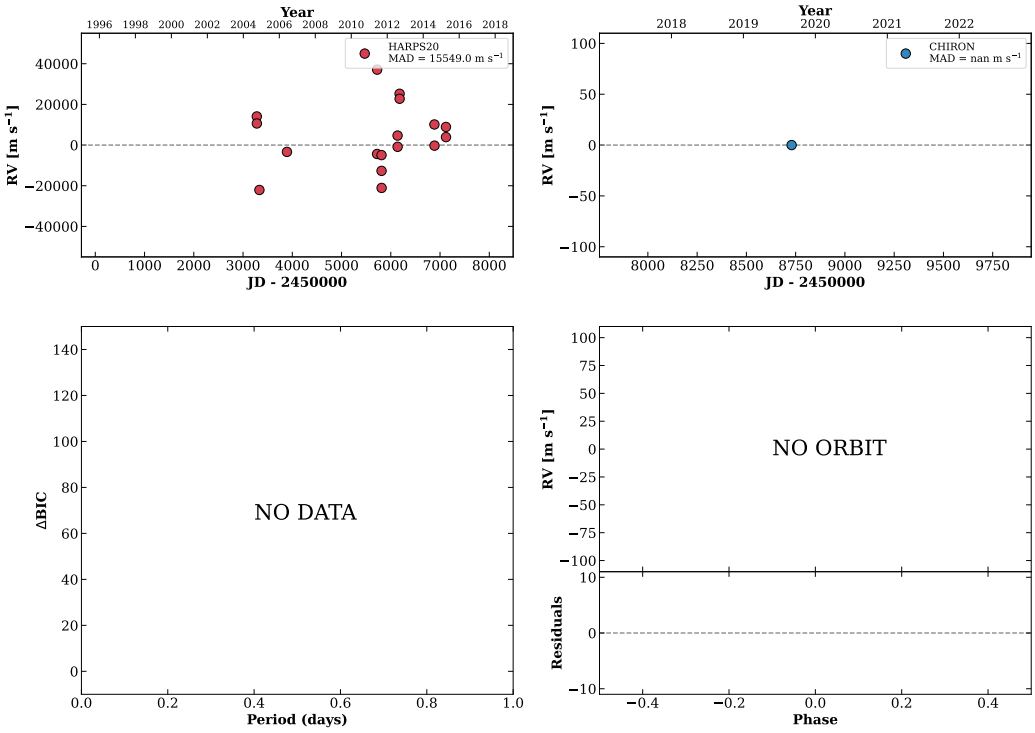

RKS1954+2013

19:54:38 +20:13:07 V = 11.1 TIC 263105734
$N_{H/H}$ = 0 N_C = 2 DY

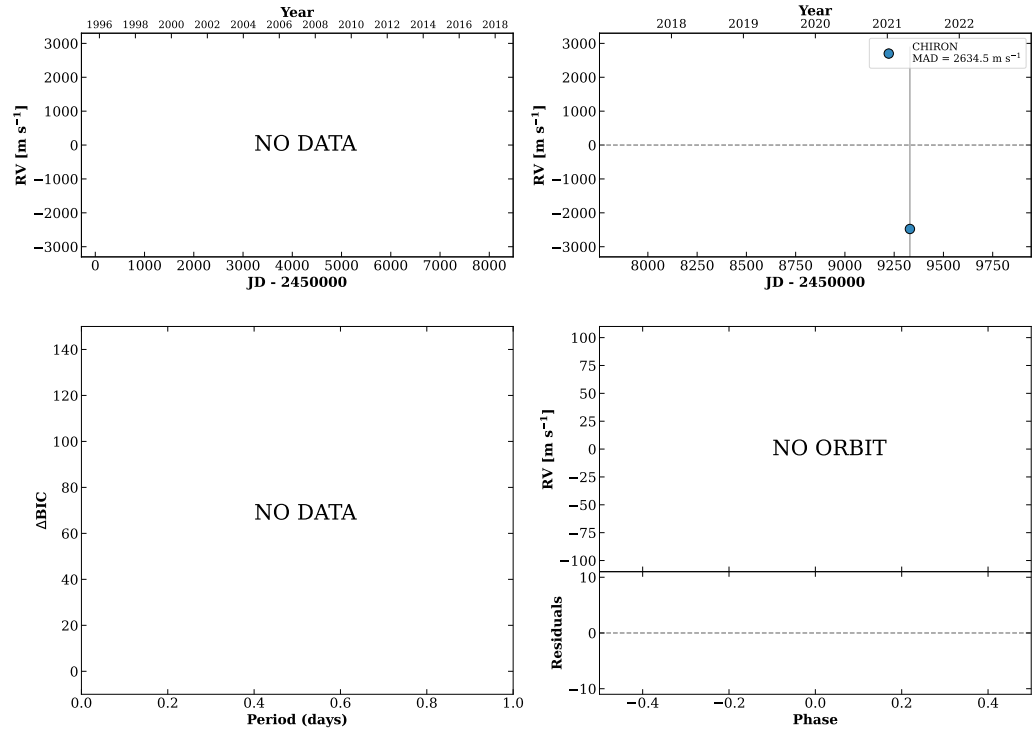

Figure 333 RV results for RKS1954-2356 (top) and RKS1954+2013 (bottom).

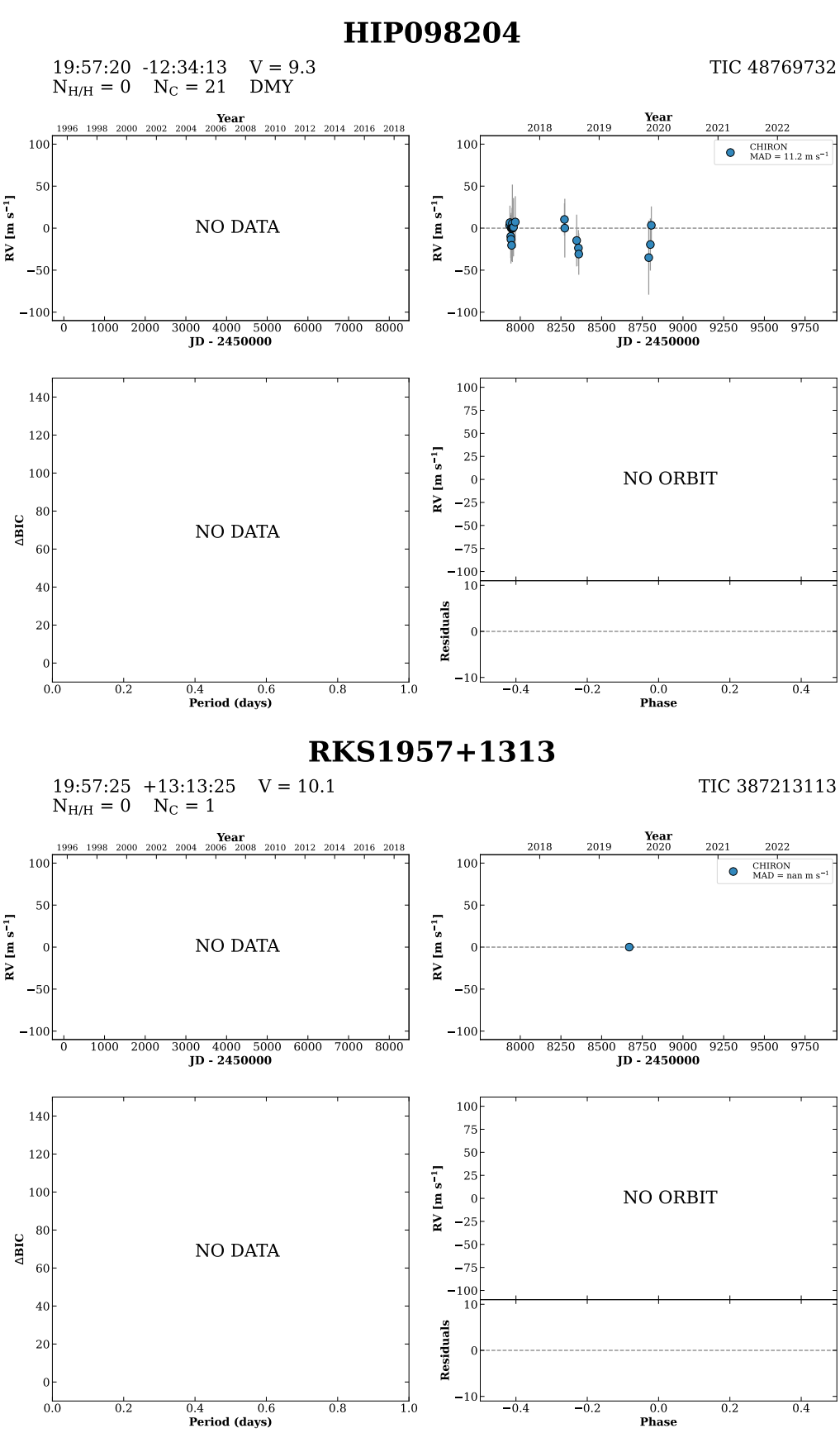

Figure 334 RV results for HIP098204 (top) and RKS1957+1313 (bottom).

RKS2000+2242

20:00:44 +22:42:39 V = 7.7 HIP098505 TIC 256364928
$N_{H/H}$ = 52 N_C = 31 DM

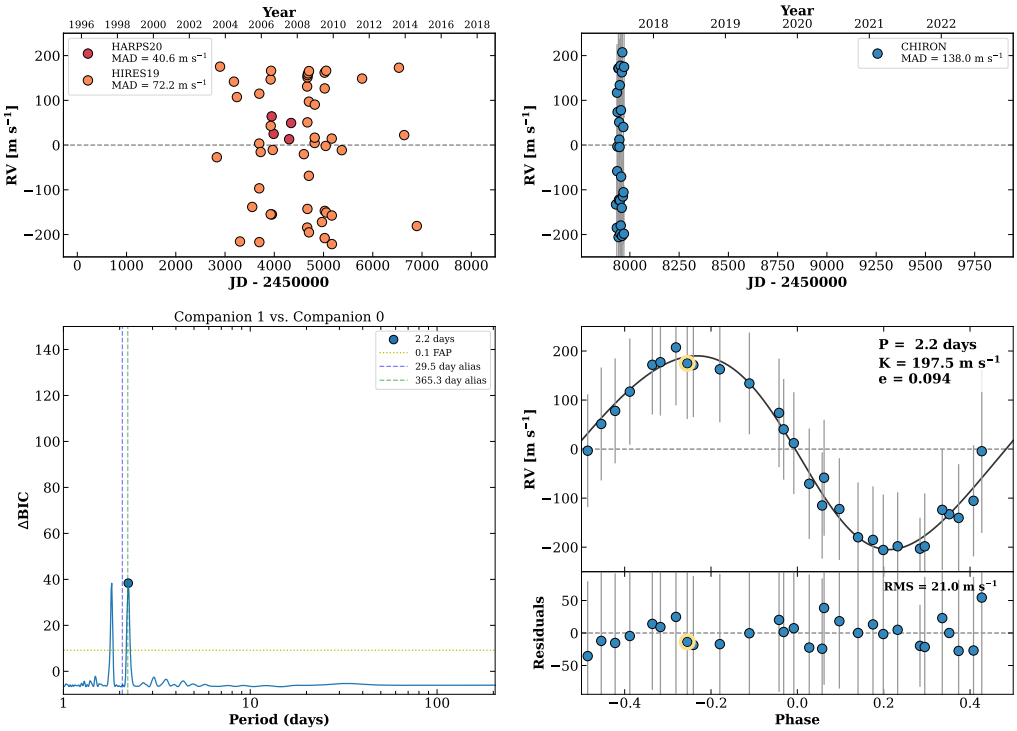

RKS2002+0319

20:02:47 +03:19:34 V = 7.5 HIP098698 TIC 345217789
$N_{H/H}$ = 34 N_C = 14 DM

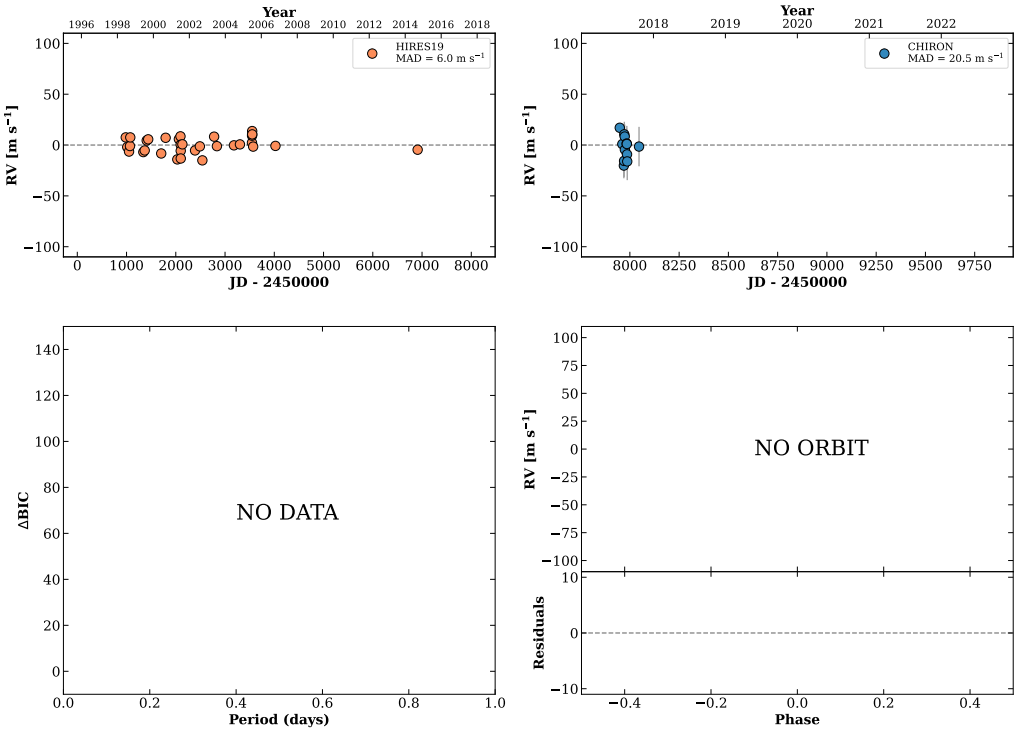

Figure 335 RV results for RKS2000+2242 (top) and RKS2002+0319 (bottom).

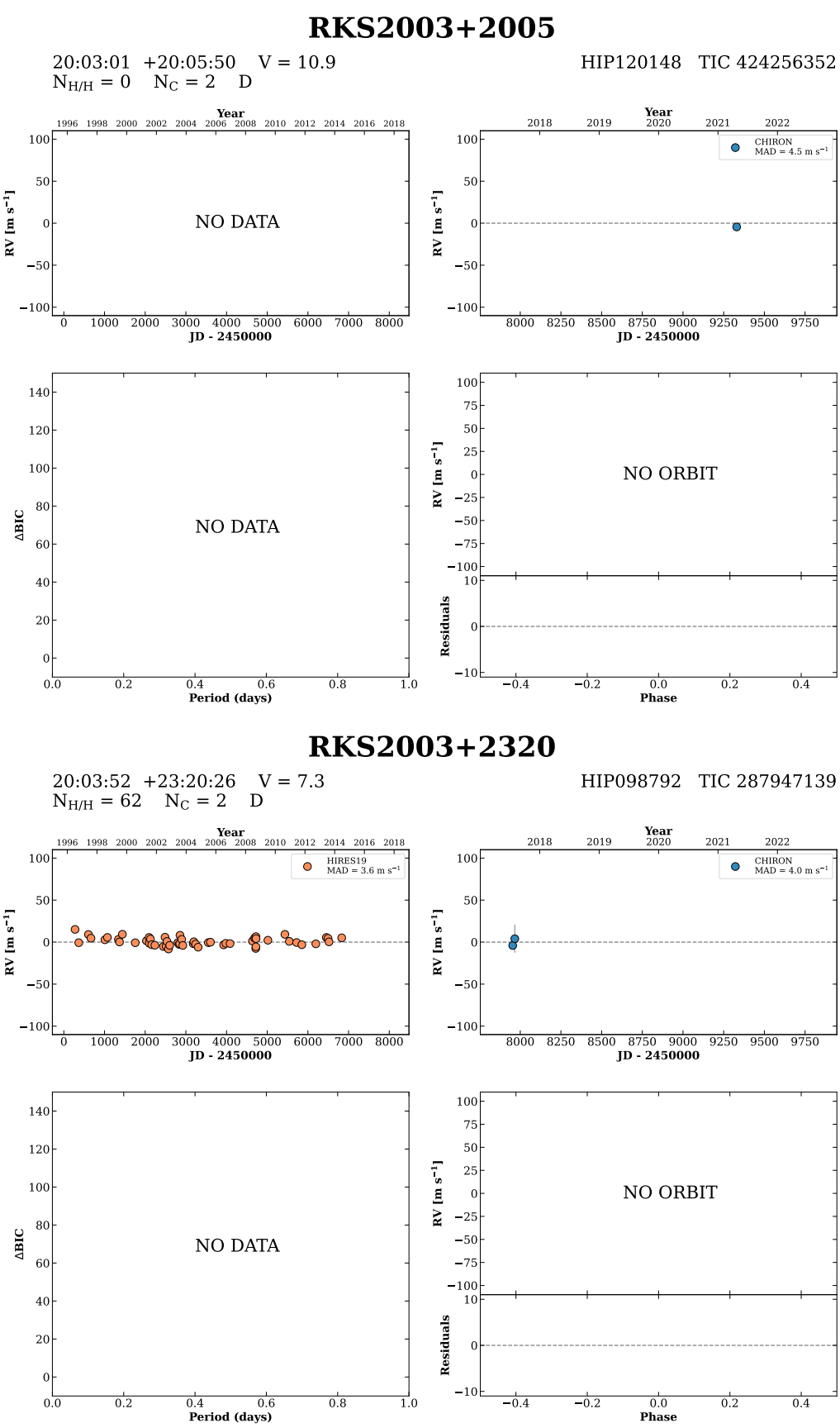

Figure 336 RV results for RKS2003+2005 (top) and RKS2003+2320 (bottom).

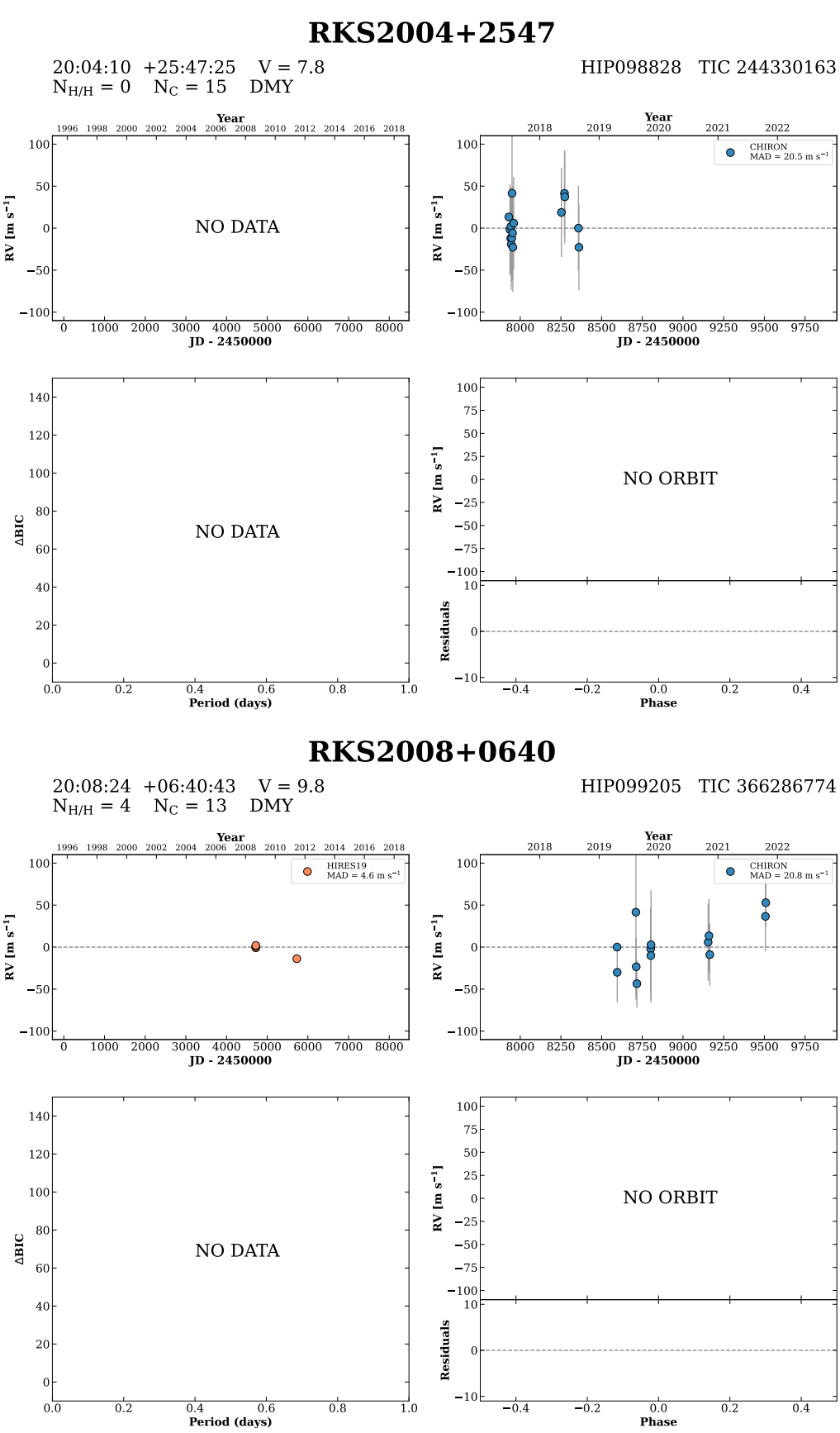

Figure 337 RV results for RKS2004+2547 (top) and RKS2008+0640 (bottom).

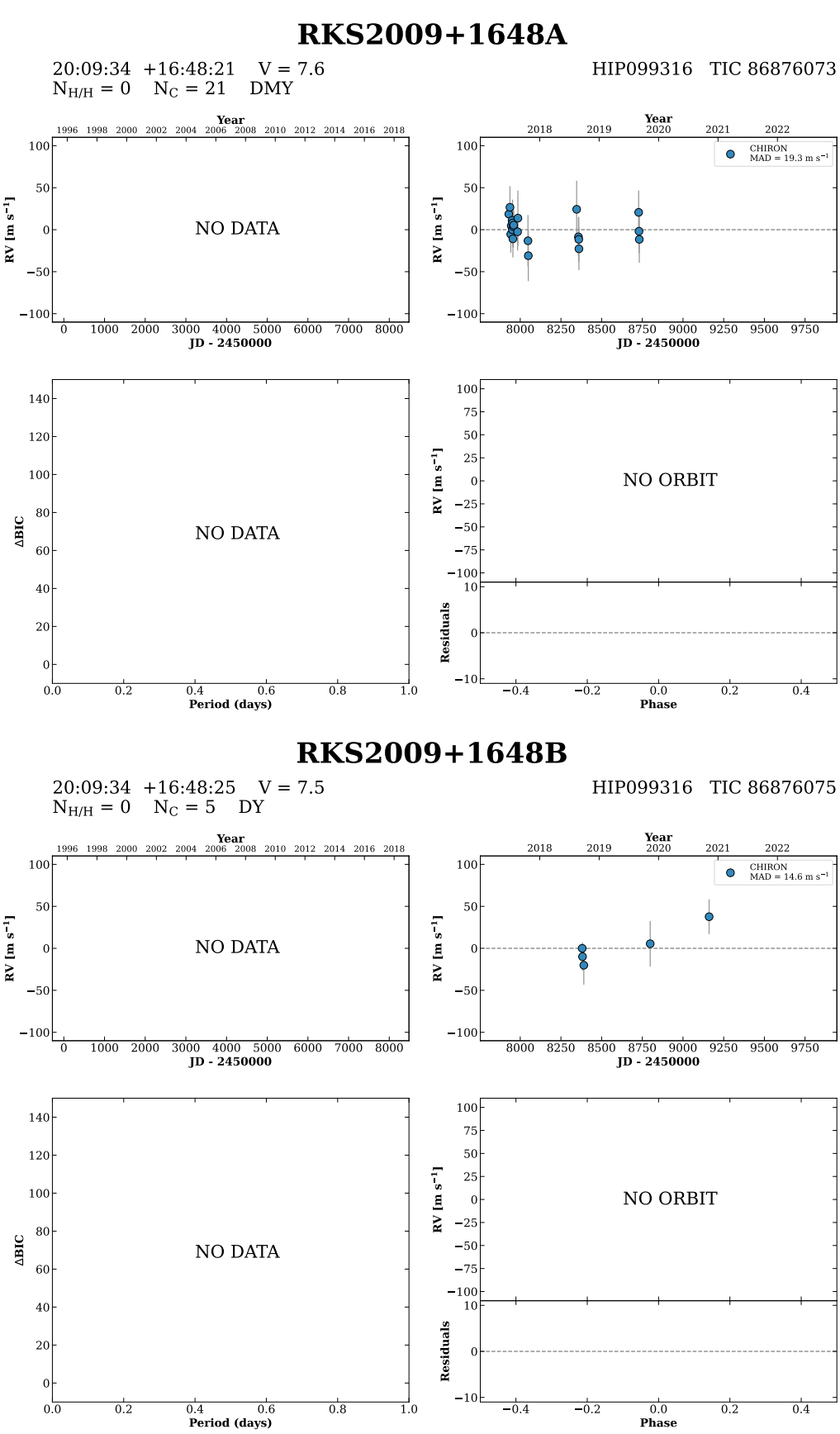

Figure 338 RV results for RKS2009+1648A (top) and RKS2009+1648B (bottom).

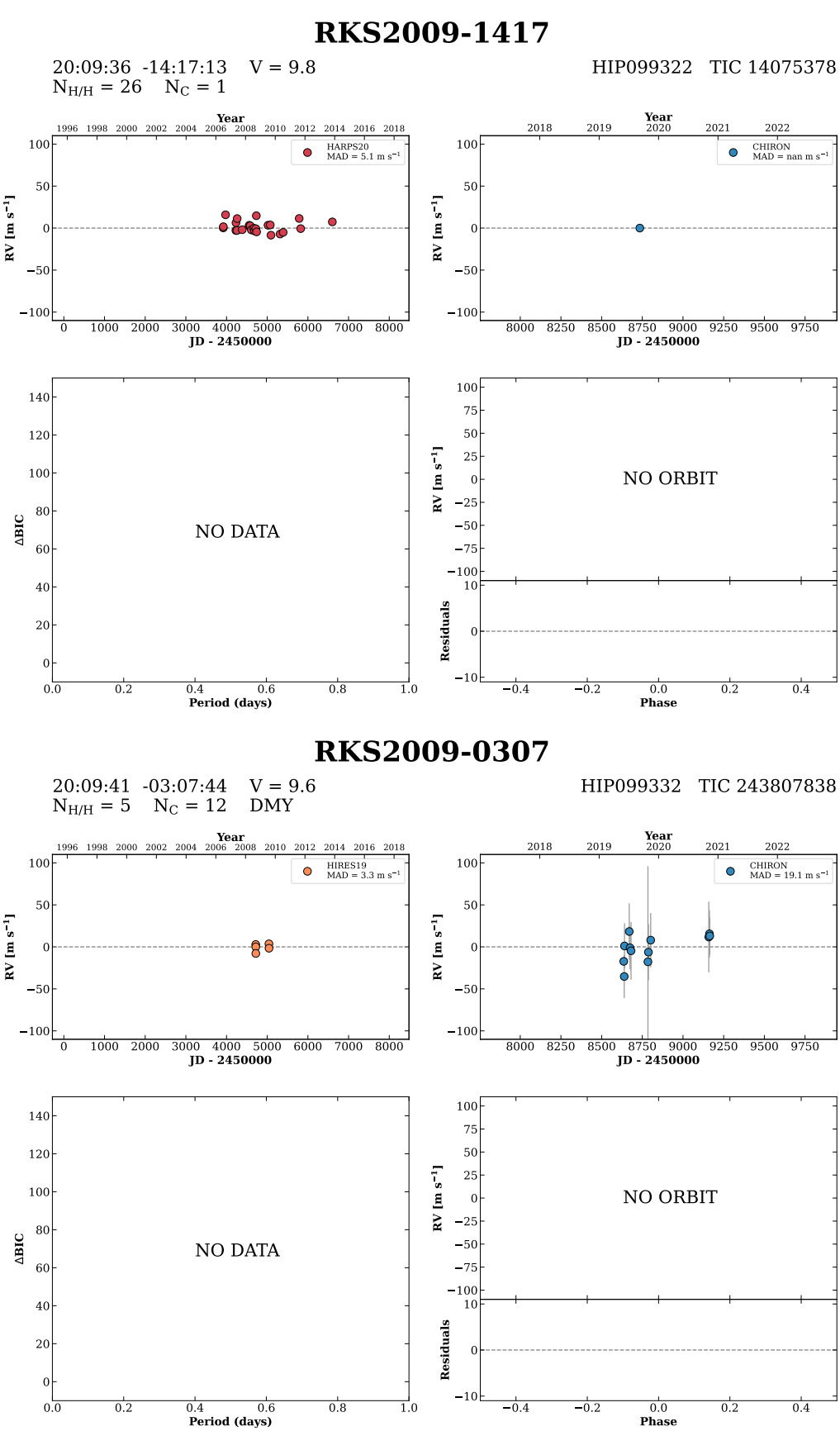

Figure 339 RV results for RKS2009-1417 (top) and RKS2009-0307 (bottom).

RKS2010-2029A

20:10:20 -20:29:36 V = 8.9 HIP099385 TIC 75231315
$N_{H/H}$ = 29 N_C = 5 DM

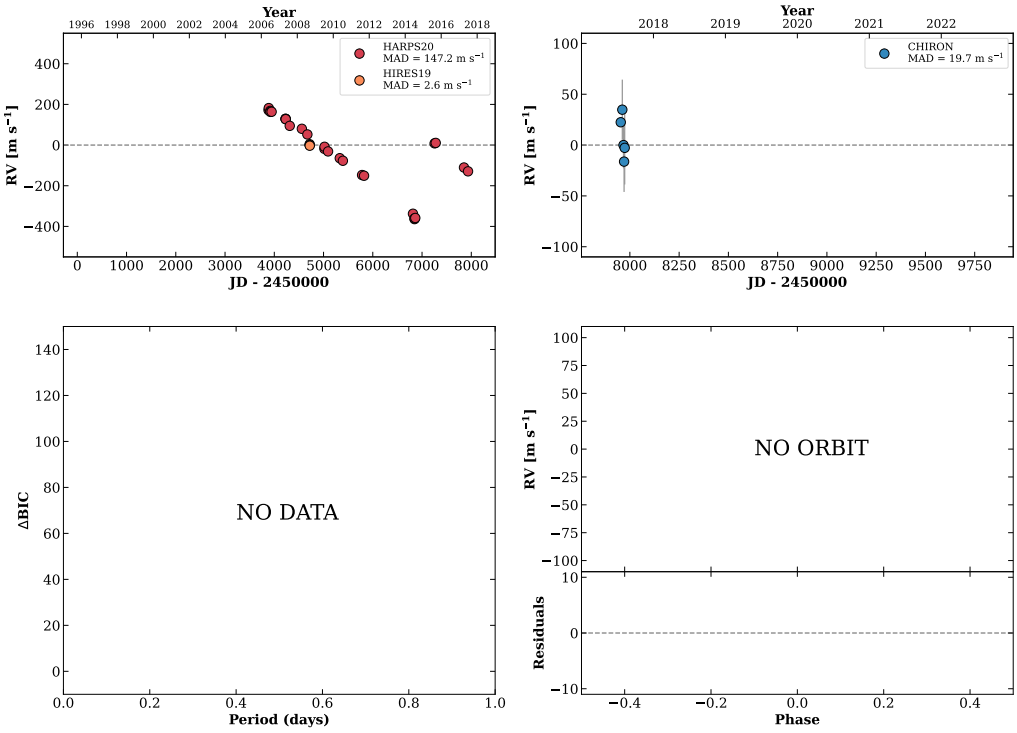

RKS2011+1611

20:11:06 +16:11:17 V = 7.4 HIP099452 TIC 87216634
$N_{H/H}$ = 63 N_C = 4 DM

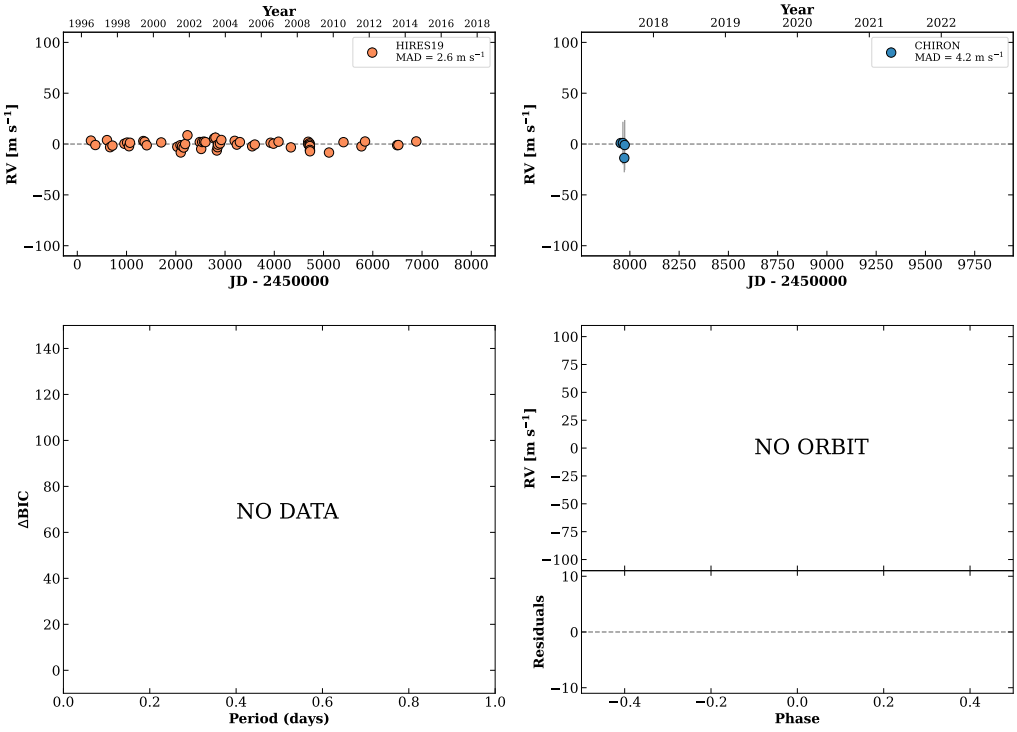

Figure 340 RV results for RKS2010-2029A (top) and RKS2011+1611 (bottom).

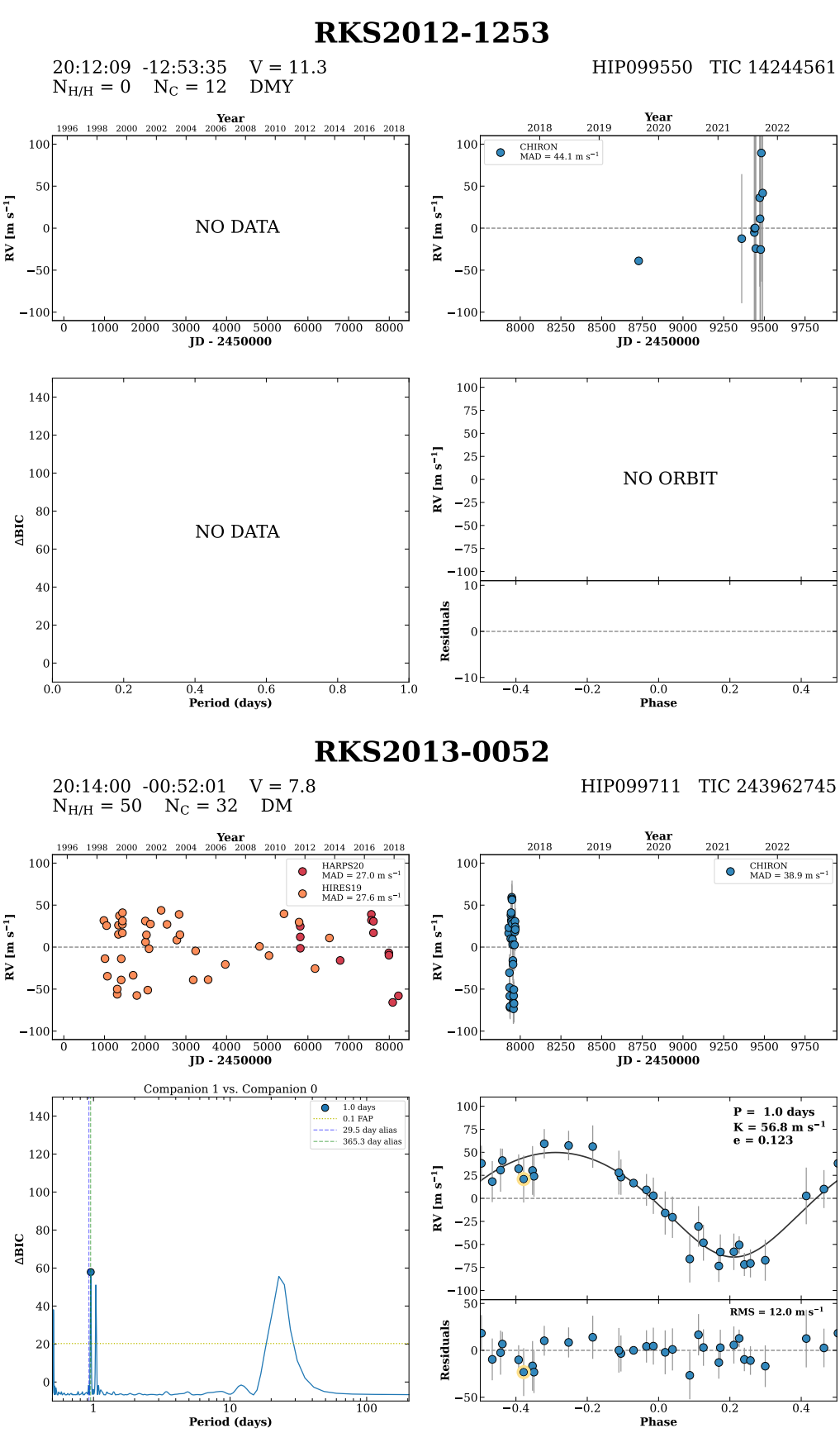

Figure 341 RV results for RKS2012-1253 (top) and RKS2013-0052 (bottom).

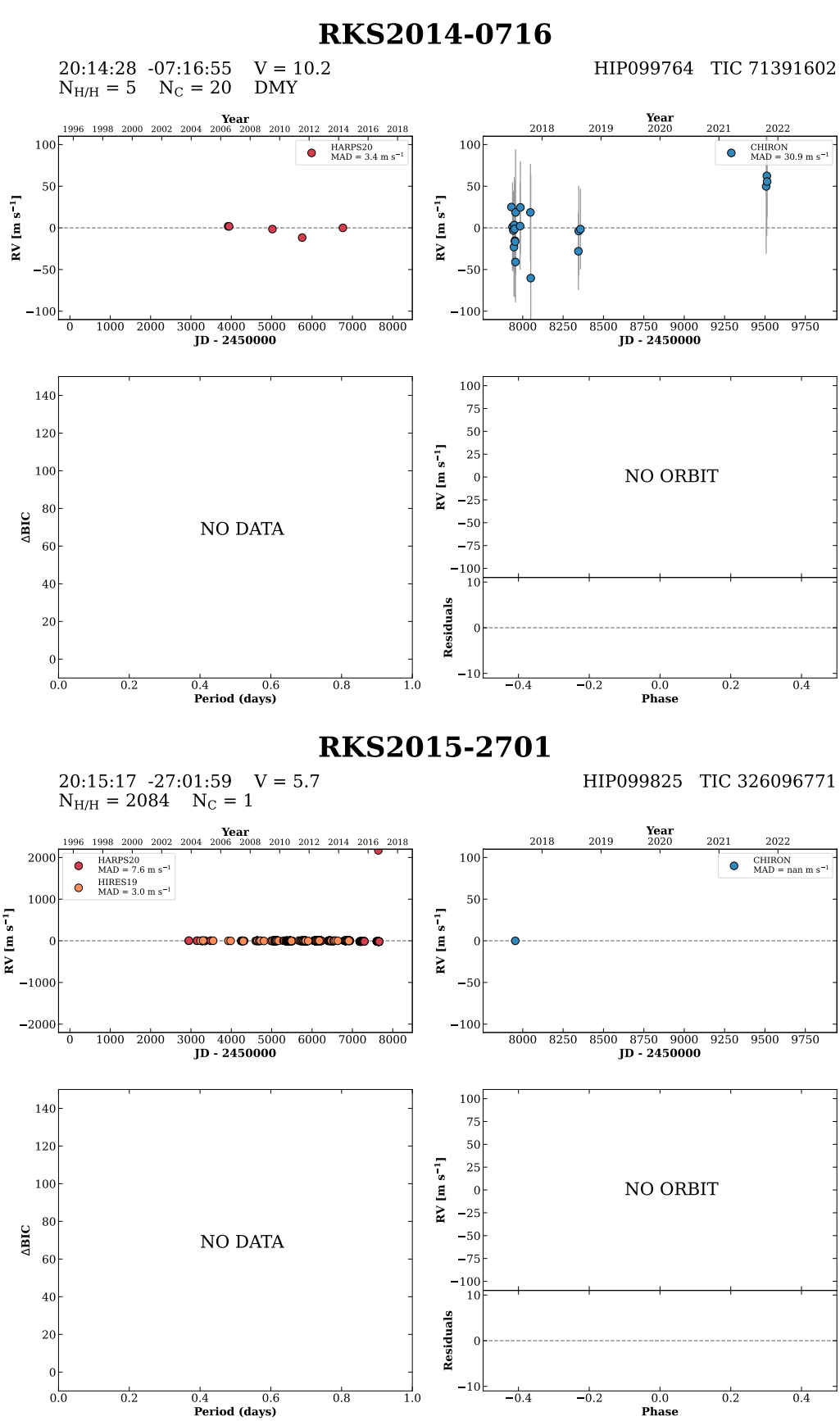

Figure 342 RV results for RKS2014-0716 (top) and RKS2015-2701 (bottom).

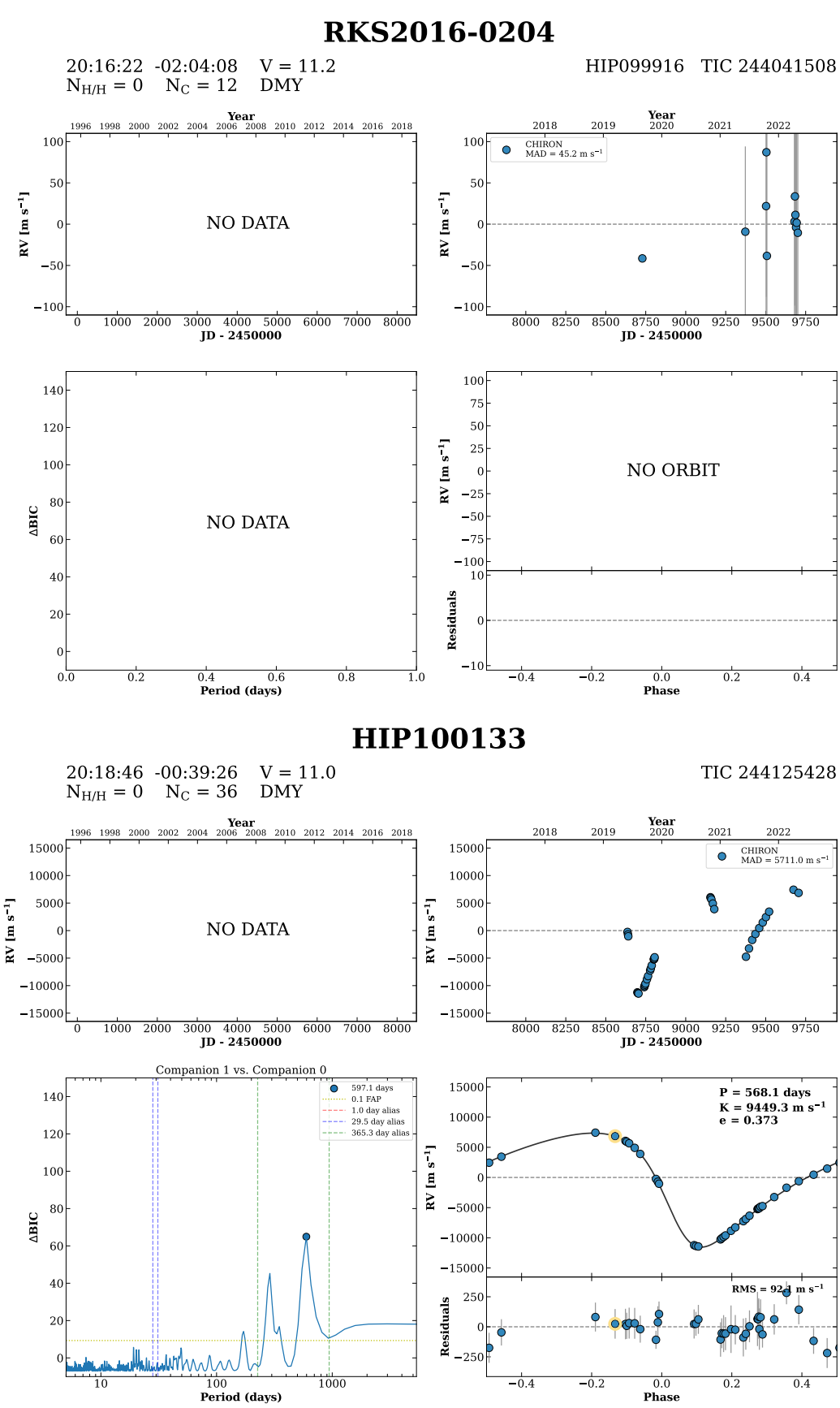

Figure 343 RV results for RKS2016-0204 (top) and HIP100133 (bottom).

RKS2030+2650

20:30:11 +26:50:34 V = 9.7 HIP101150 TIC 436446360
$N_{H/H} = 0$ $N_C = 1$

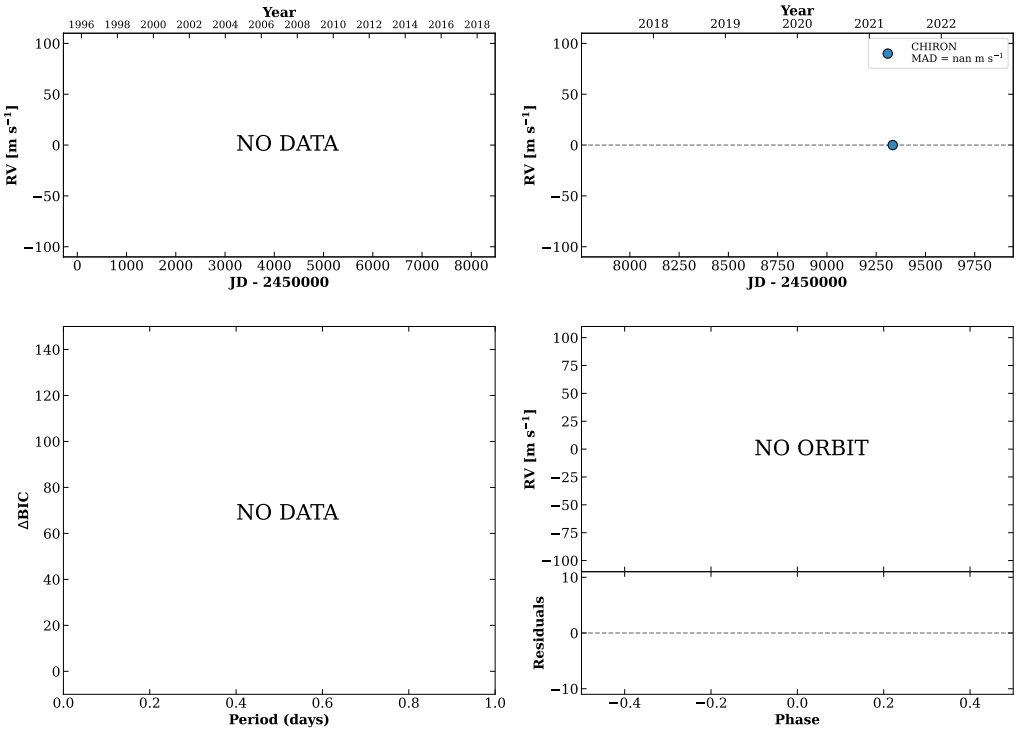

RKS2035+0607

20:35:13 +06:07:37 V = 8.9 HIP101579 TIC 375008312
$N_{H/H} = 62$ $N_C = 1$

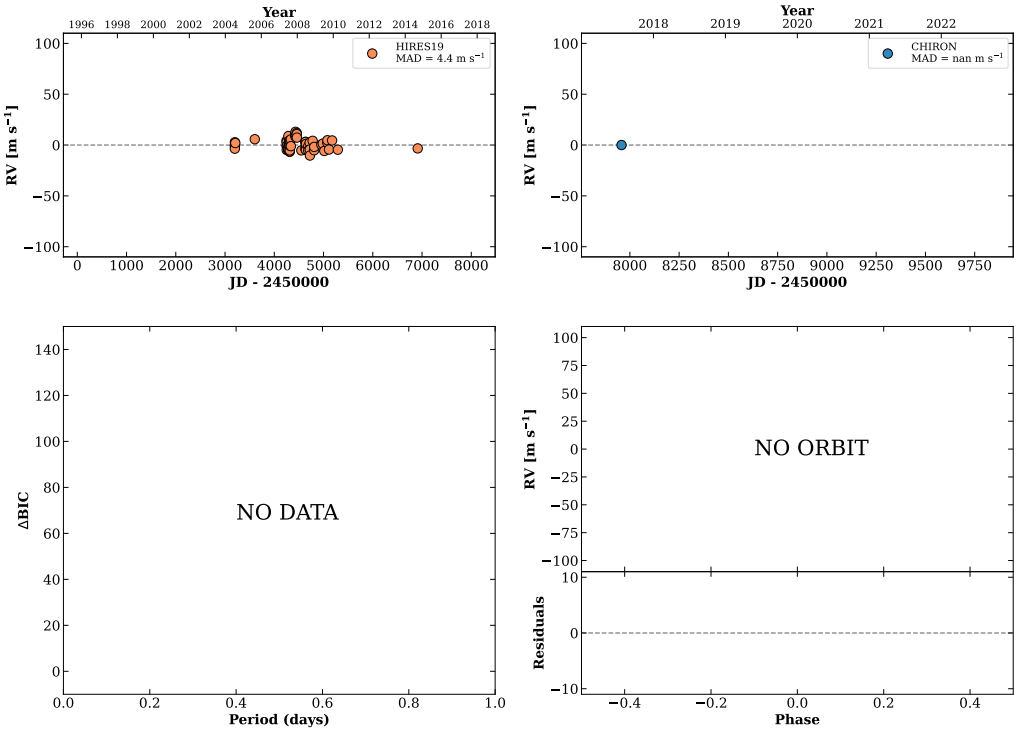

Figure 344 RV results for RKS2030+2650 (top) and RKS2035+0607 (bottom).

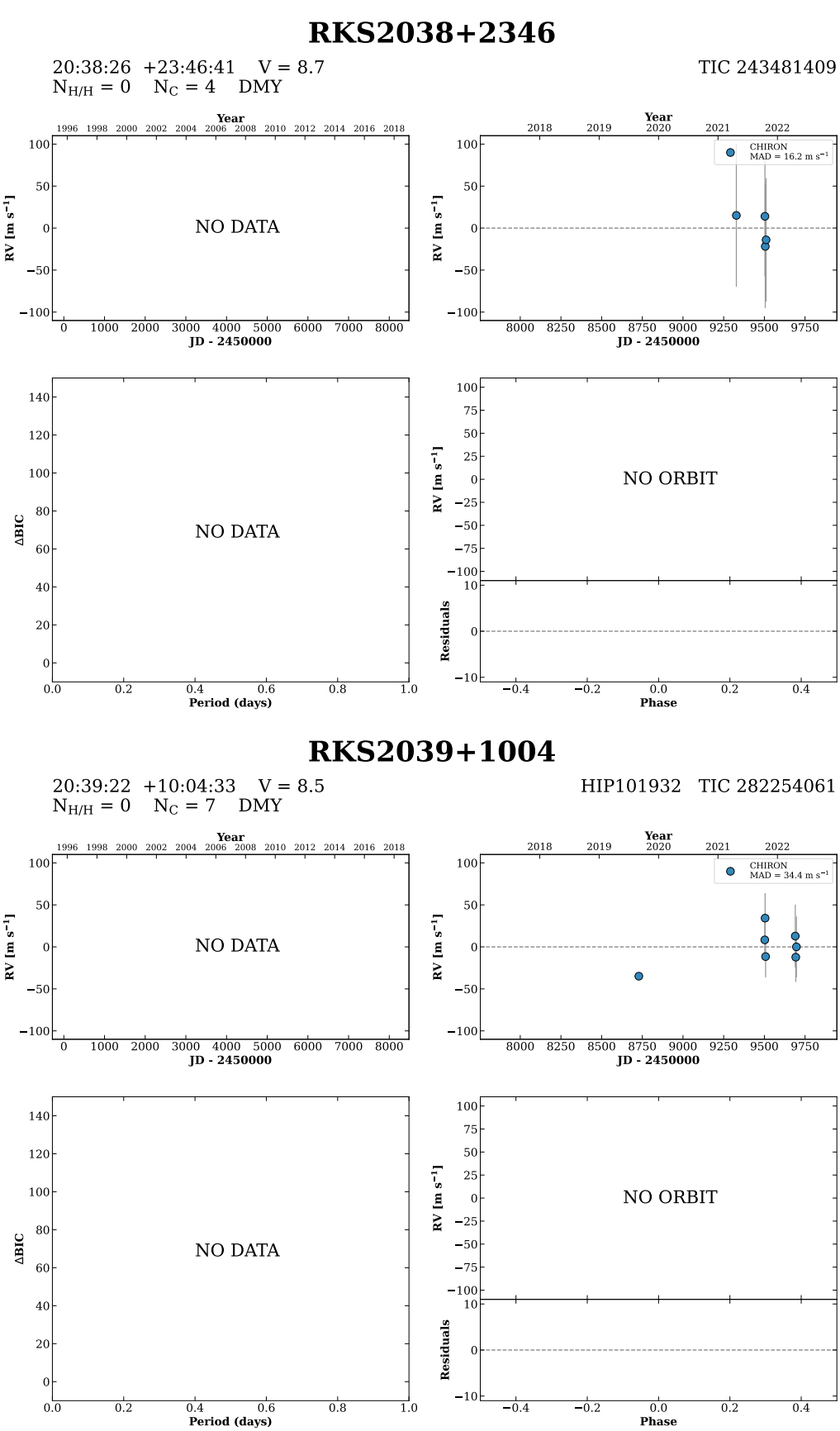

Figure 345 RV results for RKS2038+2346 (top) and RKS2039+1004 (bottom).

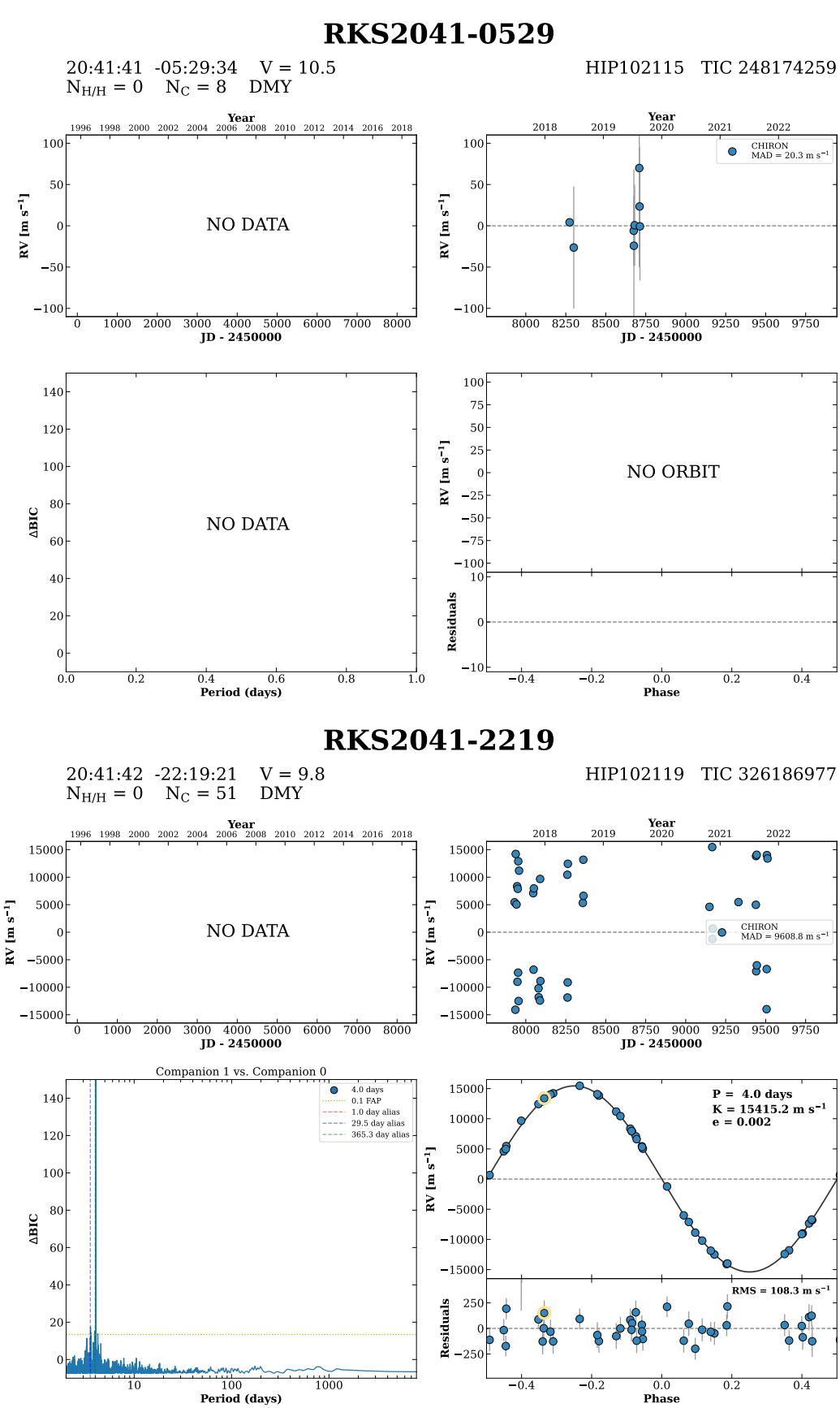

Figure 346 RV results for RKS2041-0529 (top) and RKS2041-2219 (bottom).

RKS2042-2116

20:42:06 -21:16:38 V = 9.3 TIC 271686772
$N_{H/H}$ = 0 N_C = 7 DMY

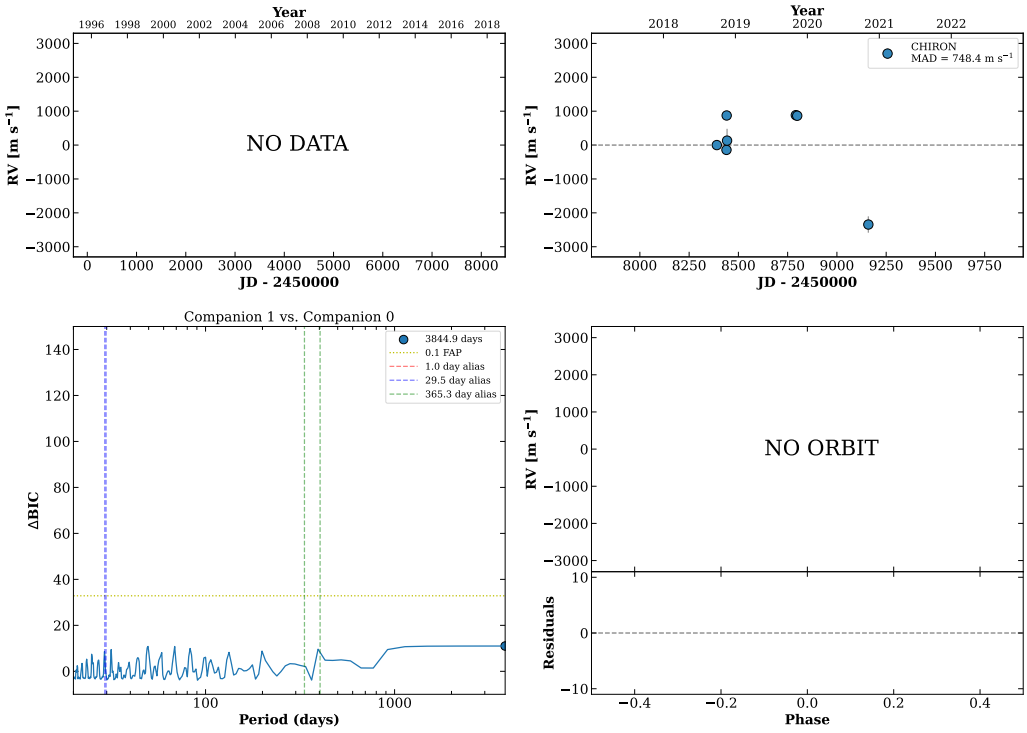

RKS2042+2050

20:42:49 +20:50:41 V = 8.3 HIP102226 TIC 331366716
$N_{H/H}$ = 0 N_C = 5 DMY

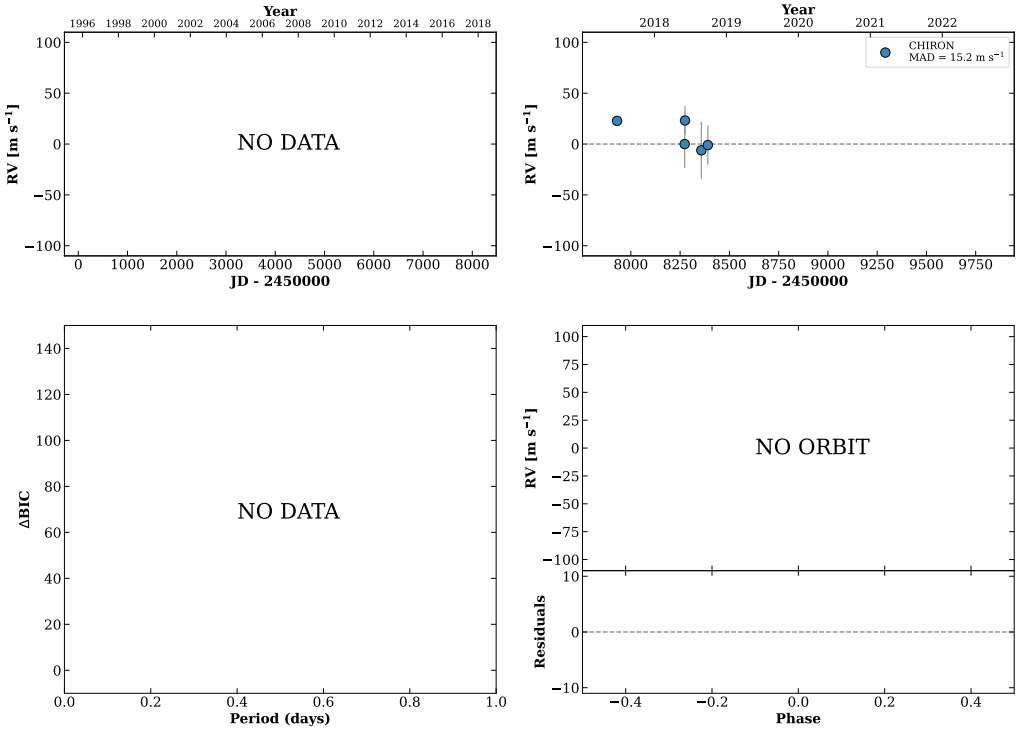

Figure 347 RV results for RKS2042-2116 (top) and RKS2042+2050 (bottom).

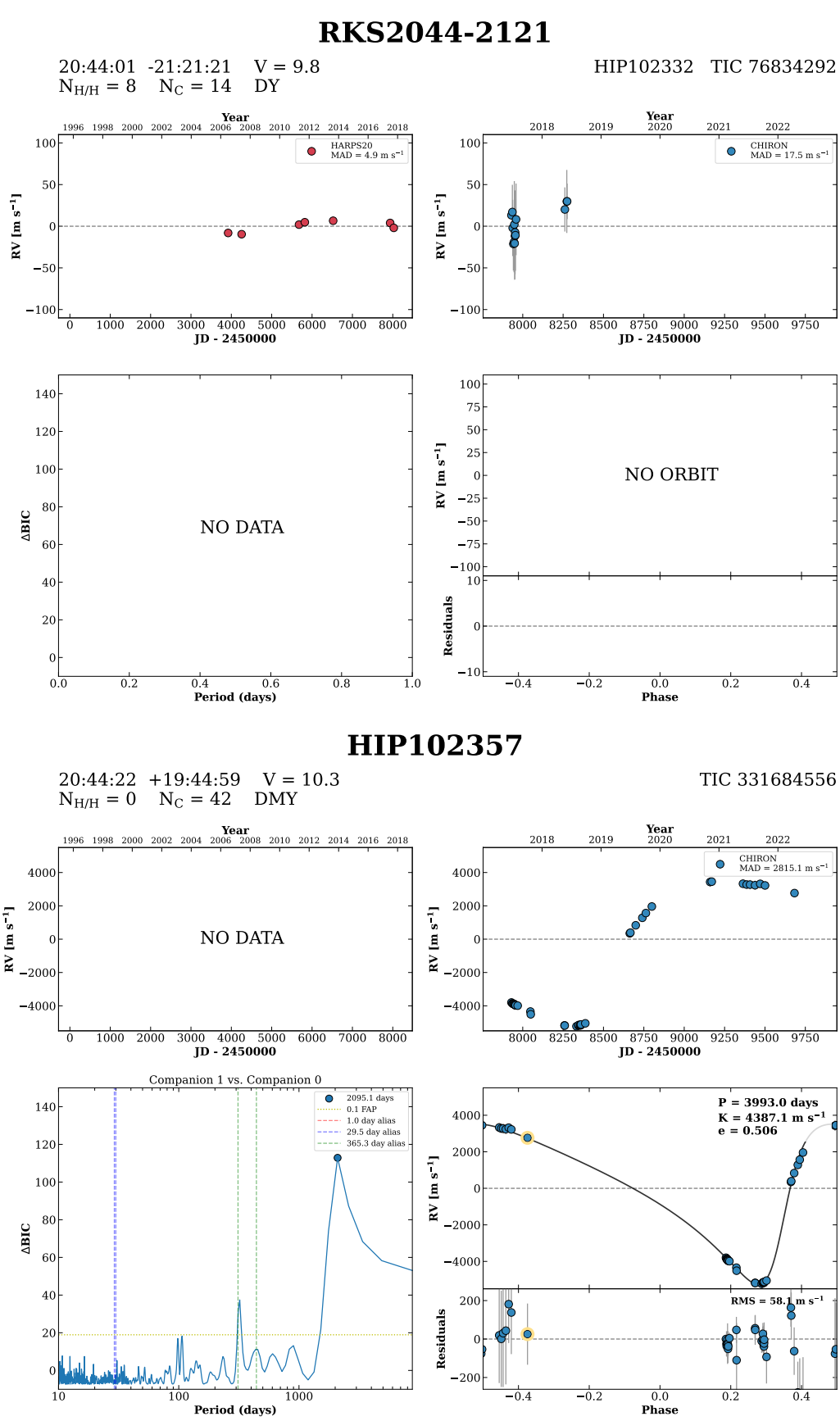

Figure 348 RV results for RKS2044-2121 (top) and HIP102357 (bottom).

RKS2046-2144

20:46:10 -21:44:45 V = 7.8 HIP102486 TIC 422364489
$N_{H/H}$ = 0 N_C = 6 DMY

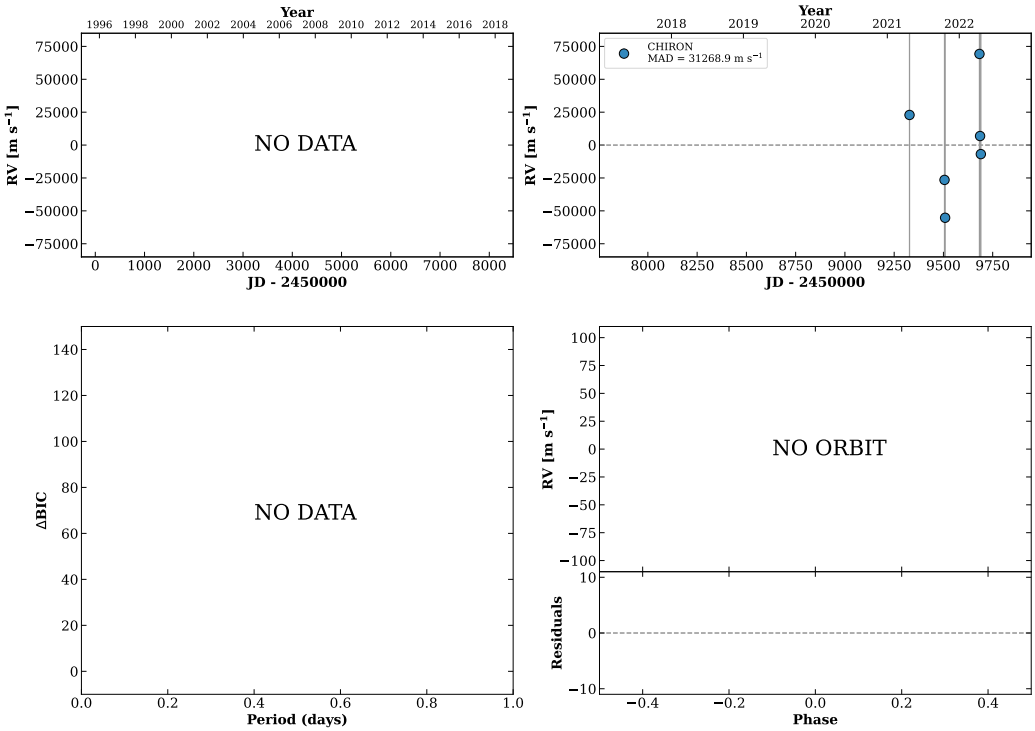

RKS2046-2304

20:46:18 -23:04:50 V = 10.7 HIP102495 TIC 422363545
$N_{H/H}$ = 9 N_C = 33 DMY

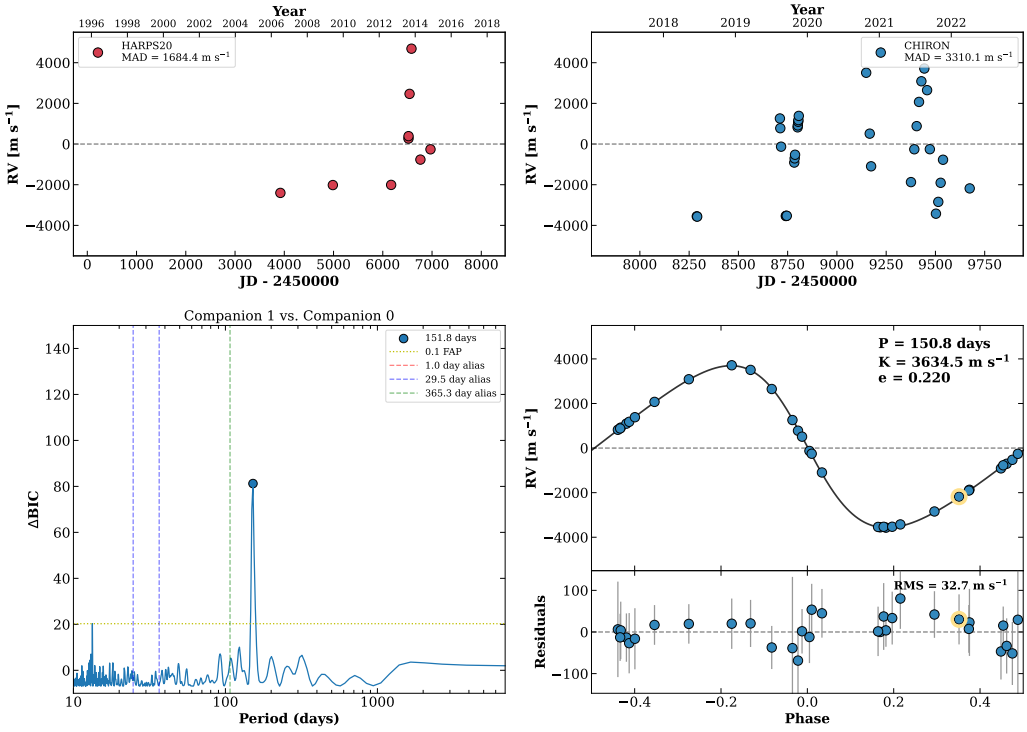

Figure 349 RV results for RKS2046-2144 (top) and RKS2046-2304 (bottom).

RKS2047+1051

20:47:17 +10:51:36 V = 9.7 HIP102582 TIC 383384592
$N_{H/H}$ = 0 N_C = 9 DMY

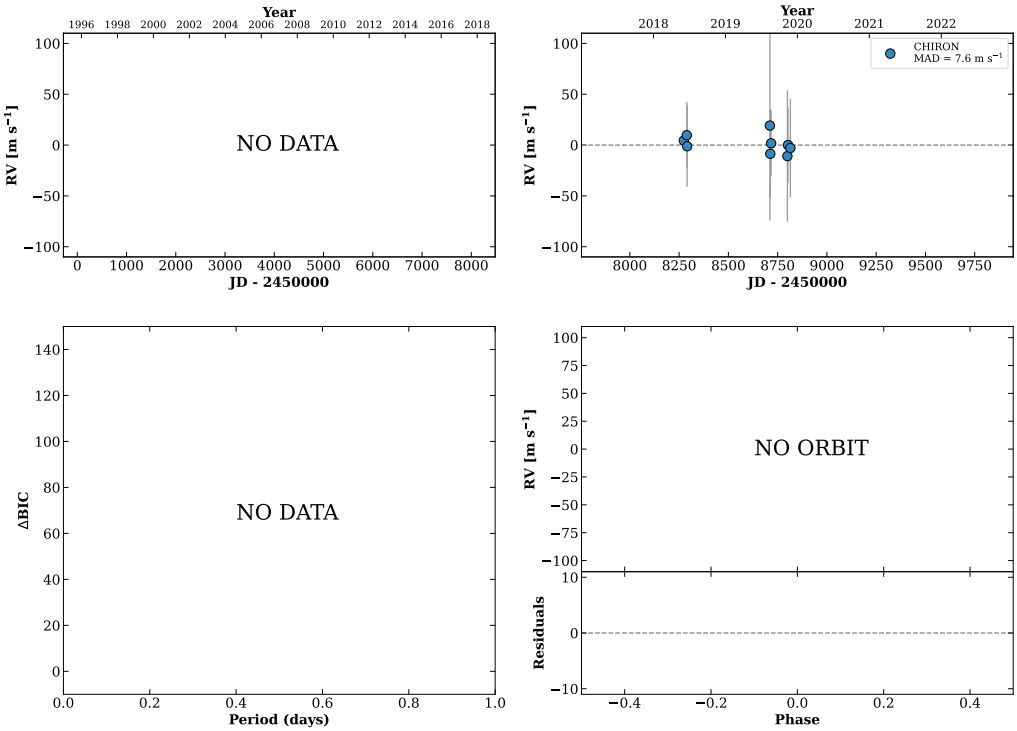

RKS2050+2923A

20:50:11 +29:23:03 V = 8.3 HIP102851 TIC 282843610
$N_{H/H}$ = 6 N_C = 29 DMY

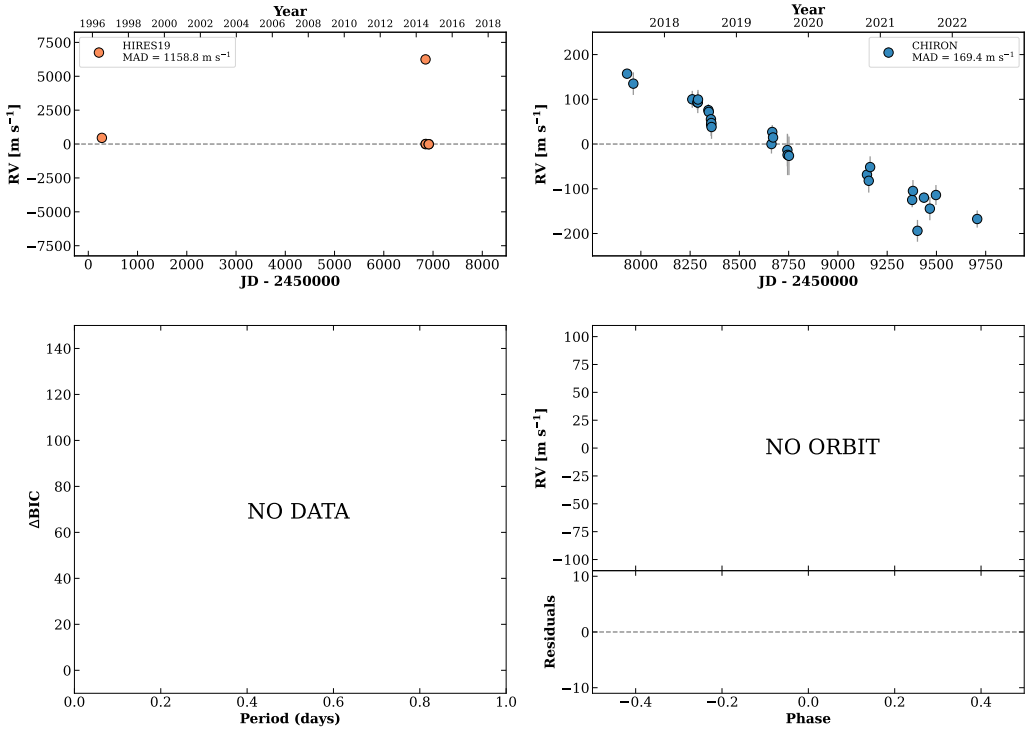

Figure 350 RV results for RKS2047+1051 (top) and RKS2050+2923A (bottom).

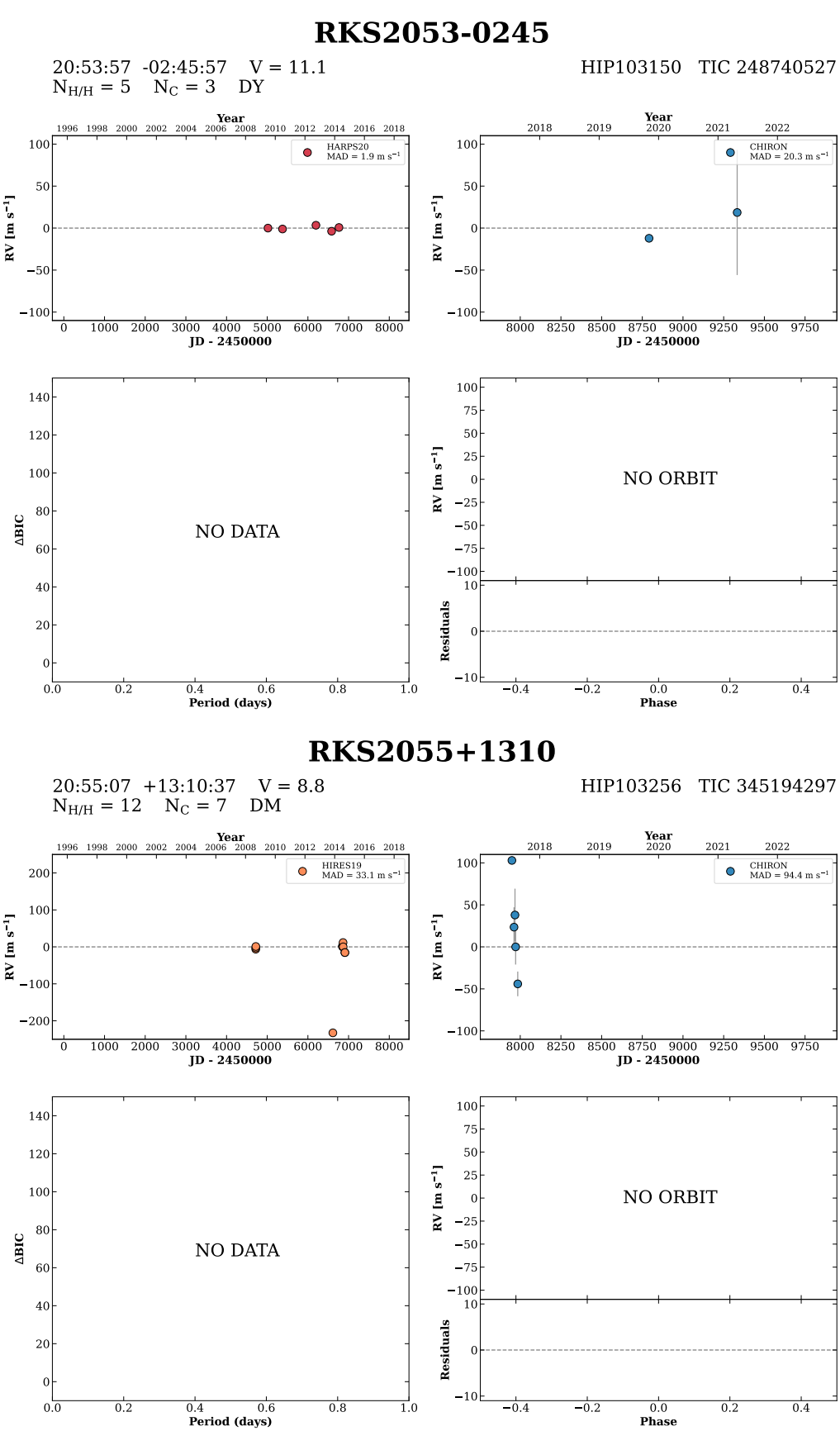

Figure 351 RV results for RKS2053-0245 (top) and RKS2055+1310 (bottom).

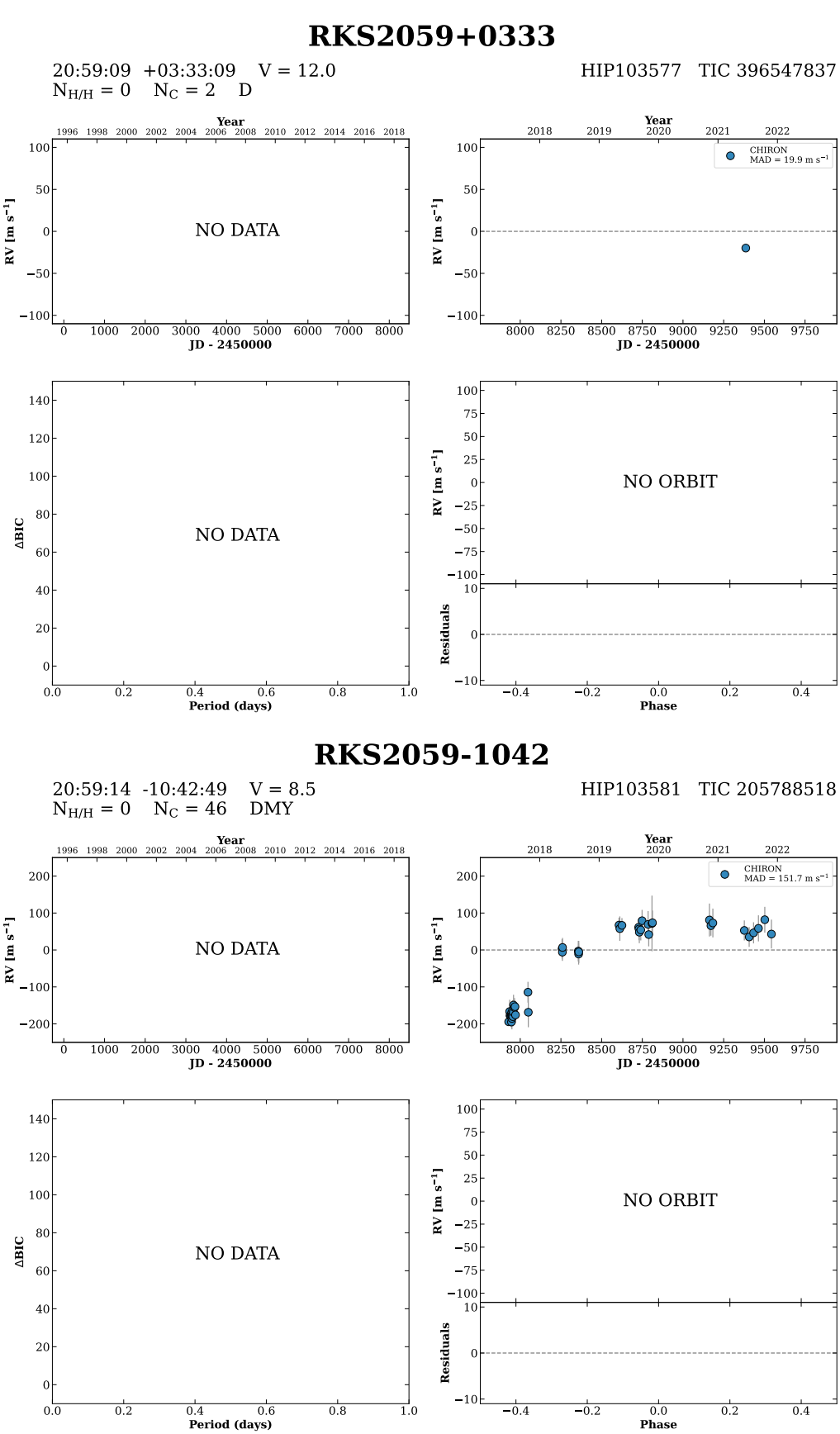

Figure 352 RV results for RKS2059+0333 (top) and RKS2059-1042 (bottom).

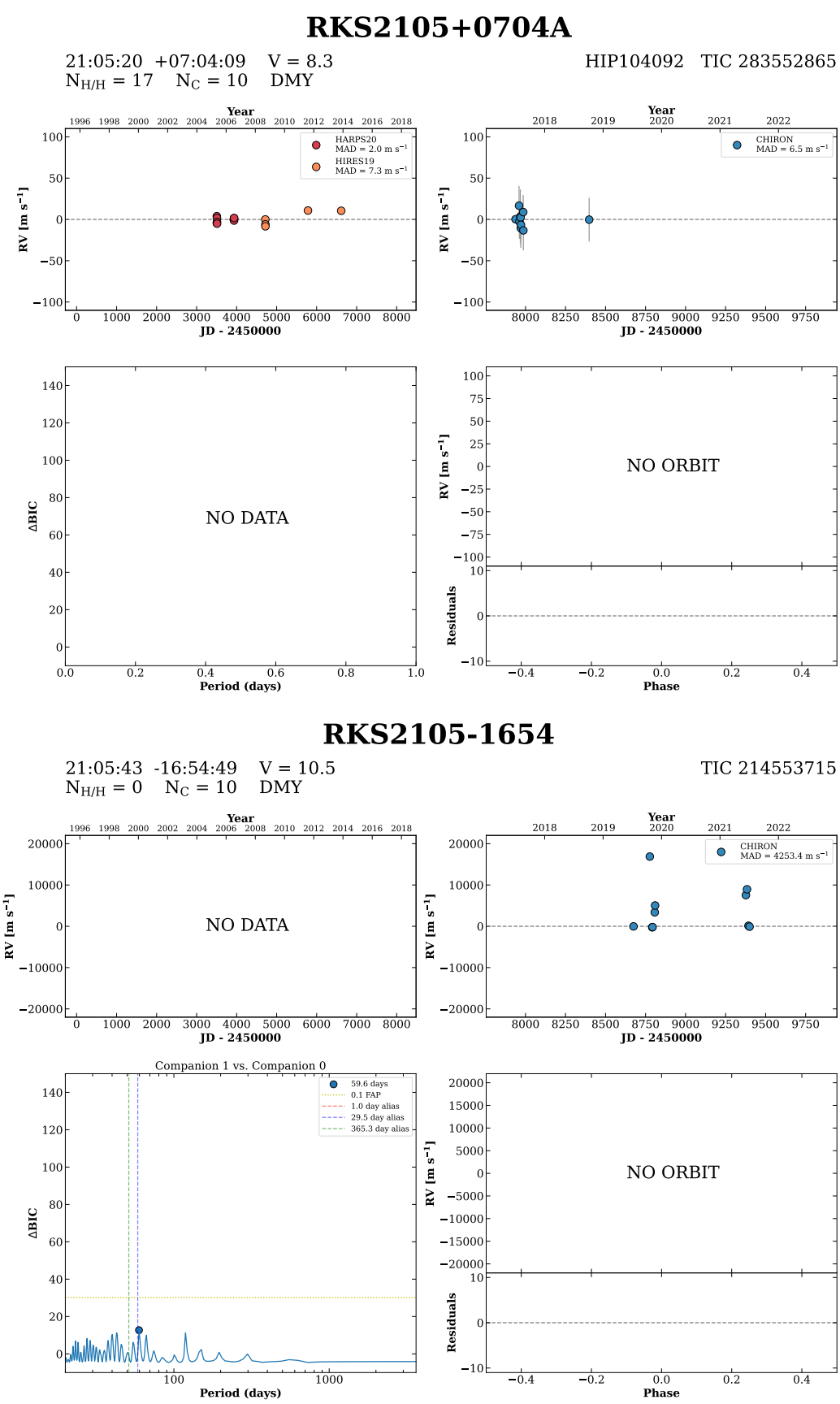

Figure 353 RV results for RKS2105+0704A (top) and RKS2105-1654 (bottom).

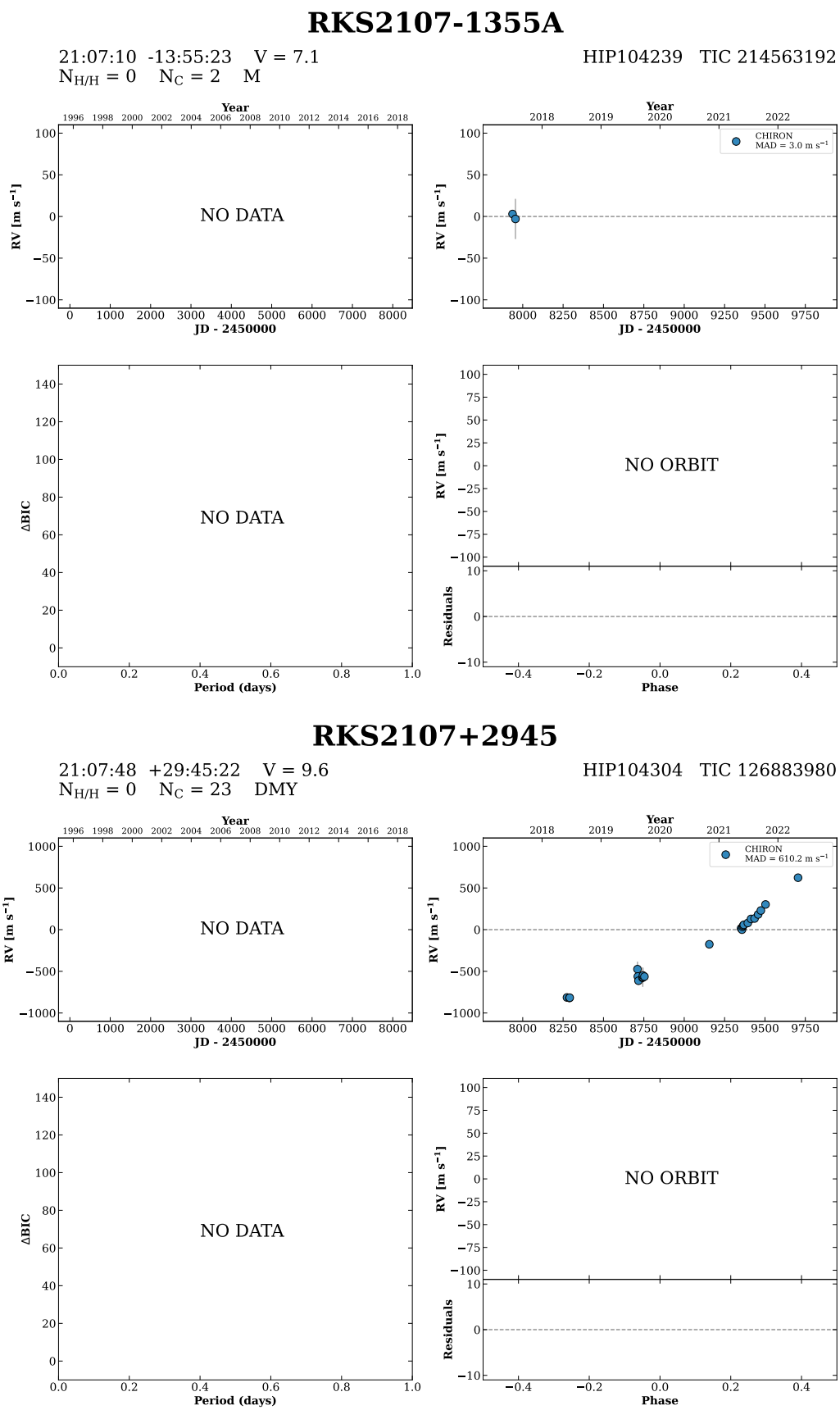

Figure 354 RV results for RKS2107-1355A (top) and RKS2107+2945 (bottom).

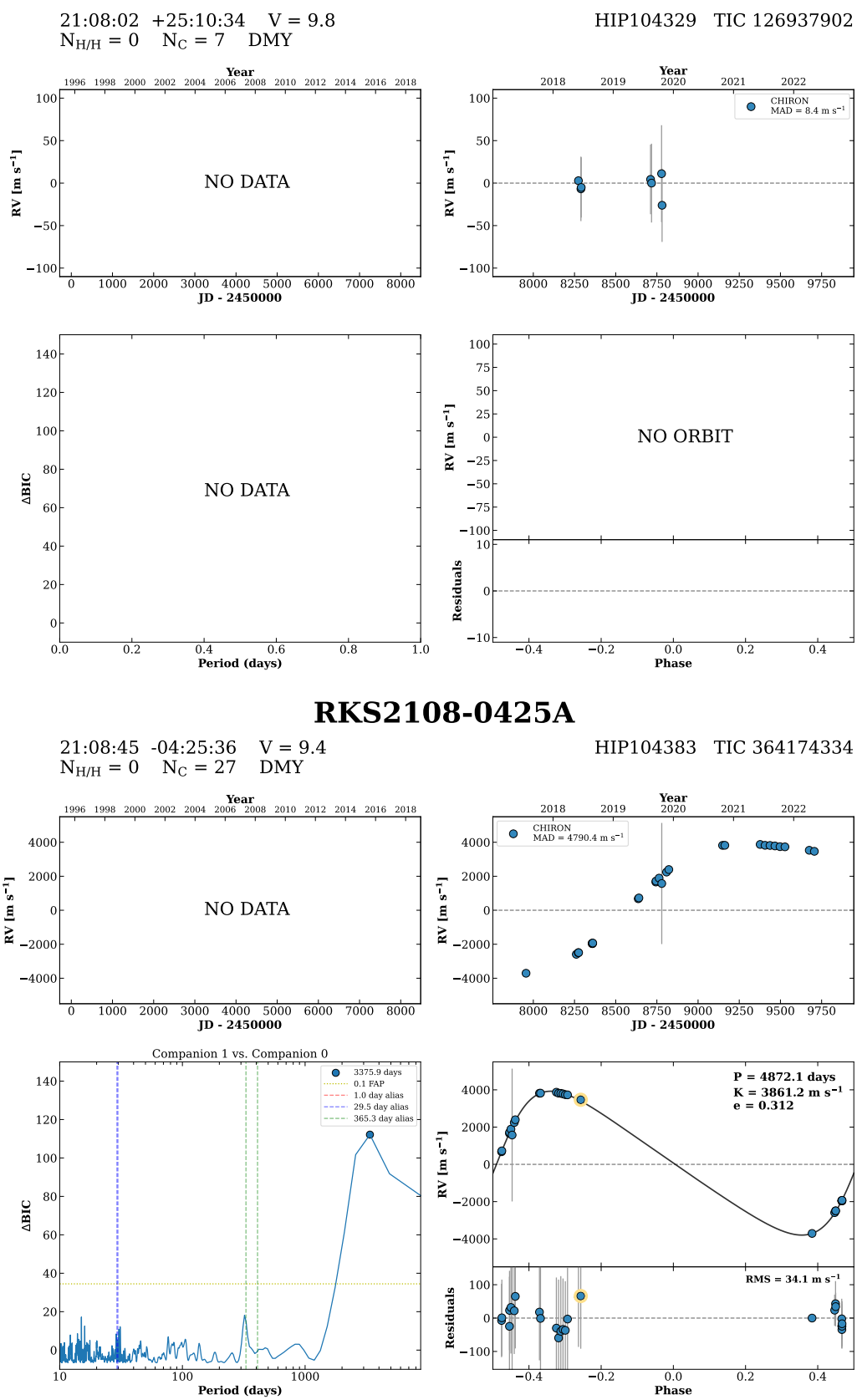

Figure 355 RV results for RKS2108+2510 (top) and RKS2108-0425A (bottom).

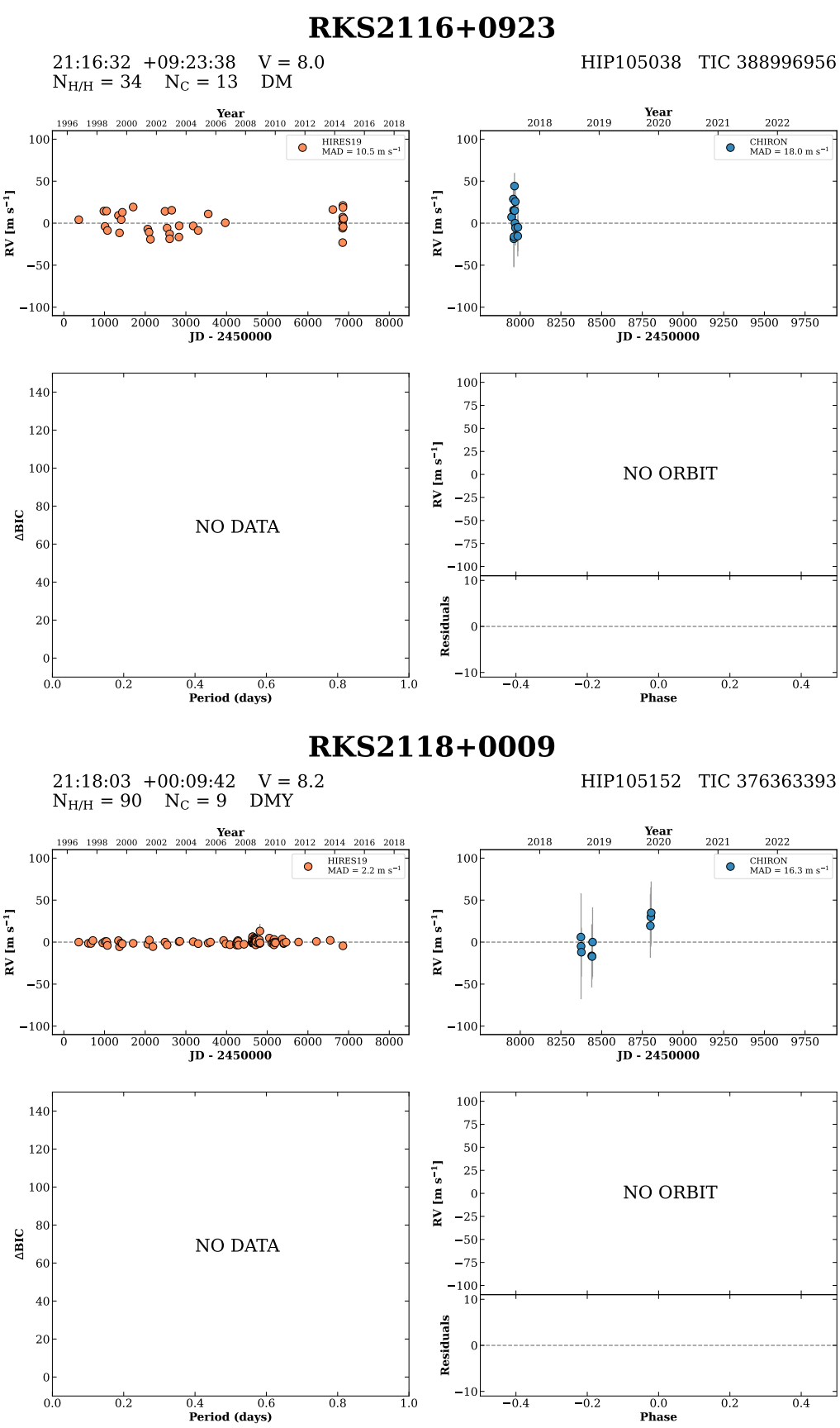

Figure 356 RV results for RKS2116+0923 (top) and RKS2118+0009 (bottom).

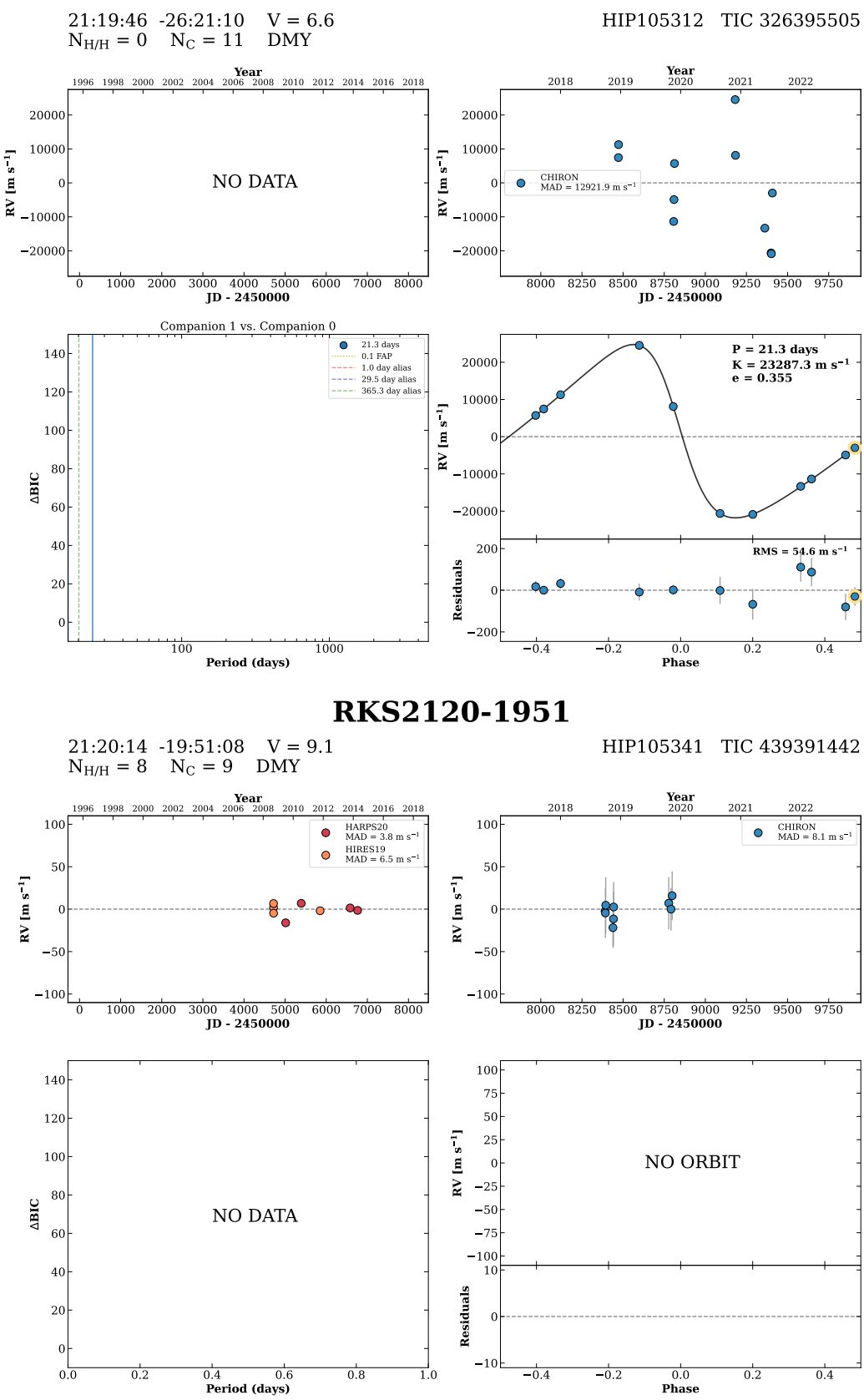

Figure 357 RV results for RKS2119-2621 (top) and RKS2120-1951 (bottom).

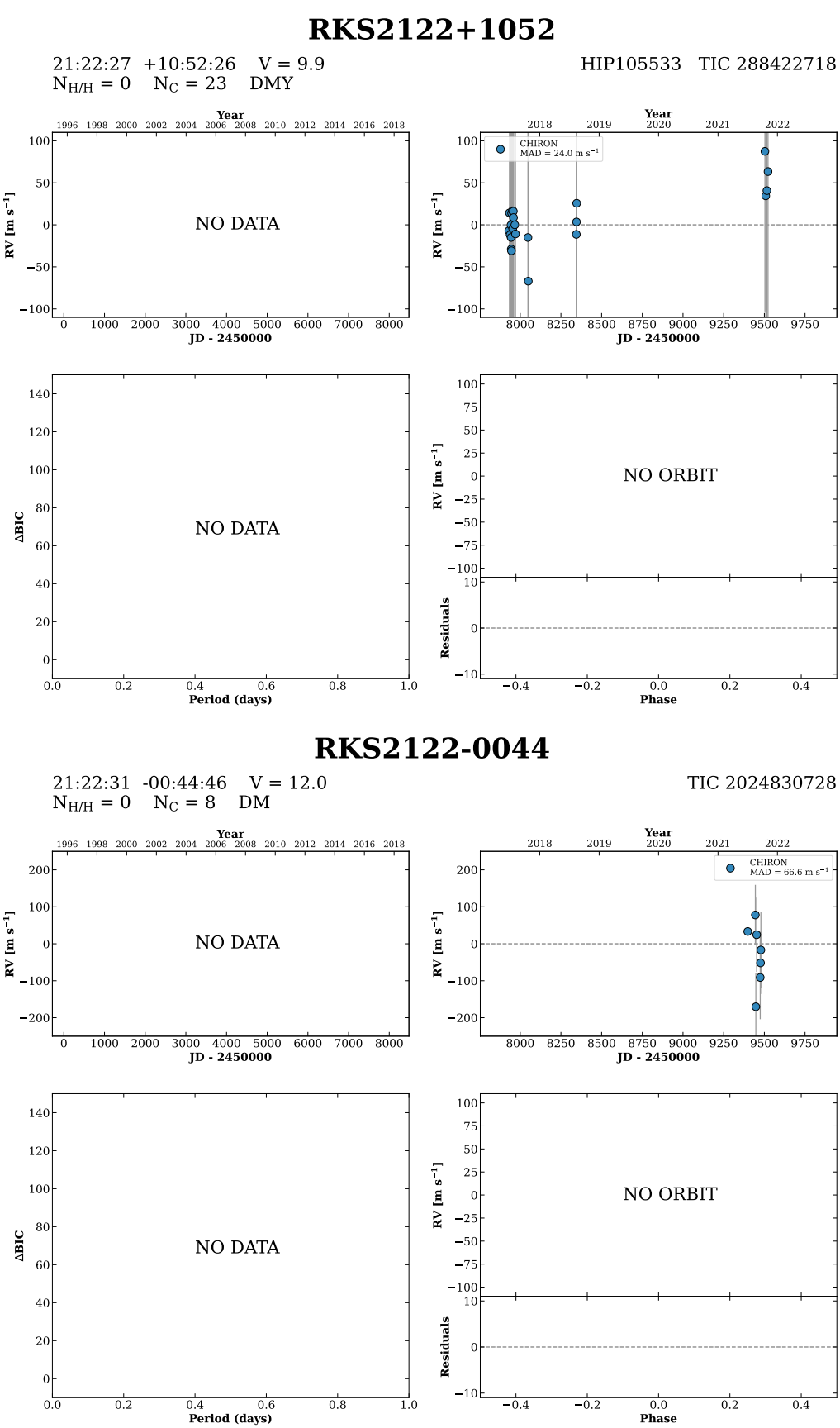

Figure 358 RV results for RKS2122+1052 (top) and RKS2122-0044 (bottom).

RKS2125+2712

21:25:29 +27:12:38 V = 8.3 HIP105791 TIC 14981454
$N_{H/H}$ = 0 N_C = 11 DMY

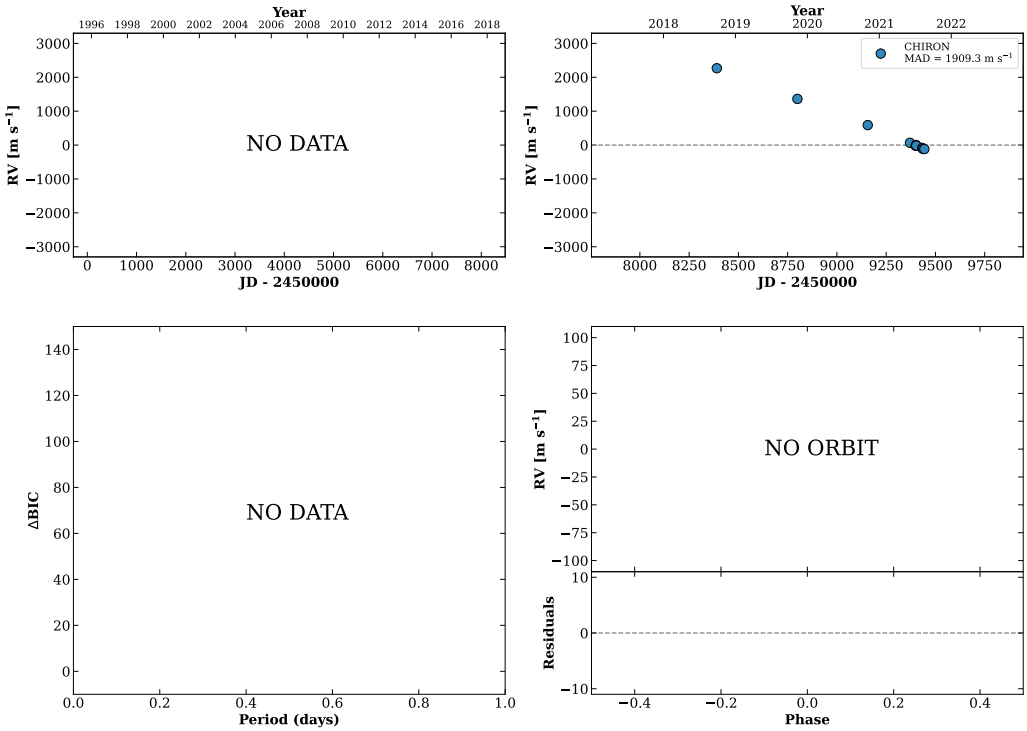

RKS2126+0344

21:26:42 +03:44:14 V = 10.5 HIP105885 TIC 352621507
$N_{H/H}$ = 0 N_C = 8 DM

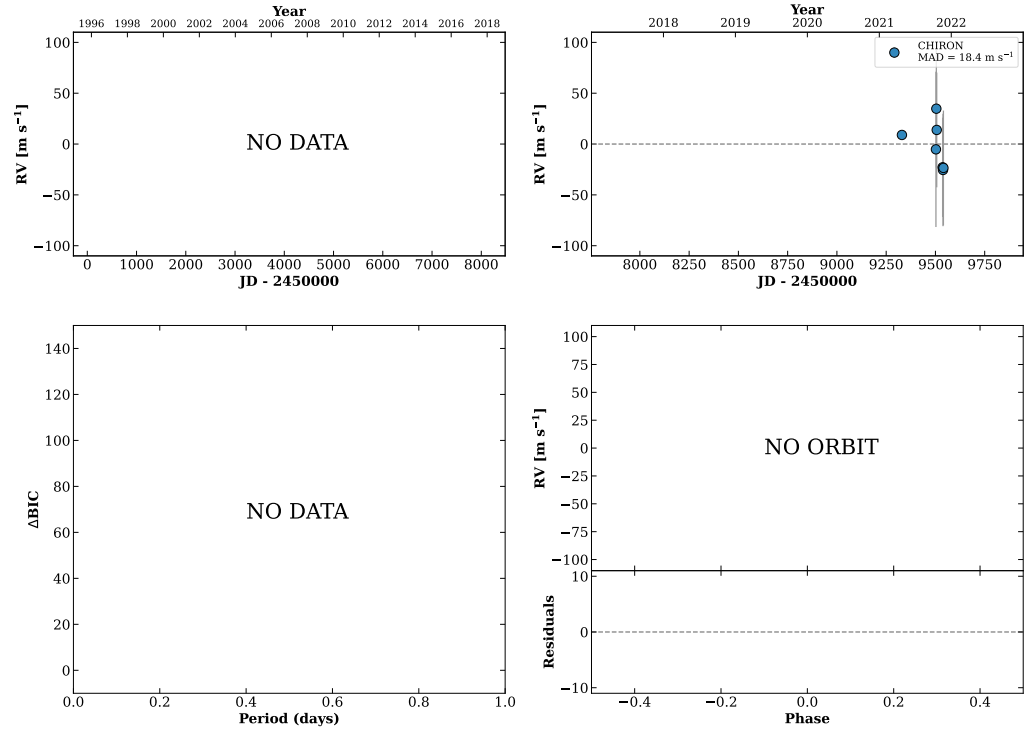

Figure 359 RV results for RKS2125+2712 (top) and RKS2126+0344 (bottom).

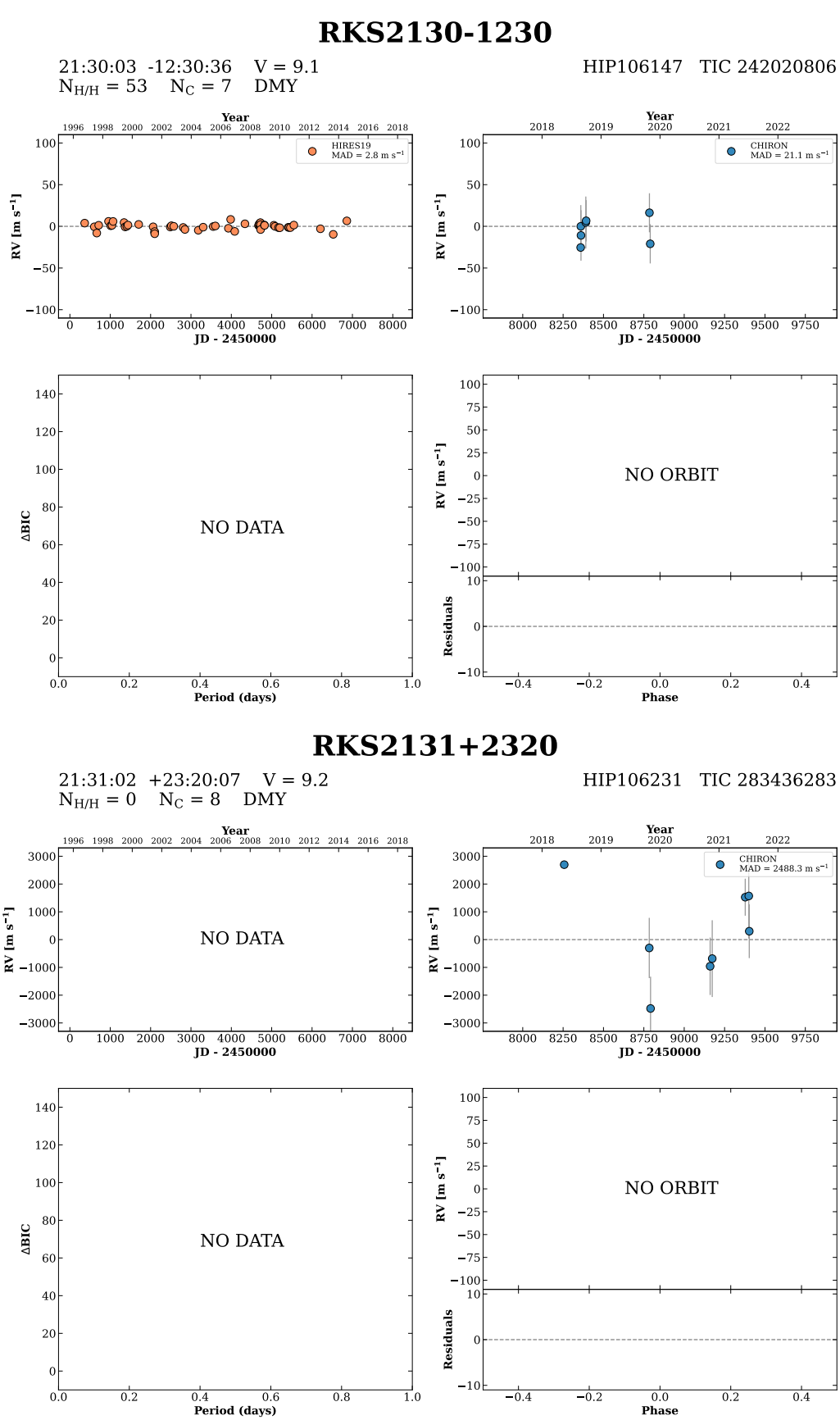

Figure 360 RV results for RKS2130-1230 (top) and RKS2131+2320 (bottom).

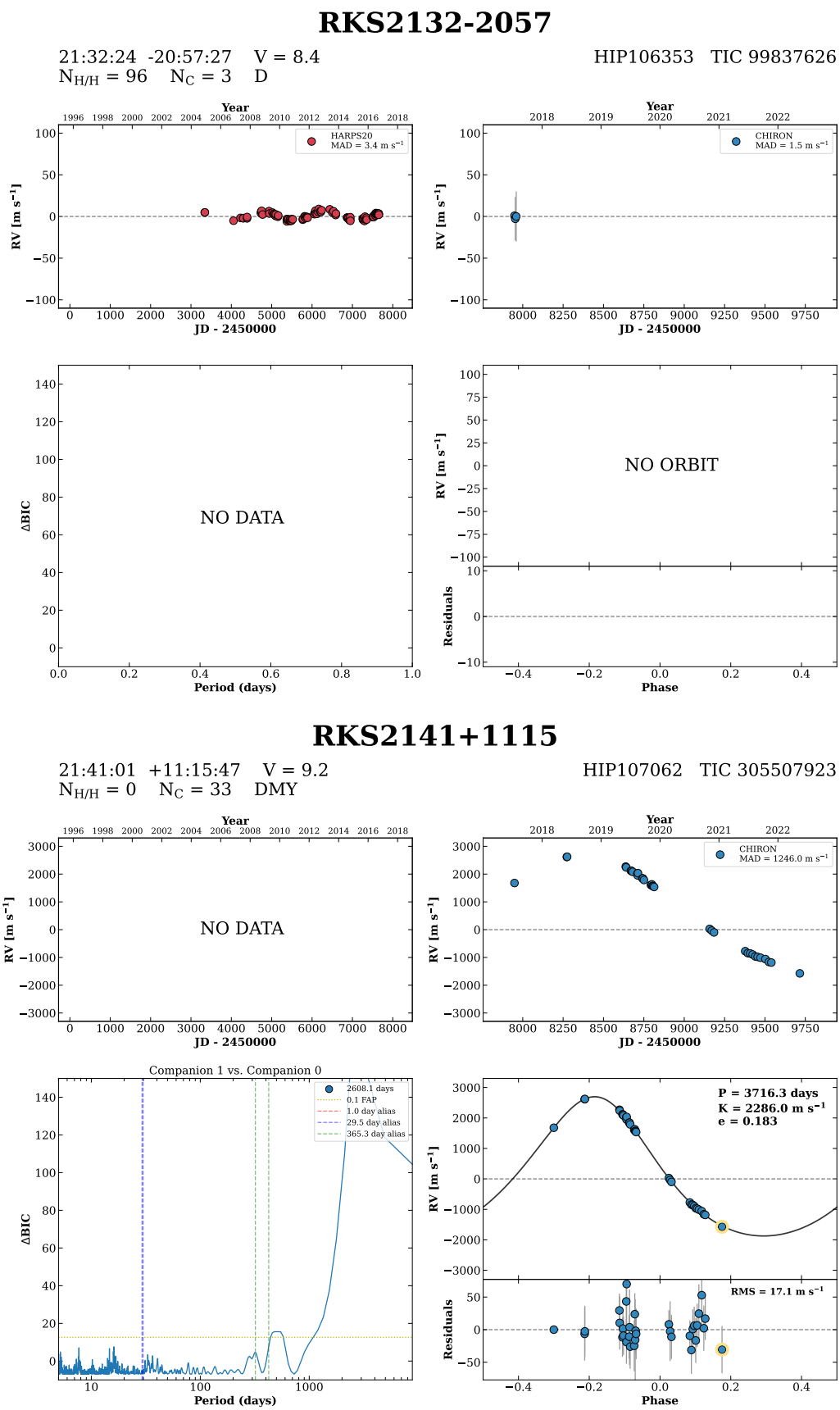

Figure 361 RV results for RKS2132-2057 (top) and RKS2141+1115 (bottom).

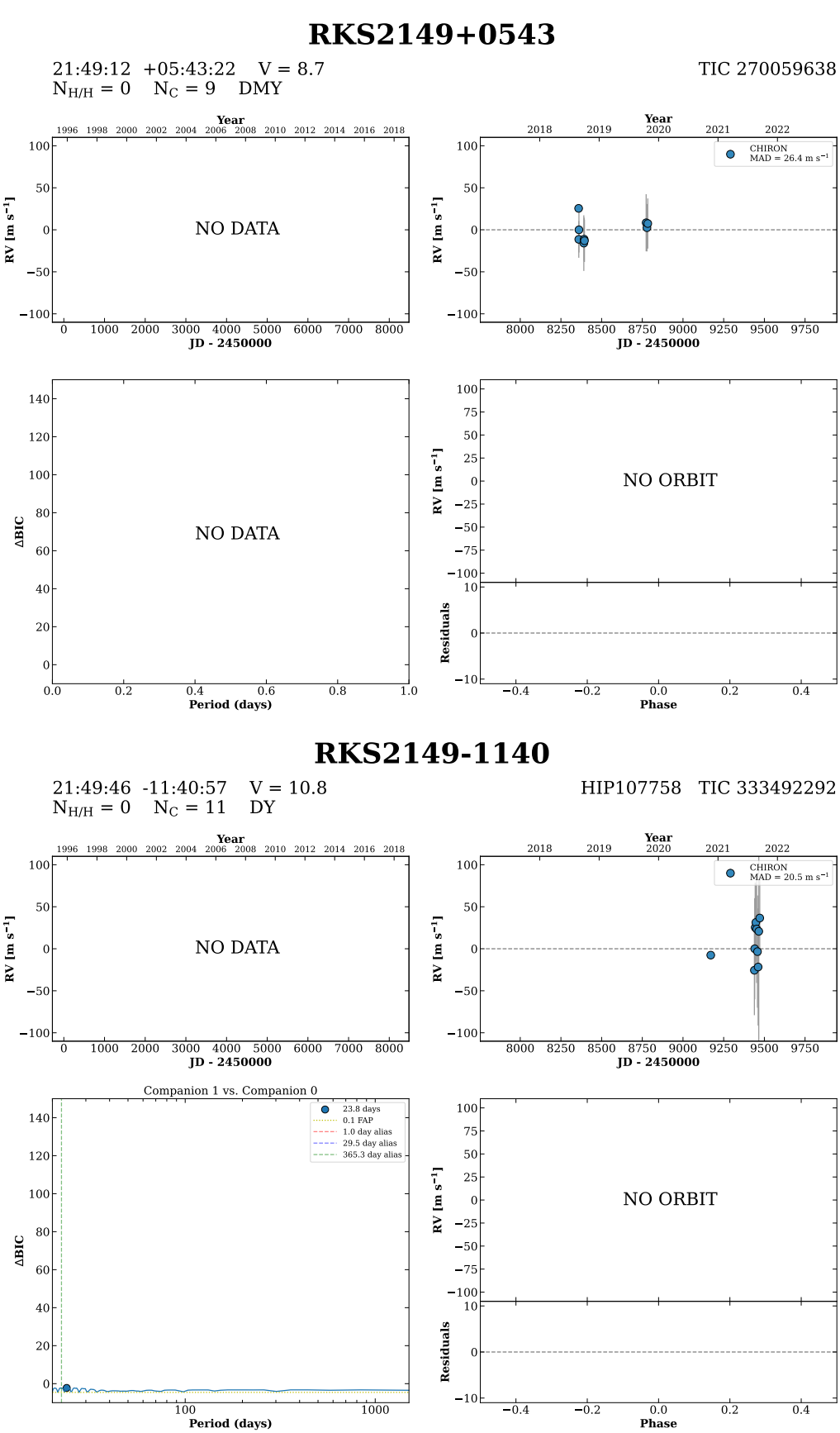

Figure 362 RV results for RKS2149+0543 (top) and RKS2149-1140 (bottom).

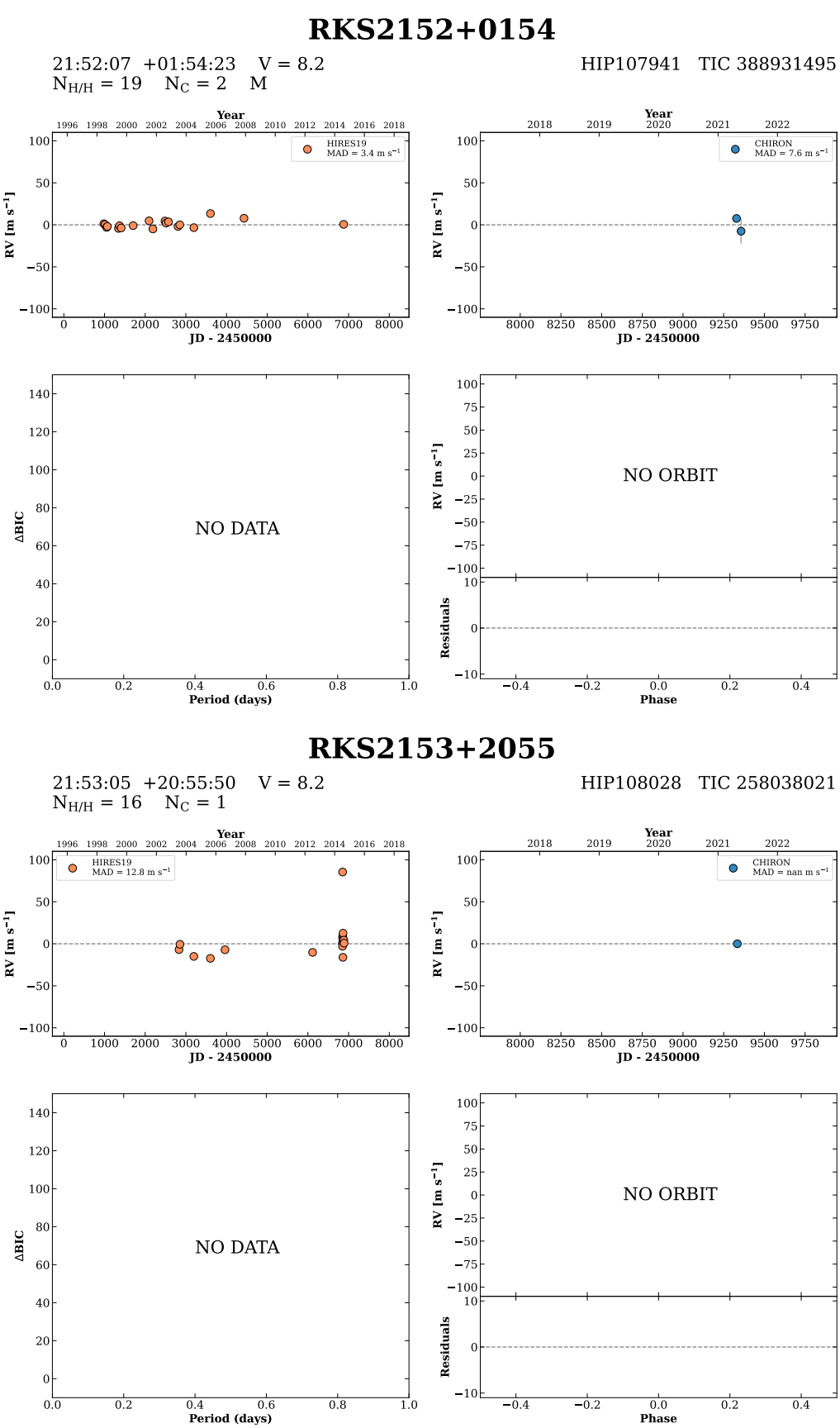

Figure 363 RV results for RKS2152+0154 (top) and RKS2153+2055 (bottom).

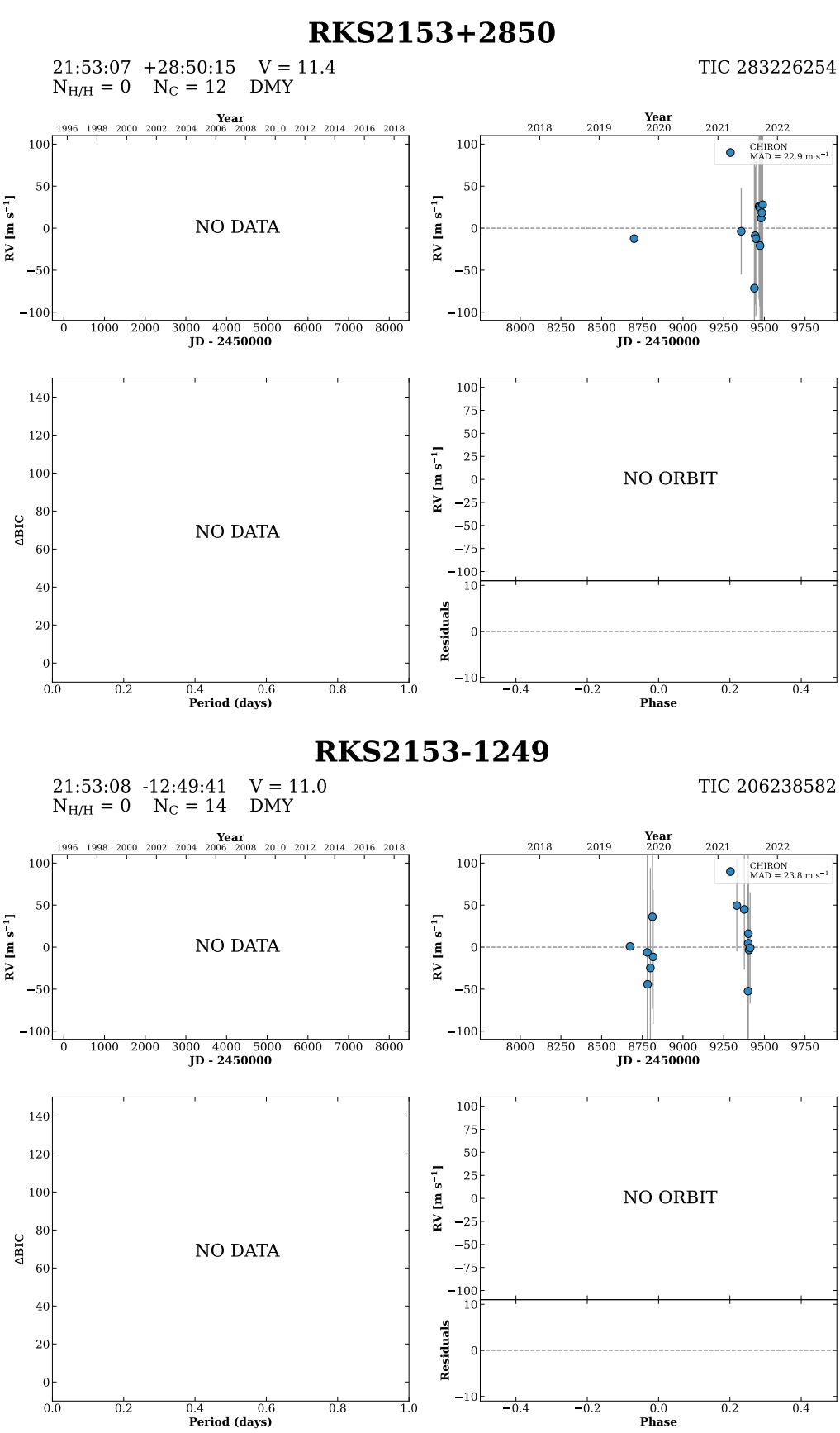

Figure 364 RV results for RKS2153+2850 (top) and RKS2153-1249 (bottom).

RKS2155-2942

21:55:42 -29:42:22 V = 8.5 HIP108241 TIC 53952985
$N_{H/H}$ = 29 N_C = 1

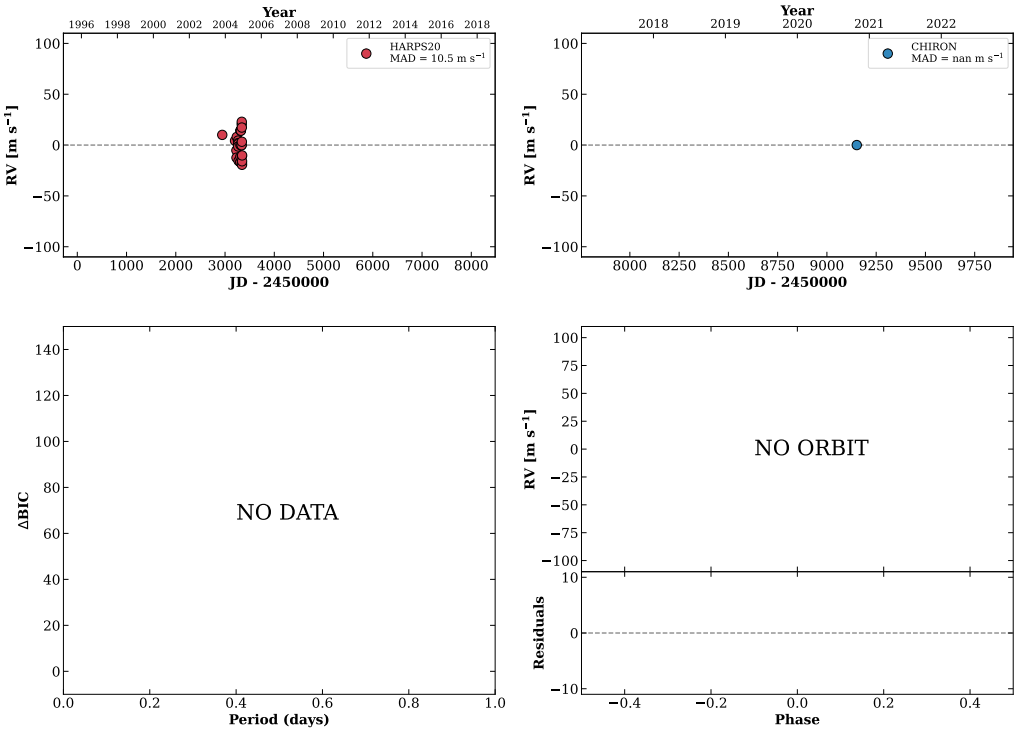

RKS2210+2247

22:10:31 +22:47:49 V = 9.2 HIP109461 TIC 258781508
$N_{H/H}$ = 0 N_C = 1

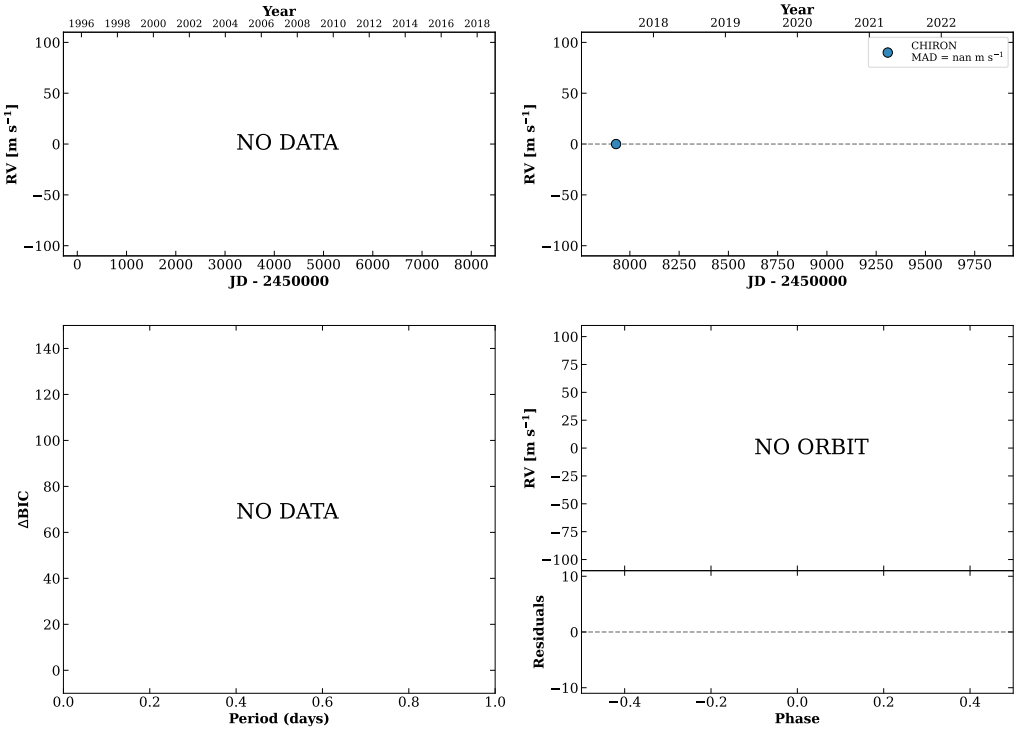

Figure 365 RV results for RKS2155-2942 (top) and RKS2210+2247 (bottom).

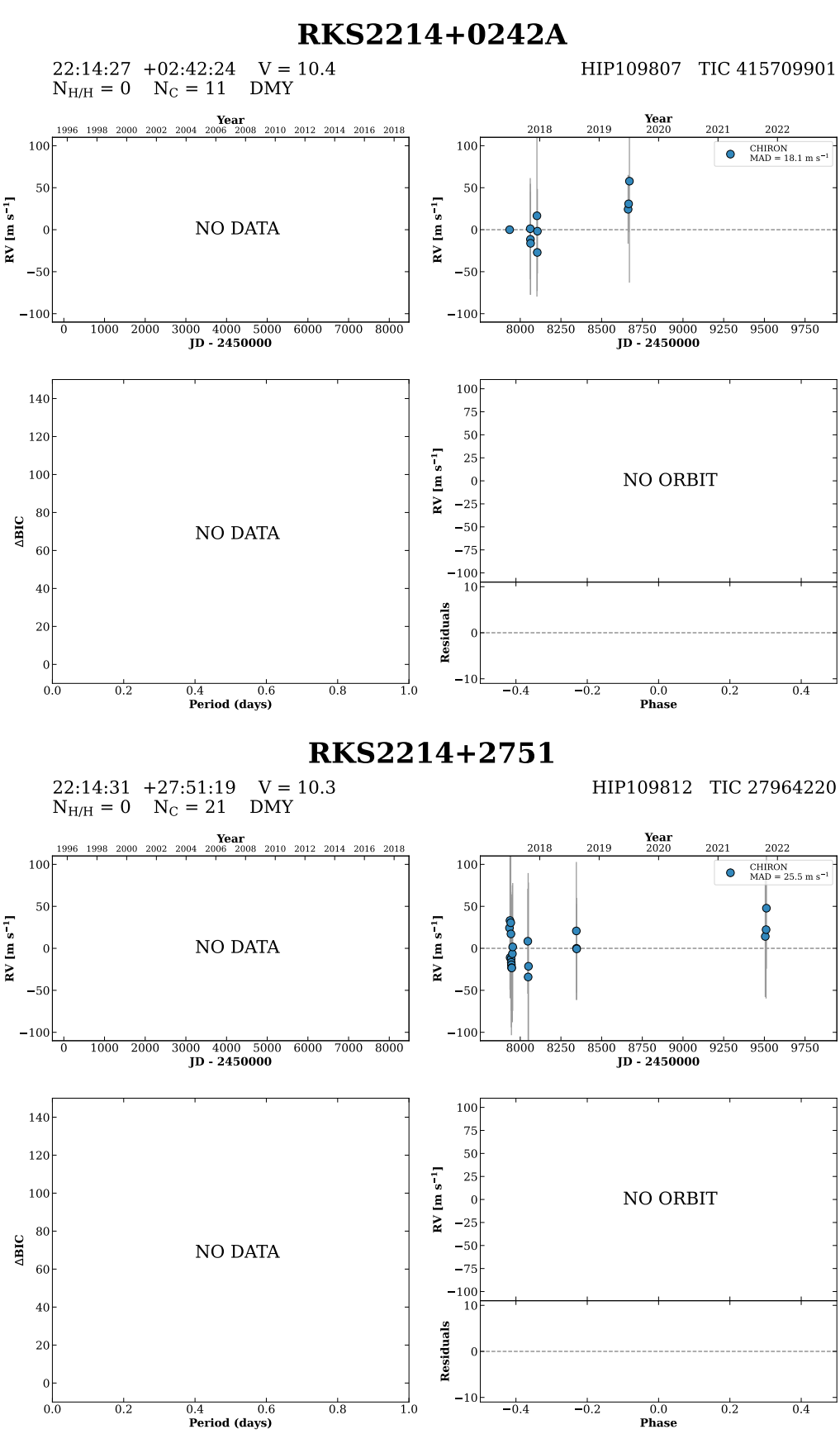

Figure 366 RV results for RKS2214+0242A (top) and RKS2214+2751 (bottom).

RKS2224+2233

22:24:46 +22:33:04 V = 8.8 HIP110640 TIC 314989124
$N_{H/H}$ = 0 N_C = 9 DMY

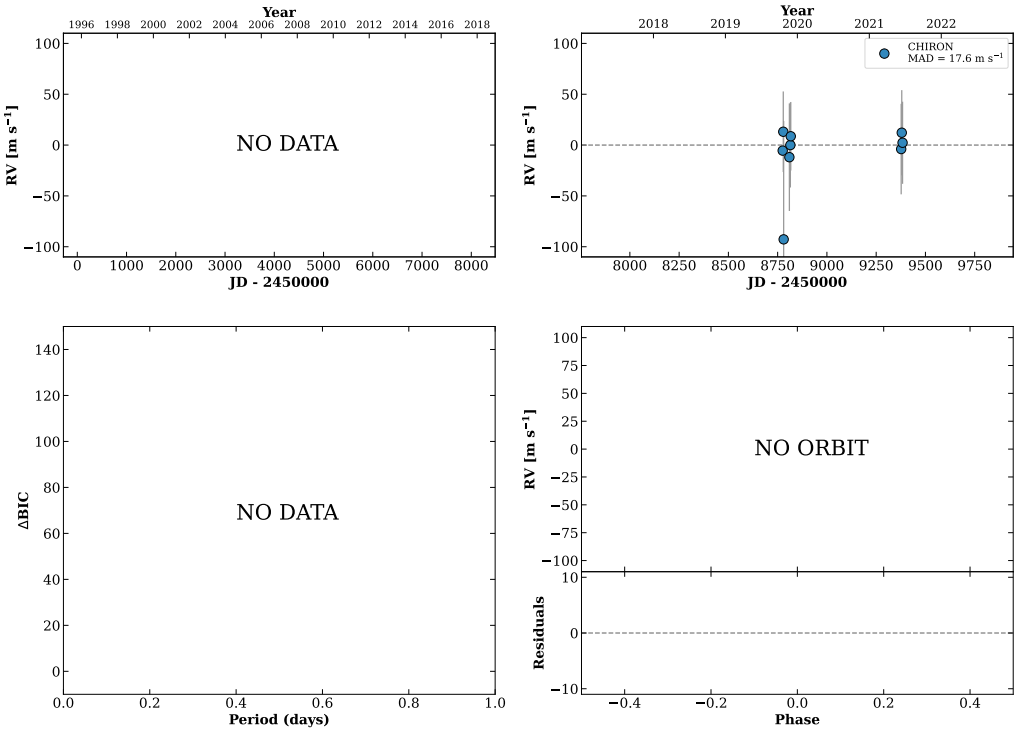

RKS2226-1911

22:26:14 -19:11:18 V = 9.2 HIP110750 TIC 69747593
$N_{H/H}$ = 13 N_C = 1

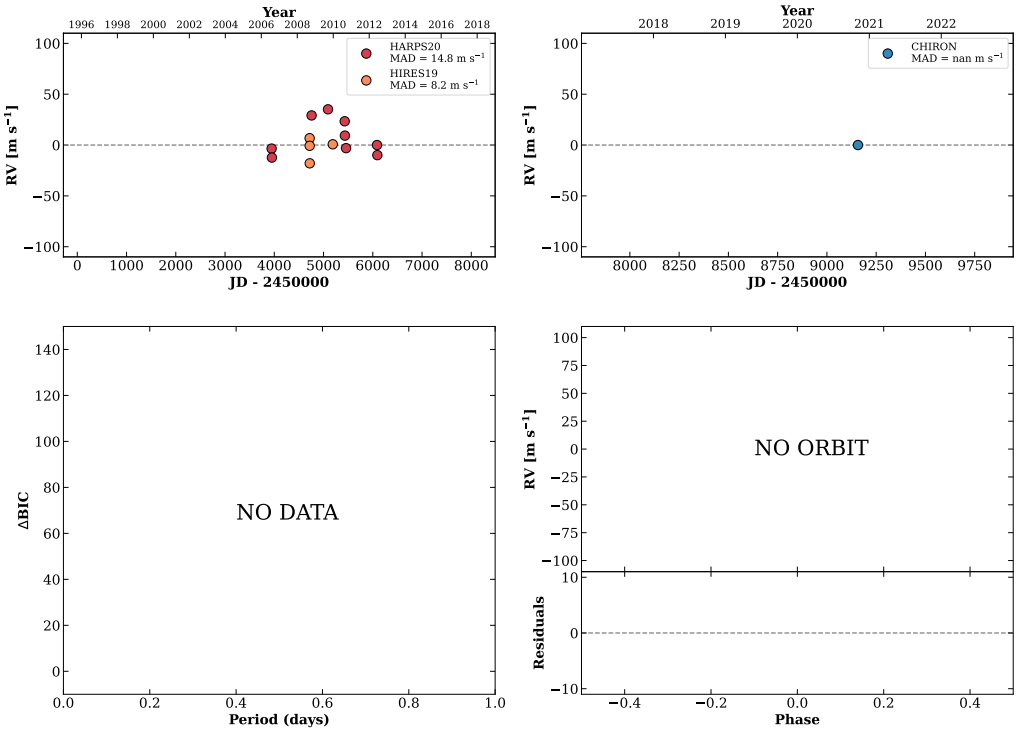

Figure 367 RV results for RKS2224+2233 (top) and RKS2226-1911 (bottom).

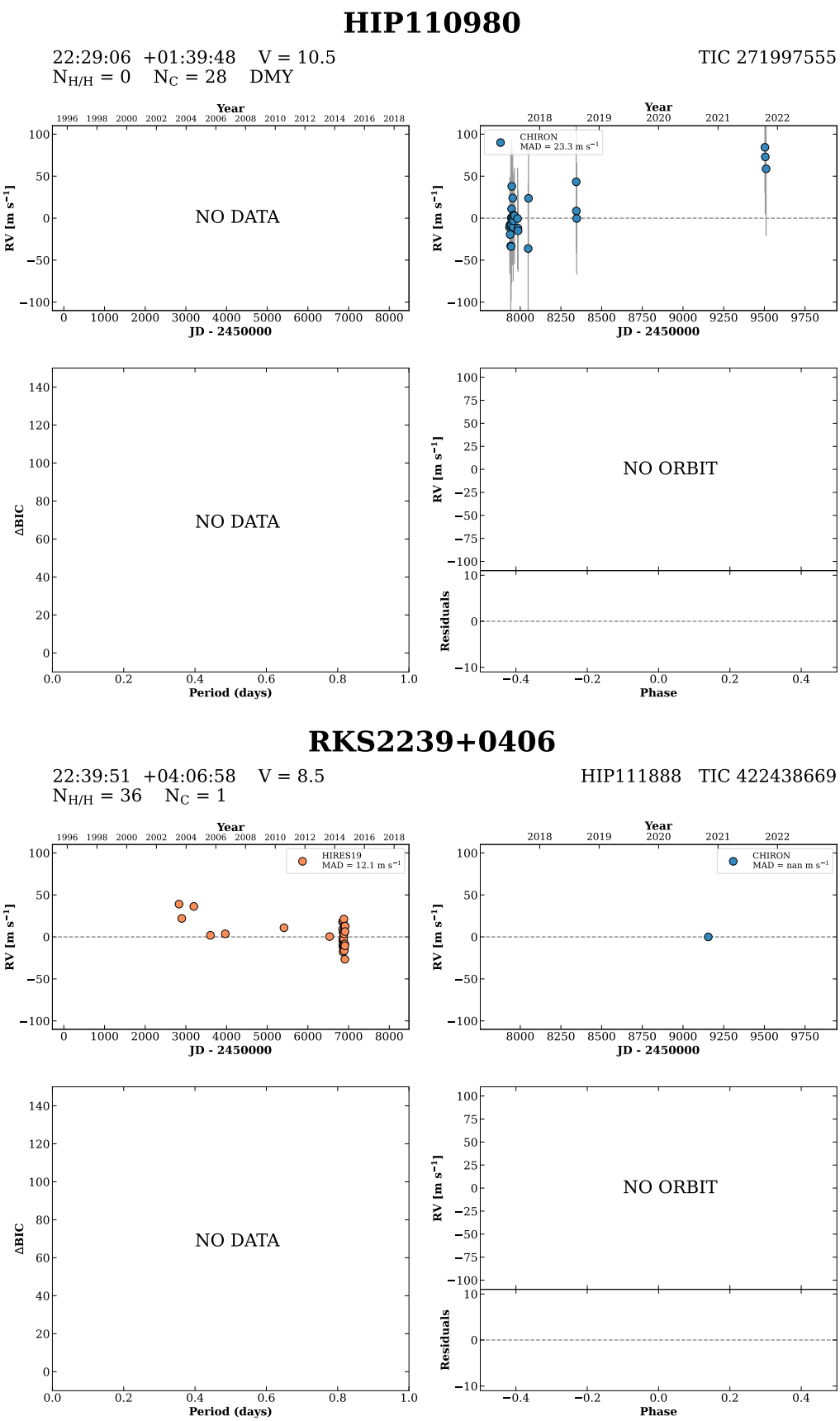

Figure 368 RV results for HIP110980 (top) and RKS2239+0406 (bottom).

RKS2240-2940

22:40:43 -29:40:28 V = 7.8 HIP111960 TIC 47295522
$N_{H/H}$ = 29 N_C = 9 DMY

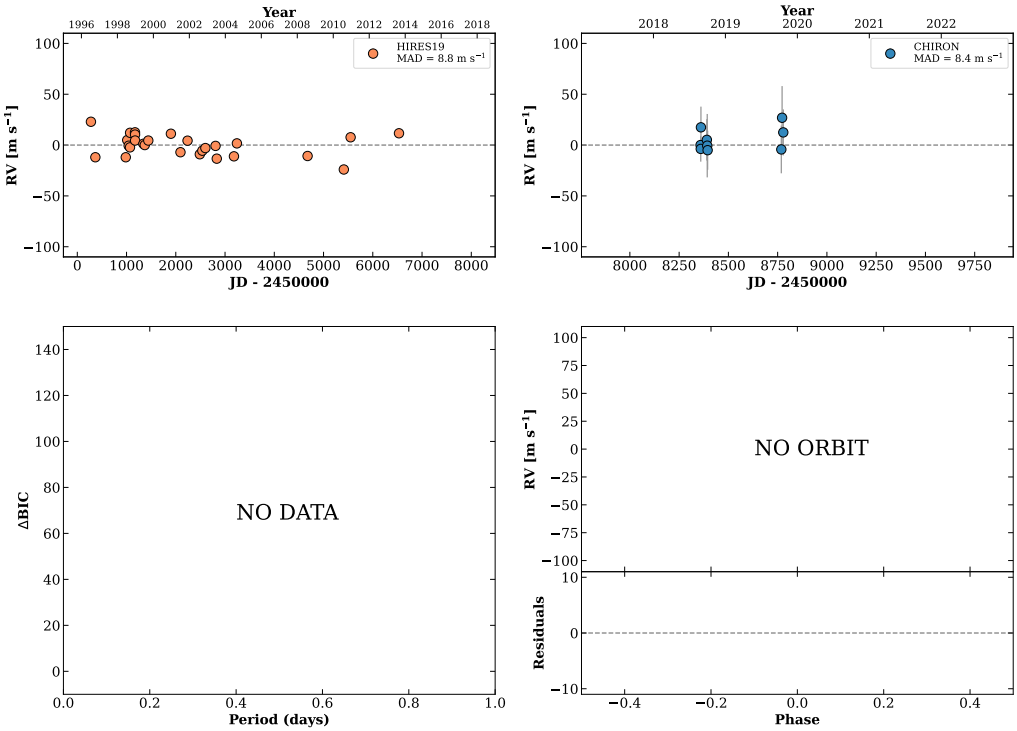

RKS2241+1849A

22:41:35 +18:49:27 V = 10.7 HIP112040 TIC 467549713
$N_{H/H}$ = 0 N_C = 2 Y

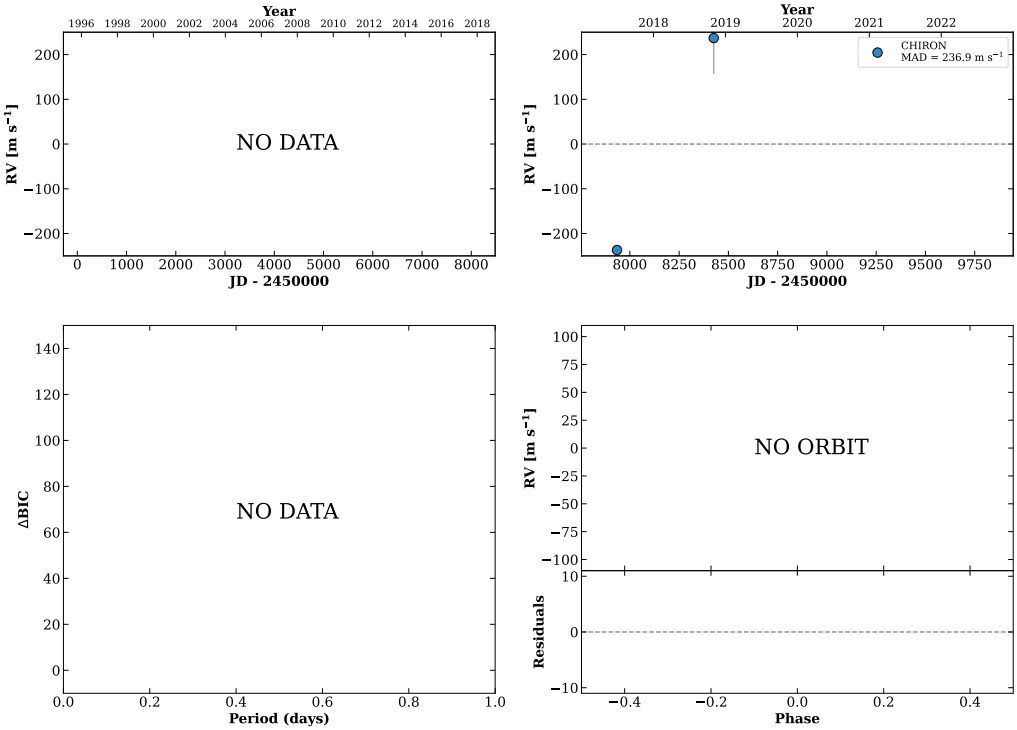

Figure 369 RV results for RKS2240-2940 (top) and RKS2241+1849A (bottom).

RKS2243-0624

22:43:21 -06:24:03 V = 8.1 HIP112190 TIC 251042502
$N_{H/H}$ = 374 N_C = 1

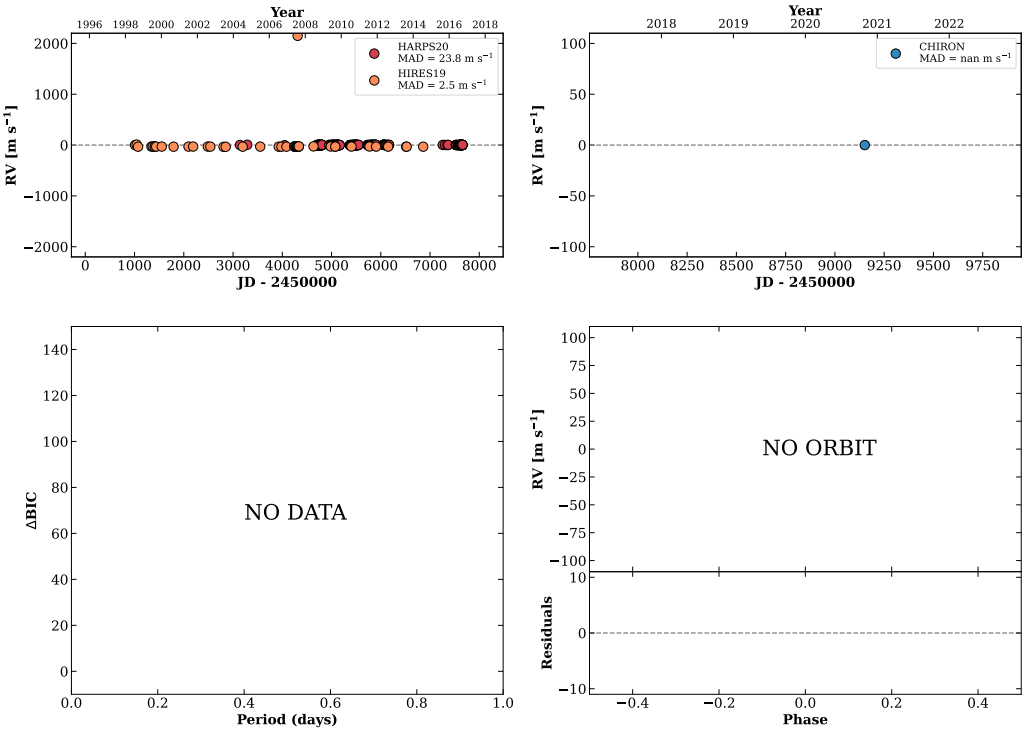

RKS2247+1823

22:47:14 +18:23:04 V = 9.0 HIP112496 TIC 434202601
$N_{H/H}$ = 2 N_C = 10 DMY

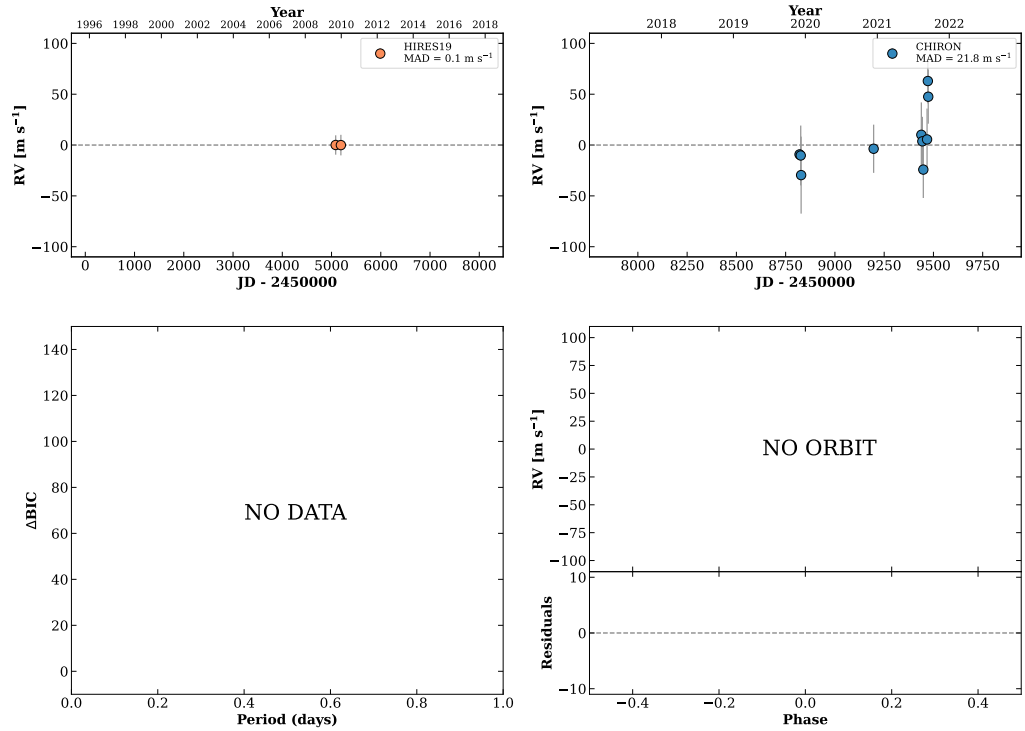

Figure 370 RV results for RKS2243-0624 (top) and RKS2247+1823 (bottom).

RKS2248+2443

22:48:36 +24:43:27 V = 10.9 HIP112610 TIC 44087301
$N_{H/H}$ = 0 N_C = 10 DY

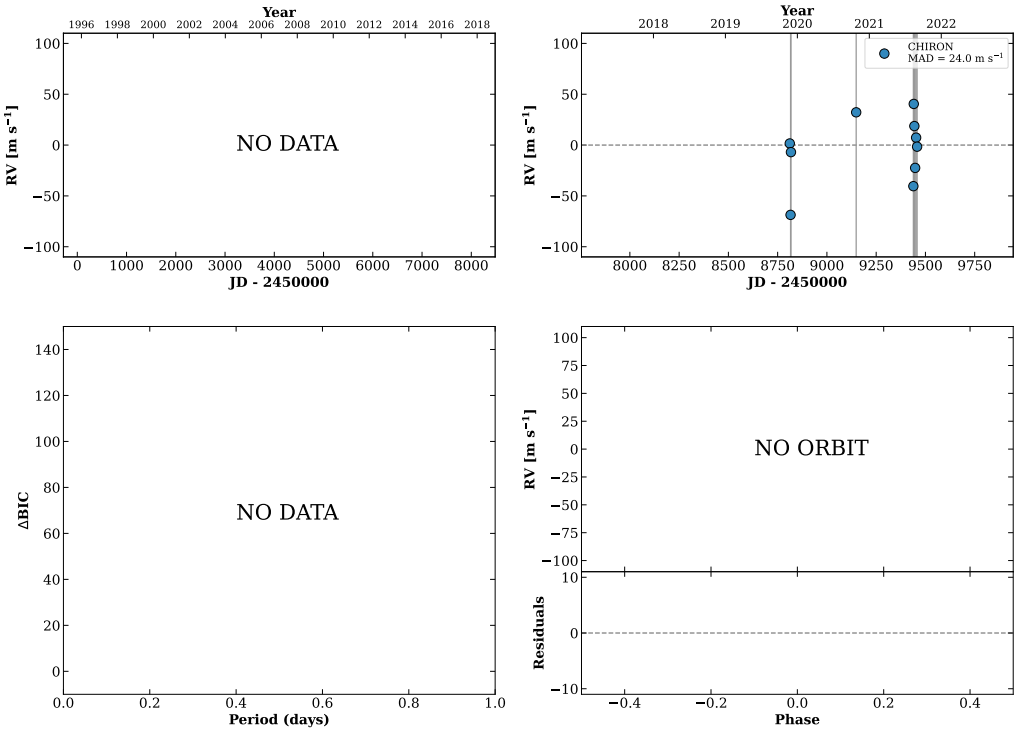

RKS2251+1358

22:51:26 +13:58:12 V = 8.3 HIP112870 TIC 60781630
$N_{H/H}$ = 260 N_C = 1

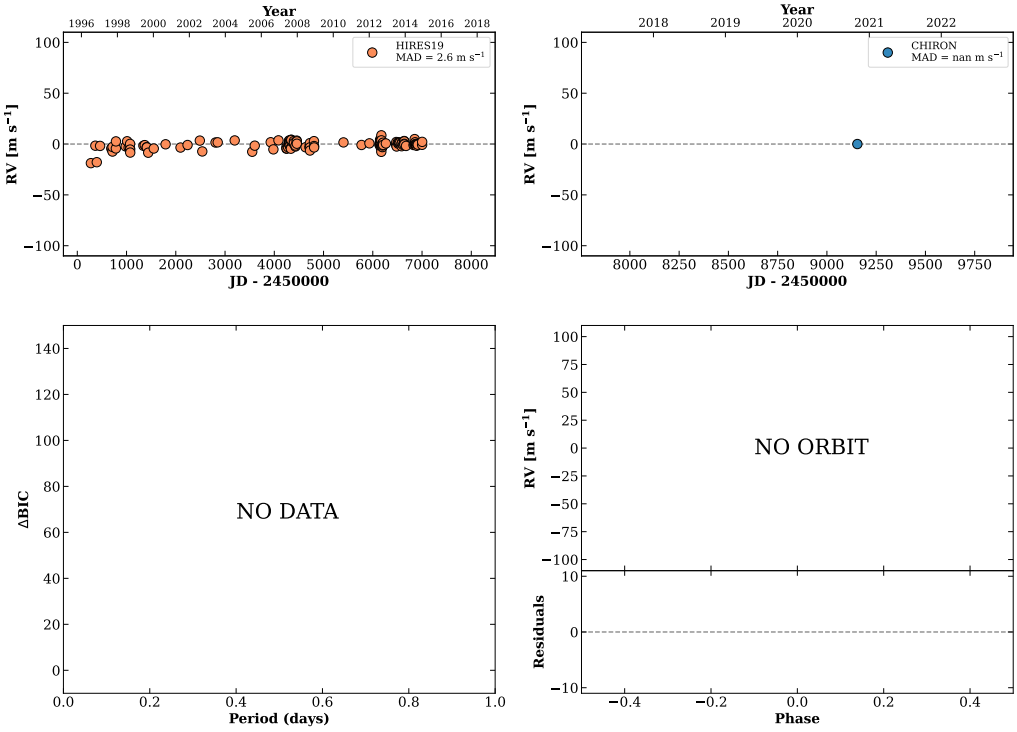

Figure 371 RV results for RKS2248+2443 (top) and RKS2251+1358 (bottom).

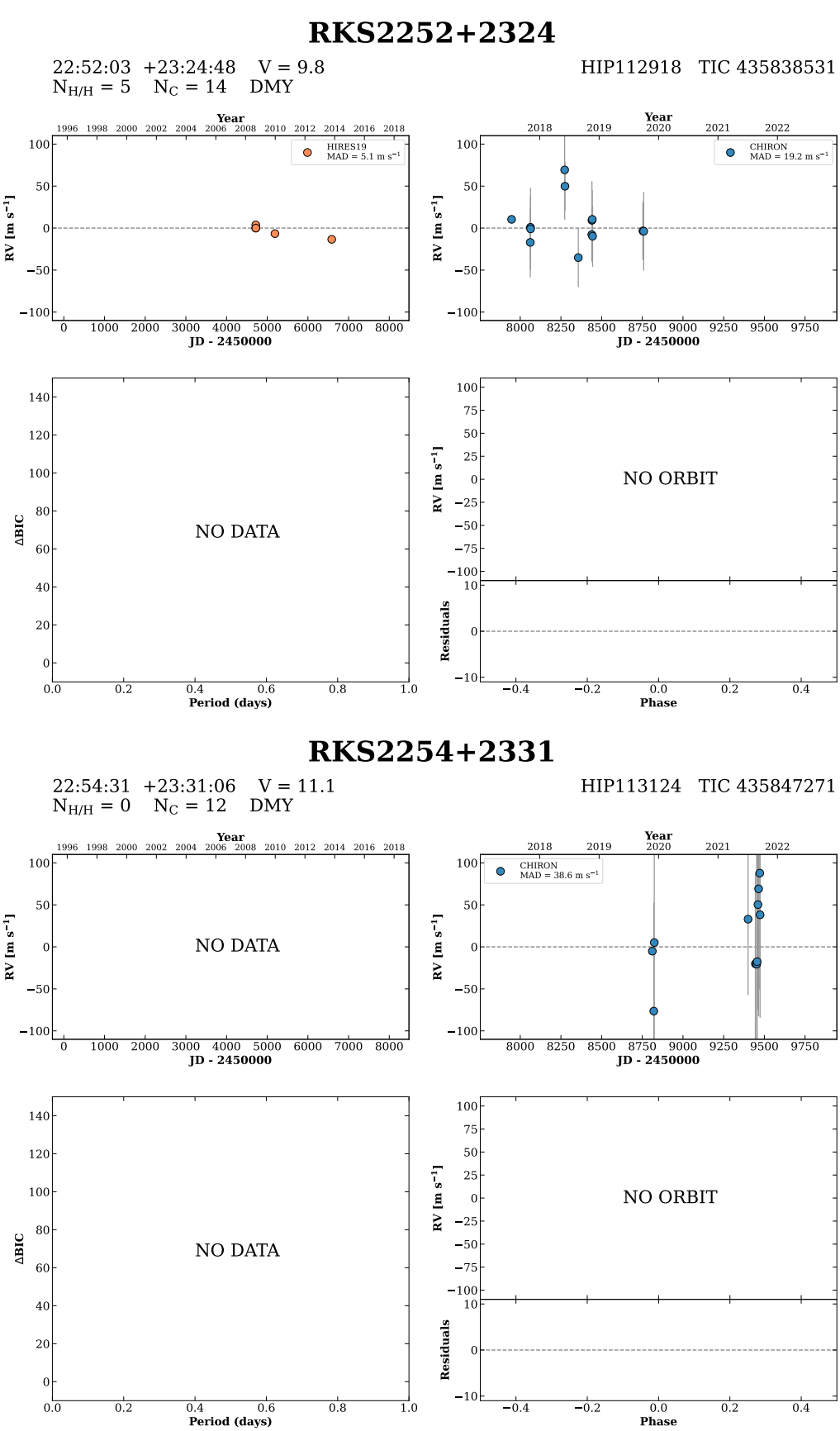

Figure 372 RV results for RKS2252+2324 (top) and RKS2254+2331 (bottom).

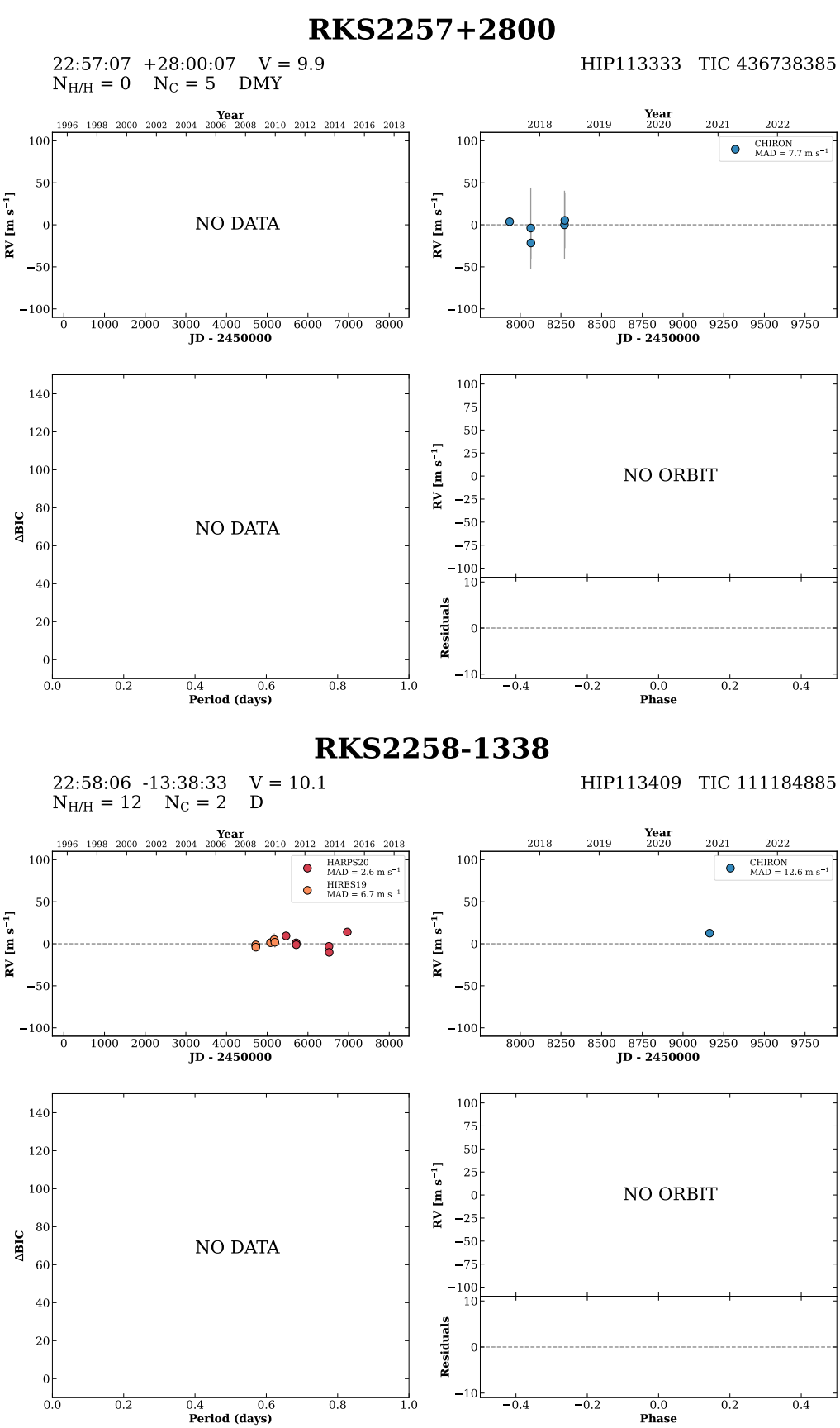

Figure 373 RV results for RKS2257+2800 (top) and RKS2258-1338 (bottom).

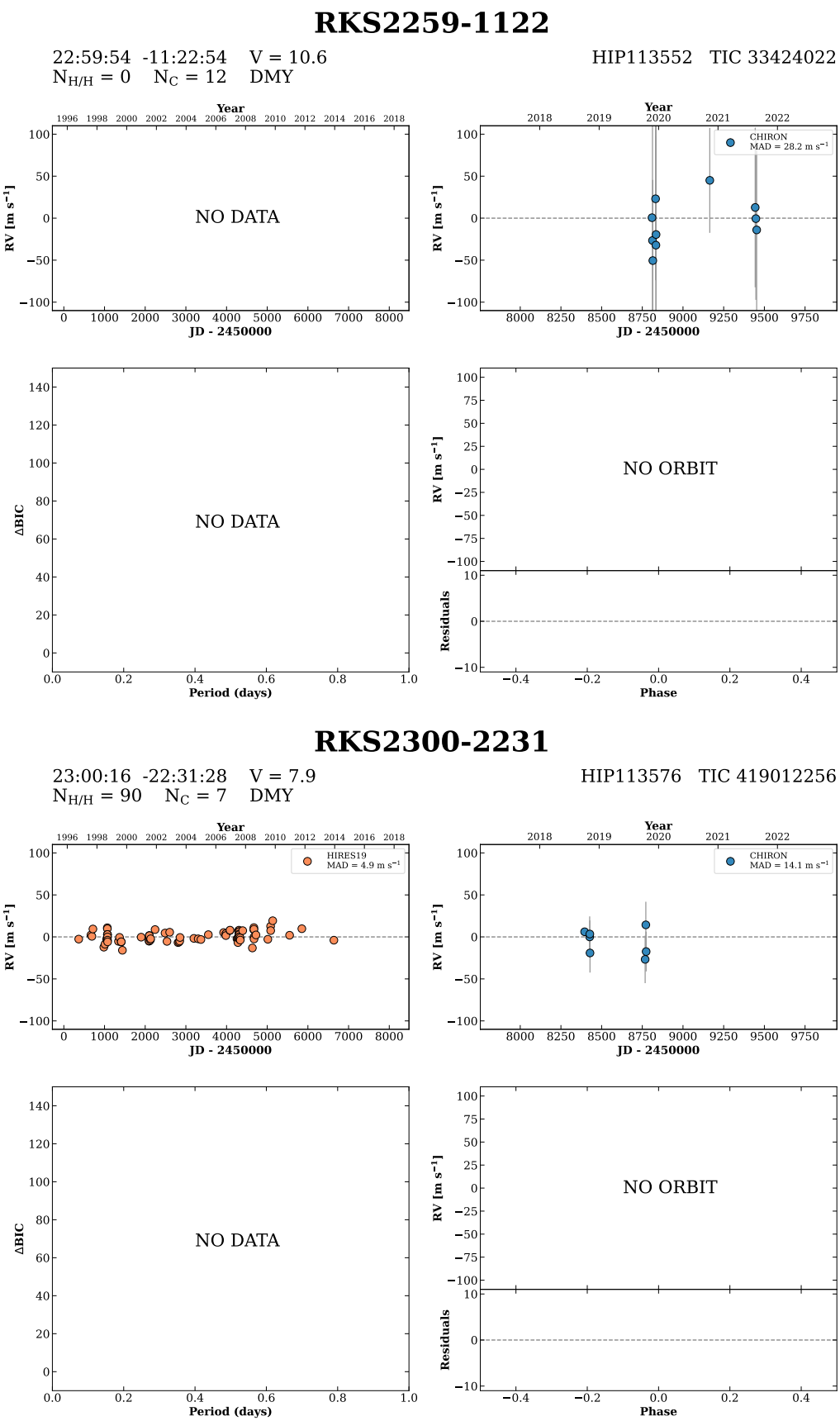

Figure 374 RV results for RKS2259-1122 (top) and RKS2300-2231 (bottom).

RKS2300-2618A

23:00:28 -26:18:43 V = 10.1 HIP113597 TIC 270377903
$N_{H/H}$ = 0 N_C = 34 DMY

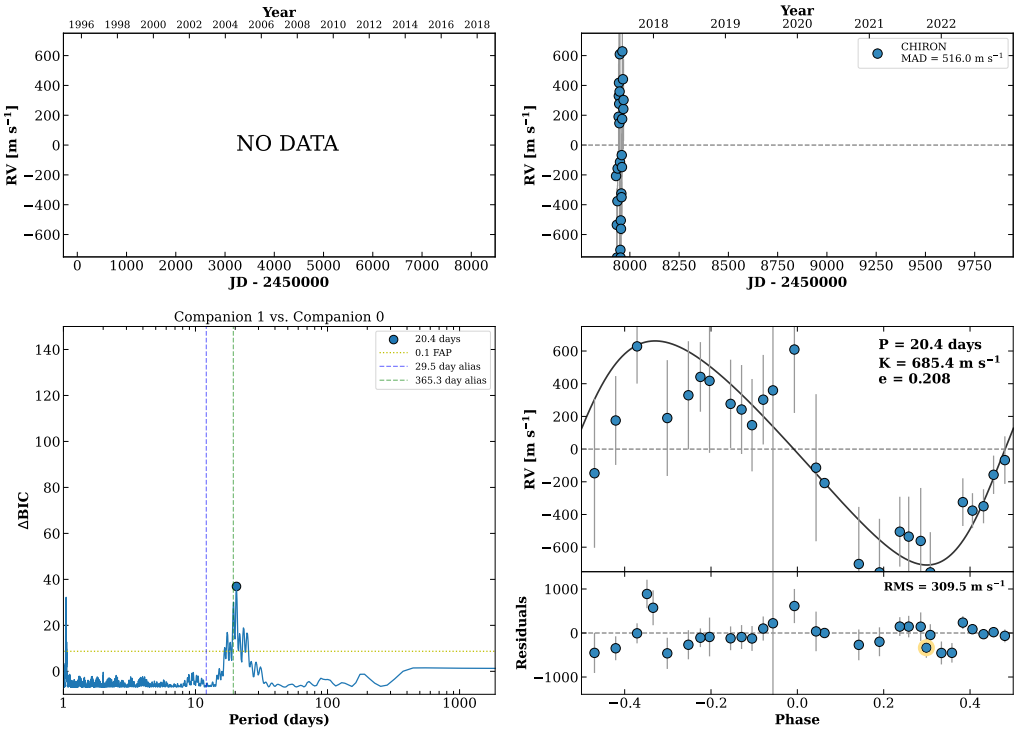

RKS2301-0350

23:01:52 -03:50:55 V = 7.5 HIP113718 TIC 278870306
$N_{H/H}$ = 0 N_C = 11 DMY

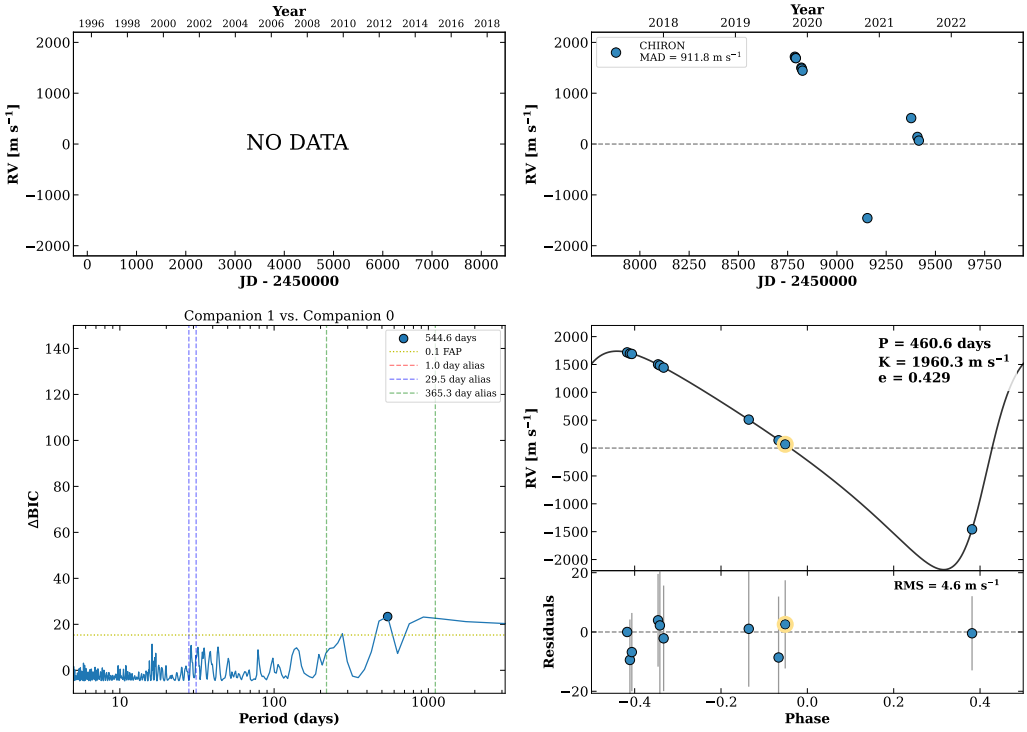

Figure 375 RV results for RKS2300-2618A (top) and RKS2301-0350 (bottom).

RKS2307-2309

23:07:07 -23:09:34 V = 9.6 HIP114156 TIC 204325307
$N_{H/H}$ = 4 N_C = 10 DY

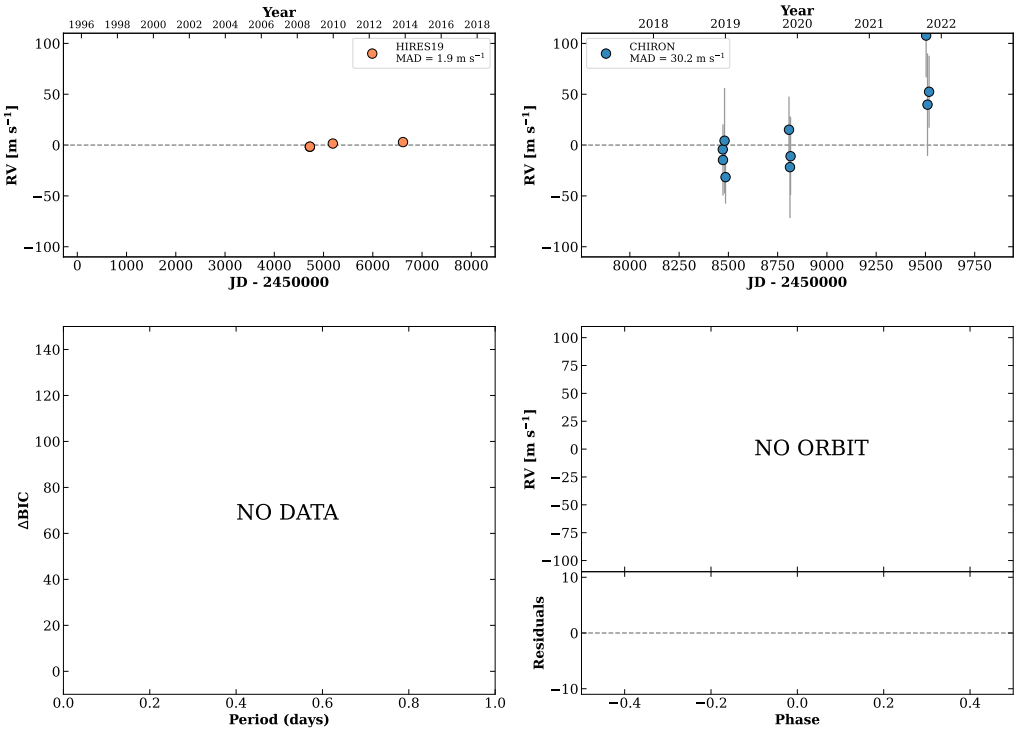

RKS2308+0633

23:08:52 +06:33:40 V = 10.9 HIP114294 TIC 402891878
$N_{H/H}$ = 0 N_C = 11 DMY

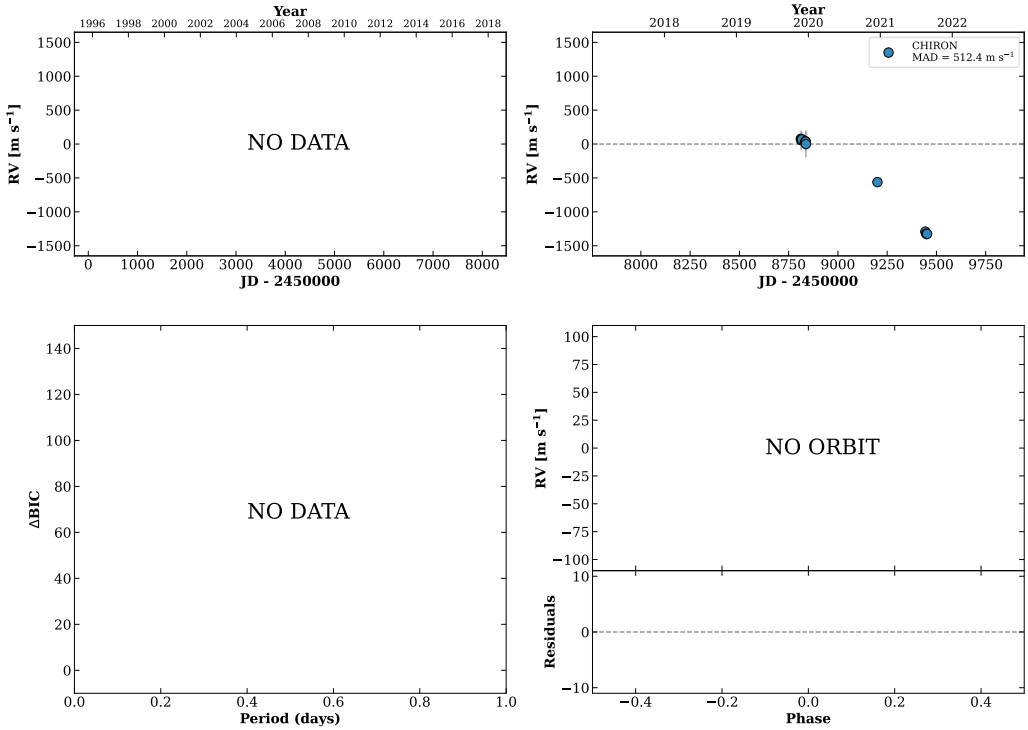

Figure 376 RV results for RKS2307-2309 (top) and RKS2308+0633 (bottom).

RKS2309-0215

23:09:11 -02:15:39 V = 8.6 HIP114322 TIC 278952345
$N_{H/H}$ = 108 N_C = 2 D

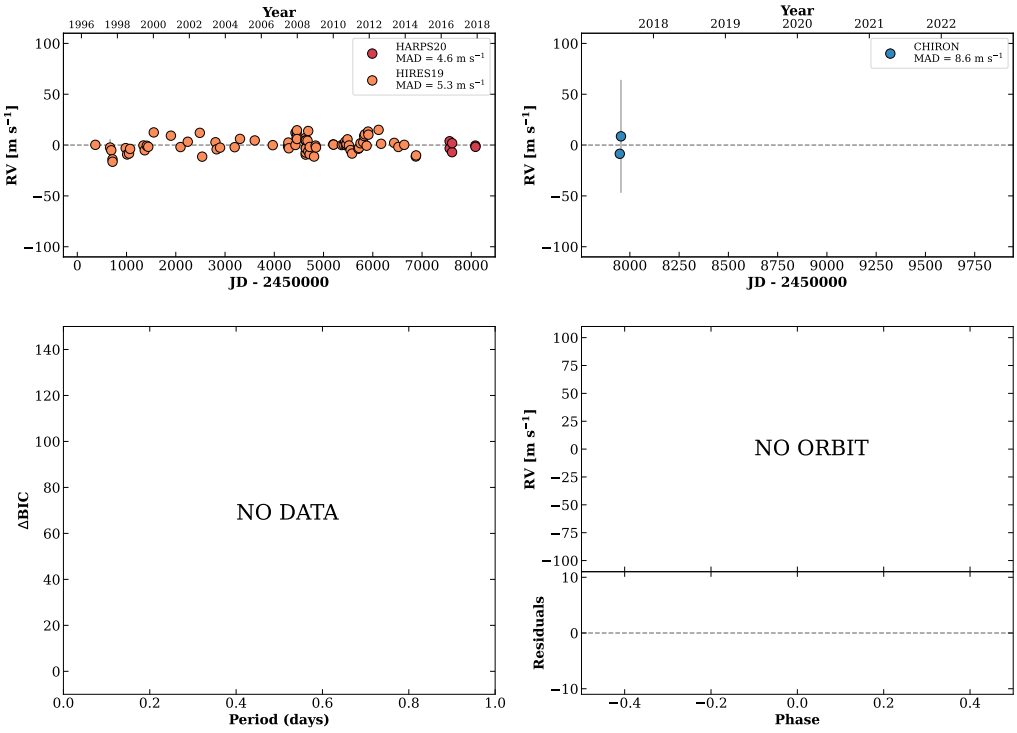

RKS2309+1425

23:09:55 +14:25:36 V = 10.3 TIC 218044102
$N_{H/H}$ = 0 N_C = 9 DMY

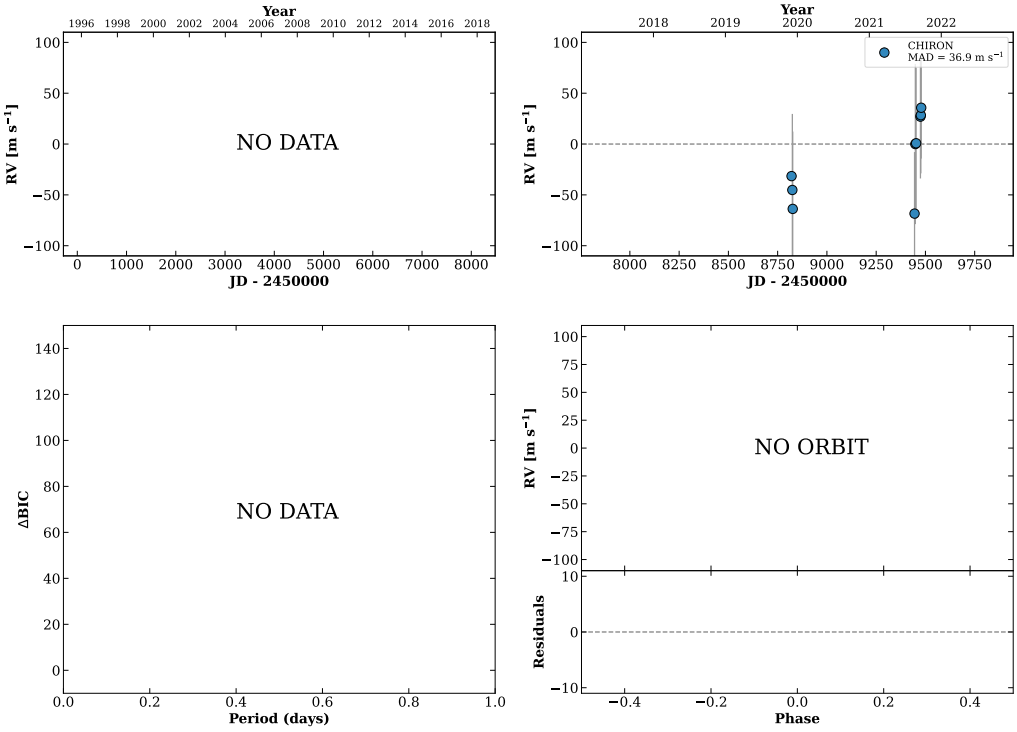

Figure 377 RV results for RKS2309-0215 (top) and RKS2309+1425 (bottom).

RKS2310-2955

23:10:49 -29:55:04 V = 8.7 HIP114455 TIC 13065840
$N_{H/H}$ = 0 N_C = 10 DMY

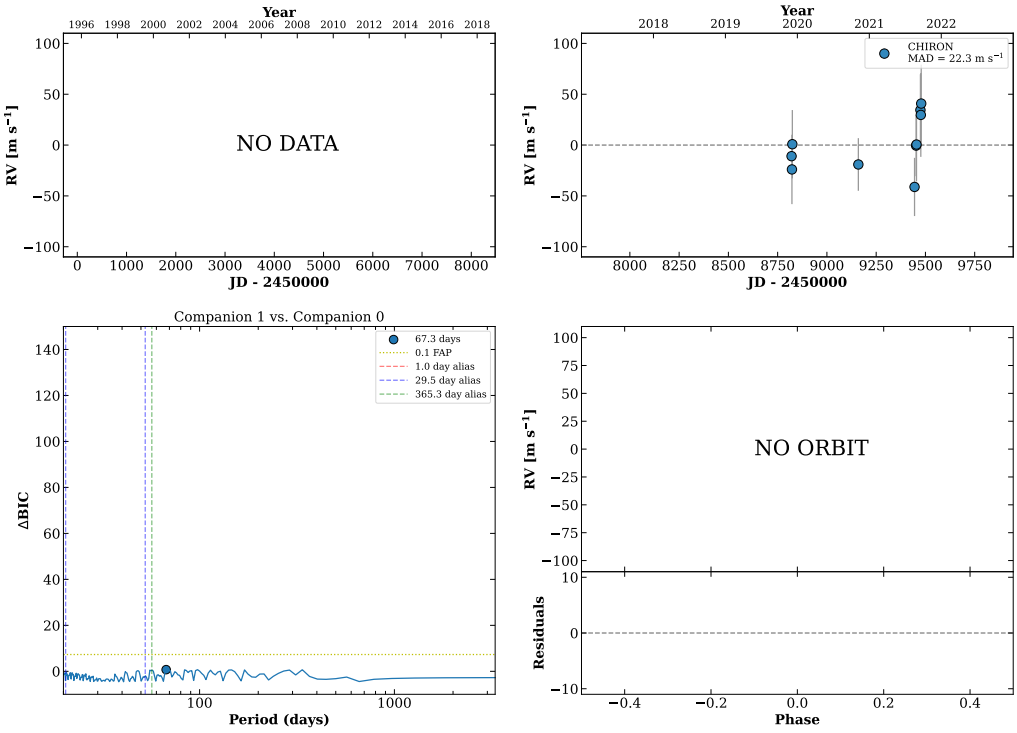

RKS2316+0541

23:16:52 +05:41:46 V = 10.5 HIP114941 TIC 262689575
$N_{H/H}$ = 0 N_C = 13 DMY

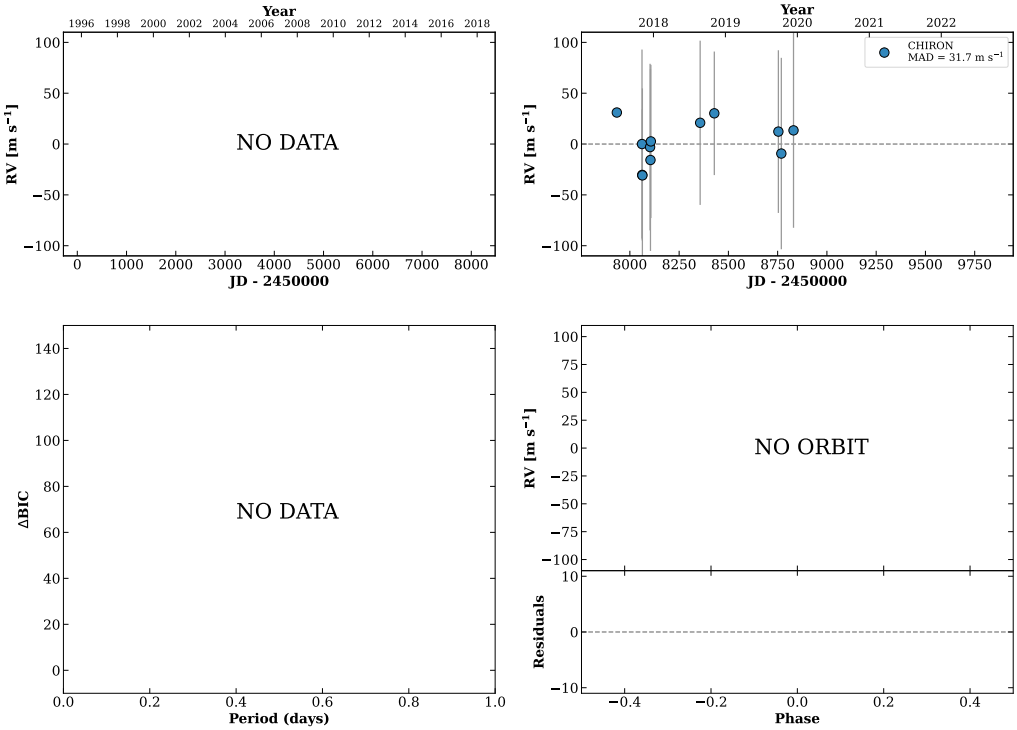

Figure 378 RV results for RKS2310-2955 (top) and RKS2316+0541 (bottom).

RKS2317-2323

23:17:00 -23:23:47 V = 10.8 HIP114954 TIC 9007748
$N_{H/H}$ = 0 N_C = 11 DMY

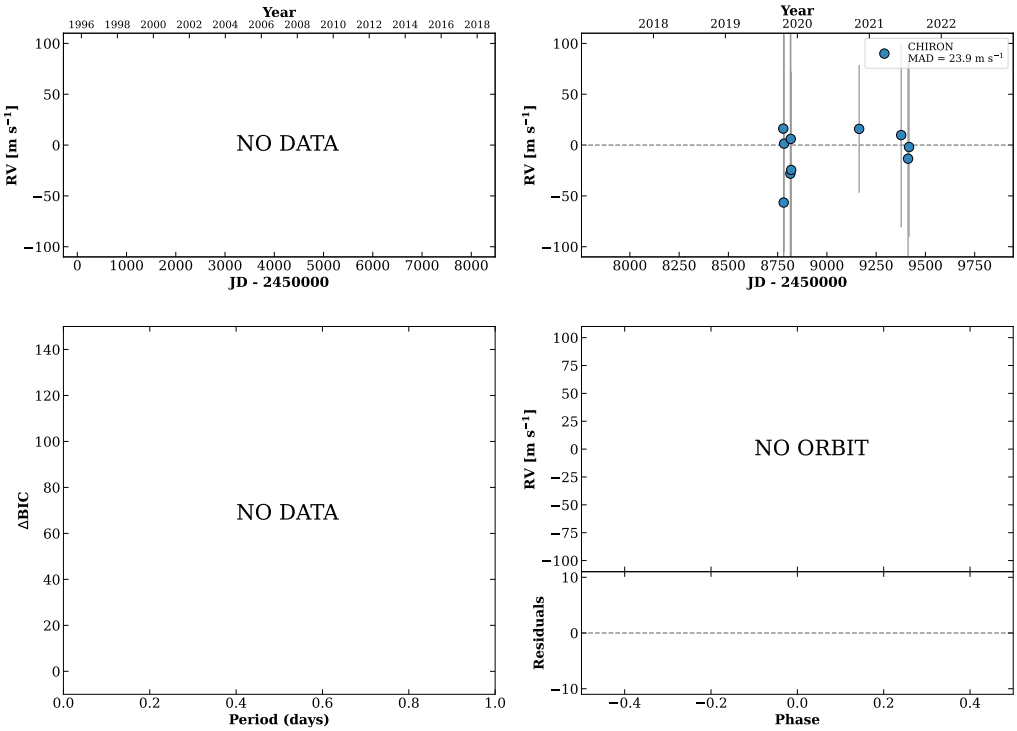

RKS2319-1327

23:19:07 -13:27:19 V = 6.9 HIP115125 TIC 214664575
$N_{H/H}$ = 68 N_C = 1

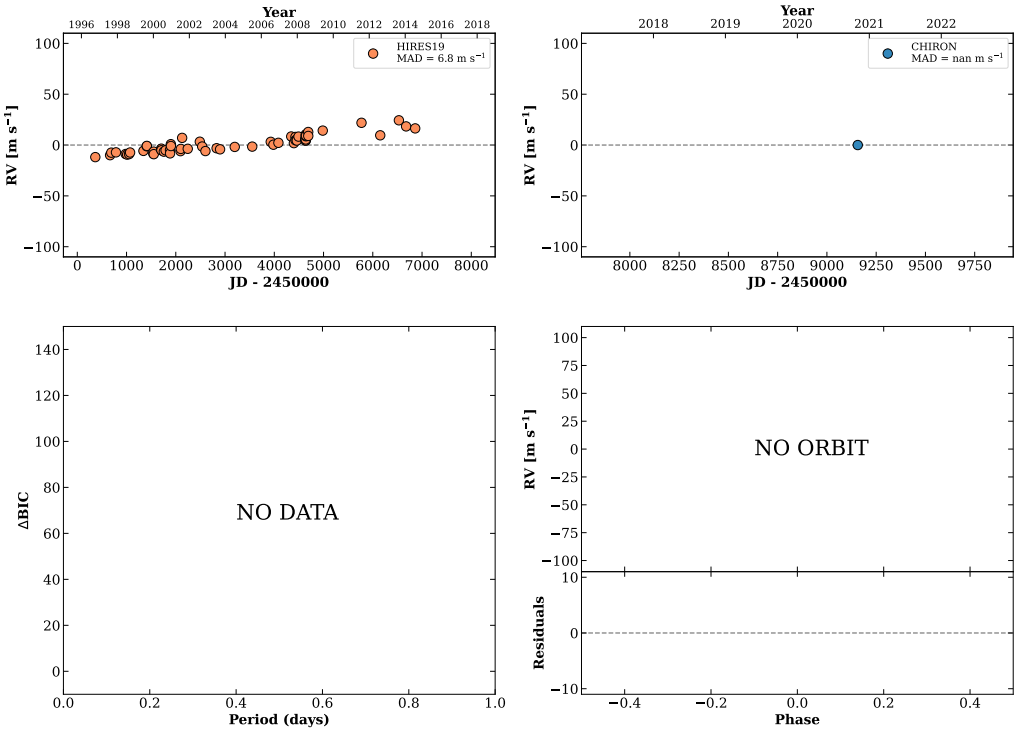

Figure 379 RV results for RKS2317-2323 (top) and RKS2319-1327 (bottom).

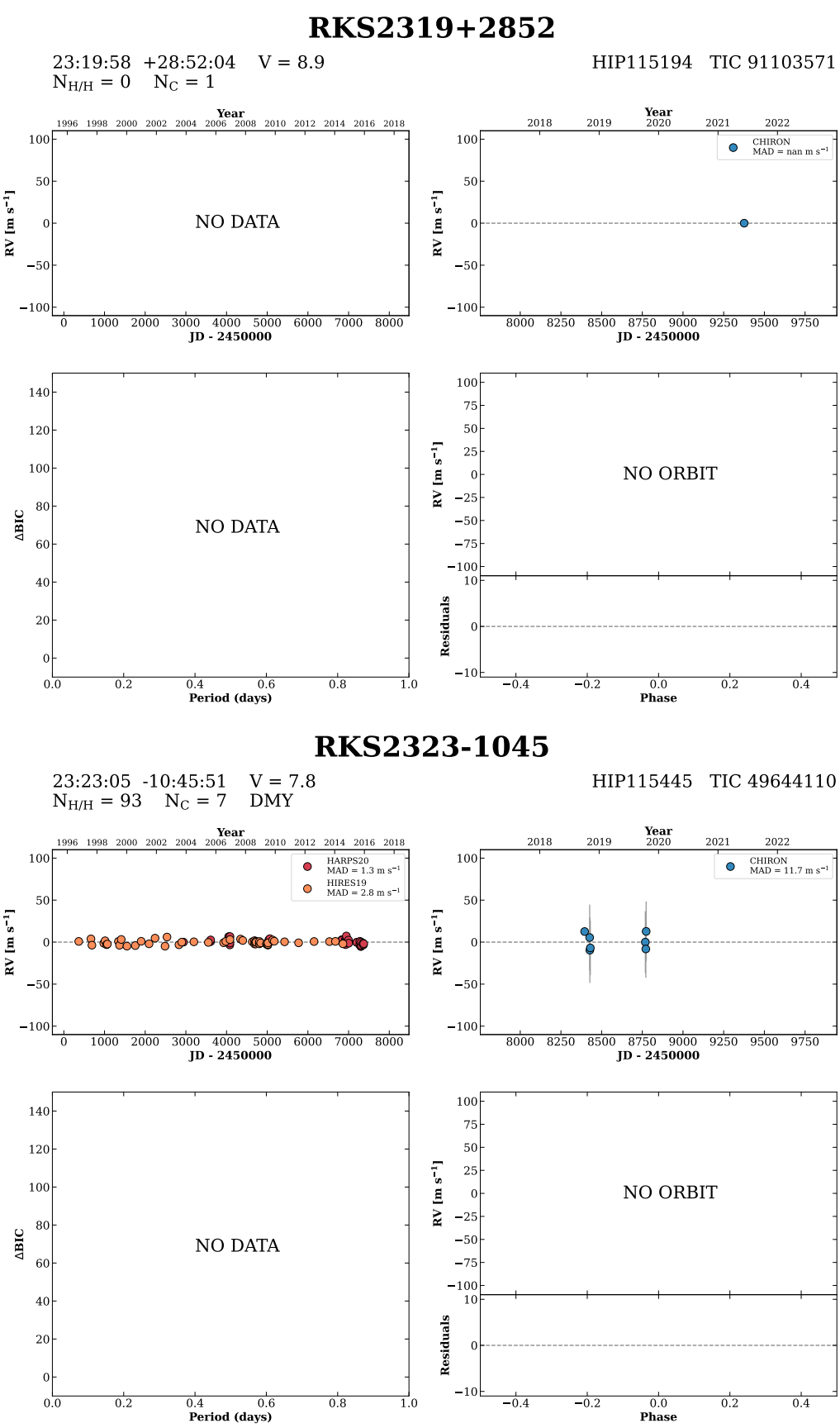

Figure 380 RV results for RKS2319+2852 (top) and RKS2323-1045 (bottom).

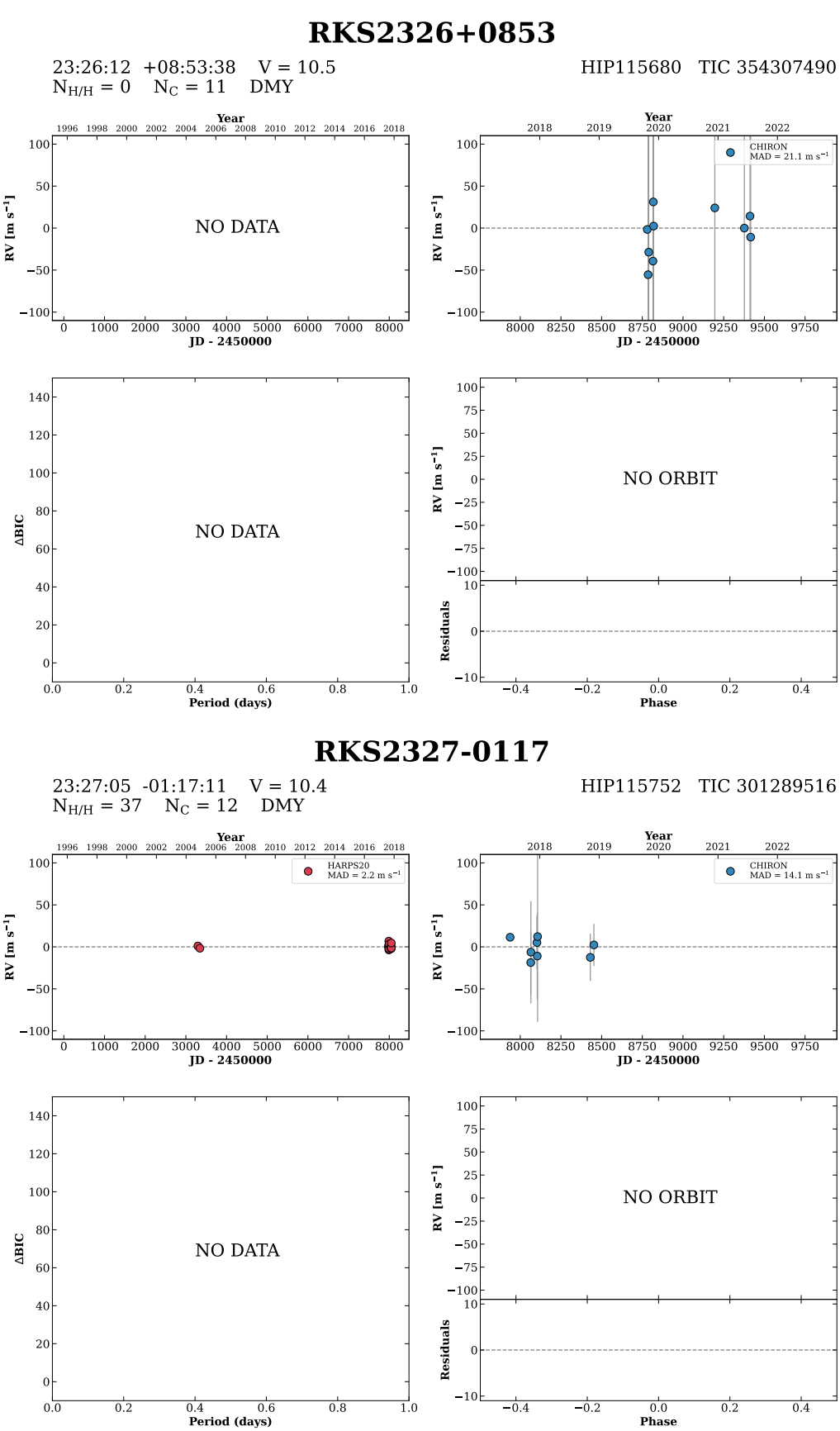

Figure 381 RV results for RKS2326+0853 (top) and RKS2327-0117 (bottom).

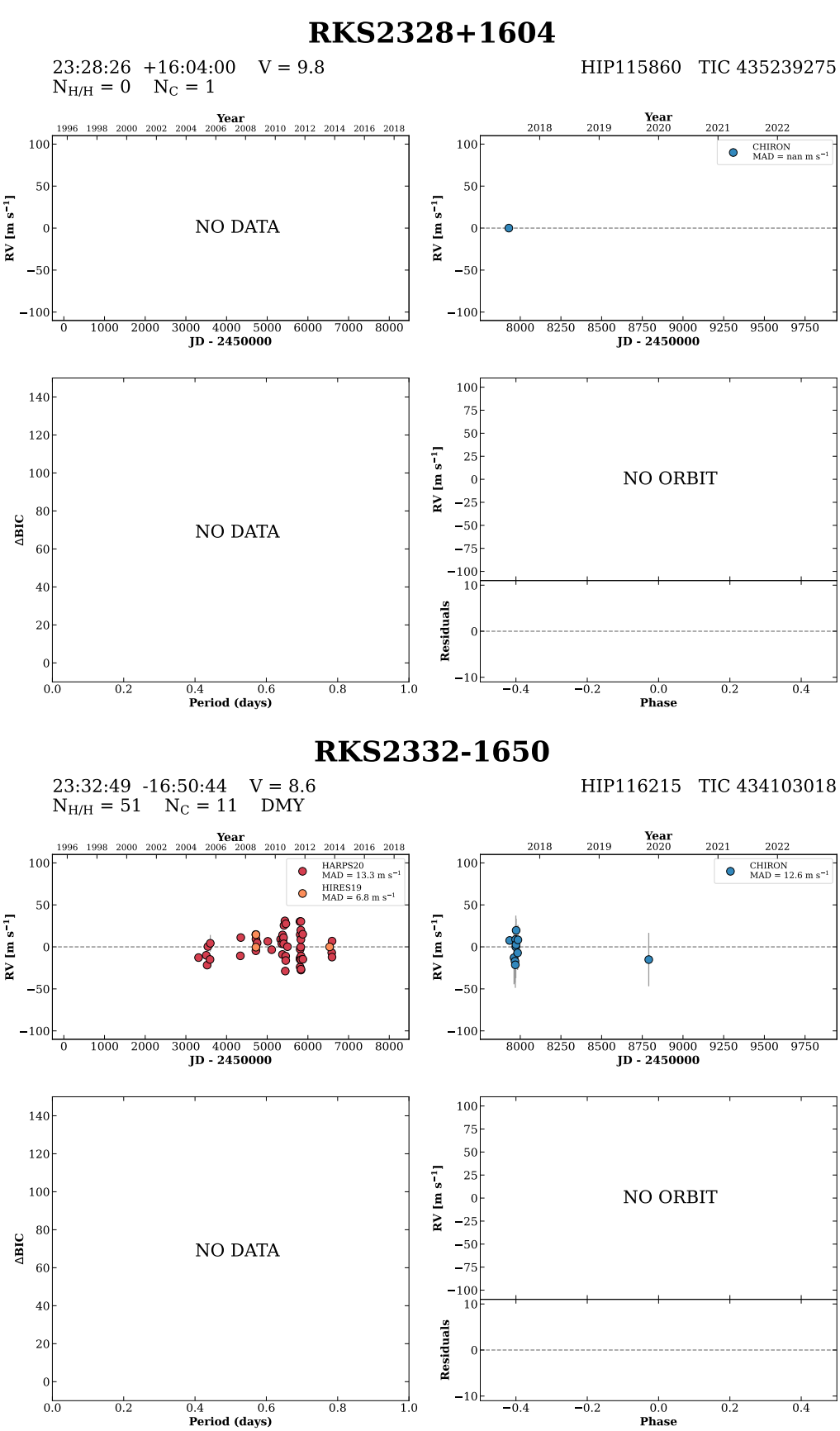

Figure 382 RV results for RKS2328+1604 (top) and RKS2332-1650 (bottom).

RKS2333-1239

23:33:24 -12:39:53 V = 8.8 HIP116258 TIC 402317981
$N_{H/H}$ = 29 N_C = 1

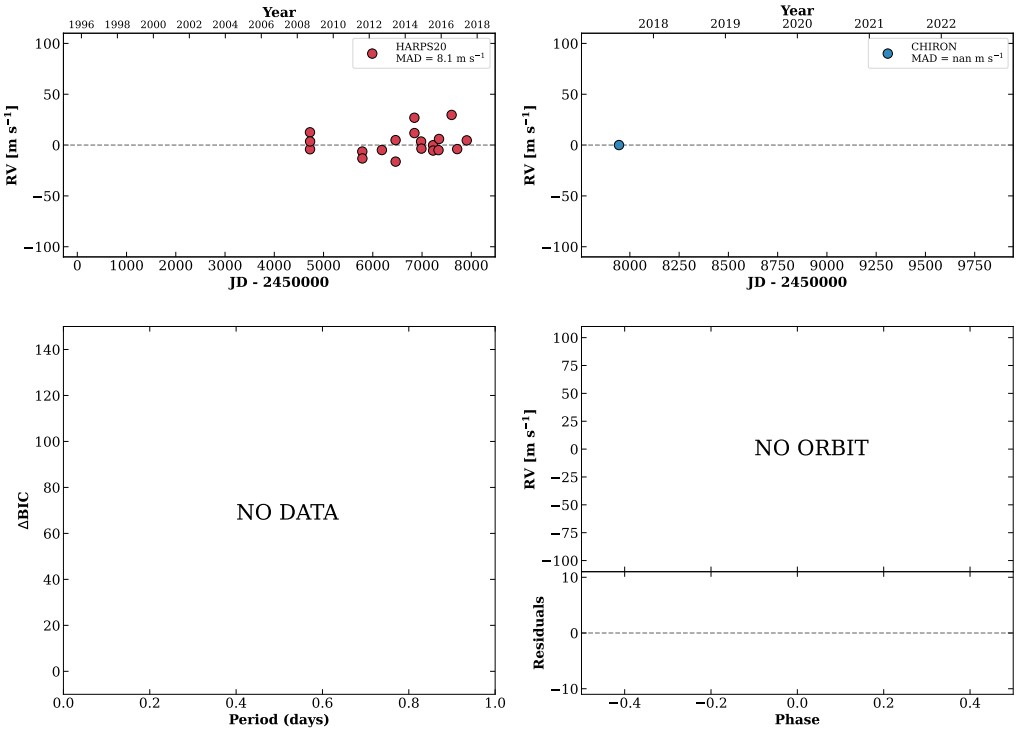

RKS2335+0136A

23:35:00 +01:36:19 V = 9.6 HIP116384 TIC 422618003
$N_{H/H}$ = 15 N_C = 11 DM

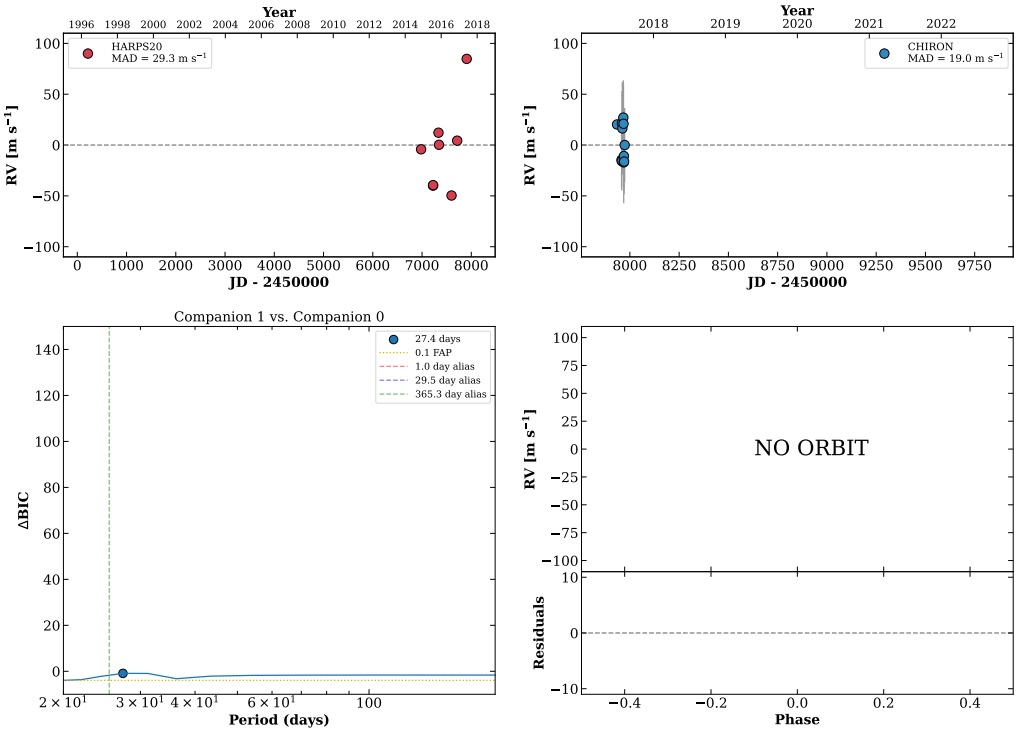

Figure 383 RV results for RKS2333-1239 (top) and RKS2335+0136A (bottom).

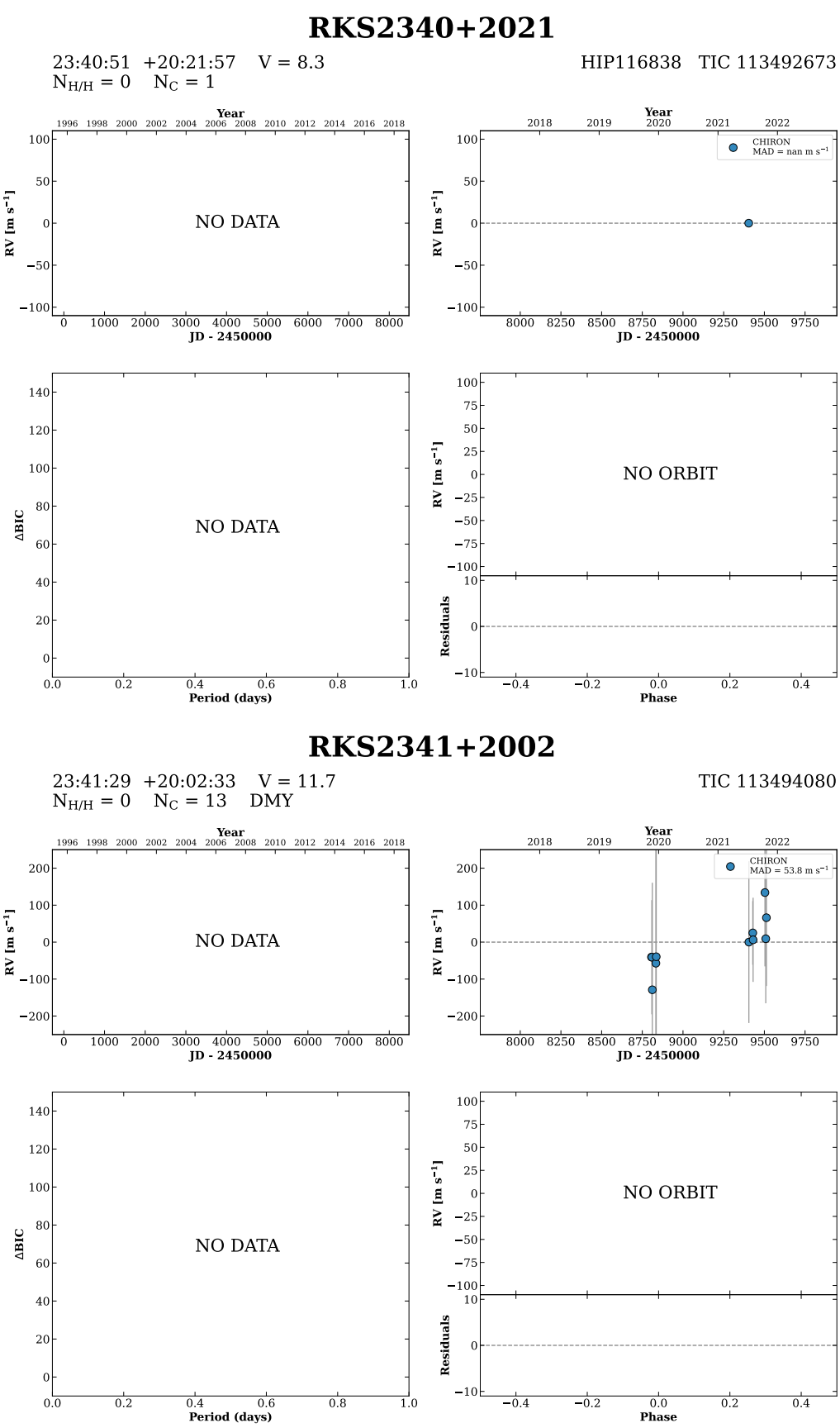

Figure 384 RV results for RKS2340+2021 (top) and RKS2341+2002 (bottom).

RKS2342-0234A

23:42:11 -02:34:36 V = 10.3 HIP116936 TIC 250107647
$N_{H/H}$ = 0 N_C = 63 DMY

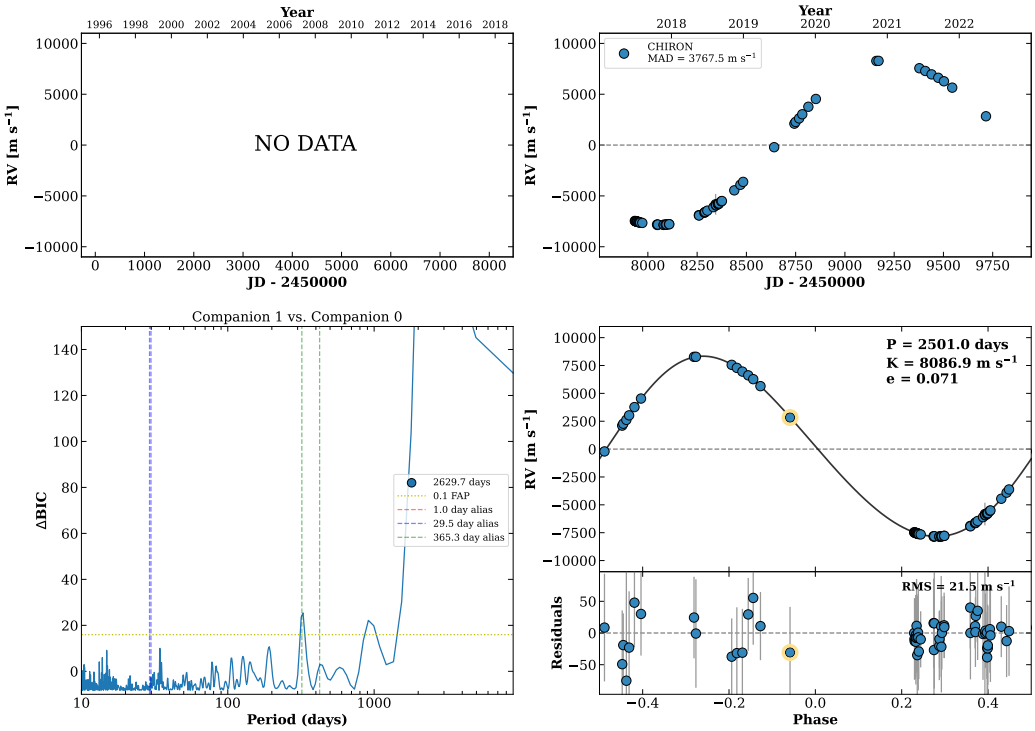

RKS2345+2933

23:45:10 +29:33:43 V = 8.4 HIP117159 TIC 56249811
$N_{H/H}$ = 0 N_C = 34 DMY

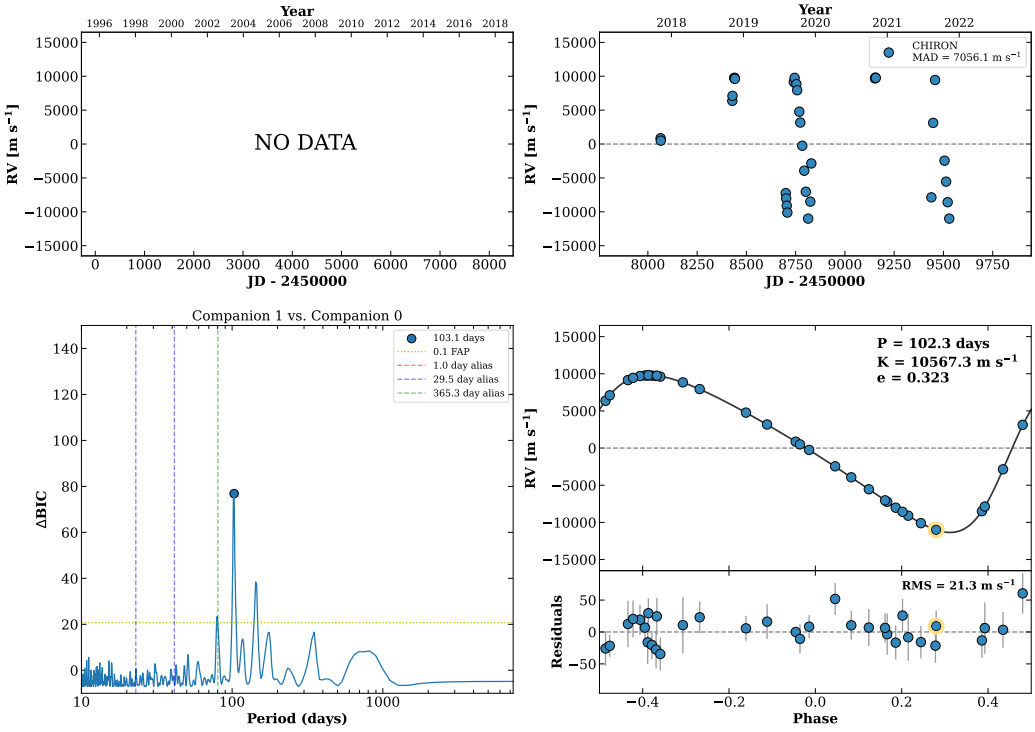

Figure 385 RV results for RKS2342-0234A (top) and RKS2345+2933 (bottom).

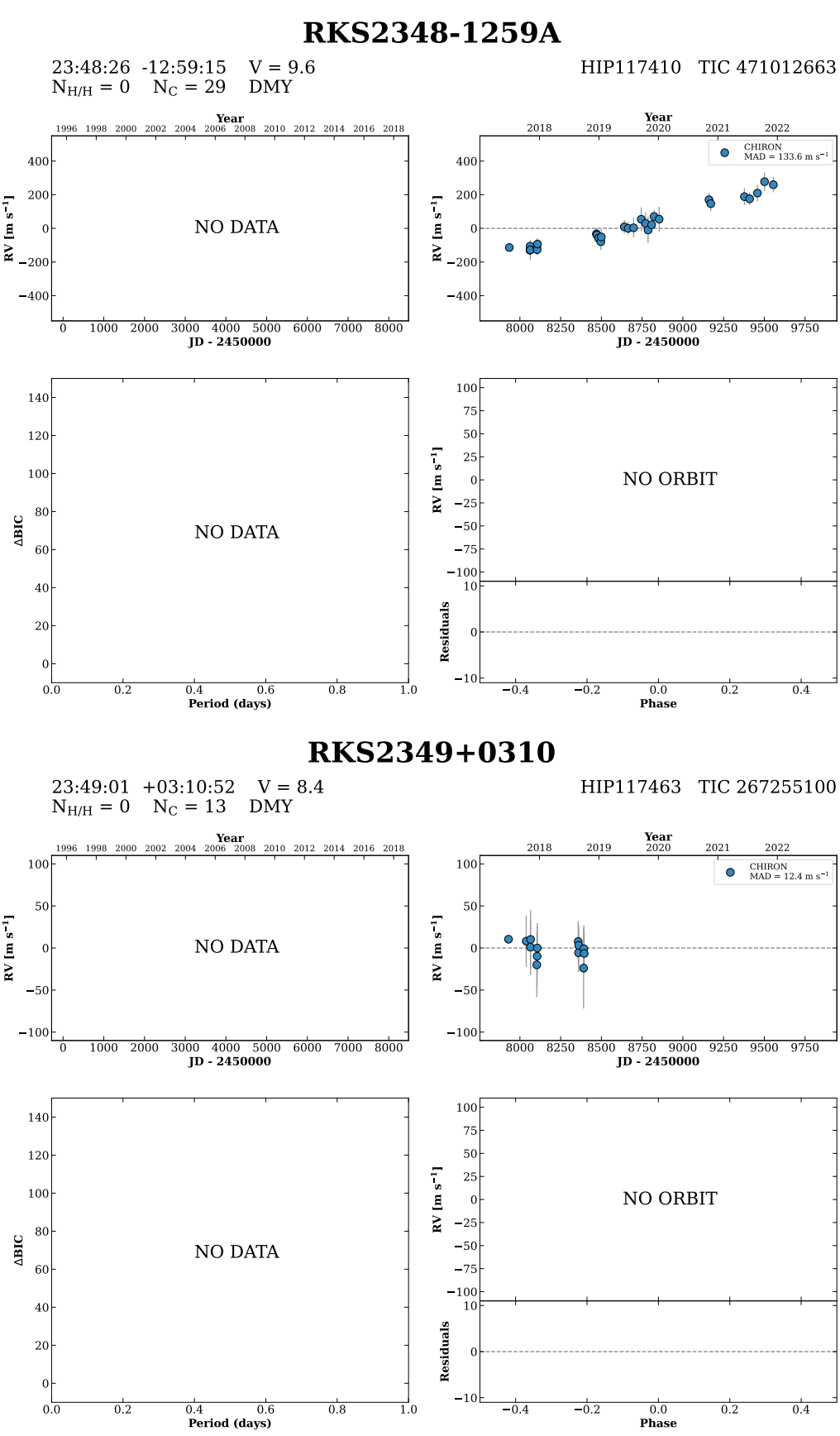

Figure 386 RV results for RKS2348-1259A (top) and RKS2349+0310 (bottom).

RKS2350-2924

23:50:15 -29:24:06 V = 7.9 HIP117542 TIC 33985272
$N_{H/H}$ = 0 N_C = 26 DMY

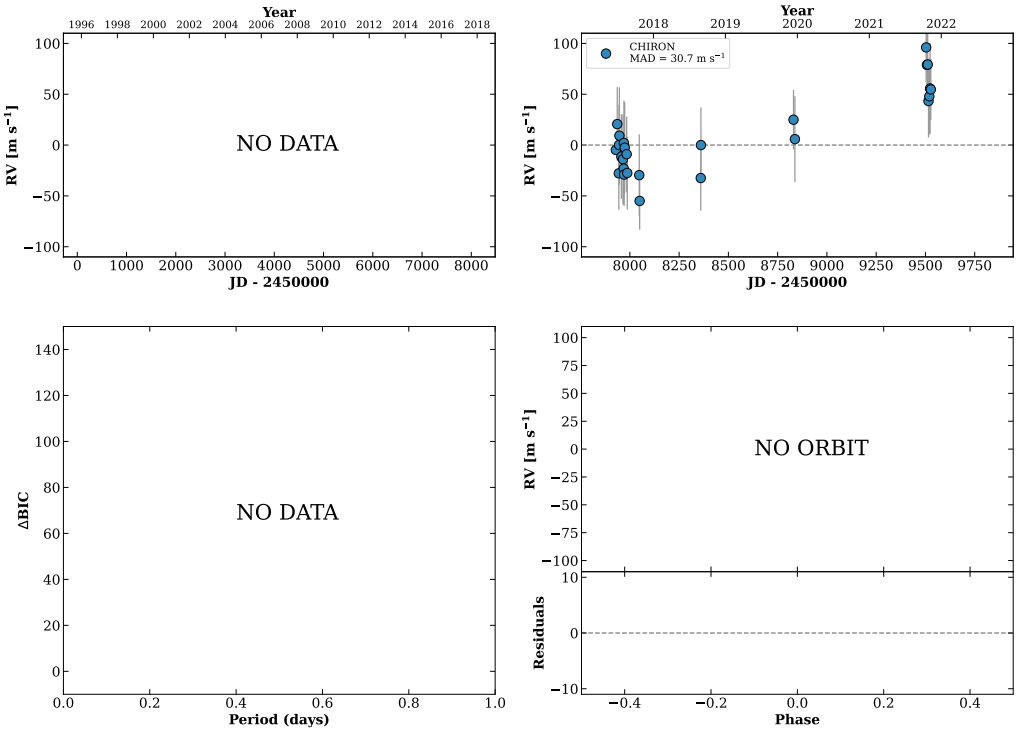

RKS2353+2901

23:53:09 +29:01:05 V = 9.8 HIP117779 TIC 406543332
$N_{H/H}$ = 0 N_C = 19 DMY

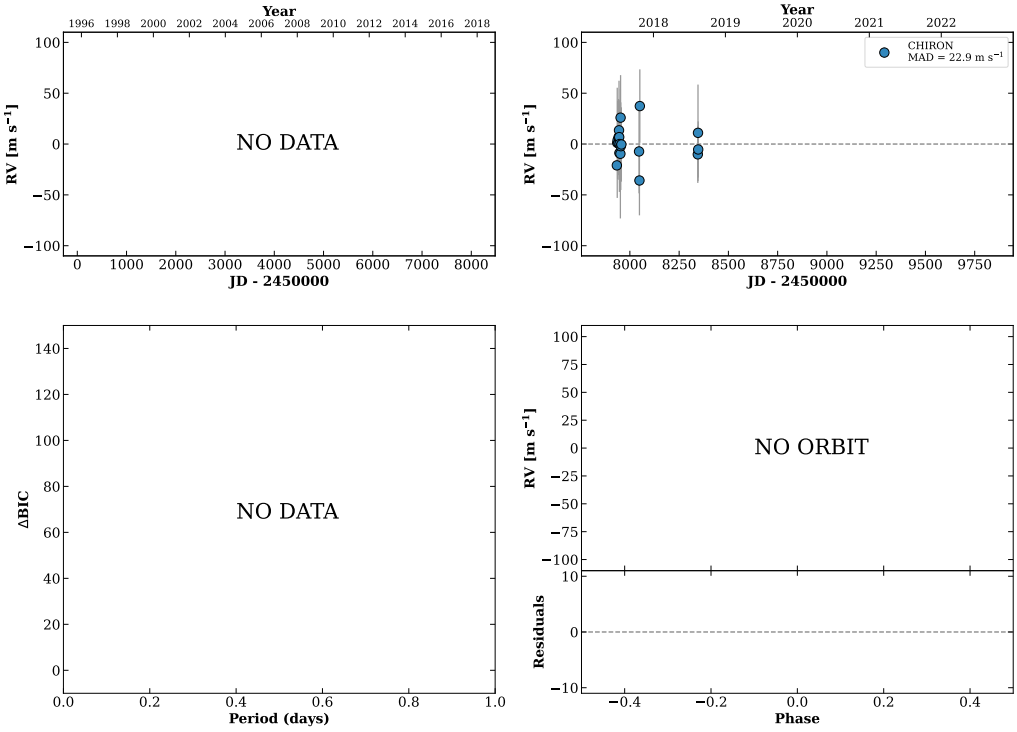

Figure 387 RV results for RKS2350-2924 (top) and RKS2353+2901 (bottom).

RKS2355+2211

23:55:27 +22:11:36 V = 8.8 HIP117946 TIC 437707246
$N_{H/H}$ = 13 N_C = 1

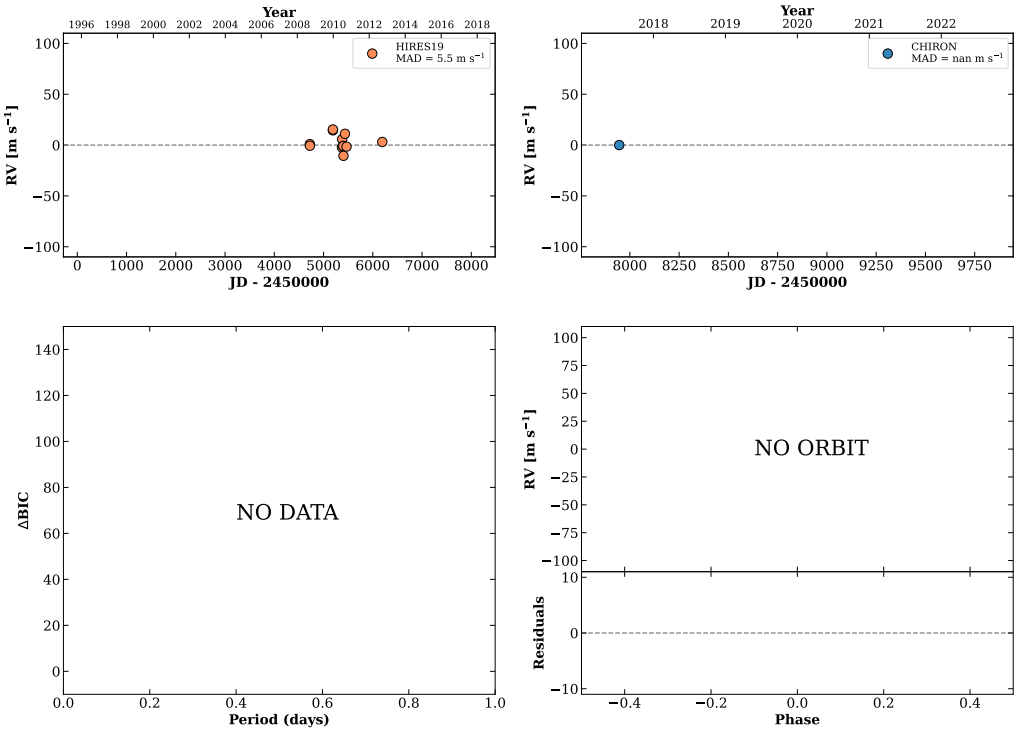

RKS2356-1445

23:56:32 -14:45:01 V = 11.7 TIC 327953001
$N_{H/H}$ = 0 N_C = 11 DMY

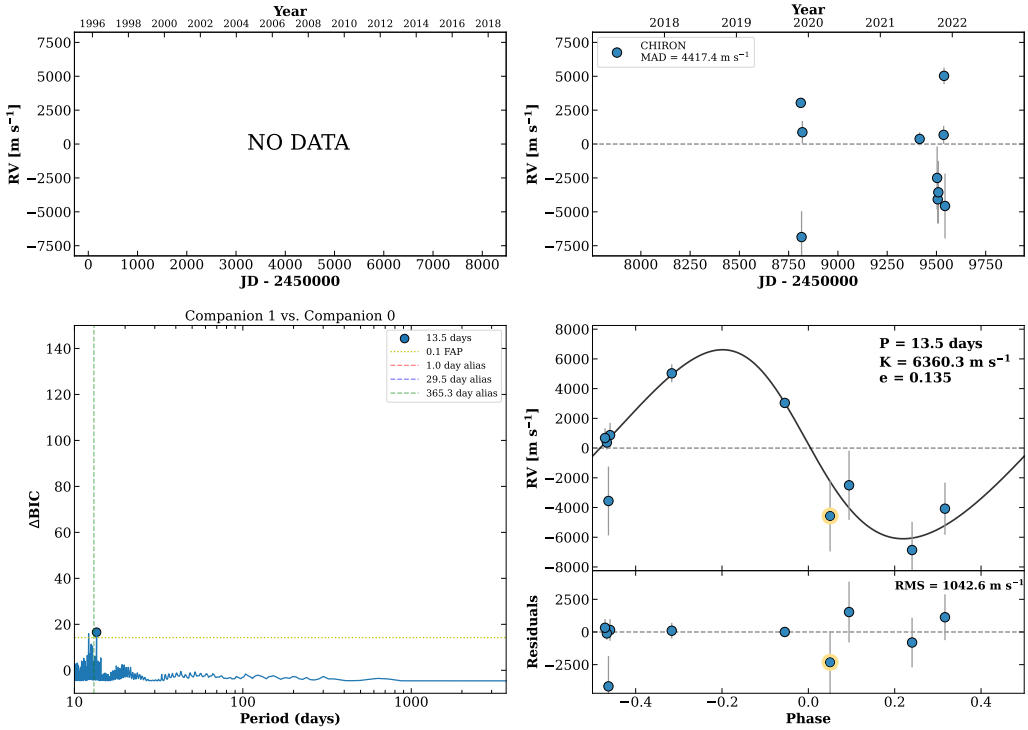

Figure 388 RV results for RKS2355+2211 (top) and RKS2356-1445 (bottom).

RKS2357-1630

23:57:14 -16:30:27 V = 10.8 HIP118086 TIC 441054056
$N_{H/H}$ = 0 N_C = 12 DMY

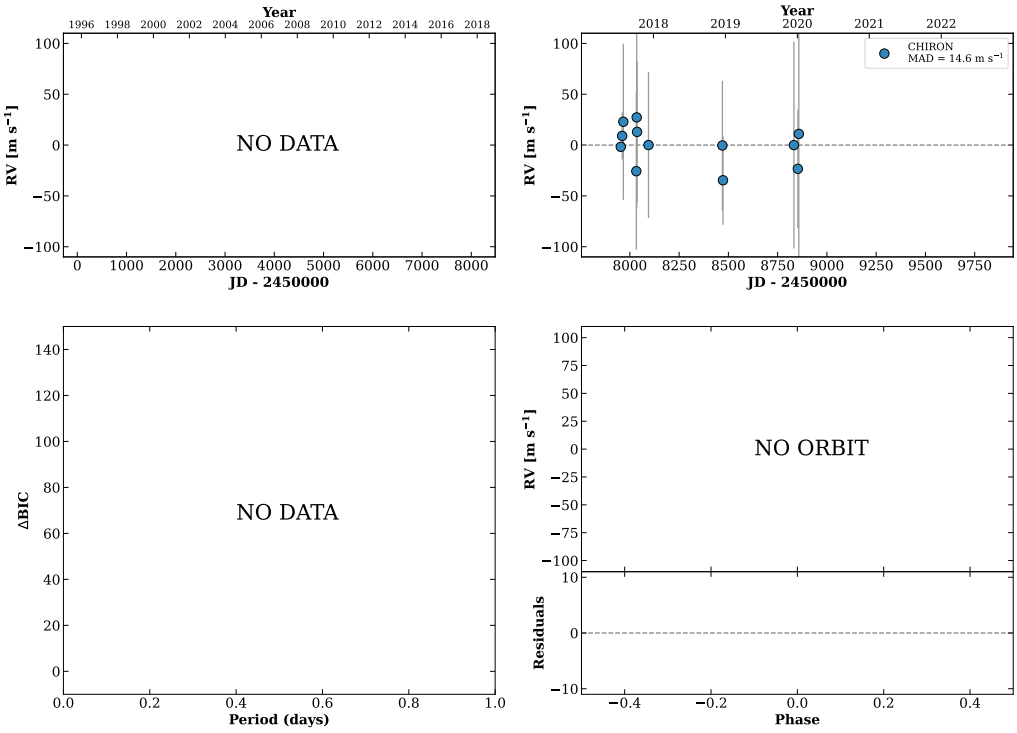

RKS2358+0949

23:58:20 +09:49:51 V = 8.3 TIC 408486919
$N_{H/H}$ = 0 N_C = 9 DMY

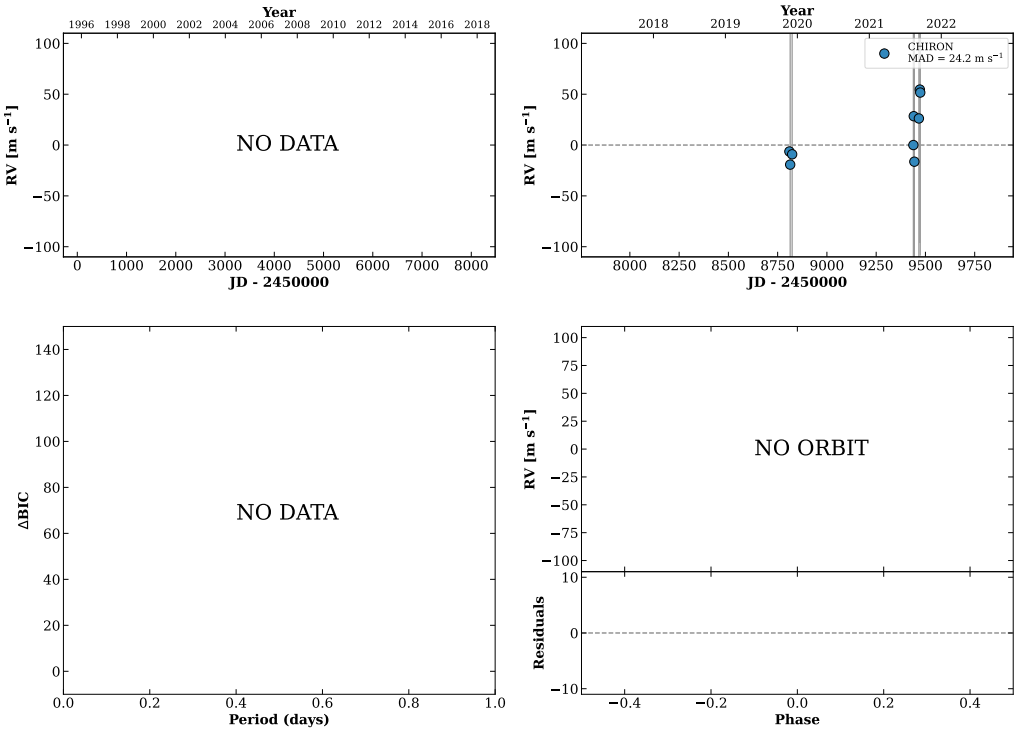

Figure 389 RV results for RKS2357-1630 (top) and RKS2358+0949 (bottom).

RKS2359-2602

23:59:14 -26:02:55 V = 8.7 HIP118261 TIC 65263849
$N_{H/H}$ = 28 N_C = 14 DM

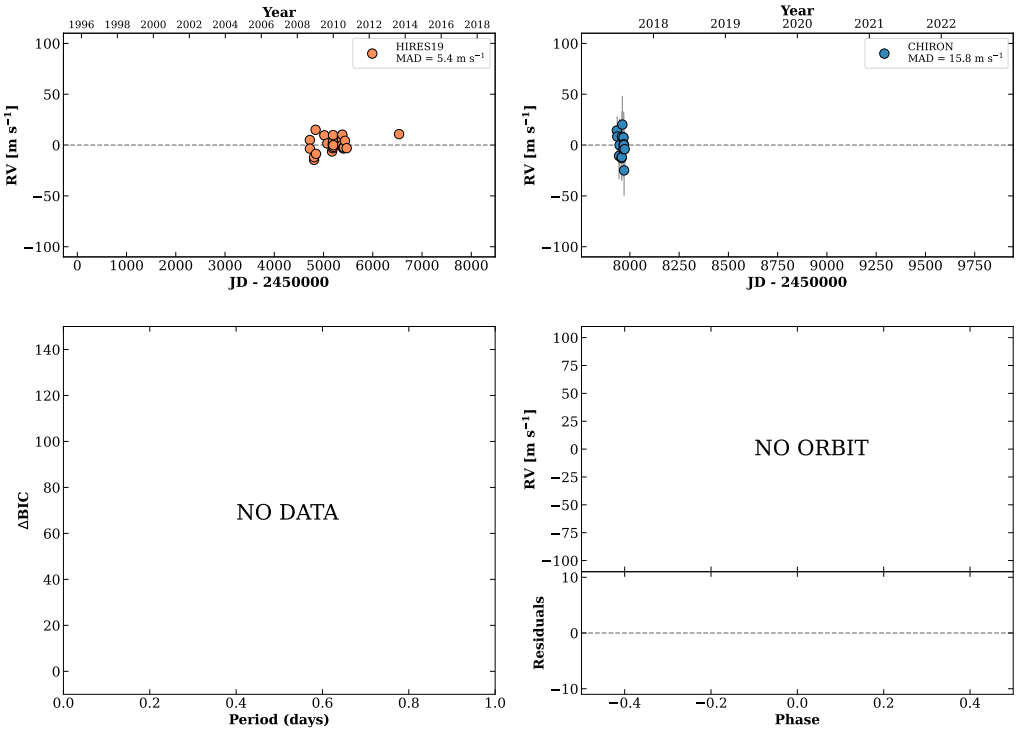

RKS2359+0639

23:59:48 +06:39:51 V = 8.9 HIP118310 TIC 401396607
$N_{H/H}$ = 0 N_C = 25 DMY

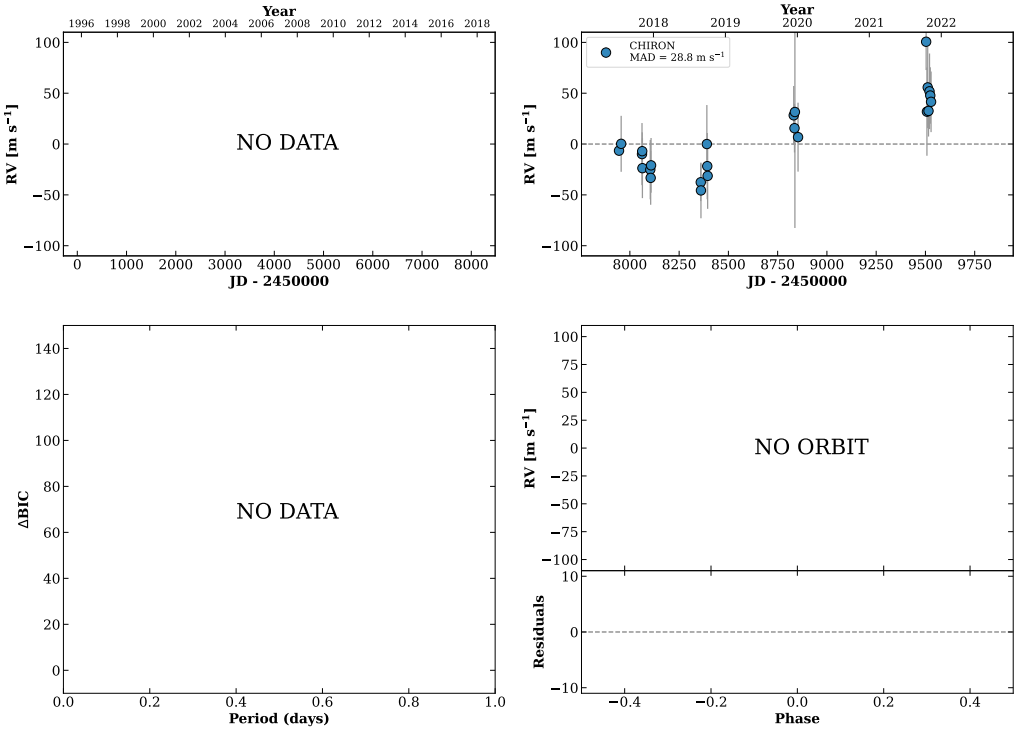

Figure 390 RV results for RKS2359-2602 (top) and RKS2359+0639 (bottom).

B Appendix

A Tables

[2]

Table 1: K dwarf Sample: Astrometry and photometry data.

RKS ID	Star Name	R.A.	Decl.	π	V	K	B_G	R_G	B_G-R_G	M_{B_G}	Sample
		hh mm ss	±dd mm ss	mas	mag	mag	mag	mag	mag	mag	
RKS0000+1659A	HIP 68	00 00 48	+16 59 17	33.16	8.79	6.34	9.02	7.82	1.21	6.63	33PC
RKS0001−2326	HD 224832	00 01 04	−23 26 25	30.14	9.40	6.87	9.63	8.35	1.27	7.02	33PC
RKS0001−1656	HIP 112	00 01 26	−16 56 54	31.97	10.75	7.22	11.00	9.19	1.82	8.53	33PC
RKS0002+1100	HIP 184	00 02 22	+11 00 22	29.52	8.48	6.46	8.70	7.66	1.04	6.05	XTRA
	HIP 400	00 04 56	+23 16 11	37.92	7.82	5.93	8.03	7.08	0.95	5.92	XTRA
RKS0007−2349	HIP 616	00 07 33	−23 49 07	30.56	8.69	6.68	8.91	7.91	1.01	6.34	33PC
	HIP 897	00 11 05	−05 47 02	41.21	10.82	7.12	11.08	9.17	1.92	9.16	XTRA
RKS0012+2705	HIP 974	00 12 04	+27 05 56	38.56	8.73	6.30	8.95	7.73	1.22	6.88	33PC
RKS0012+2142	HIP 1006	00 12 34	+21 42 48	32.01	11.75	8.04	11.97	10.08	1.89	9.50	33PC
RKS0016−1435	BD−15 36	00 16 11	−14 35 28	30.81	9.97	6.80	9.81	8.47	1.34	7.25	33PC
RKS0017+2057	G 131−51	00 18 00	+20 57 24	36.14	10.95	7.41	11.34	9.46	1.88	9.13	33PC
RKS0019−0957	HIP 1532	00 19 06	−09 57 53	49.51	9.90	6.55	10.15	8.45	1.70	8.62	25PC
RKS0019−0303	HIP 1539	00 19 12	−03 03 13	32.06	10.93	7.46	11.16	9.39	1.77	8.69	33PC
RKS0020+1738	StKM 1−25	00 20 57	+17 38 16	33.39	11.25	7.54	11.47	9.58	1.89	9.08	33PC
RKS0021+2531	BD+24 32	00 21 16	+25 31 27	35.58	9.55	6.97	9.76	8.46	1.30	7.52	33PC
RKS0022−2701	HIP 1768	00 22 24	−27 01 57	45.95	8.30	6.13	8.53	7.43	1.10	6.85	25PC
RKS0024−2701	HIP 1936	00 24 26	−27 01 36	55.71	7.93	5.56	8.15	6.98	1.16	6.87	25PC
RKS0036−0930	HIP 2839	00 36 00	−09 30 56	32.61	11.21	7.72	11.44	9.66	1.78	9.01	33PC
RKS0036+2610	BD+25 84	00 36 58	+26 10 55	43.47	9.01	6.18	9.28	7.83	1.45	7.47	25PC
RKS0039+2115	HIP 3093	00 39 22	+21 15 02	89.79	5.88	4.00	6.10	5.08	1.02	5.86	25PC
RKS0040−0713	HD 3821B	00 40 47	−07 13 51	37.79	9.93	6.83	10.23	8.65	1.58	8.11	33PC
RKS0042+2239	HIP 3378	00 42 57	+22 39 35	31.57	11.51	7.82	11.80	9.95	1.84	9.29	33PC
RKS0044−1856A	HIP 3493	00 44 37	−18 56 48	27.47	10.74	7.12	10.99	9.14	1.86	8.19	XTRA
RKS0045+0147	HIP 3535	00 45 05	+01 47 08	44.58	8.04	5.74	8.26	7.08	1.18	6.51	25PC
RKS0048+0516	HIP 3765	00 48 23	+05 16 50	134.50	5.74	3.68	5.96	4.85	1.11	6.60	25PC
RKS0051+1844A	HIP 3998	00 51 22	+18 44 21	44.95	9.22	6.24	9.47	7.97	1.49	7.73	25PC
RKS0051−2254	HIP 4022	00 51 34	−22 54 36	65.19	8.96	5.74	9.19	7.58	1.61	8.26	25PC
	HIP 4061	00 52 00	+20 34 58	31.78	11.48	7.63	11.76	9.77	1.99	9.27	XTRA
RKS0055−2940A	HIP 4353	00 55 49	−29 40 33	32.15	9.42	6.57	9.70	8.27	1.44	7.24	33PC
RKS0056−1135	HIP 4443	00 56 50	−11 35 20	39.27	11.11	7.36	11.38	9.43	1.94	9.35	33PC
RKS0057+0551	BD+05 127	00 57 45	+05 51 21	56.19	10.25	6.64	10.50	8.63	1.87	9.25	25PC
RKS0100−2536	HIP 4691	01 00 18	−25 36 53	27.60	9.96	7.21	10.18	8.82	1.36	7.38	XTRA
RKS0101−0953	HIP 4824	01 01 57	−09 53 08	29.02	10.50	7.29	10.72	9.14	1.57	8.03	XTRA

[2]All tables are created from the author of this thesis work.

Table 1: K dwarf Sample: Astrometry and photometry data.

RKS ID	Star Name	R.A.	Decl.	π	V	K	B_G	R_G	B_G-R_G	M_{B_G}	Sample
		hh mm ss	±dd mm ss	mas	mag	mag	mag	mag	mag	mag	
RKS0102−1025	HIP 4845	01 02 21	−10 25 26	47.37	10.06	6.53	10.25	8.50	1.75	8.62	25PC
RKS0102+0503A	HIP 4849	01 02 25	+05 03 41	65.76	8.16	5.51	8.40	7.10	1.30	7.49	25PC
RKS0102−2136	HIP 4855	01 02 27	−21 36 34	30.87	10.89	7.14	10.99	9.28	1.72	8.44	33PC
RKS0104−2536	HIP 5027	01 04 24	−25 36 18	37.02	9.78	6.84	10.01	8.53	1.48	7.86	33PC
RKS0104+2607	HIP 5041	01 04 32	+26 07 13	33.43	10.02	6.96	10.26	8.72	1.55	7.88	33PC
RKS0105+1523B	HIP 5110	01 05 30	+15 23 19	37.41	9.93	6.37	10.07	8.33	1.74	7.93	XTRA
RKS0105+1523A	HIP 5110	01 05 30	+15 23 24	36.65	8.66	6.48	9.36	8.07	1.29	7.18	33PC
RKS0107+2257	HIP 5286	01 07 38	+22 57 18	48.69	8.41	5.76	8.66	7.31	1.35	7.10	25PC
RKS0108+1714	HIP 5369	01 08 40	+17 14 33	34.97	10.50	7.28	10.79	9.15	1.64	8.51	33PC
RKS0112+0058	HIP 5647	01 12 32	+00 58 52	28.73	8.70	6.48	8.95	7.82	1.13	6.24	XTRA
RKS0112−2514	HIP 5663	01 12 46	−25 14 08	44.13	9.55	6.42	9.79	8.21	1.58	8.01	25PC
RKS0113+1629	HIP 5763	01 13 59	+16 29 40	31.31	9.82	6.91	10.10	8.61	1.48	7.58	33PC
RKS0116+2519	HIP 5957	01 16 39	+25 19 53	41.69	10.10	6.66	10.33	8.60	1.73	8.43	25PC
RKS0117−1530	HIP 6037	01 17 34	−15 30 12	30.82	9.76	7.17	9.98	8.71	1.27	7.42	33PC
RKS0118−0052B	G 70−50	01 18 40	−00 52 28	36.43	10.77	7.19	10.95	9.16	1.79	8.76	XTRA
RKS0118−0052A	HIP 6130	01 18 41	−00 52 03	36.27	7.99	6.04	8.22	7.22	1.00	6.02	33PC
RKS0121+2419	HIP 6342	01 21 29	+24 19 50	37.00	10.69	7.11	10.95	9.11	1.83	8.79	33PC
RKS0122−2653	HIP 6390	01 22 08	−26 53 35	32.56	8.76	6.50	9.00	7.84	1.17	6.57	33PC
RKS0123−1257B	G 272−8A	01 23 01	−12 57 30	33.31	10.28	6.66	10.60	8.74	1.86	8.21	XTRA
RKS0123−1257A	HIP 6456	01 23 03	−12 57 58	33.21	7.85	5.92	8.08	7.05	1.03	5.68	33PC
RKS0124+1254	HIP 6558	01 24 17	+12 54 27	27.28	9.52	7.06	9.75	8.51	1.24	6.93	XTRA
RKS0124+1829	HIP 6613	01 24 54	+18 30 00	31.76	8.49	6.40	8.72	7.65	1.07	6.23	33PC
RKS0125−0103	HIP 6639	01 25 09	−01 03 35	31.39	9.46	6.92	9.71	8.42	1.29	7.19	33PC
RKS0129+2143	HIP 6917	01 29 05	+21 43 23	42.75	7.74	5.37	7.97	6.77	1.19	6.12	25PC
RKS0132+2059	Wolf 1523	01 32 44	+20 59 16	38.61	12.23	8.03	12.47	10.26	2.21	10.41	33PC
RKS0133−2454	HIP 7228	01 33 09	−24 54 52	28.29	10.00	7.17	10.24	8.80	1.44	7.50	XTRA
RKS0135−2046	BD−21 262	01 35 46	−20 46 14	38.15	10.15	6.95	10.33	8.76	1.58	8.24	33PC
RKS0136+2133	HIP 7500	01 36 40	+21 33 47	28.71	9.23	6.88	9.49	8.27	1.22	6.78	XTRA
	HIP 7576	01 37 35	−06 45 38	41.59	7.66	5.75	7.88	6.90	0.98	5.97	XTRA
RKS0139+1515	HIP 7765	01 39 56	+15 15 33	40.94	8.68	6.32	9.34	7.94	1.39	7.40	25PC
RKS0142+2016	HIP 7981	01 42 30	+20 16 07	131.49	5.25	3.29	5.46	4.45	1.01	6.06	25PC
RKS0143−2136	HIP 8038	01 43 14	−21 36 56	33.62	10.77	6.98	10.42	8.85	1.57	8.06	33PC
	HIP 8039	01 43 14	−21 37 11	32.49	8.23	6.34	8.46	7.45	1.00	6.02	XTRA
	HIP 8043	01 43 16	+27 50 32	45.38	10.37	6.60	10.64	8.70	1.93	8.92	XTRA
RKS0145−2503	* eps Scl B	01 45 39	−25 03 05	35.78	8.58	...	8.80	7.68	1.12	6.57	XTRA
RKS0146+1224	HIP 8275	01 46 39	+12 24 42	41.57	8.91	6.32	9.13	7.84	1.29	7.23	25PC
RKS0150+2927	HIP 8543	01 50 08	+29 27 52	36.92	8.06	6.11	8.26	7.29	0.97	6.10	33PC
RKS0150+1817	Wolf 89	01 50 28	+18 17 47	33.02	10.85	7.24	11.01	9.22	1.79	8.60	33PC
	HIP 8768	01 52 49	−22 26 05	90.43	8.89	5.18	9.14	7.24	1.91	8.92	XTRA
RKS0200+2636	StKM 1−223	02 00 20	+26 36 00	30.42	10.97	7.59	11.24	9.52	1.73	8.66	33PC
	HIP 9603	02 03 30	−04 54 41	35.68	11.10	7.36	11.36	9.44	1.91	9.12	XTRA
	HIP 9716	02 05 00	−15 40 41	37.84	7.79	5.88	8.01	7.02	0.99	5.90	XTRA

Table 1: K dwarf Sample: Astrometry and photometry data.

RKS ID	Star Name	R.A.	Decl.	π	V	K	B_G	R_G	B_G-R_G	M_{B_G}	Sample
		hh mm ss	±dd mm ss	mas	mag	mag	mag	mag	mag	mag	
RKS0205−2804	HIP 9749	02 05 24	−28 04 11	38.29	10.89	7.16	11.14	9.22	1.92	9.05	33PC
RKS0209−1620	HIP 10037	02 09 11	−16 20 23	35.09	10.87	7.25	11.13	9.27	1.87	8.86	33PC
	HIP 10276	02 12 18	+21 58 58	29.25	8.46	6.59	8.67	7.70	0.97	6.00	XTRA
	HIP 10312	02 12 51	−17 41 12	42.51	11.09	7.34	11.36	9.42	1.94	9.50	XTRA
RKS0213−2111	HIP 10337	02 13 12	−21 11 47	42.11	9.84	6.50	10.09	8.40	1.69	8.21	25PC
RKS0214−0338	HIP 10416	02 14 14	−03 38 07	44.07	8.55	6.01	8.79	7.51	1.28	7.01	25PC
RKS0215+0729	HIP 10500	02 15 22	+07 29 39	38.77	11.88	7.82	12.16	10.01	2.15	10.10	33PC
RKS0215−1814	HIP 10542	02 15 46	−18 14 17	43.53	9.12	5.43	8.57	7.36	1.20	6.76	25PC
RKS0221−0652	HIP 11000	02 21 44	−06 52 46	36.10	9.07	6.47	9.31	8.00	1.32	7.10	33PC
RKS0222+1824	HIP 11083	02 22 42	+18 24 38	28.47	8.83	6.63	9.06	7.95	1.11	6.33	XTRA
	HIP 11452	02 27 46	+04 25 59	58.33	8.69	5.11	8.94	7.14	1.80	7.77	XTRA
RKS0229−1958A	HIP 11565	02 29 02	−19 58 45	51.29	8.78	5.83	9.01	7.55	1.45	7.56	25PC
RKS0231+0822	HIP 11707	02 31 03	+08 22 55	27.71	10.90	7.55	11.14	9.47	1.67	8.36	XTRA
RKS0231−2001	HIP 11739	02 31 31	−20 01 42	30.24	10.24	7.17	10.44	8.90	1.54	7.85	33PC
RKS0231−1516	HIP 11759	02 31 42	−15 16 24	37.08	8.67	6.40	8.90	7.76	1.15	6.75	33PC
RKS0236−2331	HIP 12110	02 36 01	−23 31 17	47.13	8.34	5.83	8.57	7.30	1.28	6.94	25PC
RKS0236−2710	HIP 12109	02 36 01	−27 10 42	30.35	9.47	6.92	9.71	8.42	1.29	7.12	33PC
RKS0236+0653	HIP 12114	02 36 05	+06 53 12	138.21	5.83	3.48	6.05	4.84	1.21	6.75	25PC
RKS0236−0309	HIP 12158	02 36 42	−03 09 22	41.09	8.10	5.94	8.35	7.23	1.12	6.42	25PC
RKS0240+0111	HIP 12493	02 40 43	+01 11 55	41.77	9.51	6.50	9.75	8.25	1.50	7.85	25PC
RKS0242+0322	BD+02 418	02 42 33	+03 22 26	40.64	10.13	6.83	10.39	8.70	1.69	8.43	25PC
RKS0243+1925A	HIP 12709	02 43 21	+19 25 45	53.56	8.23	5.54	8.47	7.13	1.34	7.11	25PC
RKS0246+2538	HIP 12926	02 46 15	+25 39 00	39.60	7.87	5.87	8.11	7.09	1.02	6.10	33PC
RKS0246+1146	HIP 12929	02 46 17	+11 46 31	61.91	8.59	5.53	8.85	7.30	1.54	7.81	25PC
RKS0246−2305	HIP 12961	02 46 43	−23 05 12	42.76	10.25	6.74	10.49	8.70	1.79	8.65	25PC
RKS0247+1922	HIP 13027	02 47 27	+19 22 21	30.24	6.90	5.64	8.26	7.34	0.92	5.66	33PC
RKS0247+2842	HIP 13065	02 47 56	+28 42 44	34.81	11.10	7.48	11.36	9.51	1.85	9.07	33PC
RKS0248−1145	HIP 13079	02 48 07	−11 45 47	35.15	10.80	7.22	11.02	9.23	1.79	8.75	33PC
RKS0248+2704	HIP 13081	02 48 09	+27 04 07	43.41	7.61	5.62	7.82	6.81	1.01	6.00	25PC
RKS0250+1542	HIP 13258	02 50 37	+15 42 36	42.76	8.88	6.13	9.14	7.74	1.40	7.29	25PC
RKS0251+1038	HIP 13342	02 51 43	+10 38 42	34.55	10.01	6.98	10.22	8.70	1.51	7.91	33PC
RKS0251−0816	HIP 13345	02 51 44	−08 16 10	32.34	9.82	6.97	10.06	8.62	1.44	7.60	33PC
RKS0252−1246	HIP 13402	02 52 32	−12 46 11	96.54	6.05	4.17	6.28	5.25	1.03	6.20	25PC
RKS0255+2652B	HD 18143B	02 55 39	+26 52 20	44.38	10.02	6.17	10.11	8.37	1.75	8.35	XTRA
RKS0255+2652A	HIP 13642	02 55 39	+26 52 24	44.37	7.52	5.43	7.82	6.75	1.07	6.06	25PC
RKS0255+2807A	HIP 13644	02 55 41	+28 07 48	30.24	11.05	7.52	11.30	9.50	1.79	8.70	33PC
RKS0257−2458	HIP 13769	02 57 13	−24 58 30	40.26	7.84	5.42	8.05	6.87	1.18	6.07	25PC
RKS0258+2646	HIP 13891	02 58 52	+26 46 27	34.02	8.21	6.13	8.43	7.38	1.05	6.09	33PC
RKS0300+0744	HIP 13976	03 00 03	+07 45 00	42.04	7.97	5.84	8.22	7.11	1.11	6.34	25PC
RKS0303+2006	BD+19 451	03 03 49	+20 06 39	46.79	8.63	5.96	8.86	7.52	1.35	7.21	25PC
RKS0306+0157	HIP 14445	03 06 27	+01 57 55	67.89	9.07	5.65	9.31	7.58	1.74	8.47	25PC
RKS0308−2445	HIP 14568	03 08 07	−24 45 35	31.03	10.23	6.66	10.48	8.68	1.80	7.94	33PC

Table 1: K dwarf Sample: Astrometry and photometry data.

RKS ID	Star Name	R.A.	Decl.	π	V	K	B_G	R_G	B_G-R_G	M_{B_G}	Sample
		hh mm ss	±dd mm ss	mas	mag	mag	mag	mag	mag	mag	
RKS0308−2410B	HIP 14589	03 08 25	−24 10 24	34.90	10.95	7.36	11.22	9.38	1.84	8.93	XTRA
RKS0308−2410A	HIP 14593	03 08 26	−24 10 03	34.92	10.12	6.97	10.35	8.78	1.57	8.07	33PC
RKS0310+1203	HIP 14729	03 10 15	+12 03 02	34.56	9.38	6.62	9.62	8.24	1.38	7.32	33PC
RKS0312−2859	* alf For B	03 12 04	−28 59 13	71.13	6.87	...	7.12	6.01	1.10	6.38	XTRA
RKS0314−2626	HIP 15095	03 14 45	−26 26 46	53.57	9.17	6.07	9.39	7.85	1.53	8.03	25PC
RKS0314+0858	HIP 15099	03 14 47	+08 58 51	43.23	7.84	5.75	8.04	6.99	1.06	6.22	25PC
RKS0320+0827	HIP 15563	03 20 29	+08 27 16	31.47	9.63	6.88	9.86	8.48	1.38	7.35	33PC
RKS0322+2709	HIP 15720	03 22 28	+27 09 22	31.50	11.01	7.42	11.27	9.43	1.83	8.76	33PC
RKS0324−0521	HIP 15919	03 25 00	−05 21 50	65.14	7.86	5.12	8.11	6.73	1.39	7.18	25PC
RKS0329−1140	HIP 16242	03 29 20	−11 40 42	47.54	9.95	6.45	10.24	8.43	1.80	8.62	25PC
RKS0329−2406	HIP 16247	03 29 23	−24 06 03	32.12	9.15	6.26	9.48	8.04	1.43	7.01	33PC
RKS0332−0927	HIP 16537	03 32 56	−09 27 30	312.22	3.72	1.78	4.00	2.88	1.12	6.47	25PC
RKS0336+0035	HD 22468B	03 36 47	+00 35 16	33.79	8.78	...	9.05	7.86	1.19	6.70	33PC
RKS0341+0336	HIP 17207	03 41 11	+03 36 41	38.71	9.61	6.15	9.85	8.11	1.75	7.79	33PC
RKS0342−2427	HIP 17346	03 42 45	−24 27 59	38.40	9.20	6.44	9.42	8.03	1.39	7.34	33PC
RKS0343−1253	HIP 17365	03 43 06	−12 53 40	35.22	10.87	7.50	11.11	9.40	1.71	8.84	33PC
RKS0343+1640	HIP 17414	03 43 53	+16 40 19	58.11	10.01	6.25	10.17	8.29	1.88	8.99	25PC
RKS0343−1906	HIP 17420	03 43 55	−19 06 39	71.66	7.10	4.84	7.32	6.18	1.14	6.59	25PC
RKS0344+1155	HIP 17496	03 44 51	+11 55 12	45.61	9.15	6.20	9.34	7.89	1.45	7.64	25PC
RKS0345−2751	HIP 17544	03 45 24	−27 51 45	48.35	8.21	5.60	8.43	7.20	1.23	6.85	25PC
RKS0348+2519	HD 23742	03 48 26	+25 19 23	30.86	8.58	6.50	8.75	7.73	1.02	6.19	33PC
RKS0348+1512	HIP 17794	03 48 33	+15 12 07	30.24	9.45	6.96	9.74	8.45	1.29	7.14	33PC
RKS0349−1329	StKM 1−413	03 49 16	−13 29 30	30.30	11.13	7.47	11.13	9.40	1.73	8.54	33PC
RKS0349+0120	HIP 17888	03 49 36	+01 20 54	30.88	8.58	6.53	8.79	7.76	1.03	6.24	33PC
RKS0350−2349	HIP 17956	03 50 20	−23 49 45	30.65	9.85	6.91	10.07	8.59	1.48	7.50	33PC
RKS0354−0649	HIP 18280	03 54 35	−06 49 34	63.71	9.02	5.63	9.26	7.55	1.72	8.28	25PC
RKS0357−2712	CD−27 1462	03 57 17	−27 12 46	34.41	10.42	6.79	10.53	8.79	1.74	8.21	33PC
RKS0357−0109	HIP 18512	03 57 29	−01 09 34	65.36	8.07	5.34	8.30	6.94	1.36	7.38	25PC
RKS0404+2634	HG 8−5	04 04 15	+26 34 25	33.33	11.23	7.63	11.46	9.64	1.82	9.08	33PC
RKS0406−2051	HIP 19165	04 06 35	−20 51 11	38.65	9.70	6.70	9.92	8.42	1.50	7.85	33PC
RKS0407+1413	LP 474−123	04 07 44	+14 13 25	32.10	10.79	7.18	11.03	9.21	1.82	8.56	33PC
RKS0408+1220	HIP 19325	04 08 31	+12 20 16	32.28	8.61	6.42	8.82	7.72	1.10	6.36	33PC
RKS0409+0918	HIP 19441	04 09 49	+09 18 20	27.77	10.10	7.26	10.31	8.87	1.44	7.53	XTRA
RKS0414+0301	HIP 19788	04 14 30	+03 01 19	31.88	8.78	6.49	9.02	7.85	1.16	6.53	33PC
RKS0415−0425A	HIP 19832	04 15 10	−04 25 06	28.50	9.38	6.32	9.58	8.07	1.51	6.85	XTRA
RKS0415−0739	HIP 19849	04 15 16	−07 39 10	198.57	4.42	2.50	4.63	3.60	1.03	6.12	25PC
	HIP 19948	04 16 42	−12 33 23	46.15	10.93	6.73	12.53	10.15	2.38	10.85	XTRA
RKS0417+2240	HIP 19981	04 17 07	+22 40 24	30.94	9.77	6.84	10.01	8.53	1.48	7.46	33PC
RKS0417+2033	HD 284336	04 17 27	+20 33 18	34.74	9.56	6.81	9.80	8.41	1.39	7.51	33PC
RKS0419−0408	HIP 20142	04 19 06	−04 08 56	34.15	10.51	7.14	10.76	9.04	1.72	8.42	33PC
RKS0420−1445	HIP 20232	04 20 11	−14 45 40	34.10	9.78	6.83	10.02	8.53	1.49	7.68	33PC
RKS0420−0902	HIP 20240	04 20 14	−09 02 13	29.39	9.81	7.13	10.06	8.69	1.38	7.40	XTRA

Table 1: K dwarf Sample: Astrometry and photometry data.

RKS ID	Star Name	R.A.	Decl.	π	V	K	B_G	R_G	B_G-R_G	M_{B_G}	Sample
		hh mm ss	±dd mm ss	mas	mag	mag	mag	mag	mag	mag	
RKS0421−1945	CPD−20 550	04 21 32	−19 45 23	40.64	10.40	7.11	10.68	8.99	1.69	8.73	25PC
RKS0427+2022	PM J04274+2022	04 27 25	+20 22 45	40.69	11.98	7.98	12.32	10.16	2.16	10.37	25PC
RKS0427+2426A	HIP 20834	04 27 53	+24 26 42	33.99	9.40	7.02	9.63	8.46	1.17	7.29	33PC
RKS0429+2155	HIP 20917	04 29 00	+21 55 22	88.96	8.30	4.88	8.56	6.81	1.75	8.31	25PC
RKS0430+0058	HIP 21006	04 30 17	+00 58 48	37.41	10.45	7.00	10.77	9.00	1.77	8.63	33PC
RKS0432+0006	G 82−29	04 32 56	+00 06 16	38.02	11.51	7.53	11.79	9.71	2.08	9.69	33PC
RKS0433+0338	TIC 672871302	04 33 19	+03 38 57	30.73	11.63	...	11.65	10.60	1.04	9.08	33PC
RKS0436+2707	HIP 21482	04 36 48	+27 07 56	57.10	8.10	5.24	8.36	6.98	1.38	7.14	25PC
RKS0436−1453	HIP 21489	04 36 54	−14 53 12	28.05	9.98	7.20	10.21	8.82	1.39	7.45	XTRA
RKS0439+0952A	HIP 21710	04 39 43	+09 52 19	36.80	9.19	6.51	9.42	8.11	1.30	7.25	33PC
RKS0440−0911	HIP 21765	04 40 29	−09 11 45	49.16	10.27	6.27	10.57	8.89	1.69	9.03	25PC
RKS0441+2054	HIP 21818	04 41 19	+20 54 05	75.54	8.09	5.15	8.18	6.79	1.39	7.57	25PC
RKS0443+2741	HIP 21988	04 43 35	+27 41 15	45.75	8.00	5.76	8.22	7.10	1.12	6.52	25PC
RKS0445+0938	StKM 1−508	04 45 27	+09 38 27	33.04	11.17	7.50	11.43	9.55	1.88	9.02	33PC
RKS0448−1056	HIP 22288	04 48 01	−10 56 01	37.74	9.53	6.60	9.72	8.28	1.44	7.61	33PC
RKS0449−1447	HIP 22424	04 49 33	−14 47 22	39.84	10.89	7.20	11.12	9.23	1.89	9.12	33PC
RKS0451+2837	HD 30754	04 51 33	+28 37 50	30.60	9.56	6.88	9.76	8.42	1.34	7.19	33PC
RKS0453+2214	HIP 22715	04 53 05	+22 14 07	37.87	8.78	6.29	9.04	7.80	1.23	6.93	33PC
RKS0454+0722B	HD 31208B	04 54 16	+07 22 08	33.78	8.31	6.28	8.59	7.52	1.07	6.23	XTRA
RKS0454+0722A	HD 31208	04 54 17	+07 22 23	33.75	8.23	6.18	8.43	7.39	1.04	6.07	33PC
RKS0455−2833	HIP 22907	04 55 42	−28 33 50	54.84	8.13	5.54	8.36	7.07	1.30	7.06	25PC
RKS0500−0545	HIP 23311	05 00 49	−05 45 13	113.02	6.23	3.71	6.45	5.20	1.25	6.72	25PC
	HIP 23431	05 02 10	+14 04 54	34.70	8.19	6.32	8.39	7.44	0.95	6.09	XTRA
RKS0503−2315A	HIP 23516	05 03 22	−23 15 01	43.10	9.28	5.92	9.53	7.85	1.67	7.70	25PC
RKS0503+0322	StKM 1−542	05 03 32	+03 22 57	31.38	11.08	7.74	11.51	9.70	1.81	9.00	33PC
RKS0506−1102	HD 32965	05 06 30	−11 02 35	32.70	9.55	6.83	9.83	8.44	1.39	7.40	33PC
RKS0506+1426	HIP 23786	05 06 42	+14 26 46	37.44	7.74	5.74	7.95	6.94	1.01	5.82	33PC
	HIP 24210	05 11 54	−09 06 47	34.88	8.04	6.13	8.25	7.27	0.98	5.96	XTRA
RKS0512+1943	HIP 24301	05 12 53	+19 43 20	32.44	9.93	7.07	10.06	8.71	1.34	7.61	33PC
RKS0513−2158	HIP 24392	05 14 00	−21 58 25	33.64	10.54	7.18	10.66	9.04	1.63	8.30	33PC
RKS0514+1952	HD 241814	05 14 17	+19 52 59	31.28	9.48	6.77	9.71	8.33	1.37	7.18	33PC
RKS0514+0039	HIP 24454	05 14 48	+00 39 43	34.54	9.97	6.99	10.23	8.74	1.49	7.93	33PC
RKS0518−2123	HIP 24783	05 18 47	−21 23 38	48.95	9.35	6.15	9.63	8.02	1.61	8.08	25PC
RKS0519−0304A	HIP 24819	05 19 13	−03 04 24	57.98	10.34	...	10.13	8.58	1.56	8.95	XTRA
RKS0519−0304B	HIP 24819	05 19 13	−03 04 26	63.65	7.77	5.05	8.04	6.74	1.30	7.06	25PC
RKS0519−1550	HIP 24874	05 20 00	−15 50 23	42.02	8.72	6.21	8.96	7.71	1.26	7.08	25PC
RKS0522+0236A	HIP 25119	05 22 37	+02 36 12	50.39	7.76	5.30	8.01	6.80	1.21	6.52	25PC
RKS0523+1719	HIP 25220	05 23 38	+17 19 27	68.66	7.93	5.23	8.17	6.81	1.36	7.36	25PC
RKS0526+1901	TYC 1304−408−1	05 26 06	+19 01 49	31.78	12.02	10.01	12.16	11.14	1.02	9.67	33PC
RKS0528−0329	HIP 25623	05 28 26	−03 29 58	77.30	7.65	4.88	7.88	6.50	1.38	7.32	25PC
RKS0533−2643	HIP 26013	05 33 05	−26 43 28	30.68	9.12	6.72	9.36	8.13	1.23	6.79	33PC
RKS0534−2328	HIP 26175	05 34 49	−23 28 08	36.09	8.80	6.48	9.02	7.88	1.15	6.81	33PC

Table 1: K dwarf Sample: Astrometry and photometry data.

RKS ID	Star Name	R.A.	Decl.	π	V	K	B_G	R_G	B_G-R_G	M_{B_G}	Sample
		hh mm ss	±dd mm ss	mas	mag	mag	mag	mag	mag	mag	
RKS0535+2805	HIP 26196	05 35 01	+28 05 55	30.46	10.08	7.00	10.30	8.76	1.55	7.72	33PC
RKS0536+1119A	HIP 26335	05 36 31	+11 19 40	87.44	8.94	5.27	9.12	7.30	1.83	8.83	25PC
	HIP 26844	05 41 59	+15 20 14	44.60	10.59	6.88	10.83	8.93	1.90	9.08	XTRA
RKS0542+0240	HIP 26907	05 42 46	+02 40 45	30.85	8.55	6.43	8.77	7.69	1.08	6.22	33PC
RKS0544−2225	V* AK Lep	05 44 27	−22 25 19	112.40	6.17	4.13	6.39	5.23	1.16	6.64	25PC
	HIP 27397	05 48 17	−11 08 05	35.54	10.97	7.28	11.23	9.33	1.90	8.98	XTRA
RKS0549−1734	HD 39071	05 49 23	−17 34 44	34.94	8.53	6.32	8.74	7.62	1.12	6.45	33PC
RKS0552−2246	BD−22 1252	05 52 32	−22 46 37	30.67	10.56	7.36	10.81	9.22	1.59	8.24	33PC
RKS0553−0559	HIP 27803	05 53 00	−05 59 41	49.31	9.70	6.30	9.95	8.24	1.71	8.41	25PC
RKS0554+0208	HIP 27918	05 54 29	+02 08 32	38.79	8.84	6.35	9.07	7.83	1.25	7.01	33PC
RKS0554−1942	TYC 5939−2260−1	05 54 30	−19 42 06	42.96	10.62	7.22	10.93	9.16	1.77	9.10	25PC
RKS0600+2101	HIP 28494	06 00 54	+21 01 16	34.33	10.02	7.00	10.24	8.73	1.52	7.92	33PC
RKS0602+0848	PM J06027+0848	06 02 44	+08 48 31	32.79	10.78	7.48	11.24	9.46	1.79	8.82	33PC
RKS0606−2754	HIP 28921	06 06 17	−27 54 21	27.98	8.95	6.78	9.17	8.08	1.10	6.41	XTRA
	HIP 28954	06 06 40	+15 32 32	63.37	6.75	4.82	6.97	5.98	0.99	5.98	XTRA
RKS0608+2630	HD 252023	06 08 13	+26 30 09	36.99	9.37	6.54	9.51	8.15	1.36	7.35	33PC
RKS0608+0928	HIP 29132	06 08 41	+09 28 42	28.52	10.39	7.33	10.59	9.06	1.53	7.87	XTRA
RKS0609+0540	HIP 29208	06 09 36	+05 40 08	32.98	8.45	6.27	8.68	7.59	1.09	6.27	33PC
RKS0609+0009	HD 291290	06 09 46	+00 09 33	31.91	10.85	7.23	11.05	9.23	1.82	8.57	33PC
RKS0610+0225	PM J06105+0225	06 10 31	+02 25 31	30.03	11.15	7.52	11.42	9.55	1.87	8.81	33PC
RKS0612+1023	TYC 734−1988−1	06 12 08	+10 23 39	32.02	9.72	6.88	9.98	8.53	1.44	7.50	33PC
RKS0614+0510A	HIP 29611	06 14 24	+05 10 05	32.83	8.39	6.22	8.63	7.55	1.08	6.21	33PC
RKS0616+2512	HIP 29810	06 16 40	+25 12 22	32.60	9.35	6.75	9.60	8.28	1.32	7.16	33PC
RKS0617+1759	HIP 29875	06 17 26	+17 59 21	32.35	10.26	7.17	10.56	8.97	1.59	8.11	33PC
RKS0618−1352	HIP 29958	06 18 22	−13 52 08	34.73	9.89	6.92	10.14	8.65	1.49	7.85	33PC
RKS0620+0215	HIP 30112	06 20 13	+02 15 32	37.23	9.83	6.70	10.06	8.48	1.58	7.91	33PC
RKS0621−2212	HIP 30225	06 21 33	−22 12 53	34.76	8.47	6.28	8.70	7.60	1.10	6.41	33PC
RKS0626+1845	HIP 30630	06 26 10	+18 45 25	67.73	6.75	4.27	7.02	5.81	1.21	6.18	25PC
RKS0629+2700	HIP 30893	06 29 06	+27 00 32	34.78	8.59	6.36	8.81	7.70	1.10	6.51	33PC
RKS0630−1148	HIP 30979	06 30 07	−11 48 32	36.99	9.11	6.41	9.34	7.98	1.36	7.18	33PC
RKS0630+2104	TYC 1340−1480−1	06 30 25	+21 04 17	32.43	11.29	8.73	11.74	10.41	1.33	9.29	33PC
RKS0631+0552	HIP 31069	06 31 11	+05 52 37	27.87	8.94	6.74	9.17	8.05	1.13	6.40	XTRA
RKS0632−2701	HIP 31148	06 32 09	−27 01 58	33.23	11.40	7.79	11.66	9.81	1.86	9.27	33PC
RKS0633+0527	HIP 31246	06 33 13	+05 27 47	33.81	7.91	6.00	8.15	7.13	1.02	5.80	33PC
RKS0637+1945	HIP 31626	06 37 05	+19 45 10	31.63	10.18	7.16	10.39	8.90	1.49	7.89	33PC
RKS0641+2357	HIP 32010	06 41 16	+23 57 28	57.89	8.08	5.55	8.32	7.06	1.27	7.14	25PC
RKS0647−1815	HIP 32530	06 47 16	−18 15 31	32.28	10.56	7.20	10.79	9.08	1.71	8.33	33PC
RKS0652−0510	HIP 32984	06 52 18	−05 10 25	114.30	6.58	4.11	6.82	5.53	1.29	7.11	25PC
RKS0652−2306	HIP 33037	06 53 00	−23 06 28	32.78	8.99	6.59	9.22	8.02	1.20	6.80	33PC
RKS0655−2008	* pi. CMa B	06 55 38	−20 08 00	33.62	9.75	6.83	10.05	8.57	1.47	7.68	33PC
RKS0658−1259A	HIP 33560	06 58 26	−12 59 31	44.41	9.14	6.19	9.40	7.91	1.48	7.63	25PC
RKS0700−2847	WT 1539	07 00 09	−28 47 02	46.02	10.78	7.12	11.02	9.13	1.89	9.34	25PC

Table 1: K dwarf Sample: Astrometry and photometry data.

RKS ID	Star Name	R.A.	Decl.	π	V	K	B_G	R_G	B_G-R_G	M_{B_G}	Sample
		hh mm ss	±dd mm ss	mas	mag	mag	mag	mag	mag	mag	
RKS0701−2556A	HIP 33817	07 01 14	−25 56 55	68.15	6.71	4.64	6.93	5.87	1.06	6.10	25PC
RKS0701+0655	HIP 33848	07 01 36	+06 55 37	35.48	8.16	6.15	8.38	7.34	1.04	6.13	33PC
RKS0702−0647	HIP 33955	07 02 43	−06 47 57	52.32	8.38	5.75	8.60	7.28	1.32	7.19	25PC
RKS0705+2728	HIP 34222	07 05 42	+27 28 15	43.76	10.14	6.78	10.41	8.71	1.70	8.62	25PC
RKS0706+2358	HIP 34317	07 06 52	+23 58 08	31.22	10.13	7.13	10.37	8.87	1.50	7.84	33PC
RKS0707+0326	HIP 34341	07 07 09	+03 26 51	38.26	9.84	6.67	10.07	8.47	1.60	7.99	33PC
RKS0708+2950	HIP 34414	07 08 04	+29 50 04	43.45	8.32	6.06	8.55	7.43	1.12	6.74	25PC
RKS0708−0958	HIP 34423	07 08 09	−09 58 07	35.30	8.85	6.51	9.09	7.91	1.18	6.83	33PC
RKS0710−1425	HIP 34673	07 10 50	−14 25 59	42.80	9.96	6.63	10.18	8.51	1.67	8.34	25PC
RKS0712−2453	HIP 34785	07 12 05	−24 53 31	35.13	10.37	6.89	10.60	8.84	1.76	8.33	33PC
RKS0713+2500	HIP 34950	07 13 53	+25 00 41	36.22	8.40	6.22	8.60	7.55	1.05	6.40	33PC
RKS0716−0339	HIP 35173	07 16 11	−03 39 57	30.13	9.01	6.67	9.25	8.06	1.20	6.65	33PC
RKS0718+1632	* lam Gem B	07 18 06	+16 32 34	32.87	9.94	6.93	10.23	8.74	1.48	7.81	33PC
RKS0720+2158	* del Gem B	07 20 07	+21 58 52	53.98	8.20	6.26	8.33	7.19	1.14	6.99	XTRA
RKS0723−2001	HIP 35851	07 23 29	−20 01 24	31.89	9.91	6.94	10.14	8.64	1.50	7.65	33PC
RKS0723+2024	BD+20 1790	07 23 44	+20 24 59	35.98	10.02	6.88	10.23	8.70	1.53	8.01	33PC
RKS0723+1257	HIP 35872	07 23 47	+12 57 53	41.57	8.19	5.89	8.42	7.25	1.18	6.52	25PC
RKS0724−1753	HIP 35943	07 24 34	−17 53 32	41.09	10.34	6.84	10.56	8.79	1.77	8.62	25PC
RKS0725−1041	LP 722−21	07 25 30	−10 42 00	30.13	11.56	7.92	11.81	9.95	1.86	9.21	33PC
RKS0726−1546	HIP 36121	07 26 27	−15 46 13	38.90	9.21	6.42	9.44	8.04	1.40	7.39	33PC
RKS0730−0340	G 112−24	07 30 18	−03 40 24	40.79	10.41	6.74	10.66	8.81	1.85	8.71	25PC
RKS0731+1436	HIP 36551	07 31 08	+14 36 51	48.19	8.94	6.13	9.18	7.79	1.38	7.59	25PC
RKS0732+1719	HIP 36637	07 32 03	+17 19 10	37.24	10.95	7.32	11.21	9.36	1.84	9.06	33PC
RKS0732−0853	HIP 36642	07 32 07	−08 53 02	34.83	10.30	7.29	10.60	9.06	1.53	8.31	33PC
RKS0734−0653	HIP 36827	07 34 26	−06 53 48	42.53	8.16	6.02	8.38	7.30	1.08	6.52	25PC
RKS0739−0335	HIP 37349	07 40 00	−03 35 51	70.92	7.18	4.88	7.40	6.25	1.15	6.66	25PC
RKS0740−0336	BD−03 2002	07 40 03	−03 36 13	71.08	8.87	5.57	9.17	7.47	1.71	8.43	XTRA
RKS0741−2921	TYC 6552−2083−1	07 41 17	−29 21 33	33.00	10.68	7.28	10.92	9.18	1.74	8.51	33PC
RKS0745+0208	HIP 37798	07 45 01	+02 08 15	37.58	10.19	6.77	10.42	8.72	1.71	8.30	33PC
RKS0752+2555	HD 63991	07 52 47	+25 55 35	45.71	8.61	6.05	8.82	7.55	1.27	7.12	25PC
RKS0752+2233	HIP 38492	07 53 00	+22 33 23	29.38	10.94	7.60	11.21	9.49	1.72	8.55	XTRA
RKS0754−2518	HIP 38594	07 54 11	−25 18 11	56.19	9.75	6.17	9.98	8.18	1.80	8.73	25PC
RKS0754−0124A	HIP 38625	07 54 34	−01 24 44	57.43	7.43	5.42	7.63	6.65	0.98	6.42	25PC
RKS0754+1914	HIP 38657	07 54 54	+19 14 11	50.34	7.76	5.45	7.99	6.83	1.16	6.50	25PC
RKS0755−1529	HIP 38702	07 55 24	−15 29 53	27.71	10.99	7.66	11.41	9.61	1.80	8.62	XTRA
RKS0757−0048	HIP 38931	07 57 58	−00 48 52	56.65	8.05	5.51	8.31	7.04	1.26	7.07	25PC
RKS0758−2537	HIP 38939	07 58 04	−25 37 36	54.10	8.42	5.83	8.66	7.37	1.29	7.32	25PC
RKS0758−1501A	HIP 38969	07 58 26	−15 01 14	31.14	9.31	6.53	9.54	8.16	1.37	7.00	33PC
	HIP 38992	07 58 50	+10 07 47	32.38	8.12	6.18	8.32	7.34	0.98	5.88	XTRA
RKS0759+2050	HIP 39064	07 59 34	+20 50 38	42.54	7.68	5.64	7.89	6.87	1.02	6.04	25PC
	HIP 39068	07 59 36	+12 59 00	29.36	8.34	6.46	8.54	7.57	0.97	5.88	XTRA
	HIP 39157	08 00 32	+29 12 44	58.48	7.00	5.09	7.17	6.24	0.94	6.01	XTRA

Table 1: K dwarf Sample: Astrometry and photometry data.

RKS ID	Star Name	R.A.	Decl.	π	V	K	B_G	R_G	B_G-R_G	M_{B_G}	Sample
		hh mm ss	±dd mm ss	mas	mag	mag	mag	mag	mag	mag	
RKS0804+1217	HD 66509C	08 04 23	+12 17 19	32.60	11.23	6.92	11.51	9.71	1.80	9.08	33PC
RKS0808+2106	HIP 39826	08 08 13	+21 06 18	56.00	9.41	6.08	9.68	7.98	1.70	8.42	25PC
RKS0813−1355A	HIP 40239	08 13 08	−13 55 01	38.94	9.38	5.82	9.77	7.96	1.81	7.72	33PC
RKS0813−1355B	BD−13 2439B	08 13 09	−13 55 01	48.03	10.28	...	9.75	8.08	1.67	8.16	XTRA
RKS0814+1301	HIP 40375	08 14 36	+13 01 22	52.12	8.79	5.89	9.03	7.58	1.45	7.61	25PC
RKS0815−2600	HIP 40459	08 15 40	−26 00 36	34.88	10.10	6.88	10.35	8.72	1.63	8.07	33PC
RKS0817+1717	LSPM J0817+1717	08 17 08	+17 17 57	35.22	9.44	6.73	9.71	8.32	1.39	7.44	33PC
RKS0818−1512A	HIP 40724	08 18 44	−15 12 08	28.85	9.82	6.86	10.07	8.60	1.47	7.37	XTRA
RKS0819+0120	HIP 40774	08 19 19	+01 20 20	44.66	8.35	6.11	8.58	7.45	1.13	6.83	25PC
RKS0820+1404	HIP 40910	08 20 55	+14 04 17	44.02	9.80	6.58	10.00	8.39	1.61	8.22	25PC
RKS0823+2150	HIP 41130	08 23 31	+21 50 58	39.73	9.52	6.55	9.73	8.27	1.46	7.73	33PC
RKS0827+2855	HIP 41443	08 27 11	+28 55 53	32.19	9.63	6.89	9.85	8.48	1.36	7.39	33PC
RKS0832−2323	BD−22 2311	08 32 33	−23 23 07	35.57	10.17	6.94	10.40	8.78	1.63	8.16	33PC
	HIP 42074	08 34 32	−00 43 34	47.40	7.32	5.42	7.53	6.55	0.98	5.91	XTRA
RKS0838−0415	G 114−7	08 38 19	−04 15 29	31.84	11.28	7.77	11.69	9.80	1.89	9.20	33PC
RKS0838−1315	HIP 42401	08 38 45	−13 15 24	31.65	9.67	6.95	9.91	8.55	1.36	7.41	33PC
RKS0839+0657	HIP 42418	08 39 00	+06 57 20	36.67	7.90	5.62	8.12	6.99	1.13	5.94	33PC
RKS0839+1131	HIP 42499	08 39 51	+11 31 22	54.16	7.63	5.44	7.82	6.75	1.06	6.49	25PC
RKS0840−0628A	HIP 42507	08 40 00	−06 28 33	38.80	9.90	6.38	10.12	8.35	1.77	8.06	33PC
RKS0848+0628	HIP 43233	08 48 26	+06 28 06	35.12	10.35	6.99	10.67	9.04	1.63	8.39	33PC
RKS0850+0751	HIP 43422	08 50 42	+07 51 52	56.19	9.76	5.60	9.31	7.63	1.68	8.06	25PC
RKS0852+2819	HIP 43587	08 52 36	+28 19 51	79.43	5.95	4.01	6.17	5.16	1.01	5.67	25PC
RKS0854−2423	HIP 43771	08 54 57	−24 23 39	29.69	8.66	6.46	8.90	7.76	1.14	6.26	XTRA
RKS0855+0132	HIP 43790	08 55 08	+01 32 47	48.69	9.99	6.35	10.21	8.37	1.84	8.64	25PC
RKS0858+2032	HIP 44072	08 58 38	+20 32 48	47.55	9.22	...	9.46	8.01	1.45	7.85	25PC
RKS0859+0151A	HIP 44109	08 59 02	+01 51 54	24.43	11.35	...	11.16	9.73	1.43	8.10	XTRA
RKS0900+2127	HIP 44259	09 00 47	+21 27 13	30.51	8.78	6.64	8.99	7.92	1.06	6.41	33PC
RKS0901+1515B	HIP 44295	09 01 17	+15 15 52	54.28	9.73	6.05	9.72	8.06	1.66	8.39	XTRA
RKS0901+1515A	HIP 44295	09 01 17	+15 15 57	54.13	9.34	5.94	9.50	7.91	1.59	8.17	25PC
RKS0904−1554	HIP 44526	09 04 21	−15 54 51	36.52	8.77	6.39	8.99	7.80	1.20	6.81	33PC
RKS0905+2517	BD+25 2037	09 05 18	+25 17 53	34.61	10.35	7.30	10.76	9.14	1.61	8.46	33PC
	HIP 44722	09 06 45	−08 48 25	68.89	9.50	5.76	9.74	7.85	1.90	8.93	XTRA
RKS0907+2252	HD 78141	09 07 18	+22 52 22	39.53	7.98	5.78	8.23	7.12	1.11	6.21	33PC
RKS0909+2725	HIP 44920	09 09 03	+27 25 55	29.61	10.26	7.20	10.50	8.95	1.55	7.85	XTRA
RKS0909+0512	HD 78727	09 09 54	+05 12 13	38.27	8.36	6.07	8.61	7.42	1.19	6.52	33PC
RKS0914+0426A	HIP 45383	09 14 54	+04 26 34	56.18	7.91	5.25	8.18	6.87	1.31	6.93	25PC
RKS0917−0323	HIP 45621	09 17 55	−03 23 14	30.64	7.78	5.72	7.99	6.95	1.04	5.42	33PC
RKS0918+2718	BD+27 1739	09 18 22	+27 18 42	47.65	9.54	6.24	9.77	8.11	1.66	8.16	25PC
RKS0919+0053	HIP 45737	09 19 28	+00 53 49	34.99	8.15	6.04	8.36	7.30	1.06	6.08	33PC
RKS0920−0545	HIP 45839	09 20 44	−05 45 14	41.36	9.10	6.27	9.33	7.92	1.41	7.41	25PC
RKS0929−0245	* tau01 Hya B	09 29 09	−02 45 03	55.37	7.18	5.14	7.41	6.36	1.04	6.12	25PC
RKS0929−0522	HIP 46549	09 29 35	−05 22 22	41.36	9.74	6.52	9.99	8.38	1.61	8.07	25PC

Table 1: K dwarf Sample: Astrometry and photometry data.

RKS ID	Star Name	R.A.	Decl.	π	V	K	B_G	R_G	B_G-R_G	M_{B_G}	Sample
		hh mm ss	±dd mm ss	mas	mag	mag	mag	mag	mag	mag	
RKS0929+0539	HIP 46580	09 29 55	+05 39 18	78.23	7.20	4.79	7.44	6.23	1.21	6.91	25PC
RKS0932+2909	StKM 1−780	09 32 11	+29 09 26	31.89	11.43	7.81	11.71	9.83	1.89	9.23	33PC
RKS0932−1111	HIP 46816	09 32 26	−11 11 05	54.67	7.82	5.45	8.01	6.87	1.15	6.70	25PC
	HIP 46843	09 32 44	+26 59 19	55.32	7.00	5.12	7.27	6.29	0.98	5.99	XTRA
RKS0937+2241	HIP 47201	09 37 11	+22 41 39	44.35	9.48	6.34	9.67	8.10	1.57	7.90	25PC
RKS0937+2231A	HIP 47261	09 37 58	+22 31 23	32.14	9.93	6.85	10.14	8.63	1.51	7.67	33PC
RKS0938+0240	HIP 47307	09 38 24	+02 40 36	33.47	11.90	8.28	12.15	10.23	1.92	9.78	33PC
RKS0947+0134	HIP 48016	09 47 17	+01 34 37	33.39	10.97	7.56	11.18	9.47	1.71	8.80	33PC
RKS0947+2618	HIP 48024	09 47 22	+26 18 13	29.43	10.86	7.34	11.09	9.31	1.79	8.44	XTRA
RKS0952+0313	HIP 48411	09 52 11	+03 13 19	48.69	8.86	5.96	9.11	7.64	1.47	7.55	25PC
RKS0952+0307	HIP 48447	09 52 39	+03 07 49	37.21	10.57	7.08	10.81	9.03	1.78	8.66	33PC
RKS0959−0911	HIP 48953	09 59 11	−09 11 00	30.25	9.88	7.14	10.11	8.75	1.36	7.51	33PC
RKS1000+2433	HIP 49018	10 00 02	+24 33 10	32.10	7.86	5.44	8.25	7.02	1.23	5.78	33PC
RKS1001−1525	HIP 49127	10 01 37	−15 25 29	39.62	8.65	6.21	8.89	7.66	1.23	6.88	33PC
RKS1004−1143	HIP 49366	10 04 38	−11 43 47	42.94	8.15	5.99	8.38	7.28	1.10	6.55	25PC
RKS1005+2629	HIP 49429	10 05 27	+26 29 16	32.77	9.12	6.65	9.35	8.10	1.25	6.92	33PC
RKS1006+0257A	HIP 49544	10 06 57	+02 57 52	45.26	10.02	6.39	10.20	8.44	1.76	8.48	25PC
RKS1008+1159	HD 87884	10 08 13	+11 59 49	41.21	8.14	5.88	8.37	7.29	1.07	6.44	25PC
RKS1011−2425	WT 1757	10 11 45	−24 25 34	33.97	11.04	7.32	11.28	9.42	1.86	8.94	33PC
RKS1020−0128	HIP 50657	10 20 43	−01 28 11	31.17	9.41	6.76	9.65	8.32	1.33	7.12	33PC
RKS1021−1743A	HIP 50696	10 21 08	−17 43 38	37.02	11.27	7.40	11.51	9.53	1.98	9.35	33PC
	HIP 50782	10 22 09	+11 18 37	36.85	7.78	5.91	8.00	7.03	0.97	5.83	XTRA
RKS1024−1024	HIP 50944	10 24 15	−10 24 21	34.36	9.98	6.92	10.22	8.71	1.52	7.90	33PC
RKS1026−0631	HIP 51127	10 26 41	−06 31 35	33.08	9.76	7.20	9.99	8.74	1.25	7.58	33PC
RKS1026+2638	HIP 51157	10 27 00	+26 38 29	32.46	8.23	6.26	8.46	7.44	1.02	6.01	33PC
RKS1028+0644	HIP 51254	10 28 10	+06 44 06	38.21	8.53	6.26	8.76	7.62	1.14	6.68	33PC
RKS1030−2114	HIP 51443	10 30 22	−21 14 12	34.00	9.64	6.82	9.86	8.44	1.42	7.52	33PC
RKS1032+0830A	HIP 51571	10 32 01	+08 30 38	33.88	10.79	7.23	11.05	9.24	1.81	8.70	33PC
RKS1036−1350	HIP 51931	10 36 31	−13 50 36	31.36	8.71	6.57	8.93	7.83	1.10	6.41	33PC
RKS1043−2903	HIP 52462	10 43 28	−29 03 51	46.43	7.72	5.66	7.95	6.89	1.06	6.29	25PC
RKS1046−2435	HIP 52708	10 46 37	−24 35 08	47.06	9.37	6.44	9.61	8.16	1.45	7.97	25PC
RKS1047+2129	HIP 52765	10 47 19	+21 29 51	29.72	10.12	7.16	10.36	8.88	1.48	7.72	XTRA
RKS1047−2217	HIP 52776	10 47 25	−22 17 12	29.76	9.91	7.12	10.16	8.75	1.41	7.53	XTRA
RKS1053−1422	HIP 53236	10 53 23	−14 22 28	30.90	9.27	6.79	9.49	8.26	1.23	6.94	33PC
RKS1054−0432	StKM 1−896	10 54 49	−04 32 31	35.45	10.39	7.08	10.81	9.05	1.76	8.55	33PC
RKS1056+0723	HIP 53486	10 56 31	+07 23 19	57.76	7.37	5.20	7.60	6.49	1.11	6.41	25PC
RKS1057+2856	HIP 53541	10 57 11	+28 56 17	35.93	8.94	6.40	9.18	7.90	1.27	6.95	33PC
RKS1059+1759	HIP 53731	10 59 35	+17 59 58	31.08	8.85	6.30	9.04	7.80	1.24	6.50	33PC
RKS1059+2526A	HD 95174A	10 59 38	+25 26 15	46.91	8.45	5.84	8.70	7.44	1.26	7.05	25PC
RKS1059+2526B	HD 95174B	10 59 39	+25 26 14	46.91	9.09	5.98	9.27	7.83	1.44	7.63	XTRA
RKS1102−0919A	HIP 54002	11 02 50	−09 19 49	32.07	9.03	6.64	9.24	8.05	1.19	6.77	33PC
RKS1105+0720	* chi Leo B	11 05 01	+07 20 10	34.37	11.06	...	11.23	9.48	1.75	8.91	33PC

Table 1: K dwarf Sample: Astrometry and photometry data.

RKS ID	Star Name	R.A.	Decl.	π	V	K	B_G	R_G	B_G-R_G	M_{B_G}	Sample
		hh mm ss	±dd mm ss	mas	mag	mag	mag	mag	mag	mag	
RKS1108−2816A	HIP 54418	11 08 06	−28 16 05	36.84	9.32	6.13	9.56	7.98	1.58	7.39	33PC
RKS1108+1546	HIP 54459	11 08 32	+15 46 03	35.48	9.75	6.82	9.96	8.54	1.42	7.71	33PC
	HIP 54513	11 09 12	−04 36 25	41.22	11.22	7.33	11.47	9.46	2.01	9.54	XTRA
RKS1111−1057	HIP 54651	11 11 11	−10 57 03	50.33	9.23	6.33	9.45	8.04	1.41	7.96	25PC
RKS1111−1459A	HIP 54677	11 11 33	−14 59 29	45.41	9.06	5.87	9.27	7.72	1.56	7.56	25PC
	HIP 54803	11 13 10	+00 14 17	41.49	10.33	6.62	10.55	8.66	1.89	8.64	XTRA
RKS1113+0428	HIP 54810	11 13 13	+04 28 56	54.46	8.70	5.85	8.95	7.50	1.45	7.63	25PC
RKS1114+2542	HIP 54906	11 14 33	+25 42 37	46.35	7.76	5.73	7.97	6.95	1.02	6.30	25PC
RKS1114−2306	HIP 54922	11 14 48	−23 06 18	43.27	9.02	6.03	9.27	7.87	1.40	7.45	25PC
RKS1115−1808B	HIP 54963	11 15 19	−18 08 40	43.56	10.26	6.65	10.27	8.55	1.73	8.47	XTRA
RKS1115−1808A	HIP 54966	11 15 21	−18 08 37	43.59	10.23	6.60	10.19	8.49	1.70	8.39	25PC
RKS1116−1441	HIP 55066	11 16 22	−14 41 36	54.73	10.00	6.46	10.23	8.43	1.80	8.92	25PC
RKS1117−2748	HIP 55119	11 17 08	−27 48 49	56.61	9.77	6.20	10.01	8.20	1.80	8.77	25PC
RKS1117−0158	HIP 55132	11 17 14	−01 58 55	30.10	9.73	6.96	10.00	8.59	1.41	7.39	33PC
RKS1121−2027	HIP 55454	11 21 27	−20 27 14	76.42	8.57	5.30	8.93	7.27	1.66	8.35	25PC
RKS1121+1811	HIP 55486	11 21 49	+18 11 24	30.79	7.93	6.03	8.20	7.21	1.00	5.65	33PC
RKS1123+0701A	HIP 55605	11 23 30	+07 01 30	31.23	10.37	7.04	10.61	8.96	1.65	8.08	33PC
RKS1124−1741	HIP 55705	11 24 53	−17 41 03	37.58	8.81	...	9.06	7.84	1.22	6.94	33PC
RKS1125+2000	HIP 55772	11 25 40	+20 00 08	31.71	8.34	6.35	8.55	7.53	1.02	6.06	33PC
RKS1126+0300B	HIP 55848	11 26 46	+03 00 23	54.91	7.57	5.26	7.81	6.62	1.18	6.50	XTRA
RKS1126+1517	BD+16 2260	11 26 50	+15 17 38	37.88	10.49	6.97	10.68	8.94	1.74	8.57	33PC
RKS1127+0358A	HIP 55915	11 27 39	+03 58 36	34.90	10.61	6.99	10.90	9.05	1.84	8.61	33PC
RKS1128+0731	HIP 55988	11 28 28	+07 31 02	35.29	10.21	7.06	10.42	8.87	1.55	8.15	33PC
RKS1131+1422	* 88 Leo B	11 31 44	+14 22 06	42.30	7.54	6.37	9.42	7.99	1.43	7.55	25PC
RKS1134−1314	HIP 56489	11 34 50	−13 14 31	33.03	10.38	7.33	10.58	9.06	1.51	8.17	33PC
RKS1135+2436A	HIP 56570	11 35 49	+24 36 43	28.65	9.34	6.87	9.57	8.35	1.21	6.85	XTRA
RKS1135+1658	HIP 56578	11 36 00	+16 58 06	31.24	9.52	6.84	9.81	8.48	1.33	7.28	33PC
RKS1139−2741	HIP 56838	11 39 08	−27 41 46	33.39	10.00	6.91	10.21	8.71	1.50	7.83	33PC
RKS1141+0508A	HIP 57058	11 41 50	+05 08 26	32.26	9.59	6.42	9.82	8.26	1.57	7.37	33PC
RKS1142+2301	HIP 57099	11 42 18	+23 01 37	32.57	11.58	7.80	11.82	9.87	1.95	9.39	33PC
	HIP 57370	11 45 42	+02 49 17	34.06	8.07	6.15	8.29	7.30	0.99	5.95	XTRA
RKS1147−1149A	HIP 57494	11 47 04	−11 49 27	38.63	9.03	6.19	9.28	7.88	1.39	7.21	33PC
RKS1152+1845	HIP 57866	11 52 08	+18 45 19	37.40	8.40	6.27	8.62	7.55	1.07	6.49	33PC
RKS1154+2844	HIP 58099	11 54 57	+28 44 15	36.38	10.49	7.00	10.74	8.96	1.77	8.54	33PC
RKS1157−2608	HIP 58293	11 57 16	−26 08 29	38.91	8.93	6.41	9.17	7.91	1.26	7.12	33PC
RKS1157+1959	HIP 58314	11 57 29	+19 59 02	35.91	8.07	6.09	8.28	7.26	1.02	6.06	33PC
RKS1157−2742	HIP 58345	11 57 56	−27 42 25	98.19	6.99	4.53	7.20	5.85	1.36	7.16	25PC
RKS1158−2355	HIP 58374	11 58 12	−23 55 26	37.71	8.70	6.31	8.94	7.72	1.22	6.82	33PC
RKS1158−2535	PM J11588−2535	11 58 51	−25 35 09	34.55	11.16	7.43	11.41	9.52	1.89	9.10	33PC
RKS1159−2021	HIP 58451	11 59 10	−20 21 14	49.08	7.92	5.61	8.15	6.98	1.16	6.60	25PC
RKS1204+0911	HIP 58863	12 04 17	+09 11 35	30.51	9.85	7.06	10.09	8.72	1.37	7.51	33PC
RKS1204−0013	HIP 58908	12 04 48	−00 13 36	34.63	10.79	8.18	11.05	9.74	1.31	8.75	33PC

Table 1: K dwarf Sample: Astrometry and photometry data.

RKS ID	Star Name	R.A.	Decl.	π	V	K	B_G	R_G	B_G-R_G	M_{B_G}	Sample
		hh mm ss	±dd mm ss	mas	mag	mag	mag	mag	mag	mag	
	HIP 58949	12 05 13	−01 30 33	30.76	8.16	6.32	8.37	7.42	0.95	5.81	XTRA
RKS1205−1852	HIP 59000	12 05 51	−18 52 31	42.72	9.99	6.62	10.23	8.52	1.71	8.38	25PC
RKS1206−2336	HD 105110	12 06 09	−23 36 09	31.40	8.58	6.53	8.82	7.76	1.06	6.31	33PC
RKS1208−0028	HIP 59198	12 08 22	−00 28 57	34.06	11.25	7.59	11.49	9.61	1.88	9.15	33PC
RKS1209−2646	PM J12093−2646	12 09 23	−26 46 47	32.30	11.01	7.40	11.25	9.43	1.82	8.80	33PC
RKS1209−1151	HD 105590B	12 09 29	−11 51 25	40.36	9.59	6.54	9.89	8.34	1.55	7.92	25PC
RKS1210−1126	LP 734−35	12 10 34	−11 27 00	32.27	11.32	7.65	11.39	9.62	1.77	8.93	33PC
RKS1215+0538A	HIP 59816	12 15 58	+05 38 25	28.65	9.45	6.47	9.95	8.50	1.45	7.24	XTRA
RKS1220−1953	HIP 60207	12 20 47	−19 53 46	33.92	8.99	6.59	9.24	8.02	1.22	6.90	33PC
	HIP 60343	12 22 21	+25 10 12	35.89	11.35	7.60	11.54	9.64	1.90	9.32	XTRA
RKS1222+0518	HIP 60352	12 22 32	+05 18 39	33.28	10.47	6.74	9.65	8.30	1.35	7.26	33PC
RKS1222+2736	HIP 60357	12 22 34	+27 36 17	33.86	10.89	7.22	11.11	9.25	1.85	8.76	33PC
RKS1223+2754	HIP 60448	12 23 35	+27 54 48	33.82	11.33	7.67	11.55	9.69	1.86	9.19	33PC
RKS1227+2701	HIP 60759	12 27 14	+27 01 29	36.47	8.91	5.74	9.02	7.79	1.23	6.83	33PC
RKS1228−1654	HIP 60853	12 28 19	−16 54 40	36.68	9.45	6.90	9.67	8.43	1.25	7.50	33PC
RKS1228−1817	HIP 60866	12 28 32	−18 17 50	42.00	9.24	6.29	9.47	7.99	1.48	7.59	25PC
RKS1229−1631	* del Crv B	12 29 51	−16 31 15	37.45	10.91	6.24	8.67	7.55	1.12	6.54	33PC
RKS1230−1323	HIP 60994	12 30 05	−13 23 34	41.33	9.20	...	9.17	7.84	1.33	7.26	XTRA
RKS1231+2013	HIP 61099	12 31 18	+20 13 04	37.94	7.91	5.90	8.13	7.10	1.03	6.02	33PC
RKS1233−1438	HIP 61329	12 34 00	−14 38 19	37.96	9.10	6.44	9.35	7.99	1.36	7.25	33PC
RKS1241+1522	HIP 61901	12 41 06	+15 22 36	70.89	7.91	5.08	8.15	6.76	1.38	7.40	25PC
RKS1241+1951	HIP 61939	12 41 37	+19 51 05	30.95	9.07	6.74	9.32	8.15	1.17	6.77	33PC
RKS1248−2448B	HIP 62471	12 48 10	−24 48 17	53.38	9.90	6.49	10.17	8.42	1.75	8.81	XTRA
RKS1248−2448A	HIP 62472	12 48 11	−24 48 24	53.38	8.90	6.03	9.13	7.70	1.43	7.76	25PC
RKS1248−1543A	HIP 62505	12 48 32	−15 43 10	39.21	7.93	5.58	8.11	6.96	1.15	6.08	33PC
RKS1250−0046	HIP 62687	12 50 44	−00 46 05	93.88	8.51	4.88	8.72	6.91	1.81	8.59	25PC
RKS1253+0645	HIP 62942	12 53 54	+06 45 46	36.53	8.24	6.15	8.46	7.41	1.05	6.27	33PC
RKS1256−2455	HIP 63157	12 56 30	−24 55 32	32.15	10.04	7.01	10.28	8.75	1.53	7.82	33PC
RKS1257−1427	HIP 63257	12 57 44	−14 27 48	39.00	9.11	6.43	9.40	8.04	1.35	7.35	33PC
RKS1259−0950	HIP 63366	12 59 02	−09 50 03	46.44	7.54	5.53	7.76	6.75	1.01	6.09	25PC
RKS1300−0242	HIP 63467	13 00 17	−02 42 17	36.69	9.78	6.77	10.01	8.50	1.51	7.84	33PC
RKS1302−2647	HIP 63618	13 02 21	−26 47 14	56.40	8.35	5.26	8.59	7.07	1.53	7.35	25PC
RKS1303−0509	HIP 63742	13 03 50	−05 09 43	48.88	7.69	5.51	7.89	6.81	1.08	6.34	25PC
RKS1306+2043A	HIP 63942	13 06 15	+20 43 45	50.90	9.44	6.04	9.73	8.01	1.72	8.26	25PC
RKS1310+0932	HIP 64262	13 10 17	+09 32 10	36.07	9.31	6.69	9.54	8.24	1.30	7.33	33PC
RKS1312−0215	HIP 64457	13 12 44	−02 15 54	47.45	7.56	5.47	7.80	6.73	1.07	6.18	25PC
RKS1316+1701	HIP 64797	13 16 51	+17 01 02	91.03	6.50	4.38	6.78	5.67	1.11	6.58	25PC
RKS1318−1446	HIP 64895	13 18 06	−14 46 48	34.30	10.88	7.50	11.11	9.40	1.72	8.79	33PC
RKS1320+0407	HIP 65121	13 20 44	+04 07 59	32.99	8.58	6.39	8.83	7.70	1.13	6.42	33PC
RKS1323+2914A	HIP 65343	13 23 33	+29 14 15	55.12	8.88	5.45	9.59	7.82	1.77	8.29	25PC
RKS1323+2914B	HD 116495B	13 23 33	+29 14 15	55.34	9.74	...	9.96	8.21	1.75	8.67	XTRA
RKS1323+0243A	HIP 65352	13 23 39	+02 43 24	60.25	7.07	5.10	7.27	6.28	0.99	6.17	25PC

Table 1: K dwarf Sample: Astrometry and photometry data.

RKS ID	Star Name	R.A.	Decl.	π	V	K	B_G	R_G	B_G-R_G	M_{B_G}	Sample
		hh mm ss	±dd mm ss	mas	mag	mag	mag	mag	mag	mag	
RKS1323+0243B	HIP 65355	13 23 41	+02 43 31	60.34	7.36	5.23	7.57	6.52	1.06	6.48	XTRA
RKS1326−2417	HIP 65574	13 26 40	−24 17 36	33.34	8.77	6.56	9.02	7.89	1.13	6.63	XTRA
RKS1327−2417	HIP 65602	13 27 03	−24 17 26	33.52	8.72	6.45	8.95	7.83	1.12	6.58	33PC
RKS1331−0219	HIP 65982	13 31 40	−02 19 03	37.76	7.32	5.31	7.54	6.54	1.00	5.42	33PC
RKS1333+0835	HIP 66147	13 33 32	+08 35 12	55.39	7.98	5.49	8.20	6.95	1.25	6.92	25PC
RKS1334−0018	HIP 66212	13 34 16	−00 18 50	37.11	7.37	5.25	7.87	6.86	1.01	5.71	33PC
RKS1334+0440	HIP 66222	13 34 22	+04 40 03	48.93	9.95	6.34	10.18	8.36	1.82	8.63	25PC
RKS1334−0820	HIP 66252	13 34 43	−08 20 31	48.73	9.24	6.12	9.42	7.92	1.50	7.86	25PC
RKS1335+0650	HIP 66283	13 35 06	+06 50 28	32.16	8.90	6.49	9.14	7.92	1.22	6.68	33PC
RKS1335−0023	BD+00 3077	13 35 25	−00 23 21	51.94	10.28	6.66	10.51	8.66	1.85	9.09	25PC
RKS1336+0746	HIP 66413	13 36 57	+07 46 01	31.77	10.00	7.19	10.21	8.83	1.38	7.72	33PC
RKS1338−0614	HIP 66587	13 38 59	−06 14 12	41.30	10.72	7.06	10.97	9.08	1.89	9.05	25PC
RKS1340−0411	HIP 66675	13 40 07	−04 11 10	66.33	9.61	6.04	9.84	8.03	1.81	8.95	25PC
RKS1341−0007	HIP 66840	13 41 56	−00 07 45	40.45	9.76	6.49	9.98	8.35	1.64	8.02	25PC
RKS1342−0141	HIP 66886	13 42 26	−01 41 11	40.67	9.24	6.33	9.46	8.01	1.45	7.50	25PC
RKS1345+1747	HIP 67090	13 45 05	+17 47 08	77.45	9.79	6.22	10.02	8.19	1.83	9.47	25PC
RKS1345−0437	HIP 67092	13 45 05	−04 37 13	33.99	10.54	7.20	10.77	9.09	1.68	8.43	33PC
RKS1345+0850	HIP 67105	13 45 15	+08 50 10	45.25	8.47	5.97	8.72	7.45	1.27	7.00	25PC
RKS1346−0027	HIP 67211	13 46 19	−00 27 29	28.69	9.31	6.91	9.55	8.37	1.18	6.84	XTRA
RKS1347+0618	HIP 67291	13 47 29	+06 18 56	31.92	10.02	7.01	10.24	8.75	1.49	7.76	33PC
RKS1347+2127	HIP 67309	13 47 42	+21 27 38	33.40	11.11	7.34	11.38	9.50	1.88	9.00	33PC
	HIP 67344	13 48 10	−10 47 20	29.22	8.32	6.43	8.53	7.54	0.99	5.86	XTRA
RKS1349+2658A	HIP 67422	13 49 04	+26 58 48	73.92	7.03	6.33	7.79	6.48	1.31	7.13	25PC
RKS1349+2658B	HD 120476B	13 49 04	+26 58 44	74.20	7.96	4.42	8.23	6.79	1.43	7.58	XTRA
RKS1349−2206	HIP 67487	13 49 45	−22 06 40	71.12	8.16	5.16	8.41	6.89	1.52	7.67	25PC
RKS1353+2748	HIP 67773	13 53 05	+27 48 24	33.90	8.36	6.35	8.58	7.56	1.02	6.23	33PC
RKS1353+1256A	HIP 67808	13 53 28	+12 56 33	45.62	9.78	6.15	10.02	8.17	1.84	8.31	25PC
RKS1359+2252	HIP 68337	13 59 19	+22 52 11	42.02	9.05	6.24	9.29	7.87	1.41	7.40	25PC
RKS1401+1529	HIP 68551	14 01 59	+15 29 39	33.84	10.62	6.90	11.34	9.51	1.83	8.99	33PC
RKS1411−1236	HIP 69357	14 11 46	−12 36 42	43.44	7.93	5.86	8.15	7.08	1.08	6.34	25PC
RKS1412+2348A	HIP 69410	14 12 42	+23 48 52	31.83	8.88	6.44	9.13	7.92	1.21	6.64	33PC
RKS1413−0657	HIP 69485	14 13 31	−06 57 32	54.68	10.14	6.57	10.40	8.56	1.83	9.08	25PC
RKS1414−1521	HIP 69562	14 14 21	−15 21 22	34.53	10.23	6.60	10.50	8.76	1.74	8.19	33PC
RKS1416+2007	HIP 69751	14 16 33	+20 07 15	30.10	8.42	5.65	8.68	7.68	0.99	6.07	33PC
RKS1418−0636A	HIP 69962	14 18 58	−06 36 13	44.38	9.10	5.85	9.35	7.71	1.64	7.58	25PC
RKS1419−2548	HD 125276B	14 19 01	−25 48 57	54.08	10.91	...	10.33	9.06	1.27	9.00	XTRA
RKS1419−0509	HIP 70016	14 19 35	−05 09 04	48.86	7.58	5.54	7.80	6.76	1.05	6.25	25PC
RKS1421+2937	HIP 70218	14 21 57	+29 37 47	68.86	8.56	5.42	8.77	7.20	1.57	7.96	25PC
RKS1424−1727A	HIP 70472	14 24 50	−17 27 08	29.38	10.71	7.28	10.94	9.25	1.68	8.28	XTRA
	HIP 70529	14 25 43	+23 37 01	61.18	9.77	5.97	9.98	8.06	1.93	8.91	XTRA
RKS1430−0838	HIP 70956	14 30 48	−08 38 47	63.36	9.40	5.77	9.63	7.81	1.83	8.64	25PC
RKS1432+1121	HIP 71086	14 32 13	+11 21 12	33.06	9.69	6.51	9.91	8.34	1.57	7.50	33PC

Table 1: K dwarf Sample: Astrometry and photometry data.

RKS ID	Star Name	R.A.	Decl.	π	V	K	B_G	R_G	B_G-R_G	M_{B_G}	Sample
		hh mm ss	±dd mm ss	mas	mag	mag	mag	mag	mag	mag	
RKS1433+0920	HIP 71190	14 33 35	+09 20 04	31.04	8.82	6.59	9.05	7.93	1.12	6.51	33PC
RKS1436+0944	HIP 71395	14 36 01	+09 44 47	61.21	7.48	5.14	7.70	6.53	1.17	6.64	25PC
RKS1437−2548	HIP 71481	14 37 05	−25 48 09	38.21	8.29	6.00	8.51	7.34	1.17	6.42	33PC
RKS1442+1930	HIP 71904	14 42 26	+19 30 13	42.24	10.08	6.66	10.26	8.56	1.70	8.39	25PC
	HIP 71914	14 42 34	+19 28 47	44.54	9.10	5.82	...	...	...	...	XTRA
RKS1444+2211	HIP 72044	14 44 12	+22 11 07	36.59	9.89	6.90	10.12	8.63	1.49	7.94	33PC
RKS1444−2215	HD 129715	14 44 36	−22 15 11	32.90	9.28	6.57	9.54	8.14	1.39	7.12	33PC
RKS1445+1350	HIP 72146	14 45 24	+13 50 47	53.16	7.87	5.61	8.09	6.97	1.13	6.72	25PC
RKS1446+2730	HIP 72200	14 46 03	+27 30 44	37.78	7.98	5.98	8.19	7.15	1.04	6.08	33PC
RKS1446+1629	HIP 72237	14 46 23	+16 29 48	56.32	9.26	6.06	9.48	7.90	1.58	8.23	25PC
RKS1447+0242	HIP 72312	14 47 16	+02 42 12	51.57	7.76	5.62	8.00	6.90	1.10	6.56	25PC
RKS1450+0648	HIP 72577	14 50 21	+06 48 54	32.26	9.08	6.72	9.31	8.13	1.18	6.85	33PC
RKS1451+0943	HD 131023B	14 51 02	+09 43 20	33.28	8.43	6.79	9.94	8.48	1.46	7.55	33PC
RKS1451+1906	* ksi Boo B	14 51 23	+19 06 07	148.21	6.85	...	7.15	5.62	1.53	8.00	25PC
RKS1451−2418	HIP 72688	14 51 40	−24 18 15	59.67	7.81	5.38	8.05	6.81	1.23	6.93	25PC
RKS1453+1909	HIP 72848	14 53 24	+19 09 10	87.91	6.01	4.32	6.22	5.18	1.04	5.94	25PC
RKS1453+2320	HIP 72875	14 53 42	+23 20 43	42.54	8.67	6.18	8.88	7.67	1.21	7.03	25PC
RKS1455−2707	HIP 73066	14 55 55	−27 07 38	36.64	9.00	6.48	9.23	7.98	1.25	7.05	33PC
RKS1457−2124	HIP 73184	14 57 28	−21 24 56	170.01	5.72	3.05	5.98	4.67	1.32	7.14	25PC
RKS1458+0445	HIP 73258	14 58 19	+04 45 35	26.39	10.49	7.31	10.66	9.09	1.56	7.77	XTRA
RKS1500−2905	TYC 6760−1510−1	15 00 10	−29 05 28	31.67	11.48	7.63	11.53	9.68	1.85	9.04	33PC
RKS1500−2427	HIP 73427	15 00 19	−24 27 15	36.33	9.92	6.80	10.15	8.60	1.55	7.95	33PC
RKS1500−1108	HIP 73457	15 00 43	−11 08 06	56.02	9.54	5.99	9.72	7.95	1.77	8.47	25PC
RKS1501+1341	StKM 1−1198	15 01 07	+13 41 39	30.70	10.96	7.53	11.24	9.48	1.76	8.68	33PC
RKS1501+1552	HIP 73512	15 01 30	+15 52 08	34.44	9.13	6.58	9.34	8.07	1.27	7.03	33PC
RKS1504+0538	HIP 73786	15 04 54	+05 38 17	52.59	9.83	6.47	10.06	8.37	1.69	8.66	25PC
RKS1504−1835A	HIP 73787	15 04 54	−18 35 27	31.93	9.50	6.44	9.74	8.19	1.54	7.26	33PC
RKS1507+2456	BD+25 2874	15 07 24	+24 56 08	52.52	10.23	6.47	10.29	8.48	1.81	8.89	25PC
RKS1509+2400A	HIP 74148	15 09 04	+24 00 58	30.65	9.32	6.74	9.56	8.26	1.30	6.99	33PC
RKS1510−1627	HIP 74234	15 10 13	−16 27 47	33.80	9.44	7.15	9.64	8.53	1.12	7.29	XTRA
RKS1510−1622	HIP 74235	15 10 13	−16 22 46	33.99	9.07	6.98	9.26	8.25	1.02	6.92	33PC
RKS1513−0347	HIP 74555	15 14 00	−03 47 53	38.87	9.84	6.91	10.05	8.62	1.44	8.00	33PC
RKS1515+0735	HIP 74682	15 15 45	+07 35 52	31.54	10.70	7.42	10.94	9.27	1.67	8.44	33PC
RKS1515+0047	HIP 74702	15 16 00	+00 47 47	63.23	6.93	4.96	7.14	6.12	1.02	6.15	25PC
RKS1517−2759	HIP 74815	15 17 21	−27 59 50	28.88	11.08	7.42	11.03	9.29	1.74	8.33	XTRA
RKS1518−1837	HIP 74926	15 18 40	−18 37 36	36.39	10.35	7.23	10.59	9.02	1.57	8.39	33PC
RKS1519+0146	* 5 Ser B	15 19 19	+01 46 05	39.77	9.89	6.75	10.34	8.64	1.69	8.34	33PC
RKS1519+2912	HIP 74981	15 19 21	+29 12 22	35.69	10.25	7.10	10.47	8.91	1.56	8.23	33PC
RKS1519+1155	BD+12 2823	15 19 35	+11 55 20	31.29	9.92	7.07	10.24	8.76	1.48	7.71	33PC
RKS1520+1522A	HIP 75090	15 20 39	+15 22 49	32.71	8.80	6.24	9.03	7.79	1.25	6.61	33PC
RKS1522−0446	HIP 75201	15 22 04	−04 46 39	52.15	9.46	6.18	9.70	8.06	1.64	8.29	25PC
RKS1522−1039	HIP 75253	15 22 37	−10 39 40	45.21	7.97	5.72	8.20	7.04	1.15	6.47	25PC

Table 1: K dwarf Sample: Astrometry and photometry data.

RKS ID	Star Name	R.A.	Decl.	π	V	K	B_G	R_G	B_G-R_G	M_{B_G}	Sample
		hh mm ss	±dd mm ss	mas	mag	mag	mag	mag	mag	mag	
RKS1522+0125	HIP 75266	15 22 43	+01 25 07	38.51	8.28	6.04	8.52	7.36	1.16	6.44	33PC
RKS1525−2642	HIP 75542	15 25 59	−26 42 21	45.13	8.82	6.16	9.04	7.73	1.31	7.31	25PC
RKS1527+1035	HIP 75672	15 27 38	+10 35 39	36.59	9.90	6.65	10.07	8.46	1.61	7.89	33PC
RKS1527+0235	HIP 75686	15 27 43	+02 35 52	35.32	10.20	6.90	10.45	8.80	1.66	8.19	33PC
RKS1528−0920A	HIP 75718	15 28 10	−09 20 53	51.14	6.89	4.89	7.10	6.10	1.01	5.65	25PC
RKS1528−0921B	HIP 75722	15 28 12	−09 21 28	48.38	7.57	5.46	7.79	6.71	1.08	6.21	XTRA
RKS1531−2916	LP 915−41	15 31 40	−29 16 29	34.79	11.29	7.54	11.62	9.63	1.99	9.33	33PC
RKS1531+1041	StKM 1−1250	15 31 40	+10 41 14	31.57	11.75	7.86	11.93	9.96	1.97	9.43	33PC
RKS1540−1802	HIP 76779	15 40 35	−18 02 56	64.23	8.92	5.69	9.15	7.52	1.63	8.19	25PC
	HIP 77408	15 48 09	+01 34 18	46.14	7.44	5.50	7.66	6.66	0.99	5.98	XTRA
RKS1552+1052A	HIP 77725	15 52 08	+10 52 28	47.29	9.40	5.82	9.61	7.81	1.80	7.98	25PC
RKS1554−2600	HIP 77908	15 54 38	−26 00 15	42.14	9.20	6.24	9.43	7.94	1.49	7.56	25PC
RKS1555+1602	HIP 77963	15 55 19	+16 02 40	30.79	8.68	6.17	8.92	7.69	1.23	6.36	33PC
	HIP 78241	15 58 32	+27 44 24	37.52	8.02	6.10	8.22	7.25	0.97	6.09	XTRA
RKS1559−0504	HIP 78336	15 59 42	−05 04 34	28.55	9.04	6.83	9.26	8.13	1.13	6.54	XTRA
RKS1600−0147A	HIP 78395	16 00 16	−01 47 56	32.61	10.28	7.15	10.50	8.94	1.56	8.07	33PC
RKS1601−2625	PM J16016−2625	16 01 40	−26 25 16	40.98	10.82	7.18	11.05	9.19	1.86	9.11	25PC
RKS1604−1126	HIP 78739	16 04 27	−11 27 00	35.84	8.02	6.11	8.23	7.22	1.02	6.01	33PC
RKS1605−2027	HIP 78843	16 05 40	−20 27 00	53.61	7.39	4.86	7.63	6.35	1.28	6.27	25PC
RKS1607−0542	HIP 78999	16 07 34	−05 42 26	30.43	10.34	7.10	10.63	8.97	1.66	8.05	33PC
RKS1608+1713	BD+17 2966	16 08 05	+17 13 45	31.27	9.13	6.75	9.37	8.16	1.20	6.84	33PC
RKS1608−1308	HIP 79066	16 08 24	−13 08 08	35.47	8.70	6.38	8.92	7.74	1.18	6.67	33PC
RKS1613+1331B	HIP 79492	16 13 18	+13 31 41	41.26	6.68	5.23	7.66	6.72	0.94	5.74	XTRA
RKS1613+1331A	HIP 79492	16 13 18	+13 31 37	41.15	6.66	5.17	7.57	6.64	0.92	5.64	25PC
RKS1615+0721A	HIP 79702	16 15 57	+07 21 25	37.14	8.70	6.06	9.51	8.17	1.33	7.36	33PC
RKS1615+0721B	HIP 79702	16 15 57	+07 21 28	37.08	9.60	...	9.88	8.43	1.45	7.73	XTRA
RKS1620−0416	HIP 80053	16 20 25	−04 16 02	34.21	10.67	7.08	10.92	9.09	1.83	8.59	33PC
RKS1621+1713	G 138−22	16 21 38	+17 13 34	30.89	10.78	7.37	10.85	9.23	1.62	8.30	33PC
RKS1624−1338	HIP 80366	16 24 20	−13 38 30	46.97	8.40	6.00	8.61	7.43	1.18	6.97	25PC
RKS1625−2156	HIP 80440	16 25 13	−21 56 15	53.81	10.30	6.72	10.62	8.74	1.88	9.28	25PC
RKS1626+1539	HIP 80539	16 26 33	+15 39 54	36.48	10.53	7.20	10.78	9.09	1.69	8.59	33PC
RKS1627+0055	HIP 80597	16 27 20	+00 55 30	35.13	9.97	6.79	10.21	8.60	1.61	7.94	33PC
RKS1627+0718	HIP 80644	16 27 57	+07 18 20	57.05	8.83	5.80	9.06	7.54	1.52	7.84	25PC
RKS1628+1824A	HIP 80725	16 28 53	+18 24 51	51.75	6.98	4.90	7.84	6.74	1.10	6.41	25PC
RKS1628+1824B	HD 148653B	16 28 53	+18 24 49	51.79	7.79	...	8.02	6.95	1.08	6.60	XTRA
RKS1629+2346	HIP 80751	16 29 14	+23 46 34	30.84	10.07	7.05	10.30	8.78	1.51	7.74	33PC
RKS1630−0359	BD−03 3952	16 30 43	−03 59 22	36.69	9.62	6.59	9.80	8.29	1.52	7.62	33PC
RKS1631−0718	TYC 5060−53−1	16 31 52	−07 18 19	44.49	11.03	8.83	11.23	10.09	1.14	9.47	25PC
RKS1632−1235	HIP 81030	16 32 58	−12 35 30	31.53	10.60	7.25	10.83	9.15	1.68	8.32	33PC
RKS1633−0933	HIP 81084	16 33 42	−09 33 12	32.17	11.27	7.55	11.46	9.59	1.87	9.00	33PC
RKS1636−0219	HIP 81300	16 36 21	−02 19 29	100.81	5.76	4.04	5.99	4.97	1.01	6.00	25PC
RKS1638−0501	HIP 81465	16 38 20	−05 01 15	24.82	10.38	7.45	10.63	9.14	1.49	7.60	XTRA

Table 1: K dwarf Sample: Astrometry and photometry data.

RKS ID	Star Name	R.A.	Decl.	π	V	K	B_G	R_G	B_G-R_G	M_{B_G}	Sample
		hh mm ss	±dd mm ss	mas	mag	mag	mag	mag	mag	mag	
RKS1646+0531	PM J16468+0531N	16 46 51	+05 31 26	30.13	10.94	7.37	11.47	9.63	1.84	8.86	33PC
RKS1647−0111	HIP 82169	16 47 18	−01 11 20	33.02	10.76	7.42	10.96	9.31	1.65	8.55	33PC
RKS1649−2426	HIP 82370	16 49 53	−24 26 49	30.09	9.59	6.89	9.81	8.46	1.35	7.20	33PC
RKS1650+1854	HIP 82389	16 50 05	+18 54 01	36.49	8.85	6.37	9.09	7.84	1.25	6.90	33PC
RKS1654+1154	HIP 82694	16 54 12	+11 54 53	49.79	10.74	7.11	10.99	9.11	1.88	9.48	25PC
RKS1659−2616	HIP 83147	16 59 33	−26 16 04	36.58	10.38	6.92	10.61	8.86	1.75	8.43	33PC
RKS1701+2256	HIP 83343	17 02 00	+22 56 09	36.30	8.77	6.39	9.05	7.81	1.23	6.85	33PC
RKS1705−0503	HIP 83591	17 05 03	−05 04 00	95.55	7.70	4.73	7.95	6.48	1.47	7.85	25PC
RKS1705−0147	HD 154361	17 05 09	−01 47 10	32.25	9.51	6.80	9.58	8.30	1.28	7.12	33PC
RKS1706−0610	HIP 83676	17 06 08	−06 10 02	33.12	8.80	6.45	9.03	7.83	1.20	6.63	33PC
RKS1712+1821	HIP 84195	17 12 38	+18 21 04	47.97	7.95	5.67	8.18	7.04	1.14	6.58	25PC
RKS1714−0824A	HIP 84303	17 14 08	−08 24 14	33.80	8.49	6.17	8.73	7.60	1.13	6.38	33PC
RKS1714−0824B	HD 155802B	17 14 08	−08 24 13	34.62	11.23	...	11.18	9.46	1.72	8.88	XTRA
RKS1715−2636A	HIP 84405	17 15 21	−26 36 06	167.82	4.33	1.84	5.31	4.26	1.06	6.44	25PC
RKS1715−2636B	HIP 84405	17 15 21	−26 36 10	167.78	5.06	...	5.31	4.26	1.05	6.43	XTRA
RKS1716−2632	HIP 84478	17 16 13	−26 32 46	168.07	6.33	3.47	6.55	5.15	1.40	7.68	XTRA
RKS1716−1210	HIP 84487	17 16 20	−12 10 41	38.31	10.47	6.91	10.56	8.83	1.73	8.48	33PC
RKS1717+2913	HIP 84607	17 17 40	+29 13 38	41.07	8.43	6.00	8.66	7.45	1.22	6.73	25PC
	HIP 84652	17 18 22	−01 46 53	44.43	10.58	6.71	10.82	8.86	1.96	9.05	XTRA
RKS1721−2106	HIP 84893	17 21 01	−21 06 43	57.26	9.67	...	9.58	8.26	1.32	8.37	XTRA
RKS1722−1457	HIP 85026	17 22 43	−14 57 37	32.66	10.89	7.43	11.14	9.37	1.77	8.71	33PC
RKS1725+0206	HIP 85295	17 25 45	+02 06 41	129.62	7.54	4.37	7.77	6.06	1.72	8.34	25PC
RKS1729−2350	HIP 85561	17 29 07	−23 50 10	54.37	9.61	6.39	9.85	8.23	1.62	8.52	25PC
	HIP 85582	17 29 20	+29 23 31	42.09	8.99	6.05	...	...	...	...	XTRA
RKS1733+0914	RX J1733.1+0914	17 33 07	+09 14 37	31.32	9.57	6.75	9.85	8.45	1.40	7.33	33PC
RKS1737+2753A	HIP 86221	17 37 11	+27 53 51	31.09	11.61	7.81	11.99	9.98	2.01	9.45	33PC
RKS1737−1314	HD 159911	17 37 46	−13 14 47	30.10	10.10	6.83	10.30	8.74	1.56	7.69	33PC
RKS1737+2257B	HIP 86282	17 37 49	+22 57 16	43.83	10.33	6.30	10.44	8.67	1.76	8.64	XTRA
RKS1737+2257A	HIP 86282	17 37 49	+22 57 20	43.84	9.93	6.29	10.18	8.50	1.69	8.39	25PC
RKS1739+0333	HIP 86400	17 39 17	+03 33 19	99.14	6.51	4.10	6.75	5.56	1.19	6.73	25PC
	HIP 86722	17 43 16	+21 36 33	39.57	7.51	5.54	7.71	6.73	0.98	5.70	XTRA
RKS1750−0603	HIP 87322	17 50 34	−06 03 01	45.07	10.11	6.54	10.40	8.55	1.85	8.67	25PC
RKS1752−0733	HIP 87464	17 52 17	−07 33 37	32.66	9.94	6.97	10.17	8.70	1.47	7.74	33PC
RKS1753+2119	HIP 87579	17 53 30	+21 19 31	40.78	8.50	6.20	8.72	7.56	1.16	6.78	25PC
RKS1754−2649	HD 314741	17 54 54	−26 49 42	36.21	10.28	6.91	10.63	8.95	1.69	8.43	33PC
RKS1755+0345	HIP 87745	17 55 25	+03 45 16	39.72	10.12	6.82	10.37	8.68	1.69	8.36	33PC
RKS1755+1830	HIP 87768	17 55 45	+18 30 01	44.36	9.22	6.30	9.43	7.96	1.46	7.66	25PC
RKS1757−2143A	HIP 87925	17 57 41	−21 43 11	33.45	9.99	6.68	10.23	8.58	1.65	7.85	33PC
RKS1803+2545	Ross 820	18 03 48	+25 45 20	35.94	10.82	7.20	11.10	9.23	1.87	8.88	33PC
RKS1804+0149	HIP 88481	18 04 02	+01 49 57	30.65	8.11	6.11	8.33	7.34	0.99	5.77	33PC
RKS1805−2929A	HD 317101A	18 05 26	−29 29 51	30.21	10.68	7.05	10.74	9.09	1.65	8.14	33PC
RKS1805+0229	HIP 88601	18 05 27	+02 29 56	195.22	6.17	1.79	6.23	4.75	1.48	7.68	25PC

Table 1: K dwarf Sample: Astrometry and photometry data.

RKS ID	Star Name	R.A.	Decl.	π	V	K	B_G	R_G	B_G-R_G	M_{B_G}	Sample
		hh mm ss	±dd mm ss	mas	mag	mag	mag	mag	mag	mag	
RKS1807−1641	TYC 6251−414−1	18 07 50	−16 41 21	38.60	10.25	7.73	10.56	9.30	1.26	8.49	33PC
RKS1809−0019	HIP 88961	18 09 32	−00 19 38	34.53	8.93	6.54	9.17	7.95	1.23	6.87	33PC
RKS1809−1202	HIP 88962	18 09 33	−12 02 20	36.63	10.50	6.99	10.73	8.96	1.78	8.55	33PC
RKS1815+1829	HIP 89449	18 15 18	+18 30 00	34.28	10.06	6.82	10.29	8.67	1.63	7.97	33PC
RKS1816+1354	HIP 89517	18 16 02	+13 54 48	54.76	10.20	6.56	10.41	8.55	1.86	9.10	25PC
RKS1817+2640	HIP 89656	18 17 50	+26 40 17	32.52	9.59	6.95	9.79	8.50	1.29	7.35	33PC
RKS1818−0642	HIP 89728	18 18 41	−06 42 04	33.56	9.28	6.72	9.51	8.22	1.28	7.13	33PC
RKS1819−0156	HIP 89825	18 19 51	−01 56 19	52.52	9.66	6.28	9.90	8.20	1.70	8.50	25PC
RKS1822+0142	HIP 90035	18 22 17	+01 42 25	37.88	10.12	6.86	10.37	8.74	1.63	8.26	33PC
RKS1826+0422	TYC 441−814−1	18 26 35	+04 22 21	31.41	12.55	8.19	12.80	10.50	2.31	10.29	33PC
RKS1829−2758	HIP 90611	18 29 22	−27 58 19	36.73	9.37	6.49	9.62	8.17	1.45	7.45	33PC
RKS1829+0903A	HIP 90626	18 29 32	+09 03 44	36.32	8.65	6.33	8.88	7.70	1.18	6.68	33PC
RKS1829−0149	HIP 90656	18 29 52	−01 49 05	53.24	8.04	5.48	8.28	6.98	1.30	6.91	25PC
RKS1831−1854	HIP 90790	18 31 19	−18 54 32	75.98	6.81	4.70	7.04	5.95	1.09	6.44	25PC
RKS1832−0347	TYC 5120−119−1	18 32 01	−03 47 43	32.32	11.44	9.55	11.81	10.80	1.01	9.35	33PC
RKS1833+2218	HIP 90959	18 33 18	+22 18 51	42.75	8.90	6.16	9.14	7.76	1.38	7.29	25PC
RKS1833−1626	HD 171075	18 33 25	−16 26 39	31.54	9.06	6.44	9.32	8.00	1.31	6.81	33PC
RKS1833−1138	HIP 90979	18 33 29	−11 38 10	36.78	10.03	6.87	10.25	8.68	1.57	8.08	33PC
RKS1834+0355	TYC 454−792−1	18 34 35	+03 55 04	46.85	10.37	8.37	10.66	9.60	1.05	9.01	25PC
RKS1847−0338	HIP 92200	18 47 27	−03 38 23	70.14	8.81	5.58	9.05	7.44	1.62	8.28	25PC
RKS1847+1226	HD 229513	18 47 41	+12 26 23	34.61	8.95	6.54	9.13	7.93	1.20	6.83	33PC
RKS1848−1008A	HIP 92250	18 48 01	−10 08 47	34.69	8.45	6.09	8.68	7.52	1.16	6.38	33PC
RKS1848+1044	HIP 92283	18 48 29	+10 44 44	59.26	7.97	5.39	8.20	6.90	1.31	7.07	25PC
RKS1848+1726	HIP 92311	18 48 52	+17 26 20	59.95	9.17	5.92	9.42	7.75	1.67	8.31	25PC
RKS1850−2655	HIP 92444	18 50 21	−26 55 25	56.62	9.65	6.18	9.94	8.16	1.78	8.70	25PC
RKS1854+2844	PM J18547+2844	18 54 44	+28 44 55	31.30	11.55	7.69	11.52	9.68	1.83	8.99	33PC
RKS1854+0051	BD+00 4050	18 54 53	+00 51 47	40.20	10.66	6.97	10.85	9.00	1.86	8.88	25PC
RKS1854+1058	HD 230017A	18 54 54	+10 58 40	53.77	9.62	5.89	9.66	7.91	1.75	8.31	25PC
RKS1855+2333A	HIP 92919	18 55 53	+23 33 24	46.84	8.16	5.64	8.35	7.14	1.21	6.70	25PC
RKS1857+0734	LP 571−80	18 57 11	+07 34 17	39.06	11.42	7.57	11.71	9.66	2.05	9.67	33PC
RKS1857−1902	HIP 93072	18 57 33	−19 02 47	38.75	10.99	...	11.25	9.37	1.88	9.19	33PC
RKS1858−1014	BD−10 4886	18 58 03	−10 14 38	30.69	9.79	7.04	10.10	8.67	1.44	7.54	33PC
RKS1858−0030	HIP 93195	18 58 56	−00 30 14	31.82	8.39	6.38	8.60	7.60	1.00	6.11	33PC
RKS1859+0759	HIP 93248	18 59 39	+07 59 14	35.43	10.81	7.15	11.07	9.19	1.88	8.82	33PC
RKS1859+1107	HD 230325	18 59 39	+11 07 05	32.96	9.22	6.64	9.44	8.15	1.29	7.03	33PC
RKS1901+0328	TYC 466−2991−1	19 01 51	+03 28 15	32.20	9.72	6.94	10.00	8.57	1.43	7.54	33PC
RKS1903−1102	HIP 93540	19 03 06	−11 02 38	35.96	8.42	6.22	8.65	7.53	1.12	6.43	33PC
	HIP 93731	19 05 08	+23 04 40	28.18	8.54	6.62	8.75	7.75	0.99	6.00	XTRA
RKS1905+1351	* zet Aql B	19 05 25	+13 51 53	39.06	11.28	12.27	11.24	9.60	1.64	9.20	33PC
RKS1907+0736	HIP 93871	19 07 02	+07 36 57	40.92	9.23	6.47	9.45	8.09	1.36	7.51	25PC
RKS1908+1627	HD 230742	19 08 03	+16 27 38	31.25	10.19	7.15	10.48	8.92	1.56	7.95	33PC
RKS1908−1640	PM J19081−1640	19 08 11	−16 40 42	37.87	10.57	7.05	10.64	8.96	1.69	8.54	33PC

Table 1: K dwarf Sample: Astrometry and photometry data.

RKS ID	Star Name	R.A.	Decl.	π	V	K	B_G	R_G	B_G-R_G	M_{B_G}	Sample
		hh mm ss	±dd mm ss	mas	mag	mag	mag	mag	mag	mag	
RKS1910+2145	TYC 1598−1505−1	19 10 32	+21 45 46	30.03	11.41	7.70	11.54	9.69	1.85	8.93	33PC
RKS1911+0500	PM J19117+0500	19 11 48	+05 00 36	36.16	11.41	7.56	11.68	9.67	2.01	9.47	33PC
RKS1914+0209A	HIP 94590	19 14 59	+02 09 55	37.22	9.85	7.18	10.47	8.96	1.51	8.32	33PC
RKS1914+0209B	HIP 94590	19 15 00	+02 09 46	37.23	11.25	7.78	11.47	9.70	1.77	9.32	XTRA
RKS1915+2453A	HIP 94622	19 15 19	+24 53 49	34.57	9.71	6.37	9.94	8.26	1.68	7.64	33PC
RKS1915+1133	HIP 94650	19 15 35	+11 33 17	37.95	8.06	5.94	8.28	7.20	1.08	6.17	33PC
RKS1923−0635A	HIP 95299	19 23 16	−06 35 07	32.10	9.66	6.81	9.92	8.50	1.42	7.46	33PC
RKS1924+2525	PM J19244+2525	19 24 27	+25 25 51	31.53	10.92	7.43	11.18	9.41	1.77	8.67	33PC
RKS1924−2203	HIP 95417	19 24 34	−22 03 44	36.19	10.91	7.43	11.16	9.37	1.78	8.95	33PC
RKS1924+0832	HIP 95429	19 24 42	+08 33 00	29.24	11.19	7.73	11.45	9.69	1.76	8.78	XTRA
RKS1928+1232A	HIP 95730	19 28 15	+12 32 09	34.57	9.17	6.35	9.41	8.05	1.35	7.10	33PC
RKS1928+1232B	HIP 95730	19 28 15	+12 32 11	37.44	12.05	...	11.29	9.50	1.79	9.16	XTRA
RKS1928+2854	PM J19284+2854	19 28 26	+28 54 10	38.62	10.85	7.24	11.09	9.25	1.85	9.03	33PC
RKS1929+0709	BD+06 4156	19 29 05	+07 09 36	37.80	10.48	7.19	10.90	9.15	1.75	8.79	33PC
RKS1930+2140	HIP 95890	19 30 05	+21 40 34	34.41	9.98	7.07	10.18	8.74	1.43	7.86	33PC
RKS1932−1116	HIP 96085	19 32 07	−11 16 30	56.52	7.53	5.33	7.75	6.63	1.12	6.51	25PC
RKS1932+0034	HIP 96121	19 32 38	+00 34 39	45.25	10.44	6.81	10.67	8.82	1.85	8.95	25PC
RKS1934+0434	HIP 96285	19 34 40	+04 34 57	69.31	9.35	5.92	9.57	7.83	1.75	8.78	25PC
RKS1936−1026B	HIP 96471	19 36 45	−10 26 32	34.83	10.09	6.80	10.28	8.71	1.58	7.99	XTRA
RKS1936−1026A	HIP 96471	19 36 46	−10 26 36	35.36	8.38	6.32	8.87	7.71	1.15	6.61	33PC
RKS1943+1005	HIP 97051	19 43 25	+10 05 22	38.39	10.00	6.84	10.21	8.64	1.57	8.13	33PC
RKS1952−2356	HIP 97805	19 52 30	−23 56 57	38.74	9.45	6.61	9.69	8.27	1.43	7.64	33PC
RKS1954−2356	HIP 97944	19 54 18	−23 56 28	70.89	6.22	4.04	6.44	5.25	1.20	5.70	25PC
RKS1954+2013	PM J19546+2013	19 54 38	+20 13 07	36.47	11.06	7.23	11.06	9.24	1.82	8.87	33PC
	HIP 98192	19 57 13	+29 49 26	36.99	7.91	5.87	8.10	7.09	1.01	5.94	XTRA
	HIP 98204	19 57 20	−12 34 13	56.26	9.29	6.01	9.47	7.89	1.59	8.22	XTRA
RKS1957+1313	HD 356314	19 57 25	+13 13 25	38.21	10.14	6.86	10.39	8.73	1.66	8.30	33PC
RKS2000+2242	HIP 98505	20 00 44	+22 42 39	50.57	7.67	5.54	7.91	6.81	1.11	6.43	25PC
RKS2002+0319	HIP 98698	20 02 47	+03 19 34	78.62	7.46	4.80	7.70	6.34	1.35	7.17	25PC
RKS2003+2005	HIP 120148	20 03 01	+20 05 50	33.34	10.88	7.27	10.84	9.17	1.68	8.46	33PC
RKS2003+2320	HIP 98792	20 03 52	+23 20 26	64.03	7.27	5.11	7.49	6.43	1.05	6.52	25PC
RKS2004+2547	HIP 98828	20 04 10	+25 47 25	45.14	7.82	5.64	8.04	6.94	1.11	6.32	25PC
RKS2008+0640	HIP 99205	20 08 24	+06 40 43	34.55	9.81	6.93	10.05	8.60	1.45	7.74	33PC
RKS2009+1648A	HIP 99316	20 09 34	+16 48 21	40.28	7.56	5.63	7.89	6.91	0.98	5.91	25PC
RKS2009+1648B	HIP 99316	20 09 34	+16 48 25	40.30	7.50	5.95	9.97	8.44	1.54	8.00	XTRA
RKS2009−1417	HIP 99322	20 09 36	−14 17 13	31.84	9.75	6.97	10.00	8.60	1.40	7.52	33PC
RKS2009−0307	HIP 99332	20 09 41	−03 07 44	32.31	9.56	6.74	9.81	8.37	1.44	7.36	33PC
RKS2010−2029A	HIP 99385	20 10 20	−20 29 36	63.28	8.91	5.70	9.15	7.54	1.61	8.16	25PC
RKS2011+1611	HIP 99452	20 11 06	+16 11 17	48.85	7.35	5.35	7.55	6.53	1.02	6.00	25PC
RKS2012−1253	HIP 99550	20 12 09	−12 53 35	35.40	11.28	7.62	11.54	9.66	1.89	9.29	33PC
RKS2013−0052	HIP 99711	20 14 00	−00 52 01	50.90	7.79	5.54	8.01	6.87	1.13	6.54	25PC
RKS2014−0716	HIP 99764	20 14 28	−07 16 55	46.20	10.19	6.73	10.42	8.68	1.73	8.74	25PC

Table 1: K dwarf Sample: Astrometry and photometry data.

RKS ID	Star Name	R.A.	Decl.	π	V	K	B_G	R_G	B_G-R_G	M_{B_G}	Sample
		hh mm ss	±dd mm ss	mas	mag	mag	mag	mag	mag	mag	
RKS2015−2701	HIP 99825	20 15 17	−27 01 59	113.65	5.73	3.50	5.95	4.88	1.07	6.23	25PC
RKS2016−0204	HIP 99916	20 16 22	−02 04 08	37.69	11.16	7.55	11.40	9.54	1.86	9.28	33PC
	HIP 100133	20 18 46	−00 39 26	35.47	11.02	7.16	11.27	9.29	1.98	9.02	XTRA
RKS2030+2650	HIP 101150	20 30 11	+26 50 34	49.03	9.69	6.35	9.94	8.26	1.69	8.40	25PC
RKS2035+0607	HIP 101579	20 35 13	+06 07 37	33.04	8.91	6.53	9.14	7.96	1.18	6.74	33PC
RKS2038+2346	HD 347103	20 38 26	+23 46 41	30.12	8.70	6.63	8.96	7.88	1.09	6.36	33PC
RKS2039+1004	HIP 101932	20 39 22	+10 04 33	33.38	8.52	6.41	8.75	7.66	1.09	6.37	33PC
RKS2041−0529	HIP 102115	20 41 41	−05 29 34	32.67	10.53	7.23	10.77	9.11	1.66	8.34	33PC
RKS2041−2219	HIP 102119	20 41 42	−22 19 21	41.39	9.83	6.61	10.11	8.49	1.61	8.19	25PC
RKS2042−2116	HD 197092	20 42 06	−21 16 38	50.53	9.28	7.18	9.49	8.42	1.07	8.01	25PC
RKS2042+2050	HIP 102226	20 42 49	+20 50 41	40.33	8.26	6.01	8.49	7.37	1.12	6.52	25PC
RKS2044−2121	HIP 102332	20 44 01	−21 21 21	38.46	9.84	6.75	10.10	8.56	1.54	8.03	33PC
	HIP 102357	20 44 22	+19 44 59	48.55	10.33	6.55	10.58	8.62	1.96	9.01	XTRA
RKS2046−2144	HIP 102486	20 46 10	−21 44 45	30.08	7.82	5.49	8.05	6.90	1.15	5.44	33PC
RKS2046−2304	HIP 102495	20 46 18	−23 04 50	28.05	10.73	7.40	10.94	9.29	1.65	8.18	XTRA
RKS2047+1051	HIP 102582	20 47 17	+10 51 36	31.63	9.72	7.00	9.96	8.63	1.33	7.46	33PC
RKS2050+2923A	HIP 102851	20 50 11	+29 23 03	49.43	8.32	5.61	8.57	7.23	1.34	7.04	25PC
RKS2053−0245	HIP 103150	20 53 57	−02 45 57	30.92	11.10	7.67	11.30	9.58	1.72	8.75	33PC
RKS2055+1310	HIP 103256	20 55 07	+13 10 37	41.51	8.83	6.18	9.04	7.73	1.31	7.13	25PC
RKS2059+0333	HIP 103577	20 59 09	+03 33 09	30.66	12.03	8.41	12.22	10.37	1.85	9.65	33PC
RKS2059−1042	HIP 103581	20 59 14	−10 42 49	30.38	8.51	6.26	8.74	7.58	1.16	6.15	33PC
RKS2105+0704A	HIP 104092	21 05 20	+07 04 09	66.47	8.30	5.31	8.53	7.02	1.51	7.64	25PC
RKS2105−1654	HD 358850	21 05 43	−16 54 49	45.64	10.46	6.69	10.55	8.73	1.83	8.85	25PC
RKS2107−1355A	HIP 104239	21 07 10	−13 55 23	57.43	7.11	5.02	7.40	6.35	1.05	6.20	25PC
RKS2107−1355B	HD 200968B	21 07 10	−13 55 27	57.56	9.99	5.32	9.97	8.19	1.78	8.77	XTRA
RKS2107+2945	HIP 104304	21 07 48	+29 45 22	27.39	9.60	7.01	9.86	8.58	1.28	7.05	XTRA
RKS2108+2510	HIP 104329	21 08 02	+25 10 34	29.32	9.84	7.06	10.08	8.69	1.39	7.42	XTRA
RKS2108−0425A	HIP 104383	21 08 45	−04 25 36	41.77	9.45	6.43	9.66	8.19	1.47	7.76	25PC
RKS2116+0923	HIP 105038	21 16 32	+09 23 38	61.87	7.95	5.39	8.15	6.89	1.26	7.11	25PC
RKS2118+0009	HIP 105152	21 18 03	+00 09 42	49.59	8.22	5.74	8.41	7.18	1.23	6.88	25PC
RKS2119−2621	HIP 105312	21 19 46	−26 21 10	54.79	6.56	4.57	6.76	5.78	0.98	5.45	25PC
RKS2120−1951	HIP 105341	21 20 14	−19 51 08	63.35	9.09	5.72	9.34	7.63	1.71	8.34	25PC
RKS2122+1052	HIP 105533	21 22 27	+10 52 26	47.16	9.91	6.44	10.16	8.40	1.76	8.53	25PC
RKS2122−0044	TIC 2024830728	21 22 31	−00 44 46	34.25	11.99	...	11.62	10.15	1.48	9.30	33PC
RKS2125+2712	HIP 105791	21 25 29	+27 12 38	40.60	8.28	6.20	8.50	7.46	1.04	6.54	25PC
RKS2126+0344	HIP 105885	21 26 42	+03 44 14	36.05	10.50	7.00	10.72	8.94	1.78	8.50	33PC
RKS2130−1230	HIP 106147	21 30 03	−12 30 36	56.43	9.11	5.88	9.32	7.70	1.62	8.08	25PC
RKS2131+2320	HIP 106231	21 31 02	+23 20 07	41.24	9.23	6.38	9.52	8.11	1.41	7.59	25PC
RKS2132−2057	HIP 106353	21 32 24	−20 57 27	34.79	8.45	6.36	8.67	7.59	1.07	6.38	33PC
RKS2141+1115	HIP 107062	21 41 01	+11 15 47	31.48	9.16	6.64	9.41	8.14	1.26	6.90	33PC
RKS2149+0543	HD 207491	21 49 12	+05 43 22	44.33	8.65	6.16	8.90	7.63	1.26	7.13	25PC
RKS2149−1140	HIP 107758	21 49 46	−11 40 57	32.61	10.85	7.35	11.10	9.32	1.78	8.67	33PC

Table 1: K dwarf Sample: Astrometry and photometry data.

RKS ID	Star Name	R.A.	Decl.	π	V	K	B_G	R_G	B_G-R_G	M_{B_G}	Sample
		hh mm ss	±dd mm ss	mas	mag	mag	mag	mag	mag	mag	
RKS2152+0154	HIP 107941	21 52 07	+01 54 23	32.58	8.19	6.18	8.42	7.37	1.05	5.98	33PC
RKS2153+2055	HIP 108028	21 53 05	+20 55 50	42.92	8.18	5.95	8.41	7.29	1.11	6.57	25PC
RKS2153+2850	StKM 1−1953	21 53 07	+28 50 15	36.97	11.43	7.79	11.71	9.83	1.88	9.55	33PC
RKS2153−1249	LP 758−74	21 53 08	−12 49 41	41.47	10.96	7.36	11.24	9.36	1.88	9.33	25PC
RKS2155−2942	HIP 108241	21 55 42	−29 42 22	30.72	8.46	6.49	8.68	7.65	1.02	6.11	33PC
RKS2210+2247	HIP 109461	22 10 31	+22 47 49	30.05	9.19	6.81	9.43	8.25	1.18	6.82	33PC
RKS2214+0242A	HIP 109807	22 14 27	+02 42 24	29.89	10.40	7.24	10.64	9.08	1.56	8.01	XTRA
RKS2214+2751	HIP 109812	22 14 31	+27 51 19	50.93	10.31	6.73	10.57	8.74	1.83	9.11	25PC
RKS2224+2233	HIP 110640	22 24 46	+22 33 04	47.80	8.83	5.76	9.16	7.73	1.43	7.56	25PC
RKS2226−1911	HIP 110750	22 26 14	−19 11 18	39.14	9.25	6.48	9.49	8.09	1.40	7.45	33PC
	HIP 110980	22 29 06	+01 39 48	45.09	10.49	6.75	10.77	8.84	1.93	9.04	XTRA
RKS2239+0406	HIP 111888	22 39 51	+04 06 58	44.43	8.48	6.14	8.71	7.53	1.18	6.95	25PC
RKS2240−2940	HIP 111960	22 40 43	−29 40 28	75.26	7.83	5.04	8.07	6.67	1.40	7.46	25PC
RKS2241+1849A	HIP 112040	22 41 35	+18 49 27	31.85	10.74	7.06	10.96	9.12	1.84	8.47	33PC
RKS2243−0624	HIP 112190	22 43 21	−06 24 03	46.27	8.11	5.78	8.34	7.16	1.17	6.66	25PC
RKS2247+1823	HIP 112496	22 47 14	+18 23 04	37.31	9.00	6.43	9.25	7.96	1.30	7.11	33PC
RKS2248+2443	HIP 112610	22 48 36	+24 43 27	33.22	10.95	7.44	11.18	9.40	1.78	8.79	33PC
RKS2251+1358	HIP 112870	22 51 26	+13 58 12	44.36	8.30	6.08	8.51	7.42	1.09	6.74	25PC
RKS2252+2324	HIP 112918	22 52 03	+23 24 48	35.76	9.79	6.82	10.03	8.52	1.51	7.80	33PC
RKS2254+2331	HIP 113124	22 54 31	+23 31 06	30.12	11.06	7.51	11.35	9.51	1.83	8.74	33PC
RKS2257+2800	HIP 113333	22 57 07	+28 00 07	27.61	9.93	7.10	10.15	8.73	1.42	7.36	XTRA
RKS2258−1338	HIP 113409	22 58 06	−13 38 33	35.81	10.13	7.02	10.36	8.81	1.56	8.13	33PC
RKS2259−1122	HIP 113552	22 59 54	−11 22 54	38.41	10.57	7.10	10.82	9.04	1.78	8.75	33PC
RKS2300−2231	HIP 113576	23 00 16	−22 31 28	121.49	7.88	4.48	8.12	6.37	1.74	8.54	25PC
RKS2300−2618B	HIP 113597	23 00 28	−26 18 44	31.47	10.57	...	10.79	9.12	1.67	8.28	XTRA
RKS2300−2618A	HIP 113597	23 00 28	−26 18 43	31.39	10.11	6.27	10.40	8.65	1.74	7.88	33PC
RKS2301−0350	HIP 113718	23 01 52	−03 50 55	61.71	7.46	5.23	7.71	6.57	1.14	6.66	25PC
RKS2307−2309	HIP 114156	23 07 07	−23 09 34	45.24	9.61	6.42	9.84	8.23	1.60	8.12	25PC
RKS2308+0633	HIP 114294	23 08 52	+06 33 40	31.22	10.90	7.25	11.13	9.28	1.85	8.60	33PC
RKS2309−0215	HIP 114322	23 09 11	−02 15 39	34.66	8.60	6.22	8.83	7.62	1.20	6.52	33PC
RKS2309+1425	AG+14 2584	23 09 55	+14 25 36	39.70	10.28	6.84	10.48	8.77	1.71	8.48	33PC
RKS2310−2955	HIP 114455	23 10 49	−29 55 04	36.34	8.65	6.32	8.88	7.71	1.17	6.68	33PC
RKS2316+0541	HIP 114941	23 16 52	+05 41 46	38.06	10.51	7.03	10.76	8.99	1.77	8.66	33PC
RKS2317−2323	HIP 114954	23 17 00	−23 23 47	43.11	10.84	7.25	11.11	9.25	1.86	9.29	25PC
RKS2319−1327	HIP 115125	23 19 07	−13 27 19	44.52	6.88	5.51	7.82	6.76	1.07	6.07	25PC
RKS2319+2852	HIP 115194	23 19 58	+28 52 04	29.99	8.88	6.74	9.07	8.03	1.04	6.45	XTRA
RKS2323−1045	HIP 115445	23 23 05	−10 45 51	52.13	7.80	5.59	8.02	6.93	1.10	6.61	25PC
RKS2326+0853	HIP 115680	23 26 12	+08 53 38	44.39	10.54	6.92	10.81	8.94	1.87	9.04	25PC
RKS2327−0117	HIP 115752	23 27 05	−01 17 11	33.69	10.37	7.19	10.60	9.02	1.59	8.24	33PC
RKS2328+1604	HIP 115860	23 28 26	+16 04 00	32.28	9.81	7.01	10.05	8.66	1.39	7.60	33PC
RKS2332−1650	HIP 116215	23 32 49	−16 50 44	68.70	8.60	5.47	8.85	7.27	1.58	8.03	25PC
RKS2333−1239	HIP 116258	23 33 24	−12 39 53	29.41	8.81	6.68	9.02	7.94	1.08	6.36	XTRA

Table 1: K dwarf Sample: Astrometry and photometry data.

RKS ID	Star Name	R.A.	Decl.	π	V	K	B_G	R_G	B_G-R_G	M_{B_G}	Sample
		hh mm ss	±dd mm ss	mas	mag	mag	mag	mag	mag	mag	
RKS2335+0136A	HIP 116384	23 35 00	+01 36 19	48.03	9.59	6.04	9.82	8.05	1.77	8.22	25PC
RKS2340+2021	HIP 116838	23 40 51	+20 21 57	39.43	8.27	5.55	8.53	7.18	1.35	6.51	33PC
RKS2341+2002	LSPM J2341+2002N	23 41 29	+20 02 33	31.37	11.73	7.66	11.78	9.89	1.89	9.26	33PC
RKS2342−0234A	HIP 116936	23 42 11	−02 34 36	41.18	10.30	6.86	10.57	8.82	1.75	8.64	25PC
RKS2345+2933	HIP 117159	23 45 10	+29 33 43	36.45	8.40	6.24	8.61	7.54	1.07	6.42	33PC
RKS2348−1259A	HIP 117410	23 48 26	−12 59 15	35.47	9.62	6.29	9.87	8.21	1.67	7.62	33PC
RKS2349+0310	HIP 117463	23 49 01	+03 10 52	40.18	8.38	6.17	8.63	7.50	1.13	6.65	25PC
RKS2350−2924	HIP 117542	23 50 15	−29 24 06	38.66	7.88	5.87	8.10	7.08	1.01	6.03	33PC
RKS2353+2901	HIP 117779	23 53 09	+29 01 05	50.22	9.75	6.39	9.98	8.28	1.70	8.48	25PC
RKS2355+2211	HIP 117946	23 55 27	+22 11 36	39.18	8.77	6.20	8.99	7.77	1.23	6.96	33PC
RKS2356−1445	TIC 327953001	23 56 32	−14 45 01	37.35	11.68	8.56	11.79	10.31	1.48	9.65	33PC
RKS2357−1630	HIP 118086	23 57 14	−16 30 27	27.24	10.76	7.60	11.19	9.47	1.73	8.37	XTRA
RKS2358+0949	HD 224476	23 58 20	+09 49 51	33.35	8.33	6.25	8.56	7.48	1.08	6.18	33PC
RKS2359−2602	HIP 118261	23 59 14	−26 02 55	43.94	8.69	6.11	8.93	7.64	1.28	7.14	25PC
RKS2359+0639	HIP 118310	23 59 48	+06 39 51	43.35	8.88	6.01	9.15	7.75	1.41	7.34	25PC

Table 2: K dwarf companion search results.

ID	Sample	Fig.	RV Survey Results						External				
			No. Obs.	Cadence	Δt	ΔRV	MAD$_{RV}$	RV Det.	No. Obs.		Companion	TESS	RKS
		No.	CHIRON	Coverage				Type	HI19	HA20	Published		Speckle
RKS/TIC					(day)	m s^{-1}	m s^{-1}				NEA/SB9/WDS	Obs./EB/PL	Obs./Det.
RKS0000+1659A	33PC	2	24	DMY	1596	271.9	68.6	T	0	0	. . ✓	. . .	✓✓
RKS0001−2326	33PC	2	9	DMY	658	84.9	17.8	F	0	0	. . ✓	. . .	. .
RKS0001−1656	33PC	3	8	DY	377	39.7	9.0	F	0	7	. . .	✓. .	✓.
RKS0002+1100	XTRA	3	1		...	...	...	.	23	0	. . ✓	✓. .	✓.
TIC 258866681	XTRA		0		...	...	...	.	43	0	. . .	. . .	. .
RKS0007−2349	33PC	4	2	Y	452	26.5	13.3	F	24	21	. . .	✓. .	✓.
TIC 301033489	XTRA	4	17	DMY	856	69.5	14.2	F	0	0	. . .	✓. .	. .
RKS0012+2705	33PC	5	8	DMY	380	38.7	11.1	F	0	0	. . .	✓. .	✓.
RKS0012+2142	33PC	5	13	DMY	730	155.4	24.5	F	0	0	. . ✓	. . .	. .
RKS0016−1435	33PC	6	12	DMY	662	132.0	28.6	F	0	0	. . ✓	. . .	. .
RKS0017+2057	33PC	6	11	DMY	671	69.8	15.1	F	0	0	. . ✓	. . .	. .
RKS0019−0957	25PC	7	13	DMY	1261	99.7	16.7	F	43	6	. . .	✓. ✓	✓.
RKS0019−0303	33PC	7	14	DMY	779	101.3	20.5	F	0	0	. . .	✓. .	✓.
RKS0020+1738	33PC	8	11	DMY	718	154.3	32.5	F	0	0	. . .	. . .	. .
RKS0021+2531	33PC	8	9	DMY	734	98.2	18.7	P	0	0	. . .	✓. .	. .
RKS0022−2701	25PC	9	51	DMY	1577	12689.6	3588.3	O	0	0	. . .	✓. .	✓.
RKS0024−2701	25PC	9	9	DM	38	52.9	9.7	F	20	6	. . .	✓. .	✓.
RKS0036−0930	33PC	10	3	DY	449	24.2	9.1	F	0	0	. . .	✓. .	✓.
RKS0036+2610	25PC	10	8	DMY	385	65.5	11.0	F	0	0	. . .	✓. .	. .
RKS0039+2115	25PC	11	11	DM	101	34.5	8.1	F	162	0	✓. ✓	✓. .	✓.
RKS0040−0713	33PC	11	1		...	...	...	F	0	0	. . ✓	. . .	. .
RKS0042+2239	33PC	12	12	DMY	790	207.4	32.6	F	0	0	. . ✓	✓. .	. .

Table 2: K dwarf companion search results.

			RV Survey Results						External				
ID	Sample	Fig.	No. Obs.	Cadence	Δt	ΔRV	MAD$_{RV}$	RV Det.	No. Obs.		Companion	TESS	RKS
		No.	CHIRON	Coverage				Type	HI19	HA20	Published		Speckle
RKS/TIC					(day)	m s^{-1}	m s^{-1}				NEA/SB9/WDS	Obs./EB/PL	Obs./Det.
RKS0044−1856A	XTRA	12	11	DMY	803	75927.5	41.9	P	0	0	. . ✓	✓. .	✓✓
RKS0045+0147	25PC	13	144	DMY	1659	122.0	18.3	F	211	4	. . .	✓. .	✓.
RKS0048+0516	25PC	13	10	DMY	1447	66.7	14.5	F	244	183	. . ✓	✓. .	✓.
RKS0051+1844A	25PC	14	13	DMY	409	43.3	9.5	F	4	0	. . ✓	✓. .	✓✓
RKS0051−2254	25PC	14	16	DMY	409	44.9	7.1	F	0	4	. . ✓	✓. .	✓.
TIC 435876741	XTRA	15	9	DMY	789	108.7	26.1	F	0	0	. . ✓	✓. .	. .
RKS0055−2940A	33PC	15	7	DMY	379	37.7	7.8	F	6	0	. . ✓	✓. .	✓✓
RKS0056−1135	33PC	16	9	DMY	730	139.4	22.9	F	0	0	. . .	✓. .	. .
RKS0057+0551	25PC	16	6	DMY	381	50.6	11.6	F	0	0	. . .	✓. .	. .
RKS0100−2536	XTRA	17	9	DMY	368	35.2	7.9	F	0	5	. . .	✓. .	✓.
RKS0101−0953	XTRA	17	14	DMY	777	69.5	14.6	F	0	0	. . .	✓. .	✓.
RKS0102−1025	25PC	18	2	M	28	12.5	1.5	F	37	5	✓. .	✓. .	✓.
RKS0102+0503A	25PC	18	3	DM	30	43.3	13.1	F	10	4	. . ✓	✓. .	✓✓
RKS0102−2136	33PC	19	10	DMY	733	555.7	156.8	P	0	0	. . ✓	. . .	. .
RKS0104−2536	33PC	19	16	DMY	401	53.5	6.2	F	0	0	. . .	✓. .	✓.
RKS0104+2607	33PC	20	1		...	...	...	.	0	0	. . .	. . .	✓.
RKS0105+1523B	XTRA		0		...	...	...	.	0	0	. . ✓	✓. .	. .
RKS0105+1523A	33PC	20	11	DMY	799	224.2	27.9	F	0	0	. . ✓	✓. .	✓.
RKS0107+2257	25PC	21	23	DMY	1432	97.2	17.2	F	0	0	. . ✓	✓. ✓	✓.
RKS0108+1714	33PC	21	12	DMY	790	91.6	22.5	F	0	0	. . .	✓. .	. .
RKS0112+0058	XTRA	22	24	DMY	1472	59204.3	16233.0	O	0	0	. . .	✓. .	✓.
RKS0112−2514	25PC	22	4	DM	29	18.7	7.6	F	20	11	. . .	✓. .	✓.

Table 2: K dwarf companion search results.

			RV Survey Results						External				
ID	Sample	Fig.	No. Obs.	Cadence	Δt	ΔRV	MAD$_{RV}$	RV Det.	No. Obs.		Companion	TESS	RKS
		No.	CHIRON	Coverage				Type	HI19	HA20	Published		Speckle
RKS/TIC					(day)	m s^{-1}	m s^{-1}				NEA/SB9/WDS	Obs./EB/PL	Obs./Det.
RKS0113+1629	33PC	23	47	DMY	1449	192.5	41.7	P	0	0	✓. .	✓. .	✓.
RKS0116+2519	25PC	23	9	DMY	395	66.7	12.0	F	0	0	. . .	✓. .	✓.
RKS0117−1530	33PC	24	7	DMY	408	23.2	4.8	F	0	0	. . .	✓. .	✓.
RKS0118−0052B	XTRA	24	9	DMY	740	100.1	22.1	F	0	0	. . ✓	. . .	. .
RKS0118−0052A	33PC	25	43	DMY	1610	176.3	31.2	T	0	0	. . ✓	✓. .	✓✓
RKS0121+2419	33PC	25	9	DMY	395	72.5	15.6	F	0	0	. . .	✓. .	✓.
RKS0122−2653	33PC	26	9	DMY	487	57.7	10.0	F	0	8	✓. ✓	✓. .	✓.
RKS0123−1257B	XTRA	26	9	DMY	734	200.0	45.7	P	0	0	. . ✓	. . .	. .
RKS0123−1257A	33PC	27	1		...	...	...	.	91	33	. . ✓	✓. .	. .
RKS0124+1254	XTRA	27	7	DMY	380	57.1	7.7	F	0	0	. . .	✓. .	✓.
RKS0124+1829	33PC	28	2	Y	472	24.8	12.2	F	13	3	. . .	✓. .	✓.
RKS0125−0103	33PC	28	12	DMY	725	50.2	9.1	F	0	6	. . .	✓. .	✓.
RKS0129+2143	25PC	29	7	DY	398	72063.5	20684.0	O	0	3	. ✓✓	✓. .	. .
RKS0132+2059	33PC	29	15	DMY	732	413.8	55.3	F	0	0	. . .	✓. .	. .
RKS0133−2454	XTRA	30	10	DMY	381	76.8	10.1	F	0	9	. . .	✓. .	✓.
RKS0135−2046	33PC	30	9	DMY	657	71.9	19.4	P	0	0	. . .	. . .	. .
RKS0136+2133	XTRA	31	11	DMY	729	84.9	20.4	P	0	0	. . .	✓. .	✓.
TIC 29900813	XTRA	31	6	DM	29	52.3	10.8	F	14	19	. . ✓	✓. .	. .
RKS0139+1515	25PC	32	7	DMY	380	43.9	9.6	F	0	0	. . ✓	. . .	. .
RKS0142+2016	25PC	32	4	DY	1453	33.0	13.2	F	399	0	. . ✓	✓. .	✓.
RKS0143−2136	33PC	33	12	DMY	783	394.3	97.4	P	0	0	. . ✓	. . .	✓✓
TIC 164752884	XTRA	33	19	DMY	1475	109.5	23.1	A	0	0	. . ✓	✓. .	. .

Table 2: K dwarf companion search results.

			RV Survey Results						External				
ID	Sample	Fig.	No. Obs.	Cadence	Δt	ΔRV	MAD$_{RV}$	RV Det.	No. Obs.		Companion	TESS	RKS
		No.	CHIRON	Coverage				Type	HI19	HA20	Published		Speckle
RKS/TIC					(day)	m s^{-1}	m s^{-1}				NEA/SB9/WDS	Obs./EB/PL	Obs./Det.
TIC 238602461	XTRA	34	14	DMY	846	37.3	13.8	F	0	0	. . .	✓. .	. .
RKS0145−2503	XTRA	34	10	DMY	719	106.4	20.9	P	0	0	. . ✓	. . .	. .
RKS0146+1224	25PC	35	1		...	...	...	.	0	0	. . .	✓. .	✓.
RKS0150+2927	33PC	35	8	DMY	393	47.6	12.7	F	0	0	. . .	✓. .	✓.
RKS0150+1817	33PC	36	11	DMY	662	76.4	16.0	F	0	0	. . .	✓. .	. .
TIC 266680951	XTRA	36	4	DM	29	13.0	2.9	F	0	15	. . .	✓. .	. .
RKS0200+2636	33PC	37	11	DMY	673	228.2	66.8	T	0	0	. . .	✓. .	. .
TIC 250393730	XTRA	37	1		...	...	...	.	0	36	. . .	✓. .	. .
TIC 257500724	XTRA	38	9	DMY	381	70.3	15.1	A	0	0	. . .	✓. .	. .
RKS0205−2804	33PC	38	3	DY	434	18.4	9.8	F	0	4	. . ✓	✓. .	. .
RKS0209−1620	33PC	39	3	DY	416	12.7	7.5	F	0	206	. . .	✓. .	✓.
TIC 306450964	XTRA		0		...	...	...	.	7	0	. . .	✓. .	. .
TIC 302411994	XTRA	39	9	DMY	344	186.7	25.3	F	0	0	. . .	✓. .	. .
RKS0213−2111	25PC	40	1		...	...	...	.	18	82	. . .	✓. .	✓.
RKS0214−0338	25PC	40	4	DM	84	10.5	3.8	F	20	11	. . .	✓. .	✓.
RKS0215+0729	33PC	41	12	DMY	430	65.4	18.6	F	0	0	. . .	✓. .	. .
RKS0215−1814	25PC	41	9	DMY	397	534.7	170.3	T	0	0	. . ✓	. . .	. .
RKS0221−0652	33PC	42	1		...	...	...	.	11	0	. . .	✓. .	✓.
RKS0222+1824	XTRA	42	8	DMY	298	33.2	8.4	F	0	0	. . .	✓. .	✓.
TIC 422844595	XTRA	43	38	DMY	533	531.8	120.2	T	0	0	. ✓✓	✓. .	. .
RKS0229−1958A	25PC	43	49	DMY	1596	1207.0	302.2	O	0	0	. . ✓	✓. .	✓✓
RKS0231+0822	XTRA	44	21	DMY	1564	88.8	14.0	F	0	0	. . ✓	✓. ✓	✓.

Table 2: K dwarf companion search results.

			RV Survey Results						External				
ID	Sample	Fig.	No. Obs.	Cadence	Δt	ΔRV	MAD$_{RV}$	RV Det.	No. Obs.		Companion	TESS	RKS
		No.	CHIRON	Coverage				Type	HI19	HA20	Published		Speckle
RKS/TIC					(day)	m s^{-1}	m s^{-1}				NEA/SB9/WDS	Obs./EB/PL	Obs./Det.
RKS0231−2001	33PC	44	1		...	...	...	.	0	11	. . .	✓. .	✓.
RKS0231−1516	33PC	45	8	DMY	392	43.6	10.5	F	0	0	. . ✓	✓. .	✓.
RKS0236−2331	25PC	45	8	DM	198	70.7	13.4	P	0	18	. . ✓	✓. .	✓.
RKS0236−2710	33PC	46	1		...	...	...	.	0	68	. . .	✓. .	. .
RKS0236+0653	25PC	46	13	DMY	824	449.6	102.0	T	116	233	. . ✓	✓. .	✓.
RKS0236−0309	25PC	47	2	M	24	19307.6	9653.2	T	16	0	. ✓.	✓. .	✓.
RKS0240+0111	25PC	47	18	DMY	1656	77.1	14.3	F	6	0	. . .	✓. ✓	✓.
RKS0242+0322	25PC	48	7	DMY	383	60.7	5.8	F	0	0	. . .	✓. .	. .
RKS0243+1925A	25PC	48	9	DMY	362	4562.4	1931.9	T	5	0	. ✓✓	✓. .	✓✓
RKS0246+2538	33PC	49	1		...	...	...	.	34	0	. . .	✓. .	✓.
RKS0246+1146	25PC	49	1		...	...	...	.	46	0	. . .	✓. .	✓.
RKS0246−2305	25PC	50	6	DM	80	52.3	14.9	P	0	48	✓. .	✓. .	✓.
RKS0247+1922	33PC		0		...	...	...	.	0	0	. . ✓	✓. .	. .
RKS0247+2842	33PC	50	9	DMY	762	85.3	20.8	F	0	0	. . .	✓. .	✓.
RKS0248−1145	33PC	51	8	DMY	367	74.1	15.3	F	0	0	. . .	✓. .	✓.
RKS0248+2704	25PC	51	3	D	5	30.8	10.2	F	16	0	. ✓✓	✓. .	. .
RKS0250+1542	25PC	52	9	DMY	386	32.6	8.7	F	23	0	. . .	✓. .	. .
RKS0251+1038	33PC	52	1		...	...	...	.	16	0	. . .	✓. .	✓.
RKS0251−0816	33PC	53	11	DMY	708	85.9	21.4	T	0	0	. . .	✓. .	. .
RKS0252−1246	25PC	53	1		...	...	...	.	0	48	. . ✓	✓. .	. .
RKS0255+2652B	XTRA	54	1		...	...	...	.	0	0	. . ✓	. . .	. .
RKS0255+2652A	25PC	54	1	Y	435	0.0	...	P	0	0	✓. ✓	✓. .	. .

Table 2: K dwarf companion search results.

			RV Survey Results						External				
ID	Sample	Fig.	No. Obs.	Cadence	Δt	ΔRV	MAD$_{RV}$	RV Det.	No. Obs.		Companion	TESS	RKS
		No.	CHIRON	Coverage				Type	HI19	HA20	Published		Speckle
RKS/TIC					(day)	m s^{-1}	m s^{-1}				NEA/SB9/WDS	Obs./EB/PL	Obs./Det.
RKS0255+2807A	33PC	55	2	Y	353	66.6	8.7	F	0	0	. . .	✓. .	✓✓
RKS0257−2458	25PC	55	1		...	...	...	.	25	0	. ✓✓	✓. .	. .
RKS0258+2646	33PC	56	10	DMY	720	17858.2	6574.7	O	0	0	. . .	✓. .	. .
RKS0300+0744	25PC	56	1		...	...	...	.	27	10	. . .	✓. .	✓.
RKS0303+2006	25PC	57	9	DMY	356	68.3	18.0	F	0	0	. . .	✓. ✓	. .
RKS0306+0157	25PC	57	12	DMY	1181	39.5	8.1	F	0	0	. . .	✓. .	✓.
RKS0308−2445	33PC	58	11	DMY	713	87694.9	28387.3	P	0	0	. ✓.	✓✓.	. .
RKS0308−2410B	XTRA	58	8	DMY	683	87.1	16.4	F	0	0	. . .	✓. .	. .
RKS0308−2410A	33PC	59	8	DMY	683	67.9	15.4	F	0	0	. . .	✓. .	. .
RKS0310+1203	33PC	59	1		...	...	...	.	10	0	. . .	✓. .	. .
RKS0312−2859	XTRA	60	1		...	...	...	.	0	0	. . ✓	✓. .	. .
RKS0314−2626	25PC	60	7	DMY	383	136.9	17.4	F	10	13	. . .	✓. .	. .
RKS0314+0858	25PC	61	8	DMY	384	23.0	7.3	F	77	0	. . .	✓. .	. .
RKS0320+0827	33PC	61	1		...	...	...	.	12	0	. . .	✓. .	. .
RKS0322+2709	33PC	62	2	DY	411	97.8	28.9	F	0	0	. . ✓	✓. .	. .
RKS0324−0521	25PC	62	1		...	...	...	.	26	0	. . .	✓. .	. .
RKS0329−1140	25PC	63	7	DMY	300	47.7	9.7	F	0	8	. . .	✓. .	✓.
RKS0329−2406	33PC	63	9	DMY	395	139537.1	47720.7	O	0	0	. . .	✓✓.	✓.
RKS0332−0927	25PC	64	31	DY	1475	56.4	7.5	F	67	541	✓. ✓	✓. .	✓.
RKS0336+0035	33PC	64	1		...	...	...	.	0	0	. . ✓	. . .	. .
RKS0341+0336	33PC	65	12	DMY	1506	39217.7	6843.3	O	0	0	. ✓.	✓. .	✓.
RKS0342−2427	33PC	65	1		...	...	...	.	5	30	. . ✓	✓. .	. .

Table 2: K dwarf companion search results.

			RV Survey Results						External				
ID	Sample	Fig.	No. Obs.	Cadence	Δt	ΔRV	MAD$_{RV}$	RV Det.	No. Obs.		Companion	TESS	RKS
		No.	CHIRON	Coverage				Type	HI19	HA20	Published		Speckle
RKS/TIC					(day)	m s^{-1}	m s^{-1}				NEA/SB9/WDS	Obs./EB/PL	Obs./Det.
RKS0343−1253	33PC	66	13	DMY	716	98.3	15.0	F	0	6	. . .	✓. .	. .
RKS0343+1640	25PC	66	9	DMY	355	84.2	20.7	T	0	0	. . ✓	✓. .	. .
RKS0343−1906	25PC	67	1		...	...	...	.	77	33	. . .	✓. .	. .
RKS0344+1155	25PC	67	8	DMY	351	38.8	7.5	F	4	0	. . .	✓. .	✓.
RKS0345−2751	25PC	68	9	DMY	355	81.9	22.4	T	0	0	. . ✓	✓. .	. .
RKS0348+2519	33PC	68	11	DMY	691	67.5	15.5	P	0	0	. . .	✓. .	. .
RKS0348+1512	33PC	69	11	DMY	726	68.1	13.6	F	0	0	. . .	✓. .	. .
RKS0349−1329	33PC	69	11	DMY	719	143.9	20.8	F	0	0	. . .	✓. .	. .
RKS0349+0120	33PC	70	2	D	1	15.4	7.0	F	0	0	. . .	✓. .	✓.
RKS0350−2349	33PC	70	1		...	...	...	.	0	11	. . .	✓. .	. .
RKS0354−0649	25PC	71	1		...	...	...	.	67	0	. . .	✓. .	. .
RKS0357−2712	33PC	71	11	DMY	692	1157.9	243.2	T	0	0	. . ✓	. . .	. .
RKS0357−0109	25PC	72	2	M	44	29.5	5.3	F	22	42	. . ✓	✓. .	✓.
RKS0404+2634	33PC	72	11	DMY	727	111.5	25.2	F	0	0	. . .	. . .	. .
RKS0406−2051	33PC	73	1		...	...	...	.	44	43	✓. .	✓. .	. .
RKS0407+1413	33PC	73	11	DMY	720	76.9	15.3	F	0	0	. . .	✓. .	. .
RKS0408+1220	33PC	74	10	DMY	733	117.8	22.0	P	0	0	. . .	✓. .	. .
RKS0409+0918	XTRA	74	7	DMY	366	41.6	13.6	F	0	0	. . .	✓. .	✓.
RKS0414+0301	33PC	75	1		...	...	...	.	29	0	. . .	. . .	. .
RKS0415−0425A	XTRA	75	34	DMY	1557	2700.9	694.8	O	0	0	. ✓.	✓. .	✓✓
RKS0415−0739	25PC	76	8	DMY	898	43.9	10.8	A	284	616	✓. ✓	✓. .	. .
TIC 70899190	XTRA	76	39	DMY	1494	8863.6	2046.5	O	0	0	. . ✓	✓. .	. .

Table 2: K dwarf companion search results.

			RV Survey Results						External				
ID	Sample	Fig.	No. Obs.	Cadence	Δt	ΔRV	MAD$_{RV}$	RV Det.	No. Obs.		Companion	TESS	RKS
		No.	CHIRON	Coverage				Type	HI19	HA20	Published		Speckle
RKS/TIC					(day)	m s^{-1}	m s^{-1}				NEA/SB9/WDS	Obs./EB/PL	Obs./Det.
RKS0417+2240	33PC	77	9	DMY	733	107.9	26.5	P	5	0	. . ✓	✓. .	. .
RKS0417+2033	33PC	77	9	DMY	741	66.0	11.8	F	0	0	. . ✓	✓. .	. .
RKS0419−0408	33PC	78	1		...	...	...	.	0	0	. . .	✓. .	. .
RKS0420−1445	33PC	78	8	DMY	1085	68.6	10.5	F	0	8	. . .	✓. .	✓.
RKS0420−0902	XTRA	79	11	DMY	811	51.9	11.0	F	0	0	. . .	✓. .	✓.
RKS0421−1945	25PC	79	13	DMY	384	57.2	15.3	P	0	0	. . .	✓. .	. .
RKS0427+2022	25PC	80	9	DMY	355	126.2	28.1	F	0	0	. . .	✓. .	. .
RKS0427+2426A	33PC	80	1		...	...	...	.	0	0	. . .	. . .	✓✓
RKS0429+2155	25PC	81	1		...	...	...	.	31	0	. . .	✓. .	. .
RKS0430+0058	33PC	81	13	DMY	760	108.0	27.6	F	0	0	. . .	✓. .	✓.
RKS0432+0006	33PC	82	11	DMY	752	134.9	26.5	F	0	0	. . ✓	✓. .	. .
RKS0433+0338	33PC	82	11	DMY	740	571.9	117.6	P	0	0	. . .	. . .	. .
RKS0436+2707	25PC	83	13	DMY	1123	20400.0	5442.5	O	0	0	. ✓✓	✓. .	✓.
RKS0436−1453	XTRA	83	15	DMY	424	45.4	8.4	F	0	0	. . ✓	✓. .	✓.
RKS0439+0952A	33PC	84	5	DM	61	1303.3	480.8	P	0	0	. ✓✓	. . .	✓✓
RKS0440−0911	25PC	84	10	DMY	391	380.0	115.1	T	0	0	. . ✓	✓. .	. .
RKS0441+2054	25PC	85	16	DMY	1243	415.4	97.5	A	0	0	. . ✓	✓. .	✓.
RKS0443+2741	25PC	85	1		...	...	...	.	42	0	. . .	✓. .	✓.
RKS0445+0938	33PC	86	11	DMY	729	124.0	25.0	F	0	0	. . .	✓. .	. .
RKS0448−1056	33PC	86	1		...	...	...	.	10	6	. . .	✓. .	✓.
RKS0449−1447	33PC	87	15	DMY	807	80.1	16.2	F	0	9	. . .	✓. .	✓.
RKS0451+2837	33PC	87	9	DMY	759	122.8	25.3	F	0	0	. . .	✓. .	. .

Table 2: K dwarf companion search results.

			RV Survey Results						External				
ID	Sample	Fig.	No. Obs.	Cadence	Δt	ΔRV	MAD$_{RV}$	RV Det.	No. Obs.		Companion	TESS	RKS
		No.	CHIRON	Coverage				Type	HI19	HA20	Published		Speckle
RKS/TIC					(day)	m s^{-1}	m s^{-1}				NEA/SB9/WDS	Obs./EB/PL	Obs./Det.
RKS0453+2214	33PC	88	7	DMY	380	37.7	7.5	F	0	0	. . ✓	✓. .	✓.
RKS0454+0722B	XTRA	88	9	DMY	751	79.8	15.0	F	0	0	. . ✓	✓. .	. .
RKS0454+0722A	33PC	89	9	DMY	751	51.2	12.4	F	0	0	. . ✓	✓. .	. .
RKS0455−2833	25PC	89	1		...	...	...	.	31	5	. . .	✓. .	✓.
RKS0500−0545	25PC	90	0	D	12	...	9.3	F	331	144	. . .	✓. .	✓.
TIC 303676299	XTRA	90	10	DMY	795	68.4	19.1	F	0	0	. . .	✓. .	. .
RKS0503−2315A	25PC	91	29	DMY	826	24282.3	7639.2	O	4	0	. . ✓	✓. .	✓✓
RKS0503+0322	33PC	91	10	DMY	728	215.4	16.3	F	0	0	. . .	✓. .	. .
RKS0506−1102	33PC	92	9	DMY	747	130.0	31.6	P	0	0	. . .	✓. .	. .
RKS0506+1426	33PC	92	5	DM	45	4173.9	1892.8	P	5	0	. ✓.	✓. .	✓.
TIC 43866397	XTRA		0		...	...	...	.	0	25	. . ✓	✓. .	. .
RKS0512+1943	33PC	93	1		...	...	...	.	0	0	. . .	✓. .	✓.
RKS0513−2158	33PC	93	7	DMY	1196	803.7	245.3	P	0	0	. . .	✓. .	✓.
RKS0514+1952	33PC	94	8	DMY	729	100.3	34.0	P	0	0	. . .	✓. .	. .
RKS0514+0039	33PC	94	6	DMY	396	47.0	8.1	F	0	0	. . .	✓. .	✓.
RKS0518−2123	25PC	95	11	DMY	435	45.7	11.5	F	0	0	. . ✓	✓. .	✓.
RKS0519−0304A	XTRA		0		...	...	...	.	0	0	. . ✓	. . .	✓✓
RKS0519−0304B	25PC	95	16	DMY	518	47.6	11.9	A	0	0	. . ✓	✓. .	✓✓
RKS0519−1550	25PC	96	10	DMY	376	59.0	12.4	F	0	0	. . ✓	✓. .	✓.
RKS0522+0236A	25PC	96	42	DMY	1237	541.0	106.9	T	0	0	. . ✓	. . .	✓✓
RKS0523+1719	25PC	97	1		...	...	...	.	10	0	. . .	✓. .	✓.
RKS0526+1901	33PC		0	DMY	734	...	9093.9	P	0	0	. . .	✓. .	. .

Table 2: K dwarf companion search results.

			RV Survey Results						External				
ID	Sample	Fig.	No. Obs.	Cadence	Δt	ΔRV	MAD$_{RV}$	RV Det.	No. Obs.		Companion	TESS	RKS
		No.	CHIRON	Coverage				Type	HI19	HA20	Published		Speckle
RKS/TIC					(day)	m s^{-1}	m s^{-1}				NEA/SB9/WDS	Obs./EB/PL	Obs./Det.
RKS0528−0329	25PC	97	1		...	...	...	.	153	285	. . ✓	✓. .	✓.
RKS0533−2643	33PC	98	8	DMY	695	137.5	29.1	P	0	51	✓. .	✓. ✓	✓.
RKS0534−2328	33PC	98	9	DMY	424	48.5	4.8	F	0	0	. . .	✓. .	✓.
RKS0535+2805	33PC	99	3	DY	342	32.4	10.9	F	9	0	. . .	. . .	✓.
RKS0536+1119A	25PC	99	2	Y	507	22.9	7.6	F	34	21	. . ✓	✓. .	✓✓
TIC 247439806	XTRA	100	9	DMY	376	91.9	23.4	F	0	0	. . .	✓. .	. .
RKS0542+0240	33PC	100	8	DMY	406	29.7	4.0	F	0	0	. . .	. . .	✓.
RKS0544−2225	25PC	101	1		...	...	...	.	14	0	. . ✓	✓. .	. .
TIC 66653445	XTRA	101	12	DMY	368	31.5	7.3	F	0	9	. . .	✓. .	. .
RKS0549−1734	33PC	102	9	DMY	762	88.3	16.5	F	0	0	. . .	✓. .	. .
RKS0552−2246	33PC	102	9	DMY	763	84.6	17.1	F	0	0	. . .	✓. .	. .
RKS0553−0559	25PC	103	1		...	...	...	.	0	120	✓. .	✓. .	✓.
RKS0554+0208	33PC	103	1		...	...	...	.	12	0	. . .	✓. .	✓.
RKS0554−1942	25PC	104	9	DMY	437	40.8	13.6	F	0	0	. . ✓	. . .	. .
RKS0600+2101	33PC	104	5	DMY	395	29.6	9.0	F	0	0	. . .	✓. .	✓.
RKS0602+0848	33PC	105	5	DY	418	51.8	14.9	F	0	0	. . .	✓. .	. .
RKS0606−2754	XTRA	105	8	DMY	368	37.5	5.8	F	0	5	. . .	✓. .	✓.
TIC 415563103	XTRA		0		...	...	...	.	23	20	. . ✓	✓. .	. .
RKS0608+2630	33PC	106	3	D	9	1001.4	352.3	T	0	0	. . .	✓. .	. .
RKS0608+0928	XTRA	106	13	DMY	381	47.7	9.9	F	0	0	. . .	✓. .	✓.
RKS0609+0540	33PC	107	10	DMY	380	46.9	11.6	F	0	0	. . ✓	. . .	✓.
RKS0609+0009	33PC	107	3	D	7	15.6	8.2	F	0	0	. . .	. . .	. .

Table 2: K dwarf companion search results.

			RV Survey Results						External				
ID	Sample	Fig.	No. Obs.	Cadence	Δt	ΔRV	MAD$_{RV}$	RV Det.	No. Obs.		Companion	TESS	RKS
		No.	CHIRON	Coverage				Type	HI19	HA20	Published		Speckle
RKS/TIC					(day)	m s^{-1}	m s^{-1}				NEA/SB9/WDS	Obs./EB/PL	Obs./Det.
RKS0610+0225	33PC	108	4	DY	435	7977.7	3842.8	T	0	0	. . .	✓. .	. .
RKS0612+1023	33PC	108	3	D	6	21.3	3.8	F	0	0	. . .	. . .	. .
RKS0614+0510A	33PC	109	31	DMY	1241	111.8	20.9	T	0	0	. . .	. . .	✓✓
RKS0616+2512	33PC	109	54	DMY	1466	10803.3	2489.1	O	0	0	. . .	. . .	✓.
RKS0617+1759	33PC	110	9	DMY	337	52.1	10.4	F	0	0	. . .	✓. .	✓.
RKS0618−1352	33PC	110	1		...	...	...	.	0	15	. . .	✓. .	✓.
RKS0620+0215	33PC	111	1		...	...	...	.	19	0	. . .	✓. .	✓.
RKS0621−2212	33PC	111	1		...	...	...	.	0	27	. . .	✓. .	✓.
RKS0626+1845	25PC	112	12	DMY	341	109480.9	37581.9	O	0	8	. ✓✓	✓. .	. .
RKS0629+2700	33PC	112	9	DMY	368	44.3	7.7	F	0	0	. . .	✓. .	✓.
RKS0630−1148	33PC	113	1		...	...	...	.	11	17	. . .	✓. .	✓.
RKS0630+2104	33PC	113	5	DMY	672	189.3	48.8	F	0	0	. . .	. . .	. .
RKS0631+0552	XTRA	114	10	DMY	367	36.4	8.0	F	0	0	. . .	✓. .	✓.
RKS0632−2701	33PC	114	12	DMY	369	106.7	20.2	F	0	6	. . ✓	✓. .	. .
RKS0633+0527	33PC	115	1		...	...	...	.	72	1158	✓. ✓	. . .	. .
RKS0637+1945	33PC	115	1		...	...	...	.	0	0	. . .	✓. .	✓.
RKS0641+2357	25PC	116	1		...	...	...	.	11	0	. . .	✓. .	✓.
RKS0647−1815	33PC	116	9	DMY	355	54.2	10.8	F	0	0	. . .	✓. .	✓.
RKS0652−0510	25PC	117	2	D	9	11.6	5.6	F	36	12	. . ✓	✓. .	✓.
RKS0652−2306	33PC	117	1		...	...	...	.	0	22	. . .	✓. .	✓.
RKS0655−2008	33PC	118	3	DM	23	40.6	13.1	F	0	0	. . ✓	. . .	. .
RKS0658−1259A	25PC	118	52	DMY	1272	756.4	146.6	T	0	0	. . ✓	✓. .	✓✓

Table 2: K dwarf companion search results.

			RV Survey Results						External				
ID	Sample	Fig.	No. Obs.	Cadence	Δt	ΔRV	MAD$_{RV}$	RV Det.	No. Obs.		Companion	TESS	RKS
		No.	CHIRON	Coverage				Type	HI19	HA20	Published		Speckle
RKS/TIC					(day)	m s^{-1}	m s^{-1}				NEA/SB9/WDS	Obs./EB/PL	Obs./Det.
RKS0700−2847	25PC	119	8	DMY	442	40.3	8.8	F	0	0	. . .	✓. .	. .
RKS0701−2556A	25PC	119	41	DMY	1557	4639.5	899.0	O	0	0	. . .	✓. .	✓✓
RKS0701+0655	33PC	120	1		...	...	...	.	17	0	. . .	✓. .	✓.
RKS0702−0647	25PC	120	1		...	...	...	.	12	7	. . .	✓. .	✓.
RKS0705+2728	25PC	121	33	DMY	1156	130.1	20.1	P	0	0	✓. ✓	. . .	✓.
RKS0706+2358	33PC	121	8	DMY	363	31.7	8.1	F	0	0	. . .	. . .	✓.
RKS0707+0326	33PC	122	30	DMY	1092	6858.1	1910.6	O	0	0	. ✓.	✓. .	✓.
RKS0708+2950	25PC	122	9	DMY	424	44.9	6.5	F	0	0	. . .	✓. .	✓.
RKS0708−0958	33PC	123	10	DMY	408	33.5	6.5	F	0	0	. . .	✓. .	✓.
RKS0710−1425	25PC	123	8	DMY	437	61.4	13.1	F	0	0	. . .	✓. .	✓.
RKS0712−2453	33PC	124	1		...	...	...	.	0	15	✓. .	✓. .	✓.
RKS0713+2500	33PC	124	8	DMY	813	58.8	12.4	F	0	0	. . ✓	. . .	✓.
RKS0716−0339	33PC	125	1		...	...	...	.	0	0	✓. .	✓. .	✓.
RKS0718+1632	33PC	125	1		...	...	...	.	0	0	. . ✓	. . .	. .
RKS0720+2158	XTRA	126	8	DMY	397	26.2	6.8	F	0	0	. . ✓	✓. .	. .
RKS0723−2001	33PC	126	9	DMY	411	37.4	7.1	F	0	0	. . .	✓. .	✓.
RKS0723+2024	33PC	127	4	DM	18	347.1	119.0	T	0	0	. . .	✓. .	. .
RKS0723+1257	25PC	127	9	DMY	450	70.4	15.9	F	0	0	. . .	✓. .	✓.
RKS0724−1753	25PC	128	10	DMY	851	67.7	16.8	F	0	7	. . .	✓. .	✓.
RKS0725−1041	33PC	128	11	DMY	663	119.5	23.4	F	0	0	. . .	✓. .	. .
RKS0726−1546	33PC	129	35	DMY	872	12622.9	3994.6	O	0	0	. . .	✓. .	✓.
RKS0730−0340	25PC	129	8	DMY	442	54.6	10.3	F	0	0	. . .	✓. .	. .

Table 2: K dwarf companion search results.

			RV Survey Results						External				
ID	Sample	Fig.	No. Obs.	Cadence	Δt	ΔRV	MAD$_{RV}$	RV Det.	No. Obs.		Companion	TESS	RKS
		No.	CHIRON	Coverage				Type	HI19	HA20	Published		Speckle
RKS/TIC					(day)	m s^{-1}	m s^{-1}				NEA/SB9/WDS	Obs./EB/PL	Obs./Det.
RKS0731+1436	25PC	130	1		...	...	...	.	9	0	. . .	✓. .	✓.
RKS0732+1719	33PC	130	33	DMY	1581	6524.6	1321.0	O	0	0	. . ✓	✓. .	✓.
RKS0732−0853	33PC	131	2	D	0	2.0	1.0	F	0	0	. . ✓	. . .	. .
RKS0734−0653	25PC	131	1		...	...	...	.	17	0	. . ✓	✓. .	✓.
RKS0739−0335	25PC	132	1		...	...	...	.	17	0	. . ✓	✓. .	✓.
RKS0740−0336	XTRA	132	1		...	...	...	.	9	0	. . ✓	✓. .	. .
RKS0741−2921	33PC	133	3	D	5	10.5	1.6	F	0	0	. . .	✓. .	. .
RKS0745+0208	33PC	133	1		...	...	...	.	13	0	. . .	✓. .	✓.
RKS0752+2555	25PC	134	8	DMY	442	60.9	12.2	F	0	0	. . .	✓. .	. .
RKS0752+2233	XTRA	134	22	DMY	397	48.3	10.0	F	0	0	. . .	✓. .	✓.
RKS0754−2518	25PC	135	1		...	...	...	.	0	17	✓. ✓	✓. .	✓.
RKS0754−0124A	25PC	135	3	DM	42	2488.7	1086.5	T	0	0	. ✓✓	✓. .	✓✓
RKS0754+1914	25PC	136	1		...	...	...	.	0	0	. ✓✓	✓. .	✓.
RKS0755−1529	XTRA	136	11	DMY	808	91.8	20.3	F	0	0	. . .	. . .	✓.
RKS0757−0048	25PC	137	1		...	...	...	.	54	69	. . ✓	✓. .	✓.
RKS0758−2537	25PC	137	1		...	...	...	.	18	0	. . ✓	✓. .	✓.
RKS0758−1501A	33PC	138	1		...	...	...	.	9	0	. . .	✓. .	✓✓
TIC 271266069	XTRA	138	10	DMY	1074	72.0	8.9	F	0	0	. . .	✓. .	. .
RKS0759+2050	25PC	139	1		...	...	...	.	54	0	. ✓.	✓. .	✓.
TIC 19064262	XTRA	139	8	DMY	405	43.6	8.7	F	0	0	. . .	✓. .	. .
TIC 171523537	XTRA		0		...	...	...	.	81	0	. . .	✓. .	. .
RKS0804+1217	33PC	140	3	D	4	346.2	115.4	F	0	0	. . ✓	. . .	. .

Table 2: K dwarf companion search results.

			RV Survey Results						External				
ID	Sample	Fig.	No. Obs.	Cadence	Δt	ΔRV	MAD$_{RV}$	RV Det.	No. Obs.		Companion	TESS	RKS
		No.	CHIRON	Coverage				Type	HI19	HA20	Published		Speckle
RKS/TIC					(day)	m s^{-1}	m s^{-1}				NEA/SB9/WDS	Obs./EB/PL	Obs./Det.
RKS0808+2106	25PC	140	11	DMY	409	46.3	9.9	F	0	0	. . ✓	. . .	✓.
RKS0813−1355A	33PC	141	3	DM	64	10850.0	4718.5	T	0	0	. . ✓	✓. .	. .
RKS0813−1355B	XTRA	141	9	DMY	426	7464.8	2364.1	O	0	0	. . ✓	. . .	. .
RKS0814+1301	25PC	142	1		...	...	...	.	27	0	. . .	✓. .	✓.
RKS0815−2600	33PC	142	1		...	...	...	.	0	32	. . .	✓. .	✓.
RKS0817+1717	33PC	143	3	D	4	23.7	3.2	F	0	0	. . .	✓. .	. .
RKS0818−1512A	XTRA	143	42	DMY	1589	6748.7	1961.5	O	0	7	. . .	✓. .	✓✓
RKS0819+0120	25PC	144	1		...	...	...	.	0	29	. . .	. . .	✓.
RKS0820+1404	25PC	144	1		...	...	...	.	23	0	. . .	✓. .	✓.
RKS0823+2150	33PC	145	1		...	...	...	.	20	0	. . .	✓. .	✓.
RKS0827+2855	33PC	145	1		...	...	...	.	8	0	. . .	✓. .	✓.
RKS0832−2323	33PC	146	3	D	4	20.9	4.5	F	0	0	. . .	. . .	. .
TIC 121286109	XTRA	146	33	DMY	518	65.9	13.0	A	0	0	. . ✓	✓. .	. .
RKS0838−0415	33PC	147	10	DMY	372	64.5	18.2	F	0	0	. . .	✓. .	. .
RKS0838−1315	33PC	147	5	DM	110	36.5	13.5	F	0	9	✓. .	✓. ✓	✓.
RKS0839+0657	33PC	148	9	DMY	371	45533.6	14879.3	O	0	0	. ✓.	✓. .	. .
RKS0839+1131	25PC	148	1		...	...	...	.	59	0	. . ✓	✓. .	✓.
RKS0840−0628A	33PC	149	37	DMY	1590	19773.5	5843.4	O	0	0	. . .	✓. .	✓✓
RKS0848+0628	33PC	149	14	DMY	816	76.6	17.2	F	0	0	. . ✓	. . .	✓.
RKS0850+0751	25PC	150	9	DM	102	187.1	47.0	T	0	0	. . ✓	. . .	. .
RKS0852+2819	25PC	150	2	M	16	81.7	35.7	P	660	88	✓. ✓	✓✓✓	. .
RKS0854−2423	XTRA	151	10	DMY	407	51.9	11.7	F	0	0	. . .	✓. .	✓.

Table 2: K dwarf companion search results.

			RV Survey Results						External				
ID	Sample	Fig.	No. Obs.	Cadence	Δt	ΔRV	MAD$_{RV}$	RV Det.	No. Obs.		Companion	TESS	RKS
		No.	CHIRON	Coverage				Type	HI19	HA20	Published		Speckle
RKS/TIC					(day)	m s^{-1}	m s^{-1}				NEA/SB9/WDS	Obs./EB/PL	Obs./Det.
RKS0855+0132	25PC	151	1		...	...	...	.	0	0	✓. .	✓. .	. .
RKS0858+2032	25PC	152	8	DMY	397	53.3	6.6	F	0	0	. . .	✓. .	✓.
RKS0859+0151A	XTRA	152	11	DMY	397	116.9	24.7	F	0	0	. . ✓	. . .	✓✓
RKS0900+2127	33PC	153	5	DM	36	1384.5	564.6	P	0	0	. ✓.	✓. .	✓.
RKS0901+1515B	XTRA		0		...	...	...	.	0	0	. . ✓	. . .	. .
RKS0901+1515A	25PC	153	11	DMY	1088	55.5	9.3	F	0	0	. . ✓	✓. .	✓.
RKS0904−1554	33PC	154	15	DMY	810	70.4	17.7	F	0	6	. . .	✓. .	✓.
RKS0905+2517	33PC	154	5	D	6	56.1	15.0	F	0	0	. . .	✓. .	. .
TIC 19976193	XTRA		0		...	...	...	.	0	26	. . ✓	✓. .	. .
RKS0907+2252	33PC	155	8	DMY	375	25743.0	7417.4	O	0	0	. ✓.	. . .	. .
RKS0909+2725	XTRA	155	8	DMY	397	38.6	8.0	F	0	0	. . .	✓. .	✓.
RKS0909+0512	33PC	156	4	DM	75	17.9	4.7	F	0	0	. . .	✓. .	. .
RKS0914+0426A	25PC	156	40	DMY	1496	1636.0	349.9	O	3	0	. . ✓	✓. .	✓✓
RKS0917−0323	33PC	157	9	DY	439	94914.7	23533.0	P	0	0	. . .	✓. ✓	. .
RKS0918+2718	25PC	157	9	DM	47	49.8	11.2	F	4	0	. . .	✓. .	. .
RKS0919+0053	33PC	158	1		...	...	...	.	16	0	. . .	✓. .	✓.
RKS0920−0545	25PC	158	1		...	...	...	.	5	29	. . .	✓. .	✓.
RKS0929−0245	25PC	159	10	DM	73	53.2	11.4	F	0	0	. . ✓	✓. .	. .
RKS0929−0522	25PC	159	7	DMY	370	29.5	7.3	F	0	8	. . .	✓. .	✓.
RKS0929+0539	25PC	160	1		...	...	...	.	0	0	. . .	✓. .	✓.
RKS0932+2909	33PC	160	3	DMY	358	138.8	25.4	F	0	0	. . .	✓. .	. .
RKS0932−1111	25PC	161	1		...	...	...	.	0	40	. . .	✓. .	✓.

Table 2: K dwarf companion search results.

			RV Survey Results						External				
ID	Sample	Fig.	No. Obs.	Cadence	Δt	ΔRV	MAD$_{RV}$	RV Det.	No. Obs.		Companion	TESS	RKS
		No.	CHIRON	Coverage				Type	HI19	HA20	Published		Speckle
RKS/TIC					(day)	m s^{-1}	m s^{-1}				NEA/SB9/WDS	Obs./EB/PL	Obs./Det.
TIC 172533278	XTRA	161	38	DMY	1199	228.8	51.7	O	0	0	. . ✓	✓. .	. .
RKS0937+2241	25PC	162	9	DMY	412	47.0	10.2	F	7	0	. . .	✓. .	✓.
RKS0937+2231A	33PC	162	18	DMY	814	86.0	16.8	T	0	0	. . .	✓. .	✓✓
RKS0938+0240	33PC	163	4	D	8	63.2	15.9	F	0	0	. . .	✓. .	. .
RKS0947+0134	33PC	163	12	DMY	413	59.1	19.1	F	0	0	. . .	✓. .	✓.
RKS0947+2618	XTRA	164	10	DMY	396	72.0	14.0	F	0	0	. . .	✓. .	✓.
RKS0952+0313	25PC	164	1		...	...	...	.	11	0	. . ✓	✓. .	✓.
RKS0952+0307	33PC	165	10	DMY	415	39.4	9.6	F	0	0	. . .	✓. .	✓.
RKS0959−0911	33PC	165	28	DMY	1293	4586.0	802.5	O	0	9	. . .	✓. .	✓.
RKS1000+2433	33PC	166	3	DY	265	78164.1	23163.5	P	0	0	. ✓✓	✓. .	. .
RKS1001−1525	33PC	166	13	DMY	786	62.3	15.6	F	0	0	. . .	✓. .	✓.
RKS1004−1143	25PC	167	1		...	...	...	.	18	0	. . ✓	✓. .	✓.
RKS1005+2629	33PC	167	8	DMY	430	38.4	5.4	F	0	0	. . .	✓. .	✓.
RKS1006+0257A	25PC	168	9	DMY	433	32.1	9.1	F	0	0	. . ✓	✓. .	✓✓
RKS1008+1159	25PC	168	10	DM	44	44.6	7.4	F	0	0	. . ✓	. . .	. .
RKS1011−2425	33PC	169	4	D	9	17.8	4.8	F	0	0	. . ✓	✓. .	. .
RKS1020−0128	33PC	169	11	DMY	413	24.9	6.8	F	0	6	. . .	✓. .	✓.
RKS1021−1743A	33PC	170	13	DMY	1108	181.6	46.6	F	0	0	. . .	✓. .	✓✓
TIC 350043652	XTRA	170	11	DMY	425	38.6	7.2	F	0	0	. . .	✓. .	. .
RKS1024−1024	33PC	171	1		...	...	...	.	0	16	. . .	✓. .	✓.
RKS1026−0631	33PC	171	34	DMY	1535	11091.2	2677.2	O	0	0	. . ✓	✓. .	✓.
RKS1026+2638	33PC	172	9	DM	153	763.5	261.4	T	0	0	. ✓.	✓. .	✓.

Table 2: K dwarf companion search results.

ID	Sample	Fig.	RV Survey Results						External				
			No. Obs.	Cadence	Δt	ΔRV	MAD$_{RV}$	RV Det.	No. Obs.		Companion	TESS	RKS
		No.	CHIRON	Coverage				Type	HI19	HA20	Published		Speckle
RKS/TIC					(day)	m s^{-1}	m s^{-1}				NEA/SB9/WDS	Obs./EB/PL	Obs./Det.
RKS1028+0644	33PC	172	9	DMY	413	38.5	9.4	F	0	0	. . .	✓. .	✓.
RKS1030−2114	33PC	173	1		...	...	...	.	20	9	. . .	✓. .	✓.
RKS1032+0830A	33PC	173	2	D	0	16.8	7.7	F	0	0	. . .	. . .	✓✓
RKS1036−1350	33PC	174	12	DMY	778	70.9	14.9	F	0	0	. . .	✓. .	✓.
RKS1043−2903	25PC	174	1		...	...	...	.	19	39	. . ✓	✓. .	✓.
RKS1046−2435	25PC	175	9	DMY	378	46.0	7.7	F	0	5	. . ✓	✓. .	✓.
RKS1047+2129	XTRA	175	7	DMY	335	49.1	8.7	F	0	0	. . .	✓. .	✓.
RKS1047−2217	XTRA	176	1		...	...	...	.	0	29	. . .	✓. .	✓.
RKS1053−1422	33PC	176	1		...	...	...	.	0	0	. . .	✓. .	✓.
RKS1054−0432	33PC	177	3	DM	15	33.5	2.1	F	0	0	. . .	✓. .	. .
RKS1056+0723	25PC	177	9	DMY	413	53.3	14.5	F	0	6	. . .	. . .	✓.
RKS1057+2856	33PC	178	19	DMY	748	1804.7	351.4	T	5	0	. . .	✓. .	✓.
RKS1059+1759	33PC	178	4	DY	342	2300.3	874.8	T	0	0	. . ✓	✓. .	. .
RKS1059+2526A	25PC	179	8	DM	47	35.4	9.4	F	0	0	. . ✓	. . .	. .
RKS1059+2526B	XTRA	179	8	DM	56	32.2	9.5	F	0	0	. . ✓	. . .	. .
RKS1102−0919A	33PC	180	19	DMY	742	129.8	25.3	T	0	0	. . .	✓. .	✓✓
RKS1105+0720	33PC	180	6	D	0	767.7	297.6	T	0	0	. . ✓	. . .	. .
RKS1108−2816A	33PC	181	29	DMY	1443	13557.8	4254.4	O	0	6	. . .	✓. .	✓✓
RKS1108+1546	33PC	181	1		...	...	...	.	12	0	. . .	✓. .	✓.
TIC 62904024	XTRA	182	10	DMY	707	81.7	15.2	F	0	0	. . .	✓. .	. .
RKS1111−1057	25PC	182	9	DMY	402	20.8	4.7	F	6	0	. . .	✓. .	✓.
RKS1111−1459A	25PC	183	26	DMY	1474	14579.6	3674.5	O	0	0	. . .	. . .	✓✓

Table 2: K dwarf companion search results.

ID	Sample	Fig.	RV Survey Results						External				
			No. Obs.	Cadence	Δt	ΔRV	MAD$_{RV}$	RV Det.	No. Obs.		Companion	TESS	RKS
		No.	CHIRON	Coverage				Type	HI19	HA20	Published		Speckle
RKS/TIC					(day)	m s^{-1}	m s^{-1}				NEA/SB9/WDS	Obs./EB/PL	Obs./Det.
TIC 425283213	XTRA	183	10	DMY	1018	240.6	38.5	F	0	0	. . ✓	. . .	. .
RKS1113+0428	25PC	184	10	DMY	409	24.0	5.8	F	4	0	. . .	✓. .	✓.
RKS1114+2542	25PC	184	2	M	35	12.8	0.7	F	452	0	✓. .	✓. ✓	✓.
RKS1114−2306	25PC	185	8	DMY	447	22.5	7.7	F	0	0	. . ✓	✓. .	✓.
RKS1115−1808B	XTRA	185	9	DMY	718	83.1	15.8	F	0	15	. . ✓	. . .	. .
RKS1115−1808A	25PC	186	8	DMY	390	23.9	5.9	F	0	0	. . ✓	✓. .	. .
RKS1116−1441	25PC	186	7	DMY	470	42.9	7.5	F	0	7	. . .	. . .	✓.
RKS1117−2748	25PC	187	7	DMY	407	10.1	2.6	F	0	6	. . .	✓. .	✓.
RKS1117−0158	33PC	187	1		...	...	...	.	0	35	. . .	✓. .	✓.
RKS1121−2027	25PC	188	21	DMY	1238	1047.8	234.6	O	0	0	. . ✓	✓. .	✓.
RKS1121+1811	33PC	188	1		...	...	...	.	7	0	✓. ✓	✓. .	. .
RKS1123+0701A	33PC	189	20	DMY	1064	273.3	77.7	O	0	0	. . ✓	. . .	✓✓
RKS1124−1741	33PC	189	1		...	...	...	.	0	0	. . ✓	. . .	. .
RKS1125+2000	33PC	190	9	DMY	348	57.8	5.4	F	0	0	. . .	✓. .	✓.
RKS1126+0300B	XTRA		0		...	...	...	.	178	38	✓. ✓	✓. .	. .
RKS1126+1517	33PC	190	11	DMY	826	71.7	19.9	F	0	0	. . .	✓. .	. .
RKS1127+0358A	33PC	191	17	DMY	1174	347.6	91.7	O	4	0	. . .	. . .	✓✓
RKS1128+0731	33PC	191	9	DMY	383	42.1	11.7	F	0	0	. . ✓	✓. .	✓.
RKS1131+1422	25PC	192	1		...	...	...	.	0	0	. . ✓	. . .	. .
RKS1134−1314	33PC	192	2	D	0	13.3	6.7	F	0	11	. . .	✓. .	✓.
RKS1135+2436A	XTRA	193	6	DMY	433	44.2	14.7	F	0	0	. . .	✓. .	✓✓
RKS1135+1658	33PC	193	5	DM	53	28.7	6.2	F	0	0	. . .	✓. .	✓.

Table 2: K dwarf companion search results.

ID	Sample	Fig.	RV Survey Results						External				
			No. Obs.	Cadence	Δt	ΔRV	MAD$_{RV}$	RV Det.	No. Obs.		Companion	TESS	RKS
		No.	CHIRON	Coverage				Type	HI19	HA20	Published		Speckle
RKS/TIC					(day)	m s^{-1}	m s^{-1}				NEA/SB9/WDS	Obs./EB/PL	Obs./Det.
RKS1139−2741	33PC	194	5	DM	67	47.0	6.3	F	0	12	. . ✓	✓. .	✓.
RKS1141+0508A	33PC	194	7	DMY	451	5666.3	1618.5	T	5	0	. ✓.	✓. .	✓✓
RKS1142+2301	33PC	195	16	DMY	1127	117.2	33.5	F	0	0	. . ✓	✓. ✓	✓.
TIC 397024052	XTRA	195	20	DM	30	152.6	39.4	O	30	24	✓. .	✓. .	. .
RKS1147−1149A	33PC	196	15	DMY	1024	65.8	15.5	F	0	0	. . ✓	✓. .	✓✓
RKS1152+1845	33PC	196	7	DMY	445	32.3	7.4	F	0	0	. . .	✓. .	✓.
RKS1154+2844	33PC	197	38	DMY	1170	1310.0	312.3	O	0	0	. . .	✓. .	✓.
RKS1157−2608	33PC	197	5	DM	67	32.5	6.4	F	0	0	. . .	✓. .	✓.
RKS1157+1959	33PC	198	1		...	...	...	.	11	13	. . .	. . .	✓.
RKS1157−2742	25PC	198	131	DMY	1787	110.3	22.6	F	104	0	. . .	✓. .	✓.
RKS1158−2355	33PC	199	7	DMY	382	31.3	6.5	F	0	4	✓. .	✓. .	✓.
RKS1158−2535	33PC	199	9	DMY	721	378.2	91.8	T	0	0	. . .	✓. .	. .
RKS1159−2021	25PC	200	1		...	...	...	.	65	88	✓. .	✓. .	✓.
RKS1204+0911	33PC	200	3	D	3	27.5	10.1	F	0	0	. . .	✓. .	✓.
RKS1204−0013	33PC	201	2	D	0	28.4	5.4	F	0	0	. . .	. . .	. .
TIC 96243602	XTRA	201	3	D	5	15.6	4.7	F	0	0	. . .	✓. .	. .
RKS1205−1852	25PC	202	46	DMY	1323	76601.3	23741.0	O	0	0	. . ✓	✓. .	✓.
RKS1206−2336	33PC	202	2	D	0	22.4	10.4	F	0	0	. . .	✓. .	. .
RKS1208−0028	33PC	203	2	D	0	25.2	9.1	F	0	0	. . .	. . .	. .
RKS1209−2646	33PC	203	2	D	0	11.6	5.8	F	0	0	. . .	✓. .	. .
RKS1209−1151	25PC	204	11	DM	179	41.4	5.8	F	0	0	. . ✓	. . .	. .
RKS1210−1126	33PC	204	2	D	0	23.9	9.2	F	0	0	. . .	✓. .	. .

Table 2: K dwarf companion search results.

ID	Sample	Fig.	RV Survey Results						External				
			No. Obs.	Cadence	Δt	ΔRV	MAD$_{RV}$	RV Det.	No. Obs.		Companion	TESS	RKS
		No.	CHIRON	Coverage				Type	HI19	HA20	Published		Speckle
RKS/TIC					(day)	m s^{-1}	m s^{-1}				NEA/SB9/WDS	Obs./EB/PL	Obs./Det.
RKS1215+0538A	XTRA	205	22	DMY	887	549.6	129.2	T	0	0	. . ✓	. . .	✓✓
RKS1220−1953	33PC	205	8	DMY	345	59.7	4.5	F	0	0	. . .	✓. .	✓.
TIC 328961501	XTRA	206	3	D	5	5.0	2.3	F	0	0	. . .	✓. .	. .
RKS1222+0518	33PC	206	1		...	...	...	.	0	0	. . ✓	. . .	. .
RKS1222+2736	33PC	207	3	D	4	33.5	9.2	F	6	0	. . .	✓. .	✓.
RKS1223+2754	33PC	207	2	D	0	10.1	5.1	F	0	0	. . .	✓. .	✓.
RKS1227+2701	33PC	208	1		...	...	...	.	0	0	. . ✓	. . .	. .
RKS1228−1654	33PC	208	1		...	...	...	.	0	33	. . .	✓. .	✓.
RKS1228−1817	25PC	209	1		...	...	...	.	0	12	. . .	✓. .	✓.
RKS1229−1631	33PC	209	1		...	...	...	.	0	2	. . ✓	. . .	. .
RKS1230−1323	XTRA	210	13	DMY	403	212.5	56.4	P	0	0	. . ✓	. . .	. .
RKS1231+2013	33PC	210	16	DMY	1199	623.6	172.2	T	0	0	. . .	✓. .	✓.
RKS1233−1438	33PC	211	7	DMY	299	34.9	5.5	F	0	0	. . .	✓. .	✓.
RKS1241+1522	25PC	211	3	D	5	21.4	5.6	F	71	0	. . ✓	✓. .	✓.
RKS1241+1951	33PC	212	4	DY	408	5893.6	2888.0	T	0	0	. ✓.	✓. .	✓.
RKS1248−2448B	XTRA	212	1		...	...	...	.	0	12	. . ✓	. . .	. .
RKS1248−2448A	25PC	213	1		...	...	...	.	0	0	. . ✓	. . .	✓.
RKS1248−1543A	33PC	213	1		...	...	...	.	0	0	. . ✓	✓. .	✓✓
RKS1250−0046	25PC	214	1		...	...	...	.	50	10	. . .	. . .	✓.
RKS1253+0645	33PC	214	13	DMY	380	36079.4	10315.1	P	0	0	. ✓.	✓. .	✓.
RKS1256−2455	33PC	215	1		...	...	...	.	0	40	. . .	✓. .	✓.
RKS1257−1427	33PC	215	9	DMY	332	246.1	49.5	T	4	0	. ✓✓	. . .	✓.

Table 2: K dwarf companion search results.

			RV Survey Results						External				
ID	Sample	Fig.	No. Obs.	Cadence	Δt	ΔRV	MAD$_{RV}$	RV Det.	No. Obs.		Companion	TESS	RKS
		No.	CHIRON	Coverage				Type	HI19	HA20	Published		Speckle
RKS/TIC					(day)	m s^{-1}	m s^{-1}				NEA/SB9/WDS	Obs./EB/PL	Obs./Det.
RKS1259−0950	25PC	216	31	DMY	347	3261.7	1073.1	O	0	0	. ✓✓	. . .	✓.
RKS1300−0242	33PC	216	14	DMY	307	74.6	10.2	F	0	5	. . .	✓. .	✓.
RKS1302−2647	25PC	217	27	DMY	1437	62000.6	18500.3	O	7	0	. . .	✓. .	✓.
RKS1303−0509	25PC	217	1		...	...	...	.	0	20	. ✓✓	✓. .	✓.
RKS1306+2043A	25PC	218	19	DMY	1672	275.1	54.9	T	0	0	. . ✓	✓. .	✓✓
RKS1310+0932	33PC	218	1		...	...	...	.	9	0	. . .	✓. .	✓.
RKS1312−0215	25PC	219	1		...	...	...	.	137	90	✓. .	✓. .	✓.
RKS1316+1701	25PC	219	1		...	...	...	.	18	0	✓. ✓	✓. .	✓.
RKS1318−1446	33PC	220	2	D	0	24.1	9.8	F	0	0	. . .	✓. .	. .
RKS1320+0407	33PC	220	1		...	...	...	.	0	0	. . .	✓. .	. .
RKS1323+2914A	25PC	221	6	DMY	765	84.4	19.5	F	0	0	. . ✓	✓. .	. .
RKS1323+2914B	XTRA	221	1		...	...	...	.	0	0	. . ✓	✓. .	. .
RKS1323+0243A	25PC	222	1		...	...	...	.	74	0	. . ✓	✓. .	✓.
RKS1323+0243B	XTRA	222	1		...	...	...	.	114	0	. . ✓	✓. .	. .
RKS1326−2417	XTRA	223	10	DMY	891	39.6	9.7	F	0	14	. . ✓	✓. .	✓.
RKS1327−2417	33PC	223	1		...	...	...	.	0	0	. . ✓	✓. .	. .
RKS1331−0219	33PC	224	1		...	...	...	.	0	0	. ✓✓	✓. .	. .
RKS1333+0835	25PC	224	1		...	...	...	.	24	0	. . .	✓. .	✓.
RKS1334−0018	33PC	225	1		...	...	...	.	0	0	. . ✓	. . .	. .
RKS1334+0440	25PC	225	1		...	...	...	.	12	0	. . .	✓. .	✓.
RKS1334−0820	25PC	226	1		...	...	...	.	0	17	. . .	. . .	✓.
RKS1335+0650	33PC	226	1		...	...	...	.	7	0	. . .	✓. .	✓.

Table 2: K dwarf companion search results.

ID	Sample	Fig.	RV Survey Results						External				
			No. Obs.	Cadence	Δt	ΔRV	MAD$_{RV}$	RV Det.	No. Obs.		Companion	TESS	RKS
		No.	CHIRON	Coverage				Type	HI19	HA20	Published		Speckle
RKS/TIC					(day)	m s^{-1}	m s^{-1}				NEA/SB9/WDS	Obs./EB/PL	Obs./Det.
RKS1335−0023	25PC	227	7	DMY	809	47.0	13.6	F	0	0	. . .	✓. .	. .
RKS1336+0746	33PC	227	1		...	...	...	.	0	0	. . .	✓. .	✓.
RKS1338−0614	25PC	228	7	DMY	821	56.9	7.6	F	0	0	. . .	. . .	. .
RKS1340−0411	25PC	228	9	DMY	348	45.1	10.2	F	0	6	. . .	. . .	✓.
RKS1341−0007	25PC	229	1		...	...	...	.	5	8	. . .	✓. .	✓.
RKS1342−0141	25PC	229	1		...	...	...	.	0	0	. . .	✓. .	✓.
RKS1345+1747	25PC	230	12	DMY	1066	59.6	15.9	F	0	0	. . ✓	✓. .	. .
RKS1345−0437	33PC	230	8	DMY	355	60.2	11.7	F	0	5	. . .	. . .	✓.
RKS1345+0850	25PC	231	9	DMY	395	134.9	13.5	F	4	4	. . .	✓. .	✓.
RKS1346−0027	XTRA	231	9	DMY	887	51.1	13.5	F	0	0	. . .	✓. .	✓.
RKS1347+0618	33PC	232	8	DMY	409	50.7	10.9	F	0	0	. . .	✓. .	✓.
RKS1347+2127	33PC	232	2	D	0	8.0	4.0	F	0	0	. . ✓	✓. .	. .
TIC 187309694	XTRA	233	9	DMY	866	85.0	19.1	A	0	0	. . .	. . .	. .
RKS1349+2658A	25PC	233	1		...	...	...	.	19	0	. . ✓	✓. .	. .
RKS1349+2658B	XTRA	234	1		...	...	...	.	22	0	. . ✓	✓. .	. .
RKS1349−2206	25PC	234	1		...	...	...	.	54	11	. . .	✓. .	✓.
RKS1353+2748	33PC	235	6	DMY	672	462.0	114.3	T	0	0	. . .	✓. .	✓.
RKS1353+1256A	25PC	235	39	DMY	973	2814.5	689.3	O	0	0	. . ✓	✓. .	✓✓
RKS1359+2252	25PC	236	1		...	...	...	.	82	0	. . .	✓. .	✓.
RKS1401+1529	33PC	236	3	DY	611	89.3	21.2	F	0	0	. . ✓	✓. .	. .
RKS1411−1236	25PC	237	1		...	...	...	.	25	12	. . ✓	. . .	✓.
RKS1412+2348A	33PC	237	10	DMY	374	30.4	8.5	F	0	0	. . .	✓. .	✓✓

Table 2: K dwarf companion search results.

			RV Survey Results						External				
ID	Sample	Fig.	No. Obs.	Cadence	Δt	ΔRV	MAD$_{RV}$	RV Det.	No. Obs.		Companion	TESS	RKS
		No.	CHIRON	Coverage				Type	HI19	HA20	Published		Speckle
RKS/TIC					(day)	m s^{-1}	m s^{-1}				NEA/SB9/WDS	Obs./EB/PL	Obs./Det.
RKS1413−0657	25PC	238	8	DMY	369	35.2	5.4	F	0	6	. . .	✓. .	✓.
RKS1414−1521	33PC	238	2	Y	354	261.7	130.9	T	0	0	. . ✓	. . .	. .
RKS1416+2007	33PC	239	1		...	...	...	.	0	0	. . ✓	. . .	. .
RKS1418−0636A	25PC	239	29	DMY	654	2088.9	490.1	T	0	0	. ✓✓	. . .	✓✓
RKS1419−2548	XTRA	240	1	D	0	0.0	...	F	0	0	. . ✓	. . .	. .
RKS1419−0509	25PC	240	1		...	...	...	.	50	43	. . ✓	✓. .	✓.
RKS1421+2937	25PC	241	9	DMY	425	48.6	13.0	F	0	0	. . .	✓. .	✓.
RKS1424−1727A	XTRA	241	8	DMY	418	66.8	23.0	F	0	0	. . .	. . .	✓✓
TIC 298434280	XTRA	242	16	DMY	277	44.5	8.5	F	0	0	. . ✓	✓. .	. .
RKS1430−0838	25PC	242	8	DMY	392	20.0	5.6	F	0	6	. . ✓	. . .	✓.
RKS1432+1121	33PC	243	1		...	...	...	.	0	0	. . .	. . .	. .
RKS1433+0920	33PC	243	9	DMY	861	38.8	8.1	F	0	0	. . ✓	✓. .	✓.
RKS1436+0944	25PC	244	1		...	...	...	.	133	0	✓. ✓	✓. .	✓.
RKS1437−2548	33PC	244	2	D	0	19.2	7.4	F	0	30	. . .	✓. .	✓.
RKS1442+1930	25PC	245	11	DMY	885	56.1	14.6	F	0	0	. . ✓	. . .	. .
TIC 287081516	XTRA	245	16	DMY	270	35.5	7.7	F	0	0	. . ✓	. . .	. .
RKS1444+2211	33PC	246	10	DMY	411	62.6	12.4	F	0	0	. . .	✓. .	✓.
RKS1444−2215	33PC	246	1		...	...	...	.	0	0	. . ✓	✓. .	. .
RKS1445+1350	25PC	247	1		...	...	...	.	13	0	. . .	✓. .	✓.
RKS1446+2730	33PC	247	7	DMY	353	34.1	6.3	F	0	0	. . .	✓. .	✓.
RKS1446+1629	25PC	248	16	DMY	313	54.1	10.0	F	0	0	. . .	✓. .	✓.
RKS1447+0242	25PC	248	2	Y	950	19.0	7.7	F	22	0	. . .	. . .	✓.

Table 2: K dwarf companion search results.

			RV Survey Results						External				
ID	Sample	Fig.	No. Obs.	Cadence	Δt	ΔRV	MAD$_{RV}$	RV Det.	No. Obs.		Companion	TESS	RKS
		No.	CHIRON	Coverage				Type	HI19	HA20	Published		Speckle
RKS/TIC					(day)	m s^{-1}	m s^{-1}				NEA/SB9/WDS	Obs./EB/PL	Obs./Det.
RKS1450+0648	33PC	249	1		...	...	...	.	19	0	. . .	✓. .	✓.
RKS1451+0943	33PC	249	1		...	...	...	.	0	0	. . ✓	. . .	. .
RKS1451+1906	25PC	250	1		...	...	...	.	0	0	. . ✓	. . .	. .
RKS1451−2418	25PC	250	2	M	20	11.4	3.9	F	68	38	. . .	✓. .	✓.
RKS1453+1909	25PC	251	10	DMY	765	10064.8	2894.1	O	0	0	. ✓.	✓. .	. .
RKS1453+2320	25PC	251	36	DMY	1757	5824.4	2274.8	O	0	0	. . ✓	✓. .	✓.
RKS1455−2707	33PC	252	18	DMY	318	59.3	12.2	F	0	0	. . .	✓. .	✓.
RKS1457−2124	25PC	252	196	DMY	1739	100.9	15.9	F	0	56	. . ✓	. . .	✓.
RKS1458+0445	XTRA	253	22	DMY	876	1627.0	550.4	O	0	0	. . .	✓. .	✓.
RKS1500−2905	33PC	253	11	DMY	849	220.1	37.9	F	0	0	. . .	. . .	. .
RKS1500−2427	33PC	254	8	DMY	794	142.4	29.4	F	11	0	. . .	✓. ✓	✓.
RKS1500−1108	25PC	254	8	DMY	325	48.4	8.9	F	0	5	. . .	. . .	✓.
RKS1501+1341	33PC	255	3	DY	541	49.0	13.1	F	0	0	. . .	. . .	. .
RKS1501+1552	33PC	255	8	DMY	875	42.2	11.0	F	0	0	. . .	✓. .	✓.
RKS1504+0538	25PC	256	18	DMY	314	60.8	10.6	F	0	0	. . .	✓. .	✓.
RKS1504−1835A	33PC	256	1		...	...	...	.	0	0	. . .	. . .	✓✓
RKS1507+2456	25PC	257	12	DMY	759	89.2	14.3	F	0	0	. . .	✓. .	. .
RKS1509+2400A	33PC	257	9	DMY	411	51.9	15.8	F	0	0	. . .	✓. .	✓✓
RKS1510−1627	XTRA	258	1		...	...	...	.	22	0	. . ✓	. . .	. .
RKS1510−1622	33PC	258	1		...	...	...	.	54	51	. . ✓	. . .	. .
RKS1513−0347	33PC	259	7	DMY	381	62.7	9.7	F	0	0	. . .	✓. .	✓.
RKS1515+0735	33PC	259	2	D	0	15.1	4.9	F	0	0	. . .	. . .	✓.

Table 2: K dwarf companion search results.

			RV Survey Results						External				
ID	Sample	Fig.	No. Obs.	Cadence	Δt	ΔRV	MAD$_{RV}$	RV Det.	No. Obs.		Companion	TESS	RKS
		No.	CHIRON	Coverage				Type	HI19	HA20	Published		Speckle
RKS/TIC					(day)	m s^{-1}	m s^{-1}				NEA/SB9/WDS	Obs./EB/PL	Obs./Det.
RKS1515+0047	25PC	260	2	M	31	34.3	17.0	F	7	0	. . ✓	. . .	✓.
RKS1517−2759	XTRA	260	28	DMY	1211	40617.2	12655.8	O	0	0	. . .	✓. .	✓.
RKS1518−1837	33PC	261	22	DMY	1529	17855.2	2878.7	O	0	0	. . .	. . .	✓.
RKS1519+0146	33PC	261	1		...	...	...	.	0	0	. . ✓	. . .	. .
RKS1519+2912	33PC	262	8	DMY	1107	123.6	28.4	F	3	0	. . .	✓. ✓	✓.
RKS1519+1155	33PC	262	1		...	...	...	.	0	0	. . .	. . .	. .
RKS1520+1522A	33PC	263	16	DMY	880	175.7	47.1	T	0	0	. . ✓	✓. .	✓✓
RKS1522−0446	25PC	263	8	DMY	324	48.3	11.7	F	0	7	. . .	✓. .	✓.
RKS1522−1039	25PC	264	2	M	34	52.3	18.1	F	126	72	. . .	✓. .	✓.
RKS1522+0125	33PC	264	1		...	...	...	.	21	0	. . .	✓. .	✓.
RKS1525−2642	25PC	265	4	DM	48	32.8	10.0	F	0	16	. . .	✓. .	✓.
RKS1527+1035	33PC	265	5	DMY	316	14.0	8.3	F	4	0	. . .	✓. .	✓.
RKS1527+0235	33PC	266	6	DMY	326	18.4	6.1	F	0	0	. . .	✓. .	✓.
RKS1528−0920A	25PC	266	1		...	...	...	.	0	0	. ✓✓	✓. .	. .
RKS1528−0921B	XTRA	267	1		...	...	...	.	28	0	. . ✓	✓. .	. .
RKS1531−2916	33PC	267	3	DY	614	64.6	32.6	F	0	0	. . .	✓. .	. .
RKS1531+1041	33PC	268	3	DY	553	163.3	55.9	F	0	0	. . .	✓. .	. .
RKS1540−1802	25PC	268	9	DMY	283	45.3	12.3	F	0	8	. . .	. . .	✓.
TIC 272595871	XTRA	269	4	DM	35	63.0	23.3	A	11	0	. . ✓	✓. .	. .
RKS1552+1052A	25PC	269	12	DMY	1460	5851.9	569.7	P	0	0	. ✓✓	✓. .	✓✓
RKS1554−2600	25PC	270	13	DMY	333	56.2	11.0	F	5	0	. . .	. . .	✓.
RKS1555+1602	33PC	270	1		...	...	...	.	0	0	. ✓.	✓. .	. .

Table 2: K dwarf companion search results.

			RV Survey Results						External				
ID	Sample	Fig.	No. Obs.	Cadence	Δt	ΔRV	MAD$_{RV}$	RV Det.	No. Obs.		Companion	TESS	RKS
		No.	CHIRON	Coverage				Type	HI19	HA20	Published		Speckle
RKS/TIC					(day)	m s^{-1}	m s^{-1}				NEA/SB9/WDS	Obs./EB/PL	Obs./Det.
TIC 258177087	XTRA		0		...	...	...	.	30	0	. . .	✓. .	. .
RKS1559−0504	XTRA	271	8	DMY	414	41.1	11.6	F	0	0	. . .	. . .	✓.
RKS1600−0147A	33PC	271	2	D	0	18.1	3.3	F	0	25	. . .	. . .	✓✓
RKS1601−2625	25PC	272	10	DMY	870	79.9	21.0	F	0	0	. . .	. . .	. .
RKS1604−1126	33PC	272	1		...	...	...	.	0	0	. . ✓	. . .	. .
RKS1605−2027	25PC	273	1		...	...	...	.	0	0	. ✓.	. . .	. .
RKS1607−0542	33PC	273	2	D	0	19.6	7.0	F	4	0	. . .	. . .	✓.
RKS1608+1713	33PC	274	1		...	...	...	.	0	0	. . .	✓. .	. .
RKS1608−1308	33PC	274	5	DMY	333	38.0	9.1	F	0	0	. . ✓	. . .	✓.
RKS1613+1331B	XTRA	275	2	M	237	5682.6	2841.3	T	94	0	. . ✓	✓. .	. .
RKS1613+1331A	25PC	275	1		...	...	...	.	111	0	. . ✓	✓. .	. .
RKS1615+0721A	33PC	276	7	DMY	339	179.2	41.5	P	0	0	. . ✓	. . .	✓.
RKS1615+0721B	XTRA		0		...	...	...	.	0	0	. . ✓	. . .	. .
RKS1620−0416	33PC	276	2	D	0	2.7	1.4	F	0	24	. . ✓	. . .	✓.
RKS1621+1713	33PC	277	1		...	...	...	.	0	0	. . .	✓. .	. .
RKS1624−1338	25PC	277	14	DMY	327	47.0	9.7	F	5	0	. . ✓	. . .	✓.
RKS1625−2156	25PC	278	9	DMY	857	81.6	13.8	F	0	6	. . .	. . .	. .
RKS1626+1539	33PC	278	6	DMY	329	40.2	15.9	F	0	0	. . .	. . .	✓.
RKS1627+0055	33PC	279	6	DMY	313	33.5	7.1	F	0	0	. . .	. . .	✓.
RKS1627+0718	25PC	279	4	DM	35	48.0	6.0	F	38	0	. . .	. . .	✓.
RKS1628+1824A	25PC	280	1		...	...	...	.	0	0	. . ✓	. . .	. .
RKS1628+1824B	XTRA	280	2	M	63	5646.8	2823.0	T	0	0	. . ✓	✓. .	. .

Table 2: K dwarf companion search results.

			RV Survey Results						External				
ID	Sample	Fig.	No. Obs.	Cadence	Δt	ΔRV	MAD$_{RV}$	RV Det.	No. Obs.		Companion	TESS	RKS
		No.	CHIRON	Coverage				Type	HI19	HA20	Published		Speckle
RKS/TIC					(day)	m s^{-1}	m s^{-1}				NEA/SB9/WDS	Obs./EB/PL	Obs./Det.
RKS1629+2346	33PC	281	1		...	...	...	.	0	0	. ✓.	✓. .	✓.
RKS1630−0359	33PC	281	1		...	...	...	.	0	0	. . ✓	. . .	. .
RKS1631−0718	25PC	282	9	DMY	722	89.7	21.8	F	0	0	. . .	. . .	. .
RKS1632−1235	33PC	282	7	DMY	418	35.5	8.3	F	0	8	. . .	. . .	✓.
RKS1633−0933	33PC	283	2	Y	666	48.4	24.2	A	0	33	. . .	. . .	✓.
RKS1636−0219	25PC	283	5	DMY	866	55.8	14.9	F	46	21	. . ✓	. . .	. .
RKS1638−0501	XTRA	284	1		...	...	...	.	0	9	. . .	. . .	✓.
RKS1646+0531	33PC	284	3	DY	633	35.9	10.4	F	0	0	. . .	. . .	. .
RKS1647−0111	33PC	285	8	DMY	464	82.2	16.5	F	0	0	. . .	. . .	✓.
RKS1649−2426	33PC	285	1		...	...	...	.	0	8	. . .	. . .	✓.
RKS1650+1854	33PC	286	1		...	...	...	.	20	0	. . .	✓. .	✓.
RKS1654+1154	25PC	286	9	DMY	734	95.0	8.5	F	0	0	. . .	. . .	. .
RKS1659−2616	33PC	287	30	DMY	1571	11729.3	2719.9	O	0	0	. . .	. . .	✓.
RKS1701+2256	33PC	287	13	DMY	1127	65.3	13.3	P	0	0	. . .	✓. .	✓.
RKS1705−0503	25PC	288	1		...	...	...	.	73	70	. . ✓	. . .	. .
RKS1705−0147	33PC	288	6	DMY	872	454.5	153.3	A	0	0	. . .	. . .	. .
RKS1706−0610	33PC	289	7	DMY	834	89.3	17.6	F	0	0	. . .	. . .	✓.
RKS1712+1821	25PC	289	4	DM	35	19.2	4.9	F	57	16	. . .	✓. .	✓.
RKS1714−0824A	33PC	290	13	DMY	1728	115.6	17.6	F	0	0	. . ✓	. . .	✓✓
RKS1714−0824B	XTRA		0		...	...	...	.	0	0	. . ✓	. . .	✓✓
RKS1715−2636A	25PC	290	6	DMY	283	237.7	86.2	P	0	0	. . ✓	. . .	. .
RKS1715−2636B	XTRA		0		...	...	...	.	0	0	. . ✓	. . .	. .

Table 2: K dwarf companion search results.

			RV Survey Results						External				
ID	Sample	Fig.	No. Obs.	Cadence	Δt	ΔRV	MAD$_{RV}$	RV Det.	No. Obs.		Companion	TESS	RKS
		No.	CHIRON	Coverage				Type	HI19	HA20	Published		Speckle
RKS/TIC					(day)	m s^{-1}	m s^{-1}				NEA/SB9/WDS	Obs./EB/PL	Obs./Det.
RKS1716−2632	XTRA	291	2	M	177	44.4	14.1	F	27	0	. . ✓	. . .	. .
RKS1716−1210	33PC	291	10	DMY	799	81.6	17.6	F	0	7	. . .	. . .	✓.
RKS1717+2913	25PC	292	1		...	...	...	.	490	0	✓. .	✓. .	✓.
TIC 58971112	XTRA	292	3	DM	36	36.5	8.7	F	0	28	. . .	. . .	. .
RKS1721−2106	XTRA	293	3	D	6	1487.5	486.9	F	0	0	. . ✓	. . .	. .
RKS1722−1457	33PC	293	15	DMY	623	162.5	26.0	F	0	0	. . .	. . .	✓.
RKS1725+0206	25PC	294	9	DM	54	40.9	6.6	F	23	0	. . ✓	. . .	✓.
RKS1729−2350	25PC	294	16	DMY	328	39.5	8.0	F	0	8	. . .	. . .	✓.
TIC 310989180	XTRA	295	29	DMY	1473	1019.2	177.5	P	4	0	. . ✓	. . .	. .
RKS1733+0914	33PC	295	1		...	...	...	.	0	0	. . .	. . .	. .
RKS1737+2753A	33PC	296	29	DMY	1461	223.6	37.4	F	0	0	. . ✓	✓. .	✓✓
RKS1737−1314	33PC	296	1		...	...	...	.	0	0	. . .	. . .	. .
RKS1737+2257B	XTRA		0		...	...	...	.	0	0	. . ✓	✓. .	. .
RKS1737+2257A	25PC	297	14	DMY	356	57.5	14.8	F	0	0	. . ✓	✓. .	✓.
RKS1739+0333	25PC	297	6	DMY	462	7730.5	1942.9	P	0	102	. ✓✓	. . .	✓.
TIC 363766517	XTRA	298	16	DMY	1509	3460.6	1018.4	T	3	0	. ✓✓	✓. .	. .
RKS1750−0603	25PC	298	2	M	27	0.7	0.3	F	0	42	. . .	. . .	✓.
RKS1752−0733	33PC	299	9	DMY	853	44.8	9.8	F	7	7	. . .	. . .	✓.
RKS1753+2119	25PC	299	2	M	25	3.1	1.3	F	2	0	. . .	✓. .	✓.
RKS1754−2649	33PC	300	9	DMY	852	1961.9	1503.7	F	0	0	. . .	. . .	. .
RKS1755+0345	33PC	300	9	DMY	800	66.7	14.4	F	0	0	. . .	. . .	✓.
RKS1755+1830	25PC	301	7	DMY	823	63.9	11.8	F	0	0	. . ✓	✓. .	✓.

Table 2: K dwarf companion search results.

			RV Survey Results						External				
ID	Sample	Fig.	No. Obs.	Cadence	Δt	ΔRV	MAD$_{RV}$	RV Det.	No. Obs.		Companion	TESS	RKS
		No.	CHIRON	Coverage				Type	HI19	HA20	Published		Speckle
RKS/TIC					(day)	m s^{-1}	m s^{-1}				NEA/SB9/WDS	Obs./EB/PL	Obs./Det.
RKS1757−2143A	33PC	301	33	DMY	1579	409.3	119.9	T	0	0	. . ✓	. . .	✓✓
RKS1803+2545	33PC	302	3	DMY	613	261.9	58.5	P	0	0	. . .	✓. .	. .
RKS1804+0149	33PC	302	6	DMY	756	4825.9	1130.4	T	0	0	. . .	. . .	. .
RKS1805−2929A	33PC	303	1		...	...	...	.	0	0	. . ✓	✓. .	. .
RKS1805+0229	25PC	303	7	DMY	424	33.0	5.6	P	0	0	. . ✓	. . .	. .
RKS1807−1641	33PC	304	1		...	...	...	.	0	0	. . .	. . .	. .
RKS1809−0019	33PC	304	14	DMY	803	57.3	11.7	F	0	0	. . .	. . .	✓.
RKS1809−1202	33PC	305	10	DMY	800	66.7	13.8	F	0	0	. . .	. . .	✓.
RKS1815+1829	33PC	305	20	DMY	1362	184.5	35.4	T	0	0	. . .	✓. .	✓.
RKS1816+1354	25PC	306	18	DMY	328	58.9	9.1	F	0	0	. . .	✓. .	✓.
RKS1817+2640	33PC	306	8	DMY	822	58.7	15.7	F	0	0	. . ✓	✓. .	✓.
RKS1818−0642	33PC	307	7	DMY	339	15.3	4.0	F	0	0	. . .	. . .	✓.
RKS1819−0156	25PC	307	20	DMY	856	55.6	11.8	F	0	5	. . .	. . .	✓.
RKS1822+0142	33PC	308	12	DMY	723	142.2	35.1	A	0	0	. . .	. . .	✓.
RKS1826+0422	33PC	308	2	D	0	34.0	17.0	F	0	0	. . .	. . .	. .
RKS1829−2758	33PC	309	13	DMY	823	52.4	12.5	F	0	8	. . .	. . .	✓.
RKS1829+0903A	33PC	309	10	DMY	790	45.9	10.4	F	0	0	. . .	. . .	✓✓
RKS1829−0149	25PC	310	2	M	31	10.9	0.3	F	71	51	. . .	. . .	✓.
RKS1831−1854	25PC	310	4	DM	44	10.9	4.0	F	47	0	. . ✓	. . .	✓.
RKS1832−0347	33PC	311	2	D	0	22.4	1.8	F	0	0	. . .	. . .	. .
RKS1833+2218	25PC	311	19	DMY	329	59.3	7.0	F	0	0	. . ✓	✓. .	✓.
RKS1833−1626	33PC	312	1		...	...	...	.	0	0	. . .	. . .	. .

Table 2: K dwarf companion search results.

			RV Survey Results						External				
ID	Sample	Fig.	No. Obs.	Cadence	Δt	ΔRV	MAD$_{RV}$	RV Det.	No. Obs.		Companion	TESS	RKS
		No.	CHIRON	Coverage				Type	HI19	HA20	Published		Speckle
RKS/TIC					(day)	m s^{-1}	m s^{-1}				NEA/SB9/WDS	Obs./EB/PL	Obs./Det.
RKS1833−1138	33PC	312	1		...	...	...	.	0	43	✓. .	. . .	✓.
RKS1834+0355	25PC	313	10	DMY	1007	104.7	29.1	F	0	0	. . .	. . .	. .
RKS1847−0338	25PC	313	6	DY	675	32.9	8.7	F	21	9	. . ✓	. . .	✓.
RKS1847+1226	33PC		0		...	...	...	.	0	0	. . .	. . .	. .
RKS1848−1008A	33PC	314	18	DMY	1578	3745.9	1058.1	T	0	0	. . ✓	. . .	✓✓
RKS1848+1044	25PC	314	4	DM	36	39.1	11.4	T	8	0	. . ✓	. . .	✓.
RKS1848+1726	25PC	315	16	DMY	355	81.6	11.2	F	0	0	. . .	. . .	✓.
RKS1850−2655	25PC	315	41	DMY	1233	85.5	13.4	F	0	7	. . .	. . .	✓.
RKS1854+2844	33PC	316	10	DMY	1013	85.0	14.8	F	0	0	. . .	✓. .	. .
RKS1854+0051	25PC	316	10	DMY	989	96.0	20.6	F	0	0	. . .	. . .	. .
RKS1854+1058	25PC	317	9	DY	1000	182.9	62.2	T	0	0	. . ✓	✓. .	. .
RKS1855+2333A	25PC	317	34	DY	370	97381.8	33155.1	O	2	0	. ✓✓	✓. .	✓✓
RKS1857+0734	33PC	318	3	DY	668	42.0	17.5	F	0	14	. . .	✓. .	. .
RKS1857−1902	33PC		0		...	...	...	.	0	0	. . ✓	. . .	. .
RKS1858−1014	33PC	318	1		...	...	...	.	0	0	. . .	. . .	. .
RKS1858−0030	33PC	319	8	DMY	759	54.7	8.6	F	0	0	. . .	. . .	✓.
RKS1859+0759	33PC	319	1		...	...	...	.	0	13	. . .	✓. .	✓.
RKS1859+1107	33PC	320	1		...	...	...	.	0	0	. . .	✓. .	. .
RKS1901+0328	33PC	320	1		...	...	...	.	0	0	. . .	. . .	. .
RKS1903−1102	33PC	321	2	D	0	3.2	0.2	F	0	171	✓. .	. . .	✓.
TIC 451627388	XTRA	321	12	DMY	1076	94.2	23.2	T	0	0	. . .	✓. .	. .
RKS1905+1351	33PC		0		...	...	...	.	0	0	. . ✓	. . .	. .

Table 2: K dwarf companion search results.

			RV Survey Results						External				
ID	Sample	Fig.	No. Obs.	Cadence	Δt	ΔRV	MAD$_{RV}$	RV Det.	No. Obs.		Companion	TESS	RKS
		No.	CHIRON	Coverage				Type	HI19	HA20	Published		Speckle
RKS/TIC					(day)	m s^{-1}	m s^{-1}				NEA/SB9/WDS	Obs./EB/PL	Obs./Det.
RKS1907+0736	25PC	322	5	DM	49	37.3	11.1	F	7	0	. . .	. . .	✓.
RKS1908+1627	33PC	322	1		...	...	...	.	0	0	. . .	. . .	. .
RKS1908−1640	33PC	323	1		...	...	...	.	0	0	. . .	. . .	. .
RKS1910+2145	33PC	323	3	DMY	684	119.6	35.8	F	0	0	. . .	✓. .	. .
RKS1911+0500	33PC	324	3	DY	651	39.8	9.3	F	0	0	. . .	✓. .	. .
RKS1914+0209A	33PC	324	4	DM	62	929.1	427.7	T	0	0	. . ✓	. . .	✓.
RKS1914+0209B	XTRA		0		...	...	...	.	0	0	. . ✓	✓. .	. .
RKS1915+2453A	33PC	325	29	DMY	885	8963.2	2084.8	O	0	0	. . ✓	. . .	✓✓
RKS1915+1133	33PC	325	7	DMY	727	57.4	11.4	F	0	8	. . .	. . .	✓.
RKS1923−0635A	33PC	326	7	DMY	746	29.8	8.0	F	0	0	. . ✓	✓. .	✓✓
RKS1924+2525	33PC	326	3	DY	639	32.0	20.9	F	0	0	. . ✓	✓. .	. .
RKS1924−2203	33PC	327	1		...	...	...	.	0	8	. . .	. . .	. .
RKS1924+0832	XTRA	327	8	DMY	502	63.5	15.3	F	0	0	. . ✓	✓. .	✓.
RKS1928+1232A	33PC	328	6	DMY	406	32.3	9.9	F	0	0	. . ✓	. . .	✓.
RKS1928+1232B	XTRA		0		...	...	...	.	0	0	. . ✓	. . .	. .
RKS1928+2854	33PC	328	3	DY	627	17.0	0.7	F	0	0	. . .	✓. .	. .
RKS1929+0709	33PC	329	1		...	...	...	.	0	0	. . .	✓. .	. .
RKS1930+2140	33PC	329	9	DMY	1043	90.2	24.3	F	0	0	. . .	✓. .	✓.
RKS1932−1116	25PC	330	6	DM	55	35.7	9.3	F	31	0	. . ✓	✓. .	✓.
RKS1932+0034	25PC	330	18	DMY	413	67.7	9.0	F	0	0	. . .	✓. .	✓.
RKS1934+0434	25PC	331	17	DMY	413	72.8	7.6	F	0	0	. . .	✓. .	✓.
RKS1936−1026B	XTRA		0		...	...	...	.	0	0	. . ✓	. . .	. .

Table 2: K dwarf companion search results.

			RV Survey Results						External				
ID	Sample	Fig.	No. Obs.	Cadence	Δt	ΔRV	MAD$_{RV}$	RV Det.	No. Obs.		Companion	TESS	RKS
		No.	CHIRON	Coverage				Type	HI19	HA20	Published		Speckle
RKS/TIC					(day)	m s^{-1}	m s^{-1}				NEA/SB9/WDS	Obs./EB/PL	Obs./Det.
RKS1936−1026A	33PC	331	2	M	140	290.6	145.2	T	0	0	. . ✓	✓. .	✓.
RKS1943+1005	33PC	332	2	D	13	12.7	1.3	F	14	0	. . .	. . .	✓.
RKS1952−2356	33PC	332	6	DMY	489	62.8	7.3	F	0	0	. . .	. . .	✓.
RKS1954−2356	25PC	333	1		...	...	...	.	0	42	. ✓✓	. . .	. .
RKS1954+2013	33PC	333	2	DY	657	5269.0	15.2	F	0	0	. . .	✓. .	. .
TIC 281827534	XTRA		0		...	...	...	.	0	0	. . .	. . .	. .
TIC 48769732	XTRA	334	21	DMY	871	45.5	9.1	F	0	0	. . ✓	✓. .	. .
RKS1957+1313	33PC	334	1		...	...	...	.	0	0	. . .	. . .	. .
RKS2000+2242	25PC	335	31	DM	41	418.9	127.4	O	119	117	✓. ✓	✓. ✓	✓.
RKS2002+0319	25PC	335	14	DM	98	42.6	7.5	F	34	0	✓. .	✓. .	✓.
RKS2003+2005	33PC	336	2	D	0	8.9	2.5	F	0	0	. . .	✓. .	. .
RKS2003+2320	25PC	336	2	D	13	8.1	3.4	F	62	0	. . .	✓. .	✓.
RKS2004+2547	25PC	337	15	DMY	431	64.3	13.5	F	0	0	. . .	✓. .	✓.
RKS2008+0640	33PC	337	13	DMY	914	96.4	20.8	F	4	0	. . .	✓. .	✓.
RKS2009+1648A	25PC	338	21	DMY	802	57.6	11.3	F	0	0	. . ✓	. . .	✓.
RKS2009+1648B	XTRA	338	5	DY	783	57.8	14.6	T	0	0	. . ✓	. . .	. .
RKS2009−1417	33PC	339	1		...	...	...	.	0	26	. . .	. . .	✓.
RKS2009−0307	33PC	339	12	DMY	529	53.6	12.7	F	5	0	. . .	✓. .	✓.
RKS2010−2029A	25PC	340	5	DM	20	51.1	9.6	F	3	26	. . ✓	. . .	✓✓
RKS2011+1611	25PC	340	4	DM	20	14.7	3.8	F	63	0	. . ✓	. . ✓	✓.
RKS2012−1253	33PC	341	12	DMY	762	128.4	30.0	F	0	0	. . .	✓. .	. .
RKS2013−0052	25PC	341	32	DM	41	132.8	38.9	O	38	31	✓. ✓	✓. .	✓.

Table 2: K dwarf companion search results.

ID	Sample	Fig.	RV Survey Results						External				
			No. Obs.	Cadence	Δt	ΔRV	MAD$_{RV}$	RV Det.	No. Obs.		Companion	TESS	RKS
		No.	CHIRON	Coverage				Type	HI19	HA20	Published		Speckle
RKS/TIC					(day)	m s^{-1}	m s^{-1}				NEA/SB9/WDS	Obs./EB/PL	Obs./Det.
RKS2014−0716	25PC	342	20	DMY	1584	122.7	19.7	F	0	5	. . .	✓. .	✓.
RKS2015−2701	25PC	342	1		...	...	...	.	250	1834	✓. .	✓. .	✓.
RKS2016−0204	33PC	343	12	DMY	972	128.6	23.9	F	0	0	. . .	✓. .	. .
TIC 244125428	XTRA	343	36	DMY	1070	18866.0	5293.4	O	0	0	. . .	✓. .	. .
RKS2030+2650	25PC	344	1		...	...	...	.	0	0	. . ✓	. . .	. .
RKS2035+0607	33PC	344	1		...	...	...	.	62	0	. . ✓	✓. .	✓.
RKS2038+2346	33PC	345	4	DMY	837	36.9	9.8	F	0	0	. . .	✓. .	. .
RKS2039+1004	33PC	345	7	DMY	968	69.1	17.3	F	0	0	. . ✓	✓. .	. .
RKS2041−0529	33PC	346	8	DMY	440	96.3	18.3	F	0	0	. . .	✓. .	✓.
RKS2041−2219	25PC	346	51	DMY	1582	29547.6	9597.9	O	0	0	. . .	. . .	✓.
RKS2042−2116	25PC	347	7	DMY	769	3227.2	488.3	P	0	0	. . ✓	. . .	. .
RKS2042+2050	25PC	347	5	DMY	461	29.3	7.7	F	0	0	. . .	✓. .	✓.
RKS2044−2121	33PC	348	14	DY	345	51.1	10.9	F	0	8	. . .	. . .	✓.
TIC 331684556	XTRA	348	42	DMY	1753	8678.8	2815.1	O	0	0	. . ✓	✓. .	. .
RKS2046−2144	33PC	349	6	DMY	1018	124511.2	14361.8	P	0	0	. . ✓	. . .	. .
RKS2046−2304	XTRA	349	33	DMY	1385	7284.4	1842.9	O	0	9	. . .	. . .	✓.
RKS2047+1051	33PC	350	9	DMY	541	30.0	6.6	F	0	0	. . .	✓. .	✓.
RKS2050+2923A	25PC	350	29	DMY	1777	351.3	81.2	T	6	0	. . .	. . .	✓✓
RKS2053−0245	33PC	351	3	DY	541	48.6	19.9	F	0	5	. . .	. . .	✓.
RKS2055+1310	25PC	351	7	DM	36	153.3	40.7	T	12	0	. ✓.	✓. .	✓.
RKS2059+0333	33PC	352	2	D	0	39.8	1.7	F	0	0	. . .	✓. .	. .
RKS2059−1042	33PC	352	46	DMY	1615	276.8	104.0	T	0	0	. . .	. . .	✓.

Table 2: K dwarf companion search results.

ID	Sample	Fig.	RV Survey Results						External				
			No. Obs.	Cadence	Δt	ΔRV	MAD$_{RV}$	RV Det.	No. Obs.		Companion	TESS	RKS
		No.	CHIRON	Coverage				Type	HI19	HA20	Published		Speckle
RKS/TIC					(day)	m s^{-1}	m s^{-1}				NEA/SB9/WDS	Obs./EB/PL	Obs./Det.
RKS2105+0704A	25PC	353	10	DMY	460	29.9	6.3	F	5	12	. . ✓	✓. .	✓✓
RKS2105−1654	25PC	353	10	DMY	725	17126.4	4222.8	P	0	0	. . .	. . .	. .
RKS2107−1355A	25PC	354	2	M	18	5.9	2.5	F	0	0	. . ✓	. . .	✓.
RKS2107−1355B	XTRA		0		...	...	...	.	0	0	. . ✓	. . .	. .
RKS2107+2945	XTRA	354	23	DMY	1431	1442.7	371.7	T	0	0	. . ✓	✓. .	✓.
RKS2108+2510	XTRA	355	7	DMY	508	37.2	3.5	F	0	0	. . .	✓. .	✓.
RKS2108−0425A	25PC	355	26	DMY	1750	7579.1	2459.8	O	0	0	. . ✓	. . .	✓✓
RKS2116+0923	25PC	356	13	DM	39	68.8	16.9	F	34	0	. . ✓	✓. .	✓.
RKS2118+0009	25PC	356	9	DMY	432	52.1	14.6	F	90	0	. . ✓	✓. .	. .
RKS2119−2621	25PC	357	11	DMY	936	45417.2	11703.6	O	0	0	. ✓✓	✓. .	✓.
RKS2120−1951	25PC	357	9	DMY	408	37.6	7.8	F	4	4	. . .	. . .	. .
RKS2122+1052	25PC	358	23	DMY	1593	154.5	22.5	F	0	0	. . .	✓. .	✓.
RKS2122−0044	33PC	358	8	DM	81	248.3	48.4	F	0	0	. . .	. . .	. .
RKS2125+2712	25PC	359	11	DMY	1053	2384.6	537.8	T	0	0	. . .	. . .	. .
RKS2126+0344	33PC	359	8	DM	211	60.3	17.2	F	0	0	. . .	. . .	. .
RKS2130−1230	25PC	360	7	DMY	431	41.7	15.8	F	53	0	. . .	. . .	. .
RKS2131+2320	25PC	360	8	DMY	1146	5176.1	2386.1	P	0	0	. . ✓	✓. .	. .
RKS2132−2057	33PC	361	3	D	11	3.7	1.5	F	0	96	✓. ✓	✓. .	✓.
RKS2141+1115	33PC	361	33	DMY	1767	4196.5	1246.0	O	0	0	. . .	✓. .	✓.
RKS2149+0543	25PC	362	9	DMY	425	41.4	8.7	F	0	0	. . ✓	. . .	. .
RKS2149−1140	33PC	362	11	DY	301	62.1	18.6	P	0	0	. . .	. . .	. .
RKS2152+0154	33PC	363	2	M	28	15.2	7.6	F	19	0	. . .	✓. .	. .

Table 2: K dwarf companion search results.

			RV Survey Results						External				
ID	Sample	Fig.	No. Obs.	Cadence	Δt	ΔRV	MAD$_{RV}$	RV Det.	No. Obs.		Companion	TESS	RKS
		No.	CHIRON	Coverage				Type	HI19	HA20	Published		Speckle
RKS/TIC					(day)	m s^{-1}	m s^{-1}				NEA/SB9/WDS	Obs./EB/PL	Obs./Det.
RKS2153+2055	25PC	363	1		...	...	...	.	16	0	. . .	✓. .	. .
RKS2153+2850	33PC	364	12	DMY	790	99.4	19.6	F	0	0	. . .	✓. .	. .
RKS2153−1249	25PC	364	14	DMY	738	121.8	22.4	F	0	0	. . ✓	. . .	. .
RKS2155−2942	33PC	365	1		...	...	...	.	0	29	. . .	✓. .	. .
RKS2210+2247	33PC	365	1		...	...	...	.	0	0	. . .	. . .	✓.
RKS2214+0242A	XTRA	366	11	DMY	736	84.9	16.7	F	0	0	. . .	✓. .	✓✓
RKS2214+2751	25PC	366	21	DMY	1579	81.9	18.4	F	0	0	. . ✓	. . .	✓.
RKS2224+2233	25PC	367	9	DMY	608	105.8	14.1	F	0	0	. . ✓	. . .	. .
RKS2226−1911	33PC	367	1		...	...	...	.	4	9	. . .	✓. .	. .
TIC 271997555	XTRA	368	28	DMY	1577	120.5	21.2	F	0	0	. . .	✓. .	. .
RKS2239+0406	25PC	368	1		...	...	...	.	36	0	. . .	✓. .	. .
RKS2240−2940	25PC	369	9	DMY	420	31.9	8.4	F	29	0	. . .	✓. .	. .
RKS2241+1849A	33PC	369	2	Y	491	473.8	236.9	T	0	0	. . .	. . .	✓✓
RKS2243−0624	25PC	370	1		...	...	...	.	62	312	✓. .	✓. .	. .
RKS2247+1823	33PC	370	10	DMY	653	92.5	17.9	F	2	0	. . .	. . .	. .
RKS2248+2443	33PC	371	10	DY	646	109.1	19.5	F	0	0	. . .	. . .	. .
RKS2251+1358	25PC	371	1		...	...	...	.	260	0	. . ✓	. . .	. .
RKS2252+2324	33PC	372	14	DMY	812	104.4	12.2	F	5	0	. . .	. . .	✓.
RKS2254+2331	33PC	372	12	DMY	662	164.3	28.8	F	0	0	. . .	. . .	. .
RKS2257+2800	XTRA	373	5	DMY	339	27.0	6.9	F	0	0	. . ✓	. . .	✓.
RKS2258−1338	33PC	373	2	D	0	25.2	2.7	F	6	6	. . .	✓. .	. .
RKS2259−1122	33PC	374	12	DMY	643	124.0	25.2	F	0	0	. . .	✓. .	. .

Table 2: K dwarf companion search results.

			RV Survey Results						External				
ID	Sample	Fig.	No. Obs.	Cadence	Δt	ΔRV	MAD$_{RV}$	RV Det.	No. Obs.		Companion	TESS	RKS
		No.	CHIRON	Coverage				Type	HI19	HA20	Published		Speckle
RKS/TIC					(day)	m s^{-1}	m s^{-1}				NEA/SB9/WDS	Obs./EB/PL	Obs./Det.
RKS2300−2231	25PC	374	7	DMY	378	41.1	12.3	F	90	0	. . .	✓. .	. .
RKS2300−2618B	XTRA		0		...	...	...	.	0	0	. . ✓	. . .	. .
RKS2300−2618A	33PC	375	34	DMY	372	2684.9	148.0	O	0	0	. ✓✓	✓. .	✓.
RKS2301−0350	25PC	375	11	DMY	629	3174.7	844.9	O	0	0	. ✓.	✓. .	. .
RKS2307−2309	25PC	376	10	DY	1047	139.2	30.2	F	4	0	. . ✓	✓. .	. .
RKS2308+0633	33PC	376	11	DMY	641	1402.6	512.4	T	0	0	. . .	✓. .	. .
RKS2309−0215	33PC	377	2	D	6	17.2	8.6	F	87	21	✓. .	✓. .	✓.
RKS2309+1425	33PC	377	9	DMY	658	104.1	26.3	F	0	0	. . ✓	. . .	. .
RKS2310−2955	33PC	378	10	DMY	658	82.0	21.3	P	0	0	. . .	✓. .	. .
RKS2316+0541	33PC	378	13	DMY	897	61.8	14.5	F	0	0	. . .	✓. .	✓.
RKS2317−2323	25PC	379	11	DMY	638	82.8	16.6	F	0	0	. . .	✓. .	. .
RKS2319−1327	25PC	379	1		...	...	...	.	68	0	. . ✓	✓. .	. .
RKS2319+2852	XTRA	380	1		...	...	...	.	0	0	. . .	. . .	✓.
RKS2323−1045	25PC	380	7	DMY	378	22.3	6.7	F	58	35	. . .	✓. .	. .
RKS2326+0853	25PC	381	11	DMY	635	97.6	21.1	F	0	0	. . .	✓. .	. .
RKS2327−0117	33PC	381	12	DMY	515	42.0	9.6	F	0	37	✓. .	✓. ✓	✓.
RKS2328+1604	33PC	382	1		...	...	...	.	0	0	. . ✓	. . .	✓.
RKS2332−1650	25PC	382	11	DMY	855	41.0	11.0	F	3	48	. . ✓	✓. .	✓.
RKS2333−1239	XTRA	383	1		...	...	...	.	0	29	. . ✓	✓. .	✓.
RKS2335+0136A	25PC	383	11	DM	39	44.1	17.5	A	0	15	. . ✓	✓. .	✓✓
RKS2340+2021	33PC	384	1		...	...	...	.	0	0	. . ✓	. . .	. .
RKS2341+2002	33PC	384	13	DMY	706	263.0	38.7	F	0	0	. . .	. . .	. .

Table 2: K dwarf companion search results.

			RV Survey Results						External				
ID	Sample	Fig.	No. Obs.	Cadence	Δt	ΔRV	MAD$_{RV}$	RV Det.	No. Obs.		Companion	TESS	RKS
		No.	CHIRON	Coverage				Type	HI19	HA20	Published		Speckle
RKS/TIC					(day)	m s^{-1}	m s^{-1}				NEA/SB9/WDS	Obs./EB/PL	Obs./Det.
RKS2342−0234A	25PC	385	63	DMY	1782	16140.7	3767.5	O	0	0	. . .	✓. .	✓✓
RKS2345+2933	33PC	385	34	DMY	1465	20809.9	7055.8	O	0	0	. . .	. . .	✓.
RKS2348−1259A	33PC	386	29	DMY	1621	407.4	101.4	T	0	0	. . ✓	✓. .	✓✓
RKS2349+0310	25PC	386	13	DMY	465	34.3	6.8	F	0	0	. . .	✓. .	✓.
RKS2350−2924	33PC	387	26	DMY	1599	151.0	30.7	T	0	0	. . ✓	✓. .	✓.
RKS2353+2901	25PC	387	19	DMY	413	73.2	11.3	F	0	0	. . ✓	. . .	✓.
RKS2355+2211	33PC	388	1		...	...	...	.	13	0	. . .	. . .	✓.
RKS2356−1445	33PC	388	11	DMY	732	11891.7	3965.9	O	0	0	. . .	. . .	. .
RKS2357−1630	XTRA	389	12	DMY	904	61.8	14.6	F	0	0	. . ✓	✓. .	✓.
RKS2358+0949	33PC	389	9	DMY	664	73.8	20.5	F	0	0	. . .	✓. .	. .
RKS2359−2602	25PC	390	14	DM	40	45.1	8.7	F	28	0	. . .	✓. .	✓.
RKS2359+0639	25PC	390	25	DMY	1584	146.2	28.4	F	0	0	. . ✓	. . .	✓.

Table 3: K dwarf Orbital Solutions.

ID RKS/TIC	Sample	Period days	K $m\,s^{-1}$	e	ω deg	T_p days	RMS $m\,s^{-1}$	No. Obs.	Comp. Name	Comp. Type	Ref.
					New Orbits						
RKS0022−2701	25PC	1157.974	6607.6	0.128	1.44	63409.388	11.3	51			this work
RKS0112+0058	XTRA	20.759	29612.5	0.148	0.28	58438.087	35.3	24			this work
RKS0229−1958A	25PC	2260.643	681.0	0.237	0.61	56912.381	21.0	49			this work
RKS0258+2646	33PC	25.038	9351.9	0.076	0.49	59426.743	10.7	10			this work
RKS0329−2406	33PC	3.981	70478.2	0.005	0.91	58216.698	12.5	9			this work
TIC 70899190	XTRA	2334.432	3700.9	0.341	1.58	58956.918	147.9	39			this work
RKS0503−2315A	25PC	267.812	12207.4	0.102	−2.08	58462.160	101.5	29			this work
RKS0616+2512	33PC	389.110	5398.7	0.062	1.38	58392.287	20.4	54			this work
RKS0701−2556A	25PC	2745.280	4756.7	0.743	−3.11	59056.230	21.8	41			this work
RKS0726−1546	33PC	121.328	6307.0	0.092	−1.94	58224.217	24.3	35			this work
RKS0732+1719	33PC	328.318	3322.8	0.217	0.55	56079.302	57.0	33			this work
RKS0813−1355B	XTRA	198.232	4842.5	0.150	2.32	58916.272	108.6	9			this work
RKS0818−1512A	XTRA	906.822	3377.7	0.466	−0.62	57611.453	24.7	42			this work
RKS0840−0628A	33PC	417.809	8410.3	0.442	0.14	58214.797	1511.7	37			this work
RKS0914+0426A	25PC	2885.500	845.7	0.176	1.57	57327.884	17.6	40			this work
TIC 172533278	XTRA	5.413	94.5	0.478	0.63	58216.873	31.3	38			this work
RKS0959−0911	33PC	2540.568	2380.5	0.500	−1.77	58936.065	15.3	28			this work
RKS1026−0631	33PC	167.438	5254.9	0.356	−2.20	58587.116	1139.6	34			this work
RKS1108−2816A	33PC	1813.439	7368.0	0.209	2.31	58581.487	86.6	29			this work
RKS1111−1459A	25PC	3858.642	8077.7	0.588	−0.36	58756.037	47.1	26			this work
RKS1121−2027	25PC	7560.127	1306.6	0.115	−2.03	57567.732	10.8	21			this work
RKS1123+0701A	33PC	4138.187	1025.8	0.407	0.32	57307.980	18.3	20			this work
RKS1127+0358A	33PC	2500.288	168.3	0.108	−1.45	56298.220	12.7	17			this work
RKS1154+2844	33PC	1725.150	965.9	0.331	1.14	58470.095	19.5	38			this work
RKS1205−1852	25PC	9.503	38300.3	0.003	−1.37	58173.003	23.4	46			this work
RKS1302−2647	25PC	21.549	32418.6	0.132	2.04	58411.206	19.0	27			this work
RKS1353+1256A	25PC	3792.566	6555.4	0.504	0.13	57321.694	14.1	39			this work
RKS1453+2320	25PC	875.799	3114.5	0.630	−2.09	60619.646	97.3	36			this work
RKS1458+0445	XTRA	1689.575	1880.1	0.765	1.76	57765.969	18.9	22			this work

Table 3: K dwarf Orbital Solutions.

ID RKS/TIC	Sample	Period days	K $m\,s^{-1}$	e	ω deg	T_p days	RMS $m\,s^{-1}$	No. Obs.	Comp. Name	Comp. Type	Ref.
RKS1517−2759	XTRA	9.198	20750.6	0.120	−2.40	59378.199	31.1	28			this work
RKS1518−1837	33PC	1635.702	11236.5	0.922	1.22	58555.874	25.9	22			this work
RKS1659−2616	33PC	94.071	5359.2	0.460	−2.29	58656.920	1159.1	30			this work
RKS1915+2453A	33PC	1020.754	4415.2	0.616	−0.82	58724.651	255.3	29			this work
TIC 244125428	XTRA	568.104	9449.3	0.373	2.21	58670.754	92.1	36			this work
RKS2041−2219	25PC	4.028	15415.2	0.002	−0.19	58259.161	108.3	51			this work
TIC 331684556	XTRA	3992.987	4387.1	0.506	−1.98	58540.542	58.1	42			this work
RKS2046−2304	XTRA	150.833	3634.5	0.220	1.50	59016.463	32.7	33			this work
RKS2108−0425A	25PC	4872.100	3861.2	0.312	−1.52	53723.407	34.1	26			this work
RKS2141+1115	33PC	3716.344	2286.0	0.183	0.19	58453.857	17.1	33			this work
RKS2342−0234A	25PC	2500.971	8086.9	0.071	−1.12	56314.315	21.5	63			this work
RKS2345+2933	33PC	102.266	10567.3	0.323	−1.80	58829.250	21.3	34			this work
RKS2356−1445	33PC	13.530	6360.3	0.135	1.27	59501.812	1042.6	11			this work
Known Stellar Orbits (SB9)											
RKS0129+2143	25PC	10.984	38870.0	0.036	192.86	46482.390	740.0	31		SB2	Halbwachs et al. (2018)
TIC 422844595	XTRA	9182.385	5600.0	0.210	229.10	37921.175	...	27		SB2	Agati et al. (2015)
RKS0236−0309	25PC	14.838	10530.0	0.216	11.30	47103.156	...	36		SB1	Imbert (2006)
RKS0243+1925A	25PC	1227.770	6476.0	0.492	119.35	46638.500	240.0	23		SB1	Halbwachs et al. (2018)
RKS0248+2704	25PC	5954.000	2957.0	0.663	110.74	48024.200	250.0	26		SB1	Halbwachs et al. (2018)
RKS0257−2458	25PC	553.890	1500.0	0.528	74.70	47489.900	380.0	32		SB1	Halbwachs et al. (2018)
RKS0308−2445	33PC	0.918	116920.0	0.000	0.00	52605.971	1080.0	31		SB2	Rozyczka et al. (2013)
RKS0341+0336	33PC	31.155	18800.0	0.388	181.60	47778.100	1550.0	...		SB2	Tokovinin (1991)
RKS0415−0425A	XTRA	716.800	1318.0	0.090	242.90	49992.200	327.0	40		SB1	Halbwachs et al. (2018)
RKS0436+2707	25PC	1.788	10454.0	0.002	323.77	46999.420	290.0	54		SB1	Halbwachs et al. (2018)
RKS0439+0952A	33PC	610.430	4596.0	0.415	269.90	56635.100	750.0	16		SB1	Sperauskas et al. (2019)
RKS0506+1426	33PC	205.800	10430.0	0.302	253.50	53893.200	200.0	48		SB1	Griffin (2013)
RKS0626+1845	25PC	6.992	56860.0	0.147	79.65	48991.973	510.0	41		SB2	Halbwachs et al. (2018)
RKS0707+0326	33PC	875.370	4561.0	0.507	328.70	55875.700	450.0	21		SB1	Sperauskas et al. (2019)
RKS0754−0124A	25PC	447.320	5850.0	0.359	227.90	46589.700	...	17		SB1	Duquennoy & Mayor (1991)

Table 3: K dwarf Orbital Solutions.

ID RKS/TIC	Sample	Period days	K $m\,s^{-1}$	e	ω deg	T_p days	RMS $m\,s^{-1}$	No. Obs.	Comp. Name	Comp. Type	Ref.
RKS0754+1914	25PC	161.119	5690.0	0.273	323.98	46586.840	420.0	24		SB1	Halbwachs et al. (2018)
RKS0759+2050	25PC	3495.000	1350.0	0.379	86.00	50177.000	560.0	66		SB1	Latham et al. (2002)
RKS0839+0657	33PC	128.250	23270.0	0.266	276.40	54785.870	240.0	28		SB2	Griffin (2009)
RKS0900+2127	33PC	120.440	3210.0	0.808	112.60	47711.390	590.0	83		SB1	Latham et al. (2002)
RKS0907+2252	33PC	160.414	16020.0	0.289	15.60	56693.950	210.0	48		SB1	Griffin (2016)
RKS1000+2433	33PC	1.070	89300.0	0.000	0.00	42849.628	...	...		SB2	Barden (1984)
RKS1026+2638	33PC	1180.600	7990.0	0.869	296.10	44583.000	700.0	86		SB1	Griffin (1987)
RKS1141+0508A	33PC	725.900	8065.0	0.164	168.00	57934.300	530.0	34		SB1	Sperauskas et al. (2019)
RKS1241+1951	33PC	1275.500	3890.0	0.187	292.00	50997.000	260.0	95		SB1	Griffin (2006)
RKS1253+0645	33PC	23.503	18040.0	0.447	21.20	54881.312	190.0	30		SB1	Griffin (2009)
RKS1257−1427	33PC	3572.100	2480.0	0.766	238.51	49872.950	340.0	41		SB1	Halbwachs et al. (2018)
RKS1259−0950	25PC	103.226	1850.0	0.141	333.00	49672.000	330.0	32		SB1	Halbwachs et al. (2018)
RKS1303−0509	25PC	216.480	13030.0	0.261	294.50	53845.300	380.0	42		SB1	Griffin (2010)
RKS1331−0219	33PC	1188.000	3140.0	0.641	355.80	49474.800	510.0	54		SB1	Latham et al. (2002)
RKS1418−0636A	25PC	6819.000	3960.0	0.306	67.10	45990.000	490.0	23		SB1	Halbwachs et al. (2018)
RKS1453+1909	25PC	125.394	18913.0	0.510	219.48	44936.898	310.0	82		SB1	Halbwachs et al. (2018)
RKS1528−0920A	25PC	889.813	36420.0	0.973	252.64	47967.519	740.0	110		SB2	Halbwachs et al. (2018)
RKS1552+1052A	25PC	1014.500	6640.0	0.367	339.60	50828.100	890.0	33		SB2	Tokovinin et al. (2000)
RKS1555+1602	33PC	24.535	37140.0	0.314	324.70	54708.895	300.0	41		SB1	Griffin (2009)
RKS1605−2027	25PC	105.947	23550.0	0.151	85.28	48948.020	560.0	25		SB2	Halbwachs et al. (2018)
RKS1629+2346	33PC	5252.000	3031.0	0.188	64.50	58096.900	230.0	15		SB1	Sperauskas et al. (2019)
RKS1739+0333	25PC	83.714	5644.0	0.210	145.50	46972.200	260.0	38		SB1	Halbwachs et al. (2018)
TIC 363766517	XTRA	2558.400	9090.0	0.936	129.60	49422.530	330.0	138		SB1	Duquennoy et al. (1996)
RKS1855+2333A	25PC	2.879	49460.0	0.003	266.70	43675.580	...	...		SB1	Imbert (1979)
RKS1954−2356	25PC	46.816	47840.0	0.686	241.17	55441.048	...	188		SB2	Fekel et al. (2017)
RKS2055+1310	25PC	2173.300	1930.0	0.459	233.58	47551.200	280.0	29		SB1	Halbwachs et al. (2018)
RKS2119−2621	25PC	21.346	24000.0	0.250	89.50	19224.110	...	...		SB1	Bopp et al. (1970)
RKS2300−2618A	33PC	20.349	41170.0	0.432	43.22	57255.933	630.0	17		SB2	Tokovinin (2016)
RKS2301−0350	25PC	453.900	2501.0	0.518	239.78	49162.200	270.0	25		SB1	Halbwachs et al. (2018)

Table 3: K dwarf Orbital Solutions.

ID RKS/TIC	Sample	Period days	K $m\,s^{-1}$	e	ω deg	T_p days	RMS $m\,s^{-1}$	No. Obs.	Comp. Name	Comp. Type	Ref.
Known Planet Orbits (NASA Exoplanet Archive)											
RKS0039+2115	25PC	62.250	16.6	0.645	243.00	53932.200	...	...	HD 3651 b	1−planet	Fischer et al. (2003)
RKS0102−1025	25PC	34.150	4.0	0.250	108.00	54702.000	...	...	HIP 4845 b	1−planet	Feng et al. (2020)
RKS0113+1629	33PC	30.014	41.1	0.054	271.08	58056.731	...	...	HIP 5763 b	1−planet	Paredes et al. (2021)
RKS0122−2653	33PC	158.991	9.4	0.200	−44.79	...	...	...	HD 8326 b	1−planet	Feng et al. (2019)
RKS0246−2305	25PC	57.435	24.7	0.170	272.00	...	...	...	HIP 12961 b	1−planet	Forveille et al. (2011)
RKS0255+2652A	25PC	10.285	3.6	0.224	60.12	50362.749	...	...	HD 18143 b	2−planet	Feng et al. (2022)
RKS0332−0927	25PC	2671.000	10.3	0.070	−19.15	60054.000	...	...	eps Eri b	1−planet	Hatzes et al. (2000)
RKS0406−2051	33PC	5.235	4.6	0.060	360.00	...	...	...	GJ 160.2 b	1−planet	Tuomi et al. (2014)
RKS0415−0739	25PC	42.378	1.8	0.040	148.97	...	...	...	HD 26965 b	1−planet	Ma et al. (2018)
RKS0533−2643	33PC	0.490	2.9	0.000	0.00	...	...	...	TOI−431 b	3−planet	Osborn et al. (2021)
RKS0553−0559	25PC	3.873	4.4	0.000	0.00	55220.500	...	...	BD−06 1339 b	2−planet	Lo Curto et al. (2013)
RKS0633+0527	33PC	3.024	33.6	0.063	114.00	51071.530	...	...	HD 46375 b	1−planet	Marcy et al. (2000)
RKS0705+2728	25PC	159.986	44.7	0.305	31.80	58023.220	...	...	HIP 34222 b	1−planet	Paredes et al. (2021)
RKS0712−2453	33PC	69.971	5.2	0.720	58.00	52965.600	...	...	GJ 2056 b	1−planet	Feng et al. (2020)
RKS0716−0339	33PC	41.516	2.8	0.160	10.73	...	...	...	HIP 35173 b	1−planet	Feng et al. (2019)
RKS0754−2518	25PC	60.722	1.9	0.170	125.00	52956.200	...	...	HIP 38594 b	2−planet	Feng et al. (2020)
RKS0838−1315	33PC	6.398	4.4	0.090	−76.00	...	...	...	HD 73583 b	2−planet	Barragán et al. (2022)
RKS0852+2819	25PC	14.652	71.4	0.000	−21.50	53021.080	...	...	55 Cnc b	5−planet	Butler et al. (1997)
RKS0855+0132	25PC	4100.000	40.0	0.370	290.00	54500.000	...	...	GJ 328 b	1−planet	Robertson et al. (2013)
RKS1114+2542	25PC	9.490	2.8	0.050	−10.00	...	...	...	HD 97658 b	1−planet	Howard et al. (2011)
RKS1121+1811	33PC	968.800	52.0	0.226	162.00	63541.000	...	...	HD 98736 b	1−planet	Ment et al. (2018)
RKS1126+0300B	XTRA	17.043	9.8	0.250	219.00	50468.700	...	...	HD 99492 b	1−planet	Marcy et al. (2005)
TIC 397024052	XTRA	4.114	63.0	0.000	143.40	53895.960	...	...	HD 102195 b	1−planet	Ge et al. (2006)
RKS1158−2355	33PC	120.878	1.8	0.190	127.74	...	...	...	HD 103949 b	1−planet	Feng et al. (2019)
RKS1159−2021	25PC	55.806	11.6	0.000	10.00	54043.150	...	...	HD 104067 b	1−planet	Ségransan et al. (2011)
RKS1312−0215	25PC	493.700	31.9	0.144	86.00	53806.000	...	...	HD 114783 b	2−planet	Vogt et al. (2002)
RKS1316+1701	25PC	10.495	10.5	0.232	259.22	52305.407	...	...	HD 115404 A b	2−planet	Feng et al. (2022)
RKS1436+0944	25PC	453.019	55.6	0.303	57.86	50198.691	...	...	HD 128311 b	2−planet	Butler et al. (2003)
RKS1717+2913	25PC	4.646	1.9	0.000	36.00	54718.570	...	...	HD 156668 b	2−planet	Howard et al. (2011)

Table 3: K dwarf Orbital Solutions.

ID RKS/TIC	Sample	Period days	K $m\,s^{-1}$	e	ω deg	T_p days	RMS $m\,s^{-1}$	No. Obs.	Comp. Name	Comp. Type	Ref.
RKS1833−1138	33PC	1634.000	14.9	0.050	343.88	55899.000	...	...	BD−11 4672 b	2−planet	Moutou et al. (2015)
RKS1903−1102	33PC	6.490	2.6	0.066	249.00	55502.900	...	...	HD 176986 b	2−planet	Suárez et al. (2018)
RKS2000+2242	25PC	2.219	205.0	0.000	20.00	57929.288	...	...	HD 189733 b	1−planet	Bouchy et al. (2005)
RKS2002+0319	25PC	11.720	5.6	0.140	254.64	...	...	...	HD 190007 b	1−planet	Burt et al. (2021)
RKS2013−0052	25PC	24.356	51.9	0.050	20.00	51979.280	...	...	HD 192263 b	1−planet	Santos et al. (2000)
RKS2015−2701	25PC	74.720	3.0	0.130	173.00	55164.300	...	...	HD 192310 b	2−planet	Pepe et al. (2011)
RKS2132−2057	33PC	1733.000	5.9	0.370	−132.00	56015.000	...	...	HD 204941 b	1−planet	Dumusque et al. (2011)
RKS2243−0624	25PC	5.760	0.8	0.000	...	...	...	...	HD 215152 b	4−planet	Delisle et al. (2018)
RKS2309−0215	33PC	225.700	8.3	0.300	44.00	50360.000	...	...	HD 218566 b	1−planet	Meschiari et al. (2011)
RKS2327−0117	33PC	1.209	4.1	0.000	...	57738.826	...	...	GJ 9827 b	3−planet	Niraula et al. (2017)
Companion Candidates											
RKS0000+1659A	33PC	3191.362	135.9	...	...	...	...	24			this work
RKS0118−0052A	33PC	3219.196	88.2	...	...	...	...	43			this work
RKS0200+2636	33PC	1346.187	114.1	...	...	...	...	11			this work
RKS0215−1814	25PC	793.726	267.4	...	...	...	...	9			this work
RKS0236+0653	25PC	1647.654	224.8	...	...	...	...	13			this work
RKS0251−0816	33PC	1415.831	43.0	...	...	...	...	11			this work
RKS0343+1640	25PC	710.091	42.1	...	...	...	...	9			this work
RKS0345−2751	25PC	710.095	41.0	...	...	...	...	9			this work
RKS0357−2712	33PC	1384.104	578.9	...	...	...	...	11			this work
RKS0440−0911	25PC	781.787	190.0	...	...	...	...	10			this work
RKS0522+0236A	25PC	2473.391	270.5	...	...	...	...	42			this work
RKS0608+2630	33PC	17.949	500.7	...	...	...	...	3			this work
RKS0610+0225	33PC	869.708	3988.8	...	...	...	...	4			this work
RKS0614+0510A	33PC	2481.451	55.9	...	...	...	...	31			this work
RKS0658−1259A	25PC	2543.258	378.2	...	...	...	...	52			this work
RKS0723+2024	33PC	35.885	173.6	...	...	...	...	4			this work
RKS0813−1355A	33PC	127.419	5425.0	...	...	...	...	3			this work
RKS0850+0751	25PC	203.521	93.6	...	...	...	...	9			this work

Table 3: K dwarf Orbital Solutions.

ID RKS/TIC	Sample	Period days	K $m\,s^{-1}$	e	ω deg	T_p days	RMS $m\,s^{-1}$	No. Obs.	Comp. Name	Comp. Type	Ref.
RKS0937+2231A	33PC	1627.614	43.0	...	...	...	...	18			this work
RKS1057+2856	33PC	1495.864	902.4	...	...	...	...	19			this work
RKS1059+1759	33PC	684.132	1150.1	...	...	...	...	4			this work
RKS1102−0919A	33PC	1484.077	64.9	...	...	...	...	19			this work
RKS1105+0720	33PC	0.058	383.8	...	...	...	...	6			this work
RKS1158−2535	33PC	1441.812	189.1	...	...	...	...	9			this work
RKS1215+0538A	XTRA	1773.381	274.8	...	...	...	...	22			this work
RKS1231+2013	33PC	2397.643	311.8	...	...	...	...	16			this work
RKS1306+2043A	25PC	3344.770	137.6	...	...	...	...	19			this work
RKS1353+2748	33PC	1344.360	231.0	...	...	...	...	6			this work
RKS1414−1521	33PC	708.121	130.9	...	...	...	...	2			this work
RKS1520+1522A	33PC	1759.377	87.8	...	...	...	...	16			this work
RKS1613+1331B	XTRA	474.386	2841.3	...	...	...	...	2			this work
RKS1628+1824B	XTRA	125.641	2823.4	...	...	...	...	2			this work
RKS1757−2143A	33PC	3157.559	204.7	...	...	...	...	33			this work
RKS1804+0149	33PC	1511.957	2412.9	...	...	...	...	6			this work
RKS1815+1829	33PC	2724.166	92.2	...	...	...	...	20			this work
RKS1848−1008A	33PC	3155.523	1873.0	...	...	...	...	18			this work
RKS1848+1044	25PC	71.718	19.6	...	...	...	...	4			this work
RKS1854+1058	25PC	2000.544	91.5	...	...	...	...	9			this work
TIC 451627388	XTRA	2152.019	47.1	...	...	...	...	12			this work
RKS1914+0209A	33PC	123.821	464.6	...	...	...	...	4			this work
RKS1936−1026A	33PC	280.787	145.3	...	...	...	...	2			this work
RKS2009+1648B	XTRA	1565.889	28.9	...	...	...	...	5			this work
RKS2050+2923A	25PC	3554.168	175.6	...	...	...	...	29			this work
RKS2059−1042	33PC	3229.368	138.4	...	...	...	...	46			this work
RKS2107+2945	XTRA	2862.119	721.3	...	...	...	...	23			this work
RKS2125+2712	25PC	2106.143	1192.3	...	...	...	...	11			this work
RKS2241+1849A	33PC	981.367	236.9	...	...	...	...	2			this work
RKS2308+0633	33PC	1282.415	701.3	...	...	...	...	11			this work

Table 3: K dwarf Orbital Solutions.

ID RKS/TIC	Sample	Period days	K $m\,s^{-1}$	e	ω deg	T_p days	RMS $m\,s^{-1}$	No. Obs.	Comp. Name	Comp. Type	Ref.
RKS2348−1259A	33PC	3241.170	203.7	...	...	...	...	29			this work
RKS2350−2924	33PC	3197.217	75.5	...	...	...	...	26			this work

Table 4: Look up table for star names.

RKS	Hipparcos	TIC	Gaia DR2	SB9	WDS	Simbad
RKS0000+1659A	HIP 68	TIC 456502768	Gaia DR2 2772904691015625984		WDS J00008+1659AB	HD 224808
RKS0001−2326		TIC 327953706	Gaia DR2 2339837370419833216		WDS J00011−2326A	HD 224832
RKS0001−1656	HIP 112	TIC 117550432	Gaia DR2 2414870582223963904			BD−17 6862
RKS0002+1100	HIP 184	TIC 403021108	Gaia DR2 2765462891378117504		WDS J00024+1100A	HD 224983
	HIP 400	TIC 258866681	Gaia DR2 2848150288954631296			HD 225261
RKS0007−2349	HIP 616	TIC 114809058	Gaia DR2 2336728947968831104			HD 283
	HIP 897	TIC 301033489	Gaia DR2 2443632711190063872			BD−06 15
RKS0012+2705	HIP 974	TIC 437739969	Gaia DR2 2856765684112654336			BD+26 8
RKS0012+2142	HIP 1006	TIC 150816111	Gaia DR2 2798963773724811904		WDS J00126+2143Aa,Ab	G 131−35
RKS0016−1435		TIC 12863584	Gaia DR2 2417069815934357248		WDS J00162−1435A	BD−15 36
RKS0017+2057		TIC 150905990	Gaia DR2 2799371898696899328		WDS J00180+2057A	G 131−51
RKS0019−0957	HIP 1532	TIC 37749396	Gaia DR2 2428162410789155328			BD−10 47
RKS0019−0303	HIP 1539	TIC 244159446	Gaia DR2 2541200830419126016			LP 644−95
RKS0020+1738		TIC 303206437	Gaia DR2 2794018509724590208			StKM 1−25
RKS0021+2531		TIC 437752575	Gaia DR2 2855386174976559488			BD+24 32
RKS0022−2701	HIP 1768	TIC 246849513	Gaia DR2 2323302296085774464			HD 1815
RKS0024−2701	HIP 1936	TIC 246852823	Gaia DR2 2322574488107786624			HD 2025
RKS0036−0930	HIP 2839	TIC 38394718	Gaia DR2 2426119449465130112			BD−10 109
RKS0036+2610		TIC 258940245	Gaia DR2 2807687883095124992			BD+25 84
RKS0039+2115	HIP 3093	TIC 434210589	Gaia DR2 2802397960855105920		WDS J00394+2115A	* 54 Psc
RKS0040−0713		TIC 3816119	Gaia DR2 2523361151179609216		WDS J00408−0714B	HD 3821B
RKS0042+2239	HIP 3378	TIC 434221364	Gaia DR2 2803019356723339392		WDS J00429+2240A	G 69−14
RKS0044−1856A	HIP 3493	TIC 114435753	Gaia DR2 2368926256202381824		WDS J00446−1856Aa,Ab	BD−19 111
RKS0045+0147	HIP 3535	TIC 257392565	Gaia DR2 2549518150551364864			HD 4256
RKS0048+0516	HIP 3765	TIC 257393898	Gaia DR2 2552925644460225152		WDS J00484+0517A	HD 4628
RKS0051+1844A	HIP 3998	TIC 435874566	Gaia DR2 2788907296779604864		WDS J00514+1844A	HD 4913
RKS0051−2254	HIP 4022	TIC 28053245	Gaia DR2 2349206308999273984		WDS J00516−2255A	HD 4967
	HIP 4061	TIC 435876741	Gaia DR2 2789773986820056064		WDS J00520+2035A	G 69−27
RKS0055−2940A	HIP 4353	TIC 63812656	Gaia DR2 5032229910174557056		WDS J00558−2941A	HD 5425
RKS0056−1135	HIP 4443	TIC 408037269	Gaia DR2 2472505371140425472			BD−12 165
RKS0057+0551		TIC 344631411	Gaia DR2 2553195883802687104			BD+05 127
RKS0100−2536	HIP 4691	TIC 63841772	Gaia DR2 2344381647681790720			CD−26 323

Table 4: Look up table for star names.

RKS	Hipparcos	TIC	Gaia DR2	SB9	WDS	Simbad
RKS0101−0953	HIP 4824	TIC 24249228	Gaia DR2 2473159374400564992			BD−10 216
RKS0102−1025	HIP 4845	TIC 24250831	Gaia DR2 2473055951588089088			BD−11 192
RKS0102+0503A	HIP 4849	TIC 344714317	Gaia DR2 2552288133874677760		WDS J01024+0504AB	HD 6101
RKS0102−2136	HIP 4855	TIC 404746289	Gaia DR2 2352443855348067584		WDS J01025−2137B	HD 6156B
RKS0104−2536	HIP 5027	TIC 326105628	Gaia DR2 5034869184758130816			HD 6378
RKS0104+2607	HIP 5041	TIC 15611379	Gaia DR2 306637167168935168			BD+25 162
RKS0105+1523B	HIP 5110	TIC 384882785	Gaia DR2 2783518212334778880		WDS J01055+1523B	HD 6440B
RKS0105+1523A	HIP 5110	TIC 384882783	Gaia DR2 2783518418493208832		WDS J01055+1523A	HD 6440A
RKS0107+2257	HIP 5286	TIC 243187830	Gaia DR2 2791782794564103808		WDS J01076+2257A	HD 6660
RKS0108+1714	HIP 5369	TIC 408251015	Gaia DR2 2784924659505377280			BD+16 120
RKS0112+0058	HIP 5647	TIC 336893636	Gaia DR2 2534953577148438528			HD 7208
RKS0112−2514	HIP 5663	TIC 11518255	Gaia DR2 5040737312674978816			HD 7279
RKS0113+1629	HIP 5763	TIC 408290683	Gaia DR2 2783854903410922496			BD+15 176
RKS0116+2519	HIP 5957	TIC 16917838	Gaia DR2 294517800251711616			G 69−62
RKS0117−1530	HIP 6037	TIC 439411675	Gaia DR2 2454812025730108672			HD 7808
RKS0118−0052B		TIC 248391510	Gaia DR2 2533723464155234176		WDS J01187−0052B	G 70−50
RKS0118−0052A	HIP 6130	TIC 248391508	Gaia DR2 2533723670313663872		WDS J01187−0052A	HD 7895
RKS0121+2419	HIP 6342	TIC 17003109	Gaia DR2 293605068161883776			Ross 788
RKS0122−2653	HIP 6390	TIC 11613065	Gaia DR2 5036553052456200320		WDS J01221−2654A	HD 8326
RKS0123−1257B		TIC 32550427	Gaia DR2 2456361654226797440		WDS J01230−1258B	G 272−8A
RKS0123−1257A	HIP 6456	TIC 32550429	Gaia DR2 2456361448068367360		WDS J01230−1258A	HD 8389
RKS0124+1254	HIP 6558	TIC 385118961	Gaia DR2 2586728480188790144			BD+12 172
RKS0124+1829	HIP 6613	TIC 456861826	Gaia DR2 2786053067672564736			HD 8553
RKS0125−0103	HIP 6639	TIC 248953025	Gaia DR2 2485808048791094784			BD−01 184
RKS0129+2143	HIP 6917	TIC 381316671	Gaia DR2 288781167053300480	SBC9 1873	WDS J01291+2143A	V* EO Psc
RKS0132+2059		TIC 126998169	Gaia DR2 288484608151416960			Wolf 1523
RKS0133−2454	HIP 7228	TIC 55857683	Gaia DR2 5038698508879942144			CD−25 636
RKS0135−2046		TIC 28127268	Gaia DR2 5138982181310063872			BD−21 262
RKS0136+2133	HIP 7500	TIC 150977490	Gaia DR2 288861019085346816			BD+20 254
	HIP 7576	TIC 29900813	Gaia DR2 2477815222028038272		WDS J01376−0645A	V* EX Cet
RKS0139+1515	HIP 7765	TIC 47140545	Gaia DR2 2589107273595379584		WDS J01399+1515B	BD+14 251
RKS0142+2016	HIP 7981	TIC 113710966	Gaia DR2 96331172942614528		WDS J01425+2016A	* 107 Psc

Table 4: Look up table for star names.

RKS	Hipparcos	TIC	Gaia DR2	SB9	WDS	Simbad
RKS0143−2136	HIP 8038	TIC 164752885	Gaia DR2 5135642002423826560		WDS J01432−2137BC	HD 10611B
	HIP 8039	TIC 164752884	Gaia DR2 5135642002423826688		WDS J01432−2137A	HD 10611
	HIP 8043	TIC 238602461	Gaia DR2 3017855377519498 24			BD+27 273
RKS0145−2503		TIC 632234616	Gaia DR2 5037943144391354368		WDS J01456−2503B	* eps Scl B
RKS0146+1224	HIP 8275	TIC 88775119	Gaia DR2 2575383100738086656			HD 10853
RKS0150+2927	HIP 8543	TIC 26895191	Gaia DR2 302447890428345088			HD 11130
RKS0150+1817		TIC 91275425	Gaia DR2 92102618725254912			Wolf 89
	HIP 8768	TIC 266680951	Gaia DR2 5134635708766250752			HD 11507
RKS0200+2636		TIC 28391317	Gaia DR2 297848079238404736			StKM 1−223
	HIP 9603	TIC 250393730	Gaia DR2 2491050180930470272			G 159−30
	HIP 9716	TIC 257500724	Gaia DR2 5147846340973892352			V* FN Cet
RKS0205−2804	HIP 9749	TIC 72588532	Gaia DR2 5021412261945549568		WDS J02053−2803A	CD−28 657
RKS0209−1620	HIP 10037	TIC 290172418	Gaia DR2 5144740907820131840			BD−17 400
	HIP 10276	TIC 306450964	Gaia DR2 100380639907919872			HD 13483
	HIP 10312	TIC 302411994	Gaia DR2 5143621433184275200			L 728−16
RKS0213−2111	HIP 10337	TIC 268804174	Gaia DR2 5124636303346779008			BD−21 397
RKS0214−0338	HIP 10416	TIC 332819192	Gaia DR2 2493069773336748928			HD 13789
RKS0215+0729	HIP 10500	TIC 337130939	Gaia DR2 2521467689076565504			Wolf 127
RKS0215−1814	HIP 10542	TIC 268859658	Gaia DR2 5143341362661301632		WDS J02158−1814A	HD 14001A
RKS0221−0652	HIP 11000	TIC 408130762	Gaia DR2 2486984045196486784			HD 14635
RKS0222+1824	HIP 11083	TIC 246972946	Gaia DR2 85973326732317056			HD 14687
	HIP 11452	TIC 422844595	Gaia DR2 2515752565074318720	SBC9 3656	WDS J02278+0426AB	HD 15285
RKS0229−1958A	HIP 11565	TIC 64008136	Gaia DR2 5130446359011574528		WDS J02290−1959A	HD 15468
RKS0231+0822	HIP 11707	TIC 258804746	Gaia DR2 22707874346819712		WDS J02310+0823A	G 4−24
RKS0231−2001	HIP 11739	TIC 64032649	Gaia DR2 5130246458348152448			BD−20 470
RKS0231−1516	HIP 11759	TIC 66574369	Gaia DR2 5145956864601439488		WDS J02321−1515B	HD 15767
RKS0236−2331	HIP 12110	TIC 64070385	Gaia DR2 5125414998097353600		WDS J02360−2331A	HD 16270
RKS0236−2710	HIP 12109	TIC 65325369	Gaia DR2 5070130934977324416			HD 16280
RKS0236+0653	HIP 12114	TIC 278962915	Gaia DR2 19316224572460416		WDS J02361+0653A	HD 16160
RKS0236−0309	HIP 12158	TIC 35722731	Gaia DR2 2495442626804315392	SBC9 2703		V* FT Cet
RKS0240+0111	HIP 12493	TIC 318753380	Gaia DR2 2501948402746099456			BD+00 444
RKS0242+0322		TIC 318802674	Gaia DR2 2502865532882650496			BD+02 418

Table 4: Look up table for star names.

RKS	Hipparcos	TIC	Gaia DR2	SB9	WDS	Simbad
RKS0243+1925A	HIP 12709	TIC 247372926	Gaia DR2 84675937371332608	SBC9 140	WDS J02433+1926AB	HD 16909
RKS0246+2538	HIP 12926	TIC 436862182	Gaia DR2 1145754724617168 64			HD 17190
RKS0246+1146	HIP 12929	TIC 387422624	Gaia DR2 25488745411919360			HD 17230
RKS0246−2305	HIP 12961	TIC 204614039	Gaia DR2 5077642283022422656			CD−23 1056
RKS0247+1922	HIP 13027	TIC 247405888	Gaia DR2 84625630419434496		WDS J02475+1922B	HD 17332B
RKS0247+2842	HIP 13065	TIC 397367857	Gaia DR2 128685947561889920			LP 298−33
RKS0248−1145	HIP 13079	TIC 36828898	Gaia DR2 5172403555223128576			BD−12 525
RKS0248+2704	HIP 13081	TIC 397368422	Gaia DR2 114832620743735808	SBC9 2276	WDS J02482+2704A	HD 17382
RKS0250+1542	HIP 13258	TIC 218291131	Gaia DR2 33439176553394048			HD 17660
RKS0251+1038	HIP 13342	TIC 387496444	Gaia DR2 22125575564953216			BD+10 378
RKS0251−0816	HIP 13345	TIC 36845881	Gaia DR2 5174322615330339456			BD−08 535
RKS0252−1246	HIP 13402	TIC 30016911	Gaia DR2 5160075762132996992		WDS J02525−1246A	HD 17925
RKS0255+2652B		TIC 436933290	Gaia DR2 116037371954842240		WDS J02556+2652B	HD 18143B
RKS0255+2652A	HIP 13642	TIC 436933294	Gaia DR2 116037204451525376		WDS J02556+2652A	HD 18143A
RKS0255+2807A	HIP 13644	TIC 436933712	Gaia DR2 116456668137575040			G 36−45
RKS0257−2458	HIP 13769	TIC 88348777	Gaia DR2 5076269164798852864	SBC9 3617	WDS J02572−2458Ca,Cb	HD 18445
RKS0258+2646	HIP 13891	TIC 34579372	Gaia DR2 115364234616059392			HD 18450
RKS0300+0744	HIP 13976	TIC 387609654	Gaia DR2 8479094371605632			V* BZ Cet
RKS0303+2006		TIC 438260486	Gaia DR2 60186343087140096			BD+19 451
RKS0306+0157	HIP 14445	TIC 328324098	Gaia DR2 630505494719360			HD 19305
RKS0308−2445	HIP 14568	TIC 88479623	Gaia DR2 5074604160596736640	SBC9 3606		V* AE For
RKS0308−2410B	HIP 14589	TIC 88479531	Gaia DR2 5074705521824867200			LP 831−72
RKS0308−2410A	HIP 14593	TIC 88479529	Gaia DR2 5074705624904081792			CD−24 1458
RKS0310+1203	HIP 14729	TIC 302499935	Gaia DR2 27775450424210816			BD+11 444
RKS0312−2859		TIC 651379982	Gaia DR2 5059348952156075392		WDS J03121−2859B	* alf For B
RKS0314−2626	HIP 15095	TIC 88533834	Gaia DR2 5073448642595674752			HD 20280
RKS0314+0858	HIP 15099	TIC 365441779	Gaia DR2 14163878724940672			HD 20165
RKS0320+0827	HIP 15563	TIC 336587521	Gaia DR2 11037726649058432			BD+07 499
RKS0322+2709	HIP 15720	TIC 29015116	Gaia DR2 117654650480415744		WDS J03224+2710A	LP 355−64
RKS0324−0521	HIP 15919	TIC 279182339	Gaia DR2 5170039502144332800			HD 21197
RKS0329−1140	HIP 16242	TIC 12570868	Gaia DR2 5162123155863791744			BD−12 662
RKS0329−2406	HIP 16247	TIC 144539611	Gaia DR2 5086152743542494592			V* AK For

Table 4: Look up table for star names.

RKS	Hipparcos	TIC	Gaia DR2	SB9	WDS	Simbad
RKS0332−0927	HIP 16537	TIC 118572803	Gaia DR2 5164707970261630080		WDS J03329−0927A	* eps Eri
RKS0336+0035		TIC 649767689	Gaia DR2 3263936658312134272	SBC9 1523	WDS J03368+0035B	HD 22468B
RKS0341+0336	HIP 17207	TIC 457140535	Gaia DR2 3271668905115228672	SBC9 1801		BD+03 515
RKS0342−2427	HIP 17346	TIC 89148220	Gaia DR2 5085376076015097600		WDS J03427−2428A	CD−24 1826
RKS0343−1253	HIP 17365	TIC 155776776	Gaia DR2 5114240352186781952			BD−13 718
RKS0343+1640	HIP 17414	TIC 434136640	Gaia DR2 43335880716390784		WDS J03439+1640A	BD+16 502
RKS0343−1906	HIP 17420	TIC 121025936	Gaia DR2 5107106033552702208			HD 23356
RKS0344+1155	HIP 17496	TIC 434138790	Gaia DR2 36590651757883392			BD+11 514
RKS0345−2751	HIP 17544	TIC 325688346	Gaia DR2 5080543413172761088		WDS J03454−2752A	HD 23588A
RKS0348+2519		TIC 35156797	Gaia DR2 66945178505314944			HD 23742
RKS0348+1512	HIP 17794	TIC 59001502	Gaia DR2 39925023848663040			BD+14 611
RKS0349−1329		TIC 156929912	Gaia DR2 5114013749714071296			StKM 1−413
RKS0349+0120	HIP 17888	TIC 256836445	Gaia DR2 3269818736284105600			HD 24002
RKS0350−2349	HIP 17956	TIC 121106297	Gaia DR2 5083970693996013952			CD−24 1905
RKS0354−0649	HIP 18280	TIC 55440009	Gaia DR2 3244915072792668416			BD−07 699
RKS0357−2712		TIC 44646065	Gaia DR2 4890157064946814208		WDS J03573−2713A	CD−27 1462
RKS0357−0109	HIP 18512	TIC 49934962	Gaia DR2 3256334497479041024		WDS J03575−0110A	HD 24916
RKS0404+2634		TIC 407932434	Gaia DR2 163302048236137600			HG 8−5
RKS0406−2051	HIP 19165	TIC 178351350	Gaia DR2 5091077112523802112			BD−21 784
RKS0407+1413		TIC 348663813	Gaia DR2 3305633918809117824			LP 474−123
RKS0408+1220	HIP 19325	TIC 389042789	Gaia DR2 3305091447260175616			HD 26129
RKS0409+0918	HIP 19441	TIC 345480097	Gaia DR2 3300315443626615040			HD 286572
RKS0414+0301	HIP 19788	TIC 396944733	Gaia DR2 3259401379007760640			HD 26794
RKS0415−0425A	HIP 19832	TIC 250158330	Gaia DR2 3203456956075394944	SBC9 3619		BD−04 782
RKS0415−0739	HIP 19849	TIC 67772871	Gaia DR2 3195919528988725120		WDS J04153−0739A	* omi02 Eri
	HIP 19948	TIC 70899190	Gaia DR2 3177244255271333248		WDS J04167−1233B	LP 714−58 B
RKS0417+2240	HIP 19981	TIC 17099206	Gaia DR2 148709810947139968		WDS J04171+2240A	HD 284310
RKS0417+2033		TIC 17145404	Gaia DR2 49295199378608000		WDS J04173+2035B	HD 284336
RKS0419−0408	HIP 20142	TIC 250188723	Gaia DR2 3203807116169000448			BD−04 797
RKS0420−1445	HIP 20232	TIC 70964316	Gaia DR2 3175952638346424832			BD−15 767
RKS0420−0902	HIP 20240	TIC 167455128	Gaia DR2 3192532758297814656			BD−09 872
RKS0421−1945		TIC 139638207	Gaia DR2 5092190299327752448			CPD−20 550

Table 4: Look up table for star names.

RKS	Hipparcos	TIC	Gaia DR2	SB9	WDS	Simbad
RKS0427+2022		TIC 17513354	Gaia DR2 144410205086676480			PM J04274+2022
RKS0427+2426A	HIP 20834	TIC 268074192	Gaia DR2 149340032971718912			HD 283668
RKS0429+2155	HIP 20917	TIC 17558287	Gaia DR2 145421309108301184			HD 28343
RKS0430+0058	HIP 21006	TIC 449098466	Gaia DR2 3278753264691218176			MCC 446
RKS0432+0006		TIC 452782929	Gaia DR2 3230595651827092864		WDS J04329+0007A	G 82−29
RKS0433+0338		TIC 672871302	Gaia DR2 3280510692293089664			Gaia DR2 3280510692293089664
RKS0436+2707	HIP 21482	TIC 125838647	Gaia DR2 151650076838458112	SBC9 258	WDS J04368+2708A	HD 283750
RKS0436−1453	HIP 21489	TIC 117748080	Gaia DR2 3173981145278199936		WDS J04070−1000C	BD−15 820
RKS0439+0952A	HIP 21710	TIC 373209819	Gaia DR2 3293515101646468352	SBC9 3620	WDS J04397+0952A	HD 286955
RKS0440−0911	HIP 21765	TIC 56096602	Gaia DR2 3185759697949251456		WDS J04406−0912B	BD−09 956B
RKS0441+2054	HIP 21818	TIC 118820774	Gaia DR2 3411339626673664000		WDS J04413+2054A	HD 29697
RKS0443+2741	HIP 21988	TIC 125918626	Gaia DR2 154660191781205120			HD 29883
RKS0445+0938		TIC 450071562	Gaia DR2 3293037741802934784			StKM 1−508
RKS0448−1056	HIP 22288	TIC 167485954	Gaia DR2 3181588219554237184			HD 30523
RKS0449−1447	HIP 22424	TIC 114921859	Gaia DR2 3173510176346843136			BD−15 869
RKS0451+2837		TIC 60129274	Gaia DR2 155141949672659072			HD 30754
RKS0453+2214	HIP 22715	TIC 18872464	Gaia DR2 3413174741644826112		WDS J04531+2214A	HD 30973
RKS0454+0722B		TIC 399757775	Gaia DR2 3288572968680438912		WDS J04543+0722B	HD 31208B
RKS0454+0722A		TIC 399757770	Gaia DR2 3288572968680438528		WDS J04543+0722A	HD 31208
RKS0455−2833	HIP 22907	TIC 682491	Gaia DR2 4879850208590379904			HD 31560
RKS0500−0545	HIP 23311	TIC 213041474	Gaia DR2 3211461469444773376			HD 32147
	HIP 23431	TIC 303676299	Gaia DR2 3391737292854784768			HD 32237
RKS0503−2315A	HIP 23516	TIC 146443052	Gaia DR2 2960883628469355008		WDS J05033−2315AB	CD−23 2363
RKS0503+0322		TIC 464831700	Gaia DR2 3238221658320206208			StKM 1−542
RKS0506−1102		TIC 43728182	Gaia DR2 3181961503752885248			HD 32965
RKS0506+1426	HIP 23786	TIC 293608218	Gaia DR2 3392089755051027712	SBC9 3564		HD 32850
	HIP 24210	TIC 43866397	Gaia DR2 3182634954624823168		WDS J05119−0907A	HD 33725
RKS0512+1943	HIP 24301	TIC 337492263	Gaia DR2 3407792804024921344			HD 241596
RKS0513−2158	HIP 24392	TIC 398842213	Gaia DR2 2962433871145965568			BD−22 1050
RKS0514+1952		TIC 337570628	Gaia DR2 3413754360367271168			HD 241814
RKS0514+0039	HIP 24454	TIC 454183305	Gaia DR2 3233691292456404992			HD 290054
RKS0518−2123	HIP 24783	TIC 408191404	Gaia DR2 2962193318618221056		WDS J05189−2124A	HD 34751

Table 4: Look up table for star names.

RKS	Hipparcos	TIC	Gaia DR2	SB9	WDS	Simbad
RKS0519−0304A	HIP 24819	TIC 672129447	Gaia DR2 3213958769589070848		WDS J05192−0304B	HD 34673B
RKS0519−0304B	HIP 24819	TIC 249076418	Gaia DR2 3213958769587525888		WDS J05192−0304A	HD 34673
RKS0519−1550	HIP 24874	TIC 442893646	Gaia DR2 2983256662869643776		WDS J05200−1550A	HD 34865
RKS0522+0236A	HIP 25119	TIC 264588636	Gaia DR2 3234412606443085824		WDS J05226+0236AB	HD 35112
RKS0523+1719	HIP 25220	TIC 47345026	Gaia DR2 3394298532176344960			* 111 Tau B
RKS0526+1901		TIC 6857595	Gaia DR2 3400750951741408768			TYC 1304−408−1
RKS0528−0329	HIP 25623	TIC 50587969	Gaia DR2 3210731015767419520		WDS J05284−0330A	HD 36003
RKS0533−2643	HIP 26013	TIC 31374837	Gaia DR2 2908664557091200768			CD−26 2288
RKS0534−2328	HIP 26175	TIC 92988866	Gaia DR2 2963680098856000128			HD 37065
RKS0535+2805	HIP 26196	TIC 74494865	Gaia DR2 3442723120208243072			HD 244957
RKS0536+1119A	HIP 26335	TIC 436248822	Gaia DR2 3339921875389105152		WDS J05365+1120A	V* V2689 Ori
	HIP 26844	TIC 247439806	Gaia DR2 3347826784173590656			MCC 467
RKS0542+0240	HIP 26907	TIC 199920519	Gaia DR2 3223331006703460352			HD 38014
RKS0544−2225		TIC 93279196	Gaia DR2 2964001014514075520		WDS J05445−2227B	V* AK Lep
	HIP 27397	TIC 66653445	Gaia DR2 3010782833390635264			L 810−58
RKS0549−1734		TIC 317281689	Gaia DR2 2967789386125779200			HD 39071
RKS0552−2246		TIC 33550619	Gaia DR2 2917283452645147392			BD−22 1252
RKS0553−0559	HIP 27803	TIC 66914642	Gaia DR2 3022099969137163904			BD−06 1339
RKS0554+0208	HIP 27918	TIC 281913005	Gaia DR2 3315907411861516160			HD 39715
RKS0554−1942		TIC 160301039	Gaia DR2 2966316109264051072		WDS J05545−1942B	TYC 5939−2260−1
RKS0600+2101	HIP 28494	TIC 429438609	Gaia DR2 3423169272278001920			HD 250268
RKS0602+0848		TIC 156566943	Gaia DR2 3323368281154260736			PM J06027+0848
RKS0606−2754	HIP 28921	TIC 37300889	Gaia DR2 2909947996398369920			HD 41842
	HIP 28954	TIC 415563103	Gaia DR2 3345968334645285376		WDS J06067+1533A	V* V1386 Ori
RKS0608+2630		TIC 81339324	Gaia DR2 3427097552448456704			HD 252023
RKS0608+0928	HIP 29132	TIC 461708344	Gaia DR2 3329457346488528384			BD+09 1105
RKS0609+0540	HIP 29208	TIC 232303637	Gaia DR2 3318883274444631296		WDS J06096+0540A	HD 42182
RKS0609+0009		TIC 232331928	Gaia DR2 3122327940136062464			HD 291290
RKS0610+0225		TIC 232369923	Gaia DR2 3315403904256700672			PM J06105+0225
RKS0612+1023		TIC 153341493	Gaia DR2 3329963877751553792			TYC 734−1988−1
RKS0614+0510A	HIP 29611	TIC 232491449	Gaia DR2 3317879695205667200			HD 43062
RKS0616+2512	HIP 29810	TIC 83179624	Gaia DR2 3426007073132962944			HD 254229

Table 4: Look up table for star names.

RKS	Hipparcos	TIC	Gaia DR2	SB9	WDS	Simbad
RKS0617+1759	HIP 29875	TIC 429717611	Gaia DR2 3370363130410784256			HD 254504
RKS0618−1352	HIP 29958	TIC 34192032	Gaia DR2 2993676867708999296			BD−13 1434
RKS0620+0215	HIP 30112	TIC 265811235	Gaia DR2 3124542635730704896			HD 288595
RKS0621−2212	HIP 30225	TIC 60175114	Gaia DR2 2937651222655480832			HD 44573
RKS0626+1845	HIP 30630	TIC 430173956	Gaia DR2 3372159045216183552	SBC9 402	WDS J06262+1845A	HD 45088
RKS0629+2700	HIP 30893	TIC 84859050	Gaia DR2 3432427499483568384			HD 257886
RKS0630−1148	HIP 30979	TIC 24952049	Gaia DR2 3000225425824867584			HD 45977
RKS0630+2104		TIC 47134740	Gaia DR2 3373041506377703040			TYC 1340−1480−1
RKS0631+0552	HIP 31069	TIC 234837298	Gaia DR2 3132002680386862208			HD 258857
RKS0632−2701	HIP 31148	TIC 172084191	Gaia DR2 2898839424265628928		WDS J06321−2702A	CD−26 3096
RKS0633+0527	HIP 31246	TIC 234928947	Gaia DR2 3131777319158581376		WDS J06332+0528A	HD 46375
RKS0637+1945	HIP 31626	TIC 55113936	Gaia DR2 3371908043029299840			HD 260564
RKS0641+2357	HIP 32010	TIC 353436550	Gaia DR2 3382815271394515072			HD 47752
RKS0647−1815	HIP 32530	TIC 49379766	Gaia DR2 2945575128080020864			BPM 72121
RKS0652−0510	HIP 32984	TIC 282210766	Gaia DR2 3101923001490347392		WDS J06523−0510A	HD 50281
RKS0652−2306	HIP 33037	TIC 78823956	Gaia DR2 2922666665878956032			HD 50590
RKS0655−2008		TIC 79215531	Gaia DR2 2932346628813361408		WDS J06556−2008B	* pi. CMa B
RKS0658−1259A	HIP 33560	TIC 147261632	Gaia DR2 2949560475474885760		WDS J06584−1300AB	HD 51849
RKS0700−2847		TIC 63354191	Gaia DR2 5608852393772621184			WT 1539
RKS0701−2556A	HIP 33817	TIC 63571394	Gaia DR2 2920772722738017920			HD 52698
RKS0701+0655	HIP 33848	TIC 270889166	Gaia DR2 3153772873178431744			HD 52456
RKS0702−0647	HIP 33955	TIC 125409404	Gaia DR2 3052753116376444800			HD 52919
RKS0705+2728	HIP 34222	TIC 91842379	Gaia DR2 884039857341503616		WDS J07057+2728A	BD+27 1311
RKS0706+2358	HIP 34317	TIC 87694489	Gaia DR2 3368634595051958656			BD+24 1529
RKS0707+0326	HIP 34341	TIC 292351181	Gaia DR2 3116065985196889216	SBC9 3737		BD+03 1552
RKS0708+2950	HIP 34414	TIC 87752739	Gaia DR2 884951489919636352			HD 53927
RKS0708−0958	HIP 34423	TIC 177524050	Gaia DR2 3046660035248293632			HD 54359
RKS0710−1425	HIP 34673	TIC 306658481	Gaia DR2 3032390401547521024			BD−14 1750
RKS0712−2453	HIP 34785	TIC 65406275	Gaia DR2 5617244278837970816			CD−24 5005
RKS0713+2500	HIP 34950	TIC 101722543	Gaia DR2 870758684590736896		WDS J07139+2501A	HD 55458
RKS0716−0339	HIP 35173	TIC 50992589	Gaia DR2 3059948148669499008			BD−03 1821
RKS0718+1632		TIC 440851540	Gaia DR2 3168265196642972288		WDS J07181+1632B	* lam Gem B

Table 4: Look up table for star names.

RKS	Hipparcos	TIC	Gaia DR2	SB9	WDS	Simbad
RKS0720+2158		TIC 184842717	Gaia DR2 866177431955017600		WDS J07201+2159B	* del Gem B
RKS0723−2001	HIP 35851	TIC 412580862	Gaia DR2 2930241682523663360			BD−19 1855
RKS0723+2024		TIC 165980070	Gaia DR2 3363049071685181056			BD+20 1790
RKS0723+1257	HIP 35872	TIC 14494641	Gaia DR2 3163201979956736000			HD 57901
RKS0724−1753	HIP 35943	TIC 412778373	Gaia DR2 3027559353615045760			BD−17 1959
RKS0725−1041		TIC 403630804	Gaia DR2 3035245970683433344			LP 722−21
RKS0726−1546	HIP 36121	TIC 386070101	Gaia DR2 3028470161558479232			HD 58760
RKS0730−0340		TIC 65068595	Gaia DR2 3060332221821297408			G 112−24
RKS0731+1436	HIP 36551	TIC 247116238	Gaia DR2 3165287719154543232			HD 59582
RKS0732+1719	HIP 36637	TIC 247128235	Gaia DR2 3169256887411823872		WDS J07320+1720Aa	G 88−36A
RKS0732−0853	HIP 36642	TIC 6677241	Gaia DR2 3053492881541639552		WDS J07321−0853B	HD 59984B
RKS0734−0653	HIP 36827	TIC 7131321	Gaia DR2 3054448838181163520		WDS J07344−0654A	HD 60491
RKS0739−0335	HIP 37349	TIC 66100263	Gaia DR2 3057712223051571200		WDS J07400−0336A	HD 61606
RKS0740−0336		TIC 66189398	Gaia DR2 3057712188691831936		WDS J07400−0336B	BD−03 2002
RKS0741−2921		TIC 125941934	Gaia DR2 5599698031766065280			TYC 6552−2083−1
RKS0745+0208	HIP 37798	TIC 266809077	Gaia DR2 3088637946087230336			BD+02 1766
RKS0752+2555		TIC 171301335	Gaia DR2 873931909508892800			HD 63991
RKS0752+2233	HIP 38492	TIC 63167717	Gaia DR2 675007406816259712			BD+22 1802
RKS0754−2518	HIP 38594	TIC 128902569	Gaia DR2 5602386058511578368		WDS J07542−2518A	CD−24 6144
RKS0754−0124A	HIP 38625	TIC 123089572	Gaia DR2 3082317193037072256	SBC9 2179	WDS J07546−0125A	HD 64606
RKS0754+1914	HIP 38657	TIC 293253336	Gaia DR2 670216834655936128	SBC9 3621	WDS J07549+1914A	HD 64468
RKS0755−1529	HIP 38702	TIC 54702151	Gaia DR2 5719262293418946432			BPM 72493
RKS0757−0048	HIP 38931	TIC 25994436	Gaia DR2 3083867749248355456		WDS J07580−0049A	HD 65277
RKS0758−2537	HIP 38939	TIC 129997166	Gaia DR2 5698188160215537920		WDS J07581−2538A	HD 65486
RKS0758−1501A	HIP 38969	TIC 689318	Gaia DR2 5725307305268686336			BD−14 2308
	HIP 38992	TIC 271266069	Gaia DR2 3147366882213649664			HD 65371
RKS0759+2050	HIP 39064	TIC 54234694	Gaia DR2 670853314448533888	SBC9 1536		HD 65430
	HIP 39068	TIC 19064262	Gaia DR2 653374000145053312			HD 65523
	HIP 39157	TIC 171523537	Gaia DR2 876370076542359936			HD 65583
RKS0804+1217		TIC 408816165	Gaia DR2 653032704866193024		WDS J08044+1217C	HD 66509C
RKS0808+2106	HIP 39826	TIC 386838171	Gaia DR2 676689831406224128		WDS J08082+2106A	BD+21 1764
RKS0813−1355A	HIP 40239	TIC 125247681	Gaia DR2 5726415887862017536		WDS J08132−1354A	BD−13 2439A

Table 4: Look up table for star names.

RKS	Hipparcos	TIC	Gaia DR2	SB9	WDS	Simbad
RKS0813−1355B		TIC 835870015	Gaia DR2 5726415887862017408		WDS J08132−1354B	BD−13 2439B
RKS0814+1301	HIP 40375	TIC 27679101	Gaia DR2 650337664425397632			HD 68834
RKS0815−2600	HIP 40459	TIC 155885021	Gaia DR2 5694469199569753472			V* V430 Pup
RKS0817+1717		TIC 186814573	Gaia DR2 656248020460761472			LSPM J0817+1717
RKS0818−1512A	HIP 40724	TIC 307629574	Gaia DR2 5723025990434513408			BD−14 2469
RKS0819+0120	HIP 40774	TIC 455179026	Gaia DR2 3089675232224086784			BD+01 2063
RKS0820+1404	HIP 40910	TIC 60285843	Gaia DR2 652005932802958976			BD+14 1876
RKS0823+2150	HIP 41130	TIC 14566446	Gaia DR2 676273597540164096			BD+22 1921
RKS0827+2855	HIP 41443	TIC 3575626	Gaia DR2 707498696972158336			BD+29 1754
RKS0832−2323		TIC 434425674	Gaia DR2 5701928217724322688			BD−22 2311
	HIP 42074	TIC 121286109	Gaia DR2 3073562610873679872		WDS J08345−0044A	HD 72760
RKS0838−0415		TIC 121419822	Gaia DR2 3071508581420749440			G 114−7
RKS0838−1315	HIP 42401	TIC 101011575	Gaia DR2 5746824674801810816			HD 73583
RKS0839+0657	HIP 42418	TIC 458680441	Gaia DR2 595390807776621824	SBC9 3680		HD 73512
RKS0839+1131	HIP 42499	TIC 443965212	Gaia DR2 602079652404802688		WDS J08398+1131A	HD 73667
RKS0840−0628A	HIP 42507	TIC 51624556	Gaia DR2 5755182715519422336			BD−05 2603
RKS0848+0628	HIP 43233	TIC 444008058	Gaia DR2 583108060303234944		WDS J08484+0629A	BD+07 2031A
RKS0850+0751	HIP 43422	TIC 437036405	Gaia DR2 596779044285041792		WDS J08507+0752A	BD+08 2131A
RKS0852+2819	HIP 43587	TIC 332064670	Gaia DR2 704967037090946688		WDS J08526+2820A	* rho01 Cnc
RKS0854−2423	HIP 43771	TIC 2220886	Gaia DR2 5653012624732870528			HD 76378
RKS0855+0132	HIP 43790	TIC 265373654	Gaia DR2 577602496345490176			BD+02 2098
RKS0858+2032	HIP 44072	TIC 203214233	Gaia DR2 684865658135318144			BD+21 1949
RKS0859+0151A	HIP 44109	TIC 800011138	Gaia DR2 576970105360152192		WDS J08590+0152B	BD+02 2116B
RKS0900+2127	HIP 44259	TIC 203227093	Gaia DR2 685029558383335168	SBC9 2324		HD 77065
RKS0901+1515B	HIP 44295	TIC 437059374	Gaia DR2 610304716643271808		WDS J09013+1516B	HD 77175B
RKS0901+1515A	HIP 44295	TIC 437059375	Gaia DR2 610304720934423424		WDS J09013+1516A	HD 77175A
RKS0904−1554	HIP 44526	TIC 1192946	Gaia DR2 5730445323098531456			HD 77825
RKS0905+2517		TIC 138660798	Gaia DR2 688430107330061056			BD+25 2037
	HIP 44722	TIC 19976193	Gaia DR2 5743705394673617664		WDS J09068−0848A	BD−08 2582
RKS0907+2252		TIC 243245964	Gaia DR2 685598040254959360			HD 78141
RKS0909+2725	HIP 44920	TIC 284992719	Gaia DR2 692114673873977472			MCC 25
RKS0909+0512		TIC 270693260	Gaia DR2 580473664802608512			HD 78727

Table 4: Look up table for star names.

RKS	Hipparcos	TIC	Gaia DR2	SB9	WDS	Simbad
RKS0914+0426A	HIP 45383	TIC 290468468	Gaia DR2 579567598502090240		WDS J09149+0427AB	HD 79555
RKS0917−0323	HIP 45621	TIC 170889511	Gaia DR2 3837451574150437120			HD 80133
RKS0918+2718		TIC 149397312	Gaia DR2 694917878769233408			BD+27 1739
RKS0919+0053	HIP 45737	TIC 290553722	Gaia DR2 3844124407140189440			HD 80367
RKS0920−0545	HIP 45839	TIC 277533870	Gaia DR2 5746426720312132608			HD 80632
RKS0929−0245		TIC 77549396	Gaia DR2 3837746380705638656		WDS J09291−0246B	* tau01 Hya B
RKS0929−0522	HIP 46549	TIC 77551910	Gaia DR2 3824731809460825728			BD−04 2639
RKS0929+0539	HIP 46580	TIC 383188202	Gaia DR2 3852570413083923072			HD 82106
RKS0932+2909		TIC 172532520	Gaia DR2 696304088053991296			StKM 1−780
RKS0932−1111	HIP 46816	TIC 46907042	Gaia DR2 5739942011185493888			V* LQ Hya
	HIP 46843	TIC 172533278	Gaia DR2 646255212109355136		WDS J09327+2659A	HD 82443
RKS0937+2241	HIP 47201	TIC 91968683	Gaia DR2 641154096631794432			BD+23 2121
RKS0937+2231A	HIP 47261	TIC 91987394	Gaia DR2 641136225272958336			BD+23 2124
RKS0938+0240	HIP 47307	TIC 453032368	Gaia DR2 3847645013308140800			Ross 888
RKS0947+0134	HIP 48016	TIC 455277453	Gaia DR2 3846345523708141568			G 53−4
RKS0947+2618	HIP 48024	TIC 239198426	Gaia DR2 646534556782461056			BD+26 2004
RKS0952+0313	HIP 48411	TIC 275249970	Gaia DR2 3847128380281953664		WDS J09522+0313A	HD 85488
RKS0952+0307	HIP 48447	TIC 275251307	Gaia DR2 3847123707357532672			MCC 559
RKS0959−0911	HIP 48953	TIC 33300879	Gaia DR2 3770491075500789504			BD−08 2813
RKS1000+2433	HIP 49018	TIC 308016265	Gaia DR2 642660938662899456	SBC9 591	WDS J10000+2433AB	V* DH Leo
RKS1001−1525	HIP 49127	TIC 332710428	Gaia DR2 5686377893489291136			HD 86972
RKS1004−1143	HIP 49366	TIC 26073633	Gaia DR2 3766401961693098368		WDS J10046−1144A	HD 87424
RKS1005+2629	HIP 49429	TIC 3906145	Gaia DR2 739100722737992064			HD 87445
RKS1006+0257A	HIP 49544	TIC 344951838	Gaia DR2 3836586468953204608		WDS J10069+0258A	BD+03 2316
RKS1008+1159		TIC 357348155	Gaia DR2 3880785530720066176		WDS J10084+1158B	HD 87884
RKS1011−2425		TIC 168078441	Gaia DR2 5473349302315731072		WDS J10118−2426A	WT 1757
RKS1020−0128	HIP 50657	TIC 143404311	Gaia DR2 3830475211527368960			HD 89668
RKS1021−1743A	HIP 50696	TIC 308020541	Gaia DR2 5669747402161003520			L 752−53
	HIP 50782	TIC 350043652	Gaia DR2 3883317121883053184			HD 89813
RKS1024−1024	HIP 50944	TIC 36841797	Gaia DR2 3767851972716355712			BD−09 3063
RKS1026−0631	HIP 51127	TIC 36892736	Gaia DR2 3775615766054509568		WDS J10267−0632A	BD−05 3063
RKS1026+2638	HIP 51157	TIC 165287825	Gaia DR2 728504488663060224	SBC9 1872		HD 90442

Table 4: Look up table for star names.

RKS	Hipparcos	TIC	Gaia DR2	SB9	WDS	Simbad
RKS1028+0644	HIP 51254	TIC 392795974	Gaia DR2 3862361392330264320			HD 90663
RKS1030−2114	HIP 51443	TIC 423437103	Gaia DR2 5475922468760821376			BD−20 3194
RKS1032+0830A	HIP 51571	TIC 392833911	Gaia DR2 3863754056950355840			BD+09 2366
RKS1036−1350	HIP 51931	TIC 386563186	Gaia DR2 3750851328223270400			V* V418 Hya
RKS1043−2903	HIP 52462	TIC 188043641	Gaia DR2 5455707157211784832		WDS J10435−2904A	V* V419 Hya
RKS1046−2435	HIP 52708	TIC 188087957	Gaia DR2 5470514142863169280		WDS J10466−2435A	HD 93380
RKS1047+2129	HIP 52765	TIC 95836951	Gaia DR2 3989171263817702656			BD+22 2271
RKS1047−2217	HIP 52776	TIC 408448101	Gaia DR2 3550084490721711872			BD−21 3153
RKS1053−1422	HIP 53236	TIC 422279710	Gaia DR2 3563850307581238400			HD 94374
RKS1054−0432		TIC 14343469	Gaia DR2 3789058803237072128			StKM 1−896
RKS1056+0723	HIP 53486	TIC 365006720	Gaia DR2 3865002247461685248			HD 94765
RKS1057+2856	HIP 53541	TIC 138763579	Gaia DR2 732983005681390592			HD 94818
RKS1059+1759	HIP 53731	TIC 97471384	Gaia DR2 3983787397757283840		WDS J10596+1800AB	HD 95175
RKS1059+2526A		TIC 82285130	Gaia DR2 3996306127913903232		WDS J10596+2527A	HD 95174A
RKS1059+2526B		TIC 82285131	Gaia DR2 3996306127914172928		WDS J10596+2527B	HD 95174B
RKS1102−0919A	HIP 54002	TIC 211445010	Gaia DR2 3759964905228025088			V* AB Crt
RKS1105+0720		TIC 903126674	Gaia DR2 3818309974359047936		WDS J11050+0720B	* chi Leo B
RKS1108−2816A	HIP 54418	TIC 168453014	Gaia DR2 3531971582843325184			CD−27 7881
RKS1108+1546	HIP 54459	TIC 77109256	Gaia DR2 3969552574763799808			HD 96692
	HIP 54513	TIC 62904024	Gaia DR2 3788517916531415552			G 163−53
RKS1111−1057	HIP 54651	TIC 143047975	Gaia DR2 3566643651231641600			HD 97214
RKS1111−1459A	HIP 54677	TIC 308076910	Gaia DR2 3562962623740696576			HD 97233
	HIP 54803	TIC 425283213	Gaia DR2 3804108716535576960		WDS J11132+0014AB	BD+01 2535
RKS1113+0428	HIP 54810	TIC 425282449	Gaia DR2 3815264842546968192			HD 97503
RKS1114+2542	HIP 54906	TIC 82308728	Gaia DR2 3997075206232885888			HD 97658
RKS1114−2306	HIP 54922	TIC 423454257	Gaia DR2 3538007420643155712		WDS J11148−2306A	HD 97782A
RKS1115−1808B	HIP 54963	TIC 423491049	Gaia DR2 3558078936688219776		WDS J11154−1807B	BD−17 3336
RKS1115−1808A	HIP 54966	TIC 423491048	Gaia DR2 3558078971047964800		WDS J11154−1807A	BD−17 3337
RKS1116−1441	HIP 55066	TIC 347626733	Gaia DR2 3561574971346845440			BD−13 3333
RKS1117−2748	HIP 55119	TIC 322777782	Gaia DR2 3531296963739811200			CD−27 7978
RKS1117−0158	HIP 55132	TIC 38064734	Gaia DR2 3790755044736796544			BD−01 2505
RKS1121−2027	HIP 55454	TIC 437261156	Gaia DR2 3545469496823737856		WDS J11214−2027A	HD 98712A

Table 4: Look up table for star names.

RKS	Hipparcos	TIC	Gaia DR2	SB9	WDS	Simbad
RKS1121+1811	HIP 55486	TIC 3819571	Gaia DR2 3977050728669174912		WDS J11218+1811A	HD 98736
RKS1123+0701A	HIP 55605	TIC 291065627	Gaia DR2 3817534337625985280		WDS J11235+0701Aa,Ab	LP 552−48
RKS1124−1741	HIP 55705	TIC 901935568	Gaia DR2 3546521385853639168		WDS J11249−1741B	* gam Crt B
RKS1125+2000	HIP 55772	TIC 3896430	Gaia DR2 3978447108436215296			HD 99303
RKS1126+0300B	HIP 55848	TIC 363549734	Gaia DR2 3812355294261019904		WDS J11268+0301B	* 83 Leo B
RKS1126+1517		TIC 67459023	Gaia DR2 3967223018862271104			BD+16 2260
RKS1127+0358A	HIP 55915	TIC 363570744	Gaia DR2 3812756203689026048			BD+04 2470
RKS1128+0731	HIP 55988	TIC 388799527	Gaia DR2 3910661735547769344		WDS J11285+0750A	Wolf 397
RKS1131+1422		TIC 219030952	Gaia DR2 3966121308211394944		WDS J11317+1422B	* 88 Leo B
RKS1134−1314	HIP 56489	TIC 157793169	Gaia DR2 3585205366015070080			BD−12 3458
RKS1135+2436A	HIP 56570	TIC 446161812	Gaia DR2 3993200561616132224			BD+25 2393
RKS1135+1658	HIP 56578	TIC 373674778	Gaia DR2 3973497278887030528			BD+17 2376
RKS1139−2741	HIP 56838	TIC 14718770	Gaia DR2 3484025454168955264		WDS J11391−2742A	CD−26 8683
RKS1141+0508A	HIP 57058	TIC 281906915	Gaia DR2 3897232781562753408	SBC9 3749		BD+05 2529
RKS1142+2301	HIP 57099	TIC 119584412	Gaia DR2 3980045523465047168		WDS J11423+2302A	LP 375−23
	HIP 57370	TIC 397024052	Gaia DR2 3799626935341796096			HD 102195
RKS1147−1149A	HIP 57494	TIC 144160090	Gaia DR2 3585636855608873984		WDS J11471−1149A	HD 102392A
RKS1152+1845	HIP 57866	TIC 272575844	Gaia DR2 3975078892003894144			HD 103072
RKS1154+2844	HIP 58099	TIC 138894223	Gaia DR2 4008018301867181952			BD+29 2228
RKS1157−2608	HIP 58293	TIC 403799988	Gaia DR2 3487784718782929920			HD 103836
RKS1157+1959	HIP 58314	TIC 202364222	Gaia DR2 3975266461816068864			V* GR Leo
RKS1157−2742	HIP 58345	TIC 403802333	Gaia DR2 3487062064765702272			HD 103932
RKS1158−2355	HIP 58374	TIC 428657118	Gaia DR2 3492633633781166336			HD 103949
RKS1158−2535		TIC 275380070	Gaia DR2 3487921092583151488			PM J11588−2535
RKS1159−2021	HIP 58451	TIC 428673146	Gaia DR2 3494677900774838144			HD 104067
RKS1204+0911	HIP 58863	TIC 397479763	Gaia DR2 3905850581902839168			HD 104828
RKS1204−0013	HIP 58908	TIC 96243247	Gaia DR2 3698712242020566528			BD+00 2888
	HIP 58949	TIC 96243602	Gaia DR2 3601738894159011328			HD 104988
RKS1205−1852	HIP 59000	TIC 398269300	Gaia DR2 3518916943846357376		WDS J12058−1853A	HD 105065
RKS1206−2336		TIC 398271125	Gaia DR2 3489706592092682752			HD 105110
RKS1208−0028	HIP 59198	TIC 56758194	Gaia DR2 3698723962986793344			Wolf 406
RKS1209−2646		TIC 402106696	Gaia DR2 3488113983859339264			PM J12093−2646

Table 4: Look up table for star names.

RKS	Hipparcos	TIC	Gaia DR2	SB9	WDS	Simbad
RKS1209−1151		TIC 152854209	Gaia DR2 3574377616021489152		WDS J12095−1151B	HD 105590B
RKS1210−1126		TIC 176866991	Gaia DR2 3580442934477012864			LP 734−35
RKS1215+0538A	HIP 59816	TIC 471012633	Gaia DR2 3894474755427985408		WDS J12160+0538A	BD+06 2573A
RKS1220−1953	HIP 60207	TIC 423529214	Gaia DR2 3515021992624319872			HD 107388
	HIP 60343	TIC 328961501	Gaia DR2 4008237753220479488			Wolf 409
RKS1222+0518	HIP 60352	TIC 377227655	Gaia DR2 3900151916215125760		WDS J12225+0518B	* 17 Vir B
RKS1222+2736	HIP 60357	TIC 328961071	Gaia DR2 4009907091045107584			BD+28 2110
RKS1223+2754	HIP 60448	TIC 97758239	Gaia DR2 4009947704255866752			Wolf 411
RKS1227+2701	HIP 60759	TIC 393800504	Gaia DR2 4008897567571892480		WDS J12272+2701A	HD 108421A
RKS1228−1654	HIP 60853	TIC 297025496	Gaia DR2 3520548825260557312			HD 108564
RKS1228−1817	HIP 60866	TIC 22481324	Gaia DR2 3517119173615245824			HD 108581
RKS1229−1631		TIC 297075867	Gaia DR2 3520585968137789184		WDS J12299−1631B	* del Crv B
RKS1230−1323	HIP 60994	TIC 952421350	Gaia DR2 3528362367203258624		WDS J12301−1324B	HD 108799B
RKS1231+2013	HIP 61099	TIC 446170645	Gaia DR2 3949377704625720192			HD 108984
RKS1233−1438	HIP 61329	TIC 1653125	Gaia DR2 3526876102361317760			HD 109333
RKS1241+1522	HIP 61901	TIC 460814512	Gaia DR2 3934198156329809152		WDS J12411+1523A	HD 110315
RKS1241+1951	HIP 61939	TIC 347334021	Gaia DR2 3948239125974974336	SBC9 2808		HD 110376
RKS1248−2448B	HIP 62471	TIC 9440488	Gaia DR2 3498481592531208576		WDS J12482−2448B	HD 111261B
RKS1248−2448A	HIP 62472	TIC 9440485	Gaia DR2 3498481519515679872		WDS J12482−2448A	HD 111261
RKS1248−1543A	HIP 62505	TIC 289989388	Gaia DR2 3523699441470095104		WDS J12485−1543A	HD 111312
RKS1250−0046	HIP 62687	TIC 53280272	Gaia DR2 3689602277083844480			HD 111631
RKS1253+0645	HIP 62942	TIC 390692143	Gaia DR2 3709422000670924416	SBC9 3684		HD 112099
RKS1256−2455	HIP 63157	TIC 228761127	Gaia DR2 3497587994520031872			CD−24 10619
RKS1257−1427	HIP 63257	TIC 2491738	Gaia DR2 3524996177995941632	SBC9 3626	WDS J12577−1428A	HD 112575
RKS1259−0950	HIP 63366	TIC 319462683	Gaia DR2 3626268998574790656	SBC9 3627	WDS J12590−0950AB	HD 112758
RKS1300−0242	HIP 63467	TIC 175740589	Gaia DR2 3685363487960149376			HD 112943
RKS1302−2647	HIP 63618	TIC 229047482	Gaia DR2 6187271616797377152			HD 113194
RKS1303−0509	HIP 63742	TIC 124612531	Gaia DR2 3677911582262521728	SBC9 3198	WDS J13038−0510AB	V* PX Vir
RKS1306+2043A	HIP 63942	TIC 347363984	Gaia DR2 3943232534138172672		WDS J13063+2044A	BD+21 2486A
RKS1310+0932	HIP 64262	TIC 390693415	Gaia DR2 3732674373792211584			BD+10 2518
RKS1312−0215	HIP 64457	TIC 292113181	Gaia DR2 3684934540986187776			HD 114783
RKS1316+1701	HIP 64797	TIC 373765355	Gaia DR2 3936909723803146368		WDS J13169+1701A	HD 115404

Table 4: Look up table for star names.

RKS	Hipparcos	TIC	Gaia DR2	SB9	WDS	Simbad
RKS1318−1446	HIP 64895	TIC 335636504	Gaia DR2 3607932305719355520			BD−14 3687
RKS1320+0407	HIP 65121	TIC 393649309	Gaia DR2 3715937504714734976			HD 116012
RKS1323+2914A	HIP 65343	TIC 459827389	Gaia DR2 1462061709995883136		WDS J13235+2914A	HD 116495A
RKS1323+2914B		TIC 1000733211	Gaia DR2 1462061709996744448		WDS J13235+2914B	HD 116495B
RKS1323+0243A	HIP 65352	TIC 393713800	Gaia DR2 3712538708114516736		WDS J13237+0243A	HD 116442
RKS1323+0243B	HIP 65355	TIC 393713801	Gaia DR2 3712538811193759744		WDS J13237+0243B	HD 116443
RKS1326−2417	HIP 65574	TIC 58465153	Gaia DR2 6193280031230266752		WDS J13267−2418B	HD 116858
RKS1327−2417	HIP 65602	TIC 58493240	Gaia DR2 6193279279612173952		WDS J13267−2418A	HD 116920
RKS1331−0219	HIP 65982	TIC 130712175	Gaia DR2 3637598641265071488	SBC9 2298	WDS J13317−0219AB	HD 117635
RKS1333+0835	HIP 66147	TIC 378993741	Gaia DR2 3719665841269118720			HD 117936
RKS1334−0018	HIP 66212	TIC 130725942	Gaia DR2 3662657851291871104		WDS J13343−0019A	HD 118036A
RKS1334+0440	HIP 66222	TIC 365159477	Gaia DR2 3714667225186824064			BD+05 2767
RKS1334−0820	HIP 66252	TIC 659763	Gaia DR2 3630092241022731136			HD 118100
RKS1335+0650	HIP 66283	TIC 379052876	Gaia DR2 3718408657097635712			HD 118206
RKS1335−0023		TIC 157838641	Gaia DR2 3662665715376647296			BD+00 3077
RKS1336+0746	HIP 66413	TIC 379078383	Gaia DR2 3718762218805509888			BD+08 2735
RKS1338−0614	HIP 66587	TIC 708973	Gaia DR2 3632451071421231360			BD−05 3740
RKS1340−0411	HIP 66675	TIC 175407829	Gaia DR2 3633926753464638592			HD 118926
RKS1341−0007	HIP 66840	TIC 61098813	Gaia DR2 3662358955927624960			HD 119217
RKS1342−0141	HIP 66886	TIC 61110114	Gaia DR2 3661492609484469504			HD 119291
RKS1345+1747	HIP 67090	TIC 72464819	Gaia DR2 1244644727396803584		WDS J13451+1747A	BD+18 2776
RKS1345−0437	HIP 67092	TIC 295680935	Gaia DR2 3633065148665344384			BD−03 3527
RKS1345+0850	HIP 67105	TIC 390730327	Gaia DR2 3725115471868587904			HD 119802
RKS1346−0027	HIP 67211	TIC 295698926	Gaia DR2 3662100605054881664			HD 119932
RKS1347+0618	HIP 67291	TIC 379137299	Gaia DR2 3721114933170707328			BD+07 2692
RKS1347+2127	HIP 67309	TIC 328936940	Gaia DR2 1250935029124246528		WDS J13477+2128A	BD+22 2632A
	HIP 67344	TIC 187309694	Gaia DR2 3613948386669881344			HD 120205
RKS1349+2658A	HIP 67422	TIC 359220741	Gaia DR2 1451450048399313664		WDS J13491+2659A	HD 120476A
RKS1349+2658B		TIC 359220744	Gaia DR2 1451450048399313792		WDS J13491+2659B	HD 120476B
RKS1349−2206	HIP 67487	TIC 437325588	Gaia DR2 6288325222245417856			HD 120467
RKS1353+2748	HIP 67773	TIC 258061897	Gaia DR2 1451877517904263680			HD 121131
RKS1353+1256A	HIP 67808	TIC 72578769	Gaia DR2 3728535399707693696		WDS J13535+1257AB	BD+13 2721

Table 4: Look up table for star names.

RKS	Hipparcos	TIC	Gaia DR2	SB9	WDS	Simbad
RKS1359+2252	HIP 68337	TIC 115110801	Gaia DR2 1250801855073489280			HD 122120
RKS1401+1529	HIP 68551	TIC 171769446	Gaia DR2 1231492609823304320		WDS J14019+1530B	GJ 536.1 B
RKS1411−1236	HIP 69357	TIC 308311310	Gaia DR2 6303961686341504512		WDS J14118−1237A	HD 124106
RKS1412+2348A	HIP 69410	TIC 307797957	Gaia DR2 1254106128033049472			V* GY Boo
RKS1413−0657	HIP 69485	TIC 5979133	Gaia DR2 3640244581637740416			BD−06 3950
RKS1414−1521	HIP 69562	TIC 157414031	Gaia DR2 6298167775459045632		WDS J14144−1521A	HD 124498A
RKS1416+2007	HIP 69751	TIC 135171752	Gaia DR2 1252050659765215616		WDS J14165+2007B	HD 125040B
RKS1418−0636A	HIP 69962	TIC 6095985	Gaia DR2 3639984066101401344	SBC9 3628	WDS J14190−0636A	HD 125354
RKS1419−2548		TIC 1056634922	Gaia DR2 6270906415441315840		WDS J14190−2549B	HD 125276B
RKS1419−0509	HIP 70016	TIC 203230367	Gaia DR2 3642413746280598784		WDS J14196−0509A	HD 125455
RKS1421+2937	HIP 70218	TIC 156641715	Gaia DR2 1284721994948665216			BD+30 2512
RKS1424−1727A	HIP 70472	TIC 335165756	Gaia DR2 6284731365410978048			LP 800−56
	HIP 70529	TIC 298434280	Gaia DR2 1254695603704323712		WDS J14257+2338A	BD+24 2733
RKS1430−0838	HIP 70956	TIC 23741668	Gaia DR2 6328672145023976960		WDS J14308−0839A	HD 127339
RKS1432+1121	HIP 71086	TIC 349606109	Gaia DR2 1178874377069433472			BD+11 2687
RKS1433+0920	HIP 71190	TIC 457920223	Gaia DR2 1176167143218779776		WDS J14336+0920A	HD 127871
RKS1436+0944	HIP 71395	TIC 349606708	Gaia DR2 1176209886733406592		WDS J14360+0945A	HD 128311
RKS1437−2548	HIP 71481	TIC 16855	Gaia DR2 6223838830917236224			HD 128356
RKS1442+1930	HIP 71904	TIC 287081520	Gaia DR2 1237696157506521600		WDS J14426+1929C	BD+20 3009
	HIP 71914	TIC 287081516			WDS J14426+1929AB	BD+20 3010
RKS1444+2211	HIP 72044	TIC 345292151	Gaia DR2 1241547437501423872			BD+22 2742
RKS1444−2215		TIC 309153368	Gaia DR2 6278792868749734912		WDS J14446−2215A	HD 129715
RKS1445+1350	HIP 72146	TIC 450354414	Gaia DR2 1185619988280226944			HD 130004
RKS1446+2730	HIP 72200	TIC 219834010	Gaia DR2 1279838754572750208			V* HO Boo
RKS1446+1629	HIP 72237	TIC 416612744	Gaia DR2 1234693112077610880			BD+17 2785
RKS1447+0242	HIP 72312	TIC 368804760	Gaia DR2 3655492127855307136			HD 130307
RKS1450+0648	HIP 72577	TIC 349670920	Gaia DR2 1159605302648975104			HD 130871
RKS1451+0943		TIC 349674634	Gaia DR2 1174143182830505856		WDS J14510+0943B	HD 131023B
RKS1451+1906		TIC 1101124559	Gaia DR2 1237090738916392832		WDS J14514+1906B	* ksi Boo B
RKS1451−2418	HIP 72688	TIC 129383	Gaia DR2 6229442835525861120			HD 130992
RKS1453+1909	HIP 72848	TIC 267365256	Gaia DR2 1236929488664453376	SBC9 820		V* DE Boo
RKS1453+2320	HIP 72875	TIC 311182515	Gaia DR2 1265702917689682944		WDS J14537+2321A	HD 131582

Table 4: Look up table for star names.

RKS	Hipparcos	TIC	Gaia DR2	SB9	WDS	Simbad
RKS1455−2707	HIP 73066	TIC 167121	Gaia DR2 6225341450996268288			HD 131719
RKS1457−2124	HIP 73184	TIC 287157634	Gaia DR2 6232511606838403968		WDS J14575−2125A	HD 131977
RKS1458+0445	HIP 73258	TIC 457927575	Gaia DR2 1158184012071254400			BD+05 2950
RKS1500−2905		TIC 440890647	Gaia DR2 6224087389269263488			TYC 6760−1510−1
RKS1500−2427	HIP 73427	TIC 440887364	Gaia DR2 6230733559097425152			CD−23 12010
RKS1500−1108	HIP 73457	TIC 192679501	Gaia DR2 6313600142709958144			HD 132683
RKS1501+1341		TIC 119738025	Gaia DR2 1182094198087372672			StKM 1−1198
RKS1501+1552	HIP 73512	TIC 119739470	Gaia DR2 1186939608392079104			HD 132950
RKS1504+0538	HIP 73786	TIC 460381297	Gaia DR2 1156846524895814144			BD+06 2986
RKS1504−1835A	HIP 73787	TIC 220232459	Gaia DR2 6257172793656011520			HD 133412
RKS1507+2456		TIC 229902009	Gaia DR2 1264654395913772416			BD+25 2874
RKS1509+2400A	HIP 74148	TIC 229904700	Gaia DR2 1263776848195725568			BD+24 2824
RKS1510−1627	HIP 74234	TIC 432234964	Gaia DR2 6307365499463905536		WDS J15103−1616C	HD 134440
RKS1510−1622	HIP 74235	TIC 432235014	Gaia DR2 6307374845312759552		WDS J15103−1616A	HD 134439
RKS1513−0347	HIP 74555	TIC 38840951	Gaia DR2 6336170195850218240			BD−03 3746
RKS1515+0735	HIP 74682	TIC 281101100	Gaia DR2 1163549697534289664			BD+08 3000
RKS1515+0047	HIP 74702	TIC 461272840	Gaia DR2 4419140645978987904		WDS J15160+0048A	HD 135599
RKS1517−2759	HIP 74815	TIC 48536669	Gaia DR2 6213898936567006464			CD−27 10303
RKS1518−1837	HIP 74926	TIC 438893825	Gaia DR2 6256550916751400320			BD−18 4031
RKS1519+0146		TIC 461308071	Gaia DR2 4421455530273467904		WDS J15193+0146B	* 5 Ser B
RKS1519+2912	HIP 74981	TIC 357501308	Gaia DR2 1272123859439770368			BD+29 2654
RKS1519+1155		TIC 445847318	Gaia DR2 1169984108299812608			BD+12 2823
RKS1520+1522A	HIP 75090	TIC 445851097	Gaia DR2 1207257552481630720		WDS J15206+1523AB	BD+15 2847
RKS1522−0446	HIP 75201	TIC 180325572	Gaia DR2 6335064087152916224			BD−04 3873
RKS1522−1039	HIP 75253	TIC 36981205	Gaia DR2 6316161317607999232			HD 136713
RKS1522+0125	HIP 75266	TIC 461330181	Gaia DR2 4420712604009198080			HD 136834
RKS1525−2642	HIP 75542	TIC 388734737	Gaia DR2 6213789290343029760			HD 137303
RKS1527+1035	HIP 75672	TIC 392982986	Gaia DR2 1165859359148269568			BD+11 2811
RKS1527+0235	HIP 75686	TIC 371228841	Gaia DR2 4421274729329022336			BD+03 3032
RKS1528−0920A	HIP 75718	TIC 37149737	Gaia DR2 6317854874752594048	SBC9 1638	WDS J15282−0921Aa,Ab	HD 137763
RKS1528−0921B	HIP 75722	TIC 37149743	Gaia DR2 6317854118838346752		WDS J15282−0921B	HD 137778
RKS1531−2916		TIC 185850907	Gaia DR2 6209995700348976896			LP 915−41

Table 4: Look up table for star names.

RKS	Hipparcos	TIC	Gaia DR2	SB9	WDS	Simbad
RKS1531+1041		TIC 393052039	Gaia DR2 1166203712446038912			StKM 1−1250
RKS1540−1802	HIP 76779	TIC 12399528	Gaia DR2 6260386975385254656			HD 139763
	HIP 77408	TIC 272595871	Gaia DR2 4422809716282811776		WDS J15482+0134A	HD 141272
RKS1552+1052A	HIP 77725	TIC 446193444	Gaia DR2 4456127942261895808	SBC9 1521	WDS J15521+1052AB	BD+11 2874
RKS1554−2600	HIP 77908	TIC 24190130	Gaia DR2 6235558525363302912			HD 142288
RKS1555+1602	HIP 77963	TIC 172653241	Gaia DR2 1193336189087814144	SBC9 3688		V* V383 Ser
	HIP 78241	TIC 258177087	Gaia DR2 1316590033811497088			HD 143291
RKS1559−0504	HIP 78336	TIC 168454208	Gaia DR2 4398623381051080064			HD 143295
RKS1600−0147A	HIP 78395	TIC 168457265	Gaia DR2 4406159365028059264			BD−01 3125
RKS1601−2625		TIC 66930631	Gaia DR2 6043237998751210880			PM J16016−2625
RKS1604−1126	HIP 78739	TIC 49777150	Gaia DR2 4343064508746082304		WDS J16044−1127B	HD 144088
RKS1605−2027	HIP 78843	TIC 48668374	Gaia DR2 6244076338858859776	SBC9 3630		HD 144253
RKS1607−0542	HIP 78999	TIC 193344911	Gaia DR2 4350344993707489920			G 153−25
RKS1608+1713		TIC 172752010	Gaia DR2 1199657143995826688			BD+17 2966
RKS1608−1308	HIP 79066	TIC 411083824	Gaia DR2 4341712281239980032		WDS J16084−1308A	HD 144840
RKS1613+1331B	HIP 79492	TIC 119985831	Gaia DR2 4464207428577214464		WDS J16133+1332B	* 49 Ser B
RKS1613+1331A	HIP 79492	TIC 119985828	Gaia DR2 4464207428579939840		WDS J16133+1332Aa,Ab	* 49 Ser A
RKS1615+0721A	HIP 79702	TIC 318628394	Gaia DR2 4450372376847499648		WDS J16160+0721A	HD 146413A
RKS1615+0721B	HIP 79702	TIC 1204484499	Gaia DR2 4450372376847499904		WDS J16160+0721B	HD 146413B
RKS1620−0416	HIP 80053	TIC 362576875	Gaia DR2 4356712162461401728		WDS J16204−0416A	MCC 760
RKS1621+1713		TIC 149689521	Gaia DR2 4466840342314357632			G 138−22
RKS1624−1338	HIP 80366	TIC 413623346	Gaia DR2 4329057039841257728		WDS J16243−1338A	V* V2578 Oph
RKS1625−2156	HIP 80440	TIC 203621441	Gaia DR2 6051948158061617024			BD−21 4352
RKS1626+1539	HIP 80539	TIC 149796418	Gaia DR2 4465681461355625984			G 138−28
RKS1627+0055	HIP 80597	TIC 5898974	Gaia DR2 4431838321653479296			BD+01 3236
RKS1627+0718	HIP 80644	TIC 318946785	Gaia DR2 4439625337884136064			HD 148467
RKS1628+1824A	HIP 80725	TIC 345662514	Gaia DR2 4467355154275146112		WDS J16289+1825A	HD 148653A
RKS1628+1824B		TIC 1205012280	Gaia DR2 4467355158571184256		WDS J16289+1825B	HD 148653B
RKS1629+2346	HIP 80751	TIC 356083397	Gaia DR2 1299173975785921536	SBC9 3764		BD+24 3014
RKS1630−0359		TIC 72368312	Gaia DR2 4357347405304553984		WDS J16307−0359A	BD−03 3952
RKS1631−0718		TIC 40673869	Gaia DR2 4351396023741669376			TYC 5060−53−1
RKS1632−1235	HIP 81030	TIC 414070454	Gaia DR2 4331055642742694400			BD−12 4542

Table 4: Look up table for star names.

RKS	Hipparcos	TIC	Gaia DR2	SB9	WDS	Simbad
RKS1633−0933	HIP 81084	TIC 40849632	Gaia DR2 4338433743723131648			LP 745−70
RKS1636−0219	HIP 81300	TIC 58092025	Gaia DR2 4358031335897026304		WDS J16364−0219A	* 12 Oph
RKS1638−0501	HIP 81465	TIC 58184907	Gaia DR2 4354023199399638912			BD−04 4138
RKS1646+0531		TIC 315475193	Gaia DR2 4434889672579861504			PM J16468+0531N
RKS1647−0111	HIP 82169	TIC 157462432	Gaia DR2 4379562449331604352			BD−00 3182
RKS1649−2426	HIP 82370	TIC 191344490	Gaia DR2 6046895455473782144			HD 151692
RKS1650+1854	HIP 82389	TIC 150553840	Gaia DR2 4559848344443069952			HD 151995
RKS1654+1154	HIP 82694	TIC 284472488	Gaia DR2 4448223656247483904			Ross 644
RKS1659−2616	HIP 83147	TIC 18364458	Gaia DR2 4112138303515401216			CD−26 11751
RKS1701+2256	HIP 83343	TIC 349490623	Gaia DR2 4571446199250804352			BD+23 3035
RKS1705−0503	HIP 83591	TIC 142456308	Gaia DR2 4364527594192166400		WDS J17050−0504A	HD 154363
RKS1705−0147		TIC 142452434	Gaia DR2 4379812214567457408			HD 154361
RKS1706−0610	HIP 83676	TIC 145389271	Gaia DR2 4364159876271314176			HD 154518
RKS1712+1821	HIP 84195	TIC 351654581	Gaia DR2 4548462729742343296			HD 155712
RKS1714−0824A	HIP 84303	TIC 1843105	Gaia DR2 4359814876901570688		WDS J17141−0824A	HD 155802A
RKS1714−0824B		TIC 1305321077	Gaia DR2 4359814881197436800		WDS J17141−0824B	HD 155802B
RKS1715−2636A	HIP 84405	TIC 79454735	Gaia DR2 4109030160308320128		WDS J17153−2636A	* 36 Oph A
RKS1715−2636B	HIP 84405	TIC 1277142190	Gaia DR2 4109030160308317312		WDS J17153−2636B	* 36 Oph B
RKS1716−2632	HIP 84478	TIC 79841001	Gaia DR2 4109034455276324608		WDS J17153−2636C	V* V2215 Oph
RKS1716−1210	HIP 84487	TIC 435045600	Gaia DR2 4141979774942939264			BD−12 4699
RKS1717+2913	HIP 84607	TIC 257715493	Gaia DR2 4575374857376398976			HD 156668
	HIP 84652	TIC 58971112	Gaia DR2 4367318326501438976			MCC 791
RKS1721−2106	HIP 84893	TIC 1455907039	Gaia DR2 4115142276696646272		WDS J17210−2107B	* ksi Oph B
RKS1722−1457	HIP 85026	TIC 429927313	Gaia DR2 4137734865485308800			BD−14 4622
RKS1725+0206	HIP 85295	TIC 327860248	Gaia DR2 4375233191015944192		WDS J17258+0207A	HD 157881
RKS1729−2350	HIP 85561	TIC 165347984	Gaia DR2 4111366313257506560			HD 158233
	HIP 85582	TIC 310989180			WDS J17293+2924AB	BD+29 3029
RKS1733+0914		TIC 302838403	Gaia DR2 4490721567368465408			RX J1733.1+0914
RKS1737+2753A	HIP 86221	TIC 311407473	Gaia DR2 4595441868000475520		WDS J17372+2754C	BD+27 2853C
RKS1737−1314		TIC 416415862	Gaia DR2 4161560427799517184			HD 159911
RKS1737+2257B	HIP 86282	TIC 349533787	Gaia DR2 4557198933740208128		WDS J17378+2257B	BD+23 3151B
RKS1737+2257A	HIP 86282	TIC 349533785	Gaia DR2 4557198933740208768		WDS J17378+2257A	BD+23 3151A

Table 4: Look up table for star names.

RKS	Hipparcos	TIC	Gaia DR2	SB9	WDS	Simbad
RKS1739+0333	HIP 86400	TIC 349491678	Gaia DR2 4377160604838377600	SBC9 1802	WDS J17393+0333A	HD 160346
	HIP 86722	TIC 363766517	Gaia DR2 4556066746008265344	SBC9 1502	WDS J17433+2137A	HD 161198
RKS1750−0603	HIP 87322	TIC 6737561	Gaia DR2 4175058204312299904			HD 162283
RKS1752−0733	HIP 87464	TIC 7095233	Gaia DR2 4171749945627705856			HD 162598
RKS1753+2119	HIP 87579	TIC 275063206	Gaia DR2 4576863905365412736			BD+21 3245
RKS1754−2649		TIC 133745276	Gaia DR2 4063811988637931904			HD 314741
RKS1755+0345	HIP 87745	TIC 325225116	Gaia DR2 4469644028247872640			BD+03 3531a
RKS1755+1830	HIP 87768	TIC 275218863	Gaia DR2 4503423641091793152		WDS J17557+1830A	BD+18 3497
RKS1757−2143A	HIP 87925	TIC 105977121	Gaia DR2 4070388266455534720		WDS J17577−2143AB	HD 163573
RKS1803+2545		TIC 320586991	Gaia DR2 4582593421793499264			Ross 820
RKS1804+0149	HIP 88481	TIC 51799658	Gaia DR2 4468231641147900928			HD 165045
RKS1805−2929A		TIC 407888149	Gaia DR2 4050315620888089472		WDS J18054−2930A	HD 317101A
RKS1805+0229	HIP 88601	TIC 398120047	Gaia DR2 4468557611977674496	SBC9 1022	WDS J18055+0230B	* 70 Oph B
RKS1807−1641		TIC 363936374	Gaia DR2 4144140276634051200			TYC 6251−414−1
RKS1809−0019	HIP 88961	TIC 250641485	Gaia DR2 4275193889350151680			HD 166184
RKS1809−1202	HIP 88962	TIC 365259442	Gaia DR2 4150826170635895424			BD−12 4935
RKS1815+1829	HIP 89449	TIC 158084063	Gaia DR2 4526375465285830656			HD 348282
RKS1816+1354	HIP 89517	TIC 406883293	Gaia DR2 4497494077967197568			BD+13 3578
RKS1817+2640	HIP 89656	TIC 258399084	Gaia DR2 4585850282613829504		WDS J18178+2640A	HD 335828
RKS1818−0642	HIP 89728	TIC 15489536	Gaia DR2 4160661607077241472			HD 168159
RKS1819−0156	HIP 89825	TIC 167913198	Gaia DR2 4270814637616488064			HD 168442
RKS1822+0142	HIP 90035	TIC 168901705	Gaia DR2 4276624250897321984			BD+01 3657
RKS1826+0422		TIC 415069167	Gaia DR2 4284152847546316288			TYC 441−814−1
RKS1829−2758	HIP 90611	TIC 324370520	Gaia DR2 4051606378878066816			HD 170209
RKS1829+0903A	HIP 90626	TIC 320508747	Gaia DR2 4480017821686413568			HD 170510
RKS1829−0149	HIP 90656	TIC 133556737	Gaia DR2 4270446404294208000			HD 170493
RKS1831−1854	HIP 90790	TIC 186271747	Gaia DR2 4093301474693288960		WDS J18313−1855A	HD 170657
RKS1832−0347		TIC 43385122	Gaia DR2 4257911555122839040			TYC 5120−119−1
RKS1833+2218	HIP 90959	TIC 258666933	Gaia DR2 4535144998232287232		WDS J18333+2219A	HD 171314
RKS1833−1626		TIC 433101580	Gaia DR2 4102812108451116672			HD 171075
RKS1833−1138	HIP 90979	TIC 217831699	Gaia DR2 4154598526336121600			BD−11 4672
RKS1834+0355		TIC 106017392	Gaia DR2 4283361027353595520			TYC 454−792−1

Table 4: Look up table for star names.

RKS	Hipparcos	TIC	Gaia DR2	SB9	WDS	Simbad
RKS1847−0338	HIP 92200	TIC 226107999	Gaia DR2 4258375617747092864		WDS J18475−0338A	HD 173818
RKS1847+1226		TIC 330191766	Gaia DR2 4504577990890909184			HD 229513
RKS1848−1008A	HIP 92250	TIC 146501718	Gaia DR2 4203266415718729856		WDS J18480−1009AB	HD 173872
RKS1848+1044	HIP 92283	TIC 93137389	Gaia DR2 4503794795019024000		WDS J18485+1045A	HD 174080
RKS1848+1726	HIP 92311	TIC 224431102	Gaia DR2 4511416609607124352			HD 229590
RKS1850−2655	HIP 92444	TIC 89684637	Gaia DR2 4072260704719970944			CD−27 13268
RKS1854+2844		TIC 290001300	Gaia DR2 2040475607275354880			PM J18547+2844
RKS1854+0051		TIC 227096293	Gaia DR2 4266702906501990016			BD+00 4050
RKS1854+1058		TIC 101292533	Gaia DR2 4311983376654646656		WDS J18550+1058A	HD 230017A
RKS1855+2333A	HIP 92919	TIC 350166984	Gaia DR2 4533301804432654976	SBC9 1105	WDS J18559+2333AB	HD 175742
RKS1857+0734		TIC 104987051	Gaia DR2 4309961232989305600			LP 571−80
RKS1857−1902	HIP 93072	TIC 1731874032	Gaia DR2 4086490824728216704		WDS J18575−1903A	LP 811−17 A
RKS1858−1014		TIC 36312951	Gaia DR2 4202329249475791104			BD−10 4886
RKS1858−0030	HIP 93195	TIC 330078921	Gaia DR2 4265754822578472576			HD 176157
RKS1859+0759	HIP 93248	TIC 222495959	Gaia DR2 4310095515150736512			BD+07 3922
RKS1859+1107		TIC 222445478	Gaia DR2 4311893972619003648			HD 230325
RKS1901+0328		TIC 228484455	Gaia DR2 4268847611328000256			TYC 466−2991−1
RKS1903−1102	HIP 93540	TIC 39554091	Gaia DR2 4199396753205879040			HD 176986
	HIP 93731	TIC 451627388	Gaia DR2 4521349425846548352			HD 177745
RKS1905+1351		TIC 1797287007	Gaia DR2 4314399312966563968		WDS J19054+1352B	* zet Aql B
RKS1907+0736	HIP 93871	TIC 197623112	Gaia DR2 4307162018124573312			HD 178126
RKS1908+1627		TIC 394650204	Gaia DR2 4513137345335832704			HD 230742
RKS1908−1640		TIC 319025953	Gaia DR2 4088716373694306048			PM J19081−1640
RKS1910+2145		TIC 9867665	Gaia DR2 4520233627713766528			TYC 1598−1505−1
RKS1911+0500		TIC 181547479	Gaia DR2 4293406921521638912			PM J19117+0500
RKS1914+0209A	HIP 94590	TIC 174696280	Gaia DR2 4267889936728497920		WDS J19149+0209A	BD+01 3942A
RKS1914+0209B	HIP 94590	TIC 174696260	Gaia DR2 4267889936728496768		WDS J19149+0209B	BD+01 3942B
RKS1915+2453A	HIP 94622	TIC 403613403	Gaia DR2 2023507806418374016		WDS J19153+2454AB	HD 338030
RKS1915+1133	HIP 94650	TIC 210208396	Gaia DR2 4312905248400130688			V* V1688 Aql
RKS1923−0635A	HIP 95299	TIC 98792665	Gaia DR2 4207995002838460800		WDS J19233−0635A	HD 182085
RKS1924+2525		TIC 109964873	Gaia DR2 2023209048496665728		WDS J19244+2526A	PM J19244+2525
RKS1924−2203	HIP 95417	TIC 118882363	Gaia DR2 6772521384023709696			CD−22 13916

Table 4: Look up table for star names.

RKS	Hipparcos	TIC	Gaia DR2	SB9	WDS	Simbad
RKS1924+0832	HIP 95429	TIC 132696054	Gaia DR2 4308259846169194112		WDS J19247+0833AB	Ross 748
RKS1928+1232A	HIP 95730	TIC 70073343	Gaia DR2 4316214125587568896		WDS J19283+1232A	HD 231512A
RKS1928+1232B	HIP 95730	TIC 1914933968	Gaia DR2 4316214125609944832		WDS J19283+1232B	HD 231512B
RKS1928+2854		TIC 111784356	Gaia DR2 2026408043220034176			PM J19284+2854
RKS1929+0709		TIC 134621509	Gaia DR2 4295497883422229888			BD+06 4156
RKS1930+2140	HIP 95890	TIC 370406321	Gaia DR2 2018148889833134080			HD 344502
RKS1932−1116	HIP 96085	TIC 100711809	Gaia DR2 4187837450005193088		WDS J19321−1116A	HD 183870
RKS1932+0034	HIP 96121	TIC 113873448	Gaia DR2 4287473578816247936			BD+00 4241
RKS1934+0434	HIP 96285	TIC 213459719	Gaia DR2 4291123545113039616			HD 184489
RKS1936−1026B	HIP 96471	TIC 242707502	Gaia DR2 4194013711756457344		WDS J19368−1027B	HD 184860B
RKS1936−1026A	HIP 96471	TIC 242707498	Gaia DR2 4193990248350991104		WDS J19368−1027A	HD 184860A
RKS1943+1005	HIP 97051	TIC 388521607	Gaia DR2 4302670684951953280			HD 355784
RKS1952−2356	HIP 97805	TIC 241940434	Gaia DR2 6863591389529611264			HD 187760
RKS1954−2356	HIP 97944	TIC 241967968	Gaia DR2 6863535898551993472	SBC9 1182	WDS J19543−2356A	HD 188088
RKS1954+2013		TIC 263105734	Gaia DR2 1826261983123386240			PM J19546+2013
	HIP 98192	TIC 281827534	Gaia DR2 2030317253745186432			HD 189087
	HIP 98204	TIC 48769732	Gaia DR2 4188997606565774976		WDS J19573−1234A	HD 188807
RKS1957+1313		TIC 387213113	Gaia DR2 4305065077668010112			HD 356314
RKS2000+2242	HIP 98505	TIC 256364928	Gaia DR2 1827242816201846144		WDS J20007+2243A	HD 189733
RKS2002+0319	HIP 98698	TIC 345217789	Gaia DR2 4247023886053586304			HD 190007
RKS2003+2005	HIP 120148	TIC 424256352	Gaia DR2 1823476232957094400			HD 351151
RKS2003+2320	HIP 98792	TIC 287947139	Gaia DR2 1833199729671740800			HD 190404
RKS2004+2547	HIP 98828	TIC 244330163	Gaia DR2 1834788970646666112			HD 190470
RKS2008+0640	HIP 99205	TIC 366286774	Gaia DR2 4250371241820042368			BD+06 4450
RKS2009+1648A	HIP 99316	TIC 86876073	Gaia DR2 1809456806859123584		WDS J20096+1648A	HD 191499A
RKS2009+1648B	HIP 99316	TIC 86876075	Gaia DR2 1809456596391861248		WDS J20096+1648B	HD 191499B
RKS2009−1417	HIP 99322	TIC 14075378	Gaia DR2 6877985989601383808			HD 191285
RKS2009−0307	HIP 99332	TIC 243807838	Gaia DR2 4223280413481383168			BD−03 4797
RKS2010−2029A	HIP 99385	TIC 75231315	Gaia DR2 6866310172545095424		WDS J20103−2030A	HD 191391
RKS2011+1611	HIP 99452	TIC 87216634	Gaia DR2 1809360187271699584		WDS J20111+1611A	HD 191785
RKS2012−1253	HIP 99550	TIC 14244561	Gaia DR2 6879662263797806976			LP 754−50
RKS2013−0052	HIP 99711	TIC 243962745	Gaia DR2 4224259562941398400		WDS J20140−0052A	HD 192263

Table 4: Look up table for star names.

RKS	Hipparcos	TIC	Gaia DR2	SB9	WDS	Simbad
RKS2014−0716	HIP 99764	TIC 71391602	Gaia DR2 4216680418835844864			BD−07 5223
RKS2015−2701	HIP 99825	TIC 326096771	Gaia DR2 6847167606385195648			HD 192310
RKS2016−0204	HIP 99916	TIC 244041508	Gaia DR2 4223848757911010816			G 24−12
	HIP 100133	TIC 244125428	Gaia DR2 4230094705509739904			LP 634−24
RKS2030+2650	HIP 101150	TIC 436446360	Gaia DR2 1856712201709083136		WDS J20302+2651AB	HD 340345
RKS2035+0607	HIP 101579	TIC 375008312	Gaia DR2 1747786539668366848		WDS J20352+0608A	HD 196124
RKS2038+2346		TIC 243481409	Gaia DR2 1819353476647202944			HD 347103
RKS2039+1004	HIP 101932	TIC 282254061	Gaia DR2 1754191229260708736		WDS J20391+1005C	HD 196794
RKS2041−0529	HIP 102115	TIC 248174259	Gaia DR2 6914228607268279936			BD−06 5559
RKS2041−2219	HIP 102119	TIC 326186977	Gaia DR2 6855358349537379840			HD 196998
RKS2042−2116		TIC 271686772	Gaia DR2 6855562789978158080		WDS J20421−2117AB	HD 197092
RKS2042+2050	HIP 102226	TIC 331366716	Gaia DR2 1817769836303393280			HD 197396
RKS2044−2121	HIP 102332	TIC 76834292	Gaia DR2 6855520385765481088			BD−21 5811
	HIP 102357	TIC 331684556	Gaia DR2 1814070838668707840		WDS J20444+1945AB	HD 352860
RKS2046−2144	HIP 102486	TIC 422364489	Gaia DR2 6855301415450400896		WDS J20462−2145A	HD 197711
RKS2046−2304	HIP 102495	TIC 422363545	Gaia DR2 6807019282894453504			CD−23 16484
RKS2047+1051	HIP 102582	TIC 383384592	Gaia DR2 1751680734976457728			BD+10 4379
RKS2050+2923A	HIP 102851	TIC 282843610	Gaia DR2 1858219151114884352			HD 198550
RKS2053−0245	HIP 103150	TIC 248740527	Gaia DR2 6916526960232473216			BD−03 5059
RKS2055+1310	HIP 103256	TIC 345194297	Gaia DR2 1758463038092175232	SBC9 3633		BD+12 4499
RKS2059+0333	HIP 103577	TIC 396547837	Gaia DR2 1731401510016752000			Wolf 901
RKS2059−1042	HIP 103581	TIC 205788518	Gaia DR2 6890278254718505088			HD 199704
RKS2105+0704A	HIP 104092	TIC 283552865	Gaia DR2 1736838805468812160		WDS J21053+0704A	HD 200779
RKS2105−1654		TIC 214553715	Gaia DR2 6882485633558785920			HD 358850
RKS2107−1355A	HIP 104239	TIC 214563192	Gaia DR2 6885342959337741184		WDS J21072−1355A	HD 200968A
RKS2107−1355B		TIC 214563193	Gaia DR2 6885342955043185664		WDS J21072−1355B	HD 200968B
RKS2107+2945	HIP 104304	TIC 126883980	Gaia DR2 1852271205513439360		WDS J21078+2945A	BD+29 4321A
RKS2108+2510	HIP 104329	TIC 126937902	Gaia DR2 1841125559219604608			BD+24 4329
RKS2108−0425A	HIP 104383	TIC 364174334	Gaia DR2 6912161147450851840		WDS J21088−0426Aa,Ab	BD−05 5480
RKS2116+0923	HIP 105038	TIC 388996956	Gaia DR2 1743592452563243136		WDS J21165+0924A	HD 202575
RKS2118+0009	HIP 105152	TIC 376363393	Gaia DR2 2689454850844597504		WDS J21180+0010A	HD 202751
RKS2119−2621	HIP 105312	TIC 326395505	Gaia DR2 6791154257817212672	SBC9 1292	WDS J21198−2621AB	HD 202940

Table 4: Look up table for star names.

RKS	Hipparcos	TIC	Gaia DR2	SB9	WDS	Simbad
RKS2120−1951	HIP 105341	TIC 439391442	Gaia DR2 6832674634380238848			HD 203040
RKS2122+1052	HIP 105533	TIC 288422718	Gaia DR2 1745568309317609088			BD+10 4534
RKS2122−0044		TIC 2024830728	Gaia DR2 2686286474944561664			Gaia DR2 2686286474944561664
RKS2125+2712	HIP 105791	TIC 14981454	Gaia DR2 1847354223872439040			HD 204079
RKS2126+0344	HIP 105885	TIC 352621507	Gaia DR2 2692798534424338304			MCC 70
RKS2130−1230	HIP 106147	TIC 242020806	Gaia DR2 6891134705556330880			HD 204587
RKS2131+2320	HIP 106231	TIC 283436283	Gaia DR2 1797276382668029440		WDS J21310+2320A	BD+22 4409
RKS2132−2057	HIP 106353	TIC 99837626	Gaia DR2 6830027182179257472		WDS J21324−2058A	HD 204941
RKS2141+1115	HIP 107062	TIC 305507923	Gaia DR2 1766575647197540480			HD 206315
RKS2149+0543		TIC 270059638	Gaia DR2 2700084315081609344		WDS J21492+0543A	HD 207491
RKS2149−1140	HIP 107758	TIC 333492292	Gaia DR2 6844229329061159040			BD−12 6102
RKS2152+0154	HIP 107941	TIC 388931495	Gaia DR2 2693778993853634304			HD 207874
RKS2153+2055	HIP 108028	TIC 258038021	Gaia DR2 1781003885454165888			HD 208038
RKS2153+2850		TIC 283226254	Gaia DR2 1896408724688348928			StKM 1−1953
RKS2153−1249		TIC 206238582	Gaia DR2 6840822904599511936		WDS J21530−1249A	LP 758−74
RKS2155−2942	HIP 108241	TIC 53952985	Gaia DR2 6617495364101129728			HD 208272
RKS2210+2247	HIP 109461	TIC 258781508	Gaia DR2 1783006542804679040			BD+22 4567
RKS2214+0242A	HIP 109807	TIC 415709901	Gaia DR2 2682914199767628032			BD+01 4594
RKS2214+2751	HIP 109812	TIC 27964220	Gaia DR2 1892539307048908928		WDS J22145+2751A	G 188−49
RKS2224+2233	HIP 110640	TIC 314989124	Gaia DR2 1875076004382831616		WDS J22248+2233A	BD+21 4747A
RKS2226−1911	HIP 110750	TIC 69747593	Gaia DR2 6821533111257080960			HD 212658
	HIP 110980	TIC 271997555	Gaia DR2 2702655587447223168			LP 640−74
RKS2239+0406	HIP 111888	TIC 422438669	Gaia DR2 2704912403783213696			HD 214683
RKS2240−2940	HIP 111960	TIC 47295522	Gaia DR2 6608490501308343168			HD 214749
RKS2241+1849A	HIP 112040	TIC 467549713	Gaia DR2 2833244072377840640			BD+18 5029
RKS2243−0624	HIP 112190	TIC 251042502	Gaia DR2 2623505219992303104			HD 215152
RKS2247+1823	HIP 112496	TIC 434202601	Gaia DR2 2833330968155957888			BD+17 4808
RKS2248+2443	HIP 112610	TIC 44087301	Gaia DR2 1876551957008238208			MCC 209
RKS2251+1358	HIP 112870	TIC 60781630	Gaia DR2 2720132500864789760		WDS J22514+1358A	HD 216259
RKS2252+2324	HIP 112918	TIC 435838531	Gaia DR2 2837037662371901184			BD+22 4725
RKS2254+2331	HIP 113124	TIC 435847271	Gaia DR2 2836968977254848384			G 67−33
RKS2257+2800	HIP 113333	TIC 436738385	Gaia DR2 1883575229265906560		WDS J22571+2800A	BD+27 4445

Table 4: Look up table for star names.

RKS	Hipparcos	TIC	Gaia DR2	SB9	WDS	Simbad
RKS2258−1338	HIP 113409	TIC 111184885	Gaia DR2 2411086582892886784			HD 217065
RKS2259−1122	HIP 113552	TIC 33424022	Gaia DR2 2604115877897249408			BD−12 6393
RKS2300−2231	HIP 113576	TIC 419012256	Gaia DR2 2396530698208685312			HD 217357
RKS2300−2618B	HIP 113597	TIC 2051974201	Gaia DR2 2382705816958084352		WDS J23005−2619B	HD 217379B
RKS2300−2618A	HIP 113597	TIC 270377903	Gaia DR2 2382705816958084224	SBC9 3524	WDS J23005−2619A	HD 217379A
RKS2301−0350	HIP 113718	TIC 278870306	Gaia DR2 2636589099125426816	SBC9 1492		HD 217580
RKS2307−2309	HIP 114156	TIC 204325307	Gaia DR2 2384342302577019264		WDS J23071−2310A	HD 218294
RKS2308+0633	HIP 114294	TIC 402891878	Gaia DR2 2665087581524066176			[R78b] 355
RKS2309−0215	HIP 114322	TIC 278952345	Gaia DR2 2638410646295370880			HD 218566
RKS2309+1425		TIC 218044102	Gaia DR2 2815543034682035840		WDS J23100+1426B	AG+14 2584
RKS2310−2955	HIP 114455	TIC 13065840	Gaia DR2 6605330195652819840			HD 218760
RKS2316+0541	HIP 114941	TIC 262689575	Gaia DR2 2664042942398600064			BD+04 4988
RKS2317−2323	HIP 114954	TIC 9007748	Gaia DR2 2384877214983800448			CD−24 17578
RKS2319−1327	HIP 115125	TIC 214664575	Gaia DR2 2411855072801159040		WDS J23191−1328B	* 94 Aqr B
RKS2319+2852	HIP 115194	TIC 91103571	Gaia DR2 2869936905701172352			HD 219953
RKS2323−1045	HIP 115445	TIC 49644110	Gaia DR2 2436812303124645504			HD 220339
RKS2326+0853	HIP 115680	TIC 354307490	Gaia DR2 2761162254723511424			G 29−33
RKS2327−0117	HIP 115752	TIC 301289516	Gaia DR2 2643842302456085888			BD−02 5958
RKS2328+1604	HIP 115860	TIC 435239275	Gaia DR2 2814457541828905728		WDS J23284+1604A	BD+15 4829
RKS2332−1650	HIP 116215	TIC 434103018	Gaia DR2 2395031273585836288		WDS J23328−1651A	HD 221503
RKS2333−1239	HIP 116258	TIC 402317981	Gaia DR2 2433113374210098048		WDS J23334−1240A	HD 221575
RKS2335+0136A	HIP 116384	TIC 422618003	Gaia DR2 2646280705713202816		WDS J23350+0136A,BC	BD+00 5017
RKS2340+2021	HIP 116838	TIC 113492673	Gaia DR2 2826159850241446784		WDS J23409+2022A	HD 222474A
RKS2341+2002		TIC 113494080	Gaia DR2 2823131829578270080			LSPM J2341+2002N
RKS2342−0234A	HIP 116936	TIC 250107647	Gaia DR2 2639991331699321472			BD−03 5691
RKS2345+2933	HIP 117159	TIC 56249811	Gaia DR2 2867826668007900800			HD 222935
RKS2348−1259A	HIP 117410	TIC 471012663	Gaia DR2 2420563960807395072		WDS J23484−1259AB	BD−13 6464
RKS2349+0310	HIP 117463	TIC 267255100	Gaia DR2 2742801956727994880			HD 223374
RKS2350−2924	HIP 117542	TIC 33985272	Gaia DR2 2327840667768506368		WDS J23502−2924A	HD 223515
RKS2353+2901	HIP 117779	TIC 406543332	Gaia DR2 2867175035571212416		WDS J23531+2901A	BD+28 4660
RKS2355+2211	HIP 117946	TIC 437707246	Gaia DR2 2847644410526748416			HD 224129
RKS2356−1445		TIC 327953001	Gaia DR2 2419161082754688896			

Table 4: Look up table for star names.

RKS	Hipparcos	TIC	Gaia DR2	SB9	WDS	Simbad
RKS2357−1630	HIP 118086	TIC 441054056	Gaia DR2 2415330079301474432		WDS J23572−1631A	G 158−12
RKS2358+0949		TIC 408486919	Gaia DR2 2759228110692738304			HD 224476
RKS2359−2602	HIP 118261	TIC 65263849	Gaia DR2 2334879397612667648			HD 224607
RKS2359+0639	HIP 118310	TIC 401396607	Gaia DR2 2745473254589480960		WDS J23598+0640A	HD 224660A

REFERENCES

Agati, J. L., Bonneau, D., Jorissen, A., Soulié, E., Udry, S., Verhas, P., & Dommanget, J. 2015, A&A, 574, A6

Arenou, F. et al. 2018, A&A, 616, A17

Arriagada, P. 2011, ApJ, 734, 70

Bakos, G. Á., Pál, A., Latham, D. W., Noyes, R. W., & Stefanik, R. P. 2006, ApJ, 641, L57

Baranec, C. et al. 2012, in Society of Photo-Optical Instrumentation Engineers (SPIE) Conference Series, Vol. 8447, Adaptive Optics Systems III, ed. B. L. Ellerbroek, E. Marchetti, & J.-P. Véran, 844704

Barden, S. C. 1984, AJ, 89, 683

Barragán, O. et al. 2022, MNRAS, 514, 1606

Bonfils, X. et al. 2013, A&A, 549, A109

Bopp, B. W., Evans, D. S., Laing, J. D., & Deeming, T. J. 1970, MNRAS, 147, 355

Bouchy, F. et al. 2005, A&A, 444, L15

Brewer, J. M., Giguere, M., & Fischer, D. A. 2014, PASP, 126, 48

Burt, J. et al. 2021, AJ, 161, 10

Butler, R. P., Marcy, G. W., Vogt, S. S., Fischer, D. A., Henry, G. W., Laughlin, G., & Wright, J. T. 2003, ApJ, 582, 455

Butler, R. P., Marcy, G. W., Williams, E., Hauser, H., & Shirts, P. 1997, ApJ, 474, L115

Butler, R. P. et al. 2017, AJ, 153, 208

Ciardi, D. R., Beichman, C. A., Horch, E. P., & Howell, S. B. 2015, ApJ, 805, 16

Cuntz, M., & Guinan, E. F. 2016, ApJ, 827, 79

Davis, A. B. et al. 2020, AJ, 160, 229

Delisle, J. B. et al. 2018, A&A, 614, A133

Dorval, P. et al. 2020, A&A, 635, A60

Duchêne, G., & Kraus, A. 2013, ARA&A, 51, 269

Dumusque, X. et al. 2011, A&A, 535, A55

Duquennoy, A., & Mayor, M. 1991, A&A, 248, 485

Duquennoy, A., Tokovinin, A. A., Leinert, C., Glindemann, A., Halbwachs, J. L., & Mayor, M. 1996, A&A, 314, 846

Eker, Z. et al. 2015, AJ, 149, 131

Evans, D. W. et al. 2018, A&A, 616, A4

Fekel, F. C., Henry, G. W., & Tomkin, J. 2017, AJ, 154, 120

Feng, F. et al. 2022, ApJS, 262, 21

——. 2019, ApJS, 242, 25

——. 2020, ApJS, 250, 29

Fischer, D. A., Butler, R. P., Marcy, G. W., Vogt, S. S., & Henry, G. W. 2003, ApJ, 590, 1081

Forveille, T. et al. 2011, A&A, 526, A141

Fulton, B. J., Petigura, E. A., Blunt, S., & Sinukoff, E. 2018, PASP, 130, 044504

Gaidos, E., Fischer, D. A., Mann, A. W., & Howard, A. W. 2013, ApJ, 771, 18

Ge, J. et al. 2006, ApJ, 648, 683

Gould, A., & Chanamé, J. 2004, ApJS, 150, 455

Gray, R. O., & Corbally, Christopher, J. 2009, Stellar Spectral Classification (Princeton University Press)

Grether, D., & Lineweaver, C. H. 2006, ApJ, 640, 1051

Griffin, R. F. 1987, The Observatory, 107, 248

——. 2006, The Observatory, 126, 338

——. 2009, The Observatory, 129, 317

——. 2010, The Observatory, 130, 125

——. 2013, The Observatory, 133, 1

——. 2016, The Observatory, 136, 179

Guilluy, G. et al. 2020, A&A, 639, A49

Guilluy, G., Sozzetti, A., Brogi, M., Bonomo, A. S., Giacobbe, P., Claudi, R., & Benatti, S. 2019, A&A, 625, A107

Halbwachs, J. L., Mayor, M., & Udry, S. 2005, A&A, 431, 1129

——. 2018, A&A, 619, A81

Hatzes, A. P. et al. 2000, ApJ, 544, L145

Henry, G. W., Donahue, R. A., & Baliunas, S. L. 2002, ApJ, 577, L111

Henry, T. J., & McCarthy, Donald W., J. 1993, AJ, 106, 773

Henry, T. J., Soderblom, D. R., Donahue, R. A., & Baliunas, S. L. 1996, AJ, 111, 439

Hinkel, N. R., Kane, S. R., Henry, G. W., Feng, Y. K., Boyajian, T., Wright, J., Fischer,

D. A., & Howard, A. W. 2015, ApJ, 803, 8

Høg, E. et al. 2000, A&A, 355, L27

Horch, E. P., Gomez, S. C., Sherry, W. H., Howell, S. B., Ciardi, D. R., Anderson, L. M., & van Altena, W. F. 2011, AJ, 141, 45

Horch, E. P., Howell, S. B., Everett, M. E., & Ciardi, D. R. 2012, AJ, 144, 165

Horch, E. P., Veillette, D. R., Baena Gallé, R., Shah, S. C., O'Rielly, G. V., & van Altena, W. F. 2009, AJ, 137, 5057

Howard, A. W. et al. 2011, ApJ, 730, 10

Huang, C. X. et al. 2020, ApJ, 892, L7

Hubbard-James, H.-S., Lesley, D. X., Henry, T. J., Paredes, L. A., & Nisak, A. H. 2022, AJ, 164, 174

Imbert, M. 1979, A&AS, 38, 401

——. 2006, Romanian Astronomical Journal, 16, 3

Jones, M. I. et al. 2019, A&A, 625, A16

Latham, D. W., Stefanik, R. P., Torres, G., Davis, R. J., Mazeh, T., Carney, B. W., Laird, J. B., & Morse, J. A. 2002, AJ, 124, 1144

Lester, K. V. et al. 2022, arXiv e-prints, arXiv:2209.09993

Lo Curto, G. et al. 2013, A&A, 551, A59

Ma, B. et al. 2018, MNRAS, 480, 2411

Malkov, O. Y., Tamazian, V. S., Docobo, J. A., & Chulkov, D. A. 2012, A&A, 546, A69

Mamajek, E. E. 2012, arXiv e-prints, arXiv:1210.1616

Marcy, G. W., Butler, R. P., & Vogt, S. S. 2000, ApJ, 536, L43

Marcy, G. W., Butler, R. P., Vogt, S. S., Fischer, D. A., Henry, G. W., Laughlin, G., Wright, J. T., & Johnson, J. A. 2005, ApJ, 619, 570

Mason, B. D., Douglass, G. G., & Hartkopf, W. I. 1999, AJ, 117, 1023

Mason, B. D., Wycoff, G. L., Hartkopf, W. I., Douglass, G. G., & Worley, C. E. 2001, AJ, 122, 3466

Mayor, M. et al. 2003, The Messenger, 114, 20

Ment, K., Fischer, D. A., Bakos, G., Howard, A. W., & Isaacson, H. 2018, AJ, 156, 213

Meschiari, S., Laughlin, G., Vogt, S. S., Butler, R. P., Rivera, E. J., Haghighipour, N., & Jalowiczor, P. 2011, ApJ, 727, 117

Meschiari, S., Wolf, A. S., Rivera, E., Laughlin, G., Vogt, S., & Butler, P. 2009, PASP, 121, 1016

Mireles, I. et al. 2020, AJ, 160, 133

Moutou, C. et al. 2015, A&A, 576, A48

——. 2005, A&A, 439, 367

Nielsen, L. D. et al. 2020, A&A, 639, A76

Niraula, P. et al. 2017, AJ, 154, 266

Nisak, A. H., White, R. J., Yep, A., Henry, T. J., Paredes, L., James, H.-S., & Jao, W.-C. 2022, AJ, 163, 278

Oh, S., Price-Whelan, A. M., Hogg, D. W., Morton, T. D., & Spergel, D. N. 2017, AJ, 153, 257

Oliva, E. et al. 2006, in Society of Photo-Optical Instrumentation Engineers (SPIE) Conference Series, Vol. 6269, Society of Photo-Optical Instrumentation Engineers (SPIE) Conference Series, ed. I. S. McLean & M. Iye, 626919

Osborn, A. et al. 2021, MNRAS, 507, 2782

Paredes, L., Henry, T., Nusdeo, D., James, H., Jao, W., & Speckle Team. 2020, in American Astronomical Society Meeting Abstracts, Vol. 235, American Astronomical Society Meeting Abstracts #235, 374.03

Paredes, L. A., Henry, T. J., Quinn, S. N., Gies, D. R., Hinojosa-Goñi, R., James, H.-S., Jao, W.-C., & White, R. J. 2021, AJ, 162, 176

Pecaut, M. J., & Mamajek, E. E. 2013, ApJS, 208, 9

Pepe, F. et al. 2011, A&A, 534, A58

Piskunov, N. E., & Valenti, J. A. 2002, A&A, 385, 1095

Pourbaix, D. et al. 2004, A&A, 424, 727

Raghavan, D. et al. 2010, ApJS, 190, 1

Redfield, S., Endl, M., Cochran, W. D., & Koesterke, L. 2008, ApJ, 673, L87

Reiners, A. et al. 2018, A&A, 612, A49

Richey-Yowell, T. et al. 2022, ApJ, 929, 169

Richey-Yowell, T., Shkolnik, E. L., Schneider, A. C., Osby, E., Barman, T., & Meadows, V. S. 2019, ApJ, 872, 17

Riddle, R. L. et al. 2015, ApJ, 799, 4

Roberts, Lewis C., J., Tokovinin, A., Mason, B. D., Riddle, R. L., Hartkopf, W. I., Law,

N. M., & Baranec, C. 2015, AJ, 149, 118

Robertson, P., Endl, M., Cochran, W. D., MacQueen, P. J., & Boss, A. P. 2013, ApJ, 774, 147

Rodríguez Martínez, R. et al. 2020, AJ, 160, 111

Rosenthal, L. J. et al. 2021, ApJS, 255, 8

Rozyczka, M., Pietrukowicz, P., Kaluzny, J., Pych, W., Angeloni, R., & Dékány, I. 2013, MNRAS, 429, 1840

Santos, N. C., Mayor, M., Naef, D., Pepe, F., Queloz, D., Udry, S., Burnet, M., & Revaz, Y. 2000, A&A, 356, 599

Santos, N. C. et al. 2003, A&A, 406, 373

Ségransan, D. et al. 2011, A&A, 535, A54

Shaya, E. J., & Olling, R. P. 2011, ApJS, 192, 2

Silverstein, M. L. et al. 2022, AJ, 163, 151

Skrutskie, M. F. et al. 2006, AJ, 131, 1163

Söderhjelm, S. 1999, A&A, 341, 121

Sperauskas, J., Deveikis, V., & Tokovinin, A. 2019, A&A, 626, A31

Stassun, K. G. et al. 2019, AJ, 158, 138

——. 2018, AJ, 156, 102

Suárez, A. et al. 2018, A&A, 612, A41

Subasavage, J. P., Bailyn, C. D., Smith, R. C., Henry, T. J., Walter, F. M., & Buxton, M. M. 2010, in Society of Photo-Optical Instrumentation Engineers (SPIE) Conference

Series, Vol. 7737, Observatory Operations: Strategies, Processes, and Systems III, 77371C

Tal-Or, L., Trifonov, T., Zucker, S., Mazeh, T., & Zechmeister, M. 2019, MNRAS, 484, L8

Tokovinin, A. 2014, AJ, 147, 87

——. 2016, AJ, 152, 11

Tokovinin, A., Fischer, D. A., Bonati, M., Giguere, M. J., Moore, P., Schwab, C., Spronck, J. F. P., & Szymkowiak, A. 2013, PASP, 125, 1336

Tokovinin, A. A. 1991, A&AS, 91, 497

——. 1992, A&A, 256, 121

Tokovinin, A. A., Balega, Y. Y., Hofmann, K. H., & Weigelt, G. 2000, Astronomy Letters, 26, 668

Trifonov, T., Tal-Or, L., Zechmeister, M., Kaminski, A., Zucker, S., & Mazeh, T. 2020, A&A, 636, A74

Tuomi, M., Jones, H. R. A., Barnes, J. R., Anglada-Escudé, G., & Jenkins, J. S. 2014, MNRAS, 441, 1545

Udry, S. et al. 2000, A&A, 356, 590

Valenti, J. A., & Fischer, D. A. 2005, ApJS, 159, 141

van Leeuwen, F. 2007, A&A, 474, 653

Vanderspek, R. et al. 2019, ApJ, 871, L24

Vogt, S. S. et al. 1994, in Society of Photo-Optical Instrumentation Engineers (SPIE) Conference Series, Vol. 2198, Instrumentation in Astronomy VIII, ed. D. L. Crawford & E. R. Craine, 362

Vogt, S. S., Butler, R. P., Marcy, G. W., Fischer, D. A., Pourbaix, D., Apps, K., & Laughlin, G. 2002, ApJ, 568, 352

Wang, S. et al. 2019, AJ, 157, 51

Ward-Duong, K. et al. 2015, MNRAS, 449, 2618

Wenger, M. et al. 2000, A&AS, 143, 9

Wilson, O. C. 1978, ApJ, 226, 379

Winters, J. G. et al. 2019, AJ, 157, 216

Wittenmyer, R. A., Endl, M., Cochran, W. D., Levison, H. F., & Henry, G. W. 2009, ApJS, 182, 97

Wittrock, J. M., Kane, S. R., Horch, E. P., Hirsch, L., Howell, S. B., Ciardi, D. R., Everett, M. E., & Teske, J. K. 2016, AJ, 152, 149

Wright, J. T., & Eastman, J. D. 2014, PASP, 126, 838

Zhou, G. et al. 2020, ApJ, 892, L21

Zucker, S. 2003, MNRAS, 342, 1291